When citing an abstract from the 2026 annual meeting, please use the format below.

[Authors]. [Abstract Title]. Program No. XXX.XX. 2026 Neuroscience Meeting Planner. Washington, DC: Society for Neuroscience, 2026. Online.

2026 Copyright by the Society for Neuroscience all rights reserved. Permission to republish any abstract or part of any abstract in any form must be obtained in writing by SfN office prior to publication.

Information is current as of November 5, 2026. See the Neuroscience 2026 Neuroscience Meeting Planner on SfN.org for the most up-to-date information.

**Poster**

**PSTR163: Transcriptional and Epigenetic Regulation of Neurogenesis**

**Location:** WCC Halls A-C

**Time:** Monday, November 16, 2026, 1:00 PM - 5:00 PM

**Program #/Poster #:** PSTR163.01/D1

**Topic:** A.01. Neurogenesis and Gliogenesis

**Support:** NSF

**Title:** EHMT1 and EHMT2 Function as Epigenetic Regulators of the Timing of Cortical Neurogenesis.

**Authors: *A. CHOUDHURI**[1], M. BAIZABAL[2];
[1]Biol., Indiana Univ. Bloomington, BLOOMINGTON, IN; [2]Biol., Indiana Univ. Bloomington, Bloomington, IN

**Abstract:** Epigenetic regulation of neural progenitor differentiation and proliferation is fundamental to mammalian cortical development. Its disruption is often implicated in neurodevelopmental disorders, which frequently arise from mutations in chromatin-modifying enzymes. However, the mechanisms by which chromatin modifications regulate cortical neurogenesis are poorly defined. The histone lysine methyltransferases EHMT1 and EHMT2 catalyze mono- and di-methylation of histone H3 lysine 9 (H3K9me1 and H3K9me2), and *EHMT1* haploinsufficiency causes Kleefstra syndrome. Despite these advances, the cooperative roles of EHMT1 and EHMT2 in regulating neurogenic gene expression programs remain elusive. To address this gap, we generated a cortex-specific double-knockout mouse model for *Ehmt1* and *Ehmt2* during early embryonic neurogenesis. We used integrative multi-omics approaches, combining single-cell transcriptomics, ChIP-seq, and chromatin accessibility profiling to elucidate the mechanisms of EHMT1/2-mediated gene regulation during cortical development. Our data indicate that loss of EHMT1/2 leads to robust and specific H3K9me2 depletion. The *Ehmt1/2* KOs exhibited cortical thinning due to disrupted neural progenitor behavior. Furthermore, our genomic data revealed repressive and activating roles for EHMT2 in the temporal execution of neurogenesis. Ultimately, we aim to uncover the mechanisms of EHMT1/2-mediated gene regulation in corticogenesis, setting up future studies with human *in vitro* models of Kleefstra syndrome.

**Disclosures: A. Choudhuri:** None. **M. Baizabal:** None.

**Poster**

**PSTR163: Transcriptional and Epigenetic Regulation of Neurogenesis**

**Location:** WCC Halls A-C

**Time:** Monday, November 16, 2026, 1:00 PM - 5:00 PM

**Program #/Poster #:** PSTR163.02/D2

**Topic:** A.01. Neurogenesis and Gliogenesis

**Support:** NINDS Grant 5R25NS130965
NINDS Grant R01NS114551
NINDS Grant U0-HG007530
NIMH Grant R01MH124808
NICHD Grant R01HD110556
NICHD Grant P50HD103525

**Title:** Investigating interactions between the disease-relevant RFX transcription factors and their roles in human cortical neurogenesis

**Authors: *J. C. GAINES**, J. J. DETERMAN, K. L. KROLL;
Developmental Biol., Washington Univ. in St. Louis, St. Louis, MO

**Abstract:** Human cortical neurogenesis is an intricate, tightly managed process centrally controlled by transcriptional regulatory networks. As major components of these networks, transcription factors (TFs) orchestrate pivotal cellular fate transitions during neurogenesis, including the differentiation of neural progenitor cells (NPCs) into neurons. Our prior work derived an epigenetic atlas by which to identify novel TFs that bind cis-regulatory elements (CREs) during cortical interneuron development. Focusing on the transition of human pluripotent stem cell (hPSC)-derived medial ganglionic eminence-like (MGE) progenitors into cortical interneurons, we identified Regulatory Factor X (RFX) 2, 3, and 4 as key regulators of neurogenesis — results of particular interest considering the recent designation of RFX 3, 4, and 7 as autism spectrum disorder risk genes. Motivated by its temporally restricted expression in NPCs, our latest work sought to characterize the regulatory functions of RFX4. We found that RFX4 restrains the onset of neuronal gene expression during both GABAergic and glutamatergic neurogenesis and functions downstream of NOTCH signaling to repress pro-neuronal and synaptic gene expression. We also found that RFX3 requires RFX4 for genome-wide binding, while others have shown that RFX TFs form homo- and heterodimers with themselves and other RFX family members. Taken together, these data suggest coordination between the RFX TFs to regulate developmental processes during cortical neurogenesis. However, the exact mechanisms by which RFX TFs control cortical development, including how they interact with both each other and other TFs, remain largely unknown. Here, we have derived CRISPRi models to enable the knockdown of RFX 1, 2, 5, and 7 in hPSCs. Complementing their differentiation into GABAergic and glutamatergic NPCs with transcriptomic, epigenetic, and cellular phenotyping analyses, we have profiled the consequences of RFX knockdown during progenitor specification and begun to characterize the functional relationships between RFX4 and the other RFX TFs. Ultimately, this work will elucidate requirements for the RFX TFs during cortical development and inform our understanding of neurodevelopmental disorders caused by mutations in the RFX genes.

**Disclosures: J.C. Gaines:** None. **J.J. Determan:** None. **K.L. Kroll:** None.

**Poster**

**PSTR163: Transcriptional and Epigenetic Regulation of Neurogenesis**

**Location:** WCC Halls A-C

**Time:** Monday, November 16, 2026, 1:00 PM - 5:00 PM

**Program #/Poster #:** PSTR163.03/D3

**Topic:** A.01. Neurogenesis and Gliogenesis

**Support:** SFARI Pilot Award SFI-AN-AR-Pilot-00010018
Washington University in St. Louis School of Medicine laboratory start-up funds
NIH Grant NS130965

**Title:** NFI transcription factors and TCF4 converge to regulate neuronal differentiation during neocortical development

**Authors: *J. E. ANTONIAK**, J. W. C. LIM, E. HOSSEN, N. A. MUNDELL, S. PAL, L. J. RICHARDS;
Dept. of Neurosci., Washington Univ. in St. Louis, St. Louis, MO

**Abstract:** The nuclear factor one (NFI) family of transcription factors consists of NFIA, NFIB, NFIC, and NFIX. In humans and mice, *NFIA*, *NFIB*, and *NFIX* are expressed at high levels in the cerebral cortex during development as well as adulthood. Haploinsufficiency of *NFIA*, *NFIB*, and *NFIX* results in human neurodevelopmental syndromes that share characteristic features with another neurodevelopmental syndrome caused by transcription factor 4 (*TCF4*) haploinsufficiency. Shared phenotypes between *NFI* and *TCF4* haploinsufficiency syndromes include intellectual disability, developmental delay, and dysgenesis of the corpus callosum. These overlapping phenotypes indicate that *NFIA*, *NFIB*, *NFIX*, and *TCF4* haploinsufficiency syndromes may have similar underlying etiologies. Additionally, recent transcriptomic, epigenomic, and proteomic studies suggest that NFIB and TCF4 may converge by binding to the same cis-regulatory elements and regulate a common set of target genes as a result. Given the shared phenotypes of *NFI* and *TCF4* haploinsufficiency syndromes and the evidence supporting molecular convergence, we investigated whether NFIB and TCF4 converge by regulating similar target genes during neocortical development. We compared bulk RNA-seq data of embryonic day 13.5 (E13.5) *Nfib* knockout (KO) and E14.5 *Tcf4* KO mouse cortical tissue and found a large overlapping set of downregulated genes involved in neuronal differentiation. We next performed Cleavage Under Targets & Release Using Nuclease (CUT&RUN) on E14.5 neocortical tissue to identify genome-wide binding of NFIB and TCF4. This revealed over 6000 shared binding sites across the genome. We further hypothesized that NFIB and TCF4 may physically interact with each other to bind to these regulatory elements. Therefore, we are currently performing GST-pulldown experiments to test this hypothesis. These ongoing experiments could reveal how these transcription factors function to regulate similar target genes and identify potential mechanisms underlying *NFI* and *TCF4* haploinsufficiency syndromes.

**Disclosures: J.E. Antoniak:** None. **J.W.C. Lim:** None. **E. Hossen:** None. **N.A. Mundell:** None. **S. Pal:** None. **L.J. Richards:** None.

**Poster**

**PSTR163: Transcriptional and Epigenetic Regulation of Neurogenesis**

**Location:** WCC Halls A-C

**Time:** Monday, November 16, 2026, 1:00 PM - 5:00 PM

**Program #/Poster #:** PSTR163.04/D4

**Topic:** A.01. Neurogenesis and Gliogenesis

**Support:** 22KK0107
JP25wm0625506

**Title:** The role of cohesin in chromatin architecture and gene regulation in the brain

**Authors: *Y. FUJITA**;
Shimane Univ., Izumo-shi, Shimane, Japan

**Abstract:** Gene expression regulated by spatial chromatin organization and nuclear architecture plays a crucial role in brain development. Our research focuses on the functions of the cohesin complex, a chromosome-associated multi-subunit protein complex, in embryonic and adult neurogenesis.Cohesin is a highly conserved nuclear protein complex composed of four core subunits, which together form a ring-like structure. The cohesin complex is best known for its essential role in sister chromatid cohesion during cell division, in which it physically encircles sister chromatids to ensure accurate chromosome segregation. Notably, cohesin subunits continue to be expressed in postmitotic cells, including NeuN-positive neurons, suggesting additional functions beyond cell-cycle regulation.Beyond its canonical role in sister chromatid cohesion, cohesin has been shown to mediate chromatin loop formation and higher-order chromatin organization, thereby contributing to the regulation of gene expression. Loss of cohesin function disrupts chromatin looping and genome architecture, leading to widespread alterations in transcriptional programs. We investigate how cohesin-dependent chromatin organization influences gene expression and contributes to the regulation of neural stem cell maintenance, neuronal differentiation, and brain development.Mutations that perturb the function of cohesin or the proteins that regulate cohesin function cause Cornelia de Lange syndrome (CdLS), a rare malformation syndrome characterized by mental retardation, limb abnormalities, and distinctive facial features. Most of these mutations do not cause overt defects in cohesion or chromosomal segregation.To investigate the potential role of cohesin in terminally differentiated cells in vivo, we generated conditional Smc3-knockout mice. We observed craniofacial abnormality and decreased spine density in cortical neurons of heterozygous Smc3-knockout mice. Heterozygous Smc3-knockout mice exhibited increased anxiety-related behavior, which is consistent with a symptom of Cornelia de Lange syndrome. Thus, neuronal cohesin contributes to neural network formation, and cohesin deficiency leads to higher brain dysfunction.

**Disclosures: Y. Fujita:** None.

**Poster**

**PSTR163: Transcriptional and Epigenetic Regulation of Neurogenesis**

**Location:** WCC Halls A-C

**Time:** Monday, November 16, 2026, 1:00 PM - 5:00 PM

**Program #/Poster #:** PSTR163.05/D5

**Topic:** A.01. Neurogenesis and Gliogenesis

**Title:** An Oncogenic lncRNA in a Developmental Role: DANCR as an Epigenetic Regulator of Early Murine Neurogenesis

**Authors: *D. YADAV**;
Biol. Dept., IISER Pune, India, Pune, India

**Abstract: An Oncogenic lncRNA in a Developmental Role: DANCR as an Epigenetic Regulator of Early Murine Neurogenesis**Dipika Yadav[1], Mansi Srivastava[2], Shreya D[1], Karishma Shaw[1], Christeena Charly[1], Nixon Abraham[1], and Sanjeev Galande[2]
1.Laboratory of Neural Circuit and Behaviour, Department of Biology, Indian Institute of Science Education and Research, Pune, Maharashtra, India2.Center of Excellence in Epigenetics, Department of Life Sciences, Shiv Nadar Institution of Eminence, Gautam Buddha Nagar, Uttar Pradesh, India.
Long non-coding RNAs (lncRNAs) orchestrate a wide range of physiological and pathological processes; however, the neurodevelopmental functions of many oncogenic lncRNAs remain largely unexplored. Here, we investigate previously uncharacterized function of the onco-lncRNA *DANCR* in early murine brain development. Building on recent evidence of its role in zebrafish embryogenesis, and given its established role in sustaining stemness across multiple cancer types, we hypothesized that *DANCR* also governs early neurodevelopmental transitions. Developmental expression profiling via quantitative RT-PCRs demonstrated that *DANCR* transcript peaks during late embryogenesis and at birth followed by a sharp downregulation during early postnatal stages. At birth, the transcript exhibits ubiquitous spatial distribution across distinct brain regions. Notably, *DANCR* has been widely annotated as primarily a cytoplasmic lncRNA, however, our subcellular fractionation assays demonstrated substantial nuclear retention. To delineate transcriptional regulatory networks driven by this nuclear pool, we performed bulk RNA-sequencing following lentivirus-mediated *DANCR* knockdown in cultured primary cortical neurons(CPCN). Transcriptomic profiling revealed the dysregulation of immediate early genes and transmembrane transporters and various other subset of genes. Furthermore, Gene Ontology (GO) analysis indicated significant enrichment in pathways governing multicellular development. Immunofluorescence assays corroborated these transcriptomic shifts, revealing distinct cell-type-specific alterations upon DANCR depletion. Ongoing calcium imaging explores DANCR-dependent neuronal activity modulation in CPCN. Finally, mechanistic studies indicate that DANCR interacts directly with the methyltransferase DNMT1, implicating it in modulation of global DNA methylation landscapes. Collectively, these findings uncover a novel physiological role for DANCR as a critical epigenetic regulator driving of early murine neural development and cellular state transitions.

**Disclosures: D. Yadav:** None.

**Poster**

**PSTR163: Transcriptional and Epigenetic Regulation of Neurogenesis**

**Location:** WCC Halls A-C

**Time:** Monday, November 16, 2026, 1:00 PM - 5:00 PM

**Program #/Poster #:** PSTR163.06/D6

**Topic:** A.01. Neurogenesis and Gliogenesis

**Title:** Patterns of Transcriptomic Expression of the Endogenous Retrovirus HML-2 in Cortical, Hindbrain, and Lower Motor Neurons

**Authors: *A. GARCIA**, D. PANDYA, J. STONE, S. DARKO, D. CASTELLANOS, A. NATH;
NINDS, NIH, Bethesda, MD

**Abstract:** Introduction Human endogenous retrovirus (HERV) sequences account for ~8% of the human genome. While unable to produce replicating virus, some can still generate transcripts and proteins. HML-2 is the youngest and most transcriptionally active HERV subgroup, with variably intact *env, gag, rec,* or *np9* gene sequences distributed across ~100 loci. Because HML-2 loci differ in genomic location, they may be differentially regulated and have distinct roles in neurons. HML-2 protein expression is associated with stemness, its overexpression impairs neuronal differentiation, and HML-2 Env is neurotoxic and associated with amyotrophic lateral sclerosis (ALS). However, locus-specific HML-2 transcription in neurons remains poorly defined. Methods Cortical neurons (CN) and lower motor neurons (LMN) were differentiated from doxycycline-inducible WTC-11 iPSC lines. Hindbrain neurons (HBN) were generated from CD34+ cord blood-derived neural stem cells (NSC). Short-read RNA-seq was performed at iPSC, day 1, and day 7 for CN and LMN cultures and in HBN at NSC and day 30. Reads were quality-checked, trimmed, and aligned to GRCh38, and HML-2 locus counts quantified using TELocal. HML-2 gene transcripts were measured by qRT-PCR as fold change (FC) relative to GAPDH. Results *Env, gag, rec,* and *np9* transcripts increased from day 1 to day 7 in CN (FC=3.4,2.7,14,1.6; $p<0.05$) and in HBN from NSC to day 30 (FC=3.8,3.2,10; $p<0.05$). In LMN, *env* and *gag* remained stable from day 1 to day 7 (FC=1, 0.8; $p>0.05$) but *rec* and *np9* decreased (FC=0.2,0.5; $p<0.05$). Neural induction yielded a drop in total HML-2 transcripts, after which expression remained relatively stable. Increases in loci-specific transcripts were seen in CN (8p23.1, 12q42.33, 19q13.12) and HBN (8p23.1, 7q34, 1q21.3), while stable/declining expression was seen in LMN (8p23.1, 7q34 1q21.3) through neuronal differentiation. 8p23.1 was among the highest-expressed loci in post-mitotic neurons across all lineages. Conclusions These exploratory data indicate that HML-2 transcript expression during neuronal differentiation is locus and lineage-specific. HML-2 genes are differentially expressed across lineages. *Rec* displays the strongest fold change increase in CN and HBN but declines in LMN. Broad reduction in HML-2 transcripts after neural induction supports prior work, but persistent expression of select loci in post-mitotic neurons suggests involvement in processes beyond stemness. The consistent expression of select loci in differentiated neurons raises the possibility that lineage-specific HML-2 loci may contribute to neuronal identity or potentially disease-relevant transcriptional states.

**Disclosures: A. Garcia:** None. **D. Pandya:** None. **J. Stone:** None. **S. Darko:** None. **D. Castellanos:** None. **A. Nath:** None.

**Poster**

**PSTR163: Transcriptional and Epigenetic Regulation of Neurogenesis**

**Location:** WCC Halls A-C

**Time:** Monday, November 16, 2026, 1:00 PM - 5:00 PM

**Program #/Poster #:** PSTR163.07/D7

**Topic:** A.01. Neurogenesis and Gliogenesis

**Title:** Investigating roles of the transferrin receptor in human cortical neurogenesis

**Authors: *Z. OU**[1], J. GUNDY[2], R. PURCELL[3];
[1]Virginia Tech., Roanoke, VA; [2]Virginia Tech., Blacksburg, VA; [3]Fralin Biomed. Res. Inst., Virginia Tech., Roanoke, VA

**Abstract:** Autism spectrum disorder (ASD) and schizophrenia (SCZ) are neurodevelopmental disorders that are associated with shortened life expectancy compared to healthy populations. In order to make earlier and more accurate diagnosis possible and help with potential treatment development, it is important to better understand the etiologies and molecular pathogenesis of these disorders. Early-life iron deficiency (FeD) is associated with increased risk for ASD and SCZ in addition to other neurodevelopmental conditions, but the reason that FeD increases the risk for these disorders not understood. Iron is imported to cells by the transferrin receptor (TFRC), which is encoded by the *TFRC* gene, and it is critical for many fundamental biological processes in the brain. 3q29 deletion (3q29Del) is a copy number variant (CNV) that results in hemizygosity of the *TFRC* gene, and leads to 20 times increased risk for ASD. It is also the strongest known genetic risk factor for SCZ, with more than 40-fold higher risk. *TFRC* is located within the 3q29Del locus and is well-positioned to serve as a mediator of environmental risk in the context of genetic risk for neurodevelopmental disorders, but its role in human neurogenesis is unclear. Here, we investigate the role of TFRC in neurogenesis in vitro via human induced pluripotent stem cell (iPSC) derived neurons and hypothesize that *TFRC* is critical for neurogenesis during brain development because of its key function in cellular iron import to meet the metabolic requirement for neuron development. We deleted *TFRC* from iPSC lines derived from neurotypical individuals using a CRISPR/Cas9 approach. Edited and mock-edited control iPSC clones were selected and characterized by Western blot and Sanger sequencing. At Neuroscience 2026 we will present the results of ongoing experiments aimed at determining the impact of *TFRC* on human cortical neurogenesis and neural cell type proportions in cortical organoids. We will further test whether restoring *TFRC* expression to 3q29Del cell lines rescues cellular phenotypes. These studies will improve our understanding of the roles for this essential iron importer in human corticogenesis.

**Disclosures: Z. Ou:** None. **J. Gundy:** None. **R. Purcell:** None.

**Poster**

**PSTR163: Transcriptional and Epigenetic Regulation of Neurogenesis**

**Location:** WCC Halls A-C

**Time:** Monday, November 16, 2026, 1:00 PM - 5:00 PM

**Program #/Poster #:** PSTR163.08/D8

**Topic:** A.01. Neurogenesis and Gliogenesis

**Support:** Campbell Foundation
NIH R21093993-02
GVSU Kindschi Fellowship
GVSU Student Summer Scholar
Michigan Economic Development Corporation

**Title:** A conserved serine in the bHLH NATO3 is phosphorylated by protein kinase A and promotes pro-dopaminergic gene expression in neural progenitors

**Authors: *M. K. DELANO-TAYLOR**[1], S. MATHEW[2], A. VANDERSLOOT[4], W. DUBE[3]; [1]Biomed. Sci., Grand Valley State Univ., Allendale, MI; [2]Grand Valley State Univ., allendale, MI; [3]Grand Valley State Univ., Allendale, MI; [4]Grand Valley State, Grand Rapids, MI

**Abstract:** Dopaminergic (DA) neurons are essential for movement, motivation, and cognition, and their dysfunction is associated with neurological disorders such as Parkinson's disease. The transcription factor Nato3, a member of the basic helix-loop-helix (bHLH) family, promotes the expression of genes required for DA neuron development, yet the mechanisms regulating its activity remain unclear. Phosphorylation may represent a key mechanism of this regulation, and Nato3 possesses a highly conserved Protein Kinase A (PKA) consensus sequence in the putative loop domain that regulates activity of other bHLH proteins. Using in vitro kinase assays with synthetic peptides representing Nato3 sequences, followed by tandem mass spectrometry, we identified kinase-specific phosphorylation patterns at serine 138 (S138). When this serine is modified to an aspartate to mimic the negative charge of phosphorylation, it can elevate dopaminergic gene expression broadly in the developing chick embryo and a more restricted set of dopaminergic genes in human embryonic stem cells. Together, these findings identify S138 as a phosphorylation site on Nato3 and demonstrates that modification of this residue can regulate dopaminergic gene expression in neural progenitors. These insights could inform future strategies for promoting dopaminergic neuron production and advance therapeutic approaches for disorders involving dopaminergic neuron loss.

**Disclosures: M.K. Delano-Taylor:** None. **S. Mathew:** None. **A. VanderSloot:** None. **W. Dube:** None.

**Poster**

**PSTR163: Transcriptional and Epigenetic Regulation of Neurogenesis**

**Location:** WCC Halls A-C

**Time:** Monday, November 16, 2026, 1:00 PM - 5:00 PM

**Program #/Poster #:** PSTR163.09/D9

**Topic:** A.01. Neurogenesis and Gliogenesis

**Support:** Universidad Católica de la Santísima Concepción FIAEC 01/2021, DIREG 09/2022, DIREG 09/2024, DI FMEI 01/2024, FGII03/2024

**Title:** Exposure-window-dependent reprogramming of embryonic cortical and interneuron development by maternal high-fat diet.

**Authors: *E. RETAMAL**[1], R. CARRAZANA[2], F. ESPINOZA[2], L. MARDONES[2], M. VILLAGRAN[2], C. ESCUDERO[3], P. VIDAL VERA[4], A. ÁVILA[2];
[1]Univ. Católica de la Santisima Concepción, Concepcion, Chile; [2]Univ. Católica de la Santísima Concepción, Concepción, Chile; [3]Basic Sci., Univ. del Bio Bio, Chillan, Chile; [4]Basic Sci., Univ. Católica De La Santísima Concepción, Concepcion, Chile

**Abstract:** Maternal obesity and high-fat diet (HFD) consumption increase offspring risk for neurodevelopmental disorders, yet whether maternal HFD acts through a uniform pathological trajectory or through exposure-window-dependent developmental reprogramming remains unclear. We recently showed that acute gestational HFD alters cortical progenitor dynamics, neuronal output, interneuron composition, and placental inflammatory signaling in a sex-dependent manner. Here, we tested whether preconception HFD exposure amplifies this phenotype or redirects corticogenesis and interneuron development through distinct trajectories. Female C57BL/6 mice were exposed to HFD for defined preconception periods and maintained on the same diet until embryonic day 15 (E15). Embryonic brains and placentas were analyzed by morphometry, immunohistochemistry, and cytokine profiling, focusing on cortical progenitors, neurogenic progression, ventral telencephalic progenitor domains, and tissue-specific inflammatory responses. Preconception HFD altered embryonic cortical development in an exposure-duration-dependent manner. Rather than linearly extending the acute gestational phenotype, extended HFD produced distinct effects on progenitor abundance, proliferative activity, progenitor-state transitions, cleavage-plane orientation, and neuronal output. These changes suggest that maternal metabolic history shifts the balance between progenitor maintenance and neurogenic progression. Prolonged HFD also modified ventral telencephalic progenitor populations associated with cortical interneuron generation. Together with our previous findings on SST- and PV-associated developmental trajectories, these data indicate that maternal HFD reprograms excitatory and inhibitory lineage development in a window-dependent manner. Placental and embryonic brain tissues exhibited divergent inflammatory and redox-associated adaptations. Placental cytokine changes were detected across HFD-exposed offspring, whereas embryonic brain responses showed sex-dependent modulation of inflammatory mediators and oxidative activity. Overall, exposure timing and duration determine the direction and cellular specificity of HFD-induced developmental disruption, identifying maternal metabolic history before conception as a determinant of embryonic cortical development and neurodevelopmental vulnerability.

**Disclosures: E. Retamal:** None. **R. Carrazana:** None. **F. Espinoza:** None. **L. Mardones:** None. **M. Villagran:** None. **C. Escudero:** None. **P. Vidal Vera:** None. **A. Ávila:** None.

**Poster**

**PSTR163: Transcriptional and Epigenetic Regulation of Neurogenesis**

**Location:** WCC Halls A-C

**Time:** Monday, November 16, 2026, 1:00 PM - 5:00 PM

**Program #/Poster #:** PSTR163.10/D10

**Topic:** A.01. Neurogenesis and Gliogenesis

**Support:** R35NS097370
R01MH125528
R01CA264932
R01CA 260729
R35NS116843
RF1AG079557

**Title:** Epigenetic maintenance of adult neural stem cell quiescence in the mouse hippocampus via Setd1a

**Authors: *T. ZHAO**[1], Y. HONG[1], G.-L. MING[2], H. SONG[3];
[1]Univ. of California, Riverside, Riverside, CA; [2]Dept Neurosci, Univ. of Pennsylvania, gladwyne, PA; [3]Neurosci., Univ. of Pennsylvania, Philadelphia, PA

**Abstract:** Quiescence, a hallmark of adult neural stem cells (NSCs), is required for maintaining the NSC pool to support life-long continuous neurogenesis in the adult dentate gyrus (DG). Whether long-lasting epigenetic modifications maintain NSC quiescence over the long term in the adult DG is not well-understood. Here we show that mice with haploinsufficiency of *Setd1a*, a schizophrenia risk gene encoding a histone H3K4 methyltransferase, develop an enlarged DG with more dentate granule cells after young adulthood. Deletion of *Setd1a* specifically in quiescent NSCs in the adult DG promotes their activation and neurogenesis, which is countered by inhibition of the histone demethylase LSD1. Mechanistically, RNA-sequencing and CUT & RUN analyses of cultured quiescent adult NSCs reveal *Setd1a* deletion-induced transcriptional changes and many Setd1a targets, among which downregulation of *Bhlhe40* promotes quiescent NSC activation in the adult DG in vivo. Together, our study reveals a Setd1a-dependent epigenetic mechanism that sustains NSC quiescence in the adult DG.

**Disclosures: T. Zhao:** None. **Y. Hong:** None. **G. Ming:** None. **H. Song:** None.

**Poster**

**PSTR163: Transcriptional and Epigenetic Regulation of Neurogenesis**

**Location:** WCC Halls A-C

**Time:** Monday, November 16, 2026, 1:00 PM - 5:00 PM

**Program #/Poster #:** PSTR163.11/Web Only

**Topic:** A.01. Neurogenesis and Gliogenesis

**Title:** Long-Read Isoform Profiling Reveals Lineage-Specific Transcript Diversity Across Human Cortical, Motor, and Dopaminergic Neuronal Development

**Authors: *J. KIM**[1], M. ALAM[2], A. DESCOEUDRES[2], S. CANZAR[2], R. SCHUBERT[1];
[1]Korea Advanced Inst. of Sci. and Technol., Daejeon, Korea, Republic of; [2]Univ. of Regensburg, Regensburg, Germany

**Abstract:** Alternative splicing and transcript isoform diversity play critical roles in establishing neuronal identity and function, yet remain incompletely characterized across distinct human neuronal lineages. Here, we generated a multi-lineage long-read transcriptomic resource spanning cortical, motor, and dopaminergic neuronal differentiation using human induced pluripotent stem cell (iPSC)-derived neural progenitor cells and mature neuronal populations. Disease-relevant models, including FMR1 knockout cortical neurons, α-synuclein (SNCA)-perturbed dopaminergic neurons, and TARDBP (A382T and G348C) mutant motor neurons, were incorporated to investigate lineage-specific transcriptomic alterations associated with neurodevelopmental and neurodegenerative disorders.Transcriptomes were profiled using PacBio and Oxford Nanopore long-read sequencing, enabling comprehensive characterization of full-length isoforms, alternative splicing events, and transcript usage across developmental stages and neuronal subtypes. Comparative analyses identified extensive lineage-specific isoform programs that distinguished cortical, motor, and dopaminergic trajectories. Neuronal maturation was accompanied by dynamic shifts in transcript usage and alternative splicing, revealing molecular signatures associated with lineage commitment and neuronal specialization. Disease-associated perturbations further altered isoform composition and splicing patterns within affected neuronal populations, highlighting transcript-level regulatory changes not readily captured by gene-level expression analyses.Together, these findings establish a framework for studying transcriptomic complexity during human neuronal development and demonstrate the value of long-read sequencing for resolving isoform-level mechanisms underlying neurological disease. This resource provides a foundation for identifying lineage-specific RNA processing events that contribute to neuronal identity, function, and vulnerability.

**Disclosures: J. Kim:** None. **M. Alam:** None. **A. Descoeudres:** None. **S. Canzar:** None. **R. Schubert:** None.

**Poster**

**PSTR163: Transcriptional and Epigenetic Regulation of Neurogenesis**

**Location:** WCC Halls A-C

**Time:** Monday, November 16, 2026, 1:00 PM - 5:00 PM

**Program #/Poster #:** PSTR163.12/D12

**Topic:** A.01. Neurogenesis and Gliogenesis

**Support:** NICHD DIR HD008962
NICHD DIR HD001205

**Title:** Mature interneuron subtypes arise from distinct spatial and temporal subdomains within the caudal ganglionic eminence

**Authors:** V. GARG[1], S. BEYENE[1], A. TANZILLO[1], A. CACCAVANO[2], V. K. CHITTAJALLU[2], A. TUCKER[1], A. C. JOHANTGES[1], Y. ZHANG[1], D. ABEBE[2], K. A. PELKEY[2], C. J. MCBAIN[2], ***T. J. PETROS**[3,1];
[1]Section on Cell. and Mol. Neurodevelopment, [2]Section on Cell. and Synaptic Physiol., [3]NICHD, Bethesda, MD

**Abstract:** Forebrain inhibitory interneurons are born from transient structures during embryogenesis known as the medial and caudal ganglionic eminences (MGE and CGE, respectively). The MGE and CGE generate distinct, non-overlapping cohorts of interneurons that can be defined by their transcriptomic, morphological, and electrophysiological characteristics. In the MGE, somatostatin-expressing (SST+) cells arise predominantly from the dorsal-posterior MGE from E12-E16 whereas parvalbumin-expressing (PV+) cells are born in the ventral-anterior MGE throughout embryogenesis. This relationship between spatiotemporal origin and mature interneuron subtypes has led to genetic insights regarding their fate and maturation. A similar organization has never been explored in the CGE, despite the significant increase in CGE-derived interneurons in primates compared to rodents. Here we harvested fluorescent cells from distinct CGE subdomains at E13.5 and E15.5 and grafted them into WT neonatal mice cortices to generate a spatiotemporal map of CGE-derived interneuron origin. Grafted cells displayed electrophysiological properties similar to distinct subtypes of mature CGE-derived interneurons. Our results indicate that there are significant spatial biases in the CGE, with specific interneuron subtypes preferentially arising from distinct CGE subdomains. These biases are relatively stable over time, implying a minimal relationship between temporal birthdate and interneuron subtype. In the future, combining these insights with spatial transcriptome profiles will generate critical insights into gene regulation of CGE-derived interneurons.

**Disclosures: V. Garg:** None. **S. Beyene:** None. **A. Tanzillo:** None. **A. Caccavano:** None. **V.K. Chittajallu:** None. **A. Tucker:** None. **A.C. Johantges:** None. **Y. Zhang:** None. **D. Abebe:** None. **K.A. Pelkey:** None. **C.J. McBain:** None. **T.J. Petros:** None.

**Poster**

**PSTR163: Transcriptional and Epigenetic Regulation of Neurogenesis**

**Location:** WCC Halls A-C

**Time:** Monday, November 16, 2026, 1:00 PM - 5:00 PM

**Program #/Poster #:** PSTR163.13/D13

**Topic:** J.01. Molecular, Biochemical, and Genetic Techniques

**Support:** Dorris Scholar Award, Frank J. Dixon Fellowship
CIRM Training Fellowship (EDU4-12811)
Stanley Center for Psychiatric Research at the Broad Institute of MIT and Harvard
National Institute of Health (R01MH137042) and SSPsyGene Consortium
Howard Hughes Medical Institute
Simons Foundation Autism Research Initiative Sex Differences Collaboration (SFARI #736613)
CIRM ReMIND-L DISC4-16295
National Institute of Health (R01HG012819, R01AT013748)
the Mathers Foundation
the One Mind Foundation
the Conrad Prebys Foundation
the Pew Charitable Trust
the McKnight Endowment

the Astera Institute
Jed McCaleb, and James Fickle

**Title:** Massively parallel in vivo multiomic Perturb-seq reveals cell type-specific gene regulatory networks in cortical development

**Authors: *X. ZHENG**[1], J. LI[1], K. KIM[2], S. SIMMONS[2], B. WU[1], X. JIN[1];
[1]The Scripps research Inst., San Diego, CA; [2]Stanley Ctr. for Psychiatric Res., Broad Inst. of MIT and Harvard, Cambridge, MA

**Abstract:** Human genetics has nominated hundreds of genes associated with neurodevelopmental disorders (NDDs), including autism spectrum disorder (ASD), but how these genes act across diverse neural cell types remains elusive. Perturb-seq couples pooled genetic perturbation with single-cell molecular phenotyping, enabling direct genotype-to-phenotype mapping in heterogeneous tissues. Using adeno-associated virus (AAV) for in vivo delivery, we established massively parallel in vivo Perturb-seq platform that perturbs genes directly in the developing mouse brain and recovers perturbation identity with single-cell transcriptomes. This approach revealed cell-type-specific effects of developmental regulators, including disruption of cortical projection neuron identity after Foxg1 perturbation. To extend this strategy to joint RNA and chromatin readouts in vivo, we developed a gRNA nuclear-anchoring approach that improves perturbation recovery in single-nucleus multiome assays, enabling perturbation identity, gene expression, and chromatin accessibility to be measured in the same cell at scale. Applying in vivo multiomic Perturb-seq to 16 NDD-associated genes and control perturbations in the developing mouse cortex, we found that genetic perturbations produced distinct effects across neuronal cell types and molecular modalities. Mef2c perturbation produced subtype-selective effects in deep-layer excitatory neurons, linking altered chromatin accessibility to downstream transcriptional changes and nominating a cell-type-specific regulatory program. Across perturbations, integrated RNA and chromatin readouts revealed diverse mechanisms by which disease-associated genes reshape neuronal identity and regulatory state. Together, this work establishes in vivo multiomic Perturb-seq as a scalable framework for causal functional genomics in the intact nervous system. By connecting genetic perturbation to cell-type-specific transcriptional and regulatory consequences in vivo, this platform provides a general strategy to interpret disease-associated genes in their native neural context.

**Disclosures: X. Zheng:** E. Ownership Interest (stock, stock options, royalty, receipt of intellectual property rights/patent holder, excluding diversified mutual funds); Scripps Research. **J. Li:** E. Ownership Interest (stock, stock options, royalty, receipt of intellectual property rights/patent holder, excluding diversified mutual funds); Scripps Research. **K. Kim:** None. **S. Simmons:** None. **B. Wu:** None. **X. Jin:** E. Ownership Interest (stock, stock options, royalty, receipt of intellectual property rights/patent holder, excluding diversified mutual funds); Scripps Research.

**Poster**

**PSTR164: Modeling Disease *In Vitro***

**Location:** WCC Halls A-C

**Time:** Monday, November 16, 2026, 1:00 PM - 5:00 PM

**Program #/Poster #:** PSTR164.01/D14

**Topic:** A.02. Stem Cells and Reprogramming

**Support:** 1UM1HG012651
19000-22-12
R35GM133600
P30CA034196

**Title:** Beyond a single reference line: a multi-ancestry iPSC resource for functional genomics across human genetic diversity

**Authors: *E. PELLEGRINO**[1], A. MELO CARRILLO[2], P. BALACHANDRAN[2], M. KOSTICH[2], C. LORIG[2], A. KENDRA[2], J. ALCOFORADO DINIZ[2], K. MERISOTIS[3], J. GAROFALO[2], S. GRUBB[2], C. BECK[2], P. ROBSON[2], W. SKARNES[4];
[1]The Jackson Labs., Farmington, CT; [3]Skarnes Lab., [2]The Jackson Lab., Farmington, CT; [4]Cell. Engin., The Jackson Lab. for Genomic Med., Farmington, CT

**Abstract:** The power of human iPSCs for disease modelling and functional genomics is increasingly constrained by a lack of diversity — not just in donor ancestry and sex, but in the depth of characterization that would make diverse lines trustworthy and widely adopted. Most studies rely on the same few reference lines, leaving the influence of genetic background on cellular phenotypes largely unexplored. Here we describe the deep characterization of the Genetic Discovery (GeDi) iPSC panel: nine clonal iPSC lines reprogrammed from donors spanning six continental ancestry groups, complemented by the well-characterized reference lines KOLF2.1J and KOLF2.2J, through integrative genomic, epigenomic, and functional studies. All lines passed comprehensive quality control, and female lines demonstrated stable X chromosome inactivation at early passage — a critical and often overlooked source of biological variability, as XCI erosion during prolonged culture can introduce variability in studies using female iPSC lines. Transcriptomic profiling across five differentiated lineages, including extra-embryonic lineages that cannot be faithfully modelled in animal models, covered over 80% of annotated protein-coding genes and uncovered stable, donor-intrinsic variability in gene expression that persists across differentiation contexts. Complementing this, whole-genome methylation analysis confirmed successful epigenomic reprogramming while revealing locus-specific variability at imprinted regions, and haplotype-resolved assemblies catalogued structural variants and regions of absence of heterozygosity that short-read sequencing alone would miss. Together, these analyses establish the GeDi iPSC panel as a deeply characterized, multi-ancestry resource openly available to accelerate functional genomic discoveries across the full breadth of human genetic diversity.

**Disclosures: E. Pellegrino:** None. **A. Melo Carrillo:** None. **P. Balachandran:** None. **M. kostich:** None. **C. Lorig:** None. **A. Kendra:** None. **J. Alcoforado Diniz:** None. **K. Merisotis:** None. **J. Garofalo:** None. **S. Grubb:** None. **C. Beck:** None. **P. Robson:** None. **W. Skarnes:** None.

**Poster**

**PSTR164: Modeling Disease *In Vitro***

**Location:** WCC Halls A-C

**Time:** Monday, November 16, 2026, 1:00 PM - 5:00 PM

**Program #/Poster #:** PSTR164.02/D15

**Topic:** A.02. Stem Cells and Reprogramming

**Title:** Enhancing In Vitro Neuro-Centric Models: Synergistic Use of iPSC-Derived Cells Across 3D, MPS, and Organ-on-a-Chip Technologies

**Authors: S. SCHACHTELE**, R. FIENE, D. MAJEWSKI, R. VAIDYANATHAN, C. B. CARLSON, *J. LIU;
FUJIFILM Cell. Dynamics, Madison, WI

**Abstract:** The translatability of animal models to human clinical outcomes remains a major challenge in neurodegenerative disease drug discovery, driving a shift toward biologically relevant human cell-based platforms. Following the FDA Modernization Act 2.0, there is increased emphasis on reducing animal testing by advancing New Approach Methodologies (NAMs), including human induced pluripotent stem cells (iPSCs), 3D organoids and spheroids, organ-on-a-chip (OoC) technologies, microphysiological systems (MPS), and AI-driven computational models. iPSC-derived neurons and glia are essential components of advanced systems integrated into 3D cultures, MPS, and OoC platforms. Cross-industry validation of iPSC-containing NAMs is ongoing for applications such as seizure liability, neurodegeneration, pain, blood-brain barrier transport, and drug discovery. Recent improvements in cell model access, media, and MPS design further enhance these models. Here, we present experimental data demonstrating the integration and synergy of FUJIFILM Cellular Dynamics' iPSC-derived iCell neurons and glia across diverse neuro-centric NAM platforms, emphasizing their scalability, purity, reproducibility, and consistent in vitro phenotypes. We optimize culture parameters for functional assays (e.g. microelectrode array, calcium imaging, and neurite degeneration) and disease modeling using patient or engineered iPSC-derived neurons. We further advance neural model complexity by incorporating iPSC-derived microglia for central neuroinflammation and macrophages for peripheral sensory inflammation. The presented results confirm that commercial iPSC-derived cells can generate complex, human-relevant tissues compatible with MPS, OoC, and 3D cultures, enhancing the physiological relevance of in vitro drug screens. Continued refinement of these platforms promises improved tissue function, better drug response predictivity, reduced animal model reliance, and facilitation of high-throughput screening. This work highlights the transformative potential of iPSC-based models and NAMs to modernize and accelerate drug discovery.

**Disclosures: S. Schachtele:** A. Employment/Salary (full or part-time):; Fujifilm Cellular Dynamics. **R. Fiene:** A. Employment/Salary (full or part-time):; Fujifilm Cellular Dynamics. **D. Majewski:** A. Employment/Salary (full or part-time):; Fujifilm Cellular Dynamics. **R. Vaidyanathan:** A. Employment/Salary (full or part-time):; Fujifilm Cellular Dynamics. **C.B. Carlson:** A. Employment/Salary (full or part-time):; Fujifilm Cellular Dynamics. **J. liu:** A. Employment/Salary (full or part-time):; Fujifilm Cellular Dynamics.

**Poster**

**PSTR164: Modeling Disease *In Vitro***

**Location:** WCC Halls A-C

**Time:** Monday, November 16, 2026, 1:00 PM - 5:00 PM

**Program #/Poster #:** PSTR164.03/D16

**Topic:** A.02. Stem Cells and Reprogramming

**Support:** R01EY035110

**Title:** Modeling CHD7-associated retinal neurodevelopmental defects using human iPSC-derived retinal organoids

**Authors: *K. H. A. PENA**[1], A. MORRIS[3], J. S. MEYER[2];
[1]Indiana Univ. Sch. of Med., Indianapolis, IN; [2]Stark Neurosciences Res. Inst., Indiana Univ. Sch. of Med., INDIANAPOLIS, IN; [3]Univ. of Kentucky, Lexington, KY

**Abstract:** Chromodomain helicase DNA-binding protein 7 (CHD7) is an ATP-dependent protein that alters chromatin structure to regulate gene expression in embryonic development, making it a key developmental timing fine-tuner. Variants in the CHD7 gene lead to CHARGE syndrome, a rare multisystem congenital disorder. Among the phenotypes associated with CHARGE syndrome, ocular abnormalities are common, particularly coloboma and optic nerve hypoplasia. While a role for CHD7 in neurogenesis has been established, the role of CHD7 in ocular morphogenesis is less clear, including how mutations in CHD7 may influence later cellular developmental events. In this study, we aim to determine how CHD7 gene variants affect retinal development using human induced pluripotent stem cell (iPSC)-derived retinal organoid models. CRISPR-Cas9 gene editing was used to generate CHD7 knock-in (Q184X) and CHD7 knockout (KO) iPSC lines. Editing was confirmed via Sanger sequencing and screening for off-target effects, and iPSC lines were differentiated to retinal organoids using a stepwise differentiation protocol. Organoids were initially screened at 45 days of differentiation, a timepoint at which retinal ganglion cell (RGC) differentiation peaks, to determine if there are any early changes in RGC specification. qRT-PCR was used to explore potential transcriptional differences in BRN3B, a key RGC gene, relative to the expression of CHX10, indicative of remaining retinal progenitor cells. We found evidence of impaired RGC differentiation, as BRN3B expression was significantly lower in Q184X and KO organoids, while CHX10 expression was significantly higher compared to isogenic controls. At later stages of differentiation, particularly day 60, we found evidence that BRN3B and CHX10 maintain their trend, suggesting a propensity for CHD7 mutants to retain a reduced number of RGCs. Ongoing studies at later retinal organoid stages (days 90 and 180) will assess photoreceptor maturation, relative rod/cone abundance, and outer segment development. Taken together, the findings of these studies suggest that pathogenic CHD7 variants impair retinal neurodevelopment by disrupting the transition from retinal progenitors to differentiated neuronal fates.

**Disclosures: K.H.A. Pena:** None. **A. Morris:** None. **J.S. Meyer:** None.

**Poster**

**PSTR164: Modeling Disease *In Vitro***

**Location:** WCC Halls A-C

**Time:** Monday, November 16, 2026, 1:00 PM - 5:00 PM

**Program #/Poster #:** PSTR164.04/D17

**Topic:** A.02. Stem Cells and Reprogramming

**Support:** Cure KCNH1 Foundation

**Title:** Precise base editing for KCNH1-related neurological disorders

**Authors: *C. SIMMONS**[1], L. BARSE[2], J. A. KEARNEY[2], A. L. GEORGE, JR[3]; [2]Pharmacol., [1]Northwestern Univ., Chicago, IL; [3]Pharmacol., Northwestern Univ. Feinberg Sch. of Med., Chicago, IL

**Abstract:** Mutations in KCNH1, encoding the human ether-á-go-go voltage-gated potassium channel (EAG1, Kv10.1), are associated with neurodevelopmental disorders including Temple-Baraitser syndrome (TBS), Zimmermann-Laband syndrome (ZLS), and epileptic encephalopathy. Affected individuals exhibit overlapping clinical features including hypotonia, developmental delay, intellectual disability, seizures, and variable presence of gingival enlargement, facial dysmorphism, abnormalities of digits. The heterozygous variant R357Q (c.1070G>A) is the most recurrent variant accounting for ~25% of known cases. Heterologous expression studies of R357Q demonstrate gain-of-function (GoF) effects including hyperpolarized voltage-dependence of activation and faster activation kinetics that contribute to generating a hyperpolarized resting membrane potential. Currently there are no effective or disease-modifying therapies for these conditions. Correcting pathogenic genetic variants at the genomic level has become feasible with base editing. Here, we present successful use of adenine base editing (ABE) to precisely correct the R357Q variant in patient-derived induced pluripotent stem cells (iPSC). Optimization of ABE for this mutation resulted in conversion of the heterozygous genotype in two different patient-derived iPSC lines to 97-98% wild-type allele without detectable insertion-deletion (indels) errors or bystander edits. We also optimized ABE to successfully convert heterozygous mutant fibroblasts obtained from Kcnh1-R357Q mice to 88% wild-type allele with less than 5% indels and bystander edits. Overall, this work provides the proof-of-concept for efficient base editing of the most recurrent KCNH1 mutation in this neurodevelopmental disorder.

**Disclosures: C. Simmons:** None. **L. Barse:** None. **J.A. Kearney:** None. **A.L. George, Jr:** None.

**Poster**

**PSTR164: Modeling Disease *In Vitro***

**Location:** WCC Halls A-C

**Time:** Monday, November 16, 2026, 1:00 PM - 5:00 PM

**Program #/Poster #:** PSTR164.05/D18

**Topic:** A.02. Stem Cells and Reprogramming

**Support:** NIH Grant F31NS137770-01

**Title:** A non-canonical role for voltage-gated sodium channel SCN3A in early human brain development

**Authors: *K. M. HELMS**[1], C. D. MAKINSON[2];
[1]Neurol., Columbia Univ. Med. Ctr., New York, NY; [2]Neurol., Columbia University, Irving Med. Ctr., New York, NY

**Abstract:** Sodium channelopathies represent a devastating class of neurodevelopmental disorders. Here, we investigate the pathophysiological consequences of a gain-of-function (GOF) SCN3A$^{I875T/+}$ variant encoding Nav1.3, associated with severe pediatric epilepsy and cortical dysplasia. SCN3A is uniquely expressed prior to neuronal excitability, suggesting a non-canonical role in early cortical development; however, mechanisms linking channel dysfunction to cortical malformation remain unclear.Using isogenic human iPSC-derived cortical organoids (hCOs), we demonstrate that SCN3A$^{I875T/+}$ initiates a pathological cascade beginning with increased persistent sodium current (INaP) and elevated intracellular calcium. Transcriptomic analysis reveals this calcium burden is not cleared extracellularly; instead, SCN3A$^{I875T/+}$ hCOs show preferential upregulation of ER and Golgi calcium uptake genes while extrusion channels remain uninduced, suggesting organellar calcium mishandling as an early defining feature of pathophysiology.Bulk RNA sequencing revealed extensive transcriptomic dysregulation emerging at 18 days in vitro, centered on a severe energetic deficit. SCN3A$^{I875T/+}$ hCOs display significantly reduced ATP alongside widespread mitochondrial and glycolytic gene dysregulation. Pharmacological dissection confirms mutant cells are critically dependent on, yet impaired in, both major energy-producing pathways. This bioenergetic crisis coincides with expanded radial glia and neural progenitor populations that persist into later stages, and with significant interneuron migration deficits in cortical-subpallial assembloids, indicating lasting consequences for circuit assembly.Together, these findings establish a novel pathogenic axis: aberrant sodium influx triggers calcium dysregulation and bioenergetic failure that derails progenitor dynamics and impairs interneuron migration, offering new mechanistic insight and therapeutic targets for sodium channelopathies.

**Disclosures: K.M. Helms:** None. **C.D. Makinson:** None.

**Poster**

**PSTR164: Modeling Disease *In Vitro***

**Location:** WCC Halls A-C

**Time:** Monday, November 16, 2026, 1:00 PM - 5:00 PM

**Program #/Poster #:** PSTR164.06/D19

**Topic:** A.02. Stem Cells and Reprogramming

**Title:** Using stem cell organoid model to investigate cerebellar malformation in NDD

**Authors: *Y. LIU**[1], C. XIA[2], L. WANG[3];
[1]university of Southern California, Los Angeles, CA; [2]USC, San Jose, CA, ; [3]Neurosciences, USC, Los Angeles, CA

**Abstract:** Genetic risk for neurodevelopmental disorders (NDDs) is highly heterogeneous, yet how diverse variants converge on region-specific developmental programmes remains poorly understood. This gap is particularly important for the human cerebellum, which is increasingly implicated in NDDs but remains difficult to study during early development. Leveraging NDD organoid atlas focused on cerebral cortex with clinical and genetic information, together with an integrated single cell transcriptomic atlas of developing human cerebellum (PCW6 - Adult), we found many NDD genes exhibit high expression in cerebellar cells. We next generated patients' iPSC derived cerebellar organoids (CerO), harbouring variants in *NARS1*, *HSPA14* and *ATP8A2*, and found NDD-CerOs reproducibly captured the early cerebellar developmental features, including ATOH1/SOX2-positive granule cell progenitors and related lineage, KIRREL2/SKOR2-positive Purkinje-lineage, and the proliferative and apoptotic compartments. Parental and non-parental CerOs were included as healthy controls. In *NARS1*-CerOs, AI-assisted brightfield image analysis revealed a reproducible reduction in CerOs size in *NARS1*-CerOs compared to control CerOs, suggesting impaired gross in *NARS1*-CerOs. We then performed quantitative immunohistochemistry and multivariate modelling, and found a significant reduction in proportion of ATOH1/SOX2 double-positive cells, suggesting impaired maintenance or expansion of rhombic lip-derived granule cell progenitors population in early cerebellar development. Next, in our multi-omics analysis, we observed WGCNA (weighted gene co-expression network analysis) modules highlighting enrichment of cerebellar disease-associated genes, including *ZIC1*, and *ZIC4* and *ATOH1* as hub genes. Moreover, proteomic profiling highlights dysregulations in pathways associated with translational regulation, cellular growth and lineage specification, consistent with function of *NARS1* and transcriptomics results. Additionally, CRISPR correction of the *NARS1* point mutation (c.50T>C) partially restored the abundance of ATOH1/SOX2+ cells and CerO size. Lastly, we observed improved gross morphologies and size in *NARS1*-CerOs when replacing FGF8 to FGF2. These results together highlight patient-derived CerOs as a scalable platform for linking NDD-associated genetic variation to region-specific developmental phenotypes. By integrating organoid atlases, clinical genetics, and patient-specific disease modeling, this framework identifies vulnerable developmental pathways to genetic perturbation and enables evaluation of targeted rescue strategies for NDDs.

**Disclosures: Y. Liu:** None. **C. Xia:** None. **L. Wang:** None.

**Poster**

**PSTR164: Modeling Disease *In Vitro***

**Location:** WCC Halls A-C

**Time:** Monday, November 16, 2026, 1:00 PM - 5:00 PM

**Program #/Poster #:** PSTR164.07/D20

**Topic:** A.02. Stem Cells and Reprogramming

**Support:** Private Funding

**Title:** Modeling MACF1-Related Neurodevelopmental Disorder Using Human Cortical Organoids

**Authors: F. MALIT**[1], J. VILLALBA[1], Z. MYERS[1], M. G. OTERO[1], V. ZHEMKOV[1], C. N. SVENDSEN[1], *M. ALLEN-SHARPLEY[2,1];
[1]Regenerative Med. Inst., Cedars-Sinai Med. Ctr., Los Angeles, CA; [2]Cedars-Sinai Guerin Children's, Los Angeles, CA

**Abstract:** Neurodevelopmental disorders are a heterogeneous group of conditions that arise from disrupted brain development, leading to impairments in motor function, communication, cognition, and behavior. MACF1-related neurodevelopmental disorder is caused by deletion or loss of function in the *MACF1* gene which encodes Microtubule-Actin Cross-Linking Factor 1 (MACF) protein. Animal models suggest that MACF1 plays a critical role in neuronal migration and axonal function; however, the mechanisms of this disorder remain poorly understood, and no human-based disease models currently exist. In this study, induced pluripotent stem cells (iPSCs) derived from a patient with a heterozygous *MACF1* deletion are used to generate cortical organoids as a platform to investigate the role of MACF1 in early brain development, including cortical lamination and neuronal migration. Immunofluorescence staining was performed at days 30, 60, and 90, to identify radial glial cells (*PAX6*), immature neuronal markers (*DCX*), and deep and early layer markers (*TBR1* and *SATB2*). At all developmental time points analyzed, *MACF1* deletion disrupted cortical organoid development as measured in expression patterning and lamination compared to healthy unaffected controls. Neural rosette formation was significantly decreased in MACF1 patient-derived organoids compared to healthy unaffected controls. These findings indicate a requirement for MACF1 in the maintenance of progenitor populations and the establishment of normal cortical architecture. Collectively, these results establish, to our knowledge, the first human stem cell-based model of MACF1-related neurodevelopmental disorder, providing a patient-specific platform for investigating disease mechanisms and developing targeted therapeutic strategies.

**Disclosures: F. Malit:** None. **J. Villalba:** None. **Z. Myers:** None. **M.G. Otero:** None. **V. Zhemkov:** None. **C.N. Svendsen:** None. **M. Allen-Sharpley:** None.

**Poster**

**PSTR164: Modeling Disease *In Vitro***

**Location:** WCC Halls A-C

**Time:** Monday, November 16, 2026, 1:00 PM - 5:00 PM

**Program #/Poster #:** PSTR164.08/D21

**Topic:** A.02. Stem Cells and Reprogramming

**Support:** Angelman Syndrome Foundation
NIH Grant NS125850

**Title:** Assessing the Functional Roles of UBE3A and GABRB3 in Patient-Derived Angelman Syndrome Neurons

**Authors: *T. M. ROBINSON**[1], C. L. SIROIS[2], S. CHAMBERLAIN[1], E. S. LEVINE[1]; [1]Univ. of Connecticut Sch. of Med., Farmington, CT; [2]Univ. of Wisconsin, Madison, Madison, WI

**Abstract:** The neurodevelopmental pathology of Angelman syndrome (AS) is driven by the loss of the maternally expressed ubiquitin protein ligase *UBE3A*, resulting in widespread neuronal hyperexcitability, ataxia, and profound language deficits. While most cases result from a large maternal 15q11-q13 deletion, which also encompasses a cluster of $GABA_A$ receptor subunits, AS can also result from rare *UBE3A* loss-of-function mutations. Dissecting the relative contributions of *UBE3A* versus neighboring genes like *GABRB3* is critical for identifying novel therapeutic targets. To isolate the specific effects of UBE3A loss, we utilized CRISPR/Cas9 and a single-stranded oligonucleotide (ssODN) template via homology-directed repair (HDR) to correct an inherited *UBE3A* missense mutation (F583S, isoform 1) in patient-derived induced pluripotent stem cells (iPSCs). While this specific point mutation preserves normal cellular UBE3A protein expression, it completely abrogates its catalytic ubiquitin ligase activity *in vitro*, offering a unique model to isolate enzymatic dysfunction even though the protein itself is still present. The ssODN included a silent mutation to prevent re-cutting and facilitate clone screening, yielding a perfectly matched isogenic control line. We differentiated these cells into neurons, and to test the specific contribution of $GABA_A$ receptor alterations, we used antisense oligonucleotides (ASOs) to knock down *GABRB3* expression in the *UBE3A* mutation neurons. Electrophysiological results revealed that *UBE3A* mutation neurons exhibited significant baseline alterations in synaptic activity and network synchrony. Resting membrane potential (RMP) was abnormally depolarized in the *UBE3A* mutation neurons compared to isogenic controls. Furthermore, *UBE3A* mutation neurons exhibited a hyperexcitable phenotype, showing an increased action potential (AP) frequency. Decreased expression of the $GABA_A$ receptor subunit gene, *GABRB3*, in *UBE3A* mutation neurons further enhanced deficits in inhibitory transmission but had no effect on baseline RMP or AP hyperexcitability phenotypes. Our analysis of this isogenic *UBE3A* mutation model successfully isolates the pathophysiological contributions of UBE3A enzymatic inactivity and demonstrates how concurrent loss of 15q cluster genes can compound neuronal phenotypes. Defining these distinct genetic drivers will help identify precise molecular targets and inform the development of more accurate translational models for Angelman syndrome.

**Disclosures: T.M. Robinson:** None. **C.L. Sirois:** None. **S. Chamberlain:** None. **E.S. Levine:** None.

**Poster**

**PSTR164: Modeling Disease *In Vitro***

**Location:** WCC Halls A-C

**Time:** Monday, November 16, 2026, 1:00 PM - 5:00 PM

**Program #/Poster #:** PSTR164.09/D22

**Topic:** A.02. Stem Cells and Reprogramming

**Support:** NIH Grant NS111986
Angelman Syndrome Foundation

**Title:** Distinct and Shared Electrophysiological Phenotypes In Models of Angelman Syndrome

**Authors: *N. BUSEL**[1], C. L. SIROIS[2], S. CHAMBERLAIN[2], E. S. LEVINE[1];
[1]Neurosci., [2]Univ. of Connecticut Sch. of Med., Farmington, CT

**Abstract:** Angelman syndrome (AS) is a severe neurodevelopmental disorder caused by loss of function of the maternal *UBE3A* gene, which encodes an E3 ubiquitin ligase responsible for targeting specific proteins for proteasomal degradation. While some patients have mutations only affecting *UBE3A*, most cases of AS arise from deletions of the 15q11-q13 region that remove *UBE3A* along with neighboring genes, including $GABA_A$ receptor subunits. Patients with the full deletion exhibit more severe characteristics, such as microcephaly and increased seizure susceptibility, compared to those with *UBE3A* mutations alone. The extent to which neighboring gene loss contributes to phenotypes beyond *UBE3A* deficiency remains incompletely understood. To parse *UBE3A*-specific contributions from broader deletion effects, I performed an electrophysiological characterization of three isogenic H9 human embryonic stem cell-derived neuronal lines: wild-type control, a CRISPR-mediated maternal *UBE3A*-specific knockout, and a CRISPR-mediated deletion of the full 15q11-q13 region (AS deletion). Recordings were conducted at two developmental windows, weeks 7-8 and weeks 9-10 *in vitro*, using whole-cell patch clamp to assess intrinsic membrane properties, action potential firing, and spontaneous synaptic transmission. Both the *UBE3A*-specific knockout and AS deletion lines exhibited increased membrane capacitance, suggesting larger cell size, when compared to controls. Voltage-clamp recordings revealed significantly reduced inward and outward current densities in the *UBE3A*-specific knockout and AS deletion lines at weeks 9-10 compared to controls, consistent with a failure to scale channel expression in proportion to membrane area. Both the *UBE3A*-specific knockout and AS deletion lines showed a higher proportion of immature or non-firing cells at weeks 7-8, though this maturational delay was more severe in the AS deletion line. Recordings of GABAergic synaptic currents revealed that both the *UBE3A*-specific knockout and AS deletions lines had a lower percentage of cells with activity at weeks 7-8 compared with controls. At weeks 9-10, the *UBE3A*-specific knockout reached levels comparable to controls, whereas the AS deletion line continued to show reduced synaptic activity. Among active cells, the *UBE3A*-specific knockout and AS deletion lines exhibited reduced event amplitude and prolonged decay kinetics compared to controls. These findings indicate that *UBE3A* loss drives deficits in neuronal maturation and channel expression, while the additional loss of neighboring genes in the 15q11-q13 region exacerbates developmental delay and impairs synaptic recruitment.

**Disclosures: N. Busel:** None. **C.L. Sirois:** None. **S. Chamberlain:** None. **E.S. Levine:** None.

**Poster**

**PSTR164: Modeling Disease *In Vitro***

**Location:** WCC Halls A-C

**Time:** Monday, November 16, 2026, 1:00 PM - 5:00 PM

**Program #/Poster #:** PSTR164.10/D23

**Topic:** A.02. Stem Cells and Reprogramming

**Support:** Rosamund Stone Zander Translational Neuroscience Center, Boston Children's Hospital Equipment and Core Resources Allocation Committee award to WAS
Congressionally Directed Medical Research Program W81XWH2110209 (MS)

**Title:** hiPSC-derived Cortical Organoid Platform to Screen Treatments for Tuberous Sclerosis Complex

**Authors: *R. HOBSON**[1], Z. YANG[2], N. TEANEY[5], F. GASPAROLI[6], W. AFSHAR SABER[3], M. SAHIN[4];
[1]Neurol., Boston Children's Hosp., Brighton, MA; [2]Boston Children's Hosp., [3]Neurol., Boston Children's Hosp., Boston, MA; [4]Dept of Neurol., Boston Children's Hosp., Needham, MA; [5]Neurobio., Tufts Univ. Sch. of Medicine, Dept. of Neurosci., Medford, MA; [6]Core for Imaging Technol. and Educ., Boston, MA

**Abstract:** Tuberous Sclerosis Disorder (TSC) is a genetic disorder with heterozygous variants in TSC1 or TSC2 which manifests as hamartomas, tubers, epilepsy and neuropsychiatric disorders. TSC1/2 are critical inhibitors in the mTOR complex 1 (mTORC1) pathway leading to mTORC1 hyperactivity. mTORC1 inhibitors, such as everolimus, are approved treatments for TSC. Yet, seizures were only reduced to near daily. Therefore, there is a critical need to uncover treatments to target the neurological symptoms of TSC. To predict treatment efficacy in reducing seizure burden, we utilized human induced pluripotent stem cells (hiPSC) as a preclinical model. Patient-derived iPSCs (LAM77) with a heterozygous frameshift mutation in TSC2 (TSC2 +/-) were used to generate an isogenic allelic series with homozygous corrected line (TSC2 +/+) and homozygous second hit mutation (TSC2 -/-). We utilized a time-series recording of the neurogenin-2 (NGN2) glutamatergic neurons co-cultured with hiPSC-derived astrocytes on MEA. We found TSC2 LOF (TSC2 -/-) had significantly increased firing rate and burst frequency compared to TSC2 +/- and TSC2 +/+. However, this bypasses critical developmental checkpoints, lacks three-dimensional structures, and exhibits less complex network dynamics. Therefore, we transitioned to accelerated cerebral cortical brain organoids containing a near pure population of glutamatergic neurons (hCO). To validate phenotype, we dissociated organoids at 36 days in vitro to co-culture with astrocytes using genetically encoded calcium indicators (hSyn-jRCaMP1b) and an automated calcium imaging pipeline. Next, we characterized 3D hCO using a high-density multielectrode array (HD-MEA). HD-MEA of 3D hCO revealed TSC2 -/- revealed a trend of increased firing rate and significantly increased inter-burst interval compared to TSC2 +/+. However, high variability and limited throughput were major drawbacks. Together, these results show that TSC seizure-like hyperactivity can be reliably recapitulated in both 2D NGN2 or glutamatergic neuron co-culture and 3D hCO models. In the future, transitioning to high-throughput 3D calcium imaging combined with HD-MEA hit validation may be a viable tool to screen cortical organoids for treatments to reduce seizure burden in TSC patients.

**Disclosures: R. Hobson:** None. **Z. Yang:** None. **N. Teaney:** None. **F. Gasparoli:** None. **W. Afshar Saber:** None. **M. Sahin:** None.

**Poster**

**PSTR164: Modeling Disease *In Vitro***

**Location:** WCC Halls A-C

**Time:** Monday, November 16, 2026, 1:00 PM - 5:00 PM

**Program #/Poster #:** PSTR164.11/D24

**Topic:** A.02. Stem Cells and Reprogramming

**Support:** GR-2021-12373376

**Title:** Molecular and functional correlates of disease severity in Dravet syndrome patient-derived GABAergic neurons

**Authors: *D. D. LI PUMA**[1,3], G. BONI[3], C. RIPOLI[1,3], M. PERULLI[2,4], D. BATTAGLIA[2,4], C. GRASSI[1,3];
[1]Dept. of Neurosci., [2]Dept. of Life Sci. and Publ. Hlth., Univ. Cattolica del Sacro Cuore, Rome, Italy; [3]Fondazione Policlinico Universitario A. Gemelli IRCCS, Rome, Italy; [4]Pediatric Neurol. and Pschiatry, Dept. di Scienze della Salute della Donna, del Bambino, Fondazione Policlinico Universitario A. Gemelli IRCCS, Rome, Italy

**Abstract:** Dravet syndrome (DS) is a severe developmental and epileptic encephalopathy caused by pathogenic variants in *SCN1A*, encoding the voltage-gated sodium channel Nav1.1. Loss of Nav1.1 function impairs the excitability of fast-spiking GABAergic interneurons, disrupting inhibitory neurotransmission and promoting network hyperexcitability. However, DS exhibits clinical heterogeneity that cannot be fully explained by *SCN1A* mutations alone. To investigate the mechanisms underlying this variability, we generated induced pluripotent stem cell (iPSC)-derived GABAergic neurons from DS patients with severe epilepsy and cognitive impairment (SISE) or milder clinical manifestations (MIME). Neuronal maturation was confirmed by the expression of neuronal markers (MAP2, GAD65/67, and VGAT), assessed by immunofluorescence and Western blot analyses. We also investigated neuronal morphology during differentiation and observed a significant reduction in neurite length in SISE neurons compared with controls, suggesting impaired neuronal development. To assess their functional consequences, we performed electrophysiological analyses at 30 days of differentiation using whole-cell patch-clamp recordings. While passive membrane properties did not differ significantly among groups, SISE neurons exhibited a reduction in action potential firing rate at higher current injections (220-280 pA; $p < 0.05$), indicating a greater impairment of neuronal excitability. In addition, action potential amplitude was significantly reduced in both DS-derived neuronal lines. Consistent with these findings, voltage-clamp recordings revealed a marked decrease in sodium current density in both DS groups compared with controls. Proteomic profiling identified disease-associated molecular signatures, with both DS-derived neuronal populations showing downregulation of proteins involved in synaptic organization, neurotransmission, and synaptic signaling, supporting widespread alterations in inhibitory network function. Collectively, these findings indicate that DS severity is not solely determined by Nav1.1 dysfunction but reflects the interplay between impaired sodium channel activity,

altered neuronal development, and synaptic dysfunction, providing insight into the mechanisms underlying phenotypic variability in DS.

**Disclosures: D.D. Li Puma:** None. **G. Boni:** None. **C. Ripoli:** None. **M. Perulli:** None. **D. Battaglia:** None. **C. Grassi:** None.

**Poster**

**PSTR164: Modeling Disease *In Vitro***

**Location:** WCC Halls A-C

**Time:** Monday, November 16, 2026, 1:00 PM - 5:00 PM

**Program #/Poster #:** PSTR164.12/D25

**Topic:** A.02. Stem Cells and Reprogramming

**Title:** High-Resolution Electrophysiological Profiling of Healthy and Dravet Syndrome Human iPSC-derived Neural Spheroids on CorePlate™ HD-MEAs

**Authors: A. L. JOLLY**[1], I. VERDUCI[2], L. DEL VECCHIO[2], A. MACCIONE[3], *P. WRIGHT[4], C. B. CARLSON[5], S. SCHACHTELE[5];
[1]3Brain, Oceanside, CA; [2]3Brain, Genova, Italy; [3]3Brain, Waedenswille, Switzerland; [4]3Brain, Pfäffikon, Switzerland; [5]FUJIFILM Cell. Dynamics, Madison, WI

**Abstract:** 3Brain's CorePlate™ HD-MEA platform delivers high-content, non-invasive electrophysiological profiling of human induced pluripotent stem cell (iPSC)-derived neural spheroids with high spatiotemporal resolution. Combined with FUJIFILM Cellular Dynamics iCell® NeuroSpheres, this integrated solution offers a scalable, ready-to-use system for investigating neural network dynamics in physiologically relevant 3D models. Using a triculture of human neural spheroids composed of fully differentiated human iPSC-derived cortical glutamatergic neurons, cortical GABAergic interneurons, and astrocytes, we demonstrate robust detection of spontaneous activity, coordinated network bursting, and functional connectivity across biological replicates. Consistent and mature neural activity measurements could be recorded as early as 3 weeks in culture with spheroids displaying well-organized network dynamics and mechanism-specific, reproducible responses to pharmacological modulation, validating both assay sensitivity and platform reliability across excitatory and inhibitory paradigms. The high-density electrode configuration of the CorePlate enabled simultaneous recording and compound dosing of multiple neural spheroids in one well, increasing technical replicate evaluation and streamlining high throughput data collection. To push beyond baseline characterization, we deployed this system in a disease-relevant context: neural spheroids incorporating SCN1A heterozygous knockout GABAergic neurons as a genetic model of Dravet syndrome. Despite no evident differences in baseline activity, the response to pharmacological modulation differed markedly between conditions. While spontaneous firing rates were largely preserved, connectivity maps and correlation analyses revealed compound-specific and genotype-dependent differences in network synchronization, nuances that standard low-density MEA approaches fail to resolve. Quantitative bursting metrics further expose subtle alterations in network dynamics linked to SCN1A dysfunction in GABAergic neurons. Together, these results

position the CorePlate™ and iCell® NeuroSphere combination as a powerful, human-relevant platform for translational research, disease modeling, and neuropharmacological screening. This ready-to-use 3D electrophysiology solution captures both global network modulation and subtle functional phenotypes in complex 3D systems where cellular architecture and biology matter most.

**Disclosures: A.L. Jolly:** None. **I. Verduci:** None. **L. Del Vecchio:** None. **A. Maccione:** None. **P. Wright:** None. **C.B. Carlson:** None. **S. Schachtele:** None.

**Poster**

**PSTR164: Modeling Disease *In Vitro***

**Location:** WCC Halls A-C

**Time:** Monday, November 16, 2026, 1:00 PM - 5:00 PM

**Program #/Poster #:** PSTR164.13/D26

**Topic:** A.02. Stem Cells and Reprogramming

**Support:** NIH Grant 3R01NS115017-04S1 (ELH)

**Title:** Characterization of SLC35A2-variants in iPSC-derived cortical organoid models of focal epilepsy

**Authors: *S. KOHRT**, E. L. HEINZEN;
UNC Chapel Hill, Chapel Hill, NC

**Abstract:** Focal cortical epilepsy accounts for approximately 60% of epilepsy cases, and 30% of these patients are described as being resistant to current therapeutic options. Somatic SLC35A2-variants present in cortical brain regions are now recognized as one of the most common causes of drug-resistant pediatric focal epilepsy. SLC35A2 encodes a protein critical for the effective transport of galactose into the Golgi body to be used in glycosylation and of proteins and lipids, a cellular process crucial for normal activity. Our lab has demonstrated SLC35A2-loss in inducible pluripotent stem cell (iPSC) models demonstrate neuronal firing dysfunction altered cell morphology, and changes in development gene expression markers. There is an ongoing need to study the maturation of cortical brain cells with SLC35A2 variation, and in a 3D model system to more closely represent the patient tissue environment. iPSC-derived cortical organoids of SLC35A2-WT vs SLC35A2-KO cell lineages reflect the precocious development phenotypes seen in monolayer cell culture. In organoids, we show the growth rates of KO versus WT vary over neurodevelopment timepoints. Immunocytochemistry studies further reveal altered rosettes and neuron morphology in KO compared to WT organoids. These morphological changes are accompanied by differing expressions of neuron development markers such as MAP2 and B3-Tubulin. Ongoing studies aim to determine the neuron firing capabilities using multielectrode array analysis, and to identify cell type populations within organoids. Together, these studies point towards precocious neurodevelopmental phenotypes that reflect our previous studies and are consistent in three-dimensional organoid models. The direct effects of SLC35A2 and glycosylation loss are still being researched, however, this data and others demonstrate the

critical need to understand the effect of glycosylation on neuron maturation, and subsequent development on epileptic symptoms.

**Disclosures: S. Kohrt:** None. **E.L. Heinzen:** None.

**Poster**

**PSTR164: Modeling Disease *In Vitro***

**Location:** WCC Halls A-C

**Time:** Monday, November 16, 2026, 1:00 PM - 5:00 PM

**Program #/Poster #:** PSTR164.14/D27

**Topic:** A.02. Stem Cells and Reprogramming

**Support:** NIH [K99 ES036290]

**Title:** A Human iPSC-Neural MEA NAM for Seizure Liability: Toward Functional Standardization

**Authors: *M. CLEMENTS**[1], M. CATO[2], K. W. CHAUDHARY[3], S. A. CHVATAL[1], A. DELAUNOIS[4], P. J. ELLINGSON[1], S. FIENE[1], C. GARRISON[3], M. KREIR[5], N. MIYAMOTO[6,7,8], K. NEWMAN[9], B. NODA[7,8], K. L. ROCKLEY[9], L. ROYER[4], T. J. SHAFER[10], C. STROCK[11], I. SUZUKI[7,8], A. M. TUKKER[12], R. H. S. WESTERINK[13], T. YOSHINAGA[6], L. A. K. ZOLKIEWSKI[9];
[1]Axion BioSystems, Atlanta, GA; [2]GSK, Collegeville, PA; [3]Bristol-Myers Squibb, Lawrenceville, NJ; [4]UCB, Braine-l'Alleud, Belgium; [5]J&J Innovative Med., Beerse, Belgium; [6]Eisai Co., Ltd., Ibaraki, Japan; [7]Tohoku Inst. of Technol., Miyagi, Japan; [8]VitroVo, Miyagi, Japan; [9]ApconiX Ltd, Macclesfield, United Kingdom; [10]Shafer Neurotox Consulting, LLC, Durham, NC; [11]Cyprotex, Watertown, MA; [12]Purdue Univ., West Lafayette, IN; [13]Utrecht Univ., Utrecht, Netherlands

**Abstract:** Human induced pluripotent stem cell (hiPSC)-derived neuronal cultures recorded on multielectrode array (MEA) platforms are increasingly being used as New Approach Methodologies (NAMs) for neurotoxicity and seizure liability assessment. These assays enable noninvasive measurement of spontaneous neuronal network activity, including firing, bursting, and synchrony, in a human-relevant *in vitro* system. However, broader adoption has been limited by variability in culture conditions, electrophysiological endpoints, and assay acceptance criteria across laboratories. To identify key determinants of assay performance, we reviewed 11 published seizure liability MEA studies and incorporated methodological insights from 11 laboratories routinely using hiPSC-neural or primary rodent neuronal cultures. Across studies, coordinated network burst activity consistently emerged as the primary electrophysiological feature associated with seizurogenic responses. Important factors influencing network behavior included astrocyte inclusion, neuronal maturation state, media handling, environmental equilibration, and compound addition methodology. Based on this analysis, we propose a functional framework for standardizing hiPSC-neural MEA seizure liability assays. Recommended baseline criteria include ≥10 active electrodes per well in 16-electrode formats,

network burst participation across ≥40% of active electrodes, Network Burst Frequency (NBF) ≥0.013 Hz, and Synchrony Index values between 0.15 and 0.85. Pharmacological responsiveness is validated using picrotoxin (10 μM), which should induce a ≥25% increase in NBF, Network Burst Duration, or Number of Spikes per Network Burst relative to vehicle controls. Importantly, this work reflects a broad cross-sector collaboration involving contributors from five pharmaceutical companies, three contract research organizations, academic laboratories, and biotechnology groups with extensive experience implementing seizure liability MEA assays. This breadth of expertise strengthens the translational relevance of the proposed recommendations and supports their utility as a consensus-driven framework for the field. Collectively, these recommendations provide an evidence-based foundation for improving reproducibility and cross-study comparability of MEA-based NAMs for seizure liability assessment and translational neuroscience research.

**Disclosures: M. Clements:** A. Employment/Salary (full or part-time):; Axion BioSystems. E. Ownership Interest (stock, stock options, royalty, receipt of intellectual property rights/patent holder, excluding diversified mutual funds); Axion BioSystems. **M. Cato:** A. Employment/Salary (full or part-time):; GSK. **K.W. Chaudhary:** A. Employment/Salary (full or part-time):; Bristol-Myers Squibb. **S.A. Chvatal:** A. Employment/Salary (full or part-time):; Axion BioSystems. E. Ownership Interest (stock, stock options, royalty, receipt of intellectual property rights/patent holder, excluding diversified mutual funds); Axion BioSystems. **A. Delaunois:** A. Employment/Salary (full or part-time):; UCB. **P.J. Ellingson:** A. Employment/Salary (full or part-time):; Axion BioSystems. E. Ownership Interest (stock, stock options, royalty, receipt of intellectual property rights/patent holder, excluding diversified mutual funds); Axion BioSystems. **S. Fiene:** A. Employment/Salary (full or part-time):; Axion BioSystems. E. Ownership Interest (stock, stock options, royalty, receipt of intellectual property rights/patent holder, excluding diversified mutual funds); Axion BioSystems. **C. Garrison:** A. Employment/Salary (full or part-time):; Bristol-Myers Squibb. **M. Kreir:** A. Employment/Salary (full or part-time):; J&J Innovative Medicine. **N. Miyamoto:** A. Employment/Salary (full or part-time):; VitroVo. **K. Newman:** A. Employment/Salary (full or part-time):; ApconiX Ltd. **B. Noda:** A. Employment/Salary (full or part-time):; VitroVo. **K.L. Rockley:** A. Employment/Salary (full or part-time):; ApconiX Ltd. **L. Royer:** A. Employment/Salary (full or part-time):; UCB. **T.J. Shafer:** A. Employment/Salary (full or part-time):; Shafer Neurotox Consulting, LLC. E. Ownership Interest (stock, stock options, royalty, receipt of intellectual property rights/patent holder, excluding diversified mutual funds); Shafer Neurotox Consulting, LLC. **C. Strock:** A. Employment/Salary (full or part-time):; Cyprotex. **I. Suzuki:** A. Employment/Salary (full or part-time):; VitroVo. **A.M. Tukker:** None. **R.H.S. Westerink:** None. **T. Yoshinaga:** A. Employment/Salary (full or part-time):; Eisai Co., Ltd. **L.A.K. Zolkiewski:** A. Employment/Salary (full or part-time):; ApconiX Ltd.

**Poster**

**PSTR164: Modeling Disease *In Vitro***

**Location:** WCC Halls A-C

**Time:** Monday, November 16, 2026, 1:00 PM - 5:00 PM

**Program #/Poster #:** PSTR164.15/D28

**Topic:** A.02. Stem Cells and Reprogramming

**Support:** NIH P50 HD103538

**Title:** Unique Phenotypic Traits of Mature Sensory Neurons from Patients with Adrenoleukodystrophy

**Authors: *M. YORKOWSKI**[1], A. FATEMI[1,2], C. L. NEMETH[1,2];
[1]Moser Ctr. for Leukodystrophies, Kennedy Krieger Inst., Baltimore, MD; [2]Dept. of Neurology, Johns Hopkins Sch. of Med., Baltimore, MD

**Abstract:** Adrenoleukodystrophy (ALD) is an X-linked genetic disorder resulting from mutations in the ATP Binding Cassette Subfamily D Member 1 (*ABCD1*) gene. *ABCD1* encodes the transporter responsible for the import of very long chain fatty acids (VLCFAs) into peroxisomes for fatty acid beta-oxidation; abnormal functioning of this process leads to the accumulation of VLCFAs in all tissues. Accumulated VLCFAs lead to, among other things, mitochondrial dysfunction, ER stress, and CNS demyelination. ALD presents in several forms, including childhood cerebral adrenoleukodystrophy (ccALD) and adrenomyeloneuropathy (AMN). In ccALD, which primarily effects young boys, the disease is fast-acting, debilitating and lethal without intervention. Contrastingly, AMN is adult-onset, resulting from slow demyelination of the spinal tracts until symptoms present themselves later in life. As these phenotypes present differently, we sought to explore phenotypic variations across sensory neuronal development and maturation. In our journey to better understand these downstream implications, we identified phenotypic traits unique to ccALD and AMN respectively, exhibited throughout their life cycles as mature neurons. We derived sensory neurons (Anatomic Inc.) from control (n = 2), AMN (n = 3), and ccALD (n = 2) patient iPSCs. Mature neurons were analyzed by microelectrode array (MEA) for electrical activity, immunocytochemistry for structural and function, and tandem mass spectrometry (LC-MS/MS) for lipid composition. Mature sensory neurons were measured by MEA for 77 days, with peak activity reached around day 42. On Day 42 in parallel cells, lipid analysis was completed by LC-MS/MS and were stained for various cell markers. Control and ccALD neurons exhibited similar maturation timelines, with comparable spontaneous electrical activity each week during the experiment. AMN neurons exhibited a delayed increase in electrical activity, only reaching similar levels of spontaneous electrical activity several weeks after their control and ccALD neuron counterparts. All ALD cells had elevated VLCFA compared to control, and AMN cells showed deficits in autophagy markers and disrupted neurofilament compared to ccALD and control. These findings demonstrate a disease relevant phenotype specific to sensory neurons. These cells may be useful to better elucidate underlying neuronal mechanisms that contribute to overall disease severity and progression. These findings may further guide understanding of ccALD and AMN differences and aid in the identification of targeted and effective therapies.

**Disclosures: M. Yorkowski:** None. **A. Fatemi:** None. **C.L. Nemeth:** None.

**Poster**

**PSTR164: Modeling Disease *In Vitro***

**Location:** WCC Halls A-C

**Time:** Monday, November 16, 2026, 1:00 PM - 5:00 PM

**Program #/Poster #:** PSTR164.16/D29

**Topic:** A.02. Stem Cells and Reprogramming

**Title:** Modeling human neurodegenerative diseases using engineered isogenic and patient-derived induced pluripotent stem cells

**Authors: *E. GEGA**[1], J. BECKWITH[2];
[1]The Jackson Lab., Farmington, CT; [2]Genet. Resource Sci., The Jackson Lab., Bar Harbor, ME

**Abstract:** In support of the initiative to include human-based disease models in study designs, The Jackson Laboratory (JAX) Cell Line Repository has been established with over 2000 iPSC-based disease models to date. The aim of this work is to highlight the power of the resource by characterizing the neurodegenerative disease models across existing iPSC collections and identify future needs of the scientific community based on literature review.
As a centralized iPSC resource, JAX performs quality control analyses, curates related information (design details, protocols, metadata), and reviews donor consent and clinical diagnosis for all candidate lines. 1500+ iPSC lines with engineered edits in isogenic backgrounds and 250+ patient-derived lines are now available, via collaborations with the iPSC Neurodegenerative Disease Initiative (iNDI), NYSCF, Rush AD, Target ALS, CZI Biohub and other donating institution. Isogenic iPSCs encompass 135 genes and 280 gene variants associated with Amyotrophic Lateral Sclerosis (ALS), Alzheimer's Disease (AD), Frontotemporal Dementia (FTD) and Parkinson's Disease (PD), featuring edits in APOE, SNCA, TARDBP, APP, FUS, GRN, PSEN1, TREM2, ABCA7, UBQLN2, SORL1, MAPT, C9orf72, etc. Many are engineered to express HALO-tagged endogenous proteins to study disease-relevant protein mislocalization.
Over 300 publications have referenced JAX iPSCs. Notably, more than 120 used iPSCs for neuronal and glial differentiation. To this end, dox-inducible cell lines that allow differentiation into cortical excitatory neurons, astrocytes and microglia were developed and later used as a background for models with GFP-organelle tagging. Similarly, Tet-inducible patient-derived lines and their corrected derivates have been developed.
A large selection of disease mutations was engineered in the KOLF2.1J (male) and FA13.1J (female) backgrounds and a selection of extensively studied gene variants in additional genetic backgrounds (e.g., African, Hispanic/Latino, East Asian, South Asian). Patient-derived iPSCs were generated from cohorts representing ALS, FTD, PD, AD, and other diseases, mostly from European or African backgrounds with even sex distribution.
The JAX Cell Line Repository is an expanding collection of iPSCs from a comprehensive representation of genetic backgrounds and sex, with engineered disease-associated gene variants and from cohorts of patients with diagnosed neurodegenerative diseases. All currently available lines are categorized as open access for genomic data restrictions, making this a powerful resource for curated neurodegenerative disease models and enabling reproducible cell-based research.

**Disclosures: E. Gega:** None. **J. Beckwith:** None.

**Poster**

**PSTR164: Modeling Disease *In Vitro***

**Location:** WCC Halls A-C

**Time:** Monday, November 16, 2026, 1:00 PM - 5:00 PM

**Program #/Poster #:** PSTR164.17/D30

**Topic:** A.02. Stem Cells and Reprogramming

**Title:** Visualizing Protein Dynamics of Neurodegenerative Disease-Associated Variants in KOLF2.1J HaloTag iPSC Lines

**Authors:** E. PELLEGRINO[1], ***E.-M. SURMANN**[1], G. NING[2], P. A. CLOW[1], J. MCDONOUGH[1], E. GEGA[1], M. R. COOKSON[3], M. WARD[4], W. SKARNES[1]; [1]The Jackson Lab., Farmington, CT; [2]Mass Gen. Brigham, Cambridge, MA; [3]Lab. Neurogenetics, Natl. Inst. Aging, NIH, Bethesda, MD; [4]NINDS, Natl. Inst. of Hlth. Office of Intramural, Bethesda, MD

**Abstract:** Isogenic induced pluripotent stem cell (iPSC) lines with engineered genetic variants are powerful tools for modeling disease. However, directly linking genotype to endogenous protein behavior in a relevant human system remains a challenge. As part of the iPSC Neurodegenerative Disease Initiative (iNDI), we generated a panel of 131 CRISPR-edited iPSC lines in the KOLF2.1J background, introducing the HaloTag® into endogenous loci in genes implicated in Alzheimer's disease and related dementias, Parkinson's disease, and amyotrophic lateral sclerosis (ALS) to enable real-time visualization of protein dynamics. This resource comprises 63 wild-type (WT) and 68 single-nucleotide variant (SNV) lines, with each HaloTag knock-in in cis with the variant allele, enabling direct readout of mutant protein behavior. Using the Janelia Fluor® 647 HaloTag® ligand in combination with live-cell high-content imaging, we assessed protein localization and subcellular distribution across all WT and SNV lines, revealing variant-specific changes in protein behavior, including mislocalization phenotypes. For example, the ALS- and frontotemporal dementia (FTD)-associated variant FUS R495X, resulting in a truncated protein, showed altered nuclear-cytoplasmic distribution, consistent with known pathogenic mechanisms. Together, these data position our HaloTag iPSC collection as a unique human cellular resource for connecting genetic variation to protein behavior, with broad utility for mechanistic studies of neurodegeneration.

**Disclosures: E. Pellegrino:** None. **E. Surmann:** None. **G. Ning:** None. **P.A. Clow:** None. **J. McDonough:** None. **E. Gega:** None. **M.R. Cookson:** None. **M. Ward:** None. **W. Skarnes:** None.

**Poster**

**PSTR164: Modeling Disease *In Vitro***

**Location:** WCC Halls A-C

**Time:** Monday, November 16, 2026, 1:00 PM - 5:00 PM

**Program #/Poster #:** PSTR164.18/D31

**Topic:** A.02. Stem Cells and Reprogramming

**Title:** Engineering an isogenic APP Swedish human iPSC derived cortical neuron model that recapitulates Alzheimer's disease-associated amyloid and tau pathology for mechanistic studies and therapeutic evaluationand tau pathology for mechanistic studies and therapeutic evaluation

**Authors: *S. CHEN**;
Cyagen Biosci., Santa Clara, CA

**Abstract:** Alzheimer's disease (AD) is characterized by progressive neurodegeneration associated with amyloid-β (Aβ) accumulation, tau pathology, synaptic dysfunction, and cognitive decline. Human induced pluripotent stem cell (iPSC)-derived neuronal models provide a physiologically relevant platform for investigating disease mechanisms in human neural cell types. However, genetic background variability often complicates the interpretation of disease-associated phenotypes. To establish a genetically defined human AD model, we introduced the APP-Swedish (APPswe) mutation (KM670L/N671L) into iPSC generated from healthy donors' peripheral blood mononuclear cells, generating an isogenic mutant-control pair.Parental and gene-edited iPSC lines were comprehensively characterized for pluripotency, donor identity, vector clearance, trilineage differentiation potential, and chromosomal stability. Both the isogenic control and APPswe-edited iPSCs clones retained typical pluripotent morphology and expressed key pluripotency markers, including NANOG, OCT4, and SOX2. Following directed differentiation, both iPSC lines generated cortical neurons with typical neuronal morphology and expression of neuronal markers NeuN and MAP2. Electrophysiological analysis demonstrated voltage-gated sodium ($Na^+$) and potassium ($K^+$) currents, evoked action potentials, and spontaneous firing activity, confirming functional neuronal maturation. To determine whether APPswe neurons develop disease-relevant AD phenotypes, we quantified amyloid and tau biomarkers following neuronal maturation. Compared with isogenic control neurons, APPswe cortical neurons exhibited a marked increase in amyloidogenic processing, characterized by significantly elevated secretion of Aβ40 (~ 5-fold) and Aβ42 (~ 3-fold). Importantly, enhanced amyloidogenic processing was accompanied by increased tau phosphorylation, with APPswe neurons displaying elevated levels of phospho-tau217 (~ 2.5-fold) and phospho-tau181 (~ 8-fold). These concurrent elevations in amyloid and phosphorylated tau biomarkers demonstrate that APPswe neurons recapitulate the two defining pathological hallmarks of AD within a controlled human genetic background.Collectively, these findings indicate that our iPSC-derived cortical neuron model captures key molecular events associated with APP mutation-driven AD pathogenesis. This provides a physiologically relevant in vitro platform for mechanistic investigations, therapeutic targets validation, and evaluation of candidate interventions targeting amyloid and tau pathology.

**Disclosures: S. Chen:** A. Employment/Salary (full or part-time):; Cyagen Biosciences.

**Poster**

**PSTR164: Modeling Disease *In Vitro***

**Location:** WCC Halls A-C

**Time:** Monday, November 16, 2026, 1:00 PM - 5:00 PM

**Program #/Poster #:** PSTR164.19/D32

**Topic:** A.02. Stem Cells and Reprogramming

**Support:** University of Illinois Chicago Center for Clinical and Translational Science (CCTS) award UL1TR002003
Community Foundation of Northern Illinois
UIC Office of Research at the College of Medicine Rockford

**Title:** Bioengineered Neurovascular Assembloids from Patient-Derived iPSCs for 3D Modeling of Alzheimer's Disease

**Authors: *N. NGUYEN**, A. MALIK, A. NAFIA, D. MAFIGU, R. CAMPOLI, B. SOSZKO, G. THAKUR, Z. CHEN, X.-J. LI, M. ALAM;
Dept. of Biomed. Sci., Univ. of Illinois in Chicago, Rockford, IL

**Abstract:** Alzheimer's disease (AD) is a progressive neurodegenerative disorder characterized by cognitive decline, amyloid-β accumulation, tau pathology, neuroinflammation, and neurovascular dysfunction. Current experimental models inadequately recapitulate human disease pathology, as animal models often fail to reproduce human-specific features and conventional two-dimensional cultures lack the complex cellular interactions of the brain microenvironment. Recent advances in patient-derived induced pluripotent stem cell (iPSC) technology have enabled the generation of disease-relevant neural and vascular cell types, providing new opportunities for human-based AD modeling. To develop a physiologically relevant neurovascular model, iPSC aggregates were differentiated into vascular organoids through sequential mesodermal and vascular lineage induction, while brain organoids were generated separately under neural induction conditions. Differentiation was validated by gene expression analysis and immunofluorescent staining. Subsequently, vascular and brain organoids were fused to generate neurovascular assembloids, and pneumatic extrusion-based 3D bioprinting was employed to achieve controlled spatial organization while preserving organoid integrity. We successfully generated vascular and brain organoids from both healthy and AD patient-derived iPSCs and confirmed lineage-specific differentiation through molecular and immunofluorescent characterization. Fusion of vascular and brain organoids resulted in the formation of neurovascular assembloids, and fluorescent imaging, including GFP-labeled patient-derived vascular organoids, demonstrated successful integration and structural organization following bioprinting. These bioengineered neurovascular assembloids provide a scalable and reproducible ex vivo platform for investigating neurovascular interactions and blood-brain barrier dysfunction in AD, with potential applications in disease modeling, mechanistic studies, and therapeutic screening.

**Disclosures: N. Nguyen:** None. **A. Malik:** None. **A. Nafia:** None. **D. Mafigu:** None. **R. Campoli:** None. **B. Soszko:** None. **G. Thakur:** None. **Z. Chen:** None. **X. Li:** None. **M. Alam:** None.

**Poster**

**PSTR164: Modeling Disease *In Vitro***

**Location:** WCC Halls A-C

**Time:** Monday, November 16, 2026, 1:00 PM - 5:00 PM

**Program #/Poster #:** PSTR164.20/D33

**Topic:** A.02. Stem Cells and Reprogramming

**Title:** Altered excitability and variation of ion channel activity in variants of ALS using iPSC-derived motor neurons and high throughput automated patch clamp

**Authors:** N. BRINKWIRTH[1], D. COLAMEO[2], ***A. R. OBERGRUSSBERGER**[1], M. RAPEDIUS[1], N. BECKER[1], E. DRAGICEVIC[1], S. PRIME[4], D. PENTON RIBAS[3], N. FERTIG[1];
[1]Nanion Technologies GmbH, Munich, Germany; [2]Electrophysiology Core Facility, Univ. of Zurich, Zürich, Switzerland; [3]Electrophysiology Core Facility, Univ. of Zurich, Zurich, Switzerland; [4]Axol Biosci., Cambridge, United Kingdom

**Abstract:** Amyotrophic lateral sclerosis (ALS) is a progressive neurodegenerative disease affecting spinal motor neurons. The expansion of GGGGCC (G4C2) repeats in the C9orf72 gene, is the most common genetic cause of ALS, associated with toxic RNA foci and dipeptide repeat proteins. SOD1 mutations cause oxidative stress and mitochondrial dysfunction, disrupting ion channels and calcium homeostasis. Mutations in TARDBP, which encodes the RNA-binding protein TDP-43 involved in RNA processing, can lead to toxic protein aggregates and dysregulated gene expression. To support ALS research and drug discovery, these genetic abnormalities were used to generate iPSC-based motor neuron models from healthy and patient donors to study the disease mechanisms of C9ORF72 expansion, TDP-43 A382T, SOD1 D109Y, plus an unaffected donor. Patch clamp remains the gold-standard for analyzing electrophysiological properties of excitable cells but remains limited by throughput. Primarily used for drug screening in heterologous expression systems, we employed high-throughput automated patch clamp (HT-APC) using the SyncroPatch 384 platform to characterize human iPSC-derived motor neurons (hiPSC-MNs). Detailed biophysical analyses revealed the presence of TTX-sensitive $Na^+$ channels with comparable steady-state activation/inactivation as well as recovery from inactivation properties between healthy and ALS-derived cells, suggesting similar $Na^+$ channel subunit composition. However, we found that ALS-derived motor neurons exhibited a significantly reduced $Na^+$ channel current density that was further studied in current clamp mode. These recordings demonstrated decreased excitability in ALS-derived neurons, reflected by alterations in action potential (AP) occurrence, amplitude, and firing response to different stimuli. These findings are consistent with previous observations of reduced synchrony, shorter, and more frequent APs in ALS-derived motor neurons. Beyond the observed morphological differences (smaller, less uniform cell bodies, thinner neurite extensions), our results indicate disease-associated ion channel remodeling, including reduced $Na^+$ - and $K^+$ current densities, while for ligand-gated channels only GABA induced currents where slightly reduced whereas response to glutamate and glycine remain unaffected. Together, these findings highlight the relevance of ion channel dysregulation in ALS pathophysiology and underscore the utility of HT-APC for unbiased, rapid, and simultaneous electrophysiological profiling of various parameters from genetically defined hiPSC-derived motor neurons relevant for ALS research and drug discovery.

**Disclosures: N. Brinkwirth:** A. Employment/Salary (full or part-time):; Nanion Technologies GmbH. **D. Colameo:** None. **A.R. Obergrussberger:** A. Employment/Salary (full or part-time):; Nanion Technologies GmbH. **M. Rapedius:** A. Employment/Salary (full or part-time):; Nanion Technologies GmbH. **N. Becker:** A. Employment/Salary (full or part-time):; Nanion Technologies GmbH. **E. Dragicevic:** A. Employment/Salary (full or part-time):; Nanion Technologies GmbH. **S. Prime:** A. Employment/Salary (full or part-time):; Axol Biosciences. **D. Penton Ribas:** None. **N. Fertig:** A. Employment/Salary (full or part-time):; Nanion Technologies GmbH.

**Poster**

**PSTR164: Modeling Disease *In Vitro***

**Location:** WCC Halls A-C

**Time:** Monday, November 16, 2026, 1:00 PM - 5:00 PM

**Program #/Poster #:** PSTR164.21/D34

**Topic:** A.02. Stem Cells and Reprogramming

**Title:** Human iPSC-Derived 3D Microphysiological Systems for Translational Neuroscience and Preclinical Safety Assessment

**Authors: *J. LAMB**[1], B. SAMSON-COUTERIE[2], K.-C. PITSA[1], M. ARGENZIANO[3], S. JAIN[1];
[2]Discovery Technologies, [3]Manufaacturing, [1]Ncardia, Leiden, Netherlands

**Abstract:** Despite advances in therapeutic development, attrition rates remain high for central nervous system (CNS) and cardiovascular programs due to the limited predictive value of conventional preclinical models. Human induced pluripotent stem cell (iPSC)-derived microphysiological systems (MPS) offer a human-relevant approach for investigating disease mechanisms and evaluating efficacy and safety liabilities.
The objective of this work was to develop and functionally characterize scalable human iPSC-derived 3D cardiac and brain microtissue platforms for quantitative assessment of tissue function, disease-relevant phenotypes, and adverse pharmacological responses.
Brain microtissues (neurospheres) were established using cortical neurons, astrocytes, and microglia. Cellular components were produced using standardized manufacturing processes and assembled using automated workflows compatible with medium- to high-throughput applications. Functional characterization included calcium imaging, multi-electrode array (MEA) electrophysiology, biomarker analysis, immunofluorescence, and molecular profiling. Disease- and safety-relevant perturbations included arrhythmogenic stimuli in cardiac tissues and Tau overexpression in brain microtissues.
Brain microtissues remained viable during long-term culture, displayed synaptic maturation by day 7, and developed complex spontaneous network activity by approximately 14 days as measured by MEA. Tau overexpression induced increased phosphorylated and aggregated Tau, recapitulating key features of neurodegenerative pathology. The platform further enabled longitudinal monitoring of neuronal network function, providing quantitative endpoints relevant for assessing disease progression and neurotoxicity.

Collectively, these findings demonstrate that human iPSC-derived brain microphysiological systems provide scalable and physiologically relevant platforms for translational research. By integrating molecular, cellular, and functional endpoints, these models support investigation of disease mechanisms while enabling earlier detection of cardiovascular and CNS safety liabilities, improving the predictive value of preclinical therapeutic development.

**Disclosures: J. Lamb:** A. Employment/Salary (full or part-time):; Ncardia. **B. Samson-Couterie:** A. Employment/Salary (full or part-time):; Ncardia. **K. Pitsa:** A. Employment/Salary (full or part-time):; Ncardia. **M. Argenziano:** A. Employment/Salary (full or part-time):; Ncardia. **S. Jain:** A. Employment/Salary (full or part-time):; Ncardia.

**Poster**

**PSTR164: Modeling Disease *In Vitro***

**Location:** WCC Halls A-C

**Time:** Monday, November 16, 2026, 1:00 PM - 5:00 PM

**Program #/Poster #:** PSTR164.22/D35

**Topic:** A.02. Stem Cells and Reprogramming

**Support:** This work was supported by grants from the U.S. National Institute of Mental Health R01MH110438 and S10MH133643 (PI: Vasudevan)
Della Martin Endowed Postdoctoral Fellowship for Mental Health at the Huntington Medical Research Institutes (Rahman MO)

**Title:** Engineering Region-Specific Human Embryonic Forebrain Endothelial Cells for Neurovascular Repair and Regeneration

**Authors: *M. RAHMAN**[1], S. TSE[2], A. VASUDEVAN[3];
[1]Huntington Med. Res. Inst. (HMRI), Pasadena, CA; [2]Huntington Med. Res. Inst. (HMRI), Los Angeles, CA; [3]Angiogenesis & Brain Develop. Lab., Huntington Med. Res. Inst., Pasadena, CA

**Abstract:** Abnormalities in neuronal, glial, and endothelial populations contribute to the pathogenesis of neuropsychiatric disorders of developmental origin and aging-related neurodegenerative diseases, for which effective treatments remain limited. Transplantation of human stem cell-derived neurons represents a promising cell-based therapeutic strategy; however, major challenges remain. In mouse xenograft studies, transplanted human neuronal precursors can differentiate in vivo but often require several months to migrate from the graft site and integrate into host circuits. In addition, neuronal survival following transplantation can be suboptimal. Such barriers significantly hinder clinical translation, particularly for patients with severe disease, where rapid integration and robust survival of grafted cells are critical determinants of therapeutic success. Our group previously discovered that endothelial cells of the embryonic periventricular vascular network serve as physical substrates and provide essential guidance cues for migrating GABAergic neurons in the developing mouse forebrain. Subsequent studies demonstrated that these specialized endothelial cells also contribute to the pathogenesis of neuropsychiatric disorders. We translated this discovery to human stem cell systems with

important therapeutic implications. We developed a differentiation protocol that generates human embryonic forebrain-like endothelial cells from both human embryonic stem cell lines and multiple control induced pluripotent stem cell (iPSC) lines. These cells express canonical endothelial markers together with forebrain-associated transcription factors, including PAX6, DLX1, DLX2, and NKX2.1. Here, we characterize the molecular identity of control iPSC-derived endothelial cells generated using our protocol and demonstrate enrichment of ventral forebrain transcription factors, including NKX2.1, relative to dorsal markers such as PAX6. We further evaluate their migratory behavior, tube-forming capacity, and neurovascular interactions in vitro and validate their developmental identity against human embryonic brain tissue. Finally, we investigate strategies to refine the differentiation protocol using additional patterning molecules to selectively generate dorsal or ventral forebrain endothelial phenotypes. Together, these studies establish a framework for engineering region-specific human forebrain endothelial cells and provide a foundation for developing neurovascular cell-based therapies aimed at restoring neural circuit function in neurological, psychiatric, and neurodegenerative disorders.

**Disclosures: M. Rahman:** None. **S. Tse:** None. **A. Vasudevan:** None.

**Poster**

**PSTR164: Modeling Disease *In Vitro***

**Location:** WCC Halls A-C

**Time:** Monday, November 16, 2026, 1:00 PM - 5:00 PM

**Program #/Poster #:** PSTR164.23/D36

**Topic:** J.04. Physiological Methods

**Title:** Rapid generation of forebrain and midbrain human iPSC-derived neural spheroids for neurotoxicity and disease modeling

**Authors: *S. SCHACHTELE**, R. FIENE, D. MAJEWSKI, X. XU, C. B. CARLSON; FUJIFILM Cell. Dynamics, Madison, WI

**Abstract:** Emerging global initiatives emphasize the need for new approach methodologies (NAMs) for pharmaceutical research and drug development. Human induced pluripotent stem cell (iPSC)-derived neurons and glia have granted access to biologically relevant in vitro models, yet more faithful representations of brain complexity are required to enhance model accuracy and predictiveness. 3D neural organoids are increasingly popular and offer tremendous promise for neurotoxicity and neurological disease research; however, they do face challenges, including lengthy differentiation (>6 weeks), protocol variability, limited high-throughput use/not yet scalable, and potential for necrotic cores. Furthermore, brain organoid generation does not yield a model with microglia, and the lack of an immune component hinders research on neuroinflammation. Here, we developed an efficient method to create brain region-specific 3D spheroids using defined combinations of fully differentiated iPSC-derived neurons and glia. Specifically, we generated forebrain neurospheres (70% glutamatergic, 30% GABAergic) and midbrain neurospheres (65% dopaminergic, 30% GABAergic, 5% glutamatergic), both containing 10% astrocytes. Using live cell imaging, we showed that cells (~25,000 cells/well) in

ultra-low attachment plates aggregate within 48-72 hours and establish a consistent diameter (~350 μm) and spheroid morphology. Quality and consistency were assessed via viability, composition, and functional assays over time. Live/Dead assays showed no necrotic core, indicating sustained viability. Immunocytochemistry verified preservation and uniform distribution of cell types throughout the spheroids. Functionally, calcium oscillation analysis (peak count, amplitude, and width) revealed distinct activity patterns in forebrain versus midbrain neurospheres, consistent across biological and technical replicates. To assess neurotoxicity screening potential, we tested a panel of compounds (GABA-A, NMDA, AMPA receptor modulators) which induced expected activity changes consistent with prior 2D co-cultures studies on MEA. These findings demonstrate the reproducibility, functional relevance, and accessibility of brain region-specific neurospheres from pre-differentiated human iPSC-derived neurons and glia, providing an economical NAM advancement for drug discovery. This baseline model supports future integration of neuroinflammatory cells or patient- and engineered iPSC-derived neural cells harboring neurodegenerative disease mutations.

**Disclosures: S. Schachtele:** None. **R. Fiene:** None. **D. Majewski:** None. **X. Xu:** None. **C.B. Carlson:** None.

**Poster**

**PSTR165: Autism: Genetic Models**

**Location:** WCC Halls A-C

**Time:** Monday, November 16, 2026, 1:00 PM - 5:00 PM

**Program #/Poster #:** PSTR165.01/D37

**Topic:** A.06. Developmental Disorders

**Support:** JSPS KAKENHI Grant Number 24KJ0093
JSPS KAKENHI Grant Number 25K16958
JSPS KAKENHI Grant Number 23K27526

**Title:** A case-control study of genetic variants with autism spectrum disorder in Japanese children revealed by targeted sequencing

**Authors:** Y. SHIOTA[1], T. NISHIYAMA[2], ***S. YOKOYAMA**[3], M. KIKUCHI[4];
[1]Child Develop., JSPS, Kanazawa city, Japan; [2]Univ. of Toyama, Toyama, Japan; [3]Kanazawa Univ., Kanazawa, Japan; [4]Kanazawa Univ., Kanazawa / Ishikawa, Japan

**Abstract:** Background: Autism spectrum disorders (ASD) are a heterogeneous group of neurodevelopmental disorders with strong hereditary predispositions. Although an increasing number of genetic variants have been implicated in the pathogenesis of ASD, little is known about the relationship between these variants and individual autistic traits. Therefore, we attempted to clarify these relationships. Methods: We performed a case-control association study of 32 Japanese children with ASD (mainly with high-functioning autism [HFA]) and 36 with typical development (TD). We explored previously reported ASD-associated genes using a next-generation sequencing panel and determined the association between Social Responsiveness

Scale (SRS) T-scores and intelligence quotient (IQ) scores. This study was approved by the Kanazawa University Medical Ethics Committee, performed in line with the principles of the Declaration of Helsinki, and were conducted in accordance with the local legislation, and institutional requirements. Written informed consent was obtained from the minors' legal guardian/next of kin for the publication of any potentially identifiable images or data included in this presentation. Results: Genotype-phenotype analyses revealed that 40 variants of 5 genes (*SCN1A*, *SHANK3*, *DYRK1A*, *CADPS*, and *SCN2A*) were associated with ASD/TD phenotypes. In particular, 10 SCN1A variants passed permutation filtering (false discovery rate <0.05). In the quantitative association analyses, 49 variants of 12 genes (*CHD8*, *SCN1A*, *SLC6A1*, *KMT5B*, *CNTNAP2*, *KCNQ3*, *SCN2A*, *ARID1B*, *SHANK3*, *DYRK1A*, *FOXP1*, and *GRIN2B*) and 50 variants of 10 genes (*DYRK1A*, S*CN2A*, *SLC6A1*, *ARID1B*, *CNTNAP2*, *SHANK3*, *FOXP1*, *PTEN*, *SCN1A*, and *CHD8*) were associated with SRS T- and IQ-scores, respectively. Conclusion: Our data suggest that these identified variants are essential for the genetic architecture of HFA.

**Disclosures: Y. Shiota:** None. **T. Nishiyama:** None. **S. Yokoyama:** None. **M. Kikuchi:** None.

**Poster**

**PSTR165: Autism: Genetic Models**

**Location:** WCC Halls A-C

**Time:** Monday, November 16, 2026, 1:00 PM - 5:00 PM

**Program #/Poster #:** PSTR165.02/D38

**Topic:** A.06. Developmental Disorders

**Support:** SFARI #SFI-AN-AR-Sex Differences-00017956-03
F32HD116501

**Title:** A massively parallel reporter assay of MECP2 cis-regulatory elements reveals genetic candidates for male-biased autism

**Authors: *R. MEYER-SCHUMAN**[1], F. CHERRY[2], K. HENNICK[4], Z. LIU[3], E. EICHLER[5], H. Y. ZOGHBI[6];
[1]Baylor Col. of Med., Houston, TX; [2]Baylor Col. of Med., Houston, TX, ; [3]Dept. of Pediatrics, Baylor Col. of Med., Houston, TX; [4]Dept. of Neurolog. Surgery, Univ. of California, San Francisco, San Francisco, CA; [5]Univ. of Washington/HHMI, Seattle, WA; [6]Mol. and Human Genet., Baylor Col. of Medicine/HHMI, Houston, TX

**Abstract:** Autism affects males four times more often than females, yet the basis of this sex bias remains unclear. One hypothesis is that hypomorphic variants in X-linked genes—genes where loss-of-function alleles cause syndromic neurodevelopmental disorders (NDDs) predominantly in females—produce milder, non-syndromic phenotypes in hemizygous males. We tested this by investigating cis-regulatory elements (CREs) of *MECP2*, a dosage-sensitive X-linked gene. Using a massively parallel reporter assay in human neurons, we mapped transcription factor binding sites within *MECP2* CREs and tested autism-associated variants for functional impact.

We identified two noncoding variants that change CRE activity, each with a male-biased phenotype. One of these, a promoter variant, disrupts NFY binding and reduces *MECP2* expression by ~30%, a magnitude that produces autism-like phenotypes in mice. These findings suggest noncoding *MECP2* variants can cause non-syndromic, male-biased autism, and provide a framework for uncovering regulatory variants in other X-linked NDD genes that may contribute to autism's missing heritability.

**Disclosures: R. Meyer-Schuman:** None. **H.Y. Zoghbi:** None.

**Poster**

**PSTR165: Autism: Genetic Models**

**Location:** WCC Halls A-C

**Time:** Monday, November 16, 2026, 1:00 PM - 5:00 PM

**Program #/Poster #:** PSTR165.03/D39

**Topic:** A.06. Developmental Disorders

**Support:** Institute for Basic Science (IBS-R002-D1)

**Title:** Slc6a20a-ASO restores NMDA receptor function in mouse and human SHANK2/3 ASD models

**Authors: *Y. OH**[1], M. BAE[2], J. D. ROH[2], E. KIM[2,1];
[1]Dept. of Biol. Sci., Korea Advanced Inst. of Sci. and Technol. (KAIST), Daejeon, Korea, Republic of; [2]Ctr. for Synaptic Brain Dysfunctions, Inst. for Basic Sci. (IBS), Daejeon, Korea, Republic of

**Abstract:** Suppressed NMDA receptor (NMDAR) function contributes to multiple brain disorders, including schizophrenia, autism spectrum disorder (ASD), and NMDAR encephalitis. Previous attempts to restore NMDAR activity by increasing ambient glycine, a critical co-agonist, through GlyT1 inhibition have yielded mixed outcomes, partly due to *GlyT1*'s extensive expression in essential brainstem regions. Slc6a20a, a glycine transporter widely expressed in cognition-relevant regions such as the cortex and hippocampus, offers a targeted alternative. Here we show that antisense oligonucleotide (ASO)-mediated *Slc6a20a* inhibition (*Slc6a20a*-ASO) normalizes ASD-related phenotypes in male *Shank2*- and *Shank3*-mutant mice, with model-dependent rescue profiles. *Slc6a20a*-ASO rescues NMDAR hypofunction and synaptic phospho-proteomic profiles in the prefrontal cortex. Furthermore, ASO targeting human *SLC6A20* rescues suppressed NMDAR function in cortical organoids harboring *SHANK2* or *SHANK3* mutations. These findings underscore the potentials of *Slc6a20a/SLC6A20*-ASO for treating disorders characterized by NMDAR hypofunction.

**Disclosures: Y. Oh:** None. **M. Bae:** None. **J.D. Roh:** None. **E. Kim:** None.

**Poster**

**PSTR165: Autism: Genetic Models**

**Location:** WCC Halls A-C

**Time:** Monday, November 16, 2026, 1:00 PM - 5:00 PM

**Program #/Poster #:** PSTR165.04/E1

**Topic:** A.06. Developmental Disorders

**Support:** Canadian Institutes of Health Research
Canada Foundation for Innovation
Ontario Research Fund: Research Infrastructure
Canada Research Chair (Tier 1)
The Azrieli Foundation
Natural Sciences and Engineering Research Council of Canada
McMaster University Startup Funds

**Title:** Autism-risk gene mutations convergently disrupt oxytocinergic modulation of sex-specific social circuits

**Authors:** A. PATWARDHAN[1], E. TSE[1], A. MOSLEMIAN[1], V. GRINEVICH[2], ***K. Y. CHOE**[1];
[1]McMaster Univ., Hamilton, ON, Canada; [2]Heidelberg Univ., Heidelberg, Germany

**Abstract:** Autism spectrum disorder (ASD) is associated with diverse genetic risk factors that frequently converge on lower sociability, yet the circuit mechanisms underlying this convergence remain unclear. Using two well-validated genetic models of ASD (*Cntnap2* or *Fmr1* knockout mice), we examined whether social investigation triggers convergent patterns of regional activity and/or network-level functional connectivity that are distinct from their wildtype littermates (n= 8-10/group). Whole-brain mapping of social investigation-evoked cellular activity (c-Fos+ cells) revealed convergent disruptions in network organization in both models, characterized by altered functional connectivity among prefrontal, reward, sensory, and amygdalar regions, which make up the social salience network (SSN). Implicating deficient oxytocin (OXT) signaling as a common driver of SSN dysfunction, chemogenetic stimulation of endogenous OXT release reorganized SSN functional connectivity and increased social investigation in both models. Importantly, the increase in the duration of social investigation events strongly correlated with higher activity levels within the paraventricular nucleus (PVN), nucleus accumbens (NAc), and lateral central amygdala (CeL), highlighting these areas as potential key SSN nodes that regulate the salient and rewarding nature of social investigation. Based on these results, we hypothesized that deficient OXT release in these regions, caused by a lack of *Cntnap2* or *Fmr1*, may be causal to their low sociability. To test this, we performed fiber photometry recordings to measure the activity dynamics of NAc and CeL neurons expressing GCaMP8f in socially interacting mice. Intriguingly, we found that social investigation triggers sex-divergent activity reductions in both models, with reduced NAc shell (NAcSh) activity in males and reduced CeL activity in females. These activity phenotypes were accompanied by a corresponding absence of socially evoked OXT release in each region, measured by GRAB-OT (Qian et al., 2023 Nat Biotech). Finally, restoring OXT signaling in a region-specific manner by optogenetically stimulating ChrimsonR-expressing OXT fibers in the NAcSh of males or the CeL of females normalized regional activity dynamics and rescued the social phenotype in both models. Together, these findings establish

deficient OXT gating of SSN activity as a shared circuit mechanism of low sociability across ASD-risk gene models and identify accumbal and amygdalar circuits as hubs that determine sociability in a sex-specific manner.

**Disclosures: A. Patwardhan:** None. **E. Tse:** None. **A. Moslemian:** None. **V. Grinevich:** None. **K.Y. Choe:** None.

**Poster**

**PSTR165: Autism: Genetic Models**

**Location:** WCC Halls A-C

**Time:** Monday, November 16, 2026, 1:00 PM - 5:00 PM

**Program #/Poster #:** PSTR165.05/E2

**Topic:** A.06. Developmental Disorders

**Support:** NIHR01GM122463
RF1AG057355
R21OD032463
The Albany Foundation
Wilder Gift
Anonymous Endowed Excellence Fund
Mulva Clinic for the Neurosciences at Dell Medical School
The CNS Advanced Summer Research Fellowship

**Title:** ASD-risk alleles bidirectionally alter penetrance of latent motor behavior in C. elegans

**Authors: *L. ROSTA**[1], G. WULFFRAAT[4], P. HERNANDEZ[2], S. IYER[2], A. C. BRUMBACK[3], J. T. PIERCE[2];
[1]Neurosci., [3]Neurol. and Pediatrics, [2]The Univ. of Texas at Austin, Austin, TX; [4]The Rockefeller Univ., New York, NY

**Abstract:** Autism spectrum disorder (ASD) is a condition characterized by symptoms such as altered social behaviors, repetitive motor behaviors, and increased sensitivity to sensory stimuli. DLG4-related synaptopathy is one such rare form of ASD caused by mutations in the synaptic scaffolding gene *DLG4* also known as *SAP90* or *PSD95*. We studied DLG4-related synaptopathy using the nematode *C. elegans* to model a patient's *DLG4* variant in the worm ortholog *dlg-1*. During phenotyping, we found that a small portion (30%) of the lab wild-type worm intersperses typical dorsoventral swimming bends with left-right bends, resembling an orchestra conductor's arm motions. This conducting behavior was significantly higher (60%) in the *dlg-1* mutant worm. The high proportion of conducting in *dlg-1* is recessive and rescuable with wild-type *dlg-1*, and was phenocopied with an independent *dlg-1* patient allele. We hypothesized that conducting might represent a phenotype that is modulated by other ASD-risk genes, so sought to test more mutants. In contrast to the *dlg-1* mutants, we found that neuroligin and neurexin mutants displayed a significantly lower proportion of conductors (10%) than wild-type. These results indicate that conducting is bidirectionally modifiable by synaptic molecules related to

ASD. Additionally, we sought to determine how sensory experience might contribute to the conducting behavior. We hypothesized that conducting might serve as a method to help the worm reorient in 3D media, so we tested whether conducting would increase if worms were reared on “3D plates” with holes pierced into the typical 2D agar surface. Interestingly, similar to wild type, each of *dlg-1*, neurexin and neuroligin mutants, showed an increased proportion of conducting when raised on textured "3D" plates. This raises the possibility that conducting represents a latent motor pattern that emerges with multidimensional sensory experience. Future studies will seek to determine the neural circuit and molecular pathways that underlie conducting to better understand how the implicated ASD-risk genes bidirectionally modulate its incidence.

**Disclosures: L. Rosta:** None. **G. Wulffraat:** None. **P. Hernandez:** None. **S. Iyer:** None. **A.C. Brumback:** None. **J.T. Pierce:** None.

**Poster**

**PSTR165: Autism: Genetic Models**

**Location:** WCC Halls A-C

**Time:** Monday, November 16, 2026, 1:00 PM - 5:00 PM

**Program #/Poster #:** PSTR165.06/E3

**Topic:** A.06. Developmental Disorders

**Support:** NRF 2022R1A6A3A13073152

**Title:** CLCN4 variants impair autophagy and cause neuronal death through epigenetic silencing of MEG3

**Authors: *D. KIM**, J. HAN;
KAIST, Daejeon, Korea, Republic of

**Abstract:** Genetic variations in *CLCN4*, which encodes the H+/Cl- exchanger CLC-4, are associated with neurodevelopmental disorders with highly variable phenotypes. However, the molecular and cellular mechanisms by which *CLCN4* variants disrupt human neurodevelopment remain poorly understood. Here, we established genome-edited brain organoid and neuronal cell systems to examine impacts of patient-relevant *CLCN4* variants. *CLCN4* variants led to early excitatory neuronal cell death, accompanied by disrupted endo-lysosomal dynamics and impaired autophagic flux. These defects were observed across variants with distinct electrophysiological phenotypes. Transcriptomic profiling identified the long non-coding RNA *MEG3* as a consistently downregulated transcripts in *CLCN4*-variant neurons. Restoring *MEG3* expression was sufficient to rescue cellular defects and improve survival of *CLCN4*-variant neurons. *CLCN4* variant decreased ERα occupancy at the *MEG3* genomic locus, accompanied by reduced active histone marks and increased DNA methylation. Together, these findings identify epigenetic regulation of *MEG3* as a mechanism linking *CLCN4* variants to impaired autophagy and early neuronal death in human neurodevelopmental disorders.

**Disclosures: D. Kim:** None. **J. Han:** None.

**Poster**

**PSTR165: Autism: Genetic Models**

**Location:** WCC Halls A-C

**Time:** Monday, November 16, 2026, 1:00 PM - 5:00 PM

**Program #/Poster #:** PSTR165.07/E4

**Topic:** A.06. Developmental Disorders

**Support:** SFARI Grant

**Title:** Identifying convergent disease mechanisms across the dysregulation of functionally distinct ASD risk genes using human cortical organoids

**Authors: *C. EISENBERG**[1], F. BIREY[2];
[1]Human Genet., [2]Psychiatry and Behavioral Sci., Emory Univ., Atlanta, GA

**Abstract:** Identifying convergent disease mechanisms across the dysregulation of functionally distinct ASD risk genes using human cortical organoids
Autism Spectrum Disorder (ASD) is a complex neurodevelopmental disorder characterized by both common as well as rare gene mutations. More than 200 rare, high-penetrance mutations in ASD-related risk genes have been identified to date, which are implicated in diverse overlapping cellular functions such as transcription regulation, chromatin remodeling, and ion channel activity. However, the mechanisms through which these divergent gene functions converge to confer risk for ASD remain unclear. Our study aims to investigate the molecular, cellular, and functional convergence of five high-confidence ASD risk genes (ADNP, POGZ, ARID1B, FOXP1, and GRIN2B) using human brain organoids and forebrain assembloids derived from induced pluripotent stem cells (hiPSCs). These models replicate human cortical development and enable the study of ASD gene function in a human context. We employ bulk RNA sequencing to identify convergent biological pathways at the molecular level, and live-cell imaging, calcium imaging, and multi-electrode arrays (MEA) to investigate cellular processes related to neuronal migration, network activity, and excitatory/inhibitory imbalance. Focusing on convergent molecular signature, we further investigate the shared signaling pathway dysregulation using antisense oligonucleotides (ASOs) to knock down our gene of interest, chromatin immunoprecipitation (ChIP) sequencing to elucidate where the protein binds, phosphoproteomics to determine what proteins become phosphorylated in the signaling pathway and live cell stimulation experiments to determine their ultimate function. By uncovering shared molecular and functional phenotypes across ASD risk genes, this study aims to contribute to the development of mutation-agnostic therapeutic strategies across genetically distinct forms of monogenic ASD.

**Disclosures: C. Eisenberg:** None. **F. Birey:** None.

**Poster**

**PSTR165: Autism: Genetic Models**

**Location:** WCC Halls A-C

**Time:** Monday, November 16, 2026, 1:00 PM - 5:00 PM

**Program #/Poster #:** PSTR165.08/E5

**Topic:** A.06. Developmental Disorders

**Support:** NIEHS P30ES030283
DOD AR230178P1

**Title:** Cannabinoid signaling and synaptic pruning in ASD

**Authors: I. TUNCALI**[1], *E. GOZAL[4], R. JAGADAPILLAI[5], M. WOLF[2], N. NAGARAJAN[2], Z.-H. SONG[3], G. N. BARNES[6];
[2]Pediatrics PRI, [3]Dept. of Pharmacol. & Toxicology, [1]Univ. of Louisville, Louisville, KY; [4]Dept of Pediatrics PRI / Univ. of Louisville, Louisville, KY; [5]Pediatric Res. Inst., [6]Dept Pediatrics PRI, Univ. of Louisville Sch. of Med., Louisville, KY

**Abstract:** Autism spectrum disorder (ASD) is a neurodevelopmental condition of increasing prevalence that lacks mechanism-based interventions. Postmortem and imaging studies indicate increased synaptic density in cortical regions of individuals with ASD, consistent with impaired synaptic pruning. Microglia are the principal mediators of synaptic pruning through complement dependent phagocytosis and immunometabolic signaling pathways, including TREM2 and Wnt/β catenin. Disruption of these pathways has been implicated in ASD risk, yet how they interact to regulate execution stage pruning remains poorly understood. Cannabidiol (CBD) is an immunomodulatory compound currently under clinical investigation in ASD; however, its effects on microglial pruning mechanisms have not been defined. We previously demonstrated that CBD administration improves ASD like behaviors in BTBR mice, a polygenic model of ASD. Based on these findings, we hypothesized that CBD administered during a critical postnatal window modulates microglial signaling pathways that support synaptic pruning execution. To test this hypothesis, BTBR and C57 control mice received CBD (35 mg/kg, i.p.) or vehicle for one week beginning at postnatal day 21. Prefrontal cortex tissue was harvested for whole cell and subcellular fractionation, and protein levels of β catenin, TREM2, and synaptic density markers (synaptophysin, PSD 95) were assessed by immunoblotting. In parallel, the BV2 microglial cell line was used to model inflammatory stress in vitro, where cells were treated with LPS in the presence or absence of CBD. Microglial migration and phagocytic capacity were quantified using scratch wound and fluorescent bead uptake assays, respectively. BTBR mice exhibited elevated cortical β catenin and reduced TREM2 relative to controls, consistent with a stress biased microglial signaling state. CBD treatment showed a trend toward normalization of these molecular alterations. In vitro, CBD significantly enhanced microglial migration and phagocytosis under inflammatory conditions, indicating restoration of microglial functional capacity rather than suppression of activation. Together, these data demonstrate that CBD modulates signaling pathways central to microglial synaptic pruning and support the concept that microglial metabolic and signaling states are reversible during defined developmental windows. These findings provide a mechanistic foundation for the current proposal, which focuses on defining execution stage pruning failure as a state based process and testing pharmacologic modulation strictly as a probe of reversibility, rather than as a therapeutic endpoint.

**Disclosures: I. Tuncali:** None. **E. Gozal:** None. **R. Jagadapillai:** None. **M. Wolf:** None. **N. Nagarajan:** None. **Z. Song:** None. **G.N. Barnes:** None.

**Poster**

**PSTR165: Autism: Genetic Models**

**Location:** WCC Halls A-C

**Time:** Monday, November 16, 2026, 1:00 PM - 5:00 PM

**Program #/Poster #:** PSTR165.09/E6

**Topic:** A.06. Developmental Disorders

**Support:** NIEHS P30ES030283
DOD AR230178P1

**Title:** Lipid alterations and microglial metabolic dysfunction in the cerebellum of ASD mouse models.

**Authors: *R. JAGADAPILLAI**[1], E. GOZAL[3], I. TUNCALI[4], N. NAGARAJAN[5], G. N. BARNES[2];
[2]Dept Neurol, [1]Univ. of Louisville Sch. of Med., Louisville, KY; [3]Pediatrics, Pharm & Tox, Physiol., Dept of Pediatrics PRI / Univ. of Louisville, Louisville, KY; [5]Pediatrics , PRI, [4]Univ. of Louisville, Louisville, KY

**Abstract:** Metabolic abnormalities are increasingly recognized as a core biological feature of autism spectrum disorder (ASD), with growing evidence implicating lipid dysregulation in disrupted neuronal development and circuit refinement. Lipids provide the structural basis for neuronal membranes and myelin and play essential roles in synaptic organization and signaling. In the developing brain, microglia regulate synaptic pruning through lipid-sensitive phagocytic and metabolic pathways, prominently involving the triggering receptor expressed on myeloid cells 2 (TREM2). TREM2 functions as a lipid and damage sensor that supports microglial survival, metabolic homeostasis, and execution-stage synaptic pruning. Loss of TREM2 signaling impairs lipid processing and clearance, leading to accumulation of neutral lipids and compromised microglial function. Ceramides represent a central lipid class linking membrane composition to cellular signaling and stress responses. Ceramide levels are regulated through de novo synthesis by ceramide synthase 2 (CERS2) and through sphingomyelin hydrolysis mediated by acid sphingomyelinase (ASM) during stress and neuroinflammation. Disruption of these pathways has the potential to impair lysosomal function and synaptic pruning execution. In this study, we examined whether reduced TREM2 signaling is associated with lipid accumulation and altered ceramide metabolism in the cerebellum of BTBR and Shank3 mouse models of ASD. Using BODIPY staining, immunofluorescence, and immunoblotting, we assessed neutral lipid accumulation, TREM2 expression, ceramide levels, and expression of CERS2 and ASM. Both BTBR and Shank3 mice exhibited increased neutral lipid accumulation relative to C57 controls, accompanied by reduced TREM2 expression. Notably, ceramide levels were decreased in ASD models and correlated with reduced CERS2 and ASM expression. These findings identify a convergent lipid metabolic phenotype in genetically distinct ASD models and

support a model in which impaired TREM2-dependent lipid handling constrains microglial execution-stage pruning in the cerebellum. Disruption of ceramide metabolism and neutral lipid clearance provides a mechanistic link between microglial metabolic stress, impaired synaptic pruning, and cerebellar circuit vulnerability. Together, these data motivate further investigation of lipid-lysosomal dysfunction as a central execution-stage bottleneck in ASD and support the development of lipid-based biomarkers to stratify neurodevelopmental risk.

**Disclosures: R. Jagadapillai:** None. **E. Gozal:** None. **I. Tuncali:** None. **N. Nagarajan:** None. **G.N. Barnes:** None.

**Poster**

**PSTR165: Autism: Genetic Models**

**Location:** WCC Halls A-C

**Time:** Monday, November 16, 2026, 1:00 PM - 5:00 PM

**Program #/Poster #:** PSTR165.10/E7

**Topic:** A.06. Developmental Disorders

**Support:** SERB CRG/2020/002462

**Title:** Mitochondrial Dysfunction and Extracellular Vesicle-Signatures in Autism Spectrum Disorder:Insights from Cybrid Model

**Authors: *N. P**[1], M. JEEJO[4], B. B R[5], K. MOHANAKUMAR[2], U. RAJAMMA[3]; [1]CDAR-Genomics, Inter Univ. Ctr. for Biomed. Res. & Super Speciality Hosp. (IUCBR & SSH), Kottaym, India; [3]CDAR-Genomics, [2]Inter Univ. Ctr. for Biomed. Res. & Super Speciality Hosp. (IUCBR & SSH), Kottayam, India; [4]CDAR-Genomics, Inter Univ. Ctr. for Biomed. research & Super Speciality Hosp. (IUCBR & SSH), Kottayam, India; [5]Shree Vidyadhiraja Homeopathic Med. College, Nemom, Thiruvananthapuram, India

**Abstract:** Extracellular vesicles (EV) are secreted nanoscale lipid bilayer particles that transport bioactive molecules and support intercellular communication. Mitochondrial DNA (mtDNA) variations and associated mitochondrial dysfunction are increasingly linked to neurodevelopmental disorders, particularly autism spectrum disorder (ASD). Using control and ASD cybrid model systems and the cybrid-derived EV, the present study examined the relationship between mitochondrial impairment, neuronal differentiation, and EV profiles. Cybrid were generated by fusing mtDNA-depleted rho0 SH-SY5Y cells with platelets from ASD probands or age-matched controls and validated by mtDNA haplogroup analysis using next-generation sequencing. Mitochondrial and nuclear-encoded electron transport chain (ETC) genes (ATP6, ATP8, NDUFS3, NDUFS5) expressions were assessed by RT-PCR along with ETC enzyme activity. Neuronal differentiation was examined by measuring neurite outgrowth and the expression of SYP and MAP2. EVs were isolated from cybrid culture spent media by ultracentrifugation and characterized using DLS, TEM and immunoblotting for flotillin-1 and Alix. Total DNA & RNA were extracted from cybrid-derived EV, quantified by spectrophotometry, and evaluated for RNA quality using Agilent Bioanalyzer-derived RNA

Integrity Numbers (RIN). PCR amplification of EV-derived DNA was then performed to detect specific encapsulated mtDNA fragments. ASD cybrids showed significant downregulation of the nuclear-encoded complex I subunits NDUFS3 and NDUFS5, upregulation of the mtDNA-encoded ATP6 gene, increased complex II activity, and evidence of mitochondrial imbalance. Neuronal differentiation was impaired, as indicated by shorter neurites and reduced SYP and MAP2 expression. Cybrid-derived EV displayed distinct nanoscale morphologies and canonical EV markers, with ASD-derived EV being smaller, suggesting ASD-specific, mtDNA-dependent changes in EV morphology. Total RNA from cybrid-derived EVs yielded small-RNA profile, enriched for fragments predominantly around 200 nucleotides and below, with RIN of 2.0-2.6, consistent with EV-associated RNA. In addition, EV-derived mtDNA was successfully amplified, with the absence of full-length mtDNA. Together, these findings show that mtDNA-driven mitochondrial dysfunction alters neuronal differentiation and the biophysical properties of the secreted EVs. These further support the potential of EV as an important biomarker for neurodevelopmental disorders such as ASD and suggest that mtDNA changes influence mitochondrial function, cellular physiology, and EV cargo composition.

**Disclosures: N. P:** None. **M. Jeejo:** None. **B. B r:** None. **K. Mohanakumar:** None. **U. Rajamma:** None.

**Poster**

**PSTR165: Autism: Genetic Models**

**Location:** WCC Halls A-C

**Time:** Monday, November 16, 2026, 1:00 PM - 5:00 PM

**Program #/Poster #:** PSTR165.11/E8

**Topic:** A.06. Developmental Disorders

**Support:** Carver Trust Research Program of Excellence
NINDS Grant R25NS130966
T32GM008629
T32GM145441
F31MH134542
T32NS007421

**Title:** Effects of Placental-Targeted Igf2 Overexpression in the 16p11.2 Deletion Mouse Model of Neurodevelopmental Disorders

**Authors: E. G. WILLIAMSON**[1,2,3], A. J. CARVER[1,3,4], B. KELVINGTON[1,5,6,7], R. FAIR[1,6,8], R. J. TAYLOR, Jr[1,3], F. FAIRBAIRN[1,3], T. ABEL[1,6,7], *H. E. STEVENS[9,1,7];
[1]Iowa Neurosci. Inst., [2]iDREAM in Neurosci. Program, [3]Dept. of Psychiatry, [4]Interdisciplinary Grad. Program in Genet., [5]Pharmacol. Grad. Program, [6]Dept. of Neurosci. and Pharmacol., [7]Hawk-IDDRC, [8]Interdisciplinary Grad. Program in Neurosci., [9]Psychiatry, Univ. of Iowa, Iowa City, IA

**Abstract:** Neurodevelopmental disorders (NDDs) are common conditions, with risk factors including genetics and conditions that affect placental signaling. The 16p11.2 microdeletion (16p) is a genetic condition associated with NDDs such as autism spectrum disorder (ASD) and intellectual disability. 16p mouse models recapitulate sex-specific ASD-relevant phenotypes on behavioral and molecular levels. Prior work has identified sex-specific differences in embryonic 16p mice and their placentas, suggesting developmental origins of NDD symptoms. Notably, at embryonic day (E)18, 16p males, but not females, had decreased placental insulin-like growth factor 2 (*Igf2*) expression compared to wildtype (WT) mice. Data on placental and postnatal IGF signaling and NDD outcomes suggest that increasing placental *Igf2* during gestation may act as a compensatory mechanism against some aspects of 16p. Our objective was to determine if overexpressing placental *Igf2* could mitigate effects of the 16p11.2 deletion on placental and neurodevelopmental outcomes in a mouse model. We investigated this by breeding WT female mice with hemizygous 16p males and injecting and electroporating either control (Con) or *Igf2* overexpression (OE) dCas9 CRISPR plasmids into placentas on E12. We assessed fetal and placental weights and brain and placental gene expression at embryonic timepoints and evaluated postnatal development and behaviors associated with 16p deficits. Data were analyzed using a linear mixed effects model with litter as a covariate. In line with previous work, Con 16p males had significantly lower body mass than Con WT males at E14 ($p<0.001$). Promisingly, OE 16p males' body mass did not differ from Con WTs ($p=0.365$) and was trend ($p=0.07$) greater than Con 16p males. No mass differences were evident in females at E14 or E18. We found no differences in self-righting behavior from P5 to P10. In the first five minutes of the open field test on P21, Con WTs traveled a similar distance (Avg = 8.92m) to OE 16p (Avg = 6.91m), while Con 16p animals moved less (Avg = 4.17m). At P21, OE 16p mice had significantly greater normalized grip strength than Con 16p mice ($p=0.005$). These initial results suggest a role for placental *Igf2* in the developmental deficits of 16p. Further analysis of embryonic and postnatal brains and postnatal behavior, including separate assessments of males and females, is ongoing. Our findings can inform approaches to reducing some symptoms of NDDs by altering placental function and the prenatal environment for fetuses with NDD risk genes.

**Disclosures: E.G. Williamson:** None. **A.J. Carver:** None. **B. Kelvington:** None. **R. Fair:** None. **R.J. Taylor:** None. **F. Fairbairn:** None. **T. Abel:** None. **H.E. Stevens:** None.

**Poster**

**PSTR165: Autism: Genetic Models**

**Location:** WCC Halls A-C

**Time:** Monday, November 16, 2026, 1:00 PM - 5:00 PM

**Program #/Poster #:** PSTR165.12/F1

**Topic:** A.06. Developmental Disorders

**Support:** Simons Foundation

**Title:** Global and local parental genome sharing among concordant and discordant siblings of ASD

**Authors: *M. JAMSANDEKAR**, I. IOSSIFOV;
Cold Spring Harbor Lab., Cold Spring Harbor, NY

**Abstract:** Autism spectrum disorder (ASD) is diagnosed four times more frequently in males than females, a disparity widely attributed to a female protective effect, the observation that females require a higher genetic burden to reach the diagnostic threshold. This model predicts that mothers, being themselves protected from ASD despite carrying risk variants, should be the primary transmitters of damaging alleles. We developed a method to test this directly by quantifying maternal and paternal genome sharing in concordant and discordant ASD sibling pairs using whole-genome or microarray genotype data (Wroten, Yoon et al., 2023). Applying this method to SSC, AGRE, and SPARK cohorts, we unexpectedly observed significantly elevated sharing of the paternal genome among concordant siblings, while maternal sharing showed no comparable signal. A complementary anti-sharing pattern in discordant siblings reinforced the finding. These results contradict the female protective model and suggest that fathers, not mothers, carry the dominant causal determinants in at least half of multiplex families. However, the initial dataset lacked statistical power to resolve individual loci contributing to the global sharing signal. To address this, we extended the study using newly ascertained WES- and WGS-sequenced families from SPARK, yielding a nearly threefold larger cohort of ~4,000 concordant and ~12,000 discordant sibling pairs. This expanded dataset robustly replicates the paternal sharing excess and additionally reveals elevated sharing of the maternal X chromosome. We further attempted to identify specific autosomal loci driving the global sharing signal. No locus reached genome-wide significance, but the three strongest candidates were found on chromosomes 7, 14, and 19 of size ranging from 3-22 Mb. The chr19 locus displays an unusual pattern of paternal anti-sharing in both concordant and discordant pairs, which is inconsistent with a straightforward autism risk model and motivating a separate investigation. The absence of genome-wide significant loci is not unexpected because a power analysis demonstrates that even this expanded cohort is substantially underpowered to detect individual loci of realistic effect size, underscoring the need for continued SPARK expansion.
Mathew Wroten, Seungtai Yoon, Peter Andrews, Boris Yamrom, Michael Ronemus, Andreas Buja, Abba M. Krieger, Dan Levy, Kenny Ye, Michael Wigler, and Ivan Iossifov. Sharing parental genomes by siblings concordant or discordant for autism. *Cell Genomics*. 2023.

**Disclosures: M. Jamsandekar:** None. **I. Iossifov:** None.

**Poster**

**PSTR165: Autism: Genetic Models**

**Location:** WCC Halls A-C

**Time:** Monday, November 16, 2026, 1:00 PM - 5:00 PM

**Program #/Poster #:** PSTR165.13/F2

**Topic:** A.06. Developmental Disorders

**Support:** T32AG000222

**Title:** Selective Vulnerability of CPN Subtypes to Circuit Dysfunction Following loss of ASD/ID gene Bcl11a

**Authors: *R. W. KIRK**[1], O. DURAK[2], J.-Y. KIM[3], D. TILLMAN[4], J. D. MACKLIS[5]; [2]Stem Cell and Regenerative Biol., [3]scrb, [4]Mol. & Cell. Biol., [5]Dept of Stem Cell and Regenerative Biology, and Ctr. for Brain Sci., [1]Harvard Univ., Cambridge, MA

**Abstract:** Precise connectivity of callosal projection neurons (CPN), which connect and integrate the cortical hemispheres via the corpus callosum, is critical for sensory, associative, and behavioral functions, and is centrally implicated in autism spectrum disorder (ASD) and intellectual disability (ID). Though transcriptional and molecular controls broadly regulating superficial layer CPN ($CPN_{SL}$) development and axon targeting are partially understood, less is known about the molecular specification and circuit functions of the transcriptionally distinct CPNSL subtypes identified in the adult mammalian cortex. Our lab recently identified that the ASD/ID risk gene *Bcl11a/Ctip1* is critical for appropriate and precise contralateral targeting of $CPN_{SL}$ projections during early development. $CPN_{SL}$-specific or forebrain-specific embryonic deletion of *Bcl11a* causes dramatic loss of correct homotopic targeting in the contralateral cortex, re-routes many axonal projections through the evolutionarily older anterior commissure, and induces strikingly aberrant yet specific *de novo* projections to the basolateral amygdala (BLA), accompanied by abnormal social behavior and cognition. However, it is unclear whether these *de novo* BLA projections arise from a subpopulation of *Bcl11a*-null $CPN_{SL}$ distinct from those that maintain imprecise contralateral projections, and whether these projection types align with transcriptionally defined $CPN_{SL}$ subtypes. We have begun to investigate these questions by dual retrograde labeling $CPN_{SL}$ projecting to either the contralateral cortex or BLA in *Bcl11a* forebrain-specific cKO mice. We observe only rare, if any, cortical neurons co-labeled from both BLA and contralateral cortex, indicating that these projections arise from entirely or nearly entirely distinct $CPN_{SL}$ subpopulations. Strikingly, CPN aberrantly projecting to BLA occupy an extremely superficial sub-layer of the cortex, suggesting that these subsets of CPN might have distinct developmental dynamics. Identification of discrete CPN projection sub-subtypes with laminar separation in *Bcl11a* cKO cortex suggests that *Bcl11a* deletion leads to $CPN_{SL}$ subtype-specific effects on gene expression and axon targeting that can be leveraged to investigate CPN subtype diversity and subtype-specific vulnerability in ASD.

**Disclosures: R.W. Kirk:** None. **O. Durak:** None. **J. Kim:** None. **D. Tillman:** None. **J.D. Macklis:** None.

**Poster**

**PSTR165: Autism: Genetic Models**

**Location:** WCC Halls A-C

**Time:** Monday, November 16, 2026, 1:00 PM - 5:00 PM

**Program #/Poster #:** PSTR165.14/F3

**Topic:** A.06. Developmental Disorders

**Title:** Functional impact of of autism-associated TRIO variants on GABAergic interneurons

**Authors: *A. TOUMI**[1], É. CHAMBERLAND[2], N. PROTZENKO[4], E. ROSSIGNOL[3];
[1]Univ. de Montréal-CHU Ste-Justine, Montréal, QC, Canada; [2]CHU Ste-Justine, Montréal, QC, Canada; [3]Univ. de Montréal, CHU Ste-Justine, Montreal, QC, Canada; [4]Sorbonne Université, CNRS, Inserm, Ctr. for Neurosci. Sorbonne Univ. (Neuro-SU), Paris 75005, France, Paris.

**Abstract:** Mutations in *TRIO* are associated with a spectrum of neurodevelopmental disorders (NDDs). *TRIO* encodes a RhoGEF (The Rho-guanine nucleotide exchange factor) that activates Rac1 and RhoA, two Rho-GTPases implicated in neuronal migration. Recent data from our group indicate that, in mice, the conditional deletion of *Trio* alters the migration and morphological development of GABAegic interneurons (INs), resulting in reduced cortical inhibition, ASD-like behavior and epilepsy in $Trio^{cKO}$ mice. However, the impacts of specific disease-causing variants on INs development remain unknown. We designed a new functional validation pipeline to address this question.We expressed mutant cDNA, carrying patient-derived variants, or the wild-type cDNA in explants of the medial ganglionic eminence of e13.5 $Trio^{cKO}$ embryos. Using FLIM-FRET-based biosensors, we monitored the pattern of RhoA and Rac1 activation in INs and HEK293 cells. Additionally, we investigated the migration dynamics and morphological development of INs using time-lapse imaging of MGE explants. We find that $Trio^{cKO}$ INs display hypoactivation of RhoA, which is reversible by re-expressing WT *Trio* cDNA. When studied in HEK293 cells, patient-derived *TRIO* variants also alter Rac1 and RhoA activation. Furthermore, when expressed in mice INs, cDNA carrying GEFD1 variants fail to rescue the deficits in IN migration and morphology observed in $Trio^{cKO}$ INs, which are reversed by expressing the $Trio^{WT}$ cDNA. Thus, our findings suggest that NDD-associated TRIO variants disrupt the development and migration of INs, and that variant pathogenecity can be efficiently assessed using our validation pipeline.

**Disclosures: A. Toumi:** None. **É. Chamberland:** None. **N. Protzenko:** None. **E. Rossignol:** None.

**Poster**

**PSTR165: Autism: Genetic Models**

**Location:** WCC Halls A-C

**Time:** Monday, November 16, 2026, 1:00 PM - 5:00 PM

**Program #/Poster #:** PSTR165.15/F4

**Topic:** B.05. Synaptic Plasticity

**Support:** R01DC019380
1R56DC022339-01A1
R03MH127401
The David M. Rubenstein Precision Medicine Center of Excellence in Hearing Fund
Lloyd B. Minor Center for Vestibular and Skull Base Sciences
R01NS146406
R35GM156374
Johns Hopkins University Provost's Undergraduate Research Award (PURA)

**Title:** Autism-associated Cntnap2 and Shank3 mutations disrupt peripheral vestibular signaling and spatial cognition

**Authors: *Y. SHU**[1], Y. CHEN[2], D. ZHOU[2], D. BALLINAS[1], X. DENG[1], S. G. SADEGHI[2], T. DEEMYAD[3];
[2]Otolaryngology - Head and Neck Surgery, [3]Psychiatry, [1]Johns Hopkins Univ., Baltimore, MD

**Abstract:** Balance, gaze, and spatial-orientation abnormalities are common in ASD and are typically attributed to central sensory-integration deficits. Because vestibular organs provide key input for posture, otolith reflexes, and spatial navigation, we tested whether ASD-associated mutations also disrupt vestibular signaling at the periphery. We compared adult male and female Cntnap2$^{-/-}$ and Shank3$^{-/-}$ mice with wild-type littermates using VsEPs to measure synchronized phasic vestibular afferent activity, contact righting and balance-beam assays to assess static and dynamic vestibular function, OCR and VOR, and Y-maze and Barnes maze tasks to assess spatial cognition. Loss of Cntnap2 caused broad vestibular impairment in both sexes. Cntnap2$^{-/-}$ mice showed reduced VsEP P1N1 amplitudes with relatively preserved latency, delayed contact righting, impaired balance-beam traversal with increased hindlimb slips, and reduced ocular counter-roll gain, while rotational VOR gain and phase were preserved. This pattern indicates preferential disruption of otolith/linear-acceleration pathways rather than global vestibular failure. Cntnap2$^{-/-}$ mice also failed to prefer the novel arm in the Y-maze and showed severe Barnes maze acquisition deficits, consistent with impaired spatial working and learning memory. Shank3$^{-/-}$ mice showed a partially overlapping but more sex-dependent phenotype. Shank3$^{-/-}$ mice had reduced VsEP amplitudes and delayed contact righting, suggesting impaired peripheral vestibular signaling and static vestibular behavior. Shank3 loss disrupted spatial working memory in both sexes, and males showed impaired Barnes maze learning. Together, these data indicate that peripheral vestibular dysfunction is a convergent but gene and sex-dependent feature of ASD mouse models. The pattern of VsEP, righting, OCR, and balance deficits suggests that altered non-quantal and/or quantal transmission at the vestibular periphery may contribute to postural and spatial-cognitive phenotypes. These findings identify the vestibular sensory periphery as an active site of ASD-relevant dysfunction and suggest that sensory-organ deficits should be considered alongside central circuit mechanisms in ASD.

**Disclosures: Y. Shu:** None. **Y. Chen:** None. **D. Zhou:** None. **D. Ballinas:** None. **X. Deng:** None. **S.G. Sadeghi:** None. **T. Deemyad:** None.

**Poster**

**PSTR166: Other Ion Channels**

**Location:** WCC Halls A-C

**Time:** Monday, November 16, 2026, 1:00 PM - 5:00 PM

**Program #/Poster #:** PSTR166.01/F5

**Topic:** B.03. Ion Channels

**Title:** Optical modulation of ion channels using Qube Opto

**Authors: *P. SCADUTO**[1], K. BODDUM[2], D. SAUTER[3], J. ROLLAND[4];
[1]Sophion Biosci. Inc., Bedford, MA; [2]R&D, Sophion Biosci., Ballerup, Denmark; [3]Sophion Biosci. A/S, Bedford, CA; [4]Axxam SpA, Bresso, Italy

**Abstract:** Optical modulation of ion channels is traditionally studied using manual patch clamp systems combined with external light sources. While this approach provides precise temporal control, it is limited by very low throughput. In the present work, we demonstrate the use of the Qube Opto 384, a 384-well automated patch clamp system equipped with 384 integrated light sources, enabling high-throughput optical modulation studies.For optogenetic applications, we evaluated Channelrhodopsin-2 (ChR2), a light-sensitive non-selective cation channel permeable to sodium, potassium, and calcium, which opens upon illumination. We also employed the chloride-conducting channelrhodopsin iC++, developed from a non-selective cation-conducting channelrhodopsin through a mutational approach, and photoactivatable adenylyl cyclase (bPAC) to modulate intracellular cAMP levels and thereby alter the biophysical properties of HCN2 channels.For optopharmacology studies, we investigated the light activation of caged compounds using Rubi-GABA. Compound activation by light enables pharmacological manipulation of receptors, ion channels, and other proteins with a high degree of temporal control. Rubi-GABA was combined with the microfluidic flow channel of the QChip 384X consumable to provide enhanced experimental control during receptor activation.HEK293-HCN2/bPAC (kindly provided by Axxam S.p.A., Milan), HEK293-ChR2, HEK293-GABAA alpha5 beta3 gamma2, and HEK293-iC++ cells were cultured according to supplier recommendations. ChR2, GABAA receptors, and HCN2/bPAC were stably expressed, whereas iC++ expression was induced 24 hours prior to the experiment. All recordings were performed at ambient temperature using QChip 384X multi-hole consumables and standard whole-cell patch clamp protocols.With the new optical feature of the Qube Opto 384, it was possible to evaluate both light-activated ion channels and photo-activated ligands. Qube Opto 384 combines automated patch clamp electrophysiology with 384 individual built-in light sources operating at 475 nm, enabling modulation of ion channels through optogenetic actuators such as channelrhodopsins or activation of photo-responsive compounds, including caged ligands. These results demonstrate the suitability of Qube Opto 384 for high-throughput optogenetic and optopharmacological applications.

**Disclosures: P. Scaduto:** A. Employment/Salary (full or part-time):; Sophion Bioscience. **K. Boddum:** A. Employment/Salary (full or part-time):; Sophion Bioscience. **D. Sauter:** A. Employment/Salary (full or part-time):; Sophion Bioscience. **J. Rolland:** A. Employment/Salary (full or part-time):; AXXAM S.p.a.

**Poster**

**PSTR166: Other Ion Channels**

**Location:** WCC Halls A-C

**Time:** Monday, November 16, 2026, 1:00 PM - 5:00 PM

**Program #/Poster #:** PSTR166.02/F6

**Topic:** B.03. Ion Channels

**Support:** NS102239
DC01919

**Title:** Targeting the Slack channel KCNT1-CYFIP1 complex to restore translational control in Fragile X syndrome

**Authors: *J. WU**[1], S. GILLIAT[2], R. A. APONTE RIVERA[2], Y. ZHANG[2], H. WANG[2], L. K. KACZMAREK[2];
[2]Pharmacol., [1]Yale Univ., New Haven, CT

**Abstract:** Fragile X syndrome (FXS), a leading genetic cause of autism spectrum disorder (ASD), is characterized by loss of the Fragile X Mental Retardation Protein (FMRP), resulting in dysregulated synaptic protein synthesis and neuronal hyperexcitability. FMRP normally suppresses translation initiation by partnering with cytoplasmic FMRP-interacting protein 1 (CYFIP1) to sequester eIF4E (eukaryotic Initiation Factor 4E) from eIF4G at the 5' cap. We previously identified the sodium-activated potassium channel KCNT1 (Slack, KNa1.1) as a critical regulator of translational control through its interaction with FMRP and CYFIP1. Upon activation, KCNT1 recruits FMRP and CYFIP1 away from eIF4E, thereby promoting cap-dependent translation initiation. Our recent work suggests that, in FMRP-deficient neurons, KCNT1 may still regulate CYFIP1 distribution, reducing CYFIP1 association with eIF4E and enhancing eIF4G recruitment. This shift may promote aberrant translation of excitability-related proteins, including the voltage-gated sodium channels NaV1.2 and NaV1.6. We further found that KCNT1 suppression, either with antisense oligonucleotides (ASOs) or the small-molecule modulator PRX2904, disrupts KCNT1-CYFIP1 binding, releases CYFIP1 back to the eIF4E complex, restores translational repression, and reduces NaV1.2 and NaV1.6 expression. These findings uncover a novel mechanism by which KCNT1 contributes to translational dysregulation in FXS and establish the KCNT1-CYFIP1 axis as a promising therapeutic target to normalize protein synthesis and neuronal excitability. Notably, CYFIP1 loss has also been implicated in ASD, suggesting that targeting KCNT1 may provide therapeutic benefit not only in FXS but also in CYFIP1-deficient forms of ASD.

**Disclosures: J. Wu:** None. **S. Gilliat:** None. **R.A. Aponte Rivera:** None. **Y. Zhang:** None. **H. Wang:** None. **L.K. Kaczmarek:** None.

**Poster**

**PSTR166: Other Ion Channels**

**Location:** WCC Halls A-C

**Time:** Monday, November 16, 2026, 1:00 PM - 5:00 PM

**Program #/Poster #:** PSTR166.03/F7

**Topic:** B.03. Ion Channels

**Title:** Exploring the mechanism of the effect of potassium solution on swallowing initiation in humans

**Authors: *N. PHETNIN**[1], M. D. SURBOYO[2], A. QUISPE SALCEDO[3], H. OHSHIMA[3], J. MAGARA[1], T. TSUJIMURA[1], M. INOUE[1];
[1]Div. of Dysphagia Rehabil., [2]Advanced Res. Ctr. for Oral and Craniofacial Sci., [3]Div. of Anat. and Cell Biol. of the Hard Tissue, Niigata Univ. Grad. Sch. of Medicine, Dentistry, and Hlth. Sci., Niigata, Japan

**Abstract: Background and objective**: The swallowing reflex can be facilitated by some chemical stimulation applied to the pharynx/larynx. Previous studies have demonstrated that potassium ions enhance the swallowing-evoked activity of the superior laryngeal nerve in rats, and certain potassium ion channels, such as Kir3.1 and Kir6.2, were involved in this facilitation. However, the effect of potassium on swallowing performance in humans remains unclear. Therefore, this study investigated the effects of potassium fluid infusion on the initiation of involuntary swallowing in humans and examined the expression of the potassium channel receptor Kir3.1, which may be involved in this process. **Methods**: Hypopharyngeal fluid stimulation consisted of 154 mM potassium chloride (KCl), distilled water (DW), and 154 mM saline (NaCl) at low rates (0.2 mL/min and 3 mL/min) performed for 1 minute in 27 volunteers. Electromyography (EMGs) of the suprahyoid muscles was performed to determine swallowing muscle activity characteristics. In addition, inward rectifier potassium channel Kir 3.1 positive cells were identified in the nodose (inferior) ganglion and epiglottis tissues obtained from human cadavers (3 females and 2 males) using crysectioning and immunohistochemistry analysis. **Results**: The number of swallowing reflexes differed significantly between DW and KCl at the higher infusion rate (3.0 mL/min). The facilitatory effects on swallowing were ranked as follows: KCl > DW > NaCl. At the lower infusion rate (0.2 mL/min), significant differences in the number of swallows and the interval between consecutive swallows were observed only between NaCl and DW and between NaCl and KCl. The area and duration, especially the peak-to-offset time, of EMG bursts were significantly larger and longer during voluntary saliva swallowing than during involuntary swallowing under all conditions. Immunohistochemical analysis revealed Kir3.1-positive cells in neurons of the nodose ganglion and in peripheral nerve endings within the epiglottis. The mean expression percentages of Kir3.1-positive expression were 30.2% in the nodose ganglion and 29.6% in the epiglottal nerve endings. **Conclusion**: Application of KCl at a higher infusion rate facilitated swallowing initiation through both chemosensory and mechanical inputs, and we suggest that the inward rectifier potassium channel Kir3.1 may play a role in potassium-facilitated swallowing reflexes in humans.

**Disclosures: N. Phetnin:** None. **M.D. Surboyo:** None. **A. Quispe Salcedo:** A. Employment/Salary (full or part-time):; Niigata University. **H. Ohshima:** A. Employment/Salary (full or part-time):; Niigata University. **J. Magara:** A. Employment/Salary (full or part-time):; Niigata University. **T. Tsujimura:** A. Employment/Salary (full or part-time):; Niigata University. **M. Inoue:** A. Employment/Salary (full or part-time):; Niigata University.

**Poster**

**PSTR166: Other Ion Channels**

**Location:** WCC Halls A-C

**Time:** Monday, November 16, 2026, 1:00 PM - 5:00 PM

**Program #/Poster #:** PSTR166.04/F8

**Topic:** B.03. Ion Channels

**Title:** Cell-type Specific Spatial Expression of Sodium-Activated Potassium Channel Isoforms

**Authors: *R. A. APONTE RIVERA**[1], J. WU[2], L. K. KACZMAREK[3];
[1]Neurosci., [2]Pharmacol., Yale Univ., New Haven, CT; [3]Yale Univ. Sch. Med., New Haven, CT

**Abstract:** Sodium-activated potassium channels (KNa) play important roles in excitability via rapid high conductance hyperpolarization in response to increases in intracellular sodium level, resulting in control of neuronal firing rates. There are two genes that encode KNa channels, Kcnt1 (Slack) and Kcnt2 (Slick). The Slack channel is known to bind several cytoplasmic signaling factors including regulators of mRNA translation. Slack channels are also subject to alternative splicing, with isoforms differing primarily at their N-terminal domains. Previous work has shown that there exist at least two isoforms of Slack channels, Slack-A and Slack-B, with the B isoform having a longer cytoplasmic N-terminal domain. Distinct Slick and Slack isoforms are capable of assembling as heterotetramers with different biophysical properties and regulation. Moreover, these KNa isoforms have been shown to express in distinct brain regions. Cell-type and neuronal subcompartment specific expression has, however, not been explored. We have now used cell-type specific whole brain open datasets to identify brain regions and cell types of interest, and immunohistochemistry to confirm spatial cell type specific isoform expression and hybrid channel expression. Unlike what has been observed in primary neuronal cortical cell cultures, mature cortical excitatory neurons have cell type, and sub-compartment specific expression of Slack isoforms. Slack-B isoforms are concentrated at the axon initial segment of cortical excitatory neurons, while Slack-A isoforms are broadly expressed in the same cell type. Moreover, Slack and Slick are differentially expressed across cell types of cerebellum. Subcompartment recruitment of Slack channel isoforms suggests that isoforms may play different roles in fine tuning neuronal excitability and neuronal firing, as well as regulation of local mRNA translation.

**Disclosures: R.A. Aponte Rivera:** None. **J. Wu:** None. **L.K. Kaczmarek:** None.

**Poster**

**PSTR166: Other Ion Channels**

**Location:** WCC Halls A-C

**Time:** Monday, November 16, 2026, 1:00 PM - 5:00 PM

**Program #/Poster #:** PSTR166.05/G1

**Topic:** B.03. Ion Channels

**Support:** NIH Grant R15NS116630

**Title:** Dynamics of synaptic BMP signaling in response to membrane voltage changes

**Authors: *M. SULKOWSKI**;
Biol., Southern Connecticut State Univ., New Haven, CT

**Abstract:** Neural activity can be described as a pattern of transient electrical impulses. Over time, the pattern of these impulses integrate to inform more durable structural changes to the neural network. Despite considerable progress, our knowledge of the molecular cascades mediating this process remains incomplete.
Our previous work identified a novel, noncanonical form of bone morphogenetic protein (BMP) signaling that responds to changes in the activity of ionotropic glutamate receptors (iGluRs). As iGluRs are the a major driver of membrane voltage changes, we hypothesize that this form of BMP signaling could serve as an adaptor between electrical activity and cellular/molecular processes.For our present study, we utilized a repressible system to express an exogenous potassium ion channel for specific time periods of larval development, causing acute changes in membrane voltage. We measured the resulting changes in localized BMP signaling using immunofluorescence. We also present our discovery of synaptic BMP immunoreactivity in mammalian brain tissue.

**Disclosures: M. Sulkowski:** None.

**Poster**

**PSTR166: Other Ion Channels**

**Location:** WCC Halls A-C

**Time:** Monday, November 16, 2026, 1:00 PM - 5:00 PM

**Program #/Poster #:** PSTR166.06/G2

**Topic:** B.03. Ion Channels

**Support:** NIH Grant R01MH112739

**Title:** Cell type-specific expression of voltage-gated ion channels in the mouse mammillary bodies

**Authors: *K. SPRINGER**[1], F. C. DRIVER[2], X. WANG[4], W. F. FLYNN[5], P. ROBSON[4], H. SOH[2], A. TZINGOUNIS[2], A. C. JACKSON[3];
[2]Physiol. and Neurobio., [1]Univ. of Connecticut, Storrs, CT; [3]Physiol. and Neurobio., Univ. of Connecticut, Storrs Mansfield, CT; [5]Single Cell Biol., [4]The Jackson Lab., Farmington, CT

**Abstract:** The mammillary bodies (MB) are a hypothalamic subregion and a node in the Papez circuit, a brain-wide circuit associated with encoding both spatial and episodic memory in mammals. Despite mounting evidence suggesting that this structure is a key component in these functions, very little is known about the cell type composition, gene expression and intrinsic properties of MB neurons, and how these properties contribute to their function within the Papez circuit. Our single cell sequencing of the MB revealed its transcriptomic and spatial organization, which consists of subpopulations of glutamatergic neurons defined by unique suites of neurochemical markers. Furthermore, MB subpopulations differentially express transcripts encoding specific voltage-gated ion channels. We found that voltage-gated sodium (Nav) and

potassium (Kv) channel family members, as well as hyperpolarization-activated cyclic nucleotide-gated (HCN) channels, are differentially expressed among neuronal subpopulations and anatomically-distinct subnuclei. Given that mutations in several of the channels within these families are strongly associated with neurodevelopmental disorders (NDDs), characterized by deficits in learning and memory, we hypothesize that these ion channels play a critical role in the function of MB neurons, and their dysfunction in disease states. Using fluorescence *in situ* hybridization (FISH) and focusing on the channels most frequently mutated in neurodevelopmental disorders, SCN1A, KCNQ2, KCNQ3 and HCN1, we found that mRNA for these channels show differential patterns of enrichment in specific MB subnuclei. Due to the differences in ion channel expression patterns, we also investigated the firing properties of neurons within MB subnuclei using slice electrophysiology. To this end, we asked if the transcriptional differences between lateral mamillary (LM) and median mammillary (MnM) neurons may be reflected in their intrinsic membrane properties. Recordings from these neurons revealed that MnM neurons fire repetitively with a lower threshold, while LM neurons have a higher threshold to fire, but burst and rapidly adapt. Taken together, these data show that MB neurons are composed of multiple distinct subpopulations, with unique patterns of voltage-gated ion channel expression, which in turn contribute to differences in their intrinsic firing properties.

**Disclosures: K. Springer:** None. **F.C. Driver:** None. **X. Wang:** None. **W.F. Flynn:** None. **P. Robson:** None. **H. Soh:** None. **A. Tzingounis:** None. **A.C. Jackson:** None.

**Poster**

**PSTR166: Other Ion Channels**

**Location:** WCC Halls A-C

**Time:** Monday, November 16, 2026, 1:00 PM - 5:00 PM

**Program #/Poster #:** PSTR166.07/G3

**Topic:** B.03. Ion Channels

**Support:** SECITHI grant CBF-2025-1-462 to ES
VIEP-BUAP grant 00758-PV/2026 to ES

**Title:** MINOCYCLINE AND DOXYCYCLINE MODULATE ACID SENSING ION CHANNEL CURRENTS

**Authors: L. CABA**[1], B. PAIZ-CANDIA[2], R. FELIX[3], *E. SOTO[4];
[1]Instituo de Fisiología, Benemérita Univ. Autónoma de Puebla, Puebla, Mexico; [2]Facultad de Ciencias Químicas, Benemerita Univ. Autonoma de Puebla, Puebla, Mexico; [3]Cell Biol., Cinvestav, Mexico City, Mexico; [4]Inst. of Physiol., Benemerita Univ. Autonoma De Puebla, Puebla, Mexico

**Abstract:** Acid Sensing Ion Channels (ASICs) are proton-activated $Na^+$ channels activated by pH widely expressed in neuronal and non-neuronal cells, where they are involved in multiple physiological and pathological processes. Minocycline (Min) and doxycycline (Dox) are second-generation tetracyclines (Ts) with neuroprotective properties in processes in which ASICs have

been implicated, such as neurodegeneration, ischemia, nociception, and inflammation. This led us to propose ASICs as potential targets of these Ts. Whole-cell voltage-clamp recordings of ASIC currents ($I_{ASIC}$) expressed in CHO (Chinese Hamster Ovary) cells were performed in control and after drug application (statistical paired T-test were applied to determine significance ($p < 0.05$)). Both Ts: Min and Dox (in μM concentration) inhibit the peak amplitude ($I_{peak}$) (10-20%; n>=6) of the ASIC 1a currents. In addition, Dox 1 mM decreases (~30%) the sustained component ($I_{sus}$) and the desensitization time constant ($T_{des}$). In ASIC 3 currents, Min (30 nM - 1 mM) enhance the $I_{peak}$ (~10%, n>=4) and Dox (0.03 - 1 mM) increases the $I_{sus}$ (~30 - 200 %) and the $T_{des}$ (~15 - 40 %; n>=5). In the ASIC 1b currents, Min 100 nM enhances the $I_{peak}$ (~25%), Min 1 mM) enhances the $I_{peak}$, $I_{sus}$ and the $T_{des}$ (100, 90 and 30 %, respectively; n=5). Dox increases the $I_{sus}$ and slows the $T_{des}$, at 100 nM it increases $I_{peak}$ (~10%) and at 0.1, 0.3 and 1mM it decreases $I_{peak}$ (~30%). Molecular docking identified the “acid pocket” as a putative common binding site for both Ts in the open and desensitized chicken ASIC1a channel (cASIC1a) (E220, D238, D350; adding D408 in the open state). In the resting state of cASIC1a, Dox binds with de acid pocket, while Min binds between the finger and thumb domain. In the open state, Min binds to the central vestibule region (E412). These findings show that Ts modulate ASIC activity and may contribute to the neuroprotective actions of Min and Dox. Moreover, they highlight Ts as starting points for the development of new molecules with improved affinity, specificity, and selectivity toward ASIC subunits, potentially expanding the therapeutic options for neuroprotection.

**Disclosures: L. Caba:** None. **B. Paiz-Candia:** None. **R. Felix:** None. **E. Soto:** None.

**Poster**

**PSTR166: Other Ion Channels**

**Location:** WCC Halls A-C

**Time:** Monday, November 16, 2026, 1:00 PM - 5:00 PM

**Program #/Poster #:** PSTR166.08/G4

**Topic:** B.03. Ion Channels

**Support:** CalciGenix LLC

**Title:** The Slow Afterhyperpolarization Modulates Spike Timing Reliability in CA1 Pyramidal Neurons

**Authors: *I. MORLEY**[1], B. NATWORA[4], D. SAFARINI[5], F. M. MULLER[2], J. R. MOYER, JR.[3];
[2]Departments of Psychological and Brain Sci., [3]Psychological and Brain Sci., [1]Univ. of Wisconsin-Milwaukee Grad. Training Program in Neurosci., Milwaukee, WI; [4]Psychological and Brain Sci., [5]Departments of Psychological and Brain Sci., Univ. of Wisconsin-Milwaukee Grad. Training Program In Neurosci., Milwaukee, WI

**Abstract:** Neurons transfer information through two axes: the firing rate and the precise timing of action potentials. While the calcium activated potassium currents that mediate the slow

afterhyperpolarization (sAHP) have been shown to modulate the firing rate of CA1 pyramidal neurons, the contribution of the sAHP to spike timing reliability has not been directly investigated. To investigate whether the sAHP modulates spike timing reliability, visually guided whole-cell recordings were performed on CA1 pyramidal neurons obtained from 400 μm hippocampal slices from male F344 rats (n = 28 cells, PND 65-95). After baseline electrophysiological properties were recorded (input resistance, threshold, SAG), each neuron was presented with five trials of a 1s depolarizing current injection ranging from 50 to 450 pA. For each ordinal action potential (e.g., 1st, 2nd, 3rd, etc ⋯), spike timing jitter was defined as the mean absolute deviation of the spike latency, for that action potential, from stimulus onset across trials. To maximize action potential sample size and contribution of the sAHP, data from 450 pA are presented, though lower current injection amplitudes yielded similar results. Following a 450pA current injection, the amplitude of the sAHP (measured 1-5s after stimulus offset) is negatively correlated with the mean spike timing jitter ($r$ = -0.61, $p < 0.001$). This relationship persists even after controlling for the average instantaneous firing rate (partial $r$ = -0.54, $p$ = 0.004), indicating that independent of firing rate, the sAHP predicts timing jitter. Preliminary results suggest that the sAHP may indeed serve as a tuning mechanism not only for spike rate but also for spike timing reliability in CA1 pyramidal neurons. These data may contribute to our understanding of how the slow AHP modulates individual neuronal and network function.

**Disclosures: I. Morley:** None. **B. Natwora:** None. **D. Safarini:** None. **F.M. Muller:** None. **J.R. Moyer, Jr.:** None.

**Poster**

**PSTR166: Other Ion Channels**

**Location:** WCC Halls A-C

**Time:** Monday, November 16, 2026, 1:00 PM - 5:00 PM

**Program #/Poster #:** PSTR166.09/H1

**Topic:** B.03. Ion Channels

**Support:** ZIACL090033
ZIACL090034
ZIACL090035

**Title:** Ligand specific control of TRPV1 pore dilation and cation permeation by RTX and capsaicin

**Authors:** Y. LIU[1], Y. LEE[1], S. A. HASSAN[1], D. E. HURT[1], M. G. DUNKELBERG[2], A. J. MANNES[4], M. R. SAPIO[2], ***M. J. IADAROLA**[3,2];
[1]Bioinformatics and Computat. Biosci. Br., NIH, NIAID, Bethesda, MD; [2]Perioperative Med., [3]NIH Clin. Ctr., Bethesda, MD; [4]Perioperative Med., NIH, Clin. Ctr., Bethesda, MD

**Abstract:** TRPV1 (transient receptor potential vanilloid 1) is a non-selective cation channel and an important target for analgesic drug development. TRPV1 activation can be triggered by diverse stimuli, including elevated temperature, low pH, and agonist ligands. Resiniferatoxin

(RTX) and capsaicin are two major TRPV1 agonists under investigation for pain treatment. Strong or prolonged TRPV1 activation induces excessive $Ca^{2+}$ influx, which can disrupt membrane integrity and ultimately inactivate or ablate nociceptive nerve axon, terminals or the neuron itself. Previous studies have shown that RTX is approximately 500-fold more potent than capsaicin, largely because of its higher binding affinity.Beyond affinity, our molecular dynamics simulations reveal that RTX induces greater TRPV1 pore dilation than capsaicin, providing a structural basis for its enhanced functional potency. To test whether this expanded pore supports increased permeation, we are evaluating a series of organic cations of different sizes to assess ligand-dependent transmembrane transport through TRPV1. Channels activated by RTX exhibited higher inward cation flux than those activated by capsaicin, supporting the role of RTX in stabilizing a more expanded and conductive pore state.Together, these findings establish a mechanistic link between ligand binding, pore expansion, and ion permeation in TRPV1. By showing that RTX promotes a larger conducting pore and enhanced cation flux, our study identifies ligand-pore allostery as an actionable design principle for TRPV1 modulation. These insights suggest that future TRPV1-targeted compounds could be optimized not only for binding affinity, but also for their ability to stabilize specific pore conformations, enabling the rational design of agonists, partial agonists, or antagonists with tunable efficacy and improved therapeutic potential.

**Disclosures: Y. Liu:** None. **Y. Lee:** None. **S.A. Hassan:** None. **D.E. Hurt:** None. **M.G. Dunkelberg:** None. **A.J. Mannes:** None. **M.R. Sapio:** None. **M.J. Iadarola:** None.

**Poster**

**PSTR166: Other Ion Channels**

**Location:** WCC Halls A-C

**Time:** Monday, November 16, 2026, 1:00 PM - 5:00 PM

**Program #/Poster #:** PSTR166.10/H2

**Topic:** B.03. Ion Channels

**Support:** NIH Grant EY028927
NIH Grant EY015128
NIH Grant EY08098
NSF Grant 2014862
Research to Prevent Blindness (New York, NY) Stein Innovation Award
Research to Prevent Blindness (New York, NY) Unrestricted Research Grant to the Department of Ophthalmology, University of Pittsburgh
Gabe Newell Unrestricted Grant to BWJ

**Title:** Life cycle of the gap junction plaque: ultrastructural analysis using TEM-based connectomics

**Authors: *C. L. SIGULINSKY**, J. R. ANDERSON, B. W. JONES;
Ophthalmology, Univ. of Pittsburgh, Pittsburgh, PA

**Abstract:** In the nervous system, gap junctions afford a powerful and dynamic alternative form of neurotransmission in the form of electrical synapses. One mechanism shown to regulate the strength of electrical transmission is the rate of assembly and disassembly of the gap junction plaque. However, much of our understanding regarding the turnover of channels within gap junction plaques has come from nonneural systems, in vitro studies and/or tagged connexin proteins, which may not recapitulate the process occurring in neural tissues. Here, we have taken advantage of the large, high-resolution, transmission electron microscopy (TEM)-based connectomics datasets of mammalian neural retina to define the nanoscale ultrastructure of neuronal gap junction plaques throughout their life cycle. Retinal Connectome 1 (RC1), derived from the retina of a healthy adult (13-month-old), light-adapted, female, Dutch Belted rabbit (Anderson et al., Molecular Vision, 2011), contains over 4800 gap junction plaques identified between retinal bipolar, amacrine, and ganglion cell neurons. Many of these plaques were found to exhibit evidence of endocytic and/or exocytic processes. Detailed analysis of over 1300 plaques revealed that intercellular gap junction channels are removed from neuronal gap junction plaques through a highly stereotyped internalization process, involving the budding of unexpectedly small vesicles with a max diameter of 150 nm. Against predictions, buds occurred predominantly from peripheral, rather than central, locations within a plaque. The observed nanoscale ultrastructure of these events indicates significant remodeling of the channels and plasma membrane within the plaque both during and after budding. Although single-bud events were observed at the majority of plaques, multi-bud events also exist, and bud internalization can occur simultaneously on opposing sides of the plaque. Internalization was documented for multiple cell classes, but appears preferentially biased. Additionally, small omega-figures, indicative of endocytic and exocytic events, were commonly observed adjacent to plaques and may indicate the addition and/or removal of unbound hemichannels. Lastly, plaques in the process of internalizing were often found adjacent to each other in the same cell, suggesting a possible diffusible signal may initiate these events. Together, these findings suggest tight regulation of channel turnover that may be unique to these neuronal connexins, presumably connexin36 and connexin45, or to this neural tissue.

**Disclosures: C.L. Sigulinsky:** None. **J.R. Anderson:** None. **B.W. Jones:** None.

**Poster**

**PSTR166: Other Ion Channels**

**Location:** WCC Halls A-C

**Time:** Monday, November 16, 2026, 1:00 PM - 5:00 PM

**Program #/Poster #:** PSTR166.11/H3

**Topic:** B.03. Ion Channels

**Title:** Electrophysiological Characterization of Human Piezo1 Channels Expressed in HEK Cells Using the SyncroPatch 384i and FLIPR Assays

**Authors:** A. DICKSON, *S. RICE, R. FINOCCHIARO, P. COCCHIARA, L. C. D. GIBSON, L. J. D. YUILL, E. PARKER, C. BROWN, L. HUTCHISON, **G. CUCINIELLO**, L.

GERRARD;
Cell. Pharmacol., Sygnature Discovery, Glasgow, United Kingdom

**Abstract:** The Piezo family comprises mechanically activated, non-selective cation ion channels that convert physical forces into electrochemical signals. Piezo1 is a widely expressed trimeric membrane protein activated by membrane tension induced by shear stress, stretch, and cell swelling. Channel activation results in rapid cation influx, particularly $Ca^{2+}$, linking mechanical inputs to intracellular signalling pathways. Piezo1 is increasingly recognised for its role in mechanosensitive signalling within the nervous system. It is expressed in neuronal and glial populations, where it contributes to $Ca^{2+}$-dependent signalling. Notably, Piezo1-mediated mechanosensing in astrocytes regulates calcium dynamics, ATP release, and processes linked to neurogenesis and synaptic function, while also contributing to neurovascular coupling and signalling in cerebral endothelial cells. Despite its biological importance, the pharmacology of Piezo1 remains limited. The agonist Yoda1 is widely used to activate Piezo1 by slowing inactivation and stabilising the open state, enabling reproducible channel activation in the presence or absence of mechanical stimuli, whereas compounds such as gadolinium ($GdCl_3$) are commonly used as non-selective inhibitors of mechanosensitive channels, including Piezo1. The lack of selective modulators limits both mechanistic studies and therapeutic exploration, highlighting the need for robust assay platforms to support drug discovery. We established recombinant HEK cell lines expressing human Piezo1 and developed protocols compatible with 384-well automated voltage-clamp electrophysiology. Piezo1 currents were reproducibly evoked by both shear stress-based mechanostimulation and Yoda1 application. These currents displayed characteristic inactivation behaviour and were consistently inhibited by $GdCl_3$, confirming reliable detection of Piezo1-dependent activity. In parallel, FLIPR-based calcium flux assays were implemented as an orthogonal, high-throughput approach to assess Piezo1 function. Yoda1-induced $Ca^{2+}$ influx signals were readily detected and inhibited by $GdCl_3$, supporting the use of fluorescence-based assays for compound screening. Together, these results demonstrate the successful development of complementary electrophysiology and calcium flux assay platforms for the study of Piezo1. This combined approach enables detailed functional characterisation alongside scalable screening, providing a strong foundation for the identification and evaluation of novel Piezo1 modulators and supporting further investigation into its roles in both physiological and pathological contexts.

**Disclosures: A. Dickson:** None. **S. Rice:** None. **R. Finocchiaro:** None. **P. Cocchiara:** None. **L.C.D. Gibson:** None. **L.J.D. Yuill:** None. **E. Parker:** None. **C. Brown:** None. **L. Hutchison:** None. **G. Cuciniello:** None. **L. Gerrard:** None.

**Poster**

**PSTR166: Other Ion Channels**

**Location:** WCC Halls A-C

**Time:** Monday, November 16, 2026, 1:00 PM - 5:00 PM

**Program #/Poster #:** PSTR166.12/H4

**Topic:** B.03. Ion Channels

**Support:** NCBRI City St George's University London Small Grant
NCBRI Staff Development Fund

**Title:** Functional PIEZO1 in hippocampal pyramidal neurons

**Authors:** A. BHAVNANI[1], S. SYLANTYEV[2], K. TÖRÖK[3], D. A. RUSAKOV[4], ***O. KOPACH**[5,6];
[1]City St George's Univ. of London, London, United Kingdom; [2]Univ. of Aberdeen, Aberdeen, United Kingdom; [3]City St George's Univ. of London, London, United Kingdom; [4]UCL Inst. of Neurol., London, United Kingdom; [5]City St George's Univ. of London, London, United Kingdom; [6]Queen Square Inst. of Neurology, Univ. Col. London, London, United Kingdom

**Abstract:** PIEZO1 is a mechanosensitive, non-selective ion channel increasingly implicated in central nervous system physiology and pathology; however, the channel expression and function in brain neurons remain debatable. Here, we combine electrophysiology and imaging approaches, including a genetically encoded, PIEZO1-specific optical sensor, GenEPi, expressed in rodent hippocampal tissue, to demonstrate PIEZO1 function in pyramidal neurons. Two-photon imaging confirmed sensor-mediated responses in pyramidal CA1 and CA3 pyramidal neurons following mechanical and pharmacological stimulation with a selective PIEZO1 agonist. Outside-out and nucleated patch-clamp recordings confirmed functional PIEZO1 activity in CA3 and CA1 neurons, while synaptic recordings revealed a role for PIEZO1 in CA3-CA1 synaptic transmission. Overall, our findings provide direct evidence for a functional PIEZO1 channel in brain neurons and establish its contribution to hippocampal synaptic activity.

**Disclosures: A. Bhavnani:** None. **S. Sylantyev:** None. **K. Török:** None. **D.A. Rusakov:** None. **O. Kopach:** None.

**Poster**

**PSTR166: Other Ion Channels**

**Location:** WCC Halls A-C

**Time:** Monday, November 16, 2026, 1:00 PM - 5:00 PM

**Program #/Poster #:** PSTR166.13/H5

**Topic:** B.03. Ion Channels

**Support:** NIH Grant GM163799
NIH Grant GM140130

**Title:** Multimodal Sensory Neurons in Fly Larvae

**Authors: *L. NI**, H. BAI, T. VADEN;
Sch. of Neurosci., Virginia Tech., Blacksburg, VA

**Abstract:** Animals must continuously detect and respond to diverse and dynamically changing environmental stimuli to survive. This process relies on specialized sensory neurons. However, the molecular and cellular mechanisms by which sensory neurons detect and integrate multiple

sensory modalities remain incompletely understood. Our recent work demonstrates that thermosensory neurons in *Drosophila* larvae possess multimodal sensory functions. In addition to detecting temperature changes, these neurons respond to other environmental stimuli, including changes in tonicity and moisture. We further identified the molecular mechanisms underlying these sensory responses. Together, these findings reveal how individual sensory neurons integrate multiple environmental cues at the molecular and cellular levels, providing insight into how animals sense and adapt to complex environmental conditions.

**Disclosures: L. Ni:** None. **H. Bai:** None. **T. Vaden:** None.

**Poster**

**PSTR166: Other Ion Channels**

**Location:** WCC Halls A-C

**Time:** Monday, November 16, 2026, 1:00 PM - 5:00 PM

**Program #/Poster #:** PSTR166.14/H6

**Topic:** B.03. Ion Channels

**Support:** NIH Grant NS139648

**Title:** Identifying the Thermosensory Structural Mechanisms of GR28B.D in fruit flies

**Authors: *A. HUDA**[1], L. NI[2];
[1]Sch. of Neurosci., Virginia Tech. Neurosci. PhD Program, Blacksburg, VA; [2]Sch. of Neurosci., Virginia Tech., Blacksburg, VA

**Abstract:** Temperature significantly influences physiological processes and behaviors, impacting chemical reactions, biomolecule activity, and species distribution. Temperature detection requires molecular mechanisms that transduce thermal stimuli into cellular signals, yet how specific receptor domains contribute to this process remains poorly understood. In *Drosophila melanogaster*, aristal heating cells rely on GR28B.D, a gustatory receptor (GR), to drive avoidance of warmth above room temperature. Among the five splice variants encoded by the *Gr28b* gene, only GR28B.D responds to temperature, suggesting that its unique first exon, predicted to encode transmembrane domains (TMs) 1-4, harbors the thermosensory domain. We hypothesize that one or more domains within TMs 1-4 of GR28B.D are necessary and sufficient to confer warmth sensation. To test this, we generated chimeric receptors by swapping the individual structural elements within the first exon of *Gr28b.d* with that of a thermally insensitive isoform. The thermosensory function of each chimeric protein was assessed using two behavioral assays and electrophysiological recordings. Preliminary data indicate that exon 1 of *Gr28b.d* is required for warmth-evoked responses and that individual domain substitutions differentially impact thermosensory output. These results begin to define the structural determinants of GR28B.D-mediated thermosensation and offer insight into how an invertebrate chemoreceptor family has been co-opted for temperature detection.

**Disclosures: A. Huda:** None. **L. Ni:** None.

**Poster**

**PSTR167: Presynaptic Structure, Organization, and Function**

**Location:** WCC Halls A-C

**Time:** Monday, November 16, 2026, 1:00 PM - 5:00 PM

**Program #/Poster #:** PSTR167.01/H7

**Topic:** B.04. Synaptic Transmission

**Title:** Ultrastructural alterations in some brain areas after pre- and early postnatal exposure of arsenic

**Authors: *T. BIKASHVILI**[1,2], M. MIKADZE[1];
[1]Neurotoxicology, Ivane Beritashvili Ctr. of Exptl. Biomedicine, Tbilisi, Georgia; [2]New Vision Univ., Tbilisi, Georgia

**Abstract:** Chronical exposure to arsenic (As) still stays problematic to many populations and the mechanisms of action is the main focus of study since they are crucial to the advancement of treating arsenic toxicity. The main goal of this research was to study the effect of As compounds on brain ultrastructural changes in rat offspring which got this toxicant via their parents during pre and early postnatal development. Offspring of Wistar rats which received arsenic at a concentration of 0; 35ppm, 70 ppm were used. Statistically significant decrease the number of neurons was observed in prefrontal and motor cortex. Electron microscopic study showed changes not only in neurons of the prefrontal and motor cortex, but also in neurons in areas of the hippocampus. Swollen mitochondria with partially degraded cristae, some with damage to the outer mitochondrial membrane, along with pathologically dilated RER components and/or focal or peripheral chromatolysis was observed in many neurons. The structures of some dendritic stems were also deranged: some contained few or no microtubules, while others were swollen and yet others contained altered mitochondria, vacuoles, or inclusions consisting of membrane structures. Cells showed a significant reduction in the number of synaptic vesicles. Along with presynaptic terminals, clear changes also occurred in the postsynaptic regions. As all damage in neurons exclusively affected the structure of cytoplasmic organelles, the nucleus remaining intact, we can assume that neuronal necrosis developed in the studied areas. In summary, this study identifies neurons damage as an apoptosis-necrosis continuum, marked by mitochondrial destruction while the cell nucleus appears intact. This data is important for future research, as it shifts scientific attention from superficial “cell counts” to the nuanced deterioration of internal cellular health.

**Disclosures: T. Bikashvili:** None. **M. Mikadze:** None.

**Poster**

**PSTR167: Presynaptic Structure, Organization, and Function**

**Location:** WCC Halls A-C

**Time:** Monday, November 16, 2026, 1:00 PM - 5:00 PM

**Program #/Poster #:** PSTR167.02/H8

**Topic:** B.04. Synaptic Transmission

**Support:** NIH grant DC01919 to LKK

**Title:** Synaptic activity regulates Tank Binding Kinase 1 to couple/uncouple Kv3.3 channels from the presynaptic actin cytoskeleton

**Authors:** Y. ZHANG[1], S. SUBRAMANIAN[2], Y. ZARAPINA[5], Q. WANG[5], E. A. JONAS[3], Y. LIU[4], ***L. K. KACZMAREK**[2];
[1]Pharmacol., [2]Yale Univ. Sch. Med., New Haven, CT; [3]Yale Univ. Sch. Med., Hamden, CT; [4]Yale Univ. Sch. Med., West HAVEN, CT; [5]Yale Univ., New Haven, CT

**Abstract:** The voltage-gated potassium channel Kv3.3 is highly expressed in principal neurons of the medial nucleus of the trapezoid body (MNTB). At active zones, Kv3.3 forms a complex with Hax-1 and actin-nucleating proteins to establish a dense F-actin cytoskeleton that regulates neurotransmitter release. Mutations in Kv3.3 disrupt this actin-nucleating capability, inhibiting endocytosis, vesicle mobilization, and synaptic transmission during repetitive firing. We have now found that, rather than simply acting as a scaffold for actin nucleation, the link between Kv3.3 and the cytoskeleton is dynamically regulated during repetitive stimulation. The binding of Kv3.3 to Hax-1 requires phosphorylation by Tank-Binding Kinase 1 (TBK1), an enzyme that is stimulated by activation of Kv3.3. We first carried out a phospho-proteomic analysis of Kv3.3 expressing cells in the presence and absence of a TBK1 inhibitor and identified three candidate TBK1 phosphorylation sites on Kv3.4. In contrast, no TBK1 sites were found on Hax-1. We next assessed whether synaptic stimulation alters TBK1 activity in the MNTB using immunostaining, western blotting and 3D-STED imaging. Presynaptic stimulation produced a decrease in TBK1 activity, dissociation of the Kv3.3-Hax-1 complex, and depolymerization of F-actin at active zones. This decrease in TBK1 activity was reversed by the phosphatase inhibitor okadaic acid. In contrast, TBK1 activity was markedly elevated during the period of recovery (endocytosis), 30 to 60 seconds after stimulation. This stimulation of TBK1 activity in the presynaptic terminals after the end of stimulation was abolished in Kv3.3$^{-/-}$ mice, confirming the role of Kv3.3 in regulating TBK1 activity. Together, our findings suggest that synaptic stimulation initially triggers a phosphatase that de-activates TBK1, disrupting the link between Kv3.3 and Hax-1 during high-frequency exocytosis. Subsequent endocytosis then requires TBK1-dependent reassembly of the Kv3.3-Hax-1-Arp2/3 complex and re-polymerization of the local actin network. Because the MNTB is critical for central auditory processing, regulating TBK1 activity may represent a novel therapeutic target for auditory processing disorders.

**Disclosures: Y. Zhang:** None. **S. Subramanian:** None. **Y. Zarapina:** None. **Q. Wang:** None. **E.A. Jonas:** None. **Y. Liu:** None. **L.K. Kaczmarek:** None.

**Poster**

**PSTR167: Presynaptic Structure, Organization, and Function**

**Location:** WCC Halls A-C

**Time:** Monday, November 16, 2026, 1:00 PM - 5:00 PM

**Program #/Poster #:** PSTR167.03/I1

**Topic:** B.04. Synaptic Transmission

**Support:** NIH Grant 5R01NS131557-03
V-SMART Fellowship
Cornelius Vanderbilt Scholarship
Immersion Vanderbilt Funding

**Title:** Palmitoyl protein thioesterase-1 (Ppt1) regulates synaptic transmission at the Drosophila neuromuscular junction

**Authors: *V. TOSCANO PASOS**[1,2], S. N. LEAHY[3,2], K. S. BROADIE[1,2];
[1]Program in Neurosci., [2]Biol. Sci., [3]Vanderbilt Univ., Nashville, TN

**Abstract:** Protein palmitoylation is the post-translational modification of covalent attachment of a palmitoyl acyl group to a cysteine residue for the purpose of protein trafficking and membrane association. The thioester bond is reversibly cleaved by palmitoyl protein thioesterase-1 (PPT1). Human *PPT1* mutations cause infantile neuronal ceroid lipofuscinosis (INCL), a fatal condition in infants and toddlers that causes motor deficits, seizures and neurodegeneration. Based on these symptoms, we hypothesized a requirement for PPT1 and protein de-palmitoylation in proper maintenance of synaptic transmission, as a key basis for neuronal viability in the nervous system. Palmitoylated synaptic proteins are involved in synapse formation (e.g. PSD-95), function (e.g. SNAP-25), and plasticity (e.g. NMDA receptors) in mechanisms regulated by palmitoylation cycling. However, the role of PPT1 and de-palmitoylation in synaptic transmission is still poorly understood. Our strategy is to employ the powerful *Drosophila* genetic system and glutamatergic neuromuscular junction (NMJ) in functional analyses of *Ppt1* in synaptic transmission. With two-electrode voltage-clamp (TEVC) recordings, we find *Ppt1* homozygous point mutants, and mutants over a *Ppt1* deficiency, exhibit a highly significant decrease in synaptic transmission strength ($p<0.001$). Ubiquitous and neuronal *Ppt1* RNAi knockdowns replicate mutant phenotype, confirming the result and demonstrating the effective knockdown. Muscle-specific *Ppt1* RNAi causes no phenotype, indicating that deficits are neuron-specific and due to a presynaptic impairment. Mutants demonstrate highly significantly decreases in synaptic vesicle (SV) loading ($p<0.001$) and unloading ($p<0.001$) of FM 1-43 dye in live imaging, revealing impaired SV cycling. Mass spectrometry of palmitoylated proteins reveals 23 neuronal proteins with increased palmitoylation in *Ppt1* mutants compared to matched controls, and >140 synaptic proteins with decreased expression. We found active zone Bruchpilot (Brp) is palmitoylated at three sites (C371, C984, C997). Quantitative proteomic analysis and confocal imaging demonstrates a highly significant decrease in Brp expression ($p<0.001$), with fewer and smaller active zones. We conclude *Ppt1* function positively regulates presynaptic active zone Brp (mammalian ELKS/CAST) to maintain neurotransmission strength. This new *Drosophila* INCL disease model enables full dissection of the *Ppt1* de-palmitoylation regulation of synaptic function.

**Disclosures: V. Toscano Pasos:** None. **S.N. Leahy:** None. **K.S. Broadie:** None.

**Poster**

**PSTR167: Presynaptic Structure, Organization, and Function**

**Location:** WCC Halls A-C

**Time:** Monday, November 16, 2026, 1:00 PM - 5:00 PM

**Program #/Poster #:** PSTR167.04/I2

**Topic:** B.04. Synaptic Transmission

**Support:** NIH R01AG051470
the Food Science Institution Foundation/Ryoushoku-kenkyukai

**Title:** Single active-zone level analysis reveals unit structure, synapse-organizer alignment, and higher concentration at SNARE protein-dense domains at mouse neuromuscular junctions

**Authors: *H. NISHIMUNE**[1], Y. BADAWI[2], N. H. TOMIOKA[3], S. SENO[4];
[1]Physical Med. and Rehabil., Univ. of Missouri, Sch. of Med., Columbia, MO; [2]Pharmacology, Toxicology & Therapeut., Univ. of Kansas Med. Ctr., Kansas City, KS; [3]Neurobio. of Aging, Tokyo Metropolitan Inst. for Geriatrics and Gerontology, Itabashi-Ku, Tokyo, Japan; [4]Bioinformatic Engin., The Univ. of Osaka, Suita, Osaka, Japan

**Abstract:** Neuromuscular junctions are large synapses with several hundred discretely distributed active zones essential for synaptic vesicle release. After a single action potential, it has been estimated that only about 20% of these active zones participate in transmitter release; however, the detailed distribution patterns of active zone proteins and vesicle fusion proteins underlying the selective use of only a fraction of the available active zones have yet to be revealed. First, this study used super-resolution microscopy to reveal the molecular distribution pattern that enabled trans-synaptic nanocolumn-like alignment of presynaptic active zones with postsynaptic junctional folds through the preferential localization of laminin β2 secreted by muscles. Second, a single active zone-level analysis revealed configurations and distribution patterns of active zone-specific proteins, including bassoon, ELKS, Munc13-1, 2, RIM2, RIM-BP1, piccolo, and P/Q-type VGCC, at mouse neuromuscular junctions. Most active zones contained combinations of these active zone-specific proteins, suggesting that the protein composition may not be the mechanism for the selective use of only some active zone regions for transmission. Third, when we focused on SNARE proteins, necessary for synaptic transmission, we revealed high-density subsynaptic areas within each neuromuscular junction. The high-density subsynaptic areas of presynaptic membrane-associated SNAREs, a synaptic vesicle-associated SNARE with the calcium sensor synaptotagmin, showed about 50% colocalization. These SNARE colocalization hotspots were surrounded by P/Q-type VGCCs and had a higher density of active zones. These distribution patterns were independently reconfirmed using computational image analysis. In summary, neuromuscular junctions have subsynaptic areas with higher-density active zones and vesicle-fusion proteins, and we hypothesize that this may contribute to the selective use of these areas for synaptic transmission.

**Disclosures: H. Nishimune:** None. **Y. Badawi:** None. **N.H. Tomioka:** None. **S. Seno:** None.

**Poster**

**PSTR167: Presynaptic Structure, Organization, and Function**

**Location:** WCC Halls A-C

**Time:** Monday, November 16, 2026, 1:00 PM - 5:00 PM

**Program #/Poster #:** PSTR167.05/I3

**Topic:** B.04. Synaptic Transmission

**Support:** Freedom Together Foundation

**Title:** Characterizing Active Zone Development, Maintenance, and Turnover at Adult Neuromuscular Junctions During Aging

**Authors: *J. M. SIDISKY**, J. T. LITTLETON;
MIT, Cambridge, MA

**Abstract:** Neurotransmitter release occurs at contact sites where a presynaptic electron-dense cytomatrix termed the active zone (AZ) aligns with postsynaptic receptor fields. Following synapse maturation, it is unclear if AZs reach a set output level that is maintained over the life of the animal, or if AZs undergo turnover during aging. At larval NMJs, the AZ population formed by a single motoneuron has a heterogeneous distribution of release probability that increases over a multi-day growth period as AZs accumulate key proteins. In the current study, we assayed if the same diversity in AZ strength exists at adult NMJs across the lifecycle. Although the abundance of the presynaptic AZ proteins Cac and BRP displayed a mild increase over time, adult AZ populations maintained a heterogenous distribution of AZ protein abundance across the lifecycle, without a change in AZ density. Similar to larvae, *Rab3* mutants disrupted adult AZ development and composition with ~50% of AZs opposed to PSDs lacking BRP and Cac. This fraction did not increase during aging in *Rab3* mutants, indicating AZs are unlikely to be continuously added in adulthood as they are in larvae. *Syd1* and *Liprin-α* adult mutants displayed a similar AZ phenotype to *Rab3* mutants with many PSDs unopposed to mature AZs. This contrasts with their role in larvae where they are more involved in establishing overall AZ number. To characterize AZ protein turnover at adult NMJs, the mEosEM photoconvertible tag was attached to BRP and postsynaptic GluRs. Animals expressing photoconverted GluRIIE$^{mEOSEM}$ and BRP$^{mEOSEM}$ revealed a slow decay of both proteins and no evidence of new AZ or PSD formation later in adulthood. These studies provide insights into how AZ maturation and maintenance is regulated over the lifetime of an aging neuron.

**Disclosures: J.M. Sidisky:** None. **J.T. Littleton:** None.

**Poster**

**PSTR167: Presynaptic Structure, Organization, and Function**

**Location:** WCC Halls A-C

**Time:** Monday, November 16, 2026, 1:00 PM - 5:00 PM

**Program #/Poster #:** PSTR167.06/I4

**Topic:** B.04. Synaptic Transmission

**Support:** NIH SC1GM136609

**Title:** Valproate Exposure Impacts Mitochondrial Function, Synaptic Function, and Behavior in Drosophila

**Authors: M. MARCHIDAN**[1], N. DE SILVA[2], A. BIEGLARIAN[2], J. QIAN[2], A. TURAEVA[2], F. ROMERO[2], F. FERREIRA[3], *P. PEIXOTO[2,1];
[1]CUNY Grad. Ctr., New York, NY; [2]CUNY - Baruch Col., New York, NY; [3]Oswaldo Cruz Inst., Rio de Janeiro, Brazil

**Abstract:** Valproate (VPA) is a widely used mood stabilizer and anti-epileptic medication that has been well-established as a human teratogen. Prenatal exposure to VPA has been linked to neurodevelopmental disorders, such as autism spectrum disorder (ASD). The biological mechanism of its teratogenic effect still needs to be elucidated. Drosophila melanogaster provides a tractable model to investigate VPA's synaptic, metabolic, and behavioral effects. Flies were raised on media with 0, 0.5, or 1 mM VPA. Synaptic function was quantified at the larval neuromuscular junction (NMJ) via miniature excitatory junction potential (mEJP) recordings, mitochondrial membrane potential was estimated by confocal imaging of MitoTracker Deep Red in larval neuromuscular preparations, and adult behavior was evaluated using the Social Space Assay and Fly Climbing Assay. Developmental VPA exposure produced male-biased, non-monotonic effects across physiological and behavioral readouts. In males, mEJP frequency was significantly reduced in the 0.5 mM group relative to controls, whereas the 1 mM group was not significantly different from controls; mEJP amplitude was unchanged. Similar trends were observed in females but did not reach statistical significance. Recordings were obtained from 71 NMJs across all conditions. Mitochondrial membrane potential also showed a dose-dependent, non-monotonic pattern in males, whereas females showed only nonsignificant trends. Confocal images were analyzed blind to treatment condition, and 1-3 NMJs were averaged per fillet prior to analysis. Significant differences were observed in males between control and 1 mM groups and between 0.5 mM and 1 mM groups. Subsequent behavioral analyses were prioritized in males. In adults, 0.5 mM males showed reduced social spacing and impaired climbing relative to controls, whereas 1 mM males were not significantly different from controls. These findings indicate that developmental VPA exposure alters mitochondrial function, spontaneous synaptic transmission, and adult behavior in a sex- and non-linear dose-dependent manner.

**Disclosures: M. Marchidan:** None. **N. De Silva:** None. **A. Bieglarian:** None. **J. Qian:** None. **A. Turaeva:** None. **F. romero:** None. **F. Ferreira:** None. **P. Peixoto:** None.

**Poster**

**PSTR167: Presynaptic Structure, Organization, and Function**

**Location:** WCC Halls A-C

**Time:** Monday, November 16, 2026, 1:00 PM - 5:00 PM

**Program #/Poster #:** PSTR167.07/I5

**Topic:** B.04. Synaptic Transmission

**Support:** NIH MH130472
NIH MH129269

**Title:** Neurotransmitters, release sites, and targets of VTA axons in the amygdala

**Authors: *J. O'CONNELL IV**[1,2], J. PEREZ-GARZA[1], L. OSTROFF[1,3,2];
[1]Physiol. and Neurobio., [2]Inst. for the Brain and Cognitive Sci., [3]Inst. of Materials Sci., Univ. of Connecticut, Storrs Mansfield, CT

**Abstract:** Projections from the ventral tegmental area (VTA) to the basolateral complex of the amygdala are the predominant source of dopamine that regulates fear- and anxiety-related behavioral states, as well as the plasticity underlying fear conditioning and extinction learning, yet their synaptic organization within amygdala microcircuits remains poorly resolved. Although dopamine is known to function as a diffuse modulatory signal via volume release, some VTA neurons are capable of releasing GABA or glutamate in addition to or instead of dopamine, potentially supporting fast synaptic transmission. Dopaminergic axons have been shown by electron microscopy (EM) to form chemical synapses in the amygdala with both excitatory and inhibitory neurons, and both excitatory and inhibitory synapse morphologies were reported. These observations suggest that VTA inputs influence amygdala function through cell type- and transmitter-specific synaptic interactions as well as broad neuromodulation, but how these inputs are organized is unknown. Whether, for example, volume transmission of dopamine and synaptic transmission occur on the same or separate axons, which combinations of neurotransmitters are present at synapses, and whether this varies within axons or by target cell type, are all open questions. Here we examine the synaptic, molecular, and ultrastructural organization of VTA axons in the adult rat amygdala using viral tracing and ultraplex microscopy with volume EM. Highly-multiplexed immunolabeling was used to identify endogenous molecules within labeled VTA axonal boutons in the amygdala and their postsynaptic cells, allowing molecular and ultrastructural classification of synaptic contacts. Ultraplex microscopy was used to integrate molecular labeling with serial-section transmission EM, enabling reconstruction of individual VTA axons and their synaptic contacts, nonsynaptic appositions, and targeted compartments while preserving molecular information. We find that axonal boutons containing both tyrosine hydroxylase (TH) and GABA, but not glutamate transporters, form chemical synapses in the lateral amygdala, and that individual TH-positive axons have structurally diverse en passant release sites for volume and classical synaptic transmission, suggesting that dopamine axons in the amygdala may utilize different modes of transmission across segregated microdomains. Together, our data indicate that VTA inputs to the amygdala are not a uniform modulatory projection, but a molecularly diverse set of synaptic afferents that differentially interface with local inhibitory and excitatory microcircuits within BLA.

**Disclosures: J. O'Connell IV:** None. **J. Perez-Garza:** None. **L. Ostroff:** None.

**Poster**

**PSTR167: Presynaptic Structure, Organization, and Function**

**Location:** WCC Halls A-C

**Time:** Monday, November 16, 2026, 1:00 PM - 5:00 PM

**Program #/Poster #:** PSTR167.08/I6

**Topic:** B.04. Synaptic Transmission

**Support:** MH129269

**Title:** Reconstruction and analysis of axons identified by higly-multiplexed molecular labeling in an EM volume

**Authors: *J. PEREZ-GARZA**[1], L. OSTROFF[1,2,3];
[1]Physiol. and Neurobio., [2]Inst. of Material Sci., [3]Inst. for the Brain and Cognitive Sci., Univ. of Connecticut, Storrs Mansfield, CT

**Abstract:** The synaptic organization of the brain is difficult to study with cell-type specificity because synapses can only be directly visualized by electron microscopy (EM), and methods for incorporating molecular information into EM volumes are limited. We have developed a method, ultraplex microscopy, that allows versatile multiplexing of labeling and imaging methods, including EM, across ultrathin sections. Here we have used a new ultraplex microscopy workflow to integrate highly-multiplexed, high-resolution immunofluorescence with volume EM for molecular profiling of cellular structures. We present quantitative data on more than 600 axons and their postsynaptic dendrites reconstructed from a 5000 $\mu m^3$ volume of adult rat amygdala imaged by transmission EM at 1.8 nm pixel resolution. Cyclic immunofluorescence was used to extend fluorescence imaging to more than 20 channels per section on individual sections taken at intervals from a long EM series, allowing dense molecular information to be extracted without compromising EM ultrastructure. Labeling localized endogenous molecules including neurotransmitters such as GABA and somatostatin and cell-type markers such as VGluT1, VGluT2, GABA, tyrosine hydroxylase, and calbindin to individual axons or dendrites. Connectivity parameters such as synapse size and the frequency of synapses within and between processes were quantified, revealing distinct microstructural features of individual cell types. This new approach offers insight into previously inaccessible features of cell type specific synaptic connectivity.

**Disclosures: J. Perez-Garza:** None. **L. Ostroff:** None.

**Poster**

**PSTR167: Presynaptic Structure, Organization, and Function**

**Location:** WCC Halls A-C

**Time:** Monday, November 16, 2026, 1:00 PM - 5:00 PM

**Program #/Poster #:** PSTR167.09/I7

**Topic:** B.04. Synaptic Transmission

**Support:** NIH R01NS119980

**Title:** Presynaptic regulation of short-term plasticity by mitochondrial fission adapters

**Authors: *M. G. HOFNER**, P. XU, R. B. RENDEN;
Physiol. and Cell Biol., Univ. of Nevada, Reno, Reno, NV

**Abstract:** Mitochondrial dynamics are crucial for meeting the energy demands of a cell. In neurons, dysregulated mitochondrial fission is a cause of several neurodegenerative diseases, yet the underlying impairments are poorly understood. The GTPase Dynamin Related Protein 1 (DRP1) promotes mitochondrial fission by severing the outer mitochondrial membrane. DRP1 is recruited to mitochondria by membrane-bound adapter proteins Mitochondrial Fission Factor (MFF), Mitochondrial Fission 1 (FIS1), MiD49 and MiD51. Using viral-mediated knockdown of DRP1; MFF; FIS1; and both MFF /FIS1 in floxed C57 mice we evaluated the role of these proteins in presynaptic function at the calyx of Held, a well-established central synapse model that allows multiple experimental approaches, in acute brain slices form 16-18 day old mice of both sexes. Our provisory electrophysiology, electron microscopy and fluorescence confocal microscopy data suggest that DRP1 is directly involved in synaptic vesicle endocytosis, as well as mitochondrial fission. Further, we observed that presynaptic knockdown of MFF and FIS1 qualitatively recapitulates impairments in synaptic transmission due to knockdown of DRP1, but quantitatively less severe. By measuring excitatory postsynaptic currents (EPSCs) during high frequency trains of synaptic activity using whole cell voltage clamp we observed that loss of both MFF and FIS1 in the presynaptic terminal increases short-term depression, decreased the paired pulse ratio, and increased the release probability. In addition, recovery of the readily releasable pool following short-term depression was also impaired. Effects of MFF or FIS1 knockdown separately were less prominent, where MFF loss diminished the readily releasable pool and slowed refilling, and FIS1 loss specifically slowed recovery following depression. Taken together, these results improve our understanding of a multifaceted role of mitochondrial fission proteins in regulating presynaptic function during neurotransmission.

**Disclosures: M.G. Hofner:** None. **P. Xu:** None. **R.B. Renden:** None.

**Poster**

**PSTR167: Presynaptic Structure, Organization, and Function**

**Location:** WCC Halls A-C

**Time:** Monday, November 16, 2026, 1:00 PM - 5:00 PM

**Program #/Poster #:** PSTR167.10/I8

**Topic:** B.04. Synaptic Transmission

**Support:** core funding from TLL

**Title:** Two mechanisms for mobilization of reserve pool synaptic vesicles by synapsin phosphorylation

**Authors:** S.-H. SONG[1], ***G. J. AUGUSTINE**[2];
[1]Temasek Lifesciences laboratory, Singapore, Singapore; [2]Temasek Lifesciences Lab., Singapore, Singapore

**Abstract:** Synapsins cluster synaptic vesicles (SVs) within the reserve pool via liquid-liquid phase separation (LLPS) at GABAergic synapses and via oligomerization-mediated crosslinking at glutamatergic synapses (*Cell Reports* 42: 113004). We have examined how protein kinases regulate mobilization of SVs from these different types of clusters.
Phosphorylation by protein kinase A (PKA) disrupted synapsin oligomerization and altered synapsin 2a (SYN2a) clustering of purified SVs. Further, both phosphomimetic and phospho-null substitutions at the PKA phosphorylation site of SYN2a failed to rescue SV mobilization during repetitive stimulation of glutamatergic synapses of synapsin triple knockout (TKO) neurons. This indicates a role for PKA in mobilization of glutamatergic SVs from their reserve pool. In contrast, neither PKA activity nor mutation of the PKA phosphrylation site altered the LLPS behavior of SYN2a or affected the ability of SYN2a to rescue GABA release in synapsin triple knockout (TKO) neurons. Thus, PKA is not involved in SV mobilization at inhibitory synapses.
The $Ca^{2+}$/calmodulin-dependent protein kinase II (CaMKII) seems to be involved in SV mobilization at inhibitory synapses: a CaMKII phospho-null mutant of SYN2a restored basal GABA release, while its phosphomimetic mutant did not. Consistent with this, CaMKII phosphorylation prevented SYN2a from undergoing LLPS.
These findings reveal distinct, kinase-specific mechanisms that differentially control mobilization of SVs from SV clusters mediated by synapsin LLPS or by oligomerization and mobilization. Mobilization of glutamatergic SVs at excitatory synapses depends on PKA phosphorylation of SYN2a, while CaMKII-dependent phosphorylation of SYN2a regulates SV mobilization at inhibitory synapses.

**Disclosures: S. Song:** None. **G.J. Augustine:** None.

**Poster**

**PSTR167: Presynaptic Structure, Organization, and Function**

**Location:** WCC Halls A-C

**Time:** Monday, November 16, 2026, 1:00 PM - 5:00 PM

**Program #/Poster #:** PSTR167.11/J1

**Topic:** B.04. Synaptic Transmission

**Support:** NIH 1F31NS141318-01
NIH NINDS 1RO1NS112365-01A1
NSF Career IOS 1750199

**Title:** Kv2/VAP Membrane Contact Sites Regulate Presynaptic Organelle Calcium Handling and Synaptic Stamina

**Authors: *C. D. PATON**, M. B. HOPPA;
Dartmouth Col., Hanover, NH

**Abstract:** Sustained synaptic transmission requires neurons to repeatedly mobilize and fuse synaptic vesicles to release neurotransmitter, a property we refer to as synaptic stamina. Our

research has identified membrane contact sites (MCSs), a conserved structural feature in cell biology, as critical regulators of presynaptic function during repetitive stimulation. We recently showed that voltage-gated potassium channel Kv2.1 dynamically regulates uptake of calcium ($Ca^{2+}$) into the presynaptic endoplasmic reticulum (ER), independent of potassium conductance. Prior studies in heterologous cells suggest that Kv2.1 forms ER-plasma membrane (ER/PM) MCSs through interactions between its FFAT motif and VAMP-associated proteins (VAPs) in the ER membrane. To define the molecular role of VAP in axons, we used a CRISPR-based knockdown (KD) approach to acutely deplete both isoforms, VAPA and VAPB. We combined this knockdown approach with noninvasive optical indicators of synaptic vesicle exocytosis and organelle (ER and mitochondria) $Ca^{2+}$ in cultured primary rat hippocampal neurons. We found that loss of VAPA/B reduced vesicle fusion by more than 50%, disrupted Kv2.1 clustering, and impaired $Ca^{2+}$ uptake into two major intracellular $Ca^{2+}$ sinks, the ER by more than 50% and mitochondria by more than 75%. Moreover, we found that the organization of synaptic vesicles is altered. The recycling pool was decreased, and synaptic vesicles were recruited to release sites less efficiently. Together, these findings support a novel presynaptic role for VAP-mediated ER-PM contact sites in sustaining vesicle mobilization, maintaining synaptic strength, and ultimately supporting synaptic stamina during repetitive activity.

**Disclosures: C.D. Paton:** None. **M.B. Hoppa:** None.

**Poster**

**PSTR167: Presynaptic Structure, Organization, and Function**

**Location:** WCC Halls A-C

**Time:** Monday, November 16, 2026, 1:00 PM - 5:00 PM

**Program #/Poster #:** PSTR167.12/J2

**Topic:** B.04. Synaptic Transmission

**Support:** NINDS RM1NS140326

**Title:** Effects of anandamide (AEA) on GABAergic synaptic transmission in rat ventrolateral periaqueductal gray (VlPAG) in persistent inflammation

**Authors: *Y. GWAK**, S. INGRAM;
Univ. of Colorado Anschutz Med. Campus, Aurora, CO

**Abstract:** Endocannabinoids are key modulators in pain regulation of the nervous system. The two main endocannabinoids in the brain, 2-Arachidonoylglycerol (2-AG) and anandamide (AEA), are synthesized in neurons and retrogradely activate cannabinoid 1 receptors (CB1Rs) on GABAergic presynaptic terminals. We previously reported that the production of 2-AG inhibits GABAergic inhibitory postsynaptic currents (IPSCs) in the vlPAG via CB1Rs in naïve rats and in inflamed rats pretreated with Complete Freud's adjuvant (CFA). Mass spectrometry HPLC studies observed a transient increase in AEA on Day 1 post-CFA, whereas 2-AG levels increased at later timepoints post-CFA (> Day 5). However, the effects of anandamide (AEA) on GABAergic neurotransmission have not been characterized throughout CFA-induced

inflammation. The present study examined the effects of AEA on GABAergic IPSCs in rats. In naïve and CFA-treated rats, endocannabinoid activation of CB1Rs is not evident in the presence of D034 (1 μM), an inhibitor of diacyl glycerol lipase (DAGL). These results suggest that the primary endocannabinoid in the vlPAG is 2-AG. However, in the presence of multiple concentrations of URB 597 (1 and 50 nM), an inhibitor of fatty acid amide hydrolase (FAAH) to augment levels of AEA, we observed significant inhibition of GABAergic IPSCs in the vlPAG. After CFA treatment (100 μl) onto the hindpaw, both concentrations of URB 597 showed similar inhibition of GABAergic IPSCs on both day 1 and day 7. The combined inhibition of 1 nM of URB 597 was 21.56 ± 6.73 % (n=9) and 50 nM was 28.97 ± 3.21 % (n=4), and did not show significant difference. In addition, inhibition of female and male groups was 24.09 ± 2.95 % (n=8) and 23.39 ± 12.34 % (n=5), and did not show significant differecnes. It is noted that the maximal effect of URB597 inhibited GABAergic IPSCs less than the maximal effect of 2-AG (~50%). Taken together, those results suggest a differential sensitivity of 2-AG and AEA on presynaptic CB1Rs in the vlPAG under inflammatory pain conditions.

**Disclosures: Y. Gwak:** None. **S. Ingram:** None.

**Poster**

**PSTR167: Presynaptic Structure, Organization, and Function**

**Location:** WCC Halls A-C

**Time:** Monday, November 16, 2026, 1:00 PM - 5:00 PM

**Program #/Poster #:** PSTR167.13/J3

**Topic:** B.04. Synaptic Transmission

**Support:** NIH Grant R01 NS126247
NIH Grant R01NS131299-01A
VA Grant I01 BX006921
VA Grant I01 BX004938

**Title:** Loss of α2δ-2 protein function in Parvalbumin-expressing neurons drives the phenotypes of global CACNA2D2 mutant mice

**Authors: *E. JEROME**[1], A. ELLINGSON[2], A. GALLAGHER[1], E. SCHNELL[1];
[1]Anesthesiol. and Perioperative Med., [2]Neurosci. Grad. Program, Oregon Hlth. & Sci. Univ., Portland, OR

**Abstract:** Voltage gated calcium channels (VGCCs) allow for depolarization-induced calcium entry into neurons and are crucial regulators of neuronal signal transduction. The CACNA2D family of channel subunit proteins contributes to VGCC trafficking and coupling of VGCCs to downstream effector mechanisms. One of the CACNA2D isoforms, α2δ-2 (CACNA2D2), is expressed throughout the brain, and the predominant CACNA2D isoform present in parvalbumin-positive (PV+) interneurons of the hippocampus and in cerebellar Purkinje cells. Global α2δ-2 loss in both humans and mice causes a range of neurological phenotypes, including epilepsy and ataxia. To determine the selective contribution of α2δ-2 function in PV+ cells to the

behavioral and molecular phenotypes of global α2δ-2 deletion, we generated PV-cell-specific conditional α2δ-2 KO mice. PV-Cre$^{+/?}$::α2δ-2$^{fl/fl}$ mice displayed gross physical and behavioral phenotypes similar to global α2δ-2 KO mice, as evidenced by reduced body weight and rotarod performance. Some, but not all, immunohistopathological alterations observed in the global a2d2 knockout mouse, such as increased cerebellar tyrosine hydroxylase expression, were recapitulated in the PV-Cre conditional KO mouse. Together, these observations suggest that loss of α2δ-2 function in PV+ cells is a significant driver of the α2δ-2 KO phenotype. Ongoing experiments are focused on assessing the functional effects of this conditional KO in Purkinje cells, and in determining the contributions of α2δ-2 to neuronal function.

**Disclosures: E. Jerome:** None. **A. Ellingson:** None. **A. Gallagher:** None. **E. Schnell:** None.

**Poster**

**PSTR167: Presynaptic Structure, Organization, and Function**

**Location:** WCC Halls A-C

**Time:** Monday, November 16, 2026, 1:00 PM - 5:00 PM

**Program #/Poster #:** PSTR167.14/J4

**Topic:** B.04. Synaptic Transmission

**Support:** NIH Grant R01 NS126247
NIH Grant R01NS131299-01A
VA Grant I01 BX006921
VA Grant I01 BX004938

**Title:** α2δ-2 functionally couples calcium entry to presynaptic release machinery in hippocampal PV+ interneurons

**Authors:** A. ELLINGSON[1], E. JEROME[3], A. GALLAGHER[4], ***E. SCHNELL**[2];
[1]Neurosci. Grad. Program, [2]OHSU, Portland, OR; [3]Anesthesiol. & Perioperative Med., [4]Oregon Hlth. & Sci. Univ., Portland, OR

**Abstract:** Voltage gated calcium channels (VGCCs) are required for many aspects of neuronal signal transduction, including action potential-dependent synaptic transmission. VGCCs consist of several different subunits, including both pore-forming α1 channels and auxiliary modulatory subunits such as β, γ, and α2δ proteins. α2δ subunits contribute to surface and subcellular trafficking of VGCCs, and mutations in genes that encode for any of the three brain α2δ isoforms cause neuronal dysfunction. Previous studies of α2δ isoforms in genetic mouse models have been complicated by isoform compensation and the mortality of double and triple knockout mutants. However, the α2δ-2 isoform is selectively expressed in parvalbumin (PV) positive neurons throughout the hippocampus, and loss of this isoform causes epilepsy in both mice and humans. To determine how α2δ-2 loss affects PV+ interneuron function, we studied synaptic function in α2δ-2 WT and KO mice selectively expressing Channelrhodopsin2 in PV+ neurons. We found that loss of α2δ-2 significantly reduces synaptic transmission from PV+ interneurons, with optically evoked inhibitory post synaptic currents decreased from ~150pA to ~50pA at identical

light stimulation intensity. This seems to occur primarily via a reduction in the probability of release of GABA-containing vesicles, as seen in a reduced paired pulse ratio. Loss of α2δ-2 leads to a loss of nanodomain coupling between calcium entry via VGCC and presynaptic vesicle release machinery, as assessed using cell-permeable fast and slow calcium chelators. This contributes to reduced feed-forward inhibition and may underlie the epileptic phenotype observed in α2δ-2 KO mice.

**Disclosures: A. Ellingson:** None. **E. Jerome:** None. **A. Gallagher:** None. **E. Schnell:** None.

**Poster**

**PSTR167: Presynaptic Structure, Organization, and Function**

**Location:** WCC Halls A-C

**Time:** Monday, November 16, 2026, 1:00 PM - 5:00 PM

**Program #/Poster #:** PSTR167.15/J5

**Topic:** B.04. Synaptic Transmission

**Support:** NIH Grant DA035714
NIH DA057866
NIH Grant DA047924

**Title:** Mutations of Asp316, Glu322, and Asp569 of human serotonin transporter attenuate HIV-1 Tat protein-induced inhibition of serotonin transport

**Authors: *J. ZHU**[1], C.-G. ZHAN[2];
[1]Pharmacol. and Toxicology, Med. Col. of George, Augusta Univ., Augusta, GA; [2]Pharmaceut. Sci., Univ. of Kentucky, Lexington, KY

**Abstract:** The lifetime prevalence of depression in people living with HIV is twice as high as in the general population. HIV-1 Trans-Activator of Transcription (Tat) protein has a great impact on the development of HIV-1 associated depression through disrupting serotonin (5-HT) transmission. Computational modeling revealed a direct human serotonin transporter (hSERT)-Tat complex and predicted Asp319, Glu322, and Asp569 as strong hydrogen bond with Tat. Mutating any of these three residues is expected to disrupt favorable hydrogen bonds and reduce Tat's effect. This study determined the mutational effects of these hSERT residues on the basal SERT function and Tat-induced inhibition of SERT-mediated 5-HT uptake. We generated single mutants (N316A, E322A, N569A), double mutants (N316A/N569A, N316A/E332A, E322A/N569A) and triple mutant (N316A/E322A/N569A). Compared to WT hSERT, no significant alterations in either maximum velocity ($V_{max}$) or affinity ($K_m$) of [$^3$H]5-HT uptake via SERT were observed in CHO cells transfected with N316A, E322A, and N569A. However, double and triple mutants significantly reduced the $V_{max}$, suggesting that these residues have overlapping or cooperative roles in supporting normal SERT function. The Ki value (inhibition constant) of recombinant $Tat_{1-86}$ ($rTat_{1-86}$) for inhibition of SERT-mediated [$^3$H]5-HT uptake was 8.3 nM in CHO cells transfected with WT hSERT. In vitro exposure to 17.5 nM and 8.5 nM $rTat_{1-86}$ resulted in 26.7 ± 4.2% and 29.8 ± 3.0% of WT hSERT-mediated specific [$^3$H]5-HT

uptake, respectively. In contrast to WT hSERT, $rTat_{1-86}$ exposure did not produce significant inhibition of hSERT-mediated 5-HT uptake in any of the mutants examined, indicating that Tat-induced inhibition of [$^3$H]5-HT uptake was completely attenuated in the mutant transporters. Ongoing studies are investigating whether the attenuation of Tat-induced inhibition of 5-HT transport by these mutants occurs through an allosteric modulatory mechanism. These results suggest that these residues play a crucial role in Tat binding and in the functional regulation of SERT. The findings provide important mechanistic insights that may support the development of allosteric modulators as a therapeutic strategy to mitigate Tat-induced dysregulation of serotonin transmission.

**Disclosures: J. Zhu:** None. **C. Zhan:** None.

**Poster**

**PSTR167: Presynaptic Structure, Organization, and Function**

**Location:** WCC Halls A-C

**Time:** Monday, November 16, 2026, 1:00 PM - 5:00 PM

**Program #/Poster #:** PSTR167.16/J6

**Topic:** B.04. Synaptic Transmission

**Support:** R01DA047924
DA035714
DA057866

**Title:** Characterization of a third generation of allosteric modulators of the human dopamine transporter and its role in attenuating HIV-1 Transactivator of Transcription protein-mediated inhibition of dopamine transport

**Authors: *A. C. JIMENEZ**[1], O. MOUKHA-CHAFIQ[2], C. AUGELLI-SZAFRAN[3], J. ZHU[4]; [1]Dept. of Pharmacol. and Toxicology, AUGUSTA UNIVERSITY, Augusta, GA; [2]Dept. of Biochem. & Mol. Genet., Univ. of Alabama at Birmingham, Birmingham, AL; [3]2Department of Biochem. & Mol. Genet., Univ. of Alabama at Birmingham, Heersink Sch. of Med., BIRMINGHAM, AL; [4]Dept. of Pharmacol. and Toxicology, Med. Col. of George, Augusta Univ., Augusta, GA

**Abstract:** The role of the HIV-1 Transactivator of Transcription (Tat) protein in the disruption of physiological dopamine (DA) neurotransmission as an allosteric inhibitor of the dopamine transporter (DAT) has been correlated with the development of HIV-associated neurocognitive disorders (HANDs) and potentiation of drug-misuse in people living with HIV (PLWH). Our previous studies demonstrated through computational modeling and pharmacological characterization that two small molecule inhibitors, SRI-32743 and SRI-47056, bind allosterically to DAT and disrupt hydrogen bonds that are key in the DAT-Tat complex. Systemic administration of SRI-32743 and SRI-47056 attenuate the increase of DA levels in the baseline of phasic DA release and alleviate the potentiation of cocaine reward in inducible Tat transgenic mice. However, optimization of SRI-32743 and SRI-47056 is required to improve the

metabolic stability in mice and human liver microsomes. This study determines the pharmacological profile of a third generation of analogs of SRI-32743 as modulators of human DAT (hDAT). Structure-activity relationship studies of SRI-32743 and SRI-47056 yielded five novel compounds with high potency to modulate hDAT. These compounds partially inhibited [$^3$H]DA uptake ($IC_{50}$= 0.043 - 0.704 μM) but displayed less binding to the orthosteric site on hDAT, thus, showing less affinity to [$^3$H]WIN35,428 binding ($IC_{50}$ values, 0.381 - 23.2 μM) in CHO cells expressing WT hDAT. Contrary to the typical inhibitors of DAT, such as GBR12909 and cocaine, these compounds display a submaximal inhibition profile ($E_{max}$ <75%) characteristic of atypical ligands of DA reuptake. For example, a new analog, SRI-50627, allosterically modulates DAT, recombinant $Tat_{1-86}$-induced 43% inhibition of hDAT was recovered by 0.1 nM of SRI-50627 via *in vitro* exposure and SRI-50627 slowed the cocaine-induced dissociation rate of [$^3$H]WIN35,428 binding in WT hDAT relative to cocaine alone. Ongoing studies are focused on investigating the effects of SRI-50627 on physiological phasic DA release and basal locomotor activity in C57BL/6J mice. These findings suggest that this new series of compounds exhibits improved potency to modulating DAT function, with SRI-50627 emerging as a particularly promising candidate for preclinical studies aimed at preventing HIV-1 Tat-mediated disruption of dopaminergic hemostasis during HIV infection.

**Disclosures: A.C. Jimenez:** None. **O. Moukha-Chafiq:** None. **C. Augelli-Szafran:** None. **J. Zhu:** None.

**Poster**

**PSTR168: Postsynaptic Structure, Organization, and Function**

**Location:** WCC Halls A-C

**Time:** Monday, November 16, 2026, 1:00 PM - 5:00 PM

**Program #/Poster #:** PSTR168.01/J7

**Topic:** B.04. Synaptic Transmission

**Support:** NIH R01AG089566
NIH R21AG068423
NIH 5R35GM156406
NIH 5R35GM156863
Charles H. Hood Foundation
Chan Zuckerberg Initiative 2024-338564
Chan Zuckerberg Initiative 2024-338564
NARSAD Young Investigator Grant
Alzheimer's Association Research Grant 23AARG-1026776
Star-Friedman Challenge for Promising Scientific Research
Esther A. & Joseph Klingenstein Fund, the Simons Foundation

**Title:** Activity dependent lipid droplet biogenesis and turnover regulate synaptic integrity

**Authors: *E. KATAFYGIOTOU**, J. CHUNG;
Mol. and Cell. Biol., Harvard Univ., Cambridge, MA

**Abstract:** Lipid droplets (LDs) are dynamic organelles responsible for the storage and utilization of fatty acids and other lipids. Dysregulation of LD metabolism has been linked to an array of neurodegenerative diseases, including Alzheimer's, Parkinson's disease, and hereditary spastic paraplegia. However, LD abundance is reported to be low in neurons under physiological conditions, and how neuronal lipids are regulated through LD, as well as why their dysregulation is associated with diseases, remain unclear. Here, using an LD indicator we developed, which is compatible with brain-cell LD imaging, we show that neurons form and turn over LDs in an activity-dependent manner. LDs formed rapidly, predominantly in dendrites, following various paradigms of neuronal activation in cultured primary neurons. Disrupting LD clearance through inhibition of autophagic LD degradation, or lipophagy, led to LD accumulation in dendritic spines and shafts, impaired postsynaptic integrity, decreased post-synaptic density, and altered spontaneous and evoked calcium kinetics. To investigate the consequence of abnormal LD accumulation in neurites, we profiled altered LD proteomes using a proximity-dependent protein labeling assay. We found abnormal enrichment of proteins involved in synaptic structure and organization under lipophagy inhibition. Taken together, our results suggest that neuronal activation induces LD formation under physiological conditions and that impaired LD clearance disrupts synaptic structure and function, potentially by sequestering synapse-related proteins on the LD surface.

**Disclosures: E. Katafygiotou:** None. **J. Chung:** None.

**Poster**

**PSTR168: Postsynaptic Structure, Organization, and Function**

**Location:** WCC Halls A-C

**Time:** Monday, November 16, 2026, 1:00 PM - 5:00 PM

**Program #/Poster #:** PSTR168.02/J8

**Topic:** B.04. Synaptic Transmission

**Support:** F31 NS139688
R01 MH122461

**Title:** Modulation of Synaptic Transmission by Ketamine in the Medial Prefrontal Cortex

**Authors: *S. R. SCHWARZ**, S. OUBRAIM, S. HAJ-DAHMANE;
Dept. of Pharmacol. and Toxicology, Jacobs Sch. of Med. and Biomed. Sci., Univ. at Buffalo, SUNY, Buffalo, NY

**Abstract:** Ketamine (KET), an open channel blocker of NMDA receptors (NMDARs), when administered at sub-anesthetic doses produces rapid (within hours) and sustained antidepressant effects in treatment-resistant depressed patients. Early mechanistic studies in both human and rodent models show that acute KET administration increases glutamate release in the prefrontal cortex (PFC). These effects have largely been attributed to the disinhibition hypothesis, which posits that KET preferentially binds to and inhibits NMDARs on GABAergic interneurons at sub-anesthetic doses and results in enhanced glutamate release and excitation of pyramidal cells

(PCs).
To further test this hypothesis and investigate KET's influence on excitation and inhibition (E/I) balance in the medial PFC (mPFC), we recorded spontaneous excitatory and inhibitory postsynaptic currents (sEPSCs and sIPSCs) in a whole-cell configuration from L5 PCs in *ex-vivo* rat brain slice electrophysiology experiments. Our sEPSC results show that in the presence of a $GABA_A$ receptor antagonist, bath perfusion of 10 μM KET increases frequency ($p = 0.02$, $n = 12$) but not amplitude ($p = 0.8$, $n = 12$). Our results also show that KET does not affect sIPSC frequency ($p = 0.4$, $n = 15$) or amplitude ($p = 0.9$, $n = 15$). These results indicate that acute KET directly causes an increase in glutamatergic synaptic transmission into PCs which is independent of GABAergic drive.
We next investigated the effects of KET on E/I ratio in evoked synaptic currents. Our results show heterogenous responses to acute KET. Indeed, in a group of L5 PCs we find a noticeable increase ($p = 0.003$, $n = 8$) in E/I ratio. In another group we find a decrease ($p = 0.1$, $n = 4$), and a third group with no change ($p = 0.8$, $n = 6$), indicating the response is cell specific. Currently, using retrograde labeling combined with electrophysiology recordings, we are identifying L5 PC subtypes that respond differently to KET in E/I ratio experiments. Collectively, our results show that KET causes an increase in mPFC glutamatergic drive which is not attributed to a reduction in GABAergic activity. Further studies are needed to elucidate mechanisms by which low-dose KET increases cortical glutamatergic synaptic transmission.

**Disclosures: S.R. Schwarz:** None. **S. Oubraim:** None. **S. Haj-Dahmane:** None.

**Poster**

**PSTR168: Postsynaptic Structure, Organization, and Function**

**Location:** WCC Halls A-C

**Time:** Monday, November 16, 2026, 1:00 PM - 5:00 PM

**Program #/Poster #:** PSTR168.03/K1

**Topic:** B.04. Synaptic Transmission

**Support:** NIH/NINDS (R01-NS110575)
NIH/NIDCD (R01-DC019916-01)
Novo Nordisk Foundation (0064289)
Boston VA Healthcare System (RR&D: BX005959)

**Title:** Responses to High-Frequency Electrical Stimulation Are Strongly Modulated by the Synaptic State of Targeted Cells

**Authors: *H. ROH**[1], J. SEO[2], S. FRIED[1,3], J.-I. LEE[1];
[1]Massachusetts Gen. Hosp., Boston, MA; [2]Univ. of Melbourne, Melbourne, Australia; [3]Boston VA Healthcare Syst., Boston, MA

**Abstract:** High-frequency electrical stimulation (HFS) is a powerful neuromodulation technique used in deep brain, spinal cord, and peripheral nerve stimulation, yet many aspects of its underlying mechanisms remain unclear. Our prior work showed that, unlike conventional single-

pulse or low-frequency stimulation, which drive neurons in a pulse-by-pulse manner, HFS modulates neuronal activity through a sustained shift in membrane potential that develops over multiple pulses. This shift either hyperpolarizes or depolarizes the neuron and, with sufficient depolarization, induces depolarization block. However, mechanistic studies of HFS to date, including ours, have been conducted in neurons largely isolated from their native circuits, and how HFS responses are reshaped in situ, particularly when strong excitatory and inhibitory synaptic input is present, remains poorly understood. To address this, we performed whole-cell patch-clamp recordings from retinal ganglion cells in explanted C57BL/6J mouse retina ($n$ = 21), delivering 2 kHz HFS (0-150 μA) while presenting light stimuli at specific time intervals to add excitatory or inhibitory synaptic input to the cell targeted by HFS; we compared firing in response to (1) HFS alone, (2) HFS with excitation, and (3) HFS with inhibition. Similar to previous work, HFS alone produced a non-monotonic firing response, peaking at 113 ± 17 Hz near 50 μA before depolarization block suppressed spiking. Adding excitation shifted the firing-rate curve leftward (peak 91 ± 25 Hz near 30 μA), whereas inhibition shifted it rightward, with firing remaining elevated at 60 μA (75 ± 31 Hz). Population analysis revealed a state-dependent, often paradoxical pattern: under weak HFS, excitation increased firing (+1200%) while inhibition suppressed it (−44%); under moderate HFS, both excitation and inhibition reduced firing (−62% and −5%, respectively); and under strong HFS, the relationship inverted, with inhibition enhancing firing (+426%) and excitation suppressing it (−52%). Thus, the same synaptic input could enhance, reduce, or invert its effect on spiking depending on the amplitude of HFS. These findings identify the synaptic state of targeted cells as a major determinant of the HFS response, indicating that stimulation outcomes cannot be predicted from HFS parameters alone. Because therapeutic HFS is delivered to active circuits whose synaptic drive varies across disease states and time, knowledge and control of circuit state may help reduce variability in neuromodulation outcomes.

**Disclosures: H. Roh:** None. **J. Seo:** None. **S. Fried:** None. **J. Lee:** None.

**Poster**

**PSTR168: Postsynaptic Structure, Organization, and Function**

**Location:** WCC Halls A-C

**Time:** Monday, November 16, 2026, 1:00 PM - 5:00 PM

**Program #/Poster #:** PSTR168.04/K2

**Topic:** B.04. Synaptic Transmission

**Support:** Wellcome Trust, 218293

**Title:** A synaptome map of the human neocortex

**Authors: *N. MARTINEZ-WISE**[1], Z. QIU[2], J. GRIFFITHS[1], B. NOTMAN[1], W. QUAH[1], D. DOMINIC[1], K. YUAN[1], C. SMITH[1], S. G. GRANT[1];
[1]Inst. for Neurosci. and Cardiovasc. Res., Univ. of Edinburgh, Edinburgh, United Kingdom; [2]Dept. of Biomed. Engin., Univ. of Strathclyde, Glasgow, United Kingdom

**Abstract:** The synaptome of the mammalian brain comprises a highly diverse population of synapses that are spatially organised into a characteristic synaptome architecture. Although this architecture has been extensively characterised in mice, its organisation in the human brain remains poorly understood. To address this, we developed a synaptome mapping pipeline to systematically analyse the molecular composition and morphology of billions of individual synapses in human post-mortem cortical tissue. Using multiplex immunofluorescent labelling of excitatory and inhibitory synaptic proteins, high-resolution spinning-disk confocal microscopy, and machine learning-based image analysis, we detected and classified individual synapse types and subtypes. Based on the combinatorial expression of presynaptic (VGLUT1, VGAT) and postsynaptic (PSD95, PSD93, GLUN1, GLUA2, GEPH) proteins, we identified 11 synapse types and 118 subtypes. We analysed 16 Brodmann areas spanning prefrontal, motor, somatosensory, auditory, visual, and limbic cortices in both hemispheres from six neurologically healthy middle-aged male donors. To enable laminar analyses, cross-sample registration, and integration with published brain-wide datasets, we developed an automated segmentation method to delineate cortical layers from Nissl-stained sections. Our findings reveal a highly structured synaptome architecture across the human neocortex and establish a resource for integration with connectomic, cellular, and transcriptomic brain atlases.

**Disclosures: N. Martinez-Wise:** None. **Z. Qiu:** None. **J. Griffiths:** None. **B. Notman:** None. **W. Quah:** None. **D. Dominic:** None. **K. Yuan:** None. **C. Smith:** None. **S.G. Grant:** None.

**Poster**

**PSTR168: Postsynaptic Structure, Organization, and Function**

**Location:** WCC Halls A-C

**Time:** Monday, November 16, 2026, 1:00 PM - 5:00 PM

**Program #/Poster #:** PSTR168.05/K3

**Topic:** B.04. Synaptic Transmission

**Title:** Evaluating CaMKIIβ's role in excitatory synaptic transmission and plasticity

**Authors: *A. WEIT**, E. T. KAVALALI, L. M. MONTEGGIA;
Vanderbilt Univ., Nashville, TN

**Abstract:** Calcium/calmodulin-dependent protein kinase II (CaMKII) is a kinase that phosphorylates serine/threonines in target proteins and is an important regulator of synaptic plasticity and learning and memory. CaMKII has two isoforms, α and β, that are highly expressed in the hippocampus. CaMKIIα through its kinase function is a critical sensor of activity-driven synaptic transmission and regulator of long term potentiation, or high activity-induced synaptic strengthening. CaMKIIβ differs by supportively trafficking CaMKIIα independently of its kinase function. CaMKIIβ, in contrast to CaMKIIα, is sensitive to low amounts of calcium/calmodulin and its protein expression is enriched in the absence of activity (i.e. tetrodotoxin (TTX) used to block action potentials). Furthermore, previous studies suggest CaMKIIβ may be involved in homeostatic plasticity mechanisms governed by lowered activity.

These findings led us to hypothesize that CaMKIIβ may be a key regulator in mechanisms of spontaneous transmission and related homeostatic upscaling pathways. To test this hypothesis, we have been evaluating the impact of CaMKIIβ expression and enzymatic activity in hippocampal neurons using whole cell patch clamp electrophysiology on basal spontaneous neurotransmission and upscaling in postsynaptic homeostatic mechanisms. We are also using confocal microscopy to investigate the understudied basal function of CaMKIIβ in the presynapse. Together, we seek to provide novel insight into the role of CaMKIIβ in synaptic transmission and synaptic homeostasis.

**Disclosures: A. Weit:** None. **E.T. Kavalali:** None. **L.M. Monteggia:** None.

**Poster**

**PSTR168: Postsynaptic Structure, Organization, and Function**

**Location:** WCC Halls A-C

**Time:** Monday, November 16, 2026, 1:00 PM - 5:00 PM

**Program #/Poster #:** PSTR168.06/K4

**Topic:** B.04. Synaptic Transmission

**Support:** Z01 HD008914- funded by the Intramural Program of NICHD

**Title:** Molecular determinants of gating differences between Drosophila Type A and type B receptors.

**Authors: *S. GOYAL**[1], M. SERPE[2], R. VICIDOMINI[3];
[1]Natl. institute of Hlth., Silver Spring, MD; [2]Natl. Inst. of Child Hlth. and Human Develop., NIH, Bethesda, MD; [3]Section on metabolic regulation, NIH/NCHID, Bethesda, MD

**Abstract:** The properties of ionotropic glutamate receptors (iGluRs) are tuned to permit diverse roles in synaptic transmission. At *Drosophila* neuromuscular junction (NMJ), two classes of iGluRs shape synaptic strength and plasticity, GluRIIA-containing Type A receptors and GluRIIB-containing Type B receptors. Both receptor complexes share three essential subunits—GluRIIC, GluRIID, and GluRIIE—as well as the obligatory auxiliary subunit Neto. Type-A and Type-B receptors compete for synaptic occupancy and have distinct gating properties, with Type-A receptors desensitizing slower than Type-B and providing most of the charge transfer. The two receptor subtypes are recruited at PSDs by different mechanisms; the high extracellular glutamate concentration at larval NMJ regulates constitutive iGluRs desensitization and controls the synaptic receptor abundance. Here, we use outside-out patch-clamp recordings from receptors expressed in HEK cells to investigate the molecular determinants underlying the distinct gating properties of these receptor subtypes. To identify domains responsible for differences in desensitization, deactivation, and recovery kinetics, we generated a series of chimeric receptors through domain swapping between GluRIIA and GluRIIB. Surprisingly, the ligand -binding domain was not the primary determinant of the observed functional differences. Instead, we found that the intracellular C-terminal tail partially contributes to the distinct gating behaviors of Type A and Type B receptors. We are currently examining additional structural

elements potentially involved in shaping their unique gating behaviors. These studies will allow us to identify the molecular features responsible for the distinct gating properties of these receptors and parse out the contribution of receptor function *vs* recruitment to the compound *in vivo* phenotypes.

**Disclosures: S. Goyal:** None. **M. Serpe:** None. **R. Vicidomini:** None.

**Poster**

**PSTR168: Postsynaptic Structure, Organization, and Function**

**Location:** WCC Halls A-C

**Time:** Monday, November 16, 2026, 1:00 PM - 5:00 PM

**Program #/Poster #:** PSTR168.07/K5

**Topic:** B.04. Synaptic Transmission

**Support:** DIP Grant (ZI 1039/1-1)
ISF Grant (1470/18; 2322/23)
the Rappaport Institute and the Allen and Jewel Prince Center for Neurodegenerative Disorders of the Brain

**Title:** TAG, DEGRADE, OBSERVE: REVEALING ACUTE CONSEQUENCES OF RAPID PROTEIN DEGRADATION AT INDIVIDUAL SYNAPSES USING AUXIN-INDUCIBLE DEGRON 2 TECHNOLOGY

**Authors: *L. ELBAUM**[1], W. YUAN[1], J. SEILER[2], N. E. ZIV[3];
[1]Technion - Israel Inst. of Technol., Haifa, Israel; [2]Inst. of Physiology, Focus Program Translational Neurosciences, Univ. Med. Ctr. of the Johannes Gutenberg Univ. Mainz, Mainz, Germany; [3]Technion Fac. of Med., Haifa, Israel

**Abstract:** Roles of particular proteins in synaptic organization and function are commonly studied by knock-out, knock-down or overexpression strategies. Such approaches are typically protracted, associated with adaptive changes and challenge the ability to observe acute consequences at individual synapses. Here we describe the use of Auxin-Inducible Degron 2 (AID2) technology and coexpressed reporters to study real-time effects of rapidly degrading postsynaptic density proteins at individual synapses. We establish the capacity of AID2 technology to rapidly degrade postsynaptic scaffold fusion proteins in cultured neurons and in vivo. We show that acute PSD-95 or gephyrin degradation leads to concomitant loss of AMPA or $GABA_A$ receptors from the same synapses. Unexpectedly, we find that acute GKAP, but not PSD-95 degradation, is associated with scaffold size reductions at the same synapses. Our findings demonstrate the utility of approaches based on acute degradation and live imaging for studying the roles of select proteins in synaptic organization.

**Disclosures: L. Elbaum:** None. **W. Yuan:** None. **J. Seiler:** None. **N.E. Ziv:** None.

**Poster**

**PSTR168: Postsynaptic Structure, Organization, and Function**

**Location:** WCC Halls A-C

**Time:** Monday, November 16, 2026, 1:00 PM - 5:00 PM

**Program #/Poster #:** PSTR168.08/K6

**Topic:** B.04. Synaptic Transmission

**Title:** Decoding the assembly of postsynaptic specializations with the ALFA/Nanobody split system

**Authors: *E. BENARYEH**, R. VICIDOMINI, T. HAN, M. SERPE;
Section on Cell. Communication, NIH/NICHD, Bethesda, MD

**Abstract:** Normal neural development and function requires recruitment and stabilization of neurotransmitter receptors at postsynaptic densities (PSDs). Disruptions in the receptor recruitment and/or stabilization at synapses have been implicated in numerous neurological and psychiatric disorders. In both flies and mammals, auxiliary proteins play essential roles in neurotransmitter receptor recruitment and synapse maturation; however, the underlying molecular mechanisms remain poorly understood. At the *Drosophila* NMJ, the auxiliary protein Neto (Neuropillin and Tolloid-like) controls the synaptic recruitment and function of glutamate receptors. We previously demonstrated that Neto-β, the predominant postsynaptic isoform, functions as a dynamic scaffold that recruits receptors as well as PSD components, including PAK (p21-activated kinase) and dPix (a Rho guanine nucleotide exchange factor), which in turn stabilize specific glutamate receptor subtypes and thereby shape synaptic strength.
Here, we combine genetics, cell biology and electrophysiology approaches to map functional motifs within the intracellular domain of Neto-β. Since synapse development is highly sensitive to Neto levels and phosphorylation states, we first developed an ALFA tag/nanobody split system suitable for structure-function studies *in vivo* (Vicidomini et al, *Nat Comm*, 2024). The ALFA system consists of a synthetic 13 amino acid epitope and a nanobody that binds this epitope with picomolar affinity both inside and outside the cell. This approach allows us to replace any interaction motif with the ALFA tag and then restore its function *in trans* by expressing nanobody-fusion proteins carrying either the missing motif or its interacting partner. For example, a *neto-β*$^{short}$ allele (lacking most of the intracellular domain), fails to recruit the PSD protein dPix and Dlg. We introduced the ALFA tag into the truncated Neto-β protein, then expressed a series of nanobody-Neto-β chimeras in larval muscles. Remarkably, a construct containing only ~100 amino acids of Neto-β fully restored Pix and Dlg accumulation at the NMJ. We are further dissecting this region to identify the minimal motifs that are necessary and sufficient for the recruitment of Pix, Dlg, and other postsynaptic components.

**Disclosures: E. Benaryeh:** None. **R. Vicidomini:** None. **T. Han:** None. **M. Serpe:** None.

**Poster**

**PSTR168: Postsynaptic Structure, Organization, and Function**

**Location:** WCC Halls A-C

**Time:** Monday, November 16, 2026, 1:00 PM - 5:00 PM

**Program #/Poster #:** PSTR168.09/K7

**Topic:** B.04. Synaptic Transmission

**Support:** AA017823
F31AA032445-01A1

**Title:** Vasopressin 1A receptor modulation of GABAergic input onto central amygdala neurons activated by withdrawal from adolescent binge ethanol exposure

**Authors: *P. PENTA**[1], F. P. VARODAYAN[2], E. I. VARLINSKAYA[3], D. F. WERNER[4]; [1]Binghamton Univ., Johnson City, NY; [2]Binghamton Univ., Vestal, NY; [3]Dept Psychol, [4]Psychology and Behavioral Neurosci., Binghamton Univ., Binghamton, NY

**Abstract:** Adolescent intermittent binge-like ethanol exposure produces sex-specific alterations in GABAergic signaling within the central amygdala (CeA), a critical region for withdrawal-related anxiety. However, CeA neurons are molecularly and functionally diverse, and the synaptic state of the subpopulation activated by ethanol withdrawal remains unknown. The hypothalamic neuropeptide arginine vasopressin (AVP) promotes anxiety-like behavior, but its role in ethanol withdrawal during adolescence is still unclear. We previously showed that withdrawal from adolescent binge ethanol exposure increases CeA AVP mRNA expression in male, but not female, rats. Consequently, AVP 1a receptor (V1aR) modulation may differentially affect GABAergic transmission in withdrawal-activated CeA neurons in a sex-dependent manner. The current study therefore assessed whether V1aR antagonism alters GABAergic input onto CeA neurons activated during withdrawal from adolescent ethanol exposure. Male and female Fos-LacZ transgenic rats received 4 g/kg ethanol or isovolumetric tap water via intragastric gavage on a two-day-on/two-day-off schedule from postnatal day (P) 28 to P53 (14 exposures). Spontaneous inhibitory postsynaptic currents (sIPSCs) were recorded from activated medial CeA neurons at baseline and following bath application of the selective V1aR antagonist SR-49059. Our findings indicate that basal and V1aR antagonist-modulated GABAergic transmission were sex-dependently reduced during withdrawal from adolescent ethanol exposure through a mixture of pre- and postsynaptic effects. Together, these findings suggest that a history of adolescent ethanol exposure disinhibits CeA neurons activated during withdrawal, and that AVP signaling may counteract these changes. Given the established role of the CeA in the transition to alcohol use disorder (AUD) and the association between adolescent alcohol use and increased AUD risk, these sex-dependent GABAergic adaptations may contribute to withdrawal-related anxiety and subsequent vulnerability to AUD.

**Disclosures: P. Penta:** None. **F.P. Varodayan:** None. **E.I. Varlinskaya:** None. **D.F. Werner:** None.

**Poster**

**PSTR168: Postsynaptic Structure, Organization, and Function**

**Location:** WCC Halls A-C

**Time:** Monday, November 16, 2026, 1:00 PM - 5:00 PM

**Program #/Poster #:** PSTR168.10/K8

**Topic:** B.04. Synaptic Transmission

**Title:** Creating a Prediction Model of Critical Protein Motifs across Post Synaptic Genes Using Human Clinical Variants

**Authors: *A. W. LEHR**[1], K. W. ROCHE[2];
[1]Brown University-NIH GPP, Bethesda, MD; [2]RBS/NINDS, NIH, Bethesda, MD

**Abstract:** Neurodevelopmental disorders (NDDs) are conditions arising from disruptions in early brain development, often first detected between 6 months and 2 years of age. This onset coincides with synaptic circuit refinement, and genetic studies identify numerous synaptic genes in NDD risk. Proteins encoded by these genes form the structural and signaling framework of the post-synaptic density(PSD), enabling activity-driven changes in membrane voltage, cytoskeletal remodeling, and downstream signaling.
Protein-protein interactions (PPIs) in the PSD are highly dynamic and often activity dependent, occurring in response to synaptic events, such as $Ca^{2+}$ influx, voltage changes, and G-protein activation. PPIs drive structural remodeling of synapses, which is mediated by short binding motifs often within intrinsically disordered regions (IDRs) of synaptic proteins, such as PDZ-domain binding motifs. However, most studies of pathogenic missense mutations have focused on structured protein domains, leaving variants within IDRs relatively understudied.
Although IDRs inherently tolerate greater sequence variability, they frequently contain short linear motifs (5-15 residues) that mediate essential PPIs. These motifs have limited evolutionary conservation, and thus predictive models may overlook pathogenic variants in these regions. As a result, variants in IDRs are often classified as benign despite IDRs representing up to 70% of the eukaryotic proteome.
To identify functionally critical IDR regions, I developed an algorithm that compares the density of clinical missense variants from ClinVar against background variation from Genome Aggregation Database (gnomAD). This approach detects hotspots enriched for clinical variants but depleted in population variation, enabling extraction of candidate sequence motifs for predictive modeling. IDRs are identified using IUPred3 to train a long short-term memory (LSTM) model capable of learning relationships based on clinically intolerant protein sequences across SynGO's 1084 postsynaptic genes. Initial validation identified hotspots overlapping with kinase-binding sites within the unstructured cytoplasmic tails of GRIN2A and GRIN2B. This model will enable identification of previously uncharacterized regulatory regions in the human synaptosome.

**Disclosures: A.W. Lehr:** None. **K.W. Roche:** None.

**Poster**

**PSTR168: Postsynaptic Structure, Organization, and Function**

**Location:** WCC Halls A-C

**Time:** Monday, November 16, 2026, 1:00 PM - 5:00 PM

**Program #/Poster #:** PSTR168.11/L1

**Topic:** B.04. Synaptic Transmission

**Support:** IITM sponsored

**Title:** Spatially distinct excitatory inputs enable direction selective retinal ganglion cells to respond to high speed motion

**Authors: *M. ALFRED**[1], S. SETHURAMANUJAM[2];
[1]Dept. of Biotech., Indian Inst. of Technol. Madras, Chennai, India; [2]Indian Inst. of Technol. Madras, Indian Institute of Technology Madras, India

**Abstract:** ON-OFF Direction Selective Ganglion Cells (DSGCs) encode for the direction of image motion over a range of speeds. While the mechanisms underlying direction selectivity have been extensively studied, the mechanisms governing velocity tuning are yet to be explored. Previous studies have identified that cholinergic excitation from Starburst Amacrine Cells (SACs) and glutamatergic excitation from bipolar cells are primary excitatory inputs to ON-OFF DSGCs. However, how these pathways interact to shape velocity tuning in ON-OFF DSGCs is yet to be determined.

To understand the mechanisms of velocity tuning in ON-OFF DSGCs, we monitored the activity of DSGCs in mouse retinal whole mount preparations. ON-OFF DSGCs exhibited high pass spiking characteristics, with firing rates saturating at higher speeds. However, we observed that both EPSCs and IPSCs were preferentially tuned to lower velocities, and the responses decreased at higher speeds. This dissociation between the spiking responses and the synaptic inputs indicates that the DSGCs tuned to higher velocities are not merely due to the magnitude of these synaptic inputs, but rather due to additional circuit mechanisms that may arise from the spatial and temporal integration of these excitatory inputs.

We examined the mechanisms underlying this dissociation by studying the spatial and temporal organization of excitatory inputs. Conductance analyses revealed that cholinergic activation preceded NMDA receptor-mediated excitation, resulting in a spatial offset between these two conductances. When the visual stimulus was restricted with a 200 μm aperture, the spatial offset was abolished that led to simultaneous activation of both acetylcholine and NMDA conductances. The spatial offset of these excitatory sources can act as a coincidence detector, boosting responses at higher speeds. This was confirmed by pharmacologically blocking either nicotinic acetylcholine receptors or NMDA receptors, which shifted the spiking responses towards lower velocities. These findings suggest that coordinated spatial integration of cholinergic and NMDA receptor-mediated excitation selectively enhances the responses to higher velocities.

**Disclosures: M. Alfred:** None. **S. sethuramanujam:** None.

**Poster**

**PSTR168: Postsynaptic Structure, Organization, and Function**

**Location:** WCC Halls A-C

**Time:** Monday, November 16, 2026, 1:00 PM - 5:00 PM

**Program #/Poster #:** PSTR168.12/L2

**Topic:** I.06. Social Cognition

**Title:** Intracellular signaling dysregulation in GRIN1 Channelopathies converge on the PSD95ome

**Authors: *A. KUNCH**[1], S. SEENIVASA[1,2], M. SULLIVAN[3], R. ZIDAN[1], N. HENKEL[5], J. VERGIS[1], A. S. IMAMI[6], P. PULVENDER[7], S. M. O'DONOVAN[8], A. J. RAMSEY[4], J. MELLER[9], R. E. MCCULLUMSMITH[8];
[1]The Univ. of Toledo, Toledo, OH; [2]The Univ. of Toledo Col. of Med. and Life Sci., Toledo, OH; [3]Pharmacol. & Toxicology, [4]Pharmacol. and Toxicology, Univ. of Toronto, Toronto, ON, Canada; [5]Neurosci. & Neurolog. Disorders, [6]Univ. of Toledo Col. of Med. Neurosci. & Neurolog. Disorders, Toledo, OH; [8]Neurosciences, [7]Univ. of Toledo, Toledo, OH; [9]Univ. of Cincinnati, Cincinnati, OH

**Abstract:** The NMDA receptor subunit gene GRIN1 encodes an essential component of glutamatergic signaling. Pathogenic GRIN1 variants cause NMDAR channelopathies and manifestations of neurodevelopmental disorders, seizures, and autism. Despite known receptor dysfunction and behavioral abnormalities, intracellular signaling dysregulation in GRIN1 channelopathies remains poorly understood. Frontal pole tissue was collected from transgenic mouse models of GRIN1 channelopathy including Grin1 Y647S heterozygous gain-of-function (GoF), Q536R heterozygous loss-of-function (LoF), and Grin1 knockdown (KD) mice, for a total of 6 genotypes stratified by sex, each with age- and sex-matched wild-type (WT) littermates. Phosphopeptides were enriched from frontal pole lysates using aluminum oxide columns, trypsin-digested, and analyzed using label-free LC-MS/MS (n=3 per genotype). Serine/threonine kinase activity was assessed using the PamStation12 platform (5 pooled biological samples, n=3 technical replicates per genotype). Differential analyses, kinase substrate enrichment, pathway enrichment using Gene Ontology (GO) and synGO, and multiomic network integration using STRINGDB and ChEA3 priors were conducted to identify cell signaling dysregulation across genotypes. PSD95/Dlg4, a crucial postsynaptic scaffolding protein that organizes NMDAR and AMPAR signaling complexes, emerged as a convergent multiomic network hub across all genotype-sex comparisons. GoF mice show broad downregulation of many kinase families and LoF and KD showing upregulation of AKT, MTOR, AMPK, MAPK, and PKC families, which are downregulated in GoF. NMDA selective glutamate receptor complex (CC) is upregulated in LoF males and downregulated in GoF males (FDR adj. $p < 0.05$). PSD95 Serine 295 is upregulated in LoF males (logFC = 0.35) and KD males (logFC = 0.74), and downregulated in GoF females (logFC = -1.42) (adj. $p < 0.05$). Other phosphosites on PSD95\Dlg4, Dlg3, Dlg1, Shank3, Ctnnb1, and Gsk3 are dysregulated in one or more channelopathy models. Downregulation of AKT and MTOR in GoF is consistent with reduced anabolic signaling and enhanced cell stress responses, promoting a stress-adaptive, catabolic state that may contribute to compensatory mechanisms that reduce NMDAR activity, while upregulation of AKT and MTOR in LoF and KD is consistent with activation of anabolic pathways that may stabilize NMDAR via the PSD. Phosphorylation of PSD95 Serine 295 promotes AMPAR recruitment and NMDAR stabilization and is increased in LoF and KD, and decreased in GoF, suggesting a compensatory effect of PSD95 phosphorylation in GRIN1 channelopathy.

**Disclosures: A. Kunch:** None. **S. Seenivasa:** None. **M. Sullivan:** None. **R. Zidan:** None. **N. Henkel:** None. **J. Vergis:** None. **A.S. Imami:** None. **P. Pulvender:** None. **S.M. O'Donovan:** None. **A.J. Ramsey:** None. **J. Meller:** None. **R.E. McCullumsmith:** None.

**Poster**

**PSTR169: Pharmacological and Non-Pharmacological Interventions for Brain Aging**

**Location:** WCC Halls A-C

**Time:** Monday, November 16, 2026, 1:00 PM - 5:00 PM

**Program #/Poster #:** PSTR169.01/L3

**Topic:** C.01. Brain Wellness and Aging

**Support:** RF1AG078677

**Title:** Exercise-induced neurological benefits in eNOS-deficient mice are negated by the inhibition of α5β1 integrin

**Authors: *A. WHITE**[1], S. ISMAEL[1], E. B. ENGLER-CHIURAZZI[2], B. OUVRIER[3], G. J. BIX[2];
[2]Neurosurg., [1]Tulane Univ., New Orleans, LA; [3]Clin. Neurosci. Res. Ctr., New Orleans, LA

**Abstract:** Vascular cognitive impairment (VCI) is a term used to describe a loss of cognitive ability arising from dysfunction of the cerebral vasculature. Due to its heterogenous etiology, specific therapeutic options for VCI are extremely limited. One treatment method that has shown promise in mouse models of VCI is exercise. However, the mechanisms behind the benefits of exercise have yet to be fully elucidated. As ischemic lesions are a common pathology of VCI and exercise-induced benefits have been thought to be related to increases in blood flow, the angiogenic receptor integrin α5β1 has become a target of interest. Therefore, we hypothesize that exercise-induced benefits act through the α5β1 integrin pathway.
To test this hypothesis, we used the small peptide ATN-161 to inhibit α5β1 integrin in the eNOS-deficient mouse model of VCI. Forty-five 17-month-old eNOS+/- mice were divided into four treatment groups: sedentary, ATN-161 only, Exercise only, and Exercise and ATN-161. The mice were allowed free access to a running wheel for a period of 30 days. eNOS+/- mice were also given 1 mg/kg of ATN-161 or a saline equivalent through intraperitoneal injection once every other day during the 30-day exercise period. At 18-mo, behavior and cognition of the mice were examined using the Open Field test, Footprint analysis test, Y-maze test, and Morris Water Maze test.
No differences were found in the Y-maze test or footprint analysis among any of the groups. However, we did find that mice in the exercise-only group spent more time in the center of the open field apparatus, indicative of less anxiety. This difference in temperament was lost when ATN-161 was added to the exercise treatment regime. We also saw that these same mice displayed a higher cognitive ability compared to the other groups through their shorter latency period in the Morris water maze test, a difference that was again lost when ATN-161 was combined with exercise treatment.
Taken together, our results demonstrate that the beneficial effects of exercise on anxiety and

cognition are abated by the further addition of ATN-161. This suggests that a functioning α5β1 integrin is important to the neurologic benefits resulting from exercise.

**Disclosures: A. White:** None. **S. Ismael:** None. **E.B. Engler-Chiurazzi:** None. **B. Ouvrier:** None. **G.J. Bix:** None.

**Poster**

**PSTR169: Pharmacological and Non-Pharmacological Interventions for Brain Aging**

**Location:** WCC Halls A-C

**Time:** Monday, November 16, 2026, 1:00 PM - 5:00 PM

**Program #/Poster #:** PSTR169.02/L4

**Topic:** C.01. Brain Wellness and Aging

**Support:** NIH Grant T32 AG071745
DoD Grant HT9425-24-1-0139

**Title:** Targeting glial senescence as a treatment for post-traumatic epilepsy following experimental traumatic brain injury

**Authors: *M. STEVENSON**[1], D. MCFALL[5], S. HANEY[2], J. SU[2], M. P. BURNS[3], P. A. FORCELLI[4];
[1]Pharmacol. and Physiol., [2]Georgetown Univ., Washington DC, DC; [3]Dept of Neurosci., [4]Dept of Pharmacol. & Physiol., Georgetown Univ., Washington, DC; [5]Georgetown Univ. Med. Ctr., Washington, WA

**Abstract:** Senescence is a phenomenon by which cells enter an anti-apoptotic state of cell cycle arrest and lose many of their homeostatic properties. While senescent cells have been demonstrated to arise as a normal part of aging, increased numbers of these cells have recently been identified in several neurodegenerative conditions, indicating their prevalence may serve to differentiate normal and pathological aging. Senescent microglia have further been shown to arise following traumatic brain injury (TBI) and epilepsy, raising the possibility that microglial senescence represents a mechanistic link between TBI and post-traumatic epilepsy (PTE), a serious complication for which no preventative treatments exist. To test this hypothesis, we used a controlled cortical impact (CCI) model to induce TBI in 3-month-old male and female C57Bl/6J mice. Immunohistochemical analysis of senescent and glial markers revealed that senescent cells emerge in the ipsilateral thalamus and contralateral hippocampus, with critical accumulation spiking by four weeks post-injury. Microglia were identified as the predominant senescent cell type. By eight weeks post-CCI, EEG recording showed that mice developed spontaneous seizures, which were associated with hippocampal memory deficits.In a separate cohort of mice, treatment with the senolytic combination of dasatinib and quercetin (D+Q) initiated one day post-injury and continued weekly for 12 weeks, rescued cognitive deficits, but not spontaneous seizures; however, delayed treatment beginning two weeks post-injury did not, defining a critical therapeutic window for administering senolytics. Single-cell RNA sequencing further identified senescence-associated transcriptomic signatures following CCI that were

normalized by D+Q treatment.These findings implicate microglial senescence as an early and targetable driver of PTE and identify senolytics as a promising preventative strategy, contingent on the timing of intervention.

**Disclosures: M. Stevenson:** None. **D. McFall:** None. **S. Haney:** None. **J. Su:** None. **M.P. Burns:** None. **P.A. Forcelli:** None.

**Poster**

**PSTR169: Pharmacological and Non-Pharmacological Interventions for Brain Aging**

**Location:** WCC Halls A-C

**Time:** Monday, November 16, 2026, 1:00 PM - 5:00 PM

**Program #/Poster #:** PSTR169.03/L5

**Topic:** C.01. Brain Wellness and Aging

**Support:** Shota Rustaveli National Science Foundation of Georgia (Project No FR-24-4786)

**Title:** Age-Dependent Effect of Alpha-Lipoic Acid on Na,K-ATPase Activity and Redox Homeostasis

**Authors: G. CHKADUA**[1,2];
[1]Iv. Beritashvili Ctr. Of Experimantal Biomedicine, Tbilisi, Georgia; [2]Georgian Natl. Univ., Tbilisi, Georgia

**Abstract:** Aging is associated with increased oxidative stress and progressive impairment of neuronal function, including alterations in Na,K-ATPase activity. In addition to its role in ion transport, Na,K-ATPase functions as a redox-sensitive signaling platform involved in Src- and ERK-dependent pathways. The present study investigated the effects of alpha-lipoic acid (ALA) on hippocampal Na,K-ATPase activity, oxidative stress markers, and signaling mechanisms in 3- and 12-month-old Wistar rats.ALA (100 mg/kg/day) was administered for one month. Aging significantly reduced total and α2/3-associated Na,K-ATPase activity, increased protein carbonylation, and reduced Src activation. In aged animals, ALA attenuated the decline in Na,K-ATPase activity, markedly reduced protein carbonylation, and increased α1-associated activity. In contrast, ALA increased protein carbonylation, enhanced SOD activity, reduced α2/3-associated activity, and suppressed Src activation in young animals. ERK activation remained unchanged across experimental groups.These findings demonstrate that ALA exerts age-dependent effects on hippocampal Na,K-ATPase function and redox homeostasis. While ALA exhibited predominantly antioxidant and protective effects in aged animals, distinct redox-modulatory responses were observed in young animals. The results highlight the involvement of Na,K-ATPase in the interplay between oxidative stress, cellular signaling, and brain aging.

**Disclosures: G. Chkadua:** None.

**Poster**

**PSTR169: Pharmacological and Non-Pharmacological Interventions for Brain Aging**

**Location:** WCC Halls A-C

**Time:** Monday, November 16, 2026, 1:00 PM - 5:00 PM

**Program #/Poster #:** PSTR169.04/L6

**Topic:** C.01. Brain Wellness and Aging

**Support:** United States Department of Agriculture
Department of Pathology and Anatomical Sciences, School of Medicine, University of Missouri.

**Title:** Dietary Elderberry and DHA Modulate Molecular Signatures of Brain Resilience and Improve Neurological Function in Aging Mice

**Authors: *W. YU**[1,2], T. MONY[3], R. LI[3], E. PAN[1], G. Y. SUN[4], J. CUI[3], A. THOMAS[1], C. M. GREENLIEF[5], Z. GU[3];
[2]Interdisciplinary Neurosci. Program, [3]Path & Ana Sci. Dept., [4]Biochem., [5]Biochem, [1]Univ. of Missouri, Columbia, MO

**Abstract:** Aging is a primary risk factor for cognitive decline and neurological disorders including Alzheimer's disease-related dementias (ADRD). Elderberry is rich in anthocyanins and polyphenols, known for their antioxidant and anti-inflammatory properties. Docosahexaenoic acid (22:6n-3, DHA) enriches brain membranes and vulnerability to oxidative stress. Both elderberry and DHA have been implicated in promoting brain resilience, their comparative and combined impacts on the aging brain remain unclear. This study investigated the effects of dietary elderberry, DHA, and their combination on neurobehavioral function, fatty acid composition and cortical proteome/phosphoproteome regulation in aging mice. A total 47 male mice (11-month-old, average 32.5 gram of body weight) were randomly assigned to control, elderberry, DHA, or combined diet groups for 12-week, followed by a battery of behavioral assessment, including anxiety-like behavior, exploratory activity, and cognitive performance. Cortical tissues (n=5 per group) were used for fatty acid analysis and proteomic and phosphoproteomic profiling. Proteomic and phosphoproteomic datasets were analyzed to identify molecular signatures and associated functional pathways using Ingenuity Pathway Analysis (IPA). Our results demonstrated that DHA supplementation increased membrane DHA and reduced arachidonic acid (20:4n-6), a precursor for pro-inflammatory prostaglandin pathways. Elderberry significantly modulated pathways associated with synaptogenesis, glutamatergic signaling, and long-term potentiation (LTP). Mechanistically, elderberry consumption was linked to the regulation of CDK5-MAPT/Tau signaling, whereas DHA primarily influenced CAMK-mediated pathways, suggesting distinct, non-redundant neuroprotective mechanisms. Behaviorally, mice receiving elderberry or DHA alone exhibited reduced anxiety-like behavior; elderberry alone additionally increased exploration and enhanced spatial memory. Crucially, phosphoproteomic signatures showed strong concordance with observed behavioral improvements. Together, these findings suggest that elderberry and DHA promote resilience in the brain and support healthy cognitive aging by modulating synaptic plasticity and mitigating age-related deficits. This study provides a robust framework for understanding the neuroprotective mechanisms of dietary interventions in brain aging.

**Disclosures: W. Yu:** None. **T. Mony:** None. **R. Li:** None. **E. Pan:** None. **G.Y. Sun:** None. **J. Cui:** None. **A. Thomas:** None. **C.M. Greenlief:** None. **Z. Gu:** None.

**Poster**

**PSTR169: Pharmacological and Non-Pharmacological Interventions for Brain Aging**

**Location:** WCC Halls A-C

**Time:** Monday, November 16, 2026, 1:00 PM - 5:00 PM

**Program #/Poster #:** PSTR169.05/L7

**Topic:** C.01. Brain Wellness and Aging

**Title:** Exploring the Effects of Prazosin and Propranolol on Long-Term Stress-Induced Neural Activation

**Authors: *J. N.-D. LAMBERT**[1], N. GULAI[2], M. ARFAN[2], L. JOHNSON-KLEINPETER[3], K. PATEL[2], B. CORBETT[4];
[1]Biol., Rutgers Univ., MOORESTOWN, NJ; [3]Biol., [2]Rutgers Univ., Camden, NJ; [4]Rutgers-Camden: Rutgers Univ. Camden, Camden, NJ

**Abstract:** Chronic stress produces lasting behavioral and neural changes that contribute to anxiety and depression like phenotypes. Noradrenergic signaling is strongly engaged during stress and is known to regulate arousal, vigilance, threat processing, and stress-related learning. Because repeated stress can convert acute neural activation into long-term molecular adaptation, pharmacological blockades of adrenergic receptors during stress may alter later plasticity-related outcomes. Prazosin (1mg/kg) and Propranolol (10mg/kg), antagonists of α1- and β-adrenergic receptors, respectively, were injected intraperitoneally to modify long-term stress-related neural adaptation in the Dentate gyrus (DG) region in male mice exposed to chronic social defeat stress. Delta FosB acted as the marker of long-term stress-related neural adaptation, and quantification focused on the dorsal blade, ventral blade, and hilus regions of the DG using threshold-based ImageJ analysis. Using a previously validated approach, defeat reduced social interaction in vehicle-treated mice. Conversely, adrenergic blockade attenuated this behavioral effect, with a significant drug × defeat interaction for social interaction ratio ($p=0.022$). In the present study, within the DG, prazosin significantly reduced ΔFosB signal in the ventral blade ($p=0.011$) and the hilus ($p=0.0261$). In contrast, propranolol significantly reduced ΔFosB signal in the dorsal blade ($p= 0.041$) and ventral blade ($p=0.018$) compared with defeat vehicle-treated mice. These findings suggest that α1 and β adrenergic signaling during defeat may contribute to region-specific stress-induced transcriptional plasticity in the dentate gyrus, especially in the ventral blade of DG. Collectively, this study supports the concept that DG is functionally heterogeneous and that noradrenergic signaling during stress may shape susceptibility-related plasticity in anatomically distinct hippocampal compartments.

**Disclosures: J.N. Lambert:** None. **N. Gulai:** None. **M. Arfan:** None. **L. Johnson-Kleinpeter:** None. **K. Patel:** None. **B. Corbett:** None.

**Poster**

**PSTR169: Pharmacological and Non-Pharmacological Interventions for Brain Aging**

**Location:** WCC Halls A-C

**Time:** Monday, November 16, 2026, 1:00 PM - 5:00 PM

**Program #/Poster #:** PSTR169.06/L8

**Topic:** C.01. Brain Wellness and Aging

**Title:** Oral NLRP3 Inhibition Improves Behavioral Phenotypes Associated with Brain Aging in Mice

**Authors:** S. YAN[1], A. BANICKI[1], M. BANICKI[1], ***Y. WANG**[1], K. WILHELMSEN[1], M. COCHRAN[1], C. RODRIGUEZ[1], C. PORTILLO[1], A. LUNDQUIST[2], C. PATIL[1], J. REBO[1], G. HARTMAN[1], R. MONTGOMERY[1], P. LEONG[1], E. MORGEN[1], K. FORTNEY[1], P. RUBIN[1]; [1]BioAge Labs, Emeryville, CA; [2]BioAge Labs, Inc., Richmond, CA

**Abstract:** Aging is accompanied by chronic neuroinflammation, blood-brain barrier (BBB) dysfunction, and progressive declines in neural function that manifest as impairments in locomotor, exploratory, social, and sleep-related behaviors. Activation of the NLRP3 inflammasome has been implicated in age-related neuroinflammation, neurodegeneration, and cognitive decline, making it an attractive therapeutic target for brain aging. In this exploratory study, we tested whether BAL-1901, a potent, orally active, CNS-penetrant NLRP3 inhibitor, could reverse behavioral phenotypes associated with advanced age in mice. Twenty-one-month-old female C57BL/6 mice received vehicle or BAL-1901 (20 mg/kg, oral gavage, once daily; n=12/group); 12-month-old vehicle-treated female mice served as younger controls (n=12). Only females were studied; sex differences were not assessed. Behavior was phenotyped continuously in group-housed animals using an AI-enabled home-cage monitoring platform (DOMEs Smart Lid, Olden Labs) with near-infrared cameras and microphones that quantify locomotor activity, sleep, feeding and drinking, exploration, and social interaction. Relative to younger controls, aged vehicle-treated mice showed deficits across behavioral domains commonly affected in brain aging and neurodegeneration, including spontaneous locomotion, exploration, social engagement, sleep, and home-cage behavioral organization. BAL-1901 significantly increased activity-related measures in aged mice, including distance traveled, average speed, awake speed, and acceleration, and significantly reduced inactivity and sleep measures, restoring these parameters toward younger-control levels. Drinking duration was likewise restored, and aging-associated changes in eating duration, spatial occupancy (front- and corner-zone preference), enrichment-tube interaction, and social distance shifted toward younger-control profiles. In parallel studies, mice of comparable age showed regional BBB leakage, suggesting the observed benefits may partly reflect modulation of neuroinflammatory pathways linked to compromised neurovascular integrity. Together, these results support NLRP3-driven neuroinflammation as a contributor to behavioral impairment in brain aging and identify NLRP3 inhibition as a promising strategy to preserve neural-circuit function and mitigate behavioral decline in aging and neurodegenerative disease.

**Disclosures: S. Yan:** A. Employment/Salary (full or part-time):; BioAge Labs. **A. Banicki:** A. Employment/Salary (full or part-time):; BioAge Labs. **M. Banicki:** A. Employment/Salary (full or part-time):; BioAge Labs. **Y. Wang:** A. Employment/Salary (full or part-time):; BioAge Labs.

**K. Wilhelmsen:** A. Employment/Salary (full or part-time):; BioAge Labs. **M. Cochran:** A. Employment/Salary (full or part-time):; BioAge Labs. **C. Rodriguez:** A. Employment/Salary (full or part-time):; BioAge Labs. **C. Portillo:** A. Employment/Salary (full or part-time):; BioAge Labs. **A. Lundquist:** A. Employment/Salary (full or part-time):; BioAge Labs. **C. Patil:** A. Employment/Salary (full or part-time):; BioAge Labs. **J. Rebo:** A. Employment/Salary (full or part-time):; BioAge Labs. **G. Hartman:** A. Employment/Salary (full or part-time):; BioAge Labs. **R. Montgomery:** A. Employment/Salary (full or part-time):; BioAge Labs. **P. Leong:** A. Employment/Salary (full or part-time):; BioAge Labs. **E. Morgen:** A. Employment/Salary (full or part-time):; BioAge Labs. **K. Fortney:** A. Employment/Salary (full or part-time):; BioAge Labs. **P. Rubin:** A. Employment/Salary (full or part-time):; BioAge Labs.

**Poster**

**PSTR169: Pharmacological and Non-Pharmacological Interventions for Brain Aging**

**Location:** WCC Halls A-C

**Time:** Monday, November 16, 2026, 1:00 PM - 5:00 PM

**Program #/Poster #:** PSTR169.07/M1

**Topic:** C.01. Brain Wellness and Aging

**Support:** NIA P01AG055365

**Title:** Cortical Impact of Auditory Training Types on Hierarchical Language Representations

**Authors: *C. STONE**[1], L. Z-RIVERA[2], E. SAJJADI[2], S. ANDERSON[3];
[1]Univ. of Maryland, Col. Park, Bethesda, MD; [3]Hearing and Speech Sci., [2]Univ. of Maryland, College Park, MD

**Abstract:** Aging and age-related hearing loss make understanding speech more difficult, as degraded processing in the auditory system distorts the fine temporal features of speech. Current research suggests that this difficulty is linked to changes in the brain's temporal dynamics, manifesting as delayed and exaggerated cortical responses to speech. These changes appear to be compensatory mechanisms, but fail to restore perception, especially listening in noisy environments or to fast speech. This study aims to explore the extent to which auditory training, with either time-compressed speech (TCS) or with speech-in-noise (SiN), can restore youthful functioning. Effects on cortical processing are analyzed in a Temporal Response Function (TRF) framework to present changes observed across hierarchical levels of linguistic neural representation (e.g., phonemes, words) for three levels of hearing loss. Participants (N=94) included a younger normal hearing (YNH) group, an older normal hearing (ONH) group, and an older hearing impaired (OHI) group. Participants underwent pre- and post-training behavioral tests to obtain their thresholds for 50% keyword recognition of TCS. All participants completed 6 hour-long adaptive training sessions, either manipulating TCS rate or SiN ratio. Before and after training, EEG was recorded for cortical responses to continuous speech, presented through audiobooks in both unprocessed and TCS conditions. After training, significant improvement in behavioral measures was observed, with a greater effect for TCS training. Notably, the TCS-trained ONH group achieved the pre-training thresholds of the YNH group. This suggests that

targeted training can partly restore rapid speech recognition, especially in older adults with normal hearing. To understand the neural basis of this improvement, TRFs of the EEG data will show how the exaggerated cortical tracking responses previously observed in older adults change with training. Our findings provide new insight into the potential for auditory training to improve speech perception for older adults. The behavioral results suggest a restoration of more youthful function, which has impactful clinical relevance for cortical plasticity in aging. Targeted training could provide a valuable toolset to help overcome problems with speech comprehension in everyday life, alleviating the need for pharmacological intervention. Future work will examine long term effects of such training and its potential in home and clinical settings. Importantly, different types of auditory training can drive neuroplastic changes that improve speech recognition.This work was supported by NIA P01AG055365

**Disclosures: C. Stone:** None. **L. Z-Rivera:** None. **E. Sajjadi:** None. **S. Anderson:** None.

**Poster**

**PSTR169: Pharmacological and Non-Pharmacological Interventions for Brain Aging**

**Location:** WCC Halls A-C

**Time:** Monday, November 16, 2026, 1:00 PM - 5:00 PM

**Program #/Poster #:** PSTR169.08/M2

**Topic:** C.01. Brain Wellness and Aging

**Support:** NIH T32 5T32GM142520-04
Georgetown Univeristy Jerome H. Fleisch & Marlene L. Cohen Endowed Fund

**Title:** Early-Life Phenobarbital Generates Acute and Long-term Neurotoxicity in the Larval Zebrafish

**Authors: *A. GHOSH**[1], E. GLASGOW[2], P. A. FORCELLI[3];
[1]Dept. of Pharmacol. & Physiol., Georgetown Univ. Med. Ctr., Washington, DC; [2]Dept. of Oncology, [3]Dept of Pharmacol. & Physiol., Georgetown Univ., Washington, DC

**Abstract: Problem**: Phenobarbital (PB) is the first-line anti-seizure medication (ASM) used to treat early-life seizures. PB exposure during critical neurodevelopmental windows, is linked to adverse neurological effects in children years after ASM exposure, and causes acute and long-term toxicity in preclinical rodent models. Despite over two decades of research into ASM-mediated neurotoxicity, nearly half of FDA-approved ASMs remain uncharacterized. This investigation used PB exposure in larval zebrafish to test the effectiveness of the platform as an efficient screen for ASM-mediated developmental neurotoxicity using histological and behavioral methodologies.
**Methods:** Following early-life PB (0uM control, 100uM, or 1000uM in E3 medium, n=7-24/group) exposure in 1-3 days post fertilization (dpf) zebrafish, the TUNEL assay was used to histologically assess acute neurotoxicity, while long-term toxicity was assessed with behavior assays after animals grew to adulthood (90+ dpf) using novel tank, light/dark, and social behavior tasks.

**Results:** PB produced region- and concentration-dependent elevations in TUNEL+ cells in larval zebrafish exposed starting in the second post-fertilization day. In the optic tectum, PB1000, but not PB100 increased the number of TUNEL+ cells. By contrast, in the brainstem, both PB100 and PB1000 increased the number of TUNEL+ cells. In frontal regions, neither concentration produced a significant increase in the number of TUNEL+ cells. Ongoing studies are evaluating narrower exposure windows. In adult animals (3 months) exposed to PB as larvae, we found a dose-dependent reduction in locomotion in the light-dark tank task, without a difference in preference for the light or dark chamber. When prompted with a social stimulus (a tank of conspecific zebrafish), PB100, but not PB1000 animals spent less time in social proximity than vehicle-treated controls. In the novel tank test, neither depth preference nor distance traveled differed amongst the treatment groups.
**Discussion:** Consistent with previous reports in rodents, these novel findings in zebrafish suggest that early-life PB exposure causes significant acute toxicity in the optic tectum and brainstem, and significantly affects some adult behavioral modalities, such as anxiety-like behavior and social drive. These data suggest that the larval zebrafish is a sensitive model system for screening ASM toxicity and that it may serve as a scalable screening platform for potential neurotoxic effects of ASMs.

**Disclosures: A. Ghosh:** None. **E. Glasgow:** None. **P.A. Forcelli:** None.

**Poster**

**PSTR169: Pharmacological and Non-Pharmacological Interventions for Brain Aging**

**Location:** WCC Halls A-C

**Time:** Monday, November 16, 2026, 1:00 PM - 5:00 PM

**Program #/Poster #:** PSTR169.09/M3

**Topic:** C.01. Brain Wellness and Aging

**Support:** 5R01AI187391-02

**Title:** Investigating The Potential Neuroprotective Effects of the Fungal Polysaccharide Glucuronoxylomannan (GXM) in adult and aged wild-type Mice

**Authors: *J. TOLLER**[1], C. WANG[6], M. HALL[1], K. ALVIÑA[2], L. MARTINEZ[3], C. L. CHARLES NINO[4], A. KELEGAMA[2], S. FIDELIA[5];
[2]Neurosci., [3]Oral Biollgy, [1]Univ. of Florida, Gainesville, FL; [4]Oral Biol., Univ. of Florida, GAINESVILLE, FL; [5]Oral Biol., Univ. of Florida, Port Saint Lucie, FL; [6]Neurosci., Univ. of Florida Dept. of Neurosci., Gainesville, FL

**Abstract:** Cryptococcus neoformans (Cn) is an encapsulated fungus that can lead to meningoencephalitis in immunocompromised individuals. Cn uses glucuronoxylomannan (GXM), the main capsular component, to evade host immune cells. GXM reduces the expression of pro-inflammatory cytokines, while also upregulating anti-inflammatory signals. Chronic neuroinflammation is a hallmark of aging and neurodegenerative diseases. We aimed to exploit this physiological phenomenon by investigating isolated GXM as a potentially neuro-modulatory

novel therapeutic approach against neuroinflammation. Therefore, we investigated the effects of GXM in reducing cognitive and physiological symptoms that concur with high neuroinflammation typical of aging. We used female adult wildtype mice (C57BL/6 strain, WT) to assess the ability of GXM to cross the Blood Brain Barrier (BBB). We validated this by using two injection methods, namely intravenous, and intraperitoneal. Mice were then processed at different times post injection: non-injected, 1, 6, and 24 hours. We then used immunohistochemistry and confocal imaging to assess where and when GXM accumulates in brain tissue. After the BBB validation we used male and female WT mice in two different age groups, adult (12-15 months old) or aged (>24 months old). Mice were then divided into two groups and injected with GXM during 7-or 15-days. Following GXM injections, mice underwent behavioral testing to assess cognitive function and exploratory behaviors. Subsequently, brain, visceral tissue, and serum samples were collected for quantification of several cytokines via ELISA. Our results indicate that GXM-treated mice exhibited reduced immobility time, increased center duration, and longer freezing latency compared with control mice. These behavioral changes are consistent with increased exploratory activity and suggest a reduction in anxiety-like behavior following GXM administration. We also observed significant differences in organ weights, including a reduction in adipose tissue mass in aged mice compared to adult mice and a decrease in spleen weight in adult male mice. Preliminary results show a significant effect of age on glucose levels, with aged mice exhibiting reduced glucose concentrations compared to adult mice, along with increased levels of the anti-inflammatory cytokine TGF-b in male adult mice. This project underscores the promising attributes of GXM as a potential therapeutic for the reduction of aging-related neuroinflammation and possibly in neurodegenerative diseases.

**Disclosures: J. Toller:** None. **C. Wang:** None. **M. Hall:** None. **K. Alviña:** None. **L. Martinez:** None. **C.L. Charles nino:** None. **A. Kelegama:** None. **S. Fidelia:** None.

**Poster**

**PSTR169: Pharmacological and Non-Pharmacological Interventions for Brain Aging**

**Location:** WCC Halls A-C

**Time:** Monday, November 16, 2026, 1:00 PM - 5:00 PM

**Program #/Poster #:** PSTR169.10/M4

**Topic:** C.01. Brain Wellness and Aging

**Support:** NIH AG072714 (BS, JLB)
Florida Department of Health Ed and Ethel Moore Alzheimer's Disease Research Program grant 21A11 (BS, JLB)
Diana Jacobs Kalman/AFAR Graduate Student Award in Geroscience

**Title:** Enhancing effects of voluntary oral Δ9THC and CBD consumption on working memory in aged rats

**Authors: *S. ZEQUEIRA**[1], B. SETLOW[2], J. L. BIZON[3];
[2]Dept. of Psychiatry, [1]Univ. of Florida, Gainesville, FL; [3]Neurosci., Univ. of Florida Dept. of Neurosci., Gainesville, FL

**Abstract:** With the increased legalization of recreational and medicinal cannabis, use is growing rapidly amongst older adults. As the number of older adults in the US is expected to reach 90 million by 2050, it is imperative to better understand the potential cognitive impacts of cannabis use in this population. Work from our lab and others has demonstrated that Δ9THC has pro-cognitive effects in aged subjects across several cognitive domains. The degree to which these benefits can be mimicked or influenced by other, non-psychoactive cannabinoids such as CBD remains unclear. In this study, we evaluated the effects of chronic oral self-administration of delta-9-tetrahydrocannabinol (THC; the primary psychoactive component of cannabis) cannabidiol (CBD; the primary non-psychoactive component of cannabis) and their combination on a delayed response task that assessed prefrontal cortex-dependent working memory in aged (23 months) Fischer 344 x Brown Norway F1 hybrid rats of both sexes. Rats were initially trained on the delayed response task until reaching stable performance prior to drug administration. Rats then consumed either plain gelatin or gelatin containing 1.0 mg/kg Δ9THC, 1.0 mg/kg CBD, or a 1:1 ratio of Δ9THC:CBD daily in their home cage. Working memory performance was assessed after three weeks of daily consumption. Results showed that chronic oral consumption of either Δ9THC, CBD, or the combination enhanced working memory accuracy. There were no main effects or interactions involving drug condition in the number of trials completed per session, indicating that task engagement was equivalent across groups. To evaluate Δ9THC and CBD pharmacokinetics, blood was collected via tail nicks at multiple timepoints after consumption and evaluated for Δ9THC and CBD as well as their major metabolites (11-OH-Δ9THC and 11-COOH-Δ9THC) via ultraperformance liquid chromatography-tandem mass spectrometry (UPLC-MS/MS). Initial data indicate that both cannabinoids were present in blood following oral consumption. Together, these results show that both CBD and Δ9THC can enhance working memory, and that the two cannabinoids do not appear to interact in their influences on this cognitive domain.

**Disclosures: S. Zequeira:** None. **B. Setlow:** None. **J.L. Bizon:** None.

**Poster**

**PSTR169: Pharmacological and Non-Pharmacological Interventions for Brain Aging**

**Location:** WCC Halls A-C

**Time:** Monday, November 16, 2026, 1:00 PM - 5:00 PM

**Program #/Poster #:** PSTR169.11/N1

**Topic:** C.01. Brain Wellness and Aging

**Support:** The Hilary and Galen Weston Foundation

**Title:** Hippocampal neurogenesis and transcriptional responses to repeated multifocal transcranial ultrasound stimulation in young and aged mice

**Authors: *D. MCMAHON**, V. JABR, S. QASIM, S.-K. WU, K. HYNYNEN;
Sunnybrook Res. Inst., Toronto, ON, Canada

**Abstract:** Transcranial ultrasound stimulation (TUS) is an emerging non-invasive neuromodulation approach with potential applications for age-related cognitive decline. While TUS has been shown to alter neural activity and plasticity-related signaling, its effects on structural markers of hippocampal plasticity in aged animals remain incompletely understood. Here, we assessed whether repeated multifocal TUS alters neurogenesis, perineuronal nets, glial reactivity, and transcriptional profiles in young and aged mice.
Methods: Young (8-10 weeks old) and aged (80-90 weeks old) C57BL/6J mice received six bilateral TUS or sham sessions over three weeks. Ultrasound was delivered using a 550 kHz focused transducer with sequential multifocal targeting intended to cover the bilateral hippocampus, nucleus reuniens, and prefrontal cortex. Sonications were delivered using 5 Hz pulse repetition frequency, 10 ms pulse duration, 1 MPa peak negative pressure, 12 s pulse trains, and 5% duty cycle, repeated six times per session across seven targets. Twenty-four hours after the final sonication, brain tissue was collected for immunofluorescent quantification of hippocampal neurogenesis markers, perineuronal nets, GFAP immunoreactivity, as well as qPCR and RNA-seq.
Results: Across age groups, TUS significantly increased BrdU+ and BrdU+/NeuN+ cell densities, consistent with enhanced survival or maturation of newly generated neurons. In aged mice, TUS significantly increased BrdU+/DCX+ cell density relative to aged sham controls (4.6-fold increase, $p < 0.05$), suggesting enhanced immature neuron generation or persistence. In the hippocampus, repeated TUS resulted in a 43% reduction in Bax/Bcl2 expression ratio relative to sham ($p < 0.05$). This shift toward pro-survival signaling may support survival or maturation of adult-born neurons. RNA-seq revealed negative enrichment of oxidative phosphorylation pathways in the hippocampus and prefrontal cortex of aged mice relative to sham. Repeated TUS did not significantly alter WFA+ perineuronal net density or WFA+/PV+ perineuronal net density across the dentate gyrus, CA1, or CA3. No evidence of astrogliosis or transcriptional indications of inflammation were observed.
Conclusion: Together, these findings suggest that repeated multifocal TUS can enhance select hippocampal neurogenesis-associated outcomes in aged and young mice, potentially driven by a shift towards pro-survival signaling.

**Disclosures: D. McMahon:** F. Consulting Fees (e.g., advisory boards); Grey Matter Neurosciences. **V. Jabr:** None. **S. Qasim:** None. **S. Wu:** None. **K. Hynynen:** F. Consulting Fees (e.g., advisory boards); Grey Matter Neurosciences.

**Poster**

**PSTR169: Pharmacological and Non-Pharmacological Interventions for Brain Aging**

**Location:** WCC Halls A-C

**Time:** Monday, November 16, 2026, 1:00 PM - 5:00 PM

**Program #/Poster #:** PSTR169.12/N2

**Topic:** C.01. Brain Wellness and Aging

**Support:** R35GM153232 (National Institutes of Health)

**Title:** Neuroprotection by Chronic Intermittent Propofol is Critically Dependent on α5-$GABA_A$ Receptors after Laparotomy in Aged Mice

**Authors: *R. NAGARAJAN**[1], J. LYU[1,2], M. KAMBALI[1], M. WANG[1,2], H.-Y. KUAN[1,2], R. A. PEARCE[4], U. RUDOLPH[1,2,3];
[1]Dept. of Comparative Biosciences, Col. of Vet. Med., [2]Neurosci. Program, [3]Carl R. Woese Inst. for Genomic Biol., Univ. of Illinois Urbana-Champaign, Urbana, IL; [4]Dept. of Anesthesiol., Univ. of Wisconsin, Madison, WI

**Abstract:** Perioperative neurocognitive disorder (PND) is a common complication in elderly patients and is mechanistically linked to surgery-induced microglial activation and hippocampal dysfunction. We previously demonstrated that chronic intermittent propofol (CIP) produces a sustained (5-day), non-canonical increase in neuronal surface expression of α5-containing $GABA_A$ receptors (α5-$GABA_A$ Rs) in the hippocampus and attenuates laparotomy-induced cognitive impairment, neuroinflammation, and caspase activation in aged C57BL/6J mice. However, whether α5-$GABA_A$ Rs are required for CIP-mediated protection remains unknown. To address this, aged (21-24 months) $\alpha5^{fl/fl}$ and global α5 knockout mice underwent exploratory laparotomy under isoflurane anesthesia and received CIP (75 mg/kg, i.p.) or vehicle every fifth day. Cognitive performance was assessed using hippocampus-dependent behavioral tests. Hippocampal tissue was analyzed by Western blot for pro-apoptotic markers (cleaved caspase-3, cleaved caspase-9, and Bax), and the microglial activation marker IBA-1, while nitrite levels were measured as an index of oxidative stress. Laparotomy induced significant cognitive deficits accompanied by increased IBA-1 expression, elevated nitrite production, and enhanced pro-apoptotic signaling. CIP prevented these molecular and behavioral abnormalities in $\alpha5^{fl/fl}$ mice but failed to confer protection in α5 knockout mice. These findings identify α5-$GABA_A$Rs as essential mediators of sustained propofol-induced neuroprotection in aging. Enhancing α5-$GABA_A$R surface expression suppresses postoperative neuroinflammation, oxidative stress, and expression of proapoptotic markers, thereby preserving hippocampal-dependent cognition and highlighting α5-$GABA_A$R-dependent inhibitory plasticity as a potential therapeutic target for PND.

**Disclosures: R. Nagarajan:** None. **J. Lyu:** None. **M. Kambali:** None. **M. Wang:** None. **H. Kuan:** None. **R.A. Pearce:** None. **U. Rudolph:** None.

**Poster**

**PSTR169: Pharmacological and Non-Pharmacological Interventions for Brain Aging**

**Location:** WCC Halls A-C

**Time:** Monday, November 16, 2026, 1:00 PM - 5:00 PM

**Program #/Poster #:** PSTR169.13/N3

**Topic:** C.01. Brain Wellness and Aging

**Support:** BrightFocus Foundation (A2022048S)
NIH-NINDS (R01 NS109226)
NIH via Goizueta Alzheimer's Disease Research Center (ADRC)
Alzheimer's Association Research Fellowship (AARFD-21-853104)

**Title:** Frequency-specific sensory stimulation reduces stress potentiated deficits in 5XFAD mice

**Authors: *T. C. FRANKLIN**[1], H. MOORE[1], A. L. PAULSON[2], K. IYER[3], A. SINGER[3], M. GOODSON[4], K. INAGAKI[3], J. MATTA[1], A. PRICHARD[6], R. DAS[3], L. WOOD[5], A. C. SINGER[7];
[1]Biomed. Engin., Georgia Inst. of Technology- Emory Univ., Atlanta, GA; [2]Biomed. Engin., Georgia Inst. of Technol., Cary, GA; [4]Biomed. Engin., [5]Inst. for Bioengineering and Biosci., [3]Georgia Inst. of Technol., Atlanta, GA; [6]Res., Durham Veterans Affairs Med. Ctr., Durham, NC; [7]Coulter Dept. of Biomed. Engin., Georgia Inst. of Technol. & Emory Univ., Atlanta, GA

**Abstract:** Chronic stress substantially increases Alzheimer's disease (AD) risk, likely through stress-induced disruption of neuroimmune function and the gut microbiome. We and others previously demonstrated that noninvasive frequency-specific audiovisual stimulation ("flicker") modulates neuroimmune signaling in brain regions implicated in stress-related and neurodegenerative disorders. In unstressed mouse models of amyloidosis, 40Hz flicker improves microglial and neuronal function. Separately, we have shown that frequency-specific flicker attenuates stress-induced behavioral, synaptic, and inflammatory phenotypes in a sex-dependent manner. However, the combined impact of chronic stress and amyloid pathology, a clinically relevant multi-hit condition in which multiple risk factors converge to accelerate disease progression, remains poorly understood, and whether flicker can mitigate stress-potentiated deficits in this context is unknown. To address this gap, male and female 5XFAD mice were exposed to 4 weeks of chronic unpredictable stress (CUS) and concomitantly treated with 10Hz or 40Hz audiovisual flicker, frequencies previously shown to ameliorate stress- or amyloid-associated pathology in isolation. We assessed stress- and flicker-induced effects on behavior, amyloid pathology, microglia, and the gut microbiome. Amyloid deposition and microglial morphology were quantified in the hippocampus using 3D image reconstruction and analysis. CUS significantly exacerbated physiological stress responses in 5XFAD mice and produced locomotor and anxiety-like behavioral impairments. Flicker mitigated these deficits in a frequency- and sex-dependent manner, with the strongest protective effects observed in males. Chronic stress promoted a pathological trend characterized by greater amyloid burden, increased accumulation of larger plaques, and reduced microglial-amyloid interactions. Frequency-specific flicker prevented stress-associated plaque accumulation and restored microglial colocalization and engulfment of amyloid. Finally, 16S rRNA sequencing revealed sex-specific stress-associated alterations in the fecal microbiome that were mitigated by chronic flicker exposure. Together, these findings identify chronic stress as a potent amplifier of AD-related pathology and demonstrate that frequency-specific flicker counteracts behavioral, neuroimmune, amyloid, and microbiome dysfunction arising from the combined effects of stress and amyloidosis. These results support noninvasive flicker as a promising strategy for reducing neurodegenerative vulnerability in populations exposed to chronic stress.

**Disclosures: T.C. Franklin:** None. **H. Moore:** None. **A.L. Paulson:** None. **K. Iyer:** None. **A. Singer:** None. **M. Goodson:** None. **K. Inagaki:** None. **J. Matta:** None. **A. Prichard:** None. **R. Das:** None. **L. Wood:** E. Ownership Interest (stock, stock options, royalty, receipt of intellectual

property rights/patent holder, excluding diversified mutual funds); Intellectual property rights/Patent holder. **A.C. Singer:** A. Employment/Salary (full or part-time):; Scientific Advisory Board for Cognito Therapeutics. E. Ownership Interest (stock, stock options, royalty, receipt of intellectual property rights/patent holder, excluding diversified mutual funds); Intellectual property rights/Patent holder.

**Poster**

**PSTR169: Pharmacological and Non-Pharmacological Interventions for Brain Aging**

**Location:** WCC Halls A-C

**Time:** Monday, November 16, 2026, 1:00 PM - 5:00 PM

**Program #/Poster #:** PSTR169.14/N4

**Topic:** C.01. Brain Wellness and Aging

**Title:** Reversing molecular brain aging dissociates from cognitive benefit: a multi-modal screen of geroprotectors and $\Delta^9$-tetrahydrocannabinol

**Authors: *A. BALAKRISHNAN**[1], L. BEHARRY[1], I. GONEHAL[2];
[1]Novaflow, San Francisco, CA; [2]Novaflow, Riverside, CA

**Abstract: Reversing molecular brain aging dissociates from cognitive benefit:a multi-modal screen of geroprotectors and Δ9-tetrahydrocannabinol**Brain aging proceeds through distinct molecular programs: neuroinflammation, synaptic loss, mitochondrial/metabolic decline, vascular degradation, and demyelination. Whether drugs that reversethese molecular signatures also preserve cognition is unclear, and “rejuvenation” claims are sel-dom tested against independent measures. From drug-free brains we trained regularized-regressionaging clocks and curated program signatures in two modalities (gene expression and DNA methy-lation), plus an orthogonal protein-level readout; we then froze these models and transfer-scoreddrug-treated versus control samples to quantify movement toward a younger molecular profile. Weevaluated two senolytics, dasatinib plus quercetin (D+Q) and navitoclax (ABT-263); rapamycinand caloric restriction (CR); and low-dose Δ9-tetrahydrocannabinol (THC) in aged rodent andhuman brain datasets, with cross-cohort replication and randomization-based controls.Senolytics broadly reversed aging signatures: D+Q lowered neuroinflammation and restored synaptic, vascular, and myelination programs in aged hippocampus, while ABT-263 acted more narrowly.Low-dose THC, which rescues memory in aged mice, did not reverse the molecular aging signature, revealing a dissociation between molecular rejuvenation and cognitive benefit. THC’s signal was faint and non-reproducible across mRNA cohorts, yet pronounced at the protein level, where it coherently suppressed mitochondrial oxidative-phosphorylation proteins in human neuronal cells, a metabolic, post-transcriptional mechanism transcriptomics misses. A reported epigeneticrejuvenation by rapamycin/CR did not survive randomization controls, and a senolytic effective in vivo failed in brain organoids lacking peripheral senescence. Reversing molecular brain aging is therefore neither equivalent to nor sufficient for cognitive benefit.By placing cognitively-beneficial and broadly clock-reversing drugs on one multi-modal instrument, we deliver what single-clock studies could not: a direct dissociation of molecular age from cognition, a relocation of THC’s measurable action to a metabolic, post-transcriptional layer, and

randomiza-tion controls that reject rejuvenation artifacts. We propose this mechanism- and modality-awarescreen as a more reliable basis for evaluating candidate brain geroprotectors than any single molecular aging clock.

**Disclosures: A. Balakrishnan:** None. **L. Beharry:** None. **I. Gonehal:** None.

**Poster**

**PSTR169: Pharmacological and Non-Pharmacological Interventions for Brain Aging**

**Location:** WCC Halls A-C

**Time:** Monday, November 16, 2026, 1:00 PM - 5:00 PM

**Program #/Poster #:** PSTR169.15/N5

**Topic:** C.01. Brain Wellness and Aging

**Title:** Metabolomic and proteomic profiling of the effects of engineered Lactococcus lactis on intestinal neurochemicals and the gut epithelial barrier

**Authors: *K. SHARMA**[1], S. NAVA[2], S. PRADHAN[1], J. OCHOA-REPARAZ[3], C. BLANTON[1];
[2]Biomed. and Pharmaceut. Sci., [1]Idaho State Univ., Pocatello, ID; [3]Boise State Univ., Boise, ID

**Abstract:** The communication between the gut and the brain occurs through complex biological networks, including shifting microbial populations and metabolic pathways. The gut microbiota produces essential amino acids and neuroactive molecules such as gamma-aminobutyric acid (GABA), dopamine, and serotonin that directly influence epithelial barrier integrity. Consequently, the intestinal epithelium serves as a dynamic interface where localized neurochemical production and barrier function are interdependent. Modulating the gut-brain axis using engineered probiotics designed to synthesize specific neuroactive molecules represents a promising therapeutic frontier. This study investigates the impact of *P8-GAD-Lactococcus lactis*, a probiotic strain engineered to express glutamate decarboxylase (GAD) and produce GABA, on the neurochemical profiles and intestinal barrier integrity of adult female Sprague-Dawley (SD) rats. To characterize the neurochemical shifts of this intervention, a targeted liquid chromatography-mass spectrometry (LC-MS) method was developed to simultaneously quantify key metabolites GABA, glutamic acid, succinic acid, and glutamine extracted from fecal, colonic, and brain tissues. Additionally, to evaluate gut barrier function and potential epithelial leakage, untargeted LC-MS/MS proteomics was performed on colon tissues to identify differentially expressed proteins, focusing on tight junction complexes, inflammatory biomarkers, and structural mucus barrier proteins. This study establishes a robust analytical framework combining targeted metabolomics and untargeted tissue proteomics to evaluate engineered probiotic interventions. These findings will clarify how localized, probiotic-derived GABA production influences both neurochemical profiles and local colonic integrity, offering crucial insights into the therapeutic potential of *P8-GAD-Lactococcus lactis* in modulating the gut-brain axis.

**Disclosures: K. Sharma:** None. **S. Nava:** None. **S. Pradhan:** None. **J. Ochoa-Reparaz:** None. **C. Blanton:** None.

**Poster**

**PSTR169: Pharmacological and Non-Pharmacological Interventions for Brain Aging**

**Location:** WCC Halls A-C

**Time:** Monday, November 16, 2026, 1:00 PM - 5:00 PM

**Program #/Poster #:** PSTR169.16/N6

**Topic:** C.01. Brain Wellness and Aging

**Support:** NIH Grant 5R01AG085279-02

**Title:** Pharmacoexposomic profiling reveals therapeutic drug-associated metabolic networks linked to cognitive impairment in aging

**Authors: *J. JEON**[1], D. C. GERMAN[2], J. R. RICHARDSON[3], Y. GO[1], D. P. JONES[1]; [1]Emory Univ., Atlanta, GA; [2]Psychiatry, U Texas Southwestern Med. Cntr., Dallas, TX; [3]Univ. of Georgia, Athens, GA

**Abstract:** Cognitive impairment is associated with substantial inter-individual metabolic variability that is not fully explained by clinical characteristics or documented medication use. Therapeutic drug exposures may contribute to this variability through interactions with endogenous metabolic pathways, yet drug-associated metabolic signatures in cognitive impairment remain poorly characterized. Therefore, we applied PharmMet- based pharmacometabolomic network analysis to identify therapeutic drug-associated metabolite communities and metabolic pathways linked to cognitive impairment. Total of 542 participants were included in this study (median: 67 years; 60% female; 50% Hispanic, 50% White), including 367 cognitively unimpaired (CU) and 175 cognitively impaired (CI). Their first-draw plasma samples were analyzed using untargeted liquid chromatography-high resolution mass spectrometry (LC-HRMS), and detected features were annotated using PharmMET, a reference database of therapeutic drug metabolites generated from human liver S9 fractions. PharmMET-annotated drug-derived features were integrated with endogenous metabolites using xMWAS to generate therapeutic drug-associated metabolic networks. Correlation-based networks were analyzed, followed by pathway enrichment analysis using Mummichog 1.0. Medication record analysis suggests a higher prevalence of antidepressant/psychiatric medications in CI (CI: 24.6% vs. CU: 17.4 %). Cardiovascular (CI: 46.9% vs. CU: 40.3%) and antidiabetic (CI: 22.3% vs. CU: 20.7%) was also more prevalent in CI. PharmMet-based annotation linked metabolites were matched across multiple medication classes. In CU, correlation analysis showed the largest clusters from cetirizine (58) and buspirone (42). In CI, the buspirone cluster expanded to 199 metabolites, and duloxetine cluster containing 201 metabolites emerged exclusively. Pathway enrichment analysis of CI clusters identified pentose phosphate pathway metabolism (p=0.0417) and fatty acid biosynthesis (p=0.0351), represented by D-ribose and 6-phosphogluconolactone. The duloxetine cluster was associated with linoleic acid metabolism (p=0.0045) and biosynthesis of unsaturated fatty acids (p=0.0196), represented by linoleic acid, palmitic acid, and stearic acid.

These findings demonstrate that PharmMet allows pharmacoexposomic profiling to detect real-world therapeutic drug exposures in human plasma and identify exposure-associated metabolic signatures linked to cognitive impairment. This approach may improve characterization of pharmacologic contributors to metabolic heterogeneity in aging populations.

**Disclosures: J. Jeon:** None. **D.C. German:** None. **J.R. Richardson:** None. **Y. Go:** None. **D.P. Jones:** None.

**Poster**

**PSTR169: Pharmacological and Non-Pharmacological Interventions for Brain Aging**

**Location:** WCC Halls A-C

**Time:** Monday, November 16, 2026, 1:00 PM - 5:00 PM

**Program #/Poster #:** PSTR169.17/N7

**Topic:** C.01. Brain Wellness and Aging

**Support:** R43 AG047722/AG/NIA NIH HHS/United States
R44 AG047722/AG/NIA NIH HHS/United States

**Title:** Speed based cognitive training increases fMRI-BOLD signals in sensorimotor regions during multitasking: a neural mechanism of transfer in healthy aging

**Authors: *C. BASAK**[1], Y. LIU[1], P. SKOLASINSKA[1], S. QIN[2], M. VOSS[3], H. LEE[4]; [1]Univ. of Texas at Dallas, Dallas, TX; [2]Natl. Univ. of Singapore, Singapore, Singapore; [3]Psychological and Brain Sci., The Univ. of Iowa, Iowa City, IA; [4]Post Sci. Corp., San Francisco, CA

**Abstract:** This study used a hybrid block- and event-related (ER) task-switching fMRI paradigm (Nashiro et al., 2018) to examine training-related transfer to cognitive control. This design assessed block-level global switch costs and trial-level mixing, local switch, and incompatibility costs, across single and dual task blocks (Basak et al., 2018; Nashiro et al., 2018; Qin & Basak, 2020).Participants from Dallas and Iowa were assigned to BrainHQ cognitive training (CT) or active control (AC) group (Lee et al., 2024). The final sample included 114 older adults with behavioral, demographic, and fMRI data: 53 CT, 61 AC; Dallas $n = 52$, Iowa $n = 62$; $M_{age} = 71.88$ years, $SD = 4.64$; 64 female, 50 male. Whole-brain Group × Time analyses showed training-related neural changes in global switch costs and sensorimotor incompatibility cost (IC). Results were cluster-corrected at $p < .05$, with cluster-forming threshold $Z > 1.96$, to detect the within subject change. Follow-up analyses on these resulting ROIs were FDR-corrected. For the block design GLM, Group × Time interactions were observed in thalamus/putamen/pallidum for Single > Dual, implicating training related change in global switching. Follow-up ANCOVA showed a significant group effect for the Single > Dual contrast, even after controlling for differences in baseline activation, $F(1,102) = 11.68$, $q = .005$. CT showed a higher increase in post-training activation than AC for Single, compared to Dual, implicating greater engagement of basal ganglia after speed-based BrainHQ training for a choice RT transfer task. The Group × Time ROI from the incompatibility cost contrast (incompatible > compatible) included

SMA/cingulate/precentral regions. Repeated measures ANOVA for this IC-sensitive region showed a significant Group × Time effect for IC, $F(1,174) = 12.17$, $q = .002$, but this did not vary by compatibility. CT, not AC, showed a post-training increase in activation, suggesting increased sensorimotor recruitment during incompatible stimulus-response (SR) mapping.Furthermore, group moderated the relationship between post-training IC activation and post-training IC Cost, $F(1,81) = 13.64$, $q = .019$. In CT, increased post-training IC activation in SMA/cingulate/precentral cluster was associated with reduced IC RT cost, $F(1,81) = 4.70$, $p = .033$, implicating BrainHQ-related sensorimotor recruitment to improved incompatible SR mapping. Additional brain regions were also observed, but they were not sensitive to cognitive control. We will discuss the impacts of CT on varieties of cognitive control, and whether these effects are site invariant or not.

**Disclosures: C. Basak:** None. **Y. Liu:** None. **P. Skolasinska:** None. **S. Qin:** None. **M. Voss:** None. **H. Lee:** A. Employment/Salary (full or part-time):; Posit Scinece Corporation. E. Ownership Interest (stock, stock options, royalty, receipt of intellectual property rights/patent holder, excluding diversified mutual funds); Posit Science Corporation.

**Poster**

**PSTR169: Pharmacological and Non-Pharmacological Interventions for Brain Aging**

**Location:** WCC Halls A-C

**Time:** Monday, November 16, 2026, 1:00 PM - 5:00 PM

**Program #/Poster #:** PSTR169.18/N8

**Topic:** C.01. Brain Wellness and Aging

**Support:** Office of Undergraduate Research – Magellan Scholar Grant to MJP
South Carolina Honors College Undergraduate Research Grant to MJP
NIH Grant P20GM109091 to JAM
NIH Grant K01AG061263 to JAM

**Title:** Targeting D-Serine Metabolism Enhances Memory and NMDA Receptor-Associated Signaling in Aged Rats

**Authors: *M. J. PITRE**, D. J. HOROVITZ, M. A. TIEMAN, A. E. SIKORA, C. D. WOHLFELD, M. A. FRICK, J. R. FADEL, J. A. MCQUAIL;
Univ. of South Carolina, Columbia, SC

**Abstract:** D-serine, an endogenous co-agonist at NMDA receptors, regulates synaptic plasticity and memory and has been investigated as a target for the treatment of age-related cognitive decline, including conditions such as mild cognitive impairment and Alzheimer's disease. However, a key unresolved question is whether age-related reductions in D-serine synthesis and availability meaningfully account for variability in memory performance, and whether enhancing this pathway remains capable of improving memory and NMDA receptor-associated signaling in the aged brain. To address this, we integrated behavioral phenotyping, metabolic analysis, protein expression, and in vivo signaling in young (4-6 months) and aged (22-24 months) F344

rats of both sexes. All animals were first assessed on a standardized hippocampus-dependent spatial learning task to quantify individual differences in performance. D-serine and related metabolites were measured in hippocampus and frontal cortex using HPLC, alongside serine racemase protein expression. In a complementary within-subjects behavioral pharmacology experiment, a subset of animals was tested on a delayed match-to-place spatial memory task following administration of a D-amino acid oxidase (DAAO) inhibitor, a pharmacological approach used to increase endogenous D-serine availability. ERK phosphorylation was subsequently assessed in hippocampus and frontal cortex as an index of NMDA receptor-associated signaling engaged during memory performance. Aging was associated with reduced hippocampal D-serine and decreased serine racemase expression, yet these measures showed weakened and less reliable relationships with spatial learning performance in aged animals. In contrast, DAAO inhibition improved memory performance across aged subjects and was accompanied by increased ERK activation in both hippocampus and frontal cortex. These effects were observed in both males and females. Together, these findings indicate that age-related changes in D-serine biology do not tightly determine cognitive outcome but instead define a pathway that can be engaged to improve memory-related signaling and behavior. By demonstrating that this system retains the capacity to support memory when appropriately activated, these results provide a clearer basis for understanding how D-serine-targeted approaches might be used to enhance cognitive function in aging and related neurodegenerative conditions.

**Disclosures: M.J. Pitre:** None. **D.J. Horovitz:** None. **M.A. Tieman:** None. **A.E. Sikora:** None. **C.D. Wohlfeld:** None. **M.A. Frick:** None. **J.R. Fadel:** None. **J.A. McQuail:** None.

**Poster**

**PSTR169: Pharmacological and Non-Pharmacological Interventions for Brain Aging**

**Location:** WCC Halls A-C

**Time:** Monday, November 16, 2026, 1:00 PM - 5:00 PM

**Program #/Poster #:** PSTR169.19/O1

**Topic:** C.01. Brain Wellness and Aging

**Support:** NIH Grant K01AG061263 to JAM
University of South Carolina Office of Vice-President of Research to PJV and JAM

**Title:** A Reverse-Translated Rodent Dual-Task Paradigm for Investigating Cognitive Aging

**Authors:** A. M. MAHONEY, L. E. STONE, H. A. DUFALA, S. M. HARDING, P. J. VENTO, ***J. A. MCQUAIL**;
Univ. of South Carolina, Columbia, SC

**Abstract:** Executive function is critical for coordinating behavior across changing task demands and is particularly vulnerable to cognitive aging. Human dual-task paradigms have revealed age-related impairments in task coordination, yet mechanistic investigation of these processes

requires translational animal models. To address this gap, we reverse-translated a block-structured dual-task paradigm from the human task-switching literature and adapted it for use in rats. Using a cross-sectional design, male and female Fischer 344 rats were tested at 7 and 26 months of age. Rats were trained in operant chambers to perform matching-to-sample and nonmatching-to-sample rules under single-task and dual-task conditions. Additional task variants manipulated executive demands through rule-memory and rule-on-demand conditions, in which rule-specific cues were available only during the sample phase or only during the choice phase, respectively. Performance accuracy declined as task demands increased. Accuracy declined from single-task to dual-task conditions and was lower during nonmatching than matching trials. Aging was associated with reduced overall accuracy, with deficits most evident under cognitively demanding conditions. In contrast, response latency was comparatively less sensitive to task demands, suggesting that age-related impairments were expressed primarily as reduced choice accuracy rather than generalized slowing. Manipulating the timing of rule information further produced distinct behavioral profiles, indicating that the paradigm engages multiple executive demands. These findings establish a reverse-translated rodent dual-task paradigm that will enable mechanistic investigation of age-related changes in executive control and experimental interrogation of the neural circuits that support task switching.

**Disclosures: A.M. Mahoney:** None. **L.E. Stone:** None. **H.A. Dufala:** None. **S.M. Harding:** None. **P.J. Vento:** None. **J.A. McQuail:** None.

**Poster**

**PSTR169: Pharmacological and Non-Pharmacological Interventions for Brain Aging**

**Location:** WCC Halls A-C

**Time:** Monday, November 16, 2026, 1:00 PM - 5:00 PM

**Program #/Poster #:** PSTR169.20/Web Only

**Topic:** C.01. Brain Wellness and Aging

**Title:** Is vigorous physical activity associated with verbal episodic memory in older adults?

**Authors: J. PHILLIPS**, *K. RODRIGUEZ;
Neuropsychology, Orlando Hlth., Orlando, FL

**Abstract:** Previous research has identified a relationship between physical activity and memory in adults, however, less is known specifically about the association between vigorous physical activity and verbal episodic memory in older adults. The present study used a confirmatory approach to examine the relationship between vigorous physical activity frequency and verbal episodic memory, measured using a delayed word recall task, in older adults. This research further underscores how physical activity may be related to memory performance in later adulthood. Data were obtained from the Midlife in the United States (MIDUS 3): Retention Early Warning Project (2018-2019). The final sample included 525 adults (M age = 62.7 years, SD = 9.49). A multiple linear regression was conducted to examine the association between vigorous physical activity frequency and delayed recall performance while controlling for age. Verbal episodic memory was assessed using a delayed word recall task. Vigorous physical

activity frequency was measured using a self-report item assessing participation in vigorous physical activity during the summer. The overall regression model was significant, $F(6, 518) = 16.4$, $p < .001$, and explained 16.0% of the variance in delayed recall performance ($R2 = .160$). Age was a significant predictor of memory performance, with older participants demonstrating poorer delayed recall. After controlling for age, participants who reported never engaging in vigorous physical activity exhibited significantly poorer delayed recall performance than those who engaged in vigorous physical activity several times per week ($p = .028$). No other physical activity frequency group differed significantly from the reference group. These results suggest that older adults who never engage in vigorous physical activity may demonstrate poorer delayed recall performance than those who engage in vigorous physical activity several times per week, independent of age. Interestingly, individuals who engaged in vigorous physical activity less than once per month did not differ significantly in delayed recall performance from those who engaged in vigorous physical activity several times per week. These findings could potentially inform clinician recommendations regarding lifestyle behaviors that support cognitive health.

**Disclosures: J. Phillips:** None. **K. Rodriguez:** None.

**Poster**

**PSTR169: Pharmacological and Non-Pharmacological Interventions for Brain Aging**

**Location:** WCC Halls A-C

**Time:** Monday, November 16, 2026, 1:00 PM - 5:00 PM

**Program #/Poster #:** PSTR169.21/O2

**Topic:** F.09. Motor Neurons and Muscle

**Title:** Systemically targeted intracellular delivery of glucose dendrimer- creatine nano-therapeutics in creatine transporter deficiency disorder.

**Authors: *D. CHERUKARAVEEDU**[1], P. VYAS[2], K. MURUGESAN[1], N. R. KALE[2], W. LIYANAGE[3], J. ALLENDE LABASTIDA[4], S. A MOHANAKRISHNAN[5], L. JU[6], M. K. PERNA[8], M. R. SKELTON[9], J. XU[3], E. W. TUCKER[10], R. KANNAN[7], S. KANNAN[2]; [1]Ctr. for Nanomedicine, Dept. of Ophthalmology, Wilmer Eye Institute, JHU SOM,, Baltimore, MD; [2]Dept. of Anesthesiol. and Critical Care Med., JHU SOM, Baltimore, MD; [3]Johns Hopkins Univ. Sch. of Med., Baltimore, MD; [4]Dept. of Pharmacol. and Toxicology, Univ. of Texas Med. Br., Galveston, TX; [5]Ctr. for Nanomedicine, Dept. of Ophthalmology, Wilmer Eye Institute, JHU SOM, Baltimore, MD; [6]Radiology, [7]Johns Hopkins Univ., Baltimore, MD; [8]Dept. of Pediatrics, Univ. of Cincinnati Col. of Med. and Div. of Neurol., Cincinnati Children's Res. Fndn., Cincinnati, OH; [9]Neurol., Cincinnati Childrens Res. Fndn., Cincinnati, OH; [10]ACCM, Johns Hopkins Hosp., Baltimore, MD

**Abstract:** Creatine transporter deficiency (CTD) is an X-linked metabolic disorder caused by pathogenic variants in SLC6A8, which encodes the creatine transporter (CrT). CTD is characterized by intellectual disability, speech delay, behavioral abnormalities, seizures, and markedly reduced brain creatine (Cr) levels. Despite its severe clinical burden, there are no FDA-approved therapies. Effective treatment requires restoration of brain creatine and

phosphocreatine (P-Cr) levels; however, defective or absent transporters limit creatine uptake across the blood-brain barrier and into neural cells. Thus, a transporter-independent strategy for intracellular creatine delivery may provide a viable therapeutic approach. To address this need, we developed a glucose dendrimer-creatine conjugate (GD-Cr) using click chemistry and an esterase-sensitive linker. The nanocarrier contains 10.3 wt% creatine and provides sustained release for up to 14 days under intracellular conditions. Following cellular uptake, creatine is released from the dendrimer, enabling intracellular delivery and participation in the Cr-P-Cr energy shuttle independent of CrT activity. In vitro studies using neuronal cells treated with creatine transporter inhibitors confirmed successful intracellular creatine delivery despite transporter blockade. For vivo evaluation, CrT−/y knockout mice were used to model CTD. Systemic GD-Cr administration increased brain creatine levels, while tissue MALDI analyses demonstrated elevations in both creatine and phosphocreatine, indicating target engagement. Treatment also improved disease-related phenotypes, including grip strength and body weight. MRI CEST imaging showed decreased creatine and increased P-Cr levels relative to baseline, suggesting enhanced intracellular utilization and conversion of creatine to phosphocreatine. Ongoing studies are evaluating pharmacokinetics, biodistribution, efficacy, and safety. Collectively, these findings support GD-mediated creatine delivery as a promising nanotherapeutic strategy for CTD.

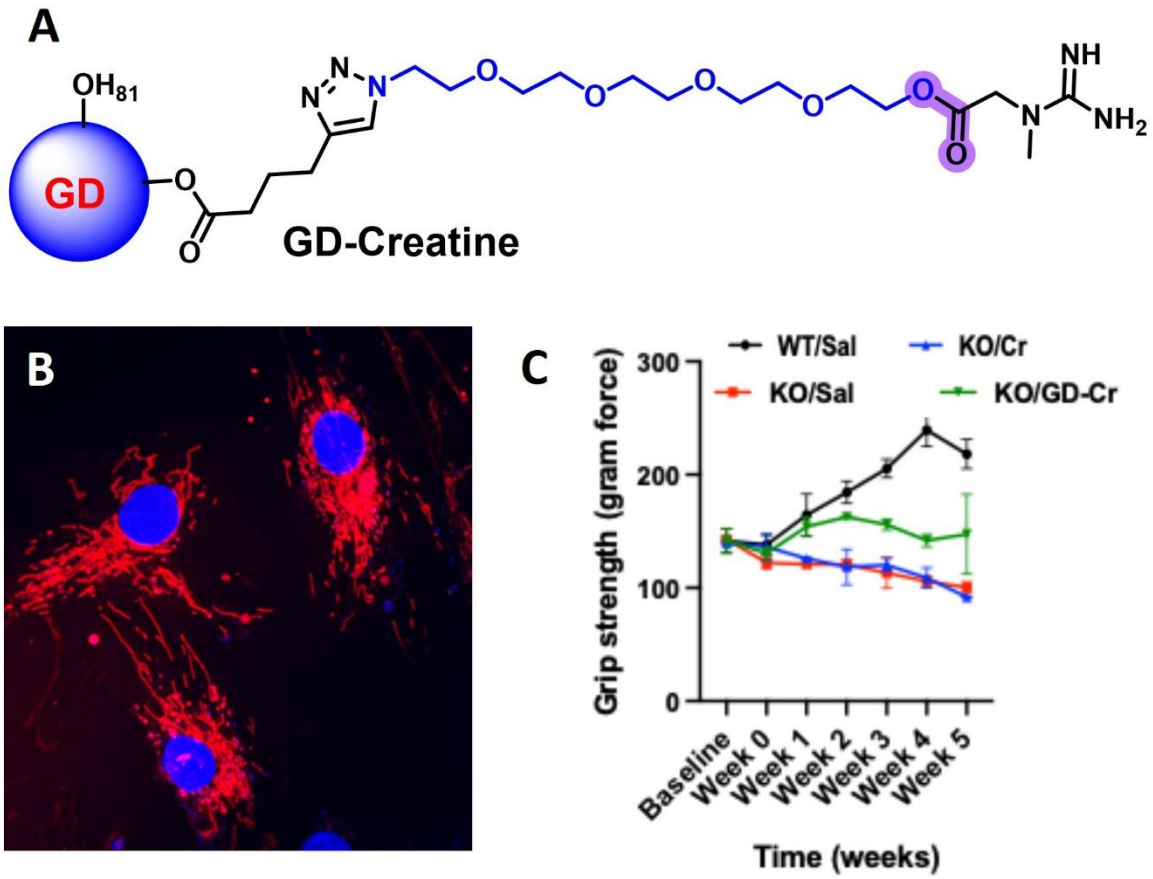



Figure 1. The chemically synthesized GD-Creatine conjugate were designed to deliver creatine intracellularly mediated by esterase activity (A). The human primary skin fibroblasts which do not have functional creatine transporter (SLC6A8) showed cellular uptake of the fluorophore (Cy-5) labeled Cy5-GD-Creatine (B). The *in-vivo* experiments proved the effective creatine delivery in mice which lacks the natural creatine transporters (KO mice) by improving their grip strength compared to the untreated KO mice (C).

**Disclosures: D. Cherukaraveedu:** None. **P. Vyas:** None. **K. Murugesan:** None. **N.R. Kale:** None. **W. Liyanage:** None. **J. Allende Labastida:** None. **S. A Mohanakrishnan:** None. **L. Ju:** None. **M.K. Perna:** None. **M.R. Skelton:** None. **J. Xu:** None. **E.W. Tucker:** None. **R. Kannan:** None. **S. Kannan:** None.

**Poster**

**PSTR170: Systemic Factors, Inflammation, and Brain Function**

**Location:** WCC Halls A-C

**Time:** Monday, November 16, 2026, 1:00 PM - 5:00 PM

**Program #/Poster #:** PSTR170.01/O3

**Topic:** C.01. Brain Wellness and Aging

**Support:** NEI, NIH Grant R21 EY034326-01A1

**Title:** An analysis of multiscale entropy in the brain dynamics of individuals with diabetic retinopathy

**Authors: *S. F. NEWBOLDS**[1], E. STACY[2], I. SLUCH[4], J. T. TOWNSEND[5], M. J. WENGER[3];
[1]Psychology, The Univ. of Oklahoma, Norman, OK; [2]Univ. of Oklahoma, Norman, OK, ; [3]Ctr. for Applied Social Res., Univ. of Oklahoma, Norman, OK; [4]Oklahoma City Veterans Admin., Oklahoma City, OK; [5]Psychological and Brain Sci., Indiana Univ., Bloomington, IN

**Abstract:** Diabetic retinopathy (DR) is a complication of diabetes caused by chronic hyperglycemia and is the leading cause of blindness among working-age adults. In 2020, DR was estimated to affect over 103 million adults globally, and its prevalence is expected to continue rising. DR manifests as retinal lesions, hemorrhages, and microaneurysms, which progressively worsen over time. These changes are associated with significant visual impairment, negatively impacting activities of daily living such as reading, working, and socializing. Importantly, individuals with DR, regardless of disease severity, also face an increased risk of developing neurodegenerative conditions compared to those with diabetes alone. Previous studies have identified higher rates of all-cause dementia, Alzheimer's disease, and vascular dementia in this population. Despite these associations, evidence regarding the impact of DR on neural dynamics remains extremely limited. The present study aims to address this gap by examining the effects of DR on brain dynamics using multiscale entropy (MSE) complexity analysis of EEG data collected during a facial perception task. MSE is a non-linear analytical method used to characterize variability in brain states associated with aging and disease. We applied MSE analyses to EEG data from a cohort of participants with DR to assess changes in complexity of brain dynamics. The findings indicate that DR alters the complexity of neural activity, providing potential biomarkers for DR-related neural effects and possible associations with increased risk of neurodegenerative diseases. Integrating behavioral and neurophysiological data, this study offers new insights into neural encoding, processing deficits, and neural resilience in individuals with DR.

**Disclosures: S.F. Newbolds:** None. **I. Sluch:** None. **J.T. Townsend:** None. **M.J. Wenger:** None.

**Poster**

**PSTR170: Systemic Factors, Inflammation, and Brain Function**

**Location:** WCC Halls A-C

**Time:** Monday, November 16, 2026, 1:00 PM - 5:00 PM

**Program #/Poster #:** PSTR170.02/O4

**Topic:** C.01. Brain Wellness and Aging

**Title:** Preclinical Evidence for Sex-Dependent Vulnerabilities to Doxorubicin-Induced Cognitive Impairment

**Authors: *C. G. FOWLER**, S. B. BOTNER, V. MUÑIZ, A. J. DITLEV, L. E. KUSUMO, E. G. VICHAYA;
Baylor Univ., Waco, TX

**Abstract:** Chemotherapy-induced cognitive impairment (CICI) is reported in over 35% of cancer survivors and is characterized by changes in memory and executive function. Understanding risk factors for developing CICI may provide valuable insight into mechanisms and treatment. Clinical evidence suggests women are more likely to develop CICI, but there are limited preclinical studies directly investigating the role of sex in symptom expression and neurobiological changes. Our study utilizes doxorubicin, a common chemotherapy used in the treatment of breast cancers as well as lymphomas, leukemias, and sarcomas. Doxorubicin is associated with CICI symptoms, including impaired executive function and short-term memory, implicating frontohippocampal dysfunction. We aimed to directly compare the behavioral and neurobiological changes associated with doxorubicin chemotherapy between male and female mice. We used 25 to 29 week-old C57BL/6 mice in a 2 (male vs. female) x 2 (+/- doxorubicin) experimental design (n = 5-6/group). Doxorubicin (5 mg/kg) or saline vehicle was administered once a week for two weeks followed by 4 weeks of rest and then another set of once weekly doses (total cumulative dose of 20 mg/kg). Body weight and health were monitored throughout the study. Two weeks after the final dose, a battery of behavioral tasks assessing cognitive impairment and affective dysfunction was conducted, including Open Field (OF), Nest Building, Novel Object Place Recognition Test (NOPRT), Puzzle Box, and Forced Swim Test (FST). Following behavior, the hippocampus and frontal cortex were collected. Changes in gene expression for markers of neuroinflammation, mitochondrial dysfunction, and blood brain barrier integrity are ongoing. Doxorubicin treatment decreased body weight in both sexes. This effect was more pronounced in male mice ($p = 0.004$), with doxorubicin-treated male mice losing 15 +/- 2% of their body weight compared to 5+/- 2% in female mice. Despite the more blunted weight loss, female mice showed a more severe effect on nest building ($p = 0.010$). There was also a trending effect that doxorubicin-treated mice demonstrated poorer learning in the puzzle box task irrespective of sex ($p = 0.066$). Preliminary tissue analysis of the male groups reveals a trend toward doxorubicin-induced oxidative stress and apoptosis in the hippocampus. Overall, our results indicate that while doxorubicin exerts effects in both male and female mice, there may be task-specific differences in performance that require further investigation. Ongoing analyses and future studies seek to investigate the neurobiological mechanisms underlying these sex differences.

**Disclosures: C.G. Fowler:** None. **S.B. Botner:** None. **V. Muñiz:** None. **A.J. Ditlev:** None. **L.E. Kusumo:** None. **E.G. Vichaya:** None.

**Poster**

**PSTR170: Systemic Factors, Inflammation, and Brain Function**

**Location:** WCC Halls A-C

**Time:** Monday, November 16, 2026, 1:00 PM - 5:00 PM

**Program #/Poster #:** PSTR170.03/O5

**Topic:** C.01. Brain Wellness and Aging

**Support:** NIA R01 AG063849-01
Charles Raison Scholarship in Depression

**Title:** Investigating heart rate variability (hrv) as a predictor of postoperative delirium (pod)

**Authors: *M. R. HESS**[1], M. I. BANKS[2], R. C. LENNERTZ, III[3];
[1]Univ. of Wisconsin-Madison, Madison, WI; [2]Dept. of Anesthesiol., Univ. of Wisconsin, Madison, WI; [3]Dept. of Anesthesiol., Univ. of Wisconsin, Madison, Madison, WI

**Abstract:** Postoperative delirium (POD) is an acute disorder of consciousness associated with poor clinical outcomes and increased risk of Alzheimer's disease and related dementias. While heart rate variability (HRV) has emerged as a promising biomarker for POD, the relationship between baseline autonomic function and POD risk remains poorly defined. HRV quantifies efferent noradrenergic and cholinergic signaling by measuring variations between R-peaks on an electrocardiogram, associating with emotional and physical wellbeing. It is thought that POD pathophysiology affects these underlying neurobiological pathways, suggesting that baseline autonomic activity may act as a predictor of POD. Here, we conducted an exploratory analysis of an ongoing prospective longitudinal cohort study, Interventions for Postoperative Delirium Biomarker-3 (IPOD-B3) registered with clinicaltrials.gov (NCT03124303), to investigate the relationship between POD and baseline HRV. This study received IRB approval from University of Wisconsin-Madison (2015-0374). Participants ≥ 65 years old undergoing non-intracranial surgery with an anticipated hospital stay of ≥ 2 days were included. Patients were excluded if they had a history of dementia, resided in a nursing home, or could not complete study assessments. We hypothesized that baseline Root Mean Squared of the Successive Differences (RMSSD), a time-domain measure of HRV, predicts POD incidence while controlling for patient age, sex, depression diagnosis, baseline cognitive scores, surgery length, and cardiac surgery type. We also hypothesized that HRV metrics would associate with a medical diagnosis of depression, such that a diagnosis of depression would associate with lower baseline RMSSD. Logistic regression assessed the relationship between delirium incidence and RMSSD. Multiple regression assessed the relationship between peak POD severity and RMSSD. All analyses were performed in R (R Studio 2023.12.1 Build 402, base 4.3.2), and statistical significance was defined as $p < .05$. No significant association was found between POD incidence ($p = .346$) or severity ($p = .311$) and baseline RMSSD, suggesting RMSSD may not be a predictor of POD. A significant association was found between a depression diagnosis and POD incidence ($p = .020$), consistent with previous reports linking baseline depression to POD. However, there was no relationship between RMSSD and depression diagnoses ($p = .372$), contrasting other reports on depression and RMSSD. Future analyses may investigate additional postoperative timepoints and individual changes in HRV through within-subjects designs.

**Disclosures: M.R. Hess:** None. **M.I. Banks:** None. **R.C. Lennertz:** None.

**Poster**

**PSTR170: Systemic Factors, Inflammation, and Brain Function**

**Location:** WCC Halls A-C

**Time:** Monday, November 16, 2026, 1:00 PM - 5:00 PM

**Program #/Poster #:** PSTR170.04/O6

**Topic:** C.01. Brain Wellness and Aging

**Support:** NIH Grant R01NS108810
NIH Grant T32GM142520
NIH Grant T32NS041218

**Title:** Aging amplifies molecular and cellular dysfunction in the dorsal striatum following acute systemic inflammation.

**Authors: *Z. A. COLON**, K. A. MAGUIRE-ZEISS;
Neurosci., Georgetown Univ. Med. Ctr., Washington, DC

**Abstract:** Aging is the primary risk factor for neurodegenerative diseases (NDDs), and chronic neuroinflammation is a common feature across these disorders. To investigate how aging influences the brain's response to systemic inflammation, we employed a peripheral lipopolysaccharide (LPS) model of acute inflammation and examined transcriptomic and proteomic changes within the dorsal striatum of young (4-month-old) and aged (20-month-old) male and female C57BL/6J mice. In aged mice, LPS exposure elicited an exaggerated inflammatory response characterized by activation of immune and autoimmune-related pathways, alongside disruptions in lipid metabolism and cellular energy homeostasis, suggesting that peripheral inflammatory insults can promote molecular signatures associated with increased neurodegenerative vulnerability. Proteomic analyses further revealed evidence of heightened inflammatory signaling, impaired proteostasis, increased cell death-related processes, and deficits in synaptic function, including reduced dopamine transporter expression. Relative to young mice exposed to LPS, aged mice displayed marked dysregulation of cell cycle pathways, with deficits in cellular division and chromatin organization. Aging also altered astrocyte reactivity, with loss of normal regulation between A1- and A2-like activation states following inflammatory challenge. In parallel, proteomic profiling demonstrated reductions in proteins associated with mitochondrial function, blood-brain barrier integrity, and vascular homeostasis. Multiple pathways involved in synaptic architecture and neurotransmission were disrupted, including significant decreases in proteins associated with dopaminergic, GABAergic, and glutamatergic signaling. Immunohistochemical analyses identified a non-canonical microglial activation phenotype in aged LPS-treated mice, characterized by elevated Iba1 expression without the expected hypertrophic morphology. Collectively, these findings demonstrate that aging amplifies the detrimental effects of systemic inflammation on the dorsal striatum, promoting widespread molecular and cellular dysfunction that converges on mechanisms implicated in neurodegeneration.

**Disclosures: Z.A. Colon:** None. **K.A. Maguire-Zeiss:** None.

**Poster**

**PSTR170: Systemic Factors, Inflammation, and Brain Function**

**Location:** WCC Halls A-C

**Time:** Monday, November 16, 2026, 1:00 PM - 5:00 PM

**Program #/Poster #:** PSTR170.05/O7

**Topic:** C.01. Brain Wellness and Aging

**Support:** U19-AG065169
T32-AG027668

**Title:** Inflammation in the Blood, Disruption in the Brain: Plasma Markers and White Matter Microstructure in Human Aging

**Authors: *E. R. PAITEL**[1], S. MISHRA[2], C. PETTIGREW[1], C. UGONNA[3], N.-K. CHEN[3], J. FRYE[3], K. P. DOYLE[3], L. RYAN[3], M. ALBERT[1], S. HO[1], A. MOGHEKAR[1], A. SOLDAN[1]; [1]Neurol., Johns Hopkins Univ. Sch. of Med., Baltimore, MD; [2]Johns Hopkins Univ., Baltimore, MD; [3]Univ. of Arizona, Tucson, AZ

**Abstract:** Introduction. Chronic inflammation is a common feature of aging and is observed across various age-related neurodegenerative diseases, including Alzheimer's disease (AD). It has, however, been challenging to develop neuroimaging measurements of brain structure directly linked to peripheral measures of neuroinflammation in human participants. Methods. This cross-sectional study examined whether plasma levels of markers related to inflammation were associated with diffusion magnetic resonance imaging (dMRI) measures of white matter microstructure, using both conventional, single-shell diffusion tensor imaging (mean diffusivity (MD)), as well as more advanced diffusion-based measures from neurite orientation dispersion and density imaging (NODDI; free-water fraction (FWF), orientation dispersion index (ODI)). Participants included 457 dementia-free later middle-aged and older adults (mean age=63.82, *SD*=7.63; 69% female). Blood plasma markers related to inflammation included two measures of systemic inflammation, (1) high-sensitivity C-reactive protein (CRP), and (2) a composite of pro-inflammatory cytokines (IL-1α, IL-1β, IL-2, IL-6, IL-8, TNF-α, TNF-β), as well as (3) glial fibrillary acidic protein (GFAP), a measure of astrocytic activation. Results. Higher cytokine composite levels were associated with higher values of all three dMRI measures (FWF, ODI, MD) in global cerebral white matter and with higher ODI in the cerebellar peduncles. Higher CRP levels were associated with higher ODI in global cerebral and cerebellar white matter. Associations with GFAP were not significant after adjusting for multiple comparisons. Results were consistent after accounting for plasma biomarkers of AD pathology (phosphorylated tau (p-tau$_{181}$)/amyloid beta (A$\beta_{42}$)). Discussion. Overall, higher levels of peripheral pro-inflammatory markers measured in plasma were associated with both cerebral and cerebellar white matter microstructure (higher FWF, ODI, and MD), supporting the view that these dMRI-based metrics are sensitive to inflammatory processes. By comparison, white matter microstructure in cognitively unimpaired participants may be less sensitive to alterations in plasma GFAP, a measure of astrocytic activation. Together, these patterns demonstrate the importance of examining multiple markers of systemic inflammation and astrocytic activation, which may capture different aspects of the inflammatory response.

**Disclosures: E.R. Paitel:** None. **S. Mishra:** None. **C. Pettigrew:** None. **C. Ugonna:** None. **N. Chen:** None. **J. Frye:** None. **K.P. Doyle:** None. **L. Ryan:** None. **M. Albert:** None. **S. Ho:** None. **A. Moghekar:** None. **A. Soldan:** None.

**Poster**

**PSTR170: Systemic Factors, Inflammation, and Brain Function**

**Location:** WCC Halls A-C

**Time:** Monday, November 16, 2026, 1:00 PM - 5:00 PM

**Program #/Poster #:** PSTR170.06/O8

**Topic:** C.01. Brain Wellness and Aging

**Support:** NRF grant RS-2026-25471870

**Title:** Two distinct extracranial lymphatic pathways drain cerebrospinal fluid and decline with age

**Authors: *J.-H. YOON**[1], H. JIN[2], G. KOH[3];
[1]Sungkyunkwan Univ., Suwon, Korea, Republic of; [2]Samsung Med. Ctr., Seoul, Korea, Republic of; [3]Inst. for Basic Sci., Daejeon, Korea, Republic of

**Abstract:** Cerebrospinal fluid (CSF) leaves the cranial cavity through extracranial lymphatic vessels, but a complete anatomical map of these outflow routes has been lacking. Here we describe two distinct extracranial lymphatic pathways through which CSF exits the skull and show that both branches deteriorate with aging. Using Prox1-GFP lymphatic reporter mice, intracisternal tracer injection (fluorescent dextrans, FluoSpheres), in vivo imaging, and whole-mount imaging of optically cleared tissues, we first identified a nasopharyngeal lymphatic plexus (NPLP) as the principal hub for CSF efflux. CSF traversing the anterior and middle skull base converges in the NPLP and drains into deep cervical lymphatic vessels (dcLVs) before reaching deep cervical lymph nodes. These deep vessels are ensheathed by smooth muscle, display tonic contractility, and are dynamically regulated by adrenergic agonists and nitric oxide. We subsequently mapped a second, parallel pathway: facial subcutaneous lymphatic vessels that collect CSF-derived tracer from the periorbital region and nasal mucosa and drain to submandibular lymph nodes (smLNs). Because these vessels lie immediately beneath the skin, the superficial route is accessible to non-invasive manipulation; gentle mechanical stimulation of the cervicofacial region augments CSF efflux through this branch. Together, these maps define an extracranial lymphatic CSF outflow architecture comprising a deep NPLP-dcLV axis and a superficial facial-smLN axis. CSF drainage declined markedly in aged mice across both branches, identifying age-related extracranial lymphatic failure as a unified mechanism of impaired CSF clearance. This route map provides an anatomical and physiological framework for therapies aimed at restoring CSF drainage in aging and neurodegenerative disease.

**Disclosures: J. Yoon:** None. **H. Jin:** None. **G. Koh:** None.

**Poster**

**PSTR170: Systemic Factors, Inflammation, and Brain Function**

**Location:** WCC Halls A-C

**Time:** Monday, November 16, 2026, 1:00 PM - 5:00 PM

**Program #/Poster #:** PSTR170.07/P1

**Topic:** C.01. Brain Wellness and Aging

**Title:** Excess ePWV as a Quantitative Marker of Early Vascular Aging and White Matter Injury

**Authors: *B. AIMAGAMBETOVA**[1], M. NAFELI SHAHRESTANI[2], B. E. LEVIN[1], T. RUNDEK[3], H. GARDENER[3], S. TOM[4];
[1]Neurol., Univ. of Miami, Miami, FL; [2]Univ. of Miami, Coral Gables, FL; [3]Univ. of Miami, Miami, FL; [4]Columbia Univ., New York, NY

**Abstract: Background:** Early vascular aging (EVA) reflects accelerated arterial stiffness relative to chronological age. Estimated pulse wave velocity (ePWV), a surrogate marker of stiffness, has been associated with cerebral small vessel disease, cognitive impairment, and dementia. However, whether EVA contributes to brain injury and cognitive decline remains unclear. **Objective:** to define EVA using excess ePWV and evaluate association with white matter hyperintensity volume (WMHV), incident cognitive impairment, incident dementia, and potential mediation through WMHV in the Northern Manhattan Study (NOMAS) MRI cohort. **Methods:** We analyzed 1,268 participants (70.5±8.9 years, 61% women, 67% Hispanic). ePWV was calculated from age and blood pressure, using a validated equation. The mean ePWV was 11.69±1.95m/s. Age-expected ePWV was estimated using a linear regression of observed ePWV on chronological age at MRI; excess ePWV was defined as the residual difference (observed minus expected), with positive residuals indicating EVA. WMHV was normalized, log2-transformed, and standardized. Outcomes were incident cognitive impairment (25%) and incident dementia (13%). Associations were evaluated using multivariable linear or logistic regression, as appropriate. Mediation by WMHV was evaluated using causal mediation models (regmedint). Models were progressively adjusted for demographics, vascular risk factors, and ApoE4 status. Age was not included in multivariable models because EVA represents age-residualized ePWV. **Results:** Positive excess ePWV (49% of the cohort) was associated with greater WMHV burden (β=0.062, 95% CI 0.000-0.124, p=0.049) but was not associated with incident cognitive impairment or dementia. Higher WMH burden was independently associated with incident cognitive impairment (OR=1.55, CI 1.31-1.84, p<0.001) and incident dementia (OR=1.75, CI 1.41-2.17, p<0.001). In contrast, conventional ePWV remained strongly associated with WMH burden (β=0.408, 95% CI 0.347-0.469, p<0.001), cognitive impairment (OR=1.57, 95% CI 1.34-1.85), and dementia (OR=1.94, 95% CI 1.58-2.40). Mediation analyses suggested possible indirect effects through WMHV, but these did not reach statistical significance in fully adjusted models.
**Conclusions:** These findings suggest that the age-related component of stiffness may contribute to the associations between conventional ePWV and cognitive outcomes. Whereas excess ePWV may serve as a quantitative marker of EVA associated with vascular brain injury, but not with cognitive decline.

**Disclosures: B. Aimagambetova:** None. **M. Nafeli Shahrestani:** None. **B.E. Levin:** None. **T. Rundek:** None. **H. Gardener:** None. **S. Tom:** None.

**Poster**

**PSTR170: Systemic Factors, Inflammation, and Brain Function**

**Location:** WCC Halls A-C

**Time:** Monday, November 16, 2026, 1:00 PM - 5:00 PM

**Program #/Poster #:** PSTR170.08/P2

**Topic:** C.01. Brain Wellness and Aging

**Title:** Association between chronic multi-symptom illness severity and health-related quality of life and deployment location in Gulf War Veterans.

**Authors: *F. MOJABI**[1], J. W. ASHFORD, Jr.[3], J. CLIFFORD[1], S. AKITT[2];
[2]WRIISC, [1]Veterans Affairs Palo Alto HCS, Palo Alto, CA; [3]Stanford Univ., Redwood City, CA

**Abstract:** Background Gulf War Illness (GWI) is a chronic multisymptom illness (CMI) affecting approximately 30-40% of Veterans deployed to the Middle East during the 1990-1991 Gulf War (GW). GWI is often characterized by persistent neurological, cognitive, pain, fatigue, and GI symptoms that substantially impair daily functioning and health-related quality of life (HRQoL). Although GWI is commonly identified using the Kansas case definition, diagnosis remains largely qualitative, limiting the ability to quantify disease burden and evaluate relationships between symptom severity and functional outcomes. This study examined associations between symptom burden and HRQoL and deployment location among GW Veterans enrolled in an NIH-VA investigative study. Methods 231 Veterans completed questionnaires, including a modified Kansas symptoms assessment and the Short-Form 36 (SF36). Symptom severity was quantified using cumulative Kansas scores derived from ratings ranging from none (0) to severe (3) across multiple symptom domains. HRQoL was assessed using eight standardized SF36 domains. General linear regression models were used to evaluate associations between symptom burden and HRQoL. Deployment location data was analyzed to investigate potential differences by location in neurological symptom severity. Results Greater Kansas symptoms severity was significantly associated with poorer HRQoL, particularly in physical functioning, vitality, and bodily pain domains (all $p<0.0001$). Increasing CMI burden corresponded to reductions in functional health measures, showing a strong relationship between symptom severity and lower quality of life. Preliminary analysis of deployment location indicated higher mean Kansas severity score among Veterans deployed to at-sea locations (2.16), Persian Gulf (2.06), and Saudi Arabian Red Sea Coast (2.06). Lower means were observed among Veterans deployed to Central Saudi Arabia (1.91), Eastern Saudi Arabia (1.89), and Bahrain (1.87). Further statistical analyses are evaluating whether these relationships are significant. Conclusion Kansas symptom severity scores are strongly associated with reduced functional health outcomes and may provide a valuable measure of disease burden in GW Veterans. Preliminary findings suggest that deployment location may contribute to symptom severity, potentially reflecting differing environmental or toxic exposures. Integrating quantitative symptom metrics with standardized HRQoL assessments may improve GWI

phenotyping and support the development of targeted interventions aimed at improving long-term neurological health and quality of life in affected Veterans.

**Disclosures: F. Mojabi:** A. Employment/Salary (full or part-time):; THE DEPARTMENT OF VETERANS AFFAIRS. **J.W. Ashford:** A. Employment/Salary (full or part-time):; THE DEPARTMENT OF VETERANS AFFAIRS. **J. Clifford:** A. Employment/Salary (full or part-time):; THE DEPARTMENT OF VETERANS AFFAIRS. **S. Akitt:** A. Employment/Salary (full or part-time):; THE DEPARTMENT OF VETERANS AFFAIRS.

**Poster**

**PSTR170: Systemic Factors, Inflammation, and Brain Function**

**Location:** WCC Halls A-C

**Time:** Monday, November 16, 2026, 1:00 PM - 5:00 PM

**Program #/Poster #:** PSTR170.09/P3

**Topic:** C.01. Brain Wellness and Aging

**Support:** VA Clinical Science Research and Development (CSR&D) grant entitled "The role of the brainstem in GWVI pathology" (1 I01 CX002182-01)
VA Office of Academic Affiliations, CA WRIISC Fellowship program
California War Related Illness and Injury Study Center

**Title:** Diffusion Tensor Imaging Assessment of the Glymphatic Function in Veterans from the Gulf War and Iraq/Afghanistan Wars

**Authors: *A. J. FURST**[1,2], Y. ZHANG[1], M. MOORE[1,2], Y. RAHIMPOUR[1,2], D. CLARK[1,2], P. J. BAYLEY[1,2], J. W. ASHFORD, Jr.[1,2];
[1]VA Palo Alto Hlth. Care Syst., Palo Alto, CA; [2]Stanford Univ., Stanford, CA

**Abstract:** Background: Chronic multisystem illness (CMI), which includes chronic fatigue, sleep difficulty, pain, neurological, respiratory, and gastrointestinal problems, is common in veterans after returning from Gulf War deployments, Operations Desert Shield/Storm (ODS/S) and Iraq/Afghanistan Wars. Diffusion Tensor Imaging along the Perivascular Space (DTI-ALPS) provides a non-invasive proxy to assess the the brain's waste-clearing "glymphatic" system function. The objective of this study was to identify impairments in glymphatic system functions and to investigate their correlations with CMI in veterans who deployed to these conflicts, utilizing DTI-ALPS for evaluation. Methods: ALPS indices were evaluated using MR-DTI of 100 ODS/S veterans (mean age = 50 ± 5 years) and 96 Iraq/Afghanistan veterans (mean age = 40 ± 10 years). Furthermore, 224 healthy controls (HC, mean age = 50 ± 15 years) were obtained from public research databases. ALPS indices were harmonized to mitigate the discrepancies in MRI sites and scans. All 196 veterans met the CDC criteria for CMI. The severity scores of chronic fatigue syndrome, sleep disturbances, and pain intensity were assessed for all veterans. ANCOVA and Pearson's correlation models were used for group comparisons and correlation analyses. A multiple linear regression model was used to identify the most important independent predictor variable. Results: Age-related ALPS reduction in veterans ($p$ = .07) was

not as remarkable as that observed in HC ($p < .001$). However, when compared to age matched HC, veterans deployed to ODS/S ($p < .001$ on left, right and bilateral hemisphere) and Iraq/Afghanistan Wars (left: $p < .001$, right: $p=.001$, bilateral: $p < .001$) had lower ALPS after adjusting for age, sex, and education. Compared to the ODS/S veterans, veterans from the Iraq/Afghanistan Wars showed slightly milder symptom severity and higher ALPS, however, these differences were not statistically significant ($p > .3$). Among all veterans, significant correlations were observed between decreased ALPS and increased severity scores of sleep disturbances ($r = -.23$, $p = .002$), pain intensity ($r = -.18$, $p = .01$), chronic fatigue ($r = -.17$, $p = .02$), and overall CMI symptoms ($r = -.18$, $p = .01$). Notably, sleep disturbance emerged as the primary factor contributing to the decrease in ALPS (*Beta* = -.18, $p = .03$). Conclusion: DTI-ALPS analysis revealed an impaired glymphatic clearance in veterans with CMI, regardless of the conflict in which they were deployed. Among the multiple chronic symptoms, sleep disturbances emerged as the primary factor linked to this glymphatic dysfunction.

**Disclosures: A.J. Furst:** None. **Y. Zhang:** None. **M. Moore:** None. **Y. Rahimpour:** None. **D. Clark:** None. **P.J. Bayley:** None. **J.W. Ashford:** None.

**Poster**

**PSTR170: Systemic Factors, Inflammation, and Brain Function**

**Location:** WCC Halls A-C

**Time:** Monday, November 16, 2026, 1:00 PM - 5:00 PM

**Program #/Poster #:** PSTR170.10/P4

**Topic:** C.01. Brain Wellness and Aging

**Support:** Jerome H. Fleisch & Marlene L. Cohen Endowed Fund at Georgetown Univeristy
Initiative for Maximizing Student Development
Pharmacological Sciences Training Grant

**Title:** The Contribution of Cellular Senescence to HIV-Associated Neurocognitive Disorders (HAND)

**Authors: *A. HUSSAIN**[1], P. A. FORCELLI[2], M. W. BURKE[3];
[1]Georgetown Univ., Washington, DC, DC; [2]Dept of Pharmacol. & Physiol., Georgetown Univ., Washington, DC; [3]Physiol. & Biophysics, Col. of Med., Washington, DC

**Abstract:** The Contribution of Cellular Senescence to HIV-Associated Neurocognitive Disorders (HAND)Advances in antiretroviral therapies have shifted Human Immunodeficiency Virus 1 (HIV-1) infection from a terminal illness to a manageable disease. These treatments, however, fail to prevent the cognitive decline and impaired daily function caused by HIV, known as HIV-associated neurocognitive disorders (HAND). Therefore, it is vital to develop an effective therapeutic strategy to combat these disorders. The HIV envelop protein, gp120, is neurotoxic and overexpression of this protein in mice triggers a range of behavioral and neuropathological changes, providing a model of some features of HAND. Similarly, the tg26 transgenic mouse line expresses 7 of 9 HIV-1 proteins, making it clinically relevant to ART-

controlled HIV-1-infected patients who lack active viral replication but suffer from continuous stress from the viral proteins. Cellular senescence, a conserved cellular aging cascade is of increasing interest in neurodegenerative disorders. Indeed, the proinflammatory state, mirrored by cognitive decline in these models resembles canonical cellular senescence pathways. However, senescence in HAND remains poorly understood. No studies have evaluated the impact of removal of senescent cells (SCs) on outcomes related to HAND. Here we addressed this gap by first profiling the accumulation of SCs in the gp120 and tg26 mouse lines. We found an age dependent increase in p16-positive SCs in the striatum, hippocampus, and amygdala of aged 11-12 month tg26 mice as compared to wild type controls. Similarly, we observed significant increases in p16 in the gp120 model by 9-10 months of age. To determine if removal of SCs would protect against gp120 induced cognitive impairment, we treated animals with a combination of dasatinib and quercetin, widely utilized senolytic agents, from 6-12 months. In 12 month animals we measured performance on the Barnes Maze and found a gp120 gene dose dependent impairment. Heterozygous animals displayed impaired learning, which was worsened in homozygous animals. Treatment with DQ returned learning to wild type control levels. These results suggest senescent cells play a role in the pathology of HAND and indicate preclinical evidence for the efficacy of senolytic therapy in HAND.

**Disclosures: A. Hussain:** None. **P.A. Forcelli:** None. **M.W. Burke:** None.

**Poster**

**PSTR170: Systemic Factors, Inflammation, and Brain Function**

**Location:** WCC Halls A-C

**Time:** Monday, November 16, 2026, 1:00 PM - 5:00 PM

**Program #/Poster #:** PSTR170.11/P5

**Topic:** D.01. Neurotoxicity, Inflammation, and Neuroprotection

**Support:** Mavri (ISF) grant6023218
Cabakoff grant 3175006868

**Title:** Dental implants and inflammation are associated with cognitive decline: clinical and murine evidence

**Authors: *Y. HOURI-HADDAD**;
Hebrew university Hadassah Med. Ctr., Jerusalem, Israel

**Abstract:** Oral health has been linked to brain health through systemic pathways. Dental implants, primarily composed of titanium (Ti), are widely used for oral rehabilitation, yet Ti's biological safety is under scrutiny due to reported neurotoxicity and neuroinflammatory potential. We investigated associations between dental implant exposure, peri-implant Inflammation (PI), and cognitive health using parallel clinical and murine approaches. In a cross-sectional clinical study, 200 cognitively healthy adults aged ≥65 underwent full dental and periodontal examination, cognitive assessment using the Montreal Cognitive Assessment (MoCA), and oral microbiome sampling. Increasing implant burden correlated negatively with

MoCA scores. PI was associated with the lowest cognitive scores compared to healthy implant carriers and controls ($p<0.001$). Periodontal disease severity was inversely correlated with cognition. Implant carriers with lower cognitive scores exhibited a pathogen-enriched oral microbiome with increased stress-related metabolic pathways potential. In the murine model, first molars were extracted from 9-month-old female mice (n=60). After 4 weeks, Ti-6Al-4V implants were placed. Ti-implanted mice, performed worse on novel object recognition, Y-maze, and nesting tests. Bulk RNA sequencing of hippocampi revealed upregulation of angiogenesis and extracellular matrix remodeling genes. Immunohistochemistry confirmed increased vascular density (isolectin), microglial activation (Iba1), and astrogliosis (GFAP) in Ti-implanted groups. Ti particles were detected in brain tissue. Together, these findings suggest that Ti dental implants, particularly under PI conditions, exert systemic neurobiological effects that may contribute to cognitive impairment.

**Disclosures: Y. houri-haddad:** None.

**Poster**

**PSTR171: Parkinson's Disease: Animal Models**

**Location:** WCC Halls A-C

**Time:** Monday, November 16, 2026, 1:00 PM - 5:00 PM

**Program #/Poster #:** PSTR171.01/P6

**Topic:** C.03. Parkinson’s Disease

**Title:** Comparisons of motor and neural phenotypes in TBI and PD Drosophila models

**Authors: *E. R. REYNOLDS**, K. DAVIS;
Lafayette Col., Easton, PA

**Abstract:** Traumatic Brain Injury (TBI) can occur as a consequence of sustained head trauma. Delayed onset symptoms can increase the risk of permanent cognitive changes and the onset of neurodegenerative diseases such as Parkinson’s Disease (PD) or Parkinson’s like behavioral symptoms. While several studies have explored the general mechanisms behind TBI and PD development, a model assessing the link between these diagnoses has not yet been established. This study explores a *Drosophila melanogaster* model of TBI in direct comparison to a PD model, assessing behavioral and neurological measures. The fly alpha-synuclein model for PD was utilized by crossing a Ddc-Gal strain to a UAS-synuclein heterozygous stain producing Ddc/synuclein flies that produce the synuclein protein in dopaminergic cells and phenocopy PD. The other products of the cross were used as controls. Four groups were established: PD, PD+TBI, TBI alone, and control flies. TBI was achieved using a fly head specific injury model (Katzenberger et al., 2013; Alphen et al., 2022) using unanesthetized five-day old flies. Climbing assays were used to assess changes in motor ability with age for all groups (Manjila and Hasan 2018). Immunohistochemistry was performed using a tyrosine hydroxylase antibody to monitor preservation of dopaminergic neurons throughout life span. The control and TBI alone showed no decrease in climbing ability over the course of the experiment. PD and PD+TBI showed decreased climbing ability initially as well as significant declines in climbing ability with age.

TBI enhanced the climbing deficits in PD flies. The immunohistochemistry data shows a pattern of dopaminergic cell loss that parallels the climbing deficits. Current work is looking at neurodegeneration using a TUNEL assay in this model system. In conclusion, TBI exacerbates PD predisposition and symptomology, but TBI has distinctive climbing and neurodegeneration phenotypes.

**Disclosures: E.R. Reynolds:** None. **K. Davis:** None.

**Poster**

**PSTR171: Parkinson's Disease: Animal Models**

**Location:** WCC Halls A-C

**Time:** Monday, November 16, 2026, 1:00 PM - 5:00 PM

**Program #/Poster #:** PSTR171.02/Q1

**Topic:** C.03. Parkinson's Disease

**Support:** Campbell Foundation

**Title:** The individual and combined effects of caffeine and EHT on symptoms of Parkinson's in rats

**Authors: J. REES**[1], K. DEVLIEG[2], *N. SWALVE[1], A. DORAN[3], S. KEKEL[3];
[1]Grand Valley State Univ., Allendale, MI; [2]Grand Valley State Univ., Wyoming, MI;
[3]Psychology, Grand Valley State Univ., Allendale, MI

**Abstract:** Parkinson's disease is the second most prevalent neurodegenerative disorder, with nearly 100,000 new diagnoses every year. While the biological mechanisms behind Parkinson's disease are relatively well-known, with symptoms resulting from progressive death of dopaminergic neurons, we still do not have well-tolerated treatments. Methods of delaying or preventing the condition are thus especially important. Coffee may have a neuroprotective effect against Parkinson's, but the mechanisms behind this effect are still understudied. Preliminary evidence suggests that caffeine and an additional component found in coffee, eicosanoyl-5-hydroxytryptamide (EHT), work together as a form of neuroprotection. How this works however, is unknown. And while Parkinson's disease shows differences in males and females, with females showing faster progression and greater mortality, little is known about how these protective effects may differ between sexes. The goal of this study is to extend the research on the individual and combined neuroprotective effects of caffeine and EHT on Parkinson's Disease. Sixty-seven male and female rats were exposed to the rotenone model of Parkinson's disease (1.5 mg/kg rotenone) for 35 days. They were divided into groups and received caffeine (20 mg/kg/day) in their water, EHT (12 mg/kg/day) in their feed, both caffeine and EHT, or the corresponding vehicles during rotenone treatment. They were then tested on a series of behavioral paradigms, including the rotarod and operant responding in a fixed-ratio model of motivation. This study allows for the determination of whether individual and combined effects of caffeine and EHT can act to prevent symptoms of Parkinson's disease. It will also be the first study to examine the sex specificity of the neuroprotective effects, providing novel information

that can be used to inform prevention and treatment of one of the most common neurodegenerative disorders.

**Disclosures: J. Rees:** None. **K. Devlieg:** None. **N. Swalve:** None. **A. Doran:** None. **S. Kekel:** None.

**Poster**

**PSTR171: Parkinson's Disease: Animal Models**

**Location:** WCC Halls A-C

**Time:** Monday, November 16, 2026, 1:00 PM - 5:00 PM

**Program #/Poster #:** PSTR171.03/Q2

**Topic:** C.03. Parkinson's Disease

**Title:** Investigating the propagation of alpha synuclein aggregation following pre-formed fibril injections in human alpha-synuclein expressing mice

**Authors: *H. SANDERS**[1], C. COMMINS[1], O. MOROZOVA[1], P. BOSCH[1], F. LIAO[1], M. MIGLIORE[2], J. STOEHR[1], T. DELLOVADE[1];
[1]AbbVie, Cambridge, MA; [2]Massachusetts Col. of Pharm. and Hlth. Sci., Boston, MA

**Abstract:** Parkinson's disease (PD) is a progressive neurodegenerative disorder characterized by Lewy bodies and neurites composed of misfolded alpha synuclein (α-syn) and the loss of midbrain dopaminergic neurons. Human histological studies have shown that α-syn pathology develops in a well-defined pattern along anatomically connected brain regions as characterized by Braak staging. This pattern is hypothesized to occur by propagation, where α-syn "seeds" pass between synaptically connected neurons. Following seed uptake endogenous monomeric α-syn is recruited and templated to the pathogenic seed material, initiating aggregation in the connected neuron. To model α-syn aggregation and spreading in vivo, researchers often use direct brain injections of pre-formed fibrils (PFFs) generated from recombinant α-syn monomer, either spontaneously formed ("hPFF") or seeded by PD brain extracted α-syn aggregates ("PD-PFF"). Here we compare α-syn pathology following the injection of hPFF's and PD-PFF's into the olfactory bulb (OB) of Tg(M83) mice, over-expressing human mutant (A53T). Brains were collected 1, 2, or 3 months post-injection and histologically characterized by staining for aggregated, phosphorylated α-syn (serine 129, "pS129") immunoreactivity (IR). Our results showed that hPFF & PD-PFF injections into the OB of transgenic mice, induced robust pS129 immunoreactivity in the OB and brain regions that are one or two synapses away from the OB, suggesting transneuronal spread of α-syn pathology. When characterizing the propagation in Tg(M83) mice we observed that hPFF's lead to greater seeding and propagation when compared with PD-PFF. These results will be compared to ongoing studies of OB seeding and propagation of hPFF and PD-PFF in Tg(hSNCA KI) mice that express wild-type human α-syn. This will help to explore the effect of mutant A53T versus wt human α-syn in combination with hPFF and PD-PFF seeds on seeding and propagation differences. Overall, these data suggest a promising in vivo approach to model α-syn propagation and the careful combination of transgenic mouse lines

and specific PFF preparations will create reliable propagation models for future research into the mechanisms of α-syn pathology seeding and spreading in PD.

**Disclosures: H. Sanders:** A. Employment/Salary (full or part-time):; AbbVie. **C. Commins:** A. Employment/Salary (full or part-time):; Abbvie. **O. Morozova:** A. Employment/Salary (full or part-time):; AbbVie. **P. Bosch:** A. Employment/Salary (full or part-time):; AbbVie. **F. Liao:** A. Employment/Salary (full or part-time):; Abbvie. **M. Migliore:** A. Employment/Salary (full or part-time):; Massachusetts College of Pharmacy and Health Sciences. **J. Stoehr:** A. Employment/Salary (full or part-time):; AbbVie. **T. Dellovade:** A. Employment/Salary (full or part-time):; AbbVie.

**Poster**

**PSTR171: Parkinson's Disease: Animal Models**

**Location:** WCC Halls A-C

**Time:** Monday, November 16, 2026, 1:00 PM - 5:00 PM

**Program #/Poster #:** PSTR171.04/Q3

**Topic:** C.03. Parkinson's Disease

**Support:** NIH/NINDS Grant R01NS119610-01

**Title:** Beyond Seeding: A Hippocampal α-synuclein model with robust neuronal loss, neuroinflammation, and cognitive deficits in wild-type mice

**Authors: *J. BYUN**, B. HUDSON, D. GRESHAM, J. LIM, A. ADEBOWALE, J. CHUNG, N. M. FILIPOV, J.-K. LEE;
Dept. of Physiol. and Pharmacol., Univ. of Georgia, Athens, GA

**Abstract:** Lewy body dementia (LBD) is characterized by the accumulation of α-synuclein (α-syn), neuroinflammation, neuronal degeneration, and progressive cognitive decline. Although several α-syn mouse models have been developed, few reproduce the hippocampal pathology and behavioral impairments associated with LBD. We therefore developed a hippocampal α-syn preformed fibril (PFF) mouse model to investigate pathological α-syn spread, neuronal loss, immune cell responses, and cognitive dysfunction. Male and female wild-type (C57BL/6) mice received stereotaxic hippocampal injection of α-syn PFFs or monomeric α-syn and were analyzed at 1- and 3-month post-injection (MPI). Immunohistochemical analyses revealed progressive accumulation and spread of phosphorylated α-syn pathology throughout hippocampal subregions, including the dentate gyrus (DG), CA2/3, CA1, and other limbic regions, including the lateral entorhinal cortex (LEnt), with minimal pathology in the Amygdala. Neuronal degeneration (FJC+) and loss (reduced NeuN) were greatest in the DG granule cell layer, where α-syn pathology was most severe. PFF α-syn-injected mice exhibited increased microglial and astrocytic reactivity in affected hippocampal regions, indicating robust neuroinflammatory activation. Moreover, in *CX3CR1$^{GFP}$/CCR2$^{RFP}$* dual-reporter mice, CCR2$^{+}$ peripheral monocytes (red) infiltrated areas of α-syn pathology alongside resident CX3CR1$^{+}$ microglia (green), indicating that the neuroinflammatory response involves recruitment of

peripheral myeloid cells. No sex differences were detected in α-syn pathology, neuronal loss, or glial reactivity. In the behavioral battery (elevated zero maze (EZM), open field test (OFT), novel location recognition test (NLRT), novel object recognition test (NORT), and Barnes maze), PFF α-syn-injected mice were impaired on hippocampal-dependent cognitive tasks, including NORT, NLRT, and Barnes maze, indicating functional deficits associated with pathological α-syn accumulation. Despite comparable histopathology between sexes, female mice exhibited greater deficits than males in EZM, OFT, and NLRT, suggesting sex-dependent vulnerability to α-syn-induced dysfunction. Together, this model reproduces key pathological, neuroinflammatory, and cognitive features of LBD and reveals sex-dependent behavioral alterations, providing a platform to study hippocampal dysfunction and to test synucleinopathy-targeted therapies.

**Disclosures: J. Byun:** None. **B. Hudson:** None. **D. Gresham:** None. **J. Lim:** None. **A. Adebowale:** None. **J. Chung:** None. **N.M. Filipov:** None. **J. Lee:** E. Ownership Interest (stock, stock options, royalty, receipt of intellectual property rights/patent holder, excluding diversified mutual funds); Co-Founder of NeuronityTx Inc..

**Poster**

**PSTR171: Parkinson's Disease: Animal Models**

**Location:** WCC Halls A-C

**Time:** Monday, November 16, 2026, 1:00 PM - 5:00 PM

**Program #/Poster #:** PSTR171.05/Q4

**Topic:** C.03. Parkinson’s Disease

**Support:** MJFF

**Title:** Characterization of scAAV2/5-hWT-aSyn-induced rat and mouse models of Parkinson’s disease.

**Authors: *M. P. HILL**[1], T. H. JOHNSTON[1], J. M. BROTCHIE[1], N. POLINSKI[2]; [1]Atuka Inc., Toronto, ON, Canada; [2]The Michael J. Fox Fndn. for Parkinson's Res., STEWART MANOR, NY

**Abstract:** A common feature of Parkinson’s Disease (PD) is the presence of pathological forms of a-synuclein (aSyn) throughout the central nervous systems of patients. One way to achieve this in animals is using adeno-associated viruses (AAV) to mediate aSyn overexpression within the targeted neuronal pathway, producing restricted neurodegeneration with limited spread to other brain regions. In this study, we evaluated a new AAV2/5 vector that overexpresses human wild-type alpha-synuclein (scAAV2/5-hWT-aSyn). The self-complementary (sc) design produces an inverted repeat aSyn genome that can fold into dsDNA without DNA synthesis and allows for faster gene expression than a standard single-stranded AAV. Female Sprague-Dawley rats and male C57BL/6 mice received unilateral intranigral (SNc) administration of scAAV2/5-hWT-aSyn (aSyn) or scAAV2/5-empty vector (EV). Extent of forelimb asymmetry was assessed via the cylinder test at baseline, 3-weeks and 6-weeks post injection. At 6 weeks, the animals

were killed and post mortem analyses performed. In rats, forelimb asymmetry became more pronounced over time and was significantly increased at both weeks 3 and 6 compared to baseline. There was a non-significant trend for forelimb asymmetry to be greater in aSyn animals compared to those that received EV at week 6. aSyn animals displayed significantly increased levels of aggregated alpha-synuclein in the striatum and reduced nigral TH+ve cell counts by 65% and striatal dopamine by 79% compared to EV. aSyn also significantly increased nigral Iba-1+ve cells by 5.2-fold. Despite the increase in striatal aggregated synuclein, there was little evidence of phosphorylated alpha synuclein (pSer129) positive cells in the SNc. In mice, forelimb asymmetry was significantly increased in aSyn animals compared to EV at both week 3 and 6. The aSyn vector significantly increased levels of striatal aggregated alpha-synuclein and reduced nigral TH+ve cell counts by 84% and striatal dopamine by 93%. The aSyn vector also significantly increased nigral Iba-1+ve cells by 4.7-fold. Unlike in rat, numerous pSer129 positive cells were observed in the SNc. This work demonstrates the potential of this vector to produce a pronounced synucleinopathy that is associated with a robust loss of markers of dopaminergic function and a substantial increase in neuroinflammation in both rats and mice.

**Disclosures: M.P. Hill:** None. **T.H. Johnston:** None. **J.M. Brotchie:** None. **N. Polinski:** None.

**Poster**

**PSTR171: Parkinson's Disease: Animal Models**

**Location:** WCC Halls A-C

**Time:** Monday, November 16, 2026, 1:00 PM - 5:00 PM

**Program #/Poster #:** PSTR171.06/Q5

**Topic:** C.03. Parkinson’s Disease

**Title:** Modeling early parkinson's disease through subthreshold dopamine depletion and α-synuclein pathology

**Authors: *H. PRISINZANO**[1], S. ROCKE[2], A. DUBUISSON[3], L. GUARDASCIONE[4], F. P. MANFREDSSON[6], C. R. BISHOP[5];
[1]Binghamton Univ., Binghamton, NY; [2]Binghamton Univ., New York, NY; [3]Binghamton Univ., washingtonville, NY; [4]Binghamton Univ., Ringwood, NJ; [5]Psychology, Binghamton Univ., Binghamton, NY; [6]Translational Neurosci., Barrow Neurolog. Inst., Phoenix, AZ

**Abstract:** Parkinson’s Disease (PD) is characterized by progressive dopaminergic cell loss and aggregations of misfolded α-synuclein. However, current rat models recapitulate either robust dopaminergic neuron loss or α-synuclein pathology that alone does not produce a consistent behavioral phenotype. Although levodopa (L-DOPA) remains the gold-standard treatment for PD, L-DOPA-induced dyskinesia (LID) is a common complication of advanced disease, and therapeutic responses in α-synuclein-based models remain inconsistent. This study aims to establish a subthreshold 6-hydroxydopamine (6-OHDA) lesion in the medial forebrain bundle (MFB) producing moderate DA depletion, which will be combined with α-synuclein pathology to examine synergistic effects on parkinsonian outcomes. Sprague Dawley rats (N=34; 17F, 17M) received a unilateral lesion to the MFB with one of four 6-OHDA doses: 0, 0.5, 1, or 2 µg

per 4 µL vehicle. Gross and fine motor function was assessed pre- and post-lesion on/off L-DOPA using the Forehand Adjusting Steps (FAS), Vermicelli Handling Test (VHT), and Rotarod. To assess LID, Abnormal Involuntary Movements (AIMs) tests were conducted over 4 days with escalating L-DOPA doses (3, 4, 6, and 12 mg/kg). Following behavioral testing, tyrosine hydroxylase (TH) immunohistochemistry of the substantia nigra pars compacta (SNc) and high-performance liquid chromatography (HPLC) of the striatum (STR) were conducted. We anticipate that escalating 6-OHDA doses will produce increasing liability for motor deficits, AIMs severity, and neurodegeneration. TH-positive cell counts and DA levels in the STR were used to generate a dose-response curve to identify the Effective Dose 50 (ED50) of 6-OHDA that produces moderate DA depletion and a detectable behavioral phenotype. To establish a novel dual lesion model, a new cohort of animals received a unilateral lesion to the MFB using the ED50 of 6-OHDA and unilateral adeno-associated virus (AAV)-mediated human α-synuclein overexpression in the SNc. Motor function was assessed at baseline, post-lesion, and post-virus on/off L-DOPA, and AIMs tests evaluated LID severity. We expect α-synuclein overexpression to potentiate neuronal dysfunction in surviving neurons, beyond the threshold for parkinsonian dysfunction, producing progressive increases in motor impairments and AIMs severity. Future work will continue investigating the dual-lesion model to establish a preclinical model that better recapitulates human PD pathology, symptomatology, and treatment response, thereby improving the predictive validity and translational relevance of preclinical findings.

**Disclosures: H. Prisinzano:** None. **S. Rocke:** None. **A. Dubuisson:** None. **L. Guardascione:** None. **F.P. Manfredsson:** None. **C.R. Bishop:** None.

**Poster**

**PSTR171: Parkinson's Disease: Animal Models**

**Location:** WCC Halls A-C

**Time:** Monday, November 16, 2026, 1:00 PM - 5:00 PM

**Program #/Poster #:** PSTR171.07/Q6

**Topic:** C.03. Parkinson’s Disease

**Title:** Psychoplastogens ibogainalog and ibogaminalog for optimizing L-DOPA treatment in a rat model of Parkinson’s Disease

**Authors: *E. YANNI**[1], C. R. BISHOP[2];
[2]Psychology, [1]Binghamton Univ., Binghamton, NY

**Abstract:** Parkinson’s Disease (PD) is a neurodegenerative disorder characterized by motor deficits such as tremor, rigidity, and bradykinesia that emerge with progressive dopamine (DA) cell loss. People with Parkinson’s (PwP) are invariably treated by DA replacement therapies like levodopa (L-DOPA) though complications often emerge such as L-DOPA-induced dyskinesia (LID), abnormal, involuntary movements that can significantly impact quality of life. Evidence suggests that this is due in part to neuroplasticity in the serotonin (5-HT) system. Therefore, adjuvant treatments that alleviate LID without diminishing L-DOPA efficacy are needed. Psychoplastogens, a novel class of drugs that appear to have sustained neurobiological effects,

have recently been identified as having therapeutic benefits by modulating the 5-HT system. For instance, ibogainalog (IBG) and ibogaminalog (DM506) dose-dependently alleviated depression-like and anxiogenic symptoms in mice. Drugs with multimodal actions on the 5-HT system have been shown to optimize L-DOPA treatment in preclinical models and PwP, however the influence of ibogalogs on PD and LID have yet to be determined. Therefore, we aimed to investigate the effects of IBG and DM506 on motor function and dyskinesia in a rat model of PD. Sprague-Dawley rats (N = 24) received a unilateral 6-OHDA lesion to the left medial forebrain bundle to elicit a hemiparkinsonian phenotype. All rats then underwent a Forepaw Adjustment Stepping (FAS) test to determine baseline motor function and 14 days of L-DOPA with Abnormal Involuntary Movements (AIMs) tests conducted on days 1, 7, and 14 to induce LID. Eleven dyskinetic rats then received acute within subjects, counterbalanced treatments of IBG (0, 5, and 10 mg/kg) just prior to L-DOPA (6 mg/kg). The remaining 13 rats underwent the same procedure but were administered DM506 (0, 20, and 40 mg/kg) with L-DOPA (6 mg/kg). AIMs assessments as well as on-treatment FAS tests were conducted on each testing day and at study end striatal DA was analyzed for lesion efficacy. Initial findings with the psychoplastogens reveal acute anti-dyskinetic effects and clear maintenance of L-DOPA efficacy. Moreover, rats treated with these compounds do not display the features of pharmacologically similar pro-hallucinatory compounds indicating a novel neurobiological mechanism and promising therapeutic characteristics.

**Disclosures: E. Yanni:** None. **C.R. Bishop:** None.

**Poster**

**PSTR171: Parkinson's Disease: Animal Models**

**Location:** WCC Halls A-C

**Time:** Monday, November 16, 2026, 1:00 PM - 5:00 PM

**Program #/Poster #:** PSTR171.08/R1

**Topic:** C.03. Parkinson’s Disease

**Support:** Ministerio de Ciencia, Innovación y Universidades (Grant No. PID2023-127802OB-I00)

**Title:** Tier-specific location of Lewy body pathology and related neuromelanin levels drive dopaminergic cell vulnerability in pigmented non-human primates

**Authors: *C. CANALES**[1], M. MARTINEZ DE ILARDUYA[1], J. CHOCARRO[1,2], D. GOMEZ-PINILLOS[1], B. SANCHEZ-ALCITURRI[1], E. LORENZO-RAMOS[1], G. ARIZNABARRETA[1], A. J. RICO[1], J. L. LANCIEGO[1,2,3];
[1]CIMA - Univ. of Navarra, Pamplona, Spain; [2]CiberNed, Pamplona, Spain; [3]Fundacion Cien, Madrid, Spain

**Abstract:** Although a differential vulnerability of dopaminergic neurons to degeneration based on their specific location within the dorsal and ventral tiers of the substantia nigra pars compacta (SNcD and SNcV, respectively) has long been postulated, the underlying mechanisms sustaining

these tier-specific differences remain poorly understood. Here, upon inducing a viral-mediated enhancement of neuromelanin (NMel) accumulation within dopaminergic neurons in non-human primates, the distribution of Lewy body-like inclusions (LBs) was analyzed within identified SNcD and SNcV neurons, together with their intracellular NMel levels. Results showed that the vast majority of intracytoplasmic inclusions were found in SNcV neurons, and indeed correlated to higher pigmentation levels. By contrast, only very few LBs were found in calbindin-positive neurons of the SNcD, which in parallel exhibited very low levels of NMel accumulation. These results postulate an additive effect made of a tier-specific location of LB burden together with high pigmentation levels as synergistic drivers sustaining the preferential vulnerability of SNcV dopaminergic neurons. Moreover, the evidence obtained here supported that NMel accumulation beyond a given threshold triggers the aggregation of endogenous α-Syn in the form of LBs; therefore, approaches intended to reduce pigmentation levels in SNcV neurons would likely induce a neuroprotective effect by preventing the subsequent aggregation of α-Syn.

**Disclosures: C. Canales:** None. **M. Martinez de Ilarduya:** None. **J. Chocarro:** None. **D. Gomez-Pinillos:** None. **B. Sanchez-Alciturri:** None. **E. Lorenzo-Ramos:** None. **G. Ariznabarreta:** None. **A.J. Rico:** None. **J.L. Lanciego:** None.

**Poster**

**PSTR171: Parkinson's Disease: Animal Models**

**Location:** WCC Halls A-C

**Time:** Monday, November 16, 2026, 1:00 PM - 5:00 PM

**Program #/Poster #:** PSTR171.09/R2

**Topic:** C.03. Parkinson’s Disease

**Support:** NIH/NINDS RO1 NS135830
NIH/NIA RF1 AG079199

**Title:** Neuromelanin accumulation in dopamine neurons induces neurodegeneration, neuroinflammation, and motor deficits in mice

**Authors: *C. MEYER**[1], K. CARTER[1], W. M. KENNEDY[1], N. E. YATES[1], A. DRUMOND-BOCK[1], L. R. LITER[1], H. BLANKENSHIP[1], A. IANNITELLI[2], D. WEINSHENKER[2], M. J. BECKSTEAD[1];
[1]Aging and Metabolism Res. Program, Oklahoma Med. Res. Fndn., Oklahoma City, OK; [2]Dept. of Human Genet., Emory Univ. Sch. of Med., Atlanta, GA

**Abstract:** The pigment neuromelanin (NM) is an oxidized catecholamine byproduct that accumulates in human dopaminergic neurons throughout life. Over time, NM particles aggregate to form granules that have established protective roles as antioxidants and chelators of toxic metals. However, NM may contribute to Parkinson's Disease (PD) neuropathology, as NM pigmentation decreases in patients, likely due to preferential degeneration of NM-containing dopamine neurons. The effect of NM in PD is understudied, partially due to the lack of NM accumulation in rodents. Therefore, to investigate the effect of NM in dopamine neurons, we

injected a *Cre*-dependent adeno-associated virus (AAV) into the substantia nigra pars compacta (SNc) of DAT$^{IRES cre}$ mice to express human tyrosinase (hTyr), an enzyme that catalyzes NM production. To vary the rate and extent of NM accumulation, we administered a low (1:100 dilution) or high (full-strength) dose of the vector. We then assessed NM accumulation, expression of hTyr and tyrosine hydroxylase (a dopamine neuronal marker) and microglia morphology in the SNc and ventral tegmental area (VTA), as well as motor function up to 16 weeks post-injection (wpi). Both doses induced hTyr expression and progressive NM formation over 16 wpi, with greater NM accumulation in the full-strength group. At 2 wpi, there was a significant reduction in tyrosine hydroxylase positive neurons in the high dose group, demonstrating that NM induces dopamine neuronal loss. Additionally, microglia in the VTA and SNc showed reduced branching complexity, reflecting a shift toward a reactive, neuroinflammatory state. After a low vector dose, NM accumulation did not affect motor function over the 16 wpi. In contrast, NM accumulation in the high dose group resulted in significant impairment in rotarod and open-field locomotion beginning at 2 wpi. In our model, greater NM accumulation, as in the full-strength group, was associated with adverse outcomes. These findings suggest that excess NM accumulation in dopamine neurons is sufficient to generate Parkinsonian phenotypes and provide a platform for further investigation of NM's contribution to PD progression.

**Disclosures: C. Meyer:** None. **K. Carter:** None. **W.M. Kennedy:** None. **N.E. Yates:** None. **A. Drumond-Bock:** None. **L.R. Liter:** None. **H. Blankenship:** None. **A. Iannitelli:** None. **D. Weinshenker:** None. **M.J. Beckstead:** None.

**Poster**

**PSTR171: Parkinson's Disease: Animal Models**

**Location:** WCC Halls A-C

**Time:** Monday, November 16, 2026, 1:00 PM - 5:00 PM

**Program #/Poster #:** PSTR171.10/R3

**Topic:** C.03. Parkinson's Disease

**Support:** Ministerio de Ciencia, Innovación y Universidades (Grant No. PID2023-127802OB-I00)

**Title:** Use of viral vectors coding for the human tyrosinase gene to induce pigmentation of dopaminergic neurons in macaques. Comparison between putaminal and nigral deliveries.

**Authors: *M. MARTINEZ DE ILARDUYA**[1], C. CANALES[1], J. CHOCARRO[1,2], D. GOMEZ-PINILLOS[1], B. SANCHEZ-ALCITURRI[1], E. LORENZO-RAMOS[1], G. ARIZNABARRETA[1], A. J. RICO[1], J. L. LANCIEGO[1,2,3];
[1]CIMA - Univ. of Navarra, Pamplona, Spain; [2]CiberNed, Pamplona, Spain; [3]Fundacion Cien, Madrid, Spain

**Abstract:** The lack of adequate animal models of Parkinson's disease (PD) currently represents the main barrier for pre-clinical testing of novel therapeutic candidates. The recent introduction

of a novel generation of rodent and non-human primate (NHPs) models based on the increased accumulation of neuromelanin (NMel) has gained increased appeal. These models reproduced the main neuropathological hallmarks that typically characterize human PD with unprecedented accuracy. Here, unilateral deliveries of adeno-associated viral vectors encoding the human tyrosinase gene (AAV9-hTyr) were performed into the substantia nigra pars compacta (SNpc) or the putamen in an attempt to induce a progressive pigmentation of SNpc neurons. Although both strategies managed to reproduce key PD signatures such as (i) ongoing pigmentation, (ii) Lewy body-like intracytoplasmic aggregates, (iii) time-dependent nigrostriatal damage, and (iv) pro-inflammatory scenario, viral vector deliveries into the SNpc resulted in a more severe nigrostriatal lesion and within shorter follow-up times. Compared with control specimens, up to 62% of dopaminergic cell loss was found upon delivery of AAV9-hTyr into the SNpc after four months in-life, whereas only an 18.5% of mean neuronal degeneration was observed following putaminal injections four and eight months post-viral administration. Similar trajectories were found when considering loss of nigrostriatal terminals, resulting in 72% loss of TH+ terminals when targeting the SNpc, compared to 15% nigrostriatal terminal damage in animals where AAV9-hTyr was delivered into the putamen. In summary, targeting the SNpc led to a faster progression and more severe nigrostriatal damage, whereas a slower and milder neurodegenerative phenotype resulted from putaminal injections. Although the development of ideal NHP models of prodromal PD is extremely challenging, those appointed here could be regarded as good choices for end-stage pre-clinical testing of disease-modifying candidates.

**Disclosures: M. Martinez de Ilarduya:** None. **C. Canales:** None. **J. Chocarro:** None. **D. Gomez-Pinillos:** None. **B. Sanchez-Alciturri:** None. **E. Lorenzo-Ramos:** None. **G. Ariznabarreta:** None. **A.J. Rico:** None. **J.L. Lanciego:** None.

**Poster**

**PSTR171: Parkinson's Disease: Animal Models**

**Location:** WCC Halls A-C

**Time:** Monday, November 16, 2026, 1:00 PM - 5:00 PM

**Program #/Poster #:** PSTR171.11/R4

**Topic:** C.03. Parkinson’s Disease

**Support:** NIH R01NS124777
NIH SIG S10-OD034258

**Title:** Modulation of D2and mGluR5 Receptor Function in Parkinson’s Disease: A PET and phMRI Study in Rats

**Authors: *I. CHEN**[1,2], Z. SUAR[2], R. GHOSH BISWAS[2], Y. LI[3], Y. SUN[4], J. WANG[1], B. G. JENKINS[2], A.-L. BROWNELL[1];
[1]Radiology, [2]Martinos Ctr. for Biomed. Imaging, [3]Massachusetts Gen. Hosp., Charlestown, MA; [4]Radiology, Massachusetts Gen. Hosp., Boston, MA

**Abstract:** Parkinson's disease (PD) is characterized by progressive dopaminergic dysfunction and altered glutamatergic signaling, yet the interaction between dopamine receptor activity and metabotropic glutamate receptor 5 (mGluR5) during disease progression remains poorly defined. To address this, we used simultaneous PET and pharmacological MRI (phMRI) in A53T α-synuclein transgenic Sprague-Dawley rats aged 3-24 months to evaluate mGluR5 and dopamine D2 receptor (D2R) function using [18F]FPEB and [18F]Fallypride, respectively, in combination with pharmacological challenges using d-amphetamine (a dopamine releaser) and MTEP (an mGluR5 antagonist). PD rats showed significantly lower basal mGluR5 binding than controls in key dopaminergic regions, indicating early glutamatergic dysfunction before overt behavioral decline. This reduction was sex dependent and, in females, correlated with age and body weight, suggesting progressive modulation of receptor-related signaling. d-Amphetamine (1mg/kg iv) increased cortical mGluR5 binding in controls but not in PD rats, with a stronger effect in female than male controls, while phMRI demonstrated blunted rCBV responses in male PD rats and no significant response in female PD rats. In contrast, basal $D_2R$ binding was largely preserved across dopaminergic regions, except for increased motor cortex binding in male PD rats. Female PD rats additionally showed lower $D_2R$ binding in motor cortex and caudate-putamen than male PD rats, further supporting sex-specific receptor alterations. MTEP (2 mg/kg iv) did not displace [$^{18}$F]Fallypride binding in any group, indicating that the PET signal reflected stable $D_2R$ binding under these conditions rather than acute competitive effects. However, phMRI after MTEP revealed robust cortical rCBV increases with minimal caudate-putamen response in male PD rats, whereas female PD rats showed decreased rCBV in caudate-putamen and thalamus with little cortical activation, highlighting striking sex-dependent differences in downstream circuit responses. Despite these clear molecular and functional imaging abnormalities, motor behavior remained normal across age, and preliminary histology showed preserved TH staining but marked α-synuclein expression, consistent with an early-stage PD phenotype even in aged animals. Together, these findings identify early, sex-dependent disruption of mGluR5- and $D_2R$-related signaling before overt motor impairment and support combined PET/phMRI as a sensitive *in vivo* platform for detecting presymptomatic circuit dysfunction, defining mechanistic biomarkers, and guiding therapeutic development in PD.

**Disclosures: I. Chen:** None. **Z. Suar:** None. **R. Ghosh Biswas:** None. **Y. Li:** None. **Y. Sun:** None. **J. Wang:** None. **B.G. Jenkins:** None. **A. Brownell:** None.

**Poster**

**PSTR171: Parkinson's Disease: Animal Models**

**Location:** WCC Halls A-C

**Time:** Monday, November 16, 2026, 1:00 PM - 5:00 PM

**Program #/Poster #:** PSTR171.12/R5

**Topic:** C.03. Parkinson's Disease

**Title:** Characterizing the role of dorsal striatal dopamine D3 receptors in L-DOPA-induced dyskinesia in hemi-parkinsonian rats

**Authors: *L. M. DOUGHTY**[1], C. R. BISHOP[2], K. E. LANZA[4], E. YANNI[2], S. ROCKE[3], J. PARK[2], H. PRISINZANO[2];
[1]Psychology, Binghamton Univ., Endicott, NY; [2]Psychology, Binghamton Univ., Binghamton, NY; [3]Binghamton Univ., New York, NY; [4]Dept. of Psychiatry, Northwestern Univ., Chicago, IL

**Abstract:** Parkinson's Disease (PD) is a progressive neurodegenerative disease characterized by the loss of niogrostriatal dopamine (DA) neurons in the substantia nigra pars compacta. L-DOPA remains the gold standard pharmacological treatment for people with PD; however its chronic use leads to the development of L-DOPA-induced dyskinesias (LID), treatment-related side effects typified by uncontrolled choreic and dystonic movements. Although the mechanisms by which LID emerges and persists are complex, DA receptors have long been implicated. While the roles of D1 (D1R)- and D2 (D2R)- receptors have been well-established, D3 receptor (D3R) upregulation and recent evidence of D1R-D3R cooperativity likely play a pronounced role in promoting and maintaining LID. Despite this, translation into effective therapeutic strategies remains limited in part due to gaps in knowledge regarding the function of the D3R in the parkinsonian brain. To address this, experiments were designed to examine whether stimulation of striatal D3R is sufficient to drive dyskinesia in L-DOPA-treated rats. To do so, Sprague-Dawley rats in experiments 1 and 2 (N=29) received unilateral 6-hydroxydopamine (6-OHDA) lesions, followed 3 weeks later by daily L-DOPA (6 mg/kg) for 2 weeks, and then again in a probe test (12 mg/kg) 5 days thereafter. Periodically rats were then rated for axial, limb, and orolingual (ALO) abnormal involuntary movements (AIMs) to capture emerging LID. Next, rats in experiments 1 and 2 were treated, in counterbalanced within-subjects designs, with the D3R preferring agonist PD128907 systemically (0, 0.1, 0.3 mg/kg) or intrastriatally (0, 0.5, 5 µl), respectively, after which AIMs were assessed. Results revealed dose-dependent D3R agonist-induced dyskinesia occurred with both systemic and intrastriatal routes. In addition, D3R-induced AIMs were positively correlated with L-DOPA-induced AIMs, but not striatal DA loss. Collectively these findings implicate an instigating role for L-DOPA in striatal D3R neuroplasticity that drives dyskinesia and support targeting aberrant D3R function for the treatment of LID.

**Disclosures: L.M. Doughty:** None. **C.R. Bishop:** None. **K.E. Lanza:** None. **E. Yanni:** None. **S. Rocke:** None. **J. Park:** None. **H. Prisinzano:** None.

**Poster**

**PSTR171: Parkinson's Disease: Animal Models**

**Location:** WCC Halls A-C

**Time:** Monday, November 16, 2026, 1:00 PM - 5:00 PM

**Program #/Poster #:** PSTR171.13/R6

**Topic:** C.03. Parkinson's Disease

**Support:** UH-NEOMED neurodegenerative disease and aging research center
CDMRP Grant HT94252310540
CDMRP Grant HT94252310588

**Title:** Modeling Cognitive Dysfunction in the Alpha-Synuclein Preformed Fibril Rat Model of Parkinson's disease

**Authors: *J. R. BECHTOLD**[1], N. AHMED[1], J. PATTERSON[2], C. J. KEMP[2], M. KUBIK[2], M. HORE[2], A. GONZALES[2], V. FIELD[1], V. SUNDARARAJAN[1], A. SALEM[1], J. ADIL[1], J. G. HOLDEN[3], C. E. SORTWELL[2], S. M. FLEMING[1];
[1]Pharmaceut. Sci., Northeast Ohio Med. Univ., Rootstown, OH; [2]Translational Neurosci., Michigan State Univ., Grand Rapids, MI; [3]Dept. of Psychology, Univ. of Cincinnati, Cincinnati, OH

**Abstract:** Cognitive dysfunction is common in Parkinson's disease (PD) with impairments in executive function typically observed early and development of dementia frequent in the later stages of the disorder. Although alpha-synuclein (α-Syn) pathology and circuit dysfunction within cortical and cholinergic pathways have been implicated in executive dysfunction and progression to dementia, there remain no targeted therapies for cognitive dysfunction in PD. The present study sought to model multiple aspects of PD-related cognitive dysfunction using α-Syn preformed fibrils (PFFs) in rats. Monomer (n=24) or α-Syn PFFs were bilaterally injected into the substantia nigra (SNc=20), striatum (Str=19), or striatum and vertical limb of the diagonal band of Broca within the basal forebrain (Str+VLDB=17) in male F344 rats at three months of age. From four to six months post-injection rats were tested on a battery of behavioral assays including cognitive measures of behavioral flexibility (set-shifting and reversal learning), attention and object memory (novel object recognition), and spatial memory (Barnes maze). In the operant test of behavioral flexibility both Str and Str+VLDB groups showed significant impairments in set-shifting and reversal learning with an increase in the number of trials to reach criterion and longer response latencies compared to monomer-injected rats. While in the novel object recognition test, the Str group showed significantly decreased attention for the objects compared to monomer and SNc groups. In the Barnes maze, spatial memory was impaired only in the Str+VLDB group compared to monomer. Taken together, the results show α-Syn PFFs can induce PD-related cognitive dysfunction in rats and will be a useful model for testing potential disease-modifying or symptomatic therapeutics targeting cognition in PD.

**Disclosures: J.R. Bechtold:** None. **N. Ahmed:** None. **J. Patterson:** None. **C.J. Kemp:** None. **M. Kubik:** None. **M. Hore:** None. **A. Gonzales:** None. **V. Field:** None. **V. Sundararajan:** None. **A. Salem:** None. **J. Adil:** None. **J.G. Holden:** None. **C.E. Sortwell:** None. **S.M. Fleming:** None.

**Poster**

**PSTR171: Parkinson's Disease: Animal Models**

**Location:** WCC Halls A-C

**Time:** Monday, November 16, 2026, 1:00 PM - 5:00 PM

**Program #/Poster #:** PSTR171.14/S1

**Topic:** C.03. Parkinson's Disease

**Support:** Aligning Science Across Parkinson's Grant: ASAP-020572, H.-Y.C.

**Title:** MitoPark mice show age-dependent impairments in instrumental learning that are dissociable from motor dysfunction

**Authors: *T. HUFF**, H.-Y. CHU;
Dept. of Pharmacol. and Physiol., Georgetown Univ. Med. Ctr., Washington, DC

**Abstract:** Parkinson's disease (PD) produces heterogeneous cognitive symptoms that are not well managed by currently available dopaminergic medications. Thus, there is a compelling need for a deeper understanding of the neurobiological mechanisms underlying cognitive impairments in PD. Recent human imaging studies of PD patients correlate substantia nigra (SN) degeneration with reinforcement-learning impairments. In the present work, we examined whether progressive nigrostriatal dopamine loss impairs instrumental learning in the MitoPark (MP) mouse -- a genetic model of nigrostriatal neurodegeneration. MP mice and littermate controls were tested across ages in a deterministic sequential task using an automated operant conditioning device. Mice earned sucrose pellets by completing a two-poke sequence within 30s; incorrect choices produced a timeout penalty. Forward (left->right) and reversal (right->left) phases were each performed in six daily 4h sessions, analyzed by linear regression across 1h bins. Primary metrics were cumulative pellets earned, poke efficiency (pellets/100 pokes), and trial accuracy (% correct).
At > 15 weeks of age (i.e., moderate stages of Parkinsonism), MP mice showed robust forward-learning impairments in all metrics, earning fewer cumulative pellets, poking less efficiently, and showing lower trial accuracy than controls. Reversal impairments across all three metrics were stronger still. Despite these deficits, MP mice showed no reduction in total poke activity, indicating preserved task engagement and motivation. At 12 weeks of age (i.e., the early motor stage of Parkinsonism), MP mice exhibited highly variable performance across all metrics of the deterministic sequential task, despite showing similar locomotor impairments in the open-field test. Thus, impairments in instrumental learning were dissociable from gross locomotor dysfunction.
Together, our findings show that MP mice develop robust, age-dependent impairments in instrumental learning that cannot be explained by reduced task engagement or gross locomotor impairment. More broadly, they support the model's usefulness for studying SN-dependent cognitive symptoms in PD. Ongoing work explores additional cognitive task assessments and tests potential preclinical treatment options for cognitive impairments in this model.

**Disclosures: T. Huff:** None. **H. Chu:** None.

**Poster**

**PSTR171: Parkinson's Disease: Animal Models**

**Location:** WCC Halls A-C

**Time:** Monday, November 16, 2026, 1:00 PM - 5:00 PM

**Program #/Poster #:** PSTR171.15/S2

**Topic:** C.03. Parkinson's Disease

**Support:** BGSU Optimal Aging Institute Small Grant
BGSU Catalyst Grant

**Title:** Examining reward sensitivity, apathy, and impulsivity in a 6-OHDA rat model of early Parkinson's Disease

**Authors: *E. SHULTZ**, S. O'NEIL, H. C. CROMWELL;
Psychology, Bowling Green State Univ., Bowling Green, OH

**Abstract:** Parkinson's Disease (PD) is a neurodegenerative disease of the dopaminergic system. While primarily considered a motor disease, it also presents with a wide variety of non-motor effects that are less understood. Additionally, medications commonly used to treat PD have side effects that can exacerbate existing symptoms and induce new ones. Among the non-motor symptoms, motivational dysfunction uniquely impacts quality of life and patient relationships. Predicting which patients are likely to exhibit motivation-related non-motor symptoms in response to medication or disease, particularly in early PD, is an area that could substantially influence treatment decisions and benefit patient wellbeing. The current study employs an aged 6-OHDA rodent model of Parkinson's Disease to examine facets of motivation such as reward sensitivity, impulsivity, and apathy prior to and after lesioning dopaminergic neurons in the striatum. The pattern of dopamine depletion in the dorsal striatum, associated with motor and executive functioning, vs. the ventral striatum, associated with affect and reward functioning, may contribute to disparate PD symptom presentation. Thus, subjects in this study are differentially lesioned and tyrosine hydroxylase (TH) cell volume, density, total cell count, and optical density are being assessed. Behavioral performance in the sucrose preference test, reward sensitivity operant test, splash test, open field test, novel object recognition task, delay discounting task, and progressive ratio task prior to and after lesioning dopaminergic neurons in the striatum is also being assessed. Finally, the effects of the first-line treatment for PD - L-DOPA - on the aforementioned aspects of motivation are being examined. This study aims to identify predictive behavioral and anatomical factors impacting presentation of motivational dysfunction.

**Disclosures: E. Shultz:** None. **S. O'Neil:** None. **H.C. Cromwell:** None.

**Poster**

**PSTR171: Parkinson's Disease: Animal Models**

**Location:** WCC Halls A-C

**Time:** Monday, November 16, 2026, 1:00 PM - 5:00 PM

**Program #/Poster #:** PSTR171.16/S3

**Topic:** C.03. Parkinson's Disease

**Support:** NSTC 1132314B182050MY3

**Title:** EEG Spectral Alterations and Their Association with Motor Impairment in a 6-OHDA-Induced Rat Model of Parkinson's Disease

**Authors: H. CHEN**[1,2], *T.-H. HSIEH[2,3];
[1]Morrison Acad. Taipei, New Taipei, Taiwan; [2]Sch. of Physical Therapy, Chang Gung Univ., Taoyuan, Taiwan; [3]Dept. of Physical Med. and Rehabil., Chang Gung Mem. Hospital, Linkou, Taoyuan, Taiwan

**Abstract:** Parkinson's disease (PD) is characterized by progressive dopaminergic degeneration and disrupted neural network activity. Quantitative electroencephalography (qEEG) is a non-invasive and cost-effective tool for assessing electrophysiological abnormalities. However, the relationship between EEG alterations and motor dysfunction in experimental PD models remains incompletely understood. Therefore, this study investigated qEEG changes and their associations with motor deficits in a 6-hydroxydopamine (6-OHDA)-induced rat model of PD. A unilateral 6-OHDA lesion was induced by stereotaxic injection into the medial forebrain bundle (MFB) to produce nigrostriatal dopaminergic degeneration. Four weeks after surgery, quantitative EEG recordings, apomorphine-induced rotation tests, and open-field assessments of locomotor activity were conducted. Spectral analysis revealed significantly increased Delta ($p < 0.01$) and Beta ($p < 0.05$) power, whereas Alpha ($p < 0.01$), Theta ($p < 0.01$), and Gamma ($p < 0.05$) power were significantly decreased in PD rats compared with sham controls. Correlation analyses demonstrated significant associations between EEG oscillatory activity and behavioral outcomes. Theta power was negatively correlated with apomorphine-induced rotations ($r = -0.79$, $p < 0.01$), while Alpha power showed a negative correlation ($r = -0.58$, $p < 0.05$) and Beta power showed a positive correlation ($r = 0.62$, $p < 0.01$). Open-field locomotor distance was negatively correlated with Delta power ($r = -0.63$, $p < 0.05$) and positively correlated with Theta power ($r = 0.71$, $p < 0.01$). These findings indicate that specific EEG frequency bands are associated with dopaminergic dysfunction and locomotor impairments in experimental Parkinsonism. qEEG may serve as a useful electrophysiological biomarker for monitoring disease severity and evaluating therapeutic interventions in PD.

**Disclosures: H. Chen:** None. **T. Hsieh:** None.

**Poster**

**PSTR171: Parkinson's Disease: Animal Models**

**Location:** WCC Halls A-C

**Time:** Monday, November 16, 2026, 1:00 PM - 5:00 PM

**Program #/Poster #:** PSTR171.17/S4

**Topic:** F.07. Rhythmic Pattern Generation

**Support:** NIH/NIEHS-1ZIAES103310-GC

**Title:** Dynamic Weight-Signatures as a Novel Biomarker of Motor Dysfunction in Mouse Models

**Authors: *A. PAPANERI**[1,2], C. T. SHOEMAKER[2,1], S. SAHA[2,1], G. CUI[2,1];
[2]DIR/NL/In Vivo Neurobio. Group, [1]NIH/NIEHS, Research Triangle Park, NC

**Abstract:** Clinical detection of motor dysfunction typically relies on neurological examination and observation of overt symptoms with clinical scoring. Instrumented approaches, including accelerometry and gait analysis, are increasingly used to quantify motor abnormalities that may be difficult to resolve by observation alone. In Parkinson's disease (PD), for example, resting tremor is typically observed in the 4-6 Hz range, highlighting the importance of capturing subtle motor fluctuations at biologically relevant timescales. Our study hypothesizes that dynamic weight signatures derived from ultra-high-frequency recordings of freely moving mice may reveal disease-associated motor changes before overt phenotype onset. Here, we tested whether high-precision weight and activity measurements can provide a simple, noninvasive screen for subclinical tremor or motor dysfunction with potential translational relevance. Using a high-precision weighing module, we recorded body weight and behavioral activity at >120 Hz with 0.1 mg sensitivity. To quantify biologically relevant fluctuations in the weight trace, we measured the normalized max-min range over time as an index of variability, dispersion, and fluctuation amplitude, and we evaluated temporal structure using autocorrelation analysis. In the Mitopark mouse model of PD, animals spend more time in non-ambulatory states and exhibit less stable locomotion than healthy controls. Although overall movement is reduced, this novel method reveals that Mitopark mice show a disproportionate increase in small, higher-frequency weight fluctuations, consistent with tremor-like or erratic motor activity. Autocorrelation curves further indicate altered motor temporal organization, potentially reflecting rapid irregular movements, freezing episodes, tremor-related oscillations, or reduced persistence of movement. Behavioral states were validated using synchronized video recordings to confirm correspondence with features observed in the weight traces. Together, these findings suggest that disease-model-specific behavioral signatures can be extracted from high-precision, ultra-fast weight measurements alone. This approach could be incorporated into rodent home-cage monitoring systems as a less invasive alternative to implanted activity sensors, although single housing may be required. If translatable, analogous sensing could potentially be embedded in household or clinical scales to enable early detection of subclinical tremor or motor dysfunction in humans.

**Disclosures: A. Papaneri:** None. **C.T. Shoemaker:** None. **S. Saha:** None. **G. Cui:** None.

**Poster**

**PSTR171: Parkinson's Disease: Animal Models**

**Location:** WCC Halls A-C

**Time:** Monday, November 16, 2026, 1:00 PM - 5:00 PM

**Program #/Poster #:** PSTR171.18/S5

**Topic:** C.03. Parkinson's Disease

**Support:** DoD Grant W81XWH-21-1-0915
NIH Grant 5R01NS104565
NIH Grant 5R01DK124098

**Title:** Robust Evaluation of Limb Dominance as a Tool for Investigating Hemispheric Vulnerability in Neurological Disease

**Authors: D. POKHAREL**[1], *K. M. LE[2], D. H. BELIGALA[3], T. SUBRAMANIAN[4], K. VENKITESWARAN[5];
[1]Howard Univ. Col. of Med., Washington, DC; [2]Howard Univ., Washington, DC; [3]Ohio Northern Univ., Perrysburg, OH; [4]Neurol., [5]Intrnl. Med., Howard Univ., Washington, DC

**Abstract:** Brain lateralization is a fundamental feature of nervous system organization and may influence vulnerability to neurological disorders characterized by asymmetric pathology, including Parkinson's disease. Reliable assessment of limb dominance in rodents is therefore essential for studies investigating hemispheric specialization and selective neurodegeneration. We compared three widely used behavioral paradigms for assessing paw preference in Sprague Dawley rats: the Collins Test, Staircase Test, and Pawedness Trait Test (PaTRaT). Thirty rats (12-48 weeks; 20 females, 10 males) completed all three assays, and laterality indices were calculated for each test. Additional cohorts (n = 173 total) were evaluated using the Collins Test to examine population-level distributions and the influence of age and sex. Repeated measures ANOVA revealed no significant differences in laterality indices across the three behavioral paradigms ($p = 0.801$). Substantial inter-test agreement was observed (Fleiss' $\kappa = 0.761$, $p < 0.001$), demonstrating robust consistency in paw preference classification across methodologies. Pairwise analyses showed the strongest agreement between the Collins and Staircase tests (Cohen's $\kappa = 0.747$). Population-level analysis revealed 43% right-pawed, 39% left-pawed, and 17% ambidextrous animals, closely matching previously reported distributions. Neither age nor sex significantly influenced paw preference outcomes. These findings establish that multiple behavioral paradigms provide reliable and consistent measures of limb dominance in rats. These findings may provide a reliable method for studying hemispheric asymmetry and selective vulnerability in Parkinson's disease and other neurological disorders.

**Disclosures: D. Pokharel:** None. **K.M. Le:** None. **D.H. Beligala:** None. **T. Subramanian:** None. **K. Venkiteswaran:** None.

**Poster**

**PSTR171: Parkinson's Disease: Animal Models**

**Location:** WCC Halls A-C

**Time:** Monday, November 16, 2026, 1:00 PM - 5:00 PM

**Program #/Poster #:** PSTR171.19/S6

**Topic:** C.03. Parkinson’s Disease

**Support:** WFT

**Title:** Characterization of the TSHR-hyt Mutant Mouse as a Potential Model for Dopaminergic Neurodegeneration and Parkinson’s Disease.

**Authors: C. TWIGGS**[1], *E. WALTERS[2];
[1]Biol., Howard Univ., Washington, DC; [2]Howard Univ. Coll Med., Washington, DC

**Abstract:** Parkinson's disease (PD) is characterized by degeneration of nigrostriatal dopaminergic neurons (DANs), but the mechanisms underlying its etiology are unclear. The

TSHR-hypothyroid (hyt) mouse harbors a dominant-negative Pro556Leu mutation in the IV transmembrane domain of the thyrotropin receptor (TSHR) that disrupts signaling and downstream effector mechanisms. Previous studies report that Tshr homozygous (hyt/hyt) mutants exhibit spontaneous circling behavior and loss of tyrosine hydroxylase (TH+) DANs in the substantia nigra (SN). In this study, we performed sib-pair mating to profile inheritance of the circling trait. Pedigree analyses show that circling segregates as an autosomal recessive trait, dependent on (+/hyt) or (hyt/hyt) zygosity, without sex bias. Directional circlers arise from allele-specific effects ($c_1$ = counterclockwise; $c_2$ = clockwise) at the same locus ($c_1 > c_2$). Circling trait displays incomplete penetrance, appearing sparsely in heterozygotes (+/hyt). When circling homozygotes (hyt/hyt) were injected with saline (0.9%) or L-DOPA (10 mg/kg), L-DOPA effectively attenuated circling within 0.5hr, and returned to baseline levels at 24hr. Immunoblotting of SN of non-circling and circling homozygotes revealed a 60% reduced TH expression alongside a 56% decrease in dopaminergic neuroprotective GPR37. Astroglial markers GFAP and IBA1 showed increases and decreases, respectively, in SN of circling mice compared to non-circlers. Preliminary analysis of the neuroprotective/neuroinflammatory regulatory factor IGF-1R, was increased (66%) in SN tissues of circlers. Collectively, our studies demonstrate that circling in TSHR-hyt mice displays incomplete penetrance, and that mice exhibiting circling behavior are dopamine-responsive. Additionally, DANs deficits in circling mutants correlate with altered expression of neuroprotective and neuroinflammatory factors. These findings suggest the importance of extrathyroidal TSHR signaling in dopaminergic homeostasis. The use of the TSHR-hyt mice as a model to elucidate mechanisms of nigrostriatal neurodegeneration and PD-related pathology is warranted.

**Disclosures: C. Twiggs:** None. **E. Walters:** None.

**Poster**

**PSTR171: Parkinson's Disease: Animal Models**

**Location:** WCC Halls A-C

**Time:** Monday, November 16, 2026, 1:00 PM - 5:00 PM

**Program #/Poster #:** PSTR171.20/S7

**Topic:** C.03. Parkinson’s Disease

**Title:** Dysregulation of Tryptophan Metabolism Heightens Neuroinflammation in Parkinson's Disease

**Authors: *N. FARSHCHI AZIZ**[1], S. KORTAGERE[2];
[1]Drexel Univ., Philadelphia, PA; [2]Microbiology and Immunol., Drexel Univ. Col. of Med., Philadelphia, PA

**Abstract:** Parkinson’s disease (PD), the second most common neurodegenerative disorder, affects over 11 million people worldwide. Traditionally defined as a CNS disorder with significant motor impairments resulting from dopaminergic neuron loss in the substantia nigra pars compacta, PD is now recognized as a multi-system disorder with prodromal non-motor symptoms, particularly gastrointestinal disturbances. These non-motor symptoms emerge at least

a decade before motor impairment is observed. These findings implicate the gut-brain axis in PD pathogenesis. A central mediator of this axis is tryptophan metabolism, which proceeds via host serotonin and kynurenine pathways and the microbiota-dependent indole pathway. We hypothesize that dopaminergic insults, whether 6-hydroxydopamine (6-OHDA)-driven or α-synuclein-mediated, disrupt tryptophan metabolism through host Kynurenine and microbial indole pathways. In adult Sprague Dawley rats lesioned with 6-OHDA, fecal analysis revealed significant decreases in protective indole metabolites including indole lactic acid ($p<0.05$), indole acrylic acid ($p<0.01$), and indole-3-carbaldehyde ($p<0.01$). Parallel brain analysis showed region-specific alterations in kynurenine metabolites, with kynurenic acid increased at the whole-brain level ($p<0.01$) and reduced in the striatum ($p<0.001$), while quinolinic acid was elevated in whole brain ($p<0.001$) but decreased in the cerebellum ($p<0.001$) and striatum ($p<0.01$). In a short-term dual-hit model we combined lipopolysaccharide (LPS)-induced gut dysbiosis with α-synuclein preformed fibrils (PFFs) lesions. As a result, striatal kynurenine metabolism shifted profoundly. Both kynurenic acid and quinolinic acid were increased with LPS alone ($p<0.0001$) but reduced when combined with PFFs ($p<0.0001$). These metabolic shifts were accompanied by elevated striatal IL-1β ($p<0.05$) and GM-CSF ($p<0.05$). Collectively, these results support that disruption of tryptophan metabolism at both microbial and host levels links gut-brain metabolic imbalance to PD-associated neuroinflammation, and that gut dysbiosis exacerbates this pathogenic cascade.

**Disclosures: N. Farshchi Aziz:** None. **S. Kortagere:** None.

**Poster**

**PSTR171: Parkinson's Disease: Animal Models**

**Location:** WCC Halls A-C

**Time:** Monday, November 16, 2026, 1:00 PM - 5:00 PM

**Program #/Poster #:** PSTR171.21/S8

**Topic:** C.03. Parkinson’s Disease

**Title:** Sex-dependent vulnerability to manganese-induced neurotoxicity and melatonin neuroprotection in Wistar rats

**Authors: *N. BOUHADDOU**;
Fac. of Sci. - Mohammed V Univ. in Rabat, Rabat, Morocco

**Abstract:** Excessive manganese (Mn) accumulation in the central nervous system induces a neurodegenerative syndrome known as manganism, characterized by motor and non-motor deficits with important similarities to Parkinson's disease. While biological sex is increasingly recognized as a modulator of neurotoxic susceptibility, its effect on Mn-induced behavioral impairment and the neuroprotective action of melatonin (MLT) remains poorly defined. This exploratory study assessed sex differences in Mn neurotoxicity and MLT neuroprotection using a comprehensive behavioral approach. Adult male and female Wistar rats (n=6/group/sex) were assigned to three groups: vehicle control, manganese dichloride (MnCl2), and MLT+MnCl2. MnCl2 (15 mg/kg i.p.) was administered daily for 21 days; MLT (20 mg/kg s.c.) was injected 30

min prior to MnCl2. An 8-test behavioral battery evaluated motor coordination (rotarod, open field), anxiety-like behavior (light-dark box, elevated plus maze), depressive-like behavior (forced swim test, sucrose preference test), and memory (novel object recognition, Y-maze). Statistical analyses were performed using two-way ANOVA (treatment x sex) with Bonferroni post-hoc correction (significance: $p<0.05$). Mn-exposed males showed significant deficits in motor coordination ($p<0.001$), locomotion ($p<0.001$), anxiety-like behavior ($p<0.05$), anhedonia ($p<0.05$), behavioral despair ($p<0.01$), and recognition memory ($p<0.05$). MLT co-treatment significantly mitigated motor ($p<0.01$) and affective impairments ($p<0.05$) in males. Mn-exposed females exhibited impairment restricted to body weight gain ($p<0.0001$) and locomotor/exploratory activity ($p=0.030$), with no significant effects on anxiety, depression, or memory. Two-way ANOVA revealed a significant treatment x sex interaction, with males exhibiting broader behavioral impairment than females. These results demonstrate that male rats are substantially more vulnerable than females to Mn-induced neurobehavioral impairment, and that MLT provides significant neuroprotection in the more susceptible sex. Biological sex should be considered a key variable in manganism research and in the design of neuroprotective strategies against Mn-related neurodegeneration.

**Disclosures: N. Bouhaddou:** None.

**Poster**

**PSTR171: Parkinson's Disease: Animal Models**

**Location:** WCC Halls A-C

**Time:** Monday, November 16, 2026, 1:00 PM - 5:00 PM

**Program #/Poster #:** PSTR171.22/T1

**Topic:** C.03. Parkinson’s Disease

**Support:** DoD NETP 13204752
NIDDK R01 DK124098
NINDS R01 NS104565
Anne M. and Phillip H. Glatfelter III Family Foundation

**Title:** Hemispheric Asymmetry of Dopaminergic Markers in a Rat Model of Paraquat and Lectin (P+L)-Induced Parkinsonism

**Authors: E. CLARK**[1], R. RODRIGUEZ[1], A. BOWERSOCK[1], B. PARTIN[1], D. POKHAREL[2], K. VENKITESWARAN[2], T. SUBRAMANIAN[2], *D. H. BELIGALA[1];
[1]Ohio Northern Univ., Ada, OH; [2]Howard Univ. Col. of Med., Washington DC, DC

**Abstract:** Parkinson’s disease (PD) is a progressive neurodegenerative disorder characterized by the selective loss of dopaminergic neurons and the development of motor and non-motor symptoms. Motor symptoms, including tremor, rigidity, and bradykinesia, are unilateral at disease onset in more than 85% of patients and often remain more severe on one side throughout disease progression. This pronounced asymmetry suggests that hemispheric differences in dopaminergic marker levels may influence disease susceptibility, progression, and underlying

neuropathology. Paw preference in rats, analogous to handedness in humans, provides a useful model for studying lateralized brain function. This study investigated hemispheric levels of dopaminergic markers during neurodegeneration in a paraquat and lectin (P+L) rat model of PD. We hypothesize that unilateral onset of neurodegeneration in this model can be due to altered expression of key dopaminergic proteins between hemispheres. Immunoblot analyses were performed to compare hemispheric expression of tyrosine hydroxylase (TH), dopa decarboxylase (DDC), and vesicular monoamine transporter 2 (VMAT2) in brain regions implicated in PD pathology, including the substantia nigra pars compacta (SNpc), dorsal striatum, ventral striatum, and ventral tegmental area. Analyses of control animals revealed no significant hemispheric differences in TH, DDC, or VMAT2 expression. When statistical comparisons were made using unpaired two-tailed t-tests (n = 6 per group), no significant hemispheric differences were observed for VMAT2 ($p = 0.09$), TH ($p = 0.51$), or DDC ($p = 0.12$) in the dorsal striatum, or for VMAT2 ($p = 0.13$), TH ($p = 0.48$), and DDC ($p = 0.28$) in the ventral striatum. Understanding the hemispheric levels of dopaminergic marker proteins may provide insight into the mechanisms underlying asymmetric disease onset and progression and contribute to the development of targeted therapeutic strategies for PD.

**Disclosures: E. Clark:** None. **R. Rodriguez:** None. **A. Bowersock:** None. **B. Partin:** None. **D. Pokharel:** None. **K. Venkiteswaran:** None. **T. Subramanian:** Other; Speaker's bureau - Supernus, Neurocrine, Acadia; Royalty CRC Press; and Founder of StereoRx.. **D.H. Beligala:** None.

**Poster**

**PSTR171: Parkinson's Disease: Animal Models**

**Location:** WCC Halls A-C

**Time:** Monday, November 16, 2026, 1:00 PM - 5:00 PM

**Program #/Poster #:** PSTR171.23/T2

**Topic:** C.03. Parkinson's Disease

**Support:** DoD Grant W81XWH-21-1-0915
NIH Grant 5R01NS104565
NIH Grant 5R01DK124098

**Title:** Evaluation of the nonmotor deficits in the Paraquat and Lectin induced body first subtype of Parkinson's Disease rat model

**Authors: *V. V. PESHATTIWAR**[1], C. C. SWAIN[3], D. POKHAREL[3], K. M. LE[1], I. NESTER[3], K. VENKITESWARAN[2], T. SUBRAMANIAN[1];
[1]Neurol., [2]Intrnl. medicine, Howard Univ., Washington, DC; [3]Dept. of Neurosciences, Univ. of Toledo Col. of Med. and Life Sci., Toledo, OH

**Abstract:** Parkinson's disease (PD) has been established as an heterogenous, multifactorial progressive neurodegenerative disorder. Recent evidence support the existence of two subtypes of PD, a body first and brain first subtype owing to variability in the disease site of onset as well

as disease progression. Animal models which could replicate the specific differences of these subtypes are important to explore the pathophysiology as well as to evaluate novel treatment options. While PD is considered to be a movement disorder, nonmotor symptoms are integral component, few often preceding the motor deficits. Epidemiological studies strongly implicate the association of environmental neurotoxins in the development of idiopathic PD. The aim of our present study was to characterize the development of nonmotor deficits with the chronic low dose exposure of environmental neurotoxin Paraquat (P) and Lectin (L) in the body first PD subtype animal model. To achieve this, we administered P+L (p.o.) daily to rats for 90 days. These animals underwent vibrissae evoked forelimb placement test (VEFPT) and cylinder test to detect the initiation and progression in motor deficits. The animals were evaluated for sleep abnormalities (REM sleep behavior disorder (RBD)) and cognitive deficits via Novel object recognition test (NORT) and Y maze test at various timepoints. After 21 weeks, post-mortem histopathological analysis was performed to assess neurodegeneration and alpha synucleinopathy in brain and gut. Onset of motor deficits initiated unilaterally from week 4 of P+L followed by gradual progression towards bilateral symptoms that were levodopa responsive. RBD, was observed in all animals regardless of the variation in their motor deficit severity. A gradual decline in the working and long-term memory was also observed in the animals over the study duration. The histopathology showed nigrostriatal dopaminergic degeneration and proteinase K resistant S129 alpha-synucleinopathy both in the gut and the brain. The replication of both progressive motor and nonmotor features in this rat model corroborates body first subtype of PD therefore making it an attractive option for testing neuroprotective experimental therapeutics and avenue to understand pathophysiological mechanisms.

**Disclosures: V.V. Peshattiwar:** None. **C.C. Swain:** None. **D. Pokharel:** None. **K.M. Le:** None. **I. Nester:** None. **K. Venkiteswaran:** None. **T. Subramanian:** None.

**Poster**

**PSTR171: Parkinson's Disease: Animal Models**

**Location:** WCC Halls A-C

**Time:** Monday, November 16, 2026, 1:00 PM - 5:00 PM

**Program #/Poster #:** PSTR171.24/T3

**Topic:** C.03. Parkinson’s Disease

**Support:** JSPS KAKENHI JP25K20487

**Title:** Weight loss associated with intestinal dysmotility in a mouse model of Parkinson’s disease featuring intranasal rotenone administration

**Authors: *K. KAWAGUCHI**, H. SATO, A. MATSUSHITA, K. HAYAKAWA, S. MORIDAIRA, K. ADACHI;
Div. of Pharmacol., Meikai Univ. Sch. of Dent., Sakado, Japan

**Abstract:** Body weight (BW) loss is a common non-motor symptom of Parkinson’s disease (PD) and may precede overt motor symptoms. In our previous study, mice receiving intranasal

rotenone developed approximately 10% BW loss beginning in the 3rd treatment week, without a significant association with motor deficits or neuronal loss in the substantia nigra pars compacta. However, the underlying mechanisms remain unknown. This study investigated the association between rotenone treatment-induced BW loss and the intestinal dysmotility in the mice and identified several factors that contribute to the dysmotility.Rotenone (0.35 mg/kg) was intranasally administered into the right nostril of male C57BL/6J mice once a day for 4 weeks. The 24-h food intake and stool output were assessed during rotenone treatment every week for 4 weeks. We examined the functional and histological changes in the upper intestinal segments using organ bath and Hematoxylin-Eosin stain, respectively, one week after 4-week rotenone treatment. Using another group of mice, we also examined smooth muscle contraction force in the intestinal segment from mice treated with 1-week rotenone, following the measurement of ATP levels in the adjacent segment, and mRNA expression levels of tyrosine hydroxylase (TH) and $M_3$ muscarinic acetylcholine receptor (mAChR).BW was gradually and significantly decreased from the 2nd week after rotenone treatment. There were no significant correlations between the rate of BW reduction and changes in food intake or stool output. The smooth muscle contraction force in the upper intestinal segment was reduced in the 4-week rotenone-treated mice compared to that in the non-treated mice without histological inflammation. There was a significant correlation between the rate of BW reduction and the peak or total value of the area under the curve of the trace in the upper intestinal contraction force. In contrast, 1-week rotenone caused a slight decrease in the acetylcholine-evoked intestinal smooth muscle contraction force, showing the reduction in the decay time of muscle contractile responses. In addition, ATP levels and mRNA expression levels of TH and $M_3$ mAChR were significantly decreased in 1-week rotenone-treated mice.These results suggested that BW loss in the rotenone-induced tardive Parkinson’s disease model mouse was associated with intestinal dysmotility, accompanying the functional changes in the intestinal tract from the early phase of rotenone treatment. Intranasal rotenone-treated mice may help clarify the mechanisms of the multifactorial non-motor symptoms of PD such as BW loss.

**Disclosures: K. Kawaguchi:** None. **H. Sato:** None. **A. Matsushita:** None. **K. Hayakawa:** None. **S. Moridaira:** None. **K. Adachi:** None.

**Poster**

**PSTR171: Parkinson's Disease: Animal Models**

**Location:** WCC Halls A-C

**Time:** Monday, November 16, 2026, 1:00 PM - 5:00 PM

**Program #/Poster #:** PSTR171.25/T4

**Topic:** C.03. Parkinson’s Disease

**Support:** FAPESP
CAPES

**Title:** Impact of Aging on Central and Peripheral Respiratory Dysfunction in a 6-OHDA Rat Model of Parkinson’s Disease

**Authors: *P. MEDEIROS**[1], L. PEDRAO[1], A. TAKAKURA[2], T. MOREIRA[3], B. FALQUETTO[2];
[2]Dept. of Pharmacol., [3]Dept. of Physiol., [1]Univ. of Sao Paulo, Sao Paulo, Brazil

**Abstract:** Parkinson's disease (PD) is a neurodegenerative disease with death of dopaminergic neurons in the Substantia Nigra (SN). It presents classic symptoms, and respiratory deficits. The disease prevails in older populations, and ageing is an aggravating factor. There is neurodegeneration in respiratory regions noted in 6-hydroxydopamine (6-OHDA) PD animal model, which reflects on the function of the respiratory system.Evaluate the effects of aging on respiratory function and anatomy of respiratory nuclei and the respiratory deficits in 6-OHDA animals.38 male rats of 12 months of age (CEUA 1342290421) were injected with 6-OHDA (24mg/ml) or vehicle into the striatum. Also, 13 young male rats were injected with vehicle into the striatum. On the 40th day, all animals were submitted to whole-body plethysmography. Half was euthanized and pulmonary mechanics was performed, and the other half underwent perfusion and brain dissection to perform immunohistochemistry. Two-way ANOVA followed by Bonferroni was applied with $p<0.05$. 6-OHDA reduced 65% of TH+ neurons in SN and old animals did not show reduction, confirming the PD model ($p<0,0001$). At normoxia, 6-OHDA animals showed reduced 28,1% respiratory frequency (fR) and 37,9% in minute ventilation (VE) ($p<0,0001$); during hypercapnia, tidal volume (VT) and VE was reduced (26% and 23%, respectively) ($p<0,0001$); in hypoxia, only VT was reduced by 24,2% ($p<0,0001$). Old animals displayed reduced VT and VE in normoxia (18,9% and 37,9%, respectively), hypercapnia (22,7% and 24,3%, respectively) and hypoxia (28,9% and 27,5%, respectively) ($p<0,0001$). We observed a 32% reduction in phox2b neurons in cNTS ($p<0,0001$), 53% in the RTN ($p=0,0003$), and in NK1R-expressing neurons in rVRG (15,2%) and preBotC (14,7%) ($p<0,0001$) in 6-OHDA but not old animals.Both aging and 6-OHDA rats showed reduced ventilation, but only 6-OHDA animals displayed central neurodegeneration, whilst aging suggests there is more peripheric neuromotor involvement.

**Disclosures: P. Medeiros:** None. **L. Pedrao:** None. **A. Takakura:** None. **T. Moreira:** None. **B. Falquetto:** None.

**Poster**

**PSTR171: Parkinson's Disease: Animal Models**

**Location:** WCC Halls A-C

**Time:** Monday, November 16, 2026, 1:00 PM - 5:00 PM

**Program #/Poster #:** PSTR171.26/T5

**Topic:** C.03. Parkinson’s Disease

**Support:** FAPESP 2023/11274-6
CAPES 001

**Title:** MINOCYCLIN TREATMENT PREVENTS INFLAMMATORY DEVELOPMENT OF MICROGLIA IN THE 6-OHDA MOUSE MODEL OF PARKINSON’S DISEASE

**Authors: *L. PEDRAO**[1], B. FALQUETTO[2], P. MEDEIROS[2];
[1]Dept. of Pharmacol., Univ. of Sao Paulo, Sao Paulo, Brazil; [2]Univ. of Sao Paulo, São Paulo, Brazil

**Abstract:** Parkinson's disease (PD) is a neurodegenerative disease with death of dopaminergic neurons in the Substantia Nigra (SN). It presents classic symptoms, and respiratory deficits. Although being idiopathic, one of the hypotheses of the development of the disease is inflammation. In 6-hydroxydopamine (6-OHDA) mouse model of PD, neurodegeneration is not restricted to SN, spreading to respiratory regions in the medulla oblongata. However, the reason why this region degenerates is also unknown. Minocycline (MINO) is an antibiotic drug, but studies show an off-label anti-inflammatory activity, which might reduce inflammation in the respiratory nuclei. Evaluate the effects of MINO in preventing the inflammation of respiratory nuclei and the outcome of treatment in the ventilation of animals. 50 male mice between 3-4 months of age (CEUA 7992180820) were injected with 6-OHDA (12mg/ml) or vehicle into the striatum. Half of both groups were treated with MINO (45 mg/kg/day, i.p.) from day 3 to day 6 after surgery. On the $6^{th}$ day, all animals were submitted to whole-body plethysmography and were euthanized. Brains were collected to perform immunohistochemistry, and the medulla oblongata was dissected to collect the respiratory nuclei and make flow cytometry. Due to low number of cells, animals were pooled (N = 2 animals). Two-way ANOVA followed by Bonferroni was applied with $p<0.05$. 6-OHDA reduced 76,3% of $TH^+$ neurons in SN of 6-OHDA animals did not show reduction, confirming the PD model ($p<0,0001$). At normoxia, 6-OHDA animals showed 17% reduction of respiratory frequency ($f_R$), with no alteration in other parameters, which was restored after treatment with MINO ($p<0,0001$); during hypercapnia and hypoxia, there was no difference between groups in the parameters analyzed. Flow cytometry for TNFα in the rVRG + preBötzinger showed in the 6-OHDA that 6% of microglia were active, and of those, 23,8% were responsive to TNFα; in the RTN, 6-OHDA group showed that 7,7% of microglia were active, and 27,1% were responsive to TNFα; in both nuclei, treatment with MINO was capable of preventing the inflammatory response ($p<0,0001$). 6-OHDA animals showed both inflammatory and respiratory impairments due to the model, and MINO could restore the respiratory function and preventing respiratory nuclei from developing an inflammatory response. **Financial support:** CAPES, FAPESP **Keywords:** Inflammation. Neural control of breathing. Parkinson’s Disease. Respiratory deficits.

**Disclosures: L. Pedrao:** None. **B. Falquetto:** None. **P. Medeiros:** None.

**Poster**

**PSTR172: Tauopathies, Synucleinopathies, and Other Related Diseases: Animal Models**

**Location:** WCC Halls A-C

**Time:** Monday, November 16, 2026, 1:00 PM - 5:00 PM

**Program #/Poster #:** PSTR172.01/Web Only

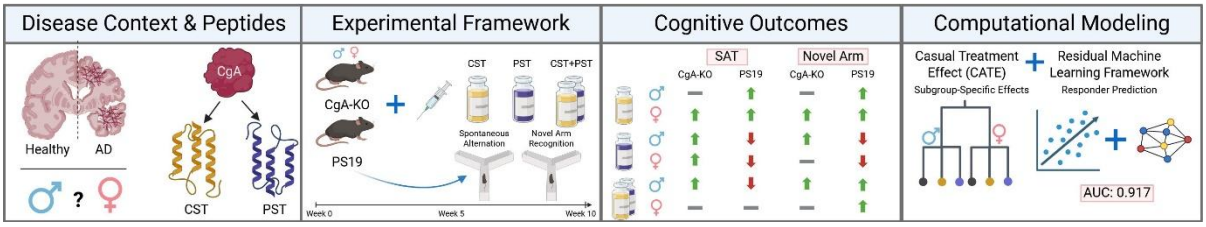
**Topic:** C.05. Tauopathies, Synucleinopathies, and Other Related Diseases

**Support:** NIH/NIA 1R21AG091126-01A1

**Title:** Uncovering Sex-Specific Memory Restoration Through Chromogranin A-Derived Peptides in Alzheimer's Disease

**Authors: R. GUHA**[1], S. K. MAHATA[2], *B. GUHA[3];
[1]Del Norte High School, San Diego, CA, San Diego, CA; [2]Med., UCSD, San Diego, CA;
[3]Independent, San Diego, CA

**Abstract:** Alzheimer's disease (AD) affects nearly 55 million people worldwide and is characterized by progressive cognitive decline associated with tau neurofibrillary tangles and β-amyloid plaques. Although nearly 66% of AD patients are females, sex-specific therapeutic strategies remain largely unexplored. Chromogranin A (CgA)-derived peptides catestatin (CST; $hCgA_{352-372}$) and pancreastatin (PST: $hCgA_{250-301}$) have been found to differentially regulate neuroinflammatory and synaptic pathways, suggesting their efficacy in treating tauopathies. This study investigates sex-dependent cognitive modulation mediated by CST and PST in CgA-knockout (CgA-KO) and PS19 mouse models. Mice (n=5-8/sex/treatment) were treated with intraperitoneal saline, CST (1 µg/g body weight), PST (0.7 µg/g body weight), or CST+PST for 10 weeks. Working memory (spontaneous alternation) and long-term spatial recognition memory (Y-maze novel arm exploration) were assessed longitudinally to quantify restoration of memory potential. For CgA-KO mice, both peptides improved cognition relative to saline; females exhibited stronger responses to CST treatment, whereas males exhibited stronger responses to PST-containing treatments. In contrast, under tau pathology, CST significantly restored cognition in both sexes ($p<0.05$), while PST caused detrimental effects to memory. A novel two-phase computational framework integrating cross-validated regularized regression-based treatment effect modeling with a residual machine-learning classifier (AUC=0.91) confirmed CST as the most effective intervention in tauopathy and revealed sex- and disease-context-specific response patterns. Collectively, these findings identify CST as a sex-aware therapeutic candidate and highlight the importance of incorporating biological sex, disease context, and computational modeling into peptide-based AD treatment strategies, advancing precision neurotherapeutics.




**Disclosures: R. Guha:** None. **S.K. Mahata:** None. **B. Guha:** None.

**Poster**

**PSTR172: Tauopathies, Synucleinopathies, and Other Related Diseases: Animal Models**

**Location:** WCC Halls A-C

**Time:** Monday, November 16, 2026, 1:00 PM - 5:00 PM

**Program #/Poster #:** PSTR172.02/T6

**Topic:** C.05. Tauopathies, Synucleinopathies, and Other Related Diseases

**Support:** NIH Grant AG085688
Freedom Together Foundation
Farmers Family Foundation

**Title:** Evidence for Motor Dysfunction and Cognitive Changes in a Novel Mouse Model for Lewy Body Dementia

**Authors: *J. SHI**[1,2], L. LI[1,2], V. L. DAWSON[1,2,3], T. M. DAWSON[1,2,3];
[1]Dept. of Neurol., [2]Neuroregeneration and Stem Cell Programs, Inst. for Cell Engin., [3]Dept. of Physiology, Pharmacol. and Therapeut., The Johns Hopkins Univ. Sch. of Med., Baltimore, MD

**Abstract:** Lewy body dementia (LBD) is the second most common neurodegenerative dementia, yet it is frequently misdiagnosed due to overlapping clinical features with Alzheimer's and Parkinson's diseases. LBD is characterized by α-synuclein (SNCA) fibrils, often accompanied by tau tangles and β-amyloid (Aβ) deposition; however, current animal models fail to capture the characteristic combination of cognitive and motor deficits seen in human patients. To address this gap, we developed a novel triple "humanized" mouse model (hLBD) expressing human SNCA (hSNCA), human tau (hMAPT), and the $APP^{NL-G-F}$ knock-in for Aβ pathology. hSNCA mice were obtained from Jackson Laboratories and $APP^{NL-G-F}$ and hMAPT from RIKEN, then backcrossed to C57BL/6. Genotypes were confirmed via PCR and gel electrophoresis. Ten-month-old male and female hLBD mice (n=12; 5 females, 7 males) and wild-type controls (n=11; 5 females, 6 males) underwent cognitive testing using the Morris water maze (MWM), including 5 days of acquisition training followed by a probe trial, and motor assessment via grip strength testing. Experimenters were blinded to genotype, and with replicated results. Trials were video-tracked using ANY-maze software. Data (mean ± SEM) were analyzed using t-tests or two-way ANOVA in GraphPad Prism 6. Sex differences were assessed. hLBD mice displayed significant cognitive impairment, taking longer to locate the platform during acquisition training (t-test, $p<0.001$), indicating deficits in learning, and approximately twice as long to locate the platform during the probe trial with fewer platform entries (t-test, $p<0.05$), indicating deficits in memory recall. Motor deficits were also evident: hLBD mice showed reduced swim speed during the probe trial consistent with bradykinesia (t-test, $p<0.05$), and forelimb-hindlimb grip strength was decreased by approximately 50% compared to controls (t-test, $p<0.01$), with males showing a more pronounced deficit (two-way ANOVA, $p<0.01$). No differences in body weight were observed in males (t-test, n.s.), eliminating weight as a confounding variable. This exploratory study demonstrates that hLBD mice recapitulate both the cognitive and motor deficits characteristic of human LBD, supporting its utility as a translational platform for mechanistic studies and therapeutic development.

**Disclosures: J. Shi:** None. **L. li:** None. **V.L. Dawson:** None. **T.M. Dawson:** None.

**Poster**

**PSTR172: Tauopathies, Synucleinopathies, and Other Related Diseases: Animal Models**

**Location:** WCC Halls A-C

**Time:** Monday, November 16, 2026, 1:00 PM - 5:00 PM

**Program #/Poster #:** PSTR172.03/T7

**Topic:** C.05. Tauopathies, Synucleinopathies, and Other Related Diseases

**Title:** EIF2B Activator BMS-986419 / EVT-8683 Prevents Integrated Stress Response and Protects from Neurological Decline in a Vanishing White Matter Disease Model

**Authors: *D. MENSCHING**[1], A. GARCIA DIAZ BARRIGA[1], N. C. CARTY[1], M. HERMANN[2], T. KRÖCHER[1], E. STRERATH[1], M. GRUEN[1], K. KOLLMANN[2], T. SAMATOV[2], B. SEIP[2], A. LUCAS[4], F. DEGLAVE[5], E. ERDOCIAIN[5], C. BROWN[4], D. WALTER[4], M. GEMKOW[1], R. B. BOYANAPALLI[6], K. J. RHODES[7], R. J. HARGREAVES[7], R. KUHN[3], Y. RUDHARD[1];
[1]Evotec SE, Hamburg, Germany; [2]Evotec Intl. GmbH, Goettingen, Germany; [3]Evotec Intl. GmbH, Hamburg, Germany; [4]Evotec (UK) Ltd., Abingdon, United Kingdom; [5]Evotec (Toulouse) SAS, Toulouse, France; [6]Bristol Myer Squibbs, LEXINGTON, MA; [7]Bristol-Myers Squibb Co., Cambridge, MA

**Abstract:** The integrated stress response (ISR) is a conserved pathway that suppresses global protein translation while promoting stress-response proteins. The GDP/GTP exchange factor eIF2B is central to this pathway by controlling ternary complex formation during translation initiation. Although acute ISR activation supports proteostasis, chronic ISR activation contributes to neurological disease, as illustrated by partial loss-of-function eIF2B mutations causing Vanishing White Matter Disease (VWMD), a rare leukodystrophy. We developed BMS-986419 / EVT-8683, a novel CNS-penetrant eIF2B activator with a favourable pharmacological profile, and show that it reduces ISR, normalizes protein translation in vitro, and prevents ISR-driven neurological and behavioural decline in vivo. In the Optic Nerve Crush model, BMS-986419 / EVT-8683 produced dose-dependent ISR suppression, retinal ganglion cell protection, and sustained activity, establishing an efficacious dose for chronic treatment studies. In the $EIF2B5^{R195H/R195H}$ (2B5ho) mouse model of VWMD, the compound showed dose-dependent reversal of ISR and normalization of body weight, alongside transcriptional rescue of synaptic transmission pathways. With 18 weeks of once-daily dosing, BMS-986419 / EVT-8683 fully normalized ISR and body weight and completely prevented astrogliosis, microgliosis, neurodegeneration, weight loss, and motor deficits. Together, these data identify BMS-986419 / EVT-8683 as a brain-penetrant ISR inhibitor with potential to treat VWMD and other neurological diseases driven by chronic ISR activation.

**Disclosures: D. Mensching:** A. Employment/Salary (full or part-time):; Evotec SE. **A. Garcia Diaz Barriga:** A. Employment/Salary (full or part-time):; Evotec SE. **N.C. Carty:** A. Employment/Salary (full or part-time):; Evotec SE. **M. Hermann:** A. Employment/Salary (full or part-time):; Evotec International GmbH. **T. Kröcher:** A. Employment/Salary (full or part-time):; Evotec SE. **E. Strerath:** A. Employment/Salary (full or part-time):; Evotec SE. **M. Gruen:** A. Employment/Salary (full or part-time):; Evotec SE. **K. Kollmann:** A. Employment/Salary (full or part-time):; Evotec International GmbH. **T. Samatov:** A. Employment/Salary (full or part-time):; Evotec International GmbH. **B. Seip:** A. Employment/Salary (full or part-time):; Evotec International GmbH. **A. Lucas:** A. Employment/Salary (full or part-time):; Evotec (UK) Ltd. **F. Deglave:** A. Employment/Salary (full or part-time):; Evotec (Toulouse) SAS. **E. Erdociain:** A. Employment/Salary (full or part-time):; Evotec (Toulouse) SAS. **C. Brown:** A. Employment/Salary (full or part-time):; Evotec

(UK) Ltd. **D. Walter:** A. Employment/Salary (full or part-time):; Evotec (UK) Ltd. **M. Gemkow:** A. Employment/Salary (full or part-time):; Evotec SE. **R.B. Boyanapalli:** A. Employment/Salary (full or part-time):; Bristol-Myers Squibb Company. **K.J. Rhodes:** A. Employment/Salary (full or part-time):; Bristol-Myers Squibb Company. **R.J. Hargreaves:** A. Employment/Salary (full or part-time):; Bristol-Myers Squibb Company. **R. Kuhn:** A. Employment/Salary (full or part-time):; Evotec International GmbH. **Y. Rudhard:** A. Employment/Salary (full or part-time):; Evotec SE.

**Poster**

**PSTR172: Tauopathies, Synucleinopathies, and Other Related Diseases: Animal Models**

**Location:** WCC Halls A-C

**Time:** Monday, November 16, 2026, 1:00 PM - 5:00 PM

**Program #/Poster #:** PSTR172.04/T8

**Topic:** C.05. Tauopathies, Synucleinopathies, and Other Related Diseases

**Support:** R01AG068330
R01AG093847
BrightFocus A20201775S
CART Fund
Cure Alzheimer's Fund
P30GM127211

**Title:** Tau pathology disrupts inhibitory control of hemodynamics and neurovascular coupling

**Authors: *R. E. IRMEN**[1,2], S. TURNER[1], A. SNIPES[1], L. JOHNSON[3], A. Q. BAUER[4], S. L. MACAULEY[2];
[2]Physiol., [1]Univ. of Kentucky, Lexington, KY; [3]Univ. of Kentucky, Lexington, KY, ;
[4]Radiology, Washington Univ. in St. Louis, St. Louis, MO

**Abstract:** Background: Primary and secondary tauopathies are characterized by progressive impairments in neuronal activity, network synchrony, and excitatory/inhibitory (E/I) imbalance. Despite extensive investigation of tau-mediated neuronal dysfunction, considerably less is known about how these changes impact the neurovascular unit and coupling. Our previous studies demonstrate that tau pathology disrupts sleep, reduces EEG beta power, alters glutamate and GABA production, and promotes cortical hyperexcitability, suggesting widespread network dysfunction. Importantly, inhibitory signaling remains a plausible therapeutic target. Because coordinated neuronal activity is a primary regulator of cerebral blood flow, we hypothesized that tau-dependent E/I imbalance contributed to neurovascular uncoupling. Methods: EEG/EMG recordings were performed on 9 month P301S and wildtype (WT) mice to assess sleep quantity, relative frequency, and oscillatory activity. Stable isotope-resolved metabolomics quantifies glucose-derived and total metabolite abundance. Wide-field optical imaging (WFOI) measured glutamatergic calcium dynamics and hemodynamics during rest and stimulation. Immunohistochemistry characterized inhibitory neuronal populations and vascular morphology. Results: Tau pathology reduces time spent in NREM and REM sleep while reducing EEG beta

power, coherence, and altering oscillatory activity. Metabolomics revealed an overall reduction in metabolite abundance; however, P301S mice exhibited an increase in $^{13}C$ labeled glutamate at the expense of GABA production. WFOI revealed increased glutamatergic calcium dynamics during stimulation in P301S mice. Despite heightened neuronal activity, P301S mice exhibited abnormal hemodynamic responses. Lectin labeling of brain vasculature revealed increased branching, length, and thickness of vessels. Additionally, preliminary data suggests P301S mice exhibit reductions in parvalbumin labeled neurons and GAD65/67 labeling. Conclusions: Tau pathology is associated with progressive network dysfunction characterized by E/I imbalance, metabolic reprogramming, impaired synchrony, and neurovascular uncoupling. Our findings support a model in which tau pathology disrupts inhibitory regulation of cerebral hemodynamics. Ongoing studies using whole-brain light sheet microscopy and single-nucleus RNA sequencing will define how tau pathology alters neuronal populations, vascular architecture, and cell-type specific transcriptional programs. Identifying mechanisms linking neuronal and vascular dysfunction may reveal novel therapeutic targets for tauopathies.

**Disclosures: R.E. Irmen:** None. **S. Turner:** None. **A. Snipes:** None. **A.Q. Bauer:** None. **S.L. Macauley:** E. Ownership Interest (stock, stock options, royalty, receipt of intellectual property rights/patent holder, excluding diversified mutual funds); A patent (Application #63/770,737) relevant to the work being presented has been filed by the University of Kentucky on behalf of Shannon Macauley (Inventor)..

**Poster**

**PSTR172: Tauopathies, Synucleinopathies, and Other Related Diseases: Animal Models**

**Location:** WCC Halls A-C

**Time:** Monday, November 16, 2026, 1:00 PM - 5:00 PM

**Program #/Poster #:** PSTR172.05/T9

**Topic:** C.05. Tauopathies, Synucleinopathies, and Other Related Diseases

**Title:** Age-Dependent Characterization of rTg4510 Mice to Guide Tauopathy Drug Screening Endpoints

**Authors: *Y. LI**;
Pharmaron Beijing Co. Ltd, Beijing, China

**Abstract: Title:** Age-Dependent Characterization of rTg4510 Mice to Guide Tauopathy Drug Screening Endpoints
**Authors:** Yinjie Li, Ce Zhong, Yufang Yan, Zhanshan Chen, Tianli Zhang, Jiameng Xu, Hong Liu, Zixuan Zhang, Yarou Pu, Jing Ma, Tong Wang, ***Fang He**.Pharmaron, Beijing, China.
**Abstract:** The rTg4510 mouse is a widely used preclinical tauopathy model that overexpresses human P301L tau and develops progressive behavioral deficits, tau pathology, neuroinflammation, and neurodegeneration. To guide model selection and endpoint design for tauopathy drug discovery, we characterized disease progression in female rTg4510 mice at an early symptomatic stage (5 months of age) and an advanced stage (8 months of age) using behavioral, pathological, and transcriptomic analyses.

Cognitive function, assessed by Morris water maze, Y-maze, and novel object recognition, was impaired at 5 months and further deteriorated at 8 months. Anxiety-related and disinhibition-like behaviors, evaluated by open field and elevated plus maze, showed trends toward increased center-zone and open-arm exploration at 5 months, with significant alterations at 8 months. Motor dysfunction, measured by hind limb clasping, was minimal at 5 months but significantly increased at 8 months. Neuroinflammatory changes also progressed with age. In the hippocampus, GFAP and IBA1 showed moderate increases at 5 months and significant increases at 8 months, whereas cortical GFAP and IBA1 were significantly elevated at both ages. Tau pathology displayed a similar region-dependent pattern, with hippocampal AT100 becoming significant at 8 months, while cortical AT8 and AT100 were significantly increased at both 5 and 8 months. Transcriptomic profiling further revealed age-dependent alterations in pathways related to long-term potentiation, neuroinflammation, and synaptic dysfunction.
These findings indicate that age selection strongly influences endpoint sensitivity in rTg4510 studies. Earlier stages particularly advantageous for prevention-oriented studies and for interventions such as tau-lowering or neuroinflammation-targeting approaches, whereas later stages provide a stronger efficacy window for assessing therapeutic benefit on established behavioral and pathological phenotypes, including targeted by anti-tau antibodies, synaptic protective compounds, and other disease-modifying strategies.
By understanding stage-specific distinctions, researchers can strategically select rTg4510 mice at different disease stages according to their investigative and therapeutic goals, thereby enhancing the efficiency and relevance of preclinical drug discovery for tauopathies.

**Disclosures: Y. Li:** A. Employment/Salary (full or part-time):; Pharmaron Beijing Co. Ltd.

**Poster**

**PSTR172: Tauopathies, Synucleinopathies, and Other Related Diseases: Animal Models**

**Location:** WCC Halls A-C

**Time:** Monday, November 16, 2026, 1:00 PM - 5:00 PM

**Program #/Poster #:** PSTR172.06/T10

**Topic:** C.05. Tauopathies, Synucleinopathies, and Other Related Diseases

**Title:** Establishing a Heterochronic Parabiosis Model in Aged α-Synuclein Preformed Fibril Mice: A Feasibility and Proof-of-Concept Study

**Authors: *R. BABARIA**[1,2], H. JO[2], S.-U. KANG[2];
[1]Johns Hopkins Univ., Baltimore, MD; [2]Johns Hopkins Sch. of Med., Baltimore, MD

**Abstract:** Aging is a major risk factor for α-synucleinopathies and related dementias, such as Parkinson's disease with dementia (PDD), and are characterized by abnormal α-synuclein (α-syn) protein accumulation. The spread of α-syn pathology can be modeled with a single intrastriatal injection of recombinant α-syn preformed fibrils (striatal-PFFs). Heterochronic blood exchange (HBE) through parabiosis, the surgical union of two mice, enables the investigation of the effects of young systemic milieu on aging mechanisms via a shared circulatory system between aged and young mice. Heterochronic parabiosis has been widely studied in aged mice,

but its application to aged α-synuclein PFF models remains unexplored. Here, we conducted a feasibility study to establish and validate this model. Male and female C56BL/6J mice aged 20-24 months (n=26) underwent unilateral intrastriatal injection of PFF or PBS prior to parabiosis. Behavioral analyses were performed before and after injection by an investigator blinded to treatment group. The mice were assigned to one of four experimental groups: heterochronic parabiosis between aged mouse with striatal-PFF injection and young mouse (HPFF, n=7 pairings), isochronic parabiosis between aged mouse with PFF and non-injected aged mouse (IPFF, n=5 pairings), heterochronic parabiosis between aged mouse with PBS and young mouse (HPBS, n=6 pairings), and isochronic parabiosis between aged mouse with PBS and non-injected aged mouse (IPBS, n=3 pairings). We assessed surgical survival, postoperative recovery, blood-sharing validation, and long-term follow-up. Cross-circulation build-up was validated by Evans blue assay with an optical absorption value at 620 nm.Prior to parabiosis, PFF-injected mice exhibited deficits compared to pre-injection baseline, including reduced rotarod latency, grip strength, Y-maze alternation, and novel object discrimination index, and an increased pole test descent time (paired analyses, all $p<0.05$). 21 pairings were created across all groups; 95% survived surgery and 86% reached the planned study midpoint (3 weeks). Body weight recovered to baseline within 2.5 weeks. Evans blue analysis demonstrated robust circulatory exchange with the recipient serum optic density reaching, on average, approximately 78% of donor levels.These findings suggest the feasibility of combining heterochronic parabiosis with an aged PFF-induced α-synucleinopathy model, while achieving high surgical survival and shared blood circulation. Ongoing analyses will evaluate α-syn pathology, neuroinflammation, and neuronal integrity to determine if exposure to young circulation can alter α-syn pathology.

**Disclosures: R. Babaria:** None. **H. Jo:** A. Employment/Salary (full or part-time):; Johns Hopkins School of Medicine. **S. Kang:** A. Employment/Salary (full or part-time):; Johns Hopkins University School of Medicine.

**Poster**

**PSTR172: Tauopathies, Synucleinopathies, and Other Related Diseases: Animal Models**

**Location:** WCC Halls A-C

**Time:** Monday, November 16, 2026, 1:00 PM - 5:00 PM

**Program #/Poster #:** PSTR172.07/T11

**Topic:** C.05. Tauopathies, Synucleinopathies, and Other Related Diseases

**Support:** Harrington Discovery Institute 2023 Cathy and Paul Douglas Scholar in Alzheimer's Discovery Award
Alzheimer's Association AARG-25-1476652

**Title:** Modulating the Hsp90 Co-Chaperone Aha1 to Reduce Pathological Tau Accumulation

**Authors: *B. OLUKADE**[1,2], D. MEZQUITE-GARCIA[1,2], L. J. BLAIR[1,2];
[1]Dept. of Mol. Med., Univ. of South Florida, Tampa, FL; [2]Byrd Alzheimer's Ctr. and Res. Inst., Tampa, FL

**Abstract:** Alzheimer disease (AD) and related tauopathies are characterized by the progressive accumulation of pathological tau species, leading to neuronal dysfunction, neurodegeneration, and cognitive decline. Despite extensive efforts to target tau pathology therapeutically, effective disease-modifying interventions remain limited. Increasing evidence suggests that disruption of molecular chaperone networks contributes to tau misfolding and aggregation, highlighting protein quality control pathways as promising therapeutic targets. The 90kDa heat shock protein (Hsp90) and its co-chaperone, ATPase homolog 1 (Aha1), influence tau dynamics. In AD human brain tissue, Aha1 colocalizes with aberrant tau, and its overexpression in tau mouse models exacerbates tau pathology and cognitive deficits. Here, we investigated whether reducing Aha1 expression could alter tau and mitigate disease-associated phenotypes in the PS19 transgenic mouse model of tauopathy. A gene-silencing strategy, adeno-associated virus (AAV)-mediated (AAV-PHP.eB) short hairpin RNA was employed through retro-orbital injection to modulate Aha1 expression, followed by behavioral, biochemical, and neuropathological assessments. Our preliminary analyses in the anterior cortex revealed a significant reduction in soluble total tau within female tau transgenic mice which was complemented by Aha1 suppression, whereas comparable effects were not observed in males. Importantly, reduction of Aha1 was well tolerated and did not adversely affect locomotor activity, anxiety-related behaviors, or working memory. Evaluation of the effects of Aha1 modulation in additional brain regions. pathological tau species is ongoing. Through this study, we will be able to determine if targeting Aha1 could be used as a strategy to regulate tau proteostasis. More broadly, these studies will provide insight into how selective modulating of protein quality control pathways may influence the progression of tau-driven neurodegeneration.

**Disclosures: B. Olukade:** None. **D. Mezquite-Garcia:** None. **L.J. Blair:** None.

**Poster**

**PSTR172: Tauopathies, Synucleinopathies, and Other Related Diseases: Animal Models**

**Location:** WCC Halls A-C

**Time:** Monday, November 16, 2026, 1:00 PM - 5:00 PM

**Program #/Poster #:** PSTR172.08/T12

**Topic:** C.05. Tauopathies, Synucleinopathies, and Other Related Diseases

**Support:** NIH Grant 5R01AG087877-03

**Title:** Common use pesticide alters TDP-43 dynamics in zebrafish

**Authors: *S. M. KIEHL**[1], R. WEEKS[2], G. FRAGOLA[3], T. J. COHEN[4];
[1]Cell Biol. and Physiol., [2]Univ. of North Carolina at Chapel Hill, Chapel Hill, NC; [3]UNC at Chapel Hill, Chapel Hill, NC; [4]Neurol., Univ. of North Carolina - Chapel Hill, Chapel Hill, NC

**Abstract:** Chronic exposure to low doses of a common use pesticide (CUP) has been epidemiologically associated with a range of neurodegenerative diseases, including amyotrophic lateral sclerosis (ALS). However, little is known about the mechanism of how these environmental exposures to CUP induce neurodegenerative pathology. Here, we examined the

effect of CUP on TAR DNA-binding protein 43 (TDP-43), whose nuclear depletion and aggregation is a hallmark of several neurodegenerative diseases, notably ALS. In HEK293 cells with GFP-tagged cytoplasmic TDP-43, we observed formation of GFP+ foci after 6 hours of exposure to CUP at concentrations as low as 3.125 μM. We next used an *in vivo* zebrafish (*Danio rerio*, ZF) model aged 21 months exposed to 1 μM CUP for 9 days. P-values were calculated using Student's t-test unless specified otherwise. Behavioral analysis of ZF by novel tank analysis showed decreased time spent in "safe" zone (133.74 s ± 89.94 [CUP N=54] vs. 215.86 s ± 86.86 [DMSO N=48]; $p < 0.01$) and increased time spent in "risk-associated" zone (98.87 s ± 87.02 vs. 38.21s ± 57.28; $p < 0.01$). Swim tunnel suggested impaired mobility with reduced time to fatigue (2120 s ± 764 [CUP N=22] vs. 2524 s ± 651 [DMSO N=24]; $p = 0.08$ with log-rank test). Harvested ZF brains (N=8) had increased mRNA levels of *tardbp* (fold change (FC) = 1.78 ± 0.77, $p = 0.03$), a ZF-specific *tardbp* homolog *tardbpl* (FC = 1.36 ± 0.18, $p = < 0.01$), and splicing variant *tardbplv1* (FC = 1.30 ± 0.29, $p = 0.28$). We used principal component analysis (PCA) and k-means clustering (k=2) to group ZF based on novel tank assay results into approximate "resilient" and "susceptible" populations and examined TDP-43 mRNA expression changes. "Resilient" populations (N=4) had elevated *tardbp* mRNA (FC = 2.83 ± 1.2, $p = 0.01$) with no significant changes in *tardbpl* ($p = 0.24$) or *tardbplv1* ($p = 0.26$) mRNA. "Susceptible" populations (N=4) had elevated *tardbpl* mRNA (FC = 1.49 ± 0.1, $p < 0.01$) with no significant changes in *tardbp* ($p = 0.87$) or *tardbplv1* ($p = 0.07$) mRNA. In summary, we observed CUP-induced formation of TDP-43 puncta, suggesting possible aggregation. The observed behavioral changes in ZF aligned with symptoms of TPD-43 proteinopathies, including reduced risk-aversion in frontotemporal dementia (FTD) and reduced mobility in ALS. Finally, CUP appeared to increase mRNA levels of TDP-43 genes and splice variants, with selective upregulation of *tardbp* in "resilient" populations and *tardbpl* in "susceptible" populations. This is the first research to associate this CUP exposure with TDP-43 dysregulation and begin to distinguish TDP-43 dynamics between zebrafish populations.

**Disclosures: S.M. Kiehl:** None. **R. Weeks:** None. **G. Fragola:** None. **T.J. Cohen:** None.

**Poster**

**PSTR172: Tauopathies, Synucleinopathies, and Other Related Diseases: Animal Models**

**Location:** WCC Halls A-C

**Time:** Monday, November 16, 2026, 1:00 PM - 5:00 PM

**Program #/Poster #:** PSTR172.09/T13

**Topic:** C.05. Tauopathies, Synucleinopathies, and Other Related Diseases

**Support:** Aligning Science Across Parkinson's ASAP-020572

**Title:** Limbic System α-Synuclein Pathology Induces Apathy-like Behavior in Mice

**Authors: *Y.-T. HUANG**[1], H.-Y. CHU[2];
[1]Dept. of Pharmacol. and Physiol., Georgetown Univ., Washington, DC; [2]Dept. of Pharmacol. and Physiol., Georgetown Univ., Washington DC, DC

**Abstract:** Alpha-synuclein (α-Syn)-related pathology plays a crucial role in the pathogenesis of Parkinson's disease (PD), a neurodegenerative disorder characterized by both motor and non-motor symptoms. Neuropsychiatric symptoms, including anxiety, depression, and apathy, are among the most prevalent non-motor manifestations of PD and substantially impair patients' quality of life. Post-mortem studies have revealed prominent α-Syn pathology in the amygdala of PD patients, indicating its potential contributions to the propagation of neuropathology and the manifestation of neuropsychiatric deficits. However, the neurobiological mechanisms by which α-Syn pathology in the amygdala contributes to these symptoms remain unclear. In this study, α-Syn preformed fibrils (PFFs) into the basolateral amygdala (BLA) of mice to induce the accumulation and propagation of α-Syn pathology. Monomeric α-Syn was injected as a control. Behavioral assessments were conducted at 1, 3, and 6 months post-injection (MPI) to examine the temporal evolution of behavioral changes. No abnormalities in motor, emotional, and cognitive function were observed in PFF-injected mice relative to controls at 1 MPI. At 3 MPI, PFF-injected mice exhibited robust apathy-like behavioral deficits and normal general motor activities. Immunohistochemical analysis revealed abundant phosphorylated α-Syn (pS129) pathology in the BLA, medial prefrontal cortex (mPFC), and nucleus accumbens (NAc) at 3 MPI, indicating propagation of α-Syn pathology to interconnected limbic and cortical regions. Our ongoing work focuses on behavioral characterization and neuropathology assessment at 6 MPI. Taken together, we report a new mouse model of synucleinopathy that exhibits apathy-like behavioral deficits and may be useful to advance our understanding of the neurobiological basis of nonmotor symptoms in PD.

**Disclosures: Y. Huang:** None. **H. Chu:** None.

**Poster**

**PSTR172: Tauopathies, Synucleinopathies, and Other Related Diseases: Animal Models**

**Location:** WCC Halls A-C

**Time:** Monday, November 16, 2026, 1:00 PM - 5:00 PM

**Program #/Poster #:** PSTR172.10/T14

**Topic:** C.05. Tauopathies, Synucleinopathies, and Other Related Diseases

**Title:** TNFR1 allosteric inhibition by peptide FKC restores neuronal viability and reduces tau pathology in tauopathy models

**Authors: *D. T. MURPHY**[1], Y. ZHONG[2], K. ABD-ELRAOUF[2], J. ZENG[2], C. LO[1];
[1]Biol., [2]Syracuse Univ., Syracuse, NY

**Abstract: TNFR1 allosteric inhibition by peptide FKC restores neuronal viability and reduces tau pathology in tauopathy models**Dylan T. Murphy[1,2], Yilin Zhong[1,2], Kholoud AbdEl-Raouf[1,2], Jialiu Zeng[2,3], Chih Hung Lo[1,2,*1]Department of Biology, Syracuse University, NY 13244, USA[2]Interdisciplinary Neuroscience Program, Syracuse University, NY 13244, USA[3]Department of Biomedical and Chemical Engineering, Syracuse University, NY 13244, USA*Correspondence: Chih Hung Lo, PhD (clo101@syr.edu)
**Abstract:** Alzheimer's disease (AD) and related tauopathies are neurodegenerative diseases

characterized by progressive neuronal death and the accumulation of pathological tau species in the brain. Tumor necrosis factor receptor 1 (TNFR1) signaling is a key mediator of neuroinflammation and cell death in tauopathy, however there are a lack of TNFR1-specific therapeutics. Targeting TNFR1-driven cell death signaling represents a promising strategy to preserve neuronal viability during disease progression. In this study, we investigate whether TNFR1 allosteric inhibitior peptide FKC can rescue neuronal viability and promote tau clearance in both in vitro and in vivo tauopathy models. PS19 transgenic mice were treated with FKC at 11 months of age, followed by behavioral tests and brain harvesting for histological and immunohistochemical analyses. Brain tissues were assessed for cell-type-specific markers, cell death markers, TNF/TNFR1 signaling pathway components, and pathological tau burden. In parallel, SH-SY5Y neuroblastoma cell were used to evaluate the effects of FKC under tau overexpression conditions, focusing on cell viability, cell death signaling, and tau levels. FKC treatment improved neuronal viability, reduced markers of cell death signaling including pMLKL and cleaved caspase-8, and decreased tau pathology in both cellular and mouse models. Together, these results suggest that inhibition of TNFR1 signaling through an allosteric mechanism may represent a potential therapeutic strategy to mitigate neurodegeneration in AD and related tauopathies.

**Disclosures: D.T. Murphy:** None. **Y. Zhong:** None. **K. Abd-ElRaouf:** None. **J. Zeng:** None. **C. Lo:** None.

**Poster**

**PSTR172: Tauopathies, Synucleinopathies, and Other Related Diseases: Animal Models**

**Location:** WCC Halls A-C

**Time:** Monday, November 16, 2026, 1:00 PM - 5:00 PM

**Program #/Poster #:** PSTR172.11/T15

**Topic:** C.05. Tauopathies, Synucleinopathies, and Other Related Diseases

**Support:** NIH R00AA029754

**Title:** Novel preclinical model of tauopathy for studying the impact of CTE and chronic alcohol-use on the brain

**Authors: *J. CARR**[1], B. WILLIAMS[3], J. L. HOFFMAN[2];
[2]Mol. Pharmacol. and Neurosci., [1]Loyola Univ. Chicago, Maywood, IL; [3]Univ. of North Carolina- Chapel Hill, Chapel Hill, NC

**Abstract: Novel preclinical model of tauopathy for studying the impact of CTE and chronic alcohol-use on the brain**Jenna Carr[1], BB Williams[2], Jessica Hoffman[1] Department of Molecular Pharmacology and Neuroscience, Loyola University Chicago Bowles Center for Alcohol Studies & Department of Psychiatry, University of North Carolina-Chapel HillChronic traumatic encephalopathy (CTE) is a neurodegenerative disorder associated with repeated mild traumatic brain injury (mTBI). Diagnosis currently relies on postmortem identification of tau pathology, and the mechanisms driving disease progression remain poorly understood. Alcohol use is

common among populations at elevated risk for CTE and may exacerbate pathology through neuroinflammation, neuronal loss, neurotransmitter dysregulation, and cognitive impairment. Because rodents do not naturally develop human-like tauopathies, improved preclinical models are needed to investigate interactions among trauma, tau pathology, and alcohol exposure.We developed a novel mouse model using a blood-brain barrier-crossing AAV expressing human tau (huTau) delivered via retro-orbital injection, resulting in widespread brain expression. This approach was combined with repeated mTBI (rmTBI) and chronic intermittent ethanol (CIE) vapor exposure to examine the independent and combined contributions of tauopathy, brain injury, and alcohol dependence to CTE-like pathology and behavior.Using the Morris Water Maze (MWM), we examined effects on spatial learning and memory. Adult male C57BL/6J mice (n=40) received retro-orbital huTau AAV (or saline), rmTBI (or sham) via a weight-drop procedure, and CIE vapor (or air) across three weeks. MWM testing was conducted over six days, including one habituation day, four acquisition days, and a probe trial. Four trials were conducted per day during habituation and acquisition.Immunohistochemistry confirmed widespread viral distribution and propagation of cleaved tau, validating this approach for inducing global huTau expression. Initial behavioral analyses suggest both ethanol and rmTBI influence spatial learning and memory, although effects were not strongly synergistic as predicted. Ongoing studies will examine molecular adaptations associated with these behavioral changes and determine how alcohol dependence modifies tau-related pathology following repeated brain injury. Development of a model that more closely recapitulates human CTE pathology may facilitate identification of shared mechanisms among CTE, alcohol use disorder, and related neurodegenerative diseases and support future therapeutic development.

**Disclosures: J. Carr:** None. **B. Williams:** None. **J.L. Hoffman:** None.

**Poster**

**PSTR172: Tauopathies, Synucleinopathies, and Other Related Diseases: Animal Models**

**Location:** WCC Halls A-C

**Time:** Monday, November 16, 2026, 1:00 PM - 5:00 PM

**Program #/Poster #:** PSTR172.12/T16

**Topic:** C.05. Tauopathies, Synucleinopathies, and Other Related Diseases

**Support:** Brain Research Foundation Fay Frank Seed Grant (BRFSG-2019-05)
Brain and Behavior Research Foundation NARSAD Young Investigator Grant (30481)
NINDS R01NS128079

**Title:** Functional and structural characterization of dendritic spine pathology in mouse models of tauopathy

**Authors: *K. CEKADA**[1,2], L. M. ADSIT[3,2], I. T. SMITH[2,1,3];
[1]Dept. of Psychological & Brain Sci., [2]Neurosci. Res. Inst., [3]Dept. of Molecular, Cell. & Developmental Biol., Univ. of California, Santa Barbara, Santa Barbara, CA

**Abstract:** Abnormal accumulation of the microtubule-associated protein tau is associated with neurodegenerative diseases, most notably frontotemporal dementia and Alzheimer's disease, but also traumatic brain injury, chronic traumatic encephalopathy, and chronic substance abuse. While spine loss and neuronal death are hallmarks of tauopathy, how pathological tau affects synaptic and dendritic activity *in vivo* remains unclear. Here, we performed immunohistochemistry to measure the tauopathy progression in the primary visual cortex (V1) of the P301S mouse model of tauopathy and employed longitudinal two-photon calcium imaging with GcaMP8m to examine the visual response properties of their layer 2/3 (L2/3) neuronal dendrites and spines. We found somatic and dendritic phosphorylated tau expression in mutant mice as young as 6 months of age. Visually evoked neuronal outputs in tau mutant mice were poorly tuned and hyperactive while synaptic responses of dendritic spines were also poorly tuned, but hypoactive compared to controls. Moreover, we found that spines that were stably retained across two imaging sessions were larger in size and more sharply tuned but less active compared to those that turned over in controls. This structure-to-function pattern was not observed in mutants. Our findings illustrate how the preferential maintenance of well-tuned inputs in healthy neural circuitry may be affected by tauopathy, resulting in neurons with poorly tuned visual responses. As a complementary model to the P301S transgenic model in which mutant human tau is expressed ubiquitously in the brain, we have generated a V1 L2/3-specific, virally transduced tauopathy model via targeted AAV-mediated Cre-dependent co-expression of P301L mutant human tau with GcaMP8m. The virally transduced model enables us to have precise control over the onset of the mutant tau expression and the proportion of transfected V1 neurons. Temporal and spatial control of expression is crucial for separating the effects of the pathological tau specifically on the visual cortical neurons from those on the lower stations of the visual pathway (e.g. retina and optic nerves). We confirmed the presence of tau+/GcaMP8m+ V1 L2/3 neurons along with tau-/GcaMP8m+ neurons, which allows for intraindividual controls, suggesting it is a promising new method to study tauopathy.

**Disclosures: K. Cekada:** None. **L.M. Adsit:** None. **I.T. Smith:** None.

**Poster**

**PSTR172: Tauopathies, Synucleinopathies, and Other Related Diseases: Animal Models**

**Location:** WCC Halls A-C

**Time:** Monday, November 16, 2026, 1:00 PM - 5:00 PM

**Program #/Poster #:** PSTR172.14/T17

**Topic:** C.05. Tauopathies, Synucleinopathies, and Other Related Diseases

**Support:** NIH Grant AG062509
NIH Grant AG041274
NIH Grant AG070761
UTHealth Houston

**Title:** Circuit-specific Tau ablation in medial septum blocks p-tau trafficking to anterior cingulate cortex and reverses delirium-like behavior in mice

**Authors: *W. ZHANG**[1], S. FU[2], Y. ZHANG[4], L.-J. WU[3], G. YANG[5], X. JIANG[6], Z. XIE[7]; [1]UTHealth Houston, Houston, TX; [3]Neurol., [2]Univ. of Texas Hlth. Sci. Ctr. at Houston, Houston, TX; [4]Anesthesia, Critical Care and Pain Med., Massachusetts Gen. Hospital/Harvard Med. Sch., Charlestown, MA; [5]Anesthesiol., Columbia Univ., New York, NY; [6]Baylor Col. of Med., Houston, TX; [7]Anesthesia, Critical Care and Pain Med., Massachusetts Gen. Hosp. and Harvard Med. Sch., Houston, TX

**Abstract:** Postoperative delirium is a common complication in older surgical patients, and postoperative pain is an important risk factor. Although incisional pain induces delirium-like behaviors and activates the anterior cingulate cortex (ACC) in mice, the upstream circuit and molecular mechanisms remain unclear. We hypothesized that pain facilitates phosphorylated Tau (p-Tau) trafficking along the medial septum (MS)-to-ACC pathway, thereby contributing to delirium-like behaviors.

Female C57BL/6J mice underwent sham treatment or plantar incision. Delirium-like behaviors were assessed using the "CAM in mice" battery at baseline and 6 hours after incision. To test pain-dependent p-Tau transfer, Cy5-labeled p-Tau441 was stereotaxically injected into the MS and quantified in the MS and ACC. To examine causality, MS Tau was disrupted using MS-targeted lentiviral CRISPR-Cas9, followed by c-Fos mapping and behavioral testing.

p-Tau441-Cy5 was detected in MS neurons in both groups, but ACC neuronal p-Tau signal was minimal in sham mice and markedly increased after incision, indicating pain-gated MS-to-ACC p-Tau trafficking. Incision also increased c-Fos density in both the MS and ACC and induced robust delirium-like behaviors. MS-targeted Tau ablation reduced pain-evoked c-Fos activation and reversed the behavioral impairments.

These findings suggest that incisional pain promotes MS-to-ACC p-Tau trafficking and associated circuit activation, contributing to delirium-like behaviors. Targeting Tau in the MS may represent a potential strategy for preventing postoperative delirium.

**Disclosures: W. Zhang:** None. **S. Fu:** None. **Y. Zhang:** None. **L. Wu:** None. **G. Yang:** None. **X. Jiang:** None. **Z. Xie:** None.

**Poster**

**PSTR172: Tauopathies, Synucleinopathies, and Other Related Diseases: Animal Models**

**Location:** WCC Halls A-C

**Time:** Monday, November 16, 2026, 1:00 PM - 5:00 PM

**Program #/Poster #:** PSTR172.15/T18

**Topic:** C.05. Tauopathies, Synucleinopathies, and Other Related Diseases

**Support:** NIH Grant R56AG083436
NIH Grant R01AG032611
NIH Grant R01NS077239
NIH Grant RF1/R01NS120488

**Title:** A novel anti-α-synuclein single-domain antibody targets aggregation-prone region to improve function, reduce pathological α-synuclein and rescue neurodegeneration

**Authors: *P. SHARMA**[1,2], E. E. CONGDON[1], Y. JIANG[1], H.-W. HUANG[2], R. PAN[3], X.-P. KONG[3], H. ERDJUMENT-BROMAGE[1], I. S. MARCHAL[1], T. A. NEUBERT[1], H. D. RYOO[2], E. M. SIGURDSSON[1,4];
[1]Dept. of Neuroscience, Inst. for Translational Neuroscience, New York Univ. Grossman Sch. of Med., New York, NY; [2]Dept. of Cell Biology, New York Univ. Grossman Sch. of Med., New York, NY; [3]Dept. of Biochem. and Mol. Pharmacology, New York Univ. Grossman Sch. of Med., New York, NY; [4]Dept. of Psychiatry, New York Univ. Grossman Sch. of Med., New York, NY

**Abstract:** Synucleinopathies are a group of neurodegenerative disorders, including Parkinson's disease, Dementia with Lewy Bodies (DLB), and Multiple System Atrophy, characterized by the accumulation of aggregated α-synuclein (α-syn) that is associated with phosphorylation on serine 129. These diseases are marked by locomotor and non-motor impairments, as well as the loss of dopaminergic (DA) neurons and mitochondrial dysfunction. We have developed several anti-α-syn single-domain antibodies (sdAbs) and demonstrated the diagnostic imaging potential of a couple of them (Jiang Y et al, Sci Adv 2023, PMID 37163602) and the acute therapeutic benefit of one in clearing α-syn in a mouse model (Jiang Y et al, Mol Neurodegener 2024, PMID 38816762). However, whether these sdAbs can suppress α-syn-mediated neuronal loss and locomotor impairment in vivo remains unclear. We evaluated the therapeutic potential of five anti-α-syn sdAbs to clear pathological α-synuclein in a culture model that consisted of primary neurons from the M83 synucleinopathy mouse model incubated with a soluble toxic α-syn fraction from a DLB brain. Three of the sdAbs targeting intracellular α-syn prevented α-syn toxicity ($p \leq 0.05$-$0.0001$), and four of them cleared α-syn ($p \leq 0.05$-$0.01$). Subsequently, we assessed their in vivo efficacy in a *Drosophila* model of synucleinopathy to dissect cellular mechanisms by expressing them in all neurons or only in DA neurons. The sdAbs differed in their efficacy to lower levels of phospho-serine 129 α-syn ($p \leq 0.05$-$0.01$), prevent loss of DA neurons ($p \leq 0.05$-$0.01$), alleviate mitochondrial dysfunction ($p \leq 0.001$-$0.0001$), improve motor function ($p \leq 0.05$-$0.0001$), and prolong survival ($p \leq 0.01$-$0.0001$) in synucleinopathy flies. The most effective sdAb, 2H1, has not been reported before. It binds strongly to the aggregation prone region of α-syn and robustly improves all these disease parameters. Additionally, proximity-dependent biotinylation of that sdAb in α-syn-expressing neurons showed, for the first time, a characteristic in vivo binding with α-syn and enrichment of α-syn-associated proteins involved in synapse/vesicle trafficking pathways, pinpointing the location of their intracellular interaction. Our findings strongly support the therapeutic benefit and clinical development of these anti-α-syn sdAbs.

**Disclosures: P. Sharma:** None. **E.E. Congdon:** None. **Y. Jiang:** None. **H. Huang:** None. **R. Pan:** None. **X. Kong:** None. **H. Erdjument-Bromage:** None. **I.S. Marchal:** None. **T.A. Neubert:** None. **H.D. Ryoo:** None. **E.M. Sigurdsson:** E. Ownership Interest (stock, stock options, royalty, receipt of intellectual property rights/patent holder, excluding diversified mutual funds); inventor on a patent that is assigned to New York University: Alpha-synuclein single domain antibodies. Patent Application No: 16/971,157. Filed February 19, 2019. Notice of Allowance July 31, 2024., US Patent Number 12162929. Issued December 10, 2024. The authors declare that they have no other competing interests.

**Poster**

**PSTR172: Tauopathies, Synucleinopathies, and Other Related Diseases: Animal Models**

**Location:** WCC Halls A-C

**Time:** Monday, November 16, 2026, 1:00 PM - 5:00 PM

**Program #/Poster #:** PSTR172.16/T19

**Topic:** C.05. Tauopathies, Synucleinopathies, and Other Related Diseases

**Support:** NIH R56 AG083436
NIH R01 AG032611
NIH R01 NS077239
NIH R01 NS120488
NIA K01 AG092910

**Title:** Cell-Type-Selective Cortical Pathology and Functional Deficits in Synucleinopathy

**Authors: *X. YANG**[1,2], C. JI[1,2], S. C. SONG[3,4], N. HARANO[1,2], Y. LIN[1,2], E. M. SIGURDSSON[1,2,5];
[1]Dept. of Neurosci., [2]Inst. for Translational Neurosci., [3]Dept. of Pathology, [4]IonLab, [5]Dept. of Psychiatry, New York Univ. Grossman Sch. of Med., New York, NY

**Abstract:** Misfolding and aggregation of α-synuclein (α-syn) is a hallmark of Parkinson's disease (PD) and other synucleinopathies such as dementia with Lewy bodies (DLB), and multiple system atrophy (MSA). Although accumulation of α-syn aggregates in motor-related brain regions accompanies motor symptoms, their early-stage impact on neuronal activity during movement execution and skill acquisition remains unclear. This study adopted a multi-disciplinary approach to elucidate the pathophysiological characteristics in a transgenic (Tg) mouse model (M83) of synucleinopathy with minimal nigrostriatal degeneration. Fine-level assessment revealed subtle motor deficits and impaired learning in a treadmill task at the early stage of disease. Training significantly increased forelimb swing time in non-Tg (nTg) mice (8-9-month-old females, n=16, $p<0.0001$), whereas this adaptation was absent in age- and sex-matched M83 mice (n=15, $p=0.6853$). In parallel, M83 mice exhibited a gradual reduction in stride length (n=15, $p<0.0001$) and an increase in step number (n=15, $p<0.0001$), while both parameters remained more stable in nTg controls (Stride length: n=16, $p<0.1951$; step number: n=16, $p<0.0061$). During running, two-photon imaging revealed cell-type-selective alterations in the motor cortex of M83 mice, with reduced $Ca^{2+}$ events in excitatory neurons but not in parvalbumin (PV)-expressing inhibitory neurons compared with nTg mice (Excitatory: n=7, $p=0.0324$; PV: n=8, $p=0.8300$, females, 8-9-month-old). In addition, the temporal response of both cell types in M83 mice were altered at movement onset, showing abnormal suppression of excitatory neurons and enhanced activation of PV neurons. This was accompanied by diminished reorganization of movement-related neuronal ensembles during learning. Cell-type specific ex vivo whole-cell recordings revealed selectively altered membrane properties in excitatory neurons, but not in PV neurons, characterized by reduced excitability and compromised repetitive firing ability. These functional deficits parallel the preferential accumulation of α-syn inclusions in excitatory rather than in PV neurons, as quantified by immunohistology in the same cortical region (Excitatory: n=11 slices, 4 mice; PV: 12 slices, 4 mice, $p= 0.0003$, females, 8-9-month-old). These results demonstrate a cell-type-selective vulnerability of cortical neurons at the early stage of synucleinopathy, leading to cortical hypoactivity and dysregulated plasticity

that could underlie early motor symptoms. We are seeking to alleviate these functional deficits in ongoing studies.

**Disclosures: X. Yang:** None. **C. Ji:** None. **S.C. Song:** None. **N. Harano:** None. **Y. Lin:** None. **E.M. Sigurdsson:** None.

**Poster**

**PSTR172: Tauopathies, Synucleinopathies, and Other Related Diseases: Animal Models**

**Location:** WCC Halls A-C

**Time:** Monday, November 16, 2026, 1:00 PM - 5:00 PM

**Program #/Poster #:** PSTR172.17/T20

**Topic:** C.05. Tauopathies, Synucleinopathies, and Other Related Diseases

**Support:** CNIR Pilot grant (Georgetown University)

**Title:** Elucidating the neuroprotective role of Claudin mediated micro-environments in preventing neuro-degeneration and cognitive decline

**Authors: *A. VARGHESE**, P. JOSHI;
Biochem. and Mol. and Cell. Biol., Georgetown Univ., Washington DC, DC

**Abstract:** Elucidating the neuroprotective role of Claudin-mediated microenvironments in preventing neurodegeneration and cognitive decline. Amal Wilson Varghese, Priyanka Joshi*. Neurodegenerative pathologies are progressively linked to the breakdown of cellular barriers, in Alzheimer's disease (AD) and Parkinsons disease (PD). In higher vertebrates, claudin is the primary regulator of paracellular permeability in the BBB. Unlike the BBB, there is less focus on the role of localized neuronal compartmentalization, which could also be critical in maintaining synaptic health. The clc-1 and nsy-4 helps maintain the compartmentalization and structural integrity of sensory neurons like AWC, the nsy-4 is essential for signal activation. We utilizes *C. elegans* to investigate claudin-like proteins (CLC) a functional analogue to mammalian tight junction proteins to preserve neuronal micro-environments.Motor deficits and hyposmia are critical early-onset hallmarks of PD, we assessed whether claudin supplementation preserved odor detection and motor reflexes. We alter the expression of claudins in specific tissues, sensory, motor neuronal regions via cell-specific promoters using RNA interference and single copy insertions. These alterations are introduced into pan neuronal Aβ expressing worms and other PD backgrounds. Impaired olfactory adaptation is also associated with neurodegeneration; however, we observed positive effects of claudin introduction within the neuronal microenvironments surrounding cholinergic regions that directly modulate motor movements. This intervention recovered foraging and sensory-stimulus compared to knockout worms. An associative learning to evaluate short-term memory in these mutants, allowed us to assay dopaminergic motor circuit defects alongside subtle memory and recall deficits. Additionally, basal slowing responses and reflex/escape behaviors were assessed to verify the overall physical and cognitive well-being of the worms. Maintaining high levels of claudins appeared to stabilize and increase the recovery of cognitive abilities, foraging, and motor reflexes. This approach

moderately shifts the therapeutic focus from clearing protein aggregates toward strengthening underlying cellular architecture. Our results provide a proof-of-concept for lifespan and health span extending strategies that target the structural integrity of the nervous system that should begin at the pre-symptomatic stages of the disease.

**Disclosures: A. Varghese:** None. **P. Joshi:** None.

**Poster**

**PSTR172: Tauopathies, Synucleinopathies, and Other Related Diseases: Animal Models**

**Location:** WCC Halls A-C

**Time:** Monday, November 16, 2026, 1:00 PM - 5:00 PM

**Program #/Poster #:** PSTR172.18/T21

**Topic:** C.05. Tauopathies, Synucleinopathies, and Other Related Diseases

**Support:** NS077239
NS120488
AG032611

**Title:** Effects of Tau Pathology on Motor Cortical Ensemble Recruitment and Sequential Activation During Motor Learning

**Authors: *N. HARANO**[1,2], C. JI[2], X. YANG[2], A. TETLOW[2], Y. LIN[2], E. M. SIGURDSSON[2,3];
[1]New York Univ., New York, NY; [2]Dept. of Neurosci., [3]Dept. of Psychiatry, New York Univ. Grossman Sch. of Med., New York, NY

**Abstract:** Tau pathology is associated with neuronal dysfunction and motor impairment, yet how pathological tau alters learning-related cortical computations remains poorly understood. Recent work from our laboratory demonstrated that 6-month-old homozygous female JNPL3 tauopathy mice exhibit neuronal hypoactivity, increased neuronal synchrony, and disrupted network engagement in the primary motor cortex, suggesting early circuit dysfunction prior to severe neurodegeneration (Ji C et al Alzheimers Dement 2024, PMID 39368113). Motor learning requires coordinated activity across excitatory neuronal ensembles and is accompanied by experience-dependent changes in population dynamics within the motor cortex. Recent studies suggest that learning-related plasticity in healthy non-transgenic mice is reflected not only in changes in neuronal activity levels but also in the temporal organization of ensemble activity (Adler et al Neuron 2019, PMID 30792151). We hypothesize that tau pathology disrupts these processes, resulting in altered excitatory ensemble dynamics during motor learning. To investigate this question, we selectively targeted layer 2/3 excitatory pyramidal neurons in primary motor cortex using CaMKIIα-driven GCaMP7s expression and performed in vivo two-photon calcium imaging in 6-month-old homozygous female JNPL3 and age-and-strain-matched non-transgenic mice during treadmill-based motor behavior and learning paradigms. Ongoing analyses characterize excitatory ensemble dynamics by quantifying calcium activity, neuronal recruitment, population coordination, and learning-related temporal organization during motor

behavior and learning. Behavioral performance is assessed in parallel using gait-based measures of motor function. These studies aim to define if and how tau pathology alters excitatory population activity and ensemble-level organization during learning. By linking tau-mediated circuit dysfunction to changes in cortical ensemble dynamics, this work may provide insight into mechanisms underlying impaired motor plasticity and behavioral dysfunction in early-stage tauopathy.

**Disclosures: N. Harano:** None. **C. Ji:** None. **X. Yang:** None. **A. Tetlow:** None. **Y. Lin:** None. **E.M. Sigurdsson:** None.

**Poster**

**PSTR172: Tauopathies, Synucleinopathies, and Other Related Diseases: Animal Models**

**Location:** WCC Halls A-C

**Time:** Monday, November 16, 2026, 1:00 PM - 5:00 PM

**Program #/Poster #:** PSTR172.19/T22

**Topic:** C.05. Tauopathies, Synucleinopathies, and Other Related Diseases

**Support:** NIH Grant AG032611
NIH Grant NS077239
NIH Grant NS120488
Alzheimers Association grant AARFD-22-926379

**Title:** Clearance of truncated tau protein ameliorates deficits in microglia calcium dynamics in tauopathy mice

**Authors: *A. M. AVILA**[1], Y. LIN[1], E. M. SIGURDSSON[1,2];
[1]Dept. of Neuroscience. Inst. for Translational Neuroscience. NYU Grossman Sch. of Med., New York, NY; [2]Dept. of Psychiatry. NYU Grossman Sch. of Med., New York, NY

**Abstract:** Amyloid-β and tau aggregates are hallmarks of Alzheimer's disease, but tau pathology has been shown to correlate better with the degree of dementia than Aβ plaques. Tau pathology is also the defining feature of primary tauopathies. Several tau immunotherapies are in clinical trials, but their mechanism of action is unclear. Microglia are the professional phagocytes of the brain that help remodel neuronal circuits and remove dead cells and protein aggregates; however, little is known about how microglia interact with neurons accumulating tau or with tau-antibody complexes. While activated microglia are found near tau aggregates, microglia away from tau lesions do not display such an activated phenotype. Microglia are highly dynamic, and their motility has been shown to be modulated by neuronal activity. However, the functional dynamics of microglia have not been well explored during the progression of tau pathology and following tau immunotherapy. Towards this aim, we crossed Tmem119CreER: tdTomatoflox: GCaMP6flox mice with the PS19 tauopathy P301S mouse model. We then visualized by two-photon imaging in awake mice the functional dynamics of microglia in the motor cortex in control and PS19 mice, as well as in PS19 mice that were acutely treated with two intravenous injections of 5G2 antibody or an IgG control (100 µg, three days apart). 5G2 is a monoclonal

mouse antibody that targets pathological truncated tau protein at Asp421. We recently reported on its beneficial effects on neuronal function and microglial Iba1 expression in awake PS19 tauopathy mice (Martin-Avila, A. et al., Cell Reports 2025, PMID 40966081). Here, we analyzed calcium profiles in microglial soma in awake, head-restrained mice after they ran for 20 min on a free-floating treadmill. PS19 mice displayed reduced ΔF/F of total calcium activity (0.064 ± 0.006, n = 3), compared to control mice (0.116 ± 0.012, n = 4, p = 0.0009) and reduced ΔF/F of peak calcium amplitude (0.208 ± 0.021), compared to control mice (0.331 ± 0.033, p = 0.0041). Preliminary results indicate that the acute tau immunotherapy restored total calcium activity in PS19 mice (5G2: 0.106 ± 0.006, n = 2), compared to control PS19 mice (IgG: 0.071 ± 0.005, n = 2, p < 0.05). The 5G2 treatment in the PS19 mice also restored peak calcium amplitude to control levels (5G2: 0.373 ± 0.032), compared to control PS19 mice (IgG: 0.273 ± 0.015, p = 0.0356). Analyses of additional mice are underway to strengthen our current findings. Together, these data show functional impairment of microglia in tauopathies that can be alleviated with an antibody that targets the Asp421 truncated pathological tau protein, further supporting its therapeutic potential.

**Disclosures: A.M. Avila:** None. **Y. Lin:** None. **E.M. Sigurdsson:** E. Ownership Interest (stock, stock options, royalty, receipt of intellectual property rights/patent holder, excluding diversified mutual funds); E.M.S. is an inventor on patents on tau immunotherapy and related diagnostics that are assigned to the New York University..

**Poster**

**PSTR173: Neuroprotective Mechanisms: Preclinical**

**Location:** WCC Halls A-C

**Time:** Monday, November 16, 2026, 1:00 PM - 5:00 PM

**Program #/Poster #:** PSTR173.01/T23

**Topic:** D.01. Neurotoxicity, Inflammation, and Neuroprotection

**Support:** NIH R01 035477

**Title:** Tooth healing following damage and inflammation requires calcitonin gene related peptide (CGRP) from sensory afferents

**Authors: *S. PETERS**;
The Ohio State Univ. Col. of Dent., Columbus, OH

**Abstract:** Dental caries affect millions of Americans every year, causing pulpitis and subsequent dental pulp necrosis. Traditional endodontics include denervation of the tooth organ, but this leaves the patient susceptible to secondary infections without a nervous system to signal immune protection responses. Vital pulp therapy offers a promising alternative to root canal treatments and tooth extractions by preserving pulp tissue and sensory innervation; however, VPT is less effective when pulpitis is established, with failures seen as necrosis or continued inflammation. Therefore, VPT implementation in dental clinics is limited by an incomplete understanding of the mechanisms that regulate pulp inflammation and healing. There is a large body of

information demonstrating significant innervation changes, such as axon sprouting and phenotypical plasticity, underneath damaged and/or infected carious dentin. Importantly, several decades of research have established that sensory afferents secrete CGRP/*Calca* during tooth injury and/or inflammation and that sensory denervation disrupts reparative dentinogenesis. To determine the role of CGRP and its receptor RAMP1 in tooth protection and repair, we performed deep dentin injuries +/- local application of lipopolysaccharide (LPS) to create models of injury and of microbial penetration into the dental pulp. Using micro-computed tomography and histology, we found that LPS application significantly reduced reparative dentin after 21 days of healing in control mice. We further performed the injury in a mouse model with global deletion of *Calca* and found reduced reparative dentin secretion as compared to wild-type mice after 21 days but similar to the control mice with LPS application. These results suggest that inflammation resolution and the presence of CGRP signals are crucial to reparative dentinogenesis. Further studies are currently underway to define the role of CGRP in pulp inflammatory and healing responses utilizing conditional RAMP1-deletion in mineralizing or immune cells. The results of these studies will provide information on cell-specific responses to CGRP during tooth inflammation and damage to incorporate into next-generation vital pulp therapies.

**Disclosures: S. Peters:** None.

**Poster**

**PSTR173: Neuroprotective Mechanisms: Preclinical**

**Location:** WCC Halls A-C

**Time:** Monday, November 16, 2026, 1:00 PM - 5:00 PM

**Program #/Poster #:** PSTR173.02/T24

**Topic:** D.01. Neurotoxicity, Inflammation, and Neuroprotection

**Support:** USA Pennsylvania State Health Department grant Project 10: 420491-04400-02 to Nune Darbinian
NIH grant to Dr. Shohreh Amini
NIH grants R01NS97846, R01NS097846-02S1, R01NS092876 and the National Institute on Alcohol Abuse and Alcoholism (NIAAA) of NIH grant R01AA031319 to Michael Selzer
Dr. Schein (MD) Neuropathology Endowed Fellowship award to Dr. Darbinyan Armine

**Title:** SARS-CoV-2- and HIV-1-Associated Neurotoxicity, Demyelination, and Axonal Loss: Therapeutic Potential of DING Protein

**Authors: *N. DARBINIAN**[1], A. DARBINYAN[2,3], S. AMINI[4], M. E. SELZER[2];
[1]Ctr. for Neural Develop. and Repair, Dept. of Neural Sci., Temple University, Lewis Katz Sch. of Med., Philadelphia, PA; [2]Neural Sci., Lewis Katz Sch. of Med. At Temple Univ., Philadelphia, PA; [3]Pathology, Yale Univ., New Haven, CT; [4]Dept. of Biology, Col. of Sci. and Technol., Temple Univ., Philadelphia, PA

**Abstract: Introduction.** COVID-19 can lead to long-lasting neurological sequelae, commonly referred to as long COVID. However, it remains unclear which patients are most susceptible to these complications, limiting the development of preventive and therapeutic strategies. Both white matter, particularly myelin, and gray matter, including neurons, appear to be affected. Here, we demonstrate alterations in myelin thickness and axonal integrity in patients with COVID-19. Identification of molecular markers associated with these neuropathological changes is critical for developing targeted therapies for long COVID. We also identified sequence similarities between SARS-CoV-2 and HIV-1 strains. Previously, we demonstrated the neuroprotective function of the human DING protein against HIV-1 transcription and replication. Therefore, we propose DING protein as a potential therapeutic strategy against COVID-19-associated neurotoxicity, including axonal, neuronal, and oligodendrocyte (OL) loss. **Methods.** To determine the nature of OL injury, tissue samples were stained with the axonal marker neurofilament-heavy chain (NF-H), followed by examination of myelin sheath morphology. Electron microscopy was used to identify axonal thinning and myelin sheath abnormalities. BLAST analysis was performed to compare SARS-CoV-2 and HIV-1 sequences. In parallel, Sholl analysis was used to assess neuronal degeneration and neurite complexity in HIV-1-injured neurons following DING protein treatment. **Results.** SARS-CoV-2-associated neural injury was associated with OL dysfunction, demyelination, and axonal degeneration. Electron microscopy revealed regions of axonal thinning accompanied by disrupted and reduced myelin sheath thickness. Although OL damage has been reported in SARS-CoV-2-infected patients, the mechanisms underlying these abnormalities remain poorly understood. Sequence analysis demonstrated similarities between SARS-CoV-2 and HIV-1 viral regions associated with neurotoxicity. In neuronal injury models, DING protein treatment reduced neuronal degeneration and preserved neurite architecture, supporting its neuroprotective role against virus-associated neural damage. **Conclusion.** These findings suggest that SARS-CoV-2-associated neurological injury involves demyelination and axonal degeneration linked to OL dysfunction. The human DING protein demonstrates neuroprotective properties against virus-induced neuronal injury and may represent a novel therapeutic candidate for long COVID-associated neurotoxicity.

**Disclosures: N. Darbinian:** None. **A. Darbinyan:** None. **S. Amini:** None. **M.E. Selzer:** None.

**Poster**

**PSTR173: Neuroprotective Mechanisms: Preclinical**

**Location:** WCC Halls A-C

**Time:** Monday, November 16, 2026, 1:00 PM - 5:00 PM

**Program #/Poster #:** PSTR173.03/T25

**Topic:** D.01. Neurotoxicity, Inflammation, and Neuroprotection

**Support:** NIH Grant DC022073

**Title:** TLR4-Dependent Inflammation Differentially Activates Neuroimmune Responses Across the Auditory Pathway Following Systemic Endotoxin Exposure

**Authors:** K. SLEIMAN[1], E. PALTJON[2], J. LABERTEAUX[3], A. HORNAK[2], S. RANGANATHAN[2], A. MANOHAR[4], G. LOPEZ GIULIANI[2], E. G. VICHAYA[5], R. R. KANE[3], ***D. D. SIMMONS**[1];
[2]Biol., [3]Chem. and Biochem., [1]Baylor Univ., Waco, TX; [4]Biol., Baylor Univ., Glenview, IL; [5]Psychology & Neurosci., Baylor Univ., Woodway, TX

**Abstract:** Acquired sensorineural hearing loss (SNHL), caused by aging, infection, noise, or ototoxic drugs, is associated with cochlear inflammation, but how immune responses evolve across the auditory pathway remains unclear. We examined the effects of systemic inflammation on peripheral and central auditory structures (e.g. spiral ganglion and cortex) as well as the hippocampus using lipopolysaccharide (LPS), a Toll-like receptor 4 (TLR4) agonist. C57Bl/6 mice were treated intraperitoneally (IP) with LPS, and auditory brainstem responses (ABRs) were recorded pre- and post-treatment. Immunofluorescence for CD45 and IBA-1 assessed immune activation. Low-dose LPS induced widespread inflammation throughout the cochlea and central auditory regions, including increased macrophages in the spiral ganglion and elevated microglia throughout the brain, without changes in hearing thresholds. In contrast, higher-dose LPS caused significant auditory deficits, including 30–40 dB SPL threshold shifts and reduced synaptic density beneath inner hair cells, alongside increased immune cell density. To confirm pathway specificity, a TLR4 inhibitor was administered IP, reducing LPS-induced auditory threshold shifts by ~50%. Similarly, a PEGylated prodrug of the TLR4 inhibitor demonstrated improved solubility and sustained inhibition of TLR4 signaling in vivo, and also reduced threshold shifts in an equivalent manner, supporting its potential for modulating neuroimmune responses in SNHL. These findings indicate that while systemic inflammation produces broad neuroimmune activation, inflammation alone is insufficient to impair auditory function; instead, a threshold or qualitative shift in TLR4 signaling is required to drive synaptic and functional deficits. We hypothesize that cochlear macrophages and central microglia exhibit context-dependent roles in maintaining homeostasis or promoting SNHL pathology.

**Disclosures: K. Sleiman:** None. **E. Paltjon:** None. **J. Laberteaux:** None. **A. Hornak:** None. **S. Ranganathan:** None. **A. Manohar:** None. **G. Lopez Giuliani:** None. **E.G. Vichaya:** None. **R.R. Kane:** None. **D.D. Simmons:** None.

**Poster**

**PSTR173: Neuroprotective Mechanisms: Preclinical**

**Location:** WCC Halls A-C

**Time:** Monday, November 16, 2026, 1:00 PM - 5:00 PM

**Program #/Poster #:** PSTR173.04/T26

**Topic:** D.01. Neurotoxicity, Inflammation, and Neuroprotection

**Support:** R01 EY032519-01A1

**Title:** Single-cell transcriptomic characterization neural progenitor cell expression in the old-world primate optic nerve head

**Authors: *K. PUCHA**[1], S. BERNSTEIN[2];
[1]Univ. of Maryland Sch. of Med., Baltimore, MD; [2]Univ. of Maryland Sch. of Med. at Baltimore, Baltimore, MD

**Abstract:** The optic nerve (ON) is comprised of axons originating from retinal ganglion cells (RGCs) whose soma are in the retina of the eye. ON axons and their corresponding cell bodies are subject to many different stressors that arise during normal function. These stressors include external compression, increases in intraocular pressure, vitreous motion/traction, torsion, and inflammation. When RGC stress exceeds the ability to counter it, RGC dysfunction and death occurs. Chronic RGC stress can occur in the ON disease glaucoma, and acute ischemic stress occurs in Non-arteritic anterior ischemic optic neuropathy (NAION). The optic nerve head (ONH) is the anterior unmyelinated portion of the ON that emerges through the eye wall as it exits the back of the eye. The ONH contains a astrocyte-neural progenitor cell (NPC) niche, other differentiated astrocytes, and oligodendrocyte progenitor cells (OPCs). In addition to giving rise to more mature cell types, these NPCs secrete trophic factors that seem to support RGC function. The NPC niche is depleted during aging, and we hypothesize that age-associated loss of NPC-trophic support may contribute to the development of glaucoma and NAION. ONH-NPCs are also centers of molecular communication and interact with a variety of cell types through secreted extracellular vesicles (EVs) carrying microRNAs (miRNAs), EV-peptides and soluble secreted proteins. In this study, we combined single-cell sequencing (scRNA seq) and miRNA-deep sequencing to understand the unique contribution of the NPC secretome. Sequencing of the EV-associated miRNAs from primary rodent ONH cultures yielded highly expressed miRNAs such as has-miR-192-5p, which significantly overlaps with apoptotic signaling pathways specifically in neurons. Additionally, scRNA seq revealed that a large portion (~80%) of astrocyte-like cells express stem-cell associated transcription factors such as Sox9 and LHX2, and receptors such as NTRK2 at high levels, demonstrating their potential to differentiate into neuronal and glial lineages. These cells secrete factors such as the FGFs, TGFs and VEGFs not expressed in high quantities in any other ONH cell type, demonstrating they are a specific regulatory niche. Our analysis is the first of its kind to characterize the vesicular and soluble secretome of the neural progenitor cell niche in the primate ONH. Many transcriptional and secreted factors are likely shared with human counterparts, demonstrating the utility of primate models when studying retinal and ONH function. This data also demonstrates that the ONH-NPC secretome may be useful to uncover therapeutic targets for conditions such as glaucoma and NAION.

**Disclosures: K. Pucha:** None. **S. Bernstein:** None.

**Poster**

**PSTR173: Neuroprotective Mechanisms: Preclinical**

**Location:** WCC Halls A-C

**Time:** Monday, November 16, 2026, 1:00 PM - 5:00 PM

**Program #/Poster #:** PSTR173.05/T27

**Topic:** D.01. Neurotoxicity, Inflammation, and Neuroprotection

**Support:** GlaxoSmithKline GW58292-11653

**Title:** Kainate-Induced Status Epilepticus Depletes NeuN (RbFox3) Antigenicity of the Retrosplenial Cortex in the Absence of Cell Loss

**Authors: *R. R. PRASAD**[1], J. HOFFMAN[2], L. K. FRIEDMAN[3];
[1]New York Med. Col., Valhalla, NY; [2]New York Med. Col., New York, NY; [3]Cell Biol. and Anat., New York Med. Col., Valhalla, NY

**Abstract:** Retigabine (RGB), an activator of KCNQ channels, can dose dependently attenuate or exacerbate kainate (KA)-induced status epilepticus (Friedman et al, 2015). Extrahippocampal structures such as the retrosplenial cortex (RSC) and cingulate cortex, involved memory, and other cognitive functions, may also be altered by seizure activity. Previously, neuronal loss and volume reduction was reported within the densely packed retrosplenial granular cortex (RSG) in response to pilocarpine-induced status epilepticus, whereas the adjacent retrosplenial agranular region (RSA) was spared. Adult rats were injected with KA via intraperitoneal (Ip) or intrahippocampal (ih) routes to induce status epilepticus in presence and absence of one or two injections of RGB. The RSC was subsequently evaluated immunohistochemically with NeuN, a neuron-specific nuclear protein and Nissl staining. One day (d) after Ip injection, moderate loss of NeuN label of the RSC was detected with KA alone or KA+1×RGB treatment. At 3 d after either route of KA administration, large patches of neurons exhibited marked depletion of NeuN immunolabeling within layers IV-V of the RSG and RSA. However, layers II-III deficits weregrossly affected by the Ip injection. Some NeuN+ neurons were very dark and irregular in shape and associated with hyperbasophilia or eosinophilia of the RSC in the absence of histological cell loss at any time point. Two doses of RGB treatment mitigated NeuN depletions observed at 3 d when the largest NeuN deficits were observed. At 28 d, persistent loss of NeuN staining continued but was found predominantly within RSC layers IV-V forming a crescent shape. Marked decreases of NeuN antigenicity in limbic cortical regions may indicate a “circuitry break” due to lack expression of RbFox3 gene variants affecting neurotransmission and transcriptional regulation in RSC neuronal populations. These changes within critical regions could be responsible for spatial navigation and memory deficits as well as other cognitive comorbidities associated with prolonged seizures.

**Disclosures: R.R. Prasad:** None. **J. Hoffman:** None. **L.K. Friedman:** None.

**Poster**

**PSTR173: Neuroprotective Mechanisms: Preclinical**

**Location:** WCC Halls A-C

**Time:** Monday, November 16, 2026, 1:00 PM - 5:00 PM

**Program #/Poster #:** PSTR173.06/T28

**Topic:** D.01. Neurotoxicity, Inflammation, and Neuroprotection

**Support:** Calcigenix, LLC

**Title:** Intrahippocampal apoaequorin infusions confer neuroprotection against oxygen-glucose deprivation in male and female rats

**Authors: *D. SAFARINI**[1], B. NATWORA[2], J. R. MOYER, JR.[3], M. MASSMAN[4];
[1]Univ. of Wisconsin-Milwaukee Grad. Student Training Program In Neurosci., Milwaukee, WI; [2]Psychological and Brain Sci., Univ. of Wisconsin-Milwaukee Grad. Training Program In Neurosci., Milwaukee, WI; [3]Psychological and Brain Sci., Univ. of Wisconsin-Milwaukee, Milwaukee, WI; [4]Psychology, Univ. of wisconsin Milwaukee, Milwaukee, WI

**Abstract:** Stroke, a leading cause of death worldwide, is characterized by interrupted blood flow to the affected area, depriving it of key nutrients, including oxygen and glucose, which results in neuronal injury, followed by neuronal death. In ischemic stroke, glutamatergic excitotoxicity and disruption of calcium homeostasis, is one of the main causes of neuronal death. Prior data from our lab have demonstrated that apoaequorin (AQ), a calcium-binding protein derived from jellyfish*Aequorea victoria*, protects male rat hippocampal neurons against subsequent oxygen-glucose deprivation (OGD), an *in vitro* model of ischemic stroke (Detert *et al*., 2013). To date, however, whether this protection is comparable in both male and female hippocampal neurons is not known. The present study sought to fill this gap by evaluating whether an intrahippocampal infusion of 4% AQ (w/v) attenuates CA1 cell death and promotes neuroprotective efficacy regardless of sex or hemisphere. Apoaequorin was prepared in stock at a concentration of 74.5mg/mL in $Ca^{2+}$ free aCSF, aliquoted, and stored at -20°C. In each experiment, one hemisphere received an infusion of AQ and the other hemisphere an infusion of vehicle ($Ca^{2+}$-free aCSF). Twenty-four hours later, 400 µm thick coronal brain slices containing the dorsal hippocampus were obtained from adult male and female Fisher 344 rats and placed in oxygenated artificial cerebrospinal fluid (aCSF). Following a 1-hr recovery, half of the slices from each animal were subjected to 5-minute of OGD and the remaining slices remained in oxygenated-aCSF as controls. Slices from each group were then transferred to oxygenated aCSF containing 0.2% trypan blue for 30-min. Slices were then fixed, subsectioned, and the number of trypan labeled neurons counted. Dead and dying neurons take up the trypan blue and thus are easily quantified. Data demonstrate that 5-minute of OGD significantly increased the number of trypan labeled neurons in the CA1 by 3-fold in males and 2.6-fold in females ($p < 0.001$ for each). Infusion of 4% AQ significantly reduced the number of trypan labeled neurons in both males and females such that there was no longer a difference between vehicle and ischemic slices. The AQ-mediated neuroprotection effect was also independent of hemisphere and occurred in both left and right hippocampus. Thus, apoaequorin exerts comparable neuroprotection in female as well as male rats. These data further support a potential role apoaequorin in protecting hippocampal neurons from ischemic stroke and should inspire additional research aimed at understanding how this neuroprotection is achieved.

**Disclosures: D. Safarini:** None. **B. Natwora:** None. **J.R. Moyer, Jr.:** None. **M. Massman:** None.

**Poster**

**PSTR173: Neuroprotective Mechanisms: Preclinical**

**Location:** WCC Halls A-C

**Time:** Monday, November 16, 2026, 1:00 PM - 5:00 PM

**Program #/Poster #:** PSTR173.07/Web Only

**Topic:** D.01. Neurotoxicity, Inflammation, and Neuroprotection

**Support:** SECIHTI 712328
SECIHTI 39783
SIREI 27928202467

**Title:** Effect of blue corn tortilla and gestational lipopolysaccharide on hematological parameters and hippocampal histology in juvenile rat offspring

**Authors: *P. F. GONZÁLEZ NIETO**[1], M. ALVARADO[2], R. I. GUZMÁN-GERÓNIMO[4], L. T. HERNANDEZ SALAZAR[3], J. F. RODRÍGUEZ-LANDA[3];
[1]Facultad de Nutrición, Xalapa, Mexico; [2]Inst. de Neuroetología, Xalapa, Veracruz, Mexico; [3]Inst. de Neuroetología, Xalapa, Mexico; [4]Inst. de Ciencias Básicas, Xalapa, Mexico

**Abstract:** During pregnancy, infectious processes can disrupt the development of brain structures (such as the hippocampus) that are critical for cognitive processes. In early life, brain maturation continues, a period marked by a peak in dendritic density and programmed neuronal pruning; the consequences of exposure to lipopolysaccharide (LPS) may remain latent until early adulthood. However, natural alternatives that can mitigate infectious processes are being sought, such as foods containing bioactive compounds of significant scientific relevance due to their biological properties. The blue corn tortilla has traditionally been proposed for this study due to its anthocyanins, which possess antioxidant and neuroprotective properties. Therefore, the objective of this study was to evaluate the effect of the blue corn tortilla on hippocampal cell density in offspring at 40 days of age (P40) exposed to LPS during gestation. Eighteen male offspring were analyzed and divided into three groups: control (CTL), LPS-G (offspring of mothers exposed to LPS during gestation), and LPS-GTM (offspring of mothers exposed to LPS during gestation and fed tortillas). The tortilla was administered throughout the entire gestation period, providing an equivalent of 6 mg/kg of anthocyanins and 10 mg/kg of polyphenols; the nixtamalization process was performed in a microwave with the addition of gallic acid to improve anthocyanin retention and biological function. LPS (50 μg/kg) was administered on embryonic days 10-14. Cell density was assessed in different regions of the hippocampus: the dentate gyrus (DG) and the Ammon's horn (CA1, CA2, and CA3), for which Nissl staining was performed. Cell counting was performed using the "ImageJ" software and expressed as the number of cells per unit area (cells/mm²). Additionally, hematological parameters were analyzed on a blood sample obtained from the right atrium of the heart and collected in an EDTA (ethylenediaminetetraacetic acid) tube. The results showed that, in terms of hematological parameters, there was a significant decrease in the LPS-GTM group compared to the CTL group in the following parameters: hemoglobin, hematocrit, mean cell volume, and mean corpuscular hemoglobin, whereas the LPS-GTM group showed a significant increase in the percentage of lymphocytes compared to the CTL group. Regarding cell density, no significant differences were observed between the groups, with the number of hippocampal cells remaining more stable, possibly due to the influence of gonadal hormones on brain organization and maturation.

**Disclosures: P.F. González Nieto:** None. **M. Alvarado:** None. **R.I. Guzmán-Gerónimo:** None. **L.T. Hernandez Salazar:** None. **J.F. Rodríguez-Landa:** None.

**Poster**

**PSTR173: Neuroprotective Mechanisms: Preclinical**

**Location:** WCC Halls A-C

**Time:** Monday, November 16, 2026, 1:00 PM - 5:00 PM

**Program #/Poster #:** PSTR173.08/T29

**Topic:** D.01. Neurotoxicity, Inflammation, and Neuroprotection

**Support:** Gates Grubstake Award; Unrestricted Grant to the Department of Ophthalmology at the University of Colorado from Research to Prevent Blindness.

**Title:** Overexpression of HSPB1 in Human iPSC-Derived Retinal Ganglion Cells Improves Survival uponTransplantation in Mouse Models

**Authors: *M. HA**[1], S. PARWEEN[2], R. NAGARAJ[3], N. VERGARA[4], M. NAM[1];
[1]Univ. of Colorado Med. Sch., Aurora, CO; [2]Opthalmology, [4]Ophthalmology, [3]Univ. of Colorado Sch. of Med., Aurora, CO

**Abstract:** Glaucoma causes irreversible vision loss through degeneration of retinal ganglion cells (RGCs), and current treatments can slow disease progression but cannot replace lost neurons. RGC transplantation is a promising strategy for vision restoration, but poor survival of transplanted cells remains a major barrier. We tested whether engineering human induced pluripotent stem cell-derived RGCs to overexpress heat shock protein beta-1 (HSPB1) could improve cell survival and transplantation outcomes. RGCs were transduced with an AAV2-HSPB1 vector and exposed to oxidative or inflammatory stress. HSPB1-overexpressing RGCs showed reduced cell death, lower apoptotic marker expression, decreased mitochondrial reactive oxygen species, and increased neurite outgrowth compared with control RGCs. To assess transplantation outcomes, control or engineered RGCs were injected into mouse eyes under uninjured conditions or after optic nerve crush. Engineered RGCs showed improved survival and localized near the ganglion cell layer, persisting after the injury. In optic nerve crush eyes, engineered RGC transplantation also improved pattern electroretinogram responses compared with control RGC transplantation. These findings suggest that HSPB1 overexpression enhances the resilience, survival, and function of transplanted human RGCs. This approach may help improve cell replacement strategies for glaucoma and other optic neuropathies.

**Disclosures: M. Ha:** None. **S. Parween:** None. **R. Nagaraj:** F. Consulting Fees (e.g., advisory boards); Ram H. Nagaraj is Chief Scientific Advisor for Eyegenex Inc. **N. Vergara:** None. **M. Nam:** None.

**Poster**

**PSTR173: Neuroprotective Mechanisms: Preclinical**

**Location:** WCC Halls A-C

**Time:** Monday, November 16, 2026, 1:00 PM - 5:00 PM

**Program #/Poster #:** PSTR173.09/T30

**Topic:** D.01. Neurotoxicity, Inflammation, and Neuroprotection

**Support:** MR15MH130900

**Title:** Lipopolysaccharide-induced astrocyte reactivity is inhibited by FDA-approved drugs

**Authors:** T. HAMAD, O. LOGUIDICE, A. WHITE, ***M. T. MANNERS**;
Rowan Univ., Glassboro, NJ

**Abstract:** Major Depressive Disorder (MDD) is a worldwide leading cause of disability, and while currently available antidepressants are effective for some patients, over 30% of patients do not respond to the available treatment options. Increasing evidence implicates chronic neuroinflammation as a key contributor to the pathophysiology of MDD. Astrocytes are responsible for maintaining neuroinflammatory homeostasis, and overactivity of astrocytes has been associated with depressive phenotypes, indicating that astrocyte-mediated inflammation may be a critical target for the treatment of MDD. Astrocytes morphology and cytokine production are important indicators of astrocyte reactivity to the environment. We hypothesized that anti-inflammatory or antidepressant drugs would reduce the reactivity of astrocytes. Here we culture primary cortical astrocytes from PND 2-5 mice, and pretreated astrocytes with currently prescribed anti-inflammatory and antidepressant drugs and then treated cells with 10 ng/ul lipopolysaccharide (LPS). We then measured cytokine expression and reactive astrocyte morphology and found that both anti-inflammatory and antidepressant drugs reduced LPS-induced TNFa secretion in astrocytes. These findings indicate that both anti-inflammatory and antidepressant agents reduce the reactivity of cultured astrocytes, and this could be a relevant approach to reduce neuroinflammation in the brain.

**Disclosures: T. Hamad:** None. **O. Loguidice:** None. **A. White:** None. **M.T. Manners:** None.

**Poster**

**PSTR173: Neuroprotective Mechanisms: Preclinical**

**Location:** WCC Halls A-C

**Time:** Monday, November 16, 2026, 1:00 PM - 5:00 PM

**Program #/Poster #:** PSTR173.10/T31

**Topic:** D.01. Neurotoxicity, Inflammation, and Neuroprotection

**Support:** SECIHTI CF2023-2024-2706

**Title:** RESVERATROL NANOFORMULATION MITIGATES DIABETES-INDUCED CEREBROVASCULAR ENDOTHELIAL DAMAGE IN MICE

**Authors: *P. AGUILERA**[1], A. Y. NAVARRO PITA[2], A. MÉNDEZ PALACIOS[3], O. MEDINA CAMPOS[5], J. PEDRAZA-CHAVERRI[6], F. SANCHEZ[7], I. M. ALQUISIRAS BURGOS[8], M. ESPINOZA[4];
[1]Inst. Nacional de Neurologia y Neurocirugia, Mexico Distrito Federal, Mexico; [2]Univ. Autónoma de Guerrero, Chilpancingo, Mexico; [3]Univ. Autónoma de Guerrero, México, Mexico; [4]Facultad de Ciencias Químico Biológicas, Univ. Autónoma de Guerrero, Chilpancingo de Los Bravo, Mexico; [5]Biología, Facultad de Química, UNAM, CDMX, Mexico; [6]Biología, Facultad de Química, UNAM, Ciudad de México, Mexico; [7]Vascular Pathology, Natl. Inst. of Neurol. and Neurosurg., Mexico City, Mexico; [8]Inst. Nacional de Neurologia y Neurocirugia Manuel Velasco Suarez, Mexico, Mexico

**Abstract:** Vascular complications associated with diabetes mellitus type 2 (DM2) are a major consequence of chronic hyperglycemia. Diabetes-induced oxidative stress and inflammation are associated with the glial response and contribute to the loss of cerebral endothelial function, leading to cerebrovascular pathology. Resveratrol (RSV), a polyphenolic compound, has demonstrated protective effects in diabetic conditions, largely attributed to its antioxidant, anti-inflammatory, and hypoglycemic properties. RSV nanoformulations (RSVn) enhance its bioavailability and tissue distribution, potentially improving its therapeutic efficacy. **Objective:** To evaluate the effect of RSVn on vascular endothelial damage in diabetic mice. **Methods:** The antioxidant activity of RSVn was assessed in vitro using DPPH and FRAP assays. A murine model of DM2 was established in neonatal male C57BL/6 mice through streptozotocin administration, followed by a high-fat diet regimen for 16 weeks. RSVn was administered intranasally (1 mg/kg/day) for 5 days. Astrocytic reactivity, endothelial response, and vascular permeability were evaluated in the cerebral cortex by immunofluorescence. **Results:** In the DPPH assay, RSVn showed a trapping capacity of 80.0% ± 0.5, similar to RSV in DMSO (84.6% ± 0.5), while VHn (vehicle, nanoformulation without RSV) showed no activity. In FRAP, RSVn (2.62 ± 0.27 Eq mM Trolox/g) showed greater reducing capacity than RSV in DMSO (1.64 ± 0.07 Eq mM Trolox/g), and VHn showed no activity. In the cerebral cortex of the DM2 group, the expression of GFAP+ (0.2690 ± 0.0389 *vs.* 0.0216 ± 0.0030) and von Willebrand factor (vWF: 186.9 ± 38.94 *vs.* 49.92 ± 22.48) was increased compared to the control group. Similar results were obtained with the Evans blue permeability assay (EBp: 193.9 ± 33.74 *vs.* 85.58 ± 10.36). Treatment with RSVn significantly decreased these parameters (GFAP+: 0.0470 ± 0.0172; vWF: 43.95 ± 14.62; EBp: 53.54 ± 16.28) compared to DM2 and DM2+VHn. **Conclusions:** *In vitro*, RSVn preserves the antioxidant activity of RSV and its reducing power; *in vivo* experiments showed that RSVn decreased astrocytic reactivity and endothelial damage while preserving the integrity of the blood-brain barrier, positioning itself as a strategy for neurovascular damage in DM2. **Acknowledgments:** SECIHTI (CF2023-2024-2706).

**Disclosures: P. Aguilera:** None. **A.Y. Navarro Pita:** None. **A. Méndez Palacios:** None. **O. Medina Campos:** None. **J. Pedraza-Chaverri:** None. **F. Sanchez:** None. **I.M. Alquisiras Burgos:** None. **M. Espinoza:** None.

**Poster**

**PSTR173: Neuroprotective Mechanisms: Preclinical**

**Location:** WCC Halls A-C

**Time:** Monday, November 16, 2026, 1:00 PM - 5:00 PM

**Program #/Poster #:** PSTR173.11/T32

**Topic:** D.01. Neurotoxicity, Inflammation, and Neuroprotection

**Support:** R01EY036020
Research to Prevent Blindness- Career Development Award
NEI NIH CORE grant P30 EY08098
Research to Prevent Blindness Unrestricted Grant to Department of Ophthalmology
Generous support from the Eye and Ear Foundation

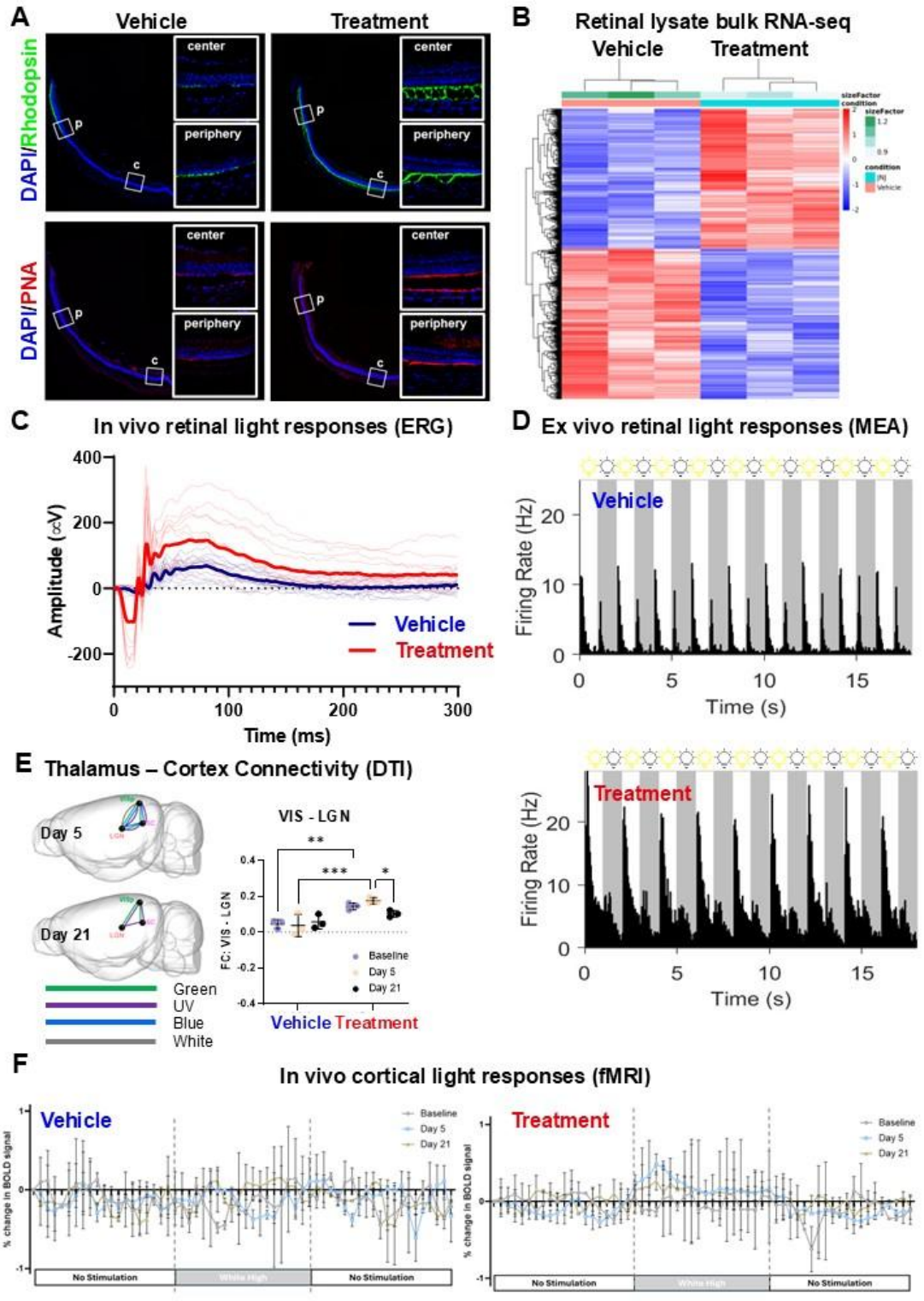
**Title:** Systemic pharmacological inhibition of the purinergic receptor P2X7 prevents retinal neurodegeneration.

**Authors: *L. AFRIMA**[1], J. ENDRES[1], M. TELIAS[2];
[1]Ophthalmology, [2]Mol. and Cell Biol., Univ. of Pittsburgh, Pittsburgh, PA

**Abstract:** Neurodegeneration of photoreceptors—the light sensing cells of the retina—causes progressive blindness, a profound burden on society. Photoreceptors can degenerate due to hundreds of inherited mutations, as in retinitis pigmentosa (RP); acquired conditions, such as age related macular degeneration and geographic atrophy; or physical injuries, including retinal detachment and phototoxicity. Although some etiologies have been mechanistically defined, many remain poorly understood, complicating efforts to develop effective neuroprotective therapies.

Evidence suggests that rod and cone death is driven by stress and apoptosis triggered through pathways downstream of the primary mutation or insult and largely independent of it. A prominent candidate mediator is the purinergic receptor P2X7, a large ATP gated cation channel that promotes calcium influx, increases reactive oxygen species, reduces mitochondrial respiration, and ultimately induces apoptosis. We repurposed a commercially available, orally delivered, brain penetrant small molecule P2X7 inhibitor to treat retinal degeneration in a mouse model of RP.

Systemic P2X7 inhibition produced robust neuroprotection, with more than 50% of photoreceptors surviving in treated mice at ages when vehicle treated controls exhibited near complete degeneration. Treated mice showed significantly improved retinal light responses measured in vivo by electroretinography and ex vivo by multi electrode arrays. Functional MRI revealed preserved thalamocortical connectivity and rescued light evoked brain activity. Behaviorally, treated mice displayed strong light aversion comparable to healthy wild type animals, whereas untreated mice at the same age exhibited no measurable light perception. These findings demonstrate that targeting P2X7 is sufficient to prevent progressive photoreceptor degeneration and preserve visual function. Systemic pharmacological inhibition of P2X7 represents a promising therapeutic strategy for preventing blindness across diverse retinal degenerative conditions.




**Disclosures: L. Afrima:** None. **J. Endres:** None. **M. Telias:** None.

**Poster**

**PSTR173: Neuroprotective Mechanisms: Preclinical**

**Location:** WCC Halls A-C

**Time:** Monday, November 16, 2026, 1:00 PM - 5:00 PM

**Program #/Poster #:** PSTR173.12/U1

**Topic:** D.01. Neurotoxicity, Inflammation, and Neuroprotection

**Title:** A Potent Allosteric SARM1 Inhibitor Protects Against Axonal Degeneration and Advances to Clinical Evaluation

**Authors: *M. LIU**, A. L. BAGDASARIAN, M. STEFFEK, W. AVERY, D. BRAUN, C. BUCHER, M. K. CAMPBELL, R. A. CRAIG II, T. Z. FISCHER, G. A. FITZGERALD, Y. HSIEH, B. HUFFMAN, L. IBRAHIM, K. W. LEXA, A. EL-SHERBENI, D. W. STEVENS, E. W. SUN, R. H. TAKAHASHI, X. WANG, E. YULYANINGSIH, B. M. FOX;
Tenvie Therapeut., Brisbane, CA

**Abstract:** Axonal degeneration is a defining pathological feature of various serious neurologic disorders. In chemotherapy-induced peripheral neuropathy (CIPN), diabetic peripheral neuropathy (DPN), and amyotrophic lateral sclerosis (ALS), it contributes directly to pain, functional decline, and disability. In addition, CIPN often leads to reduced chemotherapy dose levels and duration. Sterile alpha and TIR motif-containing 1 (SARM1), a central metabolic sensor and executor of axon degeneration, represents a compelling target for the clinical development of novel disease-modifying therapies that may prevent or slow neurodegeneration. Its relevance across CIPN, DPN and ALS is supported by genetic evidence: SARM1 deletion attenuates neuropathic phenotypes in rodent models of both CIPN and DPN, while in ALS, gain of function SARM1 mutations are enriched in patients and SARM1 loss is protective in preclinical models. Here, we report the identification of compound 121, a potent allosteric inhibitor of SARM1 that binds to the ARM domain and stabilizes the inactive conformation. This distinct mechanism of action differs from that of orthosteric inhibitors, which bind to the catalytic site in the TIR domains and stabilize the active conformation. As a result, it effectively mitigates the translational liabilities associated with that class of inhibitors. Efficacy of compound 121 was assessed in a rat model of paclitaxel-induced CIPN, and for the first time in the field in a high-fat, high-sucrose diet-induced DPN model. In the DPN model, compound 121 reduced cADPR levels in tissues, confirming target engagement and pharmacologic inhibition of SARM1 activity. Across both models, compound 121 conferred robust structural protection, preserving axonal integrity in the sciatic nerve in the CIPN model and intraepidermal nerve fiber density in the DPN model. These were associated with functional benefits, including improved sensory nerve action potential amplitude and reduced mechanical allodynia. Together, these data support the clinical development of SARM1 inhibition as a potential therapeutic strategy for peripheral neuropathies. A Phase 1 trial of our clinical-stage allosteric SARM1 inhibitor is currently ongoing to evaluate safety, tolerability, pharmacokinetics, and pharmacodynamics in healthy volunteers.

**Disclosures: M. Liu:** A. Employment/Salary (full or part-time):; Tenvie Therapeutics. E. Ownership Interest (stock, stock options, royalty, receipt of intellectual property rights/patent holder, excluding diversified mutual funds); Tenvie Therapeutics. **A.L. Bagdasarian:** A.

Employment/Salary (full or part-time):; Tenvie Therapeutics. E. Ownership Interest (stock, stock options, royalty, receipt of intellectual property rights/patent holder, excluding diversified mutual funds); Tenvie Therapeutics. **M. Steffek:** A. Employment/Salary (full or part-time):; Tenvie Therapeutics. E. Ownership Interest (stock, stock options, royalty, receipt of intellectual property rights/patent holder, excluding diversified mutual funds); Tenvie Therapeutics. **W. Avery:** A. Employment/Salary (full or part-time):; Tenvie Therapeutics. E. Ownership Interest (stock, stock options, royalty, receipt of intellectual property rights/patent holder, excluding diversified mutual funds); Tenvie Therapeutics. **D. Braun:** A. Employment/Salary (full or part-time):; Tenvie Therapeutics. E. Ownership Interest (stock, stock options, royalty, receipt of intellectual property rights/patent holder, excluding diversified mutual funds); Tenvie Therapeutics. **C. Bucher:** A. Employment/Salary (full or part-time):; Tenvie Therapeutics. E. Ownership Interest (stock, stock options, royalty, receipt of intellectual property rights/patent holder, excluding diversified mutual funds); Tenvie Therapeutics. **M.K. Campbell:** A. Employment/Salary (full or part-time):; Tenvie Therapeutics. E. Ownership Interest (stock, stock options, royalty, receipt of intellectual property rights/patent holder, excluding diversified mutual funds); Tenvie Therapeutics. **R.A. Craig II:** A. Employment/Salary (full or part-time):; Tenvie Therapeutics. E. Ownership Interest (stock, stock options, royalty, receipt of intellectual property rights/patent holder, excluding diversified mutual funds); Tenvie Therapeutics. **T.Z. Fischer:** A. Employment/Salary (full or part-time):; Tenvie Therapeutics. E. Ownership Interest (stock, stock options, royalty, receipt of intellectual property rights/patent holder, excluding diversified mutual funds); Tenvie Therapeutics. **G.A. Fitzgerald:** A. Employment/Salary (full or part-time):; Tenvie Therapeutics. E. Ownership Interest (stock, stock options, royalty, receipt of intellectual property rights/patent holder, excluding diversified mutual funds); Tenvie Therapeutics. **Y. Hsieh:** A. Employment/Salary (full or part-time):; Tenvie Therapeutics. E. Ownership Interest (stock, stock options, royalty, receipt of intellectual property rights/patent holder, excluding diversified mutual funds); Tenvie Therapeutics. **B. Huffman:** A. Employment/Salary (full or part-time):; Tenvie Therapeutics. E. Ownership Interest (stock, stock options, royalty, receipt of intellectual property rights/patent holder, excluding diversified mutual funds); Tenvie Therapeutics. **L. Ibrahim:** A. Employment/Salary (full or part-time):; Tenvie Therapeutics. E. Ownership Interest (stock, stock options, royalty, receipt of intellectual property rights/patent holder, excluding diversified mutual funds); Tenvie Therapeutics. **K.W. Lexa:** A. Employment/Salary (full or part-time):; Tenvie Therapeutics. E. Ownership Interest (stock, stock options, royalty, receipt of intellectual property rights/patent holder, excluding diversified mutual funds); Tenvie Therapeutics. **A. El-Sherbeni:** A. Employment/Salary (full or part-time):; Tenvie Therapeutics. E. Ownership Interest (stock, stock options, royalty, receipt of intellectual property rights/patent holder, excluding diversified mutual funds); Tenvie Therapeutics. **D.W. Stevens:** A. Employment/Salary (full or part-time):; Tenvie Therapeutics. E. Ownership Interest (stock, stock options, royalty, receipt of intellectual property rights/patent holder, excluding diversified mutual funds); Tenvie Therapeutics. **E.W. Sun:** A. Employment/Salary (full or part-time):; Tenvie Therapeutics. E. Ownership Interest (stock, stock options, royalty, receipt of intellectual property rights/patent holder, excluding diversified mutual funds); Tenvie Therapeutics. **R.H. Takahashi:** A. Employment/Salary (full or part-time):; Tenvie Therapeutics. E. Ownership Interest (stock, stock options, royalty, receipt of intellectual property rights/patent holder, excluding diversified mutual funds); Tenvie Therapeutics. **X. Wang:** A. Employment/Salary (full or part-time):; Tenvie Therapeutics. E. Ownership Interest (stock, stock options, royalty, receipt of intellectual property rights/patent holder, excluding diversified mutual funds); Tenvie Therapeutics. **E. Yulyaningsih:** A.

Employment/Salary (full or part-time):; Tenvie Therapeutics. E. Ownership Interest (stock, stock options, royalty, receipt of intellectual property rights/patent holder, excluding diversified mutual funds); Tenvie Therapeutics. **B.M. Fox:** A. Employment/Salary (full or part-time):; Tenvie Therapeutics. E. Ownership Interest (stock, stock options, royalty, receipt of intellectual property rights/patent holder, excluding diversified mutual funds); Tenvie Therapeutics.

**Poster**

**PSTR173: Neuroprotective Mechanisms: Preclinical**

**Location:** WCC Halls A-C

**Time:** Monday, November 16, 2026, 1:00 PM - 5:00 PM

**Program #/Poster #:** PSTR173.13/U2

**Topic:** I.08. Learning and Memory

**Title:** Behavioral analysis in mice defines anxiety- and stress-dependent cognitive alterations differentially after sevoflurane exposure

**Authors:** A. ALTUNKAYA[1], J. JIAO[1], M. VADKERTIOVA[1], G. RAMMES[1], C. TOUMA[2], M. V. SCHMIDT[3], G. SCHNEIDER[1], ***T. FENZL**[1];
[1]Tech. Univ. Munich, Munich, Germany; [2]Dept. of Behavioural Biol., Osnabrueck Univ., Osnabrueck, Germany; [3]Max Planck Inst. of Psychiatry, Munich, Germany

**Abstract: Introduction:** Preoperative anxiety (POA) and preoperative stress (POS) correlate with postoperative delirium (POD), a condition from short cognitive impairment to chronic cognitive deficits. Preoperative tests rely on subjective measures, demanding objective markers. We investigated if POA and POS as risk factors can be separated in modulating post-sevoflurane cognitive responses in mice, bridging anxiety/stress with anesthetic vulnerability. We also investigated baseline EEG to predict POA and POS phenotypes. **Methods:** 75 male mice were EEG-implanted. Fear conditioning freezing was used to classify BL/6N-mice into high-anxiety (HA) or low-anxiety (LA) groups. Water-Cross Maze (WCM, 5 days, 6 trials/day), sevoflurane exposure (1hr, 2.0%vol) and Re-Test post-anesthesia followed. A stress reactivity (SR) mouse model (CD1 background), selectively bred for extremes in HPA axis activity, was used in the same experiment flow. Based on CORT levels, mice were classified as high (HR), intermediate (IR), or low (LR) stress responders. DeepLabCut tracked body parts during WCM, Keypoint MoSeq identified behavioral syllables during WCM. **Results:** Baseline HA had diminished REMS and elevated NREMS with altered bout lengths. Spectral analysis revealed lower delta power in HA, with heightened eta/beta activity during REMS. HA markedly decreased velocity (HA -4.07%, LA +25.94%; $p<.001$) and spent more time confused (HA -1.8%, LA -37.1%; $p=.0014$) in WCM Re-Test. For "Wall" syllables, HA increased duration (HA +5.6%, LA -14.5%; $p=.024$) with smaller velocity increases (HA +5.87%, LA +21.77%; $p<.001$). "Swim" syllables showed similar patterns (duration: HA +6.1%, LA -17.7%; velocity HA: +7.14%, LA +16.28%; $p<.001$). HR showed increased REMS, compared to LR (dark-phase REMS: 5.53% vs 3.63% of recording time; $p=0.006$). All SR groups demonstrated robust WCM performance. HR showed longer escape latencies than IR and LR (training days, $p<0.05$), but higher Test and Re-Test accuracy (HR vs IR, $p=0.013$, 0.009). Sevoflurane anesthesia did not impair cognitive

performance in SR mice. **Conclusion:** Specific baseline EEG-parameters predict distinct anxiety phenotypes and vulnerability to sevoflurane-induced cognitive dysfunction. For the stress phenotypes followed sevoflurane anesthesia, a hyperactive HPA axis may be protective, maintaining enhanced cognitive performance. This research may establish objective neurophysiological markers identifying individuals at higher risk for POA/POS-POD interactions in clinical settings.

**Disclosures: A. Altunkaya:** None. **J. Jiao:** None. **M. Vadkertiova:** None. **G. Rammes:** None. **C. Touma:** None. **M.V. Schmidt:** None. **G. Schneider:** None. **T. Fenzl:** None.

**Poster**

**PSTR173: Neuroprotective Mechanisms: Preclinical**

**Location:** WCC Halls A-C

**Time:** Monday, November 16, 2026, 1:00 PM - 5:00 PM

**Program #/Poster #:** PSTR173.14/U3

**Topic:** D.01. Neurotoxicity, Inflammation, and Neuroprotection

**Support:** NIH R01 EY031696
NIH R21 EY033882
Harvard NeuroDiscovery Center Grant
Core Grant for Vision Research P30EY003790

**Title:** Epigenetic reprogramming by targeting Dnmt3a enables functional neuroregeneration and neuroprotection in the adult CNS

**Authors: *W. TAI**, K.-S. CHO, A. ASHOK, D. CHEN;
Schepens Eye Res. Inst. of Massachusetts Eye and Ear, Dept. of Ophthalmology, Harvard Med. Sch., Boston, MA

**Abstract:** Adult mammalian CNS neurons lack the capacity to regenerate axons after injury. Retinal ganglion cells (RGCs), whose axons form the optic nerve, provide an accessible CNS projection system to study neuroregeneration after injury. Through genetic screening in the RGCs, we identified DNA methyltransferase 3a (Dnmt3a) as a key epigenetic barrier to both axon regeneration and neuronal survival. Dnmt3a levels increase during the developmental loss of regenerative capacity (E16-P0) and after traumatic nerve injury in a mouse model of optic nerve crush (ONC). Genetic ablation of Dnmt3a not only promotes axon regeneration after ONC but also confers robust neuroprotection in a retinal ischemia-reperfusion (I/R) model. Adult mice carrying a conditional knockout of Dnmt3a (CKODnmt3a+/-) selectively in RGCs and their littermate controls underwent ONC. While control mice remained blind after ONC, CKODnmt3a+/- showed full-length axon regeneration into central visual targets after ONC and restored visual function, including visual acuity, light perception, positive scotopic threshold response (pSTR), and visual evoked potential. Therapeutic knockdown via intravitreal AAV-shRNA in wildtype mice similarly promoted axon regeneration and vision recovery after ONC. Moreover, in the I/R model induced by acute intraocular pressure elevation, CKODnmt3a+/-

mice exhibited significantly improved RGC survival, preserved pSTR responses, and sustained visual acuity, indicating maintained RGC function and visually guided behavior after ischemic insult. These findings reveal that Dnmt3a-mediated DNA methylation acts as a dual epigenetic regulator—suppressing both axon regeneration and neuronal survival in adult CNS neurons. Targeting Dnmt3a may represent a promising therapeutic strategy for neuroprotection and repair across CNS injuries and ischemic neuropathologies.

**Disclosures: W. Tai:** None. **K. Cho:** F. Consulting Fees (e.g., advisory boards); SunRegen Healthcare AG, FireCyte Therapeutics. **A. Ashok:** None. **D. Chen:** F. Consulting Fees (e.g., advisory boards); i-Lumen Scientific, Sichuan PriMed, Sanofi, FireCyte Therapeutics.

**Poster**

**PSTR173: Neuroprotective Mechanisms: Preclinical**

**Location:** WCC Halls A-C

**Time:** Monday, November 16, 2026, 1:00 PM - 5:00 PM

**Program #/Poster #:** PSTR173.15/U4

**Topic:** D.01. Neurotoxicity, Inflammation, and Neuroprotection

**Support:** TA-2104-37423, NMSS Career Transition Award

**Title:** NLRX1 as a Neuroprotective Regulator of Axon-Myelin Integrity During Demyelinating Stress

**Authors: *M. GHARAGOZLOO**[1], M. D. SMITH[2], G. SARDI ROGINES[2], A. SINGH[2], D. GALLEGUILLOS[2], P. A. CALABRESI[3,2];
[1]JOHNS HOPKINS UNIVERSITY, BALTIMORE, MD; [2]Johns Hopkins Univ., Baltimore, MD; [3]Univ. of Vermont, Burlington, VT

**Abstract:** Progressive MS involves chronic inflammation, mitochondrial dysfunction, neuroaxonal injury, and remyelination failure, creating an urgent need to identify CNS resilience pathways that preserve axon-myelin integrity. We tested whether NLRX1, a mitochondria-localized innate immune regulator, protects neuronal, synaptic, and myelin integrity during cuprizone (CPZ)-induced demyelination. WT and *Nlrx1*$^{-/-}$ mice were exposed to CPZ. Myelin loss was evaluated by MBP and Black-Gold staining, mature oligodendrocytes were quantified as Olig2+ASPA+ cells in the central corpus callosum, and gliosis was assessed by GFAP and Iba1 staining at 2 and 4 weeks. Bulk RNA-seq of the corpus callosum was performed after 1 week to identify injury signatures. Histology showed no significant genotype-dependent difference in demyelination or gliosis after 2 weeks of CPZ. By 4 weeks, *Nlrx1*$^{-/-}$ mice developed greater myelin loss and fewer Olig2+ASPA+ mature oligodendrocytes than WT controls, indicating increased white matter vulnerability without NLRX1. To determine whether early transcriptional changes could explain this delayed phenotype, we analyzed corpus callosum RNA-seq after 1 week of CPZ. Canonical myelin genes, including *Mbp, Plp1, Mog, Mag, Cnp, and Mobp,* were downregulated in both genotypes, indicating a shared early oligodendrocyte/myelin stress response. Pathway-level analysis revealed a major divergence in

neuronal and synaptic programs. Following CPZ exposure, *Nlrx1*$^{-/-}$ mice showed coordinated suppression of genes involved in presynaptic vesicle cycling, synaptic adhesion, glutamatergic signaling, ion-channel activity, calcium-dependent signaling, and neuronal excitability, whereas these programs were largely preserved in WT mice. These findings suggest that loss of NLRX1 renders neuronal and synaptic compartments vulnerable to early demyelinating stress. Together, these data support a model in which NLRX1 preserves axon-myelin integrity by maintaining early metabolic, neuroimmune, and synaptic resilience during demyelinating stress. Although early myelin gene suppression occurs in both genotypes, loss of NLRX1 selectively disrupts neuronal and synaptic pathways before genotype-dependent demyelination is detectable by histology. These findings identify NLRX1 as an endogenous CNS resilience pathway that protects neuronal and synaptic integrity during early demyelinating stress and limits subsequent myelin loss.

**Disclosures: M. Gharagozloo:** None. **M.D. Smith:** None. **G. Sardi Rogines:** None. **A. Singh:** None. **D. Galleguillos:** None. **P.A. Calabresi:** None.

**Poster**

**PSTR173: Neuroprotective Mechanisms: Preclinical**

**Location:** WCC Halls A-C

**Time:** Monday, November 16, 2026, 1:00 PM - 5:00 PM

**Program #/Poster #:** PSTR173.16/U5

**Topic:** D.01. Neurotoxicity, Inflammation, and Neuroprotection

**Support:** NIH Grant R01DK118082

**Title:** Edaravone Protects the Hippocampus from Brain Damage following Insulin-Induced Severe Hypoglycemia in a Diabetic Rodent Model

**Authors: *A. THOMPSON**[1], H. RILEY[2], V. PATEL[2], S. STONE[2], G. AKIN[2], L. SCHOEDER[2], M. DEVORE[3], S. J. FISHER[4];
[2]Intrnl. Med., [3]Pharmacol. and Nutritional Sci., [4]Intrnl. Medicine; Pharmacol. and Nutritional Sci., [1]Univ. of Kentucky, Lexington, KY

**Abstract:** Severe hypoglycemia is a major consequence of intensive insulin therapy in diabetes and is associated with neuronal damage, particularly within the hippocampus. Yet, effective neuroprotective treatments remain elusive. This study investigates whether post-insult administration of edaravone, a free radical scavenger and neuroprotective agent with antioxidant properties, can attenuate hippocampal injury following insulin-induced severe hypoglycemia.in a Streptozotocin (STZ)-diabetic model. Ten-week-old Sprague-Dawley rats were divided into three treatment cohorts: 1) STZ-diabetic controls (STZ+CON), 2) rats treated with insulin-induced (50U mg/kg) severe hypoglycemia (STZ+SH: 10-15mg/dL for 90 minutes), and 3) rats treated with SH followed by once daily with edaravone (3mg/kg) (STZ+SH+EDV) (n=5-6/group). One-week post-insult, rats were euthanized, perfused, and 40 μm coronal sections of the hippocampus were analyzed via immunohistochemistry for markers of cell death (Fluoro-

Jade C, Cleaved Caspase-3), neuroinflammation (Iba1/CD68), and oxidative stress (4-Hydroxynonenal). Quantitative analysis was conducted using ImageJ and one-way ANOVA. As compared to diabetic controls, severe hypoglycemia markedly increased all pathological markers: FJC (11-fold, $p<0.05$), Iba1/CD68 (12-fold, $p<0.01$), CC3 (3-fold, $p<0.05$), as well as 4HNE positive areas (3.4-fold, $p<0.001$). As compared to STZ+SH alone, STZ+SH+EDV markedly reduced all stained cells to a level not statistically different from controls (p=NS). These findings demonstrate that edaravone confers robust neuroprotection in the hippocampus following insulin-induced SH in an STZ-diabetic model. The reduction of cell death, neuroinflammation, and oxidative stress supports its therapeutic potential in mitigating hypoglycemia-related brain injury. This work advances our understanding of neuroprotective treatments in metabolic brain injury and highlights novel pathways for therapeutics in diabetes-related brain damage.

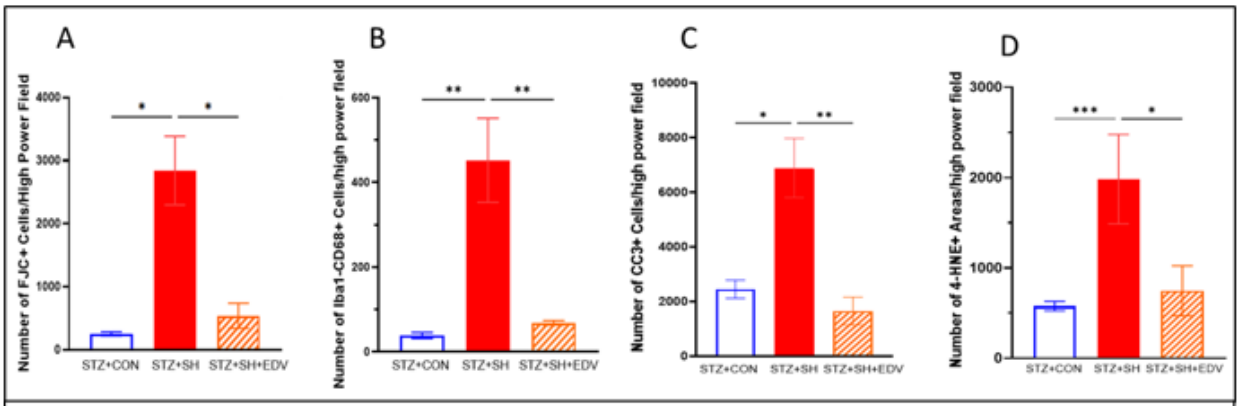



**Figure 1.** Severe hypoglycemia causes brain damage and is prevented with drug treatment in a diabetic rodent model. **A)** Graph of FJC+ cell count. **B)** Graph of Iba1-CD68+ cell count. **C)** Graph of CC3+ cell count. **D)** Graph of 4HNE+ Areas. Blue open box = STZ diabetic controls; red filled box = STZ diabetic + severe hypoglycemia group; orange hatched box = STZ diabetic + SH + edaravone group. ***p<0.001, **p<0.01, *p<0.05.

**Disclosures: A. Thompson:** None. **H. Riley:** None. **V. Patel:** None. **S. Stone:** None. **G. Akin:** None. **L. Schoeder:** None. **M. Devore:** None. **S.J. Fisher:** None.

**Poster**

**PSTR173: Neuroprotective Mechanisms: Preclinical**

**Location:** WCC Halls A-C

**Time:** Monday, November 16, 2026, 1:00 PM - 5:00 PM

**Program #/Poster #:** PSTR173.17/U6

**Topic:** D.01. Neurotoxicity, Inflammation, and Neuroprotection

**Title:** The GLP-1 Receptor Agonist Semaglutide Attenuates Neuroinflammation and Rescues Memory Deficits via a Glia-Dependent Mechanism

**Authors:** *C. DUCHEMIN, S. WAGNER, B. HUYARD, E. POIRAUD, **E. ANDRIAMBELOSON**;
NEUROFIT, ILLKIRCH, France

**Abstract: Introduction:** Glucagon-like peptide-1 receptor (GLP-1R) agonists, such as semaglutide, have shown neuroprotective potential in neurodegenerative models. However, it remains unclear whether these effects arise from indirect metabolic changes or direct central nervous system (CNS) actions. This study aims to identify the cellular targets of semaglutide within the neuroimmune axis and clarify its mechanism of action across disease-relevant models of cognitive decline. **Methods:** Efficacy was assessed using complementary in vivo and in vitro approaches. In vivo cognitive deficits were evaluated in a murine model of lipopolysaccharide (LPS)-induced inflammation and a rat model of neurotoxicity induced by intracerebroventricular (ICV) injection of amyloid-β (25-35). Memory retention in mice was evaluated by using the T-maze alternation task and in rats was quantified using the passive avoidance task (step-through latency). The involvement of the neuroimmune axis was assessed in vitro using two distinct cellular systems matched to specific stressors. LPS-induced inflammatory responses were evaluated in neuron-glia co-cultures, whereas direct neurotoxicity induced by amyloid-β (Aβ) or glutamate was assessed in pure neuronal cultures. Cells were treated in the presence or absence of semaglutide. This experimental design enables discrimination between glia-mediated and neuron-intrinsic mechanisms. **Results:** Systemic semaglutide rescued LPS-induced cognitive deficits in mice, restoring performance to baseline levels. Similarly, rats subjected to ICV amyloid-β (25-35) exhibited severe memory impairment, reflected by a marked reduction in step-through latency, which was fully prevented by semaglutide treatment. In neuron-glia co-cultures exposed to LPS, semaglutide reduced glial nitric oxide (NO) release, a key marker of neuroinflammation, and restored neuronal survival. In contrast, in pure neuronal cultures exposed to Aβ or glutamate, semaglutide failed to prevent neurotoxicity, indicating a lack of direct neuroprotective effects in the absence of glial cells. **Conclusions:** Semaglutide does not act as a direct neuronal stabilizer; rather, its neuroprotective effects are dependent on the presence of glial cells, where it functions as a neuroimmunomodulator, suppressing microglial and astrocytic neurotoxicity. By linking glia-dependent mechanisms in vitro with robust cognitive rescue in vivo, this study highlights the therapeutic relevance of targeting the neuroimmune axis with GLP-1R agonists.

**Disclosures: C. Duchemin:** None. **S. Wagner:** None. **B. Huyard:** None. **E. Poiraud:** None. **E. Andriambeloson:** None.

**Poster**

**PSTR173: Neuroprotective Mechanisms: Preclinical**

**Location:** WCC Halls A-C

**Time:** Monday, November 16, 2026, 1:00 PM - 5:00 PM

**Program #/Poster #:** PSTR173.18/U7

**Topic:** D.01. Neurotoxicity, Inflammation, and Neuroprotection

**Title:** Structural and Mechanistic Characterization of Allosteric SARM1 Inhibition Supports Clinical Translation for Neuroprotection

**Authors: *M. STEFFEK**, A. L. BAGDASARIAN, M. LIU, W. AVERY, D. BRAUN, C. BUCHER, M. K. CAMPBELL, R. A. CRAIG II, T. Z. FISCHER, G. A. FITZGERALD, Y.

HSIEH, B. HUFFMAN, L. IBRAHIM, K. W. LEXA, A. EL-SHERBENI, D. W. STEVENS, E. W. SUN, R. H. TAKAHASHI, X. WANG, E. YULYANINGSIH, B. M. FOX;
Tenvie Therapeut., Brisbane, CA

**Abstract:** SARM1 is a central executioner of programmed axon degeneration, and its NADase activity drives axon loss after injury or cellular stress. As a downstream effector of diverse axonal insults, SARM1 (an obligate octamer) represents an attractive target for neuroprotective strategies in disorders characterized by axon degeneration. In the current study, we compared two classes of SARM1 inhibitors, orthosteric and allosteric, using biochemical and biophysical analyses to define their distinct mechanisms. Building on reports that orthosteric SARM1 inhibitors can activate the protein at sub-saturating concentrations in vivo and in vitro, we investigated the basis for this effect and found that activation correlated with formation of compound-induced higher-order SARM1 oligomers. In contrast, novel internally developed allosteric inhibitors did not induce higher-order oligomerization and instead stabilized SARM1 in an inactive conformation. These compounds inhibited full-length SARM1 but not a truncated construct containing the catalytic region and lacking the regulatory ARM domain, consistent with inhibition through a regulatory site outside the orthosteric site. Allosteric inhibitors also did not induce the oligomerization-linked activation liability observed with orthosteric compounds. A cryo-EM structure localized this chemical series to the regulatory ARM domain. This structure supported an allosteric mechanism in which binding stabilizes SARM1 in an inactive conformation with restrained catalytic TIR domains and provided a foundation for structure-based drug discovery. The medicinal chemistry campaign yielded a series of highly potent and metabolically stable allosteric compounds, including an in vivo tool compound. In a mouse sciatic nerve transection model, the allosteric tool compound robustly prevented increases in plasma NfL, whereas the orthosteric compound exacerbated NfL elevation, demonstrating the superiority and translational potential of allosteric SARM1 inhibition. Together, these findings define a mechanistic distinction between orthosteric and allosteric SARM1 inhibition and show that allosteric inhibitors avoid the paradoxical activation liability associated with orthosteric compounds by stabilizing SARM1 in an inactive conformation. These findings support allosteric SARM1 inhibition as a mechanistically differentiated strategy for neuroprotection.

**Disclosures: M. Steffek:** A. Employment/Salary (full or part-time):; Tenvie Therapeutics. E. Ownership Interest (stock, stock options, royalty, receipt of intellectual property rights/patent holder, excluding diversified mutual funds); Tenvie Therapeutics. **A.L. Bagdasarian:** A. Employment/Salary (full or part-time):; Tenvie Therapeutics. E. Ownership Interest (stock, stock options, royalty, receipt of intellectual property rights/patent holder, excluding diversified mutual funds); Tenvie Therapeutics. **M. Liu:** A. Employment/Salary (full or part-time):; Tenvie Therapeutics. E. Ownership Interest (stock, stock options, royalty, receipt of intellectual property rights/patent holder, excluding diversified mutual funds); Tenvie Therapeutics. **W. Avery:** A. Employment/Salary (full or part-time):; Tenvie Therapeutics. E. Ownership Interest (stock, stock options, royalty, receipt of intellectual property rights/patent holder, excluding diversified mutual funds); Tenvie Therapeutics. **D. Braun:** A. Employment/Salary (full or part-time):; Tenvie Therapeutics. E. Ownership Interest (stock, stock options, royalty, receipt of intellectual property rights/patent holder, excluding diversified mutual funds); Tenvie Therapeutics. **C. Bucher:** A. Employment/Salary (full or part-time):; Tenvie Therapeutics. E. Ownership Interest (stock, stock options, royalty, receipt of intellectual property rights/patent holder, excluding diversified mutual funds); Tenvie Therapeutics. **M.K. Campbell:** A. Employment/Salary (full or part-time):;

Tenvie Therapeutics. E. Ownership Interest (stock, stock options, royalty, receipt of intellectual property rights/patent holder, excluding diversified mutual funds); Tenvie Therapeutics. **R.A. Craig II:** A. Employment/Salary (full or part-time):; Tenvie Therapeutics. E. Ownership Interest (stock, stock options, royalty, receipt of intellectual property rights/patent holder, excluding diversified mutual funds); Tenvie Therapeutics. **T.Z. Fischer:** A. Employment/Salary (full or part-time):; Tenvie Therapeutics. E. Ownership Interest (stock, stock options, royalty, receipt of intellectual property rights/patent holder, excluding diversified mutual funds); Tenvie Therapeutics. **G.A. Fitzgerald:** A. Employment/Salary (full or part-time):; Tenvie Therapeutics. E. Ownership Interest (stock, stock options, royalty, receipt of intellectual property rights/patent holder, excluding diversified mutual funds); Tenvie Therapeutics. **Y. Hsieh:** A. Employment/Salary (full or part-time):; Tenvie Therapeutics. E. Ownership Interest (stock, stock options, royalty, receipt of intellectual property rights/patent holder, excluding diversified mutual funds); Tenvie Therapeutics. **B. Huffman:** A. Employment/Salary (full or part-time):; Tenvie Therapeutics. E. Ownership Interest (stock, stock options, royalty, receipt of intellectual property rights/patent holder, excluding diversified mutual funds); Tenvie Therapeutics. **L. Ibrahim:** A. Employment/Salary (full or part-time):; Tenvie Therapeutics. E. Ownership Interest (stock, stock options, royalty, receipt of intellectual property rights/patent holder, excluding diversified mutual funds); Tenvie Therapeutics. **K.W. Lexa:** A. Employment/Salary (full or part-time):; Tenvie Therapeutics. E. Ownership Interest (stock, stock options, royalty, receipt of intellectual property rights/patent holder, excluding diversified mutual funds); Tenvie Therapeutics. **A. El-Sherbeni:** A. Employment/Salary (full or part-time):; Tenvie Therapeutics. E. Ownership Interest (stock, stock options, royalty, receipt of intellectual property rights/patent holder, excluding diversified mutual funds); Tenvie Therapeutics. **D.W. Stevens:** A. Employment/Salary (full or part-time):; Tenvie Therapeutics. E. Ownership Interest (stock, stock options, royalty, receipt of intellectual property rights/patent holder, excluding diversified mutual funds); Tenvie Therapeutics. **E.W. Sun:** A. Employment/Salary (full or part-time):; Tenvie Therapeutics. E. Ownership Interest (stock, stock options, royalty, receipt of intellectual property rights/patent holder, excluding diversified mutual funds); Tenvie Therapeutics. **R.H. Takahashi:** A. Employment/Salary (full or part-time):; Tenvie Therapeutics. E. Ownership Interest (stock, stock options, royalty, receipt of intellectual property rights/patent holder, excluding diversified mutual funds); Tenvie Therapeutics. **X. Wang:** A. Employment/Salary (full or part-time):; Tenvie Therapeutics. E. Ownership Interest (stock, stock options, royalty, receipt of intellectual property rights/patent holder, excluding diversified mutual funds); Tenvie Therapeutics. **E. Yulyaningsih:** A. Employment/Salary (full or part-time):; Tenvie Therapeutics. E. Ownership Interest (stock, stock options, royalty, receipt of intellectual property rights/patent holder, excluding diversified mutual funds); Tenvie Therapeutics. **B.M. Fox:** A. Employment/Salary (full or part-time):; Tenvie Therapeutics. E. Ownership Interest (stock, stock options, royalty, receipt of intellectual property rights/patent holder, excluding diversified mutual funds); Tenvie Therapeutics.

**Poster**

**PSTR173: Neuroprotective Mechanisms: Preclinical**

**Location:** WCC Halls A-C

**Time:** Monday, November 16, 2026, 1:00 PM - 5:00 PM

**Program #/Poster #:** PSTR173.19/U8

**Topic:** D.01. Neurotoxicity, Inflammation, and Neuroprotection

**Support:** Investissements d'Avenir" ANR-10-IAIHU-06
ANR grant FLAME
European Union's Horizon 2020 Research and Innovation Program ENDpoiNTs project Grant Agreement number: 825759
Neuratris
ARSEP Cashmere

**Title:** Deleterious consequences of perfluoroalkyl substances exposure on myelin functions

**Authors:** V. VALCÁRCEL HERNÁNDEZ[1], L. BUTRUILLE[2], E. MARTIN[3], C. LUBETZKI[4], B. STANKOFF[5], P. BASSEREAU[6], E. LERAY[7], S. REMAUD[8], ***B. ZALC**[9];
[1]UMR 7221, CNRS-MNHN, paris, France; [2]Museum Natl. d'Histoire Naturelle, Paris, France;, paris, France; [3]Sorbonne University, Paris Brain Inst. (ICM), Paris, France;, Paris, France; [4]Sorbonne University, Inserm, CNRS, ICM, Paris Cedex 13, France, paris, France; [5]Paris Brain Inst., orbonne University, Inserm, CNRS, ICM, Paris Cedex 13, France, Paris, France; [6]Inst. Curie, paris, France; [7]Inserm U1309 Hlth. services and management, CS 74312, Rennes France., Rennes, France; [8]CNRS MNHN 7221, PARIS, France; [9]Sorbonne University, Inserm, CNRS, ICM, Paris Cedex 13, France

**Abstract:** Although the cause of MS is not known, it is believed that MS is triggered by a combination of factors among which environmental factors contribute to the risk of developing the disease. An unexplained increasing prevalence and incidence of cases of MS occurred over the last part of the XXth century, relatesd to an increase in environmental risk factors.Perfluoroalkyl substances (PFAS) are bioaccumulative pollutants crossing placental and blood-brain barriers, exposing foetal and neonatal brains. As myelin is lipid-rich and a potential PFAS sink, early exposure may impair white-matter integrity and behaviours relevant to MS. We investigated whether exposure to legacy PFAS, perfluorooctanoic acid (PFOA) and perfluorooctane sulfonate (PFOS), affects myelin sheath stability and functionality.(1) Conditional demyelination was induced in Xenopus laevis Tg(*mbp:GFP-NTR*) tadpoles exposed to PFAS during remyelination, assessing sensory-motor consequences. (2) Mouse cerebellar slice cultures were demyelinated with lysolecithin and treated with PFAS +/- thyroid hormone (TH). (3) Following exposure in drinking water of dams during late gestation and lactation PFAS were detected in myelin of offsprings at 3 weeks and 3 months. (4) Resistance to tension and lysis tension of myelin-lipids giant unilamellar vesicles (GUVs) was assessed following PFAS exposure. (5) Spatial epidemiology examined links between geographic PFAS exposure and MS prevalence and incidence.PFOS, but not PFOA, inhibited functional remyelination in Xenopus. Similarly, remyelination of mouse cerebellar slices was reduced following PFOS exposure. This inhibition was rescued by TH co-treatment, suggesting TH-sensitive pathways. Perinatal PFOS administration during lactation accumulated in myelin of 3-week-old offspring and thinner myelin sheath and axonal damages were observed at 3-month. GUV assays demonstrated PFOS-driven alterations in myelin biophysical properties, consistent with myelin destabilization. Our findings show that PFOS acts as a myelin-targeting developmental neurotoxicant that damages myelin sheath stability and functionality. This is linked to TH-responsive remyelination and myelin-lipid perturbation. Our data highlight the relevance of PFAS exposure as a potential modifier of MS risk.

**Disclosures: V. Valcárcel Hernández:** None. **L. Butruille:** None. **E. Martin:** None. **C. Lubetzki:** None. **B. Stankoff:** None. **P. Bassereau:** None. **E. Leray:** None. **S. Remaud:** None. **B. Zalc:** None.

**Poster**

**PSTR173: Neuroprotective Mechanisms: Preclinical**

**Location:** WCC Halls A-C

**Time:** Monday, November 16, 2026, 1:00 PM - 5:00 PM

**Program #/Poster #:** PSTR173.20/U9

**Topic:** D.01. Neurotoxicity, Inflammation, and Neuroprotection

**Support:** Huffington Foundation
Freedom Together Foundation
Howard Hughes Medical Institute
NICHD-U54HD083092

**Title:** Astrocytic ACSBG1 depletion improves lipid-cytokine signaling and attenuates α-Synuclein pathology in a Parkinson's disease mouse model

**Authors: *Y. KIM**[1], B. VAIDYA[1], J. KIM[1], S. BITAR[1], H. Y. ZOGHBI[2];
[1]Baylor Col. of Med., Houston, TX; [2]Mol. and Human Genet., Baylor Col. of Medicine/HHMI, Houston, TX

**Abstract:** Astrocytes are key regulators of lipid metabolism, and dysregulated astrocytic lipid processing is implicated in Parkinson's disease (PD) pathogenesis. Our prior genome-wide screens identified ACSBG1, an astrocyte-enriched acyl-CoA synthetase, as a candidate regulator of α-synuclein (α-Syn) levels. However, how ACSBG1 links lipid reprogramming to inflammatory astrocyte activation and α-Syn pathology remains unknown. We compared the transcriptomic, cytokine, and lipid secretomes of TNF-α and IL-1α stimulated primary astrocytes from wild-type (WT) and *Acsbg1* knockout (KO) mice. In vivo, we crossed Acsbg1 KO mice with a Thy1-α-Syn PD model to assess behavior, neuroinflammation, synaptic integrity, and α-Syn levels. Following cytokine exposure, *Acsbg1* KO astrocytes mounted an attenuated inflammatory transcriptional response, secreting significantly fewer inflammatory mediators (e.g., IL-6, RANTES, MIP-3α) and less long-chain Sphingosine 20:1 than WT astrocytes. Importantly, exogenous Sphingosine 20:1 or cytokines from WT reactive astrocytes induced neuronal α-Syn phosphorylation (pS129). *In vivo*, *Acsbg1* deletion in Thy1-α-Syn mice reduced astrogliosis, rescued synaptic and behavioral deficits, and decreased total and pS129-α-Syn. These findings establish ACSBG1 as a key regulator of inflammatory astrocyte signaling that contributes to α-Syn phosphorylation via specific cytokine and lipid mediators, identifying ACSBG1 as a novel therapeutic target for modulating astrocyte-neuron communication in PD.

**Disclosures: Y. Kim:** None. **B. Vaidya:** None. **J. Kim:** None. **S. Bitar:** None. **H.Y. Zoghbi:** E. Ownership Interest (stock, stock options, royalty, receipt of intellectual property rights/patent holder, excluding diversified mutual funds); H.Y.Z. cofounded Cajal Therapeutics. F. Consulting

Fees (e.g., advisory boards); H.Y.Z. is a Director of Regeneron Pharmaceuticals board, and is on the scientific advisory board of Cajal Therapeutics, Lyterian Therapeutics, and the Column Group..

**Poster**

**PSTR173: Neuroprotective Mechanisms: Preclinical**

**Location:** WCC Halls A-C

**Time:** Monday, November 16, 2026, 1:00 PM - 5:00 PM

**Program #/Poster #:** PSTR173.21/U10

**Topic:** D.01. Neurotoxicity, Inflammation, and Neuroprotection

**Support:** Robert J. and Nancy D. Carney Endowment
Blackman Family Fund for MS
R25NS080686

**Title:** Myelin locally suppresses SARM1 activation along optic nerve axons

**Authors: *S. R. MAYORAL**[1], M. MCQUILLAN[1], V. F. YI[1], S. RIOS MENDEZ[1], G. M. MOLICA[1], C. STEIN[2], S. R. FREGOSO[1], L.-A. HASSELL[1], I. HERNANDEZ RIVERA[1], S. E. RAISSI[3], A. J. GREEN[3], C. CORDANO[3], Y. SASAKI[4];
[1]Brown Univ., Providence, RI; [2]Psychology, Hunter College, CUNY, New York, NY; [3]Neurol., UCSF, San Francisco, CA; [4]Genet., Washington Univ. St. Louis, Saint Louis, MO

**Abstract:** Myelin, a lipid-rich sheath that insulates axons, is thought to be neuroprotective, though the mechanisms underlying this protection remain unclear. To directly address this, we developed a mouse model where myelin is spatially restricted to the posterior optic nerve (ON), leaving the anterior region completely unmyelinated. After ON transection, we observed accelerated Wallerian degeneration (WD) in unmyelinated regions of the nerves compared to myelinated regions both 3- and 6-days post injury. This accelerated WD was not mediated by microglia since their ablation did not affect degeneration. While proteomics of unmyelinated ON regions showed no obvious differences in degeneration-related targets compared to myelinated regions, metabolomics revealed distinct changes linked to SARM1-mediated degeneration. Importantly, in mice with partially myelinated ONs but also lacking SARM1, degeneration was no longer accelerated, suggesting that myelin protects axons from degeneration by suppressing SARM1 activity. These findings reveal a new link between myelin and SARM1-mediated degeneration and provide insight into local axonal protection mechanisms that may guide future therapies for neurodegenerative diseases.

**Disclosures: S.R. Mayoral:** None. **M. McQuillan:** None. **V.F. Yi:** None. **S. Rios Mendez:** None. **G.M. Molica:** None. **C. Stein:** None. **S.R. Fregoso:** None. **L. Hassell:** None. **I. Hernandez Rivera:** None. **S.E. Raissi:** None. **A.J. Green:** None. **C. Cordano:** None. **Y. Sasaki:** None.

**Poster**

**PSTR173: Neuroprotective Mechanisms: Preclinical**

**Location:** WCC Halls A-C

**Time:** Monday, November 16, 2026, 1:00 PM - 5:00 PM

**Program #/Poster #:** PSTR173.22/U11

**Topic:** D.01. Neurotoxicity, Inflammation, and Neuroprotection

**Support:** 1R01CA215973
R41CA261451
BFA-2023-01

**Title:** Paclitaxel neurotoxicity is triggered by epidermal EG5 dependent microtubule fasciculation and X-ROS formation

**Authors: *S. RIEGER**;
Univ. of Miami, Coral Gables, FL

**Abstract:** Chemotherapy-induced peripheral neuropathy (CIPN) is a common dose-limiting toxicity of paclitaxel treatment, yet the cellular mechanisms initiating axon degeneration remain incompletely understood. We previously identified epidermal matrix metalloproteinase-13 (MMP-13) activation as a key contributor to sensory axon degeneration. Here, we investigated the upstream mechanisms linking paclitaxel exposure to epidermal oxidative stress and neurotoxicity.Using transgenic zebrafish and live imaging approaches, we examined the effects of paclitaxel on epidermal microtubule organization and reactive oxygen species (ROS) formation. Paclitaxel induced pronounced epidermal microtubule fasciculation characterized by increased detyrosinated microtubule bundles. Fasciculation was accompanied by nuclear deformation, elevated hydrogen peroxide production, and induction of mmp13 expression. Pharmacological inhibition of the kinesin motor EG5/KIF11 using EMD534085, ispinesib, or monastrol prevented microtubule fasciculation, suppressed ROS formation, and blocked MMP-13 upregulation. Genetic disruption of kif11 similarly reduced epidermal oxidative stress and protected sensory axons from degeneration.*In vivo* imaging demonstrated that EG5 inhibition preserved epidermal integrity and prevented degeneration of cutaneous sensory axons following paclitaxel exposure. Conversely, constitutive disruption of kif11 produced developmental abnormalities in sensory axons, indicating an important role for EG5 in regulating microtubule organization during nervous system development. Together, these findings support a model in which EG5-dependent microtubule remodeling in epidermal cells initiates a cascade of oxidative stress signaling that promotes sensory axon degeneration.These findings identify a previously unrecognized epidermal mechanism in which paclitaxel promotes EG5-dependent microtubule fasciculation, leading to ROS generation, MMP-13 activation, and sensory axon degeneration. The results establish EG5 as an upstream regulator of epithelial stress responses and reveal a critical role for epidermal microtubule organization in the pathogenesis of CIPN.

**Disclosures: S. Rieger:** E. Ownership Interest (stock, stock options, royalty, receipt of intellectual property rights/patent holder, excluding diversified mutual funds); Avantyx.

**Poster**

**PSTR174: Microglia in Alzheimer's Disease**

**Location:** WCC Halls A-C

**Time:** Monday, November 16, 2026, 1:00 PM - 5:00 PM

**Program #/Poster #:** PSTR174.01/U12

**Topic:** C.02. Alzheimer's Disease and Other Dementias

**Support:** NIH RF1 AG078299
NIH R01 AG084624
NIH R01 AG083941

**Title:** MicroRNA-223 Restores Synaptic Markers and Promotes Microglial-Mediated Clearance of Beta Amyloid in AppNL-G-F Alzheimer's Disease Model Mice

**Authors: *A. KRUNIC**[1], N. UMESH GANESH[1], M. KURKELA[2], T. TAY[3], J. TCW[6], A. FISCHER[8], I. DELALLE[4], J. K. BLUSZTAJN[5], T. J. MELLOTT[7];
[2]Chobanian & Avedisian Sch. of Med., [3]Dept. of Biol., [4]Pathology, [5]Dept Pathol, [1]Boston Univ., Boston, MA; [7]Pathology & Lab. Med., [6]Boston Univ. Chobanian & Avedisian Sch. of Med., Boston, MA; [8]German Ctr. For Neurodegenerative Dis., Goettingen, Germany

**Abstract:** The Alzheimer's disease (AD) brain is characterized by dysregulated expression of multiple microRNAs (miRNA), positioning them as promising diagnostic and therapeutic targets. The levels of glia-enriched miR-223 are altered in the brains and plasma of AD patients and is neuroprotective in models of stroke. We have previously found that intracerebroventricular injection of miR-223 in $App^{NL-G-F}$ AD model mice rescued cognitive impairment and reduced amyloid beta (Aβ) pathology. However, the mechanisms underlying these protective actions of miR-223 are not known. We performed multiplexed immunohistochemistry on 7-month-old wild type and $App^{NL-G-F}$ mice treated with miR-223 mimic or scramble control to assess its effects on Aβ pathology and levels of synaptic markers. We also performed immunofluorescence staining to assess microglial morphology and used western blotting to quantify the expression of inflammatory proteins. We found that miR-223 increases microglial clustering around plaques while promoting a ramified morphology away from plaques, accompanied by a downregulation in levels of inflammasome marker ASC. Moreover, we found that miR-223 promoted microglial phagocytosis and upregulated expression of CD11c both in vivo and in primary microglia culture. Pharmacological microglia depletion via the CSF1R inhibitor PLX5622 ablated miR-223-mediated clearance of Aβ pathology, demonstrating that microglia are necessary for miR-223-mediated enhanced plaque clearance. Additionally, miR-223 significantly reduced LAMP1-positive dystrophic neurite staining in the cerebral cortex and hippocampus, and upregulated synaptic and neuronal markers such as SYP and MAP2. Moreover, we found that miR-223-mediated rescue of synaptic markers was partially independent of Aβ clearance, suggesting a direct protective action of miR-223 on neurons. Overall, we found that miR-223 enhanced microglial clearance of Aβ pathology and ameliorated neuronal injury, and thus holds promise as a therapeutic agent for AD.

**Disclosures: A. Krunic:** None. **N. Umesh Ganesh:** None. **M. Kurkela:** None. **T. Tay:** None. **J. Tcw:** None. **A. Fischer:** None. **I. Delalle:** None. **J.K. Blusztajn:** None. **T.J. Mellott:** None.

**Poster**

**PSTR174: Microglia in Alzheimer's Disease**

**Location:** WCC Halls A-C

**Time:** Monday, November 16, 2026, 1:00 PM - 5:00 PM

**Program #/Poster #:** PSTR174.02/U13

**Topic:** C.02. Alzheimer's Disease and Other Dementias

**Support:** R01AG068330
R01AG093847
BrightFocus A20201775S
CART Fund
Cure Alzheimer's Fund
P30GM127211

**Title:** Microglia contribute to metabolic and sleep dysregulation in an APP/PS1 model of Alzheimer's Disease

**Authors: *A. JACOBS**[1,2], N. J. CONSTANTINO[3], C. ASHLEY[1], A. SNIPES[2], S. L. MACAULEY[2];
[2]Physiol., [3]Neurosci., [1]Univ. of Kentucky, Lexington, KY

**Abstract:** Alzheimer's disease (AD) is a neurodegenerative disease characterized by amyloid plaques, neurofibrillary tangles, neurodegeneration, and profound disturbances in both brain metabolism and sleep. Both AD patients and amyloid (APP/PS1) mouse models exhibit a shift toward glycolytic metabolism at the expense of oxidative metabolism. These metabolic changes are accompanied by elevated brain interstitial fluid (ISF) lactate in APP/PS1 mice and increased markers of lactate production in humans. Recent studies suggest that microglia undergo glycolytic reprogramming in the plaque microenvironment and may contribute to altered lactate metabolism. Because lactate is a key regulator of sleep/wake state transitions, dysregulated lactate metabolism may link metabolic dysfunction and sleep disruption in AD. To investigate the role of microglia on AD-related pathology, metabolism, and sleep, 9 month APP/PS1 mice were treated with the CSF1R inhibitor, PLX3397, to deplete microglia. PLX3397 treatment reduced cortical microglial abundance, decreasing Iba1+ microglia by 89%, Tmem119+ microglia by 99%, and Clec7A+ microglia by 44% ($p<0.05$). Microglial depletion reduced brain ISF lactate levels by approximately 50% and altered lactate dehydrogenase (LDH) isoenzyme expression. There was a decrease in LDH5 abundance ($p<0.0001$) and a resulting increase in LDH3 abundance, consistent with a shift away from a lactate-producing metabolic profile and toward greater metabolic flexibility. In addition, PLX3397 treatment increased total daily sleep time by approximately 45 minutes compared to untreated APP/PS1 mice ($p<0.05$). Ongoing studies using single-nucleus transcriptomics, 13C-glucose stable isotope-resolved metabolomics, and mitochondrial profiling will further determine how amyloid pathology alters brain metabolism in the presence and absence of microglia. These results highlight microglial metabolism as a potential therapeutic target in AD.

**Disclosures: A. Jacobs:** None. **N.J. Constantino:** None. **C. Ashley:** None. **A. Snipes:** None. **S.L. Macauley:** None.

**Poster**

**PSTR174: Microglia in Alzheimer's Disease**

**Location:** WCC Halls A-C

**Time:** Monday, November 16, 2026, 1:00 PM - 5:00 PM

**Program #/Poster #:** PSTR174.03/U14

**Topic:** C.02. Alzheimer's Disease and Other Dementias

**Support:** NIH R01AG097537 to AF
NIH R21AG082230 to AF
Alzheimer's Association AARF22973974
JSME funding bridge to AF
MBHI I-DID pilot grant to AF
R21AG089708 to GT
R01AG073133 to GT

**Title:** Protective microglial activation and autophagy induced by brain-derived tau oligomers from resilient Alzheimer's disease cases

**Authors:** J. GUPTARAK[1], B. TUMURBAATAR[1], T. NGUYEN[1], M. MARCATTI[1], W.-R. ZHANG[2], A. TRUPP[1], M.-A. MICCI[1,2], G. TAGLIALATELA[1,2], ***A. FRACASSI**[1,2]; [1]Univ. of Texas Med. Br., Galveston, TX; [2]Moody Brain Hlth. Inst. UTMB, Galveston, TX

**Abstract:** A subset of individuals harbors extensive Alzheimer's disease (AD) neuropathology while maintaining normal cognitive function throughout life. These resilient subjects, commonly referred to as Non-Demented with Alzheimer's Neuropathology (NDAN), provide a unique opportunity to identify mechanisms that counteract neurodegeneration. Because soluble tau aggregates are strongly associated with synaptic dysfunction and memory impairment, we investigated whether brain-derived tau oligomers (BDTO) isolated from NDAN brains elicit distinct biological responses compared with BDTO from cognitively impaired AD cases. Tau oligomers were isolated from postmortem AD and NDAN brains using immunoprecipitation-based approaches. Following biochemical characterization, BDTO were administered by intracerebroventricular injection into wild-type mice. Molecular markers of autophagy, oxidative stress, and microglial activation were evaluated together with behavioral outcomes at acute time points following exposure. Exposure to NDAN-BDTO promoted a coordinated protective response characterized by increased expression of autophagy-related proteins, including Beclin-1, ATG family members, and LC3-II. In parallel, antioxidant defenses were enhanced, as evidenced by elevated SOD1, SOD2, and catalase levels and reduced accumulation of oxidative DNA damage. NDAN BDTO also induced a microglial phenotype associated with phagocytic functions, including increased CD68 and TREM2 expression. These molecular changes were accompanied by preserved cognitive performance in the novel object recognition test, whereas mice exposed to AD BDTO exhibited impaired memory. Our findings demonstrate that tau

oligomers isolated from cognitively resilient individuals engage adaptive cellular programs rather than triggering neurotoxic cascades. Activation of autophagy, reinforcement of antioxidant pathways, and induction of beneficial microglial responses may contribute to resistance against cognitive decline despite AD pathology. Understanding the biological properties of resilience-associated tau species may reveal novel therapeutic strategies aimed at promoting brain resilience in AD.

**Disclosures: J. Guptarak:** None. **B. Tumurbaatar:** None. **T. Nguyen:** None. **M. Marcatti:** None. **W. Zhang:** None. **A. Trupp:** None. **M. Micci:** None. **G. Taglialatela:** None. **A. Fracassi:** None.

**Poster**

**PSTR174: Microglia in Alzheimer's Disease**

**Location:** WCC Halls A-C

**Time:** Monday, November 16, 2026, 1:00 PM - 5:00 PM

**Program #/Poster #:** PSTR174.04/U15

**Topic:** C.02. Alzheimer's Disease and Other Dementias

**Support:** Alzheimer's Association Research Fellowship 24AARF-1241864
Edythe M. Laudati Memorial Fund

**Title:** Microglial C1q Supports Memory Before Downstream Complement Activation in Alzheimer's Disease Mouse Model

**Authors: *T. J. PETRISKO**, S.-H. CHU, A. J. TENNER;
UC Irvine, Irvine, CA

**Abstract:** C1q, the initiating protein of the classical complement pathway, has been implicated in both neuroprotective and pathogenic processes in Alzheimer’s disease (AD), yet the factors governing these divergent effects remain unclear. While complement expression has been largely characterized in transgenic AD mouse models, its temporal regulation in humanized knock-in models has not been well defined. We therefore characterized complement expression in the SAA mouse model and examined the effects of stage-specific deletion of microglial C1q on cognitive function during amyloid progression In aging SAA mice, ThioS-positive fibrillar amyloid beta (fAβ) deposition began in the cortex by 6 months and hippocampus by 9 months of age. Notably, hippocampal C1q protein accumulation was evident by 6 months, preceding substantial local fAβ deposition, whereas cortical C1q accumulation was not observed until 13 months despite earlier plaque formation. qPCR analyses revealed increased C1q and C4 expression by 9 months, followed by increased C3 expression at 13 months. C1r expression exhibited a modest age-associated increase. To determine how the timing of C1q loss influences disease outcomes, microglial C1q was deleted either prior to fAβ formation (3 months) or following established pathology (9 months) using inducible $C1qa^{FL/FL}$ and SAA $C1qa^{FL/FL}$ mice with and without $Tmem119Cre^{ERT2}$ . Memory was assessed at 8 and 13 months using object location memory (OLM) and contextual fear conditioning (CFC). At 8 months, SAA mice

exhibited no deficits in OLM or CFC performance; however, pre-plaque microglial C1q deletion reduced OLM discrimination indices and CFC freezing behavior in SAA mice, consistent with an early neuroprotective role for C1q. By 13 months, SAA mice dispalyed memory deficits in OLM and CFC performance that were attenuated by early, but not late, C1q deletion. Together, these findings demonstrate that C1q supports memory early in disease but contributes to later cognitive decline, consistent with early hippocampal C1q accumulation and later C3 induction. These findings suggest a transition from protective, complement-independent C1q signaling to downstream complement activation associated with cognitive decline and identify a stage-dependent therapeutic window for complement-targeted intervention in AD.

**Disclosures: T.J. Petrisko:** None. **S. Chu:** None. **A.J. Tenner:** None.

**Poster**

**PSTR174: Microglia in Alzheimer's Disease**

**Location:** WCC Halls A-C

**Time:** Monday, November 16, 2026, 1:00 PM - 5:00 PM

**Program #/Poster #:** PSTR174.05/U16

**Topic:** C.02. Alzheimer's Disease and Other Dementias

**Title:** PLCG2-P522R, a microglia expressed gene associated with reduced Alzheimer’s risk, suppresses type-1 interferon signaling and prevents amyloid-beta induced mitochondrial injury.

**Authors: *A. SRIRAM**[1], V. A. MADORMO[2], M. P. SADGROVE[2], G. A. GARDEN[2]; [1]Neurosci., Perelman Sch. of Med. at the Univ. of Pennsylvania, Philadelphia, PA; [2]Neurol., Univ. of North Carolina at Chapel Hill Sch. of Med., Chapel Hill, NC

**Abstract:** Genome-wide association studies identified variants in phospholipase Cγ2 (PLCγ2) that influence AD risk. One such variant, P522R, provides robust protection against Alzheimer’s disease (AD) and other neurodegenerative diseases. How PLCγ2 (P522R) confers protection against AD is not fully understood. PLCγ2 is predominantly expressed in the brain by microglia. Microglia are the innate immune cells of the brain and exhibit both protective and pathogenic responses to AD associated proteins such as amyloid beta (Aβ). Aβ influences microglia metabolism and innate immune signaling. PLCγ2 signaling impacts several of the reported metabolic and signaling changes induced by Aβ exposure. PLCγ2 is hypothesized to serve as a central regulator of microglial immune and metabolic responses downstream of disease-associated receptors. We hypothesize that the protective variant, PLCγ2 (P522R), alters these changes in metabolism and immune signaling. To test our hypothesis, we performed RNA sequencing on primary mouse microglia expressing either PLCγ2 (P522R) or PLCγ2 (WT) under Aβ-exposed and unexposed conditions to assess differences in the transcriptional response to Aβ. We observed that PLCγ2 (WT) microglia activate a type 1 interferon transcriptional program and S100 family signaling axis in response to Aβ. However, PLCγ2 (P522R) microglia exposed to Aβ do not activate these responses. In contrast, PLCγ2 (P522R) primary mouse microglia had increased expression of oxidative phosphorylation and fatty acid metabolism pathways. Based on the altered transcriptomic responses, we hypothesized that PLCγ2 (P522R) microglia may be

protected from Aβ-induced mitochondrial damage and loss of mitochondrial membrane potential (ΔΨm). To test this hypothesis, we measured ΔΨm in live primary mouse microglia exposed to Aβ. These experiments demonstrated that PLCγ2 (P522R) microglia maintain ΔΨm across all concentrations of Aβ compared to their PLCγ2 (WT) counterparts. Taken together, these results suggest that PLCγ2 (P522R) microglia are resistant to mitochondria damage and suppress innate immune signaling programs following Aβ exposure. This study supports PLCγ2 signaling as a promising therapeutic target to address multiple features of AD pathology.

**Disclosures: A. Sriram:** None. **V.A. Madormo:** None. **M.P. Sadgrove:** None. **G.A. Garden:** None.

**Poster**

**PSTR174: Microglia in Alzheimer's Disease**

**Location:** WCC Halls A-C

**Time:** Monday, November 16, 2026, 1:00 PM - 5:00 PM

**Program #/Poster #:** PSTR174.06/U17

**Topic:** C.02. Alzheimer's Disease and Other Dementias

**Title:** Enrupatinib Selectively Modulates Neuroinflammatory Microglia, Rescues Neuronal Integrity, and Restores Cognitive Function in Alzheimer’s Disease Mouse Models

**Authors:** W. TAMAYANTI[1], Y.-N. CHANG[1], A. ARIYANTI[1], J.-R. LIN[1], C.-W. HUANG[3], T. HSIEH[1], H. HSIAO[3], H.-Y. CHENG[1], I. HUANG[1], H. ZHAO[1], S. SETIAWAN[4], H.-C. HUANG[1], A. BUEHLER[5], I. H. CHENG[1], H.-T. LEE[2], C.-Y. PAI[3], H.-K. CHEN[3], ***J.-W. TSAI**[1];
[1]Inst. of Brain Sci., [2]Inst. of Anat. and Cell Biol., Natl. Yang Ming Chiao Tung Univ., Taipei, Taiwan; [3]Elixiron Immunotherapeutics Inc., Taipei, Taiwan; [4]Intrnl. Med. Dept., Dr Sardjito Hosp., Yogyakarta, Indonesia; [5]Carle Illinois Col. of Med., Univ. of Illinois Urbana-Champaign, Urbana, IL

**Abstract:** Chronic neuroinflammation driven by activated microglia is a hallmark of Alzheimer's disease (AD) that amplifies synaptic damage, neuronal loss, and cognitive decline. To target this pathological process, we orally administered Enrupatinib (EI-1071), a novel, brain-penetrant, and highly selective CSF1R kinase inhibitor, to 5xFAD and J20 transgenic mice for 4 weeks. Behavioral assessments using the Novel Object Recognition (NOR) test demonstrated that Enrupatinib significantly alleviated cognitive impairments in both AD models, markedly increasing discrimination indices. Pathological analyses revealed that Enrupatinib preferentially eliminated plaque-associated (periplaque) microglia over homeostatic, distal populations in a dose-dependent manner, without increasing overall amyloid plaque burden, suggesting selective microglial modulation rather than broad microglial depletion. To visualize neuronal vulnerability to plaque-associated damage at single-cell resolution, we fluorescently labeled cortical neurons with EGFP via in utero electroporation. Confocal imaging demonstrated that Enrupatinib robustly rescued these neurons from plaque-induced membrane rupture, cytoplasmic fragmentation, and cell death observed in untreated AD mice. To elucidate the underlying

molecular mechanisms, we performed bulk RNA-seq, scRNA-seq, and qPCR profiling, revealing profound downregulation of pro-inflammatory pathways and disease-associated microglia (DAM) gene networks, including Trem2, Apoe, Tyrobp, Cst7, and Clec7a. Diffusion pseudotime trajectory analyses further demonstrated that Enrupatinib did not cause uniform microglial depletion but instead shifted cells away from terminal, highly cytotoxic activation states toward less inflammatory early states. Together, these findings establish Enrupatinib as a brain-penetrant CSF1R inhibitor capable of suppressing pathological neuroinflammation, preserving neuronal integrity, and restoring cognitive function through precision remodeling of disease-associated microglia, providing compelling preclinical rationale for its clinical development as a disease-modifying therapy for AD.

**Disclosures: W. Tamayanti:** None. **Y. Chang:** None. **A. Ariyanti:** None. **J. Lin:** None. **C. Huang:** A. Employment/Salary (full or part-time):; Elixiron Immunotherapeutics Inc.. **T. Hsieh:** None. **H. Hsiao:** A. Employment/Salary (full or part-time):; Elixiron Immunotherapeutics Inc.. **H. Cheng:** None. **I. Huang:** None. **H. Zhao:** None. **S. Setiawan:** None. **H. Huang:** None. **A. Buehler:** None. **I.H. Cheng:** None. **H. Lee:** None. **C. Pai:** A. Employment/Salary (full or part-time):; Elixiron Immunotherapeutics Inc. **H. Chen:** A. Employment/Salary (full or part-time):; Elixiron Immunotherapeutics Inc. **J. Tsai:** B. Contracted Research/Research Grant (principal investigator for a drug study, collaborator or consultant and pending and current grants). If you are a PI for a drug study, report that research relationship even if those funds come to an institution.; Elixiron Immunotherapeutics Inc.. E. Ownership Interest (stock, stock options, royalty, receipt of intellectual property rights/patent holder, excluding diversified mutual funds); Elixiron Immunotherapeutics Inc.. F. Consulting Fees (e.g., advisory boards); Elixiron Immunotherapeutics Inc..

**Poster**

**PSTR174: Microglia in Alzheimer's Disease**

**Location:** WCC Halls A-C

**Time:** Monday, November 16, 2026, 1:00 PM - 5:00 PM

**Program #/Poster #:** PSTR174.07/U18

**Topic:** C.02. Alzheimer's Disease and Other Dementias

**Support:** NIH Grant 1R01NS091519

**Title:** Trem2 negatively contributes to CSF-1 receptor related leukoencephalopathy in the Csf1r heterozygous mouse model

**Authors:** V. CHITU[1], J. ALVARENGA[2], J. AGUILAN[3], S. SIDOLI[4], ***E. STANLEY**[1]; [1]Developmental and Mol. Biol., Albert Einstein Col. of Med., Bronx, NY; [2]Developmental and Mol. Biol., Albert Einstein Col. of Med., The Bronx, NY; [3]Pathology, Albert Einstein Col. of Med., Bronx, NY; [4]Biochem., Albert Einstein Col. of Med., The Bronx, NY

**Abstract:** Colony stimulating factor-1 receptor (CSF-1R)-related leukoencephalopathy (CRL) is a primary microgliopathy that triggers demyelination and neuronal loss leading to adult-onset

dementia. Triggering receptor expressed on myeloid cells-2 (TREM2) is a microglial receptor that promotes the phagocytic clearance of apoptotic neurons and myelin debris by microglia and mediates gene expression changes that drive their transition to various dyshomeostatic states. In the *Csf1r*$^{+/-}$ mouse model of CRL, we have shown that elevation of *Trem2* expression and callosal demyelination occur prior to the development of symptoms, at 4-5-months of age. *Trem2* deficiency attenuated myelin pathology, normalized callosal microglial densities and morphology, prevented axonal degeneration, the loss of cortical layer V neurons, the accumulation of myelin-derived lipids in *Csf1r*$^{+/-}$macrophages and reduced the production of TNF-alpha after myelin engulfment (Biundo et al ., *Biomedicines.* 2023;11(8)). These results suggested that TREM2 contributes to microglial dyshomeostasis in CRL. In the present study, we have examined the long-term consequences of *Trem2* deficiency in the mouse model. In aged *Csf1r*$^{+/-}$ mice, *Trem2* deficiency alleviated cognitive, brain connectivity and motor coordination deficits. These effects were associated with decreased microglial activation, evidenced by decreased synapse engulfment and reduced microglial secreted phosphoprotein 1 (SPP1, osteopontin) expression. Reduction in the levels of complement proteins and markers of oligodendrocyte and neuronal damage in the cerebrospinal fluid (CSF) further indicated that *Trem2* deficiency ameliorated brain pathology. Both these animal studies indicate that endogenous TREM2 activation contributes negatively to disease progression in CRL. They are consistent with recent reports of microglial and peripheral macrophage activation, following administration of TREM2 agonists in patients with CRL and Alzheimer's disease which, together with the lack of beneficial effects, led to the discontinuation of Phase 2 clinical trials.

**Disclosures: V. Chitu:** None. **J. Alvarenga:** None. **J. Aguilan:** None. **S. Sidoli:** None. **E. Stanley:** None.

**Poster**

**PSTR174: Microglia in Alzheimer's Disease**

**Location:** WCC Halls A-C

**Time:** Monday, November 16, 2026, 1:00 PM - 5:00 PM

**Program #/Poster #:** PSTR174.08/U19

**Topic:** C.02. Alzheimer's Disease and Other Dementias

**Support:** NIA R01 AG078761
NIAID T32 AI007363-31A1

**Title:** Microglial remodeling and sustained activation induced by repeated brain resident memory T cell reactivation leads to altered pathology in the 5xFAD mouse model of Alzheimer's disease

**Authors: *T. CHEN**[1], H. N. DEGEFU[1], S. A. KLEIST[1], C. GONZALEZ CRUZ[2], A. CRUZ RIVERA[1], S. MUSIAL[1], A. SKORPUT[3], P. C. ROSATO[1];
[1]Microbiology and Immunol., [2]Integrative Neurosci. Dept., Dartmouth Col., Lebanon, NH; [3]Neurol., Dartmouth, Lebanon, NH

**Abstract:** Microglia, key mediators of Alzheimer's disease (AD) pathogenesis, respond to amyloid-beta (Aβ) plaques, a hallmark of AD pathology, and can contribute to Aβ clearance through phagocytosis. However, chronic or dysregulated microglial activation may also promote neuroinflammation and neurodegeneration. Recently, chronic viral infections, such as herpes simplex virus and cytomegalovirus, have been linked to increased risk of developing AD. CD8+ T cells are largely responsible for responding and clearing virally infected cells and have increased numbers in the brains of AD patients and mouse models. CD8+ T cell depletion in 5xFAD AD-model mice of Aβ pathology results in exacerbated pathology, suggesting a protective role. The majority of CD8+ T cells in human AD brains are resident memory T cells ($T_{RM}$), a subset of memory T cells that persist in lymphoid and non-lymphoid tissues and are poised to protect against reinfection. As chronic viruses move in and out of latency, $T_{RM}$ will also reactivate when they encounter their specific viral peptide antigen. Importantly, $T_{RM}$ reactivation in the healthy brain induces transient activation and recruitment of local immune cells, including microglia. As such, we sought to test the impact of brain $T_{RM}$ ($bT_{RM}$) recall functions on AD pathology by taking a reductionist approach to modeling $bT_{RM}$ reactivation in response to recurrent viral infection or reactivations from latency. To reactivate $bT_{RM}$, we introduced the viral peptide they are specific for intracranially three times, one month apart. Consistent with cell proliferation, we saw a significant increase in $bT_{RM}$ numbers in both 5xFAD and littermate control mice. Intriguingly, we observed sustained microglial activation as indicated by elevated MHCII expression over one month after the last $bT_{RM}$ reactivation in 5xFAD mice. These resulting microglia are a unique subset that arise in response to $bT_{RM}$ reactivation, upregulating high levels of activation and antigen-presenting genes such as H2-Ab1, H2-Eb1, and most notably Cd74, which has implications in AD. Strikingly, we observe changes in Aβ plaque size and numbers in the cortex and hippocampus of $bT_{RM}$ reactivated 5xFAD mice, and an increase in disease-associated microglia after aging. Subsequently, we note amelioration of behavioral deficits, as $bT_{RM}$ reactivated 5xFAD mice but not control 5xFAD mice habituated to the open field similarly to wildtype mice after consecutive days of testing. This data reveals unique microglial remodeling driven by repeated $bT_{RM}$ reactivation, suggesting an inflammatory and protective role of $bT_{RM}$ in AD, providing insight into neuroimmune crosstalk for guiding future AD immunotherapies.

**Disclosures: T. Chen:** None. **H.N. Degefu:** None. **S.A. Kleist:** None. **C. Gonzalez Cruz:** None. **A. Cruz Rivera:** None. **S. Musial:** None. **A. Skorput:** None. **P.C. Rosato:** None.

**Poster**

**PSTR174: Microglia in Alzheimer's Disease**

**Location:** WCC Halls A-C

**Time:** Monday, November 16, 2026, 1:00 PM - 5:00 PM

**Program #/Poster #:** PSTR174.09/U20

**Topic:** C.02. Alzheimer's Disease and Other Dementias

**Title:** Mitochondrial Complex II-Complex I Reverse Electron Transport Drives Aβ-Induced Microglial Immunometabolic Dysfunction.

**Authors: *J. MCWHIRT**, C. A. MARTINEZ, P. DA SILVA FROST, J. H. LEDO; Neurosci., Med. Univ. of South Carolina, Charleston, SC

**Abstract:** In Alzheimer's disease (AD), microglia initially help limit pathology by clearing amyloid-β (Aβ) and cell debris but later adopt chronically activated, exhausted states that exhibit impaired phagocytosis and profound immunometabolic dysfunction. In this exhausted state, microglia fail to mount appropriate inflammatory responses despite persistent Aβ exposure, contributing to ongoing neurodegeneration. The mechanisms driving this transition from protective to dysfunctional microglia, and whether targeting these pathways can restore microglial function, remain unclear. To address this, we investigated how pharmacologic inhibition of mitochondrial complexes, particularly the succinate dehydrogenase (complex II) and complex I RET axis, alters Aβ-induced immune and metabolic responses in microglial cell models. We treated BV2 and HMC3 microglial cell lines with Aβ for 24 hours in the presence or absence of a succinate dehydrogenase (SDH) inhibitor to test whether mitochondrial complex inhibition modulates Aβ-induced immunometabolic stress. Aβ induced a pattern of mitochondrial dysfunction consistent with reverse electron transport (RET)-mediated reactive oxygen species (ROS) production, increasing mitochondrial ROS in a manner sensitive to the complex I-targeted RET inhibitor S1QEL but not the complex III q-site inhibitor S3QEL, without altering fluorescence of the mitochondrial membrane potential indicator tetramethylrhodamine methyl ester (TMRM). Aβ also elevated intracellular succinate levels, and SDH inhibition further increased succinate, suggesting that excess succinate oxidation through SDH fuels RET-dependent ROS during Aβ exposure. Functionally, pharmacologic SDH inhibition reduced Aβ-induced Il1b mRNA and mature IL-1β secretion into the media in both BV2 cells supporting a model in which interrupting RET-driven mitochondrial ROS dampens inflammasome-associated cytokine production and partially restores microglial immunometabolic homeostasis. These findings indicate that RET-dependent mitochondrial ROS contributes to Aβ-induced microglial immunometabolic dysfunction and demonstrate that pharmacologic manipulation of mitochondrial complexes, including SDH, can be used to interrupt this pathway and improve microglial immunometabolic flexibility.

**Disclosures: J. McWhirt:** None. **C.A. Martinez:** None. **P. Da Silva Frost:** None. **J.H. Ledo:** E. Ownership Interest (stock, stock options, royalty, receipt of intellectual property rights/patent holder, excluding diversified mutual funds); AzoraX.

**Poster**

**PSTR174: Microglia in Alzheimer's Disease**

**Location:** WCC Halls A-C

**Time:** Monday, November 16, 2026, 1:00 PM - 5:00 PM

**Program #/Poster #:** PSTR174.10/U21

**Topic:** C.02. Alzheimer's Disease and Other Dementias

**Title:** Alzheimer's disease protective variant attenuates microglia senescence

**Authors: *V. A. MADORMO**[1,2], A. SRIRAM[2], M. P. SADGROVE[2], G. A. GARDEN[2];
[1]Univ. of North Carolina Chapel Hill, Chapel Hill, NC; [2]Neurol., Univ. of North Carolina Chapel Hill Sch. of Med., Chapel Hill, NC

**Abstract:** Aging is a primary risk factor for Alzheimer's disease (AD). A fundamental hallmark of aging that predicts health span is the accumulation of senescent cells. Senescence is a state of irreversible cell cycle arrest accompanied by cellular changes that compromise normal cellular function. This state is commonly triggered by cellular insults such as DNA damage, reactive oxygen species, or proteotoxic stressors. Emerging evidence suggests senescence of microglia, the innate immune cell of the brain, impacts the pathology of AD. Senescent microglia fail to clear pathogenic proteins and increase chronic inflammatory signaling. Many of the pathways that microglia use to process stress and enter senescence or mount a reparative response involve phospholipase C γ 2 (PLCγ2). A variant of PLCγ2 with a single substitution (P522R) provides protection against AD in humans. We hypothesize that PLCγ2 (P522R) provides protection against AD in part by altering the induction of microglia senescence. To assess the impact of PLCγ2 (P522R) on the microglia senescence response we performed RNA sequencing of primary mouse microglia expressing PLCγ2 (P522R) and PLCγ2 (WT) with and without exposure to fibrillized Aβ exposure. We observed that Aβ exposure induced senescence associated transcriptional networks, including p16 and p21, in WT microglia, but these gene expression patterns were not observed in PLCγ2 (P522R) microglia. PLCγ2 (P522R) microglia also showed lower senescence associated *TP53* target gene sets and elevated cell cycle modules. We found that these network changes are also present in publicly available RNA sequencing datasets from 5xFAD mice with PLCγ2 (P522R) and from human iPSC-derived microglia with PLCγ2 (P522R) xenotransplanted into mice. Further, we assessed senescence associated beta-galactosidase in human iPSC-derived microglia treated with two senescence inducers, etoposide and iron. Microglia with PLCγ2 (P522R) demonstrated reduced senescence associated beta-galactosidase compared to microglia with PLCγ2 (WT) in each condition. Overall, microglia with PLCγ2 (P522R) have less senescence burden than microglia with PLCγ2 (WT). Taken together, these results suggest that PLCγ2 (P522R) may confer protection against AD in part by reducing microglial senescence in AD.

**Disclosures: V.A. Madormo:** None. **A. Sriram:** None. **M.P. Sadgrove:** None. **G.A. Garden:** None.

**Poster**

**PSTR175: Neuroimmune Mechanisms and Immune-Brain Interactions**

**Location:** WCC Halls A-C

**Time:** Monday, November 16, 2026, 1:00 PM - 5:00 PM

**Program #/Poster #:** PSTR175.01/U22

**Topic:** G.04. Neuroimmunology and Neurovirology

**Support:** National Key Research and Development Program of China 2023YFA1801901
National Natural Science Foundation of China 32125017
National Natural Science Foundation of China 32150008

National Natural Science Foundation of China 82441057
Beijing Natural Science Foundation 7232086
Beijing Natural Science Foundation L244055

**Title:** Postprandial parasympathetic signals promote lung type 2 immunity via Chrm4 on ILC2s

**Authors: *H. CHEN**[1], T. LIU[2];
[1]Peking Univ., Beijing, China; [2]Cornell Univ., New York, NY

**Abstract:** While postprandial exacerbation of asthma is clinically observed, the underlying neuroimmune mechanisms remain poorly understood, with gastroesophageal reflux disease (GERD) being the dominant explanation—yet GERD-targeted therapies only partially alleviate symptoms, suggesting additional pathways. We hypothesized that feeding-induced activation of the parasympathetic nervous system (PNS), a core "rest-and-digest" response, may directly modulate lung type 2 immunity. Using whole-tissue immunolabeling, light-sheet 3D imaging, chemogenetics, vagotomy, and genetically modified mice, we assessed PNS-lung immune crosstalk in response to interleukin (IL)-33 or papain challenge. We found that food intake within 3 hours significantly enhanced lung expression of *IL-5/IL-13* and eosinophil recruitment, correlating with increased c-Fos$^+$/p-S6$^+$ neurons in the dorsal motor nucleus of the vagus (DMV) and elevated plasma levels of acetylcholine. Anatomically, 3D imaging confirmed dense cholinergic (VAChT$^+$) innervation along airways and spatial co-localization with IL-5$^+$ type 2 innate lymphoid cells (ILC2s) and Siglec-F$^+$ eosinophils. Chemogenetic activation of DMV neurons mimicked feeding-induced type 2 immunity; conversely, vagotomy, ipratropium bromide (muscarinic antagonist), or DMV-targeted hM4D(Gi) chemogenetic inhibition suppressed it. Transcriptomic profiling identified cholinergic receptor Chrm4 as highly and selectively expressed in lung ILC2s (mouse and human), but not in other immune cells; *Chrm4*$^{-/-}$ mice showed intact lung development but blunted feeding-enhanced type 2 responses and eosinophilia. Adoptive transfer experiments confirmed that Chrm4 expression specifically in ILC2s is necessary and sufficient for this effect, and *in vitro*, acetylcholine directly stimulated type 2 cytokine production in wild-type but not *Chrm4*$^{-/-}$ ILC2s. Notably, feeding alone induced baseline type 2 immunity, and in a fungal challenge model (*Aspergillus fumigatus* spores in diet), vagotomy or *Chrm4* deletion impaired pathogen clearance, indicating a physiological protective role. These findings reveal a gut-brain-lung reflex wherein postprandial PNS activity, acting via Chrm4 on ILC2s, potently enhances type 2 immunity. This mechanism likely evolved to protect against food-associated airborne pathogens and offers a novel explanation for postprandial asthma exacerbations with implications for muscarinic-targeted immunomodulation.

**Disclosures: H. Chen:** None. **T. liu:** None.

**Poster**

**PSTR175: Neuroimmune Mechanisms and Immune-Brain Interactions**

**Location:** WCC Halls A-C

**Time:** Monday, November 16, 2026, 1:00 PM - 5:00 PM

**Program #/Poster #:** PSTR175.02/U23

**Topic:** G.04. Neuroimmunology and Neurovirology

**Title:** Clinical Heterogeneity of Anti-NMDA Receptor Encephalitis: Fulminant Disease With Extreme Delta Brush Versus Late-Onset Autoimmune Psychosis

**Authors: *A. LEE**;
Edward Via Col. of Osteo. Med., Blacksburg, VA

**Abstract:** Anti-NMDA receptor encephalitis (ANRE) is an autoimmune disorder characterized by psychiatric, neurologic, and autonomic manifestations resulting from antibodies directed against the NMDA receptor subunits. Although increasingly recognized, ANRE remains frequently misdiagnosed because of its diverse clinical presentations. We describe two antibody-confirmed cases that illustrate the broad clinical spectrum of the disease and the potential for favorable outcomes following aggressive immunotherapy. Case 1 involved a 30-year-old woman who developed anxiety, insomnia, paranoia, and hallucinations following a prodromal illness. Her condition rapidly progressed to severe psychosis, catatonia-like features, dyskinesias, autonomic instability, electrographic seizures, and respiratory failure requiring intubation. Cerebrospinal fluid (CSF) demonstrated lymphocytic pleocytosis, MRI was normal, and electroencephalography (EEG) revealed extreme delta brush. Despite limited response to corticosteroids and intravenous immunoglobulin (IVIG), she improved following rituximab and plasma exchange (PLEX). A later relapse required repeat immunotherapy. Bilateral oophorectomy was negative for teratoma. At six-year follow-up, she achieved near-complete neurologic recovery. Case 2 involved a 56-year-old woman who presented with anxiety, dyspnea, progressive psychosis, encephalopathy, and autonomic dysfunction. MRI was normal, CSF showed lymphocytic pleocytosis, and EEG demonstrated only generalized slowing. Clinical improvement was limited after corticosteroids and IVIG but was marked following PLEX and rituximab. She subsequently achieved near-complete recovery with only mild residual anxiety. These cases highlight the remarkable clinical heterogeneity of ANRE, ranging from fulminant encephalitis with extreme delta brush and seizures to late-onset autoimmune psychosis with nonspecific EEG findings. Early recognition and escalation to second-line immunotherapy can result in excellent long-term outcomes even in severe disease.

**Disclosures: A. Lee:** None.

**Poster**

**PSTR175: Neuroimmune Mechanisms and Immune-Brain Interactions**

**Location:** WCC Halls A-C

**Time:** Monday, November 16, 2026, 1:00 PM - 5:00 PM

**Program #/Poster #:** PSTR175.03/U24

**Topic:** G.04. Neuroimmunology and Neurovirology

**Title:** Sex Differences in S1PR3 Signaling in Stress-Related Brain Regions: Implications for Neuroinflammation and Anxiety-Related Behavior

**Authors: *N. TAJAMAL**;
Res., Inst. of Biomed. and Genet. Engin., Islamabad, Pakistan

**Abstract:** Sphingosine-1-phosphate receptor 3 (S1PR3) is a G protein-coupled receptor that binds the bioactive lipid sphingosine-1-phosphate (S1P) and is expressed throughout the central nervous system, including brain regions involved in stress and anxiety regulation. Previous studies suggest that S1PR3 contributes to stress resilience and modulates inflammatory signaling; however, sex-specific expression of S1PR3 in stress-related brain circuits has not been fully characterized. In this study, we examined S1PR3 expression in the medial prefrontal cortex (mPFC) and dentate gyrus of male and female mice. Female mice were further stratified according to estrous cycle stage (non-proestrus/diestrus vs proestrus) to assess hormonal influences on receptor expression. Immunohistochemistry and confocal microscopy were performed to evaluate S1PR3 localization, and quantitative image analysis was conducted using ImageJ. S1PR3 expression was increased in female mice compared to males, with the highest levels observed during the proestrus phase, suggesting hormone-dependent regulation. Confocal imaging demonstrated co-localization of S1PR3 with NeuN-positive neurons in both the mPFC and dentate gyrus, indicating neuronal expression. Functional behavioral studies demonstrated that pharmacological activation of S1PR3 increased social interaction behavior, whereas inhibition of S1PR3 increased anxiety-like behavior in females. Together, these findings suggest that S1PR3 may function as a molecular interface between hormonal signaling and neuroinflammatory pathways in stress-related brain regions and may represent a potential therapeutic target for anxiety-related disorders.

**Disclosures: N. Tajamal:** None.

**Poster**

**PSTR175: Neuroimmune Mechanisms and Immune-Brain Interactions**

**Location:** WCC Halls A-C

**Time:** Monday, November 16, 2026, 1:00 PM - 5:00 PM

**Program #/Poster #:** PSTR175.04/U25

**Topic:** G.04. Neuroimmunology and Neurovirology

**Support:** Brain Behavior Research Foundation
Klingenstein-Simons Fellowship in Neuroscience
Pew Biomedical Scholars Program
Whitehall Foundation
NIH Grant 5R00NS114107
NIH Grant 5F32MH140490

**Title:** Social isolation impairs sickness recovery by altering neuro-immune responses

**Authors: *D. L. GERMUNDSON-HERMANSON**, J. A. OSTERHOUT;
Neurobio., Univ. of Utah, Salt Lake City, UT

**Abstract:** Chronic social isolation is linked to more severe symptoms and delayed recovery from infection. Sickness symptoms are considered the physiologic and behavioral outputs of peripheral immune activation. However, while immune-responsive neural circuits drive sickness symptoms, emerging evidence suggests other central pathways can also regulate immune function. Given that social isolation is encoded in the brain, how social environments affect the neural populations that may control immunity is unclear. In our own studies, we found that male but not female mice subjected to chronic social isolation exhibited significantly greater hypothermia, prolonged anorexia, and robust immune activation after bacterial lipopolysaccharides (LPS, 0.5 mg/kg i.p.) compared to group-housed counterparts, indicating greater sickness severity and recovery time. Interestingly, while sickness elevated levels of the stress hormone corticosterone (CORT), isolated sick males did not reach the CORT levels observed in sick grouped males. The blunted CORT responses suggested a potential mechanism where altered endocrine signaling drives localized glucocorticoid receptor (GR) resistance and downregulation in the brain. As GR signaling impacts neuronal excitability, disruption may impair central circuits that help control systemic inflammation. Since GR is highly expressed in the cortex, we proposed these regulatory populations may reside in regions such as the insular cortex (IC), which integrates interoceptive and social signals and has been linked to peripheral immune function. Thus, we hypothesized that isolation increases sickness severity by suppressing recovery-promoting neurons within the IC ($IC^{recovery}$ neurons), delaying recovery. Our activity pattern analysis revealed that while group-housed IC activity and GR expression tracked with sickness resolution, this pattern was delayed in isolated males, matching their prolonged recovery. We found that these changes correlated with circulating cytokine profiles during the sickness response. To determine whether $IC^{recovery}$ neurons reflected peripheral immune activity or functionally impacted recovery, we used targeted chemogenetic activation of $IC^{recovery}$ neurons in isolated TRAP2 males. Strikingly, activating $IC^{recovery}$ neurons during sickness accelerated resolution of hypothermia and pro-inflammatory cytokine levels, suggesting these neurons can modulate both sickness symptoms and peripheral immune activity. Together, our findings highlight that sickness symptoms and inflammation are not fixed responses but are dynamically modulated by central circuits based on social environment.

**Disclosures: D.L. Germundson-Hermanson:** None. **J.A. Osterhout:** None.

**Poster**

**PSTR175: Neuroimmune Mechanisms and Immune-Brain Interactions**

**Location:** WCC Halls A-C

**Time:** Monday, November 16, 2026, 1:00 PM - 5:00 PM

**Program #/Poster #:** PSTR175.05/U26

**Topic:** G.04. Neuroimmunology and Neurovirology

**Title:** Exploring the Role of Meningeal B Cells in Age-Related Cognitive Decline

**Authors: *E. OATMAN**, A. DAUGHERTY-LOPES, A. JOHNSON, J. R. LUKENS; Neurosci., Univ. of Virginia, Charlottesville, VA

**Abstract:** Age-related cognitive decline is a contributor to morbidity and reduced quality of life in elderly populations. The recent re-discovery of the meningeal lymphatics and how this system is involved in neuroimmune cross talk has sparked interest in understanding its role in brain health and aging. Interestingly, the meninges harbor a significant population of B cells derived from the skull marrow under homeostatic conditions. Recent research has demonstrated an expansion of age-related B cells and plasma cells in the meninges as well as impairment of meningeal lymphatic drainage. Additionally, systemic deletion of B cells protects from age-related health decline. However, it is not well understood how meningeal lymphatics and these expanded B cell populations are involved in neurocognitive outcomes during aging. Here, we assess learning, memory, and anxiety-like behaviors in aged wild type (WT) mice and aged mice lacking B cells ($\mu MT^{-/-}$ mice) to ascertain if B cells contribute to neurobehavioral changes during aging. We found decreased anxiety-like behaviors between aged $\mu MT^{-/-}$ mice and aged WT mice, suggestive of B cell influence in increased anxiety behaviors during aging. Additionally, we have evaluated meningeal lymphatic drainage in both groups of aged mice as well as young controls and demonstrate aged $\mu MT^{-/-}$ mice have enhanced lymphatic drainage to deep cervical lymph nodes (dcLNs) compared to aged WT mice. This suggests that age-associated B cells may contribute to dysfunction of meningeal lymphatics during aging. Utilizing flow cytometry, we immunophenotyped B cells within the draining deep cervical lymph nodes of aged mice and show expanded transitional B cells still undergoing development in aging as well as expanded activated B cells. Here, we show that accumulated B cells may contribute to anxiety behaviors and meningeal lymphatic drainage impairment during aging.

**Disclosures: E. Oatman:** None. **A. Daugherty-Lopes:** None. **A. Johnson:** None. **J.R. Lukens:** None.

**Poster**

**PSTR175: Neuroimmune Mechanisms and Immune-Brain Interactions**

**Location:** WCC Halls A-C

**Time:** Monday, November 16, 2026, 1:00 PM - 5:00 PM

**Program #/Poster #:** PSTR175.06/U27

**Topic:** G.04. Neuroimmunology and Neurovirology

**Support:** W.M. Keck Foundation
NIH Grant DK119811
NIH Grant AG082349

**Title:** Olfactory bulb microglia surrounding apoptotic cells exhibit daily changes in density and morphological complexity

**Authors: *G. L. PEARSON**, E. BURKE, M. KRASAKOVA, P. REIS, B. BACA, J. WANG, S. AKLI, I. N. KARATSOREOS;
Psychological and Brain Sci., Univ. of Massachusetts Amherst, Amherst, MA

**Abstract:** The murine olfactory bulb, a brain region that experiences high levels of neuronal turnover, regular exposures to inhaled stimuli, and robust circadian rhythms, offers a powerful model for examining how daily timing coordinates cellular maintenance, immune processes, and tissue repair. Our recently published work demonstrated that transcripts related to apoptosis and microglia function are rhythmically expressed by the olfactory bulb in a temporally organized manner throughout the day. Given this, we hypothesized that there may be a bidirectional relationship between apoptotic cells and microglia in the olfactory bulb, and that this interaction would be impacted by time of day. To test this, we immunohistochemically stained coronal sections of olfactory bulbs collected from male mice at two times of day ($n$ = 5 mice / time of day) to detect apoptotic cells (cCasp3+ with pyknotic nuclei), microglia (Iba1+ cells), and microglial lysosomes (Cd68+ puncta). We then acquired slide scanning images of these stained olfactory bulb sections. Next, in a randomized fashion, we acquired 40x z-stack confocal images of the detected apoptotic cells and quantified microglial counts and morphological characteristics, including morphological complexity using a Sholl analysis. We investigated this in several different anatomical locations within the olfactory bulb, from rostral to caudal and across different olfactory bulb layers. We found that time of day altered the cumulative frequency of microglia independent of their distance from apoptotic cells, with increased numbers of microglia at ZT0 compared to ZT12. Moreover, we found that morphological complexity, as demonstrated by Sholl analysis, was greater at ZT12 compared to ZT0. Together, these findings suggest that olfactory bulb microglia surrounding apoptotic cells vary with time of day in both number and morphology: more microglia but simpler morphology at ZT0, fewer microglia but more ramified at ZT12. This inverse relationship suggests microglial surveillance of the olfactory bulb is temporally tuned, with implications for how the tissue maintains homeostasis across the day. Future work will explore whether chronic environmental circadian desynchronization disrupts this timing and how daily timing or its dysregulation influence the number and distribution of apoptotic cells throughout the olfactory bulb.

**Disclosures: G.L. Pearson:** None. **E. Burke:** None. **M. Krasakova:** None. **P. Reis:** None. **B. Baca:** None. **J. Wang:** None. **S. Akli:** None. **I.N. Karatsoreos:** None.

**Poster**

**PSTR175: Neuroimmune Mechanisms and Immune-Brain Interactions**

**Location:** WCC Halls A-C

**Time:** Monday, November 16, 2026, 1:00 PM - 5:00 PM

**Program #/Poster #:** PSTR175.07/U28

**Topic:** G.04. Neuroimmunology and Neurovirology

**Support:** CNDD - Neurodevelopmental Disorders Internal Grant

**Title:** Maternal Immune Activation Alters Dynamic Prefrontal Cortical Responses to Repeated Novelty

**Authors: *P. DA SILVA FROST**[1], V. GLASS[4], J. MCWHIRT[2], C. MARTINEZ[3], E. AZEVEDO[3], J. H. LEDO[5];

[1]Neurosci., Med. Univ. of South Carolina, charleston, SC; [2]neuroscience, [3]Neurosci., Med. Univ. of South Carolina, Charleston, SC; [4]MUSC, Charleston, SC; [5]Neurosci., Med. Univ. of South Carolina Neurosci., Charleston, SC

**Abstract:** Autism spectrum disorder (ASD) is a heterogeneous neurodevelopmental condition characterized by sensory hypersensitivity, repetitive behaviors, and differences in social communication. Many genetic risk factors linked to ASD are associated with alterations in neuronal metabolism and cellular stress during development, driving long-lasting changes in brain excitability. Exacerbated inflammatory responses during early developmental windows are also known environmental risk factors for neurodevelopmental disorders. In mouse models, gestational increases in pro-inflammatory cytokines are sufficient to produce ASD-relevant social and repetitive behavioral phenotypes and to increase long-term neuronal excitability. Here, we investigated whether maternal immune activation (MIA) produces persistent alterations in prefrontal cortical activity during cognitive engagement with novel stimuli. Using in vivo calcium recordings during repeated novel-object exploration, we found that MIA disrupted the normal attenuation of prefrontal cortical responses across repeated interactions, consistent with impaired neuronal habituation. These findings suggest that early-life inflammatory mediators can alter the dynamic cortical adaptations required to filter repeated sensory information and support flexible behavioral responses.

**Disclosures: P. Da Silva Frost:** None. **V. Glass:** None. **J. McWhirt:** None. **C. Martinez:** None. **E. Azevedo:** None. **J.H. Ledo:** None.

**Poster**

**PSTR175: Neuroimmune Mechanisms and Immune-Brain Interactions**

**Location:** WCC Halls A-C

**Time:** Monday, November 16, 2026, 1:00 PM - 5:00 PM

**Program #/Poster #:** PSTR175.08/U29

**Topic:** G.04. Neuroimmunology and Neurovirology

**Support:** ZIC-ES103330
Z01 ES102005

**Title:** Blocking Terminal Cholesterol Synthesis in CD4+ Cells Causes Sex-Dependent Differences in Locomotion, Foraging, and Sleep in Mice

**Authors: *M. YUN**[1], P. W. F. KARMAUS[2], K. S. KONRAD[4], L. R. WILSON[5], J. D. CUSHMAN[5], M. FESSLER[3];
[1]Neurobio. Lab., Natl. Inst. of Envrn. Sci., Durham, NC; [2]Immunity, Inflammation, & Dis., [3]Clin. Res. Unit, Natl. Inst. of Envrn. Sci., Research Triangle Park, NC; [4]Publ. Hlth. and Scientific Res., Social and Scientific Systems, Inc., a DLH Holdings Corp. Co., Durham, NC; [5]Neurobio. Lab., Natl. Inst. of Envrn. Hlth. Sci., Durham, NC

**Abstract:** Cholesterol is a critical metabolite for membrane structure and cellular signaling. While systemic metabolism is well-studied, less is known about cholesterol synthesis in

proliferating immune cells, or how it influences immune regulation and in turn neurobehavior. This study examines how modifying terminal T cell cholesterol biosynthesis affects immune function and behavior, clarifying its role in immunometabolism and neuroimmune interactions. We focused on 3β-hydroxysterol Δ7-reductase (Dhcr7), an enzyme catalyzing the final steps of cholesterol synthesis. Its loss of function in humans causes Smith-Lemli-Opitz syndrome (SLOS), characterized by physical, neurodevelopmental, and immune abnormalities. Dhcr7 is upregulated during T cell activation, paralleling the cholesterol pathway's engagement for proliferation. Using a conditional knockout CD4Cre Dhcr7flox/flox mouse model (Dhcr7CD4), we examined how lacking endogenous T cell cholesterol production via deletion of Dhcr7 influences immune metabolism and behavior. In vitro, wild-type (WT) $CD8^+$ T cells showed expected impaired proliferation under lipoprotein-depleted conditions. However, Dhcr7CD4 $CD8^+$ T cells rescued proliferation, suggesting Dhcr7-deficient T cells adapt differently to extracellular cholesterol limitations. Additionally, while immune challenge tests did not show differences in T cell immune responses, Dhcr7CD4 mice displayed abnormal behavior during handling. Behavioral differences were therefore assessed using Open Field, Rotarod, SHIRPA, Grip strength, and automated home-cage Phenotyper assays that assess spontaneous behavior and an automated cognitive test (Cognition Wall). Statistical tests showed differences in activity levels between male WT and Dhcr7CD4 mice across the Open Field and spontaneous behavior assays. Both sexes also demonstrated evidence of changes in foraging behavior. Together, this data suggests that CD4+ cell-specific cholesterol biosynthesis influences immune metabolism, immune outcomes, and neurobehavioral phenotypes. Altered immunometabolism in these cells may directly contribute to activity levels, providing crucial mechanistic insights into behavioral features observed in cholesterol disorders like SLOS. While the CD4-Cre line impacts both CD4+ and CD8+ T cell lineages, our current data suggests that $CD8^+$ T cells likely drive these phenotypes. Future work using a CD8-Cre model will help distinguish the specific contributions of $CD8^+$ T cells from other $CD4^+$ populations.

**Disclosures: M. Yun:** None. **P.W.F. Karmaus:** None. **K.S. Konrad:** None. **L.R. Wilson:** None. **J.D. Cushman:** None. **M. Fessler:** None.

**Poster**

**PSTR175: Neuroimmune Mechanisms and Immune-Brain Interactions**

**Location:** WCC Halls A-C

**Time:** Monday, November 16, 2026, 1:00 PM - 5:00 PM

**Program #/Poster #:** PSTR175.09/U30

**Topic:** G.04. Neuroimmunology and Neurovirology

**Support:** NIDA Grant R01 DA057884

**Title:** The Role of the NLRP3 Inflammasome in Opioid-Induced Neurochemical Markers, Therapeutic and Adverse Effects in Male Mice

**Authors: *A. K. WILLIAMS**[1], M. RODRIGUEZ[3], D. VEERAGONI[3], C. CARBAJAL[3], F. OWENS[3], S. O. EANS[1], R. SHINOUCHI[4], B. A. TSAI[1], N. EL-HAGE[3], J. P. MCLAUGHLIN[2];

[2]Pharmacodynamics, [1]Univ. of Florida, Gainesville, FL; [3]Florida Intl. Univ., Miami, FL; [4]Dept. of Pharmacology, Showa Med. Univ. Grad. Sch. of Pharm., Sinagawa-ku, Japan

**Abstract:** Opioids are often used in combination with anti-inflammatory medications to manage severe pain. Morphine, the μ opioid receptor agonist, enhances the activity of NOD-like receptor protein 3 (NLRP3) inflammasomes, paradoxically prolonging neuropathic pain. The NLRP3 inflammasome is found primarily in immune cells but also astrocytes, microglia and neurons, and is known to facilitate opioid tolerance and opioid-induced hyperalgesia. In this study, we investigated the bidirectional interactions between the NLRP3 inflammasome and opioid-induced immune activation to establish whether NLRP3 inhibition is sufficient to modulate the antinociceptive and behavioral effects of morphine and fentanyl in male C57BL/6J mice. Pretreatment of an NLRP3 inhibitor MCC950 (40 mg/kg, i.p.) potentiated the antinociceptive effects of morphine and fentanyl (s.c.) in the 55°C warm-water tail withdrawal tests, significantly reducing the $ED_{50}$ values for morphine 3.6-fold and for fentanyl 1.8-fold ($F_{(2,88)} = 47.4$; $p < 0.0001$). When administered with morphine (3 nmol, i.c.v.), MCC950 also prevented subsequent morphine acute antinociceptive tolerance observed in control mice 8 h later. Pretreatment with MCC950 prevented morphine-induced hyperalgesia ($F_{(2,25)} = 3.30$; $p = 0.80$ for tail withdrawal latency pre vs. post chronic morphine) and ameliorated some symptoms of naloxone-precipitated withdrawal in morphine-physically dependent mice including jumping ($F_{(2,25)} = 25.5$; $p = 0.03$ vs. morphine) and teeth chattering frequencies ($F_{(2,25)} = 8.57$; $p = 0.002$ vs. morphine). MCC950 time-dependently potentiated opioid-induced respiratory depression and hyperlocomotion as well as morphine (0.1 and 1.0 mg/kg) CPP. Exposure to a single dose of morphine (10 mg/kg), fentanyl (0.1 mg/kg), or the agonists together time-dependently increased pro-inflammatory cytokines in the brain including IL-1β, IL-6, IL-18, and TNFα. Morphine exposure also decreased the expression of PSD-95 and NMDA receptors, but increased expression of AMPA receptors, suggesting ways that acute morphine may modulate synaptic plasticity in the brain. Pretreatment with MCC950 blocked many of the fentanyl-mediated increases in cytokine expression. These results support previous studies suggesting a bidirectional interaction between NLRP3 inflammasome and μ opioid systems.

**Disclosures: A.K. Williams:** None. **M. Rodriguez:** None. **D. Veeragoni:** None. **C. Carbajal:** None. **F. Owens:** None. **S.O. Eans:** None. **R. Shinouchi:** None. **B.A. Tsai:** None. **N. El-Hage:** None. **J.P. McLaughlin:** None.

**Poster**

**PSTR175: Neuroimmune Mechanisms and Immune-Brain Interactions**

**Location:** WCC Halls A-C

**Time:** Monday, November 16, 2026, 1:00 PM - 5:00 PM

**Program #/Poster #:** PSTR175.10/U31

**Topic:** G.04. Neuroimmunology and Neurovirology

**Support:** RS-2025-23323091

**Title:** Disruption of the Hyperosmotic Nucleus Pulposus Microenvironment Promotes VCAM-1 Expression and Macrophage Recruitment in Intervertebral Disc Herniation

**Authors: *H. KIM**, J. HONG, W. JEON, J. LEE, C. YEO, H. KIM;
Jaseng Med. Fndn., Seoul, Korea, Republic of

**Abstract: Disruption of the Hyperosmotic Nucleus Pulposus Microenvironment Promotes VCAM-1 Expression and Macrophage Recruitment in Intervertebral Disc Herniation**
**Authors** Hyunseong Kim, Jin Young Hong, Wan-Jin Jeon, Junseon Lee, Changhwan Yeo, Hyun Kim, Yoon Jae Lee, In-Hyuk Ha
**Disclosures** H.S.K.: None; J.Y.H.: None; W.-J.J.: None; J.L.: None; C.Y.: None; H.N.K.: None; Y.J.L.: None; I.-H.H.: None.
**Abstract**Intervertebral disc herniation is characterized by disruption of the immune-privileged nucleus pulposus (NP) environment and infiltration of inflammatory cells, particularly macrophages. Previous studies have reported increased expression of vascular cell adhesion molecule-1 (VCAM-1) in extruded NP tissue from patients with severe disc herniation, suggesting a role for VCAM-1 in inflammatory cell recruitment. However, the regulation of VCAM-1 expression in human NP cells and its contribution to macrophage recruitment remain unclear. Therefore, this study investigated the effects of inflammatory cytokines and osmotic microenvironment on VCAM-1 expression in human NP cells and evaluated its role in macrophage migration.Human NP cells were stimulated with interleukin-1β (IL-1β) or tumor necrosis factor-α (TNF-α) under defined osmotic conditions. VCAM-1 expression was assessed by quantitative PCR, immunofluorescence staining, and flow cytometry. Both IL-1β and TNF-α significantly increased VCAM-1 expression in a dose-dependent manner. Flow cytometric analysis showed that the proportion of VCAM-1-positive NP cells increased from 6.1% to 10.1% following IL-1β stimulation and from 5.7% to 20.7% following TNF-α stimulation. In contrast, increasing extracellular osmolarity from 275 to 400 mOsm/kg progressively reduced VCAM-1 expression, decreasing the proportion of VCAM-1-positive cells from 6.5% to 1.9%. Hyperosmotic conditions also suppressed cytokine-induced VCAM-1 upregulation, indicating that the native NP osmotic microenvironment limits inflammatory responsiveness. Functionally, VCAM-1-overexpressing NP cells significantly enhanced macrophage migration compared with control cells.These findings demonstrate that inflammatory cytokines promote VCAM-1 expression, whereas the native hyperosmotic NP microenvironment suppresses both basal and cytokine-induced VCAM-1 expression. Loss of this osmotic regulation during disc herniation may facilitate VCAM-1-mediated macrophage recruitment and contribute to local inflammatory responses.

**Disclosures: H. Kim:** None. **J. Hong:** None. **W. Jeon:** None. **J. Lee:** None. **C. Yeo:** None. **H. Kim:** None.

**Poster**

**PSTR175: Neuroimmune Mechanisms and Immune-Brain Interactions**

**Location:** WCC Halls A-C

**Time:** Monday, November 16, 2026, 1:00 PM - 5:00 PM

**Program #/Poster #:** PSTR175.11/U32

**Topic:** G.04. Neuroimmunology and Neurovirology

**Support:** DA051235
DA050837
AG078530
MH138309

**Title:** Continuous Digital Monitoring Improves Biological Interpretation of Inflammatory and Immune Responses in Preclinical Animal Models

**Authors: *V. KUMAR**[1], M. HASHAM[2], M. VAN GAALEN[3], P. A. GERRARD[4], A. GUIDI[4], L. SCHAEVITZ[2], C. BERGER-LIEDTKA[2], K. FUHRMAN[2], N. DITTO[2], J. ZYUZIN[2], M. C. SAUL[2], N. BRATCHER-PETERSEN[2];
[1]Jackson Lab., Bar Harbor, ME; [2]The Jackson Lab., Bar Harbor, ME; [3]Evotec, Hamburg, Germany; [4]Aptuit, Verona, Italy

**Abstract:** Systemic inflammatory and immune responses produce coordinated changes in behavior and physiology that remain difficult to characterize in preclinical models because conventional endpoints are sparse, episodic, and often insensitive to dynamic biological change. Continuous digital measures may improve longitudinal assessment of these responses, but their interpretation requires validation against underlying biological processes.
Here we define a context of use for continuous digital measures as surrogate indicators of systemic inflammatory and immune responses and apply a clinical validation framework to evaluate their biological relevance in vivo. Across three complementary murine models—graft-versus-host disease (GvHD), cachexia, and lipopolysaccharide (LPS)-induced inflammation—we assessed the extent to which continuous digital measures reflect immune-driven disease progression and capture coordinated multisystem responses and provide decision-relevant information for disease characterization.
Continuous digital measures aligned with immune-mediated disease progression and inflammatory biomarkers in GvHD, capturing early changes in activity, feeding behavior, and respiratory rate. In cachexia, measures reflected progressive disease burden through coordinated reductions in activity and increased respiratory rate. In LPS-induced inflammation, continuous digital measures identified threshold-dependent inflammatory responses and resolved their temporal dynamics. Across models, continuous monitoring provided greater temporal resolution and sensitivity than conventional intermittent assessments.
These findings demonstrate that continuous digital phenotyping provides a sensitive, longitudinal view of responses to inflammation and immune activation. By linking behavioral and physiological signals to biologically meaningful outcomes across multiple disease contexts, this work supports the use of continuous digital measures as interpretable, decision-relevant endpoints for studying neuroimmune interactions, disease-relevant endpoints for studying neuroimmune interactions and disease progression for studying neuroimmune interactions and disease progression in preclinical research. The consistency of findings across mechanistically distinct models suggests that continuous digital measures may provide a generalizable approach for quantifying inflammatory and immune-mediated pathology and may inform interpretation of behavioral and physiological outcomes in other LPS-based paradigms relevant to neuroinflammation and depression.

**Disclosures: V. Kumar:** A. Employment/Salary (full or part-time):; The Jackson Laboratory. C. Other Research Support (receipt of drugs, supplies, equipment or other in-kind support); NIDA, NIMH, NIH. E. Ownership Interest (stock, stock options, royalty, receipt of intellectual property rights/patent holder, excluding diversified mutual funds); Patent Holder. **M. Hasham:** A. Employment/Salary (full or part-time):; The Jackson Laboratory. **M. van Gaalen:** A. Employment/Salary (full or part-time):; Evotec. **P.A. Gerrard:** A. Employment/Salary (full or part-time):; (Verona) Srl, Aptuit an Evotec Company. **A. Guidi:** A. Employment/Salary (full or part-time):; Aptuit (Verona) Srl, an Evotec Company. **L. Schaevitz:** A. Employment/Salary (full or part-time):; The Jackson Laboratory. **C. Berger-Liedtka:** A. Employment/Salary (full or part-time):; The Jackson Laboratory. **K. Fuhrman:** A. Employment/Salary (full or part-time):; The Jackson Laboratory. **N. Ditto:** A. Employment/Salary (full or part-time):; The Jackson Laboratory. **J. Zyuzin:** A. Employment/Salary (full or part-time):; The Jackson Laboratory. **M.C. Saul:** A. Employment/Salary (full or part-time):; The Jackson Laboratory. **N. Bratcher-Petersen:** A. Employment/Salary (full or part-time):; The Jackson Laboratory.

**Poster**

**PSTR175: Neuroimmune Mechanisms and Immune-Brain Interactions**

**Location:** WCC Halls A-C

**Time:** Monday, November 16, 2026, 1:00 PM - 5:00 PM

**Program #/Poster #:** PSTR175.12/V1

**Topic:** G.04. Neuroimmunology and Neurovirology

**Support:** DOD Grant HT9425-23-1-0579
NIH Grant R01-DK103808

**Title:** More Gain More Pain: The Relationship Between Weight and Pain Status in a Diet Induced Model of Obesity in Mice

**Authors: *M. L. MCGRATH**[1], R. BUGESCU[2], G. M. LEINNINGER[3];
[1]Michigan State Univ., Lansing, MI; [3]Physiol., [2]Michigan State Univ., East Lansing, MI

**Abstract:** Obesity is a major health burden often complicated by associated comorbidities, such as the development of chronic pain. A large study by Stone and Broderick found that self-reported experiences of pain in a US population increased as calculated BMI increased, showing a strong positive correlation between pain and obesity. However, this relationship is complicated, as chronic pain can lead to obesity promoting behaviors, such as a more sedentary lifestyle, muddling the directionality of this relationship. Moreover, it is unclear if addressing weight status can alleviate associated pain. Here we tested the hypothesis that caloric restriction and GLP1R agonist treatment of obese mice can reduce body weight and pain, and that the degree of analgesia will correlate with the amount of weight loss. We provided adult C57/Bl6 mice of both sexes with either *ad libitum* chow (control group) or 45% high fat diet for at least 16 weeks to induce obesity. We also assessed pain status in the mice with a von Frey assay of mechanical allodynia. Body fat percentage was determined by time-dependent nuclear magnetic resonance (TD-NMR). After at least 16 weeks on diets (sufficient to induce obesity) the obese mice were

divided into four groups: 1) continued on high fat diet, 2) caloric restriction of high fat diet, 3) switch mice from high fat diet to standard chow diet, and 4) injection with semaglutide. For caloric restriction, mice were limited to seventy percent of their average daily intake. We found that mice developed significantly lower paw withdrawal thresholds within 8 weeks of starting a high fat diet, indicating a lower pain threshold. By 16 weeks on high fat diet mice had very low paw thresholds via the Von Frey test indicating that they experience significant mechanical allodynia. Interestingly, diet intervention does improve both weight and pain status, though over different time courses and mode of intervention differentially resolves pain. Our ongoing work will determine how these different groups will affect neuroinflammatory status as a possible method of central pain sensitization. Better understanding the relationship between weight and pain status, and how different modes of weight reduction alter this relationship, can help inform clinical decision making when trying to help patients who are experiencing comorbid obesity and pain.

**Disclosures: M.L. McGrath:** None. **R. Bugescu:** None. **G.M. Leinninger:** None.

**Poster**

**PSTR175: Neuroimmune Mechanisms and Immune-Brain Interactions**

**Location:** WCC Halls A-C

**Time:** Monday, November 16, 2026, 1:00 PM - 5:00 PM

**Program #/Poster #:** PSTR175.13/V2

**Topic:** G.04. Neuroimmunology and Neurovirology

**Support:** NIH Director's Pioneer Award DP-AT011979-01
This research was supported by the Allen Institute, founded by Jody Allen – chair and co-founder of Allen Family Philanthropies, and the late Paul G. Allen – investor, philanthropist, and co-founder of Microsoft.We gratefully acknowledge their vision

**Title:** Unraveling Central Mechanisms of Classically Conditioned Immune-suppression

**Authors: *A. STANLEY**, T. FINNEMORE, L. K. SCARIA, H. F. RODRIGUES, C. R. SCHMIDT, L. REMÉDIO, A. VICENTE, R. M. COSTA;
Allen Inst., Seattle, WA

**Abstract:** The brain can modulate immune responses through peripheral neuronal inputs to immune organs. Importantly, this modulation can be learned, as demonstrated by paradigms of conditioned immune suppression. During the acquisition phase of such paradigms, animals are exposed to a sensory stimulus paired with an immunosuppressive drug. Subsequently, in the evocation phase, presentation of the sensory stimulus alone is sufficient to suppress immune responses to an immune stimulant. Our goal is to identify the central brain regions—and the specific cell types within those regions—that orchestrate this learned immune response. Previous studies of conditioned immune effects have relied primarily on *in vitro* assessments, leaving the time course and magnitude of the *in vivo* response largely uncharacterized. To address this gap,

we characterized the temporal dynamics of plasma cytokine changes following administration of an immune stimulatory challenge (concanavalin A, ConA), as well as their suppression by an immunosuppressant (cyclosporine A, CSA), in awake mice. This was achieved using implanted catheters that enable stress-free, repeated blood sampling. We combined this approach with the Olink Target 48 cytokine panel, which allows simultaneous quantification of 43 immune-related proteins from small blood volumes. Using this methodology, we successfully demonstrated robust CSA mediated immune suppression *in vivo*. In parallel, we engineered an odor delivery system capable of precise and reliable presentation of olfactory conditioning stimuli, and preliminary conditioned immune suppression experiments are currently underway using this setup. Together, these foundational experiments establish the framework for investigating the central nervous system mechanisms underlying the learning and evocation of conditioned immune responses—specifically, the brain pathways that can modulate immunity.

**Disclosures: A. Stanley:** None. **T. Finnemore:** None. **L.K. Scaria:** None. **H.F. Rodrigues:** None. **C.R. Schmidt:** None. **L. Remédio:** None. **A. Vicente:** None. **R.M. Costa:** None.

**Poster**

**PSTR175: Neuroimmune Mechanisms and Immune-Brain Interactions**

**Location:** WCC Halls A-C

**Time:** Monday, November 16, 2026, 1:00 PM - 5:00 PM

**Program #/Poster #:** PSTR175.14/V3

**Topic:** D.01. Neurotoxicity, Inflammation, and Neuroprotection

**Support:** JSPS KAKENHI 16K10188
JSPS KAKENHI 19K08019
JSPS KAKENHI 22K07616
JSPS KAKENHI 25K10862

**Title:** Neuronal autoantibodies in patients initially diagnosed with psychiatric disorders or neurological disorders.

**Authors: *M. TAKAKI**[1], K. HINOTSU[2], H. KAWAI[3], T. ASADA[2], Y. OHYA[2], A. YOKODE[2], S. SAKAMOTO[1];
[1]Dept. of Neuropsychiatry, Okayama Univ. Fac. of Medicine, Dent. and Pharmaceut., Okayama, Japan; [2]Dept. of Neuropsychiatry, Okayama Univ. Grad. Sch. of Medicine, Dent. and Pharmaceut. Sci., Okayama, Japan; [3]Dept. of Psychiatry and Behavioral Sciences, Johns Hopkins Univ. Sch. of Med., Baltimore, MD

**Abstract:** Introduction Neuronal autoantibody against the NR1 subunit of NMDAR causes not only encephalitis symptoms but also symptoms similar to various psychiatric disorders. These are often misdiagnosed as various mental and neurological disorders. Early diagnosis and treatment intervention affect the prognosis. We present the results of measuring neuronal autoantibodies in patients diagnosed with psychiatric disorders or neurological disorders. Methods Between April 2014 and March 2026, neuronal autoantibodies were tested in

cerebrospinal fluid, serum, or both from 346 patients with psychiatric or neurological disorders requested by 41 institutions in Japan, including the Department of Psychiatry at Okayama University. Written consent was obtained from the patients or their legal representatives after an explanation of this study. This study was approved by the Okayama University Ethics Committee. The tests were performed by house cell-based assays using the co-expression to HEK cell of NMDAR (NR1 and NR2), Autoimmune Encephalitis Mosaic 6 (Euroimmun, Germany), NMDA, AMPA1/2, CASPR2, DPPX, LGI1, GABAB receptor, or both. Results In patients with initial diagnoses of schizophrenia (11/119), depression (2/60), epilepsy (5/56), bipolar disorder (3/25), encephalitis/encephalopathy (1/46), and post-Covid-19 infection (1/8), 19 patients were NMDAR positive and 4 patients were LGI1 positive. Most of NMDAR positive patients met the "possible" criteria for Graus's diagnostic criteria (2016) for autoimmune encephalitis, while most of LGI1 positive patients did not. All LGI1 positive patients were initially diagnosed with epilepsy, and two developed dementia symptoms over the long term. NMDAR results varied. A patient was positive only in house and six patients only in Euroimmun. Four patients were positive only in cerebrospinal fluid and negative in serum. Antibodies were negative in patients with dementia (14), dissociative or conversion disorders (11), autism spectrum disorder (8), hypersomnia (6), anxiety disorders (2), Parkinson's disease (2), or other neurological disorders (2). Most of positive patients were received steroids, plasmapheresis, high-dose immunoglobulin or rituximab and the prognosis was generally well. Discussion A small number of patients initially diagnosed with psychiatric disorders may have positive autoantibodies. The careful examination of neurological symptoms is emphasized. The different results in test method and test specimen should be careful. Results for Neural Cell Adhesion Molecule 1 (NCAM1), neurexin 1α (NRXN1α), and Dopamine-2 receptor (D2R) antibodies may also be presented.

**Disclosures: M. Takaki:** None. **K. Hinotsu:** None. **H. Kawai:** None. **T. Asada:** None. **Y. Ohya:** None. **A. Yokode:** None. **S. Sakamoto:** None.

**Poster**

**PSTR176: Ischemic and Hypoxic Injury: Neuroprotective and Therapeutic Strategies**

**Location:** WCC Halls A-C

**Time:** Monday, November 16, 2026, 1:00 PM - 5:00 PM

**Program #/Poster #:** PSTR176.01/V4

**Topic:** D.02. Ischemia

**Support:** CONDA 3P20GM130447-04S1
NIGMS CoBRE 1P20GM139762
NIH Grant 1R01NS13993
PhRMA Foundation Predoctoral Fellowship Grant 2026 PDDS 1510617

**Title:** Small Molecule-Mediated TREM1 Inhibition as a Therapeutic Strategy for Global Cerebral Ischemia

**Authors: *P. L. TIWARI**[1], H. KIM[1], R. URQUHART[1], V. DUNCAN[2], P. ABEL[1], G. JADHAV[1], J.-Y. HWANG[1];
[1]Pharmacol. and Neurosci., Creighton Univ., Omaha, NE; [2]St. Mary Col., Omaha, NE

**Abstract:** Global cerebral ischemia often caused by cardiac arrest affects over 200,000 Americans annually and leads to severe cognitive deficits or death. Although current emergency interventions restore cardiac function and cerebral blood flow, effective therapies targeting post-ischemic neurodegeneration remain limited. TREM1 is a membrane immune receptor expressed on the surface of myeloid-derived cells where it magnifies the innate pro-inflammatory immune response. Our recent studies showed that global ischemia activates TREM1 and neuroinflammation in the hippocampal CA1 in rats. Additionally, TREM1 inhibition by the peptide inhibitor LR12 demonstrated neuroprotection against ischemic insult. Therefore, we hypothesized that TREM1 inhibition could be a new therapeutic strategy. Current inhibitors, however, have limitations as potential drug candidates due to their poor cell permeation and short half-life. To address these limitations and develop small molecule TREM1 inhibitors, we first identified an $N^4$-(amino-substituted)-*N*-substituted-benzene sulfonamide pharmacophore as a hit molecule from molecular docking. Surface Plasmon resonance (SPR) analysis confirmed hit molecule's affinity to TREM1 with a Kd of 14.3 μM, but displayed poor solubility. To address this, we synthesized para-fluoro analog of hit molecule (GJ079), which showed enhanced solubility and improved affinity to TREM1 (Kd = 4.8 nM). Thus, we further modified hit molecule's structure and synthesized 44 additional analogs to enhance their pharmacological and pharmacokinetic properties through five series: Series 1 and 2 required an additional aromatic-acetamido substitutions; Series 3 featured ortho, meta and para fluoro substitution on the end phenyl ring of hit molecule; Series 4 involved the replacement of the 2-thiazolyl ring with another hetero aromatic ring in the hit molecule; and Series 5 with aromatic-amido substitution on the $N^4$- aromatic amino group. To evaluate therapeutic potential of these compounds, we first tested GJ079 under inflammatory and ischemic conditions *in vitro* and in a rat model of global ischemia *in vivo*. GJ079 reduced pro-inflammatory cytokines, attenuated neuroinflammation and prevented neuronal death, indicating its neuroprotective effect. Screening of the additional analogs identified 7 promising lead candidates as small-molecule TREM1 inhibitors. The lead small-molecule candidate will undergo pharmacokinetic profiling, safety and toxicity studies in animal models, mechanistic evaluation of TREM1 signaling, and behavioral assessments following global cerebral ischemia.

**Disclosures: P.L. Tiwari:** None. **H. Kim:** None. **R. Urquhart:** None. **V. Duncan:** None. **P. Abel:** None. **G. Jadhav:** None. **J. Hwang:** None.

**Poster**

**PSTR176: Ischemic and Hypoxic Injury: Neuroprotective and Therapeutic Strategies**

**Location:** WCC Halls A-C

**Time:** Monday, November 16, 2026, 1:00 PM - 5:00 PM

**Program #/Poster #:** PSTR176.02/V5

**Topic:** D.02. Ischemia

**Support:** AA031465
AA025744
GM121307
AA025744
AA026708
AA023610
HL141998

**Title:** Endothelial Autotaxin-LPA Signaling Orchestrates Blood-Brain Barrier Breakdown and Mitochondrial Failure in Ischemic Stroke: Convergent Evidence From Genetic Deletion and Pharmacological Inhibition

**Authors: *M. PANCHATCHARAM**[1], V. MANIKANDAN[2], S. MANIKANDAN[2], H. SUN[3], S. MIRIYALA[4];
[1]Neurol., St. Louis Univ. Sch. of Med., St. Louis, MO; [2]KHS, Kirksville, MO; [3]Cell. biology and Anat., LSUHS, Shreveport, LA; [4]Anat., ATSU, Kirksville, MO

**Abstract:** Background: Blood-brain barrier (BBB) disruption and mitochondrial dysfunction drive neurological injury after ischemic stroke. Autotaxin (ATX), the principal lysophospholipase D, generates lysophosphatidic acid (LPA), promoting endothelial dysfunction, oxidative stress, and neuroinflammation. Lipid phosphate phosphatase-3 (LPP3) counterbalances LPA signaling. The endothelial ATX-LPA-LPP3 axis, an integrator of neurovascular failure after ischemia-reperfusion, remains incompletely defined.
Methods: Transient MCAO (90 min/24 h reperfusion) was performed in C57BL/6J mice. ATX activity, LPA species, BBB integrity (Evans blue, junctional proteins), mitochondrial bioenergetics (Seahorse XF24), cerebral blood flow (laser speckle), and infarct volume (TTC/Cresyl violet) were quantified. Pharmacological inhibition (HA130, PF8380, BrP-LPA, Ki16425) and tamoxifen-inducible endothelial ATX knockout mice (ERT2 $ATX^{-/-}$; Tie2-Cre/loxP) provided causal mechanistic evidence.
Results: Ischemia-reperfusion elevated ATX mRNA ~2-fold and activity ~4-fold ($p<0.05$), with LPA accumulation confined to brain microvasculature by CD31 co-localization. BBB disruption was characterized by ~3-fold increases in Evans blue extravasation and loss of ZO-1, claudin-5, VE-cadherin, and β-catenin. Mitochondrial dysfunction was characterized by reduced basal respiration, ATP turnover, spare capacity, and maximal respiration ($p<0.001$), along with elevated superoxide levels and suppressed antioxidant enzyme activity. Pharmacological inhibition restored junctional integrity, reduced permeability, and rescued mitochondrial bioenergetics. ERT2 $ATX^{-/-}$ mice showed reduced infarct volume, decreased vascular LPA, preserved cerebral blood flow, diminished penumbral microglial activation, and reduced neuronal loss versus I/R controls ($p<0.05$), with no physiological baseline abnormalities.
Conclusions: The endothelial ATX-LPA-LPP3 axis centrally orchestrates BBB breakdown, mitochondrial failure, and neuroinflammation after ischemic stroke. Selectively activated by ischemic stress yet dispensable in adult physiology, endothelial ATX is a compelling, low-toxicity therapeutic target. These findings support ATX-LPA-LPP3-directed strategies as adjuvants to reperfusion therapy to expand treatment eligibility and improve stroke outcomes.

**Disclosures: M. Panchatcharam:** None. **V. Manikandan:** None. **S. Manikandan:** None. **H. Sun:** None. **S. Miriyala:** None.

**Poster**

**PSTR176: Ischemic and Hypoxic Injury: Neuroprotective and Therapeutic Strategies**

**Location:** WCC Halls A-C

**Time:** Monday, November 16, 2026, 1:00 PM - 5:00 PM

**Program #/Poster #:** PSTR176.03/V6

**Topic:** D.02. Ischemia

**Support:** NIH grant R01NS124846

**Title:** GalR1 Agonist Ameliorates Brain Injury in a Rodent Transient Ischemic Stroke Model

**Authors: *N. BASNET**[1], H. WANG[2];
[1]Texas Tech. Univ. Hlth. Sci. Ctr., Lubbock, TX; [2]Texas Tech. Univ. HSC, Lubbock, TX

**Abstract: GalR1 Agonist Ameliorates Brain Injury in a Rodent TransientIschemic Stroke Model**Nikita Basnet, and Hongmin Wang*Department of Neuroscience and Pharmacology, Garrison Institute on Aging, and Center of Excellence forTranslational Neuroscience and Therapeutics (CTNT)Texas Tech University Health Sciences Center, Lubbock, TX*Ischemic stroke, resulting from insufficient cerebral blood flow, remains a leading causeof mortality and long-term disability worldwide, with limited therapeutic options available.Galanin receptors (GalRs), a family of G protein-coupled receptors widely expressed inthe central nervous system, have been implicated in neuroprotective processes. Althoughgalanin has been shown to exert neuroprotective effects in ischemic stroke, and GalR1agonists have demonstrated efficacy in hemorrhagic stroke models, the specific role ofGalR1 in ischemic stroke remains poorly defined. In this study, we investigated theneuroprotective effects of GalR1 activation using a transient middle cerebral arteryocclusion (tMCAO) mouse model. Mice were treated with M617 (25 μg/kg, i.p.), aselective GalR1 agonist, either 1 hour before ischemia induction or after reperfusion toevaluate its therapeutic potential. Brain infarct volume and neurological deficit scoreswere assessed to evaluate injury severity and functional outcomes. Pretreatment withM617 significantly reduced infarct volume and improved neurological deficit scorescompared with vehicle-treated controls, indicating attenuation of ischemic brain injury andenhanced functional recovery. Importantly, post-treatment with M617 administeredimmediately after reperfusion or 3 hours later also significantly reduced brain injury,demonstrating a clinically relevant therapeutic time window. These findings demonstratethat GalR1 activation confers robust neuroprotection in experimental ischemic stroke andsuggest that pharmacological targeting of GalR1 may represent a promising therapeuticstrategy. Further studies are warranted to elucidate the underlying mechanisms andevaluate the translational potential of GalR1 agonists for stroke treatment. This work wassupported by the NIH grant R01NS124846.**Keywords:** Ischemic stroke, Galanin receptor 1 (GalR1); M617; Transient middlecerebral artery occlusion (tMCAO).

**Disclosures: N. Basnet:** None. **H. Wang:** None.

**Poster**

**PSTR176: Ischemic and Hypoxic Injury: Neuroprotective and Therapeutic Strategies**

**Location:** WCC Halls A-C

**Time:** Monday, November 16, 2026, 1:00 PM - 5:00 PM

**Program #/Poster #:** PSTR176.04/V7

**Topic:** D.02. Ischemia

**Title:** Neuroprotection via ferroptosis inhibition upon cerebral ischemia/reperfusion injury: the effect of alpha-melanocyte stimulating hormone

**Authors: *L. XIANG**[1], A. W. TAYLOR[3], A. C. LO[2];
[1]The Univ. of Hong Kong, Hong Kong, China; [2]Dept. of Ophthalmology, The Univ. of Hong Kong, Hong Kong, Hong Kong; [3]Dept. of Ophthalmology & Vision Sci., Boston Univ., Boston, MA

**Abstract:** Ischemic stroke (IS) accounts for 80-85% of all strokes and remains a leading cause of long-term disability worldwide. Current treatments primarily aim at reperfusion, achieved through surgical methods or pharmacological interventions. However, these approaches can induce ischemia-reperfusion (IR) injury, which exacerbates neurological outcomes by accelerating neuronal damage and cell death. Alpha-melanocyte stimulating hormone (α-MSH) possesses neuroprotective properties, but its underlying mechanism remains unclear. This study aims to investigate whether the regulation of ferroptosis, a form of programmed cell death characterized by iron-dependent lipid peroxidation, contributes to the neuroprotective effects of α-MSH in cerebral IR injury. In vitro, mouse Neuro-2a (N2a) cells underwent oxygen-glucose deprivation/reoxygenation (OGD/R) to model IR injury and their response to α-MSH treatment were assessed by immunocytochemistry, Western blot, malondialdehyde (MDA) assay, glutathione (GSH) assay, iron assay, and JC-1 staining for ferroptosis. In vivo, cerebral IR injury was induced in 3-month-old male C57BL/6J mice via middle cerebral artery occlusion (MCAO). Neuronal damage was evaluated by neurological deficit scoring, 2,3,5-triphenyltetrazolium chloride (TTC) staining, and Hematoxylin and eosin (H&E) staining. Iron deposits were visualized by Perl's staining, and ferroptosis-associated proteins such as glutathione peroxidase 4 (GPX4), long-chain-fatty-acid—CoA ligase 4 (ACSL4), and solute carrier family 7 member 11 (SLC7A11) were assessed by immunohistochemistry. GSH and MDA levels were assayed to evaluate ferroptosis-related metabolites. In both models, α-MSH administration significantly improved neuronal survival, decreased neurological deficits, and preserved cell morphology after MCAO. It mitigated the reduction of GPX4 and GSH levels, suppressed the increase of MDA following OGD/R and MCAO, and prevented mitochondrial membrane depolarization associated with ferroptosis. Importantly, α-MSH treatment preserved the expression of ferroptosis-related proteins (GPX4, ACSL4, SLC7A11) in the penumbra. Double immunohistochemistry with neuronal (NeuN), astrocyte (glial fibrillary acidic protein, GFAP), and microglial (ionized calcium-binding adaptor molecule 1, Iba1) markers revealed elevated ACSL4 expression across these cell types. In conclusion, α-MSH exerts potent neuroprotective effects by modulating ferroptosis upon cerebral IR injury. These findings suggest that targeting ferroptosis by α-MSH administration may serve as a promising complementary therapeutic strategy for IS.

**Disclosures: L. Xiang:** None. **A.W. Taylor:** B. Contracted Research/Research Grant (principal investigator for a drug study, collaborator or consultant and pending and current grants). If you

are a PI for a drug study, report that research relationship even if those funds come to an institution.; Palatin Technologies Inc.. F. Consulting Fees (e.g., advisory boards); Palatin Technologies Inc., ANI Pharmaceuticals Inc.. **A.C. Lo:** None.

**Poster**

**PSTR176: Ischemic and Hypoxic Injury: Neuroprotective and Therapeutic Strategies**

**Location:** WCC Halls A-C

**Time:** Monday, November 16, 2026, 1:00 PM - 5:00 PM

**Program #/Poster #:** PSTR176.05/V8

**Topic:** D.02. Ischemia

**Support:** Programa de Becas Posdoctorales UNAM

**Title:** Lippia origanoides extract exerts neuroprotective effects in the MCAO I/R rat model

**Authors: *K. L. MARTINEZ-GONZALEZ**[1], P. GARCIA-DELATORRE[2], A. M. GARÍA BORES[1], I. VALENCIA QUIROZ[3];
[1]FITOQUÍMICA, Univ. Nacional Autónoma De México, Mexico, Mexico; [2]UIM Enfermedades Neurológicas, IMSS-UIESS A Envejecimiento, Mexico City, Mexico; [3]Facultad de Estudios Superiores Iztacala, Univ. Nacional Autónoma de México (UNAM), Mexico City.

**Abstract:** Lippia origanoides extract exerts neuroprotective effects in the MCAO I/R rat model Stroke remains a leading cause of mortality and long-term disability worldwide, with cerebral ischemia accounting for the majority of cases. Ischemia/reperfusion (I/R) injury involves complex pathological mechanisms, including oxidative stress, neuroinflammation, blood-brain barrier disruption, and neuronal cell death. Therefore, identifying therapeutic strategies that target multiple pathways involved in I/R injury remains a major challenge. *Lippia origanoides* (Mexican oregano) is a plant traditionally used in Mexican medicine for the treatment of inflammatory-related disorders. Its bioactive compounds, including terpenoids, iridoids, and flavonoids, have been associated with antioxidant and anti-inflammatory properties. However, its potential neuroprotective effects in cerebral ischemia have not been fully explored. In this study, we evaluated the neuroprotective effects of orally administered *Lippia origanoides* extract in a rat model of cerebral ischemia/reperfusion induced by middle cerebral artery occlusion (MCAO). Treatment with *Lippia origanoides* extract (500mg/kg/daily/7d) reduced oxidative damage, evidenced by decreased nitric oxide production and lipid peroxidation, while increasing total antioxidant capacity. Additionally, extract administration attenuated neuroinflammatory responses, as demonstrated by reduced microglial (Iba1) and astrocytic activation (GFAP) and decreased pro-inflammatory cytokine expression in contralateral cortex at the level of bregma 1.0mm and hippocampus. Our findings demonstrate that *Lippia origanoides* extract provides neuroprotection against cerebral I/R injury, likely through modulation of oxidative stress and neuroinflammatory pathways. These results highlight the potential of this plant-derived extract as a promising therapeutic approach for limiting secondary injury mechanisms following ischemic stroke.

**Disclosures: K.L. Martinez-Gonzalez:** None. **P. Garcia-delaTorre:** None.

**Poster**

**PSTR176: Ischemic and Hypoxic Injury: Neuroprotective and Therapeutic Strategies**

**Location:** WCC Halls A-C

**Time:** Monday, November 16, 2026, 1:00 PM - 5:00 PM

**Program #/Poster #:** PSTR176.06/V9

**Topic:** D.02. Ischemia

**Support:** NIH Grant 1R01EY030841
ARPA-H THEA

**Title:** Galectin-3 Modulation Reveals a Dissociation Between Retinal Ganglion Cell Survival and Functional Recovery Following Retinal Ischemia-Reperfusion Injury

**Authors: *E. ESCH**;
Univ. of Colorado Anschutz Med. Campus, Aurora, CO

**Abstract:** Retinal ischemia-reperfusion (I/R) injury contributes to vision loss across multiple ocular diseases and induces inflammatory responses that drive neuronal degeneration. Galectin-3 (Gal-3), a β-galactoside-binding lectin upregulated following retinal injury, has emerged as a therapeutic target because genetic deletion or pharmacologic inhibition preserves retinal structure and retinal ganglion cell (RGC) survival in multiple models of neurodegeneration. As a result, Gal-3 activity is generally considered detrimental following retinal injury. However, whether structural preservation following Gal-3 inhibition translates into improved retinal function remains unknown.Adult wild-type (WT) and Gal3 knockout (Gal3KO) mice underwent unilateral retinal ischemia-reperfusion injury. Additional WT cohorts received the Gal-3 inhibitor TD139 by intraperitoneal (IP) administration or intraocular (IO) injection. Retinal function was assessed by scotopic electroretinography (ERG) at 7 and 14 days post-injury, and RGC survival was quantified by RBPMS immunolabeling.Consistent with prior reports, Gal3KO and TD139-treated animals demonstrated greater structural preservation following injury. Unexpectedly, increased RGC survival did not correspond to improved retinal function. WT animals exhibited progressive recovery of both low-intensity (0.01 cd·s/m²) and mixed rod-cone (1.0 cd·s/m²) ERG responses between 7 and 14 days post-injury. In contrast, Gal3KO animals demonstrated limited functional recovery despite increased RGC survival. Similarly, IP Gal-3 inhibition preserved retinal structure but failed to restore ERG responses to WT levels, while IO Gal-3 inhibition produced the poorest functional outcomes. Across ERG paradigms, functional recovery followed the pattern WT > WT+IP TD139 ≈ Gal3KO > WT+IO TD139.These findings challenge the assumption that structural preservation predicts functional recovery after retinal injury. While Gal-3 suppression promotes neuronal survival, it does not improve retinal physiological recovery. Together, these data reveal a dissociation between retinal structure and function and suggest that Gal-3 contributes to mechanisms of post-injury retinal circuit recovery independent of its effects on neuronal survival.

**Disclosures: E. Esch:** None.

**Poster**

**PSTR176: Ischemic and Hypoxic Injury: Neuroprotective and Therapeutic Strategies**

**Location:** WCC Halls A-C

**Time:** Monday, November 16, 2026, 1:00 PM - 5:00 PM

**Program #/Poster #:** PSTR176.07/V10

**Topic:** D.02. Ischemia

**Support:** DE-INBRE P20GM103446-23S8

**Title:** Developing A Sustained Release Single Dose Immunomodulatory Therapy for Hypoxic Ischemic Encephalopathy

**Authors: *B. COLLINS**[1,2];
[1]Univ. of Delaware, Newark, DE; [2]Nemours Children's Hlth., Newark, DE

**Abstract:** Hypoxic ischemic encephalopathy (HIE) is a common brain injury that occurs in up to 9 million infants each year globally and is a leading cause of long-term disability or death. Therapeutic hypothermia is the only effective treatment for HIE. However, this therapy is resource intensive, time sensitive, and has variable efficacy, demonstrating the critical need for additional therapies for HIE. T regulatory cells (Tregs) function as master regulators of neuroinflammation, homeostasis, and tissue regeneration. As such, neonatal Tregs are an excellent target for modulating neuroinflammation both acutely and over time following neonatal brain injury. Interleukin 33 (IL-33) is a cytokine that recruits T regulatory cells previously shown to have a neuroprotective effect after HIE when delivered systemically. We developed a single-dose sustained release injectable alginate hydrogel to deliver IL-33 directly into the brain for treatment of HIE. We used an inflammation-sensitized Rice Vannucci (RV) model of HIE with maternal intraperitoneal lipopolysaccharide exposure on gestational day 18 vs sham. We assessed functional outcomes by gait analysis (Catwalk), grip strength, and rotarod. Extent and distribution of brain injury were determined by histologic analysis of whole brain sections stained with hematoxylin and eosin. Overall, males had worse histologic and functional outcomes than females. Male mice treated with RV and a blank hydrogel displayed the lowest grip strength and the most abnormal gait, as well as the largest ventricular area increase. Males treated with RV and the IL-33 loaded gel showed similar functional and histological outcomes as the controls. The results indicate that IL-33-loaded alginate hydrogels are a promising technique for the treatment of HIE.

**Disclosures: B. Collins:** None.

**Poster**

**PSTR176: Ischemic and Hypoxic Injury: Neuroprotective and Therapeutic Strategies**

**Location:** WCC Halls A-C

**Time:** Monday, November 16, 2026, 1:00 PM - 5:00 PM

**Program #/Poster #:** PSTR176.08/V11

**Topic:** D.02. Ischemia

**Support:** PERF/CNS Elterman Award
NIH Grant K12EY015398

**Title:** Preventing DHA oxidation using deuterated DHA ameliorates neonatal hypoxic ischemic brain injury.

**Authors: *J. VITHAYATHIL**[1], F. E. JENSEN[2], D. M. TALOS[4], J. L. DUNAIEF[3];
[1]Dept. of Pediatrics, Children's Hosp. of Philadelphia, Philadelphia, PA; [2]Dept Neurol, [3]Dept. of Ophthalmology, Univ. of Pennsylvania, Philadelphia, PA; [4]Neurol., Univ. of Pennsylvania, Perelman Sch. of Medicine, Philadelphia, PA 19104, Philadelphia, PA

**Abstract: Background:** Polyunsaturated fatty acids (PUFAs), such as arachidonic acid (ARA) and docosahexaenoic acid (DHA), are highly susceptible to oxidative damage in neonatal hypoxic ischemic (HI) brain injury. While DHA supplementation is neuroprotective in rodent models of HI brain injury, it remains unclear whether this benefit is due to repletion of DHA damaged by oxidation or if it increases neuroprotective byproducts of DHA oxidation. **Methods:** Using the modified Vannucci model of neonatal HI in C57Bl/6 mice at post-natal day 9 (PND9), we characterized the temporal profile of PUFA oxidation at 6, 24, and 72 hours post-injury via mass spectrometry quantification of neuroprostanes and isoprostanes. DHA and ARA oxidation were further assessed by immunofluorescence against carboxyethylpyrrole (CEP) and 4-hydroxynonenal (HNE), respectively. To determine whether DHA oxidation contributes to neuronal injury, we utilized deuterated DHA (D-DHA) which is resistant to oxidation. Pregnant dams were started on 0.25% D-DHA diet at conception with control mice receiving equivalent standard hydrogenated DHA (H-DHA) or standard mouse diet. Percent of D-DHA incorporated into the brain was measured in post-natal rodents. Subsequently, HI injury was induced in D-DHA mice and injury severity was compared to HI injury in H-DHA and standard mouse diet. **Results:** Mass spectrometry revealed selective elevation of neuroprostanes, but not isoprostanes, at 24 hours post-HI, indicating DHA-specific oxidation in the hippocampus. CEP colocalization with TUNEL-positive cells confirmed that DHA oxidation products accumulate at sites of cell death. Pups preloaded with D-DHA achieved over 70% D-DHA incorporation into the brain by PND9 and demonstrated significantly reduced injury severity compared to those receiving hydrogenated DHA or standard chow. **Conclusion:** DHA oxidation is a key mediator of hippocampal injury following neonatal HI. Preloading the developing brain with oxidation-resistant deuterated DHA reduces injury severity, establishing DHA oxidation as a significant driver of neuronal injury and a tractable therapeutic target in neonatal HI brain injury.

**Disclosures: J. Vithayathil:** None. **F.E. Jensen:** None. **D.M. Talos:** None. **J.L. Dunaief:** None.

**Poster**

**PSTR176: Ischemic and Hypoxic Injury: Neuroprotective and Therapeutic Strategies**

**Location:** WCC Halls A-C

**Time:** Monday, November 16, 2026, 1:00 PM - 5:00 PM

**Program #/Poster #:** PSTR176.09/V12

**Topic:** D.02. Ischemia

**Support:** NIH grant (1R01NS117428-01A1)
ANR grant (ANR-21-CE17-0019-01)

**Title:** BRT_002, a Novel Purine Derivative, Improves Neuropathological and Behavioral Outcomes and Promotes Cytoskeletal Remodeling After Neonatal Hypoxic-Ischemic Brain Injury

**Authors: A. TSINTZOU**[1], C. DISDIER[2], A. BOUZID[3], X. CHEN[4], R. POIRIER[5], B. S. STONESTREET[6], *A. MABONDZO[7];
[1]CEA, DMTS, SPI, Neurovascular Unit Res. & Therapeut. Innovation Laboratory, Paris-Saclay Univ., Gif sur Yvette, France, France; [2]CEA, DMTS, SPI, Neurovascular Unit Res. & Therapeut. Innovation Laboratory, Paris-Saclay Univ., gif sur yvettes, France; [3]Univ. of Sharjah, Sharjah, United Arab Emirates; [4]Pediatrics, Kilguss Lab. 134, Women and Infants Hosp., Providence, RI; [5]Paris-Saclay Neurosci. Institute, UMR 9197, CNR, orsay, France; [6]Pediatrics, Women & Infants Hosp. of Rhode Island, Providence, RI; [7]CEA Saclay, Joliot Institute, DMTS, Paris Saclay Univ., Gif Sur Yvette Cedex, France

**Abstract:** Neonatal hypoxic-ischemic encephalopathy (HIE) is a leading cause of mortality and long-term neurodevelopmental disability in newborns worldwide. There are currently no pharmacological agents available to treat HIE in newborns. Therefore, it is essential to develop alternative and/or adjunctive novel therapeutic agents to attenuate the long-term sequela resulting from HIE. We reported that BRT_002 reduces short-term brain injury after HI. Although BRT_002 exerts short-term neuroprotection, it is important to determine whether BRT_002 has durable benefits. Sham and HI exposed male and female rats were given BRT_002 or placebo (PL), 0 min, 24 and 48 h after carotid ligation and 120 min of 8% oxygen on post-natal day 7. Sham, HI+PL and HI+BRT_002 rats were examined by motor tests for short-term, and long-term effects on memory (Novel Object Recognition test, and Morris Water Maze). Shot gun proteomic and bioinformatic analyses were carried out to determine the molecular mechanisms which support the long-term beneficial effects of BRT_002 treatment. BRT_002 improved HI-related sex-specific motor deficits. BRT_002 improved long-term and spatial learning memory in a sex-dependent manner. Hippocampal HI-induced GFAP expression and neuronal losses were reduced 60 days after treatment with BRT_002. BRT_002 treatment of HI-related brain injury exhibits durable hippocampal cellular changes and improves long-term functional outcomes. Proteomic analyses in HI animals identified changes in 350 proteins in females and 96 in males related to BRT_002 treatment. Pathway enrichment analysis revealed that cytoskeletal organization and synaptic function were among the most prominently modulated pathways in HI animals following BRT_002 treatment. Ten differentially expressed proteins (DEPs) overlapped between sexes, and were also identified as DEPs in the sham versus HI+PL comparison. Among the common DEPs, Myosin VI (Myo6), an actin-based motor protein involved in intracellular trafficking, synaptic remodeling, autophagy, and cytoskeletal organization, was identified as a central hub connecting multiple altered proteins. Myo6 was increased after HI in both sexes and normalized by BRT_002 treatment. These findings indicate that neonatal HI induces persistent

cytoskeletal and synaptic remodeling in perilesional brain tissue two months after injury. When administered early post-insult, BRT_002 treatment attenuates this long-term remodeling, with Myo6 emerging as a potential molecular marker and mechanistic hub of BRT_002 efficacy in HIE. BRT_002 could represent a promising alternative or adjunctive treatment for HIE.

**Disclosures: A. Tsintzou:** None. **C. Disdier:** None. **A. Bouzid:** None. **X. Chen:** None. **R. Poirier:** None. **B.S. Stonestreet:** None. **A. Mabondzo:** None.

**Poster**

**PSTR176: Ischemic and Hypoxic Injury: Neuroprotective and Therapeutic Strategies**

**Location:** WCC Halls A-C

**Time:** Monday, November 16, 2026, 1:00 PM - 5:00 PM

**Program #/Poster #:** PSTR176.10/V13

**Topic:** D.02. Ischemia

**Title:** Elucidating the Role of BDNF in Neonatal Stroke Recovery

**Authors: *E. PFOHL**[1], E. BURKE[1], R. PAWAR[1], S.-K. SIMS[2];
[1]Biol., Col. of Charleston, Charleston, SC; [2]Biol., Col. of Charleston Program In Neurosci., Charleston, SC

**Abstract:** INTRODUCTION: Neonatal hypoxic ischemia (HI) can result in death or lifelong functional impairments. Compounding this issue are challenges in early diagnosis and limited treatment options. Administration of brain-derived neurotrophic factor protein (BDNF) is a potential and understudied therapeutic option for ameliorating the impact of HI neonates. In adult clinical and preclinical animal studies, BDNF has been shown to improve synaptic plasticity, neuroinflammation, and aid in recovery. Intranasal administration of BDNF is a noninvasive method that bypasses the blood-brain barrier, allowing direct access to the brain. This project evaluated BDNF's role in recovery and therapeutic potential in both neonatal HI and non-HI models through intranasal delivery of the BDNF/TrkB receptor antagonist ANA-12. METHODS: Preliminarily, neonates received intranasal delivery of the BDNF antagonist ANA-12 and saline. Animals were intranasally administered 0.5mg/kg ANA-12 or 1mg/kg ANA-12 on postnatal day 7 (PND 7), followed by a motor skill analysis using 3 behavioral tasks: righting reflex, cliff avoidance, and negative geotaxis. Intranasal delivery of ANA-12 and saline continued daily until PND 14, at which point behavioral tasks were re-evaluated. In a following experiment, HI-induced neonates were administered BDNF. HI was induced on PND 7 using the modified Vannucci model and hypoxic-ischemic model by ligating the right carotid artery, followed by a 2hr exposure in an 8% oxygen/92% nitrogen-enclosed chamber, with a 2hr hypothermia treatment post-stroke. On PND 7, neonates were subjected to either 15 μg of recombinant human BDNF, 1mg/kg ANA-12, or saline via intranasal delivery from PND 8-13, administered in small increments and alternating nostrils. On PND 14, both experiments had the rat model brains harvested for immunohistochemistry and western blotting to measure BDNF levels, TrkB phosphorylation, and neuroinflammation. RESULTS: Data from the non-HI experiment indicated a negative relationship between intranasal ANA-12 administration and

reductions in recovery, TrkB receptor phosphorylation, and weight compared with saline-treated neonates. Unexpectedly, the ANA-12 groups showed less neuroinflammation, with decreased IL-6 and TNF-alpha cytokine expression in cortical and hippocampal tissues. Preliminary HI experimental data indicated a predictive relationship between ANA-12 administration and BDNF levels, with higher BDNF levels associated with better developmental outcomes. These results further indicate that neonatal rodents with lower BDNF levels are developmentally and performance restricted.

**Disclosures: E. Pfohl:** None. **E. Burke:** None. **R. Pawar:** None. **S. Sims:** None.

**Poster**

**PSTR176: Ischemic and Hypoxic Injury: Neuroprotective and Therapeutic Strategies**

**Location:** WCC Halls A-C

**Time:** Monday, November 16, 2026, 1:00 PM - 5:00 PM

**Program #/Poster #:** PSTR176.11/V14

**Topic:** D.02. Ischemia

**Support:** NIH K99NS142573
NIH K00NS124174
BWF 1280545

**Title:** Tunable Hydrogel Scaffold for Vascular Enhancement and Localized Gene Delivery After Ischemic Stroke

**Authors: *J. T. MOORE**[1], J. T. WANG[2], K. ZERA[4], K. BRADSHAW[1], M. HEFFERON[3], M. S. BUCKWALTER[1];
[2]Dept. of Neurobio., [1]Stanford Univ., Stanford, CA; [3]Stanford Univ., Menlo Park, CA; [4]Univ. of Minnesota, Duluth, MN

**Abstract:** Blood-brain barrier (BBB) dysfunction following ischemic stroke contributes to chronic neuroinflammation, vascular instability, and secondary neurodegeneration. Because BBB disruption can persist for months to years after injury, interventions that promote vascular maturation and restore barrier integrity may improve long-term neurological outcomes. Pericytes are critical regulators of BBB maintenance, and reduced PDGFB signaling has been implicated in vascular dysfunction. We developed an injectable hyaluronic acid and elastin-like protein (HELP) hydrogel platform for localized lipid nanoparticle (LNP)-mediated PDGFB gene delivery that supports endothelial cell survival and exhibits prolonged retention within the post-stroke brain without eliciting a substantial foreign body response.
We engineered HELP hydrogels to mimic properties of brain tissue. To identify optimal formulations that support brain endothelial cells, hydrogel composition, bioactivity, and stiffness were systematically varied. Murine brain endothelial cells (bEnd.3) were encapsulated within hydrogels and assessed for viability, metabolic activity, proliferation, and expression of vascular-associated genes. Scaffold material properties were characterized by rheology. To evaluate in vivo persistence and biocompatibility, fluorescently labeled hydrogels were injected into the

stroke lesion following distal middle cerebral artery occlusion and monitored longitudinally by IVIS imaging and immunohistochemistry.
Our HELP scaffold exhibited tunable stiffness within the range of native brain tissue (750-850 Pa) while maintaining high endothelial cell viability. LNP-mediated transgene expression was maintained following hydrogel encapsulation, producing robust transfection across multiple formulations (greater than 10-fold increase, log2 scale). Hydrogels remained detectable within the stroke lesion in all animals through 4 weeks (n=5) and in 2 (n=3) animals through 7 weeks, spanning a therapeutically relevant period of post-stroke vascular dysfunction.
Immunohistochemistry revealed no evidence of enhanced inflammatory responses (CD68 & GFAP) compared with sham controls at 28 days post-implantation, indicating favorable brain biocompatibility.
Together, these findings establish HELP hydrogels as a promising platform for sustained local delivery of vascular regenerative genes after stroke. The platform supports endothelial viability, sustained transgene expression, and prolonged retention, providing a foundation for future studies aimed at restoring BBB integrity and promoting neurovascular repair.

**Disclosures: J.T. Moore:** None. **J.T. Wang:** None. **K. Zera:** None. **K. Bradshaw:** None. **M. Hefferon:** None. **M.S. Buckwalter:** None.

**Poster**

**PSTR176: Ischemic and Hypoxic Injury: Neuroprotective and Therapeutic Strategies**

**Location:** WCC Halls A-C

**Time:** Monday, November 16, 2026, 1:00 PM - 5:00 PM

**Program #/Poster #:** PSTR176.12/V15

**Topic:** D.02. Ischemia

**Title:** Computational Virtual Stenting Simulation Using Contrast-Enhanced CT images of the Carotid Artery

**Authors: *T. YOKOYAMA**[1], M. NAKAZAKI[1], M. SASAKI[2], O. HONMOU[1];
[1]Sapporo Med. Univ. Sch. of Med., Sapporo, Japan; [2]Div. of Neuroscience, Dept. of Physiol., Sapporo Med. Univ., Sapporo, Japan

**Abstract:** OBJECTIVE: Carotid artery stenting (CAS) is a well-established treatment for extracranial carotid artery stenosis. Conventionally, angiographic images or contrast-enhanced CT images, which are two-dimensional (2D) images, are typically used to evaluate the vessel diameter and length for stent size selection. However, it is challenging to accurately estimate a vessel length of a three-dimensional (3D) structure from 2D images. Furthermore, there is no universally accepted method for determining the stent sizes.This study aimed to develop a method for selecting the appropriate stent size and determining the optimal stent placement using volume-based 3D images from preoperative contrast-enhanced CT scans. METHODS: We conducted a retrospective study enrolling patients with extracranial internal carotid artery stenosis who underwent CAS at Shiroishi Memorial Hospital were included.The volume-matched virtual stent (VS) images were reconstructed using contrast-enhanced CT images. The

length of this VS model was defined as the predicted total stent length and compared with the actual implanted stent (AS) length. The AS length was measured on postoperative angiographic images. The absolute difference between the length of the VS and the AS was calculated to evaluate prediction accuracy. RESULTS: The predicted VS length closely matched the measured AS length across the enrolled patients. The absolute difference between the two remained small, within a clinically acceptable range for stent size selection. Linear regression of the predicted VS length against the measured AS length showed a strong positive correlation, indicating that the volume-based prediction reliably reproduced the implanted stent length. These results support the clinical utility of this method. CONCLUSIONS: A volume-based VS model derived from preoperative contrast-enhanced CT images can accurately predict stent length, and potentially assisting the appropriate stent size selection and its optimal placement planning.

**Disclosures: T. Yokoyama:** None. **M. Nakazaki:** None. **M. Sasaki:** None. **O. Honmou:** None.

**Poster**

**PSTR176: Ischemic and Hypoxic Injury: Neuroprotective and Therapeutic Strategies**

**Location:** WCC Halls A-C

**Time:** Monday, November 16, 2026, 1:00 PM - 5:00 PM

**Program #/Poster #:** PSTR176.13/V16

**Topic:** D.02. Ischemia

**Support:** AHA 24SCEFIA1255866
AHA 24TPA1300751
NIH/NINDS 5R01NS126273-04
AHA 25TPA1475809
AHA 23TPA1069224

**Title:** Role of Long-chain acyl-CoA Synthetases in Neurovascular Dysfunction in Sickle Cell Disease

**Authors: Z. ZHANG**[1], T. YUAN[1], Y. ZHOU[1], X. TIAN[2], R. H.-C. LEE[1], *C. Y.-C. WU[1]; [1]Pharmaceut. Sci., Univ. of South Florida, Tampa, FL; [2]Toxicology and Cancer Biol., Univ. of Kentucky, Lexington, KY

**Abstract:** Sickle cell disease (SCD) is the most common severemonogenic disorder affecting 300,000 individuals worldwide annually. The mainchallenges in the treatment of SCD are the sickle-shaped red blood cells thattend to aggregate along the vessel walls leading to inflammation and vascularocclusions. Therefore, patients with SCD suffer from ischemic stroke, transientischemic attacks, and multiple organ dysfunction. One of the major hallmarks ofSCD is the low levels of omega-3 fatty acids (ω3-FA) such as docosahexaenoic acid (DHA) and eicosapentaenoicacid (EPA) in the blood. Thus, identifying the regulatory elements that controlω3-FA metabolism holds high therapeutic potential. As such, biosynthesis ofω3-FA through long-chain acyl-CoA synthetases (ACSLs) is essential for cellmember function and survival. In fact, it has been reported that downregulationof ACSL can cause ω3-FA deficiency,

as a result of cardiovascular diseases. Theimpact of ACSL on the central nervous system in pathological conditions (e.g.,SCD), however, remains largely unknown. The goal of the study is to determinethe role of ACSLs in brain circulation and neurological outcomes in SCD. Wediscovered in our pilot study that only ACSL6 expression is reduced in brainregions that are susceptible to ischemia. Based on preliminary findings, wefurther used pharmacological interventions and cell type-specific geneticapproaches to determine the effects of ACSL6 on cerebral blood flow,mitochondrial function, neuroinflammation, and neurological outcomes. Our findingsidentify ACSL6 as a critical regulator of neuronal survival during cerebral ischemiaand highlight the importance of ACSL6-mediated ω3-FA metabolism in maintainingbrain function. We conclude that ACSL6 represents a promising therapeutic targetfor preventing neurological complications in sickle cell disease.

**Disclosures: Z. Zhang:** None. **T. Yuan:** None. **Y. Zhou:** None. **X. Tian:** None. **R.H. Lee:** None. **C.Y. Wu:** None.

**Poster**

**PSTR177: Cellular Stress and Mechanisms of Degeneration**

**Location:** WCC Halls A-C

**Time:** Monday, November 16, 2026, 1:00 PM - 5:00 PM

**Program #/Poster #:** PSTR177.01/Web Only

**Topic:** D.01. Neurotoxicity, Inflammation, and Neuroprotection

**Support:** JSPS KAKENHI 20K07154
JSPS KAKENHI 23K06278

**Title:** Bortezomib-Induced Upregulation of Abhd4 Promotes Apoptosis in Peripheral Nerve Cells

**Authors: *T. OMURA**[1], Y. KONISHI[1,2], T. IJICHI[1], I. YANO[1];
[1]Kobe Univ. Hosp., Kobe, Japan; [2]Sysmex Corp., Technol. Innovation, Kobe, Japan

**Abstract:** Bortezomib (BTZ) is a first-generation proteasome inhibitor that has become a cornerstone treatment for multiple myeloma and other hematological malignancies. Peripheral neuropathy (PN) is a major adverse effect of BTZ, which occurs in approximately 20%-30% of patients and frequently necessitates dose reduction or discontinuation. There are currently no established strategies for the prevention or treatment of BTZ-induced PN, owing to a lack of understanding of the underlying mechanisms. To gain mechanistic insights, this study leveraged the clinical observation that carfilzomib (CFZ), a second-generation proteasome inhibitor with comparable antitumor effects, is associated with a substantially lower incidence of PN than BTZ. We performed a direct transcriptomic comparison of BTZ- and CFZ-treated peripheral nerve cells to identify molecular events specific to BTZ-induced neurotoxicity. Differentiated F11 cells—a hybridoma of rat embryonic dorsal root ganglion neurons and mouse neuroblastoma N18TG2-derived cells—were treated with 10 nM BTZ or CFZ. Microarray analysis performed 12 h post-treatment revealed that BTZ selectively upregulated *Abhd4* (α/β-hydrolase domain-

containing protein 4) in both mouse and rat homolog analyses, whereas CFZ did not induce any genes exceeding the cutoff threshold (log2 ratio ≥ 3). *Abhd4* was the only gene consistently identified across both homologs and was therefore prioritized for further analysis. Quantitative RT-PCR and immunoblotting confirmed the upregulation of *Abhd4* mRNA and protein after BTZ treatment, respectively; CFZ produced no significant changes. To explore the functional consequences of *Abhd4* upregulation, F11 cells were transfected with an *Abhd4*-EGFP expression vector. Flow cytometric analysis using Annexin V/PI staining demonstrated that *Abhd4* overexpression significantly increased the proportion of early apoptotic cells compared with EGFP-only controls. Collectively, these findings identify *Abhd4* as a candidate molecular signature associated with BTZ-induced PN and suggest that its upregulation may contribute to neuronal vulnerability after BTZ exposure. Further investigation is warranted to determine the role of *Abhd4* in the pathogenesis of BTZ-induced PN.

**Disclosures: T. Omura:** None. **Y. Konishi:** A. Employment/Salary (full or part-time):; Sysmex Corporation. **T. Ijichi:** None. **I. Yano:** None.

**Poster**

**PSTR177: Cellular Stress and Mechanisms of Degeneration**

**Location:** WCC Halls A-C

**Time:** Monday, November 16, 2026, 1:00 PM - 5:00 PM

**Program #/Poster #:** PSTR177.02/V17

**Topic:** D.01. Neurotoxicity, Inflammation, and Neuroprotection

**Support:** Grant-in-Aid for Scientific Research from the Ministry of Education, Culture, Sports, Science and Technology of Japan (JSPS Kakennhi Grant No. 25K09946
DAIGAKUTOKUBETSU KENKYUHI Grant (Musashino University)

**Title:** Perfluorooctanoic acid (PFOA) - induced neurotoxicity is enhanced by tamoxifen, an antagonist of estradiol

**Authors: *M. KAWAHARA**[1], K.-I. TANAKA[2], M. KATO-NEGISHI[3];
[1]Musashino Univ., Nishitokyo, Japan; [2]Dept of Bio-Analytical Chem., Musashino Univ., Tokyo, Japan; [3]Inst. of Industrial Science,, The Univ. of Tokyo, Tokyo, Japan

**Abstract:** The environmental contamination of per- and polyfluoroalkyl substances (PFAS) such as perfluorooctanoic acid (PFOA) and perfluorooctane sulfonate (PFOS) is a serious problem for human health. PFAS reportedly affect carcinogenicity, immunological system and fertility, however, little is known about their neurotoxic effects. We investigated the characteristics of PFOA-induced neurotoxicity using GT1-7 cells (immortalized hypothalamic neurons). GT1-7 cells, which were derived from murine hypothalamic neurons, possess neuronal characteristics, express neuron-specific proteins, and express the receptors of 17β-estradiol (E2). After 2 days of exposure to low concentration of PFOA (2.5~5 μM) , the oncrease of cell viability and the extension of neuronal processes were observed. However, the cells were degenerated in high concentration (more than 10 μM) . These biphasic neurotoxic effects were also observed after

exposure to E2 or E2-related compounds such as bisphenol A. Furthermore, the co-existence of tamoxifen, an antagonist of E2, exaggerated PFOA-induced neurotoxicity. PFOA-induced neurotoxicity was not affected by the co-existence of sodium pyruvate, an energy substrate, nor N-acertyl cysteine (NAC), an antioxidant.
Meanwhile, PFOA-induced neurotoxicity was attenuated by the addition of $Ca^{2+}$, and was aggravated by addition of KCl. The Ca-imaging system using Calbrite 520AM revealed that the exposure to PFOA caused the increase of intracellular $Ca^{2+}$ levels. These results suggested the involvements of estradiol and $Ca^{2+}$ homeostasis on PFOA-induced neurotoxicity. Our system will provide a good tool for the investigation of PFAS-induced neurotoxicity and the screening of protective substances against PFOA-induced neurotoxicity.

**Disclosures: M. Kawahara:** None. **K. Tanaka:** None. **M. Kato-Negishi:** None.

**Poster**

**PSTR177: Cellular Stress and Mechanisms of Degeneration**

**Location:** WCC Halls A-C

**Time:** Monday, November 16, 2026, 1:00 PM - 5:00 PM

**Program #/Poster #:** PSTR177.03/V18

**Topic:** D.01. Neurotoxicity, Inflammation, and Neuroprotection

**Support:** NIH Grant R35GM148177
NIH Grant R01GM112696

**Title:** Machine learning-driven identification of convergent neurotoxicity networks and candidate neuroprotective targets in developing mouse brain exposed to the general anesthetics propofol and sevoflurane

**Authors: *M. KIM**[1], Y. YAN[1], T. ARZUA[2], S. LOGAN[3], X. BAI[1];
[1]Dept. of Anesthesiol., The Ohio State Univ., Columbus, OH; [2]Zuckerman Inst., Columbia Univ., New York, NY; [3]Med. Col. of Wisconsin, Milwaukee, WI

**Abstract:** Emerging evidence suggests that early-life exposure to general anesthetics, including intravenous and volatile agents, may adversely affect neurodevelopment. In experimental models, anesthetic-induced developmental neurotoxicity (AIDN) involves acute neuronal injury followed by long-term deficits in learning, memory, and behavior. Given that a substantial proportion of young children, including approximately 14% before age 3, and up to 2% of pregnant women are exposed to general anesthesia, AIDN remains an important clinical concern. However, most studies have examined individual anesthetics separately, limiting the identification of shared injury pathways. We aimed to determine whether distinct general anesthetics induce a shared neurotoxicity-associated transcriptional program. To test this, postnatal day 7 (P7) mice were exposed to either propofol (50 mg/kg, intraperitoneal injection) or 3% inhalation sevoflurane for 3 or 6 hours. Acute neuronal injury was assessed by cleaved caspase-3 expression and activity. Long-term learning and memory were evaluated at P60 using the Morris water maze. Hippocampal mRNA profiles were generated by microarray and

analyzed using Ingenuity Pathway Analysis, unsupervised k-means clustering, and STRING network analysis to identify shared expression modules across anesthetic exposures, hub genes, and candidate neuroprotective targets. This integrated approach revealed both anesthetic-specific and shared injury responses. Propofol and sevoflurane exposure increased cleaved caspase-3 activity in P7 hippocampal neurons, indicating acute apoptosis. Both anesthetics caused persistent learning and/or memory deficits at P60, demonstrated by prolonged escape latency in the Morris water maze. Transcriptomic analysis identified 100 dysregulated genes after propofol exposure and 148 after 6-hour sevoflurane exposure, including 44 shared genes. Fold changes induced by propofol and sevoflurane were strongly correlated (Pearson $r = 0.78$, $p < 0.0001$), supporting a conserved transcriptional response. Machine learning and network analyses identified interconnected pathways involving mitogen-activated protein kinase signaling, metabolic regulation, immune activation, and extracellular matrix remodeling. These findings suggest that distinct general anesthetics may converge on shared developmental brain injury pathways. By combining behavioral, biochemical, transcriptomic, machine learning, and network-based analyses, this study identifies conserved molecular signatures of AIDN and highlights candidate pathways for future mechanistic and neuroprotective studies.

**Disclosures: M. Kim:** None. **Y. Yan:** None. **T. Arzua:** None. **S. Logan:** None. **X. Bai:** None.

**Poster**

**PSTR177: Cellular Stress and Mechanisms of Degeneration**

**Location:** WCC Halls A-C

**Time:** Monday, November 16, 2026, 1:00 PM - 5:00 PM

**Program #/Poster #:** PSTR177.04/V19

**Topic:** D.01. Neurotoxicity, Inflammation, and Neuroprotection

**Title:** Senolytic treatment reduces senescent astrocytes to attenuate dopaminergic neuronal loss in a-syn pre-formed fibril injected mice

**Authors: *P. WARDWELL**;
Biol. Sci. + Neurosci. Program, Boise State Univ., Meridian, ID

**Abstract:** Emerging evidence suggests that cellular senescence (CS) contributes to the progression of neurodegenerative diseases, including Parkinson's disease (PD). Cellular senescence is a state in which cells cease to proliferate in response to damage and contribute to tissue dysfunction through the release of toxic cytokines, collectively termed the Senescence-Associated Secretory Phenotype (SASP). While dopaminergic neurons are the primary cell type lost in the substantia nigra compacta (SNc) in PD, senescent glia—particularly astrocytes—are considered to mediate secondary toxicity that drives neuronal death. Using pre-formed fibrils (PFF) of α-synuclein to induce PD-like pathology, we examined the impact of senolytic (ABT-263) treatment on senescent glial burden and downstream neuroprotection. Cellular senescence was assessed through established markers using immunohistochemistry (IHC) and Western blot analyses. Using triple labelling immunohistochemistry (IHC) and confocal microscopy, we quantified GFAP-positive astrocytes, in addition to the complement protein C3 and the cyclin-

dependent kinase inhibitor p21 as markers of reactive or senescent astrocyte states, respectively. In our well-established classification model: GFAP+/C3+/p21- astrocytes are defined as reactive, GFAP+/C3-/p21+ as senescent, GFAP+/C3+/p21+ as ambiguous/transitionary, and GFAP+/C3-/p21- as healthy. PFF injection significantly elevated both C3 and p21 levels in the striatum, cortex, and SNc, while it increased colocalization of C3 and p21 within astrocytes, indicating a shift toward transitionary and senescent states. Oral ABT-263 treatment, reduced both C3 and p21 levels and decreased C3/p21 colocalization in astrocytes, suggesting a reduction in the transitionary and senescent astrocyte populations. These changes were accompanied by significant prevention or reversal of dopaminergic neuronal loss in PFF-injected brains, as verified by IHC. Taken together, these findings demonstrate that PFF-induced PD-like pathology promotes astrocyte dysfunction across a spectrum from reactive to senescent states, and that senolytic clearance of senescent astrocytes attenuates nigrostriatal neurodegeneration. Although our simplified astrocyte classification model may not fully characterize the type of damaged astrocytes, it may offer an approachable method for quantifying glial pathology in PD and Dementia with Lewy body (DLB). These results support that removal of senescent glia as a novel therapeutic strategy may slow neurodegeneration and pathological progression in human PD patients.

**Disclosures: P. Wardwell:** B. Contracted Research/Research Grant (principal investigator for a drug study, collaborator or consultant and pending and current grants). If you are a PI for a drug study, report that research relationship even if those funds come to an institution.; Yong-Hwan Kim. C. Other Research Support (receipt of drugs, supplies, equipment or other in-kind support); Dinesh Kumar Verma.

**Poster**

**PSTR177: Cellular Stress and Mechanisms of Degeneration**

**Location:** WCC Halls A-C

**Time:** Monday, November 16, 2026, 1:00 PM - 5:00 PM

**Program #/Poster #:** PSTR177.05/V20

**Topic:** D.01. Neurotoxicity, Inflammation, and Neuroprotection

**Title:** Exposure to Red 40 induces dose-dependent somatic atrophy in rat cerebellar Purkinje cells

**Authors: M. MALPICA GALICIA**[1], J. RAMIREZ MENDOZA[1], E. CHÁVEZ[2], D. MEDINA AGUINAGA[3], *N. MIRTO AGUILAR[4];
[1]Licenciatura en Biotecnología, Benemérita Univ. Autónoma de Puebla, Puebla, Mexico; [2]Inst. de Ciencias, Lab. de Patogenicidad Microbiana, Benemérita Univ. Autónoma de Puebla, HEROICA PUEBLA DE ZARAGOZA, Mexico; [3]Anatom. Sci. and neurobiology, Univ. of Louisville Anatom. Sci. & Neurobio., Louisville, KY; [4]Unidad Académica de Fisioterapia, Univ. Autónoma de Tlaxcala, Tlaxcala, Mexico

**Abstract:** Purkinje cells represent the primary output pathway and motor integration center of the cerebellum. Their high sensitivity to xenobiotic agents and systemic oxidative stress makes

them a critical target for evaluating the neurotoxic potential of food additives such as Red 40 dye. The aim was to evaluate the histopathological and morphometric effects of repeated administration of Red 40 on Purkinje cells in the rat cerebellum. Methods: Wistar rats (N=20) were assigned to four groups receiving daily oral doses of Red 40 for 45 days: G1 (control), G2 (14 mg/kg), G3 (7 mg/kg), and G4 (3.5 mg/kg). Following the experimental period, histological sections stained with H&E were obtained. Results: The linear density of Purkinje cells exhibited adaptive fluctuations, with an average increase in the G2 group (0.0276 cells/μm) compared to the G1 group (0.0195 cells/μm). However, the somatic cell area decreased from 166.08 $\mu m^2$ in the G1 and 169.57 $\mu m^2$ in the G4, to 153.99 $\mu m^2$ in the G3 group, and finally to a minimum of 127.10 $\mu m^2$ in the G2 group. The reduction in somatic area reflects atrophy and retraction of the perinuclear cytoplasmic volume in Purkinje neurons, a classic indicator of neuronal cytotoxicity. The increase in linear density observed under the G2 group does not represent cell proliferation in the central nervous tissue; rather, it indicates a compensatory tissue packing or compaction phenomenon resulting from the loss of somatodendritic volume in these neurons. Conclusions: Repeated administration of Red 40 dye exerts a neurotoxic effect on cerebellar Purkinje neurons. This effect is manifested as a marked, dose-dependent somatic atrophy.

**Disclosures: M. Malpica Galicia:** None. **J. Ramirez Mendoza:** None. **E. Chávez:** None. **D. Medina Aguinaga:** None. **N. Mirto aguilar:** None.

**Poster**

**PSTR177: Cellular Stress and Mechanisms of Degeneration**

**Location:** WCC Halls A-C

**Time:** Monday, November 16, 2026, 1:00 PM - 5:00 PM

**Program #/Poster #:** PSTR177.06/V21

**Topic:** D.01. Neurotoxicity, Inflammation, and Neuroprotection

**Support:** NSF #2413997
NASA #80NSSC25M7079

**Title:** Microtubule disruption and mitochondria mislocalization by silver nanoparticle exposure in cultured B35 cells

**Authors: *A. B. PLANTZ**, N. SPITZER;
Dept. of Biol. Sci., Marshall Univ., Huntington, WV

**Abstract:** Silver nanoparticles (AgNPs) are antimicrobial agents prevalent in the manufacturing of plastic products. However, AgNPs shed from these products can enter the body and cross the blood-brain barrier. AgNPs bioaccumulate and persist in the brain, and the effects of this chronic low exposure are not well understood. Microtubules in the cytoskeleton are critical to brain function, stabilizing neuron morphology and driving axon development and differentiation. Collapsin response mediator protein (CRMP-2) associates with microtubules to regulate function and structure and is regulated via phosphorylation (pCRMP-2). Tubulin-associated unit (Tau) is another microtubule-stabilizing protein that behaves similarly to CRMP-2. Under oxidative

stress, such as that induced by AgNPs, CRMP-2 and Tau become hyperphosphorylated and aggregate. Neurofibrillary tangles often contain both pCRMP-2 and pTau. In addition to microtubule stabilization, CRMP-2 also helps to facilitate mitochondrial transport. As CRMP-2 becomes hyperphosphorylated, it dissociates from its binding partners, inhibiting mitochondrial transport in the axons. If mitochondria are not reaching the axon terminal, the energetically demanding processes underlying presynaptic communication will be inhibited. The objective of this project was to determine how microtubule regulation and mitochondria localization are affected by AgNP exposure. Cultured B35 rat neuroblastoma cells were treated with 0 - 2.0 µg/ml AgNP, levels representative of those estimated from environmental exposure, followed by immunocytochemistry processing. We fluorescently labelled pCRMP-2 and pTau to determine how these proteins responded to AgNP exposure. We found that as AgNP exposure increases, pCRMP-2 aggregates increase in a dose-dependent manner. We also fluorescently labelled mitochondria to determine localization trends in response to AgNP exposure. We found that as AgNP exposure increases, the mitochondria become trapped in the soma as opposed to traveling along neurites. These data suggest that AgNP exposure dysregulates cytoskeletal structure and mitochondrial transport, thus disrupting downstream cellular processes in a manner consistent with neurodegenerative mechanisms. Therefore, these findings inform best practices in the use of AgNPs in manufacturing and use of consumer products.

**Disclosures: A.B. Plantz:** None. **N. Spitzer:** None.

**Poster**

**PSTR177: Cellular Stress and Mechanisms of Degeneration**

**Location:** WCC Halls A-C

**Time:** Monday, November 16, 2026, 1:00 PM - 5:00 PM

**Program #/Poster #:** PSTR177.07/V22

**Topic:** D.01. Neurotoxicity, Inflammation, and Neuroprotection

**Support:** NSF Cooperative Agreement #OIA2242771

**Title:** Silver nanoparticle exposure disrupts the mechanisms involved in synaptic plasticity in the hippocampus of rat brain

**Authors: *R. N. SMITH**, N. SPITZER;
Dept. of Biol. Sci., Marshall Univ., Huntington, WV

**Abstract:** Antimicrobial silver nanoparticles (AgNPs) are released into the environment during manufacturing and usage of products including toys, cosmetics, and surgical tools. Because of their unique physical properties, AgNPs cross the blood-brain barrier, bioaccumulate in the brain, and persist for months with no clearance. At the cellular level, this prolonged bioaccumulation disrupts critical elements underlying synaptic plasticity. We previously found that AgNP exposure induced synaptic decoupling *in vivo*. Synapses are strengthened through activation of the N-methyl-D-aspartate receptor (NMDAR) which anchors to postsynaptic density protein-95 (PSD-95), driving calcium ($Ca^{2+}$) influx. Given our previous findings that

AgNP exposure disrupts synaptic coupling, we investigated if AgNP exposure impedes NMDAR anchoring with PSD-95. Male and female Sprague Dawley rats were orally exposed to AgNPs emulsified in 10% sucrose for nine consecutive weekdays at control, low (25 mg/kg) or high (100 mg/kg) dosages to achieve brain silver levels consistent with estimated environmental exposure. One set of brains was collected one day after treatment to investigate acute effects. The second set of brains was collected after one month with no additional exposure to investigate the effect of bioaccumulated AgNPs. Using immunohistochemistry for NMDAR and PSD-95, their colocalization was quantified to assess NMDAR anchoring. After acute AgNP exposure the proportion of NMDARs colocalized with PSD-95 significantly increased in a dose-dependent manner. However, in rats exposed to bioaccumulated AgNP, colocalization was reduced. $Ca^{2+}$ entry through NMDARs must be tightly regulated as excessive $Ca^{2+}$ can become toxic and insufficient $Ca^{2+}$ promotes synaptic pruning. An inability to anchor could disrupt the mechanisms underlying learning and memory. Because excessive anchoring of NMDARs could contribute to $Ca^{2+}$ toxicity, leading to apoptosis, we quantified cleaved caspase-3 in the hippocampus of rats exposed to AgNPs. Immunoblot analysis revealed an increase in cleaved caspase-3 after acute and bioaccumulated AgNP exposure. Because cleaved caspase-3 remained elevated after bioaccumulated AgNP, the reduction in colocalizations could be attributed to apoptosis due to excessive $Ca^{2+}$ influx. These findings suggest that environmental exposure to AgNPs may interfere with synaptic plasticity and activate cellular mechanisms associated with apoptosis. As AgNPs continue to be released into the environment through manufacturing and usage of everyday products, these data emphasize the importance of informing the regulation of their usage and disposal.

**Disclosures: R.N. Smith:** None. **N. Spitzer:** None.

**Poster**

**PSTR177: Cellular Stress and Mechanisms of Degeneration**

**Location:** WCC Halls A-C

**Time:** Monday, November 16, 2026, 1:00 PM - 5:00 PM

**Program #/Poster #:** PSTR177.08/V23

**Topic:** D.01. Neurotoxicity, Inflammation, and Neuroprotection

**Title:** Micro- and Nanoplastics exposure worsens Alzheimers Disease pathology in APP/PSEN1 mice

**Authors: *M. PAVLIK**, L. GASPAR, G. COPPOTELLI, J. M. ROSS;
Univ. of Rhode Island, Kingston, RI

**Abstract:** Alzheimer's disease and related dementias (AD/ADRD) are one of the most prevalent cognitive disorders, affecting more than 6 million Americans over the age of 65. While the exact cause of AD and ADRD is still unknown, several risk factors have been identified, including genetic predisposition, lifestyle factors, and exposure to environmental toxins. In recent years, micro- and nanoplastics (MNPs), defined as plastic particles $\leq 1$ μm and $\leq 5$ mm in size, respectively, have emerged as pervasive environmental pollutants. Previous studies have shown

that MNPs can accumulate in peripheral tissues throughout the bodies of both humans and mice, raising concerns about their potential health impacts, as emerging evidence suggests they may induce inflammation, oxidative stress, and disruption of metabolic and endocrine functions following exposure through ingestion, inhalation, or dermal contact. Furthermore, MNPs have been demonstrated to cross the blood-brain barrier to accumulate through the brain, resulting in alterations in cognitive behavior and immune markers consistent with neurological disease. Consistent with this, we have previously demonstrated that short-term exposure to MNPs via drinking water (as little as three weeks) impairs cognitive function in both young and aged mice, as well as in mice carrying the APOE4 allele, the strongest genetic risk factor for sporadic Alzheimer's disease, in a sex-dependent manner. We further showed that MNPs exposure induces inflammatory responses and alters GFAP expression in the brain, suggesting a mechanistic link between environmental plastic exposure and brain pathology. Building on these findings, in the present study we investigated the effects of MNPs exposure in a transgenic mouse model of Alzheimer's disease pathology (APP/PSEN1). Following chronic exposure (3 months) to pristine polystyrene particles of 0.1 μm and 2 μm, APP/PSEN1 mice exhibited a significant increase in amyloid plaque burden. This was accompanied by exacerbated cognitive deficits, as well as reductions in synaptic density and increased immune cell death, collectively indicating that MNP exposure may accelerate key pathological features associated with Alzheimer's disease progression.

**Disclosures: M. Pavlik:** None. **L. Gaspar:** None. **G. Coppotelli:** None. **J.M. Ross:** None.

**Poster**

**PSTR177: Cellular Stress and Mechanisms of Degeneration**

**Location:** WCC Halls A-C

**Time:** Monday, November 16, 2026, 1:00 PM - 5:00 PM

**Program #/Poster #:** PSTR177.09/V24

**Topic:** D.01. Neurotoxicity, Inflammation, and Neuroprotection

**Support:** AMED-PRIME JP24gm6910013
AMED-MS7 JP24zf0127010
JSPS Research Fellowship 26KJ1474
Kyoto University Medical Innovation Graduate Program (MIP)

**Title:** Convergent maternal immune activation and peripubertal stress disrupt cerebellar learning via microglial epigenetic remodeling of Purkinje cells.

**Authors: *M. HIKOSAKA**[1], N. HOSOI[3], A. KATOH[4], K. KOBAYASHI[5], K. UEMURA[6], H. HIRAI[7], S. NARUMIYA[8], G. OHTSUKI[2];
[2]Dept. of Drug Discovery Med., [1]Kyoto Univ., Kyoto, Japan; [3]Dept. of Neurophysiol. and Neural Repair, Gunma Univ. Grad. Sch. of Med., Maebashi, Japan; [4]Physiol., Tokai University, Sch. of Med., Isehara, Japan; [5]Natl. Inst. For Physiological Sci., Okazaki, Japan; [6]Kyoto Univ. Grad. Sch. of Med., Kyoto-shi, Kyoto, Japan; [7]Gunma Univ. Grad Sch. of Med., Maebashi, Japan; [8]Kyoto Univ. Facul.Med., Kyoto, Japan

**Abstract:** Prenatal and developmental stress disrupt neural network functioning, cumulatively increasing the risk for neuropsychiatric disorders later in life. However, how cumulative developmental stress impairs cognition and learning remains elusive. The cerebellum, traditionally associated with motor coordination and learning, is now recognized to contribute to higher cognitive functions. Here, we investigated how cumulative inflammatory stress alters neural function using a two-hit (2HIT) mouse model combining maternal immune activation (MIA) and repeated social defeat stress (RSDS). We previously demonstrated cerebellum-specific microglial activation in 2HIT mice (Hikosaka et al., 2025, Communications Biology, PMID: 40033126). To further investigate how reactive microglia influence cerebellar function, we examined cerebellar-dependent learning and Purkinje cell physiology. 2HIT mice displayed impaired learning accompanied by reduced spine density, decreased synaptic transmission, attenuated $Ca^{2+}$ responses, and deficits in both synaptic and intrinsic plasticity. Importantly, microglial replacement rescued these abnormalities, indicating a causal contribution of reactive microglia to cerebellar dysfunction. To investigate the underlying mechanisms, we performed Purkinje cell-specific Patch-seq and ATAC-seq analyses. These analyses revealed coordinated alterations in gene expression and chromatin accessibility associated with impaired neuronal excitability and dendritic structure, indicating stress-induced epigenetic remodeling in Purkinje cells. Together, our findings suggest reactive microglia as key mediators linking developmental stress to long-lasting cerebellar dysfunction through epigenetic reprogramming of Purkinje cells, revealing a microglia-neuron epigenetic axis as a potential therapeutic target for stress-associated neuropsychiatric disorders.

**Disclosures: M. Hikosaka:** None. **N. Hosoi:** None. **A. Katoh:** None. **K. Kobayashi:** None. **K. Uemura:** None. **H. Hirai:** None. **S. Narumiya:** None. **G. Ohtsuki:** None.

**Poster**

**PSTR177: Cellular Stress and Mechanisms of Degeneration**

**Location:** WCC Halls A-C

**Time:** Monday, November 16, 2026, 1:00 PM - 5:00 PM

**Program #/Poster #:** PSTR177.10/V25

**Topic:** D.01. Neurotoxicity, Inflammation, and Neuroprotection

**Title:** GasderminD (GSDMD)-tagged Mitochondrion Propagates Neuroinflammation in Parkinson's Disease

**Authors: *E. R. KADIRI**;
Case Western Reserve Univ., Cleveland, OH

**Abstract:** Parkinson’s disease (PD) is a neurodegenerative disease characterized by chronically impaired motor deficits, caused by the death of dopaminergic neurons in the ventral midbrain. It has been established that, along with neuron death, mitochondrial dysfunction and increased brain inflammation are hallmarks of PD. Microglia are the brain’s resident immune cells that initiate and regulate inflammation. The Nod-like Receptor Protein 3 (NLRP3) inflammasome has been shown to be a major pathway of brain inflammation, although the mechanisms by which it

accelerates the disease course remain under-characterized. Specifically, the NLRP3 inflammasome is assembled in response to the pattern recognition of pathogen-associated molecular patterns (PAMPs), such as bacteria and viruses, and damage-associated molecular patterns (DAMPs), such as defective mitochondria. Neuron-released alpha-synuclein (α-syn) aggregates, characteristic of PD, expedite mitochondrial dysfunction, inducing NLRP3 activation, thereby triggering the subsequent secretion of pro-inflammatory cytokines and the proteolytic activation of an enzyme known as caspase-1 (casp1). Casp1 cleaves the pore-forming protein, gasdermin-D (GSDMD), which then induces inflammatory cell death by embedding and forming pores in cell membranes. Our work aims to assess the method by which GSDMD could escalate the spread of neuroinflammation in PD models by translocating to and creating pores within microglial mitochondria. Our hypothesis explores the idea that extracellular vesicles (EVs) export damaged mitochondria and cytokines to neighboring cells to propagate neuroinflammation in PD models. Overall, deducing the mitochondrial roles of GSDMD in microglia will provide the potential to establish treatments that target GSDMD-induced inflammation and improve outcomes of PD patients.

**Disclosures: E.R. Kadiri:** None.

**Poster**

**PSTR177: Cellular Stress and Mechanisms of Degeneration**

**Location:** WCC Halls A-C

**Time:** Monday, November 16, 2026, 1:00 PM - 5:00 PM

**Program #/Poster #:** PSTR177.11/V26

**Topic:** D.01. Neurotoxicity, Inflammation, and Neuroprotection

**Support:** Ralph W. and Grace M. Showalter Research Trust

**Title:** Persistent, sex-divergent neurodegenerative molecular signatures in the adult rat brain following a single PFOS exposure

**Authors: *P. BALONI**, J. R. CANNON, J. PARK;
Sch. of Hlth. Sci., Purdue Univ., West Lafayette, IN

**Abstract:** Background: Perfluorooctane sulfonate (PFOS) is a persistent environmental contaminant detected in human population worldwide, with documented neurotoxicity and epidemiological links to cognitive impairment and Alzheimer's disease (AD). Whether a single PFOS exposure can cause persistent sex-specific effects, and exhibit neurodegeneration-like molecular signatures in the adult brain, remains unknown. Methods: We administered a single oral dose of PFOS (10 mg/kg) to adult Sprague-Dawley rats (n=3/sex/timepoint; N=30) and collected whole-brain tissue at days 1, 3, 28, and 112 post-exposure. Bulk RNA-sequencing was followed by DESeq2 differential gene expression analysis, Gene Set Enrichment Analysis across GO-BP, KEGG, and Reactome databases, and Expression-Weighted Cell-Type Enrichment (EWCE) using a whole-brain single-cell reference. Results: By Day 112, male and female transcriptomic responses had diverged almost completely, sharing only 10 differentially

expressed genes (DEGs). Females showed persistent, coordinated suppression of mitochondrial oxidative phosphorylation and respiratory chain complex assembly across all four timepoints, along with suppression of ubiquitin-proteasome system (UPS) components at all three proteostasis layers (RNA processing, translation/folding, and protein disposal), partially compensated by lysosomal upregulation. At pathway-level, the DEGs drove significant downregulation of KEGG neurodegenerative disease pathways (Alzheimer, Parkinson, ALS, Huntington) at Day 112. Males showed no mitochondrial suppression at Day 112; instead, they showed persistent activation of RNA splicing machinery, broad suppression of glutamatergic, GABAergic, dopaminergic, and cholinergic synaptic pathways, complement cascade activation, and upregulation of the proteasome, but lysosomal collapse and loss of amyloid-β handling. Brain cell type enrichment analysis identified delayed microglial activation in females and astrocytic/BBB enrichment in males at Day 112, indicating sex-specific neuroinflammatory trajectories. Conclusion: These findings demonstrate that a single PFOS exposure produces persistent, sex-divergent molecular changes that persist more than 16 weeks post-exposure. PFOS exposure leading to dysregulation of mitochondrial functions, proteostasis failure, neuroinflammation, and synaptic dysfunction are concordant with the hallmarks of neurodegeneration. This work advances understanding of environmental PFAS neurotoxicity and highlights biological sex as a critical determinant of vulnerability to PFOS-induced neurodegeneration-like brain changes.

**Disclosures: P. Baloni:** None. **J.R. Cannon:** None. **J. Park:** None.

**Poster**

**PSTR177: Cellular Stress and Mechanisms of Degeneration**

**Location:** WCC Halls A-C

**Time:** Monday, November 16, 2026, 1:00 PM - 5:00 PM

**Program #/Poster #:** PSTR177.12/V27

**Topic:** D.01. Neurotoxicity, Inflammation, and Neuroprotection

**Support:** RS-2025-25459402
RS-2025-16070516

**Title:** Targeting Aurora kinase as a key modulator of neurotoxic macrophage phenotype to prevent post-stroke secondary neurodegeneration

**Authors: *Y. SEO**[1,2], S. JEE[1,2], H. KIM[1], B. G. KIM[1,2];
[1]Ajou university, Suwon-Si, Korea, Republic of; [2]Neurosci. Grad. Program, Dept. of Biomedical, Ajou university graduate schoold of medicine, Suwon-si, Korea, Republic of

**Abstract:** Macrophages are double-edged swords in the post-stroke environment, contributing to both neuroregeneration and neurodegeneration, yet the molecular switches driving their neurotoxic transition remain elusive. We previously showed that the neurotoxic potential of macrophages toward cultured cortical neurons is markedly attenuated when they are co-cultured with dorsal root ganglia neurons. RNA sequencing revealed that this neuroprotective shift is

accompanied by robust upregulation of cell cycle-related pathways in macrophages, and bioinformatic analysis identified Aurora kinase (AURK) as a central regulatory hub. Functional studies underscored the importance of AURK, as pharmacological and RNAi-mediated inhibition reversed the attenuation of macrophage neurotoxicity by the co-culture paradigm. Macrophage colony-stimulating factor (MCSF) was used to increase AURK expression in macrophages, and MCSF-treated macrophages showed a substantial reduction in neurotoxicity toward cortical neurons. *In vivo*, temporal profiling of FACS-sorted brain macrophages showed that AURK expression is markedly suppressed by 7 days post-stroke, coinciding with peak induction of the senescence marker p21. Consistent with these findings, integrative single-cell RNA sequencing results from publicly available datasets on stroke mouse models also showed that the proliferating macrophage subcluster exhibits higher expression of AURKs, accompanied by a decrease in p21 expression. In a mouse photothrombotic stroke model, splenectomy conducted 2 weeks prior to stroke induction led to a reduction of infarct volume, whereas intravenous splenocyte reconstitution exacerbated infarction, confirming the neurotoxic role of macrophages infiltrating into the brain. This exacerbation was markedly blunted when transplanted splenocytes were engineered to overexpress AURK, indicating that AURK activation may enable macrophage reprogramming, thereby reducing the neurotoxic phenotype and limiting inflammation-related post-stroke brain damage. Collectively, these findings identify AURK as a key modulator of macrophage-mediated neurotoxicity and suggest that targeting AURK signaling may offer a therapeutic strategy to limit post-stroke secondary neurodegeneration

**Disclosures: Y. Seo:** None. **S. Jee:** None. **H. Kim:** None. **B.G. Kim:** None.

**Poster**

**PSTR177: Cellular Stress and Mechanisms of Degeneration**

**Location:** WCC Halls A-C

**Time:** Monday, November 16, 2026, 1:00 PM - 5:00 PM

**Program #/Poster #:** PSTR177.13/V28

**Topic:** D.01. Neurotoxicity, Inflammation, and Neuroprotection

**Title:** Advanced Modeling of Amyotrophic Lateral Sclerosis Using a Human iPSC-Derived Motor Neuron, Astrocyte, and Microglia Tri-culture System

**Authors: *M. BSIBSI**[1], C. LOOMANS[1], L. VAN BEEK[1], N. CHUNDURI[1], H. RUETH[2], M. L. HENDRICKSON[2], A.-M. ZUURMOND[1];
[1]IQVIA Labs., Leiden, Netherlands; [2]BrainXell, Madison, WI

**Abstract:** Amyotrophic lateral sclerosis (ALS) is a progressive and complex neurodegenerative disease primarily characterized by the degeneration of motor neurons, with increasing recognition of critical contributions from non-neuronal cells, particularly astrocytes and microglia, in disease progression. A major challenge in ALS drug discovery is the limited translational success of candidate therapeutics, largely attributed to existing models—including simplified in vitro systems and animal models—that fail to recapitulate the multicellular

interactions and dynamic microenvironment present in vivo. Consequently, more physiologically relevant and complex in vitro models incorporating multiple disease-relevant cell types are needed to better mimic ALS pathology. Such advanced systems offer improved platforms for early-stage drug discovery and may reduce reliance on animal models. In this study, we established a physiologically relevant multicellular co-culture model comprising iPSC-derived motor neurons, astrocytes, and microglia. Co-cultures were generated using both wild-type (WT) cells and cells harbouring the ALS-associated TDP-43 G298S mutation. Mislocalization and aggregation of the RNA-binding protein TDP-43 represent key pathological hallmarks of ALS and central targets for therapeutic intervention. Cellular stress was induced using puromycin and the proteasome inhibitor MG132 to drive TDP-43 pathology. High-content imaging was employed to quantify TDP-43 nuclear-to-cytoplasmic translocation and aggregation, while loss of TDP-43 function was assessed by measuring mis-spliced truncated STMN2 transcripts via qPCR. In addition, multiparametric analyses were performed using cell type-specific markers to characterize phenotypic changes across neurons, astrocytes, and microglia in both WT and mutant conditions. Importantly, this multicellular co-culture system more effectively recapitulates key aspects of ALS pathobiology compared to traditional monoculture models, providing a more predictive and disease-relevant platform for therapeutic evaluation. By incorporating multicellular complexity and disease-relevant stressors, this model has the potential to enhance early-stage screening, improve translational success rates, and reduce attrition in central nervous system drug discovery

**Disclosures: M. Bsibsi:** None. **C. Loomans:** None. **L. van Beek:** None. **N. Chunduri:** None. **H. Rueth:** None. **M.L. Hendrickson:** None. **A. Zuurmond:** None.

**Poster**

**PSTR177: Cellular Stress and Mechanisms of Degeneration**

**Location:** WCC Halls A-C

**Time:** Monday, November 16, 2026, 1:00 PM - 5:00 PM

**Program #/Poster #:** PSTR177.14/W1

**Topic:** D.01. Neurotoxicity, Inflammation, and Neuroprotection

**Support:** NIH RO1 AC-M, NIMH, 7R01MH129732-04
NARSAD Young Investigator Grant (AC-M, #27202)
Startup Fund Anesthesiology Department CU Anschutz

**Title:** Sparse Complement C4 Dysregulation Drives Transcriptomic and Lipid Metabolic Alterations in the Prefrontal Cortex

**Authors: *J. E. AVILA PAGAN**[1], M. SANCHEZ CARBONELL[2], S. BOLSHAKOVA[6], Y. SABIR[3], S. CIESLEWICZ[4], A. HASCHE-KLUENDER[5], A. CRUZ-MARTIN[7];
[1]Human Med. Genet. and Genomics, Univ. of Colorado: Anschutz Med. Campus, Denver, CO; [2]Anesthesiol., Univ. of Colorado: Anschutz Med. Campus, BOULDER, CO; [3]Univ. of Colorado: Anschutz Med. Campus, Aurora, CO; [4]Univ. of Colorado: Anschutz Med. Campus, Morrison,

CO; [5]Univ. of Colorado: Anschutz Med. Campus, Denver, CO; [6]Broad Inst., Cambridge, MA; [7]Anesthesiol., Univ. of Colorado, Anschutz Med. Campus, Denver, CO

**Abstract:** In the brain, the immune complement pathway (CP) is a molecular cascade that recruits microglia to tag and eliminate unwanted synapses, debris, and pathogens, thereby playing a vital role in maintaining brain homeostasis throughout our lifespan. The CP has also been shown to influence synaptic plasticity and circuit refinement in the brain. Although complement dysregulation has been linked to various neurological and psychiatric disorders, it remains unclear how localized increases in complement activity within a small group of cells affect gene regulation across larger cortical populations. To investigate this, we overexpressed the schizophrenia (SCZ) risk gene C4 in about 2% of prefrontal cortex neurons in mice through in utero electroporation. Bulk RNA sequencing of microdissected tissue revealed widespread transcriptional changes, predominantly in untransfected cells, indicating non-cell-autonomous effects of C4 overexpression (C4-OE). Sparse C4-OE led to increased expression of genes involved in cholesterol biosynthesis, axon guidance, synaptic plasticity, cytoprotection, and neurogenesis, suggesting compensatory remodeling or abnormal plasticity. Co-expression analysis identified a C4b-containing gene module rich in genes related to dendritic development and cell cycle regulation, indicating altered circuit maturation, while immune and inflammatory gene programs were broadly suppressed, reflecting homeostatic downregulation in response to sustained complement activity. Reference-based projection of DEG signatures onto cortical single-cell transcriptomic atlases further revealed astrocyte-associated transcriptional remodeling, while MFISH and PLIN2 imaging extended these findings beyond bulk RNA-seq by showing increased *Hmgcr1* expression and increased PLIN2-positive lipid-droplet burden in neighboring GFP-negative cells. Together, these findings demonstrate that sparse neuronal C4 upregulation is sufficient to reorganize transcriptional and lipid-associated programs across the local cortical microenvironment. In addition, this work suggests altered cholesterol biosynthesis and LD burden as a candidate mechanism linking complement-associated circuit remodeling to schizophrenia.

**Disclosures: J.E. Avila Pagan:** None. **M. Sanchez Carbonell:** None. **S. Bolshakova:** None. **Y. Sabir:** None. **S. Cieslewicz:** None. **A. Hasche-Kluender:** None. **A. Cruz-Martin:** None.

**Poster**

**PSTR177: Cellular Stress and Mechanisms of Degeneration**

**Location:** WCC Halls A-C

**Time:** Monday, November 16, 2026, 1:00 PM - 5:00 PM

**Program #/Poster #:** PSTR177.15/W2

**Topic:** D.01. Neurotoxicity, Inflammation, and Neuroprotection

**Support:** Department of Defense
Eye and Ear Foundation of Pittsburgh
The Alcon Research Institution Young Investigator Award

**Title:** Immunomodulation by Matrix-Bound Nanovesicle and Fluvastatin Combination Therapy Promotes Retinal Ganglion Cell Survival and Axon Regeneration

**Authors: *K. M. HENRY**[1], D. RAJASUNDARAM[2], T. KUWAJIMA[3];
[1]Ophthalmology, Univ. of Pittsburgh, Pittsburgh, PA; [2]Pediatrics, Univ. of Pittsburgh, Sewickley, PA; [3]Dept. of Ophthalmology, Univ. of Pittsburgh, Pittsburgh, PA

**Abstract:** Retinal ganglion cells (RGCs) undergo progressive degeneration following ocular trauma and optic neuropathies, such as glaucoma, resulting in irreversible vision loss due to the limited regenerative capacity of the adult central nervous system. To identify novel therapeutics that promote optic nerve regeneration after optic nerve injury, our previous *in vitro* drug screening identified statins (HMG-CoA reductase inhibitors) as compounds that enhance axon regeneration by overcoming axonal inhibition of factors, such as myelin-associated glycoprotein. Our independent studies have shown that matrix-bound nanovesicles (MBV), extracellular matrix-derived nanoparticles, provided neuroprotective effects in an animal model of glaucoma. In this study, we investigated whether a combination of two different FDA-approved reagents, MBV and fluvastatin, the second most effective statin for axon outgrowth *in vitro* and remains clinically available, synergistically enhances RGC survival and axon regeneration following optic nerve crush (ONC) in adult C57BL/6 mice. We performed ONC followed by intravitreal injections of phosphate-buffered saline, MBV, fluvastatin, or MBV plus fluvastatin, a few minutes and two days after ONC. RGC survival was quantified by immunolabeling, and axonal regeneration was assessed by cholera toxin B anterograde axon tracing. To gain altered molecular signatures induced by the single and combined treatments, transcriptome sequencing in the retina was performed three days after injury. We found that the combined treatments provided greater neuroprotective and regeneration effects than either therapy alone two weeks after ONC. Transcriptomic analysis identified DEGs unique to the combined treatment, compared to either MBV or fluvastatin, and these DEGs were associated with immune responses. We also found that specific immune cell infiltration mediates RGC protection and axon regeneration. These findings demonstrate that MBV and fluvastatin act together to promote RGC survival and axon regeneration via enhancing recruitment of specific immune cells, suggesting that modulation of pro-regenerative immune responses may represent a novel strategy for promoting neuroprotection and optic nerve regeneration in injury/disease of the eye.

**Disclosures: K.M. Henry:** None. **D. Rajasundaram:** None. **T. Kuwajima:** E. Ownership Interest (stock, stock options, royalty, receipt of intellectual property rights/patent holder, excluding diversified mutual funds); Filed a patent application related to matrix-bound nanovesicle/statin work.

**Poster**

**PSTR177: Cellular Stress and Mechanisms of Degeneration**

**Location:** WCC Halls A-C

**Time:** Monday, November 16, 2026, 1:00 PM - 5:00 PM

**Program #/Poster #:** PSTR177.16/W3

**Topic:** D.01. Neurotoxicity, Inflammation, and Neuroprotection

**Support:** R01 DK124098-01A1
DOD - NETP - 13204752
R01 NS104565

**Title:** Comparison of inflammation and autophagy markers in two rat models exhibiting dopaminergic cell loss

**Authors: *K. VENKITESWARAN**[1], S. SENAPATI[2], M. RAMI REDDY[3], R. RIZWAN[4], C. C. SWAIN[5], V. V. PESHATTIWAR[8], D. POKHAREL[9], D. H. BELIGALA[10], I. KENNEDY[6], M. P. SUBRAMANIAN[3], K. ZAIDAT[11], K. M. LE[8], A. KIM[12], P. S. GRIGSON[13], T. SUBRAMANIAN[7,8];
[1]Intrnl. Med., Howard Univ. COM, Washington, DC; [2]Univ. of Toledo Col. of Med., Toledo, OH; [3]Univ. of Toledo, Toledo, OH; [4]Univ. of Toledo, Buford, GA; [5]Dept. of Neurosciences, [6]Univ. of Toledo Col. of Med. and Life Sci., Toledo, OH; [7]Neurology, Neurosci. and Bioengineering, Univ. of Toledo Col. of Med. and Life Sci., Maumee, OH; [8]Neurol., Howard Univ., Washington, DC; [9]Howard Univ. Col. of Med., Toledo, OH; [10]Ohio Northern Univ., Perrysburg, OH; [11]Univ. of Texas Southwestern Med. Ctr., Dallas, TX; [12]Pennsylvania State Col. of Med., Hershey, PA; [13]Neural and Behavioral Sci., Penn State Col. of Med., Hershey, PA

**Abstract:** We have demonstrated that there is loss of dopamine neurons in VTA of a high dose cocaine self-administering rat model. We also observed that there is selective neurodegeneration in substantia nigra pars compacta in the oral Paraquat and lectin - induced Parkinsonian rat model. Here we compare the inflammatory responses in these two models of DAergic neuronal loss. The P+L model during degeneration shows inflammatory astroglia (GFAP) and activated microglia (OX42). Similarly in the high drug cocaine intaking rat model exhibit astrogliosis associated inflammation and dopamine neuronal loss in the VTA region specifically. Both models show changes in expression of autophagy markers LC3b, Beclin and LAMP2A. Despite the adjacency of the two structures VTA and SNpc exhibit inflammation and neuronal loss that is specific to that nucleus in each condition while sparing the other. This raises an interesting observation that inflammation and autophagic markers are sequestered adj to neuronal injury and does not spread into adjacent structures. Additional studies to seek what additional protective factors preventing inflammation in these dopaminergic nuclei need to be evaluated.

**Disclosures: K. Venkiteswaran:** None. **S. Senapati:** None. **M. Rami Reddy:** None. **R. Rizwan:** None. **C.C. Swain:** None. **V.V. Peshattiwar:** None. **D. Pokharel:** None. **D.H. Beligala:** None. **I. Kennedy:** None. **M.P. Subramanian:** None. **K. Zaidat:** None. **K.M. Le:** None. **A. Kim:** None. **P.S. Grigson:** None. **T. Subramanian:** None.

**Poster**

**PSTR177: Cellular Stress and Mechanisms of Degeneration**

**Location:** WCC Halls A-C

**Time:** Monday, November 16, 2026, 1:00 PM - 5:00 PM

**Program #/Poster #:** PSTR177.17/W4

**Topic:** D.01. Neurotoxicity, Inflammation, and Neuroprotection

**Title:** Comparative Neurotoxicological Assessment of Environmental-like Nanoplastics Detected in Human Brain

**Authors: *J. VALERA-VEGA**[1], T. MALANKHANOVA[2], A. B. WEST[3];
[1]Pharmacol. and Cancer Biology, Integrated Toxicology and Envrn. Hlth. Program, [3]Pharmacol., [2]Duke Univ., Durham, NC

**Abstract:** Micro- and nanoplastics are increasingly recognized as persistent environmental contaminants with potential relevance to human health. Recent reports detecting plastic particles in human tissues, including the brain, raise important questions about whether environmentally relevant nanoplastics can affect neuroimmune function or neuronal viability. However, most experimental studies of nanoplastic toxicity have relied on pristine manufactured nanobeads, particularly polystyrene beads, that poorly model the irregular morphology, polymer diversity, surface oxidation, and chemical complexity of weathered environmental particles.To address this gap, we developed a production and characterization pipeline for environmental-like nanoplastics derived from polymer materials detected in human tissue and shaped by mechanical fragmentation and weathering. Here, we will compare the neurotoxicity profiles of these weathered nanoplastic fragments with those of conventional manufactured nanoplastic beads using an in vitro microglia-neuron co-culture platform. We will evaluate microglial activation, inflammatory mediator release, and the downstream effects of microglia-conditioned media on neuronal viability. Comparative analyses will determine whether polymer composition, weathering state, and particle morphology influence neuroimmune activation or neurotoxicity.This study is designed to test whether pristine manufactured nanobeads accurately represent the biological effects of environmental-like nanoplastics detected in the human brain, and to identify particle types most strongly associated with microglial inflammatory responses and neuronal injury. These findings will help prioritize nanoplastic materials for mechanistic studies and future in vivo exposure models, while providing a more physiologically relevant framework for evaluating potential neurotoxic risks of human nanoplastic exposure.

**Disclosures: J. Valera-Vega:** None. **T. Malankhanova:** None. **A.B. West:** None.

**Poster**

**PSTR177: Cellular Stress and Mechanisms of Degeneration**

**Location:** WCC Halls A-C

**Time:** Monday, November 16, 2026, 1:00 PM - 5:00 PM

**Program #/Poster #:** PSTR177.18/W5

**Topic:** D.01. Neurotoxicity, Inflammation, and Neuroprotection

**Support:** NIH grants R01NS97846, R01NS097846-02S1, R01NS092876 and NIAAA of NIH grant R01AA031319 to MS

**Title:** Biomarkers for Oligodendrocyte Injury in Fetal Brain-Derived Oligodendrocyte-Specific Exosomes as Early Indicators of Fetal Alcohol Spectrum Disorders.

**Authors:** ***U. BHARAI**[1], N. DARBINIAN[2], M. HAMPE[1], L. DRAK[1], J. HAMZE[4], J. HU[1], E. OLIVER[1], R. MOSSABEB[3], M. MORRISON[1], L. HART[1], M. E. SELZER[5], T. SA NGUANPHO[1], H. ZHAO[4];
[2]Dept. of Neural Sci., [1]Temple Univ., Philadelphia, PA; [3]Temple Univ., White Non-Hispanic, PA; [4]Lewis Katz Sch. of Med. at Temple Univ., Philadelphia, PA; [5]Neural Sci., Lewis Katz Sch. of Med. At Temple Univ., Philadelphia, PA

**Abstract: Introduction**. OL-neuron communication plays a critical role in myelin sheath and axonal development, neuronal support, and neurotrophic signaling during fetal brain maturation. Prenatal alcohol exposure disrupts these interactions, yet early, non-invasive biomarkers of such alterations remain limited. This study investigates OL proteins involved in OL-neuron communication within fetal brain-derived exosomes (FB-Es) isolated from maternal blood as potential early predictors of fetal alcohol spectrum disorders (FASD). **Methods**. FB-Es were isolated using neural-specific immunoaffinity and OL-specific markers and analyzed for mature OL signature proteins regulating OL injury, using qRT-PCR and ELISA for MBP and other targets. **Results**. Preliminary findings reveal significant dysregulation of key OL-neuron biomarkers, including MBP, in pregnancies exposed to alcohol compared with controls, reflecting early impairments in OL-neuronal crosstalk, myelin sheath, and axonal maturation. Changes in MBP expression were correlated with changes in fetal eye diameter, a characteristic feature of FASD.**Conclusions**. These results support the feasibility of using FB-E/OL-E biomarkers as novel, non-invasive markers for early detection of FASD, providing insight into the cellular mechanisms underlying alcohol-induced disruptions in fetal brain development.

**Disclosures: U. Bharai:** None. **N. Darbinian:** None. **M. Hampe:** None. **L. Drak:** None. **J. Hamze:** None. **J. Hu:** None. **E. Oliver:** None. **R. mossabeb:** None. **M. Morrison:** None. **L. Hart:** None. **M.E. Selzer:** None. **T. Sa Nguanpho:** None. **H. Zhao:** None.

**Poster**

**PSTR177: Cellular Stress and Mechanisms of Degeneration**

**Location:** WCC Halls A-C

**Time:** Monday, November 16, 2026, 1:00 PM - 5:00 PM

**Program #/Poster #:** PSTR177.19/W6

**Topic:** D.01. Neurotoxicity, Inflammation, and Neuroprotection

**Title:** Genetic ablation of SARM1 reduces axon degeneration, whereas acute SARM1 Inhibition preserves function in TDP-43-driven ALS models

**Authors:** S. VITO[1], D. REID[1], R. M. REESE[4], S. HUR[2], M. WEBER[5], ***F. I. HINZ**[3];
[2]Neurosci. department, [3]Neurosci., [1]Genentech Inc., South San Francisco, CA; [4]Neurosci., Genentech, South San Francisco, CA; [5]Dept. of Neurosci., Genentech Inc, South San Francisco, CA

**Abstract:** Amyotrophic Lateral Sclerosis (ALS) is driven by progressive loss of upper and lower motor neurons resulting in highly elevated neurofilament light chain (NfL) plasma levels and

rapid motor function decline and death. TAR DNA-binding protein 43 (TDP-43) aggregates are found in ~97% of ALS patient postmortem tissue, which through both loss and gain of function mechanisms, result in deficits in axon trafficking and mitochondrial dysfunction. SARM1, a metabolically regulated NADase, has recently been identified as the key driver of axon degeneration. Both human genetics and ALS pathology indicate that SARM1 activation may contribute to ALS disease progression, making SARM1 a relevant target. Therefore, we investigated the effect of SARM1 loss in two TDP-43 overexpression driven preclinical models of ALS: 1) the developmental TAR4/4 model, in which human wt TDP-43 is overexpressed from the Thy1 promoter and 2) the inducible rNLS8 model, in which human TDP-43 lacking the nuclear localization sequence leads to cytoplasmic TDP-43 aggregation. In both models we find that SARM1 KO reduces plasma NfL levels by approximately 50% at peak and ameliorates histological axon degeneration. However, SARM1 KO does not improve survival or motor function in the TAR4/4 model. Similarly, SARM1 KO does not improve compound muscle action potential or behavioral motor function in the rNLS8 model. Surprisingly, we find that treatment with a SARM1 small molecule inhibitor in the rNLS8 model leads not only to significant plasma NfL reduction, but also to a dose dependent improvement in motor function. These findings indicate that germline SARM1 KO animals may have developmental compensatory mechanisms which mask potential neuroprotective effects of acute SARM1 inhibition in chronic models of neurodegeneration and provide additional support that SARM1 may be a relevant target for neuroprotection.

**Disclosures: S. Vito:** None. **D. Reid:** None. **R.M. Reese:** None. **S. Hur:** None. **M. Weber:** None. **F.I. Hinz:** None.

**Poster**

**PSTR177: Cellular Stress and Mechanisms of Degeneration**

**Location:** WCC Halls A-C

**Time:** Monday, November 16, 2026, 1:00 PM - 5:00 PM

**Program #/Poster #:** PSTR177.20/W7

**Topic:** D.01. Neurotoxicity, Inflammation, and Neuroprotection

**Title:** Mechanistic understanding of the role of microtubules in the onset of Paclitaxel-induced peripheral neuropathy

**Authors: *A. BARDHAN**[1], M. MAGIERA[2], P. PULLARKAT[3], C. JANKE[2], A. GHOSE[4]; [1]Biol., Indian Inst. of Sci. Educ. and Research, Pune, Pune, India; [2]Genome Integrity, RNA and Cancer (UMR3348), Inst. Curie, Orsay, France; [3]Soft and condensed matter, Raman Res. Inst., Bengaluru, India; [4]Biol., IISER Pune, Pune, India

**Abstract:** Chemotherapy-induced peripheral neuropathy (CIPN) is a common and dose-limiting side effect of cancer treatment. Paclitaxel (PTX), a widely used chemotherapeutic drug, frequently causes sensory neuropathy, but the underlying mechanisms remain poorly understood. Because PTX targets microtubules, we investigated whether alterations in the tubulin post-translational modifications (PTMs) contribute to PTX-induced neurotoxicity.To investigate these

mechanisms, we employed primary adult mouse dorsal root ganglion (DRG) neurons, cell types primarily affected in CIPN patients, and examined the impact of PTX on tubulin PTMs in the onset of neuropathy. We find that chronic in vitro PTX exposure induced focal axonal swellings (FAS) and lysosomal accumulation, hallmarks of axonal neurodegeneration. These pathological changes were accompanied by a marked increase in Delta2 (Δ2) tubulin, an irreversible tubulin PTM. Elevation of Δ2-tubulin through overexpression of either recombinant Δ2-tubulin or cytosolic carboxypeptidase 1 (CCP1), the enzyme responsible for Δ2-tubulin generation, was sufficient to induce axonopathy in these primary DRG neurons. Conversely, pharmacological inhibition of Δ2-tubulin production attenuated PTX-induced FAS formation. Furthermore, shRNA-mediated knockdown of CCP1 reduced Δ2-tubulin levels, restored lysosomal motility, and mitigated PTX-induced axonal pathology without compromising PTX's anti-proliferative efficacy in cancer cells.Collectively, these findings identify aberrant Δ2-tubulin accumulation as a key mediator of PTX-induced sensory axon degeneration and establish CCP1 as a potential therapeutic target for preventing Paclitaxel-induced peripheral neuropathy.

**Disclosures: A. Bardhan:** None. **M. Magiera:** None. **P. Pullarkat:** None. **C. Janke:** None. **A. Ghose:** None.

**Poster**

**PSTR177: Cellular Stress and Mechanisms of Degeneration**

**Location:** WCC Halls A-C

**Time:** Monday, November 16, 2026, 1:00 PM - 5:00 PM

**Program #/Poster #:** PSTR177.21/W8

**Topic:** D.01. Neurotoxicity, Inflammation, and Neuroprotection

**Title:** Cholesterol and RGC axonal degeneration in the adult zebrafish visual system: a role in mediating axonal regeneration?

**Authors: *H. JURKIEWICZ**, M. B. VELDMAN;
Cell Biology, Neurobiology, and Anat., Med. Col. of Wisconsin, Milwaukee, WI

**Abstract:** Cholesterol dysregulation in the mammalian central nervous system (CNS), such as increased accumulation and improper trafficking, has been associated with multiple neurodegenerative disorders. Meanwhile, efficient cholesterol synthesis and recycling mechanisms in pro-regenerative vertebrates such as the adult zebrafish (*Danio rerio*) support regeneration. Therefore, we are investigating cholesterol homeostasis in the adult zebrafish visual system following optic nerve (ON) injury to understand cholesterol management during CNS regeneration and neuroprotection with the aim of discovering ways to improve cholesterol homeostasis in mammalian neurodegeneration. We hypothesize that unesterified cholesterol obtained from the degenerating ON following optic nerve crush (ONC) is re-utilized by the retinal ganglion cells (RGC) to facilitate successful RGC regeneration. We examined the availability of unesterified cholesterol in the ON following ONC by performing a cholesterol stain across early ON regeneration (0-72 hours post-injury (hpi)). We find cholesterol accumulation peaks at 6 hpi and returns to baseline by 24 hpi. These findings demonstrate the

elevated presence of unesterified cholesterol throughout the ON, shortly after injury, which is regulated and cleared by 24 hpi. To determine if RGC axonal degeneration correlates with the observed changes in unesterified cholesterol levels, we examined the time course of RGC axon degeneration in Tg(*isl2b:GFP)* transgenic zebrafish. Using whole-brain tissue clearing, we imaged RGC axonal projections in the optic tectum after ONC. Notably, axonal fragmentation was observed as early as 18 hpi. Additionally, axonal debris clearance was noted and measured as the total axonal area loss. Our results demonstrate a reduction of 40% at 48 hpi and 60% by 72 hpi. Interestingly, RGC axon degeneration does not temporally correlate with the availability of unesterified cholesterol. We decided to examine alternative sources of cholesterol, such as non-neuronal cells. Surprisingly, we have observed a reduction in the presence of mpeg+ cells at the injured ON by 3 hpi. Notably, our results also demonstrate the return of mpeg+ cells as early as 18 hpi, which remain for 7 days post-injury. This may suggest a role for mpeg+ cells in ON cholesterol homeostasis. In conclusion, our data suggests a potential role for the RGC and the microenvironment in supporting and regulating cholesterol homeostasis. We continue to examine other potential sources of cholesterol, such as astrocytes and oligodendrocytes, in addition to determining the mechanism(s) of cholesterol reuptake and their role in mediating axonal regeneration.

**Disclosures: H. Jurkiewicz:** None. **M.B. Veldman:** None.

**Poster**

**PSTR177: Cellular Stress and Mechanisms of Degeneration**

**Location:** WCC Halls A-C

**Time:** Monday, November 16, 2026, 1:00 PM - 5:00 PM

**Program #/Poster #:** PSTR177.22/W9

**Topic:** D.01. Neurotoxicity, Inflammation, and Neuroprotection

**Title:** A high throughput functional genomics screen in human neurons identifies novel genetic regulators of SARM1-dependent axon degeneration

**Authors: *A. WESTERHAUS**[1], Y. KWAK[2], R. IHRY[2];
[2]Neurosci., [1]Novartis Inst. for Biomed. Res., Cambridge, MA

**Abstract:** SARM1 is a central executioner of programmed axon degeneration and a promising therapeutic target in neurological disorders characterized by axon loss. Although inhibition of SARM1 preserves axon integrity across models of injury and disease, the molecular pathways regulating its activation are not fully understood. To identify genetic factors regulating SARM1-dependent degeneration, we performed a genome-wide arrayed CRISPR knockout screen in human pluripotent stem cell derived neurons using a lentiviral gRNA library. Neurons were challenged with vacor, a neurotoxin that induces axon degeneration through SARM1 activation. We leveraged an automated phenotyping platform that integrates high-throughput neuronal culture, high content imaging, and in silico labeling-based analysis of degeneration-associated features, such as neurite length. This platform identified genetic modifiers of SARM1 activation, including candidate cofactors and pathway components not previously implicated in SARM1-

driven axon degeneration. Follow-up validation confirmed prioritized hits and demonstrated that these genes modulate susceptibility to vacor-induced axon loss in human neurons. Mechanistic studies further revealed molecular processes that contribute to SARM1 activation in disease-relevant contexts, providing new insights into the regulation of axon degeneration. Our findings establish a scalable functional genomics framework for investigating programmed axon degeneration and expand the set of genes linked to SARM1-mediated neurodegenerative mechanisms. Collectively, this work advances understanding of SARM1 pathway regulation and supports target discovery for disorders involving pathological axon loss.

**Disclosures: A. Westerhaus:** A. Employment/Salary (full or part-time):; Anna Westerhaus is an employee at Novartis Institutes for Biomedical Research. **Y. Kwak:** A. Employment/Salary (full or part-time):; Young Don Kwak is an employee at Novartis Institutes for Biomedical Research. **R. Ihry:** A. Employment/Salary (full or part-time):; Robert Ihry is an employee at Novartis Institutes for Biomedical Sciences.

**Poster**

**PSTR177: Cellular Stress and Mechanisms of Degeneration**

**Location:** WCC Halls A-C

**Time:** Monday, November 16, 2026, 1:00 PM - 5:00 PM

**Program #/Poster #:** PSTR177.23/W10

**Topic:** D.01. Neurotoxicity, Inflammation, and Neuroprotection

**Support:** National Institute of Neurological Disorders and Stroke Grant: R01NS114397

**Title:** Early or delayed pharmacological modulation of $NAD^+$ metabolism and DLK-JNK signaling prevents SARM1 activation and preserves PNS or CNS axons in an ex vivo model of Wallerian degeneration

**Authors: *T. FAZE**[1,4], T. ASIMAKOPOULOS[4], E. KOKKINOU[2], A. M. LABUZ[4], A. ALEXANDRIS[4], V. E. KOLIATSOS[3];
[2]Dept. of Oncology, [3]Neuropathology, Neurology, Psychiatry, [1]Johns Hopkins Univ., Baltimore, MD; [4]Dept. of Pathology (Division of Neuropathology), Johns Hopkins Sch. of Med., Baltimore, MD

**Abstract:** Wallerian degeneration is an evolutionarily conserved axonal self-destruction mechanism triggered by $NAD^+$ depletion and NMN accumulation followed by the activation of the NADase SARM1 which drives metabolic collapse and axonal fragmentation. Pharmacological strategies that work upstream to prevent SARM1 activation and avoid direct orthosteric inhibition may offer a safe therapeutic potential for peripheral and central nerve injury. We investigated combination therapies consisting of a DLK-JNK inhibitor (GNE-3511), a NAMPT inhibitor (FK866), and nicotinic acid riboside (NaR; $NAD^+$ precursor)(triple regimen) or FK866 and NaR (double regimen), in sciatic and optic nerve explants serving as models of Wallerian degeneration. Nerve explants were prepared from young adult male YFP-16 mice and cultured in Neurobasal-A medium supplemented with B-27, GlutaMAX, and antibiotic-

antimycotic, containing vehicle, FK866+NaR, or FK866+NaR+GNE-35111 added from the start of culture or after 6, 12, or 24 hours. At 2, 4, or 7 days post-initiation of culture, nerves treated with early or delayed protocols were fixed in aldehydes, cleared after SHIELD processing, and taken for dual immunostaining for neurofilament light chain (NFL) and degenerative neurofilament (dNFL) to detect degenerative axonal profiles. Liquid chromatography-mass spectrometry (LC-MS) metabolomics was used to assess target engagement by measuring levels of NMN, $NAD^+$, and cADPR; the ratio NMN/$NAD^+$ served as reporter of upstream allosteric signal driving SARM1 activation and cADPR or cADPR/$NAD^+$ served as specific readouts of SARM1 catalytic activation. The dNFL/NFL ratio increased ~100-fold in sciatic nerve and ~25-fold in optic nerve explants. The double treatment significantly suppressed this ratio in both nerves, while triple treatment further reduced dNFL/NFL closer to baseline. LC-MS showed that, when compared to vehicle, sciatic nerves treated with the triple regimen had a 5-fold increase in $NAD^+$ levels and a 10% decrease in NMN, increasing the NMN/ $NAD^+$ ratio at or above baseline. The same treatment in optic nerves restored $NAD^+$ to baseline levels. Levels of cADPR/$NAD^+$ were also significantly reduced in both nerve types. These findings demonstrate that $NAD^+$ metabolic modulation enhanced by DLK-JNK inhibition preserves sciatic and optic axons ex vivo by allosterically preventing activation of SARM1.

**Disclosures: T. Faze:** None. **T. Asimakopoulos:** None. **E. Kokkinou:** None. **A.M. Labuz:** None. **A. Alexandris:** E. Ownership Interest (stock, stock options, royalty, receipt of intellectual property rights/patent holder, excluding diversified mutual funds); Patent Holder (US12364681B2): Combined MAPK and NAMPT inhibition for treatment of neuron degeneration. **V.E. Koliatsos:** E. Ownership Interest (stock, stock options, royalty, receipt of intellectual property rights/patent holder, excluding diversified mutual funds); Patent Holder (US12364681B2): Combined MAPK and NAMPT inhibition for treatment of neuron degeneration.

**Poster**

**PSTR177: Cellular Stress and Mechanisms of Degeneration**

**Location:** WCC Halls A-C

**Time:** Monday, November 16, 2026, 1:00 PM - 5:00 PM

**Program #/Poster #:** PSTR177.24/W11

**Topic:** D.01. Neurotoxicity, Inflammation, and Neuroprotection

**Support:** NIH Grant EY029795
NIH Grant EY030077
NIH Grant EY030774
NIH Grant EY035223
NIH Grant EY035223

**Title:** Metabolic Syndrome Causes Early Neurodegenerative Alteration in Ossabaw Minipig Retina

**Authors: *S. GO**;
Med. Col. of Wisconsin, Milwaukee, WI

**Abstract: Purpose:** The miniature (mini) Ossabaw pigs are proposed as a translational preclinical model for testing and developing novel therapeutics for human diseases, including cystic fibrosis, cancer, and metabolic syndrome (MetS). In recent years, pigs have gained similar attention for studying retinal abnormalities and disorders owing to their close resemblance in size, anatomy, vasculature, and pathology to the human eye compared with their rodent counterparts. **Methods:** Ossabaw minipigs were administered a Western diet for a duration of 10 weeks, during which ocular tissues were subsequently collected. Retinal sections were evaluated for pathomorphological alterations across neuronal and non-neuronal cell types using cell-type-specific immunostaining. **Results:** We found that the Western diet-fed mini pigs had reduced rhodopsin and blue opsins, significant changes in bipolar and ganglion cells, and reduced density of pre- and post-synaptic connections. Moreover, the retinas of obese mini pigs showed evidence of gliosis and microglial activation. **Conclusions:** Our findings indicate that a Western diet-induced metabolic disorder creates an early neurodegenerative milieu and further demonstrate the suitability of Ossabaw mini pigs as a model for human retinal diseases linked to MetS, including DR.

**Disclosures: S. Go:** None.

**Poster**

**PSTR177: Cellular Stress and Mechanisms of Degeneration**

**Location:** WCC Halls A-C

**Time:** Monday, November 16, 2026, 1:00 PM - 5:00 PM

**Program #/Poster #:** PSTR177.25/W12

**Topic:** D.01. Neurotoxicity, Inflammation, and Neuroprotection

**Support:** NIH Grant EY030747
Felix and Carmen Sabates / Missouri Endowed Chair in Vision Research
Challenge Grant from Research to Prevent Blindness (PK)

**Title:** RPE-specific knockout of SOD2 in aging mice impairs visual function and retinal integrity in a sex dependent manner

**Authors: *G. T. M. EDWARDS**[1], C. BUCHHOLZ[1], J. TROST[1], A. ALEXANDER[1], C. BELLAS[1], R. ZAIDI[1], C. BARNES[3], D. DAVIS[4], P. KOULEN[2];
[1]Ophthalmology, [2]Biomed. Sci. and Ophthalmology, Univ. of Missouri-Kansas City, Kansas City, MO; [3]Ophthalmology, Univ. of Missouri - Kansas City, Kansas City, MO; [4]Animal Modeling Core, Univ. of Missouri, Columbia, MO

**Abstract: Purpose.** This study investigated whether the conditional knockout (KO) of superoxide dismutase 2 (SOD2) in the retinal pigment epithelium (RPE) of aging mice affects visual function in a sex-dependent manner. The goals of the study were to measure differences in visual function following RPE-specific KO of SOD2 in aging animals, determine if such

differences are sex-specific, and identify the relevance of measured differences for the development of antioxidant therapeutic strategies for age-related macular degeneration (AMD). **Methods.** Using a tamoxifen-inducible Cre-loxP system, SOD2 was conditionally knocked out in the RPE of C57Bl/6J mice at 9 months of age (KO), with wildtype (WT) littermates as controls. Mice were grouped by sex and genotype: male WT (n=19), male RPE SOD2 KO (n=18), female WT (n=22), and female RPE SOD2 KO (n=18). Visual acuity (VA) and contrast sensitivity (CS) were quantified longitudinally (monthly at ages 5 - 14 months, i.e., before and after induction of the KO) as non-invasive measures of the opto-motor reflex. Retinal structure was imaged *in vivo* by spectral domain-optical coherence tomography (SD-OCT) at 14 months of age. Images were analyzed with Fiji/ImageJ software. Statistical analyses were performed using two-way ANOVA with Tukey's post hoc testing. **Results.** Female RPE SOD2 KO mice show greater VA decline than female WT and both male groups, at 12 months of age and persisting to 14 months ($p < 0.001$ to $p < 0.0001$). CS showed a similar age-linked reduction in female RPE SOD2 KO mice ($p < 0.001$ to $p < 0.0001$). SD-OCT quantification revealed increases in outer nuclear layer (ONL) and total retinal thickness in female RPE SOD2 KO mice compared to female WT mice ($p < 0.01$ and $p < 0.01$, respectively). **Conclusions.** Knockout of SOD2 in the RPE generates sex-specific effects in the retina, specifically visual impairment and structural changes in the outer retina of female but not male mice. These findings support a rationale for the development of sex-specific antioxidant strategies targeting SOD2 in AMD and related retinal diseases.

**Disclosures: G.T.M. Edwards:** None. **C. Buchholz:** None. **J. Trost:** None. **A. Alexander:** None. **C. Bellas:** None. **R. Zaidi:** None. **C. Barnes:** None. **D. Davis:** None. **P. Koulen:** None.

**Poster**

**PSTR177: Cellular Stress and Mechanisms of Degeneration**

**Location:** WCC Halls A-C

**Time:** Monday, November 16, 2026, 1:00 PM - 5:00 PM

**Program #/Poster #:** PSTR177.26/W13

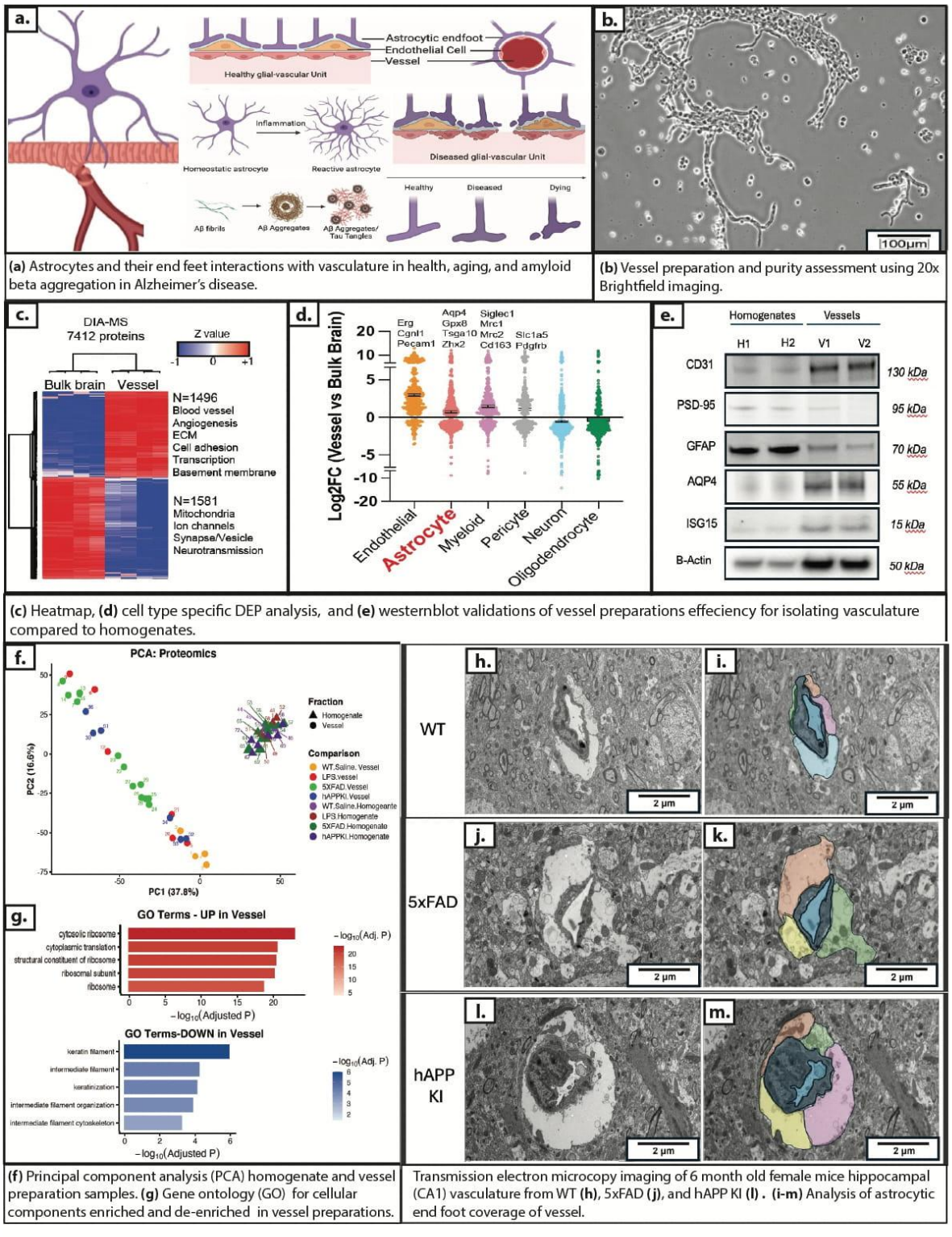
**Topic:** D.01. Neurotoxicity, Inflammation, and Neuroprotection

**Title:** Delineating distinct proteomic mechanisms of vascular dysfunction in neuroinflammation and Alzheimer's disease pathology

**Authors: *J. STAGRAY**[1], D. KOUR[2], W. E. JANG[1], M. BROMWICH[1], S. MALEPATI[1], P. KUMAR[1], U. SRIVASTAVA[2], C. ESPINOSA-GARCIA[1], S. RANGARAJU[1];
[1]Neurol., Yale Univ., New Haven, CT; [2]Neurol., Yale Univ., New haven, CT

**Abstract:** Vascular dysfunction involving cerebral microvasculature is a major pathogenic mechanism in Alzheimer's disease (Fig. a).While bulk tissue and single cell -omics studies are indicative of vascular dysfunction, proteome-level insights are limited. Understanding proteomic changes occurring in microvasculature are necessary to identify novel targets for disease modification. We applied cerebral microvascular enrichment (Fig. b-e) coupled with quantitative mass spectrometry proteomics from adult mouse brain, using LPS-induced neuroinflammation

and two models of cerebral amyloidosis (5xFAD and APP-KI-SAA) to contrast vascular changes with those occurring at the whole-brain level. MS and western blot analyses of vessel preparations showed enrichment of endothelial, astrocyte end foot and vascular macrophage markers while depletion of neuronal proteins in the vessel preparation, consistent with vessel enrichment by microscopy (Fig. f-g). Our vessel-enriched proteomics studies reveal unique molecular effects of neuroinflammation and cerebral amyloidosis that are not captured by whole brain proteomics. LPS induced neuroinflammation showed distinct increases in mRNA production with decreased extracellular matrix and synaptic transmission signatures in vessels. Amyloidosis had a larger proteomic effect on microvasculature as compared to the whole brain. In both amyloidosis models, we found increases in protein translation with decreases in vesicle transportation and mitochondrial proteins mostly distinct from the whole brain. Transmission electron microscopy revealed marked engorgement of astrocyte end feet in both amyloidosis models, corresponding to our proteomic findings (Fig. h-m). The distinct and more-pronounced effects of neuroinflammation and amyloidosis on the brain microvascular proteome are indicative of unique vulnerability of the compartment in neurodegeneration. Our ongoing analyses of proteomic and TEM data as well as integrative analyses with human brain vascular proteomes will reveal tangible targets for mechanistic studies.




**(a)** Astrocytes and their end feet interactions with vasculature in health, aging, and amyloid beta aggregation in Alzheimer's disease.

**(b)** Vessel preparation and purity assessment using 20x Brightfield imaging.

**(c)** Heatmap, **(d)** cell type specific DEP analysis, and **(e)** westernblot validations of vessel preparations effeciency for isolating vasculature compared to homogenates.

**(f)** Principal component analysis (PCA) homogenate and vessel preparation samples. **(g)** Gene ontology (GO) for cellular components enriched and de-enriched in vessel preparations.

Transmission electron microcopy imaging of 6 month old female mice hippocampal (CA1) vasculature from WT **(h)**, 5xFAD **(j)**, and hAPP KI **(l)** . **(i-m)** Analysis of astrocytic end foot coverage of vessel.

**Disclosures: J. Stagray:** None. **D. Kour:** None. **W.E. Jang:** None. **M. Bromwich:** None. **S. Malepati:** None. **P. Kumar:** None. **U. Srivastava:** None. **C. Espinosa-Garcia:** None. **S. Rangaraju:** None.

**Poster**

**PSTR177: Cellular Stress and Mechanisms of Degeneration**

**Location:** WCC Halls A-C

**Time:** Monday, November 16, 2026, 1:00 PM - 5:00 PM

**Program #/Poster #:** PSTR177.27/W14

**Topic:** D.01. Neurotoxicity, Inflammation, and Neuroprotection

**Support:** DOD/CDMRP W81XWH2220012

**Title:** Neurometabolic Alterations in Veterans with Gulf War Illness Following One Month on the Low Glutamate Diet

**Authors: *S. A. M. MCDOWELL**;
Georgetown Univ. Med. Ctr., Washington, DC

**Abstract:** Gulf War Illness (GWI) is a chronic condition that affects approximately 30% of veterans that served in the 1990-1991 Gulf War. GWI is characterized by pain, fatigue, cognitive dysfunction, mood issues, and gastrointestinal symptoms, which are thought to be connected to central nervous system dysfunction due to neurotoxic exposures during the war. Veterans with GWI (n=100) were recruited from across the US, with n=62 completing 3T Siemens Prisma-Fit MRI scanning. Participants completed a pre-diet lab visit and then received a 2-hr online dietary training session and a binder of materials on how to follow the low glutamate diet (LGD). The LGD removes exposure to free dietary glutamate (mostly from food additives) and increases consumption of foods highest in nutrients known to be protective against excitotoxicity. After 1-month on the diet, subjects returned for a post-diet lab visit where the same testing was completed. At each visit, a T1-weighted gradient echo sequence was acquired for voxel placement and later segmentation. The left dorsolateral prefrontal cortex (DLPFC), right visual cortex (V1), and left precuneus (PCU) were chosen for magnetic resonance spectroscopy (MRS) acquisition using MEGA-PRESS sequence (TE = 68 ms, TR = 2000 ms). The Matlab-based MRS preprocessing software, Osprey, was used to process, model, co-register, and segment the MEGA-PRESS data. Paired t-tests were used to compare pre- and post-intervention levels of log transformed data for glutamate (Glu), glutamine (Gln), Glx (Glu&Gln), GABA, and β-hydroxybutyrate (BHB). The pre and post-intervention metabolite differences are recorded as percent change of raw values. Changes reported are significant at the $P<0.05$ level after FDR correction. After 1-month on the low glutamate diet, there was a 99% decrease in GABA ($p=0.01$) in the DLPFC, suggesting a reduced need for inhibition. In the V1, there was a 991% increase in Gln ($p=0.02$), suggesting improved conversion of Glu to Gln, and a 96.8% decrease in BHB ($p=0.03$), suggesting improved mitochondrial function. In the PCU, there was a -7.9% decrease in Glx ($p=0.03$) and a 7.9% decrease in Glu ($p=0.036$). Glutamate decarboxylase enzymatically converts Glutamate to GABA, indicating that the decrease in GABA in the DLPFC could be attributed to a decrease in glutamate-driven excitotoxicity. A decrease in both Glu and Glx in the precuneus further supports this conclusion. Additionally, the decrease in BHB suggests improved metabolic function. Together, these findings contribute to a body of work

implicating glutamatergic excitotoxicity, neuroinflammation, and mitochondrial dysfunction as potential mechanisms underlying GWI.

**Disclosures: S.A.M. McDowell:** None.

**Poster**

**PSTR177: Cellular Stress and Mechanisms of Degeneration**

**Location:** WCC Halls A-C

**Time:** Monday, November 16, 2026, 1:00 PM - 5:00 PM

**Program #/Poster #:** PSTR177.28/W15

**Topic:** D.01. Neurotoxicity, Inflammation, and Neuroprotection

**Support:** Faneca 66 Foundation

**Title:** Mitochondrial dysfunction in GNAQ c.548G>A mutant cells in vitro

**Authors: *A. B. MANNEY**[1,2], N. F. TRUVER[1,2], M. YORKOWSKI[3], C. L. NEMETH[3,4], A. M. COMI[1,2,4,5];
[1]Neurodevelopmental Med., [2]Hunter Nelson Sturge-Weber Syndrome Ctr., [3]Moser Ctr. for Leukodystrophies, Kennedy Krieger Inst., Baltimore, MD; [4]Neurol., [5]Pediatrics, Johns Hopkins Sch. of Med., Baltimore, MD

**Abstract:** Sturge-Weber syndrome (SWS) is a congenital neurovascular disorder, primarily affecting endothelial cells in the brain, skin, and eye, caused by a somatic mosaic GNAQ c.548G>A (p.R183Q) variant. TetO-GNAQ*R183Q x Tie2-rtTA/TRE-βGal mice (Solomon et al. 2024) have enlarged vessels, blood brain barrier breakdown, decreased phospho-S6 (pS6) and abnormal Tie2 mutant endothelial cell localization. HEK293T cells were CRISPR-Cas9 edited to express GNAQ c.548G>A, single sorted, expanded, sequenced, and phenotyped against unedited controls. Seahorse XF Cell Mito Stress Test was performed to quantify mitochondrial activity (n=22 wells/genotype, normalized to cell count). Cells were stained for DAPI, α-tubulin, and either CoxIV, Tomm20, or pS6 (n=2-4 wells/genotype; 4-5 images/well taken under DAPI at 320x magnification). Image analysis (area of staining/cell) automated in ImageJ; means and independent samples t-tests assessed significance. Edited cells at low density demonstrated a 19% decrease in basal respiration (mean 2.31±0.17 pmol/min/1000 cells vs WT 2.84±0.15 pmol/min/1000 cells; $p<0.05$), a 37% decrease in maximal respiration (2.06±0.22 pmol/min/1000 cells vs WT 3.29±0.22 pmol/min/1000 cells; $p<0.01$), a 19% decrease in baseline extracellular rate of acidification (ECAR) (0.49±0.03 mpH/min vs WT 0.61±0.03 mpH/min; $p<0.05$), and a 26% increase in ECAR with oligomycin (1.04±0.06 mpH/min vs WT 0.82±0.03 mpH/min; $p<0.01$). A 53% decrease in CoxIV ($p<0.01$) and 68% decrease in pS6 staining ($p<0.01$) was demonstrated in edited cells vs WT; Tomm20 staining was unchanged. At high density, edited cells showed 25% decreased basal respiration (2.73±0.16 pmol/min/1000 cells vs WT 3.64±0.07 pmol/min/1000 cells; $p<0.01$) and 50% decreased maximal respiration (2.09±0.15 pmol/min/1000 cells vs WT 4.16±0.14 pmol/min/1000 cells; $p<0.01$); edited cells also demonstrated a 71% increase in ECAR with oligomycin (1.00±0.05 mpH/min vs WT 0.58±0.03

mpH/min; p<0.05), a 20% increase with FCCP (1.22±0.04 mpH/min vs WT 1.02±0.03 mpH/min; p<0.05), and a 50% increase with rotenone (1.10±0.05 mpH/min vs WT, 0.73±0.03 mpH/min; p<0.05). GNAQ c.548G>A HEK293T pure cultures demonstrate altered mitochondrial function; shift to reliance upon glycolysis at high cell density implies abnormal sensitivity to nutrient restriction. Analysis is underway to quantify CoxIV and Tomm20 staining at high cell density and in mutant mouse model. These data and models expand our understanding and may inform development of future treatments for SWS and other GNAQ c.548G>A-related conditions.

**Disclosures: A.B. Manney:** None. **N.F. Truver:** None. **M. Yorkowski:** None. **C.L. Nemeth:** None. **A.M. Comi:** None.

**Poster**

**PSTR177: Cellular Stress and Mechanisms of Degeneration**

**Location:** WCC Halls A-C

**Time:** Monday, November 16, 2026, 1:00 PM - 5:00 PM

**Program #/Poster #:** PSTR177.29/W16

**Topic:** J.03. Anatomical Methods

**Title:** Netrin-G2 Upregulation in the Denervated Spinal Cord Following Stroke

**Authors: *P. RHOTON**[1,2], M. KENWOOD[3], B. C. DEREBERY[4], D. BETZ[5], D. M. RAMIREZ[6], M. P. GOLDBERG[7];
[1]UTSA, San Antonio, TX; [2]Neurol., UT Hlth. SA, San Antonio, TX; [3]Neurol., UT Heath SA, San Antonio, TX; [4]Neurol., The Univ. of Texas Hlth. Sci. Ctr. at San Antonio, San Antonio, TX; [5]Neurosci., UT Hlth. San Antonio, San Antonio, TX; [6]Neurol., Univ. of Texas Southwestern Med. Ctr., Dallas, TX; [7]Neurol., Univ. of Texas Hlth. Sci. Center, San Antonio, Shavano Park, TX

**Abstract:** Stroke leaves many patients with significant motor impairment. Sprouting of the contralesional corticospinal tract (CST) into the injured spinal hemicord is associated with improved motor recovery after unilateral primary motor cortex stroke in mice. The axon guidance molecule, Netrin-G2, is upregulated in the denervated hemicord at four weeks post-stroke (J Kaiser et al 2019 PMID 30962276) and may increase reinnervation of target neurons by the cCST. Investigating the structural dynamics of this short-range axon guidance cue requires high-resolution anatomical tools capable of isolating descending circuits and spinal cord neuronal pools without disrupting baseline development. We present an intersectional viral strategy designed to evaluate Netrin-G2-mediated plasticity within the ventral horn. Targeted overexpression of a Netrin-G2-mKate2 fusion protein in spinal motor neurons was achieved by retrograde intramuscular injection of postnatal day 5 (P5) mice. Analysis of 30-micron microtome sections confirmed stable spinal cord expression of Netrin-G2-mKate2 at postnatal days P19 and P26. Netrin G2 overexpression did not induce apparent behavioral deficits, as verified by normal righting reflexes, baseline grip strength during inverted wire mesh grid-walking, and the Bederson test. Concurrently, descending Layer 5 extra-telencephalic (L5 ET)

corticospinal neurons were labeled by retro-orbital delivery of a blood-brain barrier-permeant PHP.eB capsid packaging an mGreenLantern enhancer construct. Tissue clearing and light-sheet microscopy are underway for mesoscale 3D imaging of the axonal landscape. This method will visualize potential Netrin-G2 guidance of sprouting axons toward identified motor neurons.

**Disclosures: P. Rhoton:** None. **M. Kenwood:** None. **B.C. Derebery:** None. **D. Betz:** None. **D.M. Ramirez:** None. **M.P. Goldberg:** None.

**Poster**

**PSTR177: Cellular Stress and Mechanisms of Degeneration**

**Location:** WCC Halls A-C

**Time:** Monday, November 16, 2026, 1:00 PM - 5:00 PM

**Program #/Poster #:** PSTR177.30/W17

**Topic:** D.01. Neurotoxicity, Inflammation, and Neuroprotection

**Support:** NIH BRAIN Initiative Armamentarium UF1MH128336
Roy. J. Carver Charitable Trust #25-6023
Chan-Zuckerberg Bi[o]hub
Beckman Institute Fellows Program

**Title:** Circadian Regulation of Barrier Function in Human Blood-Brain Barrier

**Authors: *C. DENG**[1], S. J. SKATCHKOV[3], A. AKALIN[2], S. ASIF[1], B. HAN[1], M. JANG[5], J. W. MITCHELL[4], M. U. GILLETTE[6];
[1]Univ. of Illinois Urbana-Champaign, Urbana, IL; [2]Univ. of Illinois Urbana-Champaign, Champaign, IL; [4]Dept. of Cell and Developmental Biol., [3]Univ. of Illinois at Urbana-Champaign, Urbana, IL; [5]Bioengineering, UIUC, Urbana, IL; [6]Dept. of Cell & Developmental Biol., Univ. of Illinois Urbana-Champaign Neurosci. Grad. Program, Urbana, IL

**Abstract:** The blood-brain barrier (BBB) is a dynamic interface that regulates molecular exchange between the circulation and the central nervous system. While circadian rhythms are known to influence vascular physiology, whether in vitro human brain microvascular endothelial cells (BMECs) exhibit daily rhythms in barrier function remains poorly understood. Here, we tested whether human primary cells and iPSC-derived BMECs show 24-hour rhythmicity in barrier integrity using transendothelial electrical resistance (TEER) as a functional readout. Human primary BMECs were cultured either as monocultures or in tricultures with pericytes and astrocytes. Cultures were synchronized with 50% serum, and TEER was measured repeatedly over time to assess temporal changes in barrier function. Cosinor analysis was used to evaluate 24-hour rhythmicity following synchronization. Both BMEC monocultures and tricultures showed significant 24-hour rhythms in TEER. Notably, the estimated peak and trough times were similar between monoculture and triculture conditions, suggesting that rhythmic regulation of barrier function may be an intrinsic property of BMECs and is preserved in a more physiologically relevant multicellular BBB model. In parallel, we tested molecular oscillation in human BMECs through E-box activity using adeno-associated virus (AAV). Because traditional

transduction showed limited efficiency in this cell type, we optimized AAV transduction across different capsid and treatment conditions. Detectable Venus signal was observed in human BMECs, indicating that AAV-mediated circadian reporter delivery is feasible. Together, these preliminary findings suggest that in vitro human BMEC barrier function is circadian regulated and that AAV-based circadian reporter strategies can be applied to in vitro human BBB models. This platform provides a foundation for investigating how the endothelial circadian clock regulates BBB permeability and how neurovascular cell interactions shape rhythmic barrier function.

**Disclosures: C. Deng:** None. **S.J. Skatchkov:** None. **A. Akalin:** None. **S. Asif:** None. **B. Han:** None. **M. Jang:** None. **J.W. Mitchell:** None. **M.U. Gillette:** None.

**Poster**

**PSTR178: Pain Imaging and Perception**

**Location:** WCC Halls A-C

**Time:** Monday, November 16, 2026, 1:00 PM - 5:00 PM

**Program #/Poster #:** PSTR178.01/W18

**Topic:** E.01. Somatosensation – Pain and Itch

**Support:** Shanghai Science and Technology Commission Fund 21Y11906000

**Title:** Widespread Reorganization of Resting-State Quasi-Perodic Brain Dynamics in Painful Diabetic Peripheral Neuropathy

**Authors:** Y. LEI[1], H. FANG[2], J. YUE[1], L. WANG[1], X. CHEN[2], Q. YANG[1], H. ZHANG[1], ***Y. FAN**[2];
[1]ShanghaiTech Univ., Shanghai, China; [2]Renji Hospital, Shanghai Jiaotong University, Sch. of medicine, Shanghai, China

**Abstract:** Painful diabetic peripheral neuropathy (PDPN) is a common complication of diabetes mellitus, but the central mechanisms remain unclear. As PDPN-related pain may involve dynamic interactions among large-scale brain networks that cannot be fully captured by static functional connectivity, quasi-periodic patterns (QPPs) were used to characterize recurrent whole-brain co-activation and temporal coordination among the networks.
23 healthy controls (HC) and 41 patients with diabetes mellitus, including 21 with PDPN and 20 with non-painful diabetic peripheral neuropathy (NDPN). Resting-state functional MRI (rsfMRI) were collected. QPPs were detected using sliding-window template-matching. Beyond group-level QPPs, individual-level QPPs were extracted to quantify subject-specific dynamics. Analyses focused on the visual, somatomotor (SM), ventral attention (VA), limbic, frontoparietal (FP), and default-mode (DM) networks. For better characterizing QPP spatiotemporal features, three summary metrics were derived: CurveOffset, PairwiseR, and PeakLag, indexing sustained network deviation, inter-network co-fluctuation, and inter-network delay, respectively (Fig. 1a). Group-level QPP showed altered brain co-activation in PDPN compared to NDPN and HC, involving visual, SM, DM, and VA networks (Fig. 1b). At the individual level, abnormalities

followed a disease-related pattern: compared to the HC, NDPN showed intermediate changes, and PDPN had the greatest changes. CurveOffset increased in the SM, DM, and visual networks and decreased in the limbic and FP networks (corrected $p < 0.001$). PairwiseR increased between the SM and VA and decreased between the VA and DM (corrected $p < 0.05$), while PeakLag was prolonged in both SM-VA ($p < 0.05$) and VA-DM ($p < 0.01$). NDPN showed relatively preserved QPP dynamics (Fig. 1c).

The findings suggest that the pain in PDPN is associated with disrupted balance among somatosensory, task control-related, and self monitoring systems, indicating potential therapeutic mechanisms for diabetes-related pain management.

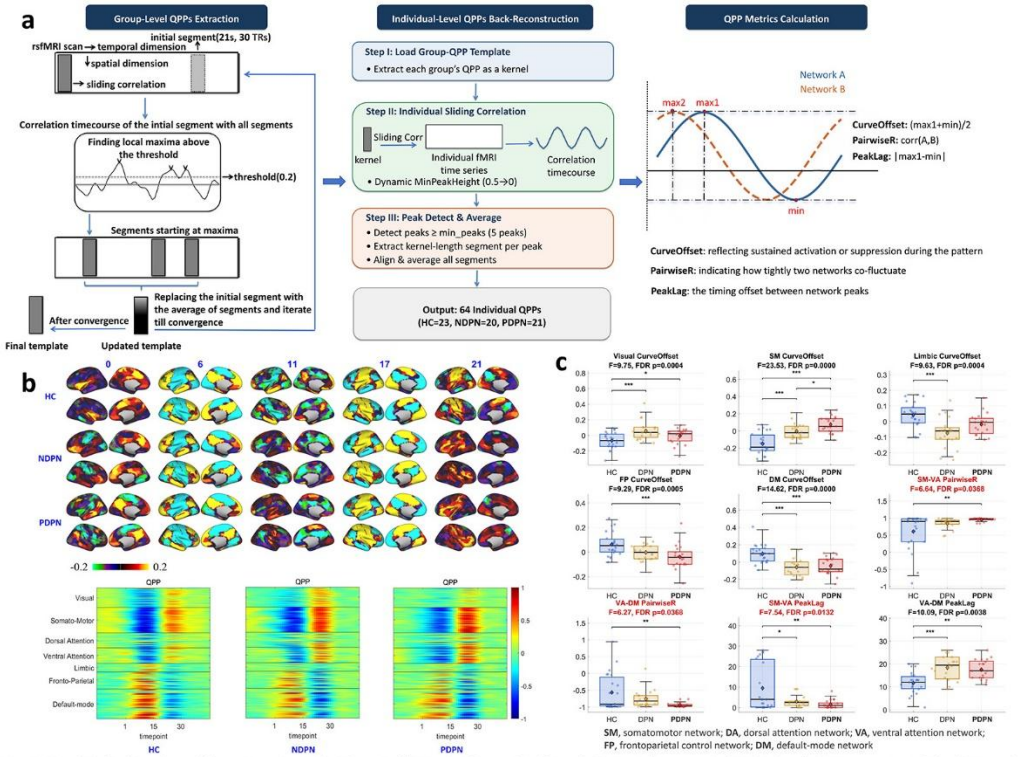



Figure 1. QPP analytical pipeline and group differences in quasi-periodic brain dynamics. (a) QPP analysis framework. Left (Group-level extraction): Preprocessed rsfMRI data from all subjects are concatenated along the temporal dimension. A random segment of fixed window length (here: 21 s / 30 TRs) is selected as the initial template. This template is correlated (sliding window, step = 1 TR) with the full concatenated time series to produce a correlation timecourse; local maxima exceeding a threshold (r = 0.2) are identified, and the corresponding time segments (centered at each maximum, equal to window length) are averaged to form an updated template, replacing the original seed. This process iterates until convergence, yielding the final group-level QPP template. Middle (Individual-level back-reconstruction): The converged group-level QPP serves as a fixed spatial-temporal kernel, which is correlated via sliding window with each subject's fMRI time series to generate a subject-specific correlation timecourse. Dynamic peak detection (minimum n peaks/subject, here ≥ 5) identifies recurrence events; detected segments are temporally aligned and averaged to produce individualized QPPs (n = 64: 23 HC, 20 NDPN, 21 PDPN). Right: Metric definitions — CurveOffset [(max + min)/2]: sustained network activation/suppression level over the QPP cycle; Pairwiser [corr(A,B)]: inter-network co-fluctuation strength; PeakLag [|max1 − max2|]: temporal delay between two networks' peak activations. (b) Group-level QPP spatial maps at key times (0, 6, 11, 17, 21s) and corresponding network activity matrices across the ~21s cycle for HC (top), NDPN (middle), and PDPN (bottom). Seven networks shown: Visual, Somatomotor, Dorsal Attention, Ventral Attention, Limbic, Frontoparietal, Default-mode. (c) Between-group comparisons of QPP metrics (ANCOVA, FDR-corrected; covariates: age, gender, education, FD, BMI). CurveOffset showed stepwise increases in Visual, SM, and DM networks and decreases in Limbic and FP networks from HC → NDPN → PDPN ($p < 0.001$). PairwiseR increased in SM–VA coupling and decreased in VA–DM coupling ($p < 0.05$). PeakLag was prolonged in both SM–VA ($p < 0.05$) and VA–DM ($p < 0.01$), indicating delayed inter-network coordination in PDPN.

**Disclosures: Y. Lei:** None. **H. Fang:** None. **J. Yue:** None. **L. Wang:** None. **X. Chen:** None. **Q. Yang:** None. **H. Zhang:** None. **Y. Fan:** None.

**Poster**

**PSTR178: Pain Imaging and Perception**

**Location:** WCC Halls A-C

**Time:** Monday, November 16, 2026, 1:00 PM - 5:00 PM

**Program #/Poster #:** PSTR178.02/W19

**Topic:** E.01. Somatosensation – Pain and Itch

**Support:** NIH: 2R01MH076136
NIH: R01DA035484
NIH: 5K01DA045735

**Title:** Stable individual differences in rating-scale use predict Neurologic Pain Signature prediction error

**Authors: *J. S. CARDOSO**[1], T. D. WAGER[2], E. R. LOSIN[3];
[1]Biobehavioral Hlth., Pennsylvania State Univ., University Park, PA; [2]Psychological and Brain Sci., Dartmouth Col., Hanover, NH; [3]Biobehavioral Hlth. Dept. & Neurosci. Dept., Penn State Univ., State College, PA

**Abstract: Background.** Pain signatures are multivariate fMRI patterns that track evoked pain when applied to new individuals. A widely validated example, the Neurologic Pain Signature (NPS), tracks within-person evoked intensity with high sensitivity and specificity but is limited between persons (Han et al., 2022). Work on newer between-person signatures (Zhang et al.) flags rating bias and scale use as unresolved confounds. This matters because these tools are validated against self-report: if a person's own rating behavior makes their reports hard to predict, then part of what looks like signature failure is really a measurement problem in inherent report variability. That possibility has been mentioned, but no one has measured, per person, how much rating-scale behavior accounts for NPS prediction error. We do so here. **Methods.** In healthy human adults (N=88; 44F/44M; ages 19-54; heat 47-49 °C; single trial fMRI) we used leave-one-subject-out models to predict trial pain ratings from trial-level NPS, taking absolute prediction error as outcome. Per-subject scale-use metrics (rating variability, range, slope) were considered, but variability and range were collinear (r=.93), so only variability indexed dispersion. Because dispersion and error on the same trials are mechanically coupled, we added an out-of-fold split half: the variability metric from one trial half, prediction error from the disjoint half, over 100 partitions each fit forward and reverse (200 fits), plus a low-trial-subject sensitivity check. Subject-level models were primary and trial-level Gamma models convergent; sex differences were not assessed. **Results.** In a confirmatory analysis, greater rating variability predicted greater held-out NPS prediction error: 16.4% greater error per 1 SD (subject level; p=.005, FDR robust), and ~14% trial-level. Out of fold, where metric and error share no trials, the effect stayed positive in all 200 fits at ~11% per SD, symmetric across direction and ~12% excluding low-trial subjects. This is only slightly below same-trial estimates, suggesting a stable within-person feature, not a same-trial arithmetic identity. Psychosocial measures did not predict error. **Conclusion.** How a person uses rating scales measurably predicts how well NPS tracks their reports, on held-out trials. This operationalizes the past hypothesized scale-use account of NPS's limited between-person performance, and bears directly on emerging between-person pain signatures that treat rating bias as a confound. Whether this dispersion reflects reporting noise that caps what any stimulus-locked signature can recover, or unmodeled variation in experience, remains for future work.

**Disclosures: J.S. Cardoso:** None. **T.D. Wager:** None. **E.R. Losin:** None.

**Poster**

**PSTR178: Pain Imaging and Perception**

**Location:** WCC Halls A-C

**Time:** Monday, November 16, 2026, 1:00 PM - 5:00 PM

**Program #/Poster #:** PSTR178.03/W20

**Topic:** E.01. Somatosensation – Pain and Itch

**Support:** American Heart Association grant 24TPA1290619

**Title:** Central Post-Stroke Pain Reduction: Evidence of Cortical and Network Reorganization in Physiological Bands

**Authors: *I. DALLASTA**[1], V. COMMURI[2], J. Z. SIMON[3], E. B. MARSH[4];
[1]Univ. of Maryland, Silver Spring, MD; [2]Univ. of Maryland Col. Park, Wheaton, MD; [3]Electrical and Computer Engin., Univ. Maryland, Col. Park, College Park, MD; [4]Neurol., Johns Hopkins Sch. of Med., Baltimore, MD

**Abstract:** Central post-stroke pain (CPSP) is a neuropathic pain syndrome that can develop following a stroke and significantly impact quality of life. It is not tied to a singular lesion location but usually involves the thalamus, sensory cortex, or brainstem. Scrambler therapy, an FDA approved, noninvasive electroanalgesia, has proven to substantially improve symptoms in about 70% of patients. Mechanisms underlying pain reduction following treatment are not well understood; however, modulation of an underlying thalamocortical dysrhythmia (TCD) is one possibility. In this study, we use magnetoencephalography (MEG) to explore the role of TCD in post-stroke pain and evaluate the changes in cortical activity and network dynamics following a single treatment session in five CPSP patients. Five stroke patients without pain and five individuals with no stroke or chronic pain were used as control groups for comparison. Source-level activity for each participant was reconstructed across all frequency bands. Network-localized Granger causality was used to estimate band-specific directional functional connectivity, and specific networks of interest including the default mode, salience, limbic and central executive networks, all implicated in TCD, were explored in secondary analyses. Differences in these measures were evaluated between patients with post-stroke pain and controls as well as responders versus non-responders. Analysis indicated increased baseline theta and gamma band activation of the dorsal anterior cingulate cortex for CPSP patients compared to control groups consistent with mechanisms described in TCD. Following treatment, further increases in theta, and increased alpha activity was observed, the opposite direction than predicted by the simplest TCD models. Functional connectivity analyses also demonstrated increased frontal lobe connectivity in patients with post-stroke pain within the theta, beta and alpha bands at baseline, as well as higher connectivity within limbic areas for multiple bands compared to controls. Traditional connectivity patterns, originally observed only in the control group without prior stroke or pain, were restored following treatment for responders, but not non-responders. Neural activity and connectivity patterns in patients with post-stroke pain offer some support for TCD as an underlying mechanism. A larger study to explore TCD as a neurophysiologic explanation for this complex syndrome is underway and will further examine changes immediately following treatment completion and at a 3-month follow-up to evaluate the durability of treatment-related effects and identify markers of sustained pain relief.

**Disclosures: I. Dallasta:** None. **V. Commuri:** None. **J.Z. Simon:** None. **E.B. Marsh:** None.

**Poster**

**PSTR178: Pain Imaging and Perception**

**Location:** WCC Halls A-C

**Time:** Monday, November 16, 2026, 1:00 PM - 5:00 PM

**Program #/Poster #:** PSTR178.04/W21

**Topic:** E.01. Somatosensation – Pain and Itch

**Support:** R35GM146774
TL1TR002016

**Title:** Default mode network connectivity as a prognostic biomarker of pain chronification following traumatic burn injury

**Authors: *C. M. AUGUSTO**[1], C. F. P. MORAN-BARISO[1], A. SIPE[1], M. L. KEASER[2], J. T. DA SILVA[2], J. E. NYLAND[1];
[1]Neurosci. and Exptl. Therapeut., Penn State Col. of Med., Hershey, PA; [2]Neural and Pain Sciences, Sch. of Dentistry, Ctr. to Advance Chronic Pain Res., Univ. of Maryland Baltimore, Baltimore, MD

**Abstract:** Persistent pain is a common but poorly understood outcome of traumatic burn injury. With more patients surviving their burn injuries, ongoing pain presents a growing complication to patient healing and quality of life. Studies utilizing functional magnetic resonance imaging (fMRI) in humans have found patterns of abnormal network connectivity in participants with chronic pain relative to healthy participants. Specifically, the Default Mode Network (DMN) has repeatedly exhibited abnormal network dynamics both at cognitive rest and during cognitive tasks. The DMN may be a useful physiological biomarker of chronic pain, but it is yet unclear whether the abnormal dynamics of the DMN contribute to pain chronification or emerge because of pain chronification. To assess this temporal question, we utilized a model of thermal burn injury in 15 male Sprague-Dawley rats undergoing longitudinal fMRI analysis. We hypothesized that intra-DMN connectivity will increase as pain persists after thermal burn injury. All rats underwent a sound-stress acclimation procedure wherein they were exposed to a pre-recorded MRI scanner noise for increasing amounts of time. During actual MRI scans, rats were lightly sedated at ~1% isoflurane. Anesthesia was used to achieve a balance between animal comfort and signal quality. After baseline measurements, 7 rats sustained a full-thickness thermal burn to the plantar surface of their right hind paw; 8 rats remained un-burned and served as controls. Longitudinal post-burn assessments included weekly Von Frey sessions and MRI scanning at the 1-, 3-, and 6-week timepoints. Two-way Mixed ANOVA of the paw withdrawal thresholds (represented as a ratio of the injured/uninjured paw) did not find a significant interaction of time and group, nor any significant main effects. Previous studies in preclinical burn models have demonstrated that burns heal quickly with minimal pain complications in rats, unlike in humans, unless there is a deliberate stress-inducing peri-injury procedure. While our results indicate that our thermal burn without peri-injury stress did not produce long-lasting pain, these results do

suggest that repeated MRI scanning did not itself become a source of stress. Preliminary MRI results indicate that the combination of the sound-stress acclimation protocol and the anesthesia during scanning resulted in minimal motion artifacts in our data. This is a considerable achievement for a scanning procedure that does not involve invasive body restraints. Further analyses will examine DMN connectivity over time to assess this network's fitness as a detectable and relevant biomarker in our model of thermal burn pain.

**Disclosures: C.M. Augusto:** None. **C.F.P. Moran-Bariso:** None. **A. Sipe:** None. **M.L. Keaser:** None. **J. T. Da Silva:** None. **J.E. Nyland:** None.

**Poster**

**PSTR178: Pain Imaging and Perception**

**Location:** WCC Halls A-C

**Time:** Monday, November 16, 2026, 1:00 PM - 5:00 PM

**Program #/Poster #:** PSTR178.05/W22

**Topic:** E.01. Somatosensation – Pain and Itch

**Support:** MRC PhD funding
Wellcome Trust PI Fellowship

**Title:** Exploring the neurocognitive basis of phantom limb sensations and pain

**Authors: *M. A. SZYMANSKA**[1], H. DIMITROV[2], V. ROOT[3], N. P. HOLMES[4], F. MANCINI[5], T. R. MAKIN[6];
[1]MRC CBU, Univ. of Cambridge, Cambridge, United Kingdom; [2]MRC CBU, Univ. of Cambridge, London, United Kingdom; [3]UCL, Bristol, United Kingdom; [4]Psychology, Univ. of Nottingham, Nottingham, United Kingdom; [5]Univ. of Cambridge, Cambridge, United Kingdom; [6]Univ. Col. London, London, United Kingdom

**Abstract:** Following limb amputation, phantom limb sensations (PLS) and phantom limb pain (PLP) often persist. We treat PLS/PLP as a neurocognitive account of inference under uncertainty: residual peripheral activity persists after limb loss, but evidence is weak while beliefs and predictions about the missing limb remain. We aim to test how this internal model is maintained under altered input and whether phantom experiences reflect individual differences in weighting prior expectations versus ambiguous evidence. We hypothesise that phantom experiences reflect increased reliance on prior predictions over degraded evidence. We test this framework with two complementary studies.
In Study 1, amputees spanning PLP severity and controls learn cue-outcome associations for painful versus non-painful thermal stimuli. We manipulate context (passive vs phantom-movement trials) and environmental statistics (stable vs volatile contingencies via reversals), and will fit reinforcement-learning models to quantify learning. Ongoing data (n=12 amputees, n=15 controls) qualitatively show higher learning accuracy and a stronger expectancy bias in amputees on surprise warm trials (pain expected, non-pain delivered) in the passive condition, consistent with pain-related priors shaping perception when predictions are violated.

Study 2 investigates sensorimotor inference under degraded peripheral evidence. Single-pulse TMS over M1 (80-120% rMT) is used to evoke movement-related sensations while high-density EMG measures motor-evoked potentials (MEPs). We compare missing versus intact hands within participants and test report-MEP coupling between groups. Preliminary data (n=5 amputees, n=6 controls) show reliable evoked sensations and MEPs in amputees, but reduced alignment: amputees report sensations despite fewer MEPs than controls, consistent with weaker coupling between peripheral evidence and perception. Planned drift diffusion modelling will capture evidence accumulation and decision thresholds.
Together, these studies operationalise how priors and evidence are integrated when evidence is weak, ambiguous, or mismatched with predictions in the phantom experience. Larger samples and modelling will test whether PLS/PLP track a shift toward prior-weighted inference and will be presented.

**Disclosures: M.A. Szymanska:** None. **H. Dimitrov:** None. **V. Root:** None. **N.P. Holmes:** None. **F. Mancini:** None. **T.R. Makin:** None.

**Poster**

**PSTR178: Pain Imaging and Perception**

**Location:** WCC Halls A-C

**Time:** Monday, November 16, 2026, 1:00 PM - 5:00 PM

**Program #/Poster #:** PSTR178.06/W23

**Topic:** E.01. Somatosensation – Pain and Itch

**Support:** 5R01NS127901-03

**Title:** Investigating the effects of early life trauma exposure on brain circuits underlying chronic pain

**Authors: *C. GUZMAN**[1], M. E. TIVARUS[2,3], P. Y. GEHA[6,4,5,3];
[1]Univ. of Rochester Neurosci. Grad. Program, Rochester, NY; [2]Imaging Sci. and Neurosci., [3]Neurosci. Grad. Program, [4]Dept. of Dent., [5]Dept. of Neurol., Univ. of Rochester, Rochester, NY; [6]Psychiatry, Univ. of Rochester Med. Ctr., Rochester, NY

**Abstract:** Exposure to childhood trauma significantly elevates the risk of developing chronic pain in adulthood, yet the neural mechanisms underlying this vulnerability remain unclear. Brain structures implicated in early life stress (ELS) are also central to chronic pain, but few studies have examined their combined impact. Here, we tested the hypothesis that ELS-exposed patients with chronic pain exhibit cumulative structural alterations in limbic regions. Because volumetric and surface area measures have yielded mixed results in both ELS and chronic pain, we applied shape analysis of limbic structures derived from high-resolution T1-weighted images, capturing localized deformations overlooked by global volumetric measures. We analyzed data from the Multidisciplinary Approach to the Study of Pelvic Pain (MAPP) cohort. Using FSL FIRST, we segmented limbic structures and performed vertex-wise shape analysis in 70 urological chronic pelvic pain (UCPP) patients and 86 healthy controls across four groups: healthy controls, trauma-

exposed controls, UCPP, and trauma-exposed UCPP. Groups were compared using ANCOVA with FSL Randomise, correcting for age, sex, BMI, and region SNR. Results revealed a significant patient-by-trauma interaction ($p<0.05$, corrected). Trauma-exposed controls showed outward expansion in right hippocampus and bilateral thalamus relative to non-exposed controls. Trauma-exposed UCPP patients also showed expansion relative to healthy controls, but to a lesser degree than non-trauma UCPP patients, indicating a significant interaction. Contrary to our hypothesis of cumulative plasticity, findings suggest compensatory mechanisms in trauma-exposed individuals. Ongoing analyses extend this work into the IMAGEN cohort (ages 14-23, four timepoints), examining resting-state functional connectivity and connectopic mapping of corticolimbic circuits across adolescence, testing whether early adversity predicts trajectory-based vulnerability to chronic pain. Together, these findings highlight the importance of accounting for trauma history in neuroimaging studies of chronic pain, with implications for identifying biomarkers of vulnerability and resilience.

**Disclosures: C. Guzman:** None. **M.E. Tivarus:** None. **P.Y. Geha:** None.

**Poster**

**PSTR178: Pain Imaging and Perception**

**Location:** WCC Halls A-C

**Time:** Monday, November 16, 2026, 1:00 PM - 5:00 PM

**Program #/Poster #:** PSTR178.07/W24

**Topic:** E.01. Somatosensation – Pain and Itch

**Support:** US Army CPMRP HT9425-23-1-1022

**Title:** Longitudinal Pain and Sensory Sensitivity Outcomes Following Rotational Ankle Fracture Repair

**Authors:** T. NGUYEN[1], H. ARELLANO[1], D. LU[1], T. DOTTO[1], L. HILL[2], K. M. NAUGLE[3], R. NATOLI[2], ***F. A. WHITE**[4,1];
[1]Anesthesia, [2]Orthopaedic Surgery, Indiana Univ. Sch. of Med., Indianapolis, IN; [3]Excercise and Kinesiology, Indiana Univ. Sch. of Human and Hlth. Sci., Indianapolis, IN; [4]Indiana University, Indianapolis, Indianapolis, IN

**Abstract: Background:** Chronic pain is a common complication following ankle fractures, with approximately 18-42% of patients reporting neuropathic pain symptoms up to one year postoperatively. Chronic post-fracture pain remains one of the most prolonged and challenging symptoms to manage after fracture repair. The underlying pathophysiological mechanisms driving the development of fracture-related chronic pain remain poorly understood. The present study aims to identify potential risk factors associated with ankle fracture-related neuropathic pain (AFNP), with a specific focus on characterizing alterations in sensory function and pain sensitivity and modulation that may contribute to its onset and progression.
**Methods:** Quantitative sensory testing (QST) was performed in 45 ankle fracture patients at 5-9 weeks, 3-5 months, and 6-9 months post-surgery, and once in 19 matched fracture-free controls.

Testing on injured and contralateral ankles included mechanical detection threshold (MDT), warm detection threshold (WDT), heat pain threshold (HPT), cold detection threshold (CDT), pressure pain threshold (PPT), mechanical temporal summation (MTS), and conditioned pain modulation (CPM) using a cold-water bath paradigm. In addition, cutaneous temperature was measured using infrared thermographic imaging. Analyses assessed (1) longitudinal changes in patients, (2) differences between patients and controls at 5-9 weeks, and (3) differences between patients with chronic neuropathic vs. non-neuropathic pain.
**Results:** Independent t-tests showed that, at 5-9 weeks post-surgery, fracture patients had higher CDTs and lower PPTs in both ankles, and higher MTS in the non-injured ankle compared to controls. Repeated-measures ANOVA indicated lower PPTs in injured vs. non-injured ankles across all time points and greater MTS in the injured ankle at 6 months only. Mixed-model ANOVA showed reduced CPM (worse pain inhibition) in chronic neuropathic vs. non-neuropathic patients across time. Skin temperature was consistently higher at the injured ankle for all visits.
**Conclusions:** The results indicate that a substantial proportion of ankle fracture patients exhibit persistent hypersensitivity and elevated skin surface temperature beyond the period of bone healing. Notably, patients with neuropathic pain demonstrated impaired conditioned pain modulation, suggesting reduced descending inhibitory control compared to those with non-neuropathic pain. Future studies will determine whether early sensory changes can serve as predictive markers for the development of post-injury neuropathic pain.

**Disclosures: T. Nguyen:** None. **H. Arellano:** None. **D. Lu:** None. **T. Dotto:** None. **L. Hill:** None. **K.M. Naugle:** None. **R. Natoli:** None. **F.A. White:** None.

**Poster**

**PSTR178: Pain Imaging and Perception**

**Location:** WCC Halls A-C

**Time:** Monday, November 16, 2026, 1:00 PM - 5:00 PM

**Program #/Poster #:** PSTR178.08/W25

**Topic:** E.01. Somatosensation – Pain and Itch

**Support:** NIH R15 NS137286-01A1

**Title:** EEG frequency oscillatory profile during processing of sensory and affective pain descriptor words in acute cold pressor pain and chronic knee osteoarthritis

**Authors: *H. FORD**[1], A. RONCK[2], M. WIRTZ[3], K. MALAVAR[4], H. STOLZ[5], A. NORRIS[2], A. PARK[6], A. L. HARRIS BOZER[1];
[1]Neurosci., [2]Tarleton State Univ., Stephenville, TX; [3]Tarleton State Univ., Georgetown, TX; [4]Tarleton Neurosci., Stephenville, TX; [5]Tarleton, Stephenville, TX; [6]Univ. of Central Arkansas, Morrilton, AR

**Abstract:** The aim of this study was to examine the profile of EEG activity associated with the cognitive processing of sensory and affective pain descriptor words in participants with and

without chronic knee osteoarthritis (OA). EEG was acquired (256 electrode Magstim EGI) from 44 participants (18 males; OA n=21, controls n=23). Participants responded to pain descriptor words acquired from the short-form McGill Pain Questionnaire at resting-state, sensory-word, and affective-word conditions during baseline and acute pain (cold pressor arm wrap). Average spectral power values for frequency bands were extracted (delta 0-3Hz, theta 4-7Hz, alpha 8-13Hz, beta 14-30Hz, gamma 31-50Hz). Mixed ANOVA analyses were computed for each electrode of interest with group as the between-subjects variable, and EEG data for each frequency band over time as the within-subjects variable. A main effect of time ($p < .05$) was observed for all electrodes of interest (C3, C4, F7, F8) in each frequency band. In the beta band at the C4 electrode, there was a main effect of group ($p = .028$), and a significant interaction effect ($p = .047$). Controls had higher beta during affective words compared to baseline. OA participants demonstrated higher beta during the processing of any pain words compared to baseline and cold pressor pain without words. A significant theta interaction was observed at F8 ($p = .023$). In both groups, higher theta was elicited during sensory and affective pain words compared to baseline. Affective words elicited more theta activity in several conditions, more often in controls. These data indicate that the cortical processing of multidimensional pain words varies across frequency bands, largely irrespective of chronic pain status. Cortical activity increased significantly over resting state conditions in response to sensory and affective words, with affective often eliciting the most activity highlighting enhanced cortical salience of affective word processing. Although chronic pain status was associated with some frequency-specific responses in beta and theta bands (especially for affective words), the overall pattern of findings is that the presence of chronic pain had little impact on the processing of pain descriptor words.

**Disclosures: H. Ford:** None. **A. Ronck:** None. **M. Wirtz:** None. **K. Malavar:** None. **H. Stolz:** None. **A. Norris:** None. **A. Park:** None. **A.L. Harris Bozer:** None.

**Poster**

**PSTR178: Pain Imaging and Perception**

**Location:** WCC Halls A-C

**Time:** Monday, November 16, 2026, 1:00 PM - 5:00 PM

**Program #/Poster #:** PSTR178.09/W26

**Topic:** E.01. Somatosensation – Pain and Itch

**Support:** NIH R15 NS137286-01A1

**Title:** Processing of sensory and affective pain descriptor words and EEG gamma band oscillations (31-50Hz) during acute cold pressor pain and chronic knee osteoarthritis

**Authors: *K. MALAVAR**[1], J. BABCOCK[2], H. STOLZ[2], H. FORD[2], A. RONCK[2], M. WIRTZ[2], A. NORRIS[2], A. PARK[3], A. L. HARRIS BOZER[2];
[1]Tarleton Neurosci., Stephenville, TX; [2]Neurosci., Tarleton State Univ., Stephenville, TX; [3]Univ. of Central Arkansas, Morrilton, AR

**Abstract:** Chronic pain is characterized by sensory, affective, and cognitive-evaluative dimensions. The aim of this study was to further examine the relationship of gamma band (31-50Hz) activity with pain perception, as participants responded to multidimensional pain descriptor words (sensory and affective) during acute pain and chronic knee osteoarthritis pain (OA). EEG data (256 electrodes; MagStim EGI) were obtained from 44 participants (18 males; OA n=21, controls n=23) as they responded to sensory and affective words taken from the short-form McGill Pain Questionnaire. Word ratings (none, mild, moderate, severe) and response times were recorded using a Chronos response box during baseline and a cold pressor arm wrap (acute pain) session. Mean spectral power values for gamma were extracted for electrodes purported to receive projections from cortical areas involved in pain processing (C3, C4, F7, F8) during both baseline and cold pressor, separated by word type (sensory and affective). Mixed ANOVAs were run with group (control/OA) as the between-subjects factor and word responses or reaction times as the within-subjects factors. For word ratings, there was a significant main effect of time and of group, $p<.001$, and a significant interaction effect, $p=.026$. OA participants rated sensory and affective words higher than the control group during baseline and during acute pain. Controls rated sensory words higher during the cold pressor, $p<.001$. For response times, there was no main effect of group or a significant interaction effect. There was a main effect of time, $p<.001$. Pearson's correlations were used to assess relationships between gamma activity and word ratings or response times. Within each time point and word type, there were no significant correlations between gamma and word ratings or response times, $p>.05$. In the current study, participants with OA pain rated pain descriptors higher at resting state and during an acute pain stimulus, indicating altered pain perception in a sample with chronic pain. However, although gamma oscillations have been implicated in pain perception, the current data indicate that gamma oscillations at these electrodes of interest may not play a role in processing multidimensional pain descriptor words.

**Disclosures: K. Malavar:** None. **J. Babcock:** None. **H. Stolz:** None. **H. Ford:** None. **A. Ronck:** None. **M. Wirtz:** None. **A. Norris:** None. **A. Park:** None. **A.L. Harris Bozer:** None.

**Poster**

**PSTR178: Pain Imaging and Perception**

**Location:** WCC Halls A-C

**Time:** Monday, November 16, 2026, 1:00 PM - 5:00 PM

**Program #/Poster #:** PSTR178.10/W27

**Topic:** E.01. Somatosensation – Pain and Itch

**Support:** NIH R15 NS137286-01A1

**Title:** EEG alpha band oscillations (8-13 Hz) during processing of sensory and affective pain descriptor words in acute cold pressor pain and chronic knee osteoarthritis

**Authors: *H. STOLZ**[1], A. NORRIS[1], K. MALAVAR[2], H. FORD[3], A. RONCK[3], M. WIRTZ[4], J. BABCOCK[5], A. PARK[7], A. L. HARRIS BOZER[6];
[1]Tarleton, Stephenville, TX; [2]Tarleton Neurosci., Stephenville, TX; [3]Tarleton State Univ.,

Stephenville, TX; [4]Tarleton State Univ., Georgetown, TX; [5]Tarleton State Univ., Gainesville, TX; [6]Neurosci., Tarleton State Univ., Stephenville, TX; [7]Univ. of Central Arkansas, Morrilton, AR

**Abstract:** Chronic pain involves sensory, affective, and cognitive dimensions. With alpha band oscillations linked to pain perception, the goal of this study was to (1) examine if participants with chronic pain due to osteoarthritis (OA) of the knee would demonstrate slower reaction times to multidimensional pain descriptor words and (2) if alpha band (8-13hz) activity in electrodes associated with pain (C3, C4, F7, F8) were associated with pain descriptor word responses. EEG signals were acquired (MagStim EGI; 256 electrodes) from 44 participants (control n=23, OA n=21; 18 males) during the presentation of pain descriptor words taken from the short form McGill Pain Questionnaire (sensory and affective). Participants rated (none, mild, moderate, severe) each word based using a Chronos response box at baseline, then during acute pain induced by a cold pressor arm wrap. Mixed ANOVAs were computed with group (control/OA) as the between subjects variable and word outcomes over time (word ratings and response times) as the within subjects variables. Results for response times indicated that there was no main effect of group or significant interaction effect, but a main effect of time, $p<.001$. Results for word ratings indicated a significant main effect of time and of group, $p<.001$, and a significant interaction effect $p=.026$. OA participants consistently rated sensory and affective words higher than controls. Controls rated the sensory pain words significantly higher during the cold pressor wrap, $p<.001$. Pearson's correlations were computed to examine the relationship of alpha activity to word ratings and response times. At the F8 electrode during the presentation of sensory words with cold pressor wrap, there was a significant positive correlation between alpha activity and word reaction times, $r=.343$, $p=.022$. Across baseline and acute pain time points, OA individuals did not require more time to respond to pain words, but submitted significantly higher ratings to pain words, supporting the idea that cognitive processing of pain and appraisal of pain stimuli differ in the presence of chronic pain. Although alpha (8-13hz) has been linked to pain perception, these data suggest alpha oscillations may play a limited role in responses to pain descriptor words.

**Disclosures: H. Stolz:** None. **A. Norris:** None. **K. Malavar:** None. **H. Ford:** None. **A. Ronck:** None. **M. Wirtz:** None. **J. Babcock:** None. **A. Park:** None. **A.L. Harris Bozer:** None.

**Poster**

**PSTR179: Non-Opioid Treatments for Persistent Pain**

**Location:** WCC Halls A-C

**Time:** Monday, November 16, 2026, 1:00 PM - 5:00 PM

**Program #/Poster #:** PSTR179.01/W28

**Topic:** E.01. Somatosensation – Pain and Itch

**Support:** NIA 5R33AG075419-04

**Title:** Overexpression of potassium channels in human iPSC derived sensory neurons demonstrates translational potential of gene therapy for chronic pain

**Authors: *C. J. SANDBERG**, R. Y. MEIR, C. A. BANNERMAN, A. H. HELD, B. WAINGER;
Massachusetts Gen. Hosp., Charlestown, MA

**Abstract:** Previously, our group validated that focal nerve delivery of AAV9-mediated potassium ($K^+$) channel overexpression enables precise spatial and cell-type specific targeting in mice and rats, establishing a promising strategy for pain modulation. We demonstrated that direct injection into the sciatic nerve results in robust expression in dorsal root ganglia sensory neurons, decreased neuronal excitability, and reduced behavioral phenotypes in models of both inflammatory and neuropathic pain. The AAV9 constructs expressed the channel transgene under the control of either the human synapsin (hSYN) promoter, a general pan-neuronal promoter, or a novel short promoter (sProm) designed for more specific targeting of nociceptors. The targeted overexpression of potassium channels via sProm reduced pain phenotypes and neuronal excitability comparable to those observed with hSYN, highlighting the potential of this novel promoter as a therapeutic strategy. To further validate the therapeutic potential of potassium channel overexpression, we assessed whether similar expression patterns could be achieved in human iPSC-derived nociceptive sensory neurons (idSNs). To generate mature and robust nociceptors, we differentiated iPSCs via a 28-day maturation process into idSNs that expressed genes with typical characteristics of nociceptors *(Scn9a*, *Scn10a*, *Trpv1*). Next, we applied either the control AAV (sProm-GFP) or the therapeutic AAV (sProm-$K^+$ Channel-GFP or hSYN-$K^+$ Channel-GFP) to day 21 idSNs and quantified expression levels 7 days post-transduction alongside co-labeling with nociceptor specific markers. On day 28, we observed evidence of successful transduction via imaging the GFP tag. Additionally, we performed electrophysiological recordings to confirm that overexpression produced functional potassium channels, resulting in increased potassium currents and decreased neuronal excitability. Overall, these initial findings demonstrate that AAV-mediated overexpression of potassium channels can occur in mature idSNs and recapitulate effects previously shown in mouse models. This work highlights the translational potential of potassium channel-based therapeutics for human pain disorders.

**Disclosures: C.J. Sandberg:** None. **R.Y. Meir:** None. **C.A. Bannerman:** None. **A.H. Held:** E. Ownership Interest (stock, stock options, royalty, receipt of intellectual property rights/patent holder, excluding diversified mutual funds); Patent filed on innovations described in poster. **B. Wainger:** E. Ownership Interest (stock, stock options, royalty, receipt of intellectual property rights/patent holder, excluding diversified mutual funds); Patent filed on innovations described in poster. F. Consulting Fees (e.g., advisory boards); Scientific advisory board member and consultant for Quralis.

**Poster**

**PSTR179: Non-Opioid Treatments for Persistent Pain**

**Location:** WCC Halls A-C

**Time:** Monday, November 16, 2026, 1:00 PM - 5:00 PM

**Program #/Poster #:** PSTR179.02/W29

**Topic:** E.01. Somatosensation – Pain and Itch

**Support:** U.S. Department of Defense CP230155

**Title:** Dose-dependent efficacy of intrathecal hiPSC derived chromaffin cell transplantation in a peripheral neuropathic pain model

**Authors: *S. JERGOVA**, B. RAHIMI, A. EESWARA, E. J. PACHECO, J. SAGEN;
Univ. of Miami, Miami, FL

**Abstract:** Chronic pain is a common and disabling consequence of peripheral or central nerve injury. Although many mechanisms and therapeutic targets have been identified, current treatments mainly provide short-term relief. Their long-term use is limited by reduced efficacy, dose escalation, tolerance, and systemic side effects, highlighting the need for more durable therapies. Prior work in our laboratory demonstrated that transplantation of adrenal medullary cells into the spinal subarachnoid space attenuates aberrant pain behaviors following peripheral nerve injury. Building on this, the present study investigates hiPSC-derived chromaffin cells sourced from human skin donors as a novel approach to sustained pain relief, with the added advantage of autologous derivation eliminating the need for immunosuppression. In the in vitro phase, chromaffin cells were differentiated from skin-derived hiPSCs and validated through immunostaining and secretion assays. To improve graft retention and limit cell dispersion post-transplantation, cells were embedded in VitroGel prior to implantation. In the in vivo phase, animals underwent unilateral sciatic nerve ligation via the chronic constriction injury model. One week later, three doses of hiPSC-derived chromaffin cells — 40k, 80k, and 160k — were transplanted intrathecally into the lumbar subarachnoid space, with fibroblasts serving as controls. Behavioral assessments including the acetone test and Von Frey were performed weekly for 12 weeks. Footprint and balance were assessed using the CatWalk test. Cell survival was evaluated at study endpoint. Rats receiving intrathecal hCC transplantation showed progressive reduction in pain behaviors across all doses, including the lowest (40k). Cell survival was confirmed by immunohistochemistry using tyrosine hydroxylase and hNuMA as chromaffin cell and human cell markers, respectively. Functional activity was validated by CSF catecholamine detection via ELISA, confirming viability and sustained function of transplanted cells. These findings establish skin fibroblast-derived hCCs as a viable and effective therapeutic strategy for peripheral neuropathic pain, with long-term survival and sustained analgesic activity supporting the potential for durable pain management. The University of Miami and J.S. and S.J. hold rights to intellectual property used in the study and may financially benefit from the commercialization of the intellectual property.

**Disclosures: S. Jergova:** None. **B. Rahimi:** None. **A. Eeswara:** None. **E.J. Pacheco:** None. **J. Sagen:** None.

**Poster**

**PSTR179: Non-Opioid Treatments for Persistent Pain**

**Location:** WCC Halls A-C

**Time:** Monday, November 16, 2026, 1:00 PM - 5:00 PM

**Program #/Poster #:** PSTR179.03/W30

**Topic:** E.01. Somatosensation – Pain and Itch

**Support:** DHA/Restoral funds

**Title:** (2R,6R)-Hydroxynorketamine is a novel analgesic in a chemotherapy-induced peripheral neuropathy mouse model.

**Authors: C. DANZY**[1], *B. CARABELLI[2], C. A. BROWNE[3], I. LUCKI[1];
[1]Pharmacol., Uniformed Services Univ. of the Hlth. Sci. (USUHS), Bethesda, MD; [2]Uniformed Services Univ. of the Hlth. Sci. (USUHS)., Bethesda, MD; [3]Dept. of Biol. Sci., Munster Technological Univ., Cork, Ireland

**Abstract:** Background: Platinum-based chemotherapeutic agents serve as standard treatments for various types of cancer. However, their clinical utility is frequently restricted by the onset of persistent pain and sensory hypersensitivity from chemotherapy-induced peripheral neuropathy (CIPN). Previous research has established that (2R,6R)-hydroxynorketamine ((2R,6R)-HNK) yields robust and prolonged antinociceptive effects in murine models of acute and chronic pain. Consequently, the primary objective of this study was to evaluate the potential analgesic efficacy of (2R,6R)-HNK using a mouse model of oxaliplatin (OXA)-induced CIPN.Methods: To induce CIPN, male C57BL/6J mice were treated with OXA (3 mg/kg, i.p.) for two 5-day cycles. Seven days post-induction, mechanical sensitivity was quantified using von Frey tests. Animals were then treated acutely with (2R,6R)-HNK (30 mg/kg, i.p.) and mechanical sensitivity was assessed at 4 and 24 hours post-injection. After a two-week washout period, mice were treated for 7 days with (2R,6R)-HNK. Mechanical sensitivity was assessed 24 hours after the last injection and then repeatedly until analgesic efficacy waned. Animals were subsequently euthanized and hippocampal tissue dissected, which was processed for GLUA1 and GLUA2 quantification using Western blot. Another cohort was treated with OXA and pre-treated with either 10 mg/kg i.p. NBQX (an AMPA receptor antagonist) or 1 mg/kg i.p. naltrexone (an opioid antagonist) 30 minutes before (2R,6R)-HNK administration. Behavioral outcomes were evaluated 24 hours later. Results: OXA administration induced mechanical hypersensitivity that was effectively reversed 4 and 24 hours after a single (2R,6R)-HNK injection. Repeated administration of (2R,6R)-HNK persistently mitigated allodynia, and paw withdrawal thresholds remained elevated for up to 21 days. AMPA blockade with NBQX completely prevented (2R,6R)-HNK-induced analgesia, while naltrexone administration yielded no effect. Western blot analysis demonstrated that OXA suppressed GLUA1 and GLUA2 receptor expression in the hippocampus and this was reversed by (2R,6R)-HNK. Conclusions: This study demonstrates that (2R,6R)-HNK confers potent long-lasting analgesia in a murine model of CIPN. Furthermore, repeated administration of (2R,6R)-HNK caused persistent analgesia that endured for weeks after treatment termination. Mechanistic assays reveal that this antinociceptive profile is dependent on AMPA receptors and not opioid receptors. Furthermore, (2R,6R)-HNK administration effectively normalizes the OXA-induced suppression of GLUA1 and GLUA2 receptor expression.

**Disclosures: C. Danzy:** None. **B. Carabelli:** None. **C.A. Browne:** None. **I. Lucki:** None.

**Poster**

**PSTR179: Non-Opioid Treatments for Persistent Pain**

**Location:** WCC Halls A-C

**Time:** Monday, November 16, 2026, 1:00 PM - 5:00 PM

**Program #/Poster #:** PSTR179.04/X1

**Topic:** E.01. Somatosensation – Pain and Itch

**Support:** University of Minnesota College of Pharmacy
University of Minnesota Center for Drug Design

**Title:** Novel guanabenz-based alpha-2 adrenergic receptor agonists for the treatment of pain

**Authors: *C. A. FAIRBANKS**[1], C. PETERSON[2], L. CAYE[3], J. NTAYAGABIRI[1], S. MORE[1], G. L. WILCOX[4];
[2]Neurosci., [3]Mol. Pharmacol. and Therapeut., [1]Univ. of Minnesota, Minneapolis, MN; [4]Dept Neurosci, Pharmacol, Univ. Minnesota Med. Sch., Minneapolis, MN

**Abstract:** Alpha 2 adrenergic receptor ($\alpha_2$-AR) agonists offer an effective, non-opioid analgesic strategy for the treatment of acute or chronic pain. While clonidine remains the best characterized $\alpha_2$-AR agonist, its use is inhibited by a side effect profile that includes hypotension and sedation, limiting patient compliance with prescribed analgesic regimens. Guanabenz (GB), an FDA-approved antihypertensive medication, provides analgesia in pre-clinical models of pain behavior but it is also limited by sedative side effects. We developed a line of $\alpha_2$-AR agonists based on GB and characterized their analgesic efficacy, side effect profile, and $\alpha_2$-AR subtype affinity utilizing *in vitro* and *in vivo* assays.
Methods: Female and male mice (21-30 g) were injected intrathecally and the warm water (52°C) tail flick (TF) assay was used as the nociceptive stimulus. Mice were pre-treated with either in-class control, the parent compound GB, or the newly developed $\alpha_2$-AR agonists and the maximum percent effect (%MPE) in extension of the tail flick latency was calculated as compared to base tail flick values. Following %MPE calculation, high effective doses were tested in the rotarod motor coordination assay and open field assay to investigate motor impairment and sedation. These compounds were also assessed in models of neuropathic pain (spared nerve injury) and inflammatory pain (complete Freund's adjuvant (CFA) injection). Compounds were also assessed for synergistic interactions in both analgesia and side effect profile.
Results: The GB-based, $\alpha_2$-AR agonists were effective in reducing pain behaviors in the TF assay. The efficacy of the GB-based compounds was inhibited by idazoxan but not naloxone co-administration, supporting action at $\alpha_2$-AR and not opioid receptors. The compounds, when co-administered, displayed a synergistic analgesic interaction. The GB-based compounds were also effective at reducing expression of pain behavior in acute and chronic rodent models of pain. Additionally, the compounds showed attenuated sedation as compared to the parent compound, guanabenz and a positive in-class control, clonidine. Pursuit of guanabenz-related analogs may represent an improved non-opioid analgesic strategy for the management of chronic pain.
Acknowledgments: These studies were supported by the College of Pharmacy and Center for Drug Design.

**Disclosures: C.A. Fairbanks:** None. **C. Peterson:** None. **L. Caye:** None. **J. Ntayagabiri:** None. **S. More:** E. Ownership Interest (stock, stock options, royalty, receipt of intellectual

property rights/patent holder, excluding diversified mutual funds); Patent Filed. **G.L. Wilcox:** None.

**Poster**

**PSTR179: Non-Opioid Treatments for Persistent Pain**

**Location:** WCC Halls A-C

**Time:** Monday, November 16, 2026, 1:00 PM - 5:00 PM

**Program #/Poster #:** PSTR179.05/X2

**Topic:** E.01. Somatosensation – Pain and Itch

**Support:** Department of Defense Peer-Reviewed Medical Research award [Grant W81XWH-19-1-0673]
College of Pharmacy, University of Minnesota

**Title:** Development of agmatine compounds for the treatment of pain

**Authors: *C. PETERSON**[1], L. CAYE[2], G. L. WILCOX[4], C. A. FAIRBANKS[3];
[2]Mol. Pharmacol. and Therapeut., [3]Pharmaceutics, Pharmacology, Neurosci., [1]Univ. of Minnesota, Minneapolis, MN; [4]Dept Neurosci, Pharmacol, Univ. Minnesota Med. Sch., Minneapolis, MN

**Abstract:** NMDA receptor antagonism is a promising, non-opioid clinical strategy to treat pain while avoiding side effects of concern, including respiratory depression, addiction, and tolerance. Agmatine, decarboxylated L-arginine, is an NMDA receptor antagonist with established pre-clinical and clinical efficacy in reducing pain and pain behaviors. However, its uptake as a therapeutic may be limited by pharmacokinetic and pharmacodynamic parameters. To address these concerns, we developed and characterized a series of agmatine-based compounds, termed the strategically-substituted agmatine (SSA) compounds, and characterized their analgesic efficacy and side effect profile.
Methods: We designed and synthesized strategically-substituted agmatine compounds (SSAs) with an intent to assess their efficacy in reducing pain behaviors in a model of post-incisional hyperalgesia. Female and male ICR mice (21-30 g) were given an incisional injury to the plantar surface of one hindpaw followed by an intravenous injection of either vehicle control or SSA3 30 mg/kg. von Frey mechanical thresholds were assessed prior to injury and following recovery from isoflurane anesthesia. In addition, open field activity was recorded and assessed to evaluate alterations in locomotion, sedation, and anxiety. The BlackBox One automated behavioral platform was used to assess gait, posture, and dynamic weight bearing. In addition to assessing analgesic efficacy, the SSA compounds were screened for side effects including drug-seeking behaviors utilizing self-administration assays as well as general toxicity scoring.
Results: We observed that increasing doses of SSA3 were effective in reducing mechanical hypersensitivity following incisional injury of the paw. Contralateral hindpaws did not display altered thresholds, indicating a lack of a sedative effect. Additionally, open field analysis did not show any alteration from vehicle control in ambulatory distance, ambulatory time, or duration in the inner zone of the apparatus. The injured paw showed increased weight bearing when a

subject was treated with SSA3 as compared to control subjects receiving vehicle, and SSA3 was not readily administered in a self-administration paradigm.
Funding was provided by Department of Defense Peer-Reviewed Medical Research award [Grant W81XWH-19-1-0673] (C.A.F.) and the College of Pharmacy of the University of Minnesota.

**Disclosures: C. Peterson:** E. Ownership Interest (stock, stock options, royalty, receipt of intellectual property rights/patent holder, excluding diversified mutual funds); PCT/US2019/060102. **L. Caye:** None. **G.L. Wilcox:** E. Ownership Interest (stock, stock options, royalty, receipt of intellectual property rights/patent holder, excluding diversified mutual funds); PCT/US2019/060102. **C.A. Fairbanks:** E. Ownership Interest (stock, stock options, royalty, receipt of intellectual property rights/patent holder, excluding diversified mutual funds); PCT/US2019/060102.

**Poster**

**PSTR179: Non-Opioid Treatments for Persistent Pain**

**Location:** WCC Halls A-C

**Time:** Monday, November 16, 2026, 1:00 PM - 5:00 PM

**Program #/Poster #:** PSTR179.06/X3

**Topic:** E.01. Somatosensation – Pain and Itch

**Support:** VCOM REAP
VCOM Virginia Tech One Health Res Grant

**Title:** Translational Evaluation of CNS4, an Agonist Concentration-Biased NMDA Receptor Modulator, Demonstrates Analgesic, Autonomic-Stabilizing, and Stress-Mitigating Effects Across Rodent and Canine Models

**Authors: *B. M. COSTA**[1,2], J. TUOHY[3], T. ISHIHARA[4], S. GOVINDASAMY[1], J. DAVIS[2], F. E. HARRISON[5], H.-L. PAN[6];
[1]Pharmacol., Edward Via Virginia Col. of Osteo. Med., Blacksburg, VA; [2]Dept. of Biomed. Sci. and Pathobiology, [3]Dept. of Small Animal Clin. Sci., Virginia Tech., Blacksburg, VA; [4]Dept. of Small Animal Clin. Sci., Virginia-Maryland Col. of Vet. Medicine, Virginia Tech., Blacksburg, VA; [5]Vanderbilt Univ. Med. Ctr., Nashville, TN; [6]Anesthesiol., Univ. Texas-MD Anderson Cancer Ctr., Houston, TX

**Abstract:** CNS4 is a novel low-affinity, agonist concentration-biased NMDA receptor modulator with GluN2 subtype-dependent effects on glutamatergic signaling. Here we evaluated the translational pharmacology of CNS4 across mice, rats, research dogs, and client-owned surgical oncology dogs. In mice, CNS4 did not produce conditioned place preference, indicating lack of reward liability compared to vehicle control. CNS4 produced dose-dependent reductions in locomotor activity without causing motor impairment on accelerating rotarod testing. CNS4 also altered thermoregulation to maintain the body temperature 0.5 to 1 °F above the vehicle group in mice and dogs. This observation is consistent with excitatory activity of NMDA

receptor-dependent thermoregulatory circuits, potentially within the hypothalamus, and contrasts with the hypothermic effects frequently reported for NMDA receptor channel blockers such as ketamine. In fear-conditioning paradigms, CNS4 did not impair fear learning or memory consolidation or fear expression during context and cue testing. CNS4 reduced acute stress-induced sucrose preference and decreased nest-building behavior at high doses, suggesting modulation of stress-responsive neural circuits. In a rat spinal nerve ligation (SNL) model of neuropathic pain, a single dose of CNS4 significantly reversed mechanical and thermal hypersensitivity, supporting analgesic efficacy in chronic neuropathic pain states. Pharmacokinetic studies in beagle dogs demonstrated measurable plasma exposure after subcutaneous and oral dosing. A 14-day acute toxicity study revealed acceptable tolerability with minimal injection site reaction. To evaluate translational clinical relevance, CNS4 was studied in client-owned surgical oncology dogs undergoing standard veterinary procedures. Preliminary findings from 14 dogs (8 CNS4-treated, 6 vehicle-treated) demonstrated stable intraoperative mean arterial pressure and heart rate in CNS4-treated animals. Post-operatively, CNS4-treated dogs exhibited improved physiologic recovery characterized by higher respiratory rate, heart rate, and body temperature toward the normal canine range despite comparable or lower post-operative analgesic burden scores. CNS4-treated dogs also required up to 8% less propofol during anesthesia maintenance. Collectively, these findings support CNS4 as a novel NMDA receptor modulator with analgesic, autonomic-stabilizing, and recovery-promoting properties without evidence of abuse liability. These results support continued translational development of CNS4 for peri-operative pain and neuropsychiatric disorders.

**Disclosures: B.M. Costa:** None. **J. Tuohy:** None. **T. Ishihara:** None. **S. Govindasamy:** None. **J. Davis:** None. **F.E. Harrison:** None. **H. Pan:** None.

**Poster**

**PSTR179: Non-Opioid Treatments for Persistent Pain**

**Location:** WCC Halls A-C

**Time:** Monday, November 16, 2026, 1:00 PM - 5:00 PM

**Program #/Poster #:** PSTR179.07/X4

**Topic:** E.01. Somatosensation – Pain and Itch

**Title:** GRT-NOP is a Selective Partial Agonist of Nociceptin/Orphanin FQ peptide (NOP) Receptors with Therapeutic Potential in Acute and Chronic Pain Disorders

**Authors: K. PASIKANTI**[1], M. PETTERSSON[1], E. SIUDA[1], R. SCHRAGE[2], S. PEIL[2], *E. NISENBAUM[1];
[1]GRT Therapeut. Inc. (Grünenthal), Cambridge, MA; [2]Grünenthal, Aachen, Germany

**Abstract:** Despite the wide range of available analgesics, effective pain management has been hindered by limitations in efficacy, safety, tolerability and/or potential for dependency and misuse. Identification of new therapies to address these challenges is urgently needed. Among new mechanisms being explored, the nociception/orphanin FQ receptor (NOP) is proposed due to its prominent neuronal expression at multiple sites of PNS and CNS somatosensory pathways

and potential to modulate pain signaling. The present studies describe the properties of a novel NOP agonist, GRT-NOP and its broad activity in suppressing pain signaling evoked by diverse stimuli in multiple species.GRT-NOP is a potent ($EC_{50}$=2.3 nM; $K_i$=2.3 nM) partial agonist ($E_{max}$=35-84% relative to nociception) of human NOP with negligible species differences in NOP affinity, but considerable selectivity versus the other human opioid receptors (mu $K_i$=3200 nM; delta $K_i$=840 nM and kappa $K_i$=3300 nM) (and 87 additional targets). GRT-NOP does not recruit β-arrestin and does not internalize NOP with prolonged stimulation compared to full NOP agonists. The major metabolite of GRT-NOP has similar properties and is expected to contribute to the overall PK/PD profile of GRT-NOP in vivo.The effects of GRT-NOP (or related compound) were tested on behavioral endpoints (i.e., paw/tail withdrawal) which served as surrogates for enhanced somatosensory signaling induced by heat, chemical activation (capsaicin), inflammation (Complete Freund's Adjuvant, CFA) or injury (Spared Nerve Injury, SNI) of peripheral nerves in rats or NHPs. Results showed that GRT-NOP dose-dependently reversed nocifensive responses in rats to either thermal or tactile stimuli following CFA treatment or SNI and these effects were durable for at least five days upon repeat dosing. In NHPs, selective NOP agonism reversed responses to acute heat stimulation alone or after capsaicin treatment. Corresponding PK measurements and predictions in PNS/CNS compartments showed that maximally efficacious doses were associated with the NOP target engagement (TE) values (defined as unbound drug concentration relative to its NOP affinity) of >90%, suggesting that full activity required appreciable CNS exposure in either species. No signs of sedation, impaired motor function or respiratory depression were observed. Collectively, these data suggest that GRT-NOP may be a promising, novel therapeutic for acute and/or chronic human pain disorders. Toward this end, the preclinical PK/PD relationships will be used to predict doses/exposures needed to achieve sufficient NOP TE values in humans for evaluation in upcoming clinical trials.

**Disclosures: K. Pasikanti:** A. Employment/Salary (full or part-time):; GRT Therapeutics Inc. **M. Pettersson:** A. Employment/Salary (full or part-time):; GRT Therapeutics Inc. **E. Siuda:** A. Employment/Salary (full or part-time):; GRT Therapeutics Inc. **R. Schrage:** A. Employment/Salary (full or part-time):; Grünenthal. **S. Peil:** A. Employment/Salary (full or part-time):; Grünenthal. **E. Nisenbaum:** A. Employment/Salary (full or part-time):; GRT Therapeutics Inc..

**Poster**

**PSTR179: Non-Opioid Treatments for Persistent Pain**

**Location:** WCC Halls A-C

**Time:** Monday, November 16, 2026, 1:00 PM - 5:00 PM

**Program #/Poster #:** PSTR179.08/X5

**Topic:** E.01. Somatosensation – Pain and Itch

**Support:** Peggy and Avinash Ahuja Foundation and the Helen Buchanan and Stanley Joseph Seeger Endowment at The University of Texas MD Anderson Cancer Center

**Title:** Nimodipine Attenuates Paclitaxel- and Nerve Injury-Induced Neuropathic Pain in Mice

**Authors: *Y. LU**[1], S. ABDI[1,2];
[2]Div. of Anesthesiology, Critical Care & Pain Medicine, Dept. of Pain Med., [1]The Univ. of Texas MD Anderson Cancer Ctr., Houston, TX

**Abstract:** Neuropathic pain from nerve injury or chemotherapeutic agents such as paclitaxel remains difficult to treat due to limited therapy options. Although L-type calcium channel blockers like nimodipine are widely used for cerebral vasospasm, their role in pain modulation is not fully understood. This study evaluated the antinociceptive effects of nimodipine in mouse models of neuropathic pain and explored its underlying mechanisms. Neuropathy was induced using four doses of paclitaxel (2 mg/kg, i.p.) to establish paclitaxel-induced peripheral neuropathy (PIPN), as well as through spared nerve injury (SNI). After the development of mechanical allodynia, mice received nimodipine (2, 10, or 20 mg/kg, i.p.), and mechanical sensitivity was assessed using von Frey filaments. Nimodipine produced dose-dependent analgesic effects in both models. In PIPN mice, a low dose (2 mg/kg) produced modest and transient relief, while higher doses (10 and 20 mg/kg) significantly increased mechanical thresholds, with onset around 30 minutes and effects lasting up to 4 hours. Similar reductions in hypersensitivity were observed in SNI mice, particularly at 10 and 20 mg/kg. Further mechanistic studies using molecular docking and computational modeling identified equilibrative nucleoside transporter 1 (ENT1) as a potential target of nimodipine. This interaction was supported by high-performance liquid chromatography and siRNA knockdown experiments, indicating that ENT1 inhibition contributes to its antinociceptive effects, likely through modulation of adenosine signaling. Collectively, these findings demonstrate that nimodipine produces robust, dose-dependent analgesia in neuropathic pain models and highlight ENT1 inhibition as a previously underrecognized mechanism, supporting its potential repurposing as a therapy for neuropathic pain.

**Disclosures: Y. Lu:** None. **S. Abdi:** None.

**Poster**

**PSTR179: Non-Opioid Treatments for Persistent Pain**

**Location:** WCC Halls A-C

**Time:** Monday, November 16, 2026, 1:00 PM - 5:00 PM

**Program #/Poster #:** PSTR179.09/X6

**Topic:** E.01. Somatosensation – Pain and Itch

**Support:** SUNY UBF Experimental Neurology Fund 0-02975

**Title:** Evaluation of prophylactic and therapeutic effects of central tumor necrosis factor blockade in paclitaxel induced peripheral neuropathy

**Authors: *M. ALHADLAQ**[1], K. INCARDONA[1], R. N. SPENGLER[2], T. A. IGNATOWSKI[1];
[1]Jacobs Sch. Of Med. And Biomed. Sci. (SUNY), Buffalo, NY; [2]Brain-Body Res. Institute™ (BBRI), Wilmington, DE

**Abstract: Background:** Paclitaxel is an effective chemotherapy drug used to treat breast, ovarian, and prostate cancers. However, despite its effectiveness, it is associated with a high incidence of paclitaxel-induced peripheral neuropathy (PIPN), which persists for over a year in approximately 64% of patients and increases in severity with cumulative chemotherapy dose. Peripheral neuropathy (PN) is a chronic neuropathic pain (NP) in which patients experience tingling, numbness, shooting pain, and burning sensations in their extremities, significantly affecting their daily quality of life. Current treatments are limited in effectiveness and are often associated with toxic side effects. The exact underlying mechanism of this neuropathy remains unclear; however, tumor necrosis factor-alpha (TNF) has been shown to contribute to pain development, where excessive accumulation of TNF in the brain disrupts the descending inhibitory pain pathway, resulting in enhanced pain sensitivity. Therefore, we hypothesized that blocking central TNF would reduce paclitaxel-induced pain behaviors, with prophylactic administration being more effective than therapeutic administration. **Methods**: Paclitaxel (4 mg/kg, intraperitoneally; i.p.) was administered to male and female Sprague-Dawley rats to induce NP. Control rats received i.p. injections of vehicle solution (CrEL) containing 4% DMSO. Anti-TNF antibody or its control IgG antibody was delivered perispinally either prophylactically (before paclitaxel administration) or therapeutically (after pain development) to assess its effects on reducing pain behaviors. Behavioral assessments of mechanical hypersensitivity and cold allodynia were evaluated. **Results**: Paclitaxel induced mechanical hypersensitivity and cold allodynia in both male and female rats equally, with no significant sex differences detected. Prophylactic administration of anti-TNF antibody reduced pain in a sex-dependent manner, decreasing mechanical hypersensitivity in males and cold allodynia in females. In contrast, therapeutic treatment showed no effect on either mechanical or cold pain reduction. **Conclusion**: These findings identify central TNF as a critical mediator in the initiation of PIPN and highlight early intervention targeting central TNF signaling as a potential strategy to prevent NP development. Overall, early TNF blockade may improve patient quality of life and reduce chemotherapy discontinuation, allowing patients to continue benefiting from paclitaxel treatment.

**Disclosures: M. Alhadlaq:** None. **K. Incardona:** None. **R.N. Spengler:** None. **T.A. Ignatowski:** None.

**Poster**

**PSTR179: Non-Opioid Treatments for Persistent Pain**

**Location:** WCC Halls A-C

**Time:** Monday, November 16, 2026, 1:00 PM - 5:00 PM

**Program #/Poster #:** PSTR179.10/X7

**Topic:** E.01. Somatosensation – Pain and Itch

**Support:** NIH 75N95024D00038

**Title:** Pharmacological characterization of rat models of chemotherapy-induced peripheral neuropathy

**Authors: *M. URBAN**[1], Y. ZHANG[1], M. CIKLIC[1], K. KROZSER[1], K. BUBAN[1], M. WOODS[1], C. CONRAD[2], S. A. WOLLER[2], S. IYENGAR[2], T. HANANIA[1];
[1]PsychoGenics, Inc., Paramus, NJ; [2]NINDS/NIH, Rockville, MD

**Abstract:** In collaboration with the NIH HEAL Initiative Preclinical Screening Platform for Pain (PSPP), we comprehensively profiled a variety of reference compounds in the rat paclitaxel and oxaliplatin models of chemotherapy-induced peripheral neuropathy (CIPN) to characterize the pharmacology associated with these models. Adult male and female Sprague Dawley rats (n=10, each sex) were used in these studies. For the paclitaxel model studies, paclitaxel (4 mg/kg, IP) was administered on alternate days (Day 1, 3, 5, 7) and effects of reference compounds on hind paw cold and mechanical allodynia were evaluated during Weeks 5 and 6, respectively. For the oxaliplatin model studies, oxaliplatin (3 mg/kg, IV) was injected 2 days per week for a period of 4 weeks and effects of reference compounds on hind paw cold and mechanical allodynia were evaluated during Weeks 6 and 7, respectively. Hind paw mechanical allodynia was measured with von Frey filaments using the "up-down" testing method, and hind paw cold allodynia was measured using the acetone test. In the paclitaxel model, hind paw cold and mechanical allodynia were maximal and stable by Week 5, whereas hind paw cold and mechanical allodynia were maximal and stable in the oxaliplatin model by Week 6. In the paclitaxel and oxaliplatin models, cold and mechanical allodynia were robustly inhibited following administration of morphine, gabapentin, or pregabalin, whereas administration duloxetine, carbamazepine, or nalfurafine primarily inhibited cold allodynia, with different effects observed in the paclitaxel and oxaliplatin models. Administration of ketoprofen, diclofenac, celecoxib or diazepam had minimal or no effect on cold or mechanical allodynia in these models. The data demonstrate that mu opioid receptor agonists and gabapentinoids are effective in inhibiting cold and mechanical allodynia in preclinical models of chemotherapy-induced peripheral neuropathy. SNRIs, sodium channel blockers, and kappa opioid receptor agonists are less effective and primarily inhibit cold allodynia, whereas NSAIDs and benzodiazepines are largely ineffective in these models. These studies highlight efforts within the NIH HEAL Initiative's PSPP program to characterize preclinical models of chemotherapy-induced peripheral neuropathy used to evaluate novel assets towards the development of novel non-opioid, non-addictive analgesics.

**Disclosures: M. Urban:** None. **Y. Zhang:** None. **M. Ciklic:** None. **K. Krozser:** None. **K. Buban:** None. **M. Woods:** None. **C. Conrad:** None. **S.A. Woller:** None. **S. Iyengar:** None. **T. Hanania:** None.

**Poster**

**PSTR179: Non-Opioid Treatments for Persistent Pain**

**Location:** WCC Halls A-C

**Time:** Monday, November 16, 2026, 1:00 PM - 5:00 PM

**Program #/Poster #:** PSTR179.11/X8

**Topic:** E.01. Somatosensation – Pain and Itch

**Support:** NIH/NINDS contract Contract No. 75N95024D00038

**Title:** In vivo PK, side effect profile, and analgesic efficacy of buprenorphine and ketorolac in male and female rats

**Authors: B. STANFIELD**[1], M. O. URBAN[1], D. BUDAC[3], C. CONRAD[4], S. A. WOLLER[5], S. IYENGAR[6], *T. HANANIA[2];
[1]Behavioral Pharmacol., [2]PsychoGenics, Inc., Paramus, NJ; [3]Behavioral Pharmacol., PsychoGenics Inc., Paramus, NJ; [4]NIH, Natl. Inst. of Neurolog. Disorders & Stroke (NINDS), Rockville, MD; [5]DTR, NIH/NINDS, Rockville, MD; [6]DTR, NINDS/NIH, Rockville, MD

**Abstract:** In collaboration with the NIH HEAL Initiative Preclinical Screening Platform for Pain (PSPP), we evaluated buprenorphine and ketorolac through the established tiered approach used to profile potential novel analgesics. First, pharmacokinetic (PK) studies were conducted to guide dosing, route of administration, and to determine the time course, supporting subsequent efficacy studies. Adult male (n=7) and female (n=7) Sprague Dawley rats were used in the PK studies for each arm. Next, the modified Irwin (n=4 male and 4 female rats) and rotarod tests (n=10 male and 10 female rats) were conducted to evaluate potential neurologic, physiologic, and motor effects that may impact outcome measures in the pain models. Analgesic efficacy was evaluated in the plantar incision and L5/L6 spinal nerve ligation (SNL) models. For both models 10 male and 10 female rats were used in each treatment arm. The rat plantar incision model is an established model of acute post-operative pain induced by incision of the skin and the plantaris muscle (Brennan et al. 1996). The model is characterized by transient hind paw tactile allodynia and spontaneous guarding behaviors. SNL is a model of peripheral neuropathic pain resulting from chronic nerve compression in which tactile and cold allodynia are produced (Kim and Chung, 1992). All experiments were conducted in a blinded manner. Power analysis was used to determine the group sizes. Side effect profile and efficacy studies showed that rats administered buprenorphine displayed low body position, reduced locomotor activity, sedation, exophthalmos, grooming, lacrimation, increased pupil size, and increased body temperature in a dose-dependent manner. Buprenorphine did not produce impairments in rotarod performance. Buprenorphine improved mechanical allodynia and spontaneous guarding behaviors in the plantar incision model and mechanical and cold allodynia behaviors in the SNL model. In side effect profile studies, ketorolac did not show observable behaviors or impairments on rotarod performance. In the plantar incision model, ketorolac showed minimal improvements on mechanical allodynia behavior in male rats but no efficacy on guarding behavior. In the SNL model, ketorolac showed minimal improvements on mechanical allodynia behavior in both male and female rats but did not show efficacy on cold allodynia. The results of these studies of clinically used compounds within the PSPP program demonstrate the validation of the models and endpoints described and highlight the goal of providing a robust platform to accelerate the discovery and preclinical development of non-opioid, non-addictive treatments for pain.

**Disclosures: B. Stanfield:** A. Employment/Salary (full or part-time):; PsychoGenics Inc. **M.O. Urban:** A. Employment/Salary (full or part-time):; PsychoGenics Inc. **D. Budac:** A. Employment/Salary (full or part-time):; PsychoGenics Inc. **C. Conrad:** None. **S.A. Woller:** None. **S. Iyengar:** None. **T. Hanania:** A. Employment/Salary (full or part-time):; PsychoGenics Inc.

**Poster**

**PSTR179: Non-Opioid Treatments for Persistent Pain**

**Location:** WCC Halls A-C

**Time:** Monday, November 16, 2026, 1:00 PM - 5:00 PM

**Program #/Poster #:** PSTR179.12/X9

**Topic:** E.01. Somatosensation – Pain and Itch

**Support:** State of Florida AWD009858

**Title:** Cell-based intrathecal delivery of CB1 acting conopeptid via engineered chromaffin cells for SCI neuropathic pain

**Authors: *B. RAHIMI**, A. EESWARA, S. JERGOVA, J. SAGEN;
Univ. of Miami, Miami, FL

**Abstract:** Chronic neuropathic pain is one of the most common and debilitating consequences of spinal cord injury (SCI), yet available treatments frequently fail to provide adequate long-term relief and carry significant systemic side effects. This study explores a novel cell-based therapeutic approach using human induced pluripotent stem cell (hiPSC)-derived chromaffin cells (hCCs) as a renewable, minimally invasive intrathecal platform for sustained local delivery of analgesic molecules. In the in vitro phase, chromaffin cells were differentiated from skin-derived hiPSCs and validated through immunostaining and secretion assays. These cells were then engineered to express and secrete newly identified CB1 receptor-acting conopeptide with strong analgesic properties. To engineer the cells, we screened a panel of AAVs to identify the most efficient transfection method and then confirmed CB1-acting conopeptide expression by immunostaining. We hypothesized that combining the endogenous catecholamine secretion of chromaffin cells with targeted cannabinoid peptide delivery would yield greater and more durable pain relief than either approach alone. In the in vivo phase, therapeutic efficacy was assessed in a rat clip-compression SCI model. Male and female animals were divided into two groups, each containing five subgroups: high-dose hCC (100k), high-dose hCC+CB1, low-dose hCC (30k), low-dose hCC+CB1, and a fibroblast control. Cells were transplanted intrathecally four weeks post-SCI in lumbar site (L5-L6), after confirmed allodynia and hyperalgesia. Behavioral outcomes — acetone test, Von Frey, and plantar heat — were assessed weekly over 12 weeks and CPP test was done with Gabapentin in the middle and end of experiment. Results demonstrated consistent generation of hiPSC-derived chromaffin cells from multiple donors, along with successful transgene expression, peptide secretion, and in vitro CB1 agonist activity. Behavioral testing showed that transplantation of high-dose hCC+CB1 significantly reduced pain-related behaviors compared with the other groups. Overall, this study supports a regenerative pain therapy that combines stem cell engineering with localized biologic delivery and highlights its translational potential as a personalized treatment for chronic SCI-related neuropathic pain.

**Disclosures: B. Rahimi:** None. **A. Eeswara:** None. **S. Jergova:** None. **J. Sagen:** None.

**Poster**

**PSTR179: Non-Opioid Treatments for Persistent Pain**

**Location:** WCC Halls A-C

**Time:** Monday, November 16, 2026, 1:00 PM - 5:00 PM

**Program #/Poster #:** PSTR179.13/X10

**Topic:** E.01. Somatosensation – Pain and Itch

**Support:** CAPES (Finance Code 001)
CNPq (314520/2023-6)

**Title:** Cannabigerol alleviates pain and anxiety-like behaviors in diabetic neuropathy: sex-dependent roles of CB1, CB2 and α2-adrenergic receptors in antinociception

**Authors: *M. V. FERREIRA**[1], L. R. RAMPIM[2], L. RAUCHBACH[2], J. M. ZANOVELI[3], J. M. CUNHA[4];
[1]Pharmacol., Univ. Federal do Paraná, Curitiba, Brazil; [2]Pharmacol., Federal Univ. of Paraná, Curitiba, Brazil; [3]Pharmacol., [4]Dept. of Pharmacol., Federal Univ. of Parana, Curitiba, Brazil

**Abstract:** Painful diabetic neuropathy is one of the most common and debilitating complications of diabetes and is frequently associated with anxiety-related symptoms. Given the limitations of current therapeutic options, alternative therapies like cannabinoids are being investigated. Cannabigerol (CBG), a phytocannabinoid with broad biological activities, shows therapeutic potential. Experimental diabetes was induced by a single injection of streptozotocin (STZ; 60 mg/kg, i.p.) in male and female adult Wistar rats (180-240 g). In the first phase, diabetic rats were treated for 14 days with vehicle or CBG (1, 3, 10, or 30 mg/kg, i.p.). Mechanical hypersensitivity was assessed by electronic von Frey at baseline and throughout treatment. Locomotor activity was evaluated in the open field test 1 h after the first CBG dose, and anxiety-like behavior was assessed in the elevated plus maze four weeks after STZ injection. In the second phase, independent cohort of diabetic rats were used to investigate the mechanisms underlying acute CBG antinociception. Animals were pre-treated with the CB1 receptor antagonist AM251 (1 mg/kg, i.p.), the CB2 receptor antagonist AM630 (1 mg/kg, i.p.), their combination, or the selective α2-adrenergic receptor antagonist atipamezole (3 mg/kg, i.p.), administered 30 min before CBG. Female rats developed mechanical hypersensitivity earlier than males; however, both sexes reached comparable nociceptive thresholds two weeks post-induction. Acute CBG reduced hypersensitivity at all tested doses in both sexes, with earlier peak effect in males. Chronic CBG fully reverted mechanical hypersensitivity in both sexes at all tested doses and attenuated anxiety-like behavior at 3 and 30 mg/kg in males, and at 3, 10, and 30 mg/kg in females, without altering locomotor activity. Mechanistically, AM251 blocked CBG antinociception by 35% in males and 63% in females, while AM630 blocked 77% in males and 42% in females. Notably, co-administration of both antagonists attenuated the antinociceptive effect by only 33% in males and failed to block the effect in females, suggesting a complex and sex-dependent interaction between CB1 and CB2-receptor-mediated pathways. In contrast, atipamezole completely abolished CBG-induced antinociception in both sexes. Collectively, these findings demonstrate sex-dependent differences in the contribution of cannabinoid receptors to CBG-induced analgesia, while identifying α2-adrenergic signaling as the predominant mechanism mediating its antinociceptive effects in diabetic neuropathy. All

experimental protocols were approved by Institutional Ethics on Animal Experimentation (CEUA-BIO-UFPR #1584).

**Disclosures: M.V. Ferreira:** None. **L.R. Rampim:** None. **L. Rauchbach:** None. **J.M. Zanoveli:** None. **J.M. Cunha:** None.

**Poster**

**PSTR179: Non-Opioid Treatments for Persistent Pain**

**Location:** WCC Halls A-C

**Time:** Monday, November 16, 2026, 1:00 PM - 5:00 PM

**Program #/Poster #:** PSTR179.14/X11

**Topic:** E.01. Somatosensation – Pain and Itch

**Support:** P50DA044118

**Title:** A fixed-ratio 1:4 Δ9-THC:cannabidiol formulation attenuates pain-stress responses in chronic pain patients and engages cortical 2-AG signaling in mice

**Authors: *R. M. KLEIN**[1], H. AVALOS[1], A. TRAN[1], F. AHMED[1], A. RAI[2], A. DAS[2], R. SINHA[3], D. PIOMELLI[4];
[1]Dept. of Anat. and Neurobio., Univ. of California, Irvine, Irvine, CA; [2]Sch. of Chem. and Biochem., Georgia Inst. of Technol., Atlanta, GA; [3]Yale Stress Ctr., Yale Univ. Sch. Med., New Haven, CT; [4]Dept. of Anat. and Neurobio., Univ. California Irvine, Irvine, CA

**Abstract:** Cannabis has long been investigated as a potential treatment for chronic pain, but its efficacy, optimal formulations, and underlying mechanisms remain incompletely established. In human experimental medicine studies from our group, co-administration of THC and CBD at a fixed 1:4 ratio attenuated experimentally provoked pain-stress responses in chronic pain patients and altered circulating levels of 2-arachidonoylglycerol (2-AG), a major endocannabinoid, with evidence linking 2-AG responses to individual variation in pain sensitivity and recovery. Adopting a reverse-translational approach, we aimed to determine whether this same THC ratio engages brain endocannabinoid signaling and to define the underlying mechanism in mice. Adult male mice received vehicle, THC (5 mg/kg), CBD (20 mg/kg), THC:CBD (5:20 mg/kg), or pharmacological pretreatments targeting cannabinoid receptors or 2-AG synthesis (n=5-7/group across experiments). Whole brain, dissected brain regions, including prefrontal cortex, remaining cortex, hippocampus, and hypothalamus, and plasma were collected 30 min after treatment. Samples were analyzed using targeted liquid chromatography tandem mass spectrometry (LC-MS/MS) for phytocannabinoids, THC metabolites, and endocannabinoid-related lipids. THC:CBD increased brain 2-AG relative to vehicle and single-drug controls. Regional profiling indicated that this response was enriched in cortex and not observed in the other regions examined. The 2-AG increase was not explained by a simple correlation between brain or plasma THC and 2-AG levels. Instead, THC:CBD shifted THC biotransformation *ex vivo*, increasing brain and plasma levels of the active metabolite 11-OH-THC and reducing levels of the inactive metabolite THC-COOH. Parallel *in vitro* assays using brain microsomes further supported an

effect of CBD on THC metabolism, with greater 11-OH-THC formation in the THC:CBD condition. Pharmacological experiments further supported a mechanism involving 2-AG synthesis and cannabinoid receptor type 1 ($CB_1$) dependence. This reverse-translational study shows that a THC:CBD 1:4 formulation that attenuates pain-stress responses in chronic pain patients recruits cortical 2-AG signaling in mice. These findings provide a mechanistic framework linking THC:CBD co-administration, altered THC metabolism, and a role for 2-AG signaling in the endocannabinoid regulation of adaptive pain-stress responses.

**Disclosures: R.M. Klein:** None. **H. Avalos:** None. **A. Tran:** None. **F. Ahmed:** None. **A. Rai:** None. **A. Das:** None. **R. Sinha:** None. **D. Piomelli:** None.

**Poster**

**PSTR179: Non-Opioid Treatments for Persistent Pain**

**Location:** WCC Halls A-C

**Time:** Monday, November 16, 2026, 1:00 PM - 5:00 PM

**Program #/Poster #:** PSTR179.15/X12

**Topic:** E.01. Somatosensation – Pain and Itch

**Support:** R01AT012053-01 (NIH/NCCIH)

**Title:** Characterizing the Neuropharmacology of Minor Cannabinoids in Neuropathy

**Authors: *N. M. MORRIS**[1], Q. W. WADE[1], K. E. VRANA[2], V. RUIZ-VELASCO[1], D. DESAI[2], N. M. GRAZIANE[1];
[1]Anesthesiol., [2]Mol. and Precision Med., Penn State Univ. Col. of Med., Hershey, PA

**Abstract: Background:** Chemotherapy-induced peripheral neuropathy (CIPN) is a debilitating side effect of cancer treatment with no FDA-approved therapies, creating a critical need for effective non-opioid analgesics. While minor phytocannabinoids are increasingly recognized for their potential therapeutic actions, many remain poorly characterized. Here, we investigated the neuropharmacology of two phytocannabinoids, cannabielsoin (CBE) and cannabifuran (CBF), in treating CIPN-associated mechanical allodynia. **Methods:** The minor cannabinoids CBE and CBF were evaluated *in vitro* using broad radioligand competition binding screens and fluorescence-based functional membrane potential assays at CB1 and CB2 receptors. *In vivo*, neuropathy was induced in male and female C57BL/6J mice using a 4-week cisplatin regimen (5 mg/kg, i.p., weekly). Mechanical allodynia and spontaneous locomotor activity were assessed 1-hour post-acute administration of CBE or CBF (10, 50, or 100 mg/kg, i.p.). Pharmacological synergy was evaluated in female mice using fixed-ratio dose combinations and Loewe additivity-based isobolographic analysis.**Results:** Functional membrane potential assays demonstrated that CBE has agonist activity at both CB1 (EC50 = 4.76 μM) and CB2 (EC50 = 5.70 μM) receptors, while CBF exhibited no agonist activity at these canonical targets. Broad radioligand binding screens revealed that CBF exhibits moderate affinity for histamine H3 receptors (Ki = 687.5 nM), whereas CBE demonstrated no measurable binding across screened non-cannabinoid targets. In behavioral studies, acute administration of CBE significantly attenuated mechanical

allodynia across all tested doses (10, 50, and 100 mg/kg) in both male and female mice. In contrast, CBF produced partial attenuation of mechanical allodynia only at higher doses (50 and 100 mg/kg) in both sexes. Neither compound altered spontaneous locomotor activity at the maximum effective dose, indicating a lack of gross motor impairment or sedation. Isobolographic analysis restricted to female mice revealed a ratio-dependent interaction where the 25:75 (CBF:CBE) dose combination demonstrated synergy.**Conclusion:** These findings demonstrate that the minor cannabinoids CBE and CBF have distinct receptor profiles, each individually attenuating mechanical allodynia while converging to produce synergistic antiallodynic actions in a ratio-dependent manner. As novel, non-sedating therapeutic agents, these structurally diverse phytocannabinoids display analgesic efficacy in neuropathic pain, providing a foundation for developing safer alternatives to opioids.

**Disclosures: N.M. Morris:** None. **Q.W. Wade:** None. **K.E. Vrana:** None. **V. Ruiz-Velasco:** None. **D. Desai:** None. **N.M. Graziane:** None.

**Poster**

**PSTR179: Non-Opioid Treatments for Persistent Pain**

**Location:** WCC Halls A-C

**Time:** Monday, November 16, 2026, 1:00 PM - 5:00 PM

**Program #/Poster #:** PSTR179.16/X13

**Topic:** E.01. Somatosensation – Pain and Itch

**Title:** Cisplatin chemotherapy induced chronic pain is attenuated by probiotics in C3H mic

**Authors: *A. GIANNOPOULOS**[1], G. CATALDO[2], M. MIAH[3];
[1]Queens College, City Univ. of New York, Hicksville, NY; [2]Psychology, Queens College, The City Univ. of New York, Flushing, NY; [3]Dept. of Psychology, Queens College, City Univ. of New York, Flushing, NY

**Abstract:** Neuropathic pain caused by damage or disease of the nervous system affects as much as 10% of the global population. Cisplatin is a common platinum based chemotherapeutic agent used in the treatment of cancer. Unfortunately, cisplatin is accompanied by a range of side effects reducing the effectiveness of treatment, affecting patient prognosis and ultimately, their survival. It also causes neuropathic pain, arising from cisplatin-induced peripheral neuropathy (CIPN) that is chronic in nature and permanent in 30-40% of patients who receive it. There is no known/effective therapy for patients who experience CIPN. Analgesics typically used to treat neuropathic pain, including opioids are relatively ineffective in alleviating pain from CIPN and exhibit their own adverse side effects such as motor impairment, tolerance, and dependence. VSL#3 probiotics contain 450 billion colony forming units (CFU) and 8 active strains of bacteria. Previous research using VSL#3 has shown the amelioration of aging effects on memory discrimination in mice older than 18 months. It has also been shown to be effective in attenuating pain, that is inflammatory/neuropathic in nature in sickle mice. We hypothesized that the VSL#3 probiotic would decrease pain and hyperalgesia in C3H mice with CIPN. Experimental mice were administered the VSL#3 probiotic (in their drinking water ad libitum) for 30 days prior to

cisplatin injections while controls received only vehicle (water) which did not alter baseline levels of pain. Cisplatin injections were administered to both groups at 1 mg/kg, i.p. for 7 consecutive days and then assessed for pain at day 15 and 30. Sensitivity to pain was assessed using a calibrated von Frey monofilament (0.4g) applied to each hindpaw and averaged to measure paw withdrawal frequency. C3H mice that were administered the probiotic for 30 days before cisplatin treatment showed a significant decrease in overall pain over 30 days compared to controls. Additionally, pretreatment with probiotics inhibited the chronicity of pain associated with CIPN. As in previous research, VSL#3 in the present study supported the idea that alternative treatments such as probiotics can be effective in reducing neuropathic pain, lacking the side effects associated with narcotic medications.

**Disclosures: A. Giannopoulos:** None. **G. Cataldo:** None. **M. Miah:** None.

**Poster**

**PSTR179: Non-Opioid Treatments for Persistent Pain**

**Location:** WCC Halls A-C

**Time:** Monday, November 16, 2026, 1:00 PM - 5:00 PM

**Program #/Poster #:** PSTR179.17/X14

**Topic:** E.01. Somatosensation – Pain and Itch

**Support:** SECIHTI Beca

**Title:** Potentiation of the Antiallodynic Effect of the Combination of a Sigma-1 Antagonist with Gabapentin in a Preclinical Model of Paclitaxel-Induced Neuropathy

**Authors: *T. GRACIDA GARCIA**[1], R. VENTURA-MARTINEZ[2], M. DECIGA-CAMPOS[1], G. E. ANGELES-LOPEZ[2];
[1]Sección de Estudios de Posgrado e Investigación, Inst. Politécnico Nacional, Mexico, Mexico; [2]Farmacologia, Facultad De Medicina UNAM, Mexico, Mexico

**Abstract:** Neuropathic pain is considered a disease of the somatosensory nervous system. In cancer patients, chemotherapy-induced neuropathy has a prevalence of 47.8% and may persist after treatment discontinuation. First-line drugs such as gabapentin provide limited relief of neuropathic pain and are associated with adverse effects. The sigma-1 receptor (σ-1R) has emerged as a relevant pharmacological target due to its role in the modulating chemotherapy-induced neuropathy. LMH-2, a selective σ-1R antagonist, has been synthesized as an optimized haloperidol analog without affinity for dopaminergic $D_2$ receptors. This study evaluated whether the coadministration of LMH-2 and gabapentin in a fixed 1:1 ratio potentiates the antiallodynic effect compared with the individual administration of each drug in a murine model of paclitaxel-induced neuropathy. It was hypothesized that this combination would produce a potentiating pharmacological interaction, allowing a reduction in the effective dose of both compounds. Methodology: Male CD1 mice weighing 25-30 g were used n = 6, and neuropathy was induced with paclitaxel (2 mg/kg every 48 h, with a total dose of 8 mg/kg). Mechanical allodynia was assessed using von Frey filaments. The antiallodynic effects of five doses of LMH-2 and

gabapentin were determined in separate groups, as was the effect of four doses of the combination of both drugs. The $ED_{50}$ values of LMH-2 and gabapentin administered individually, as well as those their 1:1 fixed-ratio combination, were determined. Pharmacological interaction was analyzed using the mathematical isobologram method. Results: Paclitaxel decreased in the withdrawal threshold from day 3 to day 8 compared with naïve mice, confirming the development of mechanical allodynia. LMH-2 and gabapentin, administered individually, showed antiallodynic effects with similar potencies, with $ED_{50}$ values of 21.3±3.9 and 24.1±1.7 mg/kg, respectively. The fixed-ratio 1:1 combination showed an experimental $ED_{50}$ significantly lower than the theoretical $ED_{50}$ (9.7±0.8 *vs*. 22.6±2.3 mg/kg, $p<0.05$, Student's t-test) and an interaction index of $\gamma = 0.43$. The isobologram analysis showed a significant potentiation of the antiallodynic effect of this combination. Conclusions: The combination of LMH-2 and gabapentin significantly potentiated the antiallodynic effect in the paclitaxel-induced neuropathy model. These results demonstrate that sigma-1 receptor inhibition in combination with gabapentin reduces the doses required for both drugs and supports a more effective and better-tolerated pharmacological strategy for the treatment of chemotherapy-associated neuropathic pain.

**Disclosures: T. Gracida Garcia:** None. **R. Ventura-Martinez:** None. **M. Deciga-Campos:** None. **G.E. Angeles-Lopez:** None.

**Poster**

**PSTR179: Non-Opioid Treatments for Persistent Pain**

**Location:** WCC Halls A-C

**Time:** Monday, November 16, 2026, 1:00 PM - 5:00 PM

**Program #/Poster #:** PSTR179.18/X15

**Topic:** E.01. Somatosensation – Pain and Itch

**Support:** TTUHSC Start-up
NIH Grant R01 DK134893

**Title:** Targeting Cellular Senescence with Polyphenol-Based Senolytics to Mitigate Diabetic Neuropathy

**Authors: V. THAKUR**[1], C. VALDEZ[1], *M. CHATTOPADHYAY[2];
[1]Mol. and Translational Med., Texas Tech. Univ. Hlth. Sci. Ctr. El Paso, El Paso, TX; [2]TTUHSC El Paso, El Paso, TX

**Abstract:** Chronic hyperglycemia in diabetes markedly increases the risk of peripheral neuropathy by inducing oxidative stress, which affects almost two-third of diabetic patients and interferes with their quality of life. Hyperglycemia also promotes the accumulation of senescent cells in multiple tissues, including the dorsal root ganglia (DRG) and spinal cord dorsal horn (SCDH). These senescent cells impair tissue repair and regeneration while sustaining a pro-inflammatory microenvironment that accelerates the progression of neuronal dysfunction. This study investigates how senescent cell accumulation plays a central role in the pathogenesis of

diabetic neuropathy. Furthermore, how treatment with a senolytic agent composed of four polyphenols—Quercetin, Epigallocatechin Gallate (EGCG), Curcumin, and Resveratrol—attenuates senescence-associated phenotypes and reduces inflammatory signaling in the DRG and SCDH of diabetic animals. Zucker Diabetic Fatty (ZDF) rats were used as an established model to investigate diabetes-related pathophysiological alterations in neuronal tissues. A group of ZDF rats received a polyphenol-based senolytic treatment with a combination of curcumin + quercetin and EGCG + resveratrol, each at 25 mg/kg, 2x/week for 6 weeks. Key biomarkers of cellular senescence, including $p16^{Ink4a}$, $p21^{Cip1}$, p53, Senescence-Associated β-galactosidase, Lamin B1, and γH2A.X, along with senescence-associated secretory phenotype (SASP) proteins such as IL-1β, TGF-β, MCP1, and MMP3, were evaluated across neuronal and non-neuronal cell populations. Senolytic treatment reduced the expression of senescence markers in sensory neurons and improved cellular homeostasis. Overall, this study highlights the therapeutic potential of targeting senescent cells using polyphenol-based senolytics to mitigate fibrotic remodeling of peripheral nerve and preserve nerve function in diabetes. The completion of this study may help optimize nutrition-based treatment options for this debilitating condition.

**Disclosures: V. Thakur:** None. **C. Valdez:** None. **M. Chattopadhyay:** None.

**Poster**

**PSTR179: Non-Opioid Treatments for Persistent Pain**

**Location:** WCC Halls A-C

**Time:** Monday, November 16, 2026, 1:00 PM - 5:00 PM

**Program #/Poster #:** PSTR179.19/X16

**Topic:** E.01. Somatosensation – Pain and Itch

**Support:** NIH HEAL grant 1RF1NS131812-01A1

**Title:** Activation of $CD8^+$ T cells resolves neuropathic pain in female mice via immunotherapy

**Authors: *S. SONG**[1], R. GUO[2], R. LI[4], R.-R. JI[3];
[1]Departments of Anesthesiol., [3]Pain Res. Division, Anesthesiol., [2]Duke Univ. Med. Ctr., Durham, NC; [4]Duke Univ., Durham, NC

**Abstract:** Chronic pain, disproportionately affecting women, involves inflammatory tolerance and sustained low-grade inflammation. During the transition from acute to chronic pain (>3 months), adaptive immune cells, particularly T cells, may modulate long-term pain persistence. However, the potential role of excessive T cell exhaustion, in promoting pain chronicity remains unclear. Programmed cell death protein-1 (PD-1) plays a crucial role in suppressing T cell function, and anti-PD-1 monoclonal antibodies (mAb) have been widely used for treating cancers as immunotherapy. However, the role of anti-PD-1 mAb in chronic neuropathic pain remains unexplored. In mouse model of the spared nerve injury (SNI) , we delivered anti-PD1 mAb via intrathecal route to target the spinal cord mechanisms of pain. Anti-PD-1 mAb (3 μg) was administered at two intervals (2 weeks and 4 weeks post SNI). We found this treatment elicited sustained analgesia across different pain modalities, including mechanical pain, cold

pain, and spontaneous pain in female mice, but not in male mice. Spinal cord RNA-seq in the spinal cord revealed the upregulated immune and T cell pathways in female mice following the treatment. This was corroborated by elevated $CD8^+$ T cell infiltration into the spinal cord. Furthermore, the analgesic effect of anti-PD-1 treatment was reversed by naloxone, suggesting that T cells may contribute to analgesia through an opioid receptor-dependent mechanism. These findings highlight that intrathecal administration of anti-PD-1 mAb may provide a promising, non-addictive strategy for treating chronic neuropathic pain by reactivating spinal immune responses and enhancing $CD8^+$ T-cell function, in a sex-dependent manner. Thus, the FDA-apporved immunotherapy may be repurposed for chronic pain management.

**Disclosures: S. Song:** None. **R. Guo:** None. **R. Li:** None. **R. Ji:** None.

**Poster**

**PSTR179: Non-Opioid Treatments for Persistent Pain**

**Location:** WCC Halls A-C

**Time:** Monday, November 16, 2026, 1:00 PM - 5:00 PM

**Program #/Poster #:** PSTR179.20/X17

**Topic:** E.01. Somatosensation – Pain and Itch

**Support:** NIH Grant R18EB035005

**Title:** Noninvasive Diagnostic Ultrasound-Guided Focused Ultrasound Enables Selective, Reversible Inhibition of Peripheral Nociceptive Fibers in a Rat Model of Acute Pain

**Authors: *N. SANGWAN**[1], L. MERGELIAN[2], M. MOHAMMADJAVADI[3], R. NAVANI[4], C. PACHARINSAK[5], K. BUTTS PAULY[3], T. ANDERSON[6];
[1]Dept. of Anesthesiology, Perioperative and Pain Med., Sch. of Medicine, Stanford Univ., Palo Alto, CA; [2]Dept. of Anesthesiology, Perioperative and Pain Med., Stanford Univ., Palo Alto, CA; [3]Dept. of Radiology, Stanford Univ., Stanford University, CA; [4]Dept. of Human Biol., Stanford Univ., Milpitas, CA; [5]Dept. of Comparative Med., Stanford Univ., Stanford, CA; [6]Anesthesiology, Perioperative and Pain Med., Stanford Univ., Palo Alto, CA

**Abstract:** Acute postoperative pain remains a significant clinical challenge, and current analgesic strategies, including local anesthetic-based peripheral nerve blocks (PNBs), are limited by invasiveness, short duration, and nonselective inhibition of motor and sensory fibers. Focused ultrasound (FUS) is an emerging neuromodulatory technology with the potential to noninvasively, selectively, and reversibly inhibit peripheral nociceptive fibers. We investigated whether diagnostic ultrasound (dUS)-guided FUS application to the sciatic nerve could prevent pain behaviors while preserving motor and non-pain sensory function in a rat hindpaw incision (HPI) model of acute pain. A total of 72 adult male and female Sprague-Dawley rats were randomized into six study arms: Control (No intervention), HPI Only, Sham FUS, FUS Only, FUS+HPI, and Local Anesthetic+HPI (n=12/group). Under dUS guidance, the sciatic nerve was identified approximately 1 cm proximal to its trifurcation, and FUS was applied transcutaneously immediately before hindpaw incision. FUS parameters were optimized to maximize nociceptive

fiber inhibition while minimizing motor and non-pain sensory inhibition. Behavioral testing was performed for up to 16 weeks. Primary outcomes included thermal withdrawal latency (modified Hargreaves) and mechanical withdrawal threshold (Randall-Selitto). Secondary outcomes included hindpaw flexion and extension.Compared with HPI Only animals, FUS+HPI animals demonstrated significant attenuation of thermal hypersensitivity from day 0 through week 5 and weeks 8-16 ($p<0.05$-$0.001$), and significant attenuation of mechanical hypersensitivity from day 0 through week 5 ($p<0.05$-$0.001$). Hindpaw flexion and extension remained preserved. Local anesthetic produced transient inhibition of nociceptive, motor, and non-pain sensory behaviors. Animals in the Sham FUS and FUS Only study arms had behaviors non-statistically different from animals in the Control study arm.Using co-aligned dUS and FUS transducers to noninvasively target the sciatic nerve, we identified a FUS parameter set that selectively and reversibly inhibited Aδ- and C-fiber-mediated acute and persistent nociceptive behaviors while preserving Aα motor and Aβ sensory function. These findings support dUS-guided FUS-induced peripheral nerve blockade as a promising noninvasive strategy for preventing acute postoperative pain and persistent pain following injury.

**Disclosures: N. Sangwan:** None. **L. Mergelian:** None. **M. Mohammadjavadi:** None. **R. Navani:** None. **C. Pacharinsak:** None. **K. Butts Pauly:** None. **T. Anderson:** None.

**Poster**

**PSTR179: Non-Opioid Treatments for Persistent Pain**

**Location:** WCC Halls A-C

**Time:** Monday, November 16, 2026, 1:00 PM - 5:00 PM

**Program #/Poster #:** PSTR179.21/Web Only

**Topic:** E.01. Somatosensation – Pain and Itch

**Support:** NIH Grant R18EB035005

**Title:** Focused Ultrasound-Mediated Peripheral Nerve Modulation in Acute Incisional Pain: Time-Dependent Changes in Nociceptor-Specific Molecular Markers

**Authors: *L. MERGELIAN**[1], N. SANGWAN[1], M. KLUKINOV[1], M. MOHAMMADJAVADI[2], L. J. DONOVAN[1], A. R. NIPPERT[1], C. PACHARINSAK[3], K. BUTTS PAULY[2], V. L. TAWFIK[1], D. C. YEOMANS[1], T. A. ANDERSON[1];
[1]Dept. of Anesthesiology, Perioperative and Pain Med., [2]Dept. of Radiology, [3]Dept. of Comparative Med., Stanford Sch. of Med., Stanford, CA

**Abstract:** Moderate-to-severe postoperative acute pain remains a prevalent and frequently inadequately managed clinical challenge. Current therapies that are available such as traditional needle- and local anesthetic-based peripheral nerve blocks (PNBs) provide effective relief for many patients, but their utility is constrained by practical limitations, including their invasiveness, relatively short duration of action, need for significant training to conduct, and non-selective nerve fiber inhibition. We utilized a novel diagnostic ultrasound-guided focused ultrasound (dUS-FUS) device to noninvasively deliver acoustic energy to the rat sciatic nerve,

producing a reversible PNB in a rodent model of acute incisional pain (hindpaw incision, HPI), and characterized the temporal changes in nociceptive (pain) marker expression compared to controls. Adult male and female Sprague-Dawley rats (200-400 g) (n = 48) were randomly assigned to the following treatment groups: No Intervention (Control), HPI Only (Disease Control), FUS+HPI(Intervention), and Local Anesthetic (LA)+HPI (0.5% Bupivacaine; Positive Control). Animals were then euthanized at 2 hours, 1 day, 3 days, and 7 days after receiving their respective treatments, and their sciatic nerves were excised, preserved, and sectioned for immunohistochemical staining for expression levels of the following pain markers: Nav1.7, Osteopontin (OPN), Transient Receptor Potential Vanilloid 1 (TRPV1), and Peripherin. Images were acquired using a Zeiss confocal microscope with a 40× oil-immersion objective and analyzed using qualitative and quantitative approaches to assess marker expression across treatment groups and time points. Compared to nerves from the HPI Only group (n = 12), nerves from the FUS+HPI group (n = 12) generally showed decreased expression of Nav1.7, TRPV1, and Peripherin across different time points, and differences were most prominent on day 1 and 7. Nerves from the LA+HPI group (n = 12) demonstrated (1) lowered Nav1.7 expression, as well as nerves from the FUS+HPI group on day 1 (notably decreased expression compared to the HPI Only group); and (2) but Nav1.7 expression on days 3 and 7 was not as low as in the FUS+HPI group. These findings suggest that preinjury FUS attenuates injury-associated nociceptive signaling and supports further investigation of dUS-guided FUS as a novel non-invasive approach for acute pain prevention and treatment.

**Disclosures: L. Mergelian:** None. **N. Sangwan:** None. **M. Klukinov:** None. **M. Mohammadjavadi:** None. **L.J. Donovan:** None. **A.R. Nippert:** None. **C. Pacharinsak:** None. **K. Butts Pauly:** None. **V.L. Tawfik:** None. **D.C. Yeomans:** None. **T.A. Anderson:** None.

**Poster**

**PSTR179: Non-Opioid Treatments for Persistent Pain**

**Location:** WCC Halls A-C

**Time:** Monday, November 16, 2026, 1:00 PM - 5:00 PM

**Program #/Poster #:** PSTR179.22/X18

**Topic:** E.01. Somatosensation – Pain and Itch

**Title:** Effects of Therapeutic Ultrasound on Chest Wall Pain and Inflammatory Responses Following Flail Chest in Rats

**Authors: *A.-K. CHOU**;
China Med. Univ. Hosp., Taichung, Taiwan

**Abstract:** Flail chest is often accompanied by persistent chest wall pain and local inflammatory responses that may delay recovery. Therapeutic ultrasound (TU) has been used in rehabilitation medicine for pain control and soft tissue disorders; however, its effects on pain and inflammation following flail chest have not been well characterized. This study examined the effects of TU on mechanical hypersensitivity and inflammatory marker expression in a rat model of flail chest.

Rats were randomly assigned to three groups: sham, flail chest (FC), and flail chest treated with therapeutic ultrasound (FC+TU). TU treatment was initiated on postoperative day (POD) 17 and continued through POD 28. Body weight was monitored throughout the experimental period. Mechanical sensitivity was assessed using von Frey filaments at predetermined time points after injury. To evaluate local inflammatory responses, the fourth rib was harvested on POD 28 for analysis of interleukin-6 (IL-6), tumor necrosis factor-α (TNF-α), and nuclear factor kappa B (NF-κB).
Body weight increased over time in all groups, and no differences in weight gain were observed among groups during the study period. Mechanical thresholds remained stable in the sham group. In contrast, rats subjected to flail chest developed mechanical hypersensitivity by POD 7 ($p<0.05$), and this response persisted through POD 14 ($p<0.001$). Following the initiation of TU treatment, force thresholds increased in the FC+TU group. Compared with untreated FC animals, force thresholds were significantly higher in TU-treated rats on PODs 21, 24, and 28 ($p<0.01$), indicating reduced mechanical hypersensitivity after treatment.
Analysis of rib tissue demonstrated increased expression of IL-6, TNF-α, and NF-κB following flail chest injury when compared with the sham group ($p<0.05$). Rats receiving TU showed lower expression of these inflammatory markers than untreated FC animals. Expression levels in the FC+TU group approached those observed in sham animals. The reduction in inflammatory marker expression was accompanied by improvement in mechanical sensitivity during the treatment period.
In summary, flail chest produced prolonged mechanical hypersensitivity and increased local expression of IL-6, TNF-α, and NF-κB in rats. Therapeutic ultrasound was associated with higher mechanical withdrawal thresholds and lower expression of inflammatory markers after injury. These findings support the use of therapeutic ultrasound as a noninvasive approach for reducing pain-related hypersensitivity and local inflammatory activity following chest wall injury.

**Disclosures: A. Chou:** None.

**Poster**

**PSTR179: Non-Opioid Treatments for Persistent Pain**

**Location:** WCC Halls A-C

**Time:** Monday, November 16, 2026, 1:00 PM - 5:00 PM

**Program #/Poster #:** PSTR179.23/X19

**Topic:** E.01. Somatosensation – Pain and Itch

**Title:** Peak Alpha Frequency as Modifiable Therapeutic Target for Pain: Effects of Preoperative Auditory Stimulation in Spine Surgery Patients

**Authors: *H. EBADI**;
Washington Univ. in St. Louis, St. Louis, MO

**Abstract:** Postoperative pain and opioid use remain major challenges following elective spine surgery, highlighting the need for non-pharmacological interventions that target the neural

mechanisms of pain. Peak alpha frequency (PAF), the dominant frequency of resting-state electroencephalographic (EEG) alpha oscillations (8-13 Hz), has emerged as a reliable, trait-like biomarker of individual pain sensitivity; slower PAF is associated with heightened pain sensitivity, whereas faster PAF is linked to greater pain tolerance. Despite robust observational evidence connecting PAF to pain outcomes in both experimental and clinical populations, no study has investigated whether PAF can be deliberately modified as a therapeutic target or whether such modification can improve postoperative outcomes. To address this gap, we conducted a randomized study of 39 adult patients (mean age 66.9 years, male & female) undergoing elective spine surgery to test whether preoperative 8 Hz auditory stimulation could shift PAF and reduce postoperative pain and opioid consumption. Patients were randomized to receive daily preoperative 8 Hz auditory stimulation (treatment, n=22) or sham stimulation (n=7). Eyes-closed resting-state EEG was recorded at three time points: enrollment, day of surgery, and day of discharge. PAF was derived using a center-of-gravity approach applied to detrended alpha-band power spectra. Treatment patients were stratified by baseline PAF into Slow (<10.1 Hz) and Fast (≥10.1 Hz) groups. Auditory stimulation produced bidirectional modulation of PAF**:** the Slow group increased ($p=0.014$) and the Fast group decreased ($p=0.003$), converging symmetrically toward ~10 Hz, whereas sham patients showed no significant change ($p=0.375$). In the Slow group, preoperative listening reduced VAS neck/back pain prior to surgery ($p=0.004$), and by postoperative day 3, pain levels had fallen below baseline values ($p=0.031$). The magnitude of individual PAF increase was strongly associated with reduced postoperative opioid consumption ($r=-0.866$, $p=0.001$), and a dose-response relationship was observed between preoperative listening duration and PAF shift magnitude ($r=0.688$, $p=0.019$). These findings provide the first evidence that PAF is not merely a static biomarker of pain susceptibility but a modifiable therapeutic target, and that a simple, home-based auditory intervention administered preoperatively can induce neurophysiological changes that translate into meaningful clinical benefits for spine surgery patients.

**Disclosures: H. Ebadi:** None.

**Poster**

**PSTR179: Non-Opioid Treatments for Persistent Pain**

**Location:** WCC Halls A-C

**Time:** Monday, November 16, 2026, 1:00 PM - 5:00 PM

**Program #/Poster #:** PSTR179.24/X20

**Topic:** E.01. Somatosensation – Pain and Itch

**Support:** NIH Grant R18 EB036591-01
Focused Ultrasound Foundation Grant

**Title:** Noninvasive magneto-acoustic spinal stimulation yields durable analgesia in neuropathic pain

**Authors: *J. R. CARTER**[1], M. J. BARTLETT[3], R. MAYER[1], U. KILIC[1], Y.-H. CHOU[2], G. BONMASSAR[4], J. G. PILITSIS[1];

[1]Neurosurg., [2]Psychology, Univ. of Arizona, Tucson, AZ; [3]Surgery, The Univ. of Arizona, Tucson, AZ; [4]Radiology, Harvard Med. Sch., Charlestown, MA

**Abstract:** Objective: Chronic neuropathic pain remains poorly managed by available therapies. Noninvasive approaches capable of directly engaging spinal pain circuits represent an unmet clinical need. LIFU and TSMS each offer complementary biophysical properties for spinal neuromodulation, but neither alone reliably achieves durable and meaningful pain relief. This study evaluates whether a novel dual stimulation strategy delivering simultaneous LIFU and TSMS through a single coaxial probe can produce effective and safe analgesia in a rodent model of peripheral neuropathic pain.
Methods: Sprague Dawley rats underwent common peroneal nerve injury (CPNI) to induce neuropathic pain. There were four cohorts - male CPNI with LIFU/TSMS (n = 6), male CPNI with sham LIFU/TSMS (n = 6), female CPNI with LIFU/TSMS (n = 7); female CPNI with sham LIFU/TSMS (n = 8). Seven days post-injury, animals received either a single 45-minute LIFU/TSMS stimulation or sham stimulation targeting T13/L1. Mechanical allodynia was assessed by von Frey filament test at one hour and daily for seven days post-treatment. Thermal sensitivity, locomotor activity, and depression-like behavior were assessed by hot plate, open field, and forced swim tests at 24 hours. Spinal cord tissue integrity was evaluated histologically using H&E and Fluoro-Jade C staining.
Results: LIFU/TSMS significantly reduced mechanical allodynia within one hour in both females ($p = 0.02$) and male ($p = 0.004$) rats compared with sham. Analgesia persisted for up to 7 days in females ($p = 0.003$) and up to 5 days in males ($p = 0.04$). Thermal hypersensitivity was significantly reduced at 24 hours in both sexes (females $p = 0.012$; males $p < 0.001$), with a larger effect in males. No spinal tissue injury or neuronal degeneration was detected in either sex.
Conclusion: A single session of LIFU/TSMS produces rapid and durable multimodal analgesia in a rodent model of neuropathic pain without detectable tissue damage, supporting multimodal spinal neuromodulation as a promising therapeutic strategy for chronic pain.

**Disclosures: J.R. Carter:** None. **M.J. Bartlett:** None. **R. Mayer:** None. **U. Kilic:** None. **Y. Chou:** None. **G. Bonmassar:** None. **J.G. Pilitsis:** None.

**Poster**

**PSTR179: Non-Opioid Treatments for Persistent Pain**

**Location:** WCC Halls A-C

**Time:** Monday, November 16, 2026, 1:00 PM - 5:00 PM

**Program #/Poster #:** PSTR179.25/X21

**Topic:** E.05. Auditory and Vestibular Systems

**Title:** Shamanic drumming reduces pain and improves mood in fibromyalgia: A role for peak alpha frequency

**Authors: *S. ELLIS**, B. R. PLUIMER, A. SRIDHAR, C. LYNSKEY, J. YEN, H. BAO, R. E. HARRIS;
Univ. of California, Irvine, Irvine, CA

**Abstract:** Fibromyalgia is a chronic pain disorder with high comorbidity rates for depression and anxiety. Despite growing recognition that affective dysregulation and altered pain processing share overlapping neural substrates, the mechanisms by which non-pharmacological interventions might simultaneously address both domains remain poorly understood. Shamanic drumming is an ancient healing practice documented across indigenous cultures for millennia, yet its clinical efficacy and neurophysiological mechanisms remain largely uncharacterized.This study investigated the effects of a shamanic drumming intervention on self-reported pain, mood, and anxiety in fibromyalgia patients, and tested whether resting-state peak alpha frequency (PAF), an index previously associated with individual differences in pain sensitivity and depression, would predict or correlate with treatment response. In this pilot study, twelve participants completed 5 individual sessions over 5 weeks with a trained shamanic practitioner. Before and after the intervention, participants completed validated assessments of depressive symptomatology (PHQ-9), mood and anxiety (MASQ), and pain severity and interference (PainDETECT, FIQR, BPI). Follow-up behavioral data were collected at 1-month, 3-months, and 6-months. EEG was collected at the baseline and final visit. Resting-state EEG recorded at baseline was analyzed for PAF.Significant pre-to-post improvements were observed in both mood ($p = 0.022$, $d = 0.870$) and pain ($p=0.027$, $d = 0.831$). Additionally, changes in affective measures were significantly correlated with changes in pain interference ($r$s = 0.914, $p < .001$). Importantly, baseline PAF significantly predicted post-intervention changes in mood and anxiety during the follow-up visits, with slower baseline PAF correlating with greater reductions in depressive and anxiety-like symptoms ($r$s = 0.803, $p = 0.009$). These findings support shamanic drumming as a candidate intervention capable of producing concurrent improvements in pain and affective symptoms in fibromyalgia. Furthermore, PAF may serve as a neurophysiological biomarker for predicting affective treatment response, with implications for individualized treatment in chronic pain populations.

**Disclosures: S. Ellis:** None. **B.R. Pluimer:** None. **A. Sridhar:** None. **C. Lynskey:** None. **J. Yen:** None. **H. Bao:** None. **R.E. Harris:** None.

**Poster**

**PSTR179: Non-Opioid Treatments for Persistent Pain**

**Location:** WCC Halls A-C

**Time:** Monday, November 16, 2026, 1:00 PM - 5:00 PM

**Program #/Poster #:** PSTR179.26/X22

**Topic:** E.01. Somatosensation – Pain and Itch

**Support:** NCI R21CA256136

**Title:** Randomized, waitlist-controlled Study of nonpharmacologic Treatment with Scrambler Therapy for Chemotherapy-Induced Painful Peripheral Neuropathy in Adolescents and Young Adults (AYA) with Cancer

**Authors: *S. ABDI**[1], J. WANG[2], S.-E. SHEN[3], X. WANG[4];
[1]Pain Med., The Univ. of Texas MD Anderson Cancer Ctr., Houston, TX; [2]Biostatistics, [3]Symptom Res., UT MD Anderson Cancer Ctr., Houston, TX; [4]Symptom Res., UT, MD Anderson Cancer Ctr., Houston, TX

**Abstract: Aim**: To demonstrate that Scrambler Therapy (ST) may be a safe and valuable alternative to pharmacologic management of chemotherapy-induced painful peripheral neuropathy (CIPN) that can effectively reduce pain and improve neuropathy and quality of life (QoL) in adolescents and young adults (AYAs) with CIPN. **Methods**: Patients with CIPN were enrolled in a prospective, randomized, waitlist-controlled clinical trial and underwent 10 ST treatments (C-30 each session lasting 45 minutes) in the Pain Management Center at MD Anderson Cancer Center. Eligible patients had moderate-to-severe CIPN-associated symptoms of pain or neuropathy (≥4 on a 0-10 scale). Patients were randomized either to immediately receive ST treatment (iST) or into the waitlist (WL) group to continue usual treatment for 4 weeks after randomization before starting ST. During treatment, eight electrodes were applied to areas of normal sensation (non-painful) adjacent to areas of pain on bilateral feet and legs. All patients completed patient-reported outcome (PRO) measurements, including the Brief Pain Inventory Short Form (BPI-SF) and Treatment-Induced Neuropathy Assessment Scale (TNAS), at baseline, weekly during the waitlist period, each day of ST treatment, weekly for 4 weeks after treatment, and monthly up to 3 months. Symptom severity comparisons between treatment groups were performed using Wilcoxon rank-sum tests. **Results**: A total of 30 patients were enrolled, ages 22-39 years old, with 15 patients randomized to each treatment group. Cronback alpha for TNAS at baseline was 0.8534. Between the iST group at week 2 post-treatment and the WL group at waitlist week 2, we observed a significant difference in mean severity of the TNAS tingling item (mean 2.27 vs. 6.10, P=.004, and hot/burning sensations (mean 0.55 vs. 4.10, P=.018). Effect stranded for week 3 post-ST. For all patients, there was a significant reduction in the BPI-SF worst pain item from day 1 of ST to the end of treatment (P = 0.0006) and 3 months post-treatment (P = 0.0002) and a significant reduction in numbness (TNAS) from day 10 to 3m (P=.015). There was no significant change in TNAS pain item scores between the end of ST and 3 months post-treatment. **Conclusion**: AYA patients with cancer who had CIPN and underwent immediate ST reported better sensory function than patients in the wait-list control group up to 3 months after therapy.

**Disclosures: S. Abdi:** None. **J. Wang:** None. **S. Shen:** None. **X. Wang:** None.

**Poster**

**PSTR179: Non-Opioid Treatments for Persistent Pain**

**Location:** WCC Halls A-C

**Time:** Monday, November 16, 2026, 1:00 PM - 5:00 PM

**Program #/Poster #:** PSTR179.27/X23

**Topic:** E.01. Somatosensation – Pain and Itch

**Title:** The NIH HEAL Initiative® Preclinical Screening Platform for Pain (PSPP): Efforts to Validate Clinically Used Therapeutics

**Authors: *S. IYENGAR**, C. CONRAD, S. SHARMA, S. A. WOLLER;
NINDS/NIH, Rockville, MD

**Abstract:** The NINDS Preclinical Screening Platform for Pain (PSPP) was developed under the NIH HEAL Initiative to facilitate the identification and development of new non-opioid, non-addictive pain therapeutics. PSPP provides researchers from academic, industry, and government institutions, an efficient, rigorous, resource to accelerate development of novel small molecule, biologic, natural product, and device treatments for pain. Such novel assets accepted into the program are profiled to evaluate their effects *in vivo* in rats in extensively validated pain related models and endpoints, paying close attention to pharmacokinetic parameters, understanding potential for neurological deficits *in vivo* and drug abuse liability *in vitro* as well as *in vivo.*The NINDS Preclinical Screening Platform for Pain (PSPP) was developed under the NIH HEAL Initiative to facilitate the identification and development of new non-opioid, non-addictive pain therapeutics. PSPP provides researchers from academic, industry, and government institutions with an efficient, rigorous resource to accelerate development of novel small molecule, biologic, natural product, and device treatments for pain. Such novel assets accepted into the program are profiled to evaluate their effects, starting with in vitro human-based assays and then assessed in a systemic array of *in vivo* rat models. The pain-related *in vivo* models and endpoints have been extensively validated, paying close attention to pharmacokinetic parameters, understanding potential for neurological deficits *in vivo*, and potential drug abuse liability *as well.*Duloxetine *(*3, 10, 30, 60 mg/kg PO), celecoxib (3, 10, 30 mg/kg, PO) and Diazepam (1, 3, 10 mg/kg, PO) were evaluated in both male and female Sprague Dawley rats in the plantar incision pain model, L5/L6 spinal nerve ligation (SNL) model of neuropathic pain, and the monosodium iodoacetate (MIA) model of osteoarthritis pain, following oral administration. Doses were selected based on pharmacokinetic studies and evaluation of side-effect profile in the modified Irwin functional observation battery and the accelerated rotarod test (duloxetine, 10, 30, 60, 100 mg/kg PO; celecoxib 3, 10, 30, 100 mg/kg PO; diazepam 1, 3, 10, 30 mg/kg PO). The results will be presented in the context of pharmacokinetic parameters.In summary, the evaluation of clinically used drugs, duloxetine, celecoxib and diazepam, showed differing profiles in the PSPP paradigm, that were consistent with their utility clinically. The NINDS PSPP program strives to accelerate the development of novel non-opioid, non-addictive therapeutics for pain.

**Disclosures: S. Iyengar:** A. Employment/Salary (full or part-time):; NINDS/NIH. E. Ownership Interest (stock, stock options, royalty, receipt of intellectual property rights/patent holder, excluding diversified mutual funds); Eli Lilly Retiree, stock. **C. Conrad:** A. Employment/Salary (full or part-time):; NINDS/NIH. **S. Sharma:** A. Employment/Salary (full or part-time):; NINDS/NIH. **S.A. Woller:** A. Employment/Salary (full or part-time):; NINDS/NIH.

**Poster**

**PSTR180: Somatosensation: Human Representations and Mechanisms**

**Location:** WCC Halls A-C

**Time:** Monday, November 16, 2026, 1:00 PM - 5:00 PM

**Program #/Poster #:** PSTR180.01/Web Only

**Topic:** E.02. Somatosensation – Touch

**Support:** Spinal Cord Injury Research Board-DOH01-C41212GM (Teale and Gupta)
Spinal Cord Injury Research Board-DOH-C37714GG (Gupta)
Stratton VA Medical Center

**Title:** Optimizing synchronization of the Barrett Upper Extremity Robotic Trainer with neurophysiological recordings

**Authors: *N. GRANT**[1], C. MCDONALD[2], E. MAHAN[2], A. TEALE[3], W. TOWNSEND[2], J. HILL[4], D. GUPTA[5];
[1]Univ. of Michigan, Ann-Arbor, Ann-Arbor, MI; [2]Barrett Technol., Newton, MA; [3]James A. Eddy Res. Institute, Sunnyview Rehabil. Hosp., Schenectady, NY; [4]Natl. Ctr. for Adaptive Neurotechnologies, Stratton VA Med. Ctr., Albany, NY; [5]NCAN, Stratton VA Med. Ctr., Natl. Ctr. for Adaptive Neurotechnologies, Stratton VA Med. Center, Albany, NY, Albany, NY

**Abstract:** *Introduction*: Brain and spinal cord injuries often result in sensory and motor impairments that may benefit from robot-based sensorimotor rehabilitation. Robotic systems such as the Barrett Upper Extremity Robotic Trainer (Burt®, Barrett Technology) provide movement training and haptic feedback to facilitate sensorimotor recovery. Real time integration with neural measurements, such as electroencephalography (EEG), enables investigation of neural responses to robot-based interactions. This requires accurate synchronization between robotic events and EEG recordings. We evaluate 2 sensor modalities and multiple placements on the robot arm to identify a robust and precise synchronization strategy. *Methods*: Inertial measurement units (IMUs) (Movella) containing tri-axial accelerometers (40-100 Hz) and piezoelectric sensors (2500 Hz) were used to detect vibrations generated by Burt® motor controllers during tasks involving single or multiple vibration sets, with long (100 ms) or short (50 ms) pulses, and both static and actively guided robot-arm movements. To assess optimal placement, sensors were mounted at the distal and proximal link, joint cover, forearm cradle, and base. Vibration onset times were identified using magnitude-based threshold detection algorithms and performance was quantified with sensitivity, precision, and temporal drift relative to Burt® generated event timestamps. *Results*: Sensor performance varied substantially by modality and placement. Among IMU configurations, sensors on the effector arm and forearm cradle demonstrated the best performance, achieving high sensitivity (91.6% and 90.6%, respectively), and precision (93.9% and 99.6%, respectively), and low drift (43 ms and 79 ms, respectively). In contrast, sensors mounted on the base arm and joint unit showed poor vibration detection performance. Piezoelectric sensors outperformed IMUs across all tasks. A clamp-mounted piezo sensor positioned at the robot base achieved highest sensitivity (100%) and precision (99.8%), and low temporal drift (4 ms) across active, passive, and long- and short-pulse paradigms. *Conclusions*: Sensor type and placement influence the accuracy of Burt® event detection and hence synchronization with EEG. Piezoelectric sensors provide greater reliability and temporal precision than IMU-based sensing. A clamp-mounted piezo sensor positioned at the robot base isolated from robot-arm movement artifacts demonstrated highly reliable event

detection with millisecond timing accuracy. This approach provides an inexpensive, practical, and robust solution for research on robotic neural sensory assessment and interventions.

**Disclosures: N. Grant:** None. **C. McDonald:** A. Employment/Salary (full or part-time):; Barrett Technology. **E. Mahan:** A. Employment/Salary (full or part-time):; Barrett Technology. **A. Teale:** None. **W. Townsend:** A. Employment/Salary (full or part-time):; Barrett Technology. **J. Hill:** None. **D. Gupta:** None.

**Poster**

**PSTR180: Somatosensation: Human Representations and Mechanisms**

**Location:** WCC Halls A-C

**Time:** Monday, November 16, 2026, 1:00 PM - 5:00 PM

**Program #/Poster #:** PSTR180.02/X24

**Topic:** E.02. Somatosensation – Touch

**Support:** Spinal Cord Injury Research Board-DOH01-C41212GM (Teale and Gupta)
Spinal Cord Injury Research Board-DOH-C37714GG (Gupta)
Stratton VA Medical Center

**Title:** Robot-Based Haptic Discrimination Training: Paradigm Development and Characterization of Sensory Neural Correlates

**Authors: *D. GUPTA**[1,2,3], A. TEALE[3], C. MCDONALD[4], E. MAHAN[4], W. TOWNSEND[4], J. HILL[1,2];
[1]Natl. Ctr. for Adaptive Neurotechnologies, Stratton VA Med. Center, Albany, NY, Albany, NY; [2]Electrical and Computer Engin., Univ. at Albany, State Univ. of New York, Albany, NY; [3]James A. Eddy Res. Institute, Sunnyview Rehabil. Hosp., Schenectady, NY; [4]Barrett Technol., Newton, MA

**Abstract:** Brain and spinal injuries frequently result in persistent motor and somatosensory impairments that limit functional independence. Although precise motor control depends critically on somatosensory input, systematic somatosensory rehabilitation remains underdeveloped. Emerging neurophysiological evidence indicates that movement impairments are closely associated with the quality of somatosensory cortical responses, and that recovery of these responses can support motor recovery. To address this gap, we describe the adaptation of robot-based motor tasks on a commercial rehabilitation robot to incorporate haptic discrimination-based conditioning. We demonstrate the feasibility of this approach for engaging the somatosensory cortex through simultaneous neural measurements.
We adapted two training tasks on the Barrett Upper Extremity Robotic Trainer (Burt®; Barrett Technology), a robotic arm with a gamified user interface: (i) a passive haptic oddball paradigm and (ii) an active haptic pulse-count discrimination task. In the passive task, participants intercepted incoming objects and perceived vibration upon contact (duration oddball: 70% standards, 20% deviants, 10% no vibration). In the active task, participants discriminated between pulse sets and responded by intercepting (2 pulses) or avoiding (3 pulses) the object. An

average of 400 trials (passive task) and 480 trials (active task) was collected across six 2-3 min runs. EEG was collected from 10 healthy adults while they engaged in these tasks, using a dry active headset (DSI-24, 300 Hz) and the BCI2000 software. Vibration onsets were marked using a piezoelectric sensor and a wireless inertial motion sensor attached to the robot end-effector. All data was obtained with informed consent; protocol was approved by the local IRB at Sunnyview Hospital.
EEG was preprocessed using notch filtering (55-65 Hz), band-pass filtering (2-40 Hz), spatial filtering (Laplacian), and baseline correction. Ocular artifacts were removed using independent component analysis and outlier trials were excluded by trial-level statistics. Further analysis was performed with epochs of 400 msec duration (-50 to 350 msec). Preliminary analysis showed P50-N80 somatosensory response to all vibration stimuli at the parietal and motor areas (i.e., electrodes P3, C3), contralateral to the hand perceiving the stimulation. Further, in the passive oddball paradigm, we observe a mismatch negativity response at approximately 150-200 msec at the fronto-central areas (Fz, Cz); and a P300 response at the central areas (Cz), as expected.

**Disclosures: D. Gupta:** None. **A. Teale:** None. **C. McDonald:** A. Employment/Salary (full or part-time):; Barrett Technology. **E. Mahan:** A. Employment/Salary (full or part-time):; Barrett Technology. **W. Townsend:** A. Employment/Salary (full or part-time):; Barrett Technology. **J. Hill:** None.

**Poster**

**PSTR180: Somatosensation: Human Representations and Mechanisms**

**Location:** WCC Halls A-C

**Time:** Monday, November 16, 2026, 1:00 PM - 5:00 PM

**Program #/Poster #:** PSTR180.03/X25

**Topic:** E.02. Somatosensation – Touch

**Support:** Spinal Cord Injury Research Board-DOH01-C41212GM (Teale and Gupta)
Spinal Cord Injury Research Board-DOH-C37714GG (Gupta)
Stratton VA Medical Cetner

**Title:** Robot-based Haptic Discrimination Training: Integration of Robotic Platform with BCI and Performance Evaluation

**Authors: *C. MCDONALD**[1], E. MAHAN[1], N. GRANT[2,3], A. TEALE[4], W. TOWNSEND[1], J. HILL[3,5], D. GUPTA[3,4,5];
[1]Barrett Technology, LLC, Newton, MA; [2]Univ. of Michigan, Ann-Arbor, Ann-Arbor, MI; [3]NCAN, Stratton VA Med. Ctr., Natl. Ctr. for Adaptive Neurotechnologies, Stratton VA Med. Ctr., Albany, NY; [4]James A. Eddy Res. Institute, Sunnyview Rehabil. Hosp., Schenectady, NY; [5]Electrical and Computer Engin., Univ. at Albany, State Univ. of New York, Albany, NY

**Abstract:** *Introduction:* Chronic upper-limb sensorimotor impairments following neurological injury substantially limit functional independence. While movement-focused rehabilitation robotics have shown promise for promoting upper-limb recovery, emerging evidence highlights

the critical role of sensory function in motor recovery. Furthermore, integrating robotic systems with neuromuscular signal measurement tools, such as electroencephalography (EEG) or electromyography (EMG), may enhance therapeutic gains by enabling closed-loop sensorimotor training. To address these needs, we a) adapted a commercial rehabilitation robotic platform (Burt®) to facilitate customizable haptic training, and b) evaluated the technical feasibility of synchronized robotic and neural signal acquisition. *Methods:* Burt® delivers upper-extremity rehabilitation in the form of virtual games that target specific joint movements, each of which include adjustable arm weight compensation, adjustable difficulty of the motor task, and specific placement and scaling of the workspace. We tested the expansion of the Burt® API to include haptic training. We adapted two single-degree-of-freedom motor tasks (shoulder abduction/adduction and shoulder flexion/extension) to include haptic stimuli presented at select times, capturing user response via robot arm movement and providing immediate visual feedback. The graphical user-interface was programmed to allow researchers to access and update bounded parameters of these activities—e.g., vibration pulse count, duration, and amplitude—to optimize experimental design. The API was also programmed to record timestamps of haptic stimuli presentation paired with robot kinematics to enable synchronization with external EEG/EMG systems. A white square presented on the screen corner, obscured from the user's view, transmitted a TTL pulse via a photodetector, encoding the stimuli presentation. We characterized the fidelity and timing of the presented vibrations as a function of the tunable parameters. *Results:* The haptic training activity prototypes were finalized after testing for visual cue presentation and response feedback timing fidelity, then utilized by collaborators in preliminary testing with human participants. Time and frequency analysis of data collected from robot motor encoders and externally attached piezoelectric sensors showed that the vibrotactile cues produced by the robot adhered closely to the commanded parameters of duration and frequency, across a range of operational durations, frequencies, and amplitudes. Event synchronization was confirmed using the external piezoelectric sensors.

**Disclosures: C. McDonald:** A. Employment/Salary (full or part-time):; Barrett Technology. **E. Mahan:** A. Employment/Salary (full or part-time):; Barrett Technology. **N. Grant:** None. **A. Teale:** None. **W. Townsend:** A. Employment/Salary (full or part-time):; Barrett Technology. **J. Hill:** None. **D. Gupta:** None.

**Poster**

**PSTR180: Somatosensation: Human Representations and Mechanisms**

**Location:** WCC Halls A-C

**Time:** Monday, November 16, 2026, 1:00 PM - 5:00 PM

**Program #/Poster #:** PSTR180.04/X26

**Topic:** E.02. Somatosensation – Touch

**Support:** CDMRP PRMRP Clinical Trial Award #PR241366

**Title:** Continuous, Multi-Degree-of-Freedom Proportional Myoelectric Control for Transradial Amputees

**Authors: *R. L. HARDESTY**[1], B. GAGNIER[1], J. LAMBRECHT[1], E. L. GRACZYK[2];
[2]Biomed. Engin., [1]Case Western Reserve Univ., Cleveland, OH

**Abstract:** Recent advances in prosthetic hardware have yielded sophisticated, multi-degree-of-freedom (DOF) prosthetic hands. However, user adoption remains limited due, in part, to restrictive and nonintuitive myoelectric control strategies. State-of-the-art commercial myoelectric devices commonly rely on classification-based strategies that constrain users to a subset of pre-defined movements that must be sequentially activated and do not provide graded force regulation. To achieve more versatile, generalizable function, transitioning to continuous and proportional control strategies is essential. To address this, we developed a myoelectric control strategy providing continuous, proportional control across 4 DOFs. The system was evaluated in two participants with acquired transradial limb loss. Eight channels of electromyography (EMG) signals were recorded using a combination of chronically-implanted intramuscular electrodes and surface electrodes while participants performed a bilateral posture-matching task guided by a virtual environment. The task protocol comprised 24 distinct postures simultaneously articulating 4 DOFs (wrist pronation/supination, wrist flexion/extension, thumb flexion/extension, and finger flexion/extension), repeated over 10 trials per posture. Mean absolute value (MAV) and waveform length (WFL) features were extracted from the EMG signals. The dataset was then partitioned into training, testing, and validation subsets, stratified by posture to ensure balanced representation across all conditions. To map EMG features to kinematic outputs, a feedforward Multilayer Perceptron (MLP) neural network was implemented. The architecture utilized a feature input layer followed by a single fully connected hidden layer configured with 10 to 12 nodes and a Rectified Linear Unit (ReLU) activation function. The network was optimized using adaptive moment estimation (ADAM) to minimize Mean Squared Error (MSE) loss, utilizing a mini-batch size of 32 and an initial learning rate of $10^{-3}$ over 2000 epochs. Model performance was evaluated by calculating the Variance Accounted For (VAF) on the validation dataset. The network achieved a mean validation VAF of 76.59%, ranging from 94.85% (wrist pronation/supination) to a low of 60.21% (thumb flexion/extension). These offline results provide a promising proof-of-concept for reconstructing continuous, multi-DOF movements using a lightweight network that can be implemented on computationally constrained, real-time systems.

**Disclosures: R.L. Hardesty:** None. **B. Gagnier:** None. **J. Lambrecht:** None. **E.L. Graczyk:** None.

**Poster**

**PSTR180: Somatosensation: Human Representations and Mechanisms**

**Location:** WCC Halls A-C

**Time:** Monday, November 16, 2026, 1:00 PM - 5:00 PM

**Program #/Poster #:** PSTR180.05/X27

**Topic:** E.02. Somatosensation – Touch

**Support:** #I01 RX003699)

**Title:** Sensitivity to temporally patterned multi-contact stimulation and its effect on the perception of tactile motion evoked by peripheral nerve stimulation

**Authors: *J. WRIGHT**[1], L. ROLDAN[2], H. LUDLOW[3], E. L. GRACZYK[2];
[2]Biomed. Engin., [1]Case Western Reserve Univ., Cleveland, OH; [3]Case Western Reserve Univ., South Euclid, OH

**Abstract:** Humans can rapidly identify the speed, pattern, and direction of tactile events occurring during movements of objects across the skin. Restoring tactile motion in individuals with limb loss is critical for stereognosis, slip feedback, and other forms of temporally varying sensory information. Previous sensory restoration studies using peripheral nerve stimulation (PNS) have largely focused on non-varying stimulation through a single electrode; much less is known about the spatiotemporal properties of multi-contact stimulation. To address this gap, we examined how two participants with upper-extremity limb loss perceived multi-contact stimulation patterns and the extent to which those patterns resembled movement across the skin. Both participants were implanted with Composite Flat Interface Nerve Electrodes (C-FINEs) around the median nerves within their residuum. In each experiment, two contacts evoking sensations in distinct parts of the hand were selected and the inter-stimulus onset interval (ISOI) between the contacts was varied. In separate sessions, participants either 1) classified the sensation as simultaneous, continuous or sequential via a forced choice paradigm or 2) completed qualitative interviews comparing perceived movement across intact skin to the electrically evoked sensations. For Experiment 1, responses were fit with cumulative Gaussian or Gaussian functions (Mean $R^2$=0.90), and judgment thresholds (JT) were defined as ISOI corresponding to 66% detection. Significant differences in mean JT were observed for both participants, with simultaneity thresholds lower than continuity thresholds and continuity thresholds lower than sequentiality thresholds (Kruskal-Wallis, $p < 0.05$). Both participants identified fully overlapped stimulation (ISOI=0s) as simultaneous at significantly above chance levels (Two Proportion Z-test , $p<0.001$). In experiment 2, one participant consistently perceived the PNS pattern to be movement across the skin and completed a follow-up experiment examining the effects of ISOI, stimulation intensity, and contact onset order on movement ratings. ISOI and stimulation intensity significantly affected perceived movement (ANOVA, $p<0.01$), whereas contact order did not. These findings establish the temporal conditions that differentiate simultaneous, continuous, and sequential percepts while demonstrating how stimulation parameters and individual differences influence tactile motion perception.

**Disclosures: J. Wright:** None. **L. Roldan:** None. **H. Ludlow:** None. **E.L. Graczyk:** None.

**Poster**

**PSTR180: Somatosensation: Human Representations and Mechanisms**

**Location:** WCC Halls A-C

**Time:** Monday, November 16, 2026, 1:00 PM - 5:00 PM

**Program #/Poster #:** PSTR180.06/X28

**Topic:** E.04. Interoception

**Support:** National Rehabilitation Center, Ministry of Health and Welfare, Korea (NRCTR-EX25007)

**Title:** Frequency- and duration-dependent modulation of onset timing and kinematic magnitude in tendon vibration-induced kinesthetic illusion

**Authors:** S. GANG, G. PARK, W. MOOJIN, H. CHEI, J. OH, S. HONG, ***K. OH**; Kyungpook Natl. Univ., Daegu, Korea, Republic of

**Abstract:** Tendon vibration selectively activates muscle spindles through Ia afferent fibers and can induce kinesthetic illusions, making it a promising approach for neurorehabilitation. However, the relationships between vibration parameters, such as frequency and duration, and the temporal and kinematic characteristics of kinesthetic illusions remain incompletely understood. This study aimed to quantify kinesthetic illusion responses in healthy adults across different vibration frequencies and durations.

Thirteen healthy adults participated in this study. This study was approved by the KNU IRB (#2025-0311). Vibration stimuli at three frequencies (65, 75, and 85 Hz) and three durations (5, 15, and 25 s) were applied in randomized order to the flexor carpi radialis tendon of the left hand using a custom-built Arduino Nano-based vibration device, while visual feedback was occluded. Participants expressed the perceived kinesthetic illusion of the left hand by moving the right wrist, and wrist flexion angles were recorded using motion capture. Illusion onset timing was additionally measured in a subset of three participants.

Illusion magnitude, represented by wrist flexion angle, generally increased with stimulus duration. The increase in illusion magnitude during the 15-25 s interval was greater than that during the 5-15 s interval, suggesting a proprioceptive drift effect over prolonged stimulation. Mean wrist angle changed nonlinearly across vibration frequencies, while variability increased at higher frequencies, indicating reduced response stability. In the subset analysis, illusion onset was shortest at 65 Hz, with a mean onset time of 2.15 s, and was progressively delayed at higher frequencies. The variability of onset timing also increased with frequency, which may reflect frequency-dependent instability in sensory processing.

These findings suggest that vibration frequencies in the 65-75 Hz range may provide efficient kinesthetic illusion induction in terms of response magnitude and onset timing. This frequency range may serve as a useful design reference for low-power and miniaturized tendon vibration devices. Furthermore, the frequency- and duration-dependent characteristics of illusion magnitude and onset provide foundational data for developing vibration-movement synchronization protocols for neurorehabilitation in patients with brain lesions.

**Disclosures: S. Gang:** None. **G. Park:** None. **W. Moojin:** None. **H. Chei:** None. **J. Oh:** None. **S. Hong:** None. **K. Oh:** None.

**Poster**

**PSTR180: Somatosensation: Human Representations and Mechanisms**

**Location:** WCC Halls A-C

**Time:** Monday, November 16, 2026, 1:00 PM - 5:00 PM

**Program #/Poster #:** PSTR180.07/X29

**Topic:** E.04. Interoception

**Title:** Proprioceptive assessment in sensory neuropathy: consistent and not-so-consistent findings across behavioral and clinical measures

**Authors: *N. M. ABI CHEBEL**[1,2], F. R. SARLEGNA[2];
[1]Inst. of physiotherapy, St. Joseph Univ. of Beirut, Beirut, Lebanon; [2]Inst. of Movement Sci., CNRS & Aix-Marseille Univ., Marseille, France

**Abstract:** It is well established that proprioception is critical for motor control (Rothwell et al. 1982; Cole & Paillard 1995; Ghez & Sainburg 1995; Hermsdorfer & Nowak 2008; Sarlegna & Sainburg 2009; Miall et al. 2021). However, we currently do not have a consensual definition of proprioception, nor do we have a consensual method to assess it. In neurotypical right-handed adults, we have used an ipsilateral passive matching task and found that proprioceptive performance was more precise for the non-preferred arm (Abi Chebel et al. 2022, 2023), but that individuals reported their preferred arm as more precise (Abi Chebel et al., in revision). Here we asked: do current behavioral tools accurately reflect the severity of proprioceptive impairments in patients with clinically-established deficits? We assessed the joint position sense of two participants with severe sensory neuropathy and compared their performance with that of age- and sex-matched controls, all right-handed. Using an ipsilateral passive matching task (Abi Chebel et al. 2023), joint position sense was assessed at the elbow and wrist of both arms. For each condition, we computed mean absolute error (accuracy) and variable error (precision) from 6 trials. Differences between each patient and their matched control group were assessed using the Crawford et al. (2010) modified t-test.We found significant proprioceptive deficits in both sensory neuropathy patients compared to matched controls. Deficits were asymmetric, with the right elbow showing the largest impairments in both patients (all $p < .01$) (Yousif et al. 2015; Miall et al. 2018). However, these deficits were smaller than expected from i) clinical tests, which failed to reveal any tendon reflex, and ii) neurophysiological testing, which failed to reveal any somatosensory-evoked potential. Additionally, in neurotypical controls, variable error was significantly larger for the right (preferred) arm compared to the left arm ($p < .02$). Overall, such inconsistencies between clinical severity and behavioral performance are consistent with new theoretical, multi-layer models of proprioceptive function (Héroux et al. 2022; Abi Chebel et al. in revision), which suggests that multiple tests are necessary to assess all aspects of proprioception.

**Disclosures: N.M. Abi chebel:** None. **F.R. Sarlegna:** None.

**Poster**

**PSTR180: Somatosensation: Human Representations and Mechanisms**

**Location:** WCC Halls A-C

**Time:** Monday, November 16, 2026, 1:00 PM - 5:00 PM

**Program #/Poster #:** PSTR180.08/X30

**Topic:** E.02. Somatosensation – Touch

**Support:** NIH NICHD R01HD117313

**Title:** Comparison between peripheral nerve stimulation and mechanical indentation across the cortical grasp network

**Authors: *P. R. BHAT**[1], B. HUTCHISON[1], W. MEMBERG[1], E. HERRING[3,2], S. BAZAREK[3,2], J. SWEET[3,2], B. AJIBOYE[1,2,4], E. L. GRACZYK[1,2,4];
[1]Biomed. Engin., [2]Sch. of Med., Case Western Reserve Univ., Cleveland, OH; [3]Neurosurg., Univ. Hosp. Cleveland Med. Ctr., Cleveland, OH; [4]FES Ctr. of Excellence, Rehab. R&D Service, Louis Stokes Cleveland Dept. of Veterans Affairs Med. Ctr., Cleveland, OH

**Abstract:** Peripheral nerve stimulation (PNS) is an sensory restoration technique for limb loss and has been shown to evoke sensory percepts in individuals with sensory-incomplete spinal cord injury (SCI). Despite its functional efficacy, users often report the PNS-evoked sensation as paresthetic. Comparing the cortical response of PNS to natural touch may objectively explain this perceptual difference. We studied how the cortical grasp network encoded PNS and mechanical indentation across stimulus levels in an individual with AIS-B C3-C5 SCI. The participant was implanted with extraneural cuff electrodes around the median and ulnar nerves, as well as 8 microelectrode arrays spanning primary somatosensory cortex (S1), primary motor cortex (M1), anterior intraparietal area (AIP), and ventral premotor cortex (6v and 6r). The participant received randomized low, medium, and high levels of either PNS or indentation for 1 second. These levels, corresponding to varying pulse width in PNS or depth for indentation, were generated from intensity matching the 30%, 60%, and 90% values of the sensory dynamic range between modalities. After each trial, the participant reported an intensity and naturalness rating on an open-ended numerical scale. For both modalities, increasing the stimulus level led to distinct increases in intensity (Kruskal-Wallis with Dunn-Sidak post-hoc, $p < 0.0001$). Increasing PNS PW had no effect on naturalness, whereas increasing indentation depth significantly increased naturalness ratings (Kruskal-Wallis with Dunn-Sidak post-hoc, $p < 0.05$). Across all levels, PNS was rated as significantly less natural than indentation (Mann-Whitney U test, $p < 0.0001$). While prior work showed S1 modulation to both modalities, we observed that M1, AIP, 6v, and 6r also responded. Demixed principal component analysis revealed that 6v, 6r, and AIP arrays displayed significantly more condition-independent features than M1 (multiple proportions chi-square test with Marascuilo post-hoc, $p < 0.003$). M1 contained the highest percentage of modality dependent features, suggesting that it plays a greater role in differentiating between PNS and mechanical indentation. These findings lay the groundwork for developing biomarkers to objectively assess artificial and natural sensory stimuli.

**Disclosures: P.R. Bhat:** None. **B. Hutchison:** None. **W. Memberg:** None. **E. Herring:** None. **S. Bazarek:** None. **J. Sweet:** None. **B. Ajiboye:** None. **E.L. Graczyk:** None.

**Poster**

**PSTR180: Somatosensation: Human Representations and Mechanisms**

**Location:** WCC Halls A-C

**Time:** Monday, November 16, 2026, 1:00 PM - 5:00 PM

**Program #/Poster #:** PSTR180.09/X31

**Topic:** E.02. Somatosensation – Touch

**Support:** DoD CDMRP SCIRP SC180308
VAMR 5I01RX002654
NIH T32EB004314
UH3NS107714

**Title:** Processing of touch information related to grasping in neuronal populations throughout human sensorimotor cortices

**Authors: *B. HUTCHISON**[1], C. M. GREENSPON[4], J. KRALL[2], A. KETTING-OLIVIER[1], W. MEMBERG[1,5], M. ABATE[1], N. SHELCHKOVA[4], P. R. BHAT[1], J. SWEET[6,3,5], R. F. KIRSCH[1,3,5], E. L. GRACZYK[1,3,5], B. AJIBOYE[1,3,5];
[1]Biomed. Engin., Case Western Reserve Univ., Cleveland, OH; [2]Biomed. Engin., Case Western Reserve Univ., Shaker Heights, OH; [3]Sch. of Med., Case Western Reserve Univ., Cleveland, OH; [4]Dept. of Organismal Biol. & Anat., Univ. of Chicago, Chicago, IL; [5]Cleveland Functional Electrical Stimulation Ctr., Louis Stokes Cleveland VA Med. Ctr., Cleveland, OH; [6]Neurolog. Surgery, Univ. Hosp., Cleveland, OH

**Abstract: Motivation** Touch is critical for hand function, providing precise details about hand-object interactions. The loss of hand function, such as from cervical spinal cord injury (SCI), impairs our ability to dexterously grasp and manipulate objects. To fully restore hand function to people with sensorimotor deficits, we need to understand how the human brain processes tactile information. **Background** Prior non-human primate studies have characterized tactile coding in primary somatosensory cortex (S1) and primary motor cortex (M1). Recent human evidence shows tactile signals are present beyond S1 and M1 including in posterior parietal, premotor, and prefrontal cortices, but how these brain regions process tactile information is not well understood. **Objective** The goal of this study is to elucidate how human sensorimotor cortices encode and process tactile location, magnitude, and timing information relevant to grasping objects from neuronal populations. **Methods** We precisely indented the fingertips of three human participants with cervical sensory-incomplete SCI—imitating the contact, hold, and release phases of object grasping. We varied the indentation location (fingertip), magnitude (depth), and timing (rate). Simultaneously, we recorded multi-unit neuronal signals from the sensorimotor cortices of the same human participants using chronically implanted microelectrode arrays. Specifically, we recorded from S1, M1, premotor (6v, 6r), inferior frontal gyrus (IFG), and anterior intraparietal (AIP) cortices. Perceived intensity was also reported. **Results** All brain regions had multi-units that robustly responded to tactile indentation (firing rate during stimulation > baseline; t-test, $p<0.05$). The dominant neural dynamics show activation is strongest during changes in contact events. The latencies of cortical response (LatenZy test, $p<0.01$) and functional connectivity results (lagged canonical correlation analysis) indicate tactile information flows from S1 to M1 then premotor cortices and from S1 to AIP. Most multi-units modulate to indentation of multiple fingers. Indentation depth and rate primarily increase neuronal population activity (linear regression coefficient, $p<0.05$). Perceived intensity also increases with indentation depth and rate (linear regression coefficient, $p<0.05$). Perceived intensity can be predicted from neural signals in S1, M1, and 6v. **Impacts** These results can help people with somatosensory loss by informing the design of biomimetic stimulation paradigms to provide tactile feedback which can be applied to people with SCI during brain machine interface (BMI) use to restore dexterous hand function.

**Disclosures: B. Hutchison:** None. **C.M. Greenspon:** None. **J. Krall:** None. **A. Ketting-Olivier:** None. **W. Memberg:** None. **M. Abate:** None. **N. Shelchkova:** None. **P.R. Bhat:** None. **J. Sweet:** None. **R.F. Kirsch:** None. **E.L. Graczyk:** None. **B. Ajiboye:** None.

**Poster**

**PSTR180: Somatosensation: Human Representations and Mechanisms**

**Location:** WCC Halls A-C

**Time:** Monday, November 16, 2026, 1:00 PM - 5:00 PM

**Program #/Poster #:** PSTR180.10/X32

**Topic:** E.02. Somatosensation – Touch

**Support:** NIH NICHD R01HD117313

**Title:** Stimulation-Evoked Sensory Percepts Feel Different During Active Tasks Compared to at Rest

**Authors: *R. BOSE**[1], A. SCHELLHOUSE[1], M. ABATE[1], W. MEMBERG[1], S. BAZAREK[2], J. SWEET[4], L. OSBORN[3], L. E. FISHER[5], B. AJIBOYE[3], E. L. GRACZYK[3];
[2]Neurolog. Surgery, [3]Biomed. Engin., [1]Case Western Reserve Univ., Cleveland, OH; [4]Univ. Hosp., Cleveland, OH; [5]Physical Med. and Rehabil., Univ. of Pittsburgh, Pittsburgh, PA

**Abstract:** Afferent suppression is a well-studied phenomenon in which afferent information is suppressed by centrally generated efferent signals while performing a motor task. The effect of afferent suppression in the context of sensory rehabilitation using artificial sensory feedback via electrical stimulation is not well studied. Here, we compared artificially evoked sensory perception at rest to perception of the same stimuli while performing a motor task to understand the role of afferent suppression in modulating artificial sensation. The experiment was performed in 14 able-bodied individuals (ABI) and 1 individual with sensory incomplete spinal cord injury (SCI). Comparing these two populations further clarifies whether an impaired spinal pathway (SCI) alters afferent suppression relative to an intact spinal pathway (ABI).In ABI, surface peripheral nerve stimulation (PNS) was delivered to the medial branch of the index finger. In the SCI participant, intracortical microstimulation (ICMS) was delivered to primary somatosensory cortex, and PNS via an implanted nerve cuff was delivered to the median nerve. The stimulation was delivered under 3 conditions: (1) Active: Participants were instructed to either perform (ABI) or attempt to perform (SCI) a grasp task in a virtual reality environment with visual feedback; (2) Passive: no movement and no visual feedback; and (3) Passive_Vis: no movement but with visual feedback. Stimulation level was set at 30%, 60% and 90% of the sensory dynamic range. Participants reported the perceived location and intensity for each stimulation level and condition.In both populations, we observed no significant differences in the percept location and size among the three conditions. In ABI, the perceived intensities for Passive and Passive_Vis conditions were significantly higher than the Active condition, across all the stimulation intensity levels ($p<0.001$, Wilcoxon signed-rank test). In the SCI participant, we did not observe a significant difference between the Active versus Passive and Passive_Vis conditions for PNS. For ICMS, we only observed a significant difference between Active and

Passive condition in the 30% stimulation level condition ($p<0.05$, Kruskal-Wallis test, Dunn-Sidak posthoc). Our findings highlight two important points: (1) afferent suppression occurs with electrically evoked sensations in humans, resulting in reduced perceived intensity during active tasks; and (2) an intact spinal cord might be essential for the descending efferent signals to cause afferent suppression at the spinal level. In future work, we plan to test whether afferent suppression also impacts task performance.

**Disclosures: R. Bose:** None. **A. Schellhouse:** None. **M. Abate:** None. **W. Memberg:** None. **S. Bazarek:** None. **J. Sweet:** None. **L. Osborn:** None. **L.E. Fisher:** None. **B. Ajiboye:** None. **E.L. Graczyk:** None.

**Poster**

**PSTR180: Somatosensation: Human Representations and Mechanisms**

**Location:** WCC Halls A-C

**Time:** Monday, November 16, 2026, 1:00 PM - 5:00 PM

**Program #/Poster #:** PSTR180.11/Web Only

**Topic:** E.02. Somatosensation – Touch

**Support:** JSPS KAKENHI (22K18263)

**Title:** Prior experience and environment-based anticipation facilitate the cutaneous rabbit illusion

**Authors: *G. ENDO**[1], M. MIYAZAKI[2];
[1]Shizuoka Univ., Hamamatsu・Shizuoka, Japan; [2]Shizuoka Univ., Hamamatsu, Japan

**Abstract:** The cutaneous rabbit illusion (CRI) is a tactile phenomenon in which the perceived locations of two successive tactile stimuli delivered to different skin sites are attracted toward each other. Notably, in the CRI, later tactile events retroactively modulate the perception of the earlier tactile events, providing a striking example of "postdiction." Previous studies reported that the CRI can be explained by Bayesian estimation models based on a prior that tactile stimuli tend to move slowly across the skin. This prior is assumed to be innately built into the brain or acquired through long-term experience. However, previous studies have also shown that short-term experience (e.g., tens to hundreds of trials) induces positive or negative aftereffects on tactile temporal perception. Here, we investigated whether recent experience modulates the postdictive component of the CRI. In the present experiments, CRI stimuli were delivered to the participants' forearm under three conditions. First, trials including actual stimulation at the middle site between the attractee (earlier) and attractor (later) stimuli were interleaved within the session (prior-stimulation condition). We hypothesized that prior experience with the actual stimuli at the middle site would facilitate the CRI in the subsequent trials. Second, no actual stimulation was delivered at the middle site throughout the session (non-prior-stimulation condition), although a stimulator was placed at the middle site. Third, no stimulator was placed at the middle site (non-stimulator condition). We included the third condition as an additional control because the presence of a stimulator at the middle site might induce anticipation of

stimulation at that location and thereby facilitate the CRI. The results showed that the illusory attractee shift was greatest in the prior-stimulation condition, supporting our hypothesis. Moreover, the illusory attractee shift in the non-prior-stimulation condition was greater than that in the non-stimulator condition, suggesting that anticipation of stimulation induced by the presence of the stimulator also enhances postdictive effects. These results demonstrate that tactile postdiction is influenced by recent sensory experience as well as anticipation based on environmental cues.

**Disclosures: G. Endo:** None. **M. Miyazaki:** None.

**Poster**

**PSTR180: Somatosensation: Human Representations and Mechanisms**

**Location:** WCC Halls A-C

**Time:** Monday, November 16, 2026, 1:00 PM - 5:00 PM

**Program #/Poster #:** PSTR180.12/Y1

**Topic:** E.02. Somatosensation – Touch

**Support:** Mitsui Chemicals, Inc.

**Title:** The influence of dynamic viscoelasticity on the occipito-parietal activities during pulling movements

**Authors: *N. KANAYAMA**[1], M. MURASE[2], H. YUI[3], T. NAKASHIMA[3];
[1]Natl. Inst. of Advanced Industrial Sci. and Technol., Tsukuba, Japan; [2]Mitsui Chemicals, Inc., Chuo-ku, Tokyo, Japan; [3]Mitsui Chemicals, Inc., Sodegaura, Japan

**Abstract:** When humans manipulate deformable objects, they must continuously regulate muscle output and posture according to changes in the object's mechanical properties. For example, when opening a sealed snack package, failure to reduce pulling force at the moment the adhesive seal begins to peel may result in unintended tearing of the entire package. This suggests that humans monitor ongoing deformation, predict imminent mechanical changes, and rapidly adjust motor output. Such adaptive control is likely supported by cortical processes in the parietal sensorimotor regions. In this study, we investigated how cortical activity is modulated by object deformation characteristics during a bilateral pulling task. Surface electromyography (EMG) and scalp electroencephalography (EEG) were recorded simultaneously while twenty healthy individuals performed controlled pulling movements. Two materials were used: a conventional elastomer material and a specially designed material with dynamically changing viscoelastic properties during pulling. Prior to the experiment, participants performed a maximal voluntary contraction (MVC), and were trained to generate pulling forces corresponding to 60% and 30% of the peak EMG amplitude recorded during MVC. During each trial, participants were instructed to produce 60% force in response to a circular cue and 30% force in response to a triangular cue presented on a display positioned 60 cm in front of them (cue-force mapping counterbalanced across participants). After cue presentation, participants maintained the target force for 5 s, then released the force and maintained posture for an additional 5 s until an

auditory signal indicated trial completion. The experiment consisted of four conditions defined by material type and force level, with 30 trials per condition. EEG analysis using ICA clustering revealed significantly greater alpha-band power suppression in the parietal cortical regions (centroid across all the involved dipoles: x, y, z = 16, -56, 31) during pulling of the dynamic viscoelastic material at 60% force compared with the conventional elastic rubber (-1.71 vs. -0.45 dB, $p < .05$, Permutation statistics with cluster correction). These findings suggest that interacting with materials whose mechanical properties change during manipulation impose greater sensorimotor processing demands for force stabilization.

**Disclosures: N. Kanayama:** B. Contracted Research/Research Grant (principal investigator for a drug study, collaborator or consultant and pending and current grants). If you are a PI for a drug study, report that research relationship even if those funds come to an institution.; Mitsui Chemicals, Inc. **M. Murase:** A. Employment/Salary (full or part-time):; Mitsui Chemicals, Inc. **H. Yui:** A. Employment/Salary (full or part-time):; Mitsui Chemicals, Inc. **T. Nakashima:** A. Employment/Salary (full or part-time):; Mitsui Chemicals, Inc..

**Poster**

**PSTR180: Somatosensation: Human Representations and Mechanisms**

**Location:** WCC Halls A-C

**Time:** Monday, November 16, 2026, 1:00 PM - 5:00 PM

**Program #/Poster #:** PSTR180.13/Y2

**Topic:** E.02. Somatosensation – Touch

**Title:** A mathematical model for predicting the illusory tactile pulling sensation induced by asymmetric vibration

**Authors:** *R. TAKAHASHI, S. ITO, **S. TAKAMUKU**;
Communication Sci. Laboratoires, NTT Inc., Atsugi, Kanagawa, Japan

**Abstract:** Asymmetric vibration, applied in the shear direction to the fingertip, can cause an illusory tactile pulling sensation despite having zero net displacement of the contact point. In this illusion, bidirectional dynamic skin deformation generated by vibratory stimulation is transformed through neural computation into a perception of a unidirectional pulling force. Investigating this process may provide important insights into the computational principles underlying our tactile force perception. In our previous study, we examined how peak asymmetries in displacement, velocity, acceleration, and jerk relate to perceived direction of the illusory pulling sensation. The results revealed that participants' responses could be explained by peak asymmetries in displacement and velocity. However, why such asymmetries explain the sensation remains unclear. In the present study, we propose a mathematical model that links asymmetric skin deformation to directional tactile perception. The model incorporates response thresholds associated with the mechanoreceptors distributed within the skin and integrates tactile responses evoked by dynamic skin deformation. We hypothesized that asymmetric vibration produces biased tactile activity after nonlinear thresholding and spatial integration, even when the overall displacement is physically balanced over time. To evaluate the model, we compared

model outputs with participants' responses obtained in behavioral experiments using asymmetric vibratory stimulation. The model reproduced the response trends to peak asymmetries in skin deformation. Importantly, the model explains the illusory pulling sensation as arising from biologically inspired computations applied to tactile stimuli, rather than from explicit peak-detection algorithms applied to displacement or velocity signals themselves. The proposed framework may be applicable, not only to asymmetric vibration, but also to a broader class of tactile force stimuli and may provide a foundation for understanding more general computational principles underlying our tactile force perception.

**Disclosures: R. Takahashi:** A. Employment/Salary (full or part-time):; NTT Inc. **S. Ito:** A. Employment/Salary (full or part-time):; NTT Inc. **S. Takamuku:** A. Employment/Salary (full or part-time):; NTT Inc..

**Poster**

**PSTR180: Somatosensation: Human Representations and Mechanisms**

**Location:** WCC Halls A-C

**Time:** Monday, November 16, 2026, 1:00 PM - 5:00 PM

**Program #/Poster #:** PSTR180.14/Y3

**Topic:** E.02. Somatosensation – Touch

**Title:** Evaluating Directional and Spatial Perception Using Vibrotactile Haptic Feedback

**Authors: *S. SUDHEENDRA**[1], A. K. FELDMAN[2], D. J. WEBER[3], D. DESPRADEL[4]; [2]Neurosci. Inst., [3]Mechanical Engin. and Neurosci. Inst., [4]Mechanical Engin., [1]Carnegie Mellon Univ., Pittsburgh, PA

**Abstract:** Vibrotactile feedback provides an intuitive way to communicate information during motor tasksand can improve both movement precision and motor learning. We developed a wearablevibrotactile haptic band using Linear Resonant Actuators (LRAs) to investigate how spatiallyencoded haptic feedback influences directional perception and movement execution duringguided drawing tasks.
The band consisted of four LRAs positioned around the forearm, each corresponding to acardinal direction: up, down, left, or right. Diagonal cues were generated through simultaneousactivation of two adjacent actuators. Vibration location encoded the direction of movement error.Two experimental paradigms evaluated directional perception and task performance. TheDirection Test presented participants with vibrotactile cues corresponding to four cardinal andfour diagonal directions, and participants identified the perceived direction. Each round included8 trial directions, and participants completed 3 rounds (24 total trials). LRAs remained activeuntil a response was entered, allowing evaluation of perception accuracy and interpretation ofspatial haptic cues.
To evaluate task performance, the Guided Drawing Task required participants to trace shapesusing a Unity-based iPad application synchronized with the wearable haptic system. Participantstraced four geometric shapes (square, circle, diamond, and triangle) under six feedbackconditions: No Feedback, Directional Haptic Feedback Only, Visual Feedback Only,

DirectionalHaptic + Visual Feedback, Uniform Haptic + Visual Feedback, and Uniform Haptic FeedbackOnly. In Visual conditions, users could see both the target trajectory and the line they weredrawing. In Directional Haptic conditions, vibrotactile cues were generated whenever the stylusdeviated from the trajectory, with vibration location indicating the direction of path deviation. InUniform Haptic conditions, all actuators vibrated simultaneously without encoding direction.Each trial consisted of 24 drawings (4 shapes × 6 conditions), and participants completed 2 trialsfor a total of 48 drawings per participant.
Preliminary results demonstrated high directional detection accuracy, with most errors occurringbetween adjacent directions. In the drawing task, Directional Haptic + Visual Feedback andUniform Haptic + Visual Feedback achieved the highest performance (~93% time on path).Directional Haptic + Visual Feedback produced the greatest improvement relative to NoFeedback (+5.2 percentage points), suggesting spatially encoded vibrotactile feedback caneffectively improve movement guidance and task accuracy.

**Disclosures: S. Sudheendra:** None. **A.K. Feldman:** None. **D.J. Weber:** None. **D. Despradel:** None.

**Poster**

**PSTR180: Somatosensation: Human Representations and Mechanisms**

**Location:** WCC Halls A-C

**Time:** Monday, November 16, 2026, 1:00 PM - 5:00 PM

**Program #/Poster #:** PSTR180.15/Y4

**Topic:** E.02. Somatosensation – Touch

**Title:** Predicating affective tactile and visual texture perception through autonomic measures using machine learning

**Authors: *M. BUFO**[1], R. H. WATKINS[2], R. ACKERLEY[2];
[1]CNRS - Aix Marseille Univ., Marseille, France; [2]CRPN, CNRS - Aix-Marseille Univ., Marseille, France

**Abstract:** Touch perception engages a broad network of autonomic and affective processes, yet thefeasibility of decoding emotional valence from multimodal physiological signals during tactileand visual stimulation remains largely unexplored. We investigated whether affective statesclassified as neutral, pleasant, or unpleasant could be discriminated from heart rate (HR), SkinConductance response (SCR), and pupil diameter (PUP) in humans, using a supervised machinelearning framework grounded in functional data analysis. The study was approved by anethical committee and all participants gave written, informed consent. 30 participantsunderwent tactile, visual, and combined visual-tactile stimulation, yielding over 2,600 trialsper modality combination. Each physiological time series was represented as a continuousfunctional object via B-spline basis expansion, with cardiac signals additionally reconstructedonto a common temporal domain through spline interpolation. Dimensionality reduction wasachieved using functional PCA. Several classifiers were evaluated, including logistic regression,support vector machines with linear, polynomial, and RBF kernels, LDA, and

QDA. A secondpipeline extended the baseline by incorporating first-order functional derivatives asindependent feature streams and pairwise cross-modal interaction features via outerproducts of functional PCA scores. Classification performance was evaluated using F1-scoresacross the affective classes (chance level ≈ 0.333). EDA measures yielded the most consistentresults, with the strongest single outcome reaching F1 = 0.382 under bimodal EDA-HR fusionwith a linear SVM in the touch condition, and F1 = 0.373 for HR under touch stimulation usingLDA in the derivative-augmented pipeline. The derivative-augmented framework did notproduce systematic improvements over the baseline, with gains appearing only in isolatedconfigurations. These findings suggest that autonomic physiological signals recorded duringaffective material exploration carry limited discriminative information for emotional valenceclassification at the individual trial level, with touch-specific conditions showing marginallyhigher discriminability than visual or pooled conditions.

**Disclosures: M. Bufo:** None. **R.H. Watkins:** None. **R. Ackerley:** None.

**Poster**

**PSTR181: Interoception: Central Circuits and Peripheral Mechanisms**

**Location:** WCC Halls A-C

**Time:** Monday, November 16, 2026, 1:00 PM - 5:00 PM

**Program #/Poster #:** PSTR181.01/Y5

**Topic:** E.04. Interoception

**Support:** JSPS KAKENHI 21K17060

**Title:** Involvement of P2X receptors on the initiation of swallowing induced by pharyngeal water stimulation in anesthetized rats

**Authors: *M. YOSHIHARA**, T. TSUJIMURA, M. TAKAKUWA, C.-R. PAN, Y. SHIYI, M. ONO, M. INOUE;
Niigata Univ., Niigata, Japan

**Abstract:** Background: Previous studies have suggested that water application to the larynx evokes the swallowing reflexes via purinergic P2X receptors and that hyposalivation condition under the blockade of muscarinic receptors by atropine facilitates these reflexes. Although swallowing evoked by laryngeal stimulation protects the airway from aspiration, that from pharyngeal stimulation mainly contributes to nutritional intake.To investigate the mechanisms underlying swallowing induced by pharyngeal stimulation, we examined the role of P2X receptors in water-induced swallowing, the effects of atropine on these reflexes in vivo, and pharyngeal water-induced ATP release ex vivo. Methods: Urethane-anesthetized male Sprague-Dawley rats were used. In vivo, swallowing was evoked by transnasal infusion of three solutions into the pharynx 40 mm from the nares (15 μl/10 s): distilled water (DW), saline, and ATP (0.1-10 mM). Swallowing events were identified by left thyrohyoid and suprahyoid electromyography. To evaluate the involvement of P2X receptors in the DW-induced swallowing, the pharynx was pretreated for 20 min using a cotton swab soaked in 50 μl of the

non-selective P2X antagonist PPADS (10 mM) or the P2X3 antagonist AF353 (1 mM), or saline as a control. Following the pretreatment, the number of DW-induced swallows was counted. Finally, DW-induced swallowing and pilocarpine induced salivary secretion were evaluated with and without intravenous administration of atropine (1 mg/kg).Ex vivo, the isolated pharynx was perfused with Krebs solution at 1 mL/min. Basal ATP release was measured during the initial Krebs solution perfusion, followed by DW perfusion for 1 min. The luminal perfusate was continuously collected throughout this 1-min DW perfusion period to determine changes in ATP release. Results: Pharyngeal DW stimulation induced significantly more swallows than saline. PPADS and AF353 significantly reduced DW-induced swallows compared to the control group. Pharyngeal ATP administration significantly increased swallows in a concentration-dependent manner. Atropine administration significantly increased pharyngeal DW-induced swallows and significantly decreased pilocarpine induced salivary secretion compared to baseline. Ex vivo, DW perfusion through the pharynx induced higher ATP concentrations in the luminal perfusate than Krebs solution.Conclusion: These findings suggest that DW stimulation induces pharyngeal mucosal ATP release, contributing to swallowing initiation via P2X3 and/or P2X2/3 receptors. Furthermore, blocking muscarinic receptors with atropine might facilitate pharyngeal water-induced swallowing.

**Disclosures: M. Yoshihara:** None. **T. Tsujimura:** None. **M. Takakuwa:** None. **C. Pan:** None. **Y. Shiyi:** None. **M. Ono:** None. **M. Inoue:** None.

**Poster**

**PSTR181: Interoception: Central Circuits and Peripheral Mechanisms**

**Location:** WCC Halls A-C

**Time:** Monday, November 16, 2026, 1:00 PM - 5:00 PM

**Program #/Poster #:** PSTR181.02/Y6

**Topic:** E.04. Interoception

**Support:** NIH-R01 HL173002
NSF 2334697

**Title:** Unique Transcriptional Adaptations of Jugular Sensory Neurons During Allergic Airway Inflammation

**Authors: *Y. WANG**[1], K. LAWSON[1], R. STEWART[1], S. TANG[2], S. WU[1], M. CHANG[1], V. YELLA[1], J. YANG[2], L. HAN[1];
[1]Sch. of Biol. Sci., Georgia Inst. of Technol., Atlanta, GA; [2]Dept. of Human Genet., Emory Univ. Sch. of Med., Atlanta, GA

**Abstract:** Vagal sensory neurons (VSNs) form a critical body-brain axis that monitors visceral physiology and coordinates protective reflexes. The vagal system is anatomically divided into jugular and nodose ganglia, which exhibit distinct peripheral innervation patterns and physiological functions. We previously demonstrated MrgprC11$^{+}$ jugular C-fibers control bronchoconstriction and airway hyperresponsiveness (AHR), yet how chronic inflammation

alters the transcriptome of these afferents to cause cellular dysfunction remains unknown. Here, we used a SMART-sequencing pipeline to map the transcriptome of airway-innervating MrgprC11$^{+}$ jugular neurons, non-airway nociceptive MrgprD$^{+}$ jugular controls, and lung-innervating mechanosensitive P2ry1$^{+}$ nodose neurons under baseline and following ovalbumin (OVA)-induced allergic lung inflammation. Histological validation via multi-channel RNAscope *in situ* hybridization confirmed that these three markers defined strictly segregated, non-overlapping subpopulations. By comparing the Phox2b$^{+}$ total nodose dataset as a reference, our filtering pipeline successfully identified distinct expression patterns for a group of jugular-associated genes. When subjected to ovalbumin (OVA)-induced inflammation, MrgprC11$^{+}$ and P2ry1$^{+}$ airway afferents exhibit sharply contrasting transcriptomic shifts despite experiencing the same peripheral inflammatory environment. Our results reveal a complete divergence in adaptive strategies between the two different jugular subtypes. Following allergic reactions, MrgprC11$^{+}$ jugular nociceptors enter a protective state of metabolic latency, systematically downregulating translation and mitochondrial oxidative phosphorylation while prioritizing cell-intrinsic proteostatic clearance pathways like autophagy. Conversely, P2ry1$^{+}$ nodose mechanoreceptors display a complete directional reversal, robustly upgrading their bioenergetic and translational mechanism to support distinct functional states. Because the transcriptomic profile of the jugular ganglion remains poorly understood, this study expands our understanding of jugular neurons, particularly distinct subpopulations under inflammatory conditions.

**Disclosures: Y. Wang:** None. **K. Lawson:** None. **R. Stewart:** None. **S. Tang:** None. **S. Wu:** None. **M. Chang:** None. **V. Yella:** None. **J. Yang:** None. **L. Han:** None.

**Poster**

**PSTR181: Interoception: Central Circuits and Peripheral Mechanisms**

**Location:** WCC Halls A-C

**Time:** Monday, November 16, 2026, 1:00 PM - 5:00 PM

**Program #/Poster #:** PSTR181.03/Y7

**Topic:** E.04. Interoception

**Support:** NIH R35HL155671

**Title:** Synergistic Interaction Between NaV1.7 and NaV1.8 blockers on Cough Causing Vagal C-fiber Terminals

**Authors: *J. S. KIM**, S. MEEKER, B. J. UNDEM;
Med., Johns Hopkins Univ. SOM, Baltimore, MD

**Abstract:** Conscious cough in guinea pigs and humans can be evoked by inhalation of selective C-fiber stimulants such as capsaicin or citric acid. In guinea pigs, conscious cough is evoked by activation of vagal neural crest-derived jugular C-fibers, but not by activation of placodal-derived nodose C-fibers. Single-neuron RT-PCR from guinea pig tracheal-specific jugular C-fiber neurons revealed expression of Nav1.7 and Nav1.8 mRNA in nearly all neurons (22 of 24 and 23 of 24, respectively).We next evaluated the effect of highly selective inhibitors of NaV1.7,

NaV1.8 and their combination on the activation of jugular C-fiber terminals. We isolated the trachea with the vagus nerve and jugular ganglion intact. Voltage threshold and citric-acid-induced action potential discharge were recorded using an extracellular electrode positioned in the jugular ganglion following stimulation of the nerve terminals in the trachea with either a concentric stimulating electrode (microprobe, tip diameter 2-3 μm) or by application of citric acid (1mM) to the receptive field. GNE8943 was used as a highly selective NaV1.7 blocker. At 3 μM, this drug abolished NaV1.7-dependent contractions of tracheal smooth muscle caused by stimulation of intrinsic parasympathetic nerves. LTGO8905 was used to block NaV1.8 (30 μM), at a concentration that reduced the NaV1.8 current in patch-clamped guinea pig neurons by >90%.Selectively blocking NaV1.7 had no effect on citric acid-induced AP discharge (n=8; 18±4 vs. 14±3 Hz; p=0.09), nor did it alter the electrical voltage threshold required to evoke a single action potential (n=9; 15±1V vs. 22±3V; p= 0.2). In contrast, selectively blocking NaV1.8, inhibited the peak AP discharge evoked by citric acid by about 35% (n=11; 14±1 vs. 7±1 Hz; p<0.0001) but did not influence the electrical voltage threshold of the terminals (n=8; 16±1 vs. 19±1 V; p=0.2).Combined blockade of NaV1.7 and 1.8 produced a much larger inhibitory effect on citric acid-induced AP discharge than either NaV1.7 or NaV1.8 inhibitor alone (n=19; 16±2 vs. 3±0.5 Hz; p<0.0001) and also significantly increased the voltage threshold (n=17; 15±1 vs. 45±8 V; p=0.007).These data show that NaV1.7 alone has no influence on chemical -induced activation of cough-causing C-fibers in guinea-pig trachea, whereas NaV1.8 significantly inhibited the response. The results also reveal a significant synergistic interaction when NaV1.7 and NaV1.8 blockers are used in combination, both in suppressing citric acid-induced AP discharge and in increasing the electrical excitability of the terminals.

**Disclosures: J.S. Kim:** None. **S. Meeker:** None. **B.J. Undem:** None.

**Poster**

**PSTR181: Interoception: Central Circuits and Peripheral Mechanisms**

**Location:** WCC Halls A-C

**Time:** Monday, November 16, 2026, 1:00 PM - 5:00 PM

**Program #/Poster #:** PSTR181.04/Y8

**Topic:** E.04. Interoception

**Support:** OT3OD030541
OT3OD025348
OT3OD025347
OT3OD025349
U24NS135547
3UC2AR082200

**Title:** SPARC: A Community Platform Bridging the Body and Brain through Open Data, Models, and Tools

**Authors: *J. BOLINE**[1], B. DE BONO[2], J. S. GRETHE[3], P. HUNTER[4], N. KUSTER[5], E. NEUFELD[5], D. P. NICKERSON[6], M. E. MARTONE[7], J. B. WAGENAAR[8];

[1]Informed Minds Inc, Walnut Creek, CA; [2]Indiana Univ. Sch. of Med., Indianapolis, IN; [3]Neurosciences, Ctr. for Res. in Biol. Systems, Neurosciences, Univ. of California San Diego, La Jolla, CA; [4]Auckland Bioengineering Institute, Univ. of Auckland, Auckland, New Zealand, Auckland, New Zealand; [5]Fndn. for Res. on Information Technologies in Society, Zurich, Switzerland; [6]Auckland Bioengineering Inst., Univ. of Auckland, Auckland, New Zealand; [7]Neurosci., UCSD, La Jolla, CA; [8]Dept. of Biostatistics, Epidemiology and Informatics, Univ. of Pennsylvania, Philadelphia, PA

**Abstract:** Understanding how the peripheral nervous system (PNS) regulates organ function and interfaces with the CNS is critical to advancing bioelectronic medicine and treating chronic pain. SPARC (RRID:SCR_017041) accelerates this understanding through open integrated data and modeling resources. The SPARC Portal (https://sparc.science) is an open-access platform supported by the SPARC Data and Resource Center (DRC). It provides NIH-compliant, HEAL-approved, and FAIR datasets, alongside computational models and interactive tools that cover various species, organs, and modalities. It is the main community repository for PNS neuroscience and systems physiology.

The SPARC Phase 2 program is publishing landmark datasets that expand our understanding of human vagal anatomy and function. REVA produced extensive multimodal imaging and segmentation of human vagus nerves from a large subject cohort. REVEAL, a large multisite clinical study, will release its first dataset by fall 2026, providing valuable new insights into the effects of vagus nerve stimulation (VNS) on multiple organs and systems.

The DRC is characterizing vagus nerve variability by registering each REVA subject to anatomical scaffolds (geometric models); normalizing scale and anatomical landmarks, and enabling population-level studies of anatomy and innervation to inform VNS device design and placement.

The DRC supports three consortia alongside SPARC, extending the Portal's focus to pain neuroscience and systems physiology. Two NIH HEAL initiatives publish data on pain: RE-JOIN is mapping sensory nerve networks innervating the temporomandibular joint and knee; PRECISION Human Pain Network provides molecular insight into the human trigeminal and dorsal root ganglia, spanning genomics, epigenomics, and proteomics. The VITAL consortium is developing multi-scale virtual patient models for cardiovascular conditions using SPARC maps as a gateway for systems physiology modeling.

To surface and support data reuse, the DRC provides a suite of tools through SPARC Apps. The o²S²PARC platform offers computational modeling and simulation, facilitating *in silico* interface safety and efficacy assessment. Map viewers and SCKAN tools allow interactive visualization and query of PNS connectivity. Dedicated REVA and PRECISION data exploration applications are also available on the Portal.

The SPARC Portal is an evolving community resource, growing in value as new data, models, and tools are added. Investigators working in PNS physiology, autonomic regulation, and pain neuroscience are encouraged to explore the Portal and consider publishing on SPARC to amplify their reach and impact.

**Disclosures: J. Boline:** None. **B. de Bono:** None. **J.S. Grethe:** E. Ownership Interest (stock, stock options, royalty, receipt of intellectual property rights/patent holder, excluding diversified mutual funds); SciCrunch Inc.. **P. Hunter:** None. **N. Kuster:** None. **E. Neufeld:** None. **D.P. Nickerson:** None. **M.E. Martone:** E. Ownership Interest (stock, stock options, royalty, receipt

of intellectual property rights/patent holder, excluding diversified mutual funds); SciCrunch Inc.. **J.B. Wagenaar:** None.

**Poster**

**PSTR181: Interoception: Central Circuits and Peripheral Mechanisms**

**Location:** WCC Halls A-C

**Time:** Monday, November 16, 2026, 1:00 PM - 5:00 PM

**Program #/Poster #:** PSTR181.05/Y9

**Topic:** E.04. Interoception

**Support:** ANID-FONDECYT 124611

**Title:** Cyclin-dependent kinase 5 (Cdk5), its activators, and receptor targets are colocalized in most mouse nodose ganglion neurons: a possible functional connection with afferent activity?

**Authors: *J. U. ALCAYAGA**;
Biología, Univ. de Chile, Fac Ciencias, Santiago, Chile

**Abstract:** The nodose ganglion (NG) of the vagus nerve (VN) contains sensory neurons that convey afferent activity from internal organs to the SNC. Several transmitter receptors (P2X) and transduction channels (TRPA1, TRPV1) have been reported to be expressed in the NG, and their responses can be modulated by post-translational modifications. Cyclin-dependent kinase 5 (Cdk5) and its activators (p35, p39) have been shown to be present in NG neurons, as well as several known (P2X, TRPA1, TRPV1) phosphorylation targets. Using immunocytochemistry, we assessed the colocalization (Pearson´s correlation coefficient, r; Manders' colocalization coefficients, MCC) of Cdk5, its activators, and targets in adult mouse NG sections and primary cultures. We recorded *in vitro* whole VN frequency discharge changes evoked by exogenously applied agonists of the abovementioned receptors and channels to the NG. Cdk5 was expressed in NG cells, both neurons (βIII tubulin$^+$) and glial cells (GFAP$^+$, GS$^+$, MBP$^+$). TRPV1 and TRPA1 were expressed in a population of neurons (45/72 and 46/62, respectively), being co-expressed in many of them (r= 0.98, MMC= 0.98, n= 30). Cdk5 colocalized with p35, p39, P2X2, TRPV1, and TRPA1 in most neurons (r= 0.73, 0.51, 0.60, 0.77; MMC= 0.99, 0.98, 0.99, 0.99; n= 139, 38, 78, 67, respectively). High colocalization values were observed for Cdk5 with TRPV1 and TRPA1 (r= 0.60, 0.70; MMC= 0.99, 0.99; n= 35, 21, respectively) in primary cultures. With an antibody against Cdk5-phosphorylated TRPV1 (p-TRPV1), we found high colocalization with Cdk5 in sections (r= 0.91; MMC= 0.99; n= 22) and cultures (r= 0.62; MMC= 0.99; n= 31). In a transgenic mouse that overexpresses TNF-alpha (TNF-alpha cTg), thus increasing p35, significantly higher levels of p35 and p-TRPV1 were observed ($p< 0.001$, Mann-Whitney test). ATP (P2X agonist), capsaicin (TRPV1 agonist), and AITC (TRPV1 agonist) applied to the NG increased the VN frequency discharge in a dose-dependent manner, with $EC_{50}$ values of 197.2 µM, 1.5 µM, and 9.5 mM, respectively, and slope (n) values of 0.85, 3.9, and 2.6, respectively. The duration of ATP-induced responses was significantly reduced by roscovitine (Cdk5 inhibitor) and in preparations from Cdk5 cKO mice. Conversely, the duration of the ATP-induced responses was significantly increased in TNF-alpha cTg preparations. Our

data show that Cdk5 is present in NG neurons, colocalizes with its activators and targets, and is basally active. Reducing its activity reduces the duration of ATP-induced responses, while increasing its activity has the opposite effect. These results suggest a possible role for Cdk5 in modulating afferent activity across different sensory modalities.

**Disclosures: J.U. Alcayaga:** None.

**Poster**

**PSTR181: Interoception: Central Circuits and Peripheral Mechanisms**

**Location:** WCC Halls A-C

**Time:** Monday, November 16, 2026, 1:00 PM - 5:00 PM

**Program #/Poster #:** PSTR181.06/Y10

**Topic:** E.04. Interoception

**Support:** Carney Graduate Award in Brain Science

**Title:** Temporal Congruency Drives the Multisensory Integration of Interoceptive and Exteroceptive Information

**Authors: *C. MCLAUGHLIN**[1], C. S. ZIMMERMAN[2], M. R. NASSAR[3], F. PETZSCHNER[1]; [2]Neurosci., [3]Metcalf Hall, [1]Brown Univ., Providence, RI

**Abstract:** The brain continuously processes signals from the external environment (exteroception) and internal bodily states (interoception) to shape our perception of the world and the body within. In the exteroceptive domain, multisensory integration across modalities such as vision and audition has long been recognized as a fundamental mechanism for forming unified percepts from distinct sensory inputs. Whether multisensory integration similarly links bodily signals with external sensory information, however, remains an open question. We used electroencephalography (EEG) and a novel heartbeat feedback task to investigate multisensory integration across interoceptive and exteroceptive channels in three independent studies. Specifically, we examined heartbeat-evoked potentials (HEPs) as objective markers of interoceptive processing, alongside stimulus-evoked potentials (SEPs) as markers of external sensory processing. We assessed how the temporal alignment between externally presented heartbeat cues and actual heartbeats modulates HEP and SEP amplitudes during the heartbeat task with auditory-visual feedback. In this task, a tone and a visually displayed heartbeat were phase-locked to an individual's cardiac cycle and periodically accelerated or decelerated. Our findings showed significant differences in HEPs, SEPs, and cardiac parameters (e.g., heart rate variability) when the stimulus was coupled to auditory-visual feedback compared to when it was uncoupled ("fasterStim HR" & "slowerStim HR"). These findings were replicated in three independent studies of healthy participants (total n= 110). Results suggest clear signs that interoceptive processing is altered by temporal locking with external information, and exteroceptive processing is altered by temporal locking with internal information. The neural and physiological markers we identified in healthy participants can inform future development of

transdiagnostic biomarkers of multisensory integration and how it is altered in mental health disorders.

**Disclosures: C. McLaughlin:** None. **C.S. Zimmerman:** None. **M.R. Nassar:** None. **F. Petzschner:** None.

**Poster**

**PSTR181: Interoception: Central Circuits and Peripheral Mechanisms**

**Location:** WCC Halls A-C

**Time:** Monday, November 16, 2026, 1:00 PM - 5:00 PM

**Program #/Poster #:** PSTR181.07/Y11

**Topic:** E.04. Interoception

**Title:** Effective Connectivity at a Large Scale: Applying regression DCM to discover connectivity within the brain's homeostatic, interoceptive, and affective sub-networks

**Authors: *J. CHE**[1], J. HADOUS[2], R. SULTAN[1], O. MUZIK[1], V. A. DIWADKAR[3]; [2]Psychiatry & Behavioral Neurosci., [1]Wayne State Univ., Detroit, MI; [3]Psychiatry & Behavioral Neurosci., Wayne State Univ. SOM, Detroit, MI

**Abstract:** Human thermoregulation has extensive brain network correlates involving regions in the brainstem and the insular cortex (Muzik et al., 2016). These functional interactions have been infrequently assessed in vivo fMRI data and mainly using undirected methods of functional connectivity (Muzik et al., Submitted). Here, we used dynamic causal modeling (DCM) typically used to investigate directed (i.e., causal) interactions in small networks (n=~8 regions). However, we circumvented this limitation using regression DCM (Frassle et al., 2017) to investigate thermoregulation induced effective connectivity (EC) in a large network (n=131 brain regions). Our implementation allowed us to capture intra and inter-lobar interactions between brain regions induced by thermoregulation (with a focus on significant *intra*-lobar interactions). fMRI data were acquired from 61 participants (28M/33F, $20 \leq \text{Age} \leq 31$) while participants were exposed to whole-body thermoregulatory challenge (25 min.; 5 min. alternating epochs for rewarming and cooling). fMRI data were processed using typical methods. First, time series from 262 regions [246 cerebral (seven lobes) and 16 brainstem regions] (Fan et al., 2016; Edlow et al., 2016) were submitted for conventional zero lag functional connectivity analyses. Pathways where each condition evoked significant connectivity ($p_{FDR}<.05$) were identified following which we computed the intersection set of effects across conditions. In each lobe, the 50$^{th}$ percentile of regions that contributed to the intersection set were submitted for rDCM analyses (n=131 regions). DCM was implemented using a sparsity constraint on the probability of each region being included in the connection (*p*-values: 0.05-0.95 at 0.05 increments, optimized over 100 iterations) to find the optimal generative model. *T*-tests were conducted to determine significant effective connectivity for all 17,030 pathways ($131^2$-131). From the full set of pathways *within* each lobe, we calculated the percentage of significant *intra*-lobar effects that were bidirectional (i.e., $R_1 \rightarrow R_2 \wedge R_2 \rightarrow R_1$) or unidirectional (i.e., $R_1 \rightarrow R_2 \neg\wedge R_2 \rightarrow R_1$). The brain stem, the limbic lobe (cingulate) and the insular cortex evinced substantial bidirectionality (14.3%, 19% and

26.7% of all possible connections), while the brainstem and the insular cortex also evinced substantial unidirectionality (16.1% and 10% respectively). These results suggest that thermoregulation evokes a substantial degree of efferent and afferent pathways *within* the brain's homeostatic (brainstem), interoceptive (insula) and affective (limbic) networks.

**Disclosures: J. Che:** None. **J. Hadous:** None. **R. Sultan:** None. **O. Muzik:** None. **V.A. Diwadkar:** None.

**Poster**

**PSTR181: Interoception: Central Circuits and Peripheral Mechanisms**

**Location:** WCC Halls A-C

**Time:** Monday, November 16, 2026, 1:00 PM - 5:00 PM

**Program #/Poster #:** PSTR181.08/Y12

**Topic:** E.04. Interoception

**Support:** CGRS-Master's (CIHR)

**Title:** Defining the Relationship between the Claustrum and the Insula: Anatomy and Interoception

**Authors: *J. P. LINDNER**[1], A. M. TAYLOR[2], J. C. JACKSON[3];
[1]Neurosci. and Mental Hlth. Institue, [2]Pharmacol., [3]Physiol., Univ. of Alberta, Edmonton, AB, Canada

**Abstract:** The claustrum is highly connected and multi-functional brain structure, with reciprocalconnections to the entire cortex, particularly the prefrontal cortex. However, one cortical regionwith poorly defined claustrum connectivity is the insula. Therefore, our first objective is todefine the anatomy between the claustrum and the insula. To execute this, we performedstereotaxic injections in C57BL/6 mice (n=10: 5F, 5M) into the anterior/posterior insula withanterograde and retrograde tracers, thereby capturing the full breadth of possible connection.Surprisingly, this tracing data showed sparse anatomical connection between the claustrum andinsula. To validate the lack of connection, we stained for the claustrum using NR2f2, a markerfor excitatory claustrum neurons, and investigated colocalization of the tracers and this marker.Specifically, in the anterior insula injections, only 1.7% of NR2f2 cells colocalized with theretrograde tracer, and 1.4% colocalized with the anterograde tracer in the claustrum region. Inthe posterior insula injections, only 1.7% of NR2f2 cells colocalized with the retrograde tracerand 2.6% colocalized with the anterograde tracer. Of the few cells that were colocalized, thesecells tended to be 100-350µm away from the claustrum core, indicating they may not becanonical claustrum cells. Therefore, in total, we found a near absence of any form ofconnectivity between claustrum and insula circuits. While these regions are not connected, theyare alike in their connections with the anterior cingulate cortex, and we postulate that thesecircuits may work in concert during interoception. The insula and anterior cingulate are majorhubs of interoception, and although the claustrum's involvement has not been well defined, itsstrong role in attention and pain indicate participation in interoceptive processing. Therefore,

oursecond objective is to investigate the role of the anterior cingulate-claustrum and anteriorcingulate-insula pathways in heart and pain interoception. Together, these studies highlight thedistinct anatomy of the claustrum and insula, and will determine how these distinct pathwaysmay orchestrate interoception.

**Disclosures: J.P. Lindner:** None. **A.M. Taylor:** None. **J.C. Jackson:** None.

**Poster**

**PSTR181: Interoception: Central Circuits and Peripheral Mechanisms**

**Location:** WCC Halls A-C

**Time:** Monday, November 16, 2026, 1:00 PM - 5:00 PM

**Program #/Poster #:** PSTR181.09/Y13

**Topic:** E.04. Interoception

**Support:** TUBITAK 2218 Fellowship Grant

**Title:** Dissecting the Role of Nitric Oxide in Vagal Sensory Neurons Using Genetically Encoded Biosensors

**Authors: *T. AKGUL CAGLAR**, S. YILDIRIM, E. EROGLU;
Istanbul Medipol Univ., Istanbul, Turkey

**Abstract:** Nitric oxide (NO) has been implicated as a versatile neuromodulator within the vagal sensory system, but its precise function remains elusive due short half-life, high diffusibility and limitations of conventional pharmacological approaches using NO donors and inhibitors. Our previous study shows that endogenous NO suppresses the spontaneous calcium ($Ca^{2+}$) activity in hippocampal neurons, and we proposed that receptor mediated NO signaling serves a critical regulatory mechanism in the nodose ganglion (NG). In the present study, we utilized a genetically encoded NO biosensor (geNOp) and $Ca^{2+}$ indicatior GCaMP6s to monitor real time intracellular NO and $Ca^{2+}$ dynamics in NG neurons. We transduced isolated NG neruons with AAV vector expressing geNOp/GCaMP6s under synapsin promoter. Endogenous NO production was induced via membrane depolarization with 50 mM potassium (KCl) and biosensor functionality was validated using 10 uM NOC-7 as a NO donor. Our results demonstrate that 90% of NG neurons exhibit robust changes in geNOp fluorescent intensity upon high KCI, revealing high capacity of endogenous NO production (n=19/22 cells). Maximum response of geNOp levels upon KCI was 5.91% ± 3.47% while averaged maximum amplitude response to NO donor was found to be 10.62% ± 1.71%. Immunolabeling with neuronal nitric oxide synthase (nNOS) antibody confirming the abundance of nNOS-positive NG neurons. To achieve further cell-type specifictiy, we will tranduce NG neurons from $Phox2b^{Cre}$ mice with geNOp and GCaMP6s. Furthermore, we will investigate receptor-mediated NO synthesis by stimulating NG neurons with transient receptor potential vanilloid type 1 (TRPV1) agonist capsaicin and purinergic receptor agonist ATP. By dissecting the interplay of receptor-mediated NO synthesis and its interaction with $Ca^{2+}$ signaling, this study will establish a foundational framework for understaing how NO signaling modulate visceral sensory transmission.

**Disclosures: T. Akgul Caglar:** None. **S. Yildirim:** None. **E. Eroglu:** None.

**Poster**

**PSTR181: Interoception: Central Circuits and Peripheral Mechanisms**

**Location:** WCC Halls A-C

**Time:** Monday, November 16, 2026, 1:00 PM - 5:00 PM

**Program #/Poster #:** PSTR181.10/Y14

**Topic:** E.04. Interoception

**Support:** NIH NIDDK 1R01DK143462
Duke CTSI Swann Lee Awards for Prevention of Chronic Diseases using Diet and Nutrition

**Title:** A gut sense for dietary protein

**Authors: *C. BEKELE**[1], S. AMIRNENI[1], B. EMREGÜL[1], E. ALWAY[4], P. WENG[5], Z. S. LORSCH[2], N. REICHER[3], D. V. BOHORQUEZ[2];
[2]Med., [3]Neurobio., [1]Duke Univ., Durham, NC; [4]Neurobio., Duke Univ. Sch. of Med., Durham, NC; [5]Johns Hopkins Univ., Baltimore, MD

**Abstract:** Dietary protein is necessary for life. However, the mechanism by which dietary protein is sensed remains incompletely understood. Our laboratory has discovered specialized gut epithelial sensory cells, known as neuropod cells, that sense sugar and help guide an animal's preference for sugar over artificial sweetener. These neuropod cells synapse with afferent fibers of the vagus nerve to rapidly convey nutritional information to the brain; however, whether neuropod cells play a role in protein-seeking behavior has not yet been explored. Here, we investigate the effect of dietary protein levels on food consumption and choice. We demonstrate that mice on diets lacking dietary protein quickly display weight loss and die. Accordingly, when given the choice, mice will preferentially consume protein-containing diets. Interestingly, this effect is apparent within minutes, occurring well before the mouse establishes a nutritional deficit for protein. Further, mice will titrate consumption according to protein content, suggesting that levels of protein in food are rapidly sensed. To evaluate the source of this sense, we determined preference for protein-containing foods in taste-blind mice. Here, we found an even more immediate preference for protein, and direct delivery of amino acids into the intestine of wild-type mice ablated protein preferences. These findings suggest that the gut senses protein and guides preferences for protein-containing foods. To explore the mechanism of this effect, we performed quantitative PCR on gut epithelial cells following protein-complete and protein-deplete diets. We find that the absence of dietary protein altered the expression of key protein-regulation genes such as FGFR1, β-Klotho, and GPRC6a selectively in neuropod cells. Together, these findings suggest a rapid gut sense for dietary protein driven by sensory neuropod cells.

**Disclosures: C. Bekele:** None. **S. Amirneni:** None. **B. Emregül:** None. **E. Alway:** None. **P. Weng:** None. **Z.S. Lorsch:** None. **N. Reicher:** None. **D.V. Bohorquez:** None.

**Poster**

**PSTR181: Interoception: Central Circuits and Peripheral Mechanisms**

**Location:** WCC Halls A-C

**Time:** Monday, November 16, 2026, 1:00 PM - 5:00 PM

**Program #/Poster #:** PSTR181.11/Y15

**Topic:** E.04. Interoception

**Support:** National Research Foundation of Korea (RS-2023-00212393)
National Research Foundation of Korea (RS-2023-00243359)
National Research Foundation of Korea (RS-2024-00345184)
National Research Foundation of Korea (RS-2022-NR068424)
National Research Foundation of Korea (RS-2023-00217798)
National Research Foundation of Korea (RS-2024-00404638)
National Research Foundation of Korea (RS-2024-00436263)
National Research Foundation of Korea (RS--2025--00521180)
National Research Foundation of Korea (RS--2025--02310437)
NRF--2022M3A9F308298213
National Research Foundation of Korea (RS--2023--00255126)
National Research Foundation of Korea (RS--2024--00404132)
Samsung Science and Technology Foundation (project no. SSTF--BA--1802--11)
the Institute for Basic Science (IBS--R042--D1)

**Title:** Complex Interplay of Neuronal, Hormonal Responses by Gut-Brain Axis to a Deficit in Essential Amino Acids

**Authors: *S. LEE**[1], G. SUH[2], B. KIM[3];
[1]Yale Univ., New Haven, CT; [2]Inst. for Basic Sci. (IBS), Ctr. for Microbiome-Body-Brain Physiology, Gwangju Inst. of Sci. and Technol. (GIST), Gwangju, Korea, Republic of; [3]Hanyang Univ. Col. of Med., Seoul, Korea, Republic of

**Abstract:** A deficit in protein can trigger a nutrient-specific appetite; however, the mechanism underlying this process remains poorly understood. Here, we found that a set of distinct neuronal and systemic mechanisms is activated in the microbiome-gut-brain axis to induce an essential amino acids (EAA)-specific appetite. In *Drosophila*, EAA deprivation increases the expression of CNMa in the gut enterocyte, which activates enteric neurons and ellipsoid body neurons in the brain to promote EAA intake through two complementary pathways: a rapid, direct neuronal gut-brain axis and a slower hormonal route. In parallel, CNMa suppresses the activity of sugar-sensing DH44 neurons, thereby reducing carbohydrate intake and biasing feeding toward EAAs. Similarly, protein deprivation in mice promotes EAA-specific appetite independently of FGF21, but this appetite requires an intact spinal pathway. Together, these findings reveal multi-layered gut-brain mechanisms that regulate nutrient-specific feeding and maintain EAA homeostasis across species.

**Disclosures: S. Lee:** None. **G. Suh:** None. **B. Kim:** None.

**Poster**

**PSTR181: Interoception: Central Circuits and Peripheral Mechanisms**

**Location:** WCC Halls A-C

**Time:** Monday, November 16, 2026, 1:00 PM - 5:00 PM

**Program #/Poster #:** PSTR181.12/Y16

**Topic:** E.04. Interoception

**Support:** R01 DK141890

**Title:** PIEZO2 is not required for distention-evoked activation of mechanosensitive vagal sensory afferent nerves in the esophagus

**Authors:** S. NAIR, J. HOOPER, S. HADLEY, K. LURYE, M. PATIL, ***T. TAYLOR-CLARK**;
Univ. of South Florida, Tampa, FL

**Abstract:** Low-threshold mechanoreceptors that innervate the esophagus play a critical role in primary and secondary peristalsis. Although both the vagal and dorsal root ganglia innervate the esophagus, immunohistochemical and functional studies have shown that almost all the esophageal low-threshold mechanoreceptors originate from the vagal ganglia (so-called Intraganglionic Laminar Endings (IGLEs)). However, the mechanism by which these afferents transduce mechanical stimuli is still not fully understood. PIEZO ion channels are mammalian mechanosensitive ion channels that have been shown to be essential for vagal afferent mechanosensation during lung inflation and as part of aortic baroreception. Previous studies have shown IGLEs express PIEZO2. Here, we investigated the role of nodose PIEZO ion channels in esophageal distention-induced mechanosensation. We used multiphoton imaging of vagal neuron GCaMP6s to measure mechanosensitive afferent activity using an ex vivo intact nodose-vagus nerve-esophagus preparation. Preliminary data from PIRT-GCaMP6s mice showed a graded, intraesophageal pressure-dependent increase in GCaMP fluorescence in a subset of nodose neurons. Pharmacological inhibition of PIEZOs using GsMTx4 significantly reduced activation by 5, 10, and 30mmHg intraesophageal pressures (n=10 ganglia). Next, we generated a vagal-specific conditional PIEZO2 knockout by crossing P2X2-Cre:GCaMP6s mice (P2X2 is expressed in all nodose neurons) with PIEZO2fl/fl mice (P2X2:GCaMP6sPIEZO2cKO). Intraperitoneal FM1-43 dye (which enters neurons through active PIEZO2 ion channels) injection showed a marked reduction in FM+ soma in the nodose ganglia of these mice when compared to control P2X2-Cre:GCaMP6s nodose ganglia (45% in controls vs 14% in KO, n= 5 mice). However, vagal cKO of PIEZO2 had no effect on the distention-induced vagal activation in ex vivo GCaMP studies (n=7 for KO and n=6 for control). Addition of GsMTx4 to the PIEZO2 cKO significantly reduced distension-evoked responses at all three pressures, suggesting a role for nodose PIEZO1 (n=6). These data suggest that nodose PIEZO2 could be redundant for sensing esophageal distention. Moreover, this function might be dependent on nodose PIEZO1.

**Disclosures: S. Nair:** None. **J. Hooper:** None. **S. Hadley:** None. **K. Lurye:** None. **M. Patil:** None. **T. Taylor-Clark:** None.

**Poster**

**PSTR181: Interoception: Central Circuits and Peripheral Mechanisms**

**Location:** WCC Halls A-C

**Time:** Monday, November 16, 2026, 1:00 PM - 5:00 PM

**Program #/Poster #:** PSTR181.13/Y17

**Topic:** E.04. Interoception

**Support:** NIH F32 Grant DK148022-01
NIH T32 Grant 5T32DC000014

**Title:** Molecular mechanisms for mechanoreception in vagal afferent neurons of the gut

**Authors: *A. BALI**[1], G. F. DE LARTIGUE[2];
[1]Monell Chem. Senses Ctr., Philadelphia, PA; [2]Univ. of Pennsylvania, Philadelphia, PA

**Abstract:** Gut distension signals give rise to feelings of fullness and meal termination as well as parasympathetic processes such as gastric emptying, gut motility, thermoregulation and glucose homeostasis. Vagal afferent neurons (VANs) are known to respond to diverse mechanical signals in the gut and suppress feeding, but the molecular mechanisms that transduce these mechanical stimuli are poorly defined. Using *in vivo* $Ca^{2+}$ imaging combined with multiplexed fluorescent *in situ* hybridization in mice with intragastric balloons, we identified Piezo2 and TRPA1 as candidate mechanosensitive ion channels expressed in non-overlapping populations of stretch-responsive VANs. These populations are distributed across previously-defined broader classes of vagal afferents, including Glp1- and Oxytocin- receptor expressing neurons. To directly test function, we selectively deleted Piezo2 or TRPA1 in stomach-innervating VANs. Loss of either channel abolished distension-induced vagal responses *in vivo*. Behavioral responses to gastric distension such as reduction in food intake and decreased locomotion require both Piezo2 and TRPA1 vagal populations. In contrast, only Piezo2 was required for distension-induced autonomic responses. All experiments were performed in mice (n= 5-10 per group). These findings identify Piezo2 and TRPA1 as key molecular transducers of gastric distension in distinct vagal mechanosensory populations, revealing parallel pathways that differentially regulate behavioral and autonomic components of eating and homeostasis.

**Disclosures: A. Bali:** None. **G.F. De Lartigue:** None.

**Poster**

**PSTR181: Interoception: Central Circuits and Peripheral Mechanisms**

**Location:** WCC Halls A-C

**Time:** Monday, November 16, 2026, 1:00 PM - 5:00 PM

**Program #/Poster #:** PSTR181.14/Y18

**Topic:** E.04. Interoception

**Title:** Stomach-Derived Sensory Signals Activate Spinal ERα Neurons to Regulate Postprandial Locomotor Activity

**Authors: *X. WU**, Y. XU;
Univ. of South Florida, Tampa, FL

**Abstract:** Meals suppress locomotor activity, but the spinal mechanisms linking postprandial visceral signals to reduced physical activity remain unclear. We investigated estrogen receptor-α-expressing neurons in the dorsal horn of T8-L2 spinal segments (ERα-$DH^{T8-L2}$). We found that refeeding reduced locomotor activity in both male and female mice and increased c-Fos expression in ERα-DHT8-L2 neurons. Retrograde viral tracing from the stomach labeled dorsal root ganglion neurons and their central terminals in the T8-L2 dorsal horn, indicating that stomach-derived sensory signals reach spinal segments containing ERα-$DH^{T8-L2}$ neurons. Chronic inhibition of ERα-$DH^{T8-L2}$ neurons increased locomotor activity, particularly during the dark cycle, increased energy expenditure, and reduced body weight despite a modest increase in food intake. Anatomical tracing showed that ERα-$DH^{T8-L2}$ neurons project to the locus coeruleus. ChR2-assisted circuit mapping further showed that ERα-$DH^{T8-L2}$ neurons provide monosynaptic glutamatergic input to LC neurons. These results identify a stomach-DRG-spinal ERα pathway that regulates postprandial locomotor activity and energy expenditure. A similar spinal interoceptive mechanism may contribute to physical inactivity and energy imbalance in obesity.

**Disclosures: X. Wu:** None. **Y. Xu:** None.

**Poster**

**PSTR181: Interoception: Central Circuits and Peripheral Mechanisms**

**Location:** WCC Halls A-C

**Time:** Monday, November 16, 2026, 1:00 PM - 5:00 PM

**Program #/Poster #:** PSTR181.15/Y19

**Topic:** E.04. Interoception

**Support:** NIH Grant HL168211

**Title:** Encoding of NTS Neurons During Physiological Dysfunction

**Authors: *M. ANDERSEN**;
Comparative Biosci., Univ. of Wisconsin Madison, Madison, WI

**Abstract:** The network-level mechanisms within the nucleus tractus solitarius (NTS), the brainstem hub for integrating cardiorespiratory afferents, and how these neurons respond to changes in afferent information, remain poorly understood. Using high-density Plexon SiNAPS recordings in anesthetized mice, we simultaneously measured neuronal activity in the NTS alongside respiratory airflow, diaphragm EMG, end-tidal CO2, carotid pulse pressure, and ECG. We developed an analysis framework combining (1) breath- and cardiac-aligned spike timing, (2) spike-triggered averages, and (3) a Poisson generalized linear model (GLM) to quantify how individual neurons encode respiratory phase, respiratory drive, blood pressure, CO2, and cardiac

phase. Across NTS units, we found highly heterogeneous but structured multimodal encoding, with most neurons driven by multiple afferent inputs. $\Delta R^2$ variance partitioning revealed distinct encoding signatures that mapped onto functional clusters identified via UMAP + HDBSCAN. Fentanyl profoundly disrupts breathing, leading to cardiorespiratory distress and within our model we found it produced rapid, ensemble-wide reconfiguration. Some NTS neuron clusters were silenced, others were strongly excited, and a subset showed preserved firing but altered encoding weights, particularly in respiratory-phase and pressure-related kernels. Despite large drug-induced changes in ventilation and autonomic output, our GLM analyses show that the structure of afferent encoding, not just firing rate, changes during opioid exposure, indicating that opioids reshape how the NTS interprets cardiorespiratory signals. These findings support a model in which opioid-induced dysregulation of NTS afferent integration contributes to failures of compensatory homeostatic reflexes during opioid overdose. Together, these data provide a high-dimensional map of multimodal encoding in the NTS during opioid perturbation and establish a framework for identifying neural substrates of respiratory and autonomic collapse.

**Disclosures: M. Andersen:** None.

**Poster**

**PSTR181: Interoception: Central Circuits and Peripheral Mechanisms**

**Location:** WCC Halls A-C

**Time:** Monday, November 16, 2026, 1:00 PM - 5:00 PM

**Program #/Poster #:** PSTR181.16/Y20

**Topic:** E.04. Interoception

**Support:** HMM 2.0 18954

**Title:** Group-Level Alignment of Periaqueductal Gray Parcellations Using Simulated Annealing

**Authors:** Y. SCHOUTENS[1], J. HALEWIJN[1], G. A. VAN KOEVERINGE[2], J. VAN DEN HURK[3], ***M. M. DE RIJK**[1];
[1]Urology, Maastricht Univ., Maastricht, Netherlands; [2]Dept. of Urology, Maastricht Univ. Med. Ctr., Maastricht, Netherlands; [3]Scannexus, Maastricht, Netherlands

**Abstract:** The periaqueductal gray (PAG) is a key midbrain node in the central control of urinary continence, linking forebrain mechanisms involved in conscious bladder control with lower brainstem circuits that coordinate reflexive micturition. Although ultra-high-field resting-state fMRI has shown that the human PAG can be divided into reproducible functional clusters, group-level mapping has been limited by the arbitrary labeling of clusters across participants. We therefore developed an exploratory simulated annealing (SA) approach to align individual PAG parcellations and generate a group-level map of intrinsic PAG organization. Seventeen healthy adult female participants underwent 7T resting-state fMRI during a full-bladder state, in which 420 T2*-weighted multiband echo planar imaging volumes were acquired (TR=1400 ms, TE=22 ms, 1.1 mm isotropic resolution). For each participant, the PAG was parcellated using Louvain community detection. SA was then used to solve the resulting cluster-label assignment problem

by minimizing total intra-group Euclidean distances between cluster centroids. To assess robustness of the alignment, performance was evaluated against permutation-based null distributions using 10,000 cluster-label shuffles for centroid distances and 1,000 permutations for spatial overlap, quantified with mean pairwise Dice coefficients. Three functional PAG clusters were identified in all participants except one participant with four clusters, in whom the two most strongly correlated clusters were merged to maintain a three-cluster solution. SA significantly reduced intra-group centroid distances beyond chance ($p \leq 0.001$) and improved spatial alignment. Results showed a group-level organization along the rostro-caudal axis, with mean Dice coefficients of 0.41 for the rostral cluster, 0.34 for the middle cluster, and 0.40 for the caudal cluster (all $p \leq 0.001$). The resulting group-level parcellation showed a bilaterally symmetrical organization of the PAG. These findings provide the first group-level intrinsic functional parcellation of the human PAG and support a rostro-caudal organizational principle relevant to brainstem control of urinary continence. More broadly, this SA-based framework offers a generalizable strategy for aligning functional parcellations of small subcortical and brainstem structures in ultra-high-field fMRI datasets.

**Disclosures: Y. Schoutens:** None. **J. halewijn:** None. **G.A. Van Koeveringe:** None. **J. Van Den Hurk:** None. **M.M. de Rijk:** None.

**Poster**

**PSTR181: Interoception: Central Circuits and Peripheral Mechanisms**

**Location:** WCC Halls A-C

**Time:** Monday, November 16, 2026, 1:00 PM - 5:00 PM

**Program #/Poster #:** PSTR181.17/Y21

**Topic:** E.04. Interoception

**Support:** NIH R01 - 5R01DK139386-03
NIH R01 - 5R01DK128475-05
NIH R01 - 5R01DK140445-02

**Title:** Molecular code of the mouse ventromedial medulla in bladder somatosensation

**Authors: *H. P. GREENHILL**[1], L. YANG[4], J. ZHENG[2], F. LIU[3], M. KAWATANI[5], Y. ZHANG[3], A. PETUKHOVA[3], M. HEITMEIER[3], V. K. SAMINENI[6];
[1]Anesthesiol., [2]Washington Univ. in St. Louis, St Louis, MO; [3]Washington Univ. in St. Louis, St. Louis, MO; [4]Anesthesiol., Washington Univ. in St. Louis Neurosci. PhD Program, St. Louis, MO; [5]Washington Univ. in St.Louis, St. Louis, MO; [6]Washington Univ., St. Louis, MO

**Abstract:** The ventromedial medulla (VMM) is a brainstem region containing essential subnuclei implicated in the descending modulation of pain and pelvic musculature through spinal circuits. Neuroanatomical studies have shown that the ventromedial medulla is multi-synaptically connected to urinary bladder afferents, and canonical ventromedial medullary “ON” and “OFF” cells have been identified in response to bladder distention. Still, these studies have not been able to provide refined VMM molecular cell types, connectivity and activity defined

atlas that may be leveraged to build mechanistic insights into bladder overactivity and pain. To identify ventromedial medulla neuronal types and projections that are involved in bladder pain and dysfunction, we employed a high-resolution multimodal map of the mouse VMM that combines spatial organization, molecular profiling, and projection patterns of medulla neurons. We combined this refined atlas of the VMM with transcriptomic sequencing of immediate early genes to identify activated or silenced cell types in the VMM in response to cystitis. Using retrograde virus injections, we identify neurons within these clusters that specifically project to the lumbosacral spinal cord, a crucial site for the integration of bladder somatosensation. By implementing computational ethology on 3D kinematic representations of freely moving mice, we show that modulation of these neurons recapitulates spontaneous pain behaviors seen uniquely in cystitis. This refined molecular and neuroanatomical understanding of the ventromedial medulla is an essential foundation for the development of specific, targeted pharmacology in the treatment of cystitis.

**Disclosures: H.P. Greenhill:** None. **L. Yang:** None. **J. Zheng:** None. **F. Liu:** None. **M. Kawatani:** None. **Y. zhang:** None. **A. Petukhova:** None. **M. Heitmeier:** None. **V.K. Samineni:** None.

**Poster**

**PSTR181: Interoception: Central Circuits and Peripheral Mechanisms**

**Location:** WCC Halls A-C

**Time:** Monday, November 16, 2026, 1:00 PM - 5:00 PM

**Program #/Poster #:** PSTR181.18/Y22

**Topic:** E.04. Interoception

**Title:** Inter-Lobar Effective Connectivity Induced During Human Thermoregulatory Challenge: Applications of Regression Dynamic Causal Modeling (rDCM)

**Authors: *R. SULTAN**[1,2], J. HADOUS[2], J. CHE[2], O. MUZIK[1], V. A. DIWADKAR[3]; [2]Psychiatry & Behavioral Neurosci., [1]Wayne State Univ., Detroit, MI; [3]Psychiatry & Behavioral Neurosci., Wayne State Univ. SOM, Detroit, MI

**Abstract:** Autonomic control in human thermoregulation results from widespread brain network interactions. These are usually investigated with functional connectivity (FC) measures (based on zero-lag correlation), but FC does not reveal directional interactions. Only effective connectivity (EC) methods such as Dynamic Causal Modeling (DCM) reveal systemic directional effects. Traditional DCM approaches are limited to modeling network interactions in small networks (n<10 regions). However, we leveraged regression DCM (rDCM), designed to investigate EC at a large scale (n>100 regions). fMRI data were acquired (n=61, 28M/33F, mean age 25.1 ± 3.4 years) using a whole-body thermoregulatory challenge (cooling and rewarming)(Muzik et al., 2024). In an initial data reduction step, functional connectivity (FC) was assessed across a 262-region connectome (based on cerebral and brainstem atlases)(Fan et al., 2016; Edlow et al., 2016) using zero-lag correlation. t-tests were used to identify pathways between pairs of regions with significant effects in both conditions (pFDR<.05). Next, we quantified the frequency with

which each of the 262 regions contributed to significant effects. In each lobe, regions in the 50th percentile were forwarded for rDCM (resulting in a network space of 131 regions in seven cerebral lobes and the brain stem) (Frassle et al., 2018). From the observed EC parameter estimates (1312-131=17,030 parameters), t-tests were used to identify pathways where the experiment evoked significant EC ($\neq 0$). Significant pathways were differentiated based on the identity of the source and target in the region pair. Across the seven cerebral lobes and the brain stem, we quantified the asymmetry in the directionality in pathways with significant EC. First, significant effects observed in each direction were expressed as a percentage of all possible pathways (e.g., 10 significant pathways from a possible total of 100 gives us a value of 10%). Then asymmetry in direction was expressed as a difference in percentages between directions (A -> B vs. B -> A). From the results, the temporal lobe evinced substantial source-target asymmetry to both the brainstem and limbic regions (+5.4% and +4.6%). In addition, the brain stem evinced substantial source-target asymmetry to the sub-cortical nuclei (+3.5%). The results suggest that rDCM successfully recovers substantial inter-mixing of efferent and afferent signals during thermoregulation. This effect was observed between regions for emotion processing (temporal and limbic), homeostatic control (brain stem) and sensory processing and motor initiation (basal ganglia and thalamus in the sub-cortical nuclei).

**Disclosures: R. Sultan:** None. **J. Hadous:** None. **J. Che:** None. **O. Muzik:** None. **V.A. Diwadkar:** None.

**Poster**

**PSTR181: Interoception: Central Circuits and Peripheral Mechanisms**

**Location:** WCC Halls A-C

**Time:** Monday, November 16, 2026, 1:00 PM - 5:00 PM

**Program #/Poster #:** PSTR181.19/Y23

**Topic:** E.04. Interoception

**Title:** Oscillatory coupling of cardiac and neural rhythms indexes the engagement of inhibitory control

**Authors: *A. YOUNG**, J. W. SCHOOLER;
Psychological and Brain Sci., Univ. of California, Santa Barbara, Santa Barbara, CA

**Abstract:** Heart rate variability (HRV), particularly high-frequency HRV, is widely studied as an index of autonomic regulation linked to emotion regulation, psychological well-being, and physical health. Recent work suggests that high-frequency HRV may be relevant to mental states not only as a downstream marker of cortico-autonomic regulation, but also as a low-frequency rhythm that organizes comparatively higher-frequency neural activity within prefrontal cortex through phase-amplitude coupling (PAC). Generalized anxiety is a compelling target for evaluating this brain-body substrate because it is characterized by autonomic and attentional dysregulation, with reduced inhibitory control contributing to persistent arousal, hypervigilance, and subjective distress. We tested whether HF-HRV-EEG PAC varies with self-reported anxiety symptomatology both at rest and during a mental arithmetic task in 22 healthy adults. At rest,

higher GAD-7 scores predicted reduced HF-HRV coupling with fronto-central theta amplitude, controlling for EEG and HRV parameters. This effect did not generalize to a posterior comparison channel. Notably, GAD-7 scores were unrelated to conventional autonomic and spectral indices. During the arithmetic task, HF-HRV-theta PAC increased relative to rest independent of changes in heart rate, HRV, or EEG band power. Critically, a significant interaction indicated that the more anxious the individual, the greater their task-related increase in HF-HRV-theta PAC. Together, these findings suggest that phase-amplitude coupling of high-frequency HRV and fronto-central EEG may reflect a regulatory mechanism that anxious individuals fail to spontaneously employ at rest, but can recruit under demand.

**Disclosures: A. Young:** None. **J.W. Schooler:** None.

**Poster**

**PSTR181: Interoception: Central Circuits and Peripheral Mechanisms**

**Location:** WCC Halls A-C

**Time:** Monday, November 16, 2026, 1:00 PM - 5:00 PM

**Program #/Poster #:** PSTR181.20/Y24

**Topic:** E.04. Interoception

**Support:** A*STAR Career Development Fund (C233312017)
National Research Foundation Fellowship Award (NRFF13-2021-0087)
NMRC-Young Individual Research Grant (OFYIRG23jul-0065)
A*STAR Strategic Research Program (Brain-Body Initiative, 21718)
NMRC-Individual Research Grant (OFIRG24jul-0096)

**Title:** A hepatic vagal circuit for inflammation sensing

**Authors: *N. ZHANG**, S. LUO;
Inst. of Mol. and Cell biology, A*STAR, Singapore, Singapore

**Abstract:** Maintaining energy homeostasis during infection requires neural mechanisms that detect peripheral inflammation and coordinate adaptive behavioural responses. As a major interface between the gastrointestinal tract and systemic circulation, the liver is ideally positioned to monitor immune challenges originating from the gut. However, the identity and function of liver-innervating sensory neurons that convey inflammatory signals to the brain remain poorly understood.Using tissue clearing and whole-organ imaging, we found that vagal sensory fibers densely innervate the hepatic portal vein, identifying this region as a major site of hepatic sensory surveillance. Projection-specific single-cell transcriptomic profiling revealed that liver-innervating vagal sensory neurons are enriched for prostaglandin receptors, suggesting a specialized role in detecting inflammatory signals. Consistent with this, hepatic inflammatory challenge activated liver-innervating vagal sensory neurons and engaged downstream brain regions involved in interoception and behavioural regulation, including the nucleus of the solitary tract (NTS), paraventricular hypothalamic nucleus (PVN), and parabrachial nucleus (PBN).Activation of this liver-vagus-brain pathway was associated with characteristic sickness

behaviors, including suppression of food intake and reduced locomotor activity. Importantly, genetic deletion of prostaglandin receptors in liver-innervating vagal sensory neurons markedly attenuated inflammation-induced circuit activation and feeding suppression. These findings identify a molecularly defined hepatic neuroimmune circuit that relays inflammatory signals to the brain through prostaglandin-sensitive vagal afferents, thereby coordinating adaptive behavioural responses during inflammation.
**Key words**: Liver-brain vagal axis; vagal sensory neurons; prostaglandin receptors; inflammation sensing; feeding regulation

**Disclosures: N. Zhang:** None.

**Poster**

**PSTR182: Neural Basis of Human Speech: Perception and Production**

**Location:** WCC Halls A-C

**Time:** Monday, November 16, 2026, 1:00 PM - 5:00 PM

**Program #/Poster #:** PSTR182.01/Y25

**Topic:** E.05. Auditory and Vestibular Systems

**Support:** NIH Grant 1R01DC018579

**Title:** Voluntary attention modulates auditory cortex encoding of speech and music in adolescent patients

**Authors: R. AGRAVAT**[1], S. GEORGES[3], J. LEISAWITZ[3], E. KITTLE[4], M. IQBAL[2], K. AUGUSTE[6], A. ANDERSON[3], H. L. WEINER[7], *L. S. HAMILTON[5];
[1]Neurosci., [2]The Univ. of Texas at Austin, Austin, TX; [3]Texas Children's Hosp., Houston, TX; [4]UC Berkeley, Emeryville, CA; [5]UC Berkeley, Berkeley, CA; [6]UCSF, SF, CA; [7]NYU Med. Ctr., New York, NY

**Abstract:** Speech and music are perceptually distinct, behaviorally relevant sounds that listeners often encounter simultaneously in natural environments. In these situations, the brain must selectively encode task-relevant acoustic information while suppressing competing sounds. To study this process, we recorded intracranial high-gamma activity (70-150 Hz) from six participants while they performed an auditory attention task. Participants watched movie clips containing simultaneous speech and music and detected targets in one stream while ignoring the other. We used a 2x2 factorial design that crossed attended stream (speech vs. music) with relative loudness (speech louder vs. music louder), allowing us to dissociate task-driven from loudness-driven influences on neural encoding. We computed spectrotemporal receptive field encoding models, and target-locked event-related potentials across four conditions. Button press responses were used to assess behavioral sensitivity via d-prime across conditions. Congruent conditions, where attentional instruction and stream loudness aligned, produced stronger STG encoding of the attended stream and higher behavioral sensitivity than incongruent conditions, where participants attended the softer stream. The incongruent conditions served as a critical test of voluntary attentional control, pitting task-demands directly against stimulus-driven factors.

These results suggest that auditory cortex flexibly prioritizes task-relevant streams, with measurable neural and behavioral costs when top-down attention and acoustic loudness conflict.

**Disclosures: R. Agravat:** None. **S. Georges:** None. **J. Leisawitz:** None. **E. Kittle:** None. **M. iqbal:** None. **K. Auguste:** None. **A. anderson:** None. **H.L. Weiner:** None. **L.S. Hamilton:** None.

**Poster**

**PSTR182: Neural Basis of Human Speech: Perception and Production**

**Location:** WCC Halls A-C

**Time:** Monday, November 16, 2026, 1:00 PM - 5:00 PM

**Program #/Poster #:** PSTR182.02/Y26

**Topic:** E.05. Auditory and Vestibular Systems

**Support:** National Institutes of Health - The National Institute on Deafness and Other Communication Disorders (NIH-NIDCD)
Marie-Josée and Henry R. Kravis Foundation

**Title:** Spatial patterns of human auditory cortical activity reflect speaker characteristics during selective attention

**Authors: *S. DINDAR**[1], X. JIANG[1], A. FIROOZI[1], V. CHOUDHARI[1], S. BICKEL[2], A. D. MEHTA[2], C. SCHEVON[3], G. M. MCKHANN, II[3], D. FRIEDMAN[4], A. FLINKER[4], N. MESGARANI[1];
[1]Electrical Engin., Columbia Univ., New York, NY; [2]Feinstein Inst., Manhasset, NY; [3]Columbia Univ. Irving Med. Ctr., New York, NY; [4]Neurol., New York Univ., New York, NY

**Abstract:** The human auditory cortex selectively represents an attended speaker in a crowded acoustic scene, yet most accounts of this process emphasize the temporal tracking of the speech envelope. Far less is known about whether more stable, time-invariant characteristics of a speaker's voice are reflected in the spatial organization of cortical activity, and how attention shapes these representations. To address this, we recorded intracranial EEG (iEEG) from six human neurosurgical patients implanted with subdural and depth electrodes. Participants listened to natural speech from eight distinct speakers, balanced for gender, while attending to a designated speaker. We then examined how neural responses across electrodes varied across speakers, and how these patterns related to the attended speaker. A subset of sites responded differentially across speakers, with the spatial patterns of activity reflecting aspects of both speaker gender and the characteristics of individual speakers. These speaker-preferential responses were distributed across the auditory cortex, and comparable patterns could be observed when more than one speaker was present. We further found that these spatial patterns were sensitive to which speaker the listener attended. Together, these findings suggest that voice characteristics that distinguish speakers are reflected in distributed, relatively time-invariant spatial patterns of human auditory cortical activity, and that these patterns are shaped by

selective attention. This spatial, feature-based representation may complement envelope-based temporal tracking and offers a candidate neural basis for attention-aware auditory technologies.

**Disclosures: S. Dindar:** None. **X. Jiang:** None. **A. Firoozi:** None. **V. Choudhari:** None. **S. Bickel:** None. **A.D. Mehta:** None. **C. Schevon:** None. **G.M. McKhann:** None. **D. Friedman:** None. **A. Flinker:** None. **N. Mesgarani:** None.

**Poster**

**PSTR182: Neural Basis of Human Speech: Perception and Production**

**Location:** WCC Halls A-C

**Time:** Monday, November 16, 2026, 1:00 PM - 5:00 PM

**Program #/Poster #:** PSTR182.03/Y27

**Topic:** E.05. Auditory and Vestibular Systems

**Title:** Decoding phonetic cue weighting from electroencephalography responses to naturalistic speech

**Authors: *C.-Y. CHANG**[1], L. D. SANDERS[2];
[2]Psychological and Brain Sci., [1]Univ. of Massachusetts Amherst, Amherst, MA

**Abstract:** Background: Although multiple acoustic cues influence listeners' phonetic categorization, their relative impact is often unequal. The current behavioral methods of estimating cue weighting are subject to variabilities in post-perceptual processes. To overcome these limitations, we propose a novel method based on representational similarity analysis of electroencephalography (EEG) data to estimate phonetic cue weighting. Methods: Representational dissimilarity matrices (RDMs) were constructed by calculating the pairwise distances between EEG responses and acoustic cues for different phonetic categories. The RDMs based on EEG and acoustic cues were then submitted as response and explanatory variables to rank-rank regression, of which the coefficients are taken as relative cue weighting. The method was tested on English listeners' EEG responses to an audiobook (OpenNeuro Accession Number: ds004408). The second and third formants (F2 and F3) were measured at the onset of all /r/ and /l/ occurrences and subtracted from the first formant (F1) for normalization. Results: As the difference between /r/ and /l/ was greater in the normalized F3 than F2, we predicted that the former receives greater cue weighting. A Wilcoxon signed rank test supported this hypothesis ($p < .05$). Furthermore, several individual listeners showed similar trends of cue weighting over time. Discussion: To summarize, our preliminary results suggested that cue weighting estimated from EEG responses to continuous speech is qualitatively comparable to that from behavioral results. Crucially, EEG as an online measure with high temporal resolution is a promising tool to elucidate the time course of cue integration.

**Disclosures: C. Chang:** None. **L.D. Sanders:** None.

**Poster**

**PSTR182: Neural Basis of Human Speech: Perception and Production**

**Location:** WCC Halls A-C

**Time:** Monday, November 16, 2026, 1:00 PM - 5:00 PM

**Program #/Poster #:** PSTR182.04/Y28

**Topic:** E.05. Auditory and Vestibular Systems

**Support:** NIH R01DC020963

**Title:** Speech-Induced Sensory Modulation in Auditory Cortex During Syllable and Sentence Production Measured with 7 Tesla fMRI

**Authors: *V. HARISH**[1], M. COLAVITO[2], A. OCAMPO[2], J. W. BOHLAND[2];
[1]Bioengineering, [2]Communication Sci. and Disorders, Univ. of Pittsburgh, Pittsburgh, PA

**Abstract:** Speaking alters activity in auditory cortex through predictive sensorimotor mechanisms thought to support fluent speech production. Although speaking-induced suppression has been extensively studied using EEG and MEG, the functional anatomy of speech-induced sensory modulation (SISM) remains incompletely understood. Here, we used 7 Tesla fMRI to characterize cortical regions modulated during self-generated speech. To date, BOLD EPI data (1.5 mm isotropic, whole brain) from 11 neurotypical adults (7 women, 4 men) have been acquired for overt speech production and passive listening tasks involving isolated syllables (SYL; n=11) and simple sentences (SENT; n=9). Participants first completed a speech localizer task contrasting speech and signal-correlated noise to identify speech-sensitive auditory cortical regions. Functional MRI data were preprocessed using fMRIPrep and analyzed using first-level univariate general linear models. Subject-specific speech-sensitive functional regions of interest (fROIs) were identified using the localizer contrast (FDR < 0.05) and mapped to auditory cortical regions defined by the Julich Brain Atlas, including Heschl's gyrus (HG), planum temporale (PT), posterior superior temporal gyrus and sulcus (pSTG/pSTS). Speech-induced sensory modulation was examined using contrasts comparing active speech production and matched passive listening (TALK>LISTEN). BOLD activation was observed throughout bilateral superior temporal and sensorimotor regions during speech production. Within speech-sensitive superior temporal cortex, SISM varied substantially across anatomically and functionally defined ROIs. PT, pSTG, pSTS, HG and neighboring auditory regions demonstrated differing magnitudes and directions of modulation. Differences between the TALK and LISTEN conditions showed similar patterns for both syllable and sentence production, although SISM appeared more spatially restricted and less variable across participants for sentences. Overlap analyses revealed speech-sensitive auditory regions across participants, supporting the reliability of the localizer-based fROI approach. These findings indicate that speech-related modulation of auditory cortex is heterogeneous and cannot be fully characterized as uniform suppression. Distinct modulation profiles were observed across PT, pSTG, pSTS, and HG suggest functional heterogeneity within superior temporal cortex during speech production. Ultra-high-field precision fMRI provides a powerful framework for resolving this functional heterogeneity and refining neurobiological models of auditory-motor integration in speech.

**Disclosures: V. Harish:** None. **M. Colavito:** None. **A. Ocampo:** None. **J.W. Bohland:** None.

**Poster**

**PSTR182: Neural Basis of Human Speech: Perception and Production**

**Location:** WCC Halls A-C

**Time:** Monday, November 16, 2026, 1:00 PM - 5:00 PM

**Program #/Poster #:** PSTR182.05/Y29

**Topic:** E.05. Auditory and Vestibular Systems

**Support:** NIH grant R01-GM109086
NIH grant R01-DC04290
NIH grant T32-NS007421

**Title:** Human intracranial responses during conversational speech in delirium

**Authors: *E. R. DAPPEN**[1], A. J. BILLIG[2], J. I. BERGER[1], A. E. RHONE[1], B. M. KRAUSE[3], M. I. BANKS[3], H. KAWASAKI[1], K. V. NOURSKI[1];
[1]The Univ. of Iowa, Iowa City, IA; [2]UCL Ear Inst., Univ. Col. London, London, United Kingdom; [3]Anesthesiol., Univ. of Wisconsin, Madison, WI

**Abstract:** Delirium is an acute and fluctuating disorder of consciousness characterized by confusion, inattention, disorganized thinking, altered mental status, and impaired comprehension. Auditory processing has previously been examined in neuropsychiatric conditions (e.g. cognitive deficits) and disorders of consciousness (e.g. coma). Impairments in attention and speech perception and production in delirium interfere with effective spoken communication. We investigated changes in cortical activity associated with conversational speech during delirium. Participants were neurosurgical patients with medically refractory epilepsy undergoing intracranial electroencephalography (iEEG) monitoring. This patient population is at risk for developing delirium following surgery (post-operative) and seizure activity (post-ictal). We simultaneously collected audio recordings of clinically validated delirium assessments and iEEG data twice daily on post-operative days 1-3 and promptly following seizures. We examined cortical activity associated with interviewer's speech ("listening"), participant's verbal responses ("speaking"), and intervening silence ("thinking"). During listening, we analyzed delta-theta (1-8 Hz) and high gamma (70-150 Hz) cortical activity using a multivariate temporal response function approach (mTRF). We examined acoustic-temporal (speech envelope and word onset) and lexico-semantic (semantic neighborhood density, word frequency, body-object interaction, and emotional valence) language features. High gamma activity during thinking and speaking was analyzed as event-related band power (ERBP). We used linear mixed effects modeling for analysis of mTRF prediction accuracy and high gamma ERBP changes. Delirium was associated with reduced cortical representation of lexico-semantic, but not acoustic-temporal features, in the superior temporal and prefrontal cortex in the 1-8 Hz band. This reflects a disruption in processing of sounds beyond their basic acoustic attributes. LME analysis did not reveal an interaction between delirium, speech features, and brain region for mTRF prediction accuracy in the high gamma band. High gamma ERBP within auditory and auditory-related cortex during speaking was comparable in delirious and non-delirious participants. High gamma ERBP was reduced in delirium during the thinking phase within anterolateral Heschl's gyrus and the anterior middle temporal gyrus. The results suggest disrupted processing beyond primary

auditory cortex and indicate that symptoms characteristic of prefrontal cortex dysfunction may not fully describe deficits in delirium.

**Disclosures: E.R. Dappen:** None. **A.J. Billig:** None. **J.I. Berger:** None. **A.E. Rhone:** None. **B.M. Krause:** None. **M.I. Banks:** None. **H. Kawasaki:** None. **K.V. Nourski:** None.

**Poster**

**PSTR182: Neural Basis of Human Speech: Perception and Production**

**Location:** WCC Halls A-C

**Time:** Monday, November 16, 2026, 1:00 PM - 5:00 PM

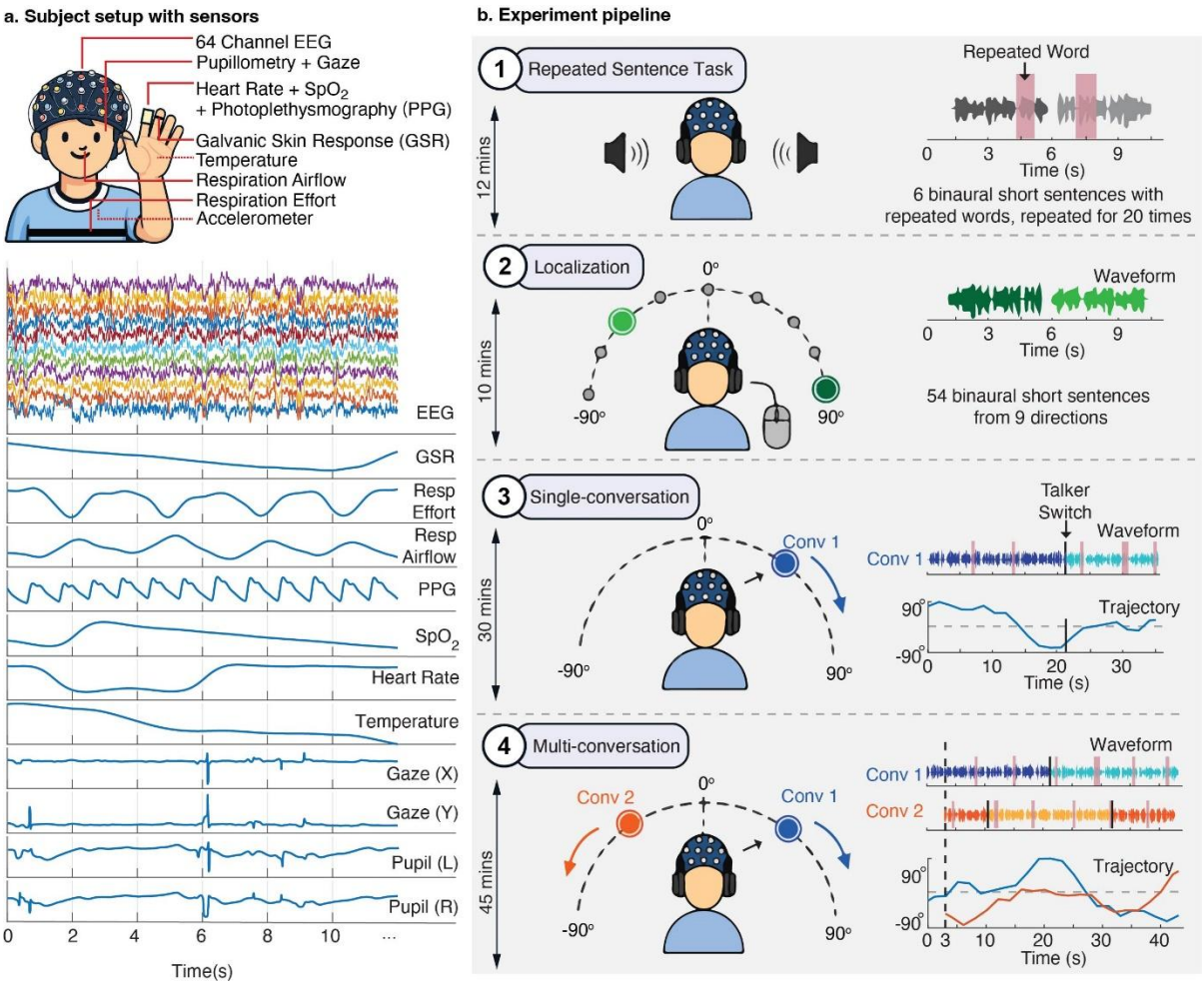
**Program #/Poster #:** PSTR182.06/Y30

**Topic:** E.05. Auditory and Vestibular Systems

**Title:** MOV-AAD: A Large-Scale Multimodal Dataset for Auditory Attention During Moving Conversations

**Authors: *X. HE**, N. MESGARANI;
Columbia Univ., New York, NY

**Abstract:** Auditory attention decoding (AAD) is often evaluated on static, simplified speech scenes, conditions that poorly match everyday listening. We introduce MOV-AAD, a large-scale dataset designed to study auditory attention under moving, naturalistic conversations. MOV-AAD combines 64-channel EEG with synchronized physiological recordings, including eye tracking, respiration, and galvanic skin response, enabling analysis of cross-modal neural, physiological markers of attention and listening effort. Crucially, the dataset uses a more ecologically valid listening paradigm featuring dynamically moving conversational speech sources and behavioral measures of attentional engagement. MOV-AAD supports research on robust AAD in realistic spatial dynamics, multimodal attention modeling, listening effort, and intersubject neural responses, and provides a resource for benchmarking selective auditory attention in naturalistic listening.




**Disclosures: X. He:** None. **N. Mesgarani:** None.

**Poster**

**PSTR182: Neural Basis of Human Speech: Perception and Production**

**Location:** WCC Halls A-C

**Time:** Monday, November 16, 2026, 1:00 PM - 5:00 PM

**Program #/Poster #:** PSTR182.07/Y31

**Topic:** E.05. Auditory and Vestibular Systems

**Support:** NIH Grant R01 DC005216
University of Minnesota College of Liberal Arts Social Science Research Grant

**Title:** Cortical representations of natural timbre across the human auditory cortex

**Authors: *Y. OU**[1], A. J. OXENHAM[2], K. N. KAY[3];
[2]Psychology, [1]Univ. of Minnesota, Minneapolis, MN; [3]Radiology, Univ. of Minnesota, Twin Cities, St Paul, MN

**Abstract:** Timbre is the perceptual attribute of sound that allows us to distinguish between different musical instruments and various speech sounds, such as vowels and speaker identities. The difficulty in developing a comprehensive understanding of timbre is reflected in its standard definition by negation—as the attribute distinguishing sounds with identical pitch, loudness, and duration. Here, we aimed to investigate timbre representations in human auditory cortex by using a wide range of naturalistic timbres. We used ultra-high-field 7-Tesla MRI to measure BOLD responses in twelve trained musicians (7 female, 5 male) to 120 naturalistic timbres, spanning Western, non-Western, and electric instruments, as well as human vocalizations. All timbres were presented using a common set of melodies in the same pitch register. Our findings show that the auditory cortex reliably encodes these diverse natural timbres, but with distinct representations across regions. Encoding and decoding analyses revealed a functional gradient in representations: primary auditory regions were best explained by spectral and spectrotemporal modulation energy; secondary regions were better explained by behavioral dissimilarity ratings and established acoustic correlates of timbre; and posterior subregions of the superior temporal gyrus demonstrated strong selectivity for human vocalizations. Together, these results indicate a progression from physical and perceptual to vocal representations of natural timbre, extending from primary to non-primary regions of the human auditory cortex.

**Disclosures: Y. Ou:** None. **A.J. Oxenham:** None. **K.N. Kay:** None.

**Poster**

**PSTR182: Neural Basis of Human Speech: Perception and Production**

**Location:** WCC Halls A-C

**Time:** Monday, November 16, 2026, 1:00 PM - 5:00 PM

**Program #/Poster #:** PSTR182.08/Y32

**Topic:** E.05. Auditory and Vestibular Systems

**Support:** NIH Grant R01-DC019394
NIH Grant T32-DC00046

**Title:** Acoustic and linguistic auditory temporal response functions encode attentional modulation during continuous active speech listening

**Authors: *K. D. LERUD**, C. FISHER, V. COMMURI, S. ANDERSON, J. Z. SIMON;
Univ. of Maryland, College Park, MD

**Abstract:** How humans accomplish the difficult task of listening successfully to a given sound in the background of many other sounds is a complex and ongoing area of research, particularly in the realm of speech and language processing, where it is known as the cocktail party problem. Here we set up a continuous and concurrent temporal response function (TRF) paradigm with both electroencephalography (EEG) and magnetoencephalography (MEG) to record and analyze

the brain's responses to continuous speech during the task of selectively attending to one out of two speakers and answering questions about the attended text.
Using TRF regressors created from a variety of acoustic and linguistic features of the ongoing speech stimuli including envelope, acoustic onset, phoneme onset, word surprisal, and cohort entropy, we analyze participants' brain responses to both the attended and unattended speaker voices at multiple signal-to-noise ratios (SNRs). As our stimuli and SNRs span a wide range of difficulty, we capture a large amount of variance in acoustic and linguistic brain responses. In addition to our novel experimental setup, we utilize state-of-the-art forward, head, and inverse modeling to obtain temporal and spatial source accuracy from the M/EEG sensor space, including individual structural MRI and tissue constraints and precise vector-valued current source solutions.
Cortical TRFs show robust effects of attentional modulation at multiple levels of an acoustic and linguistic hierarchy, with responses encoding attended speakers. Participants' TRFs also show that our tasks spanned a range of difficulty levels, with most trials existing in the "achievable with modest effort" space. Auditory TRFs in our paradigm have neural current sources ranging from midbrain and thalamus to auditory and association cortex depending on the regressors used, but effects of attentional modulation are not seen subcortically. Robust responses and attentional modulation are evident at timescales including the P50, N100, P200, and N400, all of which have important contributions from both EEG and MEG.
In addition to the TRFs themselves, we utilize sophisticated source modeling to relate the sensor space EEG and MEG to precise neural current source location and orientation. The overall picture suggests that we have made important advances in understanding the neural mechanisms underlying speech in noise processing, as well as auditory temporal processing and neural current source analysis of noninvasive human neuroimaging.

**Disclosures: K.D. Lerud:** None. **C. Fisher:** None. **V. Commuri:** None. **S. Anderson:** None. **J.Z. Simon:** None.

**Poster**

**PSTR182: Neural Basis of Human Speech: Perception and Production**

**Location:** WCC Halls A-C

**Time:** Monday, November 16, 2026, 1:00 PM - 5:00 PM

**Program #/Poster #:** PSTR182.09/Z1

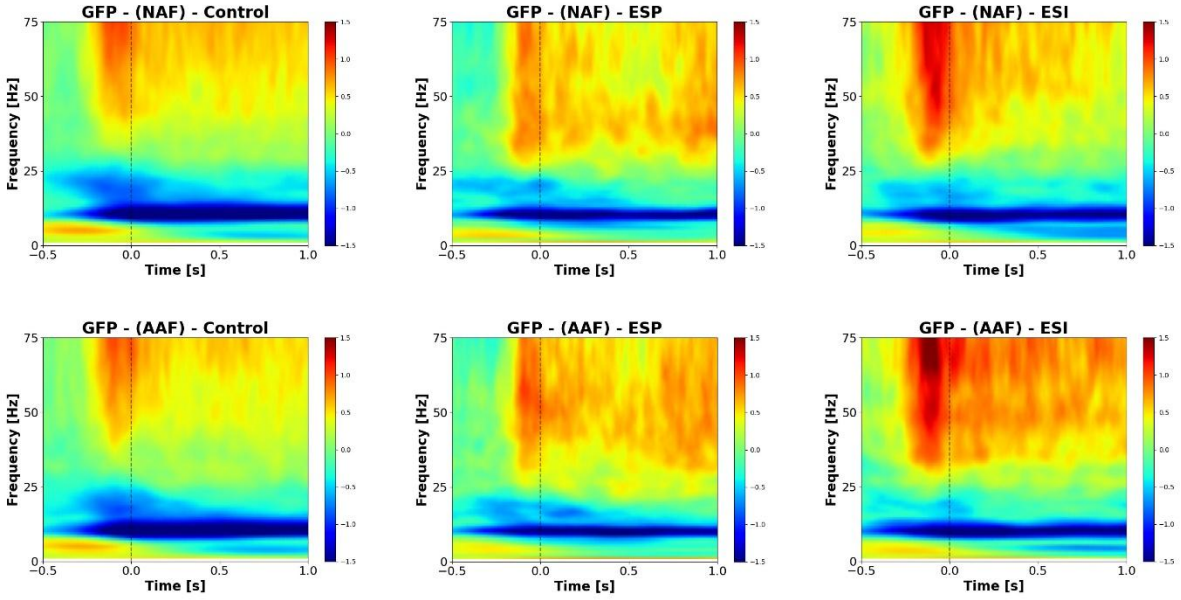
**Topic:** E.05. Auditory and Vestibular Systems

**Support:** NIH Grant 5R01DC018523-06

**Title:** Neurophysiological and Behavioural Mechanisms of Speech Motor Control Across Post-Stroke Aphasia Subtypes

**Authors: *J. SOLORZANO-RESTREPO**[1], K. RAY[1], Y. ZHANG[1], V. NEJATI[1], A. DALIRI[2], R. BEHROOZMAND[1];
[1]Speech, Language, and Hearing, The Univ. of Texas at Dallas, Richardson, TX; [2]Speech and Hearing Sci., Arizona State Univ., Tempe, AZ

**Abstract:** Fluent speech relies on motor commands with real-time sensory feedback integration. While individuals with post-stroke aphasia exhibit impaired speech compensation during Altered Auditory Feedback (AAF), the neurological mechanisms across different aphasia subtypes remain unclear. This study examined behavioral and neurological sensorimotor integration mechanisms across aphasia subgroups. 34 healthy controls and 31 individuals with chronic left-hemisphere post-stroke aphasia were recruited. Participants repeated a monosyllable ("HEAD") under non-altered (NAF) and AAF (+30% F1 shift) conditions. Speech compensation was tracked via F1 and F2 acoustic trajectories. Concurrent electroencephalography (EEG) captured Global Field Power (GFP) across theta, alpha, low-beta, high-beta, and gamma bands during pre-, early-, and late-speech epochs. Principal Component Analysis of Western Aphasia Battery-Revised metrics stratified the aphasia group into Expressive Speech-Impaired (ESI; n=16) and Expressive Speech-Preserved (ESP; n=15) subgroups. The ESP group showed a marginal trend toward an F2 deviation. Significant GFP desynchronization occurred in theta, alpha, and low-beta bands, with concurrent increments in high-beta and gamma ranges. The ESI group showed significantly increased GFP during early and late speech, alongside reduced late-speech high-beta activation. Group ESP displayed an anomalous late-speech theta power spike. Furthermore, F2 significantly predicted theta, low-beta, and high-beta activity. Categorizing aphasia by expressive deficit severity effectively isolates variations in auditory-motor integration. ESI EEG activity suggests disrupted motor planning and feedforward control. Conversely, ESP results indicate maladaptive error-monitoring systems, with disrupted auditory feedback loops preventing sensory feedback integration into articulatory corrections despite preserved basic motor execution. Future research should evaluate how these neurological patterns correlate with specific lesion profiles.




**Disclosures: J. Solorzano-Restrepo:** A. Employment/Salary (full or part-time):; The University of Texas at Dallas. B. Contracted Research/Research Grant (principal investigator for a drug study, collaborator or consultant and pending and current grants). If you are a PI for a drug study, report that research relationship even if those funds come to an institution.; NIH Grant 5R01DC018523-06. **K. Ray:** A. Employment/Salary (full or part-time):; The University of Texas at Dallas. B. Contracted Research/Research Grant (principal investigator for a drug study,

collaborator or consultant and pending and current grants). If you are a PI for a drug study, report that research relationship even if those funds come to an institution.; NIH Grant 5R01DC018523-06. **Y. Zhang:** A. Employment/Salary (full or part-time):; The University of Texas at Dallas. B. Contracted Research/Research Grant (principal investigator for a drug study, collaborator or consultant and pending and current grants). If you are a PI for a drug study, report that research relationship even if those funds come to an institution.; NIH Grant 5R01DC018523-06. **V. Nejati:** A. Employment/Salary (full or part-time):; The University of Texas at Dallas. B. Contracted Research/Research Grant (principal investigator for a drug study, collaborator or consultant and pending and current grants). If you are a PI for a drug study, report that research relationship even if those funds come to an institution.; NIH Grant 5R01DC018523-06. **A. Daliri:** A. Employment/Salary (full or part-time):; Arizona State University. **R. Behroozmand:** A. Employment/Salary (full or part-time):; The University of Texas at Dallas. B. Contracted Research/Research Grant (principal investigator for a drug study, collaborator or consultant and pending and current grants). If you are a PI for a drug study, report that research relationship even if those funds come to an institution.; NIH Grant 5R01DC018523-06.

**Poster**

**PSTR182: Neural Basis of Human Speech: Perception and Production**

**Location:** WCC Halls A-C

**Time:** Monday, November 16, 2026, 1:00 PM - 5:00 PM

**Program #/Poster #:** PSTR182.10/Z2

**Topic:** E.05. Auditory and Vestibular Systems

**Support:** NIH Grant R01 DC021140

**Title:** Can oscillatory entrainment explain cortical tracking of arrhythmic speech?

**Authors: *A. DURAN**, A. R. NIDIFFER, E. C. LALOR;
Univ. of Rochester, Rochester, NY

**Abstract:** When listening to speech, brain responses track the temporal structure of that speech. While this phenomenon is often attributed to the entrainment of ongoing neural oscillations, transient evoked responses to speech features offer a simpler explanation. Here, we directly test the extent to which oscillatory entrainment contributes to cortical tracking of natural speech. We manipulated the temporal regularity of syllables in audiobook recordings while preserving overall speech rate. In a ‘regular’ condition, syllables were rendered isochronous; in an ‘irregular’ condition, syllable intervals were drawn from uniform distributions to minimize temporal predictability. Unaltered speech served as a control condition. Both manipulated conditions remained intelligible and elicited robust cortical tracking responses in EEG. We evaluated whether oscillatory entrainment models could account for the observed neural responses. Critically, we also estimated the total explainable variance in the EEG data, providing an upper bound on the contribution entrainment mechanisms can make beyond established temporal response function (TRF) accounts. This approach offers a direct test of whether

oscillatory entrainment provides explanatory power beyond transient evoked responses in cortical speech tracking.

**Disclosures: A. Duran:** None. **A.R. Nidiffer:** None. **E.C. Lalor:** None.

**Poster**

**PSTR182: Neural Basis of Human Speech: Perception and Production**

**Location:** WCC Halls A-C

**Time:** Monday, November 16, 2026, 1:00 PM - 5:00 PM

**Program #/Poster #:** PSTR182.11/Z3

**Topic:** E.05. Auditory and Vestibular Systems

**Title:** Transcranial Direct Current Stimulation Enhances the Medial Olivocochlear Reflex and Improves Speech-in-Noise Perception

**Authors: *H. KURASHIGE**[1], S. OTSUKA[2,3,4], S. NAKAGAWA[2,3,4,5];
[1]Dept. of Med. Engineering, Grad. Sch. of Sci. and Engin., Chiba Univ., Chiba, Japan; [2]Ctr. Front Med. Eng, Chiba, Japan; [3]Grad Sch. Eng, Chiba, Japan; [4]Dept Med. Eng, Fac Eng, Chiba, Japan; [5]Ctr. Med-Tech Link, Chiba Univ. Hosp, Chiba, Japan

**Abstract:** The olivocochlear bundle, an efferent pathway extending from the brainstem to the auditory periphery, suppresses peripheral auditory responses in response to acoustic stimulation. This inhibitory action, referred to as the medial olivocochlear reflex (MOCR), has been shown to facilitate signal detection in noise —a phenomenon known as the anti-masking effect. Consequently, exogenous reinforcement of the MOCR holds promising clinical applications in rehabilitation to alleviate speech-in-noise perception difficulties, a hallmark symptom of auditory processing disorder.Corticofugal efferent projections terminate at the olivocochlear bundle, providing a pathway for top-down modulation. Previous studies have reported that invasive stimulation of the auditory cortex can modulate activity in the auditory periphery. Based on this evidence, the present study investigated whether transcranial direct current stimulation (tDCS)—a noninvasive technique that transiently modulates cortical excitability—could similarly enhance the MOCR. By assessing the relationship between tDCS-induced MOCR changes and speech-in-noise performance, we evaluated the potential contribution of MOCR modulation to improvements in speech perception in noisy environments. A 4×1 HD-tDCS montage was employed to focalize current delivery to the auditory cortex within Heschl's gyrus. The central anode was positioned at T7, with four return electrodes placed at FC5, FP9, CP5, and TP9 according to the international 10-20 system. In eleven normal-hearing male adults (aged 21-27 years), a transient enhancement of the MOCR was observed following 10 minutes of 1.0-mA anodal tDCS, accompanied by an improvement in speech-in-noise performance. Importantly, inter-individual analysis revealed that the magnitude of tDCS-induced MOCR enhancement scaled with the degree of improvement in speech-in-noise performance, specifically, participants who exhibited larger changes in MOCR strength showed greater gains in speech perception in noise. In contrast, sham stimulation—where current was restricted to the ramp-up and ramp-down phases—elicited no significant changes in either MOCR or speech-in-noise

performance. These findings suggest that tDCS potentiates the MOCR-mediated anti-masking effect, thereby facilitating speech perception in noisy environments.

**Disclosures: H. Kurashige:** None. **S. Otsuka:** None. **S. Nakagawa:** None.

**Poster**

**PSTR182: Neural Basis of Human Speech: Perception and Production**

**Location:** WCC Halls A-C

**Time:** Monday, November 16, 2026, 1:00 PM - 5:00 PM

**Program #/Poster #:** PSTR182.12/Z4

**Topic:** E.05. Auditory and Vestibular Systems

**Support:** NIDCD-R00-DC018051
NIDCD-R01- DC020960
NIDCD-F32-DC022145

**Title:** Linear spectrotemporal tuning accounts for much of phonetic feature encoding in the human auditory cortex

**Authors: *K. G. PATEL**[1], G. LIAO[2], D. BOEBINGER[2], S. V. NORMAN-HAIGNERE[3]; [1]Computer Sci., [2]Biostatistics and Computat. Biol., [3]Biostatistics & Neurosci., Univ. of Rochester, Rochester, NY

**Abstract:** Speech perception is challenging because features such as phonemes are only partially correlated with acoustic structure, making them difficult to infer from the speech signal. Our understanding of speech encoding in human auditory cortex has been shaped by studies asking whether speech features, like phonemes or phonetic features, predict neural responses beyond an acoustic baseline. Baseline choice is thus critical: it determines which aspects of neural responses are attributed to simple acoustic tuning and which are interpreted as going beyond it. Here we tested how acoustic baseline choice affects estimates of phonetic-feature encoding using intracranial recordings from 25 neurosurgical patients across two research sites. Participants heard acoustically diverse spoken sentences from 32 talkers, with added background sounds, reverberation, and spectral filtering to decouple phonetic content from acoustics. We analyzed broadband gamma responses from sound-responsive electrodes spanning primary and non-primary auditory cortex using lagged linear encoding models. We predicted neural responses from phonetic features, waveform envelope temporal response functions (TRFs), or cochleagram-based spectrotemporal receptive fields (STRFs), and fit combined models to quantify unique variance explained by each feature set. Phonetic features explained substantial unique variance relative to the envelope TRF, with the largest effects in non-primary auditory regions including planum temporale and superior temporal gyrus. In contrast, we find that throughout auditory cortex, phonetic feature models explain only a small amount of unique variance beyond linear spectrotemporal tuning, whereas spectrotemporal tuning explains substantial unique variance beyond phonetic feature models. Nonetheless, the small amount of variance explained by phonetic features concentrated in speech-selective neural populations,

suggesting they may be encoded using speech-specific mechanisms. Together, these results indicate that much of the response variance predicted by phonetic features can be captured by relatively simple linear spectrotemporal computations, highlighting acoustic baseline models as a central factor in interpreting encoding-model results.

**Disclosures: K.G. Patel:** None. **G. Liao:** None. **D. Boebinger:** None. **S.V. Norman-Haignere:** None.

**Poster**

**PSTR182: Neural Basis of Human Speech: Perception and Production**

**Location:** WCC Halls A-C

**Time:** Monday, November 16, 2026, 1:00 PM - 5:00 PM

**Program #/Poster #:** PSTR182.13/Z5

**Topic:** E.05. Auditory and Vestibular Systems

**Support:** NRF of Korea Grant RS-2024-00461617

**Title:** Changes in neural speech tracking across adverse listening conditions in age-related hearing loss

**Authors: J. PARK**[1], J. PARK[2], *Y. LIM[1];
[1]Korea Inst. of Sci. and Technol., Seoul, Korea, Republic of; [2]Bell Therapeut., Seoul, Korea, Republic of

**Abstract:** Older adults with age-related hearing loss often experience persistent difficulties understanding speech in multi-talker environments, even when elevated hearing thresholds are compensated by hearing aids. Consistent with the view that age-related hearing loss involves both peripheral auditory decline and central auditory changes, recent studies have reported enhanced cortical tracking of the temporal envelope of speech in hearing-impaired listeners. However, it remains unclear how target-speech encoding changes as listening conditions become more challenging. To examine the effects of hearing loss on the neural mechanisms of selective attention under adverse listening conditions, we compared electroencephalogram (EEG) responses to speech envelopes in 16 older adults with normal hearing (NH) and 16 with hearing impairment (HI), aged 60-78 years. Participants listened to audiobooks under three conditions of increasing listening difficulty: one-talker, dichotic two-talker, and diotic two-talker, with stimuli presented at each participant's most comfortable loudness level. We estimated the neural tracking of the acoustic envelope using temporal response functions (TRFs) while simultaneously assessing comprehension of the attended audiobook. Although both groups showed stronger tracking of attended over unattended speech, we observed distinct patterns of changes in encoding accuracy with listening difficulty. Consistent with the increasing difficulty of the task, encoding accuracy declined progressively as listening difficulty increased in NH listeners; in contrast, HI listeners showed a marked reduction not only in the diotic condition, but also in the dichotic condition. These results suggest that age-related hearing loss listeners can

track the speech envelope, but their neural ability to utilize spatial cues for maintaining target-speech encoding under adverse listening conditions may be limited.

**Disclosures: J. Park:** None. **J. Park:** None. **Y. Lim:** None.

**Poster**

**PSTR183: Photoreceptors and Retinal Circuitry**

**Location:** WCC Halls A-C

**Time:** Monday, November 16, 2026, 1:00 PM - 5:00 PM

**Program #/Poster #:** PSTR183.01/Z6

**Topic:** E.06. Vision

**Support:** NIH Grant EY026070
NIH Grant EY031411
UW 2020 WARF Discovery Award
Pilot Grant from Wisconsin National Primate Research Center
McPherson Eye Institute's David and Nancy Walsh Professorship in Vision Research
BrightFocus Foundation
Alcon Research Institute
E. Matilda Ziegler Foundation for the Blind
Deparment of Neuroscience, UW-Madison
Department of Ophthalmology and Visual Sciences, UW-Madison

**Title:** Development of photoreceptor synapses in the primate retina

**Authors: *S. E. HYMAN**[1], P. VENKIT[1], Y. CHU[2], M. HOON[2], R. SINHA[1];
[1]Dept. of Neurosci., [2]Dept. of Ophthalmology and Visual Sci., Univ. of Wisconsin - Madison, Madison, WI

**Abstract:** Retinal photoreceptors, rods and cones, transduce light into electrical signals and transmit them to second-order horizontal (HC) and bipolar (BC) cells. This signal is then relayed to ganglion cells, output neurons whose axons form the optic nerve that project to higher visual centers. Photoreceptor signal transmission occurs at specialized synapses, containing structures called ribbons that act as 'conveyor belts' to promote continuous neurotransmitter release to multiple postsynaptic partners. To optimize this signaling, rod and cone terminals form stereotypic synaptic configurations where one ribbon is opposed to central invaginating BC dendrites and lateral HC processes. Previous studies have proposed that postnatal photoreceptor synapse maturation may be one of the key limiting factors for attaining adult-like perceptual sensitivity. However, an investigation of the synaptic ultrastructure and connectivity underlying postnatal photoreceptor synaptic maturation is lacking in primate retina. To address this question, we used serial block-face scanning electron microscopy to obtain nanometer resolution images of the outer retinal synapse between photoreceptor and second-order neurons in *Macaca nemestrina* across postnatal timepoints spanning day 3, 1.5 months, 2 months, and adult. 3D reconstructions

of neuronal processes were generated and analyzed for synaptic connectivity and organization. For the rod synapse, we found the number of ribbons per rod was stable, suggesting early establishment of the presynaptic signaling infrastructure. The average number of post-synaptic partners (BC+HC) varied across timepoints, driven by a changing number of rod BC connections as the number of HC contacts remained consistent across timepoints. Thus, the number of partners that individual rods contact (synaptic divergence) can vary across development. Analysis of synaptic convergence, i.e. number of rods connecting onto individual rod BCs, also varied across timepoints. At the cone synapse, the number of ribbons per cone remained consistent across timepoints. The number of invaginating BC contacts, however, varied across timepoints. We also observed some unusual BC-photoreceptor connections at early postnatal timepoints. These findings reveal the postnatal developmental trajectory of photoreceptor synapse formation in the primate retina during a time of rapid visual and perceptual development.

**Disclosures: S.E. Hyman:** None. **P. Venkit:** None. **Y. Chu:** None. **M. Hoon:** None. **R. Sinha:** None.

**Poster**

**PSTR183: Photoreceptors and Retinal Circuitry**

**Location:** WCC Halls A-C

**Time:** Monday, November 16, 2026, 1:00 PM - 5:00 PM

**Program #/Poster #:** PSTR183.02/Z7

**Topic:** E.06. Vision

**Support:** R01 EY010699
P30 EY01730

**Title:** Beyond the triad, novel contact patterns of retinal horizontal cells

**Authors: *L. JOHNSON**[1], W.-Q. YU[2], D. M. BERSON[3], J. M. RENNA[1];
[1]Biol., Univ. of Akron, Akron, OH; [2]Allen Inst., Seattle, WA; [3]Dept. of Neurosci., Brown Univ., Providence, RI

**Abstract:** Purpose: Retinal horizontal cells (HCs) modulate rod and cone output through a GABAergic, hemichannel-, and pH-mediated signaling. Though HC modulation of signaling at the photoreceptor triad has been studied intensively, other sites of potential HC influence are less well explored due to the cells' immense complexity and the limited scale of available datasets. Here, we exploit a dataset of mouse retina to describe synaptic outputs of HCs beyond their canonical contacts at rod spherules and cone pedicles. Methods: We made complete volume reconstructions of three HC somadendritic compartments (HCd) and three HC axons and axon terminals (HCa) in an unpublished volume of adult mouse retina (>200x200 um). We mapped output synapses where vesicles in the HCs clustered at the cell membrane and a postsynaptic density was seen in the contacted cell. Results: We observed apparent non-canonical HC synaptic contacts with a variety of outer retinal neurons. HC axon terminals formed these

contacts at the highest rate with their primary non-rod photoreceptor target being bipolar cells (avg. 91.5 contacts per HCa) followed by neighboring HC axons and terminals (avg. 9.5 contacts per HCa and cone pedicles (avg. 3 contacts per HCa). All bipolar cell types were postynaptic to HC axon terminals along with evidence of synaptic machinery. These presumed synapses were distributed across the HC axon terminals with peaks near the cone pedicles bases and 10µm below in the outer plexiform layer. HC dendritic arbors formed fewer of these non-canonical contacts, but engaged in sparse, invaginating contact with rod photoreceptors (avg. 1 contact per HCd). HCs were also found postsynaptic in apposition to dendritic ribbons formed by bipolar cells (avg. 8.5 and 5.5 horizontal cell contacts per HCa and HCd compartment, respectively), with type 2 OFF bipolar cells serving as the primary presynaptic partner. Conclusions: These data resolve a long-standing need for a complete reconstruction of both HCa and HCd compartments, comprehensively mapping cell connectivity and identifying potentially novel contact patterns with synaptic partners. Our findings prompt a need for further investigation of the canonical role of HCs and lend support for a model in which HCs participate in a more diverse array of retinal circuits than currently appreciated. Their broad connectivity patterns with bipolar cells, combined with contacts from bipolar cell dendritic ribbon synapses, suggest HCs possess the anatomical capacity to influence rod- and cone-driven signals beyond the level of the photoreceptor triad and may contribute to lateral signaling and modulation of center-surround and gain control mechanisms.

**Disclosures: L. Johnson:** None. **W. Yu:** None. **D.M. Berson:** None. **J.M. Renna:** None.

**Poster**

**PSTR183: Photoreceptors and Retinal Circuitry**

**Location:** WCC Halls A-C

**Time:** Monday, November 16, 2026, 1:00 PM - 5:00 PM

**Program #/Poster #:** PSTR183.03/Z8

**Topic:** E.06. Vision

**Title:** Connectomic mapping of type 2 OFF bipolar cell circuitry in the mouse retina

**Authors: *R. J. RAMIREZ**, N. S. MALLIKARJUN, L. M. JOHNSON, J. M. RENNA; Univ. of Akron, Akron, OH

**Abstract: Purpose**: Bipolar cells transmit visual signals from photoreceptors in the outer retina to amacrine and ganglion cells in the inner retina. The mouse retina contains 15 bipolar cell types, each with distinct axonal arborization and stratification within the inner plexiform layer. Type 2 OFF cone bipolar cells receive glutamatergic input from cone photoreceptors and prominent glycinergic input from AII amacrine cells, positioning them as a major route for rod-driven signals into the OFF cone bipolar pathway. They also provide ribbon-mediated output to OFF retinal ganglion-cell dendrites, as well as, AII amacrine cell processes, while participating in an electrically coupled OFF bipolar-cell network. However, the chemical synaptic architecture of Type 2 OFF cone bipolar cells has not been comprehensively resolved. Here, we map the distribution of Type 2 bipolar-cell axonal ribbons and identify the morphologically defined

postsynaptic elements apposed to these release sites. **Methods**: Cell reconstruction was performed using the unpublished *Yu volume,* a serial block-face electron microscopy dataset taken from the ventral retina of an adult, wildtype mouse. Cells were reconstructed using the neuron tracing software, WebKnossos. All cells were characterized based on their morphology and axonal or dendritic stratification patterns in the inner plexiform layer with respect to the ON and OFF ChAT bands formed by starburst amacrine cells. **Results**: As expected, preliminary examination of type 2 OFF bipolar cell connectivity revealed frequent contacts with cells involved in the OFF pathway, such as OFF alpha-retinal ganglion cells. In addition, we observed contacts with direction-selective ganglion cells and a population of amacrine cells. Analysis of synaptic configuration revealed a high frequency of dyadic contacts in the axon terminals, implicating type 2 bipolar cells in dissemination of complex signals in the inner plexiform layer. **Conclusions:** Our findings thus far corroborate synaptic motifs previously elucidated through physiological and immunohistochemical studies. By generating a complete map of type 2 OFF bipolar cell connectivity, this study provides an anatomical reference for future exploration of OFF signaling in the mouse retina.

**Disclosures: R.J. Ramirez:** None. **N.S. Mallikarjun:** None. **L.M. Johnson:** None. **J.M. Renna:** None.

**Poster**

**PSTR183: Photoreceptors and Retinal Circuitry**

**Location:** WCC Halls A-C

**Time:** Monday, November 16, 2026, 1:00 PM - 5:00 PM

**Program #/Poster #:** PSTR183.04/Z9

**Topic:** E.06. Vision

**Support:** NIH Grant EY031333

**Title:** Conserved cooperative population modes in the mouse retina depend on intact ON-bipolar drive

**Authors: *D. BABINO**[1], J. JIN[2], S. CHEN[3], M. SHAIK[1];
[2]Neurosci. and Ophthalmology, [1]SUNY Upstate Med. Univ., Syracuse, NY; [3]Upstate Med. Univ., SYRACUSE, NY

**Abstract:** How does the retina's output organize into a population code, and what circuit builds it? Retinal coding has been studied along two parallel tracks: collective-coding work that describes ganglion-cell populations as recurring latent states, and cell-type taxonomies that catalog dozens of functional ganglion-cell types. Neither asks which cell types occupy which population states, or where that organization comes from. We bridge both. Applying hidden Markov models with Chow-Liu tree emissions to multielectrode recordings from seven wild-type mouse retinas under contrast-modulated stimuli, we find that population activity resolves into a conserved vocabulary of 9 to 12 latent modes, organized into three cell-type-defined archetypes (ON-dominant, biphasic, OFF-dominant) at reproducible stimulus phases. This vocabulary is a

hardwired feature, not a per-animal artifact: cross-animal fingerprints reach up to ~86% of the within-animal noise ceiling at the subtype level, and the mode label alone decodes single-trial stimulus phase at ~5x chance. Within it, biphasic-cell recruitment follows steep cooperative gating (Hill n~5) that ON and OFF cells lack, a quantitative signature of feature detection. Where is this cooperative code built? Two independent perturbations of the photoreceptor-to-bipolar pathway answer convergently. Acute, reversible mGluR6 blockade with L-(+)-2-amino-4-phosphonobutyric acid (L-AP4; n=4 retinas) does more than silence ON-driven firing: it disorganizes the population dynamics as a system, degrading phase-locking (per-state R ~0.83 to ~0.34) and transition determinism and erasing their normal sharpening with contrast, while eliminating biphasic and ON modes, comparatively sparing OFF, and fully recovering on washout. Chronic rd1 photoreceptor degeneration independently abolishes it (phase-locking R ~0.1 vs ~0.8 in wild-type). Pharmacology and genetics converge: a conserved, cell-type-resolved, decodable population code whose cooperative substrate requires ON-bipolar drive upstream of the ganglion cell. The collective-coding and cell-type views describe one circuit, gated at its first synapse.

**Disclosures: D. Babino:** None. **J. Jin:** None. **S. Chen:** None. **M. Shaik:** None.

**Poster**

**PSTR183: Photoreceptors and Retinal Circuitry**

**Location:** WCC Halls A-C

**Time:** Monday, November 16, 2026, 1:00 PM - 5:00 PM

**Program #/Poster #:** PSTR183.05/Z10

**Topic:** E.06. Vision

**Title:** Morphology-Dependent Voltage Responses of Reconstructed Bipolar Cells During Simulated Subretinal Stimulation

**Authors: *Y. HUANG**[1], E. JOYCE[2];
[1]Dept. of Psychological & Brain Sciences, Dept. of Statistics and Applied Probability, Univ. of California, Santa Barbara, Santa Barbara, CA; [2]UC Santa Barbara, Santa Barbara, CA

**Abstract:** Subretinal prostheses aim to restore vision in individuals with photoreceptor degenerative disease by electrically stimulating downstream retinal neurons, including bipolar cells. Because direct measurements of human bipolar cell responses to prosthetic stimulation are limited, computational modeling provides a useful approach for examining how cell morphology and spatial position may shape retinal activation. Here, we present a pipeline for simulating passive voltage responses of reconstructed human bipolar cell morphologies exposed to electric fields from a modeled subretinal prosthesis. We placed two bipolar cell reconstructions at multiple locations relative to the electric field and computed passive transmembrane voltage responses in NEURON, focusing on the axon terminal region as a readout of stimulation sensitivity. Across placements, terminal voltage varied systematically with the spatial relationship between the cell and the stimulating electrode. The simpler morphology showed larger terminal voltage responses than the more complex morphology, and terminal responses

generally decreased as the cells' dendrites were positioned farther from the electrode center. These results suggest that prosthesis-evoked bipolar cell responses depend on both cell-to-electrode position and cellular morphology. This approach provides a preliminary biophysical modeling framework for studying how subretinal stimulation may affect individual retinal neurons.

**Disclosures: Y. Huang:** None. **E. Joyce:** None.

**Poster**

**PSTR183: Photoreceptors and Retinal Circuitry**

**Location:** WCC Halls A-C

**Time:** Monday, November 16, 2026, 1:00 PM - 5:00 PM

**Program #/Poster #:** PSTR183.06/Z11

**Topic:** E.06. Vision

**Support:** NIH Grant R00EY031333

**Title:** Selective ON-Bipolar Blockade Reversibly and Dose-Dependently Dismantles Cooperative Population Modes in the Mouse Retina

**Authors: *J. JIN**[1], S. CHEN[2], M. SHAIK[1], D. BABINO[1];
[1]SUNY Upstate Med. Univ., Syracuse, NY; [2]Upstate Med. Univ., SYRACUSE, NY

**Abstract:** Retinal ganglion cells (RGCs) do not encode the visual scene as independent units; their population activity is organized into a low-dimensional repertoire of recurring, coordinated states, or "modes," that together form a collective neural code. In the healthy retina, this repertoire is stable and phase-locked to the visual stimulus, yet the synaptic origin of that organization, and whether it can be abolished and then restored, remain unresolved.
Using Hidden Markov Models with Chow-Liu tree emissions on multielectrode array recordings, we dissected RGC population modes before, during, and after selective pharmacological blockade of the photoreceptor-to-ON-bipolar synapse, the first synapse of the visual pathway. L-(+)-2-amino-4-phosphonobutyric acid (L-AP4), a selective mGluR6 agonist, was applied in paired baseline-AP4-washout recordings across four retinas, spanning sub-saturating (2.5 uM) and saturating (20 uM) doses and including a within-animal dose-response. Across the cohort, L-AP4 produced a coordinated, multi-axis collapse of the mode structure; Cell-type recruitment: biphasic-cell activity at its preferred phase fell to a few percent of baseline; Phase-locking: the per-state resultant R fell from 0.83 +/- 0.04 to 0.34 +/- 0.12; Transition determinism: the Markov branching factor rose from about 2.3 to 5.9 effective successors and lost its normal sharpening with contrast; Biphasic-dominant and ON modes were eliminated while OFF modes were comparatively spared. The collapse was near-maximal already at sub-saturating doses, and a within-animal 2.5-versus-20 uM comparison showed little further effect at 20 uM, indicating saturation at low mGluR6 occupancy. Structure recovered after washout, though variably across retinas, establishing an acute, largely reversible, ON-bipolar-specific requirement. Selective removal of ON-bipolar drive thus does not merely silence biphasic firing; it dismantles the

population mode structure as an integrated system, localizing the cooperative substrate to ON-bipolar pathway drive upstream of the ganglion cell.

**Disclosures: J. Jin:** None. **S. Chen:** None. **M. Shaik:** None. **D. Babino:** None.

**Poster**

**PSTR183: Photoreceptors and Retinal Circuitry**

**Location:** WCC Halls A-C

**Time:** Monday, November 16, 2026, 1:00 PM - 5:00 PM

**Program #/Poster #:** PSTR183.07/Z12

**Topic:** E.06. Vision

**Support:** R01EY01730
R01EY010699

**Title:** A conserved dendritic ribbon architecture in the mammalian outer retina

**Authors: *J. M. RENNA**[1], L. M. JOHNSON[1], K. SAKUTA[2], W. N. GRIMES[4], S. FLYNN[1], J. M. BALL[5], W. LI[7], C. KOIKE[3], J. S. DIAMOND[6], F. M. RIEKE[8], S. H. DEVRIES[9], D. M. BERSON[10];
[1]Univ. of Akron, Akron, OH; [2]Ritsumeikan Univ., Shiga, Japan; [3]Ritsumeikan Univ., Kusatsu, Japan; [4]NINDS/NIH, Bethesda, MD; [5]Natl. Eye Inst., [6]Natl. Inst. of Neurolog. Disorders and Stroke, NIH, Bethesda, MD; [7]Shanghai Jiao Tong Univ. Sch. of Medicine, SANS Inst. for Neurosci. and Vision Res., Shanghai, China; [8]Univ. of Washington, Seattle, WA; [9]Ophthalmology, Northwestern Univ., Chicago, IL; [10]Dept. of Neurosci., Brown Univ., Providence, RI

**Abstract: Purpose:** Bipolar cell ribbon synapses are traditionally associated with glutamatergic axon terminal signaling to amacrine and ganglion cells in the inner retina. However, using serial block-face electron microscopy (SBEM), we have identified ribbon synaptic machinery in bipolar cell outer retinal dendrites in mouse, squirrel, macaque, and human retinal tissue. Here, we seek to examine what cell types form these ribbons, what cells are in apposition to dendritic ribbons, and the molecular profile of the synaptic machinery involved. **Methods:** Cell reconstruction and ribbon synapse identification were performed in WebKnossos neuron tracing software on unpublished SBFEM images of mouse (ventral retina), squirrel, and macaque (mid-periphery) retinal tissue and published human tissue (fovea). MIRAVA-STED super-resolution microscopy was used to examine glutamate receptor profiles and ribbon clustering patterns in the outer plexiform layer of the mouse retina. **Results:** Dendritic ribbon synapses were identified in types 1, 2, 5, 6, 8, and 9 bipolar cells in mice, and DB2, DB6, and GB cells in macaque. Type 2 OFF bipolar cells exhibit the largest number of dendritic ribbons and were in similar abundance in the DB2 cells. These ribbons most frequently contact horizontal cells and other bipolar cells, particularly rod and type 3a OFF bipolar cells. Preliminary data suggest outer retinal bipolar cell ribbons are present in the cone-dominant squirrel, albeit at lower rates. Dendritic ribbons formed by bipolar cells were also observed in the adult human retina. Immunohistochemical evaluation

of dendritic ribbons in the mouse demonstrates clustering in a distinct stratum ~1-2µm below the cone terminals where RIBEYE puncta often colocalize with GluA1, GluA2, and GluA4. **Conclusions:** Our findings suggest a previously unappreciated layer of lateral processing in the outer retina. Notably, rod bipolar cells and type 3a bipolar cells are known to receive rod input, and dendritic ribbon contacts with these cells suggests a potential role in refining or sustaining rod-driven responses in the rod pathway. Furthermore, frequent contacts with horizontal cells indicate a potential role in fine-tuning feedback to the photoreceptors. Dendritic ribbons may represent an evolutionarily conserved feature of scotopic vision, facilitating local, lateral modulation of photoreceptor input within the outer plexiform layer.

**Disclosures: J.M. Renna:** None. **L.M. Johnson:** None. **K. Sakuta:** None. **W.N. Grimes:** None. **S. Flynn:** None. **J.M. Ball:** None. **W. Li:** None. **C. Koike:** None. **J.S. Diamond:** None. **F.M. Rieke:** None. **S.H. DeVries:** None. **D.M. Berson:** None.

**Poster**

**PSTR183: Photoreceptors and Retinal Circuitry**

**Location:** WCC Halls A-C

**Time:** Monday, November 16, 2026, 1:00 PM - 5:00 PM

**Program #/Poster #:** PSTR183.08/Z13

**Topic:** E.06. Vision

**Support:** Prevent Blindness Ohio

**Title:** Retinal Circuitry of the Dopaminergic Amacrine Cell

**Authors: *K. R. FARLEY**[1], L. M. JOHNSON[2], D. M. BERSON[4], K. FRANKE[5], R. LU[6], C. DAVID[9], M. SOREK[10], A. STERLING[7], A. MATSLIAH[8], G. W. SCHWARTZ[11], P. BERENS[13], T. EULER[14], J. M. RENNA[3], J. FADJUKOV[12], Z. HUANG[15];
[1]Biol., The Univ. of Akron, Akron, OH; [2]Univ. of Akron, Copley, OH; [3]Biol., Univ. of Akron, Akron, OH; [4]Dept. of Neurosci., Brown Univ. Post-Doc Dept. of Neurosci., Providence, RI; [5]Bernstein Ctr. for Computat. Neurosci., Ctr. for Integrative Neurosci., Tübingen, Germany; [6]Princeton Univ., Princeton, NJ; [7]Princeton Univ., Somerville, MA; [8]Princeton Neurosci. Inst., Princeton Univ., Princeton, NJ; [9]Ithaca Col., Ithaca, NY; [10]Princeton Neurosci. Institute, Princeton Univ., Norwood, MA; [11]Ophthalmology, [12]Northwestern Univ., Chicago, IL; [13]Inst. for Ophthalmic Res., Univ. of Tübingen, Tübingen, Germany; [14]CIN - Univ. of Tuebingen, Tuebingen, Germany; [15]Dept. of Data Sci., Hertie Inst. for AI in Brain Hlth., Tübingen, Germany

**Abstract:** Purpose: Dopamine is a primary neuromodulator of retinal light adaptation, contributing to the transition between scotopic and photopic vision via its decoupling effects on gap junctions. Dopaminergic amacrine cells (DACs) are the sole source of dopamine in the retina and modulate cell activity via their expansive arbors stratifying in the OFF sublamina of the inner plexiform layer. While the connectivity of DACs has been subject to extensive study, the full extent of DAC circuitry is yet to be comprehensively mapped. Methods: A DAC was reconstructed in Neuroglancer using the Eyewire II volume, a serial block-face electron

microscopy dataset obtained from the ventral retina of a dark-adapted adult, wildtype mouse. We identified and annotated clusters of vesicles and synaptic ribbons with adjacent postsynaptic densities in apposition to the DAC membrane and characterized the presumed pre- or postsynaptic partners. Partners were reconstructed and classified based on morphology and stratification patterns. Results: We observed a total of 746 contacts to the DAC from 605 unique cell partners and 162 contacts from the DAC to 122 unique cell partners. Presumptive DAC outputs were primarily localized to the axonal process, whereas presumptive presynaptic inputs were distributed throughout the DAC dendritic arbor. The DAC predominantly contacted short-field amacrine cells, particularly H24 (AII) amacrine cells (74.84% of total presynaptic contacts), but also contacted H22 short-field amacrine cells, H49 medium-field amacrine cells, H53 wide-field amacrine cells, type 2 cone bipolar cells, and rod bipolar cells. The most common partners contacting the DAC were short-field amacrine cells including H18, H15, H20, H24, and H17 amacrine cells as well as H41 and H30 wide-field amacrine cells, H40 medium-field amacrine cells, and type 6 cone bipolar cells via en passant ribbons. Conclusions: DACs contact a varied group of cells in the inner retina where they are well suited for a role in global dopaminergic signaling to surrounding cells. Notably, frequent contacts between DACs and AIIs along the DAC axon reveal a preferential relationship between these cell types, reinforcing the well-established role of dopamine in modulation of AII-mediated rod pathway signaling. Mapping the precise locations of these contacts provides an anatomical foundation for understanding where dopaminergic modulation of cells involved in the rod pathway and light adaptation may occur. The diverse nature of DAC synaptic connectivity explored here may inform future studies targeting specific synaptic sites to investigate functional consequences.

**Disclosures: K.R. Farley:** None. **L.M. Johnson:** None. **D.M. Berson:** None. **K. Franke:** None. **R. Lu:** None. **C. David:** None. **M. Sorek:** None. **A. Sterling:** None. **A. Matsliah:** None. **G.W. Schwartz:** None. **P. Berens:** None. **T. Euler:** None. **J.M. Renna:** None. **J. Fadjukov:** None. **Z. Huang:** None.

**Poster**

**PSTR183: Photoreceptors and Retinal Circuitry**

**Location:** WCC Halls A-C

**Time:** Monday, November 16, 2026, 1:00 PM - 5:00 PM

**Program #/Poster #:** PSTR183.09/Z14

**Topic:** E.06. Vision

**Support:** AMED JP24ek0109726

**Title:** Receptive field center-surround integration switches RGCs from position coding to global expansion detection

**Authors: *H. ISHIKANE**[1], J. UMEMOTO[2], S. MURAKAMI[3];
[1]Senshu Univ., Kanagawa, Japan; [2]Senshu Univ., Kawasaki-shi, Japan; [3]Senshu Univ., Tama-ku, Kawasaki-shi, Kanagawa, Japan

**Abstract:** The visual system is thought to have evolved under strong selective pressure to detect salient events as early as possible. In particular, expanding visual stimuli, such as looming objects, are critical cues of approaching predators or imminent collisions. Although retinal ganglion cells (RGCs) integrate signals both within and beyond the classical receptive field (RF), how surround signals interact with RF-center pathways across different spatial scales remains unclear.
Here, using multielectrode array recordings from the frog retina, we examined dimming detectors, a class of RGCs implicated in visually guided escape behavior. Large dark expanding stimuli covering both the classical RF and the surround robustly enhanced firing, whereas narrow bar stimuli confined to the surround evoked little or no response. Population decoding revealed that bar-evoked responses accurately decoded stimulus position, whereas decoding performance decreased under the large expanding stimulus condition. Mutual information analysis further demonstrated a shift from position coding toward motion-velocity coding during large dark expanding stimulation.
To investigate the underlying mechanism, we modeled RF-center responses using a linear-nonlinear (LN) model consisting of a linear filter followed by a nonlinear spike-generation process. The results showed that dark expanding stimulation in the classical RF surround left the RF-center temporal filter largely unchanged, indicating preserved feature selectivity. In contrast, surround stimulation significantly enhanced the gain of the RF-center nonlinear process.
In conclusion, this study reveals that dimming detectors dynamically switch from local position encoding to global expansion detection depending on the spatial extent of stimulus. Such context-dependent gain modulation may provide a retinal mechanism for enhancing sensitivity to behaviorally relevant looming stimuli. These findings may also contribute to the development of artificial retinal prostheses by informing stimulation strategies that exploit context-dependent gain modulation in retinal circuits.

**Disclosures: H. Ishikane:** None. **J. Umemoto:** None. **S. Murakami:** None.

**Poster**

**PSTR183: Photoreceptors and Retinal Circuitry**

**Location:** WCC Halls A-C

**Time:** Monday, November 16, 2026, 1:00 PM - 5:00 PM

**Program #/Poster #:** PSTR183.10/Z15

**Topic:** E.06. Vision

**Title:** Global sight in “blind” mice: Topological perception originates in intrinsically photosensitive retinal ganglion cells (ipRGCs)

**Authors: *L. CHEN**[1], X. ZHAO[2];
[1]Univ. of Chinese Acad. of Sci. & Inst. of Biophysics, Chinese Acad. of Sci., Beijing, China;
[2]Inst. of Biophysics, Chinese Acad. of Sci., Beijing, China

**Abstract:** Mice that retain ipRGCs but lack rod and cone phototransduction—specifically MO (rd1/rd1; cl/cl) mice—are generally considered functionally blind, limited to non-image-forming

visual responses. However, the topological approach to perceptual organization suggests a counterintuitive hypothesis: that MO mice, despite their inability to perceive local featural properties, may still retain the capacity for topological perception, since global organization based on topology forms the foundation of visual cognition. To test this hypothesis, we assessed the capacity of MO mice and other transgenic lines to perceive topological differences using various behavioral paradigms, including fear conditioning and water maze tests, and employing diverse transgenic manipulations for precise molecular-level control. The stimuli, and the training and testing paradigms, were carefully designed to prevent MO mice from using nontopological cues commonly considered basic features in pattern discrimination tasks. We controlled for confounds across a broad spectrum of nontopological features—including luminance flux, orientation, spatial frequency components, perimeter length, average edge crossings, symmetry, parallelism, and collinearity—and generalized the topological account to the discriminability of stimuli with a variety of numbers of holes, ranging from one to four. Our results consistently demonstrated that MO mice can discriminate topological differences, but not non-topological form differences. Specifically, MO mice were able to learn to discriminate stimuli based on topological distinctions, abstracted the topological invariants, and transferred this learned discriminability to novel stimuli. These findings were further validated by enhanced control conditions using gene manipulation techniques. Notably, rescuing melanopsin expression specifically in the ipRGCs of TKO (rd1/rd1; cl/cl; OPN4^cre/+; OPN4^-/-) mice restored their ability for topological discrimination, despite the loss of functional rods and cones due to mutations in both rd1 and cl. In contrast, melanopsin-deficient OPN4 knockout (OPN4^-/-) mice, which retain intact rods and cones, were unable to consistently discriminate topological properties. Together, these findings strongly indicate that ipRGCs are both necessary and sufficient for consistent discrimination of topological differences. The discovery that “global-first” topological perception originates in a specific type of neuron raises a compelling issue for connectionism: while connections are important, so too is the inner structure of cells.

**Disclosures: L. Chen:** None. **X. Zhao:** None.

**Poster**

**PSTR183: Photoreceptors and Retinal Circuitry**

**Location:** WCC Halls A-C

**Time:** Monday, November 16, 2026, 1:00 PM - 5:00 PM

**Program #/Poster #:** PSTR183.11/Z16

**Topic:** E.06. Vision

**Support:** NIH grants EY023648 (to M.T.H.D.)
NIH grants EY025555 (to M.T.H.D.)
NIH grants EY032731 (to M.T.H.D.)
NIH grants EY030628 (to M.T.H.D.)
NIH grants EY034089 (to M.T.H.D.)
Warren Alpert Distinguished Scholar (to P.M.)
Lefler Fellow (to P.M.)
Tommy Fuss Fellow (to P.M.)

**Title:** Representation of environmental illumination within the principal circadian clock

**Authors: *P. MORQUETTE**, S. MANOS, F. CAVAL-HOLME, M. H. DO;
F.M. Kirby Neurobio. Ctr., Boston Children's Hosp. and Harvard Med. Sch., Boston, MA

**Abstract:** Light is the most powerful cue for aligning the mammalian circadian clock with local time. Its effects depend on intrinsically photosensitive retinal ganglion cells (ipRGCs), which provide virtually all direct retinal input to the suprachiasmatic nucleus (SCN), the brain's principal circadian clock. Because this sensory system evolved under natural light, we hypothesized that it is tuned to natural variations associated with the solar day. To test this hypothesis, we established a novel experimental framework. First, we built a simple two-wavelength system that enables us to mimic the photopigment stimulation patterns produced by daylight in the mouse retina. Second, we developed an acute ex vivo brain-slice preparation that contains most of the SCN while preserving intact connectivity with both retinas. We prepared these explants from mice in which ipRGC axons and presynaptic terminals expressed an optical activity reporter. We imaged this reporter with multiphoton microscopy while delivering visual stimuli to the retinas.
The retina-SCN explant is robust, with light responses persisting for at least 24 hours after preparation. Using naturalistic stimulation protocols spanning 10 orders of magnitude in intensity, we find that retinal input to the SCN is a complex, distributed representation of environmental illumination. IpRGC terminals are differentially tuned to light intensity, with distinct subsets activated across a broad environmental range. Most terminals are active only within a preferred intensity range and are silent at lower or higher intensities. Terminals also vary in response kinetics, with some showing activity that persists long after illumination. Terminals with different intensity tunings and temporal profiles are intermingled within the SCN. Finally, relatively dim, twilight-like intensities are overrepresented compared with dimmer or brighter, midday-like light intensities. This bias aligns with the circadian time window during which the clock is most sensitive to light.

**Disclosures: P. Morquette:** E. Ownership Interest (stock, stock options, royalty, receipt of intellectual property rights/patent holder, excluding diversified mutual funds); Boston Children's Hospital. **S. Manos:** None. **F. Caval-Holme:** None. **M.H. Do:** E. Ownership Interest (stock, stock options, royalty, receipt of intellectual property rights/patent holder, excluding diversified mutual funds); Boston Children's Hospital.

**Poster**

**PSTR183: Photoreceptors and Retinal Circuitry**

**Location:** WCC Halls A-C

**Time:** Monday, November 16, 2026, 1:00 PM - 5:00 PM

**Program #/Poster #:** PSTR183.12/Z17

**Topic:** E.06. Vision

**Title:** Characterizing Intrinsic Iridial Photoreceptors and the Signaling Pathways in the Vertebrate Iris

**Authors: *M. T. WALKER**;
James Madison Univ., Harrisonburg, VA

**Abstract:** Over the course of a day, our visual system is tasked with operating under varying light intensities, going from bright afternoon sun to dim moonlight. The iris is an essential component of the eye that protects the retina from light damage and helps the visual system operate under these varied light conditions. To do this, the iris will constrict or dilate in response to the intensity of ambient light; this behavioral response is the pupillary light reflex (PLR). The PLR is driven by two distinct signaling pathways: the primary signaling pathway is initiated by photoreceptors in the retina and is transmitted through a multisynaptic pathway involving several central nuclei in the brain. A secondary input pathway for PLR involves an intrinsic photoresponse in the sphincter pupillae. Our research is focused on a poorly understood class of intrinsic iridial photoreceptors (IIPs) that are required for intrisic photoresponses. IIPs express the melanopsin photopigment and use an invertebrate-like phototransduction cascade to initiate light-dependent constriction. IIPs use gap junctions to transmit light activated signals to sphincter muscle cells. Gap junctions are multimeric channels that allow for rapid ion transfer between two adjacent cells. Gap junctions are composed of protein subunits called, connexins. We have been able to identify the components of the iris gap junctions across vertebrate mammalian and non-mammalian species. Our qPCR data shows that connexin 43 is a highly conserved component amongst mouse, rat, chicken, frog, and human irises and the more evolutionarily close the species are, the more connexin proteins they have in common. While the secondary pathway is sufficient to cause constriction on its own ex-vivo, it remains unclear if the two pathways converge in-vivo.

**Disclosures: M.T. Walker:** None.

**Poster**

**PSTR183: Photoreceptors and Retinal Circuitry**

**Location:** WCC Halls A-C

**Time:** Monday, November 16, 2026, 1:00 PM - 5:00 PM

**Program #/Poster #:** PSTR183.13/Z18

**Topic:** E.06. Vision

**Title:** Engineering vision in vitro: Functional light-evoked responses in laminated retinal organoids

**Authors: *A. ORTEGA**[1], J. HAGEN[1], A. CHINN[1], D.-M. ALAM EL DIN[1], B. CHICHA[2], L. SMIRNOVA[1], R. JOHNSTON[1];
[1]Johns Hopkins Univ., Baltimore, MD; [2]Johns Hopkins Univ., baltimore, MD

**Abstract:** Retinal organoids offer strong potential for studying the emergence of functional retinal circuitry and its subsequent disruption in disease. However, current organoid protocols fall short of recapitulating *in vivo* retinal architecture and function. Addressing these limitations, our lab developed the Marmoset Retinal Multi-layered Organoid (MaRMO) protocol using

marmoset iPSCs. MaRMOs are the first retinal organoid to properly laminate, produce, and maintain all major retinal cell types, effectively recreating key features of native retinal tissue. This structural fidelity enables meaningful investigation of retinal circuitry maturation and functional connectivity. Using Microelectrode arrays, MaRMOs displayed light-dependent increases in firing rate, with the response magnitude scaling with stimulus duration. Tracking action potential propagation along individual axons revealed conduction velocities consistent with unmyelinated axons. Distinct retinal ganglion cell (RGC) response subclasses were functionally identified, including ON, OFF, and ON/OFF RGCs. Lastly, we demonstrated that MaRMOs were also color perceptive. Robust responses were detected across stimuli parameters and were consistent across multiple organoids and recording sessions. In contrast, empty well controls showed no measurable response to any light stimulus. Modeling intact retinal circuitry in vitro represents a critical next step for translational vision science which will support the development of therapies aimed at restoring vision.

**Disclosures: A. Ortega:** None. **J. Hagen:** None. **A. Chinn:** None. **D. Alam El Din:** None. **B. Chicha:** None. **L. Smirnova:** None. **R. Johnston:** None.

**Poster**

**PSTR183: Photoreceptors and Retinal Circuitry**

**Location:** WCC Halls A-C

**Time:** Monday, November 16, 2026, 1:00 PM - 5:00 PM

**Program #/Poster #:** PSTR183.14/Z19

**Topic:** E.06. Vision

**Title:** Tricaine methanesulfonate (MS222) significantly impacts the response amplitude and latency of the zebrafish visual response

**Authors: *A. C. SAUNDERS**[1], M. TARCHICK[1], B. MOORE[1], J. M. RENNA[2];
[2]Biol., [1]Univ. of Akron, Akron, OH

**Abstract:** Purpose: Tricaine methanesulfonate (MS-222) is a commonly used amphibian and fish anesthetic with documented deleterious effects on visual response properties in newts, frogs and humans. Yet, the impact of MS-222 on the amplitudes and kinetics of visual responses in the zebrafish (Danio rerio) retina remains uninvestigated. Here, we use ex-vivo electroretinogram (ERG) recordings from zebrafish retinae to investigate the effects of brief exposure and prolonged exposure to MS-222 on photoreceptor and bipolar cell response properties. Methods: Under dim red light, zebrafish were anesthetized with either brief MS-222 exposure until surgical anesthesia was achieved (2 minutes) or ice-cooling as the control. Eyes were enucleated, retinae isolated, and ex-vivo ERGs recorded using 300ms 520nm flashes across five light intensities. Photoreceptor responses were isolated with $BaCl_2$, aspartic acid, and LAP4. To test the impact of prolonged exposure, isolated retinae were recorded and then perfused with 0.765 mM MS-222 for 30 minutes before subsequent recording. Results: Brief exposure to MS-222 did not significantly alter response amplitudes or kinetics. However, analysis of the synaptic transfer function revealed reduced synaptic gain at all light intensities, suggesting brief MS-222 exposure

subtly altered signal transmission between photoreceptors and bipolar cells, even though independent response properties were unimpeded. Bath applying MS-222 for 30-90 minutes during ex-vivo recordings decreased the average photoreceptor response amplitude at $10^2$ from 42µV to 16µV, at $10^3$ from 40µV to 33µV, and $10^4$ from 81µV to 62µV, but had no significant impact at the dimmest or brightest intensities of $10^1$ and $10^5$ log photons/µm². Bipolar cell response amplitudes were significantly decreased at $10^2$ from 51µV to 29µV, and $10^3$ from 75µV to 67µV, but not at other intensities. MS-222 slowed photoreceptor response kinetics at $10^3$ and $10^5$ log photons/µm² (61ms to 85ms, and 46ms to 65ms respectively). Bipolar cell kinetics were significantly impacted only at the dimmest intensities; 216ms to 355ms at $10^1$ and 230ms to 494ms at $10^2$ log photons/µm². Conclusions: Brief MS-222 exposure did not significantly alter zebrafish photoreceptor or bipolar-cell response amplitudes or kinetics, but reduced synaptic gain suggests subtle impairment of signal transfer between these cells. Prolonged exposure, however, significantly impaired retinal response amplitudes and response kinetics, highlighting MS-222 as an important experimental variable that can influence measurements of zebrafish visual function.

**Disclosures: A.C. Saunders:** None. **M. Tarchick:** None. **B. Moore:** None. **J.M. Renna:** None.

**Poster**

**PSTR183: Photoreceptors and Retinal Circuitry**

**Location:** WCC Halls A-C

**Time:** Monday, November 16, 2026, 1:00 PM - 5:00 PM

**Program #/Poster #:** PSTR183.15/Z20

**Topic:** E.06. Vision

**Support:** ZIA EY000438

**Title:** Pigment epithelium derived factor (PEDF) peptide exhibits neuroprotection in mouse models of inherited retinal degeneration

**Authors: *P. CHAMBERS**, A. BERNARDO, S. BECERRA;
Lab. of Retinal Cell and Mol. Biology, Section on Protein Structure and Function, Natl. Eye Inst., Bethesda, MD

**Abstract: Introduction:** Retinitis pigmentosa (RP) and Leber congenital amaurosis (LCA) cause progressive photoreceptor dysfunction and death, ultimately disrupting retinal circuit output. The PEDF peptide H105A has been shown to prevent progression of photoreceptor degeneration in *rd10* mice, a rapidly degenerating autosomal recessive RP model. Here, we evaluated whether H105A provides neuroprotection in two slower retinal degeneration models: $Rho^{P23H/+}$ mice, an autosomal dominant RP model carrying a mutation in rhodopsin, and $Rpe65^{-/-}$ mice, an autosomal recessive RP/LCA model lacking Rpe65. **Methods:** To define the temporal profile of neurodegeneration, retinal cell death was monitored using a fluorescent probe that detects phosphatidylserine (PS) externalization, an early marker of cell death. Independent cohorts (n=3) received fluorescent eye drops at selected timepoints from postnatal day (P)14 to P30, and fundus fluorescence was measured 24 hours later. Retinal structure and neural function

were assessed by histology, immunofluorescence, and electroretinography. Then, daily H105A eye drops were administered to *Rho*$^{P23H/+}$ mice from P15-P24 and to *Rpe65*$^{-/-}$ mice from P14-P21, with HBSS-treated littermates as controls (n=7 per group). Fluorescent fundoscopy was recorded at the end of the time course. Sex of mice was recorded but did not stratify analyses. **Results:** In *Rpe65*$^{-/-}$ mice, PS externalization was highest at P16, and declined by P28, whereas *Rho*$^{P23H/+}$ mice showed a milder increase at P19 that declined through P30, indicating a peak of PS externalization in photoreceptors in both models. PS fluorescence correlated with BAX expression in retinal sections. Early PS externalization and reductions in ERG a-wave amplitudes were detected before measurable outer nuclear layer thinning, indicating that cellular stress and functional deficits precede overt structural degeneration. H105A treatment significantly reduced PS fluorescence in *Rho*$^{P23H/+}$ mice at P19 and P25 compared with controls, but no protective effect was detected in *Rpe65*$^{-/-}$ mice. **Conclusions:** Early photoreceptor stress and cell death preceded structural retinal thinning in both slow degeneration models, highlighting a window for neuroprotective intervention before irreversible tissue loss. Topical H105A reduced an early step in retinal cell death in *Rho*$^{P23H/+}$ mice but not in *Rpe65*$^{-/-}$ mice, suggesting that its neuroprotective efficacy may depend on the underlying mechanism of photoreceptor degeneration. These findings identify H105A as a promising therapeutic peptide candidate for early neuroprotective intervention in select forms of inherited retinal disease.

**Disclosures: P. Chambers:** A. Employment/Salary (full or part-time):; National Institutes of Health, Full time. **A. Bernardo:** A. Employment/Salary (full or part-time):; National Institutes of Health, Full time. E. Ownership Interest (stock, stock options, royalty, receipt of intellectual property rights/patent holder, excluding diversified mutual funds); Patent application holder for H105A. **S. Becerra:** A. Employment/Salary (full or part-time):; National Institutes of Health, Full time. E. Ownership Interest (stock, stock options, royalty, receipt of intellectual property rights/patent holder, excluding diversified mutual funds); Patent application holder for H105A.

**Poster**

**PSTR183: Photoreceptors and Retinal Circuitry**

**Location:** WCC Halls A-C

**Time:** Monday, November 16, 2026, 1:00 PM - 5:00 PM

**Program #/Poster #:** PSTR183.16/Z21

**Topic:** E.06. Vision

**Support:** NIH 1R01EY033000
1R01EY034325
1R01EY029489
1K08EY027458
1R42EY035582
1R41EB030875
R01-HL147527
R21 GM140359-01
Foundation Fighting Blindness RC-CMM-0824-0899-JHU
University of Michigan MTRAC-FFMI grant

Michigan Medicine-Peking University Health Science Center Joint Institute
Alcon Research Institute Young Investigator Grant
Fight for Sight - International Retinal Research Foundation FFSGIA16002
Massey Foundation TBI Grand Challenge Award
Research to Prevent Blindness

**Title:** Glia CLRN1 Deficiency Triggers Photoreceptor Degeneration in Usher Syndrome Type 3A

**Authors: *Y. LEE**[1], P. NGUYEN[2], Y. PAULUS[1];
[1]Johns Hopkins Univ., Baltimore, MD; [2]Ophthalmology, Johns Hopkins Universtiy, Sch. of Med., Baltimore, MD

**Abstract:** Usher syndrome type 3A (USH3A), caused by *CLRN1* mutations, leads to progressive deaf-blindness. While transcriptomic evidence localizes *CLRN1* exclusively to Müller glia, the pathogenic mechanisms bridging this primary glial defect to non-cell-autonomous photoreceptor death remain poorly understood, and existing rodent models fail to manifest distinct retinal degeneration. To address this, we utilized CRISPR/Cas9 to develop the first *CLRN1*-null large-animal rabbit model. Retinal phenotyping was performed longitudinally from 2 months to 3 years of age using spectral domain optical coherence tomography (SD-OCT), full-field electroretinography (ffERG), and histology. For transcriptomic profiling, single-nucleus RNA sequencing (snRNA-seq) was conducted on wild-type and *CLRN1* knockout (KO) rabbit retinae at a pre-symptomatic stage (10 months), followed by differential expression and Gene Ontology enrichment analyses. *CLRN1* KO rabbits effectively recapitulated progressive deaf-blindness. SD-OCT and histology revealed selective outer nuclear layer thinning starting after 20 months, while functional visual decline was evidenced by impaired 30 Hz flicker responses. snRNA-seq confirmed exclusive *CLRN1* expression in Müller glia. In KO Müller glia, the crucial adherens junction component *CTNNA2* (α-N-catenin) was significantly downregulated, suggesting structural failure at the outer limiting membrane (OLM). Despite lacking *CLRN1* expression, photoreceptors exhibited extensive non-cell-autonomous dysregulation, marked by downregulation of the cone synaptic organizer *TENM2* and pro-fibrotic extracellular matrix remodeling in rods. Remarkably, inner retinal neurons mounted a robust proteostatic response via upregulation of HSP90 family chaperones (*HSP90AB1*, *HSP90AA1*), whereas this protective upregulation was entirely absent in vulnerable photoreceptors. These findings support an "Anchor-Shield" pathogenic model for USH3A primary *CLRN1* loss compromises the retinal structural "Anchor" (OLM integrity), while photoreceptors degenerate because they lack the proteostatic "Shield" activated by resilient inner neurons. This glia-first mechanism fundamentally distinguishes USH3A from cell-autonomous USH1/USH2 defects and identifies a 10-month pre-symptomatic therapeutic window for targeted interventions.

**Disclosures: Y. Lee:** None. **P. Nguyen:** None. **Y. Paulus:** None.

**Poster**

**PSTR183: Photoreceptors and Retinal Circuitry**

**Location:** WCC Halls A-C

**Time:** Monday, November 16, 2026, 1:00 PM - 5:00 PM

**Program #/Poster #:** PSTR183.17/Z22

**Topic:** E.06. Vision

**Support:** Research to Prevent Blindness
Fight for Sight - International Retinal Research Foundation FFSGIA16002
National Eye Institute (1R01EY033000)
National Eye Institute (1R01EY034325)
Alcon Research Institute Young Investigator Grant,

**Title:** Predicting Progression of Dry Age-related Macular Degeneration to Advanced Stages Using Machine Learning Analysis of Electronic Health Record Data

**Authors: *M. YASHAR**, L. MUNIR, Y. M. PAULUS;
Ophthalmology, Wilmer Eye Institute, Johns Hopkins Univ., Baltimore, MD

**Abstract: Objective:** Age-related macular degeneration (AMD) is a neurodegenerative disease of the retina characterized by progressive photoreceptor and retinal pigment epithelium loss, sharing key pathophysiological mechanisms with CNS neurodegeneration. Progression from dry AMD to advanced forms (geographic atrophy [GA] and neovascular AMD) is the primary determinant of vision loss. While cross-sectional risk factors are established, prediction models leveraging longitudinal real-world data remain limited. Our goal was to develop a machine learning model using electronic health record (EHR) data to predict risk of progression from dry AMD to advanced disease.**Methods:** Exploratory retrospective cohort study of dry AMD patients (ICD-10: H35.31) at Johns Hopkins, Wilmer Eye Institute (2015-2026). Predictors included demographics, ocular examination findings and history, systemic comorbidities, medications, laboratory values, and longitudinal trajectory features. Landmark Cox regression was performed at 1, 2, and 3 years post-diagnosis, with trajectory features restricted to measurements ≤ landmark time (tL) to prevent look-ahead bias. Cause-specific competing risks models were fit separately for GA and neovascular AMD. Variable selection employed univariable pre-screening ($p < 0.30$), capped at events/10 predictors, with ridge penalty ($\lambda = 0.10$) for coefficient stability. Model discrimination was assessed using Harrell's C-statistic.**Results:** The cohort included 19,026 dry AMD patients (mean age 78.6 ± 10.3 years; 62.8% female; 85.8% White, 5.9% African American) with mean follow-up of 5.0 ± 3.9 years. Of these, 571 (3.0%) progressed to GA (mean time to onset: 41.7 ± 39.2 months) and 1,687 (8.9%) to neovascular AMD (mean time to onset: 38.0 ± 47.8 months). Prospective landmark models achieved C-indices for GA of 0.675 (Year 1), 0.680 (Year 2), and 0.692 (Year 3); for neovascular AMD: 0.623, 0.625, and 0.615, respectively. Visual acuity (VA) trajectories were the strongest predictors of progression (HR 1.20-1.43). Maximum VA (LogMAR) predicted both GA (HR 1.37, $p<0.001$) and neovascular AMD (HR 1.43, $p<0.001$). Cumulative VA burden emerged as significant only at Year 3 for GA (HR 1.21, $p=0.037$). African American race was associated with lower neovascular AMD risk (HR 0.82, $p=0.014$). AREDS supplement use was associated with progression (GA: HR 1.19; neovascular AMD: HR 1.24-1.29), likely reflecting indication bias.**Conclusions:** Longitudinal EHR-derived variables improve prediction of dry AMD progression beyond baseline risk factors, supporting potential for risk-stratified monitoring in this retinal neurodegenerative disease.

**Disclosures: M. Yashar:** None. **L. Munir:** None. **Y.M. Paulus:** None.

**Poster**

**PSTR183: Photoreceptors and Retinal Circuitry**

**Location:** WCC Halls A-C

**Time:** Monday, November 16, 2026, 1:00 PM - 5:00 PM

**Program #/Poster #:** PSTR183.18/Z23

**Topic:** J.08. Methods to Modulate Neural Activity

**Support:** the MOST of China (2022ZD0210000)
the MOST of China (2022ZD0208604 and 2022ZD0208605）

**Title:** Vision Restoration Using Artificial Photoreceptors Based on Titania Nanowire Arrays

**Authors: *B. YAN**[1], R. YANG[2], J. ZHANG[1];
[1]Fudan Univ., Shanghai, China; [2]Harvard Univ., Boston, MA

**Abstract:** Retinal prostheses aim to restore vision in photoreceptor degenerative diseases, but current devices suffer from limited spatial resolution and low light sensitivity. Here we report the in vivo performance of subretinally implanted gold nanoparticle-coated titania nanowire arrays in mouse and non-human primate models of induced photoreceptor degeneration. Ex vivo patch-clamp recordings from retinal ganglion cells demonstrated that these arrays achieved a spatial resolution of 77.5 μm and a temporal resolution of 3.92 Hz. In blind mice, the arrays enabled detection of drifting gratings and flashing objects at light intensity thresholds of 15.70-18.09 $\mu W \cdot mm^{-2}$, and achieved visual acuities of 0.3-0.4 cycles per degree, as verified by visually evoked potential recordings and optomotor response tests. In rhesus monkeys, the implants exhibited excellent long-term stability over 54 weeks, enabled detection of a 10 $\mu W \cdot mm^{-2}$ light beam (0.5° beam angle) in visually guided saccade experiments, and induced plastic changes in the primary visual cortex as revealed by longitudinal in vivo calcium imaging. These results demonstrate that nanomaterial-based artificial photoreceptors represent a promising therapeutic strategy for ameliorating visual deficits in patients with photoreceptor degeneration.

**Disclosures: B. Yan:** None. **R. Yang:** None. **J. Zhang:** None.

**Poster**

**PSTR183: Photoreceptors and Retinal Circuitry**

**Location:** WCC Halls A-C

**Time:** Monday, November 16, 2026, 1:00 PM - 5:00 PM

**Program #/Poster #:** PSTR183.19/Z24

**Topic:** A.01. Neurogenesis and Gliogenesis

**Support:** NIH NEI R01 EY032136 and R01 EY012543
NIH NEI P30 EY002687

The Knights Templar Eye Foundation Pediatric Ophthalmology Career-Starter Research Grant
Research to Prevent Blindness
Members of Dr. Shiming Chen's lab

**Title:** AAV-mediated gene therapy recovering cell identity loss of cone photoreceptors in murine models of dominant cone-rod dystrophy $CRX^{E80A/+}$

**Authors: *Y. LIU**[1], C. SUN[2];
[1]Dept. of Ophthalmology and Visual Sci., Washington Univ. in St. Louis, Saint Louis, MO;
[2]Dept. of Ophthalmology and Visual Sci., Washington Univ. in St. Louis, St. Louis, MO

**Abstract:** The cone-rod homeobox (CRX) is a transcription factor regulating the development and survival of rod and cone photoreceptors. Human *CRX*$^{E80A}$ mutation in the homeodomain is linked to autosomal dominant early-onset cone-rod dystrophy (CoRD). Our previous studies reported that early-onset cone loss in *Crx*$^{E80A/+}$ knock-in mouse model recapitulated CoRD-like manifestations. *Crx*$^{E80A}$ mutation downregulated the expression of rod genes while severely disrupted the transcription regulation of cone genes. This study aimed to track cell fate of the cone lineage in *Crx*$^{E80A/+}$ mice and to develop gene therapy. We utilized *Thrb*$^{b2Cre+/-}$; *Ai6* reporter line to label fated cones in green, and immunohistochemistry (IHC) on established cone identity markers, RXRG, ARR3 and cone opsins, at postnatal day 0 (P0), P10, P14, P21 and P30. We found that cones are co-labeled by the *Ai6* reporter and IHC of cone markers in *WT* retinae at all tested ages. In contrast, *Crx*$^{E80A/+}$ cones show co-labelling at P0, but progressively lose cone markers during postnatal differentiation, becoming only detectable by the *Ai6* reporter by P30. These data suggest that *Crx*$^{E80A/+}$ cones remain viable through young adulthood despite losing cone identity during development. We further tested if *Crx*$^{E80A/+}$ mutation caused a similar loss of cone identity in cone-enriched *Nrl*$^{-/-}$;*pNrl-GFP* retinae in which *Nrl* knockout converted rods into cone-like cells. During photoreceptor differentiation, all cells in outer nuclear layers of *Nrl*$^{-/-}$;*pNrl-GFP* retinae were co-labeled by GFP and IHC of cone markers; however, *Crx*$^{E80A/+}$ mutation greatly decreased the population of co-label cells. *CRX* augmentation, the overexpression of functional *CRX*, may serve as a viable treatment strategy for *CRX*$^{E80A}$ mutation. We evaluated the therapeutic potential of *AAV2.7m8-pCrx-CRX* via subretinal injection of $10^{11}$vg/mL into the *Crx*$^{E80A/+}$;*Thrb*$^{b2Cre+/-}$;*Ai6* retinae at two treatment windows: P14 to P28, a period of progressive loss in cone identity during photoreceptor differentiation; P30 to P44, a period of absent cone identity. This therapeutic intervention resulted in co-labeled cones in treated *Crx*$^{E80A/+}$;*Thrb*$^{b2Cre+/-}$;*Ai6* retinae at both treatment windows. These preclinical data suggest that *AAV*-mediated *CRX* augmentation not only preserves cone identity during development but also recovers lost identity in underdeveloped cones in young adulthood. Altogether, this study highlights the importance of maintaining cell identity as a key therapeutic goal and unveils the potential plasticity of treatment windows for gene therapy.

**Disclosures: Y. Liu:** None. **C. Sun:** None.

**Poster**

**PSTR183: Photoreceptors and Retinal Circuitry**

**Location:** WCC Halls A-C

**Time:** Monday, November 16, 2026, 1:00 PM - 5:00 PM

**Program #/Poster #:** PSTR183.20/AA1

**Topic:** A.01. Neurogenesis and Gliogenesis

**Support:** University Undergraduate Research Fellowship, Johns Hopkins University

**Title:** MEIS2: A candidate marker of neuronal subtype maturation in human retinal organoids

**Authors: *A. L. IANNUZZI**[1], A. TAYLOR[2,1], B. GUY[1], J. S. ZHANG[1], R. JOHNSTON[1,2]; [1]The Johns Hopkins Univ. Dept. of Biol., Baltimore, MD; [2]Neurosci., The Johns Hopkins Univ., Baltimore, MD

**Abstract:** Understanding how cells in the retina develop and are maintained is important to guide stem cell based regenerative therapies for visual disorders. Human stem cell-derived retinal organoids (ROs) recapitulate key aspects of in vivo retinogenesis, offering an experimentally accessible system to analyze how genes control cell identity and maintain specific cell types. We found that MEIS2 is expressed in subtypes of retinal ganglion cells (RGCs) and amacrine cells (ACs). In organoids, ACs and RGCs were present >50 days prior to detectable MEIS2 expression, indicating that MEIS2 is activated late in the development of these cell types. MEIS2+ cells are born ~50 days before the onset of MEIS2 expression, suggesting that MEIS2 is unlikely to regulate initial fate specification and instead may function in subtype specification, maturation, or long-term maintenance. Retinoic acid (RA) is a negative regulator of MEIS2, as organoids grown in high RA had less MEIS2+ cells compared to controls. These results suggest that MEIS2 differentiates RGC and AC subtypes and is regulated by RA, informing strategies for directed differentiation and cell-replacement therapies.

**Disclosures: A.L. Iannuzzi:** None. **A. Taylor:** None. **B. Guy:** None. **J.S. Zhang:** None. **R. Johnston:** None.

**Poster**

**PSTR184: Visual Motion**

**Location:** WCC Halls A-C

**Time:** Monday, November 16, 2026, 1:00 PM - 5:00 PM

**Program #/Poster #:** PSTR184.01/AA2

**Topic:** E.06. Vision

**Support:** U19NS118246
EY013644

**Title:** Neural correlates of speed-dependent relative motion perception in area MT

**Authors: *Y. DONG**[1], A. ANZAI[1], Z. B. XU[2], X. YUAN[1], S. SHIVKUMAR[3], G. LENGYEL[4], R. M. HAEFNER[1], G. C. DEANGELIS[1];

[1]Univ. of Rochester, Rochester, NY; [2]Harvard Med. Sch., Boston, MA; [3]Indian Inst. of Technol. Gandhinagar, Palaj, India; [4]Inst. of Sci. and Technol. Austria, Klosterneuburg, Austria

**Abstract:** Motion perception is inherently relative: depending on the inferred reference frame, the same retinal velocity can correspond to different perceived object motions. Psychophysical studies have shown that perceived object motion can be repelled away from surrounding motion context, toward the relative velocity between center and surround (e.g., Johansson, 1950; Shivkumar et al., 2025). Intriguingly, this contextual influence is robust mainly at slow speeds (Rauber & Treue, 1998; Braddick et al., 2002; Chen et al., 2014). A Bayesian causal inference model offers a promising account of how observers infer hierarchical motion structure (Shivkumar et al., 2025), and predicts this speed dependence. However, the neural correlates of relative velocity perception, including its speed dependence, remain poorly understood. Responses of neurons in the middle temporal (MT) area are modulated by surrounding motion (e.g., Allman et al., 1985), and such effects may reflect causal inference computations that also underlie perception of relative motion (Lengyel et al., 2025). We first tested humans and one monkey in a binary direction-discrimination task using stimuli composed of a central motion patch and a surrounding annulus. Center and surround motions shared a common velocity component along the task-reference direction, while their motion directions varied relative to that reference. Consistent with previous work, the surround induced a repulsive perceptual bias that declined markedly as speed increased from 1 to 4 to 16 deg/s, in both humans and the monkey. We then recorded MT population activity while the monkey passively viewed stimuli with the same center-surround structure. Crucially, we included two stationary-surround controls: one in which center motion was identical to that of the moving-surround condition, and one in which its velocity matched the relative velocity between the center and surround in the moving-surround condition. These controls allowed us to test whether MT responses are better explained by retinal velocity of the center or by relative velocity between center and surround. MT responses are well described by a weighted combination of tuning for retinal and relative velocity, with stronger relative velocity weights at slow than at fast speeds. Population decoding further showed that a moving surround shifted the decoded direction toward relative velocity, and this shift weakened at higher speeds. Together, these results reveal a neural substrate for relative velocity perception and its dependence on retinal speed, suggesting that MT contributes to representations of hierarchical motion that may mediate Bayesian causal inference.

**Disclosures: Y. Dong:** None. **A. Anzai:** None. **Z.B. Xu:** None. **X. Yuan:** None. **S. Shivkumar:** None. **G. Lengyel:** None. **R.M. Haefner:** None. **G.C. DeAngelis:** None.

**Poster**

**PSTR184: Visual Motion**

**Location:** WCC Halls A-C

**Time:** Monday, November 16, 2026, 1:00 PM - 5:00 PM

**Program #/Poster #:** PSTR184.02/AA3

**Topic:** E.06. Vision

**Support:** NSF/CAREER IIS-2143440

**Title:** Motion perception as causal inference: testing the causality assumption

**Authors: *X. YUAN**[1,2,3], S. SHIVKUMAR[4], Y. DONG[2,3], A. ANZAI[2,3], G. C. DEANGELIS[2,3], R. M. HAEFNER[2,3];
[2]Brain and Cognitive Sci., [1]Univ. of Rochester, Rochester, NY; [3]Ctr. for Visual Sci., Rochester, NY; [4]Dept. of Cognitive and Brain Sci., IIT Gandhinagar, Gandhinagar, India

**Abstract:** Motion is always defined with respect to some reference frame. During perception the brain appears to flexibly and dynamically choose that reference frame. Recently, Shivkumar et al. (2025) proposed a normative model for this inference process under the assumption that the brain's choice of reference frame depends on its beliefs about the causal structure underlying its motion inputs. While this model was shown to account for several motion perception phenomena, including integration and repulsion and their dependence on motion coherence, two key questions remain open: (1) are perceived motion direction and speed inferred and perceived jointly or independently, and (2) do beliefs about the causal structure really influence motion perception as predicted by the model?To answer these questions, we conducted two psychophysical experiments. In both experiments, observers reported their perception of a central patch of coherently moving dots surrounded by an annulus of coherently moving dots. We varied the angular difference between center and surround motion while keeping the relative velocity between the two components orthogonal to the surround motion.In the first experiment, participants reported continuous motion direction estimates using a dial and subsequently made a binary speed judgment. The model predicts that perceived speed and direction are jointly inferred and therefore statistically related. Specifically for small direction differences between center and surround, when perception is based on relative motion, reports should not just be biased away from the surround but should also be perceived as slower. Our data are consistent with this prediction: when direction reports showed a larger bias, speed was also judged to be slower.In the second experiment, after approximately 1.5s, the motion direction of both center and surround dots reversed. In order to influence the subject's belief about whether center and surround were part of the same causal structure, and whether the center caused the surround, or the surround caused the center, we manipulated the temporal offset between the reversals of center and surround dots (+/−100, +/−33, 0) ms. If temporal order and synchrony contribute to causal-structure inference, these manipulations should influence motion perception. Our preliminary data support the predicted pattern: repulsion effects were stronger when the center stimulus reversed first (−100 ms) than when the surround reversed first (+100 ms), and repulsion was weakest for the largest latencies, a pattern explained by our model by assigning different probabilities to alternative causal structures.

**Disclosures: X. Yuan:** None. **S. Shivkumar:** None. **Y. Dong:** None. **A. Anzai:** None. **G.C. DeAngelis:** None. **R.M. Haefner:** None.

**Poster**

**PSTR184: Visual Motion**

**Location:** WCC Halls A-C

**Time:** Monday, November 16, 2026, 1:00 PM - 5:00 PM

**Program #/Poster #:** PSTR184.03/AA4

**Topic:** E.06. Vision

**Support:** Lilly Endowment, Inc
Simons Foundation
John Simon Guggenheim Memorial Foundation
Gordon and Betty Moore Foundation

**Title:** Contrast Distribution Shape Drives Low-Dimensional Adaptation in a Fly Visual Interneuron

**Authors: *C. EDELSON**[1], W. BIALEK[2];
[2]Joseph Henry Labs. of Physics, [1]Princeton Univ., Princeton, NJ

**Abstract:** Adaptation to the statistics of sensory inputs is a central hypothesis of efficient coding theories, and the fly visual system has proved a fruitful testing ground for these ideas. Examples of adaptation to the mean and variance of inputs are well documented. However, adaptation to the full shape of the stimulus distribution has been difficult to demonstrate, with only a few simple cases reported. Previously, we used the H1 motion-sensitive neuron in the fly visual system to characterize a hierarchy of adaptation, showing that context-dependent changes in the neuron's receptive field are confined to a low-dimensional space and improve information transmission. These adaptations largely reflect a rescaling of receptive field strength according to the maximum contrast available in the stimulus ensemble. However, because those experiments employed uniform contrast distributions, it remained unclear whether the adaptive mechanism was sensitive to the maximum contrast itself or to broader features of the underlying distribution. Here we extend that work by delivering stimuli drawn from beta distributions, which allow systematic manipulation of contrast distribution shape while preserving other stimulus statistics. Applying dimensionality reduction to the spike-triggered average velocity trajectory across these conditions, we again find that adaptive changes in the neural response occupy a low-dimensional space. The dominant dimension of this space tracks the shape of the contrast cumulative distribution function, rather than simply the maximum contrast or variance. This result suggests that the adaptive mechanism encodes distributional structure at a level beyond simple rescaling and provides new constraints on mechanistic models of contrast adaptation in the fly visual system.

**Disclosures: C. Edelson:** None. **W. Bialek:** None.

**Poster**

**PSTR184: Visual Motion**

**Location:** WCC Halls A-C

**Time:** Monday, November 16, 2026, 1:00 PM - 5:00 PM

**Program #/Poster #:** PSTR184.04/AA5

**Topic:** E.06. Vision

**Support:** NSF Grant IOS-2508419

**Title:** Population-Wide Organization of Optic Flow Response Types in the Larval Zebrafish Pretectum

**Authors:** ***Y. CHEN**[1], B. JAMES[1], S. CHALYSHKAN[1], T. BISWAS[1], F. KUBO[2], H. BAIER[3], J. FITZGERALD[1];
[1]Northwestern Univ., Evanston, IL; [2]RIKEN Ctr. for Brain Sci., Saitama, Japan; [3]Max Planck Inst. of Neurobio., Planegg, Germany

**Abstract:** Visual motion processing converts optic flow signals into compensatory behaviors, including the optokinetic response (OKR) and optomotor response (OMR), which stabilize gaze and posture during self-motion. The pretectum is a key, evolutionarily conserved region involved in this transformation across vertebrates. The larval zebrafish pretectum is accessible to whole-population calcium imaging, making it tractable for studying how populations represent visual motion for behavior. Existing characterizations of pretectal visual motion circuits rely on incomplete response repertoires. Kubo et al. (2014) recorded 3,015 pretectal neurons responding to eight monocular/binocular optic flow stimuli and characterized the circuit with abundant, interpretable response types, establishing prominent types individually while leaving less-abundant interpretable types and unassigned cells outside a unified account. Thus, how all responses relate at the population level remains unresolved, limiting efforts to uncover finer circuit mechanisms. Here, we sought to recover an interpretable functional organization of the full recorded repertoire. For each cell, we binarized eight fitted response amplitudes into a response vector and fit a Bernoulli mixture model, treating each cell as a noisy draw from a cluster with a mean response probability for each stimulus. Model selection by the Bayesian information criterion identified 13 clusters, each grouping cells with similar response patterns. Ward linkage applied to the cluster mean vectors produced a dendrogram that revealed two levels of organization. At the coarse level, clusters separated according to the dominant whole-field motion they reported: forward translation, backward translation, or rotation. These motion categories correspond to visual patterns that drive the OMR or OKR. At the fine level, clusters within each group were distinguished by the eye and direction of excitatory input supporting that report. This organization treats each cell not as an isolated response-type label, but as part of a shared response space defined by the behaviorally relevant global optic-flow pattern it reports and the eye-specific excitatory inputs that support that response. Within this hierarchy, less-abundant response types and previously unclassified cells can be placed in relation to prominent types, revealing how they fit within the full spectrum of pretectal visual motion responses. By encompassing the full recorded population, this interpretable two-level organization provides a foundation for investigating finer circuit mechanisms without relying only on a subset of named response types.

**Disclosures: Y. Chen:** None. **B. James:** None. **S. Chalyshkan:** None. **T. Biswas:** None. **F. Kubo:** None. **H. Baier:** None. **J. Fitzgerald:** None.

**Poster**

**PSTR184: Visual Motion**

**Location:** WCC Halls A-C

**Time:** Monday, November 16, 2026, 1:00 PM - 5:00 PM

**Program #/Poster #:** PSTR184.05/AA6

**Topic:** E.06. Vision

**Support:** NSF Grant IOS-2508419

**Title:** Continuous encoding of motion cues in the zebrafish pretectum

**Authors: *B. JAMES**[1], Y. CHEN[2], S. CHALYSHKAN[1], T. BISWAS[3], F. KUBO[4], H. BAIER[5], J. E. FITZGERALD[3];
[1]Northwestern Univ., Chicago, IL; [3]Neurobio., [2]Northwestern Univ., Evanston, IL; [4]RIKEN Ctr. for Brain Sci., Saitama, Japan; [5]Genes - Circuits - Behavior, Max Planck Inst. of Neurobio., Planegg, Germany

**Abstract:** Neural processing of visual motion information is an important and highly conserved aspect of both mammalian and non-mammalian vertebrate species. Relying upon evolutionary ancient brain structures, visual information pertaining to motion cues is transmitted from the retina to the pretectum, processed, and used to trigger behavioral responses such as the optomotor or optokinetic response. While in recent years a great deal of focus has been placed on analyzing pretectal responses to identify potential circuit mechanisms used to generate these behavioral responses, these analyses have largely relied upon simplistic, binary descriptions of neural responses that neglect to account for correlations between cells, responses to differing stimuli, or the continuous nature of rate-based neural responses. Consequently, most current circuit models fall short in accurately predicting neural responses, or the connectivity which gives rise to them. In this work, we utilized a combination of nonlinear regressions and stochastic mixture models to analyze previously published calcium imaging pretectal data sets (Kubo 2014). By decomposing a neuron's dynamic stimuli responses into single values using radial basis regressions, we show that individual pretectal neurons, rather than responding in a binary fashion to differing motion cue stimuli, are better described as lying on a continuum. Correlation analyses on these decomposed responses show significant continuous dependence between stimuli within single pretectal neurons. Finally, comparing the decompositions of population activity using either Gaussian mixture models that allow for continuous variation between neurons in a functional cluster with those that enforce independence using Bayesian Information Criteria shows that whole-region models of neural activity that allow for strong dependence between stimuli responses within functional clusters better explains experimentally collected data. Importantly, these findings highlight the necessity of incorporating continuous responses into models of processing in pretectal neurons. Moreover, demonstrating that neurons within functionally identified cell types show strong covariances across stimuli dimensions indicates that circuitry connection patterns are likely more sophisticated than originally proposed. Future work will both further illuminate the connectivity patterns giving rise to this continuous representation and study the potential behavioral advantages of continuous over discrete representations.

**Disclosures: B. James:** None. **Y. Chen:** None. **S. Chalyshkan:** None. **T. Biswas:** None. **F. Kubo:** None. **H. Baier:** None. **J.E. Fitzgerald:** None.

**Poster**

**PSTR184: Visual Motion**

**Location:** WCC Halls A-C

**Time:** Monday, November 16, 2026, 1:00 PM - 5:00 PM

**Program #/Poster #:** PSTR184.06/AA7

**Topic:** E.06. Vision

**Support:** National Science and Technology Innovation 2030 Major Program (2022ZD0205000)

**Title:** Measuring Hemodynamic Modulation to Optic Flow in Macaque Extrastriate Visual Cortex using functional Ultrasound Imaging (fUSI)

**Authors: *Q. LUO**[1,2], Y. GU[1,2];
[1]Syst. neuroscience, Ctr. for Excellence in Brain Sci. and Intelligence Technology, Chinese Acad. of Sci., Shanghai, China; [2]Univ. of Chinese Acad. of Sci., Beijing, China

**Abstract:** Self-motion is a crucial ability for individuals to interact wither environment, which is a process involving multiple sensory modalities including vestibular, visual, and proprioceptive (Mao & Gu 2025, Nature Reviews Neuroscience). Numerous studies have indicated that these self-motion signals are prevalently existing in neocortex, yet their properties and functions have not been well identified, partially due to limitations in each respective techniques employed in previous studies. Here we adopted functional ultrasound imaging (fUSI), a minimally invasive technique with a number of merits including high spatiotemporal resolution, high signal sensitivity, and large spatial coverage, to measure sensory hemodynamic signals in primates under self-motion condition. In our previous work, we have successfully measured vestibular-related signals during physical self-motion using fUSI in macaques (Liu et al., 2025, PNAS), validating its feasibility. In our current study, we focused on measuring the hemodynamics modulation to optic flow by imaging parietal cortex. The fUSI successfully captured hemodynamics modulation to optic flow in a number of areas in the parietal cortex including MST, VIP, LIP. In particular, across the spatial domain, fine heading directions could be successfully decoded on a trial by trial basis using fUSI data. A reference eccentricity dependent effect on heading discrimination threshold was also observed particularly in area MST, matching previous electrophysiological data. Across the temporal domain, different motion velocity profiles could also be decoded based on a single trial level. To our knowledge, such a decoding accuracy based on the fUSI data in the spatial and temporal domain are significantly better than those in fMRI. Thus, our findings suggest that fUSI holds a promising tool for studying the spatiotemporal dynamics of sensory signals, as well as their cognitive process such as perceptual decision making.

**Disclosures: Q. Luo:** None. **Y. Gu:** None.

**Poster**

**PSTR184: Visual Motion**

**Location:** WCC Halls A-C

**Time:** Monday, November 16, 2026, 1:00 PM - 5:00 PM

**Program #/Poster #:** PSTR184.07/AA8

**Topic:** E.06. Vision

**Support:** NIH R01EY035268
PHY-2317138
NSF DMS-2235451
MP-TMPS-00005320

**Title:** Short-term Synaptic Plasticity Preserves Sensitivity of the Retina to Natural Scenes

**Authors: *T. F. EDINGTON**[1], S. E. PALMER[2], W. WEI[3];
[2]Organismal Biol. and Anat., [1]Univ. of Chicago, Chicago, IL; [3]Neurobio., The Univ. of Chicago, Chicago, IL

**Abstract:** Synaptic plasticity is a key feature of the neural code, yet integrating plasticity rules into neural circuit analysis remains a challenge. Here, we use the retinal direction-selective circuit to study how short-term plasticity at multiple synapses interact and shape neural computation. We induce short-term plasticity by stimulating the retina with an "induction" motion stimulus, either confined to the receptive field (RF) center or covering both the center and surround. We found that the activity of the circuit output neuron, the direction-selective ganglion cell (DSGC), shows stronger depression when the induction motion stimulus is restricted to the RF center. This finding holds whether the induction stimulus consists of artificial drifting gratings or naturalistic footage of optic flow through grass. However, despite similar depression of DSGCs immediately after the induction stimuli, DSGC responses during the induction phase exhibit different short-term depression patterns for drifting gratings and optic flow. Drifting gratings at the RF center cause stronger DSGC depression compared to gratings covering both the center and surround; in contrast, optic flow stimuli evoke similar DSGC responses whether the motion is confined to the RF center or includes the surround. Using whole cell recordings, we find that the distinct patterns of spatial-extent dependent depression seen in the DSGC spiking responses are driven by modulation of the DSGC excitatory postsynaptic inputs, and that the dependence of this depression on spatial extent vanishes in the presence of a $GABA_A$ receptor antagonist. These findings together indicate that the presynaptic inhibition of DSGC excitatory inputs are the loci of spatial-extent dependent plasticity in DSGCs. Using a model of di-synaptic depression of a feedforward inhibitory microcircuit, we are able to replicate the different depressive properties of responses to drifting gratings and optic flow. These results reveal how visual stimuli act through a center-surround RF architecture to modulate short-term plasticity, and this mechanism more effectively preserves motion sensitivity in natural scenes compared to drifting gratings. Thus, artificial and natural visual scenes differentially recruit center-surround multi-site plasticity in a manner that is better suited to preserve motion signals in natural scenes.

**Disclosures: T.F. Edington:** None. **S.E. Palmer:** None. **W. Wei:** None.

**Poster**

**PSTR184: Visual Motion**

**Location:** WCC Halls A-C

**Time:** Monday, November 16, 2026, 1:00 PM - 5:00 PM

**Program #/Poster #:** PSTR184.08/AA9

**Topic:** E.06. Vision

**Support:** Simons Foundation Autism Research Initiative (SFARI, 967073)
NSERC Discovery Program (NSERC, RGPIN-2024-06223)
Canada Research Chair Program (CRC-2021-00326)
Ontario Early Researcher Awards program (ER24-18-272)

**Title:** Reliability and electrophysiological correspondence of functional ultrasound imaging in macaque MT/MST

**Authors: *E. RUDOLPH**[1], S. HWANG[2], H. RAMEZANPOUR[3], K. KAR[1];
[1]Biol., York Univ., Toronto, ON, Canada; [2]Biol., York Univ., North York, ON, Canada; [3]Ctr. for Vision Res., York Univ., Toronto, ON, Canada

**Abstract:** Functional ultrasound imaging (fUS) enables high-resolution mapping of stimulus-evoked changes in cerebral blood volume across mesoscopic fields of view in awake, behaving animals. However, for systems neuroscience applications, it remains important to establish what information fUS responses capture, how reliable these responses are across repeated measurements, and how closely they relate to local neuronal activity measured with electrophysiology. Here, we addressed these questions in macaque area MT/MST, a well-characterized dorsal-stream region with robust motion sensitivity. Awake macaque monkeys (n=2) viewed visual motion stimuli that parametrically varied motion evidence while we acquired fUS signals from cortical regions encompassing MT/MST using an Iconeus One system (Iconeus, Paris, France). We quantified stimulus-evoked fUS responses and assessed reliability across repeated stimulus presentations and imaging sessions. Ultrafast plane-wave imaging was performed, and the custom imaging sequence and real-time power Doppler reconstruction were executed using dedicated acquisition software (IcoScan, Iconeus, Paris, France), with an effective functional frame rate of 0.4 sec per frame. To directly evaluate the relationship between fUS signals and local neuronal activity, we also performed single-unit recordings from the same region. This allowed us to compare response functions derived from fUS pixels with neurometric functions derived from neuronal responses. We found that fUS responses in MT/MST were spatially clustered and reliably modulated by visual motion stimuli. Pixel-wise response functions showed graded changes with stimulus strength and were reproducible across measurements. Critically, fUS-derived response functions showed systematic correspondence with neuronal neurometric functions from the same cortical region, indicating that fUS preserves information about local neuronal sensitivity despite measuring a hemodynamic signal at a mesoscopic scale. These results suggest that fUS can provide reliable measurements of stimulus-dependent response structure in macaque MT/MST and recover response profiles related to electrophysiological activity. Taken together, this work evaluates the reliability and electrophysiological correspondence of fUS responses in a well-characterized visual area, clarifying the scale and type of information available from fUS measurements. We also developed fUS-studio, a freely available software environment for visualizing fUS data, generating stimulus-aligned response maps, extracting ROI signals, and comparing voxel-wise responses across conditions.

**Disclosures: E. Rudolph:** None. **S. Hwang:** None. **H. Ramezanpour:** None. **K. Kar:** None.

**Poster**

**PSTR184: Visual Motion**

**Location:** WCC Halls A-C

**Time:** Monday, November 16, 2026, 1:00 PM - 5:00 PM

**Program #/Poster #:** PSTR184.09/AA10

**Topic:** E.06. Vision

**Support:** NIH Grant 5T32EY007043-47

**Title:** Characterizing visual motion discrimination across multidimensional stimulus space using a Wishart process model

**Authors: *C. FRIEDMAN**, E. A. COOPER, J. OTERO-MILLAN;
Herbert Wertheim Sch. of Optometry and Vision Sci., Univ. of California, Berkeley, Berkeley, CA

**Abstract:** Accurate visual motion discrimination is critical for tasks supporting perception of dynamic environments, including object tracking, eye movement control, and self-motion estimation. However, human sensitivity to motion is challenging to study comprehensively because it depends on many stimulus- and observer-related factors. Fully characterizing motion sensitivity using classical psychophysical methods thus requires an untenable number of trials probing all combinations of those factors. Recent work, from the domain of colour vision, suggests that simultaneously characterizing perception across multiple stimulus factors can be achieved efficiently via a Wishart process model that exploits the smoothness of variation in visual sensitivity (Hong et al., 2025). Here, we used this technique to model motion discrimination thresholds across a 2D field of visual motion vectors within the central 2.5deg of the visual field. Four normally-sighted subjects performed an oddball discrimination task using three circular fields of random dots moving coherently according to 2D velocity vectors. Reference stimuli were sampled from a linear grid spanning -8deg/s to 8deg/s on horizontal and vertical axes, and comparator stimuli were sampled in a grid relative to the corresponding reference velocity. The Wishart process model was then fitted to the experimental data to obtain a field of covariance matrices that characterize the observer's internal uncertainty and the corresponding discrimination thresholds across the stimulus space. The resulting psychometric fields yielded preliminary findings that corroborate and extend a range of previous observations about motion sensitivity (Gros et al., 1998; Ball & Sekular, 1982; Matthews & Qian, 1999). Key results included: (1) Speed discrimination thresholds obeyed Weber's law (i.e. increasing linearly with increasing reference speed); however, this pattern is less linear for direction discrimination thresholds. (2) Overall estimates of internal noise were significantly different between cardinal and oblique motion directions. (3) Direction discrimination sensitivity was higher for motion along cardinal directions than for oblique motion, while speed discrimination sensitivity showed no axis-dependent differences. Taken together, these speed and direction sensitivity changes across motion vector space suggest that cortical processing of visual motion

speed and direction may be dissociable. Overall, applying a Wishart process model offers an efficient approach to estimating multidimensional psychometric fields and enables further investigation of visual motion parameterization.

**Disclosures: C. Friedman:** None. **E.A. Cooper:** None. **J. Otero-Millan:** None.

**Poster**

**PSTR184: Visual Motion**

**Location:** WCC Halls A-C

**Time:** Monday, November 16, 2026, 1:00 PM - 5:00 PM

**Program #/Poster #:** PSTR184.10/AA11

**Topic:** E.06. Vision

**Support:** NIH F31 EY036693
NIH R01 EY037544

**Title:** A feedforward mechanism for pattern motion encoding in primary visual cortex

**Authors: *S. M. GANNON**[1], J. MAO[1], J. J. PATTADKAL[3], L. JENNINGS[4], N. J. PRIEBE[5], L. L. GLICKFELD[2];
[2]Neurobio., [1]Duke Univ., Durham, NC; [3]Neurosci., [4]The Univ. of Texas at Austin, Austin, TX; [5]Neurosci., Univ. Texas, Austin, Austin, TX

**Abstract:** Primates and rodents perceive plaids as moving in the pattern direction of motion, which differs from the divergent directions of the component gratings. Classic models argue that pattern motion encoding arises from a two-stage computation where local component direction is represented in primary visual cortex (V1) and then integrated by pattern motion selective neurons in extrastriate cortex. However, accumulating evidence of pattern selective neurons in V1 of both primates and rodents calls this model into question. To determine whether pattern selectivity in V1 reflects the spatially-invariant computation that underlies perception, we measured neural responses in both mouse and marmosets to gratings and plaids in which we varied the starting phase of one of the component gratings. Despite no change to the perceived plaid direction, we find that responses to plaids in V1 neurons in both species are robustly modulated by stimulus phase. While a large fraction of mouse V1 neurons that are component selective at one phase remain so for 3-4 phases (30.2%), only a small fraction of pattern selective cells are similarly phase-invariant (1.9%). This differs from marmoset V1, where a similar number of neurons that are component or pattern selective are phase invariant (14.3%, 17.1%). To probe the mechanisms underlying this phase sensitivity, we built a Hubel and Wiesel-style model where V1 neurons are created by random arrangement of LGN subunit inputs. This model recapitulates phase sensitive pattern selectivity (and relative insensitivity of component cells) and predicts that receptive field characteristics like aspect ratio play a critical role. To test this prediction in vivo, we mapped the linear receptive fields of mouse V1 neurons. To determine if the spatial heterogeneity of the receptive field plays a role in generating phase sensitive pattern selectivity, we parameterized the spatial structure with model fits. We find that in mouse V1,

cells span a continuum between a Gabor and Difference of Gaussians (DoG) shape. Therefore, we fit each cell with a hybrid DoG-Gabor model. Preliminary data suggests both Gabor-like and DoG-like cells undergo modulation and that receptive field parameters, such as aspect ratio, are related to both the mean and modulation of the pattern index across phases. As a next step, we are collecting a comparable dataset from marmoset V1. Overall, our data provides an alternate mechanism for how pattern motion perception arises in V1: we propose that the pattern selectivity in V1 is generated by non-linearities in the feedforward visual pathway and its spatial-dependence must be resolved through downstream circuits to support perception.

**Disclosures: S.M. Gannon:** None. **J. Mao:** None. **J.J. Pattadkal:** None. **L. Jennings:** None. **N.J. Priebe:** None. **L.L. Glickfeld:** None.

**Poster**

**PSTR184: Visual Motion**

**Location:** WCC Halls A-C

**Time:** Monday, November 16, 2026, 1:00 PM - 5:00 PM

**Program #/Poster #:** PSTR184.11/AA12

**Topic:** E.06. Vision

**Support:** NIH Grant UL1TR002529
NSF HDR Grant 2117997
Purdue University, Health of Forces Grant

**Title:** Coordinated modulation of response gain, tuning width, and variability encodes sensory reliability across visual cortex

**Authors: *E. M. EDWARDS**[1], M. LIPTON[1], A. B. SERENO[2,3], M. C. DADARLAT[1]; [1]Biomed. Engin., [2]Psychological Sci., Purdue Univ., West Lafayette, IN; [3]Sch. of Med., Indiana Univ., Indianapolis, IN

**Abstract:** Accurate perception requires the brain to encode not only the identity of sensory features, but also the uncertainty associated with those representations. This computation is central to Bayesian accounts of perceptual decision making in which subjects incorporate both the most probable interpretation and their confidence in that estimate. Theoretical frameworks propose that sensory cortex achieves probabilistic inference by internally representing probability distributions over sensory states. For motion perception, this means encoding the likelihood of all possible movement directions, rather than encoding a single direction estimate. Despite extensive theoretical progress, the neural response properties that implement reliability encoding across sensory cortical hierarchies remain poorly characterized. To address this, we used large-scale two-photon calcium imaging to record populations of neurons across mouse primary and higher visual cortices. During imaging, mice passively viewed random dot kinematograms in which motion coherence was set to four levels (0, 20, 40, 80%), smoothly manipulating the reliability of the directional signal while holding stimulus properties constant. We find that sensory reliability is encoded by single neurons and neural populations through

coordinated changes across three response properties: response gain, directional tuning width, and trial-to-trial variability. Critically, no single property fully accounts for reliability encoding. Rather, these features act jointly to shape population-level representations of motion coherence, contributing independent predictive power for single-trial decoding of motion direction. Further, this multi-dimensional code is shared across all recorded visual areas, suggesting a conserved encoding strategy rather than area-specific computations. Nonetheless, the strength of reliability encoding scales systematically across the visual hierarchy, reflecting differences in directional information content. These results establish a unified, multi-dimensional population code for sensory reliability that is shared across visual cortex and functionally scaled by retinotopic drive and circuit specialization. Ultimately, these findings empirically constrain probabilistic theories of perception and models of visual processing.

**Disclosures: E.M. Edwards:** None. **M. Lipton:** None. **A.B. Sereno:** None. **M.C. Dadarlat:** None.

**Poster**

**PSTR184: Visual Motion**

**Location:** WCC Halls A-C

**Time:** Monday, November 16, 2026, 1:00 PM - 5:00 PM

**Program #/Poster #:** PSTR184.12/AA13

**Topic:** E.06. Vision

**Support:** NSF Grant 2212591
NIGMS Grant 2P20GM103432
NIMH R01MH046742
NINDS R35NS097343

**Title:** Sharpening of direction selective output of Xenopus tadpole tectal neurons is manifested through a developmentally-regulated decrease in their intrinsic excitability

**Authors: *K. ZHENG**[1], Y. MONDAL[2], R. L. CALABRESE[3], K. G. PRATT[4];
[1]Zoology and Physiol., Univ. of Wyoming, Laramie, WY; [2]Biol., Brandeis Univ., Waltham, MA; [3]Biol., Emory Univ., Atlanta, GA; [4]Zoology and Physiol., Univ. of Wyoming Grad. Program In Neurosci., Laramie, WY

**Abstract:** A major function of the amphibian optic tectum (superior colliculus in mammals) is identifying and tracking objects in space, a function that requires direction selective neurons. Here we describe the development of direction selectivity of tectal neurons of the Xenopus tadpole optic tectum. We measured direction selectivity of both synaptic input and action potential (spike) output across 3 key phases of retinotectal circuit formation: developmental stage 42 (approximately 5 days postfertilization, dpf), when the retinal ganglion cell axons have reached the optic tectum and have begun forming nascent synapses, stage 45 (6-7 dpf) characterized by rapid synapse formation and loss, and stage 48 (10-16 dpf), when the retinotectal projection is more refined and supporting several distinct visually guided behaviors.

Direction selectivity was measured by recording tectal neurons while bars of light moving in 4 directions (upward, downward, forward, backward) were projected onto the retina. From these recordings, a direction selectivity index (DSI) was calculated. A DSI ≥ 0.2 was considered direction selective (DS). Overall, DS synaptic input appeared broadly tuned across the three stages of development (average DSI value across stages = 0.26). DS spike output was also broadly tuned at developmental stages 42 and 45, then sharpened significantly between stages 45 and 48 (average DSI values = 0.37 and 0.56, respectively). This means that the neuron receives broadly tuned DS input and transforms it into more sharply tuned output. One mechanism underlying this transformation may involve intrinsic excitability - the ability of neurons to fire action potentials. Between developmental stages 45 and 48, we observed a marked decrease in peak Na+ currents expressed by tectal neurons, suggesting a decrease in intrinsic excitability. Consistent with this, overall spike frequencies were also lower at stage 48. But the magnitude of the decrease in spiking was not symmetrical: spike frequencies elicited by the non-preferred direction of motion were dampened more than those elicited by the preferred direction. This asymmetrical effect on spiking enhanced the difference in spike frequencies between the two directions, leading to higher DSI values. We are exploring whether a simple computational model based on a change in intrinsic excitability across stages can capture our findings.

**Disclosures: K. Zheng:** None. **Y. Mondal:** None. **R.L. Calabrese:** None. **K.G. Pratt:** None.

**Poster**

**PSTR185: Visual Learning, Memory, Categorization, and Processing**

**Location:** WCC Halls A-C

**Time:** Monday, November 16, 2026, 1:00 PM - 5:00 PM

**Program #/Poster #:** PSTR185.01/AA14

**Topic:** E.06. Vision

**Support:** KAKENHI(26K03021)

**Title:** Category separability shapes behaviorally relevant interactions across primate inferior temporal cortex

**Authors: *N. MATSUMOTO**[1], Y. SUGASE-MIYAMOTO[1], B. J. RICHMOND[2], M. A. ELDRIDGE[3,2];
[1]AIST, Tsukuba, Japan; [2]NIMH, Bethesda, MD; [3]Lab. of Neuropsychology, Newcastle Univ., Ponteland, United Kingdom

**Abstract:** Our previous lesion study has shown that removing either area TE or TEO in the inferior temporal (IT) cortex produces mild and similar categorization deficits, whereas removing both TE and TEO leads to severe deficits, suggesting that visual categorization depends on interactions across multiple areas within IT cortex (Setogawa et al., 2021). However, it remains unclear why interactions among areas are important for visual categorization. The difficulty of image categorization may increase the importance of such interactions. We addressed this question by recording simultaneously from neuronal populations in TEO,

posterior TE (pTE), and anterior TE (aTE) in two macaque monkeys performing cat/dog and car/truck categorization. DINOv2 embedding analysis showed that cat and dog images were less separable in feature space than car and truck images, indicating that they were more difficult to categorize. In both monkeys, learning of cat and dog categorization was slower, and performance was lower than for car and truck categorization. We quantified population dynamics using dynamic mode decomposition and summarized image-level interactions in three components: within-area recurrence (RC) in TEO, pTE, and aTE, feedforward (FF) interaction from TEO to pTE, pTE to aTE, and TEO to aTE, and feedback (FB) interaction from aTE to pTE, pTE to TEO, and aTE to TEO. In both monkeys, the categorization performance for cat/dog images was best predicted by within-area RC, whereas that for car/track images was best predicted by FF interaction. To test whether this image-dependent difference could arise from the same underlying attractor network principle, we built a three-area attractor network model based on Wong and Wang (2006). In the model, when category boundaries were hard to distinguish, categorization depended more on within-area RC, whereas when category boundaries were easy to distinguish, it depended more on FF interaction. A related post-lesion version of the same model accounted for the previous finding showing mild impairments after TE or TEO removal and approximately additive effects of combined lesions. Stability analysis showed that single-area lesions preserved stable attractor states in the remaining network, explaining the mild impairments; only the combined removal eliminated all attractor machinery and reduced performance to chance level. Together, these results indicate that category separability determines whether categorization relies more strongly on feedforward interaction or within-area recurrence and provide a circuit-level account of lesion vulnerability in IT cortex.

**Disclosures: N. Matsumoto:** None. **Y. Sugase-Miyamoto:** None. **B.J. Richmond:** None. **M.A. Eldridge:** None.

**Poster**

**PSTR185: Visual Learning, Memory, Categorization, and Processing**

**Location:** WCC Halls A-C

**Time:** Monday, November 16, 2026, 1:00 PM - 5:00 PM

**Program #/Poster #:** PSTR185.02/AA15

**Topic:** E.06. Vision

**Support:** Brain Science and Brain-like Intelligence Technology—National Science and Technology Major Project (2022ZD0204800) to J.C.
National Natural Science Foundation of China (No. 32500930) to J.G.

**Title:** Response format influences transfer in face-view perceptual learning

**Authors: *J. GAO**[1,2], J. LIN[2], Q. LAI[2], J. CHEN[2];
[1]South China Normal Univ., Guangzhou, China; [2]Sch. of Psychology, South China Normal Univ., Guangzhou, China

**Abstract:** Transfer is a hallmark of visual perceptual learning , yet the factors that determine its extent remain poorly understood. Previous studies have primarily examined how stimulus and task characteristics influence transfer, whereas the role of response format has received little attention. Here, we investigated whether response format affects transfer in face-view perceptual learning. Participants performed a face-view discrimination task using three-dimensional face stimuli. On each trial, two face views were presented sequentially, and participants judged whether the second face was rotated more leftward or rightward than the first. Responses were made either by key press or by oral report. Auditory feedback was provided following incorrect responses. In Experiment 1, participants were trained with face views rotated 30° leftward or 30° rightward from the frontal view. Following keypress training, learning transferred to 60° face views but not to the frontal (0°) view. In contrast, oral-report training transferred to both 0° and 60° face views. Moreover, the magnitude of transfer at 0° was significantly greater in the oral-report condition than in the keypress condition. In Experiment 2, participants were trained at the frontal view (0°). Following keypress training, no significant transfer was observed to 45° or 90° face views. In contrast, oral-report training transferred to 45° face views, but not to 90° face views. These results demonstrate that the extent of transfer in face-view perceptual learning depends on response format. Oral-report responses produced broader transfer across viewing angles than keypress responses, identifying response format as an important factor influencing perceptual learning transfer.

**Disclosures: J. Gao:** None. **J. Lin:** None. **Q. Lai:** None. **J. Chen:** None.

**Poster**

**PSTR185: Visual Learning, Memory, Categorization, and Processing**

**Location:** WCC Halls A-C

**Time:** Monday, November 16, 2026, 1:00 PM - 5:00 PM

**Program #/Poster #:** PSTR185.03/Web Only

**Topic:** E.06. Vision

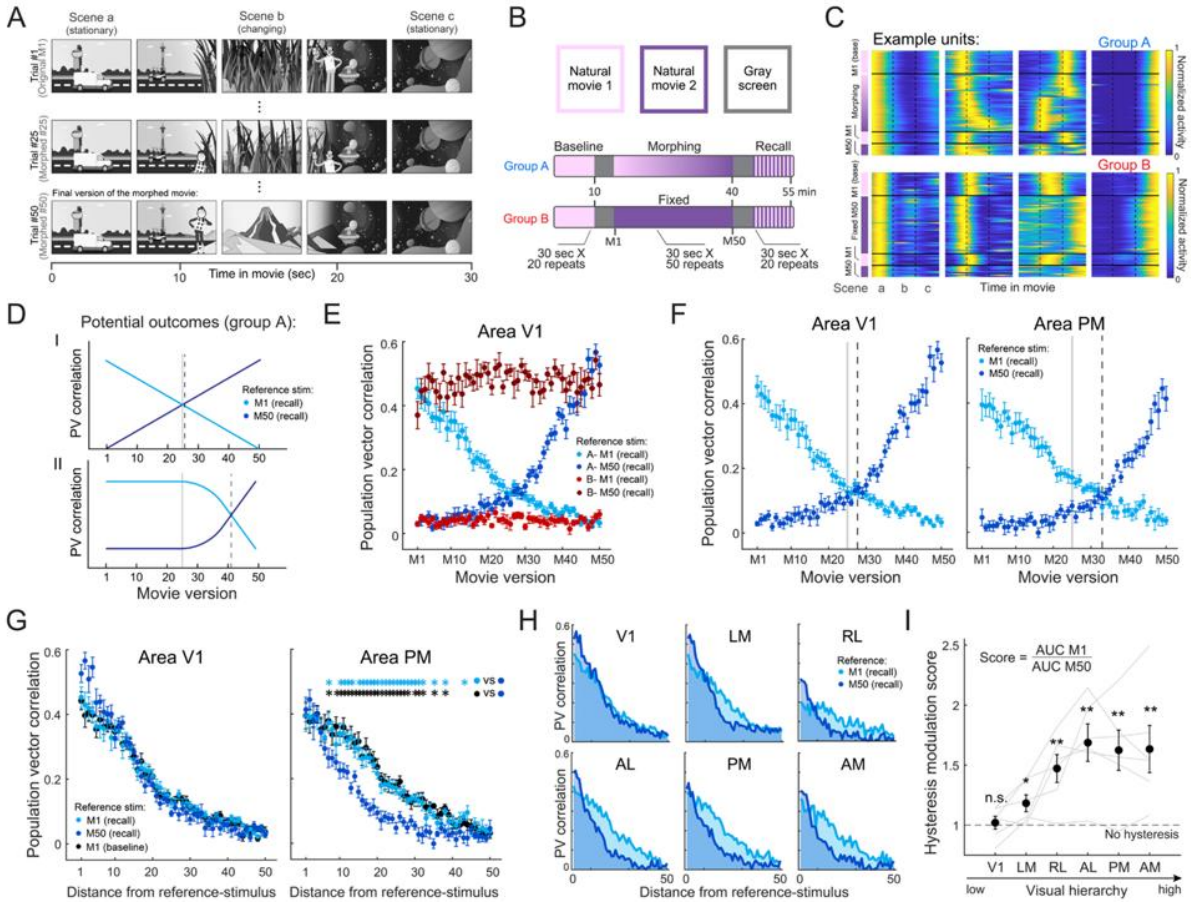
**Support:** OpenScope

**Title:** Lingering visual representations in the face of gradually changing natural stimuli

**Authors: *N. BARNEA**[1], D. DEITCH[2], A. RUBIN[3], Y. ZIV[4];
[1]Brain Sci., [2]Neurobio., [3]Weizmann Inst. of Sci., Rehovot, Israel; [4]The Weizmann Inst. of Sci., Rehovot, Israel

**Abstract:** Perception reflects an interaction between current input and prior experience. While early studies framed the visual cortex as a passive feature detector, subsequent work revealed strong history dependence. Evidence for such history-dependent effects has often come from studies using simple synthetic stimuli leaving the question of how visual representations evolve in a continuously changing world largely unresolved. Here, we recorded the neuronal activity from multiple visual cortical areas in response to a gradually changing natural movie to track how prior experience with a given stimulus affects the degree to which visual representations can

change in the future. We found that while all visual areas exhibited pronounced gradual changes in their representations as the natural movie progressively morphed, the degree by which prior experience with the stimulus impeded these changes increased along the visual hierarchy. Namely, higher-order visual representations are less susceptible to gradual changes in stimuli compared to those of lower visual areas. Overall, our results point to a possible means by which higher visual cortex supports stable perception under varying sensory input.




**Disclosures: N. Barnea:** None. **D. Deitch:** None. **A. Rubin:** None. **Y. Ziv:** None.

**Poster**

**PSTR185: Visual Learning, Memory, Categorization, and Processing**

**Location:** WCC Halls A-C

**Time:** Monday, November 16, 2026, 1:00 PM - 5:00 PM

**Program #/Poster #:** PSTR185.04/AA17

**Topic:** E.06. Vision

**Support:** NIMH R01MH116500

**Title:** Spontaneous Theta Oscillations in the Primary Visual Cortex and their Role in Visual Memory

**Authors: *K. CRAGG**[1], A. A. CHUBYKIN[2];
[2]Biol. Sci., [1]Purdue Univ., West Lafayette, IN

**Abstract:** Spontaneous theta rhythms (4-8 Hz) have been associated with the memory-related functions of the hippocampus (HPC) and have recently been shown to support synchronization between the HPC and other brain regions, including cortical areas. Similar rhythms have also been observed in the primary visual cortex (V1), and their synchronization with the retrosplenial cortex (RSC), which links the HPC to broader cortical regions, suggests they are functionally connected. To address how this functional connectivity may relate to visual learning and memory, we simultaneously recorded from V1 and HPC in Fragile X Syndrome model mice (Fmr1 KO) and wild type controls during a visual learning paradigm. We have developed two different detection algorithms to identify times of spontaneous theta rhythms in V1, which resemble visually evoked familiarity oscillations. Detected events exhibit stimulation dependent increase in their event rate and may suggest a role in the active consolidation of familiar visual stimuli following experience. Furthermore, V1 and HPC synchronize for some event types, during which the HPC theta phase leads V1. Meanwhile for theta oscillations triggered by familiar visual stimuli V1 activity leads the HPC, suggesting that triggered theta travels bottom-up while spontaneous events may travel along the inverse top-down route. Overall, this work identifies one possible mechanism for how cortical representations of visual familiarity coordinate with the HPC to facilitate visual memory encoding.

**Disclosures: K. Cragg:** None. **A.A. Chubykin:** None.

**Poster**

**PSTR185: Visual Learning, Memory, Categorization, and Processing**

**Location:** WCC Halls A-C

**Time:** Monday, November 16, 2026, 1:00 PM - 5:00 PM

**Program #/Poster #:** PSTR185.05/AA18

**Topic:** E.06. Vision

**Support:** R01EY036094
R01NS102917
Rice DPRIT Seed Fund

**Title:** Stable V1 Recordings Across Continual Learning and Sleep Reveal Cortical Reactivation in Freely Moving Mice

**Authors: *X. ZHANG**, P. ZOLOTAVIN, C. XIE, L. LUAN;
Rice Univ., Houston, TX

**Abstract:** How the brain continuously acquires new skills without overwriting previously learned memories — the continual learning problem — remains poorly understood at the circuit

level. While hippocampal replay during sleep is established as a memory consolidation mechanism, how the cortical replay drives learning and representational reorganization in sensory cortex has never been directly tested at single-neuron resolution. This project investigates whether sleep-dependent reactivation in primary visual cortex (V1) supports continual learning by linking cortical reactivation events to behavior performance and population-level representational change.
We developed a freely moving two-alternative forced-choice (2AFC) orientation discrimination task in mice, enabling continuous neural recording across learning and sleep phases within a single daily session. Using 8-shank 256-channel Nanoelectronic Threads (NET) probes, we recorded V1 population activity across 5-hour daily sessions structured as: a passive drifting-grating block (baseline tuning), pre-task sleep, active task performance, and post-task sleep. Live pose estimation (DeepLabCut) and real-time stimulus generation (Unity) enabled automated, place-specific reward delivery. We characterized V1 orientation tuning, analyzed population geometry using linear discriminant analysis (LDA), identified stimulus-selective neurons via a selectivity index, classified sleep states from LFP spectrograms, and detected a synchrony-based reactivation during sleep.
V1 neurons showed orientation and spatial-frequency tuning. LDA embedding revealed well-separated population-level representations across grating orientations and spatial frequencies. Task-relevant neurons showed distinct differential responses to task visual stimuli. Sleep state classification from LFP spectrograms reliably distinguished sleep epochs from waking. Candidate reactivation events were identified as high-synchrony bursts among stimulus-selective neurons during sleep. Ongoing analyses characterize representational drift across learning days and correlate reactivation properties with behavioral performance.
Together, these results establish the technical and analytical foundation for directly testing whether cortical reactivation drives continual learning in V1, using stable large-scale single-unit recordings across the complete learning-sleep cycle.

**Disclosures: X. Zhang:** None. **P. Zolotavin:** E. Ownership Interest (stock, stock options, royalty, receipt of intellectual property rights/patent holder, excluding diversified mutual funds); NeuralThread Inc. **C. Xie:** E. Ownership Interest (stock, stock options, royalty, receipt of intellectual property rights/patent holder, excluding diversified mutual funds); NeuralThread Inc. **L. Luan:** E. Ownership Interest (stock, stock options, royalty, receipt of intellectual property rights/patent holder, excluding diversified mutual funds); NeuralThread Inc.

**Poster**

**PSTR185: Visual Learning, Memory, Categorization, and Processing**

**Location:** WCC Halls A-C

**Time:** Monday, November 16, 2026, 1:00 PM - 5:00 PM

**Program #/Poster #:** PSTR185.06/AA19

**Topic:** E.06. Vision

**Title:** Linking neural representations to behavior using generalization

**Authors: *M. A. NUÑEZ**[1], F. DU[1], L. ZHONG[1], S. SCHRÖDER[2], C. STRINGER[1], M. PACHITARIU[1];
[1]Janelia Res. Campus, Ashburn, VA; [2]Neurosci., Univ. of Sussex, Brighton, United Kingdom

**Abstract:** Sensory-guided decisions are the result of sensorimotor transformations across many brain areas. Recent studies have localized the motor- and decision-related components of these transformations using brain-wide neural recordings. It has been more difficult to localize sensory computations in the same way. Here we developed a new approach for linking sensory computations to behavior by training mice to discriminate between two stimuli and testing their responses with new stimuli. In separate animals, we calculated the similarity of neural representations between train and test stimuli, using recordings of up to 73,000 simultaneously-recorded neurons from 9 primary and higher-order visual areas (HVAs) across layers 2 and 3. We found that neural discrimination on test but not train images correlated with behavioral discrimination, and this relation required prior visual experience as it was not present in dark-reared mice. The link between neural and behavioral performance was highest in the medial HVAs, suggesting this region is a critical component of sensory transformations and generalization. We extended this work by directly training mice to generalize: presenting mice 100 different instances from two different texture classes, and only rewarding instances from one texture class. The mice learned this task within 10 days. We observed generalization-related changes in the neural activity across brain regions, which required task engagement even after training.

**Disclosures: M.A. Nuñez:** None. **F. Du:** None. **L. Zhong:** None. **S. Schröder:** None. **C. Stringer:** None. **M. Pachitariu:** None.

**Poster**

**PSTR185: Visual Learning, Memory, Categorization, and Processing**

**Location:** WCC Halls A-C

**Time:** Monday, November 16, 2026, 1:00 PM - 5:00 PM

**Program #/Poster #:** PSTR185.07/AA20

**Topic:** E.06. Vision

**Support:** National Eye Institute Intramural Research Program at the National Institutes of Health (NIH, grant no. 1ZIAEY000570-01 to H.N.)

**Title:** Cortical face selectivity extends far into the visual periphery

**Authors: *A. ROSEMAN**[1], C. M. ZIEMBA[1], K. W. KOYANO[2,3], C. GREGG[2], H. KATTI[2], D. A. LEOPOLD[2], H. NIENBORG[1];
[1]Lab. of Sensorimotor Research, Natl. Eye Institute, NIH, Bethesda, MD; [2]Systems Neurodevelopment Laboratory, NIMH, Bethesda, MD; [3]Advanced Neuroimaging Ctr., Natl. Inst. for Quantum Sci. and Technol., Chiba-Shi, Japan

**Abstract:** Although peripheral vision is less detailed than central vision, we can identify important stimuli, like faces, when presented far from the center of gaze. However, the neural

mechanisms of face perception have been studied almost entirely near the fovea. Here, we recorded neural activity from macaque cortical face patches while presenting stimuli on a full-field, hemispheric dome display to investigate the strength and feature selectivity of face preference across nearly the entire visual field. We implanted microwire brush arrays in three fMRI-targeted face patches in two monkeys: The anterior medial face patch (AM) in inferotemporal cortex, the perirhinal face patch (PRh), and the prefrontal orbital face patch (PO). Monkeys fixated a central point while we briefly flashed images centered at different visual field locations spanning 0-80 degrees eccentricity. Images consisted of human faces, macaque faces, and non-face object images. We found that the face preference of neural populations from all areas was present in the far periphery, often up to the furthest eccentricities measured. Although selectivity was overall weaker compared to the fovea, we found that the pattern of population activity that distinguished faces and nonfaces did not differ between stimuli presented at the fovea or far in the periphery. To test the complexity of the features driving face selectivity, we created scrambled counterparts for each natural image using a synthesis procedure that disrupts higher-order visual features while maintaining low- and mid-level features. These scrambled stimuli are known to elicit similar neural responses in early visual cortex and match peripheral appearance compared to natural images under some circumstances. We found that scrambling caused a complete loss of category selectivity in PO, but a milder decrease in AM and PRh. Reductions in selectivity from scrambling were similar across the fovea and periphery, indicating that peripheral selectivity is not fully accounted for by low level features. These results indicate that the cortex maintains stable and highly selective responses to faces presented far in the visual periphery.

**Disclosures: A. Roseman:** None. **C.M. Ziemba:** None. **K.W. Koyano:** None. **C. Gregg:** None. **H. Katti:** None. **D.A. Leopold:** None. **H. Nienborg:** None.

**Poster**

**PSTR185: Visual Learning, Memory, Categorization, and Processing**

**Location:** WCC Halls A-C

**Time:** Monday, November 16, 2026, 1:00 PM - 5:00 PM

**Program #/Poster #:** PSTR185.08/AA21

**Topic:** E.06. Vision

**Title:** Visual coherence shapes the emergence of face pareidolia during early visual processing

**Authors: *S. CHEN**, A. K. ROBINSON, A. PEGNA, Z. YU, J. TAUBERT;
The Univ. of Queensland, St Lucia, Australia

**Abstract:** Face pareidolia refers to the phenomenon of perceiving illusory faces in everyday objects. Although the illusion of a face is thought to emerge rapidly, the visual mechanisms that support its formation remain poorly understood. We combined behavioral and electroencephalography (EEG) approaches to examine how object category (pareidolia images and control objects) and visual coherence (intact and scrambled) influence early visual formation of illusory faces. Behaviorally, intact pareidolia images were reliably identified as containing

both face and object information; scrambling pareidolia images only reduced the face information, demonstrating that spatial configuration is critical for the illusion. The ERP results revealed that the P1 component was sensitive to visual coherence but not object category, as evidenced by an enhanced P1 amplitude for intact compared to scrambled stimuli, regardless of the object category. This suggests that early visual responses reflect global image structure. In contrast, the N170 showed enhanced responses to pareidolia images relative to control objects during an active task, consistent with attention contributing to the perception of illusory facial features. Time-resolved decoding analyses further demonstrated that both image coherence and object category could be discriminated from neural activity beginning as early as 70 ms after stimulus onset. In contrast, decoding accuracy for scrambled images did not exceed chance levels at any time point. This indicates that scrambling abolished category-specific neural representations. Together, these findings suggest that global visual coherence is a prerequisite for face pareidolia and that early visual processing is initially driven by image structure before the emergence of face-like representations. The results provide new insight into how local object features are integrated to generate coherent percepts from ambiguous visual input.

**Disclosures: S. Chen:** None. **A.K. Robinson:** None. **A. Pegna:** None. **Z. Yu:** None. **J. Taubert:** None.

**Poster**

**PSTR185: Visual Learning, Memory, Categorization, and Processing**

**Location:** WCC Halls A-C

**Time:** Monday, November 16, 2026, 1:00 PM - 5:00 PM

**Program #/Poster #:** PSTR185.09/AA22

**Topic:** E.06. Vision

**Support:** Hitchcock Foundation to BD

**Title:** Visualizing face distortions: Prosopometamorphopsia as a window into human face perception

**Authors: *B. DUCHAINE**[1], A. REIS GONÇALVES MELLO[1], S. FORTNER[2], A. KIDDER[3]; [1]Psychological and Brain Sci., Dartmouth Col., Hanover, NH; [2]Univ. of California, Santa Barbara, Santa Barbara, CA; [3]Dartmouth College/NIMH, Akron, NY

**Abstract:** Prosopometamorphopsia (PMO) is a visual perceptual disorder in which faces are seen as distorted. Fewer than 100 cases of PMO have been described in the literature, and most reports have been brief single-case descriptions. However, because our laboratory has been contacted by more than 270 individuals who have experienced face distortions, we have been able to conduct detailed investigations of PMO as a means to better understand typical face perception and to evaluate interventions that reduce distortions. Here, we present visualizations depicting face distortions perceived by 20 individuals with PMO, accompanied by descriptions of their case histories. Our goal is to provide neuroscientists and healthcare professionals with images that communicate the character and severity of the distortions experienced in PMO.

Although distortions of face shape have been emphasized most often in previous reports, the distortions experienced by our participants frequently affect other dimensions of facial appearance, including the texture, color, and depth of facial surfaces. In some individuals, faces are altered so profoundly that judgments about age, sex, and gaze direction are severely impaired. The heterogeneity of PMO revealed by the visualizations means that experimental tasks often need to be adapted for individual participants, but this variability also provides opportunities to address a variety of theoretical questions in visual neuroscience. Many participants have reported that their descriptions of face distortions were dismissed or misunderstood in clinical contexts, and some were prescribed antipsychotic medication because their perceptual experiences were interpreted as evidence of broader psychiatric disturbance. These experiences underscore the need for greater clinical awareness of PMO. By disseminating these visualizations, we hope to encourage neuroscientists to conduct studies with PMO participants and to promote more accurate recognition of PMO and improved care for affected individuals.




**Disclosures: B. Duchaine:** None. **A. Reis Gonçalves Mello:** None. **S. Fortner:** None. **A. Kidder:** None.

**Poster**

**PSTR185: Visual Learning, Memory, Categorization, and Processing**

**Location:** WCC Halls A-C

**Time:** Monday, November 16, 2026, 1:00 PM - 5:00 PM

**Program #/Poster #:** PSTR185.10/AA23

**Topic:** E.06. Vision

**Support:** NIH/NEI (R01-EY037195)
NIH/NIMH (R01-MH122258)
NIH/NIMH (R01-MH120194)
NIH/NINDS (R21-NS128307)

NIH/NINDS (U01-NS128612)
NIH/NINDS (U01-NS108916)
NIH/NINDS (U24-NS109103)
NIH/NIBIB (R01-EB026439)
NIH/NIBIB (P41-EB018783)
Fondazione Neurone
McDonnell Center for Systems Neuroscience
NIH/NEI (K99-EY036650)
Brain and Behavior Research Foundation

**Title:** A neurocomputational network for face processing

**Authors: *Y. LI**[1], Y. WANG[2], J. ZHANG[3], H. CHO[6], P. BRUNNER[4], J. T. WILLIE[7], J. THUM[8], R. CAO[3], S. WANG[5];
[1]Biomed. Engin., Washington Univ. in St Louis, St Louis, MO; [2]NIL, [3]Radiology, [4]Dept. of Neurosurg., Washington Univ. in St. Louis, St. Louis, MO; [5]Washington Univ. in St. Louis, Saint Louis, MO; [6]Neurosurg., [7]Neurolog. Surgery, Washington Univ. Sch. of Med., Saint Louis, MO; [8]Neurosurg., Univ. of Alabama, Birmingham, Birmingham, AL

**Abstract:** The fusiform gyrus (FG) encodes visual features to represent face identities, yet how these representations are transmitted to downstream regions to support distinct cognitive demands remains poorly understood. Here, we combined intracranial electroencephalography (iEEG) and single-neuron recordings in neurosurgical patients, as well as fMRI in healthy participants during face viewing, to characterize how the FG is functionally embedded within the distributed face-processing network. Consistent with recent intracranial studies, we identified FG channels that linearly encoded feature axes, exhibiting axis-based feature coding. These axis-coding channels showed markedly stronger theta-band (3-8 Hz) phase synchronization than non-axis-coding FG channels with a distributed set of higher-order face-processing regions, including the amygdala, superior temporal sulcus (STS), medial temporal gyrus (MTG), medial temporal cortex (MTC), ventrolateral prefrontal cortex (VLPFC), and orbitofrontal cortex (OFC), beginning shortly after stimulus onset. At the cellular level, neurons in the amygdala and hippocampus were preferentially phase-locked to FG axis-coding channels, indicating that local FG visual codes are read out by medial temporal lobe (MTL) neurons through low-frequency coherence. Critically, FG connectivity reorganized as a function of the information being processed: familiarity-coding channels in the amygdala and OFC showed stronger synchronization with FG, and at the single-neuron level, hippocampal but not amygdala neurons exhibited familiarity-enhanced phase locking with the FG, OFC, and VLPFC. Social trait-coding channels in the amygdala, rostral middle frontal cortex (RFC), and OFC showed stronger FG synchronization, while the thalamus and dorsal pathway, including the inferior parietal lobule (IPL) and superior parietal lobule (SPL), exhibited stronger desynchronization. Phase slope index analyses revealed that feedforward signaling from FG to downstream regions dominated these interactions across both identity and familiarity networks. Independent fMRI functional connectivity analyses converged on this network architecture. Together, these findings identify the FG as a flexible routing hub that dynamically coordinates with distinct downstream targets depending on whether visual identity, familiarity, or social trait is being computed. Our results provide a multimodal, multiscale framework that links localized visual feature representations to distributed circuits, supporting flexible perception, memory, and social cognition.

**Disclosures: Y. Li:** None. **Y. Wang:** None. **J. Zhang:** None. **H. Cho:** None. **P. Brunner:** None. **J.T. Willie:** None. **J. Thum:** None. **R. Cao:** None. **S. Wang:** None.

**Poster**

**PSTR185: Visual Learning, Memory, Categorization, and Processing**

**Location:** WCC Halls A-C

**Time:** Monday, November 16, 2026, 1:00 PM - 5:00 PM

**Program #/Poster #:** PSTR185.11/AA24

**Topic:** E.06. Vision

**Title:** Color robustly modulates the intensity of face distortions in prosopometamorphopsia

**Authors: *A. REIS GONÇALVES MELLO**[1], D. GARSIDE[2], D. STEHR[1], B. R. CONWAY[2], B. DUCHAINE[1];
[1]Dartmouth Col., Hanover, NH; [2]NIH, Bethesda, MD

**Abstract:** Prosopometamorphopsia (PMO) is a striking visual disorder in which faces appear distorted, sometimes alongside weaker distortions to non-face objects. Individuals with PMO often find the distortions disturbing, so methods to alleviate them would be valuable. Some individuals have informally reported that hue seems to modulate the intensity of their distortions, but it is unclear whether these putative effects are real and independent of other factors influencing the color appearance of faces, such as luminance and saturation. Here, we investigated this question in four cases of PMO - V.S. (59-year-old man), Nagel (39-year-old man), Ezri (32-year-old woman), and A.S. (57-year-old woman) - using a replicated single-case experimental design (SCED). Each participant viewed live faces and non-face stimuli (hands, a human-like doll, and a ball) through combinations of colored and neutral-density filters that allowed us to test the impact of hue while controlling for lightness and chroma. Specifically, we tested perception through a neutral filter (control) and through filters of eight hues that evenly sampled the CIELAB color space at two lightness levels (L* = 53, 73) and two chroma levels (C* = 32, 52). Participants rated the intensity of distortions on a scale from zero ("no distortions") to six ("extreme distortions") across 270 randomized face trials and 180 randomized non-face trials. Regression models tailored for SCEDs showed that specific hues significantly modulated face distortions in three cases, even when accounting for lightness, chroma, and face identity (V.S., Nagel, and Ezri: all $F(8, 258) \geq 18.23$, $p < .001$); no color effects were observed for A.S. Surprisingly, cool and warm colors had opposite effects across cases. For example, for V.S. and Nagel, green and cyan decreased face distortions while pink and red increased them ($p < .05$); for Ezri, green and cyan increased face distortions while pink decreased them ($p < .01$). To illustrate these effects, we produced photorealistic visualizations of V.S.'s face distortions viewed through red and green filters, leveraging the unusual feature in his case where distortions do not appear on screens (Mello et al., 2024). Although Nagel and Ezri also perceived distortions in non-face stimuli, permutation regressions revealed no reliable hue effects on these distortions. These results indicate that hue can robustly modulate distortions in some cases of PMO, that this modulation appears specific to faces, and that the interaction of color and face distortions shows

substantial individual differences. In addition, they suggest that color may be tightly linked with face perception in typical visual systems.

**Disclosures: A. Reis Gonçalves Mello:** None. **D. Garside:** None. **D. Stehr:** None. **B.R. Conway:** None. **B. Duchaine:** None.

**Poster**

**PSTR185: Visual Learning, Memory, Categorization, and Processing**

**Location:** WCC Halls A-C

**Time:** Monday, November 16, 2026, 1:00 PM - 5:00 PM

**Program #/Poster #:** PSTR185.12/AA25

**Topic:** E.06. Vision

**Support:** NIMH Grant R21 MH129902

**Title:** BOLD response in early visual cortex following self-initiated vs. uncontrolled visual change

**Authors: *A. ALVAREZ HERNANDEZ**[1], C. Y. SANDER[2], J. THERIAULT-BROWN[1]; [1]Northeastern Univ., Boston, MA; [2]Radiology, A. A. Martinos Ctr. for Biomed. Imaging, Dept. of Radiology, Massachusetts Gen. Hosp., Charlestown, MA

**Abstract: Background:** In daily life, people exercise some control over the visual input they receive, sampling scenes at their own pace. By contrast, experimental situations, such as in-scanner screen, involve something unusual for the brain: Visual input is projected instantaneously onto the fovea. This is common in fMRI research, where the stimulus elicited BOLD response is taken to represent features of the presented stimulus. But the BOLD response may be affected by the extent of subject control over sensory input. Predictive coding accounts suggest that predictable and unpredictable sensory inputs may be processed differently; motor commands can affect sensory processing via efferent copies. We leveraged this sensorimotor link to present visual input initiated by the subject or by an uncontrolled transition. We hypothesized that subject-initiated visual change would suppress a stimulus-elicited BOLD response compared to an uncontrolled transition.**Methods:** Subjects (N=8) watched a naturalistic, first-person video of a walk through a natural scene. Throughout the video, following a cue, subjects could initiate a visual change to a black screen (fixation) with a button press (self-initiated; 6 events x 2 runs). At other times, fixation interrupted the video without subject input (uncontrolled; 6 events x 2 runs). A key element of the GLM was to set the video as an active baseline (instead of the static black fixation), to see how self-initiated vs. uncontrolled changes in visual input affect BOLD response from a naturalistic baseline. BOLD response in early visual cortex was compared between conditions.**Results:** Uncontrolled transitions to fixation, relative to the active video baseline, elicited a BOLD increase in peripheral visual cortex (V1, V2, V3), and a substantial decrease below in foveal visual cortex. This result was consistent with prior work using uncontrolled transitions in a larger sample (Theriault et al., under review). By contrast, subject-initiated transitions to fixation showed neither the foveal BOLD decrease, nor the peripheral

BOLD increase observed for the uncontrolled transition. Transitions from fixation to the video baseline (all uncontrolled) were equivalent following uncontrolled and subject-initiated transitions, showing the expected pattern of BOLD increase in foveal visual cortex (V1, V2, V3).**Conclusion**: Visual stimulus-elicited BOLD response may be modulated by expectation of change. Unexpected visual input that is not linked to a motor command through an efferent copy is associated with stronger positive and negative BOLD responses. When sensorimotor link exists the pattern of BOLD responses closely resemble baseline.

**Disclosures: A. Alvarez Hernandez:** None. **C.Y. Sander:** B. Contracted Research/Research Grant (principal investigator for a drug study, collaborator or consultant and pending and current grants). If you are a PI for a drug study, report that research relationship even if those funds come to an institution.; National Institute of Mental Health, National Institute of Health. **J. Theriault-Brown:** B. Contracted Research/Research Grant (principal investigator for a drug study, collaborator or consultant and pending and current grants). If you are a PI for a drug study, report that research relationship even if those funds come to an institution.; National Institute of Mental Health.

**Poster**

**PSTR185: Visual Learning, Memory, Categorization, and Processing**

**Location:** WCC Halls A-C

**Time:** Monday, November 16, 2026, 1:00 PM - 5:00 PM

**Program #/Poster #:** PSTR185.13/AA26

**Topic:** E.06. Vision

**Support:** NIH R01EY033835

**Title:** Functional Development of Visual Category-Selective Regions from Infancy to Childhood is Linked to Microstructural Proliferation

**Authors: *C. TYAGI**[1,2], V. S. NATU[1], D. ORTIZ[1], J. HORENZIAK[1], K. PEREZ[1], C. LIAO[3], K. GRILL-SPECTOR[1];
[1]Psychology, Stanford Univ., Stanford, CA; [2]Psychology, Ohio State Univ., Columbus, OH; [3]Radiology, Univ. of California, San Francisco, San Francisco, CA

**Abstract:** How do category-selective regions develop from infancy to childhood? Infant fMRI studies have localized category-selectivity in the parcels where they are found in adulthood. Concurrent fMRI and quantitative MRI (qMRI) studies in children have shown that different category-selective regions have differential rates of development into adolescence, which are linked to regional differences in microstructural proliferation as measured by tissue relaxation rate R1 ([s-1]). However, the developmental trajectories of category-selectivity from infancy to childhood and the potential role of microstructure in early development remain unknown. To address these gaps, we collected fMRI data using a dedicated infant coil from 13 infants ($N_{Female}$ = 5) between the ages of 3 and 6 months while they viewed colorful videos and grayscale images from 4 visual categories: faces, body parts, objects, and places. Conditions were presented in

randomized order in 16s blocks, and blank baseline presentations were interspersed between stimulus presentations. From 10 of the 13 infants, we obtained R1 measures using a qMRI fingerprinting sequence. We also incorporated an existing dataset of 27 school-age children ($N_{Female}$ = 16, ages 5-12 years) containing R1 and fMRI data during viewing of the same grayscale images. We find face-selectivity in the fusiform gyrus of 10/13 infants and 26/27 children, place-selectivity in the collateral sulcus of 4/13 infants and 27/27 children, and body-selectivity in the occipitotemporal sulcus of 7/13 infants and 25/27 children. To assess development in the regions that will eventually become category-selective in adulthood, we projected adult category-selective regions from the Kubota atlas to each individual's cortex using cortex-based alignment. We find that face-, limb-, and place-selectivity increase with age, independent of signal-to-noise ratio. This increase in selectivity is coupled with increases in the amplitude of response to the preferred category. In the same regions, we find that R1 increases with age, and these microstructural increases are linked to the development of category-selectivity.

**Disclosures: C. Tyagi:** None. **V.S. Natu:** None. **D. Ortiz:** None. **J. Horenziak:** None. **K. Perez:** None. **C. Liao:** None. **K. Grill-Spector:** None.

**Poster**

**PSTR185: Visual Learning, Memory, Categorization, and Processing**

**Location:** WCC Halls A-C

**Time:** Monday, November 16, 2026, 1:00 PM - 5:00 PM

**Program #/Poster #:** PSTR185.14/AA27

**Topic:** E.06. Vision

**Support:** ERC 2019-SyG-RELEVANCE-856495
KU Leuven Grant C14/21/111

**Title:** Mixed Representation of Primate Species Identity and Body Posture in the Macaque Superior Temporal Sulcus

**Authors: *A. BOGNÁR**[1], L. MARTINI[3], N. TAUBERT[4], M. A. GIESE[5], R. VOGELS[2]; [2]Neurosciences, [1]KU Leuven, Leuven, Belgium; [3]Hertie Inst. for Clin. Brain Res., Hertie Inst. for Clin. Brain Res., Tübingen, Germany; [4]Hertie Inst. for Clin. Brain Res., Tuebingen, Germany; [5]Dept N3, CIN / HIH, Univ. of Tuebingen, Tuebingen, Germany

**Abstract:** Bodies provide primates with information not only about posture, which is relevant for interpreting action, intention, and affect, but also about identity, such as species identity. Shape features play an important role in signaling these behaviorally relevant dimensions. In macaques, body shape is analyzed in the ventral bank of the Superior Temporal Sulcus (STS). It is unclear whether the STS neurons analyze shape with identity and posture as separable dimensions. To assess this, we generated body images depicting 5 postures of each of 5 primate species: rhesus macaque, chimpanzee, orangutan, lemur, and human. Starting from a macaque computer graphics model, the other species' meshes were aligned using multi-view anatomical

correspondences derived from the BigMaQ dataset (Martini et al., ICLR, 2026). Species-specific skeletons were retargeted and reskinned in Autodesk Maya to the macaque reference skeleton. Naturalistic macaque postures were then transferred to all aligned species models, yielding matched body postures that differed only in species identity. To minimize differences in viewpoint and scale, meshes were normalized in 3D space before perspective rendering. The 25 bodies were presented from two 3D viewpoints, each also shown mirrored. We recorded from the middle ventral bank of the STS, targeting the middle STS body patch, and the anterior STS at the level of the anterior STS body patch using Neuropixels.Two-way ANOVAs showed that the large majority of middle STS units (Kilosort4 sorted single and multi-units; n =2236; 2 monkeys) had significant main and interaction effects of the factors identity and posture. We assessed whether posture could be decoded in a species-invariant manner, and vice versa, using a cross-decoding approach. We trained a linear classifier to decode posture for one species and then tested the decoding of posture for the same and for the other species (100 resamplings of 100 units). Posture decoding generalized only partially across species, with higher performance for within-species than for cross-species testing (mean within-species: 97 % correct; cross-species accuracy: 58%), the latter depending on species differences (range cross-species decoding: 44-75%). Decoding of species showed poorer generalization across postures (mean within-posture: 95 %, cross-posture accuracy: 42% (range: 33-59%)). Anterior STS (n= 387; 1 monkey) showed a similar pattern, but with less difference between the two cross-decodings. These data suggest that posture and species identity are encoded in a mixed fashion in the ventral STS.

**Disclosures: A. Bognár:** None. **L. Martini:** None. **N. Taubert:** None. **M.A. Giese:** None. **R. Vogels:** None.

**Poster**

**PSTR185: Visual Learning, Memory, Categorization, and Processing**

**Location:** WCC Halls A-C

**Time:** Monday, November 16, 2026, 1:00 PM - 5:00 PM

**Program #/Poster #:** PSTR185.15/AA28

**Topic:** E.06. Vision

**Support:** NIMH R01MH132225

**Title:** Visual category selectivity predicts divergent aperiodic dynamics across controlled and naturalistic viewing in human intracranial EEG

**Authors: *M. RICHEY**[1], S. WALLS[2], T. J. ABEL[1], A. S. GHUMAN[2];
[1]Dept. of Neurolog. Surgery, [2]Neurolog. Surgery, Univ. of Pittsburgh, Pittsburgh, PA

**Abstract:** The relationship between the aperiodic 1/f component of neural activity and perceptual, cognitive, and behavioral response is actively debated. In particular, the extent to which task-dependent modulation of this component scales with regional category selectivity across paradigms with contrasting stimulus ecologies, such as standard category localizers versus

complex naturalistic scenes, has yet to be characterized. We recorded iEEG data from 64 left temporal electrodes in one patient performing both a Visual Category Localizer (VCL) and a Naturalistic Affective Scene Viewing (NASV) task. Using multivariate machine learning approaches, VCL category selectivity was indexed by peak cross-validated d' across six visual categories; electrodes with peak d'>=1.0 were defined as selective. The task-evoked change in aperiodic exponent (Delta 1/f, post-stimulus minus baseline; FOOOF fixed fit, 3-50 Hz) was computed per electrode for each paradigm.
VCL d' predicted NASV Delta 1/f ($r=-0.745$, $p=1.72\times10^{-12}$, $n=64$), indicating that aperiodic responses during naturalistic scene viewing carried information about independently defined visual category selectivity. Consistent with this, NASV Delta 1/f distinguished VCL-selective from non-selective contacts (AUC=0.959, permutation $p<0.0001$). All 25 VCL-selective electrodes showed negative NASV Delta 1/f (mean=-0.352) versus non-selective electrodes (mean=-0.090, n=39), and this relationship persisted after controlling for 11 spectral and data-quality covariates (partial $r=-0.378$; permutation $p=0.002$). Although VCL Delta 1/f averaged across all categories did not correlate with d' ($r=+0.126$, $p=0.321$), VCL Delta 1/f from each electrode's strongest category showed an opposite-sign relationship with d' ($r=+0.265$, $p=0.034$); Delta 1/f averaged across the other five categories did not ($r=+0.062$, $p=0.624$).
These preliminary results suggest that stimulus ecology biases the direction of aperiodic modulation in visually selective cortex. VCL isolates category discrimination under controlled stimulus conditions, whereas NASV embeds visual processing within complex naturalistic scenes that may engage broader cortical state dynamics. Stronger VCL-defined category selectivity was associated with aperiodic flattening during NASV, but relative steepening during strongest-category VCL responses. This divergence is compatible with recent work linking aperiodic slope to cognitive state and arousal dynamics, and suggests that category-selective temporal contacts may be preferentially engaged in context-dependent cortical state modulation across controlled and naturalistic viewing.

**Disclosures: M. Richey:** None. **S. Walls:** None. **T.J. Abel:** None. **A.S. Ghuman:** None.

**Poster**

**PSTR185: Visual Learning, Memory, Categorization, and Processing**

**Location:** WCC Halls A-C

**Time:** Monday, November 16, 2026, 1:00 PM - 5:00 PM

**Program #/Poster #:** PSTR185.16/AA29

**Topic:** E.06. Vision

**Title:** A Neurocomputational Framework for Object Processing

**Authors: *Y. WANG**[1], Y. LI[1], J. ZHANG[1], H. CHO[2], P. BRUNNER[3], J. WILLIE[4,1], J. THUM[5], R. CAO[1], S. WANG[1];
[1]Washington Univ. in St.Louis, St. Louis, MO; [2]Neurosurg., Washington Univ. Sch. of Med., Saint Louis, MO; [3]Dept. of Neurosurg., Washington Univ., St. Louis, MO; [4]UT Southwestern Med. Ctr. at Dallas, Dallas, TX; [5]Neurosurg., Univ. of Alabama, Birmingham, Birmingham, AL

**Abstract:** Localized visual features are encoded within the ventral temporal cortex (VTC) to represent object identities, yet how these representations are dynamically routed to downstream regions to flexibly support distinct cognitive demands remains a fundamental question. Integrating human intracranial electroencephalography (iEEG) and single-neuron recordings in neurosurgical patients with functional MRI in healthy participants, we map the multiscale network architecture embedding the VTC during object viewing. We demonstrate that VTC channels exhibiting axis-based feature coding act as communication hubs; shortly after stimulus onset, these channels initiate robust theta-band (4-8 Hz) phase synchronization with a distributed set of higher-order object-processing regions, explicitly involving the amygdala, insula, superior temporal sulcus (STS), middle temporal gyrus (MTG), medial temporal cortex (MTC), ventrolateral prefrontal cortex (VLPFC), orbitofrontal cortex (OFC), and rostral middle frontal cortex (RFC). At the cellular level, individual neurons in the amygdala and hippocampus preferentially phase-lock to these axis-coding VTC channels, providing direct evidence that local visual codes are read out via low-frequency coherence. Specifically, this routing architecture flexibly reorganizes as a function of cognitive demand: when processing behavioral memorability, memorability-coding channels within the amygdala, OFC, and STS selectively amplify their synchronization with the VTC. At the single-neuron level, this cognitive modulation manifests as memorability-enhanced phase locking within distinct sub-circuits—specifically between amygdala neurons and the VTC, OFC, and between hippocampal neurons and the VTC, insula. To validate these patterns, we examined convergent functional connectivity in an independent NSD fMRI dataset, confirming that axis-coding FG voxels show elevated connectivity with frontal areas. This supports the view of the VTC as a flexible routing engine. Depending on whether the task demands processing visual identity or memorability, the VTC selectively engages different downstream targets, demonstrating how localized visual representations plug into large-scale circuits to guide flexible thought.

**Disclosures: Y. Wang:** None. **Y. Li:** None. **J. Zhang:** None. **H. Cho:** None. **P. Brunner:** None. **J. Willie:** None. **J. Thum:** None. **R. Cao:** None. **S. Wang:** None.

**Poster**

**PSTR185: Visual Learning, Memory, Categorization, and Processing**

**Location:** WCC Halls A-C

**Time:** Monday, November 16, 2026, 1:00 PM - 5:00 PM

**Program #/Poster #:** PSTR185.17/AA30

**Topic:** E.06. Vision

**Support:** NIH Grant R01EY023915 to KGS
Bio-X Stanford Interdisciplinary Graduate Fellowship to YS

**Title:** Retinal sampling drives eccentricity-dependent receptive field organization and foveal-peripheral category biases in a topographic model of the ventral visual system

**Authors: *Y. SHAH**[1], K. GRILL-SPECTOR[2];
[1]Computer Sci., [2]Psychology, Stanford Univ., Stanford, CA

**Abstract:** The primate ventral visual stream exhibits a rich hierarchy of functional organization spanning both early and high-level visual cortex. Recent work has shown that topographic deep artificial neural networks (TDANNs; Margalit et al., 2024), trained with a combination of task and spatial constraints, can recapitulate many of these organizational motifs, including smooth orientation, spatial frequency, and color preference maps in early visual cortex, as well as category-selective regions in ventral temporal cortex (VTC). However, existing models fail to capture retinotopic features , including orthogonal eccentricity and polar angle maps in V1 (Wandell et al., 2007), systematic relationship between receptive field size and eccentricity (Dumoulin & Wandell, 2011), or foveal bias of face-selective regions and peripheral bias of place-selective regions in VTC (Levy 2001; Hasson 2002). We hypothesized that these motifs emerge in part from a fundamental property of biological vision: the non-uniform sampling of the visual field by the retina. To test this hypothesis, we developed a TDANN with a retina in which input images are sampled according to the spatial distribution of retinal ganglion cells. Training on retinally sampled ImageNet images produced several key signatures of primate visual cortex. Across five randomly seeded models, units develop receptive fields whose size increases across layers, and within a given layer, foveally positioned units have smaller receptive fields than peripherally positioned units. Despite this visual diet change, the model retained previously demonstrated biological features of TDANNs, including smooth orientation, spatial frequency, and color preference maps in V1 and category-selective topography in VTC. Notably, word-selective units cluster consistently near the fovea and place-selective units near the periphery, while face-selective units are more diffuse—plausibly reflecting the absence of egocentric gaze-centering toward faces in the training set. These organizational benefits were achieved at modest cost to visual recognition, with ImageNet top-1 accuracy decreasing from 43.4% to 35.5%. Together, these results establish that non-uniform retinal sampling is sufficient to drive eccentricity-dependent receptive field organization while remaining compatible with the emergence of topographic maps across both V1 and VTC, suggesting that the retina's spatial inhomogeneity may be a key inductive bias shaping the large-scale functional architecture of the ventral stream.

**Disclosures: Y. Shah:** None. **K. Grill-Spector:** None.

**Poster**

**PSTR185: Visual Learning, Memory, Categorization, and Processing**

**Location:** WCC Halls A-C

**Time:** Monday, November 16, 2026, 1:00 PM - 5:00 PM

**Program #/Poster #:** PSTR185.18/AA31

**Topic:** E.06. Vision

**Title:** Blurred Faces Reduce Early Visual and Face-Sensitive ERP Responses

**Authors: *I. TOVAR**[1], N. BRUNET[2];
[1]California State University, San Bernardino, San Bernardino, CA; [2]Dept. of Psychology, California State Univ. San Bernardino, San Bernardino, CA

**Abstract:** Faces typically elicit a prominent N170 component over occipito-temporal scalp regions, reflecting early face-sensitive visual processing. Previous work has shown that certain manipulations that disrupt face processing, including inversion or partial degradation, can enhance N170 amplitude, leading to the prediction that progressively blurred faces might initially increase the N170 due to increased perceptual ambiguity before decreasing once faces become unrecognizable. The present study tested this hypothesis by systematically manipulating facial blur while recording electroencephalography (EEG).Participants viewed neutral faces presented at seven levels of Gaussian blur ranging from fully intact to highly degraded. Stimuli were balanced across gender and race/ethnicity and were presented in randomized order. EEG was continuously recorded using a 64-channel actiCHamp system. Analyses focused on the P100 and N170 ERP components over occipito-temporal electrodes.Contrary to our initial prediction of a nonlinear or inverted-U relationship between blur and N170 amplitude, preliminary analyses revealed a progressive reduction in both P100 and N170 amplitudes as blur increased. The decrease appeared monotonic across blur levels, suggesting that increasing degradation weakened early visual and face-sensitive neural responses rather than amplifying them. These findings indicate that the N170 may depend more strongly on the availability of fine-grained visual information than on perceptual ambiguity alone.The results challenge the assumption that increased difficulty in face processing necessarily enhances the N170 and instead support the view that sufficient high-spatial-frequency information is required to robustly engage early face-sensitive neural mechanisms. Ongoing analyses are examining behavioral performance and potential nonlinearities at intermediate blur levels.

**Disclosures: I. Tovar:** None. **N. Brunet:** None.

**Poster**

**PSTR185: Visual Learning, Memory, Categorization, and Processing**

**Location:** WCC Halls A-C

**Time:** Monday, November 16, 2026, 1:00 PM - 5:00 PM

**Program #/Poster #:** PSTR185.19/AA32

**Topic:** E.06. Vision

**Support:** ERC 2019-SyG-RELEVANCE no. 856495
IMPRS for Intelligent Systems, Tübingen, DE

**Title:** Framework for generating highly-realistic dynamic monkey body avatars with separate control of identity and pose / motion

**Authors:** L. MARTINI[1], A. BOGNÁR[2], N. TAUBERT[1], R. VOGELS[3], ***M. A. GIESE**[4]; [1]N3, HIH / CIN, Univ. Clin. Tübingen, Tübingen, Germany; [3]Neurosciences, [2]KU Leuven, Leuven, Belgium; [4]Dept N3, CIN / HIH, Univ. of Tuebingen, Tuebingen, Germany

**Abstract:** Social signals in primates are determined not only by their content, such as facial expressions or body posture, but also by the identity of the agent. Identity determines social status within the group, which in turn influences the meaning and neural encoding of perceived

bodily signals. Manipulating identity while preserving motion and pose characteristics is impractical with natural videos. In addition, many visual features including lighting, background, and viewpoint inevitably vary across naturalistic videos. This makes dynamic, realistic avatar stimuli a powerful tool for creating highly controlled stimuli that disentangle pose, motion, and identity. METHODS: Based on a calibrated multi-camera video setup, we developed a computational framework for generating highly realistic monkey avatars with separate control of body morphology, pose, and motion. The framework uses the large-scale multi-view macaque pose dataset BigMaQ with computer graphics rendering to generate colored renderings of a monkey avatar whose morphology can be fitted to image sequences.. This allows to present identical dynamic body poses on different monkey identities (body morphologies). Identity is represented using morphable 3D surface models, enabling a generation of individual-specific avatars and even cross-species skeletal and motion retargetting. RESULTS: We demonstrate different applications of the framework. Specifically, we show how different monkey poses and dynamic behaviors can be associated not only with different individuals, but also different species-specific avatars. In addition, we demonstrate different possibilities of stimulus control, including morphing and variations of stimulus dynamics. Moreover, we demonstrate the computational advantage of disentangling identity and pose for action classification. DISCUSSION: The proposed framework provides many new possibilities for investigating the neural mechanisms of social and action vision with highly controlled stimuli. Specifically, it helps to investigate the encoding of individual and species identity in body-based social vision.

**Disclosures: L. Martini:** None. **A. Bognár:** None. **N. Taubert:** None. **R. Vogels:** None. **M.A. Giese:** None.

**Poster**

**PSTR185: Visual Learning, Memory, Categorization, and Processing**

**Location:** WCC Halls A-C

**Time:** Monday, November 16, 2026, 1:00 PM - 5:00 PM

**Program #/Poster #:** PSTR185.20/BB1

**Topic:** E.06. Vision

**Support:** NSF 1734907
NIH R01MH107797
NIH R01MH132225

**Title:** What will you look at next? Uncovering the neural processes of eye-movement guidance to objects using Intracranial Electroencephalography

**Authors: *A. ALREJA**[1], M. J. BORING[2], M. WARD[5], C. E. SCHROEDER[6], T. J. ABEL[3], A. S. GHUMAN[4];
[1]Dept. of Neurolog. Surgery, Univ. of Pittsburgh, Pittsburgh, PA; [2]Ctr. for Neurosci., [3]Dept. of Neurolog. Surgery, [4]Neurolog. Surgery, Univ. of Pittsburgh, Pittsburgh, PA; [5]David Geffen Sch. of Med., Univ. of California Los Angeles, Los Angeles, CA; [6]Nathan Kline Inst. - Translational Neurosci. Div., Nathan Kline Inst. for Psychiatric Res., Orangeburg, NY

**Abstract:** A cup of coffee, your phone, your daughter's face: We move our eyes to look at things, not coordinates in space. However, our understanding about the neural guidance of eye movements is primarily shaped by studies that examine where we will look next, not what. Thus, it remains unclear how our brain guides our eyes to things in our environment ("what" we are going to look at next). While many studies have examined the role of the dorsal "where" pathway in guiding eye movements, the role of the ventral "what" pathway in eye movement guidance remains relatively unexplored. We addressed this gap with simultaneously recorded intracranial electroencephalography and eye tracking in individuals with epilepsy during free viewing of scenes as well as during unscripted natural social interactions in the real world. In both paradigms, brain activity prior to the onset of saccades to objects could be used to predict the category of object participants looked at next: even after controlling for spatial locations of eye movements. Prediction of what a person was going to look at next was enabled not only by brain activity from areas of parietal cortex traditionally associated with eye movement guidance but also category selective regions of ventral temporal cortex. Category selective ventral cortex revealed that the spectral power and coherence of brain activity preceding a fixation differed, depending upon whether the fixation was on a face or not. These differences indicated a role for theta band activity in category selective ventral cortex, which may suggest a role for the interaction between the ventral visual stream and theta band activity in hippocampal regions for visual navigation. These results persist after controlling for the influence of parafoveal responses to the object of the next fixation which was done by comparing saccades traversing greater than 5 degrees of visual angle to smaller saccades. Prediction accuracy did not diminish for the larger saccades, suggesting that parafoveal preview was not why ventral temporal cortex predicts what people are going to look at next. These results suggest that ventral temporal cortex activity reflects what we will look at next and that interactions with hippocampus and parietal cortex may guide where to look for that object. They also raise the prospect of ventral temporal cortex playing a role in the visual guidance of eye movements.

**Disclosures: A. Alreja:** None. **M.J. Boring:** None. **M. Ward:** None. **C.E. Schroeder:** None. **T.J. Abel:** None. **A.S. Ghuman:** None.

**Poster**

**PSTR185: Visual Learning, Memory, Categorization, and Processing**

**Location:** WCC Halls A-C

**Time:** Monday, November 16, 2026, 1:00 PM - 5:00 PM

**Program #/Poster #:** PSTR185.21/BB2

**Topic:** E.06. Vision

**Support:** NSF BCS-1232530
ARCS Foundation

**Title:** Category Expertise and the Fusiform Face Area (FFA): After 30,000 Trials the FFA Is Still Not Selective for Extensively Trained Morphed Car Stimuli

**Authors: *P. H. COX**[1], Y. JUNG[2], M. RIESENHUBER[2];
[1]Lehigh Univ., Bethlehem, PA; [2]Dept. of Neurosci. and Ctr. for Neuroengineering, Georgetown Univ. Med. Ctr., Washington, DC

**Abstract:** The Fusiform Face Area (FFA) has been proposed as a domain-specific region for face perception (Kanwisher & Yovel, 2006). Alternate theories have proposed it is devoted to recognition of exemplars within a category of expertise (Bukach et al., 2006). Our previous training study (Jiang et al., 2007) showed that object-selective regions in ventral occipital temporal cortex (vOTC), particularly the right lateral occipital (rLO), became selective for the shape of trained stimuli (morphed cars) after ~5 hours of training, while the FFA did not. Yet, that training was short compared to what is commonly associated with expertise. More recently we have examined how extensive training affects neural task circuitry, consisting of ~30,000 trials over 15-20 hours (Cox et al., 2026). This amount of training resulted in automation of the car categorization task (a plateau in RT and accuracy) and representations in vOTC changing from shape- to category-selective (i.e., showing sensitivity to the category membership of the trained car stimuli rather than their shape). Due to the extent of the training, these data are uniquely situated to weigh in on the FFA expertise debate, as they enable us to assess whether additional extensive training leads to selectivity increases in the FFA, or in other areas of high-level visual cortex. In our study, 14 subjects underwent a PRE scan after initial training, with localizer (faces, objects, cars, scrambled cars) and fMRI-RA scans, followed by extensive training, and a POST scan with the localizer and fMRI-RA scans repeated. We defined the FFA by a contrast of Faces > Objects, inclusively masked by Faces > Rest. The average (±SEM) location of right FFA in MNI coordinates was [41.67 ±1.15, -49.33 ±1.97, -18.33 ±1.07]. The FFA did not become selective for trained cars over scrambled car stimuli with extensive training (univariate fMRI responses to trained cars versus scrambled car images $p = 0.22$). In contrast, a nearby posterior fusiform region (peak MNI coordinates [44 -66 -12]) did show greater responses to trained cars compared to scrambled cars ($p=0.017$)—notably, this area responded to face stimuli but not selectively, since objects also activated this area. In Cox et al. (2026), we used fMRI-RA to show that this vOTC area distinguished between car categories in the POST scan ($p < .001$, FWE-corrected $p < .05$, same vs. different car categories). In contrast, the FFA did not show selectivity for car categories in the POST scan ($p > .05$). In summary, our results provide further support that the FFA is a face-selective region and that expertise leads to selectivity increases in nearby regions of high-level visual cortex distinct from the FFA.

**Disclosures: P.H. Cox:** None. **Y. Jung:** None. **M. Riesenhuber:** None.

**Poster**

**PSTR185: Visual Learning, Memory, Categorization, and Processing**

**Location:** WCC Halls A-C

**Time:** Monday, November 16, 2026, 1:00 PM - 5:00 PM

**Program #/Poster #:** PSTR185.22/BB3

**Topic:** E.06. Vision

**Support:** NIH-NEI Grant RO1EY036881
NSF Grant 2337373

**Title:** Expanded hand representations and unique lateralization patterns in visual cortex of hearing and deaf sign language experts

**Authors: *E. DANIEL HERTZ**[1], J. GOMEZ[1,2];
[1]Princeton Neurosci. Inst., Princeton, NJ; [2]Dept. of Psychology, Princeton Univ., Princeton, NJ

**Abstract:** Childhood visual experiences shape our ability to rapidly recognize faces and objects. Across development, brain regions processing visual categories that lose relevance, such as hands, are recycled for others. How does visual cortex accommodate a childhood in which hands maintain significance? Methods: We collected structural and functional Magnetic Resonance Imaging (MRI, 3 Tesla) scans from 33 healthy adults- 11 Deaf American Sign Language (ASL) experts, (F=8, mean age=46), 11 hearing signers (state-registered interpreters or educators) who learned ASL in adulthood (F=11, mean age=47), and 11 hearing controls with no sign language experience (F=7, mean age=45). Participants completed a visual category localizer fMRI task, which allowed us to quantify the cortical surface area responsive to hands, to faces, and to their overlapping representation in ventral temporal cortex (VTC). Group comparisons were performed in Freesurfer average space, and quantified using bootstrapping analyses (1000 iterations, two-tailed CI = 95%). Results: *(1) Surface area changes:* While we find no group differences in surface area selective to faces ($p$'s $\geq 0.4$), both Deaf ($p < 0.0001$) and Hearing Signers ($p=0.04$) demonstrated a significant increase in hand-selective cortical surface area in the left VTC, with a similar trend on the right. *(2) Face-Hand Overlap shifts location:* When we compute the conjunction between face and hand selectivity in VTC, we find no group differences in the amount of overlap, but the location of shared representation is distinct across groups. Control and Hearing Signers show a majority of face-hand overlap within the hand-selective occipital-temporal sulcus, while Deaf Signers show more overlap in the face-selective lateral fusiform gyrus, in both hemispheres. *(3) No lateralization of face representations:* Both Hearing Signers and Controls show the expected rightward lateralization for face representations ($p < 0.0001$), while Deaf Signers do not ($p \geq 0.4$). *(4) No leftward viewing biases.* In an eye tracking experiment participants viewed dynamic social stimuli (clips from Hollywood movies). Interestingly, all Control participants had a leftward viewing bias ($p < 0.0001$), while Deaf Signers had symmetric viewing patterns with a slight bias towards the right visual field. Hearing Signers show an intermediate effect. Conclusion: Together, these results suggest that the acquisition of sign language expertise in both Deaf individuals and hearing interpreters who did not acquire sign language until early adulthood, is sufficient to alter the spatial topography and viewing patterns of ecologically relevant stimuli such as faces and hands.

**Disclosures: E. Daniel Hertz:** None. **J. Gomez:** None.

**Poster**

**PSTR186: Action/Sensation/Movement Selection: Human (Behavior/Physiology/Imaging) I**

**Location:** WCC Halls A-C

**Time:** Monday, November 16, 2026, 1:00 PM - 5:00 PM

**Program #/Poster #:** PSTR186.01/BB4

**Topic:** F.04. Voluntary Movements

**Title:** Kinematic evidence for heterogeneous sensorimotor control in developmental coordination disorder: Two putative profiles on a motor continuum

**Authors: *L. LIN**, Y.-T. TSENG;
Dept. of Kinesiology, Natl. Tsing Hua Univ., Hsinchu City, Taiwan

**Abstract:** Children with developmental coordination disorder (DCD) are often analyzed as a homogeneous group despite substantial inter-individual variability in sensorimotor control. We examined whether data-driven kinematic profiling could identify distinct patterns of sensorimotor performance within children with DCD.
Wrist trajectories were recorded from children with DCD (n=59) and typically developing (TD) peers (n=163) using an encoder-based manipulandum sampled at 200 Hz under full visual occlusion. Thirteen kinematic features reflecting endpoint variability, movement speed, smoothness, and trajectory deviation were extracted. Age effects were removed within each cross-validation fold to prevent data leakage. K-means clustering (k=2) was applied in the standardized feature space, while UMAP was used only for visualization.
Two putative kinematic profiles emerged within the DCD sample. A Fast-Unstable profile (n=14; mean age=4.9 yr) showed higher peak velocity (199.5 +/- 68.4 deg/s) and greater variable error (9.6 +/- 5.9 deg), consistent with unstable sensorimotor control. A Slow-Compensated profile (n=45; mean age=8.0 yr) showed near-normative endpoint stability together with slower movement, suggesting a compensation-like strategy that may reduce observable endpoint error. Partition stability was high under K-means resampling (bootstrap adjusted Rand index [ARI]=0.80), whereas agreement across clustering algorithms was modest (ARI=0.07-0.54), indicating that the profiles may reflect a graded continuum rather than discrete subtypes. XGBoost classification further showed asymmetric separability from TD participants: Fast-Unstable versus TD, ROC-AUC=0.970; Slow-Compensated versus TD, ROC-AUC=0.597; and all DCD versus TD, ROC-AUC=0.636.
These findings suggest that children with DCD may exhibit heterogeneous sensorimotor strategies, ranging from overt proprioceptive instability to compensation-like slowing. Kinematic profiling may provide mechanistic information beyond aggregate motor scores and help clarify how proprioceptive control varies across motor development.

**Disclosures: L. Lin:** None. **Y. Tseng:** None.

**Poster**

**PSTR186: Action/Sensation/Movement Selection: Human (Behavior/Physiology/Imaging) I**

**Location:** WCC Halls A-C

**Time:** Monday, November 16, 2026, 1:00 PM - 5:00 PM

**Program #/Poster #:** PSTR186.02/BB5

**Topic:** F.04. Voluntary Movements

**Support:** Wilson Foundation, affiliated with Methodist Rehabilitation, Jackson, MS

**Title:** Task-dependent asymmetries in arm and trunk kinematics during unilateral functional drinking in subacute stroke

**Authors: *B. PERRY**[1], B. TANG[1], B. SULLIVAN[2], J. SIVAK[1], A. HAYES[1], D. S. STOKIC[1]; [1]Methodist Rehabil., Jackson, MS; [2]Neurosci., Univ. of Mississippi Med. Ctr., Jackson, MS

**Abstract:** Upper-limb performance after stroke is commonly evaluated using simple, non-functional tasks, such as reaching or pointing; however, the extent and nature of kinematic differences between the more-affected (MA) and less-affected (LA) arms during ecologically valid activities such as drinking remain incompletely characterized. This study quantified asymmetries in arm and trunk kinematics during a natural unilateral drinking task in individuals with subacute stroke and examined how these asymmetries were influenced by task demands and motor impairment. Twenty-six participants with subacute stroke (19±7 days post-onset) performed unilateral drinking movements using the LA and MA arms under all combinations of eyes open or closed, cup positioned on the table at the waist or forehead height, and instruction to perform fast-accurate or fastest movements. 3-D motion capture was used to collect data and define different phases of the task (reach-to-cup, cup grasp, cup-to-mouth, drink, cup-to-table, cup release, hand-to-table). Task duration, maximum peak velocity, number of movement units (NMU), trunk displacement, and trunk contribution slope (TCS) were calculated for all phases. Linear mixed-effects models with participant-specific random intercepts evaluated the effects of side, vision, cup position, and task instruction. The MA arm demonstrated consistently longer movement durations, lower peak velocities, higher NMUs, greater trunk displacement, and lower TCS compared with the LA arm, both overall and in different phases of the drinking task (all $p<0.001$). Vision removal primarily increased movement duration, but not trunk displacement and TCS. In contrast, cup position had the most consistent effect on all measures, with high cup position increasing peak velocity, trunk displacement, and TCS. Task instruction significantly increased peak velocity but had comparatively smaller effects on trunk measures. Although the relative timing of maximal peak velocity remained relatively stable, it decreased more on the MA than the LA side in the reach phase with eyes closed and high cup position. Longer movement durations and greater NMUs correlated with greater severity of impairment. Higher-order interactions were uncommon. The results indicate the presence of task-dependent interlimb asymmetries in all phases of functional drinking in subacute stroke captured by different kinematic measures.

**Disclosures: B. Perry:** None. **B. Tang:** None. **B. Sullivan:** None. **J. Sivak:** None. **A. Hayes:** None. **D.S. Stokic:** None.

**Poster**

**PSTR186: Action/Sensation/Movement Selection: Human (Behavior/Physiology/Imaging) I**

**Location:** WCC Halls A-C

**Time:** Monday, November 16, 2026, 1:00 PM - 5:00 PM

**Program #/Poster #:** PSTR186.03/BB6

**Topic:** F.04. Voluntary Movements

**Support:** Wilson Foundation, affiliated with Methodist Rehabilitation, Jackson, MS

**Title:** Arm and trunk kinematic asymmetries are selectively reduced from unilateral to bilateral functional drinking in subacute stroke

**Authors:** B. PERRY[1], B. TANG[1], B. SULLIVAN[2], J. SIVAK[1], A. HAYES[1], ***D. S. STOKIC**[1]; [1]Methodist Rehabil., Jackson, MS; [2]Neurosci., Univ. of Mississippi Med. Ctr., Jackson, MS

**Abstract:** In our companion abstract, we reported arm and trunk asymmetries during a unilateral functional drinking task in individuals with subacute stroke. This study aimed to examine whether these asymmetries are altered during a bilateral drinking task and how visual feedback, cup position, and task instruction modify these effects. Twenty-six participants with subacute stroke (19±7 days post-onset) performed a functional drinking task under unilateral (UL) and bilateral (BL) conditions. Tasks were completed with the less-affected (LA) and more-affected (MA) arm across all combinations of visual feedback (eyes open, eyes closed), cup positioned on a table at waist or forehead height, and task instruction (fast-accurate, fastest). 3-D motion capture was used to collect data and define different phases of the task (reach-to-cup, cup grasp, cup-to-mouth, drink, cup-to-table, cup release, hand-to-table). Task duration, maximum peak velocity, number of movement units (NMU), trunk displacement, and trunk contribution slope (TCS) were calculated for all phases and analyzed using linear mixed-effects models (participant-specific random intercept) with the focus on significant interactions between movement (UL, BL) and arm (LA, MA), and additional effects of vision, cup position, and task instruction. Unilateral performance revealed task-dependent asymmetries between the LA and MA arms, both overall and across all phases of the drinking task (all $p<0.001$). Bilateral task performance selectively reduced these asymmetries (Movement × Arm interactions, $p<0.001$). The largest reductions were observed for movement duration, NMU, peak velocity timing, trunk displacement, and TCS, indicating greater temporal symmetry, smoother movements, and better arm-trunk coordination during bilateral performance. Peak velocity asymmetries were reduced but not eliminated. Despite improved interlimb symmetry, absolute trunk displacement remained increased, especially with high cup position. The most extensive bilateral effects occurred during the initial reach phase (T1), indicating that bilateral task performance mostly influences asymmetries during movement initiation. Among the experimental conditions, only the cup position significantly affected the Movement × Arm interaction for peak velocity during T1, driven primarily by reduced peak velocity of the LA arm during bilateral high cup trials. While subacute stroke patients exhibit prominent arm-trunk asymmetries during unilateral functional drinking, bilateral performance selectively reduces those asymmetries, particularly during movement initiation, despite persistent trunk compensation.

**Disclosures: B. Perry:** None. **B. Tang:** None. **B. Sullivan:** None. **J. Sivak:** None. **A. Hayes:** None. **D.S. Stokic:** None.

**Poster**

**PSTR186: Action/Sensation/Movement Selection: Human (Behavior/Physiology/Imaging) I**

**Location:** WCC Halls A-C

**Time:** Monday, November 16, 2026, 1:00 PM - 5:00 PM

**Program #/Poster #:** PSTR186.04/BB7

**Topic:** F.04. Voluntary Movements

**Support:** MND Association

**Title:** QNav, a novel closed-loop neuronavigation system for accurate placement of transcranial magnetic stimulation (TMS) of the human brain

**Authors:** J. HOWELLS[1], D. PLANINC[2], J. MIDDLETON[2], G. SAMUSYTE[3], H. TANKISI[4], B. CENGIZ[5], S. F. FARMER[2], J. C. ROTHWELL[2], H. BOSTOCK[2], ***M. KOLTZENBURG**[2]; [1]Central Clin. Sch., Univ. of Sydney, Sydney, Australia; [2]UCL Queen Square Inst. of Neurol., UCL, London, United Kingdom; [3]Dept of Neurol., Lithuanian Univ. of Hlth. Sci., Kaunas, Lithuania; [4]Dept. of Clin. Neurophysiol., Aarhus Univ. Hosp., Aarhus, Denmark; [5]Dept. of Neurol., Gazi Univ. Fac. of Med., Ankara, Turkey

**Abstract:** TMS has been extensively used for investigating mechanisms of sensorimotor control. A characteristic feature of constant intensity stimulation of the cortex is the variable amplitude of motor evoked potentials (MEPs). One potential technical source of this variability is the (often manually held) misplacement of heavy stimulating coils during a recording session. The aim of this study was to test a novel software to minimise coil misplacement. Healthy volunteers were comfortably seated in a bespoke (Edge Surgical Solutions) TMS reclining chair with head support. MEPs were recorded from intrinsic hand muscles. A (Deymed) BF70-LCQ figure of eight coil mounted on a counterweighted holder was placed over the contralateral M1. Hotspots were defined using physiological responses or anatomical landmarks. QTMS software controlled stimulus delivery of a DuoMAG MP$^{EEG}$ stimulator at frequencies of 0.1 to 1 Hz using standard stimulus protocols. Coil and head position were continuously monitored (20 Hz sampling rate) with (Rogue Research) Brainsight. From its data stream, QNav software continuously calculated and displayed at 1 decimal resolution the relative changes of head and coil placements from the hotspot in all six degrees of freedom (6DOF: X-, Y-, Z-axis, pitch, roll, yaw). Individual coordinates were recorded when stimuli were delivered. When the coil was placed on a static target, errors were < 0.1mm and <0.1° in each of the 6DOF. In subjects, it was generally possible to maintain coil position over hundreds of stimuli within ±1mm and ±1° bands and less than <0.5 mm for positional and <1° angular median errors. The software allowed separate definition of error margins for individual DOFs for gating. This enabled the manual systematic change of coil position in one dimension whilst keeping other placement parameters unchanged. Constant intensity stimulation was used to evoke MEPs targeted at 0.05, 0.2 or 1mV whilst the coil was positioned on the skull. Subsequently, the coil position was randomly changed in bands of 1mm or 1°. Positive (upward) changes in the (vertical) z-axis generally decreased MEP amplitudes with increasing distance from the skull. In some studies changes of 1-2mm almost halved the response. Whilst this change was usually monotonic, in some recordings there was an initial increase before a decrease. We conclude that QNav software facilitates the accurate manual coil placement in prolonged TMS stimulation protocols with less than 1mm positional and 1° rotational errors. Gating aids (i) in maintaining a desired coil position and (ii) exploring the effects of systematic coil misplacement on MEP amplitude variability to fixed intensity stimulation.

**Disclosures: J. Howells:** E. Ownership Interest (stock, stock options, royalty, receipt of intellectual property rights/patent holder, excluding diversified mutual funds); Royalty for Qtrac software. **D. Planinc:** None. **J. Middleton:** None. **G. Samusyte:** None. **H. Tankisi:** None. **B. Cengiz:** None. **S.F. Farmer:** None. **J.C. Rothwell:** None. **H. Bostock:** E. Ownership Interest (stock, stock options, royalty, receipt of intellectual property rights/patent holder, excluding diversified mutual funds); Royalty for Qtrac software; Co-Director of QTMS Science Ltd. **M. Koltzenburg:** E. Ownership Interest (stock, stock options, royalty, receipt of intellectual property rights/patent holder, excluding diversified mutual funds); Co-director of QTMS Science Ltd.

**Poster**

**PSTR186: Action/Sensation/Movement Selection: Human (Behavior/Physiology/Imaging) I**

**Location:** WCC Halls A-C

**Time:** Monday, November 16, 2026, 1:00 PM - 5:00 PM

**Program #/Poster #:** PSTR186.05/BB8

**Topic:** F.04. Voluntary Movements

**Title:** Automating Kinematic Time Series Segmentation: A Deep Learning Approach Using Conv-BiLSTM Networks

**Authors: F. HOUCK**, *F. A. KAGERER;
Michigan State Univ., East Lansing, MI

**Abstract:** Determining movement onset and offset in discrete reaching paradigms, such as, e.g., center-out tasks, can be surprisingly non-trivial. Traditional kinematic segmentation of human reaching movements relies heavily on threshold methods, e.g., percentage of peak velocity, that are frequently confounded by sensor artifacts, experimental perturbations, and asymptotic velocity decay at movement offsets. Despite using a refined algorithm (Teasdale 1993) for programmatically marking onset and offset, we found that about 40% of trials in our lab required manual correction. This study introduces a deep learning pipeline, a subset of machine learning which uses layered neural networks to automatically extract predictive mathematical structures directly from continuous data, to automate reach segmentation and reduce analysis overhead. We developed a convolutional bidirectional long short-term memory (Conv-BiLSTM) neural network and evaluated it on a pilot dataset of 5,521 reaches from a bimanual reaching task using joysticks (N = 18, 13 F). Each trial's movement onset and offset were estimated by the Teasdale (1993) algorithm and then manually inspected. Trials were randomly divided into 70% training, 10% validation, and 20% test splits. The architecture consisted of dual-stage convolutional layers (11- and 25- frame kernels) for multi-scale feature extraction, feeding into a 125-unit BiLSTM layer for contextual sequence-to-sequence classification. We evaluated both a 1D model (velocity) and a 3D model (velocity, acceleration, and jerk).
Though both architectures demonstrated robust performance, the 3D model achieved higher accuracy and lower error scores. A Wilcoxon signed-rank test comparing the 3D model directly to manually corrected Teasdale thresholds on matched testing trials revealed a significant difference in absolute onset errors (Model: Median = 16.67 ms, IQR = 25.00 ms; Teasdale:

Median = 8.33 ms, IQR = 58.33 ms; Z= 3.37, p = 0.0007). Crucially, for absolute offset error, the 3D model significantly outperformed the threshold method (Z = 7.06, p < 0.0001), reducing median error and variability (Model: Median = 66.67 ms, IQR = 108.33 ms; Teasdale: Median = 175.00 ms, IQR = 491.67 ms).
Our preliminary findings suggest that 1) deep learning can successfully reduce the need for manual adjustment in kinematic analysis; 2) inclusion of higher-order derivatives provides the model with critical predictive features regarding offset profiles, sharpening boundary detection of baseline noise. Future iterations will expand the model's generalizability to different data acquisition devices.

**Disclosures: F. Houck:** None. **F.A. Kagerer:** None.

**Poster**

**PSTR186: Action/Sensation/Movement Selection: Human (Behavior/Physiology/Imaging) I**

**Location:** WCC Halls A-C

**Time:** Monday, November 16, 2026, 1:00 PM - 5:00 PM

**Program #/Poster #:** PSTR186.06/BB9

**Topic:** F.04. Voluntary Movements

**Support:** State of Nebraska LB692 P2400270

**Title:** The galvanic skin response may complement sternocleidomastoid muscle activation in assessing the acoustic startle reflex.

**Authors: *S. KANNAN**, B. JOHNSON, R. L. HECKMAN;
Creighton Univ., Omaha, NE

**Abstract:** Startle-related activation of the sternocleidomastoid muscle (SCM) triggered by a loud acoustic stimulus (LAS) has been used to investigate deficits in motor planning post stroke. However, studies of shoulder movement have been limited by the role of the SCM both in the startle response and in stabilization of the head. The galvanic skin response (GSR) measures sympathetic nervous system activation and may complement the SCM as an indicator of startle. The objective of this study was to assess the relationship between SCM and GSR responses to a LAS delivered at rest to probe the acoustic startle reflex. Ten neurologically healthy adults were recruited from the community (22-71 years, 3 male). Participants were seated with a forward visual gaze. The LAS was delivered using a loudspeaker or headphones. LAS delivery method was blocked and randomized across two visits. We recorded surface electromyography from the SCM bilaterally. We identified the onset latency of muscle activation and averaged SCM amplitude over 20 ms following onset. We measured skin conductance from the palmar surface of the proximal phalanges of digits two and three on the non-dominant hand. A GSR response was indicated by an increase in skin conductance 2-5 s after LAS delivery. We calculated the GSR magnitude from baseline to maximum skin conductance after applying a logarithmic transformation. A startle response was indicated by SCM onset latency <120 ms and by presence of a GSR response. We used mixed effects models to assess the interaction between delivery

method and SCM amplitude when predicting GSR magnitude. 25% of the participants did not have a GSR response for either delivery method. The frequency of startle responses for GSR ($0.64 \pm 0.15$) and SCM (right: $0.36 \pm 0.17$, left: $0.33 \pm 0.17$) measures pooled across delivery method were not significantly different after adjusting for within participant correlation ($p = 0.25$). We found a significant positive relationship between right SCM amplitude and GSR magnitude regardless of delivery method ($\chi^2 = 5.22$, $p = 0.023$, $n = 6$, observations = 120). We did not find a significant relationship between left SCM amplitude and GSR magnitude ($\chi^2 = 0.15$, $p = 0.70$, $n = 6$, observations = 120) regardless of delivery method. GSR magnitude was greater for LAS delivery with the loudspeaker regardless of interaction with the right or left SCM amplitude ($\chi^2 = 7.22$ and 6.21, $p = 0.007$ and 0.013, respectively). Age and sex differences were not assessed. GSR may complement SCM muscle activation in assessing the startle response; however, further investigation of the neuromuscular and autonomic components of the response is warranted to guide studies of motor planning post stroke.

**Disclosures: S. Kannan:** None. **B. Johnson:** None. **R.L. Heckman:** None.

**Poster**

**PSTR186: Action/Sensation/Movement Selection: Human (Behavior/Physiology/Imaging) I**

**Location:** WCC Halls A-C

**Time:** Monday, November 16, 2026, 1:00 PM - 5:00 PM

**Program #/Poster #:** PSTR186.07/BB10

**Topic:** F.04. Voluntary Movements

**Title:** Mid-reach decisions between target options are automatically yoked to their proximity and features and are accurately replicated by a drift-diffusion model

**Authors: *I. KURTZER**[1], S. SULLIVAN[3], D. TANIS[2], T. SINGH[4], J. CASHABACK[3]; [1]New York Inst. of Technol. - Col. of Osteo. Med., Old Westbury, NY; [2]New York Inst. of Technol. - Col. of Osteo. Med., Old Westbury, NY, ; [3]Univ. of Delaware, Newark, DE, ; [4]Pennsylvania State Univ., University Park, PA.

**Abstract:** Various forces in everyday life can force us to abandon a pursued option and choose again from the available alternatives. This situation is present on multiple timescales including single reaches. We have previously shown that participants who view a target "splitting" mid-reach into two options will automatically select the one nearest the original target's location. Here we examine whether the color and shape of the options, features which powerfully impact visual search and arm movement initiation, also automatically bias mid-reach target selection. 18 participants (mean age = 22.5) reached to a target placed 20 cm ahead (MT criterion = 600-750 ms). This target was occasionally replaced mid-reach by a surrounding pair (1 cm vs 3 cm lateral). In blocked sub-experiments, the target pair also differed in color (red vs green circles) or shape (white circles vs white squares) such the near option or far option could have the same feature as the original target, e.g. both being green. Critically, participants were instructed to ignore the color or shape of the options and instead obtain the one nearest to the original target. Mid-reach decisions had lower error rates when the near target had the same feature as the

original than when different: Δ w/color = -19.2% (26.2 SD) and Δ w/shape = -7.4% (14.9 SD). The timing of these decisions was also impacted, being faster when the selected target had the same feature as the original. This occurred with trials correctly directed to the near option - Δ w/color = -29.6 ms (42.6 SD) and Δ w/shape = -10.3 ms (12.1 SD) - and incorrectly directed to the far option - Δ w/color = -38.5 ms (77.6 SD) and Δ w/shape = -67.2 ms (83.6 SD). We attempted to reproduce these results with a modified drift-diffusion model (Ulrich et. al. 2015) where one channel processes task-relevant information (here proximity) and a separate channel processes task-irrelevant information (here features). The two decision-variables have noisy trajectories that linearly sum to a common decision variable with an initial state biased to the correct boundary. The optimized model produced error rates and reaction times very similar to human performance, differing by less than 5%. Taken together, we show that options' proximity and features automatically impact online target selection and that the pattern of selection can be successfully replicated with a modified drift-diffusion model.

**Disclosures: I. Kurtzer:** None.

**Poster**

**PSTR186: Action/Sensation/Movement Selection: Human (Behavior/Physiology/Imaging) I**

**Location:** WCC Halls A-C

**Time:** Monday, November 16, 2026, 1:00 PM - 5:00 PM

**Program #/Poster #:** PSTR186.08/BB11

**Topic:** F.04. Voluntary Movements

**Support:** Goldstein Innovation Award
NIH R01MH085328

**Title:** Higher variability in effort assessment in adolescents with ADHD

**Authors: *M. UESHIMA**[1], C. SMITH[2], A. C. DERONDA[2], S. H. MOSTOFSKY[2,3,4], K. S. ROSCH[2], L. MALONE[1,3,5], V. S. CHIB[1,6];
[2]Ctr. for Neurodevelopmental and Imaging Res., [1]Kennedy Krieger Inst., Baltimore, MD; [3]Dept. of Neurol., [4]Dept. of Psychiatry and Behavioral Sci., Johns Hopkins Univ. Sch. of Med., Baltimore, MD; [5]Dept. of Physical Med. and Rehabil., Johns Hopkins Univ. Schoolf of Med., Baltimore, MD; [6]Biomed. Engin., Johns Hopkins Univ., Baltimore, MD

**Abstract:** Attention-deficit/hyperactivity disorder (ADHD) has been associated with increased intra-individual variability in behavioral performance (Castellanos et al., 2005) and avoidance of effortful tasks (Orhan et al., 2023). Individuals with ADHD also frequently exhibit impaired motor control and motor skill deficits (Kaiser et al., 2015). However, whether adolescents with ADHD display variability in their subjective assessment of effort during a motor task remains unknown. Here, we investigated motor output variability and effort assessment in adolescents with ADHD using an isometric handgrip effort assessment task. Adolescents with ADHD (n = 17; mean age, 15.1 ± 1.0 years; range, 13-16 years) and neurotypical controls (n = 20; mean age, 15.2 ± 1.5 years; range, 13-18 years) performed repeated force production trials at multiple target

exertion levels using an isometric dynamometer. During the association phase, participants generated target force levels, and during the recall phase, they estimated the exertion they had produced. Trial-level data were analyzed using linear mixed-effects models. Across participants, higher exertion levels were associated with lower success rates during force production ($p < .001$). ADHD participants demonstrated greater exertion variability during effort production compared with controls ($p = 0.03$), while exertion variability increased similarly with increasing exertion levels across groups. During the recall phase, perceived effort scaled with actual exertion levels across both groups, and no significant group differences in average effort estimation accuracy were observed. In contrast, ADHD participants exhibited greater assessment variability across exertion levels compared with controls ($p = 0.01$). Motor output variability increased similarly across groups with increasing effort demands, suggesting that elevated assessment variability in ADHD could not be fully explained by differences in motor variability. Collectively, these findings suggest that adolescents with ADHD exhibit relatively preserved average effort perception but reduced consistency of subjective effort representation. The dissociation between preserved mean estimation accuracy and elevated assessment variability may reflect unstable internal representations of exerted effort in ADHD. These findings identify assessment variability as a potential behavioral signature of altered sensorimotor processing in ADHD.

**Disclosures: M. Ueshima:** None. **C. Smith:** None. **A.C. DeRonda:** None. **S.H. Mostofsky:** None. **K.S. Rosch:** None. **L. Malone:** None. **V.S. Chib:** None.

**Poster**

**PSTR186: Action/Sensation/Movement Selection: Human (Behavior/Physiology/Imaging) I**

**Location:** WCC Halls A-C

**Time:** Monday, November 16, 2026, 1:00 PM - 5:00 PM

**Program #/Poster #:** PSTR186.09/BB12

**Topic:** F.04. Voluntary Movements

**Support:** Valentine Fund from the Psychology Department at St. Lawrence University

**Title:** Chewing Through the Pressure: Effects of Gum Chewing on Human Fine Motor Performance Under Stress

**Authors: *N. CHESTOJANOVA**[1], M. TROMMEL[2], S. V. ONYPER[1];
[1]St. Lawrence Univ., Canton, NY; [2]St. Lawrence Univ., Manlius, NY

**Abstract:** Stress can impair skilled motor performance, particularly in tasks requiring fine motor precision and attentional control. Chewing gum has been proposed as an accessible stress-regulation strategy, but its effects on motor performance and associated physiological responses remain unclear. This study tested whether gum chewing buffers stress-related changes in fine motor accuracy, cognitive performance, autonomic arousal, and prefrontal cortical oxygenation. Eighty undergraduate participants completed a 2 × 2 mixed design experiment with stress condition manipulated between subjects (high vs. low pressure) and gum/mint condition

manipulated within subjects (chewing gum vs. matched mint control, counterbalanced). Participants completed three trials of 10 dart throws in each gum/mint condition, followed by a Digit Symbol Substitution Task (DSST). Electrodermal activity (EDA), heart rate, and functional near-infrared spectroscopy (fNIRS) over prefrontal cortex were recorded across baseline, task, and recovery phases.The stress manipulation was successful subjectively: high-stress participants reported greater perceived stress than low-stress participants, $p < .001$. Contrary to predictions, gum chewing did not improve overall dart accuracy relative to mint, and stress did not moderate mean-level dart performance. However, trial-level analyses revealed a significant stress × gum/mint condition × trial interaction, $p = .002$: under high stress, dart accuracy improved linearly across trials during gum chewing but not mint, whereas under low stress, accuracy improved during mint but not gum. Gum chewing did not affect DSST performance. EDA increased during dart throwing relative to baseline but did not differ by stress or gum/mint condition. fNIRS showed a stress × gum/mint condition interaction, $p = .018$, with gum associated with lower oxygenated hemoglobin under high stress but higher oxygenated hemoglobin under low stress.These findings do not support gum chewing as a general enhancer of fine motor or cognitive performance under pressure. Instead, gum chewing may exert stress-dependent effects on prefrontal oxygenation and performance trajectories during repeated precision motor behavior.

**Disclosures: N. Chestojanova:** None. **M. Trommel:** None. **S.V. Onyper:** None.

**Poster**

**PSTR186: Action/Sensation/Movement Selection: Human (Behavior/Physiology/Imaging) I**

**Location:** WCC Halls A-C

**Time:** Monday, November 16, 2026, 1:00 PM - 5:00 PM

**Program #/Poster #:** PSTR186.10/BB13

**Topic:** F.04. Voluntary Movements

**Title:** Musical scale structure guides action selection during melodic improvisation

**Authors: *G. M. F. LIGHT**[1], O. RACCAH[2], S. D. MCDOUGLE[1];
[1]Psychology, [2]Yale Univ., New Haven, CT

**Abstract:** The use of structured memory representations to guide action is well understood in areas including spatial navigation and visuomotor association. Structured memory representations have also been studied in perception; for example, tonal structure in musical stimuli has been shown to shape the perception of music. Here, we present work that connects structured representations in memory to the domain of action by studying improvised melodies from musicians and non-musicians. Melodic improvisation is an excellent test case for research into action selection, allowing us to ask how humans sample information from a high-dimensional structured memory space to guide their behavior. Participants were asked to produce short improvised (i.e., un-planned) melodies, using one of two different empirically-selected 5-tone scales. These scales were selected based on prior perceptual research finding that they represent either a strongly-structured or weakly-structured internal musical representation.

Additionally, as a control, participants were also asked to produce random sequences (with no underlying musical structure in the auditory feedback that they received), allowing us to pinpoint the goal-directed components of improvised music production. When generating melodies using the "strongly-structured" scale, participants' (N = 30) responses were less random than responses generated with the "weakly-structured" scale and responses generated in the random sequence condition as measured by bigram entropy (both $p < .01$, two-tailed Wilcoxon signed-rank test). Moreover, preliminary results suggested that bigram transition probabilities in the strongly-structured condition could be used to predict out-of-sample participant behavior ($p < .01$, two-tailed Wilcoxon signed-rank test over Spearman $r$ values correlating out-of-sample participant behavior with the rest of the sample); this reflects a surprising level of stereotypy in improvisation across people. Together, these findings indicate that structured memory representations lead to structured action selection in melodic improvisation.

**Disclosures: G.M.F. Light:** None. **O. Raccah:** None. **S.D. McDougle:** None.

**Poster**

**PSTR186: Action/Sensation/Movement Selection: Human (Behavior/Physiology/Imaging) I**

**Location:** WCC Halls A-C

**Time:** Monday, November 16, 2026, 1:00 PM - 5:00 PM

**Program #/Poster #:** PSTR186.11/BB14

**Topic:** F.04. Voluntary Movements

**Support:** NS105759
Julius N. Frankel Foundation

**Title:** Exploratory Data for Salivary Alpha-Amylase and Pupillometry in Early Stroke Motor Recovery

**Authors: *M. SEREIKA**[1], J. A. BEAUCHAMP[1], A. ACOSTA[1], J. BAILEY[2], M. BYRNE[2], K. CAMERON[2], D. CAPINPIN[2], C. CARMONA[1], G. CLARK[3], J. P. DEWALD[1], M. FLYNN[2], J. GYARMATY[1], R. HARVEY[3], A. KEEFE[2], A. MANDANA[1], H. R. ROTH[1], S. SHETH[2], J. YAO[1], D. ZIELKE[2], M. D. ELLIS[1];
[1]Physical Therapy and Human Movement Sci., Northwestern Univ., Chicago, IL; [2]Northwestern Med. Marianjoy Rehabil. Hosp., Wheaton, IL; [3]Shirley Ryan AbilityLab, Chicago, IL

**Abstract:** Persistent upper extremity motor impairment, specifically, expression of flexion synergy and spasticity, in individuals with stroke is attributed neuromechanistically to chronically elevated levels of norepinephrine. Increased ceruleospinal monoaminergic drive to the spinal cord serves to increase excitability of spinal motor neurons, amplifying both descending input from corticoreticulospinal projections (flexion synergy) and afferent input from muscle spindles (spasticity). Increases in norepinephrine levels in early stroke recovery may be an indicator for the development of flexion synergy and spasticity. Non-invasive methods such as concentration of salivary alpha-amylase and pupillometry have been suggested as proxies for systemic and central nervous system norepinephrine levels, respectively. While impaired

pupillary light reflex is an indicator of acute brain injury, other pupillometry metrics such as dilation velocity and magnitude during a movement or cognitive task are predictive of poor generalized recovery following stroke (Modified Rankin Scale). Here, preliminary data are presented informing the working hypothesis that elevated levels of salivary alpha-amylase and asymmetry in pupil responses to light and movement tasks will be different between individuals with and without stroke and associated with motor impairment. Daily saliva swabs and pupillometry were completed for 9 participants (6 inpatient stroke, 3 control). Saliva samples were evaluated for salivary alpha-amylase concentration, and pupillometry data were processed by calculating a left/right eye laterality index of asymmetry. Salivary amylase concentration in individuals with acute stroke (81.8±2.6 U/mL) was greater than controls (14.5±7.2 U/mL) ($p=0.002$). Left/right pupil asymmetry was greater in individuals with acute stroke compared to controls for pupil light reflex ($p < 0.001$), non-paretic shoulder shrug ($p=0.01$), and paretic shoulder shrug ($p<0.001$). Increased asymmetry in individuals with acute stroke may be due to diminished light reflex and/or increased dilation with more physically and cognitively effortful movement tasks in the ipsilesional eye. Increases in salivary amylase concentration and left/right pupil function asymmetry may also be related to motor impairment, as indicated when comparing a mildly impaired individual with a severely impaired individual from the cohort. A larger study is warranted to fully evaluate proxies for norepinephrine levels as a biomarker for the development of persistent flexion synergy and spasticity.

**Disclosures: M. Sereika:** None. **J.A. Beauchamp:** None. **A. Acosta:** None. **J.P. Dewald:** None. **J. Yao:** None. **M.D. Ellis:** None.

**Poster**

**PSTR186: Action/Sensation/Movement Selection: Human (Behavior/Physiology/Imaging) I**

**Location:** WCC Halls A-C

**Time:** Monday, November 16, 2026, 1:00 PM - 5:00 PM

**Program #/Poster #:** PSTR186.12/BB15

**Topic:** F.04. Voluntary Movements

**Support:** Raynor Cerebellum Project

**Title:** Deep Brain Stimulation Improves Quality of Rhythmic Movement in Children and Young Adults with Dystonia

**Authors: *A. SEYYED MOUSAVI**[1], R. SOROUSHMOJDEHI[2], M. KASIRI[4], J. NATARAJ[5], M. ASADI[3], T. D. SANGER[6];
[1]EECS, UCI, Irvine, CA; [2]Electrical Engin. and Computer Sci., [3]Computer Engin., Univ. of California Irvine, Irvine, CA; [4]Biomed. Engin., Univ. of California, Irvine, Irvine, CA; [5]EECS, Stanford Univ., Stanford, CA; [6]Res., Children's Hosp. of Orange County, Orange, CA

**Abstract:** Deep brain stimulation (DBS) provides a direct experimental means to modulate subcortical circuits and examine how their activity influences the dynamics of human motor control. Although DBS has well-established clinical effects, its effects on continuous and

rhythmic voluntary movement, including changes in timing, smoothness, and muscle coordination under direct neuromodulation, have not been quantitatively characterized.
This study aims to quantify how direct stimulation of deep motor circuits modulates kinematic and muscular dynamics during continuous figure-eight drawing and to determine whether these effects depend on stimulation at clinically optimized versus non-optimized targets.
Seven pediatric participants with dystonia performed continuous figure-eight movements with and without stimulation. Kinematic metrics were selected to quantify distinct aspects of motor control, including the speed-accuracy trade-off (SAT), movement time (MT), out-of-path movement (OPM), coefficient of variation of speed (CV), and log-dimensionless jerk (LDJ, smoothness). Surface electromyography (EMG) signals from eight upper-limb muscles were analyzed to compute a task correlation index (TCI) reflecting task-relevant muscle activation. Analyses were performed at both subject and group levels, comparing non-optimized (G1) versus clinically optimized (G2) stimulation sites.
Stimulation at optimized targets systematically modulated movement dynamics, reducing CV and LDJ and shifting SAT toward more efficient coordination. EMG spectra showed changes in task-relevant muscle activity, indicating that DBS altered the spectral composition of motor output during continuous movement. In contrast, stimulation at non-optimized sites produced variable and often disruptive effects.
This study provides the first quantitative characterization, during invasive human neuromodulation, of how DBS modulates the integrated dynamics of movement and muscle activity. These findings establish a quantitative framework linking circuit-level stimulation to motor-system behavior and define new dynamical markers for individualized DBS tuning.

**Disclosures: A. Seyyed Mousavi:** None. **R. Soroushmojdehi:** None. **M. Kasiri:** None. **J. Nataraj:** None. **M. Asadi:** None. **T.D. Sanger:** None.

**Poster**

**PSTR186: Action/Sensation/Movement Selection: Human (Behavior/Physiology/Imaging) I**

**Location:** WCC Halls A-C

**Time:** Monday, November 16, 2026, 1:00 PM - 5:00 PM

**Program #/Poster #:** PSTR186.13/BB16

**Topic:** F.04. Voluntary Movements

**Support:** National Science and Technology Innovation 2030 Major Program

**Title:** Neural Representations for Actions with and without Haptic Feedback: Spatial Modulation and Effector Independence

**Authors: *X. WU**[1], Z. DENG[2], F. ZHU[3], J. CHEN[1];
[1]Sch. of Psychology, South China Normal Univ., Guangzhou City, China; [2]Dept. of Neurosci., Dept. of Neuroscience, Georgetown Univ., Washington, DC; [3]Zhejiang Univ., Hang Zhou, China

**Abstract:** Investigating naturalistic action within the functional magnetic resonance imaging (fMRI) environment presents inherent methodological constraints, often necessitating surrogate

paradigms such as motor imagery or pantomimed actions. However, the absence of physical haptic feedback fundamentally alters the sensory information available for closed-loop sensorimotor control. In this study, we investigated the neural divergence between actions performed with haptic feedback (HF) and without haptic feedback (NoHF) and how spatial reference frames modulate these processes. Participants were instructed to grasp a small or big object (i.e., with haptic feedback) or just open their hands a matching amount without contact with the object (i.e., NoHF) either with left or right hand at a right position or a left position. We found that HF condition does not always facilities response amplitude. For right hand in the ipsilateral, minimal differences was observed. In the contralateral, NoHF condition consistently elicited stronger activation than HF condition in higher-order sensorimotor and association cortices, suggesting increased reliance on top-down sensorimotor control in the absence of haptic confirmation. The roughly same for both hands, with slight differences: HF condition showed greater activation than NoHF condition in several subcortical regions, including the caudate nucleus, hippocampus, and thalamus. Collectively, these findings indicate that the neural processing of haptic feedback is dynamically reorganized according to the spatial reference frame. In the ipsilateral space, HF condition exhibited no robust cortical advantage, with selective activity observed only in a limited number of subcortical regions during left-hand actions, suggesting a greater reliance on relatively automated sensorimotor processing. In contrast, in the contralateral space, NoHF condition elicited widespread recruitment of sensorimotor and higher-order association cortices, indicating increased involvement of cortical networks supporting action planning, monitoring, and sensorimotor integration.

**Disclosures: X. Wu:** None. **Z. Deng:** None. **F. Zhu:** None. **J. Chen:** None.

**Poster**

**PSTR186: Action/Sensation/Movement Selection: Human (Behavior/Physiology/Imaging) I**

**Location:** WCC Halls A-C

**Time:** Monday, November 16, 2026, 1:00 PM - 5:00 PM

**Program #/Poster #:** PSTR186.14/BB17

**Topic:** F.04. Voluntary Movements

**Support:** NSF BCS 2216344

**Title:** Effort Minimization Explains Upper-Limb Reaching Patterns in Stroke and Healthy Controls

**Authors: *T. SUBASH**[1], Y. DARMON[2], N. SCHWEIGHOFER[1];
[1]Biokinesiology and Physical Therapy, USC, Los Angeles, CA; [2]Res. Inst., Casa Colina Hospital, and Centers for Healthcare, Pomona, CA

**Abstract:** Post-stroke individuals often exhibit compensatory reaching behaviors, including trunk flexion, shoulder elevation, and reduced paretic arm use. Although often viewed as maladaptive, we hypothesized that these behaviors emerge from effort-minimizing control under altered biomechanical constraints. To test this, we developed a 9-DoF (trunk flexion, lateral

flexion, and rotation; clavicular protraction and elevation; shoulder flexion, internal rotation, and abduction; elbow flexion) biomechanical model of upper-extremity reaching. Joint configurations were computed using inverse kinematics to minimize effort costs (integrated sum of joint torques) while constraining the hand to reproduce observed endpoint trajectories. Stroke impairment was modeled as reduced torque-generating capacity (weakness) of the paretic shoulder and elbow joints, thereby increasing the cost of their use. Model fitting used data from 42 individuals with stroke and 12 age-matched controls performing reaches across an obstacle to central, lateral, and contralateral targets under free-trunk and trunk-restrained conditions. Model parameters governing shoulder and elbow torque capacity were estimated by minimizing errors between simulated and observed 9-DoF kinematics from control and post-stroke reaching movements, yielding subject-specific impairment estimates. All stroke participants reached the targets with trunk restraint, indicating that compensatory behaviors reflected strategy selection rather than inability. Simulations predicted that reductions in paretic-arm torque capacity led to increased reliance on trunk and clavicular motion during reaching. Despite its mass and gravitational cost, recruiting trunk motion and clavicular elevation reduced overall movement cost relative to moving shoulder and elbow joints with reduced torque capacity. When trunk motion was restricted, reaching required greater use of paretic joints, resulting in substantially higher effort and movements closer to anatomical joint limits. Furthermore, relative effort costs computed for each limb predicted arm choice probabilities, with lower torque capacity decreasing selection of the paretic arm despite preserved reaching capability, consistent with clinically observed patterns of arm non-use following stroke. These findings suggest post-stroke compensatory behaviors, including trunk and clavicular recruitment and paretic arm non-use, emerge as adaptive, effort-minimizing solutions to altered biomechanical capacities. This framework provides a unified mechanistic account linking motor impairment, compensation, and arm choice after stroke.

**Disclosures: T. Subash:** None. **Y. Darmon:** None. **N. Schweighofer:** None.

**Poster**

**PSTR186: Action/Sensation/Movement Selection: Human (Behavior/Physiology/Imaging) I**

**Location:** WCC Halls A-C

**Time:** Monday, November 16, 2026, 1:00 PM - 5:00 PM

**Program #/Poster #:** PSTR186.15/BB18

**Topic:** F.04. Voluntary Movements

**Support:** Dystonia Medical Research Foundation
Doris Duke Charitable Foundation
Dystonia Coalition (NS065701)
Dystonia Coalition (TR001456)
Dystonia Coalition (NS116025)
American Academy of Neurology
NIH NCATS

**Title:** One Day Accelerated TMS for Focal Hand Dystonia: A Phase II Clinical Trial

**Authors:** I. XU[1], ***D. BITLIS**[2], A. FACHE[2], Z. B. SIMSEK[3], P. MULCAHEY[3], Y. LI[3], N. HAMZAH[1], A. NORAIN[3], P. LEE[3], M. LIPP[3], S. DAVE[3], K. GROZEV[2], C. RUSSELL[2], C. PETTY[2], M. LUTZ[3], A. V. PETERCHEV[2], N. BUKHARI-PARLAKTURK[3];
[1]Duke-NUS Med. Sch., Singapore, Singapore; [2]Duke Univ., Durham, NC; [3]Duke Univ. Sch. of Med., Durham, NC

**Abstract:** Background: FHD is a neurological disorder characterized by involuntary postures and pain with limited therapeutic options. We previously showed that a single session of 10 Hz repetitive transcranial magnetic stimulation (rTMS) over the primary somatosensory cortex (PSC) improves motor behavior in FHD. This study evaluated the efficacy of four sessions of 10 Hz rTMS delivered in one day to FHD patients.
Methods: The study was a double-blind, crossover design. 19 FHD participants enrolled in the clinical trial (NCT 06015672) and 15 completed one or both study arms. TMS was targeted to PSC using fMRI and electric field modeling. Each participant received a single day of four sessions of active 10 Hz rTMS (16,000 pulses at 90% resting motor threshold) and a separate day of four sessions of sham rTMS. The two study arms were delivered in randomized order with a 20-week washout. TMS effects were evaluated using behavioral assays of somatosensory temporal discrimination threshold (STDT) to measure hand sensation, kinematic writing assay to measure hand movement, a fine motor dexterity assay called 9-hole pegboard and word legibility to measure hand function. The primary outcome measure was the peak accelerations during kinematic writing. Data was statistically analyzed using a mixed-effects model for repeated measures followed by multiple comparison adjustment.
Results: Preliminary findings indicate that active TMS significantly improved sensory discrimination (STDT) (mean difference -11%, p= 0.02, mixed effects model). Active TMS also improved straightness error during kinematic writing assay (mean difference 20%, p= 0.005) but not peak accelerations during writing (mean difference -6.58%, p= 0.28). For measures of hand function, active TMS improved word legibility (7.1%, p = 0.001) and the duration to complete fine motor dexterity tasks (mean difference -4.47%, p= 0.018) for 20 weeks compared to sham TMS.
Conclusions: These findings suggest that a single day of accelerated 10 Hz rTMS to PSC may provide clinical benefit lasting up to 20 weeks, supporting its promise as a viable therapeutic option for FHD. Our study is the longest reported behavioral benefit of TMS in humans.

**Disclosures: I. Xu:** None. **D. Bitlis:** None. **A. Fache:** None. **Z.B. Simsek:** None. **P. Mulcahey:** None. **Y. Li:** None. **N. Hamzah:** None. **A. Norain:** None. **P. Lee:** None. **M. Lipp:** None. **S. Dave:** None. **K. Grozev:** None. **C. Russell:** None. **C. Petty:** None. **M. Lutz:** None. **A.V. Peterchev:** B. Contracted Research/Research Grant (principal investigator for a drug study, collaborator or consultant and pending and current grants). If you are a PI for a drug study, report that research relationship even if those funds come to an institution.; Motif. C. Other Research Support (receipt of drugs, supplies, equipment or other in-kind support); MagVenture. E. Ownership Interest (stock, stock options, royalty, receipt of intellectual property rights/patent holder, excluding diversified mutual funds); Ampa Health, Magnetic Tides. F. Consulting Fees (e.g., advisory boards); Rogue Research, Ampa Health, Magnetic Tides, Soterix Medical. **N. Bukhari-Parlakturk:** F. Consulting Fees (e.g., advisory boards); DMRF Medical and Scientific Advisory Council.

**Poster**

**PSTR187: Motor Learning: Human (Behavior/Physiology/Imaging) II**

**Location:** WCC Halls A-C

**Time:** Monday, November 16, 2026, 1:00 PM - 5:00 PM

**Program #/Poster #:** PSTR187.01/BB19

**Topic:** F.04. Voluntary Movements

**Support:** NIH Grant 1R01NS139424-01
Dorothy Foehr Huck and J.Lloyd Huck Distinguished Chair of Kinesiology and Neurology awarded to R.L. Sainburg

**Title:** Continuous theta-burst stimulation of left posterior parietal cortex impairs visuomotor adaptation but not intermanual transfer

**Authors: *P. R. RUELOS**[1], N. M. KITCHEN[2], M. WALI[3], M. YAROSSI[5], E. TUNIK[6], R. L. SAINBURG[4];
[1]Kinesiology, The Pennsylvania State Univ., University Park, PA; [2]Neurol., Penn State Univ., Hershey, PA; [3]Kinesiology, [4]Kinesiology & Neurol., Penn State Univ., University Park, PA; [5]Physical Therapy Movement and Rehabil. Sci. / Electrical and Computer Engin., Northeastern Univ., Medford, MA; [6]Dept. of Physical Therapy, Movement, and Rehabil. Sci., Northeastern Univ., Boston, MA

**Abstract:** The left posterior parietal cortex (PPC) has been implicated in visuomotor adaptation, although the precise nature of its contribution remains unclear. Previous lesion studies demonstrated that damage to the left, but not right, PPC impairs visuomotor adaptation with either arm, suggesting a lateralized role for the left PPC in visuomotor learning (Mutha et al., 2011). Consistent with this, cathodal HD-tDCS over left PPC disrupts both adaptation and intermanual transfer (Kumar et al., 2020). In contrast, anodal HD-tDCS over left, but not right, PPC facilitates intermanual transfer without affecting adaptation (Dexheimer et al., 2026). Together, these findings suggest that the neural mechanisms underlying adaptation and transfer may be partially dissociable and differentially influenced by PPC excitability. To further examine the causal role of PPC in adaptation, we utilized continuous theta-burst stimulation (cTBS), a form of repetitive transcranial magnetic stimulation that transiently suppresses cortical excitability. Healthy right-handed adults received cTBS over the left PPC, right PPC, or sham stimulation before adapting reaching movements to a 30° visuomotor rotation with the dominant right arm, followed by assessment of intermanual transfer with the left arm. Stimulation group significantly affected right-arm adaptation ($p = 0.023$). Participants receiving left PPC cTBS exhibited larger direction errors than sham ($p = 0.006$), with impairments evident during both early ($p = 0.013$) and late ($p = 0.018$) adaptation phases. Stimulation group had no significant effect on intermanual transfer. These findings support a causal role for left PPC in visuomotor adaptation and extend previous lesion work by demonstrating that transient inhibition of left PPC is sufficient to impair learning. Together with prior findings that excitatory left PPC stimulation enhances transfer without improving adaptation, these results support the hypothesis that the left PPC contributes critically to visuomotor adaptation. The absence of a corresponding effect on interlimb transfer suggests that the neural mechanisms supporting transfer may be at least partially dissociable from those supporting adaptation or may be less sensitive to transient

disruption of PPC function. Future work examining adaptation of the left arm will determine whether these effects are specific to the dominant limb or reflect a bilateral role of left PPC in visuomotor learning.

**Disclosures: P.R. Ruelos:** None. **N.M. Kitchen:** None. **M. Wali:** None. **M. Yarossi:** None. **E. Tunik:** None. **R.L. Sainburg:** None.

**Poster**

**PSTR187: Motor Learning: Human (Behavior/Physiology/Imaging) II**

**Location:** WCC Halls A-C

**Time:** Monday, November 16, 2026, 1:00 PM - 5:00 PM

**Program #/Poster #:** PSTR187.02/BB20

**Topic:** F.04. Voluntary Movements

**Support:** NIH Grant 1R01NS139424-01
Dorothy Foehr Huck and J. Lloyd Huck Distinguished Chair of Kinesiology and Neurology awarded to R.L.Sainburg

**Title:** Cathodal HD-tDCS over posterior parietal cortex does not alter visuomotor adaptation nor interlimb transfer

**Authors: *M. WALI**[1], N. M. KITCHEN[2], P. R. RUELOS[4], R. F. DOXTADER[5], M. YAROSSI[6], E. TUNIK[7], R. L. SAINBURG[3];
[1]Dept. of Kinesiology, Penn State Univ., University Park, PA; [2]Neurol., Penn State Univ., Hershey, PA; [3]Kinesiology & Neurol., Penn State Univ., University Park, PA; [4]Dept. of Kinesiology, The Pennsylvania State Univ., University Park, PA; [5]Dept. of Kinesiology, The Pennsylvania State Univ., State College, PA; [6]Physical Therapy Movement and Rehabil. Sci. / Electrical and Computer Engin., Northeastern Univ., Medford, MA; [7]Dept. of Physical Therapy, Movement, and Rehabil. Sci., Northeastern Univ., Boston, MA

**Abstract:** Lesion studies from our laboratory have shown that damage to the left, but not the right, posterior parietal cortex (PPC) impairs visuomotor adaptation in both arms. Consistent with these findings, previous studies reported that cathodal (presumably inhibitory) high-definition transcranial direct current stimulation (HD-tDCS) over left PPC disrupted both adaptation and interlimb transfer (Kumar et al., 2020). We recently showed that anodal (presumably excitatory) HD-tDCS over left PPC enhanced interlimb transfer while leaving initial adaptation intact (Dexheimer et al., 2026). These findings suggest that PPC contributions to motor learning may depend on stimulation polarity. To test this possibility, we applied cathodal HD-tDCS over the left PPC, right PPC, or sham stimulation during visuomotor adaptation in right-handed neurotypical adults (n = 20 per group). Participants first performed reaching movements with veridical visual feedback, after which a 30° visuomotor rotation was introduced during dominant-arm adaptation. The same rotation was then applied to the non-dominant arm to assess interlimb transfer. Finally, participants performed reaches with veridical feedback using the non-dominant arm to quantify aftereffects. Preliminary analyses indicate that cathodal

stimulation of neither the left nor the right PPC significantly affected adaptation to the visuomotor rotation or transfer of learning to the opposite arm. However, left PPC stimulation showed a trend toward disrupting within-movement corrections near movement end, suggesting a possible role of left PPC in late-stage online error correction. Taken together with previous lesion and neuromodulation studies, our findings suggest that the behavioral consequences of PPC disruption depend on the nature, magnitude, and timing of the neural perturbation. Our current findings, showing a trend toward impaired late movement corrections following left PPC stimulation, appear consistent with previous lesion studies implicating PPC in online adjustment of reaching movements (Gréa et al., 2002).

**Disclosures: M. Wali:** None. **N.M. Kitchen:** None. **P.R. Ruelos:** None. **R.F. Doxtader:** None. **M. Yarossi:** None. **E. Tunik:** None. **R.L. Sainburg:** None.

**Poster**

**PSTR187: Motor Learning: Human (Behavior/Physiology/Imaging) II**

**Location:** WCC Halls A-C

**Time:** Monday, November 16, 2026, 1:00 PM - 5:00 PM

**Program #/Poster #:** PSTR187.03/BB21

**Topic:** F.04. Voluntary Movements

**Title:** A computational mechanism underlying reversal between learning performance and delayed retention in context-dependent visuomotor rotation learning

**Authors: *H. GOMI**[1,2], A. OGAWA[3];
[1]Fac. of Sci. and Engin., Waseda Univ., Tokyo, Japan; [2]NTT Communication Sci. Labs., NTT, Kanagawa, Japan; [3]NTT Communication Sci. Labs., Kanagawa, Japan

**Abstract:** Contextual information facilitates difficult motor learning (Osu et al., 2004; Howard et al., 2013), and appropriate contextual cues enable adaptation to conflicting visuomotor transformations that would otherwise be impossible without such cues (Baldeo & Henriques, 2013; Abekawa et al., 2022). We recently found an unexpected dissociation in a context-dependent visuomotor rotation task. When arm movements in a given condition were closer to those in other conditions, learning performance during training was worse than in conditions in which arm movements were more distinct. However, when retention was tested after a delay, the higher-conflict conditions showed better retention. This reversal was not observed immediately after learning, suggesting that the responsible mechanism does not simply affect end-of-training performance, but instead influences how learning is stored over time. We therefore asked what computational mechanism could account for this pattern. To address this question, we constructed a two-rate learning model with fast and slow adaptive processes and simulated conditions differing in motor-state conflict. Model parameters governing retention, learning, and conflict were chosen to capture the main features of the behavioral data. The simulations reproduced the experimental findings when interference arose from assigning nearby motor states to distinct cue-dependent mappings, thereby reducing the effective contribution of fast learning and increasing reliance on slower, more persistent learning. These findings suggest that

motor-state conflict plays an important role in regulating the balance between fast and slow learning processes, thereby determining whether a learning condition preferentially supports immediate performance or durable memory. Such a mechanism may be beneficial when nearby motor states compete strongly, because it would reduce dependence on rapidly updated but unreliable learning and instead promote the formation of motor memory that is more robust over time. More broadly, our model integrates ideas from contextual interference, contextual gating of dual adaptation, and gaze-/planning-dependent motor memory to explain the dissociation between learning performance and delayed retention in context-dependent visuomotor rotation learning.

**Disclosures: H. Gomi:** None. **A. Ogawa:** None.

**Poster**

**PSTR187: Motor Learning: Human (Behavior/Physiology/Imaging) II**

**Location:** WCC Halls A-C

**Time:** Monday, November 16, 2026, 1:00 PM - 5:00 PM

**Program #/Poster #:** PSTR187.04/BB22

**Topic:** F.04. Voluntary Movements

**Title:** Movement directional similarity reverses learning performance and delayed retention in context-dependent visuomotor rotation learning

**Authors: *A. OGAWA**[1], N. SAIJO[1], S. TAKAMUKU[1], H. GOMI[2,1];
[1]Communication Sci. Laboratories, NTT, Inc., Kanagawa, Japan; [2]Sch. of Creative Sci. and Engin., Waseda Univ., Tokyo, Japan

**Abstract:** Effective contextual cues can allow successful motor learning even when opposing mappings would otherwise interfere (Osu et al. 2004; Howard et al., 2013). Understanding how interference and contextual information jointly shape motor learning and memory is therefore important. Here, we asked how the degree of movement direction similarity during learning affects subsequent retention in an opposing visuomotor rotation task in which contextual cues enable dual adaptation. In Experiment 1, we used opposing clockwise and counterclockwise visuomotor rotations, with two reach targets and their gaze relationships as contextual cues (left and right peripheral targets; Abekawa et al. 2022). Trajectory similarity (Baldeo & Henriques 2013) was manipulated according to the different cue and target combinations. Twenty-five participants made reach movements on a pen tablet. The visuomotor rotation associated with each context was gradually increased to 17° and then held constant. At the beginning of learning, trajectories under the opposing rotations were similar. As learning progressed, however, the task was designed so that, for one pair of conditions, the trajectories became more similar, whereas for the other pair they became more distinct. Cursor feedback was provided during training, and no-cursor blocks at the end of learning assessed final adaptation. End-of-training performance was higher in conditions with lower trajectory similarity, whereas retention tested 12 min later (delayed retention) was higher in conditions with higher trajectory similarity. Thus, even when contextual cues supported successful opposing adaptation, better performance at the end of

learning did not necessarily predict stronger motor memory. In Experiment 2 (n = 8), we strengthened this manipulation so that two conditions became even closer in trajectory space, and again found that conditions with better learning performance showed lower delayed retention. In Experiment 3 (n = 8), this difference was absent when retention was tested immediately after learning. These results suggest that movement similarity alters the relative contribution of fast and slow learning processes: more distinct movement-related information favors fast learning, whereas less distinct information favors slower learning. Thus, the relationship between contextual cues and motor state may play an important role in determining how motor memories are formed and retained.

**Disclosures: A. Ogawa:** None. **N. Saijo:** None. **S. Takamuku:** None. **H. Gomi:** None.

**Poster**

**PSTR187: Motor Learning: Human (Behavior/Physiology/Imaging) II**

**Location:** WCC Halls A-C

**Time:** Monday, November 16, 2026, 1:00 PM - 5:00 PM

**Program #/Poster #:** PSTR187.05/BB23

**Topic:** F.04. Voluntary Movements

**Support:** JST Moonshot R&D (JPMJMS2012)

**Title:** Online motor cortical tDCS mitigates fatigue-related impairment of force control learning: a sham-controlled parallel design study

**Authors: *S. TANAKA**, Y. KURITA, M. TAKEMI;
Grad. Sch. of Advanced Sci. and Engin., Hiroshima Univ., Higashi-Hiroshima, Japan

**Abstract:** Online motor cortical tDCS mitigates fatigue-related impairment of force control learning: a sham-controlled parallel design study Motor skill learning requires repeated practice, but practice often induces fatigue. Fatigue changes both peripheral muscle output and central sensorimotor processing, which can impair the sensory information and cortical state needed for learning. Previous work showed that motor memories formed under fatigue can persist across days and that post-practice inhibitory stimulation can attenuate their consolidation. Anodal transcranial direct current stimulation (a-tDCS) during practice is known to enhance skill consolidation in nonfatigued participants. However, whether online motor cortical a-tDCS can mitigate learning impairment when practice itself is performed under fatigue remains unclear. We tested this using a sham-controlled parallel design. Participants were assigned to an online tDCS fatigue group (N = 18), a sham tDCS fatigue group (N = 16), or a nonfatigue control group (N = 20). On day 1, the fatigue groups performed a sustained maximal force task until force output dropped to 40% of maximum. They then practiced a visuomotor force control task, in which they pressed a force sensor to move a cursor through sequential target gates. The same practice task was repeated on day 2. Electromyography during 20% maximum force production confirmed increased muscle activity after the fatigue task ($p = .014$) with no group main effect between the two fatigue groups ($p = .210$). Learning was assessed with a skill measure

combining error rate and movement time. The skill measure showed a group by set interaction ($p = .047$). On day 2, the online tDCS group and a nonfatigue control group showed higher skill than the sham tDCS fatigue group with large effect sizes (Cohen's $d > 0.8$). Movement time decreased across practice, but no group effect or group by set interaction was detected. Error rate differed across groups ($p = .005$); the sham tDCS fatigue group showed higher error rates than the nonfatigue and online tDCS groups, with no group by set interaction. Analyses of individual target gates suggested that fatigue related impairment was most evident at gates requiring fine or high force control. These findings suggest that online motor cortical a-tDCS may attenuate fatigue related impairment in force control learning by reducing accuracy loss rather than by accelerating movement.

**Disclosures: S. Tanaka:** None. **Y. Kurita:** A. Employment/Salary (full or part-time):; humanmodel inc.. E. Ownership Interest (stock, stock options, royalty, receipt of intellectual property rights/patent holder, excluding diversified mutual funds); humanmodel inc. **M. Takemi:** A. Employment/Salary (full or part-time):; Neuractice Inc.. E. Ownership Interest (stock, stock options, royalty, receipt of intellectual property rights/patent holder, excluding diversified mutual funds); Neuractice Inc..

**Poster**

**PSTR187: Motor Learning: Human (Behavior/Physiology/Imaging) II**

**Location:** WCC Halls A-C

**Time:** Monday, November 16, 2026, 1:00 PM - 5:00 PM

**Program #/Poster #:** PSTR187.06/BB24

**Topic:** F.04. Voluntary Movements

**Support:** JSPS KAKENHI (24K14608)

**Title:** Preparatory and post-movement beta-band EEG dynamics in sensory error-based motor learning

**Authors: *T. UGAI**[1], N. SENTA[2], M. TAKEMI[1];
[1]Grad. Sch. of Advanced Sci. and Engin., Hiroshima Univ., Higashi-Hiroshima, Hiroshima, Japan; [2]Grad. Sch. of Sci. and Technol., Keio Univ., Yokohama, Kanagawa, Japan

**Abstract:** Motor learning requires the brain to evaluate sensory errors and update subsequent actions. Beta-band electroencephalography (EEG) activity over sensorimotor cortex changes around movement, including foreperiod beta (FpB) before movement, event-related desynchronization (ERD) during movement, and post-movement beta rebound (PMBR) after movement. Although ERD has been widely linked to motor control and learning, it remains unclear whether preparatory and post-movement beta reflect distinct components of sensory error-based learning. We examined beta-band dynamics around movement in a visuomotor rotation task designed to isolate trial-by-trial correction. Twelve participants made reaching movements across six sessions while EEG was recorded. Brief cursor perturbations (+/-2° or +/-4°) were randomly presented to generate signed movement errors. Learning rate was defined as

the slope relating each perturbation error to the change in hand position on the next trial, when cursor feedback was removed. EEG beta power was analyzed before and after movement over the right upper limb sensorimotor area. For correlation analyses, behavioral and EEG metrics were averaged within each of the six sessions per participant. We focused on absolute perturbation error and learning rate as behavioral indices. All participants showed negative learning rates, indicating larger counter corrections after larger errors. Consistent with prior work, lower FpB power was associated with larger session-averaged absolute perturbation error ($r = -.280$, $p = .026$), whereas PMBR was not significantly associated with error size ($r = .057$, $p = .660$). Sensorimotor FpB showed a weak positive association with the session-wise learning rate, but this relation did not reach significance ($r = .23$, $p = .064$). Furthermore, PMBR was not associated with learning rate ($r = .019$, $p = .880$). PMBR in perturbation trials differed across sessions ($F(3.1, 34.2) = 3.31$, $p = .027$), peaking in the third of six sessions rather than increasing progressively across practice. These findings suggest that FpB is sensitive to sensory error size before corrective movements, whereas PMBR did not simply track error magnitude in the present task. Future analyses using single-trial correction measures, together with task designs that stabilize the hand at the endpoint, may better test how beta activity relates to error evaluation and trial-by-trial learning. Additionally, applying larger perturbations will be needed to minimize the relative influence of intrinsic motor noise.

**Disclosures: T. Ugai:** None. **N. Senta:** None. **M. Takemi:** A. Employment/Salary (full or part-time):; Neuractice Inc.. E. Ownership Interest (stock, stock options, royalty, receipt of intellectual property rights/patent holder, excluding diversified mutual funds); Neuractice Inc..

**Poster**

**PSTR187: Motor Learning: Human (Behavior/Physiology/Imaging) II**

**Location:** WCC Halls A-C

**Time:** Monday, November 16, 2026, 1:00 PM - 5:00 PM

**Program #/Poster #:** PSTR187.07/BB25

**Topic:** F.04. Voluntary Movements

**Title:** Bilateral Contribution of Somatosensory Cortex in Motor Memory Consolidation

**Authors: *R. JAIN**, N. KUMAR;
Indian Inst. of Technol., Hyderabad, India

**Abstract:** Humans maintain accurate movements in changing environments through motor adaptation. Although motor control is traditionally considered contralateral, the dominant left hemisphere contributes to movements of both limbs, producing hemispheric asymmetries in regions such as the primary motor cortex and the posterior parietal cortex (PPC). Whether the primary somatosensory cortex, a key substrate for motor memory consolidation, exhibits similar asymmetry or remains predominantly contralateral is unknown. To address this question, participants adapted to a gradual 30° visuomotor rotation during a point-to-point reaching task performed with the non-dominant left hand. Immediately following adaptation, continuous theta-burst stimulation (cTBS) was applied over either the contralateral right somatosensory cortex,

the ipsilateral left somatosensory cortex, or a sham stimulation site. Motor memory consolidation was assessed on the following day using retention trials. Participants were then re-exposed to an abrupt 30° rotation to characterize relearning. Retention was significantly reduced following the disruption of both contralateral and ipsilateral somatosensory cortex in comparison to sham. These findings suggest that bilateral contribution of somatosensory cortex in motor memory consolidation. These findings challenge a strictly contralateral model of somatosensory function, indicating that the ipsilateral hemisphere contributes to the offline stabilization of motor memories, possibly through its role in storing effector-independent movement representations or interlimb sensorimotor transfer.

**Disclosures: R. Jain:** None. **N. Kumar:** None.

**Poster**

**PSTR187: Motor Learning: Human (Behavior/Physiology/Imaging) II**

**Location:** WCC Halls A-C

**Time:** Monday, November 16, 2026, 1:00 PM - 5:00 PM

**Program #/Poster #:** PSTR187.08/BB26

**Topic:** F.04. Voluntary Movements

**Support:** Rheumatology Research Foundation, Investigator Award
Cleveland Clinic Neurological Institute, Clinician Scientist Award

**Title:** Determining if adults with knee osteoarthritis have impairments in locomotor learning

**Authors:** S. PRICE[1], S. DARADKEH[1], M. STREICHER[1], J. MIHY[1], S. M. MORTON[2], L. A. FREY LAW[3], J. WILLSON[4], E. HUSNI[1], ***P. CORRIGAN**[1];
[1]Cleveland Clin., Cleveland, OH; [2]Physical Therapy, Univ. of Delaware, Newark, DE; [3]Univ. of Iowa, Iowa City, IA; [4]East Carolina Univ., Greenville, NC

**Abstract: Problem statement/motivation:** Knee osteoarthritis (KOA) is a leading cause of chronic pain and disability. Gait retraining, including modifications of foot progression angle (FPA) (e.g., external rotation to reduce medial knee joint loading), has been proposed as a viable treatment for slowing structural progression and reducing pain. However, adults with KOA have maladaptive brain activity in motor and pain networks that could impair consolidation of new motor patterns. This study aimed to determine if adults with KOA have impaired acquisition, retention, and transfer when learning an FPA modification. **Methods:** Adults with (n= 32; 29 F; age= 63±8 y; BMI= 22±3 kg/m$^2$; knee pain (0-10) with walking = 2±2) and without (n= 17; 12 F; age= 60±8 y; BMI= 23±5 kg/m$^2$) KOA were enrolled. Participants walked on a treadmill in a 3D motion capture environment. The walking paradigm, which aimed to increase FPA by 10° (i.e., external rotation), included learning blocks and phases of measuring retention and transfer (Fig 1a). Acquisition was assessed as change in FPA for each learning block relative to baseline FPA. To assess absolute retention and transfer, performance in each retention or transfer phase was assessed relative to the preceding learning block (i.e., subtracting FPA during R1, T1, and T2 from FPA during L1, L2, and L3, respectively, and taking the absolute value). Two 2 (group)

x 3 (blocks/phases) ANCOVA models were constructed; one testing differences in acquisition and the other testing differences in absolute retention and transfer. **Results:** Stepwise changes in FPA are shown in Fig 1b for each group. ANCOVA models showed no significant interactions or main effects of group or period in acquisition (Fig 1c), absolute retention, or absolute transfer (Fig 1d). **Conclusion:** Adults with KOA and minimal pain do not have impairments in acquisition or immediate retention and transfer of a FPA modification, suggesting that gait retraining could be a viable treatment for those with little-to-no pain. Further work is needed to determine generalizability to adults with KOA and more severe pain.

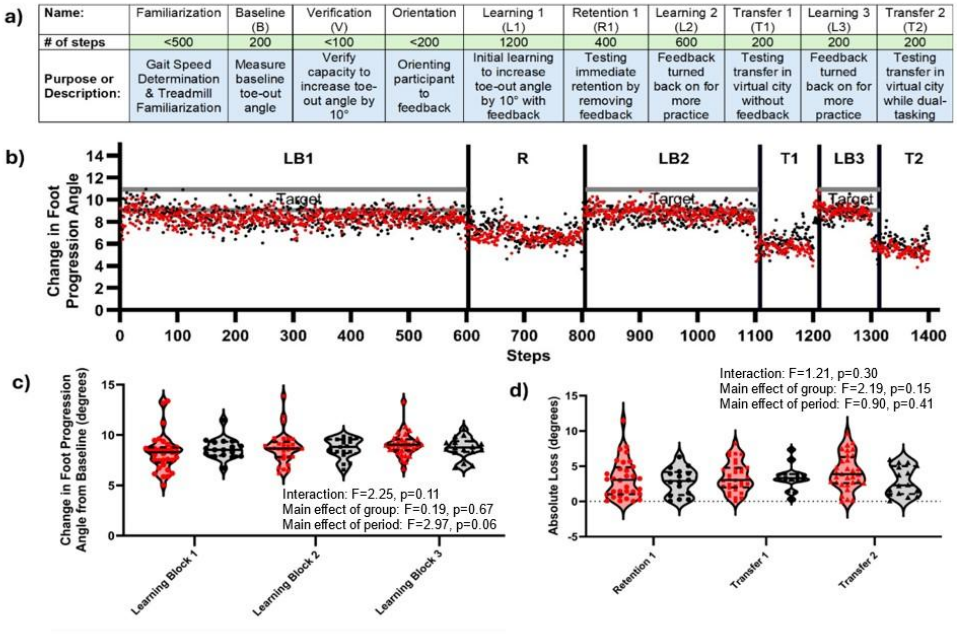



**Figure 1**. a) Walking paradigm, b) stepwise changes in FPA c) violin plots for learning blocks, and d) violin plots for absolute loss during retention and transfer phases. Adults with and without KOA are shown in red and black, respectively.

**Disclosures: S. Price:** None. **S. Daradkeh:** None. **M. Streicher:** None. **J. Mihy:** None. **S.M. Morton:** None. **L.A. Frey Law:** None. **J. Willson:** None. **E. Husni:** None. **P. Corrigan:** None.

**Poster**

**PSTR187: Motor Learning: Human (Behavior/Physiology/Imaging) II**

**Location:** WCC Halls A-C

**Time:** Monday, November 16, 2026, 1:00 PM - 5:00 PM

**Program #/Poster #:** PSTR187.09/BB27

**Topic:** F.04. Voluntary Movements

**Support:** UT San Antonio, College for Health, Community and Policy

**Title:** The Influence of Retention Interval and Performance Stability on Motor Memory Decay

**Authors: *S.-W. PARK**;
The Univ. of Texas at San Antonio, San Antonio, TX

**Abstract:** Assessing learned motor skills after an adequate retention interval is essential for investigating motor learning. While recent studies evaluate motor retention over several days, few have directly investigated the relationship between retention interval length and memory decay within this time scale. Furthermore, conflicting evidence exists regarding whether prolonged intervals induce warm-up decrements due to temporary memory loss or facilitate offline learning. To test the hypothesis that motor memory decay scales with retention interval length, a virtual throwing task was adopted to analyze motor learning processes during practice over two daily sessions. Eighty-four healthy participants (mean age: 21.8 years; 30 males, 54 females) practiced the task across two sessions. In Session 1, participants completed 4 blocks of 60 trials. In Session 2, they performed a single block of 60 trials. The retention interval between sessions varied across participants from 1 to 16 days (mean: 4.0 days). Performance metrics included the number of successful throws within a block, the minimum distance error between the trajectory and the virtual ball, variability of the distance error, and the variability of the execution variables (release angle and velocity). Performance changes were calculated across all 5 blocks. Fifty-seven out of the 84 participants demonstrated significant performance improvements by the end of Session 1. Within this cohort, the retention interval length did not significantly correlate with any performance metric that measures performance changes between the end of Session 1 and the start of Session 2 ($p > 0.05$, uncorrected). This independence remained even when analyzing smaller trial windows from the end of Session 1 and the beginning of Session 2. In contrast, distance error variability at the end of Session 1, an indicator of performance stability, was strongly correlated with the degree of retention at the beginning of Session 2 ($r = 0.67$, $p = 0.00005$). These findings indicate that motor memory consolidation is strongly associated with the stability of motor performance rather than the length of the retention interval. These results challenge the conventional assumption that retention interval duration dictates memory decay, highlighting the need for further studies to elucidate the mechanisms underlying motor memory consolidation.

**Disclosures: S. Park:** None.

**Poster**

**PSTR187: Motor Learning: Human (Behavior/Physiology/Imaging) II**

**Location:** WCC Halls A-C

**Time:** Monday, November 16, 2026, 1:00 PM - 5:00 PM

**Program #/Poster #:** PSTR187.10/Web Only

**Topic:** F.04. Voluntary Movements

**Support:** Department of Science and Technology, Government of India

**Title:** Error size and contextual experience bias model-free versus model-based reinforcement mechanisms in exogenous task-error-driven adaptation

**Authors:** S. VAASANTHI, ***P. K. MUTHA**;
Indian Inst. of Technol. Gandhinagar, Gandhinagar, India

**Abstract:** The sensorimotor system adapts to exogenously induced task errors by engaging reinforcement learning (RL) mechanisms. Yet, how the motor system arbitrates between model-free (MF) versus model-based (MB) RL processes during learning remains unclear. Here we asked whether this arbitration is governed by error-magnitude and contextual cues. We used a center-out reaching task in which participants reached from a start position to one of four targets. Following baseline trials target perturbations were introduced by displacing the target (target jumps) at movement onset, creating externally-induced task errors. Interspersed no-jump catch trials without visual feedback and a subsequent washout phase were used to quantify after-effects, a signature of MF stimulus-response caching. In Experiment 1, jump magnitudes (7.5°-90°) systematically shaped the learning strategy engaged. Small perturbations (≤15°) produced reliable after-effects (2-3°) with minimal reaction time changes, consistent with MF caching. In contrast, large perturbations (≥60°) led to elevated reaction times and no after-effects, consistent with MB planning. Intermediate perturbations (30°) elicited mixed signatures, suggesting arbitration between mechanisms. Error magnitude thus acts as a natural switch between RL systems. We next examined whether a predictive cue indicating jump direction prior to movement onset could override the default MF caching observed for small perturbations. In Experiment 2, a cued group showed near-zero after-effects while an uncued group showed robust after-effects (1.34°-2.29°), with significant between-group differences from the first catch block onward. However, suppressed after-effects under cuing are ambiguous since they could reflect genuine MB-like learning or mere reliance on an explicit strategy that masks MF caching without replacing it. Experiment 3 resolved this ambiguity by removing the cue after an initial cued training session. If cuing only masked MF learning, after-effects should re-emerge once the cue is withdrawn. However, participants trained with cues showed significantly reduced after-effects in a subsequent no-cue session, compared to a group trained without cues throughout. This indicated a genuine disruption of MF caching and a shift toward MB-like learning following cue-guided experience. Together, these results show that engagement of MF and MB processes is governed by error magnitude, and that contextual cues can durably shift the system from its default MF strategy to an MB-like one, even when conditions revert to those that would otherwise favor MF caching.

**Disclosures: S. Vaasanthi:** None. **P.K. Mutha:** None.

**Poster**

**PSTR187: Motor Learning: Human (Behavior/Physiology/Imaging) II**

**Location:** WCC Halls A-C

**Time:** Monday, November 16, 2026, 1:00 PM - 5:00 PM

**Program #/Poster #:** PSTR187.11/BB28

**Topic:** F.04. Voluntary Movements

**Support:** NASA Grant #80NSSC20K1499

**Title:** Bimanual coordination during gravitational transitions simulated with parabolic flight and lower-body negative pressure

**Authors: *R. RAO**[1], M. WEINRICH[2], R. ABBOTT[1], O. PINTO NETO[3,4], B. J. DUNBAR[1], D. M. KENNEDY[2], A. DIAZ ARTILES[1,2];
[1]Aerospace Engin., [2]Kinesiology and Sport Mgmt., Texas A&M Univ., College Station, TX; [3]Applied Physiol. and Kinesiology, Cal State Univ. - San Marcos, San Marcos, CA; [4]Biomed. Engin., Anhembi Morumbi Univ., Sao Jose dos Campos, Brazil

**Abstract:** Microgravity is known to induce sensorimotor performance deficits, but less is known about transitions between gravity levels (g-transitions) that astronauts will experience on future missions to the Moon and Mars. Parabolic flight (PF) is the gold standard for investigating such g-transitions, but cost and operational complexity limit broader research applications. In this study, we examined bimanual coordination (BMC) performance during transitions from hypogravity conditions (0 g, 0.25 g, 0.50 g, 0.75 g) to hypergravity (1.8g) during PF. We then evaluated the potential of lower-body negative pressure (LBNP) as a ground based analog for these g-transitions. For the PF arm of the study, 12 right-handed, astronaut-like adults performed 4 BMC tasks in all selected gravity conditions and a 1 g baseline. The selected BMC tasks (0°/1:1 (control), 1:2, 90°, 180°) span bimanual frequency and relative phase and were performed continuously through the parabolic maneuver to characterize performance across the g-transition. Tasks were performed using isometric contractions from the left and right triceps, and a controllable cursor on an external headset Lissajous display allowed participants to monitor their progress. The LBNP study arm follows the PF protocol and asks participants to perform the same BMC tasks while sealed inside an LBNP device to the iliac crest. Pressure is manipulated using a sequence of 22 s at 0 mmHg, 15 s at −50 mmHg, 30 s at 0 mmHg, repeated 10x to mimic the parabolas experienced in the PF arm. PF participants were able to complete all tasks in all gravity levels and maintained timing across the g-transition window. ANOVA revealed a significant gravity effect ($p < 0.001$) in the change in normalized peak force pre/post transition (ΔNormPF). ΔNormPF was significantly larger in 0 g than any partial-g level ($\bar{\Delta}$: 0 g = 0.42 ± 0.20, 0.25 g = 0.29 ± 0.13, 0.50 g = 0.23 ± 0.08, 0.75 g = 0.20 ± 0.06; all $p < 0.001$), and a dose-response effect was observed, indicating partial-g may be protective against g-transition disruptions. Normalized force variance was also disrupted ($\bar{\Delta}$: 0 g = 0.20 ± 0.16, 0.25 g = 0.12 ± 0.09, 0.50 g = 0.10 ± 0.07, 0.75 g = 0.10 ± 0.08). ANOVA revealed a significant gravity effect ($p < 0.001$). Post hoc analysis showed significant differences between 0 g and partial-gs (0 g v 0.25 g: $p = 0.003$; all other $p < 0.001$) and 0.25 g compared to 0.75 g ($p = 0.036$). Preliminary (n=5) LBNP peak force timeseries are comparable to curves from PF, with the greatest disruptions in the 1:1 and 90° tasks, indicating promise as a PF analog. However, irregularities in disruption timing potentially implicate subject anticipation as a confounding factor.

**Disclosures: R. Rao:** None. **M. Weinrich:** None. **R. Abbott:** None. **O. Pinto Neto:** None. **B.J. Dunbar:** None. **D.M. Kennedy:** None. **A. Diaz Artiles:** None.

**Poster**

**PSTR187: Motor Learning: Human (Behavior/Physiology/Imaging) II**

**Location:** WCC Halls A-C

**Time:** Monday, November 16, 2026, 1:00 PM - 5:00 PM

**Program #/Poster #:** PSTR187.12/BB29

**Topic:** F.04. Voluntary Movements

**Support:** NIH Grant R01NS117699
Simons Foundation International SFI-AN-NCSCN-00007276

**Title:** Contextual uncertainty de-multiplexes motor-memory updating across arms in bimanual control

**Authors: *A. S. NAIK**[1], C. A. VELAZQUEZ-VARGAS[1], S. SHIVKUMAR[1], J. N. INGRAM[2], M. LENGYEL[2,3], D. M. WOLPERT[1,2];
[1]Zuckerman Inst., Columbia Univ., New York, NY; [2]Dept. of Engin., Univ. of Cambridge, Cambridge, United Kingdom; [3]Dept. of Cognitive Sci., Central European Univ., Budapest, Hungary

**Abstract:** Many everyday actions require choosing between the hands. When contextual cues are certain, the hand choice is obvious; when cues are uncertain, the choice becomes ambiguous. Such choices create a motor credit-assignment problem: if movement produces an error, should learning update only the memory for the hand used, or also the memory for the alternative hand that might have been appropriate? When context clearly specifies the acting hand, error can be assigned to the corresponding hand-specific memory. When context is ambiguous, the same error may instead be assigned in proportion to the learner's belief about which hand context was active. Across two studies, we tested whether contextual uncertainty shifts error assignment from hand-specific updating to belief-weighted demultiplexing across arms.
Participants made left- or right-hand reaches to targets cued by random dots. Dot direction indicated the active hand/context, and dot coherence controlled contextual uncertainty. Force-field direction was coupled to dot direction, so cue-consistent choices produced the expected hand-specific perturbation, whereas wrong-hand choices produced a force field opposite to that hand's expectation.
Study 1 tested whether contextual uncertainty updates memories of both hands. In Exp. 1a, participants learned opposing force fields under uncertainty. During testing, the right hand continued to experience context-dependent fields while the left hand was error-clamped. Left-hand adaptation remained elevated despite no explicit error feedback. In a control without random-dot cues but matched target sequence and feedback contingencies (Exp. 1b), left-hand adaptation decayed near zero and was significantly lower than in Exp. 1a over the final 10 blocks ($p < .001$), suggesting that uncertainty promotes belief-weighted updating across hands.
Study 2 tested whether error in one hand demultiplexes memory updating across hands. In Exp. 2a, participants trained under uncertainty, underwent washout, and then experienced gradual reinstatement of the right-hand force field while the left hand remained error-clamped. As right-hand adaptation recovered, left-hand adaptation also rebounded. Across control experiments, left-hand adaptation remained near zero both when uncertainty was removed (Exp. 2b; $p < .01$) and when both hands were error-clamped after washout (Exp. 2c; $p < .001$), showing that cross-hand updating required uncertainty and was not explained by spontaneous recovery.

These results show that bimanual memories are organized by inferred context structure. Under uncertainty, error in one hand can be demultiplexed across arm-specific memories.

**Disclosures: A.S. Naik:** None. **C.A. Velazquez-Vargas:** None. **S. Shivkumar:** None. **J.N. Ingram:** None. **M. Lengyel:** None. **D.M. Wolpert:** None.

**Poster**

**PSTR187: Motor Learning: Human (Behavior/Physiology/Imaging) II**

**Location:** WCC Halls A-C

**Time:** Monday, November 16, 2026, 1:00 PM - 5:00 PM

**Program #/Poster #:** PSTR187.13/BB30

**Topic:** F.04. Voluntary Movements

**Title:** Age-related enhancement of implicit visuomotor adaptation depends on consistency in error direction

**Authors: I. ANDREWS**[1], Y. ZHOU[2], *O. A. KIM[1];
[1]Neurosci., Bates Col., Lewiston, ME; [2]Industrial and Organizational Psychology, New York Univ., New York, NY

**Abstract:** Healthy aging is associated with distinct changes in motor learning, yet findings regarding implicit reach adaptation vary between studies using different methodologies. While older adults exhibit enhanced implicit adaptation during tasks with “error-clamped” feedback (Vandevoorde & de Xivry, 2019; Cisneros et al., 2026), this age-related enhancement is absent in other paradigms, such as force-field adaptation (Hermans et al., 2024). A key methodological difference is error consistency: error-clamps fix the error direction regardless of participant behavior, whereas force-field adaptation tasks allow observed errors to vary dynamically. Here, we investigated how error consistency shapes age-related differences in implicit learning across three experiments. First, using a traditional block design, we replicated the finding that older adults (65+ years) show enhanced implicit adaptation compared to younger adults (18-35 years). Second, we transitioned to a single-trial learning paradigm where error directions were fully counterbalanced; under these conditions, age differences in implicit adaptation were completely eliminated. Finally, we tested the impact of changing error history by exposing participants to a block of errors in one direction followed by a block of salient errors in the opposite direction. We found that this directional switch significantly reduced subsequent implicit adaptation in older adults, rendering adaptation levels comparable to performance of younger controls. Taken together, these findings demonstrate that age-related enhancements in implicit adaptation depend on the presentation of directionally consistent errors. While the underlying mechanism requires further investigation, with interference between competing implicit memories and interference from explicit awareness of changes in reaching behavior offering compelling alternative explanations, our results indicate that controlling error-direction history is a critical, yet overlooked, variable when evaluating motor adaptation in aging populations.

**Disclosures: I. Andrews:** None. **Y. Zhou:** None. **O.A. Kim:** None.

**Poster**

**PSTR187: Motor Learning: Human (Behavior/Physiology/Imaging) II**

**Location:** WCC Halls A-C

**Time:** Monday, November 16, 2026, 1:00 PM - 5:00 PM

**Program #/Poster #:** PSTR187.14/BB31

**Topic:** F.04. Voluntary Movements

**Title:** Sensorimotor adaptation to viscous-curl force field in adults who stutter

**Authors:** S. GARUD[1], H. MARGULIS[2], ***K. S. KIM**[3];
[1]Sch. of Hlth. Sci., [2]Biomed. Engin., [3]Speech, Language, and Hearing Sci., Purdue Univ., West Lafayette, IN

**Abstract:** Developmental stuttering is a neurodevelopmental disorder that is characterized by involuntary disruptions in the fluency of speech production. Previous studies demonstrated that people who stutter show reduced sensorimotor learning during adaptation tasks, in which movements are updated in response to sensory errors. Interestingly, reduced sensorimotor learning in people who stutter has been reported not only in speech auditory-motor adaptation (i.e., updating speech movements in response to altered auditory feedback), but also in upper limb visuo-motor adaptation (i.e., updating arm movements in response to altered visual feedback), suggesting that adaptation difficulties in stuttering may generalize across different effector systems. Nonetheless, upper limb adaptation in stuttering individuals has only been examined in the context of visuomotor learning, and it remains unknown which whether limited adaptation extends to other types of upper limb adaptation tasks. In the current study, we examined adaptation to viscous-curl force-field in adults who stutter. We recruited individuals who stutter and sex-, age-, and handedness-matched non-stuttering controls to perform arm-reaching and return movements while holding a Kinarm End-Point handle (BKIN Technologies). Following a design similar to that used by Smith et al. (2006) to examine fast and slow adaptation processes, participants completed a total of 352 return movements, consisting of 55 null trials (i.e., no force), 132 clockwise force-field trials, 15 counterclockwise force-field trials, and 150 force-channel (i.e., the handle movement was constrained toward the target) trials. Preliminary data from 11 adults who stutter and 6 adults who do not stutter indicated that both groups adapted to the viscous-curl force-field. Moreover, the overall magnitude of adaptation and de-adaptation in both groups was consistent with previous reports in the literature. Together, these findings suggest that sensorimotor adaptation difficulties in people who stutter may not extend to upper limb force-field adaptation tasks.

**Disclosures: S. Garud:** None. **H. Margulis:** None. **K.S. Kim:** None.

**Poster**

**PSTR187: Motor Learning: Human (Behavior/Physiology/Imaging) II**

**Location:** WCC Halls A-C

**Time:** Monday, November 16, 2026, 1:00 PM - 5:00 PM

**Program #/Poster #:** PSTR187.15/BB32

**Topic:** F.04. Voluntary Movements

**Support:** NIH Grant R01 DC020707

**Title:** Feedback delay and lack of practice interfere not only with sensorimotor adaptation but also with de-adaptation: enhancing retention by preventing relearning

**Authors: L. PARONI**[1], H. WANG[2], *L. MAX[1];
[1]Univ. of Washington, Seattle, WA; [2]Otolaryngology - Head & Neck Surgery, Univ. of California, San Francisco, San Francisco, CA

**Abstract:** Changes in motor behavior resulting from sensorimotor adaptation are known to decay once the perturbation is removed and veridical feedback is restored. However, the mechanisms underlying this return to baseline behavior, and how it can be minimized, remain unclear. A widely held assumption is that de-adaptation is driven by *forgetting* of the recalibration of motor behavior. Other evidence suggests that the underlying process, instead, involves primarily *relearning* of baseline motor commands; i.e., a new phase of adaptation. To directly assess which mechanism is the primary factor contributing to the decay of adapted movements, we leveraged the known fact that both lack of practice and feedback delays interfere with adaptation and asked whether they also interfere with de-adaptation. After speech auditory-motor adaptation to a formant-shift perturbation, the first half of the washout phase included either delayed auditory feedback or no speaking at all. If de-adaptation reflects mostly forgetting, not speaking (i.e., not practicing) should facilitate a return to baseline behavior. In contrast, if relearning is the primary driving factor, both delayed feedback and absence of practice can be expected to slow down the return to baseline. Three groups of healthy adults (n=22 per group) completed the auditory-motor adaptation task with all formants in the produced monosyllabic words upshifted in real-time by 250 cents during the perturbation phase. During the first half of washout (early washout), a Control group received non-frequency-shifted (NFS) real-time auditory feedback, a Delay group received NFS auditory feedback delayed by 115 ms, and a No-Speaking group remained silent and, thus, received no auditory feedback. During the second half of washout (late), all groups received NFS real-time auditory feedback. All groups showed similar adaptation during the perturbation phase. At the end of early washout, de-adaptation was significantly reduced in the Delay group vs the Control group; thus, feedback delay interfered with de-adaptation. Upon resuming speech at the start of late washout, the No-Speaking group also showed a similar reduction in de-adaptation vs the Control group; thus, lack of practice interfered with de-adaptation. For both the Delay and No-Speaking groups, de-adaptation remained reduced throughout late washout whereas the Control group de-adapted completely. Findings suggest that de-adaptation reflects, at least in part, a process of relearning that depends on practice and real-time feedback, and that the retention of adapted motor actions can be improved by interfering with the relearning of baseline behavior.

**Disclosures: L. Paroni:** None. **H. Wang:** None. **L. Max:** None.

**Poster**

**PSTR187: Motor Learning: Human (Behavior/Physiology/Imaging) II**

**Location:** WCC Halls A-C

**Time:** Monday, November 16, 2026, 1:00 PM - 5:00 PM

**Program #/Poster #:** PSTR187.16/CC1

**Topic:** F.04. Voluntary Movements

**Support:** R01DC022097

**Title:** Acquisition and retention of speech perceptual memory

**Authors: *N. RAO**[1], M. TIEDE[2], D. J. OSTRY[3];
[1]Yale Child Study Center, Yale Sch. of Med., [2]Dept. of Psychiatry, Yale Sch. of Med., Yale Univ., New Haven, CT; [3]McGill Univ., Montreal, QC, Canada

**Abstract:** Speech production offers a unique signature to understand learning and memory as it involves a highly integrated processing of auditory and somatosensory signals. Our previous work showed that each of the somatosensory and auditory cortices is critical in retaining speech motor memory. However, humans also possess a complex ability to perceive speech sounds. When learning to perceive novel sounds, how durable is the new learning, and which cortical brain areas retain the new learning? In this experiment, participants were trained to distinguish speech sounds composed of vowel-consonant-vowel sequences (VCVs) in which the focal consonant contrast (place) was not part of their native language but was distinctive in the recorded source language. On each trial, a pair of VCVs differing in the consonant place feature was presented acoustically, followed by a different VCV matching one of the two C categories (ABX paradigm). Participants indicated which of the initial VCVs the test VCV sounded closest to, and feedback was provided on their accuracy. Learning was assessed by accuracy and reaction time. To test for the cortical substrates of this learning, transcranial magnetic brain stimulation (TMS) was delivered following learning to either motor, auditory, or somatosensory cortex. Following training and TMS, tests for retention were conducted 24 hours later. We hypothesized that if an area is not involved in perceptual learning and retention, disruption of its activity should have no effect on speech perceptual memory, whereas if an area is involved, an impairment should be observed.

**Disclosures: N. Rao:** None. **M. Tiede:** None. **D.J. Ostry:** None.

**Poster**

**PSTR187: Motor Learning: Human (Behavior/Physiology/Imaging) II**

**Location:** WCC Halls A-C

**Time:** Monday, November 16, 2026, 1:00 PM - 5:00 PM

**Program #/Poster #:** PSTR187.17/CC2

**Topic:** F.04. Voluntary Movements

**Support:** SNF_214621
PIO-03 22-2
113.845 IP-LS

**Title:** Timing of auricular vagus nerve stimulation influences motor adaptation in healthy participants

**Authors:** M. QUAST[1], O. LAMBERCY[1], D. DONEGAN[2], ***P. VISKAITIS**[1];
[2]D-HEST, [1]ETH Zurich, Zurich, Switzerland

**Abstract:** Motor disorders arising from stroke and spinal cord injury impose a profound global health burden, yet conventional rehabilitation approaches yield limited long-term recovery. Auricular vagus nerve stimulation (aVNS) has emerged as a promising non-invasive neuromodulatory intervention: growing evidence demonstrates that aVNS can enhance motor learning and cortical plasticity, and movement-paired aVNS has shown superior outcomes over unpaired stimulation in post-stroke rehabilitation. Despite this progress, the precise timing of aVNS relative to movement execution remains poorly understood, representing a critical gap in translating the intervention into optimised clinical protocols. The present study examined five stimulation conditions in healthy adults (n=114) across a 5-day longitudinal visuomotor adaptation paradigm comprising baseline, adaptation, washout, and retention phases. Stimulation was administered exclusively during the adaptation phase, in which participants moved a robotic handle (arm occluded) to reach on-screen targets while countering a visuomotor rotation perturbation. Participants were blinded to group assignment and experimental rationale. Conditions included premotor aVNS, motor aVNS, success aVNS, randomly-timed aVNS, and a motor-paired earlobe sham, each compared against a no-stimulation control. Only the motor-paired aVNS group reached a 28% success threshold (the minimum attained by all participants in this demanding task) in significantly fewer trials than the no-stimulation control. No other timing condition produced a statistically significant effect. This pattern suggests that aVNS efficacy in motor adaptation may depend on precise temporal coupling with active movement execution, rather than general arousal or reward-based mechanisms. Future analyses should establish whether null results in other conditions reflect true timing insensitivity or limitations in task sensitivity and difficulty, and whether findings generalise across tasks and clinical populations. Establishing whether closed-loop delivery systems can leverage this timing sensitivity would represent a meaningful step toward more targeted rehabilitation protocols for stroke and spinal cord injury.

**Disclosures: M. Quast:** E. Ownership Interest (stock, stock options, royalty, receipt of intellectual property rights/patent holder, excluding diversified mutual funds); Skaaltec AG. **O. Lambercy:** E. Ownership Interest (stock, stock options, royalty, receipt of intellectual property rights/patent holder, excluding diversified mutual funds); Skaaltec AG. **D. Donegan:** E. Ownership Interest (stock, stock options, royalty, receipt of intellectual property rights/patent holder, excluding diversified mutual funds); Skaaltec AG. **P. Viskaitis:** E. Ownership Interest (stock, stock options, royalty, receipt of intellectual property rights/patent holder, excluding diversified mutual funds); Skaaltec AG.

**Poster**

**PSTR187: Motor Learning: Human (Behavior/Physiology/Imaging) II**

**Location:** WCC Halls A-C

**Time:** Monday, November 16, 2026, 1:00 PM - 5:00 PM

**Program #/Poster #:** PSTR187.18/CC3

**Topic:** F.04. Voluntary Movements

**Support:** Texas A&M University

**Title:** Targeted Transcranial Ultrasound Modulation of Hippocampal-Striatal Contributions to Human Motor Sequence Learning

**Authors: *W. WANG**, Y. LEI;
Dept. of Kinesiology and Sport Mgmt., Texas A&M Univ., College Station, TX

**Abstract:** Motor sequence learning is thought to emerge from dynamic interactions between hippocampal systems that support explicit sequence discovery and striatal systems that support procedural skill acquisition. However, causal evidence for how these deep brain systems contribute to human motor learning remains limited, partly because conventional noninvasive stimulation methods have limited access to subcortical targets. Transcranial ultrasound stimulation (TUS) provides a spatially focused, noninvasive approach for modulating deep neural circuits. To our knowledge, this study is among the first behavioral and EEG-compatible human investigations comparing hippocampal and striatal TUS targets during motor sequence learning. We developed a repeated-measures pilot paradigm combining targeted TUS, typing-based sequence learning, and EEG. Participants completed sessions involving hippocampal, striatal, and sham stimulation. Each session included a random tapping baseline, an explicit sequence discovery phase, visible-guided sequence execution, hidden sequence execution, resting-state EEG, and post-stimulation repetitions of the visible and hidden tasks. Behavioral outcomes included accuracy, reaction time, inter-press interval, inter-press interval variability, correct sequence completion, discovery performance, and awareness reports. EEG was collected during resting periods to assess stimulation-related changes in neural dynamics. Preliminary data support the feasibility and sensitivity of this multimodal approach. Participants showed learning-related changes across repeated sequence blocks, including faster execution and measurable differences between visible-guided and hidden sequence performance. The task also captured individual variability in explicit discovery and hidden execution, providing behavioral markers to dissociate hippocampal-dependent discovery from striatal-dependent procedural execution. Ongoing analyses assess whether hippocampal and striatal TUS differentially modulate pre-to-post behavioral change and EEG dynamics compared with sham. This work establishes a translational framework for causally probing the contributions of the hippocampus and striatum to human motor sequence learning. By integrating deep brain TUS, behavioral decomposition of sequence learning, and EEG, this paradigm may help clarify how explicit and procedural learning systems interact during skill acquisition and may inform future neuromodulation approaches for motor rehabilitation and basal ganglia-related disorders.

**Disclosures: W. Wang:** None. **Y. Lei:** None.

**Poster**

**PSTR188: Posture and Gait: Aging, Injury, and Disease**

**Location:** WCC Halls A-C

**Time:** Monday, November 16, 2026, 1:00 PM - 5:00 PM

**Program #/Poster #:** PSTR188.01/CC4

**Topic:** F.06. Posture and Gait

**Support:** Gobierno de Navarra 0011-0537-2023-000062

**Title:** Dynamic Mode Decomposition for discovering biomechanical biomarkers of gait alterations

**Authors: *J. ULAYAR**[1,2], N. K. GUT[3], J. MENA-SEGOVIA[4], M. VALENCIA[5,2];
[1]Physiological monitoring and control, Ctr. de Investigación Médica Aplicada, Univ. de Navarra, PAMPLONA/IRUÑA, Spain; [2]IdiSNA - Inst. de Investigación Sanitaria de Navarra, Pamplona, Spain; [3]CMBN, Rutgers Univ. Newark, Newark, NJ; [4]Ctr. for Mol. and Behavioral Neurosci., Rutgers The State Univ. of New Jersey, Newark, NJ; [5]Physiological Monitoring and Control Lab., CIMA-Universidad de Navarra, Pamplona, Spain

**Abstract:** Freezing of gait is a common symptom of Parkinson's disease patients, leading to movement impairment and falls, greatly reducing their quality of life. Understanding the spatiotemporal dynamics that govern healthy and parkinsonian gaits may lead to better diagnosis and better evaluation of the effectiveness of treatments. In this work, we used a spinal cord injury and a 6-OHDA mouse models of Parkinson's disease to investigate potential gait alterations. Our aim was to identify biomechanical biomarkers that could serve to identify deficits that may reflect early or progressive features of the disease and potentially drive smart neuromodulation systems. We hypothesize that gait in healthy rodents obey oscillatory patterns of relatively constant frequency while parkinsonian ones show additional interfering motor patterns impeding normal behavior. Using the data-driven method called dynamic mode decomposition (DMD), a dimensionality reduction technique, we are able to isolate and describe the main movement patterns involved in walking mice as damped/driven oscillators. With this analysis, a deeper understanding of the motor patterns can be reached and may lead to the discovery of visual spatiotemporal biomarkers for the disease.

**Disclosures: J. Ulayar:** None. **N.K. Gut:** None. **J. Mena-Segovia:** None. **M. Valencia:** None.

**Poster**

**PSTR188: Posture and Gait: Aging, Injury, and Disease**

**Location:** WCC Halls A-C

**Time:** Monday, November 16, 2026, 1:00 PM - 5:00 PM

**Program #/Poster #:** PSTR188.02/CC5

**Topic:** F.06. Posture and Gait

**Title:** From YouTube to diagnosis: interpretable multi-disorder gait classification with generative rescue

**Authors:** ***M. CAIOLA**[1], T. THOMPSON[1], A. BUTALA[2], E. MOUKHEIBER[2], O. RASTOGI[3], W. CHU[3], S. OSTADABBAS[3], L. MORO-VELAZQUEZ[2], T. THEBAUD[2], N. DEHAK[2], A. WEITZ[1];
[1]Credence, McLean, VA; [2]Johns Hopkins Univ., Baltimore, MD; [3]Northeastern Univ., Boston, MA

**Abstract: Background**. Movement-disorder diagnosis depends on tacit clinician judgment of subtle gait abnormalities — a workflow that does not extend to real-world video, the modality most readily available for population-scale screening. Existing video-based gait classifiers rely on opaque embeddings or validate only in lab settings; neither supports clinician-in-the-loop adoption. **Methods**. We assembled a 4-class real-world video cohort of 220 subjects — 135 healthy controls (HC), 18 Parkinson's disease (PD), 6 multiple sclerosis (MS), 61 stroke — from publicly-available sources. A video-based 3D human-motion model extracted per-frame body pose, from which we computed 434 named biomechanical features (joint rotations, per-axis components, angular velocities, bilateral symmetry, frequency-domain measures) over a 24-joint skeleton. A random-forest classifier on these features was evaluated under 5-fold subject-level cross-validation. To address class imbalance and enable clinician-watchable explanations, a class-conditional variational autoencoder (FiLM-VAE) produced two outputs from one decoder: (1) synthetic minority-class feature vectors for SMOTE-style training-set balancing, and (2) per-class 3D body-mesh sequences decoded from centroid features, bridged via NVIDIA's Kimodo motion-diffusion into continuous stride dynamics. **Results**. Per-disorder one-vs-all discrimination was consistent across cohorts: balanced accuracy 0.90-0.94 (mean 0.917), AUC 0.928-0.961, and sensitivity at 95% specificity 53-88%. FiLM-VAE feature reconstruction reached per-class r = 0.78-0.98 (mean 0.87), with MS at r = 0.98 despite only 43 training windows. Under top-1 multi-class evaluation, SMOTE-style rescue lifted under-represented classes (MS from 7% to 23%, PD from 42% to 61%) while preserving HC and stroke. Decoded per-class centroid meshes recovered disease-specific kinematic signatures without decode-time class labels, including the hip range-of-motion hierarchy (HC > PD ≈ Stroke > MS). **Conclusions**. Real-world video supports interpretable multi-disorder neurological screening when features are grounded in named clinical kinematics, with one generative model delivering both small-N rescue and clinician-watchable explanations.

**Disclosures: M. Caiola:** None. **T. Thompson:** None. **A. Butala:** None. **E. Moukheiber:** None. **O. Rastogi:** None. **W. Chu:** None. **S. Ostadabbas:** None. **L. Moro-Velazquez:** None. **T. Thebaud:** None. **N. Dehak:** None. **A. Weitz:** None.

**Poster**

**PSTR188: Posture and Gait: Aging, Injury, and Disease**

**Location:** WCC Halls A-C

**Time:** Monday, November 16, 2026, 1:00 PM - 5:00 PM

**Program #/Poster #:** PSTR188.03/CC6

**Topic:** F.06. Posture and Gait

**Support:** UIC AHS EXITO Pilot Award

**Title:** Electrocortical activity during curb stepping in young and older adults

**Authors: J. SUN**, C. KUESTER, D. SAMSON, *C. LIU;
Kinesiology and Nutr., Univ. of Illinois Chicago, Chicago, IL

**Abstract:** Curbs are ubiquitous in daily walking and pose significant fall risk, especially for older adults. Safe walking requires proper cortically mediated processes such as motor planning and visuospatial processing. Yet, we have little understanding of how cortical activity contributes to greater fall risk during everyday walking tasks such as curb negotiation in older adults. Sensorimotor cortex beta-band (13-30 Hz) and posterior parietal alpha-band (8-13 Hz) are of particular interest given their roles in motor planning and visuospatial processing during obstacle crossing and uneven terrain walking (Nordin et al., 2019; Liu et al., 2024, 2025). We hypothesize that alpha and beta power will desynchronize more during curb negotiation than during flat walking, and that such desynchronization will be greater in older adults. So far, 17 young adults (24±4 yr) and 11 older adults (71±4 yr) completed trials: straight walking on a flat surface and walking then stepping onto a curb (a custom-made wooden platform 0.13 m × 1.15 m × 0.9 m). We recorded 120-channel mobile EEG along with body-worn motion sensors. EEG was preprocessed in EEGLAB (filtering, artifact rejection, AMICA, ICLabel, and DIPFIT). Independent components were clustered across participants into four regions of interest: left and right sensorimotor areas, parieto-occipital area, and supplementary motor area. Epochs were defined by gait cycle, anchored on the heel strike nearest to curb step-on, and time-warped for normalization. Event-related spectral perturbations (ERSP; 4-50 Hz) were computed and baseline-normalized to mean power across the full gait cycle. Our preliminary results showed stronger alpha and beta desynchronization prior to curb stepping compared to flat walking across all four clusters for both older and young adults. Our next step will be to perform statistical analysis to investigate age-related effects on cortical control of curb negotiation. Our results may ultimately inform neural modulation interventions to improve walking function and reduce fall risk in older adults.

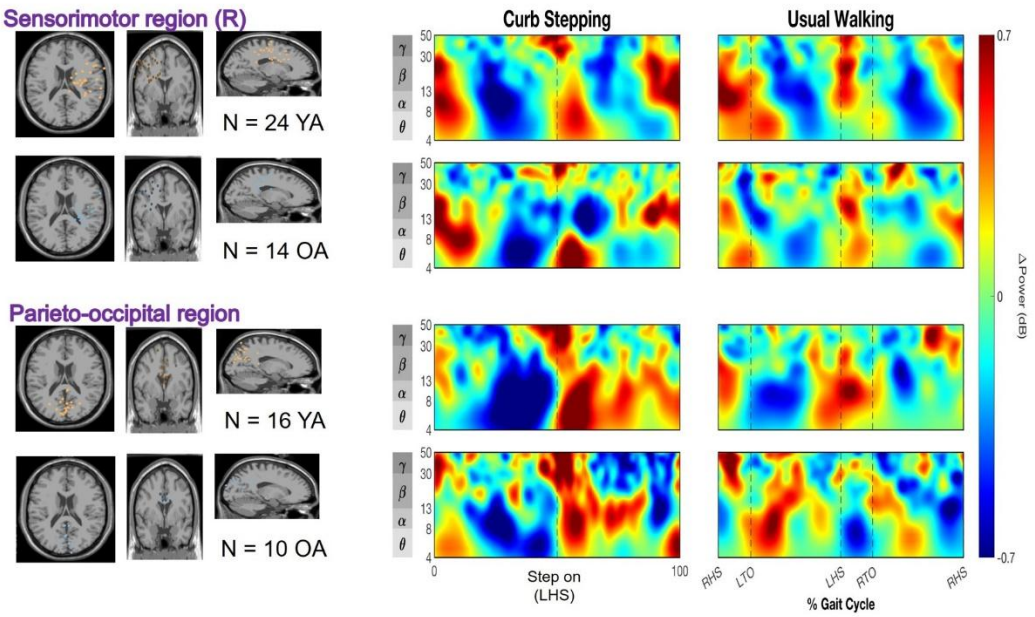



Figure 1: Dipole location and event-related spectral perturbations for young (YA) and older adults (OA) in the sensorimotor and parieto-occipital region.

**Disclosures: J. Sun:** None. **C. Kuester:** None. **D. Samson:** None. **C. Liu:** None.

**Poster**

**PSTR188: Posture and Gait: Aging, Injury, and Disease**

**Location:** WCC Halls A-C

**Time:** Monday, November 16, 2026, 1:00 PM - 5:00 PM

**Program #/Poster #:** PSTR188.04/CC7

**Topic:** F.06. Posture and Gait

**Support:** NIA Grant: F31AG081129
NINDS Grant: R01AG072756

**Title:** Cognitive-motor challenge differentially modulates cortical motor contributions to standing balance control in young versus older adults

**Authors: *C. F. MASON**[1], D. DUNOFF[3], N. A. BAUNE[2], S. EDAVALAPATI[1], T. LEONE[2], J. L. MIRDAMADI[2], R. RAJASHREE[2], A. J. LOPEZ[2], M. R. BORICH[2], L. H. TING[4], T. M. KESAR[2];
[2]Rehabil. Med., [1]Emory Univ., Atlanta, GA; [3]Neurosci. BS Program, Georgia Inst. of Technol., Atlanta, GA; [4]Biomed. Engin., Emory Univ. and Georgia Inst. of Technol., Atlanta, GA

**Abstract:** Older adults (OA) demonstrate greater cortical engagement than younger adults (YA) during balance, contributing to impaired balance and falls risk. Here, we test the hypothesis that in OA, as balance challenge increases, competing cognitive and motor demands modulate cortical engagement dual-task performance. We evaluated cortical motor engagement, as well as cognitive and balance task performance, during cognitive-balance dual-tasks of varying difficulty in n=17 YA and n=21 OA. Transcranial magnetic stimulation (TMS) was used to measure corticospinal excitability (CSE) of tibialis anterior (TA) and soleus (SOL) ankle muscles during seated, quiet standing (QS), and standing in a narrow stance on foam (NSfoam) tasks. Each postural task was performed individually (without a cognitive task, e.g. NoCog) as well as during easy (0-back) and difficult (2-back) cognitive tasks. During QS, in the presence of cognitive dual-task challenge, OA showed an increase in CSE (TA NoCog vs 2-back: $\beta$=70.84, SE=27.01, z=2.62, p=0.026), and prioritized the cognitive task, while balance performance worsened. During QS, in the presence of cognitive challenge, YA showed similar degradation of performance of cognitive and balance tasks, and an increase in CSE (TA NoCog vs 2back: $\beta$=98.04, SE=37.16, t(3209)=2.64, p=0.023). Interestingly, during the NSfoam dual-task, both YA and OA maintained cognitive and balance task performance, but their CSE changed in opposite ways, decreasing in YA (SOL: $\beta$=-59.5, SE=21.76, t(3190)=-2.73, p=0.017) and increasing in OA (TA: $\beta$=69.56, SE=26.27, z=2.65, p=0.024) during 2back compared to NoCog. Our results suggest that as dual-task difficulty increases, OA consistently engage cortical motor resources, while YA may switch from cortical to subcortical control. In addition, we have collected data on n=6 OA with mild cognitive impairment (MCI). Ongoing and future analyses will compare MCI outcomes with our healthy OA cohort to inform how cognitive impairments modulate cortical motor contributions to balance in aging. The dynamic task-dependent role of cortical and subcortical motor circuits in balance control should be considered in future studies when identifying neurophysiological biomarkers to predict fall risk, and precision (p)rehabilitation strategies to reduce falls.

**Disclosures: C.F. Mason:** None. **D. Dunoff:** None. **N.A. Baune:** None. **S. Edavalapati:** None. **T. Leone:** None. **J.L. Mirdamadi:** None. **R. Rajashree:** None. **A.J. Lopez:** None. **M.R. Borich:** None. **L.H. Ting:** None. **T.M. Kesar:** None.

**Poster**

**PSTR188: Posture and Gait: Aging, Injury, and Disease**

**Location:** WCC Halls A-C

**Time:** Monday, November 16, 2026, 1:00 PM - 5:00 PM

**Program #/Poster #:** PSTR188.05/CC8

**Topic:** F.06. Posture and Gait

**Support:** National Research Foundation of Korea (NRF) grant funded by the Korean government (MSIT) 2021R1C1C1005188
NRF grant funded by MSIT 2022R1F1A1074729
NRF grant funded by MSIT RS-2025-24534079
National Research Council of Science & Technology (NST) grant by MSIT

GTL25071-000
NST-KBSI Grant (S610000)

**Title:** Walking direction recruits anterior inferior parietal and left inferior frontal cortex beyond speed-related posterior parietal activation in aging

**Authors: *S. TAK**[1,2,3], T. CHU[4,1], I. JUNG[5];
[1]Bioimaging and Translational Res. Unit, Korea Basic Sci. Inst., Cheongju, Korea, Republic of; [2]Grad. Sch. of Analytical Sci. and Technol., Chungnam Natl. Univ., Daejeon, Korea, Republic of; [3]Bio-Analytical Sci., Univ. of Sci. and Technol., Daejeon, Korea, Republic of; [4]Biomed. Engin., Univ. of Toronto, Toronto, ON, Canada; [5]Dept. of Rehabil. Med., Wooridul Spine Hosp., Seoul, Korea, Republic of

**Abstract:** Age-related decline in gait automaticity requires older adults to increasingly rely on executive prefrontal networks, a phenomenon recognized as neural compensation. While functional near-infrared spectroscopy (fNIRS) studies have widely documented prefrontal over-recruitment during complex walking tasks, the specific neural substrates mediating adaptation to walking speed versus non-routine spatial demands (direction) remain poorly understood. This study examines fNIRS activation maps during forward walking (FW) and backward walking (BW) to dissociate speed- and direction-related cognitive-motor compensation in the aging brain. We recorded fNIRS signals from healthy young (n = 40) and older (n = 40) adults across three conditions: FW at 2 km/h, FW at 4 km/h, and BW at 2 km/h. General linear models identified activation clusters, with sex and walking ability as covariates. Group activation maps were thresholded at FDR-corrected $p < 0.05$; the isolated effects of speed (FW 4 km/h > 2 km/h) and direction (BW > FW), and their between-group differences, were examined at an uncorrected threshold $p < 0.005$. Older adults showed widespread over-recruitment across frontal, motor, and parietal regions in all conditions relative to young adults, consistent with age-related neural inefficiency. At the exploratory threshold, the two task demands engaged dissociable inferior parietal subregions in older adults: increased speed preferentially recruited the angular gyrus (posterior IPL, BA 39), consistent with spatial attention and integration, whereas directional change preferentially recruited the supramarginal gyrus (anterior IPL, BA 40), consistent with sensory-motor integration and body-schema updating. Notably, directional change additionally engaged the left inferior frontal gyrus (Broca's area), an effect not observed for the speed contrast. These findings suggest that age-related compensation is not limited to general prefrontal over-recruitment but is organized along the anterior-posterior axis of the inferior parietal lobule according to the type of locomotor demand. When automaticity is challenged by non-routine directional changes, older adults appear to recruit anterior parietal cortex for postural and body-schema reconfiguration together with left inferior frontal cortex, possibly reflecting an added cognitive, verbally mediated component supporting safe locomotion.

**Disclosures: S. Tak:** None. **T. Chu:** None. **I. Jung:** None.

**Poster**

**PSTR188: Posture and Gait: Aging, Injury, and Disease**

**Location:** WCC Halls A-C

**Time:** Monday, November 16, 2026, 1:00 PM - 5:00 PM

**Program #/Poster #:** PSTR188.06/CC9

**Topic:** F.06. Posture and Gait

**Title:** A comprehensive evaluation of mobility: validation of the functional ambulation & stair test in older adults

**Authors: *E. C. HELLER**[1], A. ROSENFELDT[2], E. ZIMMERMAN[3], S. DAVIDSON[4], J. L. ALBERTS[5];
[1]Cleveland Clinic, Lerner Res. Institute, Dept. of Biomed. Engin., Cleveland, OH; [2]Cleveland Clin. Fndn., Cleveland, OH; [3]Ctr. for Neurolog. Restoration, Cleveland Clinic, Neurolog. Inst., Cleveland, OH; [5]Biomed. Engin., [4]Cleveland Clin., Cleveland, OH

**Abstract: A Comprehensive Evaluation of Mobility: Validation of the Functional Ambulation & StairTest in Older AdultsAbstract**Falls have devastating consequences for older adults. The Functional Ambulation & Stair Test(FAST) was developed to characterize older adult mobility and eventual fall risk. Currently, thebest predictor of a future fall is a previous fall. This means that critical intervention time is notbeing utilized to prevent potentially catastrophic falls. This project aimed to assess the criterionvalidity of the FAST assessment by comparing the relationship between FAST outcomes andexisting gold-standard clinical assessments of mobility and fall risk. A secondary aim wasassessing the FAST's capacity to elicit dual-task effects in older adults. The FAST is a multi-faceted mobility assessment combining stair navigation, turning and level-ground walking; totaltime and time spent in each phase are the calculated outcomes. Data from 199 older adults age 62and older (138 female, 69.3%) completing the FAST, Berg Balance Scale (BBS), Timed Up andGo (TUG), and Ten Meter Walk Test (10MWT) at comfortable and fast speed were evaluated.Relationships between the FAST and clinical outcomes were evaluated with Spearman'scorrelations. The FAST and TUG were assessed under single- and dual-task conditions; linearmixed models evaluated the dual-task effects for overall FAST time and each phase. Spearman'scorrelations between the FAST and the BBS, TUG, 10MWT comfortable and 10MWT fast were-0.65, 0.88, -0.79, and -0.83, respectively. Participants experienced an 8.6% and 13.2% dual-taskcost in the FAST and TUG, respectively. The greatest dual-task cost during the FAST was in thegait initiation, walking, and wide turn phases. Agreement between the FAST and gold-standardclinical mobility assessments confirm the criterion validity of the FAST. Delineation of mobilityphases via the FAST offers insight into specific mobility deficits. Future work is needed toevaluate the FAST as a fall risk assessment in older adults.

**Disclosures: E.C. Heller:** None. **A. Rosenfeldt:** None. **E. Zimmerman:** None. **S. Davidson:** None. **J.L. Alberts:** None.

**Poster**

**PSTR188: Posture and Gait: Aging, Injury, and Disease**

**Location:** WCC Halls A-C

**Time:** Monday, November 16, 2026, 1:00 PM - 5:00 PM

**Program #/Poster #:** PSTR188.07/CC10

**Topic:** F.06. Posture and Gait

**Support:** Edward and Barbara Bell Endowed Chair

**Title:** First-Time Falls are Predicted by a New Complex Mobility Assessment

**Authors: *S. DAVIDSON**[1], E. C. HELLER[4], E. ZIMMERMAN[2], A. ROSENFELDT[5], J. L. ALBERTS[3];
[1]Cleveland Clin., Brook Park, OH; [3]Biomed. Engin., [2]Cleveland Clin., Cleveland, OH; [4]Cleveland Clinic, Lerner Res. Institute, Dept. of Biomed. Engin., Cleveland, OH; [5]Cleveland Clin. Fndn., Cleveland, OH

**Abstract:** The best predictor of a future fall is a prior fall, meaning there is limited ability to predict conversion from a non-faller to a faller. Predicting first-time falls would facilitate early interventions that could prevent the costly adverse events of falls. A new complex mobility assessment, the Functional Ambulation & Stair Test (FAST), includes straight line walking, turning, and stair navigation. Trials are collected in single task (ST) and dual task (DT) conditions and can be parsed into eight phases with varying motor control demands (gait initiation, walking on level ground, a "Wide Turn", walking on level ground and transitioning to the stairs, ascending the stairs, a “Tight Turn” on the stair landing, and descending the stairs). The aim of this project was to assess the ability of the FAST to predict first-time falls. A secondary aim was to compare the predictive value of the FAST with an existing balance assessment.
Data were collected from 156 healthy older adults (77.9 ± 8.5 years old, 71% female) with no history of falls in the prior 6 months. A clinical gold standard of balance assessment (the Berg Balance Scale, BBS) was concurrently administered. Prospective falls were recorded for 12 months. First-time fall prediction was conducted with elastic net models validated using nested, stratified 10-fold cross-validation. Covariates included age, sex, and living location. Separate models were generated for the FAST and the BBS.
During the follow-up period, 72 (46%) participants fell a total of 122 times, with new fallers averaging 1 [1, 2] falls. The FAST model AUC was 0.61, with the strongest predictors of a first-time fall being time to complete the Tight Turn in both ST and DT conditions and the DT cost of time to complete the Wide Turn phase. The BBS model AUC was 0.50, indicating the BBS model was no better at predicting first-time falls than random chance.
Slower performance during the Tight Turn and increased DT cost of the Wide Turn phases of the FAST are predictive of first-time falls among healthy older adults. The predictive power of the FAST model was greater than the current clinical gold standard in balance assessment, which performed no better than random chance. The results highlight the importance of assessing performance on complex, real-world tasks when considering potential conversion from non-faller to faller. Future research should assess the first-time fall prediction power of the FAST among a larger and more diverse sample.

**Disclosures: S. Davidson:** None. **E.C. Heller:** None. **E. Zimmerman:** None. **A. Rosenfeldt:** None. **J.L. Alberts:** None.

**Poster**

**PSTR188: Posture and Gait: Aging, Injury, and Disease**

**Location:** WCC Halls A-C

**Time:** Monday, November 16, 2026, 1:00 PM - 5:00 PM

**Program #/Poster #:** PSTR188.08/CC11

**Topic:** F.06. Posture and Gait

**Support:** Research supported by the National Science Foundation (NSF) under Grant No. 2340997 contributed to the development of ideas in this work.

**Title:** Wearable IMU-Based Gait Impairment Classification Toward Normal Pressure Hydrocephalus Screening

**Authors: A. RAM**[1], J. NJOKU[2], *D. SHUKLA[3];
[1]Santa Clara High Sch., Santa Clara, CA; [2]Univ. of Wyoming, LARAMIE, WY; [3]Univ. of Wyoming, Laramie, WY

**Abstract:** Normal pressure hydrocephalus (NPH) is a potentially reversible neurological disorder affecting older adults worldwide, with an estimated 700,000 adults in the United States living with the condition. NPH is characterized by progressive gait impairment, cognitive decline, and urinary dysfunction. Because gait disturbance is often the earliest and most treatment-responsive symptom, objective gait assessment may improve screening and treatment planning; however, current diagnostic pathways often rely on invasive cerebrospinal fluid procedures. This study aimed to develop and evaluate a subject-independent machine learning pipeline for IMU-based gait impairment classification as a foundation for future NPH screening applications.

The proposed framework was evaluated using a publicly available inertial measurement unit (IMU) gait dataset consisting of 20 subject-visits from 10 stroke patients. Gait impairment was defined using the Functional Ambulation Category, with scores below 4 classified as impaired and scores of 4 or higher classified as functional. Twenty-four spatiotemporal gait parameters describing gait performance, variability, and symmetry were extracted from a validated foot-mounted IMU pipeline and used as input features. Seven classifiers were benchmarked under leave-one-subject-out cross-validation with per-fold standard scaling to prevent data leakage: Random Forest, Logistic Regression, Linear Discriminant Analysis, K-Nearest Neighbors, Support Vector Machine, XGBoost, and Naive Bayes.

Random Forest achieved the highest performance, with 90.0% accuracy and an area under the receiver operating characteristic curve (AUROC) of 0.985, followed by Logistic Regression with an AUROC of 0.953 and Linear Discriminant Analysis with an AUROC of 0.906. Support Vector Machine achieved an AUROC of 0.815, while K-Nearest Neighbors exhibited 100% sensitivity but 0% specificity, and Naive Bayes performed near the chance level with an AUROC of 0.535. Feature importance analysis identified walking speed, stride length, and swing-time symmetry index as the strongest predictors of gait impairment, aligning with gait domains commonly affected in NPH, including reduced gait velocity, shortened stride length, and impaired gait symmetry.

These findings demonstrate that clinically interpretable IMU-derived gait parameters can distinguish impaired from functional gait under subject-independent evaluation. Although validation in NPH cohorts is required, this work identifies Random Forest as a promising

approach for future wearable-sensor-based screening studies targeting NPH-relevant gait dysfunction.

**Disclosures: A. Ram:** None. **J. Njoku:** None. **D. Shukla:** None.

**Poster**

**PSTR188: Posture and Gait: Aging, Injury, and Disease**

**Location:** WCC Halls A-C

**Time:** Monday, November 16, 2026, 1:00 PM - 5:00 PM

**Program #/Poster #:** PSTR188.09/CC12

**Topic:** F.06. Posture and Gait

**Support:** NIH Grant AG068054

**Title:** Gait signatures of Alzheimer's disease progression in adults with Down syndrome

**Authors: *A. BARRY**[1], B. T. CHRISTIAN[2], S. HARTLEY[1];
[1]Univ. of Wisconsin-Madison, Madison, WI; [2]Univ. of Wisconsin Madison, Madison, WI

**Abstract: Background:** Individuals with Down syndrome (DS) are genetically at-risk for Alzheimer's disease (AD), with greater than 90% of adults with DS developing AD dementia by age 70 years. While cognitive decline in DS-AD is well documented, the motor and gait changes associated with disease progression remain poorly understood. Identifying these changes could yield accessible, low-burden screening tools and improve fall risk prevention. **Objectives:** 1) Examine the age-related trajectory of gait impairments in adults with DS; 2) identify gait features that differentiate clinical AD status groups, and 3) evaluate associations between gait and cognitive performance. **Methods:** Cross-sectional baseline data from 326 adults with DS (aged 25-71; M = 42.3 years) in the Alzheimer Biomarker Consortium-Down syndrome were analyzed. Gait was evaluated with the Tinetti Gait Assessment across 8 items during two 15-foot walks (usual and rapid pace). Global cognitive functioning, episodic memory, and executive function were assessed using direct measures. LOESS smoothing and piecewise linear models characterized age trajectories. Kruskal-Wallis tests compared clinical AD status groups, and regression models examined gait-cognition associations ($p < 0.002$) controlling for age, intellectual disability, orthopedic conditions, body mass index, APOE4 status, and clinical AD status. **Results:** Gait performance declined gradually between the mid-30s and mid-40s, followed by an accelerated period of decline between ages 48-57, coinciding with mean age of participants with mild cognitive impairment (M = 53.6, SD = 7.0) and dementia (M = 56.5, SD = 6.2). Performance on all Tinetti items (except step symmetry) was lower among adults with dementia than those who were cognitively stable. Hesitancy during gait initiation, step discontinuity, path deviation, and trunk sway were also related to poorer cognitive functioning. Poor walking stance (29%) and foot clearance (11%) were common impairments but were not associated with cognitive outcomes. **Conclusions:** Gait changes coincide in time with DS-AD clinical onset. Hesitancy in gait initiation, step discontinuity, path deviation, and trunk sway had the strongest associations with cognitive decline. These features may serve as clinically

meaningful signs of DS-AD on screening tools. Wide stance and foot clearance, in contrast, may reflect lifelong DS motor characteristics rather than AD-specific changes.

**Disclosures: A. Barry:** None. **B.T. Christian:** None. **S. Hartley:** None.

**Poster**

**PSTR188: Posture and Gait: Aging, Injury, and Disease**

**Location:** WCC Halls A-C

**Time:** Monday, November 16, 2026, 1:00 PM - 5:00 PM

**Program #/Poster #:** PSTR188.10/CC13

**Topic:** F.06. Posture and Gait

**Support:** NIH Grant T32MH119168
NSF Career Award 1847891

**Title:** Executive control network tract disconnection is associated with across-context locomotor switching deficits after stroke

**Authors: *N. W. BRANTLY**[1], S. BHASKAR[2], J. CHOI[3], D. M. MARISCAL[1], A. M. WEINSTEIN[4], H. T. KARIM[4], G. TORRES-OVIEDO[5];
[1]Bioengineering, [2]Biol. Sci., Univ. of Pittsburgh, Pittsburgh, PA; [3]Bioengineering, Univ. of Pittsburgh, PITTSBURGH, PA; [4]Psychiatry, [5]Dept. of Bioengineering, Univ. of Pittsburgh, Pittsburgh, PA

**Abstract:** Across-context locomotor switching is the ability to alter walking patterns when shifting between familiar contexts, and it is important for community walking, such as transitioning from walking on an icy to a dry sidewalk in the winter. Stroke survivors often experience paretic leg motor deficits that impair walking, including across-context locomotor switching deficits. Yet, the brain networks underlying locomotor switching after stroke remain unknown. The Executive Control Network (ECN) is known to be important for task switching and may play an important role in locomotor switching. To identify these brain networks, we recruited 40 participants with chronic stroke (16 female, mean age 63.8 +/- 11.1 years SD) who completed a split-belt treadmill adaptation paradigm (900 strides, 2:1 belt-speed ratio, +/- 33% of 85% of the 6-Minute Walk Test speed). Across-context locomotor switching performance was evaluated by modeling overground post-adaptation walking using a piecewise linear mixed-effects model to estimate the step length asymmetry at the first overground stride. To characterize each participant's brain lesion, we collected T1-weighted MRI data, performed automatic lesion segmentation via SynthStrokeSPM, normalized to the MNI template using enantiomorphic lesion masking, and, finally, resegmented the lesions automatically in the MNI-transformed T1 images. We computed disconnection probabilities for an atlas of 60 brain tracts using the BCBToolkit Tractotron tool. We then performed principal components (PC) regression between the top two components from sparse Principal Components Analysis and the step length asymmetry estimate of across-context locomotor switching. We found a statistically significant association between disconnection of PC2 and worse locomotor switching ($p=0.022$), but not

PC1 (p=0.519) (model R2 = 0.134). PC2 is composed of 17 neural tracts, 14 of which are relevant to the ECN. These results suggest that the ECN may play a key role in across-context locomotor switching, which has meaningful implications for post-stroke gait rehabilitation. Rehabilitation strategies that engage or compensate for ECN dysfunction may help improve across-context locomotor switching in stroke survivors.

**Disclosures: N.W. Brantly:** None. **S. Bhaskar:** None. **J. Choi:** None. **D.M. Mariscal:** None. **A.M. Weinstein:** None. **H.T. Karim:** None. **G. Torres-Oviedo:** None.

**Poster**

**PSTR188: Posture and Gait: Aging, Injury, and Disease**

**Location:** WCC Halls A-C

**Time:** Monday, November 16, 2026, 1:00 PM - 5:00 PM

**Program #/Poster #:** PSTR188.11/CC14

**Topic:** F.06. Posture and Gait

**Support:** NIH Grant K01 AG073467

**Title:** Visuospatial Function Explains Self-Selected Walking Speed Independent of Maximal Walking Capacity in Chronic Stroke: A Pilot Study

**Authors: *Y. JIAO**[1], S. KETTLETY[2], M. KELLY[1], K. A. LEECH[1];
[1]Div. of Biokinesiology and Physical Therapy, USC, Los Angeles, CA; [2]Kennedy Krieger Inst., Johns Hopkins Univ., Baltimore, MD

**Abstract:** Self-selected walking speed (SSWS) is clinically important after stroke, but motor impairment alone does not fully explain its variability. Prior studies have linked global cognition and domains such as executive function and attention to post-stroke gait; however, it remains unclear which cognitive domains are most relevant to SSWS when considered together, particularly when controlling for differences in walking capacity between people. This study aimed to explore whether specific cognitive domains were associated with SSWS after accounting for maximal walking capacity (fastest walking speed; FWS) and motor impairment (lower-extremity Fugl-Meyer; FM-LE). Forty-two chronic-stroke adults completed a 10-meter walk at SSWS and FWS, the FM-LE, and battery cognitive assessments including: Trail Making Test-B and the Repeatable Battery for the Assessment of Neuropsychological Status that provides subscale scores for Immediate Memory, Visuospatial/Constructional, Language, Attention, and Delayed Memory). Given the multiple candidate cognitive domains, we used multivariable regression with best-subset selection by minimum Bayesian Information Criterion to identify cognitive domains that best explain SSWS while limiting model complexity. FM-LE and FWS were forced as covariates so that the residual variance reflected habitual speed selection among participants with comparable motor function and maximal walking ability. As a control, we repeated the best-subsets analysis with FWS as the outcome and FM-LE forced as a covariate to test whether the cognitive contribution was specific to SSWS not FWS. For SSWS, the best model included FWS, FM-LE, and Visuospatial/Constructional skills (adjusted $R^2$ =

0.87; Visuospatial std $\beta = 0.13$, $p = 0.041$; FWS std $\beta = 0.83$, $p < 0.001$; FM-LE n.s.), indicating SSWS was positively associated with visuospatial/constructional function when controlling for maximal walking capacity. In the FWS control model, no cognitive domain was retained (adjusted $R^2 = 0.37$), suggesting that this finding is more specific to habitual speed selection. Although a recent domain-specific study found no cognitive predictors of 10MWT without motor impairment and FWS adjustment, our findings suggest that visuospatial/constructional function helps explain how stroke survivors use their maximal walking capacity. This may reflect prior proposals of visuospatial contributions to spatial awareness, safety judgments, and movement planning during gait. Larger real-world walking studies are needed to test whether cognitive domains contribute to daily walking behavior.

**Disclosures: Y. Jiao:** None. **S. Kettlety:** None. **M. Kelly:** None. **K.A. Leech:** None.

**Poster**

**PSTR188: Posture and Gait: Aging, Injury, and Disease**

**Location:** WCC Halls A-C

**Time:** Monday, November 16, 2026, 1:00 PM - 5:00 PM

**Program #/Poster #:** PSTR188.12/CC15

**Topic:** F.06. Posture and Gait

**Support:** U.S. Army Medical Research Award No. W81XWH2210684

**Title:** Dynamic knee valgus during the long-latency reflex period following landing impact in post-rehabilitation ACL patients

**Authors:** A. JONES[1], B. SHAFFER[4], A. WIGGINS[2], C. ONKS[5], T. MURPHY[5], J. E. NYLAND[6], ***R. A. CREATH**[3];
[1]Exercise Sci., Lebanon Valley Col., Lebanon, PA; [3]Exercise Sci., [2]Lebanon Valley Col., Annville, PA; [4]West Virginia Sch. of Osteo. Med., Lewisburg, WV; [6]Neural and Behavioral Sci., [5]Penn State Col. of Med., Hershey, PA

**Abstract:** Post-rehabilitation ACL reconstruction patients experience substantially increased likelihood of re-injury. Despite the increased re-injury rate, they rarely exhibit clinical injury risk factors after they return to normal activities. This study evaluated inter-knee velocity to detect dynamic knee valgus movement, a common risk factor, induced by landing impact forces following drop jumps. Twenty post-rehabilitation adult ACL subjects (10f) and 20 healthy controls (10f) performed five drop jumps from a 0.3-meter height box. Inter-knee velocity was calculated as the first derivative of the inter-knee joint center distance with respect to time as determined by motion capture. Velocities were compared at maximum ground reaction force (GFRmax) and 50 ms after GFRmax using unpaired, one-sided t-tests. No significant group differences were observed for inter-knee velocity or distance at GRFmax, nor were any inter-knee distance differences observed at 50 ms after GRFmax. However, inter-knee velocity measured 50 ms after GRFmax showed a significant group difference and provided the clearest characterization of dynamic knee valgus movement. The average movement was <5 mm, which

may explain why it escaped clinical detection. The timing of the movement suggests that knee valgus movement occurred during the long-latency reflexive response period following GRFmax rather than as a direct mechanical consequence of initial ground contact. These findings support inter-knee velocity, shortly after GRFmax, as a potentially useful measure for identifying subtle knee valgus movements caused by landing impact forces.

**Disclosures: A. Jones:** None. **B. Shaffer:** None. **A. Wiggins:** None. **C. Onks:** None. **T. Murphy:** None. **J.E. Nyland:** None. **R.A. Creath:** None.

**Poster**

**PSTR188: Posture and Gait: Aging, Injury, and Disease**

**Location:** WCC Halls A-C

**Time:** Monday, November 16, 2026, 1:00 PM - 5:00 PM

**Program #/Poster #:** PSTR188.13/CC16

**Topic:** F.06. Posture and Gait

**Support:** University of South Dakota

**Title:** Frequency-Specific EEG Burst Dynamics Reveal Cortical Signatures of Parkinson's Disease and Freezing of Gait

**Authors:** M. LEEDOM[1], M. PALLAB[1], S. STUART[2], M. MANCINI[3], ***A. SINGH**[1]; [1]Univ. of South Dakota, Vermillion, SD; [2]Oregon Hlth. & Sci. Univ., Portland, OR; [3]Oregon Hlth. and Sci. Univ., Portland, OR

**Abstract:** Parkinson's disease (PD) is associated with abnormal oscillatory activity in basal ganglia-cortical motor networks, but conventional spectral power analyses may overlook the transient, burst-like structure of neural rhythms. Freezing of gait (FOG), a disabling and poorly understood gait disturbance, may further involve cognitive-motor network dysfunction reflected in theta-band dynamics. Here, we examined whether resting-state EEG burst metrics provide frequency-specific markers of PD and FOG severity.

Resting-state EEG data were analyzed from 237 participants across three study sites, including 88 healthy controls and 149 individuals with PD, 73 of which reporting FOG (PDFOG+) and 76 not reporting FOG (PDFOG−). To harmonize data across acquisition systems, analyses were restricted to 11 common EEG channels. Burst dynamics were quantified in theta, alpha, low-beta, and high-beta bands using amplitude-envelope thresholding. Primary burst metrics included burst rate, median burst duration, median burst amplitude, and time in burst. Hypothesis-driven analyses focused on mid-frontal Cz channel, with exploratory topographic analyses across all 11 channels. FOG severity associations were examined using study site-standardized FOGQ z-scores.

Compared with controls, people with PD showed altered low-beta burst timing, characterized by more frequent but shorter low-beta bursts at mid-frontal Cz. These effects were supported by topographic maps, suggesting a spatially distributed low-beta abnormality in PD. In three-group analyses, low-beta burst rate and duration differed across controls, PDFOG−, and PDFOG+

groups; however, PD-only adjusted models did not show robust PDFOG+ vs PDFOG− differences after accounting for disease duration and motor severity. In contrast, FOG severity was most consistently associated with theta amplitude-related burst metrics, including median and high-amplitude theta burst measures.
These findings suggest dissociable oscillatory signatures in PD and FOG: low-beta burst timing abnormalities may reflect general PD-related motor network dysfunction, whereas theta burst amplitude may related to FOG severity and cognitive-motor network burden. Burst-based EEG metrics may provide scalable biomarkers for probing PD motor network dysfunction and FOG-related pathophysiology.

**Disclosures: M. Leedom:** None. **M. Pallab:** None. **S. Stuart:** None. **M. Mancini:** None. **A. Singh:** None.

**Poster**

**PSTR188: Posture and Gait: Aging, Injury, and Disease**

**Location:** WCC Halls A-C

**Time:** Monday, November 16, 2026, 1:00 PM - 5:00 PM

**Program #/Poster #:** PSTR188.14/CC17

**Topic:** F.06. Posture and Gait

**Support:** NIH Grant R01 HD110389

**Title:** Effects of Levodopa on walking in people with Parkinson's disease

**Authors: *J. L. O. L. LIRA**[1], K. TSUJI[2], C. BATISTA[4], W. LIU[5], F. BAKER-ALCALÁ[6], P. I. BURGOS[3], M. MANCINI[2];
[1]Neurol., Oregon Healthy and Sci. Univ., Portland, OR; [3]Kinesiología/Neurociencia, [2]Oregon Hlth. and Sci. Univ., Portland, OR; [4]Neurol., OHSU, portland, OR; [5]Neurol., Oregon Hlth. & Sci. Univ., Portland, OR; [6]Oregon Hlth. & Sci. Univ., Portland, OR.

**Abstract: Title: Effects of Levodopa on walking in people with Parkinson's disease** Gait disturbances in Parkinson's disease (PD), such as reduced stride length and increased gait variability, contribute to reduced independence and increased fall risk. These impairments are often exacerbated during cognitive dual-task (DT) gait. While the effects of levodopa on spatiotemporal gait parameters during single-task (ST) walking are well established, the influence of levodopa in broader gait domains (e.g., upper limb and variability) under DT conditions remains less consistent. We hypothesize that Levodopa would improve multiple gait domains under ST and DT walking, but would have limited effects on gait variability. Therefore, we aimed to evaluate the effects of Levodopa in multiple gait domains in ST and DT walking in people with PD. Forty-one participants with mild-to-moderate PD were tested in their "*Off*" (after 12 hours of medication washout) and "*On*" (1 hour after their last dose of medication) medication on different days. Gait parameters were measured with 6 wearable sensors (Opals APDM) in ST and cognitive DT (a modified Continuous Performance Test during walking). Subsequently, average and variability (standard deviations) of gait parameters were extracted

from MobilityLab V2R software. Standardized Response Mean (SRM) with confidence intervals (CI 95%) were calculated. Differences between "*Off*" and "*On*" were analyzed using paired t-tests, with False Discovery Rate (FDR) adjustment for multiple comparisons. No outliers were identified. Therefore, no individuals from our sample were removed. During ST walking, levodopa showed small but significant improvements in stride length, turn velocity, and arm range of motion (SRMs<0.50; p≤0.03). During DT walking, levodopa showed small but significant effects in turn velocity and arm range of motion (SRMs < 0.50; p ≤ 0.03). A moderate effect on stride length (SRM < 0.80; p < 0.03) was found. Levodopa did not show any significant changes in gait variability during ST walking and DT walking (SRMs < 0.30; p > 0.05). Our preliminary findings suggest that levodopa may improve different gait domains (pace, turning, upper limb) in ST and DT walking in people with PD. This responsiveness in DT conditions may reflect levodopa's ability to support gait control under elevated cognitive demands. In contrast, no change in gait variability may suggest a continued reliance on non-dopaminergic systems, which are known to contribute to gait instability.

**Disclosures: J.L.O.L. Lira:** None. **K. Tsuji:** None. **C. Batista:** None. **W. Liu:** None. **P.I. Burgos:** None. **M. Mancini:** None.

**Poster**

**PSTR188: Posture and Gait: Aging, Injury, and Disease**

**Location:** WCC Halls A-C

**Time:** Monday, November 16, 2026, 1:00 PM - 5:00 PM

**Program #/Poster #:** PSTR188.15/CC18

**Topic:** F.06. Posture and Gait

**Support:** R01 HD110389

**Title:** Walking while enhancing arm coordination: cortical activation and gait during a motor dual task in people with Parkinson's disease

**Authors: *K. TSUJI**, P. I. BURGOS, J. L. LIRA, C. BATISTA, M. MANCINI;
Neurol., Oregon Hlth. and Sci. Univ., Portland, OR

**Abstract:** Gait impairment in people with Parkinson's disease (PD) reflects altered cortical control of walking; a concurrent task worsens it. Using functional near-infrared spectroscopy (fNIRS), we examined cortical activation and gait during single-task walking (ST) and a motor dual-task (DT) in healthy adults and people with PD. 36 older, healthy adults (HC) and 32 people with PD, (tested OFF dopaminergic medication) completed 2-minute overground walking under ST and a motor DT in which they voluntarily enhanced coordination of the contralateral arm and leg. Oxygenated-hemoglobin activation was recorded over the prefrontal cortex (PFC), supplementary motor area (SMA), primary motor (M1), and primary somatosensory (S1) cortex; gait speed, stride length, stride-time variability, and arm range of motion were measured using wearable sensors (Opals APDM). The ST-to-DT change in activation was tested within group with paired t-tests (per ROI available data; outliers excluded by Tukey fences). In ST, overall

cortical activation was lower in people with PD than HC (M1 Cohen's d = -0.99, S1d = -0.62, both $p < .02$). From ST to DT, cortical activation increased in people with PD in every region, most strongly in sensorimotor cortex (M1 $\Delta = +0.29$, $d = 0.92$; S1 $\Delta = +0.24$, $d = 0.80$; both $p < .001$; SMA $\Delta = +0.24$, $p = .04$; PFC $\Delta = +0.09$, $p = .05$). Instead, in HC, cortical activation increased only in PFC from ST to DT ($\Delta = +0.14$, $p = .01$; SMA, M1, S1 non significant). Behaviorally, people with PD walked more slowly with shorter, more variable strides than HC in both ST and DT (stride length $d = -1.04$; gait speed $d = -0.71$ to $-0.84$; stride-time variability $d = +0.73$; all $p < .005$ at ST), and reduced arm swing was more pronounced under the DT (arm ROM $d = -1.04$, $p < .001$). Exploratory within-PD correlations linked greater dual-task activation to less stable gait: higher M1 and S1 activation were correlated to more variable stride time (M1 $r = +0.57$, $p < .001$; S1 $r = +0.45$, $p = .009$) and longer double support (M1 $r = +0.44$, $p = .009$). A motor dual task enhancing arm swing during gait produced a reorganized cortical control of gait in people with PD off medication compared to healthy controls: specifically sensorimotor cortex is under-engaged during unchallenged walking but is mobilized when demand increases, while prefrontal activation remains persistently low. The fact that greater dual-task recruitment accompanied less stable gait suggests this mobilization reflects effortful compensation rather than efficient control, identifying cortical targets for gait-directed therapy.

**Disclosures: K. Tsuji:** None. **P.I. Burgos:** None. **J.L. Lira:** None. **C. Batista:** None. **M. Mancini:** None.

**Poster**

**PSTR188: Posture and Gait: Aging, Injury, and Disease**

**Location:** WCC Halls A-C

**Time:** Monday, November 16, 2026, 1:00 PM - 5:00 PM

**Program #/Poster #:** PSTR188.16/CC19

**Topic:** F.06. Posture and Gait

**Title:** Sensorimotor effects of ankle stretching on gait: Impact of age and Parkinson’s disease

**Authors: T. M. GAUSS**, G. MIZELL, N. GONZALEZ, A. M. HIGHTOWER, *J. M. HONDZINSKI;
Kinesiology, Louisiana State Univ., Baton Rouge, LA

**Abstract:** Ankle rigidity in older adults (OA) and people with Parkinson’s disease (PD) impair gait initiation, propulsion, and stability. Increased ankle rigidity limits center of pressure displacement and ankle plantar flexor power, contributing to slower walking velocity, shorter step length, and greater gait variability. Proprioception deficits, also prominent in OA and PD, may further impair gait by reducing sensorimotor control and stability. Stretching can improve ankle range of motion (ROM) and gait performance in older persons; however, effects of stretching ankle muscles on gait, proprioception, and ROM in PD remain unclear. Thus, we investigated whether acute bilateral stretching of ankle plantar flexors and dorsiflexors would improve ankle ROM, ankle proprioception, and gait parameters in healthy young adults (YA), OA, and PD. We assessed ankle ROM and proprioception abilities of 20 YA, 20 OA, and 20 PD

in addition to gait kinematics during comfortable and fast paced walking before and after bilateral ankle stretching. Results revealed fewer proprioception errors and increased ROM at the ankle for participants, with the greatest ROM gains observed in PD post-stretch. During comfortable walking, stretching increased gait velocity, cadence, step length, and single support time, while decreasing step time across groups. During fast walking, OA and PD increased velocity and cadence and decreased step time after stretching, whereas YA showed no change, likely reflecting their near-maximal gait capacity pre-stretch. Correlations revealed group-specific relationships. Greater dorsiflexion gains in OA associated with decreased cadence, slower velocity, and greater step time variability, suggesting use of a more cautious gait strategy in those achieving greater increases in flexibility. In YA, greater ROM gains associated with greater gains in variability in step length and velocity and suggest that greater post-stretch flexibility can accompany more variable spatiotemporal gait. In PD, greater improvements in proprioception associated with wider steps when walking fast, particularly in tremor-dominant PD, and may reflect a strategy that people with PD use to improve stability. Evidently, people with the greatest increases in flexibility after acute bouts of ankle stretching alter their control strategies differently than those with fewer changes in flexibility. Overall, findings support acute bouts of ankle stretching as a promising intervention to enhance flexibility, position sense, and certain gait kinematics and that gait control strategies depend on age, disease status, walking speed, and degree of flexibility achieved post-stretch.

**Disclosures: T.M. Gauss:** None. **G. Mizell:** None. **N. Gonzalez:** None. **A.M. Hightower:** None. **J.M. Hondzinski:** None.

**Poster**

**PSTR188: Posture and Gait: Aging, Injury, and Disease**

**Location:** WCC Halls A-C

**Time:** Monday, November 16, 2026, 1:00 PM - 5:00 PM

**Program #/Poster #:** PSTR188.17/CC20

**Topic:** F.06. Posture and Gait

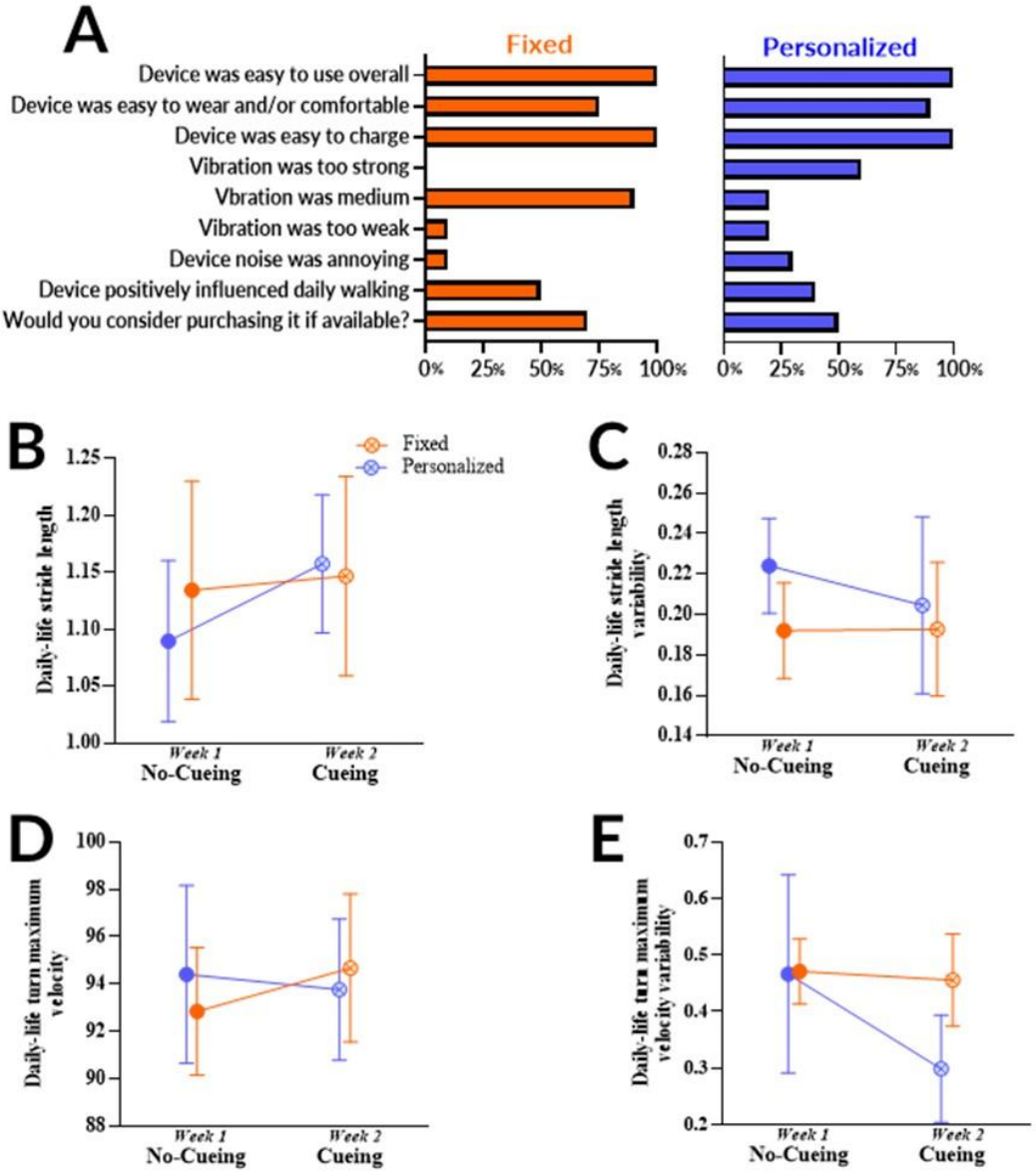
**Support:** NIH GRANT R01 HD110389

**Title:** Effects of Personalized versus Fixed Tactile Cueing on Daily-life Walking in Parkinson's Disease: a pilot study

**Authors: *C. BATISTA**[1], F. B. HORAK[2], W. LIU[3], P. I. BURGOS[4], L. A. KING[3], M. MANCINI[5];
[1]Neurol., OHSU, portland, OR; [2]OHSU, Portland, OR; [3]Neurol., Oregon Hlth. & Sci. Univ., Portland, OR; [4]Kinesiología/Neurociencia, [5]Oregon Hlth. and Sci. Univ., Portland, OR

**Abstract: Introduction:** Cueing, which involves using external temporal or spatial stimuli such as auditory, visual, or tactile cues, improves gait in Parkinson's disease (PD). Our previous work demonstrated that personalized, tactile cueing delivered to the wrist improved gait stability and the quality of turning in individuals with PD. However, the effects of personalized cueing in the

real world remain unknown for this specific cueing modality. This is an exploratory analysis of an ongoing randomized clinical trial (RCT) where we test the hypothesis that personalized (step-synchronized) but not fixed tactile cueing will improve the quality of turning and gait during daily life. **Objective:** To evaluate the practicality and impact of a personalized cueing intervention on daily-life walking in people with PD. **Methods.** The ongoing double-blinded, RCT (NCT05818189) was designed to assess the effects of personalized versus fixed cueing on gait automaticity in people with PD. Participants will wear two instrumented socks (one per foot) and a lumbar Opal sensor for 3 weeks to measure gait and turning at home, with the first and third weeks without cueing and the second week with personalized or fixed cueing. Here, we have compared the effects of no cueing (first week) vs. cueing (second week) on daily-life mobility. **Results.** We have enrolled 14 people with PD who were randomized to personalized (n=6) and fixed (n=8) cueing at home, respectively. Both types of cueing were feasible, enjoyable, without adverse events, and reached similar doses at home (average: 340 minutes for fixed and 246 minutes for personalized, $p$=0.101). Personalized cueing, but not fixed, increases the daily-life stride length (effect size=0.40) and decreases the daily-life stride length variability (effect size=-0.35) and daily-life turn peak velocity variability (effect size=-0.39) compared to no cueing. **Conclusion.** Personalized tactile cueing is feasible for people with mild-to-moderate PD and may potentially have an impact on their daily-life walking.




**Disclosures: C. Batista:** None. **F.B. Horak:** None. **W. Liu:** None. **P.I. Burgos:** None. **L.A. King:** None. **M. Mancini:** None.

**Poster**

**PSTR188: Posture and Gait: Aging, Injury, and Disease**

**Location:** WCC Halls A-C

**Time:** Monday, November 16, 2026, 1:00 PM - 5:00 PM

**Program #/Poster #:** PSTR188.18/CC21

**Topic:** F.06. Posture and Gait

**Support:** NIH Grant NS126609
NIH Grant NS088679

**Title:** Progression of stepping deficits during gait initiation in people with Parkinson's disease with and without REM sleep without atonia

**Authors: *R. TAPORCO**[1,2], S. L. AMUNDSEN HUFFMASTER[2], J. CHUNG[2], Y. CHOI[2], M. N. PETRUCCI[2], R. L. SUMMERS[3], M. E. LINN-EVANS[2], E. E. LECY[4], C. MAUPIN[2], M. HOWELL[2], C. D. MACKINNON[2];
[1]Dept. of Neurol., [2]Neurol., [3]Dept. of Rehabil. Medicine, Divisions of Rehabil. Sci. and P, [4]Neurosci., Univ. of Minnesota, Twin Cities, Minneapolis, MN

**Abstract:** We have previously shown that the expression and progression of gait deficits in Parkinson's disease (PD) is influenced by the presence of rapid eye movement sleep without atonia (RSWA), possibly due to degeneration of brainstem areas that control muscle tone during both wakefulness and sleep. We hypothesized that impairments in the execution of the first two steps of gait initiation would also progress at an increased rate in those with PD and RSWA (PD+RSWA), compared to PD without RSWA (PD-RSWA).24 people with PD (12 PD+RSWA, determined via overnight polysomnography; mean time since diagnosis = 2.2 ± 1.8 years), performed a self-initiated stepping task while off-medications (12+ hours) at baseline and 3-year follow-up (mean 35 ± 7 months). Participants were instructed to pause and then walk forward quickly, starting with a specified foot. 12 trials were performed for each participant (6 trials per leg). Ground reaction forces and whole-body kinematics were collected from force platforms (Kistler Inc., at 1000 Hz) and an 8-camera motion capture system (SIMI Reality Motion Systems, GmbH, at 100 Hz). Outcome measures were first and second step length, width, duration, and speed. Linear mixed-effects models (RStudio) explored the effects of group, visit, most affected and least affected side (MA vs. LA), visit (V1, V2), and their interactions. Significance was set at $p < 0.05$, with post hoc follow-ups using Tukey adjustments.First and second step lengths and durations significantly decreased at follow-up. First step length showed significant effects of side (MA < LA), group x visit (PD+RSWA < PD-RSWA at V1), and group x visit x side interactions (PD+RSWA < PD-RSWA on MA side at V2). Step duration had a main effect of side, such that the 1st and 2nd steps of the MA leg were shorter. Average step speed of the 1st step had effects of side (LA > MA) and group by visit by side (PD-RSWA at V1: LA > MA, PD+RSWA at V2: LA > MA). 1st and 2nd step widths had effects of side (MA > LA, whenever MA was stepping), and 2nd step width also had a group by visit by side interaction (MA PD-RSWA > MA PD+RSWA at V1).Overall, those with PD had more impaired gait initiation at the 3-year follow-up visit, characterized by shorter and wider steps, and longer step durations. Differences between groups seen at baseline were reduced at 3-year follow-up and were side-dependent. Altogether, this work suggests that the presence of RSWA affects the presentation and progression of gait initiation impairment in PD.

**Disclosures: R. Taporco:** None. **S.L. Amundsen Huffmaster:** None. **J. Chung:** None. **Y. Choi:** None. **M.N. Petrucci:** None. **R.L. Summers:** None. **M.E. Linn-Evans:** None. **E.E. Lecy:** None. **C. Maupin:** None. **M. Howell:** None. **C.D. MacKinnon:** None.

**Poster**

**PSTR188: Posture and Gait: Aging, Injury, and Disease**

**Location:** WCC Halls A-C

**Time:** Monday, November 16, 2026, 1:00 PM - 5:00 PM

**Program #/Poster #:** PSTR188.19/CC22

**Topic:** F.06. Posture and Gait

**Title:** The influence ofstretch on the relationship between standing posture and gait

**Authors: *T. M. GAUSS**, J. M. HONDZINSKI;
Louisiana State Univ., Baton Rouge, LA

**Abstract:** People with Parkinson's disease (PD) can reveal problems with standing posture and gait compared to age-matched controls. However, the relationship between standing postural control and gait remains unclear despite the continuous postural regulation required during walking. Inconsistent findings in previous work demonstrate significant associations between greater postural sway and more cautious gait patterns or no direct relationship between these variables. Recently, we determined that stretching antagonist muscle pairs of the ankles of young adults (YA), older adults (OA), and people with PD produced changes in gait variables but not postural sway. Interestingly, within group correlations with range of motion (ROM) revealed differences for postural sway and gait variables based on disease presence and age. We examined relationships between eyes-closed postural sway (center of pressure; CoP) and comfortable and fast gait before and after 45 s of bilateral static ankle stretching in 20 YA, 20 OA, and 20 PD participants. Several significant correlations persisted before and after stretching. Greater area of the ellipse containing 95% of the CoP and CoP in the anterior-posterior direction ($CoP_{AP}$) negatively correlated with single support percentage (SS), velocity, and step length (SL), indicating that participants with increased sway walked slower, took shorter steps, and spent less time in single support during comfortable and fast walking. Greater $CoP_{AP}$ variability negatively correlated with gait velocity before and after stretching. Persistent correlations showed upward shifts in regression lines without slope changes, indicating stretch-induced gait changes despite unchanged sway. Moreover, CoP in the mediolateral direction ($CoP_{ML}$) and $CoP_{ML}$ variability initially negatively correlated with SL, SS, velocity, and increased SL variability, but these associations disappeared after stretching. Reduced spread in values across participants following stretching likely contributed to non-significant post-stretch associations. In PD, increases in $CoP_{ML}$ and $CoP_{ML}$ variability also associated with increased comfortable and fast step time post-stretch to suggest that stretching helped several people with PD step faster but sway more and with greater variability in the ML direction while standing still. Together, these data show that participants with greater sway in the AP direction, regardless of stretched state, consistently produced more cautious gait patterns. In addition, people with PD experiencing greater standing sway in the ML direction after stretching may step faster to limit the effects of ML instability on gait progression.

**Disclosures: T.M. Gauss:** None. **J.M. Hondzinski:** None.

**Poster**

**PSTR188: Posture and Gait: Aging, Injury, and Disease**

**Location:** WCC Halls A-C

**Time:** Monday, November 16, 2026, 1:00 PM - 5:00 PM

**Program #/Poster #:** PSTR188.20/CC23

**Topic:** F.06. Posture and Gait

**Support:** PF-PRF-1045114

**Title:** Circuit mechanisms for skilled gait deficits in a mouse model of Parkinson’s disease

**Authors: *R. M. PAZ**, A. B. NELSON;
Neurol., UCSF, San Francisco, CA

**Abstract:** Walking gait is a fundamental motor function essential for survival and adaptive behavior. Gait impairments are among the most debilitating symptoms of Parkinson's disease, as they respond poorly to current pharmacological and surgical treatments, severely limit mobility, and contribute to falls and hospitalizations. Gait emerges from the coordinated activity of multiple neural circuits that integrate sensory and motor information to generate appropriate motor commands. While spinal central pattern generators produce the rhythmic muscle activity required for locomotion, voluntary control of gait depends on supraspinal networks, including the basal ganglia-thalamocortical circuit. In people with PD, gait deficits are closely associated with abnormal activity throughout the basal ganglia and motor cortex. These regions are interconnected through the motor thalamus, which receives inhibitory GABAergic input from basal ganglia output nuclei and maintains reciprocal connections with motor cortex. Previous studies in animal models of PD suggest that pathological basal ganglia output may disrupt normal thalamocortical activity necessary for movement. However, whether this circuit contributes directly to parkinsonian gait deficits remains poorly understood. Here, we developed a quantitative framework combining high-speed video recordings and markerless motion tracking to characterize gait kinematics and quantify gait impairments in a mouse model of PD. We then integrated this platform with in vivo single-unit electrophysiology to examine motor thalamus activity during locomotion in healthy and parkinsonian mice. We found that motor thalamus neurons encode distinct gait features and exhibit robust gait modulation. Dopamine neuron loss produced pronounced gait impairments that were accompanied by profound alterations in motor thalamus activity. Finally, using a combination of slice electrophysiology and in vivo optogenetics, we investigated the contribution of inputs from the substantia nigra pars reticulata, the principal basal ganglia output nucleus in rodents, to these deficits. Together, our findings identify the motor thalamus as a critical node in the neural control of gait and provide mechanistic insight into the circuit dysfunction underlying gait disturbances in PD.

**Disclosures: R.M. Paz:** None. **A.B. Nelson:** None.

**Poster**

**PSTR188: Posture and Gait: Aging, Injury, and Disease**

**Location:** WCC Halls A-C

**Time:** Monday, November 16, 2026, 1:00 PM - 5:00 PM

**Program #/Poster #:** PSTR188.21/Web Only

**Topic:** F.06. Posture and Gait

**Support:** Shanghai Municipal Science and Technology Major Project 2018SHZDZX05
National Natural Science Foundation of China 82461160319
National Natural Science Foundation of China 92168105

**Title:** A PONTINE CENTER ORCHESTRATES THE SPEED-ACCURACY TRADEOFF FOR ACTION AND FUNCTIONAL RECOVERY AFTER STRIATAL HEMORRHAGIC INJURY

**Authors: *Y. ZHANG**[1], Y. LI[2,1], C. JI[3];
[1]Inst. of Neurosci. (ION) Ctr. for Excellence in Brain Sci. and Intelligence Technol. (, Shanghai, China; [2]Neurol., Boston Children's Hosp., Shanghai, China; [3]Chinese Acad. of Sci. Ctr. for Excellence in Brain Sci. and Intelligence Technol., Nanjing, China

**Abstract:** Successful interaction with the environment relies on the ability to execute rapid and precise movements. Although a fundamental tradeoff exists between speed and accuracy, the neural mechanisms that regulate this balance remain poorly understood. Here, we identified a population of neurons in the pons that exhibit task-related activity during precision-demanding motor behaviors. Using chemogenetic and closed-loop optogenetic manipulations, we demonstrate that activation of these neurons enhances movement accuracy at the expense of speed in a skilled forelimb single-pellet reaching task, whereas their inhibition disrupts task execution. Further circuit analyses revealed that pontine neurons integrate striatal inputs to selectively modulate precision-demanding motor control. Notably, activating these neurons ameliorates motor deficits after striatal hemorrhagic injury. In summary, these findings identify a pontine circuit that integrates striatal inputs to regulate the speed-accuracy tradeoff in motor control and highlight a potential target for restoring motor precision after striatal injury.

**Disclosures: Y. Zhang:** None. **Y. Li:** None. **C. Ji:** None.

**Poster**

**PSTR189: Early-Life Stress: Circuit Mechanisms and Effects on Behavior**

**Location:** WCC Halls A-C

**Time:** Monday, November 16, 2026, 1:00 PM - 5:00 PM

**Program #/Poster #:** PSTR189.01/CC24

**Topic:** G.03. Stress and the Brain

**Support:** NSF Grant # 2309589
NSF Grant # 2440448

**Title:** Chronic Optogenetic Activation of Hypothalamic AgRP1 Neurons Drives Hyperlocomotion and Altered Thigmotaxis in Larval Zebrafish Open Field Test

**Authors: *H. MEHRABI**, E. JUNG;
Univ. of Illinois Chicago, Chicago, IL

**Abstract:** Hypothalamic Agouti-Related Peptide 1 (AgRP1) neurons regulate feeding behavior in zebrafish larvae. In mammals, AgRP neurons modulate anxiety-like behavior under food restriction and chronic stress, but whether AgRP1 activation similarly affects anxiety in zebrafish remains unknown. We used Tg(AgRP1:ChR2-Kaede) transgenic larvae, in which AgRP1 neurons are selectively activated by blue light (470 nm), to examine whether chronic or acute optogenetic stimulation alters thigmotaxis in a larval open field test (OFT).Four groups of 7-days post-fertilization (dpf) larvae were tested: wild-type (ABWT, n=39) and transgenic (AgRP, n=11) controls under standard rearing, and wild-type (ABWT_stim, n=53) and transgenic (AgRP_stim, n=41) groups chronically exposed to periodic blue-light stimulation (45 s on per 5-min cycle) from 2-7 dpf. Transgenic fish were screened at 6 dpf for Kaede fluorescence to confirm ChR2 expression. OFT used a custom circular arena illuminated by an LED matrix. Each trial comprised a 10-min red-light baseline followed by 10-min blue-light stimulation, recorded at 30 fps (EthoVision XT; noise threshold >5 mm/frame; samples excluded if >11% of frames were undetected). Thigmotaxis was quantified as time and distance in the inner zone (25% of arena area). Sex was not assessed, as gonads are undifferentiated at 7 dpf.Wilcoxon signed-rank tests (paired, within-group) showed AgRP_stim fish had significantly increased inner-zone time ($p=0.050$) and distance ($p=0.009$) during blue-light stimulation versus baseline, indicating reduced thigmotaxis. Mean velocity also increased significantly in AgRP_stim ($p=0.004$), but not in ABWT_stim ($p=0.968$) or non-stimulated controls. Between-group Kruskal-Wallis analysis of stimulation-minus-baseline velocity deltas was significant ($H=20.46$, $p<0.001$); Dunn post-hoc tests (Bonferroni-corrected) showed AgRP_stim exceeded both ABWT ($p=0.001$) and AgRP ($p=0.002$). Zone-preference deltas did not differ significantly between groups, suggesting the inner-zone shift in AgRP_stim may be partly locomotion-driven. Importantly, baseline inner-zone occupancy differed between AgRP_stim and ABWT_stim ($p=0.002$), indicating chronic AgRP1 activation alters developmental behavioral baselines.Chronic activation of hypothalamic AgRP1 neurons produces robust hyperlocomotion and a trend toward reduced thigmotaxis in larval zebrafish OFT, establishing a framework for studying hunger-circuit modulation of anxiety-like states.

**Disclosures: H. Mehrabi:** None. **E. Jung:** None.

**Poster**

**PSTR189: Early-Life Stress: Circuit Mechanisms and Effects on Behavior**

**Location:** WCC Halls A-C

**Time:** Monday, November 16, 2026, 1:00 PM - 5:00 PM

**Program #/Poster #:** PSTR189.02/CC25

**Topic:** G.03. Stress and the Brain

**Support:** Fundacion Alicia Koplowitz
PND Grant 2025I031
RYC2022-035438-I

**Title:** Toward Precision Psychiatry: Sex- and Glutamate-Dependent Stress Vulnerability in DAT Transgenic Rats

**Authors: *M. PARDO**[1], S. GIMENEZ GOMEZ[2], Á. COLOMINA[2], M. ESTEVE[2], P. MATAS NAVARRO[2], A. PERROTE DOMINGO[2];
[1]Univ. of Valencia/IDM, Valencia, Spain; [2]Univ. de Valencia, Valencia, Spain

**Abstract:** Stress-related disorders exhibit substantial inter-individual variability in susceptibility, symptom presentation, and treatment response. While genetic background, biological sex, and environmental exposures are recognized contributors to this variability, the mechanisms underlying distinct vulnerability trajectories remain poorly understood. Here, we developed a translational framework to investigate how dopamine transporter (DAT) dysfunction interacts with early-life stress and sex to shape behavioral outcomes and treatment responsiveness.Wild-type (WT), heterozygous (HET), and knockout (KO) DAT transgenic rats were exposed or not to maternal separation (MS) during early postnatal development. Behavioral assessments in early adulthood included measures of anxiety-like behavior, depressive-like behavior, locomotor activity, and reward-related responses. In parallel, environmental and pharmacological interventions, including voluntary wheel running and sertraline treatment, were evaluated as potential modulators of vulnerability phenotypes. Ongoing molecular analyses are examining glutamatergic pathways and stress-related markers as candidate mechanisms underlying these behavioral profiles.Preliminary findings indicate that DAT-related vulnerability is highly domain- and sex-dependent. Rather than producing a uniform stress-sensitive phenotype, HET animals exhibit selective alterations in specific behavioral domains, with the magnitude and direction of effects differing between males and females. Importantly, treatment efficacy also varies according to genotype, sex, and behavioral endpoint, suggesting the existence of distinct vulnerability and resilience profiles that are differentially responsive to intervention. Emerging molecular data further suggest that alterations in glutamatergic signaling may contribute to these divergent trajectories.These findings support a model in which stress vulnerability emerges from interactions among genetic susceptibility, sex, and underlying neurobiological mechanisms rather than from environmental exposure alone. By identifying biologically distinct vulnerability profiles and their differential responsiveness to intervention, this DAT transgenic model provides a translational platform for the development of individualized therapeutic strategies and precision psychiatry approaches for stress-related disorders.

**Disclosures: M. Pardo:** None. **S. Gimenez Gomez:** None. **Á. Colomina:** None. **M. Esteve:** None. **P. Matas Navarro:** None. **A. Perrote Domingo:** None.

**Poster**

**PSTR189: Early-Life Stress: Circuit Mechanisms and Effects on Behavior**

**Location:** WCC Halls A-C

**Time:** Monday, November 16, 2026, 1:00 PM - 5:00 PM

**Program #/Poster #:** PSTR189.03/CC26

**Topic:** G.03. Stress and the Brain

**Support:** T32HL007249
ORWH-NIMH 3U54MH118919
ORWH-NIMH 3U54MH118919-04S3

**Title:** Mid-gestation maternal immune activation in rats impacts both maternal and offspring outcomes

**Authors: *M. MARTINEZ**[1], S. A. TOBET[2], T. M. HALE[1];
[1]Univ. of Arizona, Phoenix, AZ; [2]Colorado State Univ., Loveland, CO

**Abstract:** Maternal immune activation (MIA) can occur during pregnancy due to exposure to infectious diseases or other inflammatory conditions. Resiquimod (RQ), a toll-like receptor 7 agonist, induces systemic inflammatory responses that mimic responses to viral infections. We have previously shown that RQ-induced MIA in rats during late gestation attenuated maternal weight gain and delayed female pubertal onset, increased anxiety-like behavior after puberty, and attenuated adult weight gain in offspring. We have also shown that RQ-induced MIA in mice during mid-gestation reduced prepubertal body weights, delayed the day of eye opening and female pubertal onset, and increased male anxiety-like behavior in offspring. The current project investigates the impact of mid-gestation MIA with RQ in rats on both maternal and offspring outcomes. Pregnant rat dams were weighed throughout gestation and received a single vehicle (phosphate-buffered saline) or RQ (1 mg/kg, s.c.) injection on gestation day 14. Maternal behavior was assessed using a pup retrieval test on postnatal day (PND) 5. Offspring timing of eye opening (PND 12-15) and weekly weights were assessed. An open field test assessed offspring anxiety-like behavior before (PND 23-28) and after puberty (PND 56+). RQ-induced MIA attenuated maternal gestational weight gain following injection (mixed-effects model, REML; time: $p < 0.0001$; time × injection: $p = 0.0032$). Unlike our prior studies, RQ-injected dams exhibited impaired maternal caregiving behavior during the early postnatal period, evident by a significant increase in the latency to retrieve the first pup back to the nest site (unpaired t-test, $p = 0.0127$). Offspring of RQ-injected dams experienced significantly earlier (~1 day) eye opening than their vehicle counterparts, regardless of sex (two-way ANOVA; exposure, $p = 0.0268$). Offspring of RQ-injected dams also had attenuated adult weight gain compared to their vehicle counterparts, regardless of sex (three-way ANOVA; week, $p < 0.0001$; sex, $p < 0.0001$; exposure, $p = 0.0351$; week × sex, $p < 0.0001$). RQ-induced MIA did not significantly impact the timing of pubertal onset or open field assessments before or after puberty. Taken together, the results suggest that the effects of RQ-induced MIA during mid-gestation in rats extend to the maternal condition. The results further suggest that the timing of MIA and the species of interest play a significant role in experimental outcomes.

**Disclosures: M. Martinez:** None. **S.A. Tobet:** None. **T.M. Hale:** None.

**Poster**

**PSTR189: Early-Life Stress: Circuit Mechanisms and Effects on Behavior**

**Location:** WCC Halls A-C

**Time:** Monday, November 16, 2026, 1:00 PM - 5:00 PM

**Program #/Poster #:** PSTR189.04/CC27

**Topic:** G.03. Stress and the Brain

**Title:** Parental Stress Induces Hyperactivity in Drosophila melanogaster Offspring Independent of Octopaminergic Signaling

**Authors:** K. COLLAZO, K. GARO, ***B.-S. WANG**;
Biol., St. Joseph's Univ., Brooklyn, NY

**Abstract:** Parental stress is an established risk factor for attention deficit hyperactivity disorder (ADHD) and related neurodevelopmental disorders, yet the neurobiological mechanisms linking parental stress experience to offspring behavioral phenotypes remain poorly understood. We used Drosophila melanogaster to investigate whether two forms of parental stress, circadian disruption and nutritional restriction, induce hyperactivity in offspring, and to identify neuromodulatory pathways mediating this effect. Wild-type Oregon-R parents were exposed to orbital shaker stress (300 rpm, 48h) or low-nutrient food (25% yeast, 48h) during egg laying; progeny were raised under normal conditions and assessed using an open-field locomotion assay. Both stressors induced significant hyperactivity in offspring relative to controls, measured by mean speed and total distance traveled, with nutritional stress producing a markedly more severe phenotype. To investigate the role of octopaminergic signaling, known to mediate starvation-induced hyperactivity in Drosophila, we examined locomotion in homozygous TβH mutant progeny lacking octopamine. Contrary to our hypothesis, parental stress-induced hyperactivity persisted in octopamine-deficient offspring under both stress conditions, demonstrating that octopamine is not required for this intergenerational phenotype. Direct comparison of wild-type and TβH mutant offspring revealed a stressor-dependent divergence: circadian stress produced greater hyperactivity in TβH mutants than wild-types, while nutritional stress produced greater hyperactivity in wild-types, suggesting that octopamine plays a bidirectional modulatory role that depends on stressor type rather than being strictly required for the phenotype. These findings establish Drosophila as a tractable model for dissecting the neuromodulatory basis of intergenerational stress-induced behavioral phenotypes, and motivate further investigation into the parallel monoaminergic pathways, including serotonergic and dopaminergic systems, through which parental stress shapes offspring behavior.

**Disclosures: K. Collazo:** None. **K. Garo:** None. **B. Wang:** None.

**Poster**

**PSTR189: Early-Life Stress: Circuit Mechanisms and Effects on Behavior**

**Location:** WCC Halls A-C

**Time:** Monday, November 16, 2026, 1:00 PM - 5:00 PM

**Program #/Poster #:** PSTR189.05/CC28

**Topic:** G.03. Stress and the Brain

**Title:** Maternal Early Life Stress Disrupts Auditory Cortex Glial Development and Sex-Specific Neuroplasticity in Offspring

**Authors:** ***B. KOSE-OZKAN**[1], J. MILLER[2], M. ROGIDO[2], E. A. ECKMAN[1], A. AUBER[3], P. LLOYD[3], A. FOSTER[3], S. COWHIG[4], C. MUNOZ-BALLESTER[3], A. GUNGOR AYDIN[1];

[1]Biomed. Res. Inst. of New Jersey, Cedar Knolls, NJ; [2]Pediatrics, Atlantic Hlth. Morristown Med. Ctr., Morristown, NJ; [3]Univ. of Maryland, Baltimore, MD; [4]Seton Hall Univ., South Orange, NJ

**Abstract:** Maternal early life stress is a potent risk factor for psychopathologies across generations, with offspring showing heightened vulnerability to neurodevelopmental and psychiatric disorders (Barclay et al., 2022). The prenatal period is a particularly sensitive window, and maternal experiences, such as stress before or during pregnancy, can shape the offspring's brain development. Yet, how this intergenerational stress signal alters auditory cortex development, plasticity, and behavior remains unknown. We used the social isolation rearing (SIR) model in Sprague-Dawley rats (n= 7; n=7 group housed controls), isolating females from weaning for 7 weeks (prior to mating), to examine how early life stress in mothers alters offspring auditory cortex (AC) development and adult auditory learning, neuroplasticity, and function. We found that SIR dams exhibited a depressive-like phenotype, reduced sucrose preference, and blunted habituation in the forced swim test, without altered body weight. Astrocytes shape cortical synapse maturation (Ribot et al. 2021), and disrupted astrocyte-interneuron signaling may destabilize the circuitry underlying auditory cortical plasticity (Faust et al., 2024). To establish developmental mechanisms, we quantified Ki67+ proliferating cells and S100B+ astrocytes at P7, P14, and P21 in offspring AC. SIR offspring showed elevated glial proliferation and S100B+ cell density at P7 that normalized by P14, suggesting disrupted glial scaffolding during a critical window of AC maturation. In adulthood, offspring underwent auditory brainstem response (ABR) recording (n= 24; male & female) and auditory training to assess learning and training-induced neuroplasticity. Effects were sex-specific and most pronounced in males. Male SIR offspring learned the auditory discrimination more slowly, reached a lower d-prime ceiling, and lacked training-induced ABR amplitude increases seen in controls; neural selectivity for the rewarded tone emerged in controls but was absent in SIR offspring. Females showed smaller, more variable deficits. These findings indicate that maternal early life stress disrupts offspring AC glial development and compromises sex-specific neuroplasticity in adulthood. Ongoing analyses of astrocyte maturation, PV-interneurons, and corticosterone will define the trajectory linking early glial changes to adult circuit dysfunction.

**Disclosures: B. Kose-Ozkan:** None. **J. Miller:** None. **M. Rogido:** None. **E.A. Eckman:** None. **A. Auber:** None. **P. Lloyd:** None. **A. Foster:** None. **S. Cowhig:** None. **C. Munoz-Ballester:** None. **A. Gungor Aydin:** None.

**Poster**

**PSTR189: Early-Life Stress: Circuit Mechanisms and Effects on Behavior**

**Location:** WCC Halls A-C

**Time:** Monday, November 16, 2026, 1:00 PM - 5:00 PM

**Program #/Poster #:** PSTR189.06/CC29

**Topic:** G.03. Stress and the Brain

**Title:** Nature vs. Nuture: Investigating the Intergenerational Effects of Early Life Stress

**Authors: *S. SULLIVAN**, L. R. HALLADAY;
Univ. of Arizona, Tucson, AZ

**Abstract:** Exposure to early life stress (ELS) can have profound impacts on the brain and social behavior, as it disrupts neural circuitry involved in stress regulation. Our lab uses a mouse model of ELS, maternal separation with early weaning (MSEW): pups are separated from the dam for 4h on postnatal days (P)2-5, 8h on P6-16, and weaned early on P17; controls remain with the dam undisturbed until weaning on P21. Animals exposed to MSEW reliably exhibit robust socioemotional deficits, which in prior work, we determined to be mediated primarily by the bed nucleus of the stria terminalis (BNST), a region involved in anxiety regulation and response to stress. One of our current goals is determining whether and how these ELS-induced alterations are intergenerationally inherited through epigenetic mechanisms. To do this, we bred MSEW females (F1) with naive males to produce offspring (F2) to assess for potential ELS-like alterations. We compared MSEW offspring (F2; n=60) against non-stressed (NS) and cross-fostered controls. Adult F2 mice were run in behavioral assays including 2-period social interaction to assess social motivation, the 3D radial arm maze to assess anxiety-like behavior, and cued fear conditioning to assess learning and memory. Female F2 mice raised by MSEW dams displayed reduced social motivation and potentiated anxiety-like behavior vs. offspring raised by NS dams-mirroring MSEW-induced effects of F1 mice. These effects persisted across all groups raised by MSEW dams, regardless of biological background, suggesting that maternal care is the primary driver of observed effects. Ongoing studies are exploring whether neural MSEW alterations similarly are driven by environmental, rather than epigenetic mechanisms. These studies have the potential to inform prevention strategies for individuals exposed to stressors during critical developmental periods, as well as provide a better understanding of the lasting impact of those stress-induced effects.

**Disclosures: S. Sullivan:** None. **L.R. Halladay:** None.

**Poster**

**PSTR189: Early-Life Stress: Circuit Mechanisms and Effects on Behavior**

**Location:** WCC Halls A-C

**Time:** Monday, November 16, 2026, 1:00 PM - 5:00 PM

**Program #/Poster #:** PSTR189.07/CC30

**Topic:** G.03. Stress and the Brain

**Support:** NIMH R01 MH130825

**Title:** Brain-wide mapping of attachment deficits in a mouse model of childhood adversity

**Authors: *Z. A. MACDOWELL KASWAN**, A. KAFFMAN;
Psychiatry, Yale Sch. of Med., New Haven, CT

**Abstract:** Maternal attachment is a suite of evolutionarily conserved behaviors exhibited by offspring towards their caregivers. These behaviors promote normal development by providing a cognitive “safe base” from which offspring can explore their environment. Attachment behaviors

can be classified into distinct attachment styles that emerge in response to the predictability and quality of care received. When offspring needs are met consistently, secure attachment develops. In contrast, rates of insecure attachment (avoidant, anxious, or disorganized) increase when caregiving is inconsistent and/or fails to meet those needs. In humans, insecure attachment is associated with psychiatric disorders and poorer physical health throughout life. Early life adversity (ELA) is a major risk factor for insecure attachment and is also associated with higher rates of mental and physical illness. Randomized control trials have shown that attachment-based interventions improve ELA-associated deficits, suggesting that attachment may mediate this relationship. However, the neurobiological mechanisms linking ELA and attachment remain poorly understood, in part due to a lack of animal models. To address this gap, we demonstrated that the limited bedding (LB) paradigm of ELA, a poverty-like model characterized by environmental deprivation and fragmentation of care, induces an avoidant-like attachment style in mouse pups across multiple developmental stages. Compared to control (CTL) pups, LB pups had elevated baseline serum corticosterone at post-natal day (P)7, produced fewer distress vocalizations during isolation at P8, were less likely to approach their anesthetized dam at P13 and P16, and exhibited increased anxiety-like behavior at P18. Pup weight was inversely correlated to the dams' movement, a relationship the persisted past weaning in male, but not female, suggesting greater male vulnerability. To characterize neural circuitry involved in avoidant attachment, brains form P13 CTL and LB pups were cleared and stained for cFos following the maternal affiliation test. CTL brains showed greater cFos immunoreactivity than LB brains in several regions, including limbic areas such as the amygdala and hippocampus, and regions involved in social behavior such as the paraventricular nucleus of the hypothalamus (PVN). We replicated the reduction in PVN cFos expression, and found that the affected cell population does not express oxytocin or arginine vasopressin. Together, these data establish a robust mouse model for ELA-induced attachment deficits and provide novel insight into the neural circuits underlying attachment behavior.

**Disclosures: Z.A. MacDowell Kaswan:** None. **A. Kaffman:** None.

**Poster**

**PSTR189: Early-Life Stress: Circuit Mechanisms and Effects on Behavior**

**Location:** WCC Halls A-C

**Time:** Monday, November 16, 2026, 1:00 PM - 5:00 PM

**Program #/Poster #:** PSTR189.08/DD1

**Topic:** G.03. Stress and the Brain

**Support:** NIMH R01MH130825
NIMH 1R01MH136490

**Title:** Childhood deprivation produces persistent deficits in contextual fear conditioning that are reversed by early enrichment

**Authors: *L. GIULIANO**, A. RIOS, J. GIEGERICH, A. PASTOR, A. KAFFMAN; Psychiatry, Yale Sch. of Med., New Haven, CT

**Abstract:** Childhood neglect and deprivation (CND) causes cortical thinning and persistent cognitive deficits. Although early enrichment (EE) can mitigate some of these impairments, the cellular mechanisms through which CND and EE influence cognitive function remain poorly understood, partly because of the limited availability of animal models that accurately recapitulate childhood neglect. To address this gap, we recently showed that mice exposed to prolonged impoverished conditions using the limited bedding (LB) paradigm exhibit deficits resembling those observed in children exposed to CND, including avoidant attachment, hyperactivity, cortical thinning, and impaired contextual fear conditioning (CFC). LB impaired CFC in adolescent males, but not females, and these deficits were reversed by adding toys to LB cages from postnatal day (P)14-25, a condition termed LBT. Here, we show that contextual memory deficits persist into adulthood in LB mice. Consistent with our adolescent findings, adult LB males exhibited impaired freezing behavior. In contrast to adolescent females, adult LB females displayed significant freezing deficits comparable to those observed in males. Preliminary studies further indicate that LBT normalized freezing behavior in both adult males and females, suggesting a long-lasting therapeutic effect. To investigate the mechanisms through which LB and LBT influence hippocampal function, we quantified neuronal activation during memory retrieval using the immediate-early gene (IEG) product c-Fos. Despite robust behavioral deficits, no significant differences in c-Fos expression were detected in CA1 or the dentate gyrus. Previous studies, however, suggest that activity-regulated cytoskeleton-associated protein (Arc), another IEG, may provide a more sensitive marker of hippocampal activation during CFC. Ongoing studies are examining whether LB and LBT alter Arc expression in hippocampal subregions. Together, these findings demonstrate that LB causes persistent CFC deficits in both adult male and female mice that can be reversed by brief enrichment early in life, providing a unique model for investigating how deprivation and enrichment shape adult cognitive function.

**Disclosures: L. Giuliano:** None. **A. Rios:** None. **J. Giegerich:** None. **A. Pastor:** None. **A. Kaffman:** None.

**Poster**

**PSTR189: Early-Life Stress: Circuit Mechanisms and Effects on Behavior**

**Location:** WCC Halls A-C

**Time:** Monday, November 16, 2026, 1:00 PM - 5:00 PM

**Program #/Poster #:** PSTR189.09/DD2

**Topic:** G.03. Stress and the Brain

**Support:** NIH R01MH115215
NIH R01ES035856

**Title:** Automated labeling of behavioral outputs in control and early-life stressed mice

**Authors: *T. LAGO**[1], M. BOMPOLAKI[3], K. ONO[1], M. MITELBERG[4], L. KING[1], S. A. DOMINGUEZ[3], J. NYE[2], E. D. LEONARDO[1,3], A. DRANOVSKY[1,3];
[2]Biomed. Engin., [1]Columbia Univ., New York, NY; [3]Systems Neurosci. / Psychiatry, New York State Psychiatric Inst., New York, NY; [4]Res. Fndn. For Mental Hyg., Fort Lee, NJ.

**Abstract:** Early life stress (ELS) is a risk factor for mood and anxiety disorders, the most common mental health issues affecting the US population. The limited nesting and bedding paradigm (LBN) is a common experimental model to study ELS in rodents but has produced inconsistent results in behavioral tasks. Recent advances in computer vision and the development of technology for automated labeling are potential solutions to the variability that comes from human scoring. Different tasks measure diverse aspects of behavior, from location to interaction. We have constructed two computational pipelines to automate scoring in mice performing a navigational working memory and a social interaction task. The pipelines were tested in two cohorts consisting of male and female mice (n = 98) aged 4 and 10 months. To maximize consistency, behavioral tasks were recorded from a top view camera and performed at the same time of day. The videos were then processed with DeepLabCut (DLC) until tracking reached a 60% confidence threshold. We then used custom scripts in MATLAB and Python to measure behaviors and found that while this approach yielded robust results for studying navigation, it fell short in detecting interaction behaviors. Hence, we turned to Simple Behavioral Analysis (SimBA), an open-sourced machine learning software that we were able to train to detect social interaction. Like DLC, SimBa models were trained to reach a confidence threshold of 60%. The two computational pipelines were validated against a ground truth subsample using human expert scoring. Following validation, the pipelines were applied to a large dataset of ELS and control mice. This approach allowed us to unambiguously demonstrate the effects of ELS across behavioral tasks using a standardized method. We were also able to determine the role of age and sex on the tested behaviors. Overall, this work solidifies and extends our understanding of the impact of ELS on behavior while dramatically increasing throughput for behavioral analysis. It also underscores the value of automated, data-driven approaches in behavioral neuroscience research.

**Disclosures: T. Lago:** None. **M. Bompolaki:** None. **K. Ono:** None. **M. Mitelberg:** None. **L. King:** None. **S.A. Dominguez:** None. **J. Nye:** None. **E.D. Leonardo:** None. **A. Dranovsky:** None.

**Poster**

**PSTR189: Early-Life Stress: Circuit Mechanisms and Effects on Behavior**

**Location:** WCC Halls A-C

**Time:** Monday, November 16, 2026, 1:00 PM - 5:00 PM

**Program #/Poster #:** PSTR189.10/DD3

**Topic:** G.03. Stress and the Brain

**Support:** NIH Grant R01 MH132680
NIH Grant P50 MH096889
Bren Foundation
Dr. Lorna Carlin Scholar Award

**Title:** Novel $CRH^{+}$/GABA Basolateral Amygdala-Nucleus Accumbens Projection Governs Motivated Behaviors in a Sex- and Stress-Dependent Manner

**Authors: *L. TANIGUCHI**[1,2], C. M. GOODPASTER[4], Y. CHEN[3], G. DE CARVALHO[2], M. T. BIRNIE[3], A. PAUL[2], A. CHIANG[2], D. KARTHIKEYAN[2], A. PAUL[2], L. Y. CHEN[2], L. A. DENARDO[4], T. Z. BARAM[2,3];
[2]Anat. and Neurobio., [3]Pediatrics, [1]UC Irvine, Irvine, CA; [4]Physiol., UCLA, Los Angeles, CA

**Abstract:** **Rationale**: Early-life adversity (ELA) is a risk factor for human affective disorders involving dysregulated reward behaviors. In our limited bedding and nesting mouse model, ELA induces anhedonia-like behaviors in adult male mice while increasing motivation for palatable food rewards and sex cues in adult females, indicating sex-dependent disruption of reward circuit function. We identified a novel corticotropin-releasing hormone ($CRH^+$)/GABA-expressing projection from the basolateral amygdala (BLA) to the nucleus accumbens (NAc) that governs reward-seeking deficits in adult ELA males, but not in females. **Methods**: Adult male and female CRH-Cre mice raised in control or ELA conditions received excitatory or inhibitory Cre-dependent DREADDs in the BLA, with clozapine N-oxide or vehicle delivered to the NAc medial shell during reward behaviors. Cell identity was determined via immunostaining and electrophysiology. Brain-wide $CRH^+$ BLA axonal projections were mapped using tissue clearing, light sheet fluorescence microscopy, and deep learning pipelines. Given the absence of differences observed with bilateral chemogenetic manipulations and considering that ipsilateral and contralateral projections may serve opposing or distinct functional roles, we are currently examining interhemispheric and intrahemispheric projections separately. **Results**: Chemogenetic manipulations in male mice revealed inhibitory effects of the $CRH^+$/GABA BLA-NAc projection on reward behaviors, whereas neither excitation nor inhibition influenced female behaviors. Molecular and electrophysiological cell identities of the projection did not vary by sex. By contrast, comprehensive whole-brain mapping uncovered significant differences in NAc innervation patterns that were both sex- and ELA-dependent, including selective changes in innervation of other brain regions. **Conclusions**: The $CRH^+$/GABA BLA-NAc projection that influences reward behaviors in males is structurally and functionally distinct in females, uncovering potential mechanisms for the profound sex-specific impacts of ELA on reward behaviors. Further investigation of this projection will provide deeper insight into intrinsic sex differences in reward circuit organization and the effects of ELA on reward behaviors, which underlie many mood disorders.

**Disclosures: L. Taniguchi:** None. **C.M. Goodpaster:** None. **Y. Chen:** None. **G. de Carvalho:** None. **M.T. Birnie:** None. **A. Paul:** None. **A. Chiang:** None. **D. Karthikeyan:** None. **A. Paul:** None. **L.Y. Chen:** None. **L.A. DeNardo:** None. **T.Z. Baram:** None.

**Poster**

**PSTR189: Early-Life Stress: Circuit Mechanisms and Effects on Behavior**

**Location:** WCC Halls A-C

**Time:** Monday, November 16, 2026, 1:00 PM - 5:00 PM

**Program #/Poster #:** PSTR189.11/DD4

**Topic:** G.03. Stress and the Brain

**Support:** Postdoctoral fellowship from the George E. Hewitt Foundation for Medical Research

**Title:** Effects of early life adversities on development and maturation of hippocampal networks dynamics and memory function

**Authors: *T. AUER**[1], L. MA[2], J. GELINAS[1], T. BARAM[3];
[1]UC Irvine, Irvine, CA; [2]Dept. of Biomed. Engin., Univ. of California, Irvine, Irvine, CA;
[3]Anatomy/Neurobiology; Pediatrics, Univ. of California Irvine, Irvine, CA

**Abstract:** Background: Experiencing early-life adversity (ELA), such as chaotic environments and neglect, is a potent risk factor for persistent cognitive deficits, particularly memory impairments. While epidemiological studies link ELA to poor cognitive outcomes, the underlying mechanisms by which ELA disrupts the maturation of hippocampal-dependent memory systems during early postnatal development remain poorly understood. The functional maturation of the hippocampus is characterized by a sequence of neuronal activities, which are initially intrinsically generated but modulated by sensory inputs from the environment to allow the development of mature network rhythms required for complex memory processes. We investigate the novel hypothesis that ELA interferes with these early organizing network activities, resulting in aberrant brain circuit formation and life-long memory problems. Methods: We use a validated rodent model of ELA involving limited bedding and nesting material from postnatal days 2-10, which generates chronic stress in the pups due to chaotic and unpredictable maternal sensory signals, and reliably induces memory deficits in adult mice. Acute, high-resolution *in vivo* electrophysiology using silicon probes monitors hippocampal network activity of awake, head-fixed pups with and without prior ELA exposure, establishing the effects of patterned vs. unpredictable sensory input as well as acute sensory stimulation on network dynamics. Physiological hippocampal activity mimicking endogenous sharp waves will then be induced via optogenetic stimulation in ELA pups to evaluate its ability to restore network maturation and rescue memory functions. Results: High-quality *in vivo* hippocampal recordings were successfully obtained from mouse pups at P6/7 and P13/14 in both CTL and LBN groups. Hippocampal sharp waves were detected as early as P6 in both conditions, demonstrating that early network activity is accessible during a critical window of hippocampal development. By P13/14, sharp wave-ripple complexes were identified in both CTL and LBN pups. Preliminary observations suggest differences in sharp wave-ripple dynamics between groups, providing initial evidence that ELA may alter the developmental trajectory of hippocampal network activity. Conclusion: This work leverages advanced developmental electrophysiology recordings to uncover the mechanisms linking ELA with memory deficits in adulthood. If disrupted early network activity is confirmed as a causal factor for cognitive dysfunction, this project would have broad implications for preventing cognitive disorders rooted in early-life stress.

**Disclosures: T. Auer:** None. **L. Ma:** None. **J. Gelinas:** None. **T. Baram:** None.

**Poster**

**PSTR189: Early-Life Stress: Circuit Mechanisms and Effects on Behavior**

**Location:** WCC Halls A-C

**Time:** Monday, November 16, 2026, 1:00 PM - 5:00 PM

**Program #/Poster #:** PSTR189.12/DD5

**Topic:** G.03. Stress and the Brain

**Support:** NIH Grant R21MH135346-01A1

**Title:** Serotonergic hypo-excitability and history of early life stress promote loss during social competition

**Authors: *S. WOODS**[1], A. KISNER[3], R. BAHR[4], M. WYNALDA[5], A. M. POLTER[2]; [2]Dept. of Pharmacol. and Physiol., [1]George Washington Univ., Washington, DC; [3]The George Washington Univ., Chevy Chase, MD; [4]The George Washington Univ., Washington, DC; [5]The George Washington Sch. of Med. and Hlth. Sci., Washington, DC

**Abstract:** Early postnatal development is a critical period for brain plasticity, where adverse childhood experiences are poised to disrupt cognitive and emotional circuits. These early life stressors (ELS)- abuse, neglect, resource scarcity, etc.- have been known to increase likelihood of anxiety-like and depressive-like behaviors in clinical settings and animal models. Social deficits are a key component of many psychiatric diseases, but much less is known about the neural mechanisms underlying stress-induced social adaptations. To investigate these circuits, we modeled ELS in rodents using the limited bedding and nesting (LBN), which simulates a resource-deficient environment in early postnatal life. Two key preliminary findings suggest that 1) ELS-exposure elicits a robust subordinate phenotype during adult social competition, and simultaneously that 2) adult serotonergic (5-HT) neurons of the dorsal raphe nucleus (DRN) are significantly less excitable after ELS exposure. This project aims to determine whether these findings are mechanistically linked by using several approaches to social competition using the dominance tube test assay, with additional video analysis of effortful behaviors. First, using acute fluoxetine administration in control animals, we show that increasing 5-HT levels may increase winning in males (63.89% ± 9.74, p=0.0679), but not females (25% ± 9.26, p=0.0005). Building on this, we then asked whether fluoxetine would rescue the ELS phenotype in social competition, but we did not see significant differences in their performance against a control opponent in either males (sal: 39.39% ± 6.06, flx: 35.56% ± 10.52, p=0.4779) or females (sal: 41.67% ± 11.70, flx: 42.22% ± 8.89, p=0.9002). Finally, to precisely replicate ELS-induced 5-HT neuronal hypoactivity, we used viral insertion of a Cre-dependent Kir2.1 channel directly into DRN 5-HT neurons in a PetCre+ mouse model. Our results showed that Kir2.1 mice again showed a subordinate-like phenotype, without any ELS exposure, in males (30.3% ± 10.5, p=0.015) and females (12.5% ± 8.768, p=0.001). Future experiments will use a reciprocal viral approach to help unravel the complex relationship between this neuronal population, stress, and competitive outcomes.

**Disclosures: S. Woods:** None. **A. Kisner:** None. **R. Bahr:** None. **M. Wynalda:** None. **A.M. Polter:** None.

**Poster**

**PSTR189: Early-Life Stress: Circuit Mechanisms and Effects on Behavior**

**Location:** WCC Halls A-C

**Time:** Monday, November 16, 2026, 1:00 PM - 5:00 PM

**Program #/Poster #:** PSTR189.13/DD6

**Topic:** G.03. Stress and the Brain

**Support:** NIMH RO1MH096093
NINDS F99NS139535
NIA P30AG08404
Harvey Family Endowment (UNM)
Zilkha Neurogenetic Institute
Beckman Institute at Caltech

**Title:** Early Life Adversity Reorganizes Coordinated Activity Across Prefrontal-Limbic Circuitry.

**Authors: *T. W. USELMAN**[1], R. E. JACOBS[2], E. L. BEARER[1,3];
[1]Pathology, Univ. of New Mexico Sch. of Med., Albuquerque, NM; [2]Zilkha Neurogenetic Inst., USC Keck Sch. of Med., Los Angeles, CA; [3]Biol. and Biol. Engin., Caltech, Pasadena, CA

**Abstract:** Early life adversity (ELA) is associated with persistent dysfunction of prefrontal-limbic circuitry manifested by altered behavior in response to threat. Whether ELA alters coordinated activity within this circuitry is a major question in the field. Here, we applied structural equation modeling (SEM) to neuroimaging data of longitudinal Mn(II)-enhanced MRI (MEMRI) of adult (11 - 13 wk, n = 23) standard (Std) and ELA-reared mice. ELA was induced via limited bedding and nesting material from P2-P9. Following systemic $MnCl_2$ administration (0.3 mmol/kg IP), MEMRI images were acquired at 100 μm isotropic resolution in an 11.7T Bruker MR scanner before, during, and 8 days after acute threat (TMT) monitored by video recording. SEM was verified by reproducing results from a UCLA online workshop ($Cos\theta$ = 1.00, MAD = 0.00). MEMRI covariance was validated on known olfactory circuitry ($\chi^2$ $p > 0.05$, CFI > 0.90, SRMR < 0.08) and fit selectively to threat exposure when a connection to the amygdala was included. Permutation testing of the olfactory-amygdala circuit produced significantly poorer fit after replacing regions or jumbling subject identities or regional order ($p < 0.001$; 10,000 permutations), showing that circuit hypotheses can be falsified by SEM. Applying SEM to literature-derived defensive and reward circuit models revealed additional connections required for statistically good fit, including LC→mPFC and AMY→ACB, identifying new components to be integrated into larger circuit hypotheses. Path strength of these two components exhibited differences between ELA and Std mice ($\Delta\beta = 0.285$ and $-1.900$; FDR $p < 0.05$). To examine larger-scale influence of prefrontal cortical regions, we developed Structurally Informed Co-Activation among Projection Targets (SINAPTs), integrating anterior cingulate (ACA) projection anatomy from stereotactic MEMRI data (Bearer et al. 2023) with systemic MEMRI data used to model coordination along ACA projections via piecewise-SEM. The ACA projectome derived from Std mice exhibited statistically good fit to Std across conditions (Fisher's C $p \geq 0.12$), but statistically poor fit to ELA ($p < 0.006$) with 76 significant residual interactions identified between unconnected regions ($p < 0.05$ directional separation). Average path magnitudes in the ACA projectome were significantly altered by ELA ($F_{(1,50)} = 29.54$, $p < 0.0001$), though differences converged between groups after threat ($F_{(2,50)} = 3.21$, $p = 0.049$). Together, these findings: 1) establish SEM as a framework for testing neural circuit

hypotheses in MEMRI data; and 2) demonstrate that prefrontal-limbic circuit coordination is reorganized based on cumulative stress.

**Disclosures: T.W. Uselman:** None. **R.E. Jacobs:** None. **E.L. Bearer:** None.

**Poster**

**PSTR189: Early-Life Stress: Circuit Mechanisms and Effects on Behavior**

**Location:** WCC Halls A-C

**Time:** Monday, November 16, 2026, 1:00 PM - 5:00 PM

**Program #/Poster #:** PSTR189.14/DD7

**Topic:** G.03. Stress and the Brain

**Title:** Prosocial behavior in adult rats after early life adversity: An investigation of neuronal identities in the prefrontal cortex

**Authors: *J. HICKMAN-MAYNARD**, J. M. BRETON;
Smith Col., Northampton, MA

**Abstract:** Experiencing adversity such as insecure housing, food insecurity, domestic violence, and/or neglect early in life affects the neurological development of attention, mood, and other psychological qualities. Our lab is particularly focused on identifying how early life adversity (ELA) impacts the development of brain regions associated with empathy, including the amygdala, the nucleus accumbens, and the prefrontal cortex (PFC). Prior work in our lab modeled the impact of ELA on empathy via a helping behavior task with adult rats, to test how ELA might change the motivation to aid a distressed individual. We previously found that ELA rats exhibited an increase in helping behavior in comparison to control rats, and that overall PFC activation, tracked by neural activity markers, correlated with helping behavior. Here, we explored the cellular identity of active neurons within the PFC to determine whether or not excitatory or inhibitory neurons were more prominently active in ELA rats than control rats during the task. Using immunohistochemistry, we quantified cells positive for the immediate early gene c-Fos and its colocalization with CaMKII, an excitatory neuronal marker. Specifically, we analyzed colocalization within four subregions of the PFC: the prelimbic cortex (PrL), the medial orbitofrontal cortex (MO), the ventral orbitofrontal cortex (VO), and the lateral orbitofrontal cortex (LO). We found a consistent percentage (~50%) of excitatory neurons active following the task, on average, irrespective of rearing condition or sex. This suggests that there is no difference in cell type activation between rats who did or did not experience ELA, regardless of their different performances in the helping behavior task. However, we found a wide range of variability; for an individual rat, between 20% to 80% of excitatory neurons exhibited colocalization with c-Fos across regions. This large variation warrants further study. In future research, we may look further into other cell types active within the PFC and also examine cell-specific activity within other brain regions, like the amygdala. Overall, these findings illustrate that excitatory neuronal activity within the PFC may not be the key element underlying differences in empathetic behavior following ELA.

**Disclosures: J. Hickman-Maynard:** None. **J.M. Breton:** None.

**Poster**

**PSTR189: Early-Life Stress: Circuit Mechanisms and Effects on Behavior**

**Location:** WCC Halls A-C

**Time:** Monday, November 16, 2026, 1:00 PM - 5:00 PM

**Program #/Poster #:** PSTR189.15/DD8

**Topic:** G.03. Stress and the Brain

**Support:** Apoyo al Cuerpo Académico de Neurofisiología (UV-CA-33)

**Title:** Long-Term Effects of Prenatal Restraint Stress on Anxiety-Like Behavior and Pentylenetetrazol-Induced Seizures in Adult Male and Female Rats

**Authors: *L. LOPEZ-MERAZ**[1], J. GARCÍA-RAMÍREZ[2], B. MARTÍNEZ-ROJAS[6], L. ESCALANTE RENDÓN[2], C. MORGADO-VALLE[2], J. MARTÍNEZ-QUIROZ[3], L. BELTRAN-PARRAZAL[4], L. I. GARCÍA[6], L. D. CHI-CASTAÑEDA[5];
[1]Inst. de Investigaciones Cerebrales, [3]Facultad de Q.F.B., [2]Univ. Veracruzana, Xalapa, Mexico; [5]Brain Res. Inst., [4]Univ. Veracruzana, Xalapa-Enriquez, Mexico; [6]Inst. de Investigaciones Cerebrales, Xalapa, Mexico

**Abstract:** Prenatal stress involves exposure to adverse maternal life events during gestation, which can increase the risk of neurodevelopmental and psychiatric sequelae in the offspring. Although experimental evidence suggests that gestational stress can acutely induce transient anxiety-like behaviors and exacerbate seizure severity, its definitive, long-term impact on these neurobehavioral profiles remains controversial and is still under investigation. In this study, we investigated the effects of prenatal restraint stress on anxiety-like behavior and seizure susceptibility in adult male and female Wistar rats. Pregnant dams were subjected to restraint stress twice daily from gestational day (GD) 12 to GD20, while control dams remained undisturbed. Anxiety-like behavior was evaluated in adult offspring at postnatal day 60 (P60) using the elevated plus maze (EPM), followed by the evaluation of spontaneous locomotor activity in the open field test. At P67, seizures were induced via repetitive, low-dose pentylenetetrazol (PTZ) administration. Estrous cycle stages were determined in all female offspring immediately following behavioral testing, and rats were categorized into proestrus-estrus or metestrus-diestrus phases. Our findings indicate that prenatal stress does not induce prominent long-term alterations in anxiety-like behavior in either sex. Although stressed males spent more time in the EPM open arms compared to controls, other anxiety-related parameters—including the anxiety index and total locomotor activity—remained unchanged. Regarding seizure susceptibility, the incidence of *status epilepticus* (SE) was similar across groups, regardless of sex or estrous cycle phase. Notably, stressed males and females in the metestrus-diestrus phases required a higher cumulative dose of PTZ to reach SE compared to their respective controls. Taken together, these data suggest that prenatal restraint stress exerts a limited, long-term programmed effect on seizure thresholds in adult Wistar rats. This work was supported by the Neurophysiology Academic Group (UV-CA-333).

**Disclosures: L. Lopez-Meraz:** None. **J. García-Ramírez:** None. **B. Martínez-Rojas:** None. **L. Escalante Rendón:** None. **C. Morgado-Valle:** None. **J. Martínez-Quiroz:** None. **L. Beltran-Parrazal:** None. **L.I. García:** None. **L.D. Chi-Castañeda:** None.

**Poster**

**PSTR189: Early-Life Stress: Circuit Mechanisms and Effects on Behavior**

**Location:** WCC Halls A-C

**Time:** Monday, November 16, 2026, 1:00 PM - 5:00 PM

**Program #/Poster #:** PSTR189.16/DD9

**Topic:** G.03. Stress and the Brain

**Title:** Early life stress protects against adult-stress-induced increases in anxiety-like behavior in mice

**Authors: *K. E. LEICHT**, B. D. SACHS;
Psychological and Brain Sci., Villanova Univ., Villanova, PA

**Abstract:** Early life stress (ELS) is linked to a wide range of adverse consequences, including an increased rate of mental illness, but the mechanisms linking early life stress to psychopathology are not well known. Various mouse models of ELS have been developed, but there are conflicting reports regarding their long-term effects. For example, several papers suggest that ELS increases susceptibility to adult stress, but other groups have reported no effects of ELS on susceptibility or that ELS confers stress resilience. Among studies that report ELS-induced increases in susceptibility, several evaluated only a single behavioral outcome [e.g., sucrose preference test - (SPT)]. The current work examines whether neonatal maternal separation combined with early weaning (NMSEW) alters susceptibility to a range of behavioral changes induced by three days of sub-chronic stress (3DS), including potential alterations in body weight and sleep, as well as behavior in the novel object recognition test (NORT), open field test (OFT), social interaction test (SIT), and SPT. Our results suggest that NMSEW protects against some of the anxiety-inducing effects of 3DS. Specifically, in the OFT, 3DS reduced center time in control mice, but not in NMSEW mice, suggesting that ELS had a protective effect. Surprisingly, the mice exposed to ELS also had increased body weight at post-natal day 17 compared to the control group, suggesting that maternal care may not have been substantially impaired. No significant group differences in body weight were observed following 3DS, but a significant 3DS by sex interaction was observed, in which males increased their weight slightly while females slightly decreased their body weights. Both ELS and 3DS increased the number of sleep episodes without impacting total sleep time, indicating that sleep architecture is disturbed by the stressors, not sleep duration. Behavior in both the NORT and SIT were also impacted by the stressors, but it is not clear that either memory or sociality are directly impacted. In the NORT, NMSEW mice exhibited increased exploration of both the novel and familiar objects, while 3DS-exposed mice interacted with both objects less than controls. NMSEW mice made more nonsocial zone entries than control. In females, 3DS reduced nonsocial entries but had no effect on males. No effects were found in the SPT. Together, these findings do not support previous reports that NMSEW

increases susceptibility to adult stress. Instead, they suggest that NMSEW may confer resilience to a subset of the effects of stress.

**Disclosures: K.E. Leicht:** None. **B.D. Sachs:** None.

**Poster**

**PSTR189: Early-Life Stress: Circuit Mechanisms and Effects on Behavior**

**Location:** WCC Halls A-C

**Time:** Monday, November 16, 2026, 1:00 PM - 5:00 PM

**Program #/Poster #:** PSTR189.17/DD10

**Topic:** G.03. Stress and the Brain

**Title:** Adolescent Social Isolation Alters Behavioral, Endocrine, and Locus Coeruleus Responses to Acute Stress

**Authors: *D. L. MONASTERIO**, N. KERN, S. BOZARTH, S. DE GUZMAN, D. J. CHANDLER;
Neurosci., Rowan-Virtua Sch. of Osteo. Med., Stratford, NJ

**Abstract:** Adolescent social isolation is a potent developmental stressor that produces long-lasting alterations in behavioral and neural responses to stress and increases vulnerability to stress-related neuropsychiatric disorders. The locus coeruleus (LC), the brain's primary source of norepinephrine, plays a critical role in coordinating arousal, vigilance, and physiological responses to stress. Previous studies have demonstrated that chronic stress can alter LC activity and downstream stress circuitry; however, the impact of adolescent social isolation on LC-associated stress responsivity remains incompletely understood. Therefore, we investigated how adolescent social isolation influences behavioral, endocrine, and neural responses to acute stress. Male and female rats were either socially isolated or group housed throughout adolescence and later exposed to one of two acute stress paradigms: combined restraint stress and predator odor exposure or the Defensive Shock Probe Burying (DSPB) test. Anxiety-like behaviors were assessed using the Open Field Test (OFT) and Elevated Plus Maze (EPM). Serum corticosterone levels were measured to evaluate physiological stress responsivity, and cFos immunohistochemistry was used to assess stress-induced neural activation within the LC. Previous work in our laboratory demonstrated that socially isolated rats exhibit altered anxiety-like and stress-coping behaviors relative to group-housed controls, as assessed by the OFT and EPM, including reductions in active coping behaviors and defensive burying. Here, we examined how these behavioral alterations are affected by subsequent acute stress exposure. Preliminary analyses revealed elevated corticosterone concentrations following acute stress in both groups, with socially isolated animals displaying an exaggerated hormonal response. A trend toward higher corticosterone concentrations was observed in females. Similarly, LC cFos expression was elevated in socially isolated animals relative to group-housed controls following acute stress exposure, with a trend toward greater LC activation in females.Together, these preliminary findings suggest that adolescent social isolation alters behavioral, endocrine, and neural responses to stress and that biological sex may further modulate stress responsivity. These results

support a potential role for LC-associated stress circuitry in mediating the long-term consequences of adolescent social isolation and may provide insight into mechanisms underlying vulnerability to stress-related neuropsychiatric disorders.

**Disclosures: D.L. Monasterio:** None. **N. Kern:** None. **S. Bozarth:** None. **S. de Guzman:** None. **D.J. Chandler:** None.

**Poster**

**PSTR189: Early-Life Stress: Circuit Mechanisms and Effects on Behavior**

**Location:** WCC Halls A-C

**Time:** Monday, November 16, 2026, 1:00 PM - 5:00 PM

**Program #/Poster #:** PSTR189.18/DD11

**Topic:** G.03. Stress and the Brain

**Title:** Dysregulation of Locus Coeruleus circuits as a mechanism for social isolation-induced behavioral change

**Authors: *N. D. KERN**[1], D. MONASTERIO[2], D. J. CHANDLER[3];
[1]Dept. of Neurosci., Rowan Univ., Delanco, NJ; [2]Dept. of Neurosci., Rowan Univ., Union, NJ; [3]Dept. of Neurosci., Rowan Univ., Stratford, NJ

**Abstract:** Chronic social isolation is a prominent stressor that is associated with numerous neuropsychiatric and somatic disease states. Despite receiving much attention during the COVID19 pandemic, social isolation continues to be a major public health concern, and so it is important to understand the impact that it has on stress-responsive circuits in the brain to drive long-term changes in behavior. The locus coeruleus-norepinephrine (LC-NE) system plays a key role in mediating stress response and affective behavior. In normal physiological conditions, the LC promotes brain function and behavioral compensation by enhancing noradrenergic neurotransmission throughout the brain; however, traumatic and chronic stress can dysregulate LC function and drive persistent neuroadaptations that extend beyond the stressful experience itself. While many studies have explored LC neuroadaptation in response to acute and chronic stressors, much of the literature focuses on addition of a noxious stimulus as a stress paradigm. On the other hand, LC dysfunction as a result of the removal of an appetitive stimulus such as social contact remains unexplored. Recent findings show that the LC is modular and functionally heterogenous, displaying circuit-specific activation and inhibition in response to stress. Our lab has shown that LC projections to the central amygdala (CeA) and medial prefrontal cortex (mPFC) have distinct roles in mediating anxiety-like behavior and undergo opposing physiological adaptations following stressor exposure. Here, we explore how the circuit-specific LC-to-CeA and LC-to-mPFC projections are affected by six weeks of social isolation stress. Using whole-cell patch-clamp electrophysiology, we found that LC-to-mPFC projection neurons from socially isolated animals exhibit a reduced firing rate and a higher activation gap, indicative of reduced activity within the circuit, consistent with our findings from the acute stress model. Based on this data, we hypothesize that LC-to-CeA neurons will be hyperactive and hyperexcitable following six weeks of social isolation stress. We further aim to show that

activation and inhibition of each of these circuits in group housed and socially isolated animals will produce distinct effects on social, exploratory, and stress coping behavior. Such findings will provide novel insights to mechanisms for social isolation-induced behavioral change and further develop the view of LC as a heterogenous regulator of brain function in normal physiological and disease states.

**Disclosures: N.D. Kern:** None. **D. Monasterio:** None. **D.J. Chandler:** None.

**Poster**

**PSTR189: Early-Life Stress: Circuit Mechanisms and Effects on Behavior**

**Location:** WCC Halls A-C

**Time:** Monday, November 16, 2026, 1:00 PM - 5:00 PM

**Program #/Poster #:** PSTR189.19/DD12

**Topic:** G.03. Stress and the Brain

**Support:** UWRF USE Grant
UWRF Dykstra Award

**Title:** Adolescent social isolation enhances nicotine reward learning and is accompanied by distinct, region-specific dendritic remodeling

**Authors:** J. GUILLIAMS, A. OLSTAD, S. O'MEARA, R. WYANT, E. ASHBACH, M. DEZENTJE, E. MAHONEY, G. KEELER, ***D. G. EHLINGER**;
Univ. of Wisconsin-River Falls, River Falls, WI

**Abstract:** Adolescence is a sensitive period of brain development marked by increased susceptibility to the effects of chronic stress, which may enhance vulnerability to substance use and its long-lasting impact on brain structure. In this study, we examined the effect of adolescent social isolation on nicotine reward and dendrite remodeling across a network of brain regions implicated in both drug reward and social stress. During adolescence (postnatal day P35-P49) or adulthood (P60-74), male and female C57BL/6J mice were exposed to either social isolation (SI) stress or standard rearing (SR) conditions and nicotine exposure (0.35mg/kg) during a modified nicotine conditioned place preference (CPP) procedure. On approximately P49 (adolescent) or P74 (adulthood) brains were processed for Golgi-Cox staining, and dendrite length and branching was assessed in the nucleus accumbens shell, dorsal hippocampus, anterior cingulate cortex, and amygdala. Our behavioral results show that adolescent SI mice more rapidly develop nicotine CPP compared to adolescent SR mice under an administration protocol that does not similarly affect adult mice. Adolescent, but not adult, nicotine exposure induces increased branching and length of dendrites in the nucleus accumbens shell that is independent of social isolation stress exposure, while other brain regions exhibit unique impacts of age and social isolation stress that are often independent of nicotine exposure. Ongoing research will determine the extent and timing of dendrite remodeling across these brain areas and whether these factors correlate with the onset of behavioral effects. Collectively, we report that adolescent social isolation stress enhances the rewarding effects of nicotine, while these two factors induce unique

structural changes across a network of brain regions implicated in social stress and drug reward. These results inform our understanding of the unique and combined impacts of stress and drug exposure on adolescent brain development and vulnerability.

**Disclosures: J. Guilliams:** None. **A. Olstad:** None. **S. O'Meara:** None. **R. Wyant:** None. **E. Ashbach:** None. **M. Dezentje:** None. **E. Mahoney:** None. **G. Keeler:** None. **D.G. Ehlinger:** None.

**Poster**

**PSTR189: Early-Life Stress: Circuit Mechanisms and Effects on Behavior**

**Location:** WCC Halls A-C

**Time:** Monday, November 16, 2026, 1:00 PM - 5:00 PM

**Program #/Poster #:** PSTR189.20/DD13

**Topic:** G.03. Stress and the Brain

**Support:** UWRF USE Grant
UWRF Dykstra Award

**Title:** The effect of early life gut dysbiosis on anxiety response, hippocampal neural activity, and cellular damage

**Authors: *R. WYANT**[1], J. GUILLIAMS[1], A. OLSTAD[1], E. ASHBACH[1], D. G. EHLINGER[2]; [2]Dept of Psychological Sci., [1]Univ. of Wisconsin-River Falls, River Falls, WI

**Abstract:** Bacterial metabolites travel from the gut to the central nervous system and modulate key neural functions including anxiety-related responses. In adults, links between mental illness and gut-microbiome-brain-axis imbalances are established. Therefore, it is of interest to evaluate potential sensitive periods in infancy and early childhood relating to cognitive processing, emotional processing, and the risk of mental illness. In this study we are evaluating the effect of antibiotic induced gut dysbiosis on anxiety-like behaviors in a mouse model. Post weaning groups (P21-P38) or adult groups (P60-P77) consisting of male and female C57BL/6J mice were exposed to either antibiotic (ABX) treated water designed to completely deplete the gut microbiome or standard drinking water as a control (CON) for two weeks. Locomotor and anxiety-related behaviors were assessed through an open field test (OFT), light/dark box (LDBox), and elevated plus maze (EPM). Post weaning antibiotic treated mice exhibited decrease locomotor activity in the OFT, and a trend towards disrupted anxiety-like behavior in the LDBox was observed. Ongoing research is continuing to assess the effect of treatment on behavior through increased sample sizes as well as examining neural activity (c-Fos) and markers for oxidative stress in both neurons and glial cells of the hippocampus via immunofluorescence imaging. Our results suggest that postweaning microbiome depletion influences anxiety-like behavior, while continued analyses will assess structural and functional changes related to these observed behaviors.

**Disclosures: R. Wyant:** None. **J. Guilliams:** None. **A. Olstad:** None. **E. Ashbach:** None. **D.G. Ehlinger:** None.

**Poster**

**PSTR189: Early-Life Stress: Circuit Mechanisms and Effects on Behavior**

**Location:** WCC Halls A-C

**Time:** Monday, November 16, 2026, 1:00 PM - 5:00 PM

**Program #/Poster #:** PSTR189.21/DD14

**Topic:** G.03. Stress and the Brain

**Support:** NIH DA052909
NIH DA038588
NIH MH 078105
Emory National Primate Research Center (ENPRC) Base Grant OD P51OD011132

**Title:** Long-term effects of early life adversity on brain dopamine and serotonin receptors in nonhuman primates: Implications for comorbid anxiety and cocaine use disorder

**Authors: *N. B. BRING**[1], J. H. ACEVEDO-POLO[1], E. R. SIEBERT[1], J. KHAN[1], M. I. ROUGH[2], E. L. MORIN[1], B. A. BEESLEY[1], Z. YANG[1], R. J. VOLL[1], L. N. CHAVAN[1], M. M. GOODMAN[1], A. M. KAZAMA[1], J. A. NYE[3], M. A. NADER[2], M. SANCHEZ[1];
[1]Emory Univ., Atlanta, GA; [2]Wake Forest Univ. Sch. of Med., Winston Salem, NC; [3]Med. Univ. of South Carolina, Charleston, SC

**Abstract:** Early life adversity (ELA) is a risk factor for comorbid anxiety and cocaine (COC) use disorder (CUD), although the neurobiological mechanisms remain unclear. This study examined long-term effects of ELA on adolescent and adult rhesus macaque brain serotonin (5HT) and dopamine (DA) receptors in corticolimbic regions involved in reward and emotional control. We used PET neuroimaging to measure DA D2/D3, 5HT1A, and 5HT2A receptor binding potential (BP), baseline acoustic startle response (STRL) as a proxy for anxiety, and i.v. COC self-administration (SA) under fixed-ratio (FR) and progressive-ratio (PR) schedules to assess the reinforcing effects of COC and motivation to seek the drug, respectively. Our findings suggest altered maturation of D2/D3, 5HT1A and 5HT2A receptors from adolescence to adulthood in ELA animals (n=7; 4M, 3F) compared to Controls (n=7; 4M, 3F) in medial prefrontal cortex (mPFC), orbitofrontal cortex (OFC), subgenual cingulate (SGC), amygdala (AMY) and nucleus accumbens (NAcc). DA and 5HT receptor BP were lower in animals with ELA, particularly in adolescence, with normalization in some regions by adulthood. ELA resulted in elevated STRL across both ages ($F(1,10)=4.205$, $p=.067$), and STRL in adulthood significantly predicted the reinforcing effects of COC under FR ($rho=.569$, $p=.034$). Elevated STRL reflects increased anxiety, supporting the hypothesis that high anxiety is a risk factor for CUD. Associations between adult BP data and behavioral outcomes suggest an important role of D2/D3 and 5HT2A receptors in OFC, SGC and AMY in modulating STRL and COC SA. Specifically, elevated STRL was predicted by lower 5HT2A receptor BP in OFC ($rho=-.692$, $p=.006$). Lower D2/D3 receptor BP in OFC ($rho=.596$, $p=.024$) and SGC ($rho=.628$, $p=.016$), but higher 5HT2A receptor BP in SGC ($rho=-.722$, $p=.004$) predicted greater sensitivity to the reinforcing strength of COC under PR. In addition, developmental increases in AMY D2/D3

receptor BP predicted both the reinforcing effects and strength of COC (FR - rho=-.684, p=.007, PR - rho=.729, p=.003, respectively), suggesting an important role of AMY DA receptor maturation in psychostimulant misuse. Altogether, our findings suggest that ELA disrupts the adolescent maturation of DA and 5HT receptors in reinforcement and emotional circuits. These data also provide preclinical evidence implicating the comorbidity between anxiety and CUD and reveal important roles of D2/D3 and 5HT2A receptors in the AMY, OFC and SGC - but not the mPFC - as neurobiological predictors of anxiety and COC use.

**Disclosures: N.B. Bring:** None. **J.H. Acevedo-Polo:** None. **E.R. Siebert:** None. **J. Khan:** None. **M.I. Rough:** None. **E.L. Morin:** None. **B.A. Beesley:** None. **Z. Yang:** None. **R.J. Voll:** None. **L.N. Chavan:** None. **M.M. Goodman:** None. **A.M. Kazama:** None. **J.A. Nye:** None. **M.A. Nader:** None. **M. Sanchez:** None.

**Poster**

**PSTR189: Early-Life Stress: Circuit Mechanisms and Effects on Behavior**

**Location:** WCC Halls A-C

**Time:** Monday, November 16, 2026, 1:00 PM - 5:00 PM

**Program #/Poster #:** PSTR189.22/DD15

**Topic:** G.03. Stress and the Brain

**Support:** NIH DA052909
NIH DA038588
NIH MH 078105
Emory National Primate Research Center (ENPRC) Base Grant OD P51OD011132

**Title:** Long-Term Effects of Early Life Adversity on Brain Serotonin and Dopamine Signaling using PET: Responses to Chronic Cocaine, Abstinence, and Associations with Relapse

**Authors: *A. L. LANDSTEIN**[1], J. H. ACEVEDO-POLO[1], M. I. ROUGH[2], E. R. SIEBERT[1], J. KHAN[1], R. VOLL[1], L. CHAVAN[1], M. GOODMAN[1], J. NYE[3], M. A. NADER[2], M. SANCHEZ[1];
[1]Emory Univ., Atlanta, GA; [2]Wake Forest Univ. Sch. of Med., Winston-Salem, NC; [3]Med. Univ. of South Carolina, Charleston, SC

**Abstract:** Early life adversity (ELA) is a risk factor for substance use disorder (SUD), but the neurobiological mechanisms remain unclear. This study examined long-term effects of ELA on adult rhesus monkey brain dopamine (DA) and serotonin (5HT) receptors, in particular DA $D_2/D_3$, $5HT_{1A}$ and $5HT_{2A}$ receptors, in corticolimbic regions involved in reward and drug misuse. For this, we used PET imaging and i.v. cocaine (COC) self-administration (SA). In addition to baseline PET scans, we examined dynamic changes in DA and 5HT receptors following chronic COC SA (total intake: 100 mg/kg) and 5 weeks of abstinence. Finally, the role of $D_2/D_3$, $5HT_{1A}$ and $5HT_{2A}$ receptor availability and their dynamic responses to COC and abstinence were examined as predictors of COC-induced reinstatement (preclinical model of relapse). Overall,

PET findings showed lower levels of 5HT receptors in dorsolateral prefrontal cortex (dlPFC), orbitofrontal cortex (OFC), and nucleus accumbens (NAcc) in animals with ELA compared with Controls (e.g. $5HT_{2A}$: dlPFC: $F_{(1,8)}$=6.810, $p$=0.031; OFC: $F_{(1,8)}$=8.834, $p$=0.018; and log10 NAcc: $F_{(1,8)}$=6.042, $p$=0.039), with a more limited impact on $D_2/D_3$ receptors. In terms of dynamic responses to chronic COC and abstinence, the responses varied across regions, receptors and group, although a general upregulation of $5HT_{1A}$ and $5HT_{2A}$ receptors was found following COC use, particularly robust in dlPFC ($F_{(2,16)}$=62.840, $p$<0.001; $F_{(2,16)}$=8.988, $p$=0.002, respectively). Animals with ELA showed blunted receptor upregulation following chronic COC and failure to return to baseline, compared to Controls. Multiple linear regression analyses revealed that $5HT_{2A}$ receptor levels in NAcc predicted COC-induced reinstatement; in particular, higher upregulation in response to chronic COC, blunted downregulation after abstinence, and higher receptor levels at abstinence all significantly predicted higher reinstatement (β=0.604, $p$ =0.022; β=-0.749, $p$=0.028; β=0.659, $p$=0.026, respectively). Overall, these findings suggest an important role of 5HT receptors in reward circuitry, responses to chronic COC and abstinence and as important biomarkers predicting risk for COC relapse following chronic COC use. The findings also suggest that pharmacotherapies targeting 5HT receptors are promising through their modulation of DA signaling and circuit changes associated with cocaine use disorder.

**Disclosures: A.L. Landstein:** None. **J.H. Acevedo-Polo:** None. **M.I. Rough:** None. **E.R. Siebert:** None. **J. Khan:** None. **R. Voll:** None. **L. Chavan:** None. **M. Goodman:** None. **J. Nye:** None. **M.A. Nader:** None. **M. Sanchez:** None.

**Poster**

**PSTR189: Early-Life Stress: Circuit Mechanisms and Effects on Behavior**

**Location:** WCC Halls A-C

**Time:** Monday, November 16, 2026, 1:00 PM - 5:00 PM

**Program #/Poster #:** PSTR189.23/DD16

**Topic:** G.03. Stress and the Brain

**Support:** 5P20GM121312-02

**Title:** Interoceptive processing as a neural pathway from childhood trauma to emotional regulation difficulties in depression and comorbid anxiety

**Authors: *S. A. AGUILAR**[1], M. P. PAULUS[1], M. MISAKI[1,2,3];
[1]Laureate Inst. for Brain Res., Tulsa, OK; [2]Oxley Col. of Hlth. and Natural Sci., Univ. of Tulsa, Tulsa, OK; [3]Sch. of Community Med., Univ. of Oklahoma Col. of Med., Tulsa, OK

**Abstract:** Childhood trauma (CT) is a major risk factor for depression, anxiety, and difficulties in emotion regulation. Interoception, the perception and interpretation of internal bodily signals, may represent one pathway linking early-life stress to later emotional dysfunction. The insula is central to interoceptive processing, yet the neural basis of the association between CT and emotion regulation difficulties remains unclear. This study examined whether CT severity was associated with altered insular activity during interoceptive attention in healthy controls (HC),

individuals with major depressive disorder (MDD), and individuals with MDD and comorbid anxiety (MDD+ANX). The sample included 343 participants: HC (n = 94), MDD (n = 79), and MDD+ANX (n = 170). CT severity and emotion regulation difficulties were assessed using the Childhood Trauma Questionnaire (CTQ) and the Difficulties in Emotion Regulation Scale (DERS), respectively. During fMRI, participants completed an Interoceptive Attention task involving cardiac, respiratory, and exteroceptive attention blocks. First-level GLMs generated Heart-Exteroception and Lungs-Exteroception beta images. These images were entered into a voxelwise linear mixed-effects model within a bilateral insula mask, testing Group, CTQ, and Group × CTQ effects, with contrast type as a repeated measure and age, sex, and mean motion as covariates. Multi-group mediation analyses tested whether mean right insula activity mediated the CTQ-DERS association using bootstrapped 95% confidence intervals. The linear mixed-effects analysis identified a Group × CTQ interaction in the right insula ($p < .001$, 18 voxels; peak MNI = 41.5, 17.5, −0.5; $F = 9.22$). Higher CTQ scores were associated with greater insula activation during interoceptive conditions relative to exteroception in MDD ($r = .44$) but lower activation in MDD+ANX ($r = -.22$), demonstrating opposing trauma-related slopes across the clinical groups. This association was minimal in HC ($r = .05$). Although CTQ scores were significantly correlated with DERS scores across all groups, the right insula response did not significantly mediate the CTQ-DERS association in any group. These findings suggest that anxiety comorbidity alters how childhood trauma relates to interoceptive neural processing, highlighting the need for clinical approaches tailored to the presence of anxiety. The absence of mediation indicates that localized right insula activity alone may not account for trauma-related emotion regulation difficulties. Broader insula-centered networks and connectivity may provide a more complete account of this pathway.

**Disclosures: S.A. Aguilar:** None. **M.P. Paulus:** None. **M. Misaki:** None.

**Poster**

**PSTR189: Early-Life Stress: Circuit Mechanisms and Effects on Behavior**

**Location:** WCC Halls A-C

**Time:** Monday, November 16, 2026, 1:00 PM - 5:00 PM

**Program #/Poster #:** PSTR189.24/DD17

**Topic:** G.03. Stress and the Brain

**Support:** NIH/NCCIH K23AT010643

**Title:** Hippocampal Asymmetry as a Structural Affective Correlate in Pediatric Chronic Widespread Pain

**Authors: *J. COSTA CRUZ**[1], J. ZHANG[1], M. SOLTI[1], A. MRITTIKA[2], M. MITCHESON[5], C. LAMPERT[2], M. BOSQUET ENLOW[3], D. BORSOOK[4], P. GRANT[1], B. AHTAM[1], S. NELSON[2];
[1]Fetal-Neonatal Neuroimaging and Developmental Sci. Ctr. (FNNDSC), Harvard Univ. / Boston Children's Hosp., Boston, MA; [2]Pain and Stress Studies Lab., [3]Biobehavioral Res. Lab., [4]Ctr. for

Pain and the Brain, Boston Children's Hosp., Boston, MA; [5]Univ. of Rhode Island, Providence, RI

**Abstract:** Pediatric chronic widespread pain (CWP) is a complex condition frequently compounded by childhood adversity and emotional distress. While neuroimaging points to the hippocampus as a key mediator of stress and affective regulation in chronic pain, specific structural correlates for these pathways in adolescents remain poorly understood. This study evaluated whether hippocampal volumetric asymmetry serves as a stress-modulated structural marker selectively associated with affective, rather than somatosensory, dimensions in adolescents with CWP.

High-resolution 3T T1-weighted structural MRI was acquired from a complete-case cohort of adolescents with CWP (n = 25; mean age = 15.4 ± 1.5 years, 80.0% female). Hippocampal volumes were extracted via FreeSurfer to calculate an Asymmetry Index (AI) [(R-L)/((R+L)/2)]. Cumulative early-life adversity was assessed using the Childhood Trauma Events Survey (CTES), dichotomized into high vs. low stress. Clinical measures included PROMIS Depression, the Functional Disability Inventory (FDI), and the Pain Catastrophizing Scale (PCS). To capture systemic exhaustion, a cumulative Allostatic Load (AL) risk score was constructed incorporating cardiometabolic and neuroendocrine data (Cortisol, DHEA) using binary extremes. Analyses employed exact non-parametric methods (Mann-Whitney U, Spearman's rho).

Adolescents with high cumulative stress had significantly altered hippocampal AI compared to the low-stress group ($p = 0.015$). AI showed a positive trend with depressive symptom severity ($rho = 0.32$, $p = 0.12$), but no association with physical disability (FDI; $rho = 0.12$, $p = 0.57$) or pain catastrophizing (PCS; $rho = 0.06$, $p = 0.78$). A control analysis showed a null correlation between AI and the cumulative Allostatic Load risk construct incorporating neuroendocrine data ($rho = -0.177$, $p = 0.397$), indicating this structural alteration is not merely reflecting systemic physiological wear-and-tear.

Findings suggest cumulative stress modulates hippocampal asymmetry in pediatric CWP. Although the downstream correlation with depression was a non-significant trend, the stress-driven structural alteration, contrasted against entirely null associations with functional pain and AL outcomes, provides preliminary evidence for a distinct affective pathway. This supports recent models identifying the hippocampus as a mediator in adversity-driven comorbidity and highlights AI as a candidate structural biomarker.

**Disclosures: J. Costa Cruz:** None. **J. Zhang:** None. **M. Solti:** None. **A. Mrittika:** None. **M. Mitcheson:** None. **C. Lampert:** None. **M. Bosquet Enlow:** None. **D. Borsook:** None. **P. Grant:** None. **B. Ahtam:** None. **S. Nelson:** None.

**Poster**

**PSTR190: Energy Metabolism**

**Location:** WCC Halls A-C

**Time:** Monday, November 16, 2026, 1:00 PM - 5:00 PM

**Program #/Poster #:** PSTR190.01/DD18

**Topic:** G.05. Brain Blood Flow, Metabolism, and Homeostasis

**Title:** The Impact of Gender on Four Weeks of Intermittent Fasting on Body Composition, Stress Levels, and Sleep Quality in Healthy Adults

**Authors:** A. MOHAMMAD, N. DAHER, ***G. S. BAINS**;
Loma Linda Univ., Loma Linda, CA

**Abstract: Introduction**: Intermittent fasting (IF) has emerged as a dietary plan for weight management by alternating periods of fasting/eating. This study examined the effects of a structured IF program over four weeks by gender. **Methods**: Twenty-eight participants (10 males and 18 females) with mean± SD age of 42.4±10.4 years participated in an eight-week self-controlled study and adhered to four-weeks of IF. Majority were moderately/extremely active (71.4%, n=20). Participants fasted for 16 hours from last meal to start of first meal the following day. Participants consumed normal daily caloric intake within an 8-hour period. Body composition was determined using InBody 770. Pittsburgh Sleep Quality Index, Cohen Perceived Stress Scale, and a hunger level survey were administered at baseline, post 4 weeks and post 8 weeks. **Results**: Significant change was shown in mean weight, BMI, visceral fat, stress, and sleep over time ($p=0.016$, $p=0.032$, $p=0.002$, $p=0.001$ and $p=0.021$ respectively). There was a significant decrease in mean ± standard error in weight, BMI, visceral fat, and stress post 8 weeks versus post 4 weeks (beginning of fasting), and improvement in sleep and this did not differ by gender (p-value for interaction between gender and time >0.05). For body fat %, there was a significant decrease in mean body fat % for males over time ($p=0.049$), and mainly between baseline and post 8 weeks (29.7±2.8 vs. 28.7 ±2.9, $p=0.001$). but not for females ($p=0.301$). In terms of skeletal muscle mass, dry lean mass, and hunger, there were no significant changes over time, and this did not differ by gender ($p>0.05$). **Conclusion**: Findings demonstrate that IF over a four-week period may lead to improvements in body composition, stress levels, and sleep quality regardless of gender. Results highlight the potential benefits of IF as an approach for enhancing wellness in weight management, stress reduction, and improvement of sleep quality. Further research is warranted to expand these positive findings.

**Disclosures: A. Mohammad:** None. **N. Daher:** None. **G.S. Bains:** None.

**Poster**

**PSTR190: Energy Metabolism**

**Location:** WCC Halls A-C

**Time:** Monday, November 16, 2026, 1:00 PM - 5:00 PM

**Program #/Poster #:** PSTR190.02/DD19

**Topic:** G.05. Brain Blood Flow, Metabolism, and Homeostasis

**Title:** A tale of two curves: Combining a modified oral glucose tolerance test with an ischemic forearm exercise test in fatigue evaluation.

**Authors: *A. D. KONSTANTINIDOU**[1], D. G. TSAMIS[1], N. A. FLARIS[1], A. FLARIS[2];
[1]Protypon Neuromuscular Ctr., Thessaloniki, Greece; [2]Surgery, TTUHSC of El Paso, El Paso, TX

**Abstract:** Fatigue is a daily issue in an outpatient neuromuscular clinic that is under reported, yet it can be life threatening. It can silently cause muscle damage and arrhythmia (Demirtas, A.O et al, J Interv Card Electrophysiol 55, 115-120, 2019) and even death, without an underlying anatomical structural damage. This is especially important in young athletes, some few of whom end up living a borderline life on the edge of the glucose cliff. A largely normal neurological exam and unrevealing laboratory evaluation except for random low normal glucose levels and upper normal/elevated lactate levels led us to evaluate our non-diabetic patients with a modified oral glucose tolerance test (OGTT). No specific dietary or exercise interventions were followed at the time of the evaluation. 140 patients were evaluated (white, 62 male, 78 female, age 14-79, mean 50 years). A fasting modified OGTT was performed. Glucose, insulin, creatine phosphokinase (CPK) and serum lactate were measured at 0 min. Following the ingestion of a glucose load of 75gr, repeat measurements at 15 min, 60 min and 120 min were obtained. A modified lactate/ammonia ischemic test (IFET) was also performed (Munsat T.L., Neurology, 1970) as per our standard protocol in 112 of these patients. Baseline lactate and ammonia levels were obtained after an observed 45 min rest period of the patient. Following a one min grip of a Jamar hand-held dynamometer to maximum strength, 1, 3, 5 and 15 min samples were obtained. In the OGTT 44% of patients had low (<70mg/dL, 24%) or borderline low (70-80mg/dL, 20%) glucose. Even with the lowest glucose levels at the end of the OGTT (45mg/dL) no patient experienced any significant clinical symptoms of hypoglycemia, except feeling more tired. In the same test, elevated lactate (>18mg/dL) was noted during the test in 42% of the patients, supporting the current concept of lactate being an alternative metabolic fuel for these patients. Analysis of the IFET data, in the patients that had an OGTT done as well, revealed that a subset of these patients had high resting lactate (11/112) or delayed clearance of lactate (74/112) indicative of mitochondrial dysfunction. This data set suggests that hypoglycemia, even severe, may masquerade as fatigue, a non-descriptive and nonspecific symptom.

**Disclosures: A.D. Konstantinidou:** None. **D.G. Tsamis:** None. **N.A. Flaris:** None. **A. Flaris:** None.

**Poster**

**PSTR190: Energy Metabolism**

**Location:** WCC Halls A-C

**Time:** Monday, November 16, 2026, 1:00 PM - 5:00 PM

**Program #/Poster #:** PSTR190.03/DD20

**Topic:** G.05. Brain Blood Flow, Metabolism, and Homeostasis

**Support:** National Science and Technology Innovation 2030 Grant 2022ZD0206100
National Science and Technology Innovation 2030 Grant 2024YFA180270

**Title:** Non-invasive induction of synthetic hypothermia via a specific brainstem mechanism

**Authors: *P. TIAN**, X. WANG, P. LI, Z. ZHANG;
Inst. of Neuroscience, Chinese Acad. of Sci., Shanghai, China

**Abstract:** Inducing hypothermia to drastically suppress metabolism presents promising clinical applications for humans. Although targeting the hypothalamus effectively induces hypothermia in rodents, the broader translatability of current approaches remains a challenge. This study aims to evaluate a novel non-invasive artificial induction method for synthetic hypothermia and investigate its underlying neural mechanisms. We applied a non-invasive artificial induction method in rodent models. Neural mechanisms were investigated by assessing the activation of neurons within the brainstem dorsal vagal complex (DVC) and observing the effects of ablating these specific neurons. Furthermore, we evaluated the method's safety profile and its neuroprotective efficacy against acute ischemic injury. The artificial induction method robustly induced prolonged hypothermia (tens of hours) in rodents, significantly reducing energy expenditure alongside physical and neural activities. This hypothermic effect is mediated by the activation of DVC neurons; conversely, ablation of these neurons severely disrupts temperature homeostasis. The method exhibits a safe profile with no observable tissue toxicity and provides profound neuroprotection against acute ischemia. A DVC-dependent neural pathway fundamentally regulates temperature homeostasis. This non-invasive artificial induction method provides a safe, physio-pharmacological platform for synthetic hypothermia, showcasing profound neuroprotective potential for future translational applications.

**Disclosures: P. Tian:** None. **X. Wang:** None. **P. Li:** None. **Z. Zhang:** None.

**Poster**

**PSTR190: Energy Metabolism**

**Location:** WCC Halls A-C

**Time:** Monday, November 16, 2026, 1:00 PM - 5:00 PM

**Program #/Poster #:** PSTR190.04/DD21

**Topic:** G.05. Brain Blood Flow, Metabolism, and Homeostasis

**Support:** Korea Institute of Science and Technology (2E33713)
National Research Foundation of Korea (NRF) grant funded by the Korea government (MSIT) (RS-2023-NR076437)

**Title:** Lipid-Enriched Gintonin from Korean Red Ginseng Marc Alleviates Obesity via Oral and Central Administration in Diet-Induced Obese Mice

**Authors:** *H. RHIM[1], **Y. TAMANNA**[1,2], Y. LEE[1,2], W. KIM[1,3], L. BONGGI[4], R. LEE[5], H. HWANG[6], M.-H. NAM[1,2,7], S. NAH[5], M. KIM[1,2,7];
[1]Brain Sci. Institute, Korea Inst. of Sci. and Technol. (KIST), Seoul, Korea, Republic of; [2]Div. of Bio-Medical Sci. & Technology, KIST School, Univ. of Sci. and Technol. (UST), Seoul, Korea, Republic of; [3]Dept. of Life Science, Korea Univ., Seoul, Korea, Republic of; [4]Dept. of Food Sci. and Nutrition, Pukyong Natl. Univ., Busan, Korea, Republic of; [5]Ginsentology Res. Lab. and Dept. of Physiology, Col. of Vet. Med., Ginsentology Res. Lab. and Dept. of Physiology, Col. of Vet. Medicine, Konkuk Univ., Seoul, Korea, Republic of; [6]Univ. of Seoul, Seoul, Korea, Republic of; [7]KHU-KIST Dept. of Converging Sci. and Technology,, KHU-KIST Dept. of Converging Sci. and Technology, Kyung Hee Univ., Seoul, Korea, Republic of

**Abstract: Lipid-enriched gintonin from Korean red ginseng marc alleviates obesity via oral and central administration in diet-induced obese mice****Authors**T. Yasmin[12], Y. Lee[12], W.S. Kim[13], B. Lee[4], R. Lee[5], H. Hwang[6], M.-H. Nam[127], S.-Y. Nah[5]*, M.S. Kim[127]*, H. Rhim[1]*[1]Brain Science Institute, KIST, Seoul, Korea; [2]KIST School, UST, Seoul, Korea; [3]Korea University, Seoul, Korea; [4]Pukyong National University, Busan, Korea; [5]Konkuk University, Seoul, Korea; [6]University of Seoul, Seoul, Korea; [7]KHU, Seoul, Korea.**Disclosures H. Rhim:** None. **Yasmin.T.:** None. **Y. Lee:** None. **W. Kim:** None. **L. Bonggi:** None. **R. Lee:** None. **H. Hwang:** None. **M. Nam:** None. **S. Nah:** None. **M. Kim:** None.**AbstractBackground:** Korean red ginseng marc (KRGM), a by-product of Korean red ginseng (KRG) processing, retains numerous bioactive compounds with potential health benefits. Among them, KRGM-derived gintonin (KRGM-gintonin) is particularly rich in lysophosphatidic acid (LPA) and phospholipids, which have been linked to favorable metabolic effects. This study investigated the anti-obesity potential of KRGM-gintonin in high-fat diet (HFD)–induced obese mice, focusing on its impact on weight regulation, liver health, and energy metabolism. **Methods:** Obese mice (C57BL/6N, 4 weeks, male) were administered KRGM-gintonin either orally for 25 weeks or through intracerebroventricular (ICV) injection for 14 weeks. Throughout the study, body weight, food intake, metabolic parameters, liver tissue morphology, behavioral performance, and thermogenic gene expression were carefully monitored to evaluate treatment effects. **Results:** Both oral and ICV administration of KRGM-gintonin significantly reduced body weight gain in HFD-fed obese mice without altering food intake, suggesting enhanced energy expenditure. Treatment through both routes improved physical performance and increased metabolic rate. Oral KRGM-gintonin also alleviated fatty liver, reduced plasma triacylglycerol and cholesterol levels, and promoted the expression of thermogenesis-related genes, including uncoupling protein-1 (UCP1) and hormone-sensitive lipase (HSL), specifically in brown adipose tissue. Additionally, oral administration lowered tumor necrosis factor-α (TNF-α) expression, indicating anti-inflammatory activity and further supporting metabolic health. **Conclusion:** KRGM-gintonin exerts strong anti-obesity effects, primarily through oral administration, with supportive evidence from central ICV action. These findings highlight its potential as a functional therapeutic agent for obesity prevention and management, offering dual benefits in metabolic regulation and inflammation control.

**Disclosures: H. Rhim:** None. **Y. Tamanna:** None. **Y. Lee:** None. **W. Kim:** None. **L. Bonggi:** None. **R. Lee:** None. **H. Hwang:** None. **M. Nam:** None. **S. Nah:** None. **M. Kim:** None.

**Poster**

**PSTR190: Energy Metabolism**

**Location:** WCC Halls A-C

**Time:** Monday, November 16, 2026, 1:00 PM - 5:00 PM

**Program #/Poster #:** PSTR190.05/DD22

**Topic:** G.05. Brain Blood Flow, Metabolism, and Homeostasis

**Support:** NIH: NS110069; AG070507, NS126920
Georgia Research Alliance

**Title:** Cortical energy metabolism under normal conditions and when functional hyperemia is blocked

**Authors: *O. B. OJO**[1], K. XIE[1], J. A. FILOSA[1], F. BARROS[2], P. J. O'HERRON[1];
[1]Physiol., Augusta Univ., Augusta, GA; [2]Ctr. for Scientific Studies, Valdivia, Chile

**Abstract:** Functional hyperemia ensures that the supply of oxygen and nutrients to active neurons matches their energy demand. Its impairment is associated with various pathological conditions, including diabetes, neurodegenerative diseases, and vascular disorders. However, evidence suggests that functional hyperemia may exceed the tissue's needs, making it unclear how vital the increase in blood flow is for healthy neural function. This study investigates energy metabolism under normal conditions and when functional hyperemia is blocked. An opsin mouse model was used to control vessel diameter while monitoring metabolite levels with two-photon microscopy in the mouse primary visual cortex. Functional hyperemia was activated by visual stimulation and blocked by optogenetic vasoconstriction. A phosphorescent dye, Oxyphor 2P, was used to measure extracellular oxygen levels, and AAVs encoding fluorescent sensors, ATeam1.03YEMK and SypHer3s, were used to monitor ATP and pH levels in neurons and astrocytes. The changes in oxygen, ATP and pH levels were monitored in the visual cortex of mice before, during, and after blockade of functional hyperemia. The findings show the cortical energy metabolism in response to visual stimulation, both with and without functional hyperemia. Blocking functional hyperemia alters energy balance in the visual cortex. This study advances our understanding of the complex interactions between cerebral blood flow, neuronal activity, and cortical metabolism that collectively regulate neurovascular function.

**Disclosures: O.B. Ojo:** None. **K. Xie:** None. **J.A. Filosa:** None. **F. Barros:** None. **P.J. O'Herron:** None.

**Poster**

**PSTR190: Energy Metabolism**

**Location:** WCC Halls A-C

**Time:** Monday, November 16, 2026, 1:00 PM - 5:00 PM

**Program #/Poster #:** PSTR190.06/DD23

**Topic:** G.05. Brain Blood Flow, Metabolism, and Homeostasis

**Title:** Microglial cGAS regulates glucose homeostasis and feeding behavior during energy deficit

**Authors: *J. QIU**[1], Q. LIU[2], J. C. BEAN[3], Y. XU[2];
[1]Univ. of South Florida, Lutz, FL; [2]Univ. of South Florida, Tampa, FL; [3]Baylor Col. of Med., Houston, TX

**Abstract:** The cyclic GMP-AMP synthase (cGAS) is a classical pattern recognition receptor that has recently been implicated in sensing metabolic stress via mitochondrial DNA leakage. While peripheral cGAS activation drives metabolic disorders, its role in central nutrient sensing remains elusive. Here, leveraging a hypothalamic single-cell RNA sequencing dataset, we

discovered that *Cgas* is highly enriched in microglia compared to other central cell types. Intriguingly, opposite to its peripheral regulation, microglial *Cgas* expression is selectively upregulated during fasting rather than high-fat diet feeding. To explore the functional role of microglial cGAS in response to energetic deficits, we generated a microglia-specific conditional knockout mouse model ($Cgas^{MGKO}$) by crossing $Tmem119^{CreER}$ and $Cgas^{flox/flox}$ mice. Under basal conditions, no baseline alterations were observed in body weight, food intake, or circulating blood glucose levels. However, upon nutrient deprivation, $Cgas^{MGKO}$ mice exhibited a hyper-reactive foraging response and maladaptive risk-taking behavior, manifested by a significant increase in center duration within the open field test and open-arm time in the elevated plus maze. Furthermore, in response to an acute cellular glucose crisis induced by 2-deoxy-D-glucose (2-DG), $Cgas^{MGKO}$ mice mounted an exaggerated systemic glycemic spike, indicating that microglial cGAS acts as a critical homeostatic regulator of state-dependent metabolic responses. Mechanistically, patch-clamp electrophysiology within the ventromedial hypothalamus (VMH) revealed that microglial cGAS deletion disrupts homeostatic network plasticity during energy deficits. While prolonged fasting successfully silences glucose-excited (GE) neurons and recruits glucose-inhibited (GI) counterregulatory neurons in control mice, fasted $Cgas^{MGKO}$ mice exhibit a state of central metabolic insensitivity, characterized by the aberrant persistence of active GE neurons and a failure to robustly expand the functional GI population. This localized network rigidity leaves the hypothalamus highly vulnerable to acute bioenergetic challenges, driving systemic autonomic overreaction. Together, our findings unravel an unappreciated, non-canonical function of microglial cGAS in central metabolic sensing and whole-body energy homeostasis, bridging the gap between neuroimmunology and systemic metabolism.

**Disclosures: J. Qiu:** None. **Q. Liu:** None. **J.C. Bean:** None. **Y. Xu:** None.

**Poster**

**PSTR190: Energy Metabolism**

**Location:** WCC Halls A-C

**Time:** Monday, November 16, 2026, 1:00 PM - 5:00 PM

**Program #/Poster #:** PSTR190.07/DD24

**Topic:** G.05. Brain Blood Flow, Metabolism, and Homeostasis

**Support:** NIH Intramural Research grant

**Title:** Beta-arrestin-1 regulates the activity of MC4R neurons in vivo

**Authors: *M. RASHID**[1], O. F. GAVRILOVA[1], Z. CUI[1], Y. HE[2], D. HASPULA[1], J. WESS[1]; [1]NIH, Bethesda, MD; [2]Natl. Heart Lung and Blood Inst., NIH, bethesda, MD

**Abstract: Introduction:** Melanocortin-4 Receptor (MC4R)-expressing neurons in the hypothalamus are critical nodes in the central regulation of energy balance and glucose homeostasis. In vitro studies have shown that MC4Rs can recruit both beta-arrestin-1 and -2 (Barr1 and Barr2, respectively). While a recent study elucidated the role of Barr2 in regulating the activity of MC4R-expressing neurons, the potential functional role of Barr1 expressed by this

group of neurons remains unexplored. To address this question, we generated mice lacking Barr1 specifically in MC4R neurons (MC4R-barr1-KO mice). MC4R-barr1-KO mice maintained on regular chow showed no significant metabolic differences, as compared to control littermates. However, when challenged with a high-fat diet (HFD), MC4R-barr1-KO mice developed pronounced metabolic impairments, including increased body weight and food intake, elevated adiposity, and marked glucose and insulin intolerance. However, acute anorectic responses to the MC4R agonist MTII were preserved in the mutant mice, indicating that acute MC4R-mediated feeding suppression does not require the presence of Barr1. Strikingly, virus-mediated re-expression of Barr1 in MC4R neurons of the paraventricular nucleus (PVN), a region enriched in MC4R-expressing neurons, fully rescued these metabolic deficits, normalizing body weight, food intake, adiposity, and glucose homeostasis. Since Barr1 can translocate to the nucleus and regulate transcription, we performed RNA sequencing studies to identify genes regulated by Barr1 in MC4R neurons of the PVN. We found that the expression of Histone Deacetylase 4 (HDAC4), an epigenetic regulator of numerous metabolic genes, was drastically reduced in PVN MC4R neurons of MC4R-barr1-KO mice.To test the potential involvement of HDAC4 in mediating the Barr1-dependent metabolic effects, we used a viral strategy to increase the expression of HDAC4 in PVN MC4R neurons of MC4R-barr1-KO mice. Remarkably, this approach completely prevented all metabolic phenotypes displayed by HFD MC4R-barr1-KO mice. Complementary in vitro studies further supported a requirement for Barr1 for maintaining robust HDAC4 expression. Together, these findings uncover a novel functional role of Barr1 in MC4R neurons. We found that Barr1 is required for the proper expression of HDAC4, which regulates multiple metabolically important genes to protect mice against the metabolic stress associated with the consumption of a calorie-dense diet. This Barr1-HDAC4 axis represents a potential therapeutic target for combating obesity and related metabolic disorders.

**Disclosures: M. Rashid:** None. **O.F. Gavrilova:** None. **Z. Cui:** None. **Y. he:** None. **D. Haspula:** None. **J. Wess:** None.

**Poster**

**PSTR190: Energy Metabolism**

**Location:** WCC Halls A-C

**Time:** Monday, November 16, 2026, 1:00 PM - 5:00 PM

**Program #/Poster #:** PSTR190.08/DD25

**Topic:** G.05. Brain Blood Flow, Metabolism, and Homeostasis

**Support:** SECIHTI-907564

**Title:** Differential Hypothalamic Proteomic Adaptations Underlie Susceptibility and Resistance to Cafeteria Diet Induced Weight Gain

**Authors: *S. GUZMAN**[1], C. D. GUTIERREZ REYES[2], B. A. MARICHAL-CANCINO[1], R. ROMERO[1], C. H. LÓPEZ-LARIZ[1];
[1]Univ. Autónoma de Aguascalientes, Aguascalientes, Mexico; [2]Texas Tech. Univ., Lubbock, TX

**Abstract: Differential Hypothalamic Proteomic Adaptations Underlie Susceptibility and Resistance to Cafeteria Diet-Induced Weight Gain**

[1]Sergio Guzmán-Rodríguez, [2]Cristian D. Gutiérrez-Reyes, [1]Ricardo Romero-Guevara, [1]Carlos H. López-Lariz, and [1]Bruno A. Marichal-Cancino

[1]Department of Physiology and Pharmacology, Center of Basic Sciences, Autonomous University of Aguascalientes, Aguascalientes 20100, Mexico[2]Department of Chemistry and Biochemistry, Texas Tech University, Lubbock, TX 79409, USA

**Abstract**Food environments that promote obesity, characterized by the excessive consumption of highly palatable foods rich in fats and sugars, can rapidly disrupt metabolic homeostasis and alter central mechanisms involved in energy balance regulation. In this study, we investigated behavioral traits and hypothalamic proteomic profiles associated with differential susceptibility to weight gain in rats exposed to a cafeteria-style diet for 10 weeks. Preadolescent male Sprague-Dawley rats were given access to either standard chow or a cafeteria-style diet. Behavioral outcomes were assessed using the open field test, followed by quantitative hypothalamic proteomic profiling by LC-MS/MS. Exposure to the cafeteria-style diet resulted in two distinct phenotypes: one group exhibited sustained weight gain throughout the experimental period, whereas another subgroup showed delayed weight gain and eventually reached body masses comparable to control animals, indicating an obesity-resistant phenotype. Behavioral analyses revealed no significant differences in locomotor activity, exploratory behavior, or anxiety-related among the experimental groups. In contrast, proteomic analysis showed that obesity-resistant rats exhibited a greater number of hypothalamic protein expression changes compared with control animals. For example, increased Ndufa9 expression and together with a relative decrease in Atp5pd/Tomm70, suggests active remodeling of hypothalamic energy metabolisms. In obese rats, Nap1l4, Ywhag, and Rps8 did not display similarly adaptive expression profiles, suggesting that resistance to diet-induced obesity is associated with a distinctive molecular signature in the hypothalamus. Overall, these findings indicate that obesity-resistant animals do not simply resemble control rats but instead represent a biologically distinct phenotype. From an evolutionary perspective, efficient energy storage under conditions of abundance may reflect an ancestral physiological response, whereas resistance to obesity may represent an adaptive trait that helps counteract excessive weight gain in specific environmental contexts.

**Disclosures: S. Guzman:** None. **C.D. Gutierrez Reyes:** None. **B.A. Marichal-Cancino:** None. **R. Romero:** None. **C.H. López-Lariz:** None.

**Poster**

**PSTR190: Energy Metabolism**

**Location:** WCC Halls A-C

**Time:** Monday, November 16, 2026, 1:00 PM - 5:00 PM

**Program #/Poster #:** PSTR190.09/DD26

**Topic:** G.05. Brain Blood Flow, Metabolism, and Homeostasis

**Title:** Inflammation as a Mediator of Diet and Depression

**Authors: *J. HAM**, R. E. HARTMAN;
Loma Linda Univ., Loma Linda, CA

**Abstract:** Depression is associated with both systemic inflammation and poor diet quality, which may be a modifiable behavioral pathway related to neurobehavioral risk. This study tested whether inflammatory burden mediated the association between diet quality and depressive symptoms in adult women using National Health and Nutrition Examination Survey (NHANES) August 2021-August 2023 data. Participants were women age 20 years and older with valid dietary, laboratory, sleep, and Patient Health Questionnaire-9 (PHQ-9) data (n=717). The analysis was conducted using structural equation modeling with weighted least squares means and variance-adjusted estimation. Diet Quality was modeled as a latent factor indicated by dietary fiber, choline, and vitamin D intake. Inflammatory Burden was modeled as a latent factor indicated by high-sensitivity C-reactive protein, alpha-1-acid glycoprotein, and ferritin. Depression was modeled as a latent factor indicated by the nine PHQ-9 items. Short sleep was included as an observed predictor of Depression. The primary mediation model demonstrated acceptable fit, scaled $\chi^2(101) = 367.82$, $p < .001$, CFI =.961, RMSEA =.061, and SRMR = .063. All Diet Quality indicators loaded significantly (β=.49-.81, *ps* < .001). High-sensitivity C-reactive protein and alpha-1-acid glycoprotein loaded strongly on Inflammatory Burden (β = .71 and .84, *ps* <.001). Ferritin loaded weakly but significantly on Inflammatory Burden (β = .17, $p < .001$). The PHQ-9 items loaded significantly on Depression (β = .66-.90, *ps* < .001). Higher Diet Quality was associated with lower Inflammatory Burden (β= -.21, $p < .001$) and lower Depression (β = -.19, $p < .001$), while higher Inflammatory Burden was associated with greater Depression (β = .12, $p = .010$). The indirect effect from Diet Quality to Depression through Inflammatory Burden was significant (β = -.03, $p = .020$), supporting partial mediation. These findings suggest that systemic inflammation may partially explain the association between diet quality and depressive symptoms in adult women, while diet quality also appears to have direct associations with depression independent of inflammation. Results support further investigation of diet and inflammatory biomarkers as modifiable correlates of depressive symptoms.

**Disclosures: J. Ham:** None. **R.E. Hartman:** None.

**Poster**

**PSTR190: Energy Metabolism**

**Location:** WCC Halls A-C

**Time:** Monday, November 16, 2026, 1:00 PM - 5:00 PM

**Program #/Poster #:** PSTR190.10/DD27

**Topic:** G.05. Brain Blood Flow, Metabolism, and Homeostasis

**Support:** SECIHTI doctoral fellowship No. 1133116

**Title:** NEUROENDOCRINE AND OVARIAN ALTERATIONS ASSOCIATED WITH OBESITY-INDUCED REPRODUCTIVE DYSFUNCTION IN FEMALE ZUCKER RATS

**Authors: *E. A. ROJAS**[1], A. DIAZ[2,1], B. VENEGAS MENESES[3];
[1]Fac. of Chem. Sci., [2]Inst. of physiology, Benemérita Univ. Autónoma de Puebla, Puebla, Mexico; [3]Fac. of Biol. Sci., BUAP, Puebla, Mexico

**Abstract:** Obesity is a major risk factor for metabolic and reproductive disorders, including Polyendocrine Metabolic Ovarian Syndrome (PMOS). It is currently recognized that these disorders do not solely depend on ovarian dysfunction but involve multiple components of the hypothalamic-pituitary-ovarian (HPO) axis. However, it remains unclear which components of the HPO axis are altered by genetic obesity and contribute to ovulatory dysfunction. This study aims to characterize neuroendocrine, hormonal, metabolic, and ovarian alterations associated with genetic obesity in female Zucker rats in order to identify potential sites of dysfunction within the HPO axis related to impaired reproductive function. Female Zucker obese (fa/fa) and control rats were evaluated during pubertal and adult stages. Metabolic and reproductive parameters, including body weight, Lee index, food intake, vaginal opening, and estrous cyclicity, were assessed. In addition, hypothalamic markers involved in energy balance and reproductive regulation, pituitary gonadotropins, and ovarian proteins associated with gonadotropin responsiveness and steroidogenesis were analyzed using immunohistochemical and biochemical approaches. Preliminary observations indicate that obese females exhibit increased body weight and adiposity accompanied by alterations in reproductive parameters compared with controls. These findings suggest that genetic obesity affects specific components of the HPO axis and promotes ovulatory dysfunction through integrated neuroendocrine, metabolic, and ovarian mechanisms.These findings provide insight into the neurobiological basis of obesity-associated reproductive dysfunction and contribute to understanding the mechanisms involved in metabolic and reproductive disorders such as PMOS.

**Disclosures: E.A. Rojas:** None. **A. Diaz:** None. **B. Venegas Meneses:** None.

**Poster**

**PSTR190: Energy Metabolism**

**Location:** WCC Halls A-C

**Time:** Monday, November 16, 2026, 1:00 PM - 5:00 PM

**Program #/Poster #:** PSTR190.11/DD28

**Topic:** G.05. Brain Blood Flow, Metabolism, and Homeostasis

**Support:** Mark Foundation Emerging Leader Award

**Title:** Synthetic torpor reveals tumor-specific metabolic vulnerabilities in breast cancer

**Authors: *A. BATTISON**[1], A. M. GOMEZ[1], Y. WU[2], L. BOYD[4], J. C. BORNIGER[3];
[2]Neurosci. and cancer, [3]Neuroscience/Cancer Ctr., [1]Cold Spring Harbor Lab., Cold Spring Harbor, NY; [4]Univ. of Connecticut, Storrs Mansfield, CT

**Abstract:** During torpor, mammals enter a profound hypometabolic state in which body temperature, metabolic rate, and locomotor activity plummet, allowing survival of energetically hostile conditions such as food deprivation or extreme cold. While torpor occurs naturally across

diverse heterotherms, it can be experimentally recapitulated by activating a hypothalamic circuit centred on QRFP-expressing neurons ("Q neurons") in the preoptic area. Given the known roles of metabolic rate in neuroprotection and immune regulation, we reasoned that torpor might also reshape the tumour microenvironment and cancer progression. To test this, we delivered Gq-DREADDs to the hypothalamus of QRFP-cre mice and induced synthetic torpor in tumor-bearing animals alongside controls once or twice during cancer progression. Synthetic torpor suppressed the growth of orthotopic EO771 breast tumors, with over 50% of animals ultimately showing complete regression of the tumor. To map the molecular consequences of torpor, we performed an integrated multi-omics analysis encompassing proteomics, lipidomics, and metabolomics from the same samples across tumor, visceral organs, and plasma from torpid and euthermic animals in both EO771 and B16 melanoma models, with and without tumor burden. Untargeted metabolomic and lipidomic profiling revealed striking tissue-selective changes in lipid metabolism during torpor. Suppression of oxidative phosphorylation pathway components were among the most consistently shifted features across liver, plasma, inguinal white adipose tissue (IWAT), and tumor, pointing to a system-wide remodeling of fatty-acid handling. In tumor membranes specifically, samples from mice that underwent synthetic torpor displayed an enrichment of polyunsaturated fatty acid-containing phospholipids alongside evidence of lipid peroxidation. These membrane remodeling changes were accompanied by evidence of lipid peroxidation, suggesting that torpor-induced reprogramming of the tumor lipidome may promote ferroptotic cell death as a mechanism of tumor suppression. Collectively, these findings position Q-neuron-mediated torpor as a multi-layered metabolic intervention that constrains tumor growth through both systemic energy restriction and tumor-intrinsic induction of ferroptosis.

**Disclosures: A. Battison:** None. **A.M. Gomez:** None. **Y. Wu:** None. **L. Boyd:** None. **J.C. Borniger:** None.

**Poster**

**PSTR190: Energy Metabolism**

**Location:** WCC Halls A-C

**Time:** Monday, November 16, 2026, 1:00 PM - 5:00 PM

**Program #/Poster #:** PSTR190.12/DD29

**Topic:** G.05. Brain Blood Flow, Metabolism, and Homeostasis

**Support:** CAPES
CNPq
FAPERJ

**Title:** Proton Motive Force Controls Brain Mitochondrial Glucose Phosphorylation and Redox Homeostasis

**Authors: *C. CARVALHO**, A. GALINA;
Inst. of Med. Biochem. Leopoldo de Meis (IBqM), Federal Univ. of Rio de Janeiro, Rio de Janeiro, Brazil

**Abstract:** Brain mitochondria are major sources of reactive oxygen species (ROS), making the regulation of mitochondrial membrane potential (ΔΨm) a central determinant of redox homeostasis in the central nervous system. Mitochondrial hexokinase (mHK) is known to limit ROS generation by modulating ΔΨm; however, whether the proton motive force reciprocally regulates mHK activity and mitochondrial glucose phosphorylation remains unknown. Here, we investigated how distinct energetic states influence the redox and phosphorylative functions of mHK in isolated mouse brain mitochondria.Mitochondria were energized with glycerol-3-phosphate (G3P) or succinate to establish different ΔΨm magnitudes. Oxygen consumption and ROS production were assessed by high-resolution respirometry, ΔΨm by fluorimetry, mHK activity by spectrophotometry, and glucose-6-phosphate (G6P) production by nuclear magnetic resonance (NMR). Low-ΔΨm states generated by G3P oxidation markedly reduced the sensitivity of mHK to G6P feedback inhibition, preserving enzyme activity and sustaining mitochondrial glucose phosphorylation. Consistent with this, $^{13}$C-NMR analyses revealed persistent $^{13}$C-G6P production even in the presence of inhibitory concentrations of unlabeled G6P, whereas glucose phosphorylation was largely suppressed under high-ΔΨm conditions supported by succinate. Pharmacological reduction of ΔΨm during succinate oxidation using TTFA or partial cytochrome c oxidase inhibition with KCN reproduced the low-ΔΨm phenotype, demonstrating that the energetic state itself, rather than substrate identity, governs mHK regulation. Moreover, ROS production was more responsive to mHK activation under low-ΔΨm conditions, indicating enhanced redox control. Collectively, our findings identify the proton motive force as a central regulator of mitochondrial glucose phosphorylation and redox homeostasis in brain mitochondria. By modulating mHK sensitivity to G6P, low-ΔΨm states sustain glucose utilization and strengthen ROS control, revealing a previously unrecognized mechanism through which mitochondrial energetic state coordinates glucose metabolism and redox homeostasis in the brain.

**Disclosures: C. Carvalho:** None. **A. Galina:** None.

**Poster**

**PSTR190: Energy Metabolism**

**Location:** WCC Halls A-C

**Time:** Monday, November 16, 2026, 1:00 PM - 5:00 PM

**Program #/Poster #:** PSTR190.13/DD30

**Topic:** G.05. Brain Blood Flow, Metabolism, and Homeostasis

**Support:** RO1NS091299-09

**Title:** Investigating altered glycolysis at the synapse in the context of TDP-43 proteinopathies

**Authors: *S. LANGBERG**[1], S. LOGANATHAN[3], R. SHARMA[4,5], B. LOVELL[4], K. PATHAK[4,5], P. FORSTMEIER[2], N. A. HALL[2], P. PIRROTTE[4,5], D. C. ZARNESCU[2]; [2]Cell and Biol. Systems, [1]Penn State Col. of Med., Hershey, PA; [3]Dept. of Immuno-Oncology, Beckman Res. Inst. of City of Hope, Duarte, CA; [4]Integrated Mass Spectrometry Shared Resource, Translational Genomics Res. Inst. & City of Hope Comprehensive Cancer Ctr.,

Phoenix, AZ; [5]Early Detection and Prevention Div., Translational Genomics Res. Inst., Phoenix, AZ

**Abstract:** Amyotrophic lateral sclerosis (ALS) is a progressive neurodegenerative disease characterized by the progressive loss of motor neurons. A hallmark pathological trait of ALS involves proteinopathy of TAR DNA Binding Protein, or TDP-43. TDP-43 is a DNA/RNA binding protein that resides in the nucleus under normal conditions with many functions relating to RNA metabolism and processing. In 97% of ALS cases regardless of etiology, TDP-43 mislocalizes from the nucleus into the cytoplasm and forms toxic cytoplasmic inclusions, leading to a nuclear loss of function and a cytoplasmic gain of function. Additionally, altered metabolic homeostasis has been observed years prior to motor symptom onset in many ALS patients, including elevated resting energy expenditure, and prognosis has been associated with body mass index. We have previously performed metabolomics on overexpression models of TDP-43 in *Drosophila* and identified pyruvate, the end product of glycolysis, to be elevated, consistent with findings from patient plasma samples. Transcript levels of phosphofructokinase (PFK, the enzyme catalyzing one of the rate-limiting steps in glycolysis) were also elevated in the context of TDP-43, and modulating PFK expression affected locomotion in larvae expressing TDP-43, highlighting PFK as a potential therapeutic target. To investigate how enhancing glycolysis is neuroprotective in the context of TDP-43, we used genetic interactions and pharmacological approaches in overexpression and CRISPR models of TDP-43. We found that overexpressing PFK in the context of TDP-43 improves lifespan, eclosion, and larval turning times, some of which are dependent on its catalytic activity. Endogenous PFK is enriched in synaptic boutons at the neuromuscular junction when TDP-43 is overexpressed and co-overexpression of PFK and TDP-43 improves synaptic vesicle endocytosis deficits. Additionally, chronic terazosin treatment (which enhances PGK1 activity) also improves eclosion in both overexpression and CRISPR models of TDP-43. To bolster these findings, we isolated synaptosomes from central synapses in Drosophila expressing TDP-43 panneuronally and performed proteomics. KEGG pathway analysis using DAVID highlighted different metabolic pathways and showed that glycolysis is upregulated in the context of TDP-43 proteinopathy. Preliminary metabolic flux experiments investigating altered breakdown of glucose due to TDP-43 indicate sex- and variant- dependent differences in the breakdown of glucose. These studies highlight several synapse associated metabolic alterations and the neuroprotective potential of glycolysis in the context of TDP-43 proteinopathy.

**Disclosures: S. Langberg:** None. **S. Loganathan:** None. **R. Sharma:** None. **B. Lovell:** None. **K. Pathak:** None. **P. Forstmeier:** None. **N.A. Hall:** None. **P. Pirrotte:** None. **D.C. Zarnescu:** None.

**Poster**

**PSTR191: Cardiovascular Regulation**

**Location:** WCC Halls A-C

**Time:** Monday, November 16, 2026, 1:00 PM - 5:00 PM

**Program #/Poster #:** PSTR191.01/Web Only

**Topic:** G.06. Autonomic Regulation

**Title:** A Novel Wavelet-Based Approach for Cardiovascular Autonomic Assessment Using Interbeat Interval and Systolic Blood Pressure Dynamics

**Authors: *I. ROMERO FRAGOSO**[1], J. ACEVES BUENDIA[3], A. SÁINZ JIMENEZ[2]; [1]UNAM, Coyoacan, Mexico; [2]UNAM, Ciudad de México, Mexico; [3]Dept. de Neurologia y Psiquiatria, INCMNSZ, Mexico City, Mexico

**Abstract:** Noninvasive assessment of cardiovascular autonomic regulation is commonly based on heart-rate variability and conventional spectral indices, including the low-frequency/high-frequency ratio. However, these approaches are usually derived from heart-rate information alone, rely on quasi-stationary assumptions, and may fail to incorporate relevant blood-pressure-derived dynamics. This creates an opportunity for methodological approaches that integrate interbeat interval and systolic blood pressure information while characterizing cardiovascular autonomic behavior from a non-stationary perspective. This exploratory study evaluated two continuous-wavelet-transform-derived variables, I and J, and their composite ratios as candidate indices for autonomic signal characterization during supine and orthostatic conditions. I was derived from interbeat interval dynamics, whereas J was derived from systolic blood pressure dynamics. Their associations with baroreflex sensitivity-related variables were assessed and compared with conventional Welch-derived high-frequency power, low-frequency power, and low-frequency/high-frequency ratio. I showed strong positive associations with baroreflex sensitivity-related markers in both supine and orthostatic conditions and aligned with established parasympathetic-related heart-rate variability indices. J provided complementary systolic-blood-pressure-derived information, showing significant relation with the presence of Mayer Waves, particularly during orthostatic challenge. The composite ratio J/I showed the strongest ratio-based association with baroreflex sensitivity-related markers, especially during orthostatic stress, and demonstrated greater consistency with BRS sensitivity markers than the conventional Welch-derived low-frequency/high-frequency ratio. These findings suggest that the proposed wavelet-based I/J framework may provide a more temporally resolved and physiologically integrative approach for exploratory cardiovascular autonomic assessment. The method may improve characterization of autonomic imbalance severity by combining interbeat interval and systolic blood pressure dynamics.

**Disclosures: I. Romero Fragoso:** None. **J. Aceves Buendia:** None. **A. Sáinz Jimenez:** None.

**Poster**

**PSTR191: Cardiovascular Regulation**

**Location:** WCC Halls A-C

**Time:** Monday, November 16, 2026, 1:00 PM - 5:00 PM

**Program #/Poster #:** PSTR191.02/Web Only

**Topic:** G.06. Autonomic Regulation

**Title:** Impact of Hypothyroidism on Cardiac Autonomic functions in Nepalese Menopausal Female

**Authors: *D. R. NIROULA**;
Birat Med. Col. Teaching Hosp. & K M (Krishna Mohan) Univ., Budhiganga, Morang, Nepal

**Abstract: Presentation Type:** Poster**Title: Impact of Hypothyroidism on Cardiac Autonomic functions in Nepalese Menopausal Female.**
**Corresponding Author and Presenter:** Dilli Ram Niroula**Organizational Affiliation:** PhD Candidate of KM University, Mathura, UP, India & Junior faculty member of Birat Medical College Teaching Hospital, Budhiganga-2, Morang, Nep
**Abstract Introduction**: The autonomic nervous system (ANS) maintains cardiovascular homeostasis through a balanced interaction between sympathetic and parasympathetic activities. Hypothyroidism, a prevalent endocrine disorder in Asian populations, is known to disturb this autonomic equilibrium, leading to alterations in both sympathetic and parasympathetic functions. Therefore, the present study was designed to evaluate the impact of hypothyroidism on cardiac autonomic functions in Nepalese menopausal females.**Methods**: A hospital-based cross-sectional study was conducted on 80 premenopausal females aged 35–45 years, including 40 hypothyroid patients and 40 age-matched healthy controls. Cardiac autonomic function tests were performed using standard procedures. Sympathetic activity was assessed through the postural hypotension test and sustained handgrip test, whereas parasympathetic activity was evaluated using resting and standing blood pressure measurements, deep breathing test, Valsalva maneuver and heart rate variability (HRV) analysis. **Result**s: The mean age of the participants was 36.20 ± 3.8 years. Among hypothyroid female subjects, 82.5% (n = 33) exhibited autonomic dysfunction, with 75% (n = 30) showing sympathetic dysfunction, 62.5% (n = 25) demonstrating parasympathetic dysfunction.**Conclusion**: In hypothyroid female, sympathetic activity assessed by postural hypotension and sustained handgrip tests showed significant changes in diastolic blood pressure. Parasympathetic activity examined by deep breathing and Valsalva maneuver also demonstrated significant alterations. Heart rate variability analysis at rest revealed sympathovagal imbalance. In contrast, the parasympathetic response assessed by heart rate changes upon standing did not show significant differences. Hence, autonomic dysfunction in hypothyroidism is common in Nepalese menopausal female, with a greater incidence of sympathetic dysfunction relative to parasympathetic dysfunction.

**Disclosures: D.R. Niroula:** None.

**Poster**

**PSTR191: Cardiovascular Regulation**

**Location:** WCC Halls A-C

**Time:** Monday, November 16, 2026, 1:00 PM - 5:00 PM

**Program #/Poster #:** PSTR191.04/EE1

**Topic:** G.06. Autonomic Regulation

**Title:** Autonomic, cardiovascular, and endocrine coupling

**Authors: *A. ROBLES-CABRERA**;
Univ. Nacional Autónoma de México, Mexico City, Mexico

**Abstract: AbstractIntroduction** The autonomic nervous system and the endocrine system regulate cardiovascular physiology, and their alterations—such as those occurring in type 2 diabetes mellitus (T2DM)—are linked to the development of cardiovascular complications. Sex hormones are key regulators of both the cardiovascular system and neural tissue. During postmenopause, the decline in hormone production can increase the risk of cardiovascular and autonomic diseases, especially in the presence of metabolic disorders like T2DM. However, evidence regarding whether sex hormones are related to autonomic activity remains inconclusive. The objective of this study was to evaluate the correlation between sex hormones and cardiac autonomic activity, measured via heart rate variability (HRV), in women with well-controlled T2DM and in healthy women as a control group.**Subjects and methods** In this study, four groups of women were formed based on their health status (control or T2DM) and fertility status (premenopausal or postmenopausal). Five serum sex hormones were measured (estradiol, progesterone, testosterone, LH, and FSH), and HRV indices in the time and frequency domains were determined under three conditions: supine position, active standing, and rhythmic breathing. In the full sample (n=118), Pearson bivariate correlations and multiple linear regressions were used to analyze the relationship between sex hormones, HRV indices, and other independent variables such as blood glucose levels and age. A p-value $< 0.05$ was considered statistically significant.**Results** No differences were found in sex hormones or HRV indices when comparing the healthy and T2DM groups. All Pearson bivariate correlations between sex hormones and HRV indices were significant: estradiol, progesterone, and testosterone showed positive correlations, whereas LH and FSH presented negative correlations in both time-domain indices (SDNN, RMSSD, pNN20) and frequency-domain indices (PLF and PHF). Regression models adjusted for mean inter-beat intervals confirmed the association between all sex hormones and HRV indices. Estradiol maintained its significance in regression models for specific HRV indices during the supine and active standing conditions, even after adjusting for age and glucose levels.**Conclusions** All sex hormones correlate with HRV indices. Regression analysis confirms that this correlation is independent of the mean inter-beat interval. However, in models adjusted for age and glucose levels, only estradiol maintained significance.

**Disclosures: A. Robles-Cabrera:** None.

**Poster**

**PSTR191: Cardiovascular Regulation**

**Location:** WCC Halls A-C

**Time:** Monday, November 16, 2026, 1:00 PM - 5:00 PM

**Program #/Poster #:** PSTR191.05/EE2

**Topic:** G.06. Autonomic Regulation

**Support:** FAMES scholarship program

**Title:** Data-driven closed-loop vagus nerve stimulation for human cardiovascular regulation: An in silico study using nonlinear model predictive control

**Authors: M. DELIZÉE**[1], *M. V. KOTHARE[2], A. VANDE WOUWER[3], R. VADIGEPALLI[4]; [1]Univ. of Mons, Hennuyères, Belgium; [2]Chem. & Biomolecular Eng., Lehigh Univ., Bethlehem, PA; [3]U. of Mons, Mons, Belgium; [4]U. of New Mexico, Albuquerque, NM

**Abstract:** Cardiovascular diseases including heart failure, arterial hypertension, and atrial fibrillation affect hundreds of millions of people worldwide. A common causal mechanism is autonomic imbalance characterized by sympathetic overactivation and withdrawal of vagal tone. Vagus nerve stimulation (VNS) directly augments parasympathetic tone and represents a promising therapeutic avenue. However, existing clinical systems deliver fixed, pre-programmed stimulation without adapting to the patient's real-time hemodynamic state. This limitation has been implicated in the failure of several large clinical trials to meet their primary endpoints, motivating the development of adaptive closed-loop controller approaches. We employ a pulsatile human cardiac model to develop a data-driven controller design for *in silico* validation. As a first step, a systematic open-loop characterization over 140 stimulation conditions is conducted using this human cardiovascular-baroreflex digital twin . The neural fulcrum concept, originally defined for heart rate (HR), is extended to mean arterial pressure (MAP) and stroke volume (SV), revealing a monotonically hypotensive MAP response and a biphasic SV response across the stimulation parameter space. A two-layer Long Short-Term Memory (LSTM) network trained on 896 open-loop stimulation trials then serves as the internal prediction model of a nonlinear model predictive controller (NMPC). The surrogate achieves per-output autoregressive test errors of 0.70 bpm, 0.62 mmHg, and 0.87 mL, and evaluates one cardiac cycle in under 85 ms. An offset-free disturbance observer compensates model-plant mismatch across physiological conditions. Three closed-loop scenarios are evaluated. Under nominal conditions, the controller drives HR, MAP, and SV to target setpoints with steady-state errors below 0.5 bpm, 1.0 mmHg, and 0.5 mL, and settling times between 9 and 17 cardiac cycles. Under hypertensive conditions, the offset-free formulation achieves tracking within 1.3 bpm, 1.9 mmHg, and 1.1 mL. Under exercise conditions, a dedicated surrogate retrained on exercise-specific data reduces steady-state errors to below 3.5 bpm, 1.2 mmHg, and 1.7 mL. These results demonstrate the feasibility of data-driven closed-loop VNS across a range of physiological conditions in a human cardiovascular model.

**Disclosures: M. Delizée:** None. **M.V. Kothare:** None. **A. Vande Wouwer:** None. **R. Vadigepalli:** None.

**Poster**

**PSTR191: Cardiovascular Regulation**

**Location:** WCC Halls A-C

**Time:** Monday, November 16, 2026, 1:00 PM - 5:00 PM

**Program #/Poster #:** PSTR191.06/EE3

**Topic:** G.06. Autonomic Regulation

**Title:** Optimizing Heart-Rate Variability Biofeedback Components for Resting HRV and Amyloid-Beta Outcomes: A Randomized Factorial Design Study

**Authors: *C. SUH**[1], H. YOO[2], K. NASHIRO[3], M. MATHER[3];
[1]Scripps Col., La Cañada Flintridge, CA; [2]USC, Gardena, CA; [3]USC, Los Angeles, CA

**Abstract:** Heart-rate variability (HRV) biofeedback is a promising noninvasive intervention for enhancing autonomic regulation, yet the specific protocol components and combinations responsible for physiological and biomarker change remain unclear. This is especially relevant for aging and Alzheimer's disease research, where autonomic function may be linked to amyloid-beta biology. This study aimed to identify which components of a paced-breathing HRV biofeedback intervention influence HRV-related physiology and plasma amyloid-beta outcomes. Participants (N = 130) were randomized in a 2^6 factorial design across 64 cells defined by six two-level factors: breathing frequency, graphical heart-rate feedback, pace selection, positive-emotion instructions, auditory pacing, and reward structure. Participants completed baseline and post-intervention physiological assessments, plasma biomarker collection, and at-home HRV biofeedback training. Resting HRV measures included pre-to-post changes in log-transformed RMSSD, low-frequency power, and high-frequency power, while plasma outcomes included amyloid-beta 40, amyloid-beta 42, and the amyloid-beta 42/40 ratio. Effects of intervention components were evaluated using factorial modeling, with LASSO-based variable selection followed by ordinary least squares regression. Analyses focused on main effects and two-way interactions, with false discovery rate correction applied for multiple comparisons.
For resting HRV measures, the absence of graphical heart-rate feedback was associated with greater increases in log LFP, whereas auditory pacing was linked to greater increases in log RMSSD. Several two-way interactions were also identified. Slower breathing was associated with higher log LFP under completion-based rewards but lower log LFP under performance-based rewards, suggesting that motivational framing may influence engagement with prolonged respiratory cycles. Furthermore, auditory pacing appeared beneficial without graphical feedback but detrimental when feedback was present, suggesting a possible attentional-load effect. No significant main effects were observed for plasma amyloid-beta measures. However, several two-way interactions were identified for Aβ42, indicating that lower Aβ42 levels depended on specific combinations of breathing frequency, reward structure, graphical feedback, pace selection, and positive-emotion instructions.
HRV biofeedback components and their interactions differentially influenced resting HRV and Aβ outcomes. Factorial optimization may help refine scalable interventions for cognitive aging and Alzheimer's disease risk.

**Disclosures: C. Suh:** None. **H. Yoo:** None. **K. Nashiro:** None. **M. Mather:** None.

**Poster**

**PSTR191: Cardiovascular Regulation**

**Location:** WCC Halls A-C

**Time:** Monday, November 16, 2026, 1:00 PM - 5:00 PM

**Program #/Poster #:** PSTR191.07/EE4

**Topic:** G.06. Autonomic Regulation

**Title:** Frontal midline theta and vagally mediated heart rate variability in cortical-autonomic regulation during meditation

**Authors: *D. T. HOMANS**[1], R. VYAS[2], E. ZHANG[2], A. NAVARRO-CEBRIAN[2]; [1]Psychology, Univ. of Maryland Col. Park, Frederick, MD; [2]Univ. of Maryland, College Park, MD

**Abstract:** Meditation has been associated with emotional wellbeing, attentional regulation and autonomic functioning. However, the neurophysiological mechanisms underlying these relationships are not completely understood. The neurovisceral integration model proposes that cortical regions involved in attentional and emotional regulation, particularly the medial prefrontal cortex (mPFC) and anterior cingulate cortex (ACC), show top-down influence over autonomic regulation through vagal pathways (via the amygdala and nucleus ambiguus). Within this framework, ACC-generated frontal midline (FM) theta and vagally mediated heart rate variability (HRV) may reflect coordinated cortical-autonomic regulation. Previous research has shown correlations between meditative state, frontal midline theta, attentional states and parasympathetic activity. In this study, we examine the relationship between theta oscillatory activity and vagal tone during meditation using simultaneous EEG and heart rate recordings obtained from meditators. Based on preliminary data, vagal tone (mean z-transformed RMSSD, SD1, and HF power) was positively associated with midline theta power (mean z-transformed midline theta), Spearman $\rho = 0.51$, $p = 0.0075$, permutation $p = 0.0074$, $n = 26$. These findings suggest that coordinated theta oscillatory activity and vagal regulation may reflect a broader neurophysiological trait related to cortical-autonomic integration. Ongoing analyses with additional subjects will further clarify the relationship between meditation, attentional neural systems, and autonomic regulation. Clarifying the relationship between theta oscillatory activity and vagal regulation may provide insight into the mechanisms relevant to non-pharmacological interventions targeting dysregulated attentional and autonomic processes, including panic disorders, trauma-related disorders, and ADHD.

**Disclosures: D.T. Homans:** None. **R. Vyas:** None. **E. Zhang:** None. **A. Navarro-Cebrian:** None.

**Poster**

**PSTR191: Cardiovascular Regulation**

**Location:** WCC Halls A-C

**Time:** Monday, November 16, 2026, 1:00 PM - 5:00 PM

**Program #/Poster #:** PSTR191.08/EE5

**Topic:** G.06. Autonomic Regulation

**Title:** Heartbeat-Evoked Potentials in Primate Anterior Cingulate Cortex Are Modulated by Peripheral Autonomic Blockade

**Authors: *J. DAHILL-FUCHEL**[1], M. CARDENAS[3], J. J. ALLEN[2], K. M. GOTHARD[4]; [1]Psychology, Univ. of Arizona, New York City, NY; [2]Psychology, Univ. of Arizona, Tucson, AZ; [3]Univ. of Pittsburgh, Pittsburgh, PA; [4]Physiol., Univ. Arizona, Col. Med., Tucson, AZ

**Abstract:** The heartbeat-evoked potential (HEP) reflects cortical processing of cardiac afferent signals and is considered a neural index of interoception. Disruption of this cardiac-cortical processing via peripheral autonomic manipulation provides a means of causally probing the contribution of visceral afferent feedback to cortical activity. Here, local field potentials (LFPs) were recorded from the anterior cingulate cortex (ACC) of a non-human primate performing an approach-avoidance conflict task. Glycopyrrolate, a peripherally acting muscarinic antagonist that blocks parasympathetic effects without crossing the blood-brain barrier, reduced tolerance to aversive stimuli and altered the properties of task-related neurons in the ACC. We asked whether glycopyrrolate also altered HEP amplitude in these areas. LFP signals were recorded with 32-channel V-probes spanning the upper and lower banks of the sulcal ACC (areas 24c extending toward 23c), bandpass filtered (0.1-30 Hz), common average referenced, and epoch-ed around cleaned R-peaks (−100 to 400 ms). HEPs were computed per contact and per trial block (PRE: pre-administration; POST: post-administration), and a nonparametric permutation test (1,000 iterations) assessed whether scalar HEP amplitude in a 150-350 ms post-R-peak window differed significantly between PRE and POST drug administration at each contact. False discovery rate correction ($q < 0.05$) was applied across contacts within each session. Across five glycopyrrolate sessions (305 total contacts after exclusion of artifact-contaminated channels) and five control (saline) sessions (303 contacts), glycopyrrolate was associated with a significantly higher proportion of contacts showing PRE vs. POST differences in HEP amplitude compared to saline (37.0% vs. 23.4%; $\chi^2(1) = 13.35$, $p = 0.0003$, $\varphi = 0.148$). This effect was bidirectional, as significant differences consisted in both increases and decreases in POST relative to PRE HEP amplitude (44.2% positive, 55.8% negative) with no consistent directional bias (sign test: $p = 0.259$), suggesting that glycopyrrolate did not uniformly suppress or enhance HEP amplitude. These findings suggest that strictly peripheral parasympathetic blockade destabilizes cardiac-cortical processing in the ACC, consistent with visceral afferent feedback contributing to the ongoing calibration of interoceptive representations in primate cingulate cortex.

**Disclosures: J. Dahill-Fuchel:** None. **M. Cardenas:** None. **J.J. Allen:** None. **K.M. Gothard:** None.

**Poster**

**PSTR191: Cardiovascular Regulation**

**Location:** WCC Halls A-C

**Time:** Monday, November 16, 2026, 1:00 PM - 5:00 PM

**Program #/Poster #:** PSTR191.09/EE6

**Topic:** G.06. Autonomic Regulation

**Support:** NIH R01 HL170626

**Title:** Functional parasympathetic circuits regulating ventricular electrophysiology identified by targeted neuromodulation of the ventral interventricular ganglionated plexus

**Authors: R. ALAM**[1], S. SHARMA[1], L. BALUPARI[1], N. R. JANI[2], S. AVASTHI[2], M. VASEGHI[2], *J. D. TOMPKINS[1,2];
[2]Geffen Sch. of Medicine, Dept. of Medicine, Div. of Cardiol., [1]UCLA, Los Angeles, CA

**Abstract:** The intrinsic cardiac nervous system (ICNS) is a network of neurons on the epicardial surface of the heart organized into ganglionated plexi (GPs) that integrate autonomic input and locally regulate cardiac electrical and mechanical function. Despite its importance in cardiac regulation, parasympathetic circuits regulating ventricular function are poorly defined. We used comparative neuroanatomy, ex vivo electrophysiology, and in vivo physiological studies to investigate the role of the ventral interventicular GP (VIV-GP), a GP implicated in ventricular regulation. VIV-GP ganglia were isolated from pig and human donor hearts. Immunohistochemistry for vesicular acetylcholine transporter (VAChT), protein gene product 9.5, and tyrosine hydroxylase demonstrated similar neurochemical composition, neuronal morphology and ganglion organization in both species. Adjacent sections of left ventricular (LV) myocardium contained VAChT-immunoreactive fibers and varicosities running parallel to LV myocytes, consistent with cholinergic parasympathetic innervation of the LV in both species. Intracellular recordings from VIV-GP neurons identified key roles for 4-aminopyridine (4-AP)-sensitive voltage-gated $K^+$ channels and apamin-sensitive $Ca^{2+}$-activated $K^+$ channels in regulating neuronal excitability. Combined application of 4-AP and apamin increased neuronal excitability, spontaneous firing, and synaptically evoked action potentials. To determine whether enhanced VIV-GP excitability influences LV function in vivo, 4-AP and apamin were microinjected into the VIV-GP of anesthetized pigs. Hemodynamic and electrophysiological responses, including heart rate, LV systolic pressure, and effective refractory period (ERP), were assessed before and after right and left vagus nerve stimulation (RVNS and LVNS). Targeted neuromodulation of the VIV-GP significantly prolonged ventricular ERP and augmented LVNS-evoked bradycardia and reductions in LV contractility, while RVNS responses were unchanged. Importantly, topical application of apamin and 4-AP to the LV epicardium produced no measurable electrophysiological or hemodynamic effects, with or without vagal stimulation, supporting a localized mechanism mediated through VIV-GP neurons rather than direct myocardial actions. These findings identify functional parasympathetic circuits within the VIV-GP that regulate LV electrophysiological and mechanical properties. They establish the pig heart as a translational model for investigating targeted ICNS neuromodulation and support the VIV-GP as a potential therapeutic target for ventricular arrhythmias and heart failure.

**Disclosures: R. Alam:** None. **S. Sharma:** None. **L. Balupari:** None. **N.R. Jani:** None. **S. Avasthi:** None. **M. Vaseghi:** None. **J.D. Tompkins:** None.

**Poster**

**PSTR191: Cardiovascular Regulation**

**Location:** WCC Halls A-C

**Time:** Monday, November 16, 2026, 1:00 PM - 5:00 PM

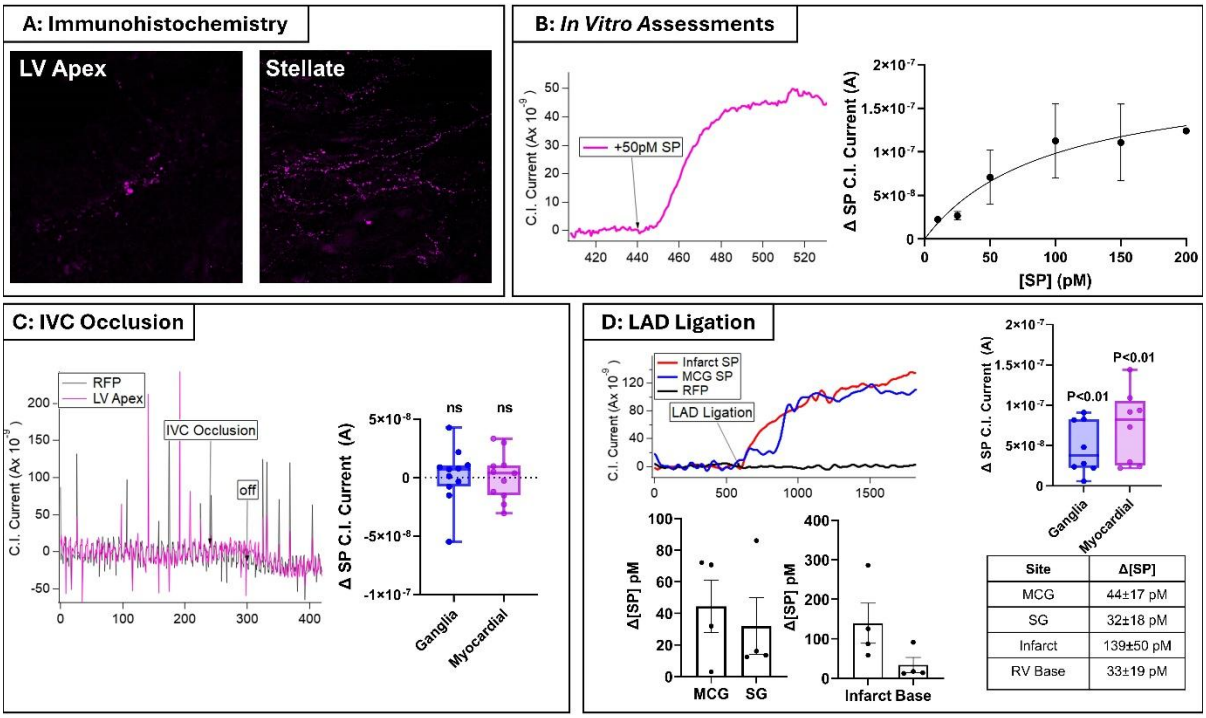
**Program #/Poster #:** PSTR191.10/EE7

**Topic:** G.06. Autonomic Regulation

**Title:** In vivo real-time detection of substance P in porcine myocardium and post-ganglionic thoracic sympathetic ganglia during myocardial ischemia

**Authors: *S. AVASTHI**[1], A. KAO[1], N. JANI[1], C. SMITH[2], M. VASEGHI[1];
[1]UCLA, Los Angeles, CA; [2]Case Western Reserve Univ., Cleveland, OH

**Abstract:** Substance P (SP) is released by nociceptive neurons in sensory ganglia (such as dorsal root ganglia, DRG) and in the heart in response to noxious stimuli such as myocardial ischemia. Exposure of peripheral autonomic neurons to SP increases their excitability *ex vivo*. Cardiac sensory fibers with cell bodies in the DRG pass through post-ganglionic sympathetic ganglia, such as the stellate ganglia (SG) and middle cervical ganglia (MCG), before reaching the spinal cord. It is unknown if these fibers release SP onto post-ganglionic neurons during myocardial ischemia that could lead to more direct activation of post-ganglionic sympathetic neurons than pathways using spinal reflexes. We developed capacitive immunoprobes (C.I.) for detection of SP. Electrodes coated with antibodies against SP or red fluorescent protein (RFP, control) were exposed to variable concentrations of SP to assess detection. A best fit curve between C.I. current and SP concentration was used to convert currents measured *in vivo* to SP concentration. Five pigs underwent sternotomy and bilateral SG and MCG exposure. SP probes were placed in the MCG, SG, left ventricular apex (LVa), and right ventricular base (RVb). SP levels were measured during inferior vena cava (IVC) occlusion for 1 min (for mechanoreceptor activation) and left anterior descending coronary artery (LAD) ligation (for nociceptor activation) before the 2nd diagonal branch for 30 min. RFP probes were placed in the RVb, away from ischemia. SG and LVa were stained for SP and imaged with confocal microscopy. Images of the LVa and SG confirmed the presence of SP-positive fibers (figure). IVC occlusion decreased blood pressure but resulted in no significant change in SP current in the myocardium, SG, or MCG (figure). After LAD ligation, significant increases in interstitial SP in the MCG, SG, and LVa, with lesser changes at the RVb were observed (figure). C.I. can detect SP release in the heart during ischemia. We additionally report release of SP in cardiac-innervating post-ganglionic sympathetic ganglia (SG and MCG) during ischemia, a novel finding of this study.




**Disclosures: S. Avasthi:** None. **A. Kao:** None. **N. Jani:** None. **C. Smith:** None. **M. Vaseghi:** None.

**Poster**

**PSTR191: Cardiovascular Regulation**

**Location:** WCC Halls A-C

**Time:** Monday, November 16, 2026, 1:00 PM - 5:00 PM

**Program #/Poster #:** PSTR191.11/EE8

**Topic:** G.06. Autonomic Regulation

**Support:** NHLBI grant HL176932

**Title:** Orexin neurons contribute to the strength of the peripheral chemoreflex

**Authors: *S. M. MAPLES**[1], D. D. KLINE[2], K. J. CUMMINGS[3];
[2]Biomed. Sciences/Dalton CRC, [1]Univ. of Missouri, Columbia, Columbia, MO; [3]Biomed. Sci., Univ. of Missouri, Columbia, MO

**Abstract:** Orexin neurons in the lateral and perifornical hypothalamus contribute to a diverse array of functions related to state, feeding and the control of cardiorespiratory and sympathetic function. Elevated strength of the reflex is associated with cardiovascular disease, such as hypertension and heart failure. Previously our group showed that blocking orexin (Ox) receptors

reduced the strength of the peripheral chemoreflex. As orexin has been identified in the blood, here we tested the hypothesis that directly inhibiting orexin neurons would reduce the strength of the reflex. We crossed commercially-available, validated Orexin-Cre (Ox-Cre+) mice with Cre-dependent Gi DREADD mice (Cd-Gi+).We exposed Ox-Cre+/Cd-Gi+ mice to two episodes of graded hypoxia, taking O2 from 21% to 8% O2. The 1st exposure was preceded by systemic injection of vehicle, while the 2nd was preceded by systemic C21 (1 mg/kg;n=6) to inhibit orexin neurons, or alternatively a second vehicle administration (n=6). We measured the change in respiratory frequency (f), tidal volume (Vt) and overall ventilation (Ve) from baseline (normoxia), comparing the 1st and 2nd exposure to 15% O2 (mild hypoxia) and 10% O2 (moderate hypoxia). Inhibition of Ox neurons significantly reduced the change in Ve from the 1st to 2nd exposure (p=0.03), an effect mediated by a reduced change in f. Vehicle had no such effect. Inhibition was associated with changes in the hypoxia-induced activation (cFos) of neurons in the hypothalamus and brainstem. This is the first evidence that Ox neurons directly contribute to the strength of the peripheral chemoreflex. Ox neurons may be considered targets for strategies aimed at reducing peripheral chemoreflex strength to reduce the burden of downstream cardiovascular diseases.

**Disclosures: S.M. Maples:** A. Employment/Salary (full or part-time):; University of Missouri, Columbia. B. Contracted Research/Research Grant (principal investigator for a drug study, collaborator or consultant and pending and current grants). If you are a PI for a drug study, report that research relationship even if those funds come to an institution.; NHLBI grant HL176932. **D.D. Kline:** None. **K.J. Cummings:** B. Contracted Research/Research Grant (principal investigator for a drug study, collaborator or consultant and pending and current grants). If you are a PI for a drug study, report that research relationship even if those funds come to an institution.; NHLBI grant HL176932.

**Poster**

**PSTR191: Cardiovascular Regulation**

**Location:** WCC Halls A-C

**Time:** Monday, November 16, 2026, 1:00 PM - 5:00 PM

**Program #/Poster #:** PSTR191.12/EE9

**Topic:** G.06. Autonomic Regulation

**Support:** NIH Grant R01 HL1331000

**Title:** Methylation of transient receptor potential melastatin-subfamily member 7 (Trpm7) in the carotid body attenuated obesity-induced hypertension

**Authors: *M. SHIN**[1], A. ROY[1], O. PAUDEL[2], J. SHAM[2], W.-Y. TANG[3], V. POLOTSKY[1]; [1]George Washington Univ., Washington, DC; [2]Johns Hopkins Univ., Baltimore, MD; [3]Univ. of Pittsburgh, Pittsburgh, PA

**Abstract: RATIONALE**: Obesity is a major cause of hypertension. We have previously shown mice with diet-induced obesity (DIO) have high levels of leptin receptor *Lepr$^b$* and *Trpm7* gene

expression in CB, and pharmacological inhibition and gene knockdown of $LEPR^b$ and TRPM7 in CB treat DIO-induced hypertension. Furthermore, we have demonstrated that leptin increases *Trpm7* expression in the carotid body type I glomus cells via epigenetic mechanisms demethylating the *Trpm7* promoter. Leptin binding to $LEPR^b$ activates gene transcription *via* phosphorylation of the transcription factor Signal Transducer and Activator of Transcription 3 (STAT3). We hypothesize that leptin demethylates the *Trpm7* promoter at the pSTAT3 site and that methylation of this region using specific methylated oligonucleotides *in vivo* will decrease CB *Trpm7* gene expression, carotid sinus nerve (CSN) activity, and blood pressure (BP) in DIO mice. **METHODS:** We performed *in silico* analysis of the *Trpm7* promoter to identify putative pSTAT3 binding site(s) and generated methylated oligonucleotides (Met-oligo) complimentary to the STAT3 binding site of the *Trpm7* promoter. The Met-oligo were tested in the PC-12 cell culture, which are phenotypically similar to the CB type I cells. Then, Met-oligo were applied to the CB area in DIO male mice for 2 weeks. CSN activity was measured ex vivo (n = 5 in the Met-oligo group vs n = 5 in the control oligo group). BP was measured by telemetry at baseline and after treatment (n = 6 in the Met-oligo group vs n = 8 in the control group) in DIO male mice. **RESULTS**: *In silico* analysis of the *Trpm7* promoter showed that it contains putative binding sites for the transcription STAT3 and revealed CG dinucleotides (CpGs) where DNA methylation occurs. Leptin demethylated the STAT3 binding site of the Trpm7 promoter and increased Trpm7 gene expression, and these effects was abolished by Met-oligo both in vitro in PC-12 cells and in vivo in the CB of DIO mice. Leptin increased CSN activity in normoxic and hypoxic chemoreflex and these effects were abolished by Met-oligo. CB administration of the Met-oligo attenuated obesity-induced hypertension during the day, when animals were predominantly asleep, decreasing mean arterial pressure (MAP) by 5.3 ± 2.1 mmHg ($p<0.05$), whereas MAP was increased by 1.4 ± 5.5 mmHg in the control group. **CONCLUSION**: Methylation of the *Trpm7* promoter at the leptin-dependent pSTAT3 binding site in the CB abolished the leptin-induced increase in CSN activity and chemoreflex and attenuated obesity-induced hypertension.

**Disclosures: M. Shin:** None. **A. Roy:** None. **O. Paudel:** None. **J. Sham:** None. **W. tang:** None. **V. Polotsky:** None.

**Poster**

**PSTR191: Cardiovascular Regulation**

**Location:** WCC Halls A-C

**Time:** Monday, November 16, 2026, 1:00 PM - 5:00 PM

**Program #/Poster #:** PSTR191.13/EE10

**Topic:** G.06. Autonomic Regulation

**Support:** NIH Grant HL154512

**Title:** RCAN1-calcineurin signaling in the paraventricular nucleus drives chronic stress-induced hypertension

**Authors: *J.-J. ZHOU**[1], J.-Y. SHAO[2], S.-R. CHEN[3], H. CHEN[2], H.-L. PAN[2];
[2]Anesthesiol. and Perioperative Med., [3]Anesthesiol., [1]The Univ. of Texas MD Anderson Cancer Ctr., Houston, TX

**Abstract: RCAN1-calcineurin signaling in the paraventricular nucleus drives chronic stress-induced hypertension**

Jing-Jing Zhou,[1] Jian-Ying Shao,[1] Shao-Rui Chen,[1] Hong Chen,[1] Hui-Lin Pan*
[1]Department of Anesthesiology and Perioperative Medicine, The University of Texas MD Anderson Cancer Center, Houston, Texas 77030, USA
*Correspondence to: Hui-Lin Pan, Department of Anesthesiology and Perioperative Medicine, Unit 110, The University of Texas MD Anderson Cancer Center, 1515 Holcombe Boulevard, Houston, TX 77030, Email: huilinpan@mdanderson.org

**Abstract (no more than 250 words)** Prolonged stress promotes persistent hypertension in genetically predisposed individuals by increasing sympathetic tone. The hypothalamic paraventricular nucleus (PVN) is central to this process, driving excessive sympathetic outflow through enhanced glutamatergic N-methyl-D-aspartate receptor (NMDAR) activity. However, the molecular mechanisms underlying this effect remain unclear. We investigated the role of calcineurin, a $Ca^{2+}$/calmodulin-dependent protein phosphatase, in regulating NMDAR activity and sympathetic outflow in stress-induced hypertension using borderline hypertensive rats (BHR), the first-generation offspring of spontaneously hypertensive rats and Wistar-Kyoto rats. BHR exposed to 42 days of unpredictable stress exhibited reduced calcineurin phosphatase activity and increased interaction between calcineurin and regulator of calcineurin 1 (RCAN1), an endogenous inhibitor, in the PVN. RCAN1 serine phosphorylation was markedly increased, while inhibition of dual-specificity tyrosine-phosphorylation-regulated kinase 1 (DYRK1) normalized this phosphorylation. Whole-cell recordings in brain slices revealed that disrupting RCAN1-calcineurin interactions with an RCAN1-mimicking peptide reduced stress-induced increases in both presynaptic and postsynaptic NMDAR activity in spinally projecting PVN neurons. In vivo, microinjection of this peptide into the PVN attenuated elevated renal sympathetic nerve activity and arterial blood pressure in stressed BHR, without affecting unstressed controls. These findings indicate that prolonged stress impairs calcineurin activity via enhanced RCAN1-mediated inhibition in the PVN. Reduced calcineurin function subsequently potentiates synaptic NMDAR activity in presympathetic neurons, driving increased sympathetic output and contributing to stress-induced hypertension. **Key words**: Calcineurin, Regulator of Calcineurin 1, Synaptic plasticity, Hypothalamus, Autonomic nervous system, Sympathetic nervous system, Borderline Hypertensive Rats

**Disclosures: J. Zhou:** None. **J. Shao:** None. **S. Chen:** None. **H. Chen:** None. **H. Pan:** None.

**Poster**

**PSTR191: Cardiovascular Regulation**

**Location:** WCC Halls A-C

**Time:** Monday, November 16, 2026, 1:00 PM - 5:00 PM

**Program #/Poster #:** PSTR191.14/EE11

**Topic:** G.06. Autonomic Regulation

**Title:** Understanding the significance of Brain Regions of the Pain Sensing Pathway in Cardiac Remodeling After Myocardial Infarction

**Authors: *A. MONDAL**[1], P. DUTTA[2];
[1]Med., Univ. of Pittsburgh, Pittsburgh, PA; [2]Univ. of Pittsburgh, Pittsburgh, PA.

**Abstract:** The nervous and cardiovascular systems are intricately linked through the heart-brain axis. Emergingevidence further implicates the brain in regulating peripheral immunity. However, how brain activity isaltered following myocardial infarction (MI) and how specific neural circuits orchestrate post-MI cardiacrecovery remain understudied. Chest pain is a predominant manifestation of acute MI and is associatedwith increased mortality up to one-year post-event, raising the question of whether nodes within thepain-sensing pathway contribute to cardiac remodeling and post-MI heart failure. To address this, weperformed an unbiased neuronal mapping using tamoxifen-inducible TRAP2;Rosa-tdTomato mice topermanently label activated neurons. Relative to sham controls, MI induced by coronary artery ligationresulted in heightened neuronal activation in the insular cortex (InCtx), anterior cingulate (ACC), andperiaqueductal gray (PAG)— three pain-pathway nodes also known to be involved in cardiovascularregulation. Based on these preliminary data, we hypothesized that **these regions of the pain-sensingpathway modulate cardiac inflammation and remodeling after MI**. To test this hypothesis, weselectively silenced neuronal population of each region using a chemogenetic approach. Cardiacfunction was assessed by serial echocardiography at various time points after MI. Moreover, weevaluated cardiac fibrosis by histology and immunohistochemistry (IHC). Given the importance ofinflammation in post-MI cardiac healing, peripheral inflammatory leukocyte populations and cardiacmacrophage subsets (reparative vs. inflammatory) were also profiled using immunohistochemistryand/or flow cytometry. Inhibition of ACC or PAG neurons have not been found significantly alter post-MI inflammation and cardiac function. In contrast, insular cortex inhibition significantly reduced ejectionfraction at 1-1.5 months following MI, exacerbated infarct fibrosis, elevated circulating inflammatorymonocytes ($Ly6C^{high}$), and neutrophils, expanded cardiac inflammatory ($CCR2^{+}$) macrophages, anddepleted reparative $TIM4^{+}/LYVE1^{+}$ macrophages. Based on these initial findings, we conclude thatinhibition of insular cortex neurons following MI worsens cardiac function and exacerbatesinflammation, establishing the insular cortex as a central regulator of post-MI cardiac healing. Whetheractivation of InCtx can reverse this phenotype remains to be determined. Our future studies will employscRNA-seq and MALDI in the infarcts of MI hearts to integrate transcriptomic and metabolomic profilesand to elucidate the underlying mechanisms.

**Disclosures: A. Mondal:** A. Employment/Salary (full or part-time):; Graduate Student Assistant.

**Poster**

**PSTR191: Cardiovascular Regulation**

**Location:** WCC Halls A-C

**Time:** Monday, November 16, 2026, 1:00 PM - 5:00 PM

**Program #/Poster #:** PSTR191.15/EE12

**Topic:** G.06. Autonomic Regulation

**Support:** IYBF, DBT, India (HRD-17011/6/2025-HRD-DBT
Exploratory Research Project (RF20210649BTRFER008967)
Ministry of Human Resource & Development-CoE/IoE (11/9/2019-U.3(A)).

**Title:** Neurogenic hypertension and cyclooxygenase: What is the brain telling us?

**Authors: *G. GODARA**[1], S. TIWARI[1], S. SEKAR[1], K. VALLINAYAGAM[1], D. SUNIL[1], B. S[2], N. SUNDARESAN[2], N. AJ[1];
[1]Biotech., Indian Inst. of Technol. Madras, Chennai, India; [2]Dept. of Microbiology and Cell Biol., Indian Inst. of Science, Bengaluru, Bengaluru, India

**Abstract:** Hypertension is one of the leading causes of death worldwide. Cyclooxygenase (COX), a rate-limiting enzyme in the prostanoid pathway, is linked to neurogenic hypertension. Using the normotensive BPN/3J and hypertensive BPH/2J mouse model of neurogenic hypertension, we measured cyclooxygenase expression in different cardio-regulatory brain regions. Blood pressure was measured using a non-invasive device after 5-days of acclimatisation. The mean arterial pressure (MAP) in BPH/2J male mice (162 ± 9 mmHg) was significantly higher than that of the BPN/3J male mice (108 ± 9 mmHg). Similarly, MAP was higher in BPH/2J female mice (154 ± 6 mmHg) compared to BPN/3J female mice (106 ± 11 mmHg). After brain tissue collection, the forebrain and the hindbrain were sectioned using a cryotome. Cardio-regulatory regions like the organum vasculosum laminae terminalis (OVLT), subfornical organ (SFO), paraventricular nucleus (PVN), nucleus tractus solitarius (NTS), and rostral ventrolateral medulla (RVLM) were punched from the brain sections of both BPN/3J and BPH/2J male & female mice. Compared with normotensive control mice, we observe higher COX expression in the PVN of male hypertensive mice, but not in female hypertensive mice. Our data suggest an altered COX enzyme expression in the brain of neurogenic hypertensive mice. Further studies will help elucidate the role of brain prostanoids in the development of neurogenic hypertension.

**Disclosures: G. Godara:** None. **S. Tiwari:** None. **S. Sekar:** None. **K. Vallinayagam:** None. **D. Sunil:** None. **B. S:** None. **N. Sundaresan:** None. **N. Aj:** None.

**Poster**

**PSTR191: Cardiovascular Regulation**

**Location:** WCC Halls A-C

**Time:** Monday, November 16, 2026, 1:00 PM - 5:00 PM

**Program #/Poster #:** PSTR191.16/EE13

**Topic:** G.06. Autonomic Regulation

**Support:** NIH R01 NS126376
Neilsen SCIRTS award 1342305

**Title:** Kilohertz-Frequency Block in Small Fibers

**Authors: *M. K. JANTZ**, K. APLAON, N. A. PELOT, W. M. GRILL;
Biomed. Engin., Duke Univ., Durham, NC

**Abstract:** Kilohertz-frequency block (KHF) is a neuromodulation method in which a high-frequency signal is applied to arrest transmission of neural activity. Eliminating or downregulating neural activity has potential clinical applications in reducing pain and regulating autonomic functions such as blood pressure. However, many of these pain and autonomic signals are carried in small unmyelinated fibers, and prior characterization of block with KHF signals has almost exclusively been based on the response of large somatic fibers.
Here, we completed two distinct experiments. First, we applied KHF signals to the sciatic nerve and its branches to characterize the effects of KHF on transmission in slow- and fast-conducting fibers. Second, to determine the impact of these signals on a clinically relevant functional outcome, we applied low-frequency and KHF signals to the splanchnic sympathetic circuit while monitoring blood pressure.
In urethane-anesthetized rats, we instrumented the common peroneal branch of the sciatic nerve with three cuff electrodes (Micro-Leads Neuro Inc.) to deliver a test stimulus, deliver the KHF signal, and record compound action potentials. We applied KHF signals at a range of frequencies (0.5-19 kHz) and measured responses before, during, and after the KHF signal.
Fast fibers (conduction velocities > 2 m/s) were blocked at 5-19 kHz and block thresholds were ~0.5-3 mA. At the higher tested frequencies (11 and 19 kHz), slow fiber (conduction velocities < 2 m/s) block thresholds were substantially higher, often exceeding 20 mA. At lower frequencies (0.5, 1, 2, 5 kHz), slow fiber block thresholds were comparatively low, typically ~2-4 mA. The presence of block at low frequencies as well as the sharp increases in block threshold at higher frequency were consistent with previous model results.
We then instrumented urethane anesthetized rats with a blood pressure catheter (Millar LLC) in the carotid artery and used hook electrodes to apply signals to the thoracic sympathetic chain and the greater splanchnic nerve, which regulate vasoconstriction in the splanchnic vasculature bed in the abdomen. We evoked both increases and decreases in blood pressure with stimulation and KHF signals applied to the sympathetic circuit.
KHF block is widely discussed as a potential intervention to manage pain and modulate autonomic function, but the response of small fibers to KHF signals is not well understood. This work characterized the response of small fibers to a range of KHF signal parameters and demonstrated that KHF block has potential functional applications to modulate autonomic signals such as blood pressure.

**Disclosures: M.K. Jantz:** None. **K. Aplaon:** None. **N.A. Pelot:** None. **W.M. Grill:** None.

**Poster**

**PSTR191: Cardiovascular Regulation**

**Location:** WCC Halls A-C

**Time:** Monday, November 16, 2026, 1:00 PM - 5:00 PM

**Program #/Poster #:** PSTR191.17/EE14

**Topic:** G.06. Autonomic Regulation

**Support:** NIH Grant 5250096101

**Title:** Single-nucleus RNA sequencing reveals cell-type heterogeneity of differential gene expression in the paraventricular hypothalamicnucleus following angiotension II hypertension in a model of post-menopause

**Authors: *D. N. SILBERSTEIN**[1], W. HU[3], H. U. TILGNER[2], T. A. MILNER[1], M. J. GLASS[4]; [1]Brain and Mind Res. Inst., [2]Weill Cornell Med., New York, NY; [3]Weill Cornell Med. Col., NEW YORK, NY; [4]Brain and Mind Res. Inst., Weill Cornell Med. Col., New York, NY

**Abstract:** Hypertension is a leading contributor to cardiovascular and cerebrovascular diseases with well-established sex differences. Men are more likely to develop hypertension through mid-life, whereas following menopause, women's rates equalize to or even exceed those of men. Central mechanisms underlying menopausal hypertension remain poorly understood. The hypothalamic paraventricular nucleus (PVN) is a critical coordinator of sympathetic and neuroendocrine signaling and is involved in neurogenic hypertension. A mouse model of accelerated ovarian failure (AOF) induced by 4-vinylcyclohexene diepoxide (VCD) has been used to demonstrate that AOF hypertension is mediated by glutamate-dependent plasticity in the PVN. Importantly, intact cycling females are protected from angiotensin II (AngII)-induced hypertension, whereas post-AOF females develop hypertension, reflecting the increased risk observed in postmenopausal women. The PVN contains diverse neuronal phenotypes that differ in gene expression and function; however cell-type-specific contributions of these populations to hypertension in comparison to males or non-hypertensive females remain unresolved. We performed single-nucleus RNA sequencing (snRNA-seq) on PVN micropunches from male, vehicle-treated female (oil), and post-AOF female mice (N=3) infused subcutaneously with either slow-pressor AngII or saline. Various cell types were identified including astrocytes, microglia, oligodendrocyte lineages, as well as vasopressin, oxytocin, corticotropin releasing hormone, and other peptidergic neuronal phenotypes. Preliminary analysis of differential gene expression revealed sex- and hypertension-dependent dysregulation of genes implicated in synaptic plasticity and other processes linked to neurogenic hypertension. These data will inform cell-type-specific neuroendocrine mechanisms underlying sex differences in neurogenic hypertension during ovarian failure.

**Disclosures: D.N. Silberstein:** None. **W. Hu:** None. **H.U. Tilgner:** None. **T.A. Milner:** None. **M.J. Glass:** None.

**Poster**

**PSTR191: Cardiovascular Regulation**

**Location:** WCC Halls A-C

**Time:** Monday, November 16, 2026, 1:00 PM - 5:00 PM

**Program #/Poster #:** PSTR191.18/EE15

**Topic:** G.06. Autonomic Regulation

**Support:** NIH R01-HL-136710
R01- HL-098602

**Title:** Maternal Serotonin Excess Reprograms Brainstem Serotonergic Development and Autonomic Regulation in Neonates

**Authors: *E. AHMADZADEH**[1], K. J. CUMMINGS[2];
[1]Dalton Cardiovasc. Res. Center, Univ. of Missouri, Columbia, MO; [2]Dept. of Pathobiology and Integrative Biomed. Sci., Univ. of Missouri, Columbia, MO

**Abstract:** Adverse pregnancy conditions, including preeclampsia, fetal growth restriction, and maternal infection/inflammation, increase the risk of sudden infant death syndrome (SIDS). Emerging evidence, including our previous findings in fetal growth restriction, indicates that these conditions are associated with increased maternal and placental serotonin (5-HT) signaling. 5-HT is a key regulator of brainstem circuits underlying cardiorespiratory control, chemoreception, arousal, and autoresuscitation, and brainstem serotonergic abnormalities are a hallmark of SIDS. We hypothesized that pregnancy-associated 5-HT excess disrupts maturation of neonatal brainstem cardiorespiratory circuits. We used continuous infusion of 5-hydroxytryptophan (5-HTP), the immediate precursor of serotonin (5-HT), in pregnant Sprague-Dawley rats from gestational day 14-21; controls received saline. Serum and medullary 5-HIAA levels, brainstem 5-HT and 5-HT2A receptor expression, and cardiovascular function were assessed in neonatal offspring (n=6/group/age). Separate cohorts were exposed to chronic intermittent hypoxia (CIH) or normoxia. 5-HTP treatment produced no significant effects on neonatal body weight or gross morphology. Serum 5-HIAA was elevated at P0 ($p=0.006$), whereas medullary 5-HIAA was reduced ($p=0.008$), with normalization by P5. Brainstem 5-HT immunoreactivity was reduced at P1 ($p=0.04$) and P5 ($p=0.001$), accompanied by increased 5-HT2A receptor expression at P1 ($p=0.02$) and P5 ($p=0.022$). CIH further reduced 5-HT and 5-HT2A receptor expression. Functionally, 5-HTP-exposed offspring exhibited reduced heart rate ($p=0.01$) and increased VLF and LF HRV power ($p<0.001$), indicating altered autonomic regulation. These findings demonstrate that a mild maternal 5-HT excess is sufficient to alter neonatal brainstem serotonergic signaling and autonomic function in the absence of overt growth restriction. Maternal 5-HT elevation may represent a developmental vulnerability in neonatal cardiorespiratory control that amplifies the effects of placental insufficiency, hypoxia, and inflammation on SIDS risk.

**Disclosures: E. Ahmadzadeh:** None. **K.J. Cummings:** None.

**Poster**

**PSTR192: Sleep Regulation: Anatomy, Pharmacology, Behavior**

**Location:** WCC Halls A-C

**Time:** Monday, November 16, 2026, 1:00 PM - 5:00 PM

**Program #/Poster #:** PSTR192.01/EE16

**Topic:** G.07. Biological Rhythms and Sleep

**Support:** AMED-Moonshot Grant JP21zf0127005
JSPS KAKENHI 22H04918
JSPS KAKENHI 22K21351
JSPS DC1 Grants 25KJ0669
JST-SPRING Grant HJI06015

**Title:** CRBN-independent hypnotic effects of thalidomide derivatives

**Authors: *M. NISHIDA**[1,2], T. HASEGAWA[1,3], K. KATO[1,3], M. KAUSHIK[1], H. FUNATO[4,1], T. ITO[5], Y. YAMAGUCHI[6], H. HANDA[5], T. SAITOH[1,7], M. YANAGISAWA[1,8];
[1]Univ. of Tsukuba, Intl. Inst. for Integrative Sleep Med. (WPI-IIIS), TIAR, Tsukuba, Ibaraki, Japan; [2]SIGMA, Univ. of Tsukuba, Ibaraki, Japan; [3]Grad. Sch. Pure Appl. Sci., Univ. of Tsukuba, Ibaraki, Japan; [4]Fac. Med., Toho Univ., Tokyo, Japan; [5]Inst. of Med. Sci., Tokyo Med., Tokyo, Japan; [6]Sch. Life Sci. Technol., Sci. Tokyo, Tokyo, Japan; [7]Grad. Sch. Comp. Hum. Sci., Univ. of Tsukuba, Ibaraki, Japan; [8]Dept. of Mol. Genetics, Univ. of Texas Southwestern Med. Ctr., Dallas, TX

**Abstract:** Thalidomide was introduced in the 1950s as a sedative and hypnotic drug marketed as "a safe and harmless medication for pregnant women and children." However, it was later discovered that its use during pregnancy leads to severe birth defects.[1] Recent studies have shown that thalidomide binds to cereblon (CRBN), a component of the ubiquitin ligase complex, triggering abnormal protein degradation responsible for its teratogenic effects.[2,3] Meanwhile, our group generated non-thalidomide-binding CRBN variant mutant mice and found dose-independent increases in sleep after the thalidomide administration, indicating that the hypnotic effects of thalidomide are mediated by a target molecule distinct from CRBN.[4] Therefore, we hypothesize that modifying the chemical structure responsible for thalidomide's teratogenicity will retain its sleep-inducing properties while eliminating its harmful effects.
X-ray crystal structure revealed that thalidomide forms H-bonds with CRBN at the glutarimide group. Thus, we designed and synthesized three thalidomide derivatives (derivatives A, B, and C) with modifications to the glutarimide moiety to disrupt thalidomide-CRBN binding and investigated their effects on sleep-wake regulation. Thalidomide-induced hypnotic effects are characterized by increased non-rapid eye movement sleep (NREMS) duration and enhanced delta power during NREMS in mice. Thalidomide and all derivatives were intraperitoneally administered to wild-type C57BL/6 mice (10-14 weeks old), and electroencephalography/electromyography (EEG/EMG) was measured 24 hours after administration. Derivative A exhibited hypnotic effects comparable to those of thalidomide. In contrast, derivative B increased NREMS duration without enhancing delta power during NREMS, whereas derivative C completely lacked these hypnotic effects. These findings indicate that the structural element modified in derivative C is essential for the hypnotic effects of thalidomide. Collectively, our pharmacological analyses suggest that the hypnotic effects of thalidomide are mediated by a molecular mechanism distinct from its CRBN-binding interface.
[Reference][1] *Teratology*, 60, 306-321 (1999). [2] *Science*, 327, 1345-1350 (2010). [3] *Nat. Chem. Biol.*, 15, 1077-1084 (2019). [4] *Proc. Natl. Acad. Sci. USA.*, 117, 23106-23112 (2020).

**Disclosures: M. Nishida:** None. **T. Hasegawa:** None. **K. Kato:** None. **M. Kaushik:** None. **H. Funato:** None. **T. Ito:** None. **Y. Yamaguchi:** None. **H. Handa:** None. **T. Saitoh:** None. **M. Yanagisawa:** None.

**Poster**

**PSTR192: Sleep Regulation: Anatomy, Pharmacology, Behavior**

**Location:** WCC Halls A-C

**Time:** Monday, November 16, 2026, 1:00 PM - 5:00 PM

**Program #/Poster #:** PSTR192.02/EE17

**Topic:** G.07. Biological Rhythms and Sleep

**Support:** HP, USUHS, APG-70-12224
MDO, APG-70-12756
CDRMP, TP240634

**Title:** Trifluoperazine modulates aquaporin-4 polarization and sleep architecture but compromises cell-specific neurovascular integrity pathways in models of hypobaric hypoxia

**Authors:** D. L. DICKSTEIN[1], V. TSYTSAREV[2], X. XU[2], C. D. STIMPSON[1], B. C. PERRY[1], C. A. BROWNE[3], D. P. PERL[4], ***Z. GALDZICKI**[5];
[1]The Henry M. Jackson Fndn. for the Advancement of Military Medicine, Inc., Dept. of Pathology, Sch. of Medicine, Uniformed Services Univ. of the Hlth. Sci., Bethesda, MD; [2]The Henry M. Jackson Fndn. for the Advancement of Military Medicine, Inc., Dept. of Anatomy, Physiol. and Genetics, Sch. of Medicine, Uniformed Services Univ. of the Hlth. Sci., Bethesda, MD; [3]Biol. Sci., Munster Technological Univ., Cork, Ireland; [4]Pathology, Uniformed Services Univ., Bethesda, MD; [5]USU, Dept. of Anat, Physiol & Genetics, Sch. of Medicine, USU, Bethesda, MD

**Abstract:** Exposure to high altitude (HA) hypobaric hypoxia drives a cascade of physiological changes impacting metabolism, glymphatic function, and sleep patterns. We evaluated the therapeutic potential of trifluoperazine (TFP), an FDA-approved drug and potent calmodulin (CaM) inhibitor, in a murine model of hypobaric hypoxia (1 to 3 week simulated HA exposure at 5000 meters) where C57BL/6J mice received systemic TFP (10 mg/kg) or saline under HA or normobaric conditions. Behavioral and sleep architecture alterations were monitored via continuous telemetry and correlated with terminal hippocampal vascular density and aquaporin-4 (AQP4) localization. Behaviorally, HA impaired contextual fear memory recall, which remained unaffected by intraperitoneal TFP administration (10 mg/kg), though significant dose-dependent motor impairments were evident in a beam walk assay. Telemetry revealed that while HA exposure and TFP independently reduce wakefulness, TFP reduces wakefulness to the greatest extent in HA-exposed animals. For these TFP+HA animals, activity periods during dark and light phases were similar, demonstrating that TFP under hypobaric conditions disrupts circadian rhythms. Furthermore, hypobaric hypoxia itself increased REM sleep duration, an effect persisting after animals returned to normal conditions. In contrast, TFP reduced REM sleep duration, particularly in HA exposed cohorts. Regarding deep sleep, hypobaric conditions reduced slow-wave sleep (SWS) duration primarily during the light phase and less so during the dark phase; this deficit rapidly disappeared upon return to normal conditions. Crucially, TFP significantly increased SWS duration in HA-exposed animals, while only slightly altering control mice. At the molecular level, TFP significantly increased the astrocytic AQP4 polarization index

within the hippocampal dentate gyrus, reducing perivascular localization despite stable total protein expression. Conversely, stereological quantification (Space Balls probe) showed that TFP had no effect on neurovascular density in the CA1 region or posterior parietal cortex. These findings show TFP's effects are significantly stronger following HA hypoxia. However, because microglia are indispensable for maintaining blood-brain barrier tight-junction integrity under hypoxic stress, TFP's anti-phagocytic multitarget activity likely suppresses vital neuroimmune barrier support. Thus, highly selective, nondopaminergic CaM countermeasures are required to enhance fluid clearance without inducing sleep architectural liabilities or compromising microglial defenses in extreme environments.

**Disclosures: D.L. Dickstein:** None. **V. Tsytsarev:** None. **X. Xu:** None. **C.D. Stimpson:** None. **B.C. Perry:** None. **C.A. Browne:** None. **D.P. Perl:** None. **Z. Galdzicki:** None.

**Poster**

**PSTR192: Sleep Regulation: Anatomy, Pharmacology, Behavior**

**Location:** WCC Halls A-C

**Time:** Monday, November 16, 2026, 1:00 PM - 5:00 PM

**Program #/Poster #:** PSTR192.03/EE18

**Topic:** G.07. Biological Rhythms and Sleep

**Title:** Efficacy and Safety of Samelisant, an H3 Receptor Inverse Agonist, for the Treatment of Narcolepsy with or without Cataplexy: A Phase 3 Study

**Authors: *V. GOYAL**[1], P. JAYARAJAN[2], V. BENADE[2], A. K. SHINDE[2], S. JETTA[2], R. SUBRAMANIAN[2], S. PANDEY[2], R. ABRAHAM[2], A. MOHAMMED[2], V. CHINNEDDULA[2], R. NIROGI[2], V. JASTI[2];
[1]Suven Life Sci. Ltd, Hyderabad, India; [2]Suven Life Sci. Ltd., Hyderabad, India

**Abstract:** Narcolepsy is a rare neurological disorder characterized by a dysregulated sleep-wake cycle, with core clinical features including excessive daytime sleepiness (EDS), cataplexy, hypnopompic/hypnagogic hallucinations, and sleep paralysis. Current treatment options are for symptomatic management of narcolepsy, but they have limitations, with disease comorbidities further limiting treatment choices. Histamine 3 (H3) receptor blockade has been demonstrated to be a viable approach for the management of symptoms of narcolepsy. Samelisant (SUVN-G3031) is a selective and orally active H3 receptor inverse agonist. A Phase 2 clinical study in patients with narcolepsy (NCT04072380) indicated that the treatment with Samelisant significantly improved EDS symptoms. Samelisant is currently being evaluated in a Phase 3, double-blind, placebo-controlled, randomized study evaluating the efficacy and safety for the treatment of narcolepsy with or without cataplexy (NCT07540364; EU CT Number: 2026-527000-24-00). Study will assess the effect of Samelisant as compared to placebo, in approximately 240 patients recruited from the North America and Europe. Key inclusion criteria included a diagnosis of narcolepsy with or without cataplexy according to ICSD-3-TR/DSM-5-TR criteria; for participants with narcolepsy type 1 (NT1), an average of ≥4 weekly cataplexy events during the final 2 weeks of screening; an Epworth Sleepiness Scale (ESS) score ≥12 at

both Screening and Baseline; and a mean Maintenance of Wakefulness Test (MWT) sleep latency of <12 minutes at Baseline. The primary endpoint is the change from baseline in ESS total score at Week 12. Secondary endpoints include change from baseline in mean MWT score, Clinical Global Impression of Severity of Illness (CGI-S) score, Weekly Cataplexy Rate (WCR) in participants with NT1, and Narcolepsy Severity Scale for Clinical Trials (NSS-CT) score in participants with NT1 at Week 12. Results from this Phase 3 study will further characterize the efficacy and clinical utility of Samelisant in the treatment of narcolepsy.

**Disclosures: V. Goyal:** A. Employment/Salary (full or part-time):; Suven Life Sciences Ltd. **P. Jayarajan:** A. Employment/Salary (full or part-time):; Suven Life Sciences Ltd. **V. Benade:** A. Employment/Salary (full or part-time):; Suven Life Sciences Ltd. **A.K. Shinde:** A. Employment/Salary (full or part-time):; Suven Life Sciences Ltd. **S. Jetta:** A. Employment/Salary (full or part-time):; Suven Life Sciences Ltd. **R. Subramanian:** A. Employment/Salary (full or part-time):; Suven Life Sciences Ltd. **S. Pandey:** A. Employment/Salary (full or part-time):; Suven Life Sciences Ltd. **R. Abraham:** A. Employment/Salary (full or part-time):; Suven Life Sciences Ltd. **A. Mohammed:** A. Employment/Salary (full or part-time):; Suven Life Sciences Ltd. **V. Chinneddula:** A. Employment/Salary (full or part-time):; Suven Life Sciences Ltd. **R. Nirogi:** A. Employment/Salary (full or part-time):; Suven Life Sciences Ltd. **V. Jasti:** A. Employment/Salary (full or part-time):; Suven Life Sciences Ltd.

**Poster**

**PSTR192: Sleep Regulation: Anatomy, Pharmacology, Behavior**

**Location:** WCC Halls A-C

**Time:** Monday, November 16, 2026, 1:00 PM - 5:00 PM

**Program #/Poster #:** PSTR192.04/EE19

**Topic:** G.07. Biological Rhythms and Sleep

**Title:** Modulation of mouse histaminergic neurons and hippocampal and caudal hypothalamic network activity by endothelin-1 and norepinephrine

**Authors: *L. WEGMANN**[1], O. A. SERGEEVA[2];
[1]Inst. of Neural and Sensory Physiol., Heinrich-Heine-University Düsseldorf, Düsseldorf, Germany; [2]Inst. of Clin. Neurosciences and Med. Psychology, Heinrich-Heine-University Düsseldorf, Duesseldorf, Germany

**Abstract:** Norepinephrine (NE), released primarily from neurons of the locus coeruleus (LC), is a key neuromodulator in the regulation of cortical arousal. We have shown previously that Endothelin-1 (ET-1), a potent vasoconstrictor with some neuromodulatory functions, enhances the firing rate of central wake-promoting histaminergic neurons (HN) in brain slices of the caudal hypothalamus (cHPT). It also increases and synchronizes the activity of cultured neurons of cHPT grown on microelectrode arrays (MEAs). In contrast, ET-1 inhibits the activity of hippocampal (HPC) neurons, taken as a positive control. The effects of ET-1 on firing frequency of HN and cHPT are relatively small and develop delayed, indicating that other neuromodulators

may indirectly be involved. It has been shown that ET-1 enhances extracellular NE-levels in cHPT and modulates the activity of tyrosine hydroxylase. Therefore, we hypothesized that ET-1 and NE may synergistically modulate the activity of HN, which prompted us to study pharmacological responses and receptor expression profiles in a parallel fashion. Although aminergic inputs from LC are well characterized, there is no evidence that NE changes the firing properties of HN directly. Using single-cell RT-PCR, we studied now the co-expression pattern of adrenoreceptors (adra1 and adra2) and ET-receptors ($ET_A$ and $ET_B$) in identified dentate gyrus granule cells (DGgc) (n=13) and HN (n=14). The effects of ET-1 and NE on firing frequency were evaluated in mouse primary cultures of HPC and cHPT with MEA recordings and in identified HN using patch-clamp recordings in brain slices. Single-cell RT-PCR detected a high expression of adra1 and adra2 (both 85%) in DGgc, whereas the detection probability of adra2 (43%) but not adra1 (93%) was lower in HN. DGgc expressed only $ET_B$ (54%), whilst both $ET_A$ (7%) and $ET_B$ receptor (64%) were expressed in HN. In cHPT cultures, NE did not alter firing frequency but increased it in the presence of yohimbine (adra2-antagonist) and reduced it in the presence of prazosin (adra1-antagonist). HPC firing was inhibited by NE in a yohimbine-sensitive way, whilst co-application of prazosin did not significantly impair NE effects. These results correspond to the higher detection probability of adra2 in DGgc compared to HN ($p=0.046$). Patch-clamp recordings revealed that in 42% of HN adra2 can be pharmacologically detected, whereas in the majority of cells adra1 was dominant. We conclude that NE and ET-1 synergistically modulate HPC and HN, inducing inhibition and excitation, respectively. The responsiveness of HN to ET-1 and NE may influence the allostatic regulation of wakefulness, which awaits further analysis *in vivo.*

**Disclosures: L. Wegmann:** None. **O.A. Sergeeva:** None.

**Poster**

**PSTR192: Sleep Regulation: Anatomy, Pharmacology, Behavior**

**Location:** WCC Halls A-C

**Time:** Monday, November 16, 2026, 1:00 PM - 5:00 PM

**Program #/Poster #:** PSTR192.05/EE20

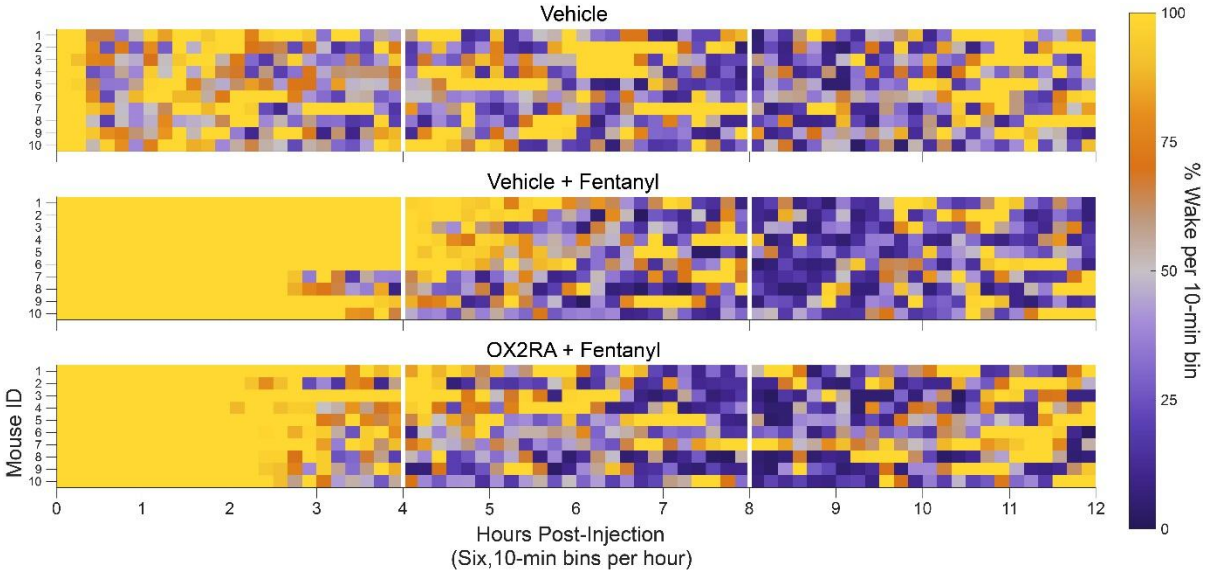
**Topic:** G.07. Biological Rhythms and Sleep

**Title:** A hidden Markov model provides novel insights into fentanyl-induced alterations in sleep dynamics of C57BL/6J mice that were not reversed by an orexin-2 receptor antagonist

**Authors: N. E. KALCHTHALER**, N. W. COOPER, J. FRAZIER, H. A. BAGHDOYAN, *R. LYDIC;
Psychology & Neurosci., Univ. of Tennessee, Knoxville, TN

**Abstract:** Dual orexin receptor antagonists are used to treat insomnia (10.1038/s41398-025-03571-5) and can diminish opioid-induced sleep disruption. Systemic administration of JNJ-10397049, an orexin-2 receptor antagonist (OX2RA), decreases fentanyl-induced sleep disruption in C57BL/6J (B6) mice (https://tinyurl.com/3vauhhmh). The present study used a hidden Markov model (HMM) (10.1007/s10928-011-9215-3) to quantify temporal features of

fentanyl-induced sleep disruption. Experiments were IACUC approved. Adult, male B6 mice (n = 10) were individually housed under a 12:12 light/dark cycle. Sleep states were scored via telemetric recordings of EEG and EMG. Treatment conditions included: 1) vehicle (15% DMSO); 2) vehicle followed by a sleep-disruptive dose of fentanyl (0.3 mg/kg); and 3) JNJ-10397049 (10 mg/kg) followed by fentanyl. Dependent measures were number and duration of wake and sleep episodes (non-rapid eye movement and rapid eye movement sleep combined). Measures were obtained during 30, 12-h, dark-period recordings. A two-state HMM quantified the probability of state transitions from wake to sleep, sleep to sleep, and sleep to wake. Sleep stability was defined as the probability of ($sleep_{t+1}$ | $sleep_t$). State transitions were analyzed in three time-blocks after injection (h 1-4, 5-8, 9-12). In h 1 to 4 sleep self-return was: 88.86% (vehicle), 79.82% (vehicle+fentanyl), and 77.84% (OX2RA+fentanyl). Higher percentages reflect sleep stability; lower percentages reflect greater sleep fragmentation. Thus, although the OX2RA increased the number of sleep episodes during h 1 to 4, the OX2RA did not mitigate the fentanyl-induced sleep fragmentation during this time-block. By h 5 to 8 h, sleep self-return was: 91.87% (vehicle), 89.82% (vehicle+fentanyl), and 90.92% (OX2RA+fentanyl). At 9 to 12 h, sleep self-return was: 92.35% (vehicle), 94.05% (vehicle+fentanyl), and 93.26% (OX2RA+fentanyl). Therefore, by h 5 to 8 and h 9 to 12, all treatment conditions converged toward a greater probability of sleep self-return (~90 to 94%), indicating sleep stability.




**Disclosures: N.E. Kalchthaler:** None. **N.W. Cooper:** None. **J. Frazier:** None. **H.A. Baghdoyan:** None. **R. Lydic:** None.

**Poster**

**PSTR192: Sleep Regulation: Anatomy, Pharmacology, Behavior**

**Location:** WCC Halls A-C

**Time:** Monday, November 16, 2026, 1:00 PM - 5:00 PM

**Program #/Poster #:** PSTR192.06/EE21

**Topic:** G.07. Biological Rhythms and Sleep

**Support:** NIH R01DA061243

**Title:** Impact of fentanyl-xylazine co-administration on sleep and the role of FGF21 in male and female mice

**Authors: *M. GAMBLE**[1], S. J. VILCA[1], G. GUINDON[1], R. W. LOGAN[2];
[1]Psychiatry, Univ. of Massachusetts Chan Med. Sch., Worcester, MA; [2]Psychiatry, Univ. of Massachusetts Chan Med. Sch., Hopkinton, MA

**Abstract: Background:** Recent shifts in the illicit opioid supply have led to widespread exposure to alpha-2-adrenergic agonists such as xylazine combined with the synthetic opioid fentanyl. This study aimed to characterize the preclinical effects of chronic fentanyl-xylazine co-exposure compared to either drug alone, with a specific focus on sleep-wake and immune signaling which are altered in opioid use. Notably, qualitative studies have reported potentially unique sleep-related effects and immune signaling changes due to fentanyl-xylazine, but quantitative investigations of fentanyl-xylazine on sleep and immune signaling remain scarce. **Methods:** Adult male and female C57BL/6J mice (12 weeks old, balanced by sex) were chronically administered saline, fentanyl (320ug/kg}, xylazine (5\mg/kg), or a fentanyl-xylazine combination for 7 days. Sleep-wake architecture was assessed via piezoelectric recordings. To evaluate the role of alpha-2-adrenergic signaling in sleep disruptions, the antagonist yohimbine was administered. To investigate systemic molecular shifts associated with chronic substance exposure, blood serum was analyzed via proteomics to quantify cytokine-related profiles. Additionally, the functional role of the brain penetrant hepatokine Fibroblast Growth Factor 21 signaling in the brain was evaluated in vivo through targeted biological modulation during the exposure paradigm. **Results:** Chronic fentanyl-xylazine co-exposure significantly modified sleep patterns with clear sex-dependent divergences. Co-exposed mice exhibited impaired non-rapid eye movement sleep recovery and increased rapid eye movement sleep. Additionally, fentanyl-xylazine uniquely reduced sleep bout durations compared to fentanyl alone. Yohimbine antagonism reversed these sleep architecture changes in a sex-selective manner. Peripheral molecular profiling revealed significantly elevated levels of plasma FGF21 specifically in the fentanyl-xylazine co-exposure group compared to the fentanyl-only and xylazine-only cohorts. Furthermore, experimental modulation of the FGF21 signaling effectively altered addiction-related behavioral responses, establishing a link between this metabolic factor and behavioral phenotype. **Conclusions:** These findings demonstrate that xylazine adulteration fundamentally alters the chronic phenotype of fentanyl exposure. The data underscore critical sex-specific responses to the drug combination on sleep-wake architecture and identify FGF21 as a novel, translationally relevant target of interest for opioid use disorder, sharing pathophysiological parallels with alcohol use disorder.

**Disclosures: M. Gamble:** None. **S.J. Vilca:** None. **G. Guindon:** None. **R.W. Logan:** None.

**Poster**

**PSTR192: Sleep Regulation: Anatomy, Pharmacology, Behavior**

**Location:** WCC Halls A-C

**Time:** Monday, November 16, 2026, 1:00 PM - 5:00 PM

**Program #/Poster #:** PSTR192.07/EE22

**Topic:** G.07. Biological Rhythms and Sleep

**Title:** Investigating the Contribution of the Locus Coeruleus to Opioid-induced Sleep Dysregulation

**Authors: *N. C. MIRANDA**[1], E. C. ANCELL[3], D. C. WITTEN[3], L. LI[2], M. R. BRUCHAS[4]; [2]Anesthesiol. and Pain Med., [1]Seattle Children's Res. Inst., Seattle, WA; [3]Dept of Statistics, [4]Dept. of Anesthesiol. and Pain Med., Univ. of Washington, Seattle, WA

**Abstract:** Sleep disruption is an underappreciated aspect of opioid use disorder, yet the underlying neural mechanisms of opioid-induced sleep dysregulation remain unclear. The locus coeruleus (LC), as the principal norepinephrine (NE) input into the cortex, is well-known to modulate sleep-wake states. Because opioids acutely inhibit LC function, we tested whether changes in noradrenergic signaling contribute to sleep disturbances during morphine exposure and withdrawal. We modeled subacute opioid use and withdrawal using an escalating morphine dosing paradigm (10-50 mg/kg over 5 days) followed by 3 days of natural withdrawal. A corresponding saline group was used as a control. Simultaneous fiber photometric, EEG/EMG, and behavioral recordings were performed in Dbh-cre mice expressing GCaMP6s in LC-NE neurons. Additional photometry experiments examined NE release using GRAB_NE2m in the downstream paraventricular thalamus (PVT) in wildtype mice, and the upstream inhibitory peri-LC activity using jGCaMP8f in Vgat-cre mice. Data were analyzed using ANOVA with Tukey's post-hoc tests. Viral expression was confirmed by histology. In our escalating morphine dosing paradigm, we did not observe significant changes in LC-NE activity during the days of morphine administration, but we found a significant increase in the event amplitude and an increased trend in event frequency in LC-NE activity during withdrawal days 1 ($p=0.028$) and 3 ($p=0.047$). On withdrawal day 1, these changes were associated with increased NREM delta power ($p=0.012$), reduced wakefulness ($p=0.040$), increased wake bout frequency ($p=0.049$), shorter wake bout duration ($p=0.032$), and a higher number of microarousals ($p=0.003$) compared with saline-treated controls ($n=7$/group). However, we did not find an altered relationship between LC-NE activity and EEG during days of morphine administration or during withdrawal. Additionally, we piloted mice to examine opioid-induced changes upstream and downstream of LC-NE activity and found peri-LC inhibitory activity ($n=6$) and PVT NE release ($n=6$) did not change during the days of opioid administration. However, both measures showed a reduction in amplitude activity during withdrawal (peri-LC: $p=0.037$; PVT NE: $p=0.043$). Morphine withdrawal increased LC-NE activity and altered sleep-related measures, while preliminary data suggest that these changes are associated with reduced peri-LC inhibition and PVT NE signaling. Together, these findings support a possible role for disrupted noradrenergic signaling contributing to sleep disruption, especially during opioid withdrawal. However, causality remains to be determined.

**Disclosures: N.C. Miranda:** None. **E.C. Ancell:** None. **D.C. Witten:** None. **L. Li:** None. **M.R. Bruchas:** None.

**Poster**

**PSTR192: Sleep Regulation: Anatomy, Pharmacology, Behavior**

**Location:** WCC Halls A-C

**Time:** Monday, November 16, 2026, 1:00 PM - 5:00 PM

**Program #/Poster #:** PSTR192.08/EE23

**Topic:** G.07. Biological Rhythms and Sleep

**Support:** R01 NS120395
R01 NS129552

**Title:** Pharmacological blockade of the kappa opioid receptor reduces sleep fragmentation and improves restorative sleep in aged mice

**Authors: *R. J. DOUGHERTY**[1], R. C. VIZIN[2], J. MARCA[2], C. KOPRUSZINSKI[2], A. THROWER[1], S. PATEL[1], E. NAVRATILOVA[2], S. L. COWEN[1], F. PORRECA[2];
[1]Dept. of Psychology, [2]Dept. of Pharmacol., Univ. of Arizona, Tucson, AZ

**Abstract:** Problems with initiating sleep, maintaining it, and achieving sufficient restorative sleep commonly occur with aging and are associated with a variety of negative health outcomes. Despite this, the mechanisms underlying age-related sleep disruptions are not yet fully understood. Recent preclinical evidence suggests that dynorphin, an endogenous agonist of the kappa opioid receptor (KOR), is involved in the regulation of arousal and sleep, and that administration of the KOR antagonist norbinaltorphimine (nor-BNI) can restore normal sleep patterns in a mouse model of chronic pain. Prior studies have also found links between elevated levels of brain dynorphin and aging, but the potential link between KOR signaling and age-related sleep disruption has yet to be investigated. Here, we evaluated whether pharmacological blockade of the KOR with nor-BNI can reduce sleep fragmentation and increase restorative sleep in aged mice. Aged (≥20 months old.; n = 19) and young adult (3 months old.; n = 17) male and female mice were implanted with EEG/EMG headmounts. After a recovery period, sleep was evaluated through EEG/EMG recordings performed for a 24-h baseline cycle, followed by a single injection of nor-BNI (10 mg/kg, i.p.). Two days later, EEG/EMG was recorded again for another 24-h cycle. We found that aged mice showed sleep fragmentation characterized by reduced NREM sleep duration, shorter bouts of NREM sleep, and increased awakenings compared to young adults. Aged mice also exhibited impaired regulation of normal sleep/wake brain oscillatory states defined by suppressed delta band power and increased theta power during NREM sleep, and conversely, elevated delta power and suppressed theta power while awake. Pharmacological blockade of the KOR with antagonist nor-BNI decreased wake time, increased NREM and REM sleep time during the light phase, and improved sleep fragmentation by reducing the number of wake and NREM bouts and increasing NREM bout duration in aged mice. Nor-BNI also increased delta power and decreased theta power during NREM sleep in aged mice, suggesting enhanced restorative sleep. Analyses assessing sex differences suggested that the effects of nor-BNI on improving sleep in aged mice were not sexually dimorphic. These results suggest that KOR signaling promotes age-related sleep disruption, and that pharmacological blockade of the KOR with antagonist drugs such as nor-BNI may improve sleep fragmentation and restorative sleep, highlighting KOR antagonists as a potential therapeutic strategy for sleep disturbances in aging.

**Disclosures: R.J. Dougherty:** None. **R.C. Vizin:** None. **J. Marca:** None. **C. Kopruszinski:** None. **A. Thrower:** None. **S. Patel:** None. **E. Navratilova:** None. **S.L. Cowen:** None. **F. Porreca:** E. Ownership Interest (stock, stock options, royalty, receipt of intellectual property rights/patent holder, excluding diversified mutual funds); Catalina Pharma, NuvieBio. F. Consulting Fees (e.g., advisory boards); Astra-Zeneca, Voyager, SiteOne Therapeutics, Nektar, Amgen, Acadia, Blackthorn, Teva, Eli Lilly, Hoba, Allergan, Abbvie, Ipsen, Proximagen.

**Poster**

**PSTR192: Sleep Regulation: Anatomy, Pharmacology, Behavior**

**Location:** WCC Halls A-C

**Time:** Monday, November 16, 2026, 1:00 PM - 5:00 PM

**Program #/Poster #:** PSTR192.09/EE24

**Topic:** G.07. Biological Rhythms and Sleep

**Title:** Age-related sleep fragmentation regulated by the hippocampus

**Authors: *S. NAGASHIMA**[1], Y. MUKAI[1], S. YAMAGUCHI[1], Z. ZHOU[1,2], H. NORIMOTO[1]; [1]Lab. for Neuroethology, Grad. Sch. of Science, Nagoya Univ., Nagoya, Japan; [2]Res. Inst. of Envrn. Med. Nagoya Univ., Nagoya, Japan

**Abstract:** Aging disrupts sleep. In particular, sleep fragmentation, characterized by frequent awakenings during the sleep period, is commonly observed in older adults. Sleep fragmentation not only impairs cognitive and behavioral performance but also increases the risk of neurological disorders. However, the neural mechanisms underlying age-related sleep fragmentation remain poorly understood. In this study, we focused on the hippocampus, a brain region best known for its roles in learning and memory. First, we labeled excitatory and inhibitory neurons in the hippocampus with fluorescent proteins and examined their projection patterns. We found that neurons from specific hippocampal subregions project to the lateral hypothalamus (LH), a key center for sleep-wake regulation. To investigate the role of the hippocampus in sleep fragmentation, we pharmacologically lesioned hippocampal neurons in aged mice (1.5-2 years old) and monitored sleep-wake states using electroencephalogram (EEG) and electromyogram (EMG) recordings. Hippocampal lesions reduced sleep fragmentation and increased the duration of sleep episodes in aged mice. Additionally, chemogenetic suppression of hippocampal neuronal activity reduced the number of microarousals in aged mice. These findings suggest that the hippocampus contributes to sleep regulation and a previously unrecognized hippocampus-hypothalamus circuit involved in age-related sleep fragmentation. To further investigate the neuronal dynamics underlying this pathway, we are currently performing simultaneous recordings from the hippocampus and LH. Ongoing analyses are examining how hypothalamic neuronal activity is modulated by hippocampal oscillations, including sharp wave ripples and theta oscillations, with the goal of elucidating circuit mechanisms linking hippocampal activity to sleep stability during aging.

**Disclosures: S. Nagashima:** None. **Y. Mukai:** None. **S. Yamaguchi:** None. **Z. Zhou:** None. **H. Norimoto:** None.

**Poster**

**PSTR192: Sleep Regulation: Anatomy, Pharmacology, Behavior**

**Location:** WCC Halls A-C

**Time:** Monday, November 16, 2026, 1:00 PM - 5:00 PM

**Program #/Poster #:** PSTR192.10/EE25

**Topic:** G.07. Biological Rhythms and Sleep

**Support:** NIH Grant R01 AG071675
NIH Grant TL1 TR002016
NIH Grant UL1 TR002014
Children's Miracle Network Research Grant (2022-2025) and Trainee Grant (2023-2025)
Penn State Center for Biodevices Grace Woodward Seed Grant (2025)

**Title:** Dopamine $D_1$ receptor agonists as a therapeutic strategy for age-related sleep disruption

**Authors: *A. P. BASSETT**[1,2], J. FANG[3], Y. YANG[1,2];
[1]Neurosci. and Exptl. Therapeut., Penn State Univ. Col. of Med., Hershey, PA; [2]Penn State Neurosci. Inst., Hershey, PA; [3]Psychiatry and Behavioral Hlth., Pennsylvania State Univ. Col. of Med., Hershey, PA

**Abstract:** Sleep is a dynamic physiological process that changes naturally throughout the course of aging. Although regarded as nonpathological, sleep disruption is commonly observed in healthy aging sleep and is characterized by increased sleep fragmentation and excessive daytime sleepiness, reflecting altered sleep-wake architecture. Importantly, aging is also associated with a gradual alteration in regional dopaminergic signaling due to decreased dopamine production and changes in receptor density. Since dopamine is crucial for the regulation of brain circuits gating sleep and arousal, developing therapies that can restore these age-related changes in dopaminergic input may reduce sleep disruption. Dopamine $D_1$ receptor ($D_1R$) agonists have been investigated for their potential in alleviating cognitive deficits and sleep disruption in young and diseased (e.g., Parkinson's) models. These prior studies, however, did not consider sleep disruption in normal aging as a distinct neurobiological condition different from those observed in young or neurodegenerative disease states. Therefore, it remains unclear whether $D_1R$-targeted interventions, including dosing and treatment timing paradigms studied in young or disease models, can be effectively translated to aging. In this study, we conducted continuous 24-hour EEG/EMG sleep recordings in aged male Fischer rats (22 mo.) and examined the acute effect of two $D_1R$ agonists on sleep architecture. Specifically, we used a prototypical (SKF 38393) and a new generation (PF-06256142) $D_1R$ agonist. Subjects were assigned to an experimental group and received a single dose (100 nmol/kg) of SKF 38393, PF-06256142, or vehicle, three hours prior to light onset. We hypothesize that timing of $D_1R$ agonist administration is critical for attenuating age-related sleep disruption and does so by restoring high arousal wake prior to sleep. Our results indicate that these compounds increase subjects' wake duration immediately following administration and temporarily decrease REM sleep duration prior to their predominant rest phase. These findings suggest that $D_1R$ agonists may reduce premature REM

sleep, thereby promoting more restorative sleep later during the predominant rest phase. Continued exploration of these compounds will clarify the role of $D_1R$ signaling in regulating dopamine-dependent sleep stages in aged adult rats, providing a foundation for the development of therapeutics that will markedly improve sleep's restorative properties. In turn, the use of these compounds may also indirectly improve age-related declines in sleep-dependent neuronal processes, including cognition and glymphatic clearance.

**Disclosures: A.P. Bassett:** None. **J. Fang:** E. Ownership Interest (stock, stock options, royalty, receipt of intellectual property rights/patent holder, excluding diversified mutual funds); J. F. is the owner of Biosoft Studio and is the owner and creator of SleepMaster™ and SleepAnalysis™ programs which were used for data collection and analysis in this study.. **Y. Yang:** None.

**Poster**

**PSTR192: Sleep Regulation: Anatomy, Pharmacology, Behavior**

**Location:** WCC Halls A-C

**Time:** Monday, November 16, 2026, 1:00 PM - 5:00 PM

**Program #/Poster #:** PSTR192.11/EE26

**Topic:** G.07. Biological Rhythms and Sleep

**Support:** National Natural Science Foundation of China (no. 82288101)
National Natural Science Foundation of China (no.82501781).

**Title:** A gut microbiota-bile acid-TGR5 axis regulates sleep behaviors

**Authors: *Z. WANG**[1], L. LU[2];
[1]Inst. of Brain Sci. and Brain-inspired Research, Shandong First Med. Univ., Jinan, China; [2]Inst. Mental Health,Peking Univ. Sixth Hosp., Beijing City, China

**Abstract:** The gut microbiota has emerged as an important regulator of sleep, yet the mechanisms underlying gut-brain metabolic communication remain poorly understood. Here, we found that sleep deprivation altered gut microbial composition and bile acid profiles in humans. Depletion of the gut microbiota in mice disrupted bile acid homeostasis and led to profound changes in sleep-wake behaviors. Both central and peripheral administration of the TGR5 agonist INT777 promoted sleep and reduced wakefulness. These effects were associated with marked alterations in bile acid metabolomic profiles in the serum and hypothalamus. Mechanistically, selective knockdown of TGR5 in lateral hypothalamic area (LHA) orexin neurons increased wakefulness, whereas TGR5 overexpression in the LHA produced the opposite phenotype. Electrophysiological recordings further revealed that activation of TGR5 by INT777 modulated the intrinsic excitability of orexin neurons. In addition, we identified *Haemophilus parainfluenzae* as a key commensal bacterium that promotes sleep-related behaviors. Collectively, our findings establish a gut microbiota-bile acid-TGR5 signaling axis that regulates sleep by modulating the activity of LHA orexin neurons.

**Disclosures: Z. Wang:** None. **L. Lu:** None.

**Poster**

**PSTR192: Sleep Regulation: Anatomy, Pharmacology, Behavior**

**Location:** WCC Halls A-C

**Time:** Monday, November 16, 2026, 1:00 PM - 5:00 PM

**Program #/Poster #:** PSTR192.12/EE27

**Topic:** D.01. Neurotoxicity, Inflammation, and Neuroprotection

**Title:** Sleep Deprivation-Induced Neurobehavioral Alterations: Evidence for Social and Affective Vulnerability Without Motor Deficits

**Authors: *A. ALI**[1], A. S. AHMAD[1], M. AHMED[2];
[1]Dept. of Neurol., Henry Ford Hlth., Detroit, MI; [2]Henry Ford Hlth., DETROIT, MI.

**Abstract: Sleep Deprivation-Induced Neurobehavioral Alterations: Evidence for Social and Affective Vulnerability Without Motor Deficits**Abid Ali, Mena Fatma, Mohammad Nematullah, Md Saddam Hussain, Mohammad Ejaz Ahmed, Shailendra Giri, Abdullah Shafique Ahmad*
**Background:** Sleep is a fundamental homeostatic process, and its disruption is increasingly recognized as a primary modulator of neuroimmune function. Chronic sleep deprivation (SD) triggers systemic inflammation and alters pro-inflammatory signaling, contributing to significant neurobehavioral decline. This study aimed to characterize the specific physiological profile and behavioral changes induced by 12 days of prolonged sleep loss in a murine model.**Methods:** Mice were divided into control and SD groups, with the latter subjected to a sleep deprivation protocol of 8 hours/day for 12 days. We monitored systemic markers of homeostasis (food/water intake, body weight) and conducted a comprehensive behavioral battery. This included the hanging wire and narrow beam tests (motor function), elevated plus maze (EPM) and open field activity (anxiety/exploration), and the social interaction and sucrose splash tests (affective/motivational behavior).**Results:** SD mice significantly increased water intake, while food consumption and body weight remained stable, suggesting stress-axis activation rather than general metabolic failure. Behaviorally, a clear divergence emerged. Gross motor coordination and muscular strength were largely preserved, indicating that 12 days of SD does not cause primary motor impairment. However, SD mice exhibited profound affective deficits, including increased anxiety-like responses in the EPM (reduced open-arm exploration) and impaired social engagement. Notably, the sucrose splash test revealed diminished grooming behavior, signifying a loss of motivation and self-care.**Conclusion:** These findings demonstrate that chronic sleep disturbance is sufficient to drive specific neurobehavioral dysfunctions, primarily social and motivational, independent of physical fatigue. These alterations align with neuroimmune dysregulation and stress-axis imbalance. Our results highlight sleep disruption as a critical, independent risk factor for psychiatric-like phenotypes, emphasizing the need for sleep-centric interventions in maintaining neurobehavioral health.

**Disclosures: A. Ali:** None. **A.S. Ahmad:** None.

**Poster**

**PSTR192: Sleep Regulation: Anatomy, Pharmacology, Behavior**

**Location:** WCC Halls A-C

**Time:** Monday, November 16, 2026, 1:00 PM - 5:00 PM

**Program #/Poster #:** PSTR192.13/EE28

**Topic:** G.07. Biological Rhythms and Sleep

**Title:** Neuromodulatory Disruption Links Peripheral Inflammation to Sleep-like Brain States

**Authors: *M. XU**;
ION, Chinese Acad. of Sci., Shanghai City, China

**Abstract:** Systemic immune activation potently drives sleep-like states, yet the neural circuitry underlying this process remains elusive. We demonstrate that peripheral lipopolysaccharide (LPS) challenge initiates neuronal activation in the nucleus tractus solitarius, culminating in NREM-like EEG synchrony. This brain-state shift is accompanied by a robust surge in norepinephrine (NE) and serotonin (5-HT). Critically, pharmacological suppression of 5-HT transmission significantly attenuated these EEG abnormalities, positioning serotonergic modulation as a key node in this pathway. We thus delineate a causal chain in which peripheral inflammation disrupts brainstem neuromodulatory systems, precipitating global brain-state dysregulation. Our findings establish a new framework for how immune-neural communication hijacks sleep-wake circuits, offering new mechanistic insight into neuroinflammatory sleep disturbances.

**Disclosures: M. Xu:** None.

**Poster**

**PSTR192: Sleep Regulation: Anatomy, Pharmacology, Behavior**

**Location:** WCC Halls A-C

**Time:** Monday, November 16, 2026, 1:00 PM - 5:00 PM

**Program #/Poster #:** PSTR192.14/EE29

**Topic:** G.07. Biological Rhythms and Sleep

**Title:** Environmental Temperature Modulates Sleep Apnea and Respiratory-Neural Coupling

**Authors: *K. DEHDAR**[1,2], E. NEUBERG[1,2], B.-M. GU[1,2,3];
[1]Ctr. for Discovery and Innovation, Hackensack Meridian Hlth., Nutley, NJ; [2]Neurosci. Inst., Hackensack Meridian JFK Univ. Med. Ctr., Edison, NJ; [3]Dept. of Neurol., Hackensack Meridian Sch. of Med., Nutley, NJ

**Abstract:** Environmental temperature critically influences sleep architecture and respiratory physiology. Previous studies have shown that environmental temperature affects deep sleep and slow-wave activity. However, its effects on sleep apnea remain unclear, particularly in rodent

models. Moreover, to our knowledge, no study has investigated the effect of environmental temperature on respiratory-neural coupling, despite emerging evidence that respiration can shape neural activity across distributed brain networks. Therefore, we examined temperature-dependent changes in sleep apnea and respiration-neural coupling. We focused on substantia nigra pars reticulata (SNr), a basal ganglia output structure, as this area has shown state-dependent coupling to the respiratory rhythm and has recently been recognized as being involved in both sleep and respiratory regulation. Simultaneous local field potential (LFP) recordings from the SNr and motor cortex (M1), together with diaphragm electromyographic (EMG) recordings, were obtained in freely behaving adult mice across sleep-wake cycles. Two different temperature conditions (23°C and 30°C) were maintained for each sleep session by an under-floor heating system. Respiratory rate, spontaneous apnea frequency, and respiration-neural coupling were quantified across non-rapid eye movement (NREM) sleep, rapid eye movement (REM) sleep, and quiet wakefulness. Higher environmental temperature significantly reduced respiratory rate and increased spontaneous apnea frequency. Elevated temperature also enhanced respiration-neural coupling across behavioral states, indicating stronger entrainment of neural oscillations to respiratory rhythms under warmer conditions. Together, these findings demonstrate temperature-dependent changes in respiration and the entrainment of neural oscillations to the respiratory rhythm. These results identify temperature as an important modulator of respiration-brain interactions and reveal a novel link between thermal state, breathing dynamics, and respiratory coupling within basal ganglia circuits during sleep.

**Disclosures: K. Dehdar:** None. **E. Neuberg:** None. **B. Gu:** None.

**Poster**

**PSTR192: Sleep Regulation: Anatomy, Pharmacology, Behavior**

**Location:** WCC Halls A-C

**Time:** Monday, November 16, 2026, 1:00 PM - 5:00 PM

**Program #/Poster #:** PSTR192.15/EE30

**Topic:** G.07. Biological Rhythms and Sleep

**Support:** NIH Grant R21 F076418
Gilmore Fellowship University of Michigan Sleep Disorder Center Award G028528

**Title:** Electrophysiologic characterization of sleep-wake patterns in the newly established Dec2-disrupted Grass Rat (DDGR) model of natural short sleep.

**Authors: *D. BEREZHNOI**[1], A. BRANNOCK[1], L. YAN[3], B. O. WATSON[2], N. OGNJANOVSKI[2];
[2]Dept. of Psychiatry, [1]Univ. of Michigan, Ann Arbor, MI; [3]Psychology, Michigan State Univ., East Lansing, MI

**Abstract:** The dec2 gene (Bhlhe41 Gene ID: 117715269) codes for a transcriptional repressor binding to many downstream gene targets, is thought of as a negative component of the circadian

clock and is known to underlie a rare phenotype in humans - Familial Natural Short Sleep (FNSS). Currently there is no reliable animal model to study the function of this gene, and the only reported results are from dec2-P384R mouse model, in which NREM and REM were just 6% and 2% reduced. However, mice used are nocturnal and the lack of melatonin in C57BL/6J mice hinders the translational potential of the current model. We address these limitations by utilizing Nile Grass Rat (Arvicanthis niloticus), a diurnal rodent model, in our research. The main objective of this study is to characterize the contribution of dec2 gene to the regulation of the sleep-wake cycle. We focused on the hDec2-P384R (P324 in rodents) mutation and used CRISPR gene editing to make 3 gene-edited lines, which we named Dec2-disrupted Grass Rats (DDGR). These consist of one in-frame (D9) and two frame shift mutations (D4, D20) in the gene of interest. Initial phenotypic characterization of sleep-wake patterns in those lines was performed with actigraphy system in the home cage, and all animals demonstrated increased activity, with the bigger D20 frame shift mutation (20bp from Y318-P324) getting the most prominent change in the activity patterns compared to WT littermates. We further observe both a decrease in the total sleep (~2hrs) and delay in the sleep onset in the dark phase (~1hr) when comparing DDGRs to WT controls. To better understand the microstructure of sleep we performed electrophysiologic characterization of sleep-wake patterns using animals implanted with cranial EEG screws. EEG was recorded along with actigraphy chronically for multiple days where we assessed 3 brain states: wake, NREM and REM. Analysis of this data revealed changes in DDGRs were specific to the dark phase: higher NREM sleep bout length in the middle of the dark phase and changed distribution of REM sleep periods over the course of the night. The spectral power of EEG signal has also shown the increase in multiple bands (delta and theta frequencies) both between the WT and mutants, as well as between different mutant lines. Overall, we have successfully established and characterized DDGR animal model, showing distinct behavioral and electrophysiological phenotypes. This extended phenotypic characterization confirms the role of dec2 in the overall regulation of sleep-wake cycle, but also points to the nuanced role it may play in regulating the microstructure of the night sleep cycle.

**Disclosures: D. Berezhnoi:** None. **A. Brannock:** None. **L. Yan:** None. **B.O. Watson:** None. **N. Ognjanovski:** None.

**Poster**

**PSTR192: Sleep Regulation: Anatomy, Pharmacology, Behavior**

**Location:** WCC Halls A-C

**Time:** Monday, November 16, 2026, 1:00 PM - 5:00 PM

**Program #/Poster #:** PSTR192.16/EE31

**Topic:** G.07. Biological Rhythms and Sleep

**Support:** R01 NS078410

**Title:** Sex-Specific Regulation of REM and NREM Recovery Sleep After Stress

**Authors: *M. R. RALSTON**, M. KAHAN, T. NG, E. LEE, K. TAMAI, K. N. PAUL; Integrative Biol. and Physiol., UCLA, Los Angeles, CA

**Abstract:** Sex differences in the prevalence and severity of sleep impairments are well-documented and are often more pronounced under pathological conditions. One such condition is insomnia, a significant public health concern that disproportionately affects women and is frequently associated with stress. Sleep is regulated by a homeostatic mechanism that allows the body to recover from sleep loss during subsequent sleep opportunities. However, sex differences in recovery from sleep loss are often influenced by the stress associated with sleep deprivation. To investigate these sex differences, we characterized sleep architecture using electroencephalographic/electromyographic (EEG/EMG) recordings in the Four Core Genotype (FCG) mouse model, which dissociates phenotypic sex from chromosomal sex and enables precise manipulation of genetic and hormonal variables. This mouse line features four distinct urogenital groups (males: $XY^{Sry}$, $XX^{Sry}$; females $XY^{-}$, $XX^{-}$). After 24 hours of baseline recording in adults, we subjected the mice to 1 hour of restraint stress (RS) or gentle handling (GH) sleep deprivation during the light phase in a 12-hour light:12-hour dark cycle. We recorded recovery sleep following either RS or GH and compared sleep architecture across experimental groups (male n=17, female n=17). Initial findings have revealed that compared to female mice, male mice exhibit increased NREM sleep, increased REM sleep, and decreased wake amount (NREM: $XY^{Sry}$ $p<0.05$; REM: $XY^{Sry}$ , $XX^{Sry}$ $p<0.05$; wake: $XY^{Sry}$ , $XX^{Sry}$ $p<0.001$; Kruskal-Wallis test; Wilcox post-hoc test) during the 18-hour recovery period following stress. After performing prepubertal gonadectomy (GDX) surgery at postnatal day 21 (male n=14, female n=14; Kruskal-Wallis test; Wilcox post-hoc test), sex differences in recovery sleep were eliminated across all experimental groups, which suggests that gonadal hormones may play an organizational role during development and are a potential driving factor behind these sex differences in adulthood.

**Disclosures: M.R. Ralston:** None. **M. Kahan:** None. **T. Ng:** None. **E. Lee:** None. **K. Tamai:** None. **K.N. Paul:** None.

**Poster**

**PSTR192: Sleep Regulation: Anatomy, Pharmacology, Behavior**

**Location:** WCC Halls A-C

**Time:** Monday, November 16, 2026, 1:00 PM - 5:00 PM

**Program #/Poster #:** PSTR192.17/EE32

**Topic:** G.07. Biological Rhythms and Sleep

**Support:** AMED Grant JP21zf0127005
KAKENHI Grant 24K09680
JST-SPRING Grant HJI06015
JSPS DC1 Grants 25KJ0694

**Title:** A neural circuit for sleepiness in the $Sik3^{Sleepy}$ mutant mice

**Authors: *K. FAN**[1,2], D. KUMAR[1,2], M. KAYAMARE[1,2], D. M. HIEN[1,2], T. FUJIYAMA[1,2], Y. ISHIKAWA[1,2], J. DIAZ[1,2], H. FUNATO[1,2,3], M. YANAGISAWA[1,2,4];
[1]Intl. Inst. for Integrative Sleep Med. (WPI-IIIS), Univ. of Tsukuba, Ibaraki, Japan; [2]Tsukuba

Inst. for Advanced Res. (TIAR), Univ. of Tsukuba, Ibaraki, Japan; [3]Toho Univ. Sch. of Med., Tokyo, Japan; [4]Dept. of Mol. Genetics, Univ. of Texas Southwestern Med. Ctr., Dallas, TX

**Abstract:** A neural process that regulates sleepiness in mammals remains elusive. *Sleepy* ($Sik3^{Slp/+}$) mutant mice, which spend more time in non-rapid eye movement sleep (NREMs) and display a higher sleep pressure, as reflected by increased NREMs EEG delta spectral power, is a suitable model mouse to investigate the neural mechanism of sleepiness. We selected claustrum, a subcortical nucleus that coordinates delta activity, as a candidate neural site to study sleepiness. We found that a lower activity of claustrum neuronal population during NREMs driven by reduced intrinsic cellular excitability underlies increased delta spectral power in *Sleepy* mice. Chemogenetic inhibition of these neurons increases NREMs delta power. Furthermore, overexpression of SIK3 (SLP) in the claustrum neurons of wild-type mice was sufficient to increase delta power. These results indicate that the intrinsic excitability of claustrum neurons plays a crucial role in determining sleep pressure.

**Disclosures: K. Fan:** None. **D. Kumar:** None. **M. Kayamare:** None. **D.M. Hien:** None. **T. Fujiyama:** None. **Y. Ishikawa:** None. **J. Diaz:** None. **H. Funato:** None. **M. Yanagisawa:** None.

**Poster**

**PSTR192: Sleep Regulation: Anatomy, Pharmacology, Behavior**

**Location:** WCC Halls A-C

**Time:** Monday, November 16, 2026, 1:00 PM - 5:00 PM

**Program #/Poster #:** PSTR192.18/FF1

**Topic:** G.07. Biological Rhythms and Sleep

**Support:** JSPS KAKENHI 25K09830
JSPS KAKENHI 25KK0088

**Title:** Sleep-wake control by neurotensinergic neurons in the lateral hypothalamus

**Authors: *F. NAGANUMA**[1], M. KHANDAY[2], K. HIRANO[1], T. YOSHIKAWA[1], R. VETRIVELAN[2];
[1]Neuropharm., Hokkaido University, Grad. Sch. of Med., Sapporo, Hokkaido, Japan; [2]Dept. of Neurol., Beth Israel Deaconess Med. Ctr., Boston, MA

**Abstract:** The role of the lateral hypothalamus (LH) in arousal regulation has been well established, but this region is heterogeneous and contains several neurochemically distinct cell populations. Neurons expressing orexins (OX) are considered a primary arousal-regulating cell population in this region. Although cytotoxic lesions of the LH reduce daily wake levels, selective loss of OX neurons alone does not alter wake amounts, suggesting the presence of additional wake-promoting populations within the LH. In this regard, we have recently identified another peptidergic population expressing neurotensin ($Nts^{LH}$), which promotes robust arousal when activated using optogenetic or chemogenetic methods (F. Naganuma et al., PLoS Biol. 2019). However, their precise contribution to normal arousal remains unclear. To address this

issue, we first monitored $Nts^{LH}$ neuronal activity across sleep-wake cycles using in vivo calcium imaging. For this, we injected Cre-dependent adeno-associated viral vectors encoding GCaMPs into the LH of Nts-Cre mice expressing Cre recombinase selectively in Nts neurons. We performed photometry recordings together with polysomnography during the light period. We found that $Nts^{LH}$ neuron activity increased concomitantly with wake onset and remained high throughout the wake episode. Activity was also elevated during various wake-related behaviors, including locomotion. While activity also increased during NREM-to-REM transitions, we then selectively ablated these neurons by injecting a Cre-dependent AAV encoding diphtheria toxin A subunit (AAV-DTA) into the LH of Nts-Cre mice. We found that loss of $Nts^{LH}$ neurons markedly reduced total wake time, increased wake fragmentation and EEG delta power during wakefulness, and decreased locomotor activity, demonstrating that $Nts^{LH}$ neurons are essential for maintaining normal arousal levels. Although these neurons were also highly active during REM sleep, their loss did not alter REM sleep levels, indicating that they are not necessary for REM sleep regulation.

**Disclosures: F. Naganuma:** None. **M. Khanday:** None. **K. Hirano:** None. **T. Yoshikawa:** None. **R. Vetrivelan:** None.

**Poster**

**PSTR192: Sleep Regulation: Anatomy, Pharmacology, Behavior**

**Location:** WCC Halls A-C

**Time:** Monday, November 16, 2026, 1:00 PM - 5:00 PM

**Program #/Poster #:** PSTR192.19/FF2

**Topic:** G.07. Biological Rhythms and Sleep

**Title:** Orexin/ataxin-3 model mice show sleep and neurochemical phenotypes reminiscent of narcolepsy type I (NT1)

**Authors: *D. D. AGUILAR**, S. MANCA, P. BATHALA, P. KRISHNASWAMI, Y. CHEN, M. LEVIT, S. COLLINS, L. GUO, B. ZHANG, S. SARDI, J. C. DODGE, S. GIERA, E. H. JENSEN;
Sanofi, Cambridge, MA

**Abstract:** Narcolepsy Type I (NT1) is a rare neurodegenerative disease characterized by the loss of orexin or orexin-producing neurons. Orexin or hypocretin plays a critical role in regulating central nervous system (CNS) and peripheral functions including the maintenance of wakefulness, food and energy homeostasis, and stress. In NT1 patients, orexin loss leads to excessive daytime sleepiness (EDS), cataplexy, weight gain, hypertension, and many other psychiatric and cognitive issues. Importantly, novel treatments are urgently needed for NT1 patients because current treatments leave many debilitating symptoms unaddressed. Here, we describe the characterization of narcolepsy-related phenotypes in the orexin/ataxin-3 model of NT1, which are reported to feature orexin neuron loss starting after postnatal day 4. We previously presented that orexin/ataxin-3 mice have differences in weight gain, nighttime activity, and orexin A levels. Using electroencephalogram/electromyography (EEG/EMG), we

demonstrate narcoleptic sleep phenotypes including lower nighttime wake bout length, enhanced REM sleep, and potential cataplexy in orexin/ataxin-3 mice. Additional behavioral changes include enhanced grooming, resting, and sniffing in the open field assay. Olink and MSD panels revealed an enhanced inflammatory profile and higher leptin levels in the plasma of orexin/ataxin-3 mice, while an internally developed SIMOA assay confirmed lower orexin A levels in the plasma and brain. RNA sequencing from the prefrontal cortex showed a downregulation of genes associated with locomotion, sleep/wake regulation, and dopaminergic signaling. Indeed, we observed a decrease in dopamine levels in the brain and altered dopamine turnover in the blood of orexin/ataxin-3 mice. In summary, our results show that orexin/ataxin-3 mice have neurochemical phenotypes that complement their behavioral deficits. They recapitulate many aspects of narcolepsy and demonstrate the potential of these mice as a preclinical model for the development of novel therapies for NT1. Disclosures: This study was funded by Sanofi. All authors are Sanofi employees and may hold shares and/or stock options in the company. All in vivo studies were conducted according to IACUC approved protocols in an accredited institution following institutional, local, state, and country requirements.

**Disclosures: D.D. Aguilar:** A. Employment/Salary (full or part-time):; Sanofi. E. Ownership Interest (stock, stock options, royalty, receipt of intellectual property rights/patent holder, excluding diversified mutual funds); Sanofi. **S. Manca:** A. Employment/Salary (full or part-time):; Sanofi. E. Ownership Interest (stock, stock options, royalty, receipt of intellectual property rights/patent holder, excluding diversified mutual funds); Sanofi. **P. Bathala:** A. Employment/Salary (full or part-time):; Sanofi. E. Ownership Interest (stock, stock options, royalty, receipt of intellectual property rights/patent holder, excluding diversified mutual funds); Sanofi. **P. Krishnaswami:** A. Employment/Salary (full or part-time):; Sanofi. E. Ownership Interest (stock, stock options, royalty, receipt of intellectual property rights/patent holder, excluding diversified mutual funds); Sanofi. **Y. Chen:** A. Employment/Salary (full or part-time):; Sanofi. E. Ownership Interest (stock, stock options, royalty, receipt of intellectual property rights/patent holder, excluding diversified mutual funds); Sanofi. **M. Levit:** A. Employment/Salary (full or part-time):; Sanofi. E. Ownership Interest (stock, stock options, royalty, receipt of intellectual property rights/patent holder, excluding diversified mutual funds); Sanofi. **S. Collins:** A. Employment/Salary (full or part-time):; Sanofi. E. Ownership Interest (stock, stock options, royalty, receipt of intellectual property rights/patent holder, excluding diversified mutual funds); Sanofi. **L. Guo:** A. Employment/Salary (full or part-time):; Sanofi. E. Ownership Interest (stock, stock options, royalty, receipt of intellectual property rights/patent holder, excluding diversified mutual funds); Sanofi. **B. Zhang:** A. Employment/Salary (full or part-time):; Sanofi. E. Ownership Interest (stock, stock options, royalty, receipt of intellectual property rights/patent holder, excluding diversified mutual funds); Sanofi. **S. Sardi:** A. Employment/Salary (full or part-time):; Sanofi. E. Ownership Interest (stock, stock options, royalty, receipt of intellectual property rights/patent holder, excluding diversified mutual funds); Sanofi. **J.C. Dodge:** A. Employment/Salary (full or part-time):; Sanofi. E. Ownership Interest (stock, stock options, royalty, receipt of intellectual property rights/patent holder, excluding diversified mutual funds); Sanofi. **S. Giera:** A. Employment/Salary (full or part-time):; Sanofi. E. Ownership Interest (stock, stock options, royalty, receipt of intellectual property rights/patent holder, excluding diversified mutual funds); Sanofi. **E.H. Jensen:** A. Employment/Salary (full or part-time):; Sanofi. E. Ownership Interest (stock, stock options, royalty, receipt of intellectual property rights/patent holder, excluding diversified mutual funds); Sanofi.

**Poster**

**PSTR192: Sleep Regulation: Anatomy, Pharmacology, Behavior**

**Location:** WCC Halls A-C

**Time:** Monday, November 16, 2026, 1:00 PM - 5:00 PM

**Program #/Poster #:** PSTR192.20/FF3

**Topic:** G.07. Biological Rhythms and Sleep

**Support:** F31HL165896
R01NS131664

**Title:** Loss of C1ql3 from hypocretin/orexin neurons alters vigilance state stability

**Authors: *L. BOYD**[1], W. P. ARMSTRONG, IV[2], D. C. MARTINELLI[4], M. E. CARTER[5], A. C. JACKSON[3];
[1]Univ. of Connecticut, Storrs Mansfield, CT; [2]Physiol. and Neurobio., Univ. of Connecticut, Storrs, CT; [3]Physiol. and Neurobio., Univ. of Connecticut, Storrs Mansfield, CT; [4]Neurosci., Univ. of Connecticut Hlth., Farmington, CT; [5]Biol., Williams Col., Williamstown, MA

**Abstract:** The hypocretin/orexin (H/OX) neuropeptides are exclusively expressed by a subpopulation of neurons in the vertebrate lateral hypothalamic area (LHA) and is a critical regulator of sleep-wake and motivated behaviors. Loss of H/OX signaling through deletion of the neuropeptides, their receptors, or ablation of H/OX neurons produces key features of the human sleep disorder narcolepsy with cataplexy, including excessive daytime sleepiness, fragmented sleep-wake states, and episodes of emotion-triggered muscle weakness. Using single-cell transcriptomic analysis of the LHA, we identified several molecular markers enriched in H/OX neurons, including complement C1q-like protein 3 (C1QL3), a secreted synaptic adhesion protein implicated in synaptic stability in other neural circuits. Given the role of H/OX neurons in maintaining wakefulness, we investigated whether loss of C1ql3 from H/OX neurons alters sleep-wake behavior. We performed 24-hour EEG/EMG recordings in C1ql3 conditional knockout (cKO) mice and littermate controls. Spectral analyses revealed increased theta power (4-9 Hz) during wakefulness and elevated high-theta power (~7-9 Hz) during rapid eye movement (REM) sleep, as well as decreased beta power (16-24 Hz) during non-rapid eye movement (NREM) sleep. Several of these spectral abnormalities resemble EEG alterations reported in narcolepsy and excessive daytime sleepiness in humans. We also observed increased delta power (0.5-4 Hz) during NREM sleep, another feature reported in narcolepsy patients. In addition, C1ql3 cKO mice exhibited alterations in sleep-related events, including sleep spindles and hypersynchronous paroxysmal theta events. Prominent sex differences were observed in spectral measures across NREM and REM sleep, along with modest alterations in sleep architecture during the early dark phase. Notably, we found no evidence of cataplexy in C1ql3 cKO mice, indicating that loss of C1ql3 is not sufficient to recapitulate severe narcoleptic phenotypes. Together with anatomical evidence of synaptic deficits following C1ql3 deletion, these findings suggest that C1QL3 contributes to H/OX circuit function and promotes normal sleep-wake regulation and wake-state stability.

**Disclosures: L. Boyd:** None. **W.P. Armstrong:** None. **D.C. Martinelli:** None. **M.E. Carter:** None. **A.C. Jackson:** None.

**Poster**

**PSTR193: Internal State, Feeding, and Physical Activity in Motivated Behavior**

**Location:** WCC Halls A-C

**Time:** Monday, November 16, 2026, 1:00 PM - 5:00 PM

**Program #/Poster #:** PSTR193.01/FF4

**Topic:** H.03. Motivation

**Support:** NIH Grant R01HD114146

**Title:** Hypothalamic AgRP Neurons Regulate Pupil Size in Response to Hunger

**Authors: *Y. YANG**, H. LIU, Y. XU;
Univ. of South Florida, Tampa, FL

**Abstract: Hypothalamic AgRP Neurons Regulate Pupil Size in Response to HungerAuthors***Yuxue Yang[1]; Hailan Liu[1]; Yong Xu[1].[1]Center for Molecular Psychiatry, Department of Psychiatry and Behavioral Neurosciences, University of South Florida, Tampa, FL, 33613, USA.
**Disclosures**Yuxue Yang: None; Hailan Liu: None; Yong Xu: None.
**Abstract**Pupil size is associated with various neurobehavioral processes, including wakefulness, exploration, learning, and nutritional states. However, the neural mechanisms linking hunger and pupil size remain unclear. Here we show that hungry individuals with a normal BMI exhibited an increase in pupil size, which subsequently decreased after feeding, while the obese subjects displayed the opposite pattern. Similarly, in mice, pupil size increased after a 24-hour fasting and decreased after refeeding. Mechanistically, we show that agouti-related protein (AgRP)-expressing neurons in the arcuate nucleus of the hypothalamus (ARC) innervate the iris sphincter muscle of the eyes, and importantly, optogenetic stimulation of AgRP neurons led to pupil dilation. Collectively, these findings indicate that AgRP neurons dilate pupils through a direct innervation, likely an evolutionarily conserved mechanism that facilitates food seeking and survival in hungry animals.

**Disclosures: Y. Yang:** None. **H. Liu:** None. **Y. Xu:** None.

**Poster**

**PSTR193: Internal State, Feeding, and Physical Activity in Motivated Behavior**

**Location:** WCC Halls A-C

**Time:** Monday, November 16, 2026, 1:00 PM - 5:00 PM

**Program #/Poster #:** PSTR193.02/FF5

**Topic:** H.03. Motivation

**Support:** NIH Grant DK139062
NIH Grant HL153274

**Title:** Opposing Sex-Specific Effects of mPFC-LHA Circuit Activation on Food Motivation

**Authors: *B. BARNHRT**[1], M. PHAM[3], L. SCHMIDT[4], U. SINGH[2], G. DENG[5], O. MUSTAFA[4], J. JIANG[2], H. CUI[2];
[2]Cell Biol., [1]Univ. of Oklahoma Hlth. Sci. Ctr., Oklahoma City, OK; [3]Dept. of Neurosci. & Pharmacol., [5]Neurosci. and Pharmacol., [4]Univ. of Iowa, Iowa City, IA

**Abstract:** Sex differences in depression, anxiety, and eating disorders are a well-documented phenomena and insights into the underlying neural circuitry could inform more effective, personalized treatment options for these neuropsychiatric disorders. Both the lateral hypothalamus (LHA) and medial prefrontal cortex (mPFC) are implicated in stress and feeding behavior and there is evidence suggesting they exhibit sex differences. Recent work has identified direct mPFC to LHA projections which are stress-sensitive and alter food motivation in male mice, yet whether this circuit functions similarly in females is unknown. Using chemogenetic and optogenetic approaches to manipulate the activity of mPFC to LHA projecting cells and fiber photometry to record their activity, we demonstrate that increasing the activity of this circuit had opposing effects on food motivation: female mice exhibited increased food motivation while food motivation was suppressed in male mice. Notably, natural responsiveness of LHA-projecting mPFC neurons to feeding and stressors did not differ between males and females, suggesting possible sex differences of synaptic connections in the LHA. These findings reveal an mPFC-LHA neural circuit which may contribute to sexually dimorphic feeding responses to stress and offers insights into the neurocircuitry underlying observed sex differences in neuropsychiatric disorders.

**Disclosures: B. Barnhrt:** None. **M. Pham:** None. **L. Schmidt:** None. **U. Singh:** None. **G. Deng:** None. **O. Mustafa:** None. **J. Jiang:** None. **H. Cui:** None.

**Poster**

**PSTR193: Internal State, Feeding, and Physical Activity in Motivated Behavior**

**Location:** WCC Halls A-C

**Time:** Monday, November 16, 2026, 1:00 PM - 5:00 PM

**Program #/Poster #:** PSTR193.03/FF6

**Topic:** H.03. Motivation

**Support:** SECIHTI CBF-2025-I-3173

**Title:** GLP-1 receptor expression in the lateral hypothalamic area and nucleus accumbens of male and female rats exposed to a cafeteria diet: effect of time restricted feeding on this anorexigenic circuit

**Authors: *P. MORALES ARGUELLO**[1], C. GARCIA-LUNA[2];
[1]Natl. Inst. of Psychiatry, Mexico City, Mexico; [2]Mol. Neurophysiol., Natl. Inst. of Psychiatry, CDMX, Mexico

**Abstract:** Obesity is a growing pandemic. Consumption of palatable food (PF) (high in sugars and lipids) is a key factor disease development. Prolonged PF consumption contributes to the malfunction of neuronal circuits that regulate feeding, including reduced glucagon-like peptide-1 (GLP-1) synthesis, an anorexigenic peptide, in neurons of the nucleus of the solitary tract (NTS). These neurons project to structures involved in homeostatic and hedonic circuits, such as the lateral hypothalamic area (LHA) and the nucleus accumbens (NAc), that express GLP-1 receptor (GLP-1R). LHA is a key integrative site projecting to the NAc, linking homeostatic and reward signals. Administration of a GLP-1R antagonist in the LHA increases PF intake, whereas a GLP-1R agonist reduces food intake. Time-restricted feeding (TRF) is a dietary intervention against obesity, characterized by an 8h food availability in the activity phase, with beneficial effects on weight loss, reduced hyperphagia, and the restoration of anorexic circuits function. However, it remains unclear if CAF intake may alter GLP-1R expression in LHA or NAc, its association with body weight gain, and if TRF may reverse those alterations. The aim of the study was to determine the effect of CAF on GLP-1R expression in LHA and NAc and body weight gain, and if TRF may prevent CAF-induced alteration. 52 male (M, n=26) and female (F, n=26) Wistar rats were fed either with chow or with chow and CAF, and divided into four groups: 1) Chow-fed rats with food available 24h (C-chow), 2) CAF-fed rats with chow and CAF available 24H (C-CAF), 3) TRF chow-fed rats with 8h food availability (TRF-chow), 4) TRF CAF-fed rats with chow and CAF food available 8h/day (TRF-CAF) for four weeks. Body weight was recorded weekly and food intake daily. GLP-1R expression in the LHA and NAc was evaluated by Western blot. Body weight gain in M-TRF-CAF rats decreased 9% compared with C-CAF group, whereas female TRF-CAF rats showed an 11% reduction compared with C-CAF rats. F-TRF-CAF rats consumed 75% more energy from chow than F-C-CAF. CAF intake decreased 11% in male TRF-CAF rats compared with M-C-CAF group, while female TRF-CAF rats reduced CAF intake by 19% compared with F-C-CAF. Total caloric intake in F-TRF-CAF rats decreased by 15% compared with F-C-CAF. GLP-1R expression in LHA was 43% higher in M-TRF-CAF than in M-C-CAF rats. GLP-1R expression in the NAc of F-TRF-CAF was 60% higher than in F-C-CAF group. TRF induced sex-dependent effects. In males, TRF reduced CAF intake and increased GLP-1R expression in LHA, suggesting that TRF effects may be mediated by LHA. In females, TRF decreased CAF intake and body weight gain, associated to enhanced GLP-1R expression in the NAc.

**Disclosures: P. Morales Arguello:** None. **C. Garcia-Luna:** None.

**Poster**

**PSTR193: Internal State, Feeding, and Physical Activity in Motivated Behavior**

**Location:** WCC Halls A-C

**Time:** Monday, November 16, 2026, 1:00 PM - 5:00 PM

**Program #/Poster #:** PSTR193.04/FF7

**Topic:** H.03. Motivation

**Support:** NSF-IOS 1901546

**Title:** The effect of orexin receptor-1 antagonism on feeding preferences and the gut microbial communities of female rats

**Authors:** A. ROACH, N. COLE, Z. MENSAH, A. SMITH, ***K. A. RICHARDSON**; Pharmacol., Howard Univ. Col. of Med., Washington, DC, DC

**Abstract:** Background: Orexin (or hypocretin) hypothalamic peptides regulate food intake and possibly maladaptive feeding behaviors. The brain-gut-microbiome axis may play a pivotal role in the pathophysiology of these behaviors. We contend that the orexin system may be involved in bidirectional communication of the brain-gut-microbiome axis and contribute to mechanisms that lead to excessive food consumption. Our goal was to determine the effect of repeated orexin receptor-1 antagonism (SB-334867) on palatable food preference and the impact on gut microbiota communities. Methods: Female Sprague Dawley rats (n=8/group, 250-300g) were categorized as high preferring (HP) or low preferring (LP) based upon their consumption of palatable food (PF, high fat, sugar pellets) across nine, intermittent feeding tests. Rats were administered SB (20mg/kg, IP) and given a feeding test to determine the impact of SB on PF consumption. The HP and LP rats were given several days of regular chow and then a no-drug feeding test to ensure a return to baseline for PF intake. Each rat received five SB-challenge tests. Feces were collected before SB and after each SB-test, 6 weeks post SB, and 3 months post-SB. DNA was extracted and PCR amplified the V4 region of the 16S rRNA genes, then sequenced on Illumina MiSeq platform. Sequences were processed and analyzed using Mothur v.1.40.5. Results: There was a significant reduction in PF intake only for HP rats ($p<0.05$) versus pre-SB consumption levels. The number of amplicon sequencing variants observed after 5 days of SB was significantly higher than for pre-SB ($p<0.005$), day 1 SB20 ($p<0.05$), and day 3 SB20 ($p<0.005$). Beta diversity was significantly affected by the number of days administered SB20mg/kg, evidenced by significant shifts in the microbial communities in response to diet and time (Bray-Curtis ANOSIM, $p<0.001$). Repeated administration of SB at 20 mg/kg reduced PF intake over time and led to shifts in microbial communities. Alpha and beta diversity were significantly affected by the number of days SB20mg/kg was administered. Additional analyses are underway to determine any differences in the microbial communities at 6 weeks and 3 months post-SB. Conclusion: These data will advance knowledge of the influence of the orexin system on the brain-gut-microbiome axis and help to delineate microbial-dependent, functional pathways that impact food choice and reduce hedonic feeding states in future studies.

**Disclosures: A. Roach:** None. **N. Cole:** None. **Z. Mensah:** None. **A. Smith:** None. **K.A. Richardson:** None.

**Poster**

**PSTR193: Internal State, Feeding, and Physical Activity in Motivated Behavior**

**Location:** WCC Halls A-C

**Time:** Monday, November 16, 2026, 1:00 PM - 5:00 PM

**Program #/Poster #:** PSTR193.05/FF8

**Topic:** H.03. Motivation

**Support:** PAPIIT-DGAPA IN203124

**Title:** Sugar pre-exposure changes behavior, not preference: Insights from licking microstructure in rats

**Authors: *M. OLVERA-CALTZONTZIN**[1], G. VERA[2], M.-I. MIRANDA[3];
[1]Univ. Nacional Autonoma de Mexico, Queretaro, Mexico; [2]Neurobiología Conductual y Cognitiva, Inst. de Neurobiología, Juriquilla. UNAM, Querétaro, Mexico; [3]Inst. Neurobiologia-UNAM, Queretaro, Qro., Mexico

**Abstract:** The hedonic and caloric properties of sweet solutions influence appetitive behavior and learning. While sugar consumption is commonly assessed using measures of volume intake or preference, these metrics do not capture the organization, rhythm, and speed of consumption behavior. Evidence suggests that familiarization with highly hedonic stimuli, such as sugar, can differentially modify subsequent learning about sweet tastes. Here, we examined whether prior acute or chronic sucrose exposure alters preference and licking microstructure in male and female Wistar rats. Rats were given measured access to either sucrose solution or water for 14 days and were subsequently assessed using a two-bottle choice paradigm over six consecutive days. Different solution pairings (water, sugar, saccharin, and fructose) were compared across sessions. Results showed that prior sugar exposure did not affect preference behavior. In contrast, analysis of licking microstructure revealed location (bottle location)- and sex-dependent differences that were not evident in the preference measures. Sex differences in preference, with females exhibiting either greater or lower preference than males depending on the condition, were observed when rats chose between sucrose and water, but were absent when sucrose was compared with alternative sweeteners such as fructose. This finding suggests that appetitive responses were driven by reward properties specific to sugar rather than by sweet taste alone. In both acutely and chronically exposed rats, sugar elicited more reinforcing consumption patterns than fructose or saccharine, characterized by shorter intervals between licking bursts, indicating a faster resumption of licking following pauses. In males, chronic sugar exposure reduced the differences between sucrose and fructose, suggesting diminished satiety-related control of consumption. However, the effect of sugar in promoting rapid re-engagement with the solution persisted across all experimental conditions. Taken together, these findings demonstrate that conventional preference measures may fail to detect important differences in appetitive behavior. In contrast, licking-microstructure analysis enables the identification of significant changes associated with chronic sugar consumption and reveals motivational differences in the preference for sweet solutions that depend on both the consumption context and the animals' sex.

**Disclosures: M. Olvera-Caltzontzin:** None. **G. Vera:** None. **M. Miranda:** None.

**Poster**

**PSTR193: Internal State, Feeding, and Physical Activity in Motivated Behavior**

**Location:** WCC Halls A-C

**Time:** Monday, November 16, 2026, 1:00 PM - 5:00 PM

**Program #/Poster #:** PSTR193.06/Web Only

**Topic:** H.03. Motivation

**Support:** NIH Grant P60 AA006420
NIH Grant R01 AA028879
The Mark Pearson Endowed Fellowship

**Title:** Rgs7bp modulates sucrose intake in a sex- and concentration-dependent manner in a two-bottle choice, concentration-response assay

**Authors: *K. N. TRINH**[1,2], P. C. BENSING[2], K. A. MARTEMYANOV[3], E. P. ZORRILLA[4]; [1]UCSD, San Diego, CA; [2]Scripps Res. Inst., La Jolla, CA; [3]Dept. of Neurosci., The Scripps Res. Inst., Jupiter, FL; [4]Mol. Med., Scripps Res., San Diego, CA

**Abstract:** Obesity can be driven by hedonic feeding, characterized by the consumption of palatable, often calorie-dense foods, beyond homeostatic energy requirements. While genetic factors are known to influence both reward processing and obesity, the specific molecular regulators involved remain under-explored. This study investigates the regulator of G protein signaling 7 binding protein (RGS7BP) as a novel contributor to sucrose consumption and metabolic outcomes. Adult male and female *Rgs7bp* knockout (KO; M: $n = 10$, F: $n = 7$) and wild-type (WT; M: $n = 6$, F: $n = 8$) mice were evaluated using a two-bottle choice assay across varying sucrose concentrations (0.5, 1, 2, 4, 8, 16, and 32%) over two testing blocks with four days without sucrose in between. In each test block, each sucrose solution was given for 48 hours in an increasing concentration order.While no genotype-related differences in sucrose solution intake were observed in Test 1 , a three-way ANOVA of Test 2 intake (g/day) revealed a significant Concentration x Sex x Genotype interaction ($F(6, 162) = 2.41$, $p = 0.0341$). In Test 2, KO male mice consumed less sucrose solution than WT male mice at the peak 8% concentration (13.1 +/- 0.8 g/day vs. 14.9 +/- 1.3 g/day) , while KO female mice displayed a marked escalation in consumption, consuming more than WT females at both 8% (19.5 +/- 1.9 g/day vs. 14.2 +/- 1.5 g/day) and 16% sucrose (14.7 +/- 2.5 g/day vs. 8.8 +/- 0.7 g/day). In contrast, a mixed-effects analysis of sucrose preference (%) yielded no significant three-way interactions in either block ($p = 0.0630$ for Test 1; $p = 0.8659$ for Test 2), with preference remaining robustly high (>80%) across cohorts. Total caloric adjustments were reflected in daily home-cage chow intake, where a mixed-effects model revealed a significant Concentration x Sex x Genotype interaction ($p = 0.0042$), tracking a drop to a nadir at the 8% and 16% sucrose steps (5.5 to 7.0 kcal/day across cohorts) as liquid sucrose intake peaked. Furthermore, a significant Time x Genotype interaction on body weight ($F(2, 54) = 4.58$, $p = 0.0144$) indicated that KO mice gained significantly more weight over the course of the study; KO males increased from a baseline of 22.6 +/- 1.1 g to 28.2 +/- 1.3 g at the end of testing, while KO females increased from 18.5 +/- 0.5 g to 22.1 +/- 0.9 g. Meanwhile, a three-way ANOVA of percent body fat showed no significant Time x Sex x Genotype interaction ($p = 0.3660$). These results identify that *Rgs7bp* deficiency modulates sucrose intake in a concentration- and sex-specific manner and weight gain in response to sucrose exposure. These findings suggest that *Rgs7bp* may be a critical regulator of reward-based food intake and obesity-related outcomes.

**Disclosures: K.N. Trinh:** None. **P.C. Bensing:** None. **K.A. Martemyanov:** None. **E.P. Zorrilla:** None.

**Poster**

**PSTR193: Internal State, Feeding, and Physical Activity in Motivated Behavior**

**Location:** WCC Halls A-C

**Time:** Monday, November 16, 2026, 1:00 PM - 5:00 PM

**Program #/Poster #:** PSTR193.07/FF10

**Topic:** H.03. Motivation

**Support:** NIGMS R35GM147504
NIGMS, U54 GM104941
P20 GM103446

**Title:** From perception to valence: Fox neurons assign state-dependent valence to taste in Drosophila

**Authors: *L. SHAO**;
Univ. of Delaware, Newark, DE

**Abstract:** Assigning valence—appeal or aversion—to gustatory stimuli and relaying it to higher order brain regions to guide flexible behaviors is crucial to survival. Yet the neural circuits that transform taste into motivationally relevant signals remain poorly defined in any model system. In *Drosophila melanogaster*, substantial progress has been made in mapping the sensorimotor pathways encoding intrinsic valence for feeding and the architecture of the dopaminergic reinforcement system. However, where and how "effective" (i.e., real-time) valence is first imposed on a taste has long been a mystery. Here, we identified a pair of subesophageal zone interneurons in *Drosophila*, termed Fox, that impart reinforcing positive valence to sweet taste and convey this signal to the mushroom body, the fly's associative learning center. We show that Fox neuron activity is necessary and sufficient to drive appetitive behaviors and can override a tastant's intrinsic neutral or aversive valence without impairing taste quality discrimination. Furthermore, Fox neurons relay the positive valence to specific dopaminergic neurons that mediate appetitive memory formation. Our findings reveal a circuit mechanism through which effective valence is bestowed upon sweet sensation and transformed into a reinforcing signal that supports learned sugar responses. Preliminary data further suggest that Fox function may extend beyond sweetness: Fox may amplify real-time valence for the tastant most valuable to the animal's current physiological state, including during sugar-protein choice. Fox neurons thus form a convergent-divergent "hourglass" circuit motif, acting as a bottleneck for valence assignment and distributing motivational signals to higher-order centers. This architecture confers both robustness and flexibility in reward processing—an organizational principle that may generalize across species.

**Disclosures: L. Shao:** None.

**Poster**

**PSTR193: Internal State, Feeding, and Physical Activity in Motivated Behavior**

**Location:** WCC Halls A-C

**Time:** Monday, November 16, 2026, 1:00 PM - 5:00 PM

**Program #/Poster #:** PSTR193.08/FF11

**Topic:** H.03. Motivation

**Support:** NIH 5R21DA056241-02

**Title:** Dopamine neurons enable a nutrient-specific work-reward tradeoff in Drosophila

**Authors: *P. BLACK**[1], K. STAPLETON[1], A. ROTHENFLUH[2];
[2]Psychiatry, [1]Univ. of Utah, Salt Lake City, UT

**Abstract:** Understanding the neural basis of internal states is a focus of neuroscience research. Dysregulated internal states are a hallmark of many psychiatric illnesses, yet we are only beginning to uncover how internal states are generated, maintained, and utilized to guide behavior. Research using Drosophila melanogaster to investigate internal state has been held back by available assays. In particular, the typical assay for feeding motivation, bitterness conflict, is confounded by starvation. As a consequence of this, how flies generate changes in their decision making in conditions of deprivation is not well understood. To address this, we developed a novel assay with a non-confounded barrier to feeding, food hardness, via agarose. We validated our novel assay using three basic motivators, finding that flies became more willing to work for protein, sugar, and salt when they had faced prior specific deprivations. After validating our assay, we then set out to find populations of neurons that could be responsible for the internal states created by nutrient-specific motivations. We found that a broad population of dopamine neurons were required for protein drive, yet inessential for sugar or salt drives, a comparison which had, to our knowledge, never been carried out. To ensure rigor, we replicated every experiment on multiple days, with a total n of between 45 and 60 (135-180 animals). After finding a broad neuronal population with a specific role in internal state, we then turned to the recently released Drosophila Brain Simulation in order to generate single-neuron candidates that could provide the circuitry needed to drive the motivated feeding we observed. The simulation suggested a subpopulation of central brain dopamine neurons that could change behavior in our assay conditions. Importantly, highly specific split-GAL4 driver lines were available for the candidates found using the simulation. We tested these dopaminergic neurons using thermogenetic tools, finding that activity in a specific class of neuron was essential for flies to work for an essential nutrient and resist low-effort, low-value temptations.

**Disclosures: P. Black:** None. **K. Stapleton:** None. **A. Rothenfluh:** None.

**Poster**

**PSTR193: Internal State, Feeding, and Physical Activity in Motivated Behavior**

**Location:** WCC Halls A-C

**Time:** Monday, November 16, 2026, 1:00 PM - 5:00 PM

**Program #/Poster #:** PSTR193.09/FF12

**Topic:** H.03. Motivation

**Support:** R01MH125898

**Title:** Goal-directed and habitual processes govern voluntary wheel running in rats

**Authors: *M. A. ABDIN**[1], M. K. TANNER[1], A. A. HOHORST[2], F. MAWLID[1], B. N. GREENWOOD[3];
[1]Univ. of Colorado Denver, Denver, CO; [2]Integrative Biol., Univ. of Colorado Denver, Morrison, CO; [3]Psychology, Univ. of Colorado Denver, DENVER, CO

**Abstract:** Physical inactivity is a risk factor for chronic disease and premature mortality. Despite these risks, exercise adherence is low. To maintain physical activity over time, exercise needs to become habitual, regardless of initial intentions. Thus, understanding the neural mechanisms underlying formation of habitual exercise could reveal targets to promote long-term adherence. Rodent voluntary wheel running (VWR) could be a pre-clinical model for studying these mechanisms, but the translational validity of VWR is limited because it is unclear why rodents run on wheels. Many reasons have been proposed, from thermoregulation and energy balance, to foraging and compulsive stereotypy. We propose that, although many processes could modulate VWR, the primary motivational processes underlying VWR are the same as those determining human exercise behavior, namely goal-directed and habitual processes. A hallmark of habitual behavior is insensitivity to outcome omission, whereby a habitual behavior persists even when the anticipated outcome is absent. Wheels in cages of adult male and female Long Evans rats were locked on the second, fifth, and twenty-eighth days of VWR and attempts to run were quantified using Noldus EthoVision XT. We observed that, compared to baseline measured on the days before and after wheel locking, attempts to run were reduced during wheel lock on the second day of VWR, indicating sensitivity to outcome omission and goal-directed control of VWR. By the twenty-eighth day, attempts to run persisted despite outcome omission, indicating habitual control. Females displayed resistance to outcome omission earlier than males. These data are consistent with prior work suggesting that VWR becomes habitual in females more readily than in males. Since habitual VWR could be a healthy behavior or a compulsion, we tested whether VWR persisted in the face of punishment, as compulsive behavior will continue despite punishment, but healthy habits will not. After 28 days of VWR, attempts to run were paired with electric shock. Data analysis is ongoing. Data provide the first direct evidence that VWR is governed by similar goal-directed and habitual processes as human physical activity and suggest that VWR is a valid translational model for studying exercise motivation.

**Disclosures: M.A. Abdin:** None. **M.K. Tanner:** None. **A.A. Hohorst:** None. **F. Mawlid:** None. **B.N. Greenwood:** None.

**Poster**

**PSTR193: Internal State, Feeding, and Physical Activity in Motivated Behavior**

**Location:** WCC Halls A-C

**Time:** Monday, November 16, 2026, 1:00 PM - 5:00 PM

**Program #/Poster #:** PSTR193.10/FF13

**Topic:** H.03. Motivation

**Support:** NIH 068283

**Title:** Sex differences in striatal dopamine release during and after voluntary physical activity

**Authors: *M. K. TANNER**[1], A. A. HOHORST[1], C. SANCHEZ MENDOZA[1], J. WESTERMAN[2], B. N. GREENWOOD[1];
[1]Psychology, Univ. of Colorado Denver, Denver, CO; [2]Neurosci. and Psychology, Univ. of Colorado, Boulder, CO

**Abstract:** Despite the benefits of regular exercise, adherence to long-term exercise is low. Identifying mechanisms that motivate exercise could reveal novel strategies to increase exercise participation and its benefits. Rodent voluntary wheel running (VWR) is used to study biological processes underlying exercise motivation. VWR is sex divergent; whereby female rats escalate running behavior and reach a plateau faster than males. We have found that the nucleus accumbens (NAc) and dorsomedial striatum (DMS) govern VWR during acquisition, whereas the dorsolateral striatum (DLS) supports its maintenance. Importantly, the transition to DLS-control of VWR occurs more rapidly in females. Dopamine (DA) supports functions of striatal subregions and VWR produces adaptations in DA systems consistent with a hyperdopaminergic state. However, the role of DA in mediating sex differences in acquisition and maintenance of VWR is unknown, and direct evidence for a hyperdopaminergic state following VWR is lacking. Here, we used fast-scan cyclic voltammetry to investigate sex differences in DA release dynamics during VWR and to test whether VWR produces a hyperdopaminergic state. We found in adult, male Long Evans rats that DA release during VWR shifts from the DMS during acquisition to the DLS during maintenance, consistent with the causal role of these regions in governing VWR during these phases. The magnitude and frequency of DA release during VWR in these regions at these timepoints were greater in males than females, but females displayed greater DA release in the DLS during acquisition compared to males. After 28 days of VWR, we found that stimulus-evoked DA release is potentiated in the DLS, but not DMS or NAc, of both sexes, thus providing evidence of a hyperdopaminergic state in the DLS. Interestingly, female estrous phase impacts the magnitude of stimulus-evoked DA release in all 3 striatal subregions. Given the sex difference in DA release in the DLS during acquisition of VWR, we used inhibitory intersectional chemogenetics to test the role of DLS DA. We found that the causal role of DA in the DLS paralleled sex differences in DA release dynamics during VWR, whereby inactivating the SN-DLS pathway reduced VWR during acquisition in females, but not males, and reduced VWR during maintenance in males, but not females. Results reveal that DA in the DLS facilitates the transition to habitual voluntary exercise and suggest that DLS DA could be a target for increasing exercise adherence.

**Disclosures: M.K. Tanner:** None. **A.A. Hohorst:** None. **C. Sanchez Mendoza:** None. **J. Westerman:** None. **B.N. Greenwood:** None.

**Poster**

**PSTR193: Internal State, Feeding, and Physical Activity in Motivated Behavior**

**Location:** WCC Halls A-C

**Time:** Monday, November 16, 2026, 1:00 PM - 5:00 PM

**Program #/Poster #:** PSTR193.11/FF14

**Topic:** H.03. Motivation

**Support:** NIH 068283

**Title:** Sex differences in the activity of mesolimbic dopamine neurons during exercise

**Authors: *J. L. SLIM**[1], J. A. QUIGLEY[2], C. SANCHEZ MENDOZA[1], S. M. MELLERT[2], A. A. HOHORST[1], M. K. TANNER[1], B. N. GREENWOOD[1];
[1]Psychology, [2]Integrative Biol., Univ. of Colorado Denver, Denver, CO

**Abstract:** Physical activity can protect against the development of stress-related mental health disorders; however, the underlying mechanisms aren't clear. Rodents given access to running wheels are similarly protected from the depressive and anxiety-like behavioral consequences of stress. Interestingly, sex differences exist in the duration of voluntary exercise required to produce stress protection: males require 6 weeks of running, whereas females require only 3 weeks. The nucleus accumbens (NAc) is a brain region critical for exercise-induced stress resistance, and where dopamine (DA) is important for exercise reward. What remains unclear about the relationship between the NAc and stress resistance is the signal elicited by exercise and responsible for producing the NAc plasticity required for stress resistance. We propose that DA in the NAc determines the rate at which VWR enables stress resistance, such that a bout of VWR will activate NAc-projecting DA neurons to a greater extent in females compared to males. To test this hypothesis, we injected a retrograde viral tracer into the NAc of female and male Sprague Dawley rats. Rats were then allowed to run in wheels for 3 weeks. After the last running bout, rats were euthanized via a transcardial perfusion, and the activity of NAc-projecting midbrain DA neurons was quantified with immunohistochemistry for the neural activation marker cFos. Tissue will be mounted on slides for analysis, and cell counts will be performed using ImageJ. We expect that after a history of 3 weeks of exercise, an exercise bout will activate NAc-projecting midbrain neurons more in females than in males. Data collection is ongoing, but this result would support the hypothesis that NAc dopamine is the signal driving rapid stress protection from exercise in females.

**Disclosures: J.L. Slim:** None. **C. Sanchez Mendoza:** None. **S.M. Mellert:** None. **A.A. Hohorst:** None. **M.K. Tanner:** None. **B.N. Greenwood:** None.

**Poster**

**PSTR193: Internal State, Feeding, and Physical Activity in Motivated Behavior**

**Location:** WCC Halls A-C

**Time:** Monday, November 16, 2026, 1:00 PM - 5:00 PM

**Program #/Poster #:** PSTR193.12/FF15

**Topic:** H.03. Motivation

**Support:** NIH 068283
NIGMS 5T34GM149812

**Title:** The time of day at which exercise occurs determines how much exercise impacts behavioral and dorsal raphe nucleus response to stress

**Authors: *A. J. VALDEZ**[1], M. K. TANNER[2], J. D. WESTERMAN[2], C. SANCHEZ MENDOZA[2], B. N. GREENWOOD[3];
[1]Univ. of Colorado Denver, DENVER, CO; [2]Univ. of Colorado Denver, Denver, CO;
[3]Psychology, Univ. of Colorado Denver, DENVER, CO

**Abstract:** Physical activity reduces the risk of future stress-related mental disorders, including anxiety. However, it remains unknown how much exercise is required for stress protection, or if the time of day of exercise impacts its stress-protective effects. Both male and female rodents allowed to run voluntarily on in-cage running wheels are protected from social avoidance and exaggerated shock-elicited fear resulting from inescapable stress. We have previously found that these protective effects are mediated by constraint of serotonergic activity in the dorsal raphe nucleus (DRN), which is sensitive to circadian rhythms. Prior work has exclusively allowed ad libitum access to exercise. Consequently, it remains unclear if exercise limited to certain times of day will enable stress protection. The goals of this project are to examine whether restricting access to voluntary wheel running to 3 hours can enable behavioral and neurochemical stress protection, and whether these effects are influenced by the time of day at which exercise occurs. Female and male adult Sprague Dawley rats were randomly assigned to exercise or sedentary groups. Different exercise groups were allowed to run only during the first 3 hours (relative morning) or the last 3 hours (relative evening) of the active cycle. Following 3 weeks of these housing conditions, rats were either exposed to inescapable tail shock or left in their home cage. Running restricted to the relative morning but not the relative evening, protected both sexes from exaggerated shock-elicited fear, but not social avoidance. Despite the partial stress protection produced by morning exercise, RNAscope revealed that stress-induced activity of DRN serotonin neurons was not constrained by morning exercise. These data suggest that morning exercise is more beneficial than evening exercise at enabling stress protection, but restricted access does not elicit the full behavioral or neurochemical protection typically elicited by *ad libitum* access. Exercise adaptations in DRN projection sites, which mediate the protective effect of morning exercise against stress-induced exaggerated fear, are currently being examined.

**Disclosures: A.J. Valdez:** None. **M.K. Tanner:** None. **J.D. Westerman:** None. **C. Sanchez Mendoza:** None. **B.N. Greenwood:** None.

**Poster**

**PSTR193: Internal State, Feeding, and Physical Activity in Motivated Behavior**

**Location:** WCC Halls A-C

**Time:** Monday, November 16, 2026, 1:00 PM - 5:00 PM

**Program #/Poster #:** PSTR193.13/FF16

**Topic:** H.03. Motivation

**Support:** R01MH125898

**Title:** Low-dose psilocybin as a potential facilitator of exercise-induced stress resistance

**Authors: *A. A. HOHORST**[1], M. K. TANNER[1], S. M. MELLERT[1], C. SANCHEZ MENDOZA[1], J. SLIM[1], J. GRIGSBY[2], B. N. GREENWOOD[3];
[1]Univ. of Colorado Denver, Denver, CO; [2]Psychology; Med., Univ. of Colorado Denver, Ward, CO; [3]Psychology, Univ. of Colorado Denver, DENVER, CO

**Abstract:** Regular physical activity reduces the risk for future stress-related mental health disorders, such as depression, generalized anxiety disorder, and post-traumatic stress disorder. Despite the stress-protective effects of exercise, many adults do not achieve the recommended minimum amount of physical activity, highlighting the need to identify strategies that reduce the exercise threshold required for stress-protective effects. Psilocybin, a compound found in “magic mushrooms” is converted to psilocin, which has psychedelic properties. Psilocybin can reduce symptoms of existing stress-related disorders and is thought to open a “plasticity window,” potentially enabling shorter durations of exercise to confer stress-resistance. However, whether this combined intervention is sufficient to promote stress-resistance remains unknown. Adult male Sprague Dawley rats received saline or low-dose psilocybin (0.1 or 0.5 mg/kg, i.p.). Rats were further divided into locked wheel or voluntary wheel running groups. Rats received their assigned dose of psilocybin paired with wheel running or locked wheel conditions every other day for 10 days. Rats ran for 2 hours immediately after receiving drug. Two days after the last treatment, rats were exposed to an inescapable stressor and subsequent effects on stress behaviors were analyzed. A separate cohort was used to determine whether a higher dose of psilocybin (1 mg/kg) alone is sufficient to promote stress resistance at a higher dose. Preliminary results indicate that repeated administration of 0.1 and 0.5 mg/kg psilocybin did not protect against the behavioral consequences of inescapable stress when administered alone, supporting their use as subthreshold doses for future combination with exercise. Short-duration exercise alone was also insufficient to promote stress resistance. However, a higher dose of psilocybin, 1 mg/kg, administered one week prior to stress exposure was sufficient to prevent stress-induced social avoidance and reduce fear expression. The behavioral effects of pairing low-dose psilocybin with short-duration exercise are currently being analyzed. These findings have the potential to reveal novel and practical prophylactic strategies to reduce the risk of future stress-related disorders.

**Disclosures: A.A. Hohorst:** None. **M.K. Tanner:** None. **S.M. Mellert:** None. **C. Sanchez Mendoza:** None. **J. Slim:** None. **J. Grigsby:** None. **B.N. Greenwood:** None.

**Poster**

**PSTR193: Internal State, Feeding, and Physical Activity in Motivated Behavior**

**Location:** WCC Halls A-C

**Time:** Monday, November 16, 2026, 1:00 PM - 5:00 PM

**Program #/Poster #:** PSTR193.14/FF17

**Topic:** H.03. Motivation

**Support:** NIH Grant R01MH125898

**Title:** Ovarian hormonal state at exercise initiation determines long-term voluntary exercise behavior in female rats: Role of the nigrostriatal pathway

**Authors: *M. HSIEH**[1], M. K. TANNER[1], K. M. KORTH[4], A. A. HOHORST[2], J. FREUND[1], J. WESTERMAN[5], C. SANCHEZ MENDOZA[1], B. N. GREENWOOD[3];
[1]Univ. of Colorado Denver, Denver, CO; [2]Integrative Biol., Univ. of Colorado Denver, Morrison, CO; [3]Psychology, Univ. of Colorado Denver, DENVER, CO; [4]Univ. of Colorado Anschutz, Aurora, CO; [5]Univ. of Colorado Boulder, Boulder, CO

**Abstract:** Despite the well-established health benefits of exercise, adherence to physical activity remains low, highlighting the need to identify biological factors that regulate the initiation and persistence of exercise behavior. Here, we tested whether ovarian hormone state at the onset of voluntary wheel running (VWR) influences both immediate and long-term exercise behavior in female rats. Females that initiated VWR during proestrus (Pro) ran farther, spent more time running, and ran at higher speeds on the first day of wheel access than females initiating VWR outside of Pro. Remarkably, initiating VWR during Pro also produced persistent increases in running distance, duration, speed, and escalation across subsequent weeks, despite normal cycling through other estrous phases. In contrast, exogenous estradiol (E2) administered at VWR initiation did not alter day-1 behavior, but increased running distance and duration across subsequent weeks without affecting running speed or escalation. To determine whether dorsal striatal dopamine contributes to these effects, we inhibited the substantia nigra (SN) to dorsolateral striatum (DLS) pathway on the first day of VWR. This manipulation reduced running distance and duration during the first hour of VWR specifically in Pro animals and prevented the long-term effects of initiating VWR during Pro, while leaving running speed unaffected. These findings identify behavioral initiation as a critical window during which hormones and nigrostriatal signaling influence future engagement in physical activity. Furthermore, analysis of VWR architecture reveals that distinct features of VWR behavior can be dissociated mechanistically and thus could be used to investigate separate motivational processes underlying physical activity.

**Disclosures: M. Hsieh:** None. **M.K. Tanner:** None. **K.M. Korth:** None. **A.A. Hohorst:** None. **J. Freund:** None. **J. Westerman:** None. **C. Sanchez Mendoza:** None. **B.N. Greenwood:** None.

**Poster**

**PSTR193: Internal State, Feeding, and Physical Activity in Motivated Behavior**

**Location:** WCC Halls A-C

**Time:** Monday, November 16, 2026, 1:00 PM - 5:00 PM

**Program #/Poster #:** PSTR193.15/FF18

**Topic:** H.03. Motivation

**Support:** R01MH125898

**Title:** Effects of exercise onaggression issexdependent

**Authors: *F. MAWLID**[1], C. M. BELLER[2], B. N. GREENWOOD[3], J. WESTERMAN[4], M. K. TANNER[1], C. SANCHEZ MENDOZA[1];
[2]Psychology, [1]Univ. of Colorado Denver, Denver, CO; [3]Psychology, Univ. of Colorado Denver, DENVER, CO; [4]Univ. of Colorado Boulder, Denver, CO

**Abstract:** Effects of exercise on aggression is sex dependentCiana Beller, Filsan Mawlid, Margaret K Tanner, Jessica D Westerman, Carolina SanchezMendoza, Benjamin N GreenwoodDC – College of Liberal Arts and Sciences, Psychology DepartmentDC – College of Liberal Arts and Sciences, Biology DepartmentAggression is associated with stress and mood-related disorders. Exercise is a promising non-pharmaceutical option for improving mental health, yet its effects on aggression, particularlyacross sexes, are not well understood. Existing pre-clinical research has focused on male-typicalrodent models of aggression and overlooked sex-specific aggression patterns. Female and malerodents express aggression differently; males typically display offensive behaviors and femalesdisplay defensive behaviors. However, most aggression models measure only offensiveaggression. The goal of this study is to understand the effects of exercise on offensive anddefensive aggressive behaviors in both sexes of adult, Sprague Dawley rats. Additionally, wealso examine the contribution of ovarian hormones to the female pattern of aggression. Wehypothesize that exercise will reduce aggression in both sexes, but sex-specific patterns willemerge which will be dependent on ovarian hormones in females. Rats remained sedentary orwere allowed to run voluntarily in wheels for 6 weeks prior to being exposed to a 3-minutejuvenile social exploration task during which aggressive behaviors were measured. We observeda sex-specific pattern of aggression, with males presenting higher levels of offensive aggressionand females presenting higher levels of defensive aggression. Furthermore, exercise reducedaggression in males, but not in females. Ovariectomy reduced defensive aggressive behaviors infemales, suggesting that the presence of ovarian hormones is necessary for the female pattern ofaggression. However, exercise still did not reduce aggression in ovariectomized females. Thesefindings indicate that aggression is regulated between the sexes and exercise influencesaggression in a sex-specific manner. These results further suggest that ovarian hormonescontribute to the female-specific pattern of aggression, but do not fully explain the lack ofexercise effects observed in females. Overall, this work highlights the importance of includingboth sexes and multiple forms of aggression when investigating the behavioral effects of exerciseand could inform the use of exercise as a sex-specific treatment for aggression.

**Disclosures: F. Mawlid:** None. **C.M. Beller:** None. **B.N. Greenwood:** None. **J. Westerman:** None. **M.K. Tanner:** None. **C. Sanchez Mendoza:** None.

**Poster**

**PSTR193: Internal State, Feeding, and Physical Activity in Motivated Behavior**

**Location:** WCC Halls A-C

**Time:** Monday, November 16, 2026, 1:00 PM - 5:00 PM

**Program #/Poster #:** PSTR193.16/FF19

**Topic:** H.03. Motivation

**Support:** UNAM-DGAPA-PAPIIT IN214524
Becas SECIHTI CVU 1140678.

**Title:** Brain plastic changes induced by sexual behavior and running wheel in female rats evaluated by manganese-enhanced magnetic resonance imaging (MEMRI).

**Authors: *L. MENDOZA**[1], R. G. PAREDES[2], L. GAYTAN[3], J. A. AGUILAR MORENO[4]; [1]Conducta sexual y Plasticidad D11, Inst. De Neurobiología, UNAM, Queretaro, Mexico; [2]Conducta sexual y Plasticidad D11, UNA ENES/INB, Querétaro, QRO, Mexico; [3]Intituto de Neurobiología, UNAM, Querétaro, Mexico; [4]Lab. D11, Inst. De Neurobiología, Querétaro, Mexico

**Abstract:** Sexual behavior and exercise on the running wheel are two motivated behaviors that induce a positive reward state and permanent plastic changes, including neurogenesis and increases in brain signal intensity, as evaluated by manganese-enhanced magnetic resonance imaging (MEMRI). **Aims:** Evaluate and compare longitudinally plastic changes induced by paced mating (PM) and running wheel (RW), assessed by MEMRI. We also evaluated whether subjects who had the opportunity to display RW+PM in the same session would show a greater increase in brain signal intensity. **Method:** Female Wistar rats (19 subjects per group) were ovariectomized and hormonally supplemented to induce behavioral receptivity. They were randomly assigned to the following groups: Control, Paced Mating (PM), Running Wheel (RW), Open Field (OF), and Running Wheel+ Paced Mating (RW+PM). The OF, the RW, and the RW+PM groups were tested for their respective motor behaviors for 1 hour, 5 days a week, for 10 weeks. The PM groups mated once a week for 10 weeks. Subjects were injected with 16 mg/kg MnCl2 24 hours before the test on sessions 1, 5, and 10, and were scanned immediately thereafter. **Results:** The groups that performed one motivated behavior, the RW group and PM group, showed greater activation of the whole-brain and higer signal intensity as measured by MEMRI along the weeks of testing. The PM group showed greater whole-brain signal activation in session 10 than RW+PM, OF, and control groups (Cohen's D >0.8). The RW and RW+PA groups showed greater whole-brain signal activation in session 10 compared to the control group (Cohen's D 0.8). In the OF group, whole-brain signal activation did not persist. **Conclusion:** The RW+PM group did not show higher intensity in the SBN and MRS than the groups that performed one motivated behavior. The results of the present experiment further confirm that female paced mating and exercise on a running wheel induce long lasting brain plastic changes from the first time the behaviors are displayed.

**Disclosures: L. Mendoza:** None. **R.G. Paredes:** None. **L. Gaytan:** None. **J.A. Aguilar Moreno:** None.

**Poster**

**PSTR193: Internal State, Feeding, and Physical Activity in Motivated Behavior**

**Location:** WCC Halls A-C

**Time:** Monday, November 16, 2026, 1:00 PM - 5:00 PM

**Program #/Poster #:** PSTR193.17/FF20

**Topic:** H.03. Motivation

**Support:** NIH Grant MH096050
NIH Grant DK095908
Maine INBRE Grant P20GM103423

**Title:** Developmental thyrotoxicosis alters reward-related behavior and brain gene expression in adult mice

**Authors: *L. DOUGLAS**[1], A. HERNANDEZ[2];
[1]Maine Hlth. Inst. for Research/University of Maine Grad. Sch. for Biomed. Sci. and E, Biddeford, ME; [2]Mol. medicine, MaineHealth Inst. for Res., Scarborough, ME

**Abstract:** Timely thyroid hormone (T3) signaling is essential for brain development, yet its role in programming adult reward circuitry remains poorly understood. To investigate the long-term consequences of developmental T3 excess, we utilized global *Dio3* knockout (KO) mice, which lack the T3-inactivating enzyme DIO3 and consequently experience developmental thyrotoxicosis. We hypothesized that developmental T3 excess produces enduring alterations in reward system-related behavior and gene expression. We evaluated adult WT and *Dio3* KO littermates of both sexes. *Dio3* KO mice exhibited enhanced motivation for palatable food in a self-administration runway task, reaching the goal box significantly faster than WT on the test day (WT n=42, KO n=46; $p = 0.046$), and showed increased conditioned place preference (CPP) for palatable food (WT n=17, KO n=25; $p = 0.029$). In a separate cohort, KO mice also displayed significantly greater morphine CPP (WT n=11 [4M/7F], KO n=10 [5M/5F]), indicating enhanced sensitivity to opioid reward. After repeated morphine administration, KO mice exhibited increased tail-flick latency, a measure of nociceptive sensitivity used to assess analgesic tolerance to morphine, consistent with reduced tolerance development ($p = 0.024$), and showed fewer naloxone-precipitated withdrawal jumps (WT n=15 [6M/9F], KO n=14 [6M/8F]; $p < 0.05$). Attenuation of withdrawal behavior was driven primarily by male KO mice, which did not show withdrawal jumps. Post-withdrawal analyses revealed elevated *Crh* expression in the amygdala, suggesting dysregulation of stress-responsive circuitry independent of withdrawal severity. Bulk RNA sequencing of WT and KO female striata revealed extensive differential gene expression (WT n=9, KO n=8; 487 genes, $p < 0.05$), including upregulation of genes associated with indirect-pathway medium spiny neurons (*Adora2a*, *Drd2*, *Ppp1r1b*, and *Gpr88*), whereas male KO striatum showed a comparatively attenuated response (WT n=6, KO n=6; 51 genes, $p < 0.05$). In the amygdala, *Hcrtr1* was among the most significantly altered genes regardless of sex (padj=0.00003). RNAScope confirmed cell type-specific expression differences in key reward-circuit genes including *Ppp1r1b*, *Drd2*, *Gpr88*, and *Hcrtr1* across striatum and amygdala. Together, these findings demonstrate that developmental T3 excess produces lasting alterations in reward processing, opioid responsivity, stress signaling, and reward-circuit gene expression. Our results identify developmental DIO3 activity as a key regulator of reward circuit maturation and dependent behavior.

**Disclosures: L. Douglas:** None. **A. Hernandez:** None.

**Poster**

**PSTR193: Internal State, Feeding, and Physical Activity in Motivated Behavior**

**Location:** WCC Halls A-C

**Time:** Monday, November 16, 2026, 1:00 PM - 5:00 PM

**Program #/Poster #:** PSTR193.18/FF21

**Topic:** H.03. Motivation

**Support:** R01 NS126816

**Title:** Effects of left versus right vagus nerve stimulation on cFos expression in catecholaminergic nuclei in naive rats

**Authors: *M. RAJENDRAN**[1], N. Y. KOPCHENKO[3], M. ALI[2], A. SYEDA[2], A. ASLAM[4], J. PEMBO[5], E. NGUYEN[6], C. A. THORN[3];
[1]Sch. pf Behavioral and Brain Sci., [2]The Univ. of Texas at Dallas, Richardson, TX; [3]Neurosci., Univ. of Texas at Dallas, Richardson, TX; [4]Univ. of Texas at Dallas, Murphy, TX; [5]NA, Metairie, LA; [6]UT Dallas, HOUSTON, TX

**Abstract:** SFN abstract, 2026 Effects of left versus right vagus nerve stimulation on cFos expression in catecholaminergic nuclei in naive rats Meena Rajendran, Nicholas Y. Kopchenko, Jordan Pembo, Mina Ali, Anshrah Syeda, Ethan Nguyen, Catherine A. Thorn Previous research shows that right vagus nerve stimulation (r-VNS), but not left VNS (l-VNS), reinforces operant behavior and drives dopaminergic neuronal activity in the ventral tegmental area (VTA) and substantia nigra pars compacta (SNc). In these previous studies, rats were habituated to the training environment and behavioral apparatus using food reinforcers that have the potential to drive plasticity within vagal-to-midbrain pathways prior to the acquisition of VNS-reinforced behaviors. Therefore, in the current study, our aim is to determine the extent to which r-VNS drives greater midbrain activation than l-VNS in training-naïve subjects. In a first experiment, adult male and female Long-Evans rats were randomly assigned to receive r-VNS, l-VNS, or sham stimulation and surgically implanted with a stimulating cuff electrode on either the left or right cervical vagus nerve. After recovery, rats were habituated for 3 days to the testing environment and stimulator cables. On day 4, rats received a single 30-minute treatment session in which 30-second trains of VNS (or sham stimulation) were delivered every 5 minutes (pulse amplitude: 0.8 mA, pulse frequency: 30 Hz, pulse width: 200 μs biphasic). Animals were transcardially perfused 90 minutes after completion of the session. Brains were extracted and immunohistochemistry was performed on slices from the VTA, SNc, and locus coeruleus (LC) to label cFos and tyrosine hydroxylase (TH) expression. In a second experiment, rats received 5 daily 2-hour sessions in which r-VNS, l-VNS, or sham stimulation was delivered (train duration: 0.5 ms, intertrain interval: 30 sec, pulse amplitude: 0.8 mA, pulse frequency: 30 Hz, pulse width: 200 μs biphasic) to mimic the stimulation administered during our prior self-administration studies. Preliminary results from both experiments indicate that VNS may increase cFos expression in the LC and in the dopaminergic midbrain nuclei in naïve rats. However, no significant differences are observed between l-VNS and r-VNS groups. If confirmed, these results suggest that the right-side biased, reward-related effects of VNS may be altered by behavioral experience, including prior food exposure, hunger/satiety state, or operant training procedures.

**Disclosures: M. Rajendran:** None. **N.Y. Kopchenko:** None. **M. Ali:** None. **A. Syeda:** None. **A. Aslam:** None. **J. Pembo:** None. **E. Nguyen:** None. **C.A. Thorn:** None.

**Poster**

**PSTR193: Internal State, Feeding, and Physical Activity in Motivated Behavior**

**Location:** WCC Halls A-C

**Time:** Monday, November 16, 2026, 1:00 PM - 5:00 PM

**Program #/Poster #:** PSTR193.19/FF22

**Topic:** H.03. Motivation

**Support:** NIH DP1 MH140021

**Title:** Peripheral inflammation drives amotivation through a vagal-brainstem-dopamine circuit in arthritis

**Authors: *K. ZANG**[1], M. OTSU[2], F. ZHANG[2], X. ZHU[2], D. AHMADI[2], M. ZHU[2], Y. HU[3], C. PHAM[3], A. KEPECS[2];
[1]Neurosci., Washington Univ. Med. Campus, Saint Louis, MO; [2]Neurosci., [3]Rheumatology, Washington Univ. in St. Louis, Saint Louis, MO

**Abstract:** Inflammatory diseases such as rheumatoid arthritis (RA) produce motivational deficits — reduced effort, withdrawal from rewarding pursuits — that are clinically distinct from pain yet poorly understood mechanistically. Here, using the K/BxN serum transfer arthritis model and multiple motivation-related behavior tasks, we show that experimental inflammatory arthritis in mice induces a selective deficit in foraging and effortful reward-seeking. Arthritis-derived cytokines act on vagal afferents of the nodose ganglion: conditional deletion of their receptors in vagal sensory neurons improves motivation without altering joint inflammation. Vagal input recruits the nucleus tractus solitarius (NTS) and its downstream projections, and silencing the projection partially restores motivation in progressive-ratio performance. In healthy mice, optogenetic activation of the NTS recruits pathways that suppress dopamine release in the nucleus accumbens. These findings define a body-to-brain interoceptive circuit that converts peripheral inflammation into amotivation by gating dopaminergic drive, identifying a tractable target for inflammation-associated behavioral symptoms.

**Disclosures: K. Zang:** None. **M. Otsu:** None. **F. Zhang:** None. **X. Zhu:** None. **D. Ahmadi:** None. **M. Zhu:** None. **Y. Hu:** None. **C. Pham:** None. **A. Kepecs:** None.

**Poster**

**PSTR194: Post-Traumatic Stress Disorder and Other Psychiatric Disorders: Human Studies and Therapeutic Approaches**

**Location:** WCC Halls A-C

**Time:** Monday, November 16, 2026, 1:00 PM - 5:00 PM

**Program #/Poster #:** PSTR194.01/FF23

**Topic:** H.07. Post-Traumatic Stress Disorder and Other Psychiatric Disorders

**Support:** NIH Grant UH3 NS103549
NIH Grant 5R01MH130597-04
Johns Hopkins Applied Physics Laboratory Independent Research & Development Program

**Title:** Behaviorally Informed Neural Subspaces from Natural Conversation Predict Depressive Symptom States

**Authors: *G. BEZOLD**[1], R. HINGORANI[1], B. S. ROBINSON[1], H. YI[1], K. KABOTYANSKI[2], S. RAJESH[4], T. MERK[2], A. GHAZAVI[5], A. ALIJANPOUROTAGHSARA[4], S. CHILUKURI[4], G. WITTEN[4], K. MIRPOUR[4], T. FRACZEK[2], L. JIVNANI[6], B. A. WESTER[1], M. S. FIFER[1], W. K. GOODMAN[3], N. POURATIAN[4], S. A. SHETH[2], N. R. PROVENZA[2];
[1]Johns Hopkins Applied Physics Lab., Laurel, MD; [2]Neurosurg., [3]Psychiatry, Baylor Col. of Med., Houston, TX; [4]Neurolog. Surgery, UT Southwestern Med. Ctr., Dallas, TX; [5]Bioengineering, Univ. of Texas At Dallas, Dallas, TX; [6]Electrical and Computer Engin., Rice Univ., Houston, TX

**Abstract:** The limbic system has a causal role in modulating one's subjective affect and affective behavior, as evidenced by studies with direct electrical stimulation of the brain. Currently, however, the precise neural mechanisms that subserve different manifestations of one's affect remains unknown. Here, we analyzed intracranial and audiovisual recordings from patients undergoing inpatient intracranial monitoring as part of a clinical trial for deep brain stimulation (DBS) therapy for treatment-resistant depression (TRD; N = 3). Specifically, we examined the extent to which neural correlates of fine-grained behavioral features (e.g., facial action units; FAUs) predict depression severity (measured using the Computerized Adaptive Test–Depression Inventory; CAT-DI). First, we identified specific combinations of spectral features across multiple electrode locations, including the anterior cingulate cortex, amygdala, orbitofrontal cortex, and the prefrontal cortex, that accounted for major variations in behavioral features during natural conversations between each patient and members of the clinical research team. Next, we used the same neural combinations to reduce the dimensionality of the data during separate time periods in which the same patients provided CAT-DI responses. We found that we could reliably predict depression severity from the low-dimensional neural space using contemporaneous data. Finally, we identified the neural dimensions that were most predictive of clinical states, mapping it back to the corresponding behavioral features. These results altogether suggest that behaviorally informed neural subspaces can help identify robust neural biomarkers for DBS for mental health symptoms as well as understand the precise links between natural behavior and clinical states.

**Disclosures: G. Bezold:** None. **R. Hingorani:** None. **B.S. Robinson:** None. **H. Yi:** None. **K. Kabotyanski:** None. **S. Rajesh:** None. **T. Merk:** None. **A. Ghazavi:** None. **A. Alijanpourotaghsara:** None. **S. Chilukuri:** None. **G. Witten:** None. **K. Mirpour:** None. **T. Fraczek:** None. **L. Jivnani:** None. **B.A. Wester:** None. **M.S. Fifer:** None. **W.K. Goodman:** None. **N. Pouratian:** None. **S.A. Sheth:** None. **N.R. Provenza:** None.

**Poster**

**PSTR194: Post-Traumatic Stress Disorder and Other Psychiatric Disorders: Human Studies and Therapeutic Approaches**

**Location:** WCC Halls A-C

**Time:** Monday, November 16, 2026, 1:00 PM - 5:00 PM

**Program #/Poster #:** PSTR194.02/FF24

**Topic:** H.07. Post-Traumatic Stress Disorder and Other Psychiatric Disorders

**Support:** NIH Grant R01 MH139889
NIH Grant UH3 NS136631
NIH Grant R01 MH130597
NIH Grant UM1NS132207
Gordon and Mary Cain Pediatric Neurology Research Foundation
McNair Foundation

**Title:** Automated Time-Aligned Warehouse and Query-able Index for Clinical Neuroscience

**Authors: *T. M. FRACZEK**[1], Y. ZHOU[2], A. MARTINEZ BROTONS[10], T. MERK[3], T. P. KUTCHER[11], R. HANISH[12], J. ZHOU[13], V. GOBO[1], W. K. GOODMAN[4], B. Y. HAYDEN[2,14], S. R. HEILBRONNER[5,15], J. A. HENNIG[6,16], S. A. SHETH[7,8,9,16,14], J. A. HERRON[17,18], N. R. PROVENZA[7,16,13,14];
[2]Dept. of Neurosurg., [1]Baylor Col. of Med., Houston, TX; [3]Baylor Col. of Med., HOUSTON, TX; [4]Psychiatry, Baylor Col. of Med., Bethesda, MD; [5]Neurosci., Baylor Col. of Med., Houston, TX; [6]Dept. of Neurosci., Baylor Col. of Med., Pittsburgh, PA; [7]Neurosurg., [8]Dept. of Neurosci., [9]Dept. of Psychiatry & Behavioral Sci., Baylor Col. of Med., Houston, TX; [10]Escuela Técnica Superior de Arte y Tecnología, Valencia, Spain; [12]Electrical and Computer Engin., [13]Dept. of Bioengineering, [14]Neuroengineering Initiative, [15]Dept. of Electrical and Computer Engin., [16]Dept. of Electrical and Computer Engin., [11]Rice Univ., Houston, TX; [17]Dept. of Neurolog. Surgery, [18]Electrical and Computer Engin., Univ. of Washington, Seattle, WA

**Abstract:** Modern clinical neuroscience studies increasingly combine neural recordings, video, audio, wearable sensors, and behavioral assessments collected across independent acquisition systems. Integrating these heterogeneous data streams remains a major challenge because they are sampled at different frequencies, stored in different formats, and often collected over extended periods. In translational neuromodulation research for neuropsychiatric disorders, neural, behavioral, and contextual data are essential for quantifying rapid changes in emotional and cognitive state. Large-scale longitudinal analyses and multimodal machine-learning approaches require these data streams to be reliably synchronized, organized, and accessible within a unified computational framework. To address these challenges, we have extended DataNet, our scalable infrastructure that includes a robust time-synchronization framework, a Neurodata without Borders (NWB)-based warehouse, and an extensible DataJoint-based index. To perform reliable and verifiable synchronization across complex distributed acquisition systems, we use a directed-acyclic graph representation that tracks synchronization relationships among modalities over time. Synchronized and pre-processed data are continuously incorporated

into NWB files spanning the recording period, enabling efficient retrieval. Native storage in NWB also facilitates data sharing and reproducibility. Metadata, quality metrics, and derived analyses are organized within a hierarchical DataJoint index schema that supports rapid data discovery, provenance tracking, and reproducible workflows. This framework allows researchers to add new analyses and metrics or integrate novel predictive models directly into the searchable index. For example, facial-action-unit outputs derived from videos can be used to automatically label smiles in the index, facilitating analyses of neural correlates of increased valence. Together, these components provide a scalable framework for synchronizing, storing, and querying complex multimodal datasets. By reducing technical barriers to multimodal data integration, DataNet accelerates the development of neural and behavioral biomarkers and supports future precision-neuromodulation approaches for neuropsychiatric disorders.

**Disclosures: T.M. Fraczek:** None. **Y. Zhou:** None. **A. Martinez Brotons:** None. **T. Merk:** None. **T.P. Kutcher:** None. **R. Hanish:** None. **J. Zhou:** None. **V. Gobo:** None. **W.K. Goodman:** E. Ownership Interest (stock, stock options, royalty, receipt of intellectual property rights/patent holder, excluding diversified mutual funds); Nview LLC, OCDscales LLC. **B.Y. Hayden:** None. **S.R. Heilbronner:** None. **J.A. Hennig:** None. **S.A. Sheth:** F. Consulting Fees (e.g., advisory boards); Boston Scientific, NeuroPace, Abbott, Koh Young, Zimmer Biomet. Other; co-founder of Motif Neurotech. **J.A. Herron:** None. **N.R. Provenza:** None.

**Poster**

**PSTR194: Post-Traumatic Stress Disorder and Other Psychiatric Disorders: Human Studies and Therapeutic Approaches**

**Location:** WCC Halls A-C

**Time:** Monday, November 16, 2026, 1:00 PM - 5:00 PM

**Program #/Poster #:** PSTR194.03/FF25

**Topic:** H.07. Post-Traumatic Stress Disorder and Other Psychiatric Disorders

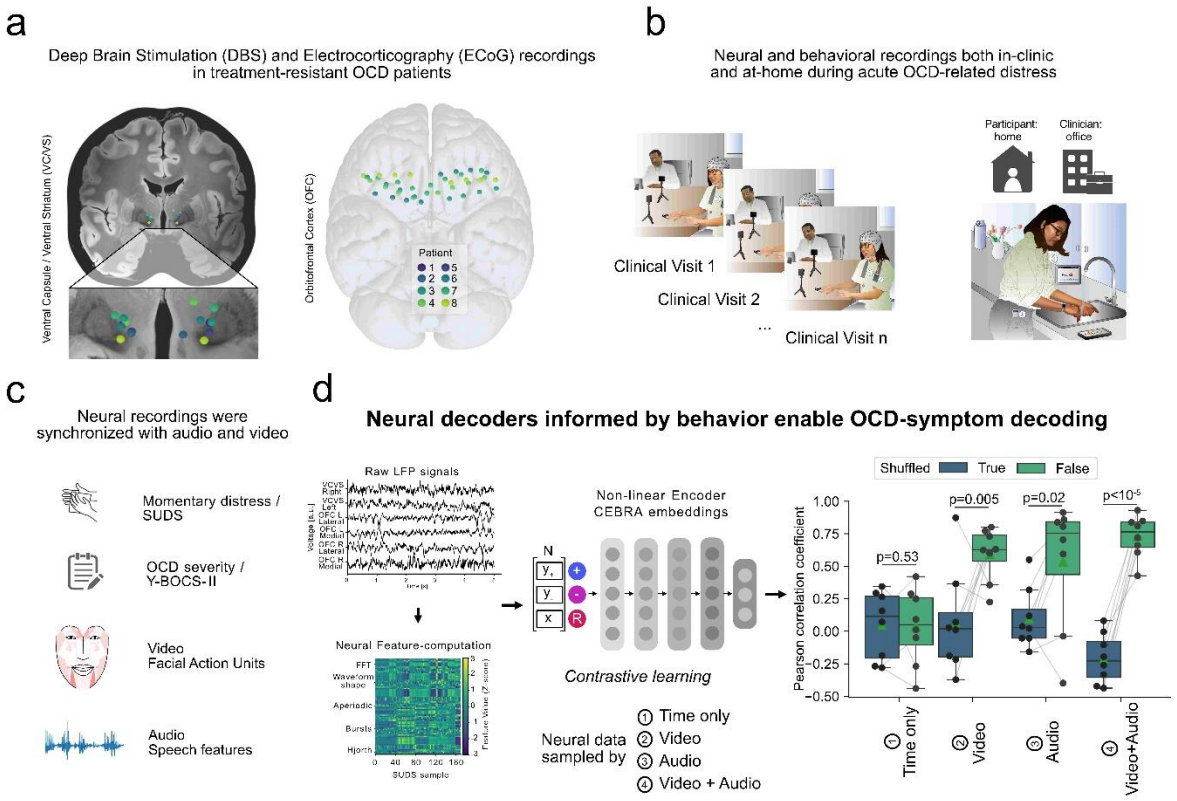
**Support:** NIH Grant UH3NS10054
McNair Foundation
Gordon and Mary Cain Pediatric Neurology Research Foundation

**Title:** Behavior-Informed Neural Decoding of Acute Distress and Long-term Symptom Severity in OCD

**Authors: *T. MERK**[1], G. BEZOLD[7], R. HINGORANI[9], A. WIESE[10], B. S. ROBINSON[8], J. R. ALTMAN[2], M. OCHOA[11], T. HAMRE[3], V. M. BELAVADI[4], M. AVENDANO-ORTEGA[10], S. SOUBRA[3], G. REYES[3], T. FRACZEK[3], E. STORCH[10], W. K. GOODMAN[5], S. A. SHETH[6], N. R. PROVENZA[6];
[1]Baylor Col. of Med., HOUSTON, TX; [2]Baylor Col. of Med., Glen Head, TX; [3]Baylor Col. of Med., Houston, TX; [4]Neurosurg., Baylor Col. of Med., Cypress, TX; [5]Psychiatry, [6]Neurosurg., Baylor Col. of Med., Houston, TX; [7]Johns Hopkins Applied Physics Lab., Washington, DC; [8]Johns Hopkins Applied Physics Lab., Clarksville, MD; [9]Johns Hopkins Univ. APL, Lakewood,

OH; [10]Dept. of Psychiatry and Behavioral Sciences, Baylor Col. of Med., Houston, TX; [11]Rice Univ., Houston, TX

**Abstract:** Deep brain stimulation (DBS) is an effective therapy for treatment-resistant psychiatric disorders. However, identifying optimal stimulation parameters often requires months of iterative clinical adjustments. To enable more objective treatment monitoring, we sought to develop neural decoders of obsessive-compulsive disorder (OCD) symptom severity and acute OCD-related distress. Because symptom expression may be reflected in both neural activity and behavior, we also evaluated whether behavioral measures extracted from synchronized video and audio recordings could improve symptom decoding from neural signals. We recorded intracranial neural signals from the ventral capsule/ventral striatum (VC/VS) DBS target and orbitofrontal cortex (OFC) electrocorticography in nine participants enrolled in a clinical trial of DBS for treatment-resistant OCD (Fig. a). We collected >200 hours of synchronized neural, video, and audio recordings during acute symptom provocation during exposure and response prevention (ERP) therapy and longitudinal clinical interviews across study visits (Fig. b). We extracted neural features, facial action units, and speech characteristics from these recordings (Fig. c), and developed decoders of acute distress and OCD symptom severity using contrastive learning within the CEBRA framework. OFC features showed significantly stronger correlations with both symptom severity and acute distress than VC/VS features alone ($p < 10^{-5}$), and showed distinct signatures for momentary distress and symptom severity within patients. We then developed high-performance neural decoders that predicted OCD symptom severity (Pearson's $R = 0.73 \pm 0.16$, $p < 10^{-5}$). Behavior-guided contrastive learning improved decoding performance compared to self-supervised decoding ($p < 10^{-5}$) and enabled significant decoding compared to shuffled labels (Fig. d).These findings suggest that jointly modeling neural and behavioral signals can improve symptom tracking and may facilitate more efficient DBS programming strategies for OCD.




**Disclosures: T. Merk:** None. **G. Bezold:** None. **R. Hingorani:** None. **A. Wiese:** None. **B.S. Robinson:** None. **J.R. Altman:** None. **M. Ochoa:** None. **T. Hamre:** None. **V.M. Belavadi:** None. **M. Avendano-Ortega:** None. **S. Soubra:** None. **G. Reyes:** None. **T. Fraczek:** None. **E. Storch:** None. **W.K. Goodman:** None. **S.A. Sheth:** None. **N.R. Provenza:** None.

**Poster**

**PSTR194: Post-Traumatic Stress Disorder and Other Psychiatric Disorders: Human Studies and Therapeutic Approaches**

**Location:** WCC Halls A-C

**Time:** Monday, November 16, 2026, 1:00 PM - 5:00 PM

**Program #/Poster #:** PSTR194.04/FF26

**Topic:** H.07. Post-Traumatic Stress Disorder and Other Psychiatric Disorders

**Support:** NIH Brain UH3NS136631
McNair Foundation
Gordon and Mary Cain Pediatric Neurology Research Foundation
NIH R01 MH139889
NIH UH3 NS136631

**Title:** Restoration of Sleep Spindles after Response to Ventral Capsule/Ventral Striatum DBS in Psychiatric Disorder

**Authors: *J. ZHOU**[1], T. MERK[4], W. COON[8], R. HANISH[2], T. P. KUTCHER[3], T. FRACZEK[5], S. SOUBRA[5], T. HAMRE[5], H. BENTLEY[5], N. MOUKADDAM[5], R. HINGORANI[10], H. YI[9], J. A. HERRON[11], W. K. GOODMAN[6], S. A. SHETH[7], N. R. PROVENZA[7];
[1]Bioengineering, [2]Electrical and Computer Engin., [3]Rice Univ., Houston, TX; [4]Baylor Col. of Med., HOUSTON, TX; [5]Baylor Col. of Med., Houston, TX; [6]Psychiatry, Baylor Col. of Med., Bethesda, MD; [7]Neurosurg., Baylor Col. of Med., Houston, TX; [9]Res. and Exploratory Develop. Dept., [8]Johns Hopkins Univ. Applied Physics Lab., Laurel, MD; [10]Johns Hopkins Univ. APL, Lakewood, OH; [11]Dept. of Neurolog. Surgery, Univ. of Washington, Seattle, WA

**Abstract:** Successful deep brain stimulation (DBS) for psychiatric disorders including depression and obsessive-compulsive disorder (OCD) often coincides with improved sleep regularity and continuity. However, the relationship between intracranial neural activity during sleep and symptom improvement after DBS remains unknown. First, we analyzed longitudinal, 24/7 onboard ventral capsule/ventral striatum (VC/VS) DBS recordings from 17 OCD patients. We observed a significant reduction in phasic nighttime 9 Hz power following treatment response ($p=0.048$). Because this frequency range overlaps with sleep spindle activity (10-16 Hz), we hypothesized that symptom improvement is linked to DBS-induced changes in sleep microarchitecture. To test this hypothesis, we utilized dense, high-resolution recordings from an apartment-style monitoring environment where patients stayed for 24-48-hour periods with continuous neurobehavioral recording. We collected VC/VS local field potential (LFP) data (250 Hz time-domain) onboard the DBS device simultaneously with scalp EEG data using the CGX Patch. LFP data were synchronized to EEG data using recorded network timestamps. Sleep stage labels were generated for 30 second epochs using ezscore-f, a sleep staging model fine-tuned for forehead EEG devices. We extracted sleep spindles that were detected during NREM2 and NREM3 sleep for both the LFP and EEG time series, and computed various spindle features including density, frequency, and amplitude. We then compared spindle characteristics before and after DBS activation and clinical response. Scalp EEG and VC/VS LFP data were collected from 5 DBS patients (2 OCD, 3 TRBD) encompassing ~125 hours over 16 nights before and after DBS activation. In the responder patient (TRBD001), both scalp (L: $p<1e-5$, R: $p<1e-5$) and intracranial (L: $p<1e-5$, R: $p<1e-5$) spindle frequencies increased significantly after clinical response was achieved. Other patients who are not yet responders trend towards increased spindle frequency although these changes are not consistently significant. These findings suggest that successful DBS therapy may be associated with normalization of sleep microarchitecture, reflected by shifts in spindle frequency detectable in both scalp EEG and intracranial VC/VS recordings. Such increases in intracranial spindle frequencies may explain the observed decrease in nighttime 9 Hz power after response as well as improved thalamocortical circuit integrity. An understanding of pathological sleep microarchitecture and how DBS affects this circuitry will inform future personalized treatment plans in psychiatry.

**Disclosures: J. Zhou:** None. **T. Merk:** None. **W. Coon:** None. **R. Hanish:** None. **T.P. Kutcher:** None. **T. Fraczek:** None. **S. Soubra:** None. **T. Hamre:** None. **H. Bentley:** None. **N. Moukaddam:** None. **R. Hingorani:** None. **H. Yi:** None. **J.A. Herron:** None. **W.K. Goodman:** None. **S.A. Sheth:** E. Ownership Interest (stock, stock options, royalty, receipt of intellectual

property rights/patent holder, excluding diversified mutual funds); Motif Neurotech. F. Consulting Fees (e.g., advisory boards); Boston Scientific, Zimmer Biomet, Koh Young, Neuropace. **N.R. Provenza:** None.

**Poster**

**PSTR194: Post-Traumatic Stress Disorder and Other Psychiatric Disorders: Human Studies and Therapeutic Approaches**

**Location:** WCC Halls A-C

**Time:** Monday, November 16, 2026, 1:00 PM - 5:00 PM

**Program #/Poster #:** PSTR194.05/FF27

**Topic:** H.07. Post-Traumatic Stress Disorder and Other Psychiatric Disorders

**Support:** R01 MH130597
NIH UH3NS136631
McNair Foundation
Gordon and Mary Cain Neurology Research Foundation

**Title:** Directional asymmetry of cortico-subcortical connectivity between SCC/VCVS deep brain stimulation targets and prefrontal cortex in treatment-resistant depression

**Authors: *R. BAO**[1], S. CHAMARTHI[1], L. MATTAR[1], R. MATHURA[1], D. OSWALT[4], A. ALLAWALA[5], E. BARTOLI[1,6], A. GHAZAVI[9], A. ALIJANPOUROTAGHSARA[9], S. CHILUKURI[9], S. RAJESH[9], G. WITTEN[9], K. MIRPOUR[9], S. J. MATHEW[2], W. K. GOODMAN[2], N. POURATIAN[9], S. R. HEILBRONNER[3,6], S. A. SHETH[1,2,3,6,7], N. R. PROVENZA[1,6,7,8];
[1]Neurosurg., [2]Psychiatry, [3]Neurosci., Baylor Col. of Med., Houston, TX; [4]Neurosurg., Univ. of Pennsylvania, Philadelphia, PA; [5]Neurosurg., Univ. of California San Francisco, San Francisco, CA; [6]Electrical and Computer Engin., [7]Neuroengineering Initiative, [8]Bioengineering, Rice Univ., Houston, TX; [9]Neurolog. Surgery, Univ. of Texas, Southwestern Med. Ctr., Dallas, TX

**Abstract:** The subcallosal cingulate cortex (SCC) and ventral capsule/ventral striatum (VCVS) are promising neuromodulation targets for neuropsychiatric disorders with known functional connectivity to prefrontal cortical regions. However, the electrophysiological signature of these cortico-subcortical interactions remains incompletely characterized. Here, we examined whether cerebro-cerebral evoked potentials (CCEPs) demonstrate symmetric, bidirectional connectivity between the SCC/VCVS and prefrontal cortical regions, including the dorsolateral prefrontal cortex (dlPFC), ventromedial prefrontal cortex (vmPFC), and orbitofrontal cortex (OFC). We analyzed CCEPs in four treatment-resistant depression patients undergoing SCC/VCVS deep brain stimulation (DBS) with concurrent stereo-electroencephalography. For detected evoked peaks (10-150 ms post-stim; prominence ≥10 μV; width 7.5-40 ms), we z-scored each against a pre-stimulation baseline. We then computed a CCEP asymmetry index per electrode pair as forward minus reverse z-scored responses. Positive index values indicate that stimulation of DBS regions elicited greater responses in cortex than cortical stimulation elicited in DBS regions. We tested per-pair asymmetry with Wilcoxon signed-rank tests and SCC versus VCVS differences

with Mann-Whitney U tests. We found that SCC stimulation evoked responses across all cortical targets (dlPFC: 4/4; vmPFC: 2/2; OFC: 2/2 patients), whereas VCVS stimulation evoked responses in the dlPFC (4/4) and OFC (2/2) across patients but engaged the vmPFC in only 1/2 patients. Moreover, stimulation at both the SCC and VCVS elicited greater responses in the dlPFC than the reverse direction ($p \leq 0.002$). At the vmPFC and OFC, however, SCC and VCVS connectivity profiles differed significantly ($p = 0.02$ and $p < 0.001$, respectively): cortical stimulation elicited greater responses in the VCVS than VCVS stimulation elicited in cortex ($p < 0.001$), whereas SCC responses showed no significant directional differences, indicating symmetric connectivity. Within-patient analyses at the OFC revealed the same pattern ($p < 0.001$). In conclusion, CCEP connectivity between the DBS targets and prefrontal cortex was largely asymmetric. Although the SCC and VCVS engaged overlapping cortical regions, their directional profiles diverged in the vmPFC and OFC. These findings position the SCC and VCVS to differentially impact prefrontal-limbic circuitry relevant to treatment-resistant depression. Future work will examine differences in response timing across directions and second-order evoked potentials to further characterize these network interactions.

**Disclosures: R. Bao:** None. **S. Chamarthi:** None. **L. Mattar:** None. **R. Mathura:** None. **D. Oswalt:** None. **A. Allawala:** None. **E. Bartoli:** None. **A. Ghazavi:** None. **A. Alijanpourotaghsara:** None. **S. Chilukuri:** None. **S. Rajesh:** None. **G. Witten:** None. **K. Mirpour:** None. **S.J. Mathew:** F. Consulting Fees (e.g., advisory boards); Abbott, AtaiBeckley, Boehringer-Ingelheim, Delix Therapeutics, Douglas Pharma, Engrail Therapeutics, Freedom Biosciences, Merck, Motif Neurotech, Neumora, Signant Health, Sunovion, Xenon Pharma. **W.K. Goodman:** C. Other Research Support (receipt of drugs, supplies, equipment or other in-kind support); Received donated devices from Medtronic. E. Ownership Interest (stock, stock options, royalty, receipt of intellectual property rights/patent holder, excluding diversified mutual funds); Receives royalties from Nview, LLC and OCDscales, LLC. F. Consulting Fees (e.g., advisory boards); Biohaven Pharmaceuticals. **N. Pouratian:** F. Consulting Fees (e.g., advisory boards); Abbott, Boston Scientific, Medtronic, and BrainLab. **S.R. Heilbronner:** None. **S.A. Sheth:** E. Ownership Interest (stock, stock options, royalty, receipt of intellectual property rights/patent holder, excluding diversified mutual funds); Motif Neurotech. F. Consulting Fees (e.g., advisory boards); Boston Scientific, Zimmer Biomet, Koh Young, NeuroPace, Abbott. **N.R. Provenza:** None.

**Poster**

**PSTR194: Post-Traumatic Stress Disorder and Other Psychiatric Disorders: Human Studies and Therapeutic Approaches**

**Location:** WCC Halls A-C

**Time:** Monday, November 16, 2026, 1:00 PM - 5:00 PM

**Program #/Poster #:** PSTR194.06/FF28

**Topic:** H.07. Post-Traumatic Stress Disorder and Other Psychiatric Disorders

**Support:** NIH grant UH3NS136631
McNair Foundation

Gordon and Mary Cain Neurology Research Foundation
NIH R01 MH139889

**Title:** Reduced neural predictability in ventral striatum after DBS is associated with OCD symptom relief and increased reward sensitivity

**Authors: *R. R. HANISH**[1], J. ZHOU[2], T. MERK[3], S. SOUBRA[4], V. M. BELAVADI[4], G. T. NITCHEU[4], T. A. HAMRE[4], R. BAO[4], Z. PERRY[4], T. M. FRACZEK[4], V. R. GATES[4], M. LIBOWITZ[7], B. M. KIOUS[8], B. J. MICKEY[9], J. A. HERRON[10], B. SHOFTY[7], E. A. STORCH[5], W. K. GOODMAN[6], S. A. SHETH[4], N. R. PROVENZA[4];
[1]Electrical and Computer Engin., [2]Dept. of Bioengineering, Rice Univ., Houston, TX; [3]Baylor Col. of Med., HOUSTON, TX; [4]Neurosurg., [5]Psychiatry and Behavioral Sci., [6]Psychiatry, Baylor Col. of Med., Houston, TX; [7]Neurosurg., [8]Psychiatry, Univ. of Utah, Salt Lake City, UT; [9]Dept. of Psychiatry, Univ. of Utah Sch. of Med., Salt Lake City, UT; [10]Dept. of Neurolog. Surgery, Univ. of Washington, Seattle, WA

**Abstract:** Objective neural biomarkers of clinical status or target engagement in psychiatric disorders have the potential to facilitate individualized neuromodulation strategies. We studied chronic intracranial low-frequency neural recordings from a deep brain stimulation (DBS) device implanted in the ventral capsule/ventral striatum (VC/VS) of 24 patients with severe treatment-resistant obsessive-compulsive disorder. Our previous work (Provenza et al., 2024) showed that neural predictability decreased after significant improvement in symptoms, which often occurs weeks to months after DBS activation. Our goal was to identify early neural biomarkers that can successfully predict eventual symptom improvement. We trained a linear autoregressive model by sliding a 3-day window over the left-hemisphere 8.79±2.5 Hz neural power time series in each patient (train: days 1-2, test: day 3). We compared model predictions to ground truth and calculated daily $R^2$. We next fit a logistic regression model using this feature to derive a decision boundary between the symptom-burdened and symptom-unburdened states. Clinical states were measured using standardized clinical scales. In patients with sufficient pre- and post-DBS data, neural predictability decreased within days after DBS activation in eventual responders. The change in neural predictability from baseline ($\Delta R^2$) just 14 days after beginning stimulation accurately predicted eventual symptom improvement in 10 of 11 patients (p=4.77e-3), while responders required an average of 230 days to respond ($\sigma$=215). A significant decrease in neural predictability after DBS activation may reflect rapid engagement and functional modulation of targeted circuitry, suggesting that stimulation first destabilizes pathological shorttimescale predictability before longer-term clinical improvement emerges. Because the observed effects were measured in the ventral striatum, a region strongly implicated in reward processing, we hypothesize that the observed decreased neural predictability may be associated with more flexible reward processing and increased reward sensitivity after DBS. In future work, we will test this by probing reward sensitivity during a naturalistic task and investigating associated VS neural dynamics throughout treatment.

**Disclosures: R.R. Hanish:** None. **J. Zhou:** None. **T. Merk:** None. **S. Soubra:** None. **V.M. Belavadi:** None. **G.T. Nitcheu:** None. **T.A. Hamre:** None. **R. Bao:** None. **Z. Perry:** None. **T.M. Fraczek:** None. **V.R. Gates:** None. **M. Libowitz:** None. **B.M. Kious:** None. **B.J. Mickey:** None. **J.A. Herron:** F. Consulting Fees (e.g., advisory boards); Panaxium, Mindmorphic. **B. Shofty:** None. **E.A. Storch:** B. Contracted Research/Research Grant (principal investigator for a drug study, collaborator or consultant and pending and current grants). If you

are a PI for a drug study, report that research relationship even if those funds come to an institution.; International OCD Foundation, Wellcome Trust, NIH, MHNTI. E. Ownership Interest (stock, stock options, royalty, receipt of intellectual property rights/patent holder, excluding diversified mutual funds); Rethinking Behavioral Health, NView, OCD Scales, LLC, Elsevier, Wiley, Oxford, American Psychological Association, Guildford, Springer, Routledge, Jessica Kingsley. F. Consulting Fees (e.g., advisory boards); Brainsway, Biohaven Pharmaceuticals. **W.K. Goodman:** E. Ownership Interest (stock, stock options, royalty, receipt of intellectual property rights/patent holder, excluding diversified mutual funds); Nview, LCC, OCDscales, LLC. **S.A. Sheth:** E. Ownership Interest (stock, stock options, royalty, receipt of intellectual property rights/patent holder, excluding diversified mutual funds); Motif Neurotech. F. Consulting Fees (e.g., advisory boards); Boston Scientific, Zimmer Biomet, Abbott, Koh Young, Neuropace. **N.R. Provenza:** None.

**Poster**

**PSTR194: Post-Traumatic Stress Disorder and Other Psychiatric Disorders: Human Studies and Therapeutic Approaches**

**Location:** WCC Halls A-C

**Time:** Monday, November 16, 2026, 1:00 PM - 5:00 PM

**Program #/Poster #:** PSTR194.07/FF29

**Topic:** H.07. Post-Traumatic Stress Disorder and Other Psychiatric Disorders

**Support:** NIH Grant UH3 NS103549
McNair Foundation
Gordon and Mary Cain Neurology Research Foundation

**Title:** Reward-Evoked ACC-mOFC Beta Coherence Indexes Depression Severity

**Authors: *S. CHAMARTHI**[1], J. XIAO[2], R. MATHURA[2], S. J. MATHEW[3], W. K. GOODMAN[3], S. R. HEILBRONNER[2], E. BARTOLI[2], B. Y. HAYDEN[2], J. A. HENNIG[4], N. POURATIAN[5], S. A. SHETH[2], N. R. PROVENZA[2];
[2]Neurosurg., [3]Psychiatry, [4]Neurosci., [1]Baylor Col. of Med., Houston, TX; [5]Neurolog. Surgery, UT Southwestern Med. Ctr., Dallas, TX

**Abstract:** Depression is marked by a reduced ability to experience reward from typically pleasurable stimuli, contributing to anhedonia and motivational disengagement. These symptoms reflect dysfunctions in neural circuitry that underlie reward evaluation and adaptive decision making. In our previous work, we found that beta-band (12-30 Hz) activity in the anterior cingulate cortex (ACC) mediates reward biases and is accordingly blunted in depression. While this implicates local beta oscillations in outcome evaluation and tracking, the network-level significance of these signals in depression remains unclear. We investigated this interplay during the probabilistic reward task in epilepsy (controls; n=15) and treatment-resistant depression (TRD; n=4) patients undergoing stereo-EEG monitoring. Focusing on beta-band interactions, we examined intrahemispheric magnitude-squared coherence, a commonly used measure of phase-synchronized communication, between the ACC and the medial (mOFC) and lateral orbitofrontal

cortices (lOFC) following reward receipt. Relative to epilepsy controls, TRD patients demonstrated significantly lower post-reward beta coherence between ACC-mOFC (296-544ms; two-sided cluster-based permutation test, p=0.004) and ACC-lOFC (382-613ms, p=0.013). Across both cohorts, ACC-mOFC beta coherence was further significantly correlated with depression severity (Pearson correlation, p=0.006), as assessed by the Beck Depression Inventory. To then evaluate whether these prefrontal coherence features could predict cohort membership, we trained a support vector machine classifier using a radial basis function kernel and leave-one-subject-out cross-validation. The classifier achieved an accuracy of 81.0%, an F1 score of 0.826, and an area under the receiver operating characteristic curve of 0.840, supporting the utility of these neural metrics in capturing clinically relevant group differences. Together, these findings identify reduced intrahemispheric beta synchrony within prefrontal reward networks as a robust signature of depression, with the magnitude of these disruptions further tracking individual differences in symptom burden. If validated in larger clinical cohorts, this mechanistic biomarker could support patient-level diagnostic classification and help guide future neuromodulatory therapies that target precise dysfunctional circuits underlying TRD.

**Disclosures: S. Chamarthi:** None. **J. Xiao:** None. **R. Mathura:** None. **S.J. Mathew:** C. Other Research Support (receipt of drugs, supplies, equipment or other in-kind support); Boehringer-Ingelheim, Engrail Therapeutics, Merck, Neurocrine, Sage Therapeutics. F. Consulting Fees (e.g., advisory boards); Almatica Pharma, Biohaven, BioXcel Therapeutics, Boehringer-Ingelheim, Brii Biosciences, Clexio Biosciences, COMPASS Pathways, Delix Therapeutics, Douglas Pharmaceuticals, Eleusis, Engrail Therapeutics, Freedom Biosciences, Janssen, Liva Nova, Levo Therapeutics, Merck, Neumora, Neurocrine, Perception Neurosciences, Praxis Precision Medicines, Relmada Therapeutics, Sage Therapeutics, Signant Health, Sunovion, Xenon Pharmaceuticals, XW Pharma. **W.K. Goodman:** C. Other Research Support (receipt of drugs, supplies, equipment or other in-kind support); Medtronic. F. Consulting Fees (e.g., advisory boards); Biohaven Pharmaceuticals. **S.R. Heilbronner:** None. **E. Bartoli:** None. **B.Y. Hayden:** None. **J.A. Hennig:** None. **N. Pouratian:** F. Consulting Fees (e.g., advisory boards); Abbott, Boston Scientific, Medtronic, BrainLab. **S.A. Sheth:** E. Ownership Interest (stock, stock options, royalty, receipt of intellectual property rights/patent holder, excluding diversified mutual funds); Motif Neurotech. F. Consulting Fees (e.g., advisory boards); Boston Scientific, NeuroPace, Abbott, Zimmer Biomet, Koh Young. **N.R. Provenza:** None.

**Poster**

**PSTR194: Post-Traumatic Stress Disorder and Other Psychiatric Disorders: Human Studies and Therapeutic Approaches**

**Location:** WCC Halls A-C

**Time:** Monday, November 16, 2026, 1:00 PM - 5:00 PM

**Program #/Poster #:** PSTR194.08/FF30

**Topic:** H.07. Post-Traumatic Stress Disorder and Other Psychiatric Disorders

**Title:** Circulatory microRNAs as potential diagnostic biomarkers for suicide in Veterans with bipolar disorder

**Authors: *S. GUPTA**[1], C. HEJL[1], C. CHAN[2], M. GOODMAN[2], P. SZESZKO[2], R. SEIM[3], R. GULERIA[1];
[1]Biomarkers & Genet., VISN17 Ctr. of Excellence, Waco, TX; [2]James J. Peters VA Med. Ctr., Bronx, NY; [3]VISN 17 Ctr. of Excellence, Waco, TX

**Abstract:** Bipolar disorder (BD) is a complex neuropsychiatric condition characterized by recurrent episodes of depression, mania and associated behavioral changes. Increasing evidence suggests that immune-inflammatory dysregulation contributes to BD pathophysiology and influence illness severity. The combination of BD diagnosis and Veteran status confers particularly high risk for future suicide attempts. MicroRNAs (miRNAs), key regulators of brain homeostasis and function, are emerging as promising biomarkers and therapeutic targets in BD. However, the modulation of inflammatory-associated miRNAs in BD patients with suicide attempts (SA+) and without suicide attempts (SA−) remain unclear. We investigated circulating inflammatory-related miRNAs in the serum of Veterans with BD-SA+, Veterans with BD-SA−, and Veteran healthy-control (HC) participants. Individuals with BD met DSM-5 criteria for a bipolar spectrum illness and were assessed using the Structured Clinical Interview for DSM-5 Research Version. SA history was assessed with the Columbia-Suicide Severity Rating Scale (C-SSRS); individuals were classified as SA+ if they had any lifetime history of self-directed potentially injurious behavior, including actual, interrupted, or aborted suicide attempts. HCs had no lifetime history of major mood or psychotic disorders, suicidal behaviors, or substance use disorder within the past three months. Using the human inflammatory response and autoimmunity miRCURY LNA miRNA PCR panel (84 miRNAs), we identified a panel of dysregulated circulating miRNAs (n=3). Six miRNAs, which included miR-98-5p, miR-125a-5p, miR-145-5p, miR-195-5p, miR-374-5p, and miR-454-3p, were validated by independent qRT-PCR analyses across three group comparisons: HC vs BD-SA+, HC vs BD-SA− and BD-SA+ vs BD-SA− (n=15, $p<0.05$). Bioinformatic analyses (KEGG and Gene Ontology enrichment) revealed candidate target genes involved in neuroinflammatory signaling. Unsupervised clustering highlighted three miRNAs, which included miR-125a-5p, miR-195-5p, and miR-454-3p, and their corresponding target genes GDNF, IGF1, and CCL2. qRT-PCR validation showed that miR-125a-5p was upregulated with concurrent downregulation of GDNF, while miR-195-5p and miR-454-3p were downregulated alongside increased IGF1 and CCL2 expression, indicating inverse regulatory relationships (n=15, $p<0.05$). This study identifies, for the first time, a distinct miRNA signature differentiating BD-SA+ from BD-SA−Veterans. These six miRNAs demonstrate potential peripheral biomarkers for BD with suicidal behavior although further studies are needed to confirm their clinical utility.

**Disclosures: S. Gupta:** None. **C. Hejl:** None. **C. Chan:** None. **M. Goodman:** None. **P. Szeszko:** None. **R. Seim:** None. **R. Guleria:** None.

**Poster**

**PSTR194: Post-Traumatic Stress Disorder and Other Psychiatric Disorders: Human Studies and Therapeutic Approaches**

**Location:** WCC Halls A-C

**Time:** Monday, November 16, 2026, 1:00 PM - 5:00 PM

**Program #/Poster #:** PSTR194.09/FF31

**Topic:** H.07. Post-Traumatic Stress Disorder and Other Psychiatric Disorders

**Support:** NIH Grants K01-MH121653, R01-MH129426, R01-EB026439, U24-NS109103, U01-NS108916, U01-NS128612, R01-EY037195, P41-EB018783, R01-MH120194
Brain and Behavior Research Foundation
McDonnell Center for Systems Neuroscience
Fondazione Neurone
American Epilepsy Society Research and Training Fellowship for clinicians

**Title:** Right amygdala ablation reduces maladaptive negative interpretation bias and symptoms in a patient with PTSD

**Authors: *T. XIE**[1], S. VAN ROOIJ[4], S. SUN[5], N. BRYSON[2], P. DEMAREST[2], H. PARK[2], L. MACCOTTA[3], S. WANG[3], P. BRUNNER[2], J. T. WILLIE[2];
[2]Neurosurg., [3]Radiology, [1]Washington Univ. Sch. of Med., Saint Louis, MO; [4]Psychiatry and Behavioral Sci., Emory Univ. Sch. of Med., Atlanta, GA; [5]Frontier Res. Inst. for Interdisciplinary Sci., Tohoku Univ., Sendai, Japan

**Abstract:** *Background:* Negative interpretation bias -- the tendency to perceive ambiguous stimuli as threatening -- is a core cognitive distortion underlying post-traumatic stress disorder (PTSD). The amygdala, a key structure in fear processing, is implicated in PTSD-related hypervigilance and heightened fear perception, yet direct causal evidence linking amygdala function to negative interpretation bias remains limited.
*Methods:* We present a unique prospective case of a male index patient with refractory epilepsy and comorbid chronic PTSD, who underwent stereoelectroencephalography-guided radiofrequency ablation (SEEG-guided RFA) targeting the right amygdala. The index patient and 16 control subjects also performed a facial emotion discrimination task.
*Results:* Before ablation, the patient exhibited heightened negative interpretation bias, judging ambiguous faces as more fearful compared to control groups of epilepsy patients without PTSD. Intracranial SEEG recordings revealed that this cognitive bias was associated with increased late-phase event-related potential (L-ERP) differentiation between fearful and happy faces in the right amygdala. Immediately following focal right amygdala ablation, negative interpretation bias and PTSD symptom severity were significantly reduced, while seizure frequency remained unchanged. Notably, reductions in L-ERP amplitude after ablation closely tracked decreases in fear perception, highlighting L-ERP as a potential biomarker of negative interpretation bias and therapeutic response.
*Conclusions:* Our findings provide causal evidence from an n-of-1 study that the right amygdala supports maladaptive negative interpretation bias in a patient with PTSD and that right amygdala ablation can contribute to the relief of PTSD symptomatology.

**Disclosures: T. Xie:** None. **S. van Rooij:** None. **S. Sun:** None. **N. Bryson:** None. **P. Demarest:** None. **H. Park:** None. **L. Maccotta:** None. **S. Wang:** None. **P. Brunner:** None. **J.T. Willie:** None.

**Poster**

**PSTR194: Post-Traumatic Stress Disorder and Other Psychiatric Disorders: Human Studies and Therapeutic Approaches**

**Location:** WCC Halls A-C

**Time:** Monday, November 16, 2026, 1:00 PM - 5:00 PM

**Program #/Poster #:** PSTR194.10/FF32

**Topic:** H.07. Post-Traumatic Stress Disorder and Other Psychiatric Disorders

**Support:** Defence Research and Development Canada (DRDC), Innovation for Defence Excellence and Security (IDEaS) Program

**Title:** Multivariate Associations Between Resting-State MEG Spectral Features and PTSD Symptom Dimensions

**Authors: *M. ALI**[1,2,4], M. SABERI[4], N. KELARDASHTI[5], P. R. JOHNSTON[5], O. VARTANIAN[1,6], T. A. SCHWEIZER[7], B. T. DUNKLEY[1,3,4];
[1]Grad. Dept. of Psychology, [2]Collaborative Specialization in Neurosci., [3]Collaborative Specialization in Neurosci. (CSIN), Univ. of Toronto, Toronto, ON, Canada; [4]Neurosciences & Mental Hlth. (NMH) Program, [5]Neurosci. Mental Hlth. (NMH) Program, The Hosp. for Sick Children Res. Inst., Toronto, ON, Canada; [6]Defence Res. and Develop. Canada (DRDC), Toronto, ON, Canada; [7]St. Michael's Hosp., Toronto, ON, Canada

**Abstract:** Posttraumatic stress disorder (PTSD) is increasingly recognized as a heterogeneous condition characterized by disturbances in neural systems supporting memory, cognition, and emotional regulation. Despite this heterogeneity, most electrophysiological studies continue to rely on categorical diagnostic comparisons and univariate approaches, limiting characterization of how continuous symptom dimensions relate to large-scale neural dynamics. Here, we used canonical correlation analysis (CCA) to examine multivariate associations between PTSD symptom dimensions and resting-state magnetoencephalography (MEG) spectral features. Resting-state MEG data were acquired from 151 trauma-exposed Canadian Armed Forces members and veterans during a five-minute eyes-open recording. Symptom severity was assessed using the PTSD Checklist Military Version (PCL-M). Reexperiencing, avoidance/withdrawal, and hyperarousal symptom dimensions were examined while controlling for anxiety (GAD-7), depression (PHQ-9), and concussion diagnosis. Source-resolved oscillatory power was quantified across canonical frequency bands, and regional aperiodic slope and offset parameters were estimated to capture complementary aspects of neural population activity. CCA was used to identify multivariate relationships linking symptom dimensions with coordinated patterns of spectral variation. Significant canonical functions were identified across delta, theta, beta, and low gamma frequency bands, as well as regional aperiodic slope and offset measures. Distinct combinations of reexperiencing, avoidance/withdrawal, and hyperarousal symptoms were associated with partially separable patterns of oscillatory and aperiodic neural variation. Multivariate loadings implicated distributed cortical and subcortical regions commonly associated with memory, salience, and cognitive control processes, suggesting that PTSD symptom dimensions are linked to dissociable neurophysiological profiles rather than a single shared neural disturbance. These findings demonstrate that variability in PTSD symptom expression is associated with coordinated alterations in resting-state neural dynamics. By

integrating oscillatory and aperiodic spectral features within a multivariate framework, this study advances dimensional approaches to trauma-related psychopathology. It identifies candidate neurophysiological markers associated with specific symptom dimensions across trauma-exposed individuals.

**Disclosures: M. Ali:** None. **M. Saberi:** None. **N. Kelardashti:** None. **P.R. Johnston:** None. **O. Vartanian:** None. **T.A. Schweizer:** None. **B.T. Dunkley:** None.

**Poster**

**PSTR194: Post-Traumatic Stress Disorder and Other Psychiatric Disorders: Human Studies and Therapeutic Approaches**

**Location:** WCC Halls A-C

**Time:** Monday, November 16, 2026, 1:00 PM - 5:00 PM

**Program #/Poster #:** PSTR194.11/GG1

**Topic:** H.07. Post-Traumatic Stress Disorder and Other Psychiatric Disorders

**Support:** National Institute on Drug Abuse Intramural Research Program
NIDA Grant UH3DA048734

**Title:** PTSD Symptom Clusters and Substance-Specific Craving Associations in Substance Use Disorder

**Authors: *E. SENKO**[1], T. LIU[1], J. ELLIS[2], A. HUHN[2], J. HEMMONS[1], B. CURTIS[1]; [1]Natl. Inst. on Drug Abuse (NIDA), Baltimore, MD; [2]Johns Hopkins Sch. of Med., Baltimore, MD

**Abstract:** Post-traumatic stress disorder (PTSD) and substance use disorder (SUD) frequently co-occur, yet specific PTSD symptom clusters (avoidance, hyperarousal, and re-experiencing) may be differentially associated with craving across substances, potentially reflecting distinct neurobehavioral pathways. This study examined whether PTSD symptom severity and PTSD symptom clusters were associated with craving across primary substance groups. A total of 6783 participants (69.5% male) receiving SUD treatment across 75 facilities in the United States completed surveys at treatment intake. PTSD symptom severity was measured using the PCL-6. Craving was assessed using validated substance-specific craving scales corresponding to the participants' primary substance group. During the intake survey, participants reported their primary substance as either alcohol, stimulants, cocaine, methamphetamine, opioids, heroin, marijuana, or benzodiazepines as their primary substance. For analysis, cocaine, methamphetamine, and stimulant responses were combined into a single stimulants group, while heroin and opioid responses were combined into a single opioids group. Linear regressions examined associations between PTSD symptom severity/clusters and craving, while interaction regressions tested whether these associations differed across substance groups. MANOVA examined differences in PTSD symptom-cluster profiles across substance groups. PTSD symptom severity significantly predicted craving across all substance groups (all ps $< 0.01$). PTSD-craving associations differed modestly across substances overall, $F(4, 6754) = 2.68$, $p =$

0.030, although Tukey-adjusted pairwise comparisons were nonsignificant. In symptom-cluster analyses, hyperarousal demonstrated the strongest overall association with craving ($\beta = .27$, $p < 0.001$), while re-experiencing was the only symptom cluster whose craving associations significantly differed across substance groups, $F(4, 6754) = 5.31$, $p < 0.01$. PTSD symptom-cluster profiles also differed significantly across substance groups overall, Pillai's Trace = .017, $F(12, 20334) = 9.49$, $p < .001$, $\eta^2p = .006$. These findings suggest that PTSD symptom clusters are differentially associated with craving across substance groups. Hyperarousal symptoms demonstrate the strongest overall association with craving, whereas re-experiencing symptoms may be more relevant to substance-specific craving processes. Improved understanding of these relationships may inform targeted interventions for individuals with co-occurring PTSD and SUD.

**Disclosures: E. Senko:** None. **T. Liu:** None. **J. Ellis:** None. **A. Huhn:** None. **J. Hemmons:** None. **B. Curtis:** None.

**Poster**

**PSTR194: Post-Traumatic Stress Disorder and Other Psychiatric Disorders: Human Studies and Therapeutic Approaches**

**Location:** WCC Halls A-C

**Time:** Monday, November 16, 2026, 1:00 PM - 5:00 PM

**Program #/Poster #:** PSTR194.12/GG2

**Topic:** H.07. Post-Traumatic Stress Disorder and Other Psychiatric Disorders

**Support:** AMED JP21zf0127005 (to M.S.)
AMED JP21km0908001 (to M.S.)
AMED JP23wm0525003 (to M.S.)
JSPS KAKENHI 24H00894 (to M.S.)
JSPS KAKENHI 23H02784 (to M.S.)
JSPS KAKENHI 22H00469 (to M.S.)
JSPS KAKENHI 26H02428 (to M.S.)
JSPS KAKENHI 25KJ0664 (to C.K.)
Takeda Science Foundation (to M.S.)

**Title:** Sound exposure during sleep in individuals with PTSD: a first-in-human, open-label feasibility study

**Authors: *M. SAKAGUCHI**[1], K. INO[2], K. ZEMPO[4], A. HORI[7], T. MARUYAMA[8], M. TOMINAGA[9], Y. SUGAYA[10], M. OBA[3], L. SATO[5], H. SEKIBA[5], C. KAWAKAMI[5], G. BACHMAN[5], I. WAKI[6], H. KITAGAWA[5], M. YANAGISAWA[5], Y. KIM[2];
[1]Kobe Univ., Kobe, Japan; [2]Dept. of Behavioral Medicine, Natl. Inst. of Mental Hlth., [3]Dept. of Clin. Data Science, Natl. Ctr. Hosp., Natl. Ctr. of Neurol. and Psychiatry (NCNP), Kodaira, Japan; [4]Inst. of Systems and Information Engin., [5]Intl. Inst. for Integrative Sleep Med. (WPI-IIIS), [6]Tsukuba Clin. Res. & Develop. Org. (T-CReDO), Univ. of Tsukuba, Tsukuba, Japan; [7]Hori Mental Clin., Fukushima, Japan; [8]Clin. Res. Promotion Ctr., The Univ. of Tokyo Hosp.,

Tokyo, Japan; [9]S'UIMIN Inc., Tokyo, Japan; [10]Dept. of Neurophysiology, Grad. Sch. of Med., The Univ. of Tokyo, Tokyo, Japan

**Abstract:** Trauma-focused psychotherapies remain the most effective treatments for post-traumatic stress disorder (PTSD), yet their reliance on conscious re-engagement with traumatic memories produces high distress and dropout rates that limit clinical reach. Whether therapeutic re-exposure can instead be delivered during sleep—when memory reactivation drives reorganization—has not been tested in people with PTSD, in whom sleep architecture is itself disrupted [1]. Here, we report a first-in-human, open-label feasibility study of sound exposure during sleep (SES) [2], in which personalized trauma-related auditory cues were presented to participants with PTSD during slow-wave sleep. Thirteen participants provided written informed consent, of which six completed the overnight SES session with sleep monitoring. SES was tolerated without procedure-attributable adverse events, and the macro-architecture of slow-wave sleep was preserved. Two sequential SES protocol versions differed in the permitted Subjective Units of Distress Scale (SUDS; 0-100) for the sleep-delivered sound: the original version (n = 2) capped SUDS at 30-40, and an amended version (n = 4) applied no ceiling SUDS. In post hoc analyses of pre-specified secondary outcomes, the no-ceiling amended protocol was associated with reductions in sound-evoked SUDS (mean difference -65.5%; 95% confidence interval: -104.2 to -26.7; nominal p = 0.012) and PCL-5 intrusion score (-7.0; nominal p = 0.015). These results establish the feasibility and safety of delivering personalized trauma-related sounds during sleep in people with PTSD and motivate sham-controlled efficacy trials of a fundamentally new therapeutic paradigm. Study registration: jRCT1030230706. References: [1] Sekiba et al. REM sleep rhythm impairment in people with PTSD. medRxiv 2025. doi:10.1101/2025.07.02.25330609. [2] Ino et al. Sound Exposure During Sleep (SES) in PTSD Patients: An Open-Label Feasibility Study. medRxiv 2026. https://www.medrxiv.org/content/10.64898/2026.05.02.26352243v1

**Disclosures: M. Sakaguchi:** E. Ownership Interest (stock, stock options, royalty, receipt of intellectual property rights/patent holder, excluding diversified mutual funds); SES-related patent (inventor; assigned to Kobe University and NCNP). **K. Ino:** None. **K. Zempo:** None. **A. Hori:** E. Ownership Interest (stock, stock options, royalty, receipt of intellectual property rights/patent holder, excluding diversified mutual funds); Pending international patent on physician sound-determination instrument (listed inventor; JP-2026-027927). **T. Maruyama:** None. **M. Tominaga:** A. Employment/Salary (full or part-time):; S'UIMIN Inc.. **Y. Sugaya:** None. **M. Oba:** None. **L. Sato:** None. **H. Sekiba:** None. **C. Kawakami:** None. **G. Bachman:** None. **I. Waki:** None. **H. Kitagawa:** E. Ownership Interest (stock, stock options, royalty, receipt of intellectual property rights/patent holder, excluding diversified mutual funds); S'UIMIN Inc. (equity holder). **M. Yanagisawa:** E. Ownership Interest (stock, stock options, royalty, receipt of intellectual property rights/patent holder, excluding diversified mutual funds); S'UIMIN Inc. (equity holder). Other; S'UIMIN Inc. (board chairperson). **Y. Kim:** E. Ownership Interest (stock, stock options, royalty, receipt of intellectual property rights/patent holder, excluding diversified mutual funds); Pending international patent on physician sound-determination instrument (listed inventor; JP-2026-027927).

**Poster**

**PSTR194: Post-Traumatic Stress Disorder and Other Psychiatric Disorders: Human Studies and Therapeutic Approaches**

**Location:** WCC Halls A-C

**Time:** Monday, November 16, 2026, 1:00 PM - 5:00 PM

**Program #/Poster #:** PSTR194.13/GG3

**Topic:** H.07. Post-Traumatic Stress Disorder and Other Psychiatric Disorders

**Support:** Neurovalens Ltd.
VA Grant I01CX002872

**Title:** Effect of Electrical Vestibular System Stimulation on PTSD Symptom Clusters

**Authors: V. R. VASQUEZ**, R. A. YOSHIDA, R. C. TOLBERT, *J. R. HOWLETT, P. COLVONEN;
VA San Diego Healthcare Syst., San Diego, CA

**Abstract:** Dysregulation of the vestibular system is linked to heightened autonomic arousal, anxiety, insomnia, and symptoms of posttraumatic stress disorder (PTSD). It is hypothesized that vestibular dysregulation causes an increase in arousal by overstimulating the limbic system. Electrical Vestibular System Stimulation (VSS) is a safe, noninvasive technique that may normalize vestibular dysfunction and has been shown to reduce anxiety. A recent randomized controlled trial found that 12 weeks of VSS treatment significantly reduced symptoms of PTSD compared to sham treatment, but the effect of VSS on specific PTSD symptom clusters has not been examined. We performed a follow-up analysis of data from the randomized, double blind controlled clinical trial, examining the effects of 12 weeks of VSS treatment (N = 108) compared to sham treatment (n = 93) on each symptom cluster in individuals with PTSD. We hypothesized that avoidance and arousal symptoms of PTSD treated would improve with VSS over time, while re-experiencing and negative cognition would not be affected. Results showed cluster B (re-experiencing) did not improve significantly with VSS compared to sham treatment (p =.078), while cluster C (avoidance; p = .002), cluster D (negative alterations in cognition and mood; p = .001) and cluster E (arousal and reactivity; p = .009) improved significantly with VSS compared to sham treatment. VSS may be a promising treatment for a range of PTSD symptoms, including avoidance, negative alterations in cognition/mood, and arousal/reactivity, while the effect on intrusion/re-experiencing symptoms is less clear.

**Disclosures: V.R. Vasquez:** None. **R.A. Yoshida:** None. **R.C. Tolbert:** None. **J.R. Howlett:** None. **P. colvonen:** B. Contracted Research/Research Grant (principal investigator for a drug study, collaborator or consultant and pending and current grants). If you are a PI for a drug study, report that research relationship even if those funds come to an institution.; Neurovalens Ltd..

**Poster**

**PSTR194: Post-Traumatic Stress Disorder and Other Psychiatric Disorders: Human Studies and Therapeutic Approaches**

**Location:** WCC Halls A-C

**Time:** Monday, November 16, 2026, 1:00 PM - 5:00 PM

**Program #/Poster #:** PSTR194.14/GG4

**Topic:** H.07. Post-Traumatic Stress Disorder and Other Psychiatric Disorders

**Title:** Examining the Underlying Neurobiology of Psychological Trauma in Physical Inactivity

**Authors: *G. SAIKIA**[1], O. ODIA[2], P. J. CLARK[1];
[1]Dept. of Food Sci. and Human Nutr., [2]Dept. of Genet. and Genomics, Iowa State Univ., Ames, IA

**Abstract:** Physical inactivity represents a growing global health burden, with approximately one in five adults meeting recommended physical activity guidelines (Garcia-Hermoso et al., 2023). Despite the well-established benefits of exercise for physical and mental health, a substantial proportion of the population remains insufficiently active (Reddigan et al., 2011; Admiraal et al., 2011). Prior traumatic experience has been identified as a risk factor for physical inactivity (Winning et al., 2017; de Assis et al., 2008; Vancampfort et al., 2016); however, the biological mechanisms linking trauma exposure to reduced physical activity remain poorly understood. This study aims to examine whether adverse childhood experiences are associated with brain volumetric changes that mediate chronic physical inactivity. We utilize data from the UK Biobank cohort (N ≈ 500,000; ages 40-69), incorporating wrist-worn accelerometry from ~ 100,000 participants, PTSD diagnoses ascertained via the Mental Health Questionnaire (PCL-based) and ICD-10 NHS records (~9,000 cases), MRI-derived brain volumetric measures, inflammatory biomarkers, and genome-wide genetic data. Covariates include age, sex, BMI, smoking status, alcohol consumption, and sleep. Longitudinal outcomes assessed through linked electronic health records. We hypothesize that higher trauma scores will be negatively associated with objectively measured physical activity levels. We further hypothesize that this relationship will be partially mediated by neuroanatomical differences in regions previously implicated in threat appraisal, emotional regulation, and reward-motivated behavior. Particularly, impaired anterior cingulate and infralimbic fear extinction, heightened prelimbic threat expression, and insular misattribution of exercise sensations as threatening collectively explain lower physical activity in high trauma individuals. In addition, trauma-driven amygdala hyperactivation, dorsal striatal dopaminergic disruption, and ventral striatal reward blunting converge to mechanistically explain why high trauma individuals are expected to exhibit significantly lower physical activity levels than low trauma counterparts. These regions are especially relevant given their roles in fear processing, interoception, and motivational salience, all of which may explain why higher trauma burden translates into reduced voluntary movement. Data collection is underway, and preliminary accelerometer data suggest that individuals reporting higher childhood trauma scores show measurably reduced physical activity levels, consistent with our central hypothesis.

**Disclosures: G. Saikia:** None. **O. Odia:** None. **P.J. Clark:** None.

**Poster**

**PSTR194: Post-Traumatic Stress Disorder and Other Psychiatric Disorders: Human Studies and Therapeutic Approaches**

**Location:** WCC Halls A-C

**Time:** Monday, November 16, 2026, 1:00 PM - 5:00 PM

**Program #/Poster #:** PSTR194.15/GG5

**Topic:** G.06. Autonomic Regulation

**Support:** CDMRP Gulf War Illness Reseach Program #11488016

**Title:** Heart Rate Variability is Associated with Autonomic Symptom Burden in Veterans with Gulf War Illness Receiving Yoga Therapy

**Authors: A. BROWN**, *P. J. BAYLEY;
VA Palo Alto / Stanford Univ., Palo Alto, CA

**Abstract:** Gulf War Illness (GWI) is a chronic multisymptom condition characterized by pain, fatigue, cognitive difficulties, and autonomic dysfunction. Although autonomic dysfunction is a prominent feature of GWI, the relationship between objective physiological markers of autonomic regulation and subjective autonomic symptom burden remains poorly characterized. We analyzed autonomic outcomes among Veterans with GWI who participated in a 10-week yoga therapy intervention to treat chronic pain (n = 39; 79.5% male; age = 53.8 ± 7.2 years). Autonomic symptoms were assessed using the Composite Autonomic Symptom Score-31 (COMPASS-31), including total, orthostatic, vasomotor, secretomotor, gastrointestinal, bladder, and pupillomotor domains. Heart rate variability (HRV) measures included mean heart rate, root mean square of successive differences (RMSSD), standard deviation of normal-to-normal intervals (SDNN), high-frequency HRV (HF-HRV), low-frequency HRV (LF-HRV), and related indices of autonomic regulation. Assessments were obtained at baseline, week 10 (end-of-treatment), and week 34 (six-month follow-up). Treatment effects, predictive associations, and cross-sectional physiological-subjective associations were evaluated using mixed-effects models and Spearman correlations with Benjamini-Hochberg false discovery rate (FDR) correction. Treatment-related effects on COMPASS-31 outcomes and HRV did not survive correction for multiple comparisons. However, two baseline physiological predictors of subsequent COMPASS-31 improvement survived FDR correction ($p < .05$). Higher baseline Mean HR predicted greater bladder symptom improvement from week 10 to week 34 ($\rho = .563$, $p = .004$, $q = .025$), while higher baseline HF-HRV predicted greater improvement in overall autonomic symptom burden during the same interval ($\rho = -.487$, $p = .021$, $q = .043$). In addition, lower HRV was associated with greater bladder and gastrointestinal symptom burden; LF-HRV was inversely associated with bladder symptoms ($\rho = -.552$, $p = .001$, $q = .013$) and gastrointestinal symptoms ($\rho = -.442$, $p = .011$, $q = .045$), while SDNN was inversely associated with bladder symptoms ($\rho = -.464$, $p = .008$, $q = .045$). These findings demonstrate significant physiological-subjective autonomic convergence in Veterans with GWI receiving yoga therapy and support HRV as an objective correlate of autonomic symptom burden, highlighting the value of integrating physiological and self-report measures when characterizing autonomic dysfunction in GWI.

**Disclosures: A. Brown:** None. **P.J. Bayley:** None.

**Poster**

**PSTR194: Post-Traumatic Stress Disorder and Other Psychiatric Disorders: Human Studies and Therapeutic Approaches**

**Location:** WCC Halls A-C

**Time:** Monday, November 16, 2026, 1:00 PM - 5:00 PM

**Program #/Poster #:** PSTR194.16/GG6

**Topic:** H.07. Post-Traumatic Stress Disorder and Other Psychiatric Disorders

**Title:** Clozapine CNS Pharmacokinetic Model: Insights into Active Brain Concentrations, Receptor Occupancy, and Cognitive Impairment

**Authors: *P. BURKAT**;
Univ. of Pennsylvania, Philadelphia, PA

**Abstract: Introduction:** Clozapine (CLOZ) is an effective treatment for treatment-resistant schizophrenia. It has a high affinity multi-receptor profile that underlies its unique efficacy. CLOZ is metabolized by the cytochrome P450 system to N-desmethylclozapine (NDMC) which contributes to both efficacy and adverse effects. CLOZ-induced cognitive impairment is a complex and significant adverse effect mediated in part by muscarinic receptor antagonism; however, histamine receptor antagonism likely also plays a critical role. This study aimed to develop a CLOZ-NDMC CNS pharmacokinetic model to estimate active human brain concentrations, predict multi-receptor occupancies, and to further elucidate mechanisms underlying CLOZ-induced cognitive impairment in human subjects. **Methods:** Data and initial parameter values were obtained from PubMed and DrugBank searches. PBPK models for CLOZ and NDMC were developed with PK-Sim software. Pharmacodynamic models for cognitive impairment with NDMC brain concentration passed as the regressor were developed with the Monolix Suite 2024 platform. P-glycoprotein blood brain barrier efflux transporter maximum reaction velocities and affinity constants for CLOZ and NDMC were optimized using a Monte Carlo algorithm. To estimate CLOZ and NDMC active brain concentrations, P-glycoprotein transporter concentration was reduced 9.88-fold for the human model. D1, D2, and 5-HT2A receptor occupancies as functions of CLOZ brain concentrations were estimated with the Gaddum-Schild equation for two ligands binding to the same receptor. **Results:** The confirmed PBPK model accounted for CLOZ and NDMC plasma concentrations following a single 12.5 mg peroral dose, and predicted steady state plasma concentrations for 100 mg twice daily CLOZ dosing. Steady state CLOZ and NDMC unbound plasma concentrations were similar for both compounds. Peak active brain concentrations for CLOZ and NDMC following a single 50 mg CLOZ dose were 12 ± 2.6 nM and 3 ± 1 nM, respectively. The kinetic profile of NDMC brain concentration following a single CLOZ dose directly corresponds to the time courses of attention and memory impairment, and mood improvement in human subjects. Prediction of D1, D2, and 5-HT2A receptor occupancies suggests an allosteric interaction between CLOZ and NDMC binding sites at each receptor. **Conclusions:** This CLOZ-NDMC model predicts human steady state plasma concentrations and multi-receptor occupancies with active brain concentrations for both compounds. NDMC likely contributes to CLOZ-induced cognitive impairment in humans via histamine H1 antagonism, while mood improvement may be associated with delta opioid agonism.

**Disclosures: P. Burkat:** None.

**Poster**

**PSTR194: Post-Traumatic Stress Disorder and Other Psychiatric Disorders: Human Studies and Therapeutic Approaches**

**Location:** WCC Halls A-C

**Time:** Monday, November 16, 2026, 1:00 PM - 5:00 PM

**Program #/Poster #:** PSTR194.17/GG7

**Topic:** H.07. Post-Traumatic Stress Disorder and Other Psychiatric Disorders

**Support:** NIH U01DA048279
NIH R01DA047880
NIMH Intramural Research Program (HBCC): ZIC MH002903

**Title:** Single-Nucleus Transcriptomic Profiling Reveals Disease- and Age-Associated Molecular Programs in the Human Ventral Midbrain

**Authors: *S. SINGH**;
Icahn Sch. of Med. at Mount Sinai, New York, NY

**Abstract:** Schizophrenia (SCZ) and bipolar disorder (BD) are highly heritable psychiatric disorders, yet how genetic risk manifests within disease-relevant cell types remains unclear. Most genomic studies have focused on the cortex, leaving the ventral midbrain, a key hub of dopaminergic signaling and a major target of antipsychotic medications, poorly characterized at cellular resolution. Here, we generated a large-scale single-nucleus RNA-sequencing resource of the human ventral midbrain comprising 219,187 nuclei from 184 postmortem donors (86 controls, 68 SCZ, and 30 BD cases). Integrative clustering and annotation defined a hierarchical cellular taxonomy consisting of 9 major cell classes and 17 transcriptionally distinct subclasses. Cell-type-resolved differential expression analyses identified 5,604 differentially expressed genes (DEGs) in SCZ (2,421 upregulated and 3,183 downregulated) and 1,833 DEGs in BD (967 upregulated and 866 downregulated). In SCZ, selective vulnerability was marked by transcriptional downregulation in oligodendrocyte precursor cells (OPCs), mural cells, and inhibitory GABAergic neurons. Similarly, BD-associated transcriptional downregulation was concentrated within inhibitory GABAergic neurons, immune cells, and mural cells. Pathway analyses revealed that downregulated genes in SCZ GABAergic neurons were enriched for neurotransmitter release and synaptic signaling pathways, whereas downregulated genes in BD GABAergic neurons were enriched for protein translation and ribosomal pathways. BD-associated immune-cell alterations additionally showed dysregulation of cholesterol biosynthesis, SREBP-mediated lipid metabolism, and mTOR signaling pathways. Disease-associated signatures converged with psychiatric genetic risk loci. We also analyzed aging-associated transcriptional changes in control donors. Aging was associated with substantial transcriptional remodeling across neuronal, glial, immune, and vascular populations. Comparison of age- and disease-associated signatures revealed both shared and distinct molecular programs, with convergence on neuronal, glial, immune, and vascular pathways alongside disease-specific alterations in neurotransmission, protein translation, and lipid metabolism. These findings establish a single-cell atlas of the human ventral midbrain across aging and psychiatric disease and identify cell populations selectively vulnerable to schizophrenia and bipolar disorder.

**Disclosures: S. Singh:** None.

**Poster**

**PSTR194: Post-Traumatic Stress Disorder and Other Psychiatric Disorders: Human Studies and Therapeutic Approaches**

**Location:** WCC Halls A-C

**Time:** Monday, November 16, 2026, 1:00 PM - 5:00 PM

**Program #/Poster #:** PSTR194.18/GG8

**Topic:** H.07. Post-Traumatic Stress Disorder and Other Psychiatric Disorders

**Support:** Department of Biotechnology
Government of India
Pratiksha Trust
Rohini Nilekani Philanthropies

**Title:** CALM-Brain: The CBM-ADBS Longitudinal Multimodal Brain data resource for neuropsychiatric disorders

**Authors: *H. GUBBI VANI**[1], G. MOHAN[2], U. S. BHALLA[1], R. PADINJAT[1], J. REDDY YC[3];
[1]NCBS-TIFR, Bangalore, India; [2]institute of experimental epileptology and cognition research, Uniklinikum Bonn, Bonn, Germany; [3]NIMHANS, BENGALURU, India

**Abstract:** Severe psychiatric and neurodegenerative disorders inflict an immense burden on individuals, families, and healthcare systems globally. Early diagnosis remains challenging due to the complex and heterogeneous nature of these disorders and their underlying biological mechanisms. CALM-Brain (CBM-ADBS Longitudinal Multimodal Brain data resource ) is the data repository for one of the largest and most comprehensive neuropsychiatric cohorts from India, designed to address these challenges by uniquely integrating clinical, imaging, genomic, and multimodal brain function data from multiply-affected families in a longitudinal design. CALM-Brain hosts data from a prospective longitudinal study of patients and their unaffected family members, obtained as part of the CBM collaboration between NIMHANS and NCBS. Subjects include patients with severe neuropsychiatric disorders including schizophrenia (SCZ), bipolar disorder (BD), obsessive-compulsive disorder (OCD), dementia, and addiction. First-degree unaffected relatives and healthy controls are included in the cohort. Subjects undergo assessments every two years that cover clinical evaluations, neuropsychological assessments, neuroimaging, and life events. Data modalities include structural and functional MRI, electroencephalography (EEG), functional near-infrared spectroscopy (fNIRS), eye tracking, standardised clinical and neuropsychological assessments. Whole-exome sequence data and Human Induced Pluripotent Stem Cell lines (IPSCs) have been obtained for a subset of participants. The latest curated release includes data from 2,282 subjects across 942 families, in the age range of 16-92 years. 56% of the subjects are male and 44% are female. Structural MRI data has been acquired for 821 subjects across 918 sessions, reflecting longitudinal assessments for a subset of subjects. The MRI dataset was preprocessed using several pipelines including

defacing, cortical segmentation, and volumetric measures. EEG, fNIRS, and eye-tracking data have been obtained for subsets of the cohort. Data is organised as per the Brain Imaging Data Structure (BIDS) format using Almirah, an in-house Python package. The CALM-Brain web interface supports searching and listing available data upon registration, prior to full access. CALM-Brain provides ready-to-use tutorials and demonstration analyses, and on-server data analysis tools. Data access is provided following submission and evaluation of institutional ethical approvals and data use agreements, with a commitment to broad dissemination for maximum use of this resource.

**Disclosures: H. Gubbi Vani:** None. **G. Mohan:** None. **U.S. Bhalla:** None. **R. Padinjat:** None. **J. Reddy YC:** None.

**Poster**

**PSTR194: Post-Traumatic Stress Disorder and Other Psychiatric Disorders: Human Studies and Therapeutic Approaches**

**Location:** WCC Halls A-C

**Time:** Monday, November 16, 2026, 1:00 PM - 5:00 PM

**Program #/Poster #:** PSTR194.19/GG9

**Topic:** H.07. Post-Traumatic Stress Disorder and Other Psychiatric Disorders

**Support:** NRF Grant RS-2024-00456412

**Title:** Altered P60m Attentional Modulation of Somatosensory Responses in Somatic Symptom Disorder

**Authors: *N. ON**[1], S. KANG[3], S. KIM[1], Y. BAE[1], C. PARK[3], S. KIM[3], J. KANG[3], D.-W. KIM[1,2];
[1]Dept. of Biomed. Engin., [2]Res. Ctr. for Healthcare and Biomed. Engin., Chonnam Natl. Univ., Yeosu-si, Korea, Republic of; [3]Dept. of Psychiatry, Inst. of Behavioral Sci. in Med., Yonsei Univ. Col. of Med., Seoul, Korea, Republic of

**Abstract:** Somatic symptom disorder (SSD) is characterized by excessive attention to bodily sensations and may be associated with altered sensory processing and attentional regulation. However, objective neurophysiological markers explaining these abnormalities remain limited. Symptom distress in SSD may be related to how bodily sensations are attended to and interpreted. Therefore, examining somatosensory evoked responses under different attentional conditions may provide insight into the pathophysiology of SSD. The present study examined the effects of attention on early and mid-latency event-related field (ERF) components. The goal was to identify group differences in attention-based modulation of somatosensory responses and to evaluate whether these responses could provide a physiological rationale for future dmPFC - related neuromodulation studies. A total of 32 participants were included in the analysis, comprising 15 normal controls (NC) and 17 patients with SSD. The experiment consisted of two attentional conditions. Participants were instructed to focus on and count the electrical stimuli in the Attend condition and to disregard them in the Ignore condition. Peak amplitudes of the major

somatosensory ERF components, including N20m, P35m, N45m, P60m, and N150m, were extracted from the MEG signals. Attentional modulation was quantified using a normalized modulation index (MI) comparing Attend and Ignore responses across four sequential stimuli. Group differences in mean MI were assessed using independent-samples t-tests. Overall amplitude analysis showed a significant group difference in the N45m component ($p = 0.03$). In the attentional modulation analysis, P60m showed the most consistent group-related pattern across stimulus order. In the P60m component, the NC group exhibited stable positive MI values across stimuli, whereas the SSD group showed reduced MI values. N45m also showed a group-related tendency in modulation, but its MI pattern was more variable than that of P60m. When MI values were averaged across stimuli, no ERF component showed a statistically significant group difference in mean MI (all $p > 0.17$). These findings suggest that P60m may serve as a candidate marker reflecting altered attention-based somatosensory modulation in SSD. In this context, the dmPFC may be involved in symptom appraisal, catastrophizing, and anxiety in SSD. Therefore, future studies should examine whether dmPFC-targeted noninvasive brain stimulation can modulate excessive attention to bodily sensations and negative symptom appraisal.

**Disclosures: N. On:** None. **S. Kang:** None. **S. Kim:** None. **Y. Bae:** None. **C. Park:** None. **S. Kim:** None. **J. Kang:** None. **D. Kim:** None.

**Poster**

**PSTR194: Post-Traumatic Stress Disorder and Other Psychiatric Disorders: Human Studies and Therapeutic Approaches**

**Location:** WCC Halls A-C

**Time:** Monday, November 16, 2026, 1:00 PM - 5:00 PM

**Program #/Poster #:** PSTR194.20/GG10

**Topic:** H.07. Post-Traumatic Stress Disorder and Other Psychiatric Disorders

**Title:** Sexual Dysfunction and Pharmacological Factors in Patients Receiving Antipsychotics: An Exploratory Cross-Sectional Study

**Authors: *K. SHIMIZU**[1], K. INADA[2], H. MURAOKA[3], R. SUZUKI[5], T. NISHIKAWA[4]; [1]Dept. of Psychiatry, Kitasato Univ. Grad. Sch. of Med. Sci., Sagamihara-shi Minami-Ku, Japan; [2]Dept. of Psychiatry, Kitasato Univ. school of medicine, Kanagawa, Japan; [3]Dept. of Psychiatry, Kitasato University, Sch. of Med., Kanagawa, Japan; [4]Dept. of Psychiatry, Kitasato University, Sch. of Med., Kanagawa sagamihara, Japan; [5]Kitasato Univ. Sch. of Med., Sagamihara / Kanagawa, Japan

**Abstract:** Antipsychotic-induced sexual dysfunction may reduce treatment satisfaction, adherence, and quality of life, but is often underassessed in routine clinical practice. This exploratory cross-sectional study evaluated sexual dysfunction with the Arizona Sexual Experiences Scale (ASEX) and examined associations with pharmacological factors and receptor-affinity profiles in patients receiving antipsychotics. Patients receiving antipsychotics who completed all five ASEX items were included. The primary outcome was the ASEX total score. Secondary outcomes were ASEX-defined sexual dysfunction and ASEX item scores.

Sexual dysfunction was defined as a total score ≥19, any item ≥5, or any three items ≥4. Pharmacological factors included D2 partial agonism, prolactin-elevating drugs, strong anticholinergic antipsychotics, α1 blockade, H1 blockade, 5-HT1A partial agonism, benzodiazepine use, and antidepressant use. Total and item scores were analyzed using multivariable linear regression, and sexual dysfunction using multivariable logistic regression, adjusted for age, sex, chlorpromazine-equivalent dose, benzodiazepine use, and antidepressant use. Ki values were converted to pKi for receptor-affinity analyses. False discovery rate correction was applied to item-level and receptor analyses. Of 138 patients with complete ASEX data, 136 receiving antipsychotics were analyzed. The mean ASEX total score was 21.43, and 72.1% met criteria for sexual dysfunction. D2 partial agonism, prolactin-elevating drugs, and strong anticholinergic antipsychotics were not clearly associated with the total score or sexual dysfunction. Benzodiazepine use was independently associated with higher total score (adjusted $\beta=2.41$, $p=0.005$) and sexual dysfunction (adjusted odds ratio=3.47, $p=0.008$). Antidepressant use showed a worsening trend. In item-level analyses, antipsychotics with 5-HT1A partial agonism were associated with better orgasm satisfaction ($\beta=-0.54$, $p=0.027$), but this association did not remain significant after false discovery rate correction. Receptor-affinity analyses showed no significant associations after correction. Overall, 88.2% reported that the questionnaire facilitated disclosure of sexual dysfunction. Sexual dysfunction was common among patients receiving antipsychotics. Benzodiazepine use may be associated with sexual dysfunction, while 5-HT1A partial agonism may be protectively associated with orgasm satisfaction. Questionnaire-based assessment may facilitate disclosure in routine care. Ethics approval was obtained from the Kitasato University Hospital Ethics Committee (B25-186).

**Disclosures: K. Shimizu:** None. **K. Inada:** D. Fees for Non-CME Services Received Directly from Commercial Interest or their Agents (e.g., speakers' bureaus); EA Pharma Co., Ltd., Viatris Pharmaceuticals Japan Inc., Eisai Co., Ltd., Otsuka Pharmaceutical Co., Ltd., Ono Pharmaceutical Co., Ltd., Kyowa Kirin Co., Ltd., Kowa Pharmaceutical Co., Ltd., Shionogi & Co., Ltd., Sumitomo Pharma Co., Ltd., Daiichi Sankyo Company, Limited., Takeda Pharmaceutical Company Limited, MSD K.K., Mitsubishi Tanabe Pharma Corporation., Nipro Corporation, Nippon Chemiphar Co., Ltd., Eli Lilly Japan K.K., Boehringer Ingelheim Japan, Inc., Nexera Pharma K.K., Novartis Pharma K.K., Nobelpharma Co., Ltd., Pfizer Japan Inc., Meiji Seika Pharma Co., Ltd., Mochida Pharmaceutical Co., Ltd., Janssen Pharmaceutical K.K., Lundbeck Japan K.K., Yoshitomi Pharmaceutical Industries, Ltd. **H. Muraoka:** D. Fees for Non-CME Services Received Directly from Commercial Interest or their Agents (e.g., speakers' bureaus); EA Pharma Co., Ltd., Viatris Pharmaceuticals Japan Inc., Eisai Co., Ltd., MSD K.K., Otsuka Pharmaceutical Co., Ltd., Shionogi & Co., Ltd., Sumitomo Pharma Co., Ltd., Daiichi Sankyo Company, Limited., Takeda Pharmaceutical Company Limited., Meiji Seika Pharma Co., Ltd., Mochida Pharmaceutical Co., Ltd., Lundbeck Japan K.K.. **R. Suzuki:** None. **T. Nishikawa:** None.

**Poster**

**PSTR194: Post-Traumatic Stress Disorder and Other Psychiatric Disorders: Human Studies and Therapeutic Approaches**

**Location:** WCC Halls A-C

**Time:** Monday, November 16, 2026, 1:00 PM - 5:00 PM

**Program #/Poster #:** PSTR194.21/GG11

**Topic:** H.07. Post-Traumatic Stress Disorder and Other Psychiatric Disorders

**Title:** Antipsychotic-Associated Sexual Dysfunction in Schizophrenia: A Network Meta-Analysis With Bayesian Receptor Affinity Correlation Analysis

**Authors: *H. MURAOKA**[1], S. OCHI[2], H. YASUDA[3], H. TAKEUCHI[4];
[1]Dept. of Psychiatry, Kitasato University, Sch. of Med., Kanagawa, Japan; [2]Ehime Univ. Grad. Sch. of Med., Toon / Ehime, Japan; [3]Dept. of Psychiatry, Sekito Hosp., Izumo, Shimane, Japan; [4]Dept. of Psychiatry, Chiba Univ. Grad. Sch. of Med., Chiba, Japan

**Abstract:** Objective: Sexual dysfunction is common in schizophrenia and may impair quality of life and adherence. The authors compared sexual dysfunction risk across antipsychotics in schizophrenia spectrum disorders and explored associations with receptor-binding profiles. Methods: MEDLINE and Embase were searched from inception to February 24, 2026, supplemented by reference screening. Eligible randomized clinical trials compared antipsychotic monotherapy with another antipsychotic or placebo and reported sexual dysfunction outcomes. Random-effects frequentist network meta-analyses used risk ratios. The primary outcome was any sexual dysfunction; secondary outcomes were ejaculatory dysfunction, erectile dysfunction, and loss of libido. Certainty was assessed with Confidence in Network Meta-Analysis. Bayesian analyses examined associations between drug-specific risk estimates and dopamine $D_2$, serotonin 5-$HT_{2C}$, and $\alpha_1$ adrenergic receptor-binding profiles. Results: Fifty trials including 15,914 participants were analyzed. For any sexual dysfunction, aripiprazole (risk ratio, 0.44; 95% CI, 0.31-0.63), ziprasidone (0.64; 0.52-0.80), and quetiapine (0.71; 0.61-0.84) were associated with lower risks than risperidone, whereas sertindole showed higher risk (2.89; 1.74-4.82). Sertindole had the highest risk of ejaculatory dysfunction, and aripiprazole was associated with lower erectile dysfunction risk than risperidone. Systematic assessment yielded higher absolute risk estimates than spontaneous reporting. Bayesian analyses suggested pharmacological patterns involving $D_2$ antagonism across domains, 5-$HT_{2C}$ antagonism for ejaculatory dysfunction, and $\alpha_1$ antagonism for erectile dysfunction. Conclusions: Antipsychotics differ meaningfully in sexual dysfunction risk, with exploratory receptor analyses suggesting domain-specific pharmacological patterns. These findings support routine assessment of sexual function and may inform individualized antipsychotic selection.

**Disclosures: H. Muraoka:** None. **S. Ochi:** None. **H. Yasuda:** None. **H. Takeuchi:** None.

**Poster**

**PSTR194: Post-Traumatic Stress Disorder and Other Psychiatric Disorders: Human Studies and Therapeutic Approaches**

**Location:** WCC Halls A-C

**Time:** Monday, November 16, 2026, 1:00 PM - 5:00 PM

**Program #/Poster #:** PSTR194.22/GG12

**Topic:** H.07. Post-Traumatic Stress Disorder and Other Psychiatric Disorders

**Support:** NIH Grant R00AA031333

**Title:** Reward reactivity, sex, and menstrual cycle influences on PTSD and alcohol use associations

**Authors: *S. H. LIPETZKY**[1], G. DEAN[1], C. A. HINOJOSA[2];
[1]Dept. of Psychology, Univ. of New Mexico, Albuquerque, NM; [2]Dept. of Psychology, The Univ. of New Mexico, Albuquerque, NM

**Abstract:** Although males report higher rates of alcohol consumption and greater exposure to potentially traumatic events, females are at greater risk of developing co-occurring posttraumatic stress disorder (PTSD) and alcohol use disorder (AUD) after experiencing a traumatic event. While the neural mechanisms that underlie each disorder have been examined extensively separately, few studies have examined the reward-related neural substrates of this co-occurrence, especially in relation to sex differences. Prior work highlights how fluctuations of ovarian steroid hormones that fluctuate across the menstrual cycle, estradiol (E2) and progesterone (P4), can exert direct effects on the brain and cognition. To further probe this relationship, we are recruiting males and naturally cycling females who have experienced at least one traumatic event in their lifetime to complete self-report assessments before undergoing scanning procedures (n=120). Participants will report PTSD symptom severity, alcohol use, and craving daily over a 28-day period for males or one menstrual cycle for naturally cycling females. Once done with the assessment protocol, participants will complete a validated monetary reward task inside a 3T MRI scanner using a 5-echo sequence. For naturally cycling females, scanning will take place during their menses, when E2 and P4 levels are at their lowest. The monetary reward task requires participants to determine via button press whether a card presented has a value that is higher or lower than five. After making their decision, the card will flip, and a number will appear in the center of the card for 500 ms, along with feedback: either a green check mark indicating that the participant guessed correctly, or a red ‘x’ indicating that the participant incorrectly guessed the card value. If the participant guesses correctly, they will receive $1, while if they guess incorrectly, $0.50 will be deducted from their totals. Participants will be unaware that the outcomes are predetermined to yield 20 gain trials and 20 loss trials. We predict that greater bilateral nucleus accumbens activation and ventromedial prefrontal cortex activation to reward versus loss trials will be associated with greater covariance between daily PTSD symptoms and alcohol use behaviors, particularly in females compared to males. This work will elucidate the biobehavioral mechanisms underlying the female vulnerability to co-occurring PTSD and AUD and reflects the need to assess the female menstrual cycle in neuroscience research.

**Disclosures: S.H. Lipetzky:** None. **G. Dean:** None. **C.A. Hinojosa:** None.

**Poster**

**PSTR195: Mechanisms of Polysubstance and Cannabinoid Use**

**Location:** WCC Halls A-C

**Time:** Monday, November 16, 2026, 1:00 PM - 5:00 PM

**Program #/Poster #:** PSTR195.01/GG13

**Topic:** H.08. Drugs of Abuse and Addiction

**Title:** AMPED UP: Effects of intermittent energy drinks, alone and mixed with alcohol, in mice

**Authors: L. FIELDS**, *J. N. BERRY;
Psychology, Butler Univ., Indianapolis, IN

**Abstract:** Energy drink (ED) usage among adolescents and young adults has skyrocketed in recent years, and the combination of EDs and alcohol (AmED) has become increasingly more common amongst these age groups as well. Like EDs alone, the combination is highly addictive and previous research has shown that AmEDs can increase the risk of binge drinking and other potentially harmful behavior. Preclinical animal models have investigated caffeine consumption and withdrawal, but relatively few studies have examined EDs and AmEDs using animal models. Thus, we sought to investigate the consumption of, preference for, and withdrawal from EDs containing various amounts of caffeine or AmEDs using an intermittent access (IA) model. In experiment 1, adolescent male and female C57BL/6J mice (N=32) were exposed to a 2-bottle choice paradigm with a secondary bottle of either water (control), sugar-free Redbull alone, sugar-free Ghost, or sugar-free Celsius. In experiment 2, adolescent male and female mice (N=32) were exposed to a 2-bottle choice paradigm with a secondary bottle of either water (control), sugar-free Red Bull alone, 10% alcohol, or 10% alcohol mixed with sugar-free Red Bull (AmED). After 4 weeks of IA to the EDs or AmEDs, all mice were examined for anxiety-like behavior in the open field test (OFT) approximately 6 hours after final removal of bottles. In experiment 1, a 2-way (time by treatment group) ANOVA revealed significant main effects of time and treatment group for caffeine consumption in both male and female mice, suggesting that the IA paradigm can be used to study various EDs. In experiment 2, a 2-way ANOVA revealed a significant interaction such that adolescent male mice consumed significantly more caffeine and alcohol when Red Bull was combined with alcohol rather than either substance alone, particularly in weeks 1 and 2. However, adolescent female mice consumed similar amounts of alcohol with or without Red Bull. No significant main effects or interactions were observed in the OFT in either experiment. These results suggest that the consumption of AmEDs may vary according to sex of the animal. These experiments demonstrate the utility of the IA paradigm for examining the effects of EDs and AmEDs in a mouse model.

**Disclosures: L. Fields:** None. **J.N. Berry:** None.

**Poster**

**PSTR195: Mechanisms of Polysubstance and Cannabinoid Use**

**Location:** WCC Halls A-C

**Time:** Monday, November 16, 2026, 1:00 PM - 5:00 PM

**Program #/Poster #:** PSTR195.02/GG14

**Topic:** H.08. Drugs of Abuse and Addiction

**Title:** The role of accumbal adenosine activity in caffeine’s systemic effects on behavioral inhibition during alcohol self-administration

**Authors: *L. HODA**[1], H. N. CARLSON[2];
[1]Neurosci. and Psychology, [2]Neuroscience, Psychology, Lake Forest Col., Lake Forest, IL

**Abstract: The role of accumbal adenosine activity in caffeine's systemic effects on behavioral inhibition during alcohol self-administrationLettia Hoda '27, Hannah Carlson**Department of Neuroscience Lake Forest College, Lake Forest, IL 60045Polysubstance use, the concurrent use of two or more drugs, is a common but understudied phenomenon. In 2022 alone, nearly half of the deaths caused by drug overdose involved multiple substances. Polysubstance use between stimulants and depressants is especially hazardous due to the masking of interoceptive cues, potentially increasing the risk of overdose. Caffeine and alcohol are among the most used and available drugs worldwide and are frequently used together due to the alertness that caffeine promotes. Previous studies have shown that by binding to and inhibiting adenosine receptors in the central and peripheral nervous system, caffeine prevents somnolence and promotes impulsive behavior independent of alcohol. Given the popularity of caffeine use in general, and beverages containing both caffeine and alcohol, the impact of caffeine use on drug-related decision making is an important clinical consideration. To that end, the present study assesses the impact of acute caffeine administration on alcohol self-administration in a behavioral conflict task, the Maladaptive Alcohol Self-Administration Task (MAST). The MAST involves 25 discrete trials of 30 second sipper tube access signaled by a cue light. During the first 10 second of sipper access, an auditory cue indicates that licking will result in mild foot shock. For the remaining 20 seconds, the auditory cue is discontinued, and licking has no programmed consequences. Sixteen adult Long-Evans rats (n=8 male, n=8 female) trained to perform the MAST and implanted with bilateral guide cannulae above the nucleus accumbens core were administered caffeine (0, 5, and 10mg/kg; i.p.) and/or adenosine A2 receptor agonist CGS 21680 (0, 0.5μL/side) in a counterbalanced Latin square design. Results suggest that both systemic caffeine and adenosine manipulation within the nucleus accumbens core produce meaningful behavioral change in performance, engagement, and intake during the MAST. Acute caffeine administration produces observable changes in alcohol directed behavior, which are influenced by concurrent A2 receptor activation in the nucleus accumbens core. Taken together, these data elucidate the impact that caffeine use has on alcohol intake.

**Disclosures: L. Hoda:** None. **H.N. Carlson:** None.

**Poster**

**PSTR195: Mechanisms of Polysubstance and Cannabinoid Use**

**Location:** WCC Halls A-C

**Time:** Monday, November 16, 2026, 1:00 PM - 5:00 PM

**Program #/Poster #:** PSTR195.03/GG15

**Topic:** H.08. Drugs of Abuse and Addiction

**Support:** R01AA031680

**Title:** Novel Therapeutic Approaches to Treating Polysubstance Abuse: Alcohol and Nicotine Co-Use

**Authors: C. A. RANDALL**[1], *P. A. RANDALL[2];
[1]Anesthesiol., Penn State Univ., Hershey, PA; [2]Penn State Col. of Med., Hershey, PA

**Abstract:** Alcohol and nicotine are two of the most commonly co-use drugs with as many as 85% of adult heavy drinkers also smoking. This creates a challenge not only in developing therapeutics that can target drug effects on two fronts but effectively modeling pre-clinically. The Randall lab has successfully developed an animal model in which rats voluntarily self-administer alcohol and nicotine. Moreover, this model was designed so that rats could deliver these drugs via the most common human routes (alcohol liquid for oral consumption and nicotine vapor for inhalation) giving it considerable translational value. Following this development, one of the major goals for our lab has been to identify and screen targets for therapeutic advancement. One such target is the nicotinic alpha 7 receptor. This receptor plays an important role in nicotine's anti-inflammatory actions. Here, we show that activating this receptor decreases alcohol intake and disrupts nicotine intake in both males and females. Opposite the alpha7 receptor, we show that directly acting on pro-inflammatory receptors - particularly TLR3 and 4 - we can modulate alcohol and nicotine intake. Finally, there is growing interest in understanding the role of GLP-1 in modulating drug-seeking behavior. Previous work has shown that GLP-1 agonists are capable of decreasing alcohol and nicotine seeking on their own but to date no studies have looked at the two drugs in combination. Here we show that the GLP-1 agonist tirzepatide decreases aspects of both alcohol and nicotine seeking in both males and females. Together, these studies point in several new directions for potential therapeutics for alcohol and nicotine co-use.

**Disclosures: C.A. Randall:** None. **P.A. Randall:** None.

**Poster**

**PSTR195: Mechanisms of Polysubstance and Cannabinoid Use**

**Location:** WCC Halls A-C

**Time:** Monday, November 16, 2026, 1:00 PM - 5:00 PM

**Program #/Poster #:** PSTR195.04/GG16

**Topic:** H.08. Drugs of Abuse and Addiction

**Support:** R21 DA063305-01A1
UMN College of Pharmacy
This research was supported by the National Institutes of Health's National Center for Advancing Translational Sciences, grants 1T32TR004376 and 1UM1TR004405.

**Title:** xylazine-induced neuroadaptations and fentanyl self-administration in mice

**Authors: *L. CAYE**[1], C. PETERSON[2], K. F. KITTO[2], G. L. WILCOX[4], C. A. FAIRBANKS[3]; [1]Pharmacol., [2]Neurosci., [3]Pharmaceutics, Pharmacology, Neurosci., Univ. of Minnesota, Minneapolis, MN; [4]Dept Neurosci, Pharmacol, Univ. Minnesota Med. Sch., Minneapolis, MN

**Abstract:** Xylazine, an alpha 2 adrenergic agonist, has increasingly been detected as an adulterant in samples of illicitly manufactured fentanyl. The physiological effects of this drug mixture remain to be understood but anecdotal reports suggest users have begun seeking out this mixture due to its "sedative, calming effects," a more intense, immediate and a longer-lasting high[1]. Questions remain as to how xylazine adulteration impacts fentanyl's reinforcing properties. To investigate these questions and more, we performed long-access fentanyl self-administration studies in combination with xylazine (3,10mg/kg pre-treatment) to better understand xylazine's effect on the motivational and rewarding properties of fentanyl. Simultaneously, we conducted additional studies on the same cohort of mice to investigate the sedative, gastrointestinal, analgesic, opioid-induced hyperalgesia, and withdrawal properties of repeated xylazine administration in fentanyl-consuming mice. Additionally, we investigated the receptor subtype responsible for xylazine-mediated sedation using functional knock-out mouse lines. Our investigation revealed that consistent pretreatment with 10 mg/kg xylazine resulted in tolerance to the sedative effects of xylazine as well as tolerance to the analgesic component of xylazine. However, these mice did not develop tolerance to the gastrointestinal inhibitory effects of xylazine at this dose. Our investigation also revealed that upon increasing the fixed ratio in our self-administration studies, the xylazine pre-treated mice showed potentiated lever responding in the first six hours of the long access sessions at both xylazine doses tested. Following withdrawal and reinstatement of fentanyl responding, the previously xylazine (10mg/kg) pre-treated group continued to show elevated fentanyl seeking relative to the saline group in response to increased fixed ratios. Finally, we demonstrated that the sedative effect of xylazine is mediated by the $\alpha_{2A}$ adrenergic receptor. Together, these findings suggest that repeated xylazine pretreatment produces a dose-related tolerance to selected side effects. They also suggest that xylazine pre-treatment may potentiate responding for fentanyl at elevated response requirements, and this potentiated fentanyl seeking may persist long after the final xylazine exposure.

**Disclosures: L. Caye:** None. **C. Peterson:** None. **K.F. Kitto:** None. **G.L. Wilcox:** None. **C.A. Fairbanks:** None.

**Poster**

**PSTR195: Mechanisms of Polysubstance and Cannabinoid Use**

**Location:** WCC Halls A-C

**Time:** Monday, November 16, 2026, 1:00 PM - 5:00 PM

**Program #/Poster #:** PSTR195.05/GG17

**Topic:** H.08. Drugs of Abuse and Addiction

**Title:** Sex- and estrous cycle-dependent modulation of psychostimulant effects on ventral striatal dopamine release

**Authors: *R. POWERS**[1], L. FORD[1], J. WOOLLEY[2], J. T. YORGASON[3];
[1]Wake Forest Univ. Grad. Sch. of Arts and Sci., Winston-Salem, NC; [2]Brigham Young Univ., Provo, UT; [3]Translational Neurosci., Wake Forest Univ. Sch. of Med., Winston-Salem, NC

**Abstract:** Psychostimulants are some of the most widely prescribed and abused medications in the United States. Clinical evidence has emerged suggesting sexually dimorphic responses to psychostimulants. Here we investigate sex- and estrous cycle-dependent differences in dopamine transmission in the nucleus accumbens core in the presence of cocaine, methylphenidate, and methamphetamine via fast-scan cyclic voltammetry in mice brain slices. We did not observe a significant sex- or estrous cycle-dependent difference in dopamine transmission across all three psychostimulants based on measuring peak height, tau, and $V_{max}$ in both tonic (single pulse) and phasic (5Hz, 20Hz, and 100Hz) electrically evoked dopamine stimulation. These data suggest that sexually dimorphic behavioral responses to psychostimulants involve more factors than dopamine release kinetics in the ventral striatum.

**Disclosures: R. Powers:** None. **L. Ford:** None. **J. Woolley:** None. **J.T. Yorgason:** None.

**Poster**

**PSTR195: Mechanisms of Polysubstance and Cannabinoid Use**

**Location:** WCC Halls A-C

**Time:** Monday, November 16, 2026, 1:00 PM - 5:00 PM

**Program #/Poster #:** PSTR195.06/GG18

**Topic:** H.08. Drugs of Abuse and Addiction

**Title:** Compartment-specific hypofunction of dopamine D2 receptors differentially gates addiction vulnerability to distinct drug classes

**Authors: *S. LEE**[1], J. SHIN[4], D. DIAZ-URBINA[2], E. MURRAY[5], R. BOCK[6], V. A. ALVAREZ[3];
[2]NIMH, [3]Lab. on Neurobio. of Compulsive Behaviors, [1]NIH, Bethesda, MD; [4]NIAAA, Natl. Inst. on Alcohol Abuse and Alcoholism, Rockville, MD; [5]Univ. of Rochester Neurosci. Grad. Program, Rochester, NY; [6]Lab. for Integrative Neurosci. / Section on Neuronal Structure, Natl. Inst. On Alcohol Abuse and Alcoholism / NIH, Bethesda, MD

**Abstract:** Substance use disorder (SUD) affects millions worldwide, yet only a subset of individuals who use addictive substances develop addiction. Repeated drug exposure therefore does not inevitably lead to SUD, suggesting that vulnerability and resilience factors shape individual risk. Reduced availability of striatal dopamine D2 receptor (D2R) is associated with SUD vulnerability, but the mechanistic contributions of distinct D2R populations remain elusive. To address this, we generated male and female mice with selective D2R haploinsufficiency either in midbrain dopamine neurons (auto-D2KD), targeting autoreceptors that provide feedback inhibition of dopamine synthesis, release, and neuronal firing, or in D2-expressing medium spiny neurons (MSN-D2KD), targeting postsynaptic heteroreceptors that modulate basal ganglia output, along with wildtype controls. Intravenous drug self-administration revealed

compartment-specific vulnerability: auto-D2KD mice exhibited heightened addiction-like phenotype for cocaine, including increased futile seeking, punishment-resistant intake, and abstinence-associated craving. In contrast, MSN-D2KD mice showed heightened addiction-like phenotype for fentanyl. We hypothesized that differences in dopamine release dynamics and/or receptor levels may underlie this drug selectivity. Using fast-scan cyclic voltammetry in *ex vivo* brain slices, we found that auto-D2KD mice exhibit enhanced phasic dopamine release during high-frequency stimulation, and that cocaine further amplifies and prolongs dopamine signals relative to controls. In contrast, fentanyl self-administration produced a doubling of striatal D2-like ligand binding compared with drug-naive mice, as measured by autoradiography. This fentanyl-induced increase was blunted in auto-D2KD mice, suggesting that fentanyl intake may upregulate D2 autoreceptors on dopamine neurons. Ongoing voltammetry experiments are testing this hypothesis. Together, these findings dissociate the contributions of presynaptic D2 autoreceptors and postsynaptic D2 heteroreceptors to addiction vulnerability and suggest that the cellular source of reduced striatal D2R availability may predict susceptibility to distinct drug classes.

**Disclosures: S. Lee:** None. **J. Shin:** None. **D. Diaz-Urbina:** None. **E. Murray:** None. **R. Bock:** None. **V.A. Alvarez:** None.

**Poster**

**PSTR195: Mechanisms of Polysubstance and Cannabinoid Use**

**Location:** WCC Halls A-C

**Time:** Monday, November 16, 2026, 1:00 PM - 5:00 PM

**Program #/Poster #:** PSTR195.07/GG19

**Topic:** H.08. Drugs of Abuse and Addiction

**Support:** Department funds
Johns Hopkins Children's Center Innovation Award
Bridge Funding from Virginia Commonwealth University School of Medicine to the VCU Center of Drug Addiction Bioanalytical Core
National Institute of Justice award 15PNIJ-23-GG-01421-COAP
THC was provided by the NIDA Drug Supply Program

**Title:** Perinatal health and sensorimotor processing outcomes of full-term prenatal cannabinoid exposure (PCE) using a translational model of vaporized delta-9-tetrahydrocannabinol (THC) administration in rats

**Authors: *B. W. JENKINS**[1], C. F. MOORE[1], P. TIWARI[1], A. H. LICHTMAN[3], J. POKLIS[3], L. L. JANTZIE[2], E. M. WEERTS[1];
[1]Div. of Behavioral Biology, Psychiatry and Behavioral Sci., [2]Pediatrics, Johns Hopkins Univ. Sch. of Med., Baltimore, MD; [3]Pharmacol. and Toxicology, Virginia Commonwealth Univ., Richmond, VA

**Abstract: Introduction:** Use of cannabinoid products during pregnancy is a major public health concern.The Δ9-tetrahydrocannabinol (THC) in these products is readily transferred to the fetal brainduring gestation. Prenatal cannabinoid exposure (PCE) is associated with increased risk of birthcomplications and lasting neuropsychiatric impairments in offspring. We established a novelmodel of PCE using THC vapor exposure across the human-equivalent full-term prenatal periodin rats. The current study examined how full-term PCE affects perinatal health measures andoffspring sensorimotor processing using this model. **Methods:** Pregnant female Sprague Dawley rats were exposed to THC (200 mg/ml, n = 13) or vehicle (100% propylene glycol, n = 8)vapor daily during gestation, through birth, until postnatal day (PD) 10 (i.e., human-equivalentfull-term). Perinatal health measures (dam food intake, dam/pup body weights, total gestationdays, litter size, and litter sex ratio) were assessed in THC- and vehicle-exposed rats. Insubsets of THC-exposed rats, concentrations of THC and metabolites (11-hydroxy-Δ9-tetrahydrocannabinol [11-OH-THC], 11-nor-9-carboxy-Δ9-tetrahydrocannabinol [THCCOOH])were quantified in the brains (dams, pups) and plasma (dams) on gestational day (GD) 20 (n =4 dams, 24 pups) or PD 10 (n = 2 dams, 33 pups). Remaining pups (n = 36) were weaned onPD 21 and tested in adolescence and adulthood for potential cognitive-affective deficits usingthe acoustic startle response test of sensorimotor processing. **Results:** Compared to controls,THC vapor decreased dam food intake, total gestation days, and offspring postnatal weights.On GD 20, dam THC concentrations were 14.8 ng/ml (plasma) and 80.5 ng/g (brain); fetalconcentrations of THC, 11-OH-THC, and THCCOOH were 12% 118%, and 75% of damplasma. On PD 10, dam THC concentrations were 68.9 ng/ml (plasma) and 125.0 ng/g (brain).Pup brain THC and 11-OH-THC concentrations were 29.6 and 9.8 ng/g, respectively;THCCOOH was not detected. PCE produced sensorimotor impairments in offspring with sex-dissociable effects: compared to controls, females had increased baseline and fear-potentiatedstartle reactivity, while males had intact baseline startle but increased fear-potentiated startleand disrupted sensorimotor gating, in adulthood. **Conclusion:** Full-term PCE produced highTHC and 11-OH-THC concentrations in fetal brains, disrupted perinatal health measures, andhad sex-specific effects on the cognitive and affective components of the acoustic startle reflex.Future directions include investigating brain network dysconnectivity and underlying immunedysregulation in offspring with PCE.

**Disclosures: B.W. Jenkins:** None. **C.F. Moore:** None. **P. Tiwari:** None. **A.H. Lichtman:** None. **J. Poklis:** None. **L.L. Jantzie:** None. **E.M. Weerts:** None.

**Poster**

**PSTR195: Mechanisms of Polysubstance and Cannabinoid Use**

**Location:** WCC Halls A-C

**Time:** Monday, November 16, 2026, 1:00 PM - 5:00 PM

**Program #/Poster #:** PSTR195.08/GG20

**Topic:** H.08. Drugs of Abuse and Addiction

**Support:** NIH Grant R00DA054205

**Title:** Adolescent delta-9-tetrahydrocannabinol (THC) impacts GABAergic involvement in inhibitory control in adulthood

**Authors:** C. FORBES, T. REESE, V. KATTLER, ***S. J. STRINGFIELD**;
Neurosci., Univ. of Pittsburgh, Pittsburgh, PA

**Abstract:** Among both adults and adolescents, cannabis remains the most widely used illicit substance in the United States. Cannabis use during adolescence presents specifically detrimental effects due to the ability of exogenous cannabinoids to alter the trajectory of neural development. Adolescent exposure to delta-9-tetrahydrocannabinol (THC), the primary psychoactive component in cannabis, has been shown to promote long-lasting alterations in neuronal functions and is associated with an increased likelihood of developing neuropsychiatric disorders including mood and anxiety disorders, schizophrenia, and substance use disorders. Adolescent THC exposure may act on specific regions of the brain, including the prefrontal cortex, that undergo protracted growth and restructuring during the adolescent development period. The prefrontal cortex is required for executive functioning, and exposure to THC during adolescence may disrupt the ability of PFC circuits to exert top-down control over impulsive behaviors. To measure this, adolescent male and female Sprague Dawley rats completed intravenous THC self-administration from postnatal day 32-51. Rats expressed the genetically encoded calcium sensor AAV1.mDLX.GCaMP8f unilaterally in the prelimbic prefrontal cortex and were implanted with optic fibers prior to beginning behavioral training in adulthood. Rats were trained to perform a differential reinforcement of low rates of responding task (DRL) to measure response inhibition behavior, and the influence of GABAergic neurotransmission in performing the response. For this task, rats are trained to nose poke on a FR2 schedule of reinforcement to receive a sucrose pellet reward. Rats learn to withhold responses for an unsignaled delay period that ranges from 4-12 seconds between the first and second response. Premature responses result in a timeout period. Fiber photometry recordings were conducted during performance of the DRL task. We found that male and female adolescents self-administer escalating doses of THC. Sex-differences emerged for performance on the DRL task, with male animals performing the task with higher accuracy than females. Adolescent THC exposure impacted behavioral performance on the DRL based on sex. GABAergic activity was blunted during task performance in THC-exposed animals. These results demonstrate that adolescent THC exposure produces lasting effects on both behavior and neuronal activity in adulthood.

**Disclosures: C. Forbes:** None. **T. Reese:** None. **V. Kattler:** None. **S.J. Stringfield:** None.

**Poster**

**PSTR195: Mechanisms of Polysubstance and Cannabinoid Use**

**Location:** WCC Halls A-C

**Time:** Monday, November 16, 2026, 1:00 PM - 5:00 PM

**Program #/Poster #:** PSTR195.09/GG21

**Topic:** H.08. Drugs of Abuse and Addiction

**Support:** Center for Medicinal Cannabis Research
Scheibel Scholarship

**Title:** Elucidating the Mechanisms Underlying Myrcene-Induced Anti-Allodynia in Chronic Neuropathic Pain

**Authors: *N. BONAVENTURE**[1], J. NGUYEN[2], M. RICE[2], C. M. CAHILL[3];
[1]UCLA, San Diego, CA; [3]Psychiatry and Biobehavioral Sci., [2]UCLA, Los Angeles, CA

**Abstract:** Phytocannabinoids such as Δ9-tetrahydrocannabinol and cannabidiol have been extensively studied for their potential analgesic properties. We and others reported that myrcene, a cannabis-derived monoterpene, produces anti-allodynic effects in preclinical models that engage the endocannabinoid system. Myrcene dose-dependently attenuates mechanical allodynia via CB1 receptor-dependent mechanisms, despite lacking direct CB1 receptor activity. This study aimed to determine to what extent myrcene's effects depend on CB1 receptor signaling and endocannabinoid synthesis pathways.

Adult male and female C57BL/6J mice underwent baseline mechanical threshold assessment using electronic von Frey. All experiments were conducted blind to treatment. Neuropathic pain was induced via unilateral chronic constriction injury (CCI) of the sciatic nerve. Mechanical thresholds were reassessed 10 days post-surgery. Mice received various treatments prior to administration of myrcene. Separate cohorts were treated with vehicle, SR141716 (3 mg/kg): centrally penetrant CB1 antagonist, MRI-1891 (3 mg/kg): peripherally restricted CB1 antagonist, DO34(30 mg/kg): DAGL inhibitor (blocks 2-AG synthesis) or LEI401 (30 mg/kg): NAPE-PLD inhibitor (blocks AEA production). A within-subject, counterbalanced design was used across treatment days. Data was analyzed by a one-way ANOVA then a Tukey's post hoc analysis.

CCI significantly reduced mechanical thresholds relative to baseline, confirming robust allodynia. Myrcene reversed CCI-induced allodynia. This anti-allodynic effect was: blocked by SR141716, indicating dependence on CB1 receptor signaling but unaffected by MRI-1891, suggesting a central (rather than peripheral) CB1 mechanism. The treatment with DO34 also prevented myrcene anti-allodynic action, implicating 2-AG signaling in mediating myrcene's effects.Importantly, DO34 alone did not alter mechanical thresholds, indicating that its effect is specific to modulation of myrcene efficacy rather than baseline nociception. Ongoing studies are evaluating the contribution of AEA signaling via NAPE-PLD inhibition.

Our findings support a model in which myrcene produces anti-allodynia through indirect engagement of central CB1 receptor signaling, potentially via enhancement of endocannabinoid tone, particularly 2-AG. This work refines the mechanistic understanding of terpene-endocannabinoid interactions and highlights myrcene as a modulator of pain-relevant CB1 pathways. Such insights may inform the development of non-cannabinoid therapeutics that leverage endogenous cannabinoid signaling for the treatment of neuropathic pain.

**Disclosures: N. Bonaventure:** None. **J. Nguyen:** None. **M. Rice:** None. **C.M. Cahill:** None.

**Poster**

**PSTR195: Mechanisms of Polysubstance and Cannabinoid Use**

**Location:** WCC Halls A-C

**Time:** Monday, November 16, 2026, 1:00 PM - 5:00 PM

**Program #/Poster #:** PSTR195.10/GG22

**Topic:** H.08. Drugs of Abuse and Addiction

**Title:** Sex-stratified MAP estimation reveals bimodal risky choice acquisition trajectories in the Rat Gambling Task

**Authors: *S. A. EZE**;
Neurosci. & Behavior, Barnard Col. of Columbia Univ., New York, NY

**Abstract:** Computational modeling of the rat Gambling Task (rGT) typically yields group-mean parameter estimates that obscure individual-level heterogeneity in learning dynamics. Here we report a striking bimodal distribution of residuals for learned disadvantageous option values (V3, V4)--absent for advantageous options (V1, V2)--indicating that this cohort contains discrete subpopulations differing fundamentally in how punishment-paired choice representations are acquired, independent of treatment condition. Using maximum a posteriori (MAP) estimation in male and female Long-Evans rats (N = 39; Female Control n = 10, Female THC n = 10, Male Control n = 9, Male THC n = 10) exposed to either a THC-containing or vehicle control edible during adolescence (PND 29-49), we estimated session-wise reward learning rate (eta+), punishment learning rate (eta-), inverse temperature (beta), and learned option values (V1-V4) across 30 rGT acquisition sessions organized into six 5-session blocks. Linear mixed-effects models (sex x group x block; random intercepts by subject; error bars +/-SEM) revealed a generalized inverted-U trajectory for eta+ shared across all groups--peaking at B3 (S11-15) before declining--consistent with a mid-acquisition shift from exploratory prediction-error-driven updating toward exploitation. Beta showed a complementary pattern, with males beginning at higher exploitation and declining, while females showed more variable trajectories, supporting a sex-differentiated exploration-exploitation transition hypothesis. Disadvantageous option values (V3, V4) showed significant block x sex interactions (both $p < .001$), with females progressively devaluing risky options and males diverging into high-V3/V4 and low-V3/V4 subpopulations--the source of the observed bimodality. THC exposure most selectively disrupted advantageous value acquisition (sex x group interactions: V1 $p < .01$, V2 $p < .05$), suggesting adolescent cannabis shifts sex-dependent acquisition of adaptive rather than maladaptive option representations. These bimodal phenotypes motivate future work linking computational subtypes to dopaminergic circuit function via fiber photometry (GrabDA) in NAc and BLA, with classification of fluorescence features by behavioral phenotype and integration with proteomics data.

**Disclosures: S.A. Eze:** None.

**Poster**

**PSTR195: Mechanisms of Polysubstance and Cannabinoid Use**

**Location:** WCC Halls A-C

**Time:** Monday, November 16, 2026, 1:00 PM - 5:00 PM

**Program #/Poster #:** PSTR195.11/GG23

**Topic:** H.08. Drugs of Abuse and Addiction

**Support:** Shirley and Stefan Hatos Foundation

**Title:** Characterization of an endogenous endocannabinoid system in the Pacific hagfish (Eptatretus stoutii), a vertebrate/invertebrate transition species

**Authors: S. CHEN**[1], G. VENUMBAKA[1], J. SIU[1], A. ROMERO[1], A. JEON[1], E. WHITEHOUSE[1], R. SETIA[1], P. R. O'NEILL[2], *C. J. EVANS[1];
[1]Psychiatry and Biobehavioral Sci., [2]Hatos Ctr. for Neuropharm., UCLA, Los Angeles, CA

**Abstract:** The mammalian endocannabinoid system is a widespread signaling network with two primary cannabinoid receptors (CNR1 and CNR2) and the enzymes that synthesize and degrade two endogenous ligands: N-arachidonoylethanolamine (AEA) and 2-arachidonoylglycerol (2-AG). Evolutionary analyses of this system remain limited, with some evidence suggesting early invertebrate origins. The Pacific Hagfish (Eptatretus stoutii) is a vertebrate/invertebrate transition species that diverged from the mammalian lineage more than 400 million years ago, and provides a window into the evolutionary origins of the endocannabinoid system. To investigate this, human CNR1 and CNR2 were aligned with short-read mRNA transcripts obtained from seven male and four female specimens. We sampled transcripts from 7 unique tissues: the anterior brain, posterior brain, notochord, gut, gonads, blood, and heart. E. stoutii transcripts homologous to human cannabinoid receptors and the metabolic enzymes synthesizing and degrading AEA and 2-AG were identified using sequence pseudo-alignments. We then assembled these to generate a consensus sequence for the E. stoutii cannabinoid receptor (esCNR). A comprehensive phylogenetic analysis was performed with multiple sequence alignments, comparing esCNR against various vertebrate and putative invertebrate receptors implicated in the endocannabinoid system. In silico structural analysis identified putative binding pockets and conserved ligand-receptor interactions. Functional evaluation of endogenous ligands and selective agonists at the esCNR was performed using a bioluminescence resonance energy transfer assay. We found that E. stoutii expressed a lone G-protein coupled receptor highly homologous to both human CNR1 and CNR2 receptors. esCNR was predominantly expressed in the brain and notochord, with limited expression in peripheral tissues, consistent with the distribution of the human CNR1. We did not find a detectable sex difference in esCNR expression. esCNR also clustered with other vertebrate CNR1s rather than CNR2s. Phylogenetically, this distinguished it from previously reported putative invertebrate cannabinoid receptors, which clustered with human lysophospholipid and sphingolipid receptors. Functionally, esCNR was robustly activated by both 2-AG and AEA, which closely mirrors the profile of human CNR1. Interestingly, esCNR also responded to a human CNR2-selective agonist (RNB 61). Together, these findings suggest that CNR1-like endocannabinoid signaling emerged early in vertebrate evolution.

**Disclosures: S. Chen:** None. **G. Venumbaka:** None. **J. Siu:** None. **A. Romero:** None. **A. Jeon:** None. **E. Whitehouse:** None. **R. Setia:** None. **P.R. O'Neill:** None. **C.J. Evans:** None.

**Poster**

**PSTR195: Mechanisms of Polysubstance and Cannabinoid Use**

**Location:** WCC Halls A-C

**Time:** Monday, November 16, 2026, 1:00 PM - 5:00 PM

**Program #/Poster #:** PSTR195.12/GG24

**Topic:** H.08. Drugs of Abuse and Addiction

**Support:** CIC-MMMP

**Title:** Affinin and bornyl decatriene show potential pharmacological activity on cannabinoid receptors

**Authors: *D. GODÍNEZ-GAUTHEREAU**[1], K. ALONSO HURTADO[2], R. ESPINOSA LUNA[2], M. M. MARTINEZ-PACHECO, Sr.[2];
[1]Facultad de Químico Farmacobiología, [2]Inst. de Investigaciones Químico Biológicas, Univ. Michoacana de San Nicolás de Hidalgo, Morelia, Mexico

**Abstract:** Cannabis is a plant that is consumed globally due to its psychoactive and pain reduction properties. Cannabinoids interact with Cannabinoid receptors found in human cells. Cannabinoid receptors are part of a family of proteins called G-Protein coupled receptors (GPCRs), and the most prominent are Cannabinoid Receptor 1 (CB1R) and Cannabinoid Receptor 2 (CB2R), which are found in neurons and immune cells, respectively. Affinin and bornyl decatriene are compounds that are extracted from Heliopolis longipes, a medicinal plant endemic to the Sierra de Alvarez and Sierra Gorda region in Mexico. Heliopolis longipes has been used for centuries due to its analgesic and anti-inflammatory properties. The aim is to determine the energetic affinity by in silico analysis of both affinin and bornyl decatriene on CB1R and CB2R, in search of a functional alternative to cannabinoids that have similar properties without generating a psychoactive response. CB1R and CB2R crystal structures were extracted from Protein Data Bank (PDB), and were adjusted in Autodock Tools. Affinin and bornyl decatriene molecular structures were extracted from ChemSpider and later adjusted manually on Maestro. The molecular docking was made in Autodock Tools. The results were visualized in Discovery Studio. Our results show that affinin and bornyl decatriene molecules bind in a stable way to previously documented binding sites on both CB1R and CB2R. Furthermore, these results suggest that affinin and bornyl decatriene possess favorable interaction energies on CB1R and CB2R. These results suggest the existence of pharmacological activity due to affinin and bornyl decatriene binding to CB1R and CB2R; hence, further research integrating in vivo experiments is strongly recommended to comprehensively describe the pharmacological profile of these ligands as well as their mechanism of action.

**Disclosures: D. Godínez-Gauthereau:** None. **K. Alonso Hurtado:** None. **R. Espinosa Luna:** None. **M.M. Martinez-Pacheco:** None.

**Poster**

**PSTR195: Mechanisms of Polysubstance and Cannabinoid Use**

**Location:** WCC Halls A-C

**Time:** Monday, November 16, 2026, 1:00 PM - 5:00 PM

**Program #/Poster #:** PSTR195.13/HH1

**Topic:** H.08. Drugs of Abuse and Addiction

**Title:** Stress-related neuroadaptations following adolescent exposure to the synthetic cannabinoid 5F-MDMB-PICA

**Authors: *F. CARIA**[1], A. M. LIBSTER[3], S. DESFOR[4], F. TELESE[5], G. DI CHIARA[6], M. A. DE LUCA[2];
[1]biomedical science, Univ. of Cagliari, monserrato, Italy; [2]Biomed. Sci., Univ. of Cagliari, Monserrato, Italy; [3]Psychiatry, UCSD, La jolla, CA; [4]Biol., [5]Psychiatry, UCSD, La Jolla, CA; [6]Univ. Cagliari, 09124 Cagliari, Italy

**Abstract:** Synthetic cannabinoids (SC) constitute the largest group of novel psychoactive substances worldwide and pose significant risks for developmental neurobiology (EMCDDA, 2022). Among them, 5F-MDMB-PICA is a potent full agonist at CB1/CB2 receptors, previously shown to enhance mesolimbic dopamine (DA) transmission in adolescent but not adult mice (Musa et al., 2020). Given the pivotal role of endocannabinoid signalingin in regulating the hypothalamic-pituitary-adrenal (HPA) axis and stress responses (Hillard et al., 2016; Loomba & Patel, 2025), we hypothesized that adolescent self-administration of 5F-MDMB-PICA induces long-term dysregulation of stress reactivity and emotional regulation. In adolescent mice, intravenous self-administration (IVSA) of 5F-MDMB-PICA at selected doses (1-5 µg/kg/25 µl) revealed an inverted U-shaped dose-response, with maximal responding at 2.5 µg/kg/25 µl (FR1-3, PR schedules). Adult mice that had self-administered 5F-MDMB-PICA (2.5 µg/kg/25 µl) during adolescence exhibited altered stress-related phenotypes: increased aggression, reduced social interaction and anhedonia. Neurochemically, these mice displayed a delayed and blunted dopaminergic response in the medial prefrontal cortex (mPFC) following an olfactory stressor, as assessed via in vivo microdialysis. Complementing this, fiber photometry recordings showed reduced calcium transients of excitatory neurons in the mPFC during aversive stimuli, consistent with impaired cortical stress-reactivity and emotional regulation. These changes correlate with disrupted DA signalling, suggesting that adolescent exposure to 5F-MDMB-PICA induces a maladaptive “stress-vulnerable” phenotype.Our findings indicate that 5F-MDMB-PICA IVSA is acquired at lower doses compared to the prototypical SCRA JWH-018 (Margiani et al., 2022), pointing to a higher abuse liability. Importantly, the adolescent exposure induced persistent neurobehavioral changes in stress-reactivity circuits, underscoring the adolescent period as a window of vulnerability. These results highlight the need to consider SC exposure not only from a reward/addiction perspective, but critically for its long-term impacts on stress regulation and emotional resilience.

**Disclosures: F. Caria:** None. **A.M. Libster:** None. **S. Desfor:** None. **F. Telese:** None. **G. Di Chiara:** None. **M.A. De Luca:** None.

**Poster**

**PSTR195: Mechanisms of Polysubstance and Cannabinoid Use**

**Location:** WCC Halls A-C

**Time:** Monday, November 16, 2026, 1:00 PM - 5:00 PM

**Program #/Poster #:** PSTR195.14/HH2

**Topic:** H.08. Drugs of Abuse and Addiction

**Support:** NIAAA R15AA027909 to ESO
William Paterson University

**Title:** Genetic variability contributes to distinct behavioral phenotypes in mice with or without type 2 cannabinoid receptors

**Authors: *E. S. ONAIVI**;
Biol., William Paterson Univ., Wayne, NJ

**Abstract:** The discovery of additional lipid mediators, enzymes, receptors, paracannabinoids, has expanded the endocannabinoid system (ECS) into the endocannabinoidome (eCBome). Previous findings from our laboratory demonstrated that the deletion of mu-opioid receptor (MOR) and CB2R cannabinoid receptors (CB2Rs) from either dopamine neurons or microglia differentially altered motor activity and nociception, accompanied by genotype-dependent changes in cytokines and chemokines. The present study examined the hypothesis that genetic variability contributes to distinct behavioral phenotypes in mice with or without CB2Rs. Eleven genetic strains of naïve male and selected female mice were used to characterize the baseline behavioral responses using tail-flick and wheel-running (WRA) activity tests. Behavioral analysis included five-minute WRA assessments and tail-flick latency measurements for nociceptive sensitivity with a cut-off time of 12 seconds. In selected mouse strains, including SERT knockout (KO), lacking the serotonin transporter gene, BTBR mice as a model of autism spectrum disorders (ASDs), and C57BL/6J, wild-type controls, were subjected to tube restriction for one hour daily for 5 days. Anhedonia was evaluated using 2% sucrose consumption while tail-flick latencies were measured on days 1, 3, and 5 following tube restriction. The Results revealed significant strain- dependent differences in WRA and tail-flick latencies particularly in dopamine neuron- and microglia-specific CB2R conditional knockout mice, which exhibited lower tail-flick latencies and reduced WRA, respectively. Strains with higher WRA displayed shorter tail-flick latencies, suggesting an inverse relationship between motor activity and pain sensitivity. Genetic background influenced activity and nociception across the mouse strains. In selected strains, tail-flick and sucrose preference tests revealed distinct behavioral responses to acute stress, further emphasizing the impact of genetic background on WRA and nociceptive sensitivity. Overall, these findings demonstrate that genetic background is a critical factor influencing behavioral outcomes and be considered in the design and interpretation of preclinical studies.

**Disclosures: E.S. Onaivi:** None.

**Poster**

**PSTR195: Mechanisms of Polysubstance and Cannabinoid Use**

**Location:** WCC Halls A-C

**Time:** Monday, November 16, 2026, 1:00 PM - 5:00 PM

**Program #/Poster #:** PSTR195.15/HH3

**Topic:** H.08. Drugs of Abuse and Addiction

**Support:** NIDA DA000523-17

**Title:** 5F-MDMB-PINACA and related compounds with methyl-3,3-dimethylbutanoate (MDMB) head groups induce potent cannabinoid-like effects in C57BL/6J mice

**Authors: *N. R. GONZALEZ**, A. D. MAITLAND, D. WALTHER, M. H. BAUMANN, G. C. GLATFELTER;
Designer Drug Res. Unit, Natl. Inst. on Drug Abuse Intramural Res. Program, Baltimore, MD

**Abstract:** Synthetic cannabinoid receptor agonists (SCRAs) mimic the psychoactive effects of delta-9-tetrahydrocannabinol (THC) via activation of cannabinoid-1 receptors (CB1), but they are associated with increased risk of hospitalizations and overdose. Since 2025, 5F-MDMB-PINACA has been the most frequently detected SCRA in human case work. The current study examined the cannabinoid-like effects of 5F-MDMB-PINACA and related compounds bearing a methyl-3,3-dimethylbutanoate (MDMB) head group (i.e., MDMB-4en-PINACA and MDMB-FUBINACA) as compared to their methyl-3-methylbutanoate (MMB) counterparts. *In vitro* CB1 affinity, potency, and efficacy were assessed using [$^{3}$H]rimonabant and [$^{35}$S]GTPγS binding assays in mouse brain membranes. For *in vivo* measures, groups of C57BL/6J mice (n=12/drug; 6 female) received subcutaneous (sc) SCRA (0.001-3 mg/kg) or vehicle injections. Cannabinoid-like effects were evaluated using the Triad Test, which sequentially measures body temperature, catalepsy bar latency, and hot plate latency every 30 min for 2 h. Agonist reversal studies examined effects of rimonabant (3 mg/kg, sc) given 30 min after 5F-MDMB-PINACA (0.03 mg/kg, sc). All SCRAs inhibited [$^{3}$H]rimonabant binding and acted as CB1 agonists *in vitro*. MDMB-FUBINACA showed the highest CB1 affinity ($K_i$ = 0.86 nM) and functional potency ($EC_{50}$ = 2.78 nM). Compounds containing MDMB head groups displayed 3- to 10-fold greater CB1 affinities and potencies than their MMB counterparts (MDMB analog $K_i$ range = 0.86 - 3.90 nM vs. MMB analog $K_i$ range = 11.7 - 64.2 nM; MDMB analog $EC_{50}$ range = 2.78 - 15.4 nM vs. MMB analog $EC_{50}$ range = 18.4 - 97.6 nM). In mouse experiments, all SCRAs produced dose-dependent hypothermia, catalepsy, and antinociception compared to vehicle controls. MDMB-FUBINACA was the most potent compound *in vivo* ($ED_{50}$ range = 0.01-0.02 mg/kg), and MDMB-containing analogs were always more potent than MMB comparators. In the reversal studies, rimonabant effectively antagonized the effects of 5F-MDMB-PINACA within 30 min of administration. Our findings show that SCRAs containing an MDMB head group exhibit greater CB1 affinity/potency *in vitro* and more robust cannabinoid-like activity *in vivo* than their MMB counterparts, regardless of tail group motif. Clandestine chemists continue to exploit the MDMB head group for newly-emerging SCRAs, portending grave risk to cannabinoid users who are inadvertently exposed to the drugs.

**Disclosures: N.R. Gonzalez:** None. **A.D. Maitland:** None. **D. Walther:** None. **M.H. Baumann:** None. **G.C. Glatfelter:** None.

**Poster**

**PSTR195: Mechanisms of Polysubstance and Cannabinoid Use**

**Location:** WCC Halls A-C

**Time:** Monday, November 16, 2026, 1:00 PM - 5:00 PM

**Program #/Poster #:** PSTR195.16/HH4

**Topic:** H.08. Drugs of Abuse and Addiction

**Support:** National Institute on Drug Abuse R01

**Title:** Disruption of CB1 Receptor Phosphorylation Sites Reduces Cannabinoid Tolerance and Enhances Antinociceptive Responses in 8-Point Mutant Mice

**Authors: *D. M. CORTEZ**[1], S. MATEEN[1], K. M. DESCHEPPER[2], B. R. RORABAUGH[3], B. K. HIRSCHE[4,1], S. PASHIKANTI[1], D. J. MORGAN[5,1];
[1]Biomed. & Pharmaceut. Sci., Idaho State Univ., Pocatello, ID; [2]Biomed. Sci., [3]Pharmaceut. Sci., Marshall Univ., Huntington, WV; [4]Biol., Brigham Young Univ. - Idaho, Rexburg, ID; [5]Biomed. & Pharmaceut. Sci., Idaho State Univ. Biomed. Sci. Grad. Program, Pocatello, ID

**Abstract:** The cannabinoid type 1 receptor (CB1R) mediates the analgesic effects of endogenous and exogenous cannabinoids; however, chronic cannabinoid exposure produces receptor desensitization, internalization, and tolerance that limit long-term therapeutic efficacy. Phosphorylation of specific serine and threonine residues within the CB1R C-terminal domain promotes β-arrestin recruitment and receptor trafficking, processes that are critical for receptor regulation. To investigate the role of phosphorylation-dependent CB1R desensitization in cannabinoid tolerance, we utilized an 8-point mutant (8PM) mouse model in which eight key phosphorylation sites (S426A, S430A, T461A, S463A, S465A, T466A, T468A, and S469A) are replaced with alanine, preventing receptor phosphorylation and subsequent β-arrestin recruitment. Cannabinoid-induced antinociception was evaluated using the tail-flick experiment after repeated treatment with $\Delta^9$-THC and CP55,940 in wild-type (WT) and 8PM mice. Consistent with our hypothesis, 8PM mice exhibited enhanced antinociceptive and hypothermic responses relative to WT controls throughout the treatment period. Tolerance to the hypothermic and antinociceptive effects of these was reduced in 8PM mice. These findings suggest that disruption of phosphorylation-dependent receptor regulation preserves cannabinoid efficacy during chronic treatment. The observed phenotype is consistent with impaired β-arrestin recruitment, reduced receptor desensitization, and diminished receptor internalization in 8PM mice. Ongoing studies are examining CB1R trafficking, β-arrestin2 interactions, receptor downregulation, and G-protein signaling to define the molecular mechanisms underlying the altered behavioral responses. Collectively, these results demonstrate that phosphorylation-dependent CB1R regulation is a critical determinant of cannabinoid tolerance. Targeting receptor conformations or signaling pathways that minimize β-arrestin-mediated desensitization may represent a promising strategy for the development of cannabinoid therapeutics with improved long-term analgesic efficacy and reduced tolerance liability.

**Disclosures: D.M. Cortez:** None. **S. Mateen:** None. **K.M. DeSchepper:** None. **B.R. Rorabaugh:** None. **B.K. Hirsche:** None. **S. Pashikanti:** None. **D.J. Morgan:** None.

**Poster**

**PSTR196: Pharmacological and Molecular Mechanisms in Substance Use Disorders**

**Location:** WCC Halls A-C

**Time:** Monday, November 16, 2026, 1:00 PM - 5:00 PM

**Program #/Poster #:** PSTR196.01/HH5

**Topic:** H.08. Drugs of Abuse and Addiction

**Support:** NIH Grant DA044242

**Title:** Low doses of nicotine and minor tobacco alkaloids interact to potentiate intravenous self-administration and dopamine increase in the nucleus accumbens in male Wistar rats

**Authors: *Z. DING**, X. TAN;
Penn State Col. of Med., Hershey, PA

**Abstract:** Nicotine (NIC) is the major tobacco alkaloid and the primary addictive component. Several minor tobacco alkaloids also possess their own abuse potential, including nornicotine (NOR), cotinine (COT), and anabasine (ANA). How these minor alkaloids may influence NIC abuse potential remains largely unknown. FDA proposed rulemaking to reduce NIC content in cigarettes to minimally addictive or non-addictive levels. Clinical studies showed that low NIC cigarettes reduced NIC intake and dependence, cigarette smoking, and toxicant exposure. However, such cigarettes remained reinforcing and continued to sustain smoking, suggesting that non-NIC constituents may contribute to sustaining the reinforcing effects of very low doses of NIC. The objective of this study was to determine interactions between addictive minor alkaloids and low doses of NIC in producing addiction-related effects. Intravenous self-administration (IVSA) was conducted to assess reinforcing effects under a fixed ratio (FR) 1 schedule for 10 sessions and a FR2 schedule for 5 sessions. Rats were allowed to self-administer NIC, a minor alkaloid, and a mixture of NIC and a minor alkaloid with each compound tested at 0.00375 mg/kg/infusion. Microdialysis was conducted to determine the stimulating effects of these compounds on extracellular dopamine (DA) levels in the nucleus accumbens. During microdialysis, rats received a subcutaneous injection of NIC, a minor alkaloid, or a mixture of NIC and a minor alkaloid. NIC, NOR, and ANA were tested at 0.1 mg/kg. COT was tested at 0.5 mg/kg. COT or NOR alone did not support IVSA. Rats started to increase active responses for NIC from session 8, for the NIC+COT mixture from session 4, and for the NIC+NOR mixture from session 6. Average number of infusions per session toward the end of FR1 sessions were greater for the NIC+COT mixture (~23/session) and the NIC+NOR mixture (~34/session) than that for NIC (~7/session), COT (~14/session), or NOR (~10/session). In microdialysis, COT, NOR, or ANA did not increase DA levels. NIC slightly increased DA levels (~130% of baseline). DA levels were significantly elevated for the NIC+COT mixture (~180% of baseline), the NIC+NOR mixture (~240% of baseline), and the NIC+ANA mixture (~220% of baseline). These results indicate that low doses of NIC and minor alkaloids interacted to augment IVSA and DA increase, suggesting that these non-NIC constituents may enhance the abuse potential of very low doses of NIC. Such interactions may contribute to sustaining reinforcing effects of low NIC cigarettes and highlight the importance of removing addictive minor alkaloids to maximize the effects of NIC reduction.

**Disclosures: Z. Ding:** None. **X. Tan:** None.

**Poster**

**PSTR196: Pharmacological and Molecular Mechanisms in Substance Use Disorders**

**Location:** WCC Halls A-C

**Time:** Monday, November 16, 2026, 1:00 PM - 5:00 PM

**Program #/Poster #:** PSTR196.02/HH6

**Topic:** H.08. Drugs of Abuse and Addiction

**Support:** TRDRP Grant T36DT10372
TRDRP Grant T34IR8049
TRDRP Grant T33IP6417

**Title:** 6-methyl nicotine and nicotinamide produce distinct behavioral effects in adolescent male and female Sprague-Dawley rats

**Authors: *N. ALAMMARI**[1], S. LOTFIPOUR[2];
[1]Pharmaceut. Sci., [2]Emergency Medicine, Pharmacology, & Pathology, Univ. of California, Irvine, Irvine, CA

**Abstract:** Adolescent nicotine exposure can alter reward-related neurodevelopment and increase vulnerability to substance use disorders. Following the recent regulation of synthetic nicotine, “nicotine-free” products have emerged that contain analogues such as 6-methyl nicotine (6MN) and nicotinamide (NAM). Despite increasing exposure, the behavioral effects of these compounds, particularly during adolescence, remain unknown. It's hypothesized that 6MN and NAM would produce acute behavioral effects distinct from nicotine that differ by sex. On postnatal day 28, adolescent male and female Sprague-Dawley rats received intravenous exposure to saline (SAL), nicotine (NIC), 6MN, or NAM, followed immediately by a 30-min open-field assay. A dose-finding approach was used to identify behaviorally active doses and compare their effects relative to a nicotine reference condition. Ambulatory counts were used as a measure of locomotor activity, and percent center time was used as an anxiety-like measure. Data are presented as mean ± SEM. Male (N=20) and female (N=19) rats were analyzed separately using one-way ANOVAs followed by Bonferroni-corrected multiple comparisons. Preliminary analyses revealed compound-, dose-, and sex-dependent behavioral effects. In males, the highest 6MN dose increased locomotor activity compared with SAL, whereas lower 6MN doses did not increase activity. NAM also increased locomotor activity in males compared with SAL and produced greater activity than NIC. In females, NIC increased locomotor activity compared with SAL, whereas NAM produced lower activity than NIC. Direct sex comparisons revealed greater NIC-induced locomotor activity in females than males, whereas males showed greater activity than females following the highest 6MN dose. Center-time effects diverged from locomotor effects where 6MN did not significantly alter center time and NAM produced greater center time in males than females. These data support evaluation of nicotine analogues as biologically active compounds with potential relevance to adolescent addiction vulnerability.

**Disclosures: N. Alammari:** None. **S. Lotfipour:** None.

**Poster**

**PSTR196: Pharmacological and Molecular Mechanisms in Substance Use Disorders**

**Location:** WCC Halls A-C

**Time:** Monday, November 16, 2026, 1:00 PM - 5:00 PM

**Program #/Poster #:** PSTR196.03/HH7

**Topic:** H.08. Drugs of Abuse and Addiction

**Support:** NIH Maine IDeA Network of Biomedical Research Excellence ( MAINE INBRE) grant P20GM103423

**Title:** Sex-specific effects of acute GLP-1R agonism on locomotion and anxiety-like behaviors during nicotine withdrawal

**Authors: *D. AMOAH**, E. ESKIN, S. EPSTEIN, S. MATTHEWS, P. ELLIOTT, Z. DODGE, R. ORTEZ, R. J. HERMAN;
Dept. of Psychology, Colby Col., Waterville, ME

**Abstract: Rationale:** Nicotine Use Disorder remains a leading cause of preventable death, with relapse rates remaining high due in part to withdrawal-related anxiety. Glucagon-like peptide-1 receptor agonists such as semaglutide have been shown to reduce nicotine intake and relapse-related behaviors; however, their effects on anxiety-like behavior during nicotine withdrawal remain unclear. **Objective:** The present study investigated whether acute semaglutide administration attenuates anxiety-like behaviors during precipitated nicotine withdrawal in male and female rats. **Methods:** Nicotine dependence was induced in male and female Sprague-Dawley rats via minipump implantation. Nicotine withdrawal was precipitated using mecamylamine following acute semaglutide or vehicle administration. Anxiety-like behavior and locomotor activity were assessed using the Elevated Plus Maze (EPM) and Open Field Test.**Results:** Anxiety-like behavior was increased during precipitated nicotine withdrawal in both sexes. Female rats exhibited heightened anxiety-like behavior in the EPM, while nicotine dependent males showed increased anxiety-like behavior across both behavioral assays. Acute semaglutide administration did not attenuate withdrawal-induced anxiety-like behavior in either sex. Sex-dependent effects on locomotor activity were observed upon semaglutide treatment.**Conclusion:** Our findings indicate that acute semaglutide administration is insufficient to reduce anxiety-like behavior during precipitated nicotine withdrawal. Sex-dependent interactions with locomotor activity may suggest that behavioral outcomes were influenced by treatment context. Further studies employing chronic dosing and expanded behavioral measures may elucidate the effect on anxiety-like behaviors.

**Disclosures: D. Amoah:** None. **E. Eskin:** None. **S. Epstein:** None. **S. Matthews:** None. **P. Elliott:** None. **Z. Dodge:** None. **R. Ortez:** None. **R.J. Herman:** None.

**Poster**

**PSTR196: Pharmacological and Molecular Mechanisms in Substance Use Disorders**

**Location:** WCC Halls A-C

**Time:** Monday, November 16, 2026, 1:00 PM - 5:00 PM

**Program #/Poster #:** PSTR196.04/HH8

**Topic:** H.08. Drugs of Abuse and Addiction

**Support:** AGR350-26

**Title:** Effects of GLP-1R Deletion in Triangular Septal Nucleus Neurons on the Motivational Properties of Nicotine

**Authors: *D. VÁZQUEZ CARRILLO**, P. J. KENNY;
Friedman Brain Inst., Icahn Sch. of Medicine, Mount Sinai, New York, NY

**Abstract:** Tobacco smoking (whose main addictive component is nicotine) increases the risk of cancer, cerebrovascular, cardiovascular, and respiratory diseases. GLP-1 receptor (GLP-1R) agonists (Exedin-4, Semaglutide, Liraglutide, among others) may reduce tobacco use and relapse during abstinence in humans. GLP-1R agonists decrease nicotine consumption in mice and rats, while *Glp1r* knockout mice exhibit increased nicotine intake. The populations of GLP-1Rs in the brain that mediate these effects are unclear. Here, we report that GLP-1Rs are densely expressed in the triangular septal nucleus (TSn), a largely unexplored region of the posterior septum. To investigate the role of GLP-1R-expressing (GLP-1R+) neurons in the TSn in regulating the motivational properties of nicotine, we generated conditional knockout (cKO) mice with *Glp1r* deletion restricted to TSn neurons using an AAV-mediated intersectional strategy in mice. cKO and control mice underwent intravenous nicotine self-administration (IVSA) for 39 days with nicotine unit doses ranging from 0.01 to 0.25 mg/kg/infusion. After stabilizing intake on the higher nicotine doses, the effects of acute semaglutide injection (0.1 mg/kg) were assessed. The TSn, lateral septum (LSn), pontine gray (PG), and nucleus tractus solitarius (NTS) were collected for *Glp1r* expression analyses. Fluorescence in situ hybridization (FISH) confirmed partial but successful *Glp1r* deletion in 75% of viral injections. Unexpectedly, cKO mice exhibited reduced nicotine self-administration at the 0.1 and 0.25 mg/kg nicotine doses compared with control mice. Semaglutide treatment also produced a reduction in nicotine intake in both controls and cKO mice. *Glp1r* expression was increased in the TSn of cKO mice. Likewise, GLP-1R levels were increased in the LSn, and PG. This indicates that partial *Glp1r* deletion in the TSn drives region-specific upregulation in *Glp1r* expression. Compensatory adaptations in GLP-1R signaling may therefore explain the decreased nicotine intake in cKO mice. These findings indicate that GLP-1R+ neurons in the TSn contribute to behavioral responses to GLP-1 agonists. Understanding the function of GLP-1Rs in this region may provide insight into neural mechanisms relevant to tobacco and other substance use disorders and the potential therapeutic utility of GLP-1R agonists.

**Disclosures: D. Vázquez Carrillo:** None. **P.J. Kenny:** None.

**Poster**

**PSTR196: Pharmacological and Molecular Mechanisms in Substance Use Disorders**

**Location:** WCC Halls A-C

**Time:** Monday, November 16, 2026, 1:00 PM - 5:00 PM

**Program #/Poster #:** PSTR196.05/HH9

**Topic:** H.08. Drugs of Abuse and Addiction

**Title:** Exercise's and NACHO's impact on Nicotine Reward, Cognition, Anxiety and Depression

**Authors: *K. A. MARQUEZ**[1], A. GONZALEZ[3], J. SAWAH[2], Z. HASSAN[4], H. MCCAMY[4], Y. SHERAFAT[4];
[1]Psychology, [2]California State Univ. San Marcos, San Marcos, CA; [3]California state Univ. San Marcos, San Marcos, CA; [4]California State University, San Marcos, San Marcos, CA

**Abstract:** Exercise has been shown to be a beneficial method for reducing nicotine seeking, anxiety and depressive-like behaviors while also increasing cognitive abilities both in rodent models and humans. When mice engage in moderate exercise, they have been shown to exhibit an increase in alpha-7 nicotinic receptors, along with an enhancement in cognitive abilities and a decrease in nicotine withdrawal behaviors. Nicotinic receptors have been shown to be dependent on the chaperone protein NACHO for their assembly, expression, and function. For this research study, we investigated the differences in cognition, nicotine seeking, anxiety- and depressive-like behaviors between NACHO Knockout (KO) mice and wild-type mice. Among both the NACHO KO mice and the wildtype groups half of the mice exercised daily for three weeks, the other half did not exercise. Results from this study revealed that among the exercise group, NACHO KO ran significantly more. Both exercise groups exhibited significantly less anxiety-like behaviors compared to the non- exercising NACHO KO mice. Results also showed that among the wildtype mice, those that exercised had better memory function compared to those that did not exercise. Results from the Forced Swim test revealed that those in the exercise group regardless of NACHO expression exhibited significantly lower levels of depressive-like behaviors compared to those in the non-exercising groups. Findings from the CPP experiment revealed that mice in the exercising groups had a higher preference for the nicotine chamber compared to the non-exercising groups. The results from this study reveal that exercise can be beneficial for anxiety-like and depressive-like behaviors regardless of NACHO's presence. These findings also reveal that when NACHO is present, exercise enhances memory. Lastly, these findings indicate that exercise may potentially increase nicotine seeking rather than decreasing, like previous studies have found. Future studies should investigate how exercise impacts the expression of NACHO to better understand how their relationship impacts the behaviors examined in this study.

**Disclosures: K.A. Marquez:** C. Other Research Support (receipt of drugs, supplies, equipment or other in-kind support); PI Start up fund. **A. Gonzalez:** C. Other Research Support (receipt of drugs, supplies, equipment or other in-kind support); PI Start up fund. **J. Sawah:** C. Other Research Support (receipt of drugs, supplies, equipment or other in-kind support); PI Start up fund. **Z. Hassan:** C. Other Research Support (receipt of drugs, supplies, equipment or other in-kind support); PI Start up fund. **H. McCamy:** C. Other Research Support (receipt of drugs,

supplies, equipment or other in-kind support); PI Start up fund. **Y. Sherafat:** C. Other Research Support (receipt of drugs, supplies, equipment or other in-kind support); PI Start up fund.

**Poster**

**PSTR196: Pharmacological and Molecular Mechanisms in Substance Use Disorders**

**Location:** WCC Halls A-C

**Time:** Monday, November 16, 2026, 1:00 PM - 5:00 PM

**Program #/Poster #:** PSTR196.06/HH10

**Topic:** H.08. Drugs of Abuse and Addiction

**Title:** Preliminary Effects of Clavulanic Acid in Nicotine Dependent Adults

**Authors: *N. J. HENIGMAN**[1], S. UPTON[2], B. FROELIGER[3];
[1]Psychological Sci., Univ. of Missouri - Columbia, Columbia, MO; [2]Psychology; Psychiatry, Univ. of Missouri, Columbia, Columbia, MO; [3]Psychological Sci., Univ. of Missouri Columbia, Columbia, MO

**Abstract:** Work in animal models demonstrates that medications that upregulate glutamate transporter (GLT-1) restore the balance in frontostriatal glutamate and blocks reinstated drug seeking. The β-lactamase inhibitor, clavulanic acid, has been shown to restore GLT-1 and block reinstated drug seeking in rodent models. However, there is currently a dearth of mechanistic work in humans on the effects of clavulanic acid for disrupting drug use and no reports on clavulanic acid for treating nicotine dependence pathophysiology. We conducted a pilot randomized, placebo-controlled, double-blind study of clavulanic acid to examine safety and tolerability as well as the effects on inhibitory control and resting-state functional connectivity following the administration of a 3-day course of clavulanic acid to nicotine dependent adults (Age: M= 45.6; FTND: M=5.44; Pack Years: M=23.9) who smoke (N=25). No significant treatment-related adverse events emerged and the blind was successful. As compared to the placebo group, those who received clavulanic acid exhibited increased rsFC in frontostriatal circuitry i.e., between the nucleus accumbens and ventromedial prefrontal cortex ($F_{1,22} = 8.99$, $p=.007$, $D =.85$) and improved inhibitory control task performance ($t(23) = 1.60$, $p=.06$; $D = .29$). These findings provide proof of concept and support for further examination of the effects of clavulanic acid on neural and behavioral mechanism underlying nicotine dependence, and potential values of reducing smoking behavior.

**Disclosures: N.J. Henigman:** None. **S. Upton:** None. **B. Froeliger:** None.

**Poster**

**PSTR196: Pharmacological and Molecular Mechanisms in Substance Use Disorders**

**Location:** WCC Halls A-C

**Time:** Monday, November 16, 2026, 1:00 PM - 5:00 PM

**Program #/Poster #:** PSTR196.07/HH11

**Topic:** H.08. Drugs of Abuse and Addiction

**Support:** NIDA IRP - Z1A DA000633

**Title:** MRI-1867, a Novel Peripherally Acting CB1 Receptor Antagonist, Shows Promise in Treating Opioid Use Disorders in Rodents

**Authors: *Z. XI**;
Natl. Inst. on Drug Abuse, Baltimore, MD

**Abstract:** The cannabinoid CB1 receptor (CB1R) plays an important role in addiction-related behaviors and has therefore been a therapeutic target in the development of medications for substance use disorders. Rimonabant, the first CB1R antagonist and inverse agonist, was tested in humans for the treatment of obesity and cigarette smoking. Preclinical studies also demonstrated that rimonabant is highly effective in reducing drug-taking and drug-seeking behaviors. However, severe central CB1R-mediated side effects—such as depression and suicidal ideation—led to its market withdrawal and the termination of further development of this class of drugs. This underscores the urgent need to develop novel, safer CB1R antagonists that retain anti-addiction efficacy without causing adverse central nervous system (CNS) effects. In this study, we explored MRI-1867, a peripherally restricted CB1 receptor inverse agonist/antagonist, as a novel therapeutic approach for opioid use disorders. Because this compound does not cross the blood-brain barrier, we assumed that it avoids the rimonabant-like neuropsychiatric side effects associated with centrally acting CB1 antagonism. In adult male rats, we assessed the effects of MRI-1867 using a series of behavioral assays, including intravenous drug self-administration, optical intracranial self-stimulation (oICSS), hot plate analgesia testing, and open-field locomotion assessments. Systemic administration of MRI-1867 yielded three key findings: (1) a significant reduction in heroin self-administration and reinstatement of heroin seeking - and to a lesser extent, in cocaine self-administration - without impairing locomotor activity; (2) inhibition of dopamine-dependent oICSS maintained by contingent optical stimulation of midbrain dopamine neurons in DAT-Cre mice; and (3) enhancement of oxycodone-induced analgesia. These results demonstrate that peripheral CB1R antagonism or inverse agonism can effectively reduce opioid-taking an seeking behaviors while enhancing analgesic effects, suggesting that MRI-1867 holds promise as a therapeutic agent for opioid use disorders. Future research will focus on identifying cell type-specific sites of peripheral CB1R expression and determining whether deletion of CB1R in peripheral sensory neurons will alter the effects of MRI-1867 on opioid reward and analgesia.

**Disclosures: Z. Xi:** None.

**Poster**

**PSTR196: Pharmacological and Molecular Mechanisms in Substance Use Disorders**

**Location:** WCC Halls A-C

**Time:** Monday, November 16, 2026, 1:00 PM - 5:00 PM

**Program #/Poster #:** PSTR196.08/HH12

**Topic:** H.03. Motivation

**Title:** Pharmacodynamic and pharmacokinetic interactions between carbamazepine and psilocybin

**Authors:** ***M. A. SAKIB**[1], S. OBENG[2], L. R. MCMAHON[3];
[2]Pharmaceut. Sci., [1]Texas Tech. Univ. Hlth. Sci. Ctr., Amarillo, TX; [3]Office of Res., Texas Tech. Univ. Hlth. Sci. Ctr., Lubbock, TX

**Abstract:** Psilocybin is being investigated for the treatment of several neuropsychiatric disorders; however, little is known about interactions with other neuropsychotropic agents. Reports of seizures when classic psychedelics were combined with lithium highlight the need to evaluate interactions between psychedelics and mood-stabilizing medications. This study examined interactions between psilocybin and carbamazepine, an FDA-approved drug for bipolar disorder and epilepsy. Male (n=4) and female (n=4) Sprague-Dawley rats were trained to discriminate the 5-HT2A agonist, DOI (0.32 mg/kg). During drug discrimination studies, the pre-treatment time for carbamazepine and psilocybin was 30 min and 15 min, respectively. Psilocybin fully substituted for DOI ($ED_{50}$=0.45 mg/kg), and carbamazepine enhanced the discriminative stimulus effects of psilocybin, producing a 10.2-fold leftward shift in the dose-response function. In pharmacokinetic studies, psilocybin (0.32 mg/kg, i.v.) was administered alone or following carbamazepine pretreatment (3.2 mg/kg, i.v.; 5 min pretreatment), and plasma psilocin concentrations were quantified by LC-MS/MS. Carbamazepine did not increase psilocin half-life (29.8 ± 0.03 vs. 28.2 ± 1.43 min), reduced $AUC_{inf}$ from 1866 ± 566 to 1001 ± 142 min×ng/mL while increasing apparent clearance (74.7 ± 37.4 vs. 120 ± 38.3 mL/min). These findings reveal that the enhanced psilocybin-appropriate responding by carbamazepine is not attributable to increased plasma psilocin exposure.

**Disclosures: M.A. Sakib:** None. **S. Obeng:** None. **L.R. McMahon:** None.

**Poster**

**PSTR196: Pharmacological and Molecular Mechanisms in Substance Use Disorders**

**Location:** WCC Halls A-C

**Time:** Monday, November 16, 2026, 1:00 PM - 5:00 PM

**Program #/Poster #:** PSTR196.09/HH13

**Topic:** H.03. Motivation

**Support:** NIDA Grant R21DA058174
NIDA Grant R01DA062540

**Title:** Single-nucleus multiome profiling reveals non-additive sgACC molecular states in comorbid opioid use disorder and major depression

**Authors:** ***M. K. FISH**[1], S. SAMBARE[2], C. SRINIVASAN[4], B. N. PHAN[5], A. R. PFENNING[6], M. L. SENEY[7], R. W. LOGAN[3];
[1]Psychiatry & Neurobio., UMass Chan Med. Sch., Worcester, MA; [2]Univ. of Massachusetts

Chan Med. Sch., Worcester, MA; [3]Psychiatry, Univ. of Massachusetts Chan Med. Sch., Hopkinton, MA; [5]Computat. Biol., [6]Computat. Biol. Dept., [4]Carnegie Mellon Univ., Pittsburgh, PA; [7]Dept. of Psychiatry, Univ. of Pittsburgh, Pittsburgh, PA

**Abstract:** Opioid use disorder (OUD) and major depressive disorder (MDD) frequently co-occur, yet the molecular architecture of their comorbidity remains poorly defined. Given the role of the subgenual anterior cingulate cortex (sgACC) in affective regulation, stress responsivity and reward processing, we generated single-nucleus multiome profiles from postmortem human sgACC of 24 donors balanced across control, MDD-only, OUD-only and comorbid OUD/MDD (COM) groups. Profiles were of high quality across modalities (mean 11,883 UMIs and 3,677 genes per GEX nucleus; mean 6,875 ATAC fragments, 6.98 TSS enrichment and 0.30 FRIP per ATAC nucleus). Using cell-type pseudobulk models fitted in limma across 22 cell types, with shared covariates and modality-specific surrogate variables, we tested three prespecified contrasts: OUD-associated effects [(OUD+COM)/2−CTL], MDD-associated effects [(MDD+COM)/2−CTL] and COM non-additivity [COM−OUD−MDD+CTL], with FDR correction across contrast families. COM non-additivity was widespread but cell-type-specific, identifying 14,337 DEGs across cell-type expression models and 9,152 DARs across cell-type accessibility models. Collapsing repeated features across cell types yielded 8,580 unique DEGs and 9,037 unique DARs. Among significant non-additive features, 56% of DEGs and 31% of DARs showed a COM-resembles-control pattern, whereas the remainder diverged from the linear expectation based on OUD-only and MDD-only effects. Enrichment analyses revealed sparse, cell-type-specific programs rather than a convergent pathway, implicating oxidative phosphorylation, sterol and cholesterol biosynthesis, synaptic signaling, small-GTPase signaling, membrane trafficking and immune processes. These findings indicate that OUD/MDD comorbidity reflects a distinct sgACC molecular state rather than an additive extension of either disorder alone.

**Disclosures: M.K. Fish:** None. **S. Sambare:** None. **C. Srinivasan:** None. **B.N. Phan:** None. **A.R. Pfenning:** None. **M.L. Seney:** None. **R.W. Logan:** None.

**Poster**

**PSTR197: Hallucinogens: Neural Mechanisms of Action**

**Location:** WCC Halls A-C

**Time:** Monday, November 16, 2026, 1:00 PM - 5:00 PM

**Program #/Poster #:** PSTR197.01/HH14

**Topic:** H.08. Drugs of Abuse and Addiction

**Support:** The Science Insititute of the Meditz College of Arts and Sciences at Fairfield University

**Title:** The Interoceptive Actions of Tryptamine Analogs: Psilocybin, Baeocystin, Norbaeocystin, and Aeruginascin

**Authors: E. ALT**[1], D. TAYLOR[1], K. GERRISH[1], E. FILLAS[1], C. FUSCO[1], V. SGAGLIONE[1], A. JONES[2], *K. SCHMIDT[1];
[1]Fairfield Univ., Fairfield, CT; [2]Miami Univ., Oxford, OH

**Abstract:** Tryptamine compounds including psilocybin, baeocystin, norbaeocystin, and aeruginascin are found naturally in psychedelic mushrooms. Administration of psilocybin is sufficient to produce psychedelic effects believed to occur through its action at the serotonin 2a receptor and measured in rodents via the head twitch response. Interestingly, baeocystin, norbaeocystin, and aeruginascin do not produce head twitch responses. In this study, we used drug discrimination to determine whether baeocystin, norbaeocystin, and aeruginascin substitute for psilocybin. Male and female Long-Evans rats were trained to discriminate 1.0 mg/kg psilocybin from saline in a two-lever discrimination paradigm. Preliminary data show dose effect curves comparing baeocystin, norbaeocystin, aeruginascin, LSD (positive control), and cocaine (negative control) to psilocybin.

**Disclosures: E. Alt:** None. **D. Taylor:** None. **K. Gerrish:** None. **E. Fillas:** None. **C. Fusco:** None. **V. Sgaglione:** None. **A. Jones:** None. **K. Schmidt:** None.

**Poster**

**PSTR197: Hallucinogens: Neural Mechanisms of Action**

**Location:** WCC Halls A-C

**Time:** Monday, November 16, 2026, 1:00 PM - 5:00 PM

**Program #/Poster #:** PSTR197.02/HH15

**Topic:** H.08. Drugs of Abuse and Addiction

**Support:** NIH Grant DA047645
NIH Grant GM152169

**Title:** Behavioral and genetic mechanisms of psychedelic drug action in C. elegans

**Authors: *A. M. WHITE**, A. D. BAUER, K. C. CORSALE, B. W. WINJUM, C. R. NEUBERT, S. FAUMONT, W. M. ROBERTS, S. R. LOCKERY;
Inst. of Neurosci., Univ. of Oregon, Eugene, OR

**Abstract:** Psychedelics have shown remarkable promise for treating intractable psychiatric conditions. Genetically tractable invertebrate models could provide a powerful complement to studies in mammals. Accordingly, we assessed the potential of *C. elegans* as a model organism for investigating psychedelic drug action. We screened the psychedelic drugs 2,5-dimethoxy-4-iodoamphetamine (DOI), psilocin, dimethyltryptamine (DMT) and lysergic acid diethylamide (LSD) for effects on *C. elegans* locomotion. Only LSD had significant effects; a 30-minute 50 μM LSD exposure decreased forward speed and increased the probability of reverse locomotion. Although psychedelics have particularly high affinity for the serotonin 2A receptor, recent work has demonstrated that LSD potently activates nearly all human serotonin, dopamine, and adrenergic receptors. Therefore, we investigated whether complex polypharmacology underlay LSD's effects on *C. elegans* locomotion. We screened for locomotor effects of 50 μM LSD in

deletion mutants for each of the 17 *C. elegans* monoaminergic receptor genes (6 for serotonin, 4 for dopamine, 3 for octopamine, 4 for tyramine) and in 6 mutants with multiple monoaminergic receptor gene deletions. The effects of LSD on locomotion were reduced or eliminated in most mutants but increased in several others. Multiple monoaminergic pathways are likely involved in LSD's effects on locomotion and bidirectional regulation is a possibility.
To understand how LSD modulates the kinematics of worm locomotion, we conducted high-resolution locomotion tracking experiments in N2 worms exposed to vehicle or 50 μM LSD for 30 minutes. Previous work showed that random search behavior in *C. elegans* was well fit by a hidden Markov model with 4 locomotory states: Forward (F), Reverse (R), and 2 distinct Pause states (X and Y). We applied this 4-state model to the behavior of LSD-exposed and control worms. LSD specifically increased a subset of the transition rates between states, with notable effects on RY transitions and FX transitions. To place these findings in a neuronal context, we mapped them onto a minimal model comprising a pair of reciprocally inhibitory, neuron-like units, one each for forward and reverse locomotion. Preliminary results from this approach suggest that LSD decreases the excitability of neurons promoting forward locomotion, thereby destabilizing the forward state. This is consistent with increased probability of reverse locomotion. Together, we showed that LSD affects *C. elegans* locomotion through multiple aminergic pathways and used behavioral analysis and modeling to develop testable hypotheses regarding LSD's effect on neural activity.

**Disclosures: A.M. White:** None. **A.D. Bauer:** None. **K.C. Corsale:** None. **B.W. Winjum:** None. **C.R. Neubert:** None. **S. Faumont:** None. **W.M. Roberts:** None. **S.R. Lockery:** None.

**Poster**

**PSTR197: Hallucinogens: Neural Mechanisms of Action**

**Location:** WCC Halls A-C

**Time:** Monday, November 16, 2026, 1:00 PM - 5:00 PM

**Program #/Poster #:** PSTR197.03/HH16

**Topic:** H.08. Drugs of Abuse and Addiction

**Support:** NIH F31 (1F31EY038625-01)

**Title:** The inhibitory mechanism underlying psychedelic disruption of visual processing

**Authors: *C. A. KNOX**, A. C. KWAN;
Biomed. Engin., Cornell Univ., Ithaca, NY

**Abstract:** Serotonergic psychedelics, such as psilocybin, are known to profoundly alter visual perception, producing both elementary and complex hallucinations. However, the mechanisms by which psychedelics alter visual information processing remain unclear. I hypothesize that psychedelic-driven changes in interneuron activity within the primary visual cortex underlie the altered visual state accompanying the psychedelic experience. Using *in vivo* large-scale extracellular Neuropixels recordings combined with optogenetic cell-type tagging, I have quantified both spontaneous and visually evoked firing changes within two interneuron

populations after psilocybin treatment within the mouse primary visual cortex. Additional experiments begin to elucidate the role of serotonin receptors that mediate interneuron responsiveness to psilocybin, utilizing an inducible Cre strategy. Through this work, I aim to advance our understanding of how psychedelics affect early visual information processing and to provide broader insight into the neural basis of hallucinations.

**Disclosures: C.A. Knox:** None. **A.C. Kwan:** B. Contracted Research/Research Grant (principal investigator for a drug study, collaborator or consultant and pending and current grants). If you are a PI for a drug study, report that research relationship even if those funds come to an institution.; Boehringer Ingelheim, Eli Lilly, Empyrean Neuroscience, Freedom Biosciences, Helus Pharma, Otsuka, Xylo Bio, Intra-Cellular Therapies.

**Poster**

**PSTR197: Hallucinogens: Neural Mechanisms of Action**

**Location:** WCC Halls A-C

**Time:** Monday, November 16, 2026, 1:00 PM - 5:00 PM

**Program #/Poster #:** PSTR197.04/HH17

**Topic:** H.08. Drugs of Abuse and Addiction

**Support:** Trone Family Eminent Scholar Chair Gift

**Title:** The Impact of Fluoxetine on the Aversive Effects of LSD: Implications for Changes in LSD Aversive Effects

**Authors: *R. CRUPI**[1], K. JIMENEZ[1], W. SHISTER[1], A. L. RILEY[2], N. SANEL[1], M. TRAVAGLIA[1];
[2]Neurosci., [1]American Univ., Washington, DC

**Abstract:** Given reports that antidepressant history can reduce the subjective effects of a variety of psychedelics, assessing how such a history impacts its therapeutic efficacy in clinical populations resistant to traditional antidepressants is critical to understanding the utility of the psychedelics in this setting. A related issue is the impact of traditional antidepressants (especially those based with serotonergic action) on the adverse effects produced by psychedelics that could affect compliance. Recent work by Becker and colleagues (2022) has reported that a number of behavioral effects (fear, anxiety, “bad drug effects”) induced by LSD were reduced by pretreatment with fluoxetine (a selective serotonin reuptake inhibitor - SSRI), while other adverse effects (e.g., nausea) as well as the “good drug effects” induced by LSD were unaffected. To extend this analysis, the present studies examined if exposure to the selective serotonin reuptake inhibitor fluoxetine impacted the aversive effects of LSD as assessed in a taste avoidance procedure, a behavioral index of drug toxicity (Riley and Tuck, 1985). While taste avoidance is generally robust and rapidly acquired, pre-exposure to the drug generally reduces or attenuates the avoidance induced by that drug and those with similar neurochemical actions. To address this issue, following the determination of a dose of LSD that induced intermediate taste avoidance that developed gradually over conditioning in male Sprague-

Dawley rats (Experiment 1), a second set of subjects in Experiment 2 was exposed to fluoxetine (10 mg/kg) or vehicle every 4$^{th}$ day for a total of five injections prior to taste avoidance conditioning in which a novel saccharin solution was followed by 50 ug/kg LSD for a total of six trials. Subjects were then assessed over six sessions in which they were given saccharin but no LSD (i.e., extinction). All animals injected with LSD during conditioning acquired LSD-induced taste avoidance that was not affected by fluoxetine pre-exposure. Further, conditioned subjects extinguished the LSD-induced avoidance over extinction, again with no effect of pre-exposure. The failure to see an overall effect of LSD history on taste avoidance conditioning is consistent with the work of Becker et al. (2022) who reported that fluoxetine did not weaken LSD-induced nausea and argues that the effects seen with antidepressant history are task dependent. This failure to see an effect of fluoxetine on LSD is likely due to the non-overlapping receptor mediation of their aversive effects (fluoxetine - primarily 5-HT$_{2C}$ and LSD - primarily 5-HT$_{2A}$).

**Disclosures: R. Crupi:** None. **K. Jimenez:** None. **W. Shister:** None. **A.L. Riley:** None. **N. Sanel:** None. **M. Travaglia:** None.

**Poster**

**PSTR197: Hallucinogens: Neural Mechanisms of Action**

**Location:** WCC Halls A-C

**Time:** Monday, November 16, 2026, 1:00 PM - 5:00 PM

**Program #/Poster #:** PSTR197.05/HH18

**Topic:** H.08. Drugs of Abuse and Addiction

**Support:** UMD BBI Seed Grant
UMD MPower Award
NIH T32DC000046

**Title:** Serotonergic psychedelics alter sensory processing in mouse auditory cortex

**Authors:** K. J. DONALDSON, K. CHERKAS, N. K. GILL, J. THOMAS, J. W. PUTNAM, K. J. ALGUARD, ***N. A. FRANCIS**;
Univ. of Maryland, College Park, MD

**Abstract:** Psychedelics profoundly alter sensory perception, yet their effects on auditory processing remain poorly understood despite the central role of sound and music in psychedelic experience and therapy. Understanding these effects requires linking drug-induced changes across scales, from individual neurons to brain-wide networks, and determining whether psychedelics with distinct serotonergic receptor profiles produce different effects on auditory circuits. To investigate, we used a multiscale approach spanning receptor expression, neuronal activity, regional brain responses, and behavior. We compared serotonin 2A receptor gene (Htr2a) expression across layers of primary auditory cortex (A1), measured A1 layer 2/3 activity with two-photon calcium imaging during psilocybin and 2,5-dimethoxy-4-iodoamphetamine (DOI) treatment, used fMRI to compare psilocybin-induced activity in A1 and secondary auditory cortex (A2), and assessed auditory-motor gating behavior during DOI treatment. Allen

Brain Cell Atlas analysis showed that 48.9% of A1 cells were Htr2a-positive, with enrichment in layers 4 (68.7%), 2/3 (52.7%), and 5 (51.5%). Htr2a-positive proportions were higher in GABAergic than glutamatergic neurons (69.3% vs. 59.9%). In awake Thy1-GCaMP6s mice, A1 layer 2/3 excitatory neurons were imaged during pure-tone presentation in untreated (n=6), psilocybin-treated (n=8; 4 mg/kg), and DOI-treated (n=9; 4 mg/kg) cohorts. Psilocybin suppressed responses more than DOI, and the two drugs produced distinct changes in response adaptation, latency, frequency selectivity, variance, and functional connectivity, indicating broad, drug-specific modulation of auditory coding. At the regional scale, 9.4T fMRI in seven CBA mice under light dexmedetomidine/isoflurane anesthesia was performed before and after psilocybin treatment (4 mg/kg). Complex sounds evoked time-locked facilitative and suppressive responses in both A1 and A2, with psilocybin tending to increase facilitative and decrease suppressive voxel counts. Preliminary results also suggest increased functional connectivity. In auditory-motor gating experiments, DOI did not initially alter acoustic startle responses or prepulse inhibition (PPI; n=10) compared with saline-treated controls (n=12), but repeated testing after DOI revealed greater startle habituation and enhanced PPI associative learning. Ketanserin pretreatment (n=13) suppressed habituation and associative learning. Together, these results identify auditory cortex as an Htr2a-rich sensory circuit where serotonergic psychedelics reshape sensory processing, which may impact sound-guided behavior.

**Disclosures: K.J. Donaldson:** None. **K. Cherkas:** None. **N.K. Gill:** None. **J. Thomas:** None. **J.W. Putnam:** None. **K.J. Alguard:** None. **N.A. Francis:** None.

**Poster**

**PSTR197: Hallucinogens: Neural Mechanisms of Action**

**Location:** WCC Halls A-C

**Time:** Monday, November 16, 2026, 1:00 PM - 5:00 PM

**Program #/Poster #:** PSTR197.06/HH19

**Topic:** H.08. Drugs of Abuse and Addiction

**Title:** Discriminative Stimulus Properties of Psilocybin and Substituted Tryptamines on Mesolimbic Area

**Authors: *S. KANG**[1], D.-S. KANG[1], T.-Y. CHOI[2], M. OH[3], J. LEE[4], S. JEONG[5], Y. JEONG[7], K. KIM[8], C. LEE[9], S.-J. PARK[10], N. LIM[11], T. NA[12], B. LEE[13], J.-S. BAE[14], S. CHANG[15], J. KOO[6];
[1]Korea Brain Res. Inst., Daegu, Korea, Republic of; [2]Emotion, Cognition & Behavior Res. Group, Korea Brain Res. Inst. (KBRI), Daegu, Korea, Republic of; [3]Korea Brain Res. Inst. (KBRI), Deagu / Daegu-gwangyeoksi, Korea, Republic of; [5]Emotion, Cognitive, & Behavior Res. Group, [6]Emotion, Cognitive & Behavior Res. Group, [4]Korea Brain Res. Inst. (KBRI), Daegu, Korea, Republic of; [7]KBRI, Deagu, Korea, Republic of; [8]Content Mgmt. - AB 245, Ctr. for Cognition and Sociality, Daejeon, Korea, Republic of; [9]Inst. for Basic Sci., Daejeon, Korea, Republic of; [10]Ministry of Food and Drug Safety, Cheongju-si, Chungcheongbuk-do, Korea, Republic of; [11]Ministry of Food and Drug Safety, Cheongju, Chungcheongbuk-do, Korea, Republic of; [12]Ministry of Food and Drug Safety, Cheongju-si, Chungcheongbuk-do, Korea,

Republic of; [13]Univ. of Daegu Haany, Gyeongsan-si, Korea, Republic of; [14]Sch. of Med., Kyungpook Natl. Univ., Daegu, Korea, Republic of; [15]Daegu Haany Univ., Suseong-Gu Daegu, Korea, Republic of

**Abstract:** Substance Use Disorder (SUD) remains a critical global health issue shaped by complex biological, psychological, and environmental factors. Tryptamines, hallucinogenic compounds structurally related to serotonin, have gained attention due to their psychoactive properties and increasing presence in illicit drug markets. Although psilocybin is regarded as having low addictive potential, repeated use may still result in compulsive, reward-driven behaviors, and its precise impact on brain reward circuitry remains poorly understood. We examined the discriminative stimulus properties of psilocybin in mice and evaluated the substitution potential of synthetic tryptamines, including 4-OH-MET, 5-MeO-2-TMT, and 4-AcO-DALT, while assessing their influence on neural activity and neurotransmitter release in the nucleus accumbens (NAc). Drug discrimination assays revealed that 4-substituted tryptamines showed generalization or partial generalization to the psilocybin discriminative stimulus, whereas 5-MeO-2-TMT did not. Psilocybin and its 4-substituted analogs selectively reduced extracellular GABA levels in the NAc shell and elevated spontaneous firing rates of NAc neurons. Whole-cell patch-clamp recordings further demonstrated that psilocin selectively suppressed tonic, but not phasic, GABAergic currents in NAc medium spiny neurons. To investigate the causal role of NAc shell GABAergic tone in mediating the discriminative stimulus effects of psilocybin, muscimol (GABA-A agonist) and baclofen (GABA-B agonist) were microinfused into the NAc shell, which significantly attenuated psilocybin-appropriate discriminative responding. These findings suggest that psilocybin and its 4-substituted analogs promote NAc neuronal excitability by reducing tonic GABAergic inhibition, with NAc shell GABAergic tone playing a critical role in mediating their discriminative stimulus properties.

**Disclosures: S. Kang:** None. **D. Kang:** None. **T. Choi:** None. **M. Oh:** None. **J. Lee:** None. **S. Jeong:** None. **Y. jeong:** None. **K. Kim:** None. **C. Lee:** None. **S. Park:** None. **N. Lim:** None. **T. Na:** None. **B. Lee:** None. **J. Bae:** None. **S. Chang:** None. **J. Koo:** None.

**Poster**

**PSTR197: Hallucinogens: Neural Mechanisms of Action**

**Location:** WCC Halls A-C

**Time:** Monday, November 16, 2026, 1:00 PM - 5:00 PM

**Program #/Poster #:** PSTR197.07/HH20

**Topic:** A.07. Development of Neural Systems

**Title:** Psilocybin induces immediate-early gene expression in nucleus accumbens somatostatin interneurons

**Authors: A. DONG**[1], Z. XU[2], W. CHEN[3], Z. CHEN[3], *C. WANG[3];
[1]Sewickley Acad., Pittsburgh, PA; [2]Univ. of pittsburgh, Pittsburgh, PA; [3]Ctr. for Genomics, Loma Linda Univ., Loma Linda, CA

**Abstract:** Psilocybin has emerged as a promising therapeutic agent for emotional and motivational disorders. The nucleus accumbens (NAc) is a key brain region involved in regulating emotional and motivational response. Using single-nucleus RNA-sequencing (snRNA-seq), we investigated whether a single dose of psilocybin would activate interneurons in the mouse NAc, quantifying neuronal activation as an immediate-early-gene score. Of all sampled interneurons, somatostatin interneurons (SST-INs) were the dominant subtype, constituting ~86% of the total interneuron population. After psilocybin administration, SST-INs elevated gene expression of the activity markers *Fos* and *Egr1*. This activation was associated with serotonin receptor expression. Specifically, the interneurons that responded to psilocybin were mostly *Htr2c*-positive, and the *Htr2c*-positive interneurons were the ones that exhibited activation. These results suggest 5-HT2C as an entry point for SST-INs, a role that was previously believed to be mediated by 5-HT2A. Activated interneurons further up-regulated translation and neuropeptide programs while simultaneously down-regulating Gq/cAMP effectors and synaptic-scaffold genes. Notably, activated SST-INs upregulated *Penk*, the precursor of enkephalin, which is depleted in the NAc during stress and negative affective states. While 5-HT2C is recognized as an antidepressant target, NAc SST-N could act as a candidate cell type for psilocybin's benefits in depression and other emotional-motivational disorders. Together, these findings indicate 5-HT2C receptors on NAc interneurons as a potential target for psilocybin’s effects on emotional and motivational behaviors.

**Disclosures: A. Dong:** None. **Z. Xu:** None. **W. Chen:** None. **Z. Chen:** None. **C. Wang:** None.

**Poster**

**PSTR197: Hallucinogens: Neural Mechanisms of Action**

**Location:** WCC Halls A-C

**Time:** Monday, November 16, 2026, 1:00 PM - 5:00 PM

**Program #/Poster #:** PSTR197.08/HH21

**Topic:** H.08. Drugs of Abuse and Addiction

**Support:** JC Bose Fellowship Project (JCB/2021/000014)
Department of Atomic Energy, India

**Title:** Neural Circuit Mechanisms Underlying the Psychedelic-Induced Head-Twitch Response in Rodents

**Authors: *R. VURUPUTURI**[1], V. REGHUNATH[3], V. A. VAIDYA[2];
[1]Dept. of Biol. Sci., [2]Biol. Sci., Tata Inst. of Fundamental Res., Mumbai, India; [3]Dept. of Biol. Sci., Indian Inst. of Sci. Educ. and Research, Pune, MUMBAI, India

**Abstract:** The renewed interest in serotonergic psychedelics has led to major advances in understanding their cellular, molecular, and behavioral effects, while the mechanisms underlying these effects remain poorly understood. The serotonin 2A receptor (5-$HT_{2A}$R) is widely recognized as the principal mediator of the actions of classical psychedelics, including their hallucinogenic and therapeutic effects. However, the necessity of subjective hallucinatory

responses in humans for the therapeutic benefits is unresolved and is actively debated. In addition, the neural circuit mechanisms through which 5-$HT_{2A}$R signaling mediates these distinct behavioral outcomes remain to be elucidated. To address this gap, we systematically investigated the circuit mechanisms underlying the head twitch response (HTR) induced by the serotonergic psychedelic 2,5-dimethoxy-4-iodoamphetamine (DOI) in rodents. HTR, a stereotypical head-shake, is a well-characterised and a widely studied behavior, which serves as a reliable proxy for the hallucinatory activity of psychedelics and 5-$HT_{2A}$R activity. Using a combination of anatomical, pharmacological, and genetic approaches, including cell type-specific conditional knockout and rescue strategies, we examined the contribution of multiple 5-$HT_{2A}$R-expressing neuronal populations and circuits to DOI-induced head-twitch response. Our findings demonstrate that the prefrontal cortex (PFC) is not the primary driver of HTRs, challenging prevailing assumptions in the field. Furthermore, the ventral hippocampus, which is essential for the anxiolytic effects of DOI, does not initiate the HTR, revealing a circuit-level dissociation between distinct behavioral effects of psychedelics. Targeted infusions of DOI into the ventral hippocampus, motor cortex, and dorsolateral striatum similarly rule out these regions as the major contributors. Ongoing studies are investigating additional candidate regions, including the somatosensory cortex, and exploring the possibility that the HTR emerges from a distributed neural network rather than a single anatomical locus. Together, these findings reveal circuit-specific roles of 5-$HT_{2A}$R signaling in mediating distinct behavioral effects of serotonergic psychedelics and provide mechanistic insight into the neural substrates underlying psychedelic-induced behaviors.

**Disclosures: R. Vuruputuri:** None. **V. Reghunath:** None. **V.A. Vaidya:** None.

**Poster**

**PSTR197: Hallucinogens: Neural Mechanisms of Action**

**Location:** WCC Halls A-C

**Time:** Monday, November 16, 2026, 1:00 PM - 5:00 PM

**Program #/Poster #:** PSTR197.09/HH22

**Topic:** H.08. Drugs of Abuse and Addiction

**Support:** NIH Grant 1U01NS115587-01
JHU Discovery Grant

**Title:** Multi-region chronic Neuropixels recordings reveal psilocybin-induced network alterations

**Authors: *T. E. DEWEESE**[1,2], A. CHENG[2], S. KOUKUNTLA[2], A. R. GRAVES[3], A. CHARLES[2], K. L. TAMASHIRO[4], T. HARRIS[2,5];
[1]Cross-Disciplinary Program in Grad. Biomed. Sci., [2]Biomed. Engin., [3]Neurosci., [4]Dept of Psychiatry & Behavioral Sci., Johns Hopkins Univ., Baltimore, MD; [5]HHMI Janelia Res. Campus, Ashburn, VA

**Abstract:** An estimated 40 million Americans suffer from depression, 12 million of whom are resistant to traditional antidepressants. Psychedelics offer a novel approach to treating psychiatric disorders, including severe depression and post-traumatic stress disorder (PTSD). Unlike conventional antidepressants, psychedelics produce rapid and long-lasting therapeutic effects after a single dose. However, despite immense clinical potential, a mechanistic understanding of how psychedelics reconfigure neural networks across the brain to alter cognition and emotional state remains elusive. Here, we investigated how psilocybin alters large-scale neural dynamics across multiple brain regions. We performed long-term, high-density in vivo electrophysiology using multiple chronically implanted Neuropixels probes in head-fixed, adult C57BL/6 mice, across medial prefrontal cortex, thalamus, and ventral hippocampus (n=12). This approach enabled us to track and correlate changes in brain-wide activity over a 10-day period following a single dose of psilocybin. Each animal served as its own baseline saline control, receiving either a subcutaneous injection of psilocybin (1 m/kg) or a saline vehicle control. We found that psilocybin suppresses neural activity brain-wide in a highly cell-type and region-specific manner. Beyond broad suppression, psilocybin significantly alters both local and global functional connectivity. These results demonstrate that psilocybin does not simply cause global suppression or desynchronization of the brain, but rather actively restructures functional neural connectivity. Ultimately, these findings provide critical insights into the long-term network-level mechanisms that underlie the unique, durable therapeutic actions of psychedelic compounds.

**Disclosures: T.E. DeWeese:** None. **A. Cheng:** None. **S. Koukuntla:** None. **A.R. Graves:** None. **A. Charles:** None. **K.L. Tamashiro:** None. **T. Harris:** None.

**Poster**

**PSTR197: Hallucinogens: Neural Mechanisms of Action**

**Location:** WCC Halls A-C

**Time:** Monday, November 16, 2026, 1:00 PM - 5:00 PM

**Program #/Poster #:** PSTR197.10/HH23

**Topic:** H.08. Drugs of Abuse and Addiction

**Support:** R01 MH136708
R01 DA061433

**Title:** Effects of psilocybin on cognitive flexibility in rats

**Authors: *J. HENNESSEY**[1], B. KURTOGLU[1], D. R. OLIVEIRA, Sr.[2], J. MCCORVY[3], J. R. MANTSCH[1];
[1]Pharmacol. and Toxicology, [3]Cell Biology, Neurobiology, and Anat., [2]Med. Col. of Wisconsin, Milwaukee, WI

**Abstract:** Rationale: Cognitive flexibility is known to be impaired across a variety of neuropsychiatric diseases and promotion of cognitive flexibility has been proposed as a transdiagnostic therapeutic mechanism of psychedelic-assisted therapy. However, the exact subtypes of cognitive flexibility and time scale on which this occurs is unknown and preclinical

studies have shown conflicting results. We sought to use different models of cognitive flexibility to see how each is affected by psilocybin treatment through time.Methods: Adult male and female Sprague-Dawley rats (8-10 weeks old upon arrival) were trained to perform cognitive flexibility tasks in an operant chamber. First, a within-session continuous attentional set-shifting task was used to assay the effects of psilocybin (1 mg/kg, i.p.) on familiar attentional set-shifts acutely (20 min.) and after 24h. Then, a novel set-shifting task was used, and trials to criterion on a novel set-shift was assayed 20min., 24h, and 5d after psilocybin. Finally, trials to criterion in a reversal learning task was measured in these same rats 24h or 72h after psilocybin. Results: Acute psilocybin significantly increased omissions and latency to respond in all tasks and did not promote performance over saline on familiar set-shifts at either time point. In novel set-shifts, acute performance was not affected while there was a trend toward improved performance at later time points. Performance on reminder trials of a previously learned rule was impaired by acute psilocybin. Finally, there was a significant reduction in trials to criterion in reversal learning at both time points.Conclusions: Psilocybin has selective effects for certain subtypes of cognitive flexibility and its effects on cognitive flexibility vary with time; acute psilocybin did not promote cognitive flexibility in any task in our hands, in contrast to other reports. In all tasks, acute psilocybin impaired operant responding and previous rule recall.

**Disclosures: J. Hennessey:** None. **B. Kurtoglu:** None. **D.R. Oliveira:** None. **J. McCorvy:** None. **J.R. Mantsch:** None.

**Poster**

**PSTR197: Hallucinogens: Neural Mechanisms of Action**

**Location:** WCC Halls A-C

**Time:** Monday, November 16, 2026, 1:00 PM - 5:00 PM

**Program #/Poster #:** PSTR197.11/HH24

**Topic:** H.08. Drugs of Abuse and Addiction

**Support:** F31DA066218
DPI DA051608

**Title:** Restoring cognitive flexibility after adolescent cocaine exposure using psilocybin

**Authors: *J. BENVILLE**[1], H. LO[1], D. TRAN[1], K. HANIN[1], R. BATISTA-BRITO[1], L. L. SJULSON[2];
[1]Dominick P. Purpura Dept. of Neurosci., [2]Dominick P. Purpura Dept. of Neurosci. and Dept. of Psychiatry and Behavioral Sci., Albert Einstein Col. of Med., Bronx, NY

**Abstract:** Background: Cocaine use disorder (CUD) has no FDA-approved biologically based treatments. Most individuals initiate cocaine use during adolescence, a critical period of medial prefrontal cortex (mPFC) development. Adolescent cocaine exposure (ACE) produces lasting mPFC dysfunction that impairs cognitive flexibility. These effects are not seen with adult exposure, highlighting adolescence as a window of vulnerability. Neural ensembles in the mPFC support flexible decision-making and may become locked into rigid states following ACE.

Psilocybin, a serotonergic psychedelic under investigation for substance use disorders, reopens a developmental critical period that may be beneficial in changing maladaptive behaviors, but whether it restores prefrontal function and cognitive flexibility after ACE is unknown.
Methods: We combined a head-fixed Go/No-Go reversal learning task, electrophysiology, and two-photon calcium imaging to investigate the long-term effects of ACE and the therapeutic potential of psilocybin. Three complementary approaches were used: (1) Neuropixels recordings to characterize ACE-induced alterations in mPFC neural dynamics outside of behavior, (2) behavioral assessment of reversal learning following ACE and psilocybin treatment, and (3) concurrent two-photon calcium imaging during behavior to identify neural ensemble activity associated with latent behavioral states and task performance.
Results: Neuropixels recordings revealed that ACE induces immature mPFC activity patterns in adulthood, including altered theta and gamma oscillatory dynamics and juvenile-like phase-locking profiles. ACE produced persistent deficits in cognitive flexibility, reflected by altered engagement during reversal learning. Psilocybin normalized reversal performance, restoring behavioral measures to control levels. Hidden Markov modeling identified three distinct latent behavioral states (engaged, biased, and disengaged), and psilocybin restored state occupancy to control levels during early reversal learning in ACE animals. Concurrent two-photon calcium imaging revealed stable mPFC ensemble activity during reversal learning, enabling identification of neural representations associated with task performance.
Conclusion: ACE produces persistent behavioral and neurophysiological immaturity in adulthood, disrupting adaptive state dynamics required for cognitive flexibility. Psilocybin restores behavioral state organization during reversal learning, suggesting its therapeutic effects may emerge through reorganization of prefrontal circuit function.

**Disclosures: J. Benville:** None. **H. Lo:** None. **D. Tran:** None. **K. Hanin:** None. **R. Batista-Brito:** None. **L.L. Sjulson:** None.

**Poster**

**PSTR197: Hallucinogens: Neural Mechanisms of Action**

**Location:** WCC Halls A-C

**Time:** Monday, November 16, 2026, 1:00 PM - 5:00 PM

**Program #/Poster #:** PSTR197.12/HH25

**Topic:** H.08. Drugs of Abuse and Addiction

**Title:** Dissecting psilocybin action from kinematic behavior to medial prefrontal cortex calcium dynamics across dose and time in mice

**Authors: *H. A. BAKER**[1], S. C. PIANTADOSI[2], A. ENGLISH[2], M. R. BRUCHAS[2], G. D. STUBER[2];
[1]Anesthesiology, Perioperative, and Pain Med., Stanford, Palo Alto, CA; [2]Anesthesiol. and Pain Med., Univ. of Washington, Seattle, WA

**Abstract:** Psilocybin induces a psychedelic state in humans characterized by profound subjective experiences that are poorly understood mechanistically. These behavioral phenotypes,

along with the global changes seen on brain-wide imaging, likely arise from a complex interplay of neurotransmitter systems and circuits that remain incompletely understood. Preclinical models allow multimodal integration of receptor pharmacology, circuit-level recording, and quantitative behavioral analysis. To that end, we have developed an integrative pipeline in mice using a linear track with high-fidelity pose tracking, 1-photon calcium imaging of medial prefrontal cortex dynamics in real-time during freely-moving behavior, and single-nucleus RNA sequencing. In 10-minute-long recording sessions after intraperitoneal injection of psilocybin, with doses spanning from 0 (saline) to 5 mg/kg in both male and female mice, we found dose-dependent reorganization of spontaneous movement across multiple kinematic parameters. Locomotor speed declined at 3 and 5 mg/kg, whereas postural kinematics and head-body coordination were altered at 1 mg/kg, even when mean speed was preserved. At 5 mg/kg, longer (2 hour) recordings showed acute locomotor suppression followed by partial recovery in a manner consistent with known pharmacokinetic parameters. MiniScope imaging in the linear track identified dose- and time-dependent changes in medial prefrontal cortex population activity after psilocybin administration, with lower and higher doses producing distinct temporal profiles. Additional imaging with selective serotonin agonists revealed related but non-identical effects, suggesting a multi-pathway convergence with psilocybin. Single nucleus RNA sequencing further showed transcriptional suppression at 5 mg/kg, especially in excitatory neurons. Together, these results connect psilocybin dose and time since administration to changes in locomotion, neural activity, and gene expression.

**Disclosures: H.A. Baker:** None. **S.C. Piantadosi:** None. **A. English:** None. **M.R. Bruchas:** None. **G.D. Stuber:** None.

**Poster**

**PSTR197: Hallucinogens: Neural Mechanisms of Action**

**Location:** WCC Halls A-C

**Time:** Monday, November 16, 2026, 1:00 PM - 5:00 PM

**Program #/Poster #:** PSTR197.13/HH26

**Topic:** H.08. Drugs of Abuse and Addiction

**Support:** ZIA DA000522

**Title:** Psychedelic-like effects of bufotenin are modulated by 5-$HT_{1A}$ receptor activity and breakdown by monoamine oxidase A

**Authors: *G. GLATFELTER**[1], N. GONZALEZ[1], M. H. BAUMANN[2];
[1]Designer Drug Res. Unit, Natl. Inst. on Drug Abuse Intramural Res. Program, Baltimore, MD;
[2]Designer Drug Res. Unit, IRP, NIDA, NIH, Baltimore, MD

**Abstract:** Tryptamine-based psychedelics induce psychoactive effects in humans and animals via actions at serotonin 2A receptors (5-$HT_{2A}$), but these compounds are generally non-selective. Bufotenin (5-hydroxy-*N*,*N*-dimethyltryptamine) is a naturally occurring 5-$HT_{2A}$ agonist that targets various serotonin receptors and other targets. Disparate accounts of the psychoactivity of

bufotenin have been reported in humans, along with variable psychedelic-like effects in rodent models. To address these inconsistencies, we examined the acute dose-related effects of subcutaneous bufotenin (0.03 - 30 mg/kg) on 5-$HT_{2A}$-mediated head twitch responses (HTRs), along with serotonin 1A (5-$HT_{1A}$)-mediated motor suppression (distance traveled) and body temperature decreases (°C) in C57BL/6J mice ($n$ = 4 - 6/ dose) over 60 min test sessions. Then, we tested the effects of bufotenin on the same endpoints after pretreatment with a 5-$HT_{1A}$ antagonist (WAY-100635, 3 mg/kg), a monoamine oxidase A inhibitor (clorgyline, 3 mg/kg), or their combination. On its own, bufotenin increased the number and rate of HTRs, but effects were limited to the first 5 - 10 min post drug administration. Further, bufotenin produced dose-related decreases in motor activity and body temperature from 1 - 30 mg/kg. Pretreatment with WAY100635, and its combination with clorgyline, elevated and extended the time-course for HTRs and blocked or attenuated locomotor suppression and hypothermic effects of 3 and 10 mg/kg bufotenin. In contrast, clorgyline pretreatment alone did not elevate HTR counts or effect duration, but did enhance motor suppression and hypothermic effects of bufotenin. Blocking 5-$HT_{1A}$ enhanced psychedelic-like effects of bufotenin, while the combined pretreatment with clorgyline extended the duration of these effects. Interestingly, clorgyline pretreatment on its own did not enhance psychedelic-like effects of bufotenin, suggesting that slowing bufotenin metabolism enhances its effects at non-5-$HT_{2A}$ receptor targets that inhibit HTR events. Overall, these results indicate that other serotonergic targets of bufotenin (i.e., 5-$HT_{1A}$) modulate its psychoactive potential in the HTR paradigm and these effects can be extended by inhibiting metabolism of the drug by monoamine oxidase A.

**Disclosures: G. Glatfelter:** None. **N. Gonzalez:** None. **M.H. Baumann:** None.

**Poster**

**PSTR197: Hallucinogens: Neural Mechanisms of Action**

**Location:** WCC Halls A-C

**Time:** Monday, November 16, 2026, 1:00 PM - 5:00 PM

**Program #/Poster #:** PSTR197.14/HH27

**Topic:** H.08. Drugs of Abuse and Addiction

**Support:** R01MH084894
T32-DA007027
FCT 2024.04513.BD

**Title:** Role of mGluR2 in Psychedelic Neural and Behavioral Plasticity

**Authors: *J. MALTMAN**[1,2], S. POTUKANUMA[1], M. FIORILLO[3], G. GABRIEL[1], J. SILVERMAN[4], S. SAHA[1], J. T. WOLSTENHOLME[2], J. GONZÁLEZ-MAESO[2];
[2]Pharm/Tox, [1]Virginia Commonwealth Univ., Richmond, VA; [3]Virginia Commonwealth Univ., Sandy Hook, VA, ; [4]Virginia Commonwealth Univ., Richmond, VA.

**Abstract: Rationale:** Psychedelics show promise for treating psychiatric and inflammatory diseases, but limited understanding of mechanisms underlying therapeutic versus hallucinogenic

effects restricts clinical use. Classical psychedelics such as psilocybin and lysergic acid diethylamide (LSD) produce hallucinogenic effects primarily through serotonin 2A receptor (5-$HT_{2A}$R) agonism, yet its role in therapeutic outcomes remains unclear. The metabotropic glutamate receptor 2 (mGluR2), an inhibitory G protein-coupled receptor, interacts with 5-$HT_{2A}$R through heteromerization and signaling crosstalk in frontal cortex (FC) pyramidal neurons (PNs). mGluR2s are also required for the psychedelic-induced head twitch response (HTR), a rodent measure of hallucinogenic potential. Despite this role in acute psychedelic signaling, its contribution to post-acute effects remains unknown. We investigated how mGluR2 influences post-acute behavioral and plasticity effects of psychedelics, including sex- and cell type-specific mechanisms.**Methods:** Studies used 2,5-dimethoxy-4-iodoamphetamine (DOI), selected for its high 5-$HT_2$ receptor specificity. Doses producing maximal HTR were administered (2 mg/kg males, 1 mg/kg females). Male and female wildtype (WT), global mGluR2 knockout (KO; 129S6/SvEv), and FC PN-specific conditional knockout mice (Emx1-Cre × $Grm2^{loxP/loxP}$; cKO; C57BL/6J) were assessed for HTR, anxiety-like behavior, locomotion, fear acquisition and extinction, and neuroplasticity. Dendritic spine density on FC PNs was quantified 24 h after DOI administration using HSV-GFP labeling. Western blotting confirmed reduced mGluR2 expression in FC, but not hippocampus, of cKO mice.**Results:** DOI significantly accelerated cued fear extinction in WT males but not females; this effect was absent in male cKO mice. Male cKOs and both sexes of global KOs exhibited reduced HTR, whereas female cKO mice displayed increased HTR relative to WT controls. Male cKOs also showed greater freezing during fear acquisition and expression and reduced basal locomotor activity. Significant effects of sex, genotype, spine type, and drug on FC-PN dendritic spine density indicated that DOI-induced structural plasticity in the FC is modulated by mGluR2 signaling in a sex-dependent manner.**Conclusions:** These findings identify a role for cortical pyramidal mGluR2 in regulating hallucinogenic and therapeutic-like effects of psychedelics and reveal sex differences. Understanding mGluR2-mediated mechanisms may guide development of next-generation psychedelic-inspired therapeutics with enhanced efficacy and reduced hallucinogenic liability.

**Disclosures: J. Maltman:** None. **S. Potukanuma:** None. **M. Fiorillo:** None. **J. Silverman:** None. **S. Saha:** None. **J.T. Wolstenholme:** None. **J. González-Maeso:** None.

**Poster**

**PSTR198: Cognitive and Neural Mechanisms of Attention in Humans**

**Location:** WCC Halls A-C

**Time:** Monday, November 16, 2026, 1:00 PM - 5:00 PM

**Program #/Poster #:** PSTR198.01/HH28

**Topic:** I.01. Attention

**Title:** Behavioral and neural changes during prolonged questionnaire responding

**Authors: *R. TAKAHASHI**[1], M. HAMAKAWA[3], C. T. Q. TRAN[1], J. ZHANG[1], H. KITAMURA[1], T. OKAMOTO[1,2];

[1]Grad. Sch. of Systems Life Sci., [2]Fac. of Arts and Sci., Kyushu Univ., Fukuoka City, Japan; [3]SSRI Co., Ltd., Tokyo, Japan

**Abstract:** Crowdsourced online questionnaires are widely used for large-scale surveys; however, prolonged questionnaire completion may induce cognitive and attentional changes associated with reduced response quality. Objective evaluation of such internal-state changes using physiological indicators remains limited. In this study, we examined behavioral and neural changes associated with prolonged questionnaire responding by evaluating behavioral performance and electroencephalographic (EEG) activity. To simulate a prolonged questionnaire environment under controlled laboratory conditions, we employed a within-subjects design with 29 participants (14 females, aged 18-26 years) who completed an approximately 30 to 40-minute computerized survey. The questionnaire consisted of three main components: a modified Stroop task, a recall task requiring topic-related information retrieval, and a set of burden-inducing questions. Each task type was repeated five to six times throughout the survey, with a different set of questions presented in each repetition. In addition, each task was preceded by a 20-second countdown period. Descriptive data showed response times per question block tended to decrease progressively from the start to the end of the questionnaire. Significant task-related changes in EEG amplitude were observed in alpha, beta, and gamma bands relative to rest. In contrast, during the countdown periods, significant changes were observed only in beta-band amplitude. Occipital alpha-band amplitude was suppressed midway through the questionnaire, suggesting increased attentional engagement during this time window. Furthermore, significant increases in beta and gamma-band amplitude were observed across multiple channels, suggesting increased cognitive processing demands. Notably, standard errors of EEG measures tended to increase toward the end of the questionnaire, whereas behavioral measures remained relatively stable. These observations may reflect individual differences in respondents' internal neural activity despite relatively uniform behavioral responses. Overall, the present findings indicate that EEG-derived electrophysiological measures can provide additional information about individual differences in internal states during prolonged questionnaire responding, which may not be evident from behavioral responses alone. These results support the potential utility of EEG-derived measures for informing the design and evaluation of prolonged questionnaire paradigms.

**Disclosures: R. Takahashi:** None. **M. Hamakawa:** None. **C.T.Q. Tran:** None. **J. Zhang:** None. **H. Kitamura:** None. **T. Okamoto:** None.

**Poster**

**PSTR198: Cognitive and Neural Mechanisms of Attention in Humans**

**Location:** WCC Halls A-C

**Time:** Monday, November 16, 2026, 1:00 PM - 5:00 PM

**Program #/Poster #:** PSTR198.02/HH29

**Topic:** I.01. Attention

**Support:** China Scholarship Council

**Title:** Investigating the effects of rTMS over the right posterior parietal cortex on the N2pc elicited by task-relevant and task-irrelevant fearful faces

**Authors: *C. YAN**[1], M. STEFANOU[2], C. CATMUR[1];
[1]Psychology, [2]Neuroimaging, King's Col. London, London, United Kingdom

**Abstract:** Emotional faces have been shown to elicit attentional shifts, as indexed by the N2pc component, when presented simultaneously with neutral faces, although such effects appear to depend on task relevance. The present study investigated the role of the right posterior parietal cortex (rPPC) in modulating the N2pc toward emotional faces using a combined Transcranial Magnetic Stimulation with simultaneous Electroencephalogram (TMS-EEG) approach. Forty participants completed both a task-relevant face position task and a task-irrelevant line direction task in a within-subject design. On each trial, a fearful and a neutral face with overlaid lines were presented simultaneously. Dual-pulse 10Hz rTMS was applied over the rPPC on each trial, starting 50 ms after stimulus onset, with vertex stimulation serving as a control condition. A 2 (face position: left, right) × 2 (task type: face position, line direction) × 2 (stimulation site: rPPC, vertex) repeated-measures ANOVA was conducted on reaction times. Behaviourally, a significant interaction between face position and stimulation site was observed, with a right-hemifield disadvantage (slower responses for fearful faces on the right than on the left) in the vertex condition. This asymmetry was attenuated following rPPC stimulation. EEG analyses are currently ongoing to examine whether disruption of the rPPC modulates the N2pc elicited by fearful faces.

**Disclosures: C. Yan:** None. **M. Stefanou:** None. **C. Catmur:** None.

**Poster**

**PSTR198: Cognitive and Neural Mechanisms of Attention in Humans**

**Location:** WCC Halls A-C

**Time:** Monday, November 16, 2026, 1:00 PM - 5:00 PM

**Program #/Poster #:** PSTR198.03/HH30

**Topic:** I.01. Attention

**Support:** RS-2024-00348130
RS-2025-02304581

**Title:** Cross-species comparison of neural and gaze responses during narrative-driven movie viewing

**Authors: *R. KIM**[1,2], H. WANG[4], Q. ZHU[5], J. HAN[6], K. HEO[2], E. HONG[3], M. FEILONG[7], Y. ZHANG[6], J. GUO[8], M. GOBBINI[9], J. V. HAXBY[6], W. VANDUFFEL[4], W. SHIM[3,2];
[2]Dept. of Intelligent Precision Healthcare Convergence, [3]Dept. of Biomed. Engin., [1]Sungkyunkwan Univ., Suwon, Korea, Republic of; [4]Dept. of Neurosciences, KU Leuven, Leuven, Belgium; [5]CEA DRF/JOLIOT/NEUROSPIN, CEA, Univ. Paris-Saclay, Gif-sur-Yvette Cedex, France; [6]Dept. of Psychological and Brain Sci., Dartmouth Col., Hanover, NH; [7]Dept. of

Psychology, Univ. of South Carolina, Columbia, SC; [8]Sch. of Behavioral and Brain Sci., UT Dallas, Richardson, TX; [9]Dept. of Med. and Surgical Sci., Univ. of Bologna, Bologna, Italy

**Abstract:** Macaques are a critical model for studying the human brain, yet recent findings suggest that anatomically homologous regions do not always exhibit functional equivalence across species. Moreover, direct functional comparisons of neural responses to complex, naturalistic stimuli remain limited. Here, we investigated how narrative context differentially shapes eye-brain coupling in humans and nonhuman primates. We collected fMRI and in-scanner eye-tracking data from humans and rhesus macaques as they watched the same narrative-driven documentary film. We hypothesized that human gaze would be modulated by top-down, narrative-driven attention, whereas macaque gaze would be driven more strongly by bottom-up sensory features. To analyze gaze and brain responses, we quantified narrative importance, reflecting story relevance and central-characters involvement, and low-level visual features of each scene using human annotations and automated video segmentation methods. Behavioral analyses revealed that humans rapidly and robustly fixated on the main character in scenes of high narrative importance, even after accounting for low-level visual features. In contrast, macaque gaze patterns were driven primarily by low-level visual features, showing little or no sensitivity to narrative importance. Mirroring this behavioral dissociation, voxel-wise encoding modeling showed that narrative importance explained significant variance in human default mode network (DMN) regions involved in narrative processing, whereas no such effects were observed in macaque cortex beyond visual areas. These findings suggest that human visual exploration during naturalistic viewing is shaped not only by sensory features but also by top-down narrative context, reflecting an active, meaning-oriented mode of visual processing that contrasts with the more bottom-up, sensory-driven gaze and neural responses observed in macaques.

**Disclosures: R. Kim:** None. **H. Wang:** None. **Q. Zhu:** None. **J. Han:** None. **K. Heo:** None. **E. Hong:** None. **M. Feilong:** None. **Y. Zhang:** None. **J. Guo:** None. **M. Gobbini:** None. **J.V. Haxby:** None. **W. Vanduffel:** None. **W. Shim:** None.

**Poster**

**PSTR198: Cognitive and Neural Mechanisms of Attention in Humans**

**Location:** WCC Halls A-C

**Time:** Monday, November 16, 2026, 1:00 PM - 5:00 PM

**Program #/Poster #:** PSTR198.05/HH32

**Topic:** I.01. Attention

**Support:** NINDS Grant R01NS021135
NIMH Conte Center P50MH109429

**Title:** A single cortical circuit implements fast and slow visual search

**Authors: *M. PAGNOTTA**[1], H. ZHUANG[3], K. SLAMA[1], K. D. LAXER[4], T. ENDESTAD[5], A.-K. SOLBAKK[6], J. J. LIN[7], R. T. KNIGHT[2];

[1]UC Berkeley, Berkeley, CA; [2]Psychology and Neurosci., UC Berkeley, el cerrito, CA; [3]Univ. of California, Berkeley, Emeryville, CA; [4]Neurosci., CPMC, San Francisco, CA; [5]Univ. of Oslo, Oslo, Norway; [6]Univ. of Oslo, Dept. of Psychology, Oslo, Norway; [7]Dept. of Neurol., Univ. of California, Davis, Sacramento, CA

**Abstract:** A foundational question in neuroscience is how the brain produces different behaviors from a fixed anatomical substrate. One account holds that cognitive flexibility requires distinct, dedicated circuits, selectively recruited by task demands. An alternative proposes that flexibility arises from dynamically reconfiguring the oscillatory coordination of a shared circuit. Visual search offers a decisive test: for four decades, the behavioral dissociation between feature ("Pop-out") and conjunction ("Search") search has been attributed to distinct cortical networks and distinct frequency bands of inter-areal coherence. Whether these search modes reflect segregated systems or a common architecture remains unresolved. To distinguish these possibilities, we recorded iEEG from 19 presurgical epilepsy patients (1,150 electrodes spanning occipital, parietal, frontal, premotor, and medial temporal cortex) during a visual search task. On each trial, participants identified a target among distractor stimuli. In the Search condition, the target shared its color with the distractors and was defined by a conjunction of features; in the Pop-out condition, the target differed from distractors by a single feature. We report four convergent findings. First, time-frequency analysis revealed the same oscillatory signatures in both conditions: broadband high-frequency activity (HFA; 70-150 Hz) increased while alpha/beta power suppressed, propagating through the same posterior-to-frontal cortical hierarchy, with no condition-specific frequency bands. Second, dynamic time warping showed that the Search neural trajectory is a temporally stretched version of the Pop-out trajectory. The degree of temporal stretching predicted individual differences in reaction time ($\rho$=0.75, p=0.0005), directly linking neural temporal dilation to behavioral slowing. Third, alpha-band (~8-10 Hz) inter-areal synchrony coordinated the same posterior cortical network in both conditions, with directed coupling shifting systematically between time windows in a manner consistent with temporal scaling of information flow. Fourth, alpha phase gated local high-frequency activity (70-150 Hz) at the same preferred phase in both conditions, demonstrating that the oscillatory machinery is shared across search modes; only the duration over which it is engaged differs. Together, these findings establish that cognitive flexibility in visual search arises not from switching between dedicated circuits, but from temporal scaling of a single alpha-coordinated architecture. The same neural hardware operates at different speeds.

**Disclosures: M. Pagnotta:** None. **H. Zhuang:** None. **K. Slama:** None. **K.D. Laxer:** None. **T. Endestad:** None. **A. Solbakk:** None. **J.J. Lin:** None. **R.T. Knight:** None.

**Poster**

**PSTR198: Cognitive and Neural Mechanisms of Attention in Humans**

**Location:** WCC Halls A-C

**Time:** Monday, November 16, 2026, 1:00 PM - 5:00 PM

**Program #/Poster #:** PSTR198.06/II1

**Topic:** I.01. Attention

**Support:** Fondecyt 1230383

**Title:** Beyond Oscillations: Aperiodic Brain Activity and Arousal Shape Sustained Attention

**Authors: *T. OSSANDON**[1], T. BOSCH[2], V. MEDEL[3];
[1]Pontificia Univ. Catolica De Chile, Santiago, Chile; [2]Pontificia Univ. Catolica de Chile, Santiago, Chile; [3]Psychiatry, Pontificia Univ. Católica de Chile, Santiago, Chile

**Abstract:** Brain rhythms do not occur on a flat spectral background. During cognitive engagement, oscillatory changes are embedded within broadband shifts of aperiodic brain activity, making it difficult to determine whether spectral effects reflect rhythmic coordination or changes in cortical state. Here, we used high-density EEG and pupillometry during a multiple object tracking (MOT) task to test whether separating periodic and aperiodic activity reveals distinct physiological components of sustained attention.Forty healthy adults performed an MOT task with parametrically varied attentional load (2-4 targets). Pupil diameter was recorded continuously as an index of arousal. EEG spectra were analyzed using time-resolved spectral parameterization, allowing separation of the aperiodic 1/f component from oscillatory activity. For each participant, we estimated load-dependent changes in theta power, aperiodic exponent, and pupil diameter, and related these measures to task accuracy.Theta modulation became evident only after accounting for the aperiodic background. Traditional spectral analyses produced broader and less specific theta effects, whereas aperiodic correction revealed a clear load-dependent increase in frontal midline theta. This effect survived correction for multiple comparisons across electrodes ($qFDR < 0.05$), indicating that frontal theta associated with attentional control is partially obscured in raw spectral estimates. However, individual differences in theta modulation were not significantly related to accuracy ($r = 0.15$, $p = 0.554$).In contrast, aperiodic activity carried behavioral information about attentional state. The aperiodic exponent increased with load over frontolateral regions, and individual aperiodic responses predicted task accuracy ($r = 0.53$, $p = 0.0235$). Pupil dilation also increased with load and predicted performance ($r = 0.57$, $p = 0.0065$). Critically, the strongest behavioral association emerged when both measures were considered jointly: a combined index of pupil-linked arousal and aperiodic activity predicted accuracy better than either marker alone ($r = 0.66$, $p = 0.00396$).Together, these results suggest that sustained attention depends on the coordinated interaction of distinct physiological mechanisms. Theta activity indexes the recruitment of control networks, aperiodic activity reflects cortical state, and pupil-linked arousal captures neuromodulatory engagement. Separating these components reveals how rhythmic coordination, cortical state, and neuromodulation jointly support successful attentional performance.

**Disclosures: T. Ossandon:** None. **T. Bosch:** None. **V. Medel:** None.

**Poster**

**PSTR198: Cognitive and Neural Mechanisms of Attention in Humans**

**Location:** WCC Halls A-C

**Time:** Monday, November 16, 2026, 1:00 PM - 5:00 PM

**Program #/Poster #:** PSTR198.07/II2

**Topic:** I.01. Attention

**Title:** Hemispheric asymmetries in visual crowding

**Authors: *V. WISEMAN**[1], S. SHEREMATA[2], S. HONG[3];
[1]Florida Atlantic Univ. Neurosci. Grad. Program, Boca Raton, FL; [2]Dept. of Psychology, Northeastern Univ., Boston, MA; [3]Psychology, Florida Atlantic Univ., Boca Raton, FL

**Abstract:** Visual crowding reflects a fundamental limit of attention and occurs when a target that is easily identified in isolation becomes difficult to recognize when surrounded by distractors. Visual crowding studies have found a right visual field advantage, attributed to a reading bias, as language is left lateralized in the brain. Additionally, rightward visual field and hemispheric asymmetries have been reported in fMRI and EEG studies under high task demand in visual attention tasks, hypothesized to reflect the right intraparietal area dynamically allocating attentional resources across the visual field. While the role of attention in crowding is debated, prior work has yet to test whether the rightward visual field bias in crowding is due to spatial attention or language processing. We hypothesize that visual attention underlies crowding and is dynamically allocated under high task demand. However, neural data from non-language-related crowding stimuli are required to confirm this effect. Specifically, if attentional mechanisms contribute to crowding, then pre-cueing will modulate behavioral and neural effects. Furthermore, if attentional mechanisms are asymmetrically organized and flexibly allocate resources under increased load, then higher task demand (cue absence) should produce rightward visual-field and right-hemisphere biases.Our findings show that visual crowding is reliably modulated by attention at the behavioral level ($p < .001$) and engages a consistent contralateral selection, as indexed by the N2pc (Left target cue-present: $p = .0131$; Right target cue-present: $p = .0068$; Left target cue-absent: $p = .0013$; Right target cue-absent: $p = .0013$). However, no evidence for fixed hemispheric or rightward visual-field bias was present with non-language stimuli (Behavior: $p < .081$; N2pc: $p = .1197$). Alpha activity showed temporally and conditionally specific modulation rather than a sustained pattern, as a selective Cue × Hemisphere interaction ($p = .019$) emerged only in the N2pc-related time window (156-215ms), driven by cue-dependent hemispheric differences without consistent cue-present asymmetry (Cue Absent trials: $p = .023$; Cue Present trials: $p = .229$). We show that attentional mechanisms contribute to crowding, as pre-cues improved behavioral performance and reduced interference. Although attentional load influenced neural dynamics, there was no consistent evidence that cue absence produced rightward visual-field or right-hemisphere biases. Instead, effects were time-specific without stable hemispheric asymmetry, indicating flexible rather than systematically lateralized allocation of resources.

**Disclosures: V. Wiseman:** None. **S. Sheremata:** None. **S. Hong:** None.

**Poster**

**PSTR198: Cognitive and Neural Mechanisms of Attention in Humans**

**Location:** WCC Halls A-C

**Time:** Monday, November 16, 2026, 1:00 PM - 5:00 PM

**Program #/Poster #:** PSTR198.08/II3

**Topic:** I.01. Attention

**Support:** P50MH132642
RO1 EY017699
R01 MH137624

**Title:** Thalamocortical coupling supports attention under cue uncertainty

**Authors: *X. LIU**[1], X. LIU[3], S. KASTNER[2], M. J. ARCARO[4];
[1]Psychology, Princeton Univ., Princeton Junction, NJ; [2]Princeton Neurosci. Inst., Princeton Univ., Princeton, NJ; [4]Psychology, [3]Univ. of Pennsylvania, Philadelphia, PA

**Abstract:** Frontal and parietal networks support everyday behaviors that require integrating information and adapting as goals shift. These processes rely on flexible coordination across brain-wide cortical networks, yet how that coordination is achieved remains poorly understood. Through their widespread cortical connectivity, higher-order thalamic nuclei, including pulvinar (PUL) and mediodorsal nucleus (MD), are well positioned to perform such coordination. To test whether PUL and MD act as integrative hubs whose activity reflects a behaviorally relevant combination of the cortical areas they interconnect, 30 participants completed a novel fMRI task combining perceptual decision making and spatial attention. On each trial, participants maintained central fixation while two gratings were presented in the left and right peripheral visual fields. A central cue (a cloud of red and blue dots) indicated the likely target location with 80% validity, with uncertainty manipulated by varying color coherence. After a delay, a near-threshold orientation change appeared at one grating. Participants reported the change location, followed by a rating of their cue confidence on a 5pt scale. At rest, PUL and MD showed distinct thalamocortical coactivation profiles. Activity flow mapping revealed that these profiles predicted task-evoked cortical activation across task phases. PUL better predicted cue-related cortical responses, whereas MD better predicted delay-related responses. This intrinsic architecture suggests stable thalamocortical coupling across task epochs, but leaves open how brain activity is shaped by changing cognitive demands. To this end, we found that task-evoked activity was modulated by cue color coherence. At high coherence, a significant spatial attention effect emerged during delay periods in visual cortex and intraparietal sulcus, with greater activation contralateral to the cued location. This effect diminished as coherence decreased, paralleling the decline in the behavioral endogenous attention effect. During cue perception, prefrontal cortex, anterior cingulate cortex (ACC), anterior insula, and MD were negatively modulated by coherence. Individual differences in ACC modulation strength predicted those at MD, suggesting MD engages a broader frontal-MD circuit to track cognitive effort. Preliminary findings indicate that retrospective confidence rating positively modulated MD and dorsal PUL activity. Together, these findings point to a dual role of higher-order thalamus, evaluating the reliability of task-relevant sensory evidence while regulating cortical information transmission according to cognitive demand.

**Disclosures: X. Liu:** None. **X. Liu:** None. **S. Kastner:** None. **M.J. Arcaro:** None.

**Poster**

**PSTR198: Cognitive and Neural Mechanisms of Attention in Humans**

**Location:** WCC Halls A-C

**Time:** Monday, November 16, 2026, 1:00 PM - 5:00 PM

**Program #/Poster #:** PSTR198.09/II4

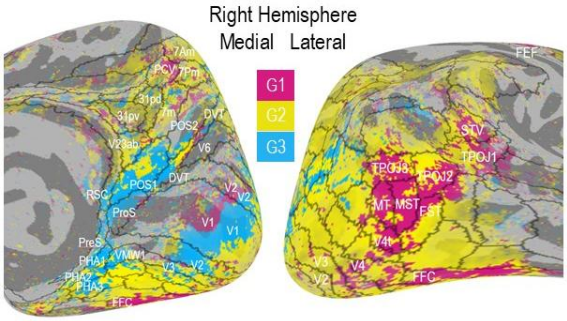
**Topic:** I.01. Attention

**Support:** JSPS KAKENHI JP23K17462
JSPS KAKENHI JP25H01145
Takeda Science Foundation

**Title:** Stacked encoding models reveal human cortical maps of three attention systems discovered in self-supervised Vision Transformers

**Authors: *T. YAMAMOTO**[1,2], S. KITAZAWA[1,3,4];
[1]Grad. Sch. of Medicine, Osaka Univ., Osaka, Japan; [2]Osaka Neurolog. Inst., Osaka, Japan; [3]Grad. Sch. of Frontier Biosciences, Osaka Univ., Osaka, Japan; [4]Ctr. for Information and Neural Networks (CiNet), Osaka, Japan

**Abstract:** Vision transformers (ViTs) trained by self-distillation with no labels (DINO) show attention maps similar to human gaze. We found that class-token attention heads in DINO ViTs form three groups: G1, focusing on the figure center; G2, covering the whole figure; and G3, sampling the background. We asked whether these systems have neural correlates in human cortex.We analyzed the Natural Scenes Dataset, with 7T fMRI responses to 9,000-10,000 natural images from each of 8 participants. We extracted G1, G2, and G3 features from DINO ViTs, fitted ridge models, and combined predictions by voxelwise stacking to map each system.G1 provided the most striking finding. Although the stimuli were still images, G1-related predictions were strongest in lateral motion-related cortex, including V4t, MT, MST, FST, and TPOJ2/3, where correlations reached r = 0.5-0.6. G1 also appeared around ~4° eccentricity in V1 and reached lateral intraparietal cortex and frontal eye field (FEF) despite fixation. These results suggest that G1 may predict how the attended object is likely to move next and where covert attention should be allocated. Separately, G1 extended into static object/face-related cortex, including V4 and fusiform face complex (FFC), suggesting representation of the selected object.G3 extended from peripheral V1/V2/V3 into medial scene- and background-related cortex, including POS1, ProS, retrosplenial cortex (RSC), parahippocampal region, and precuneus. In the precuneus, G1, G2, and G3 coexisted, consistent with representing a figure relative to the ground. Between lateral G1 and medial G3, G2 occupied a broad territory, consistent with a figure-wide representation distinct from figure-center selection and background coding.Thus, self-supervised artificial attention provides a route to discovering organizing principles of the human visual brain. The G1/G2/G3 framework extends the classical figure-ground dichotomy to a three-component architecture and links covert target selection, attended-object motion prediction, and background-centered coordinates.




**Disclosures: T. Yamamoto:** A. Employment/Salary (full or part-time):; Osaka Neurological Institute. **S. Kitazawa:** None.

**Poster**

**PSTR198: Cognitive and Neural Mechanisms of Attention in Humans**

**Location:** WCC Halls A-C

**Time:** Monday, November 16, 2026, 1:00 PM - 5:00 PM

**Program #/Poster #:** PSTR198.10/II5

**Topic:** I.01. Attention

**Support:** RS-2025-00522357

**Title:** Class-conditional ERP shift alignment improves single-trial decoding in a P300-based BCI

**Authors: *J. KIM**, S.-P. KIM;
Dept. of Biomed. Engineering, UNIST, Ulsan Natl. Inst. of Sci. and Technol., Ulsan, Korea, Republic of

**Abstract:** P300-based brain-computer interfaces usually require repeated stimulus presentations to obtain reliable selections. Although repetition improves final decision accuracy by averaging or accumulating evidence, it also slows communication and may obscure how single-trial neural evidence changes across repetitions. We asked whether repetition-dependent ERP changes can be characterized from the perspective of a decoder, and whether later repetitions can be used as training-time information to improve first-presentation decoding without requiring repeated test-time stimulation. We analyzed single-trial EEG from a P300-based BCI dataset using block-wise train/test splits. First, we quantified how target and non-target ERPs changed across stimulus repetitions and how these changes affected linear decoding geometry. We then applied a class-conditional ERP shift-alignment procedure: for each class, round-to-round ERP differences were estimated from the training data and used to transform later-round training trials toward the first-presentation feature space. Decoders were then tested only on first-presentation trials. To avoid inflation from candidate imbalance, performance was evaluated using candidate-balanced macro accuracy, with additional negative controls using global, swapped-class, and sign-flipped shifts. First-presentation decoding was substantially improved by class-conditional shift alignment.

Under the primary linear SVM analysis, candidate-balanced macro accuracy increased by approximately 9.7 percentage points relative to the unshifted first-presentation baseline. The effect replicated with logistic regression and was smaller but directionally consistent with diagonal LDA. Negative controls did not reproduce the improvement: global shifts provided little benefit, whereas swapped-class or sign-flipped shifts impaired performance. Mechanistic analyses showed that the beneficial shift was not localized to a single canonical P300 channel or time window. Instead, the improvement depended on distributed time-by-channel structure, especially outside Pz, and was aligned with the decoder's class-separating direction. These results suggest that repeated P300 stimulation does more than simply increase signal-to-noise ratio for averaging. Later repetitions reveal class-conditional changes in ERP geometry that can be used as privileged training information to improve first-presentation decoding. This approach may help reduce repetition requirements in P300-based BCIs while providing a decoder-centered account of how ERP responses evolve across repeated target detection.

**Disclosures: J. Kim:** None. **S. Kim:** None.

**Poster**

**PSTR198: Cognitive and Neural Mechanisms of Attention in Humans**

**Location:** WCC Halls A-C

**Time:** Monday, November 16, 2026, 1:00 PM - 5:00 PM

**Program #/Poster #:** PSTR198.11/II6

**Topic:** I.01. Attention

**Title:** Arousal attenuates rhythmic attentional sampling

**Authors: *O. R. CHRISTIANO**[1,2], M. MOROZ[1,2], R. F. HELFRICH[1,2,3];
[1]Psychology, [2]Wu Tsai Inst., [3]Interdepartmental Neurosci. Program, Yale Univ., New Haven, CT

**Abstract:** An emerging body of work suggests that sustained attention is not continuous, but samples visual space in discrete cycles, producing periodic fluctuations in perceptual sensitivity in the theta frequency range (~3-8 Hz). Moreover, attentional processing fluctuates on multiple timescales. Such fluctuations depend, in part, on physiological arousal, which is thought to alter the efficiency and stability of attentional control. While converging evidence indicates that arousal dynamics comprise a major source of variability in sustained attentional performance, it remains unclear whether arousal modulates rhythmic attentional sampling. If theta rhythmicity actively serves attention, it should intensify under high arousal as the brain exploits a useful computational strategy. If it reflects an inherent constraint of the neural architecture, high arousal should attenuate rhythmic sampling as perception becomes more continuous. Here, we test these opposing accounts by examining whether pre-stimulus arousal state, indexed by pupil diameter, modulates subsequent attentional sampling behavior, and whether such modulations are accompanied by differences in ongoing neural activity measured via MEG. First, we show that the magnitude and stability of theta-rhythmic fluctuations in reaction time vary as a function of arousal level, with high-arousal states associated with faster reaction times, reduced power, and lower reaction-time variability than low-arousal states. We then replicate these behavioral

patterns in a second experiment, and characterize arousal-dependent differences in oscillatory, aperiodic, and evoked neural activity accompanying attentional sampling behavior. Taken together, these results suggest that rhythmic attentional sampling is not fixed, but varies as a function of ongoing arousal state and its associated neural dynamics. More broadly, these findings identify arousal as a key source of variability in the temporal dynamics of attention, linking classical theories of arousal to contemporary models of rhythmic attentional sampling.

**Disclosures: O.R. Christiano:** None. **M. Moroz:** None. **R.F. Helfrich:** None.

**Poster**

**PSTR198: Cognitive and Neural Mechanisms of Attention in Humans**

**Location:** WCC Halls A-C

**Time:** Monday, November 16, 2026, 1:00 PM - 5:00 PM

**Program #/Poster #:** PSTR198.12/II7

**Topic:** I.01. Attention

**Title:** The Level of Attentional Engagement During Rapid Serial Visual Presentation Modulates Incidental Visual Memory for Stream Content

**Authors: *L. QUINN**[1], A. KIMATA[1], W. F. ASAAD[2];
[1]Dept. of Neuroscience, Brown Univ., Providence, RI; [2]Neurosurg., Brown Univ., Westwood, MA

**Abstract:** Rapid serial visual presentation (RSVP) paradigms have been widely used to characterize the limits of visual attention in rapidly changing, visually dense environments, yet less is known about how overall attentional engagement during target identification influences incidental memory for surrounding stream content. Here, we employed a modified RSVP paradigm in which subjects (n=52) were asked to identify and report a cued target within a 10-image stream. Following target response, subjects then reported whether they saw the probe image (non-cue, non-target image from the 10-image RSVP stream). Both the target image and probe image were randomly interleaved across trials. All subjects performed above chance (16.7%) on target identification, while the identification of the probe image proved considerably more difficult for participants. Bayesian logistic regression analyses revealed that correct target identification was associated with a modest but reliable increase in probe image recall accuracy ($\beta = 0.125$, 95% HDI [0.038, 0.218], OR = 1.13, pd = 0.997). Interestingly, the probe image position relative to the cued target did not differentially modulate correct recall performance ($\beta = -0.005$, 95% HDI [-0.023, 0.013], OR = 0.995, pd = 0.720), suggesting that probe recall was not driven by temporal proximity to the target acquisition window. Together, these findings suggest that trials in which the target was correctly identified may have higher overall attentional engagement, supporting the idea that attentional engagement facilitates incidental memory for surrounding stream content.

**Disclosures: L. Quinn:** None. **A. Kimata:** None. **W.F. Asaad:** None.

**Poster**

**PSTR198: Cognitive and Neural Mechanisms of Attention in Humans**

**Location:** WCC Halls A-C

**Time:** Monday, November 16, 2026, 1:00 PM - 5:00 PM

**Program #/Poster #:** PSTR198.13/II8

**Topic:** I.01. Attention

**Support:** U.S. National Institute of Mental Health Award R21MH129630
U.S. National Science Foundation Graduate Research Fellowship Program

**Title:** Capturing spontaneous thoughts at rest using real-time fMRI-triggered experience sampling

**Authors: *T. BOUNYARITH**, D. BRAUN, A. KUCYI;
Psychological and Brain Sci., Drexel Univ., Philadelphia, PA

**Abstract:** Much of mental life is characterized by spontaneous thoughts that occur independently of external stimuli. The neural correlates of spontaneous thought have traditionally been studied using random-onset experience sampling, in which thought probes that ask participants to report their ongoing mental experiences are delivered at random time intervals during neuroimaging. A major limitation of random-onset experience sampling is that it is not time-precise or targeted in its delivery of thought probes. To address this limitation, we developed and validated a novel paradigm called real-time fMRI-triggered experience sampling (rt-fMRI-ES) in which a set of thought probes are presented to participants based on increased ongoing blood-oxygen-level-dependent (BOLD) activity. In our pre-registered, proof-of-concept study, healthy adults (N=60) completed six 8-minute runs of rt-fMRI-ES using two run-counterbalanced regions of interest (ROIs): (1) the dorsal anterior insular cortex (daIC), implicated in high physiological arousal; and (2) the posteromedial cortex (PMC), implicated in internally-guided mental experiences. In addition to the two brain-triggered trial types, experience sampling trials were presented after a 100-second refractory period ("time-out" trials). We pre-registered two hypotheses: (H1) Ratings of ongoing arousal would be significantly higher for trials triggered by increased daIC activity compared to other trial types; and (H2) Ratings of external-attention to a visual fixation cross would be significantly lower for trials triggered by increased PMC activity compared to other trial types. After applying pre-registered exclusion criteria, 42 participants (1243 total trials) and 49 participants (1429 total trials) were included in H1 and H2 analyses, respectively. Contrary to H1, there was no significant difference between trials triggered by increased daIC activity and other trial types, building upon growing evidence for a discordance between physiological arousal and subjective affective arousal. We found evidence in support of H2, as external-attention ratings were significantly lower for trials triggered by PMC activation compared to other trial types. However, exploratory secondary analyses revealed a stronger significant effect of PMC-triggering on capturing higher perseverative thinking, based on a multi-dimensional composite of ratings for multiple thought probes. Taken together, we successfully demonstrated that rt-fMRI-ES is capable of efficiently capturing spontaneous thoughts of interest based on real-time estimates of ongoing neural activity.

**Disclosures: T. Bounyarith:** None. **D. Braun:** None. **A. Kucyi:** None.

**Poster**

**PSTR198: Cognitive and Neural Mechanisms of Attention in Humans**

**Location:** WCC Halls A-C

**Time:** Monday, November 16, 2026, 1:00 PM - 5:00 PM

**Program #/Poster #:** PSTR198.14/II9

**Topic:** I.01. Attention

**Support:** NIH R01-EY035300

**Title:** Attentional capture depends on the interaction between task-relevance of both feature and spatial location of distracting stimulus

**Authors: *S. E. PURNELL**[1], D. D. THAYER[3], T. C. SPRAGUE[2];
[2]Psychological and Brain Sci., [1]UC Santa Barbara, Goleta, CA; [3]Univ. of California, Santa Barbara, Goleta, CA

**Abstract:** In highly variable environments, selectively attending to relevant stimulus features and locations is necessary to guide behavior. Restricting attention to task-relevant locations can enhance stimulus processing at attended locations and reduce the influence of stimuli at unattended locations (Kastner et al., 1999). Evidence suggests that visual search is supported by a priority map that integrates salience and relevance signals from feature-selective 'feature dimension maps', which individually index the relative importance of stimuli based on stimulus feature(s) and task demands, respectively (Thayer & Sprague, 2023; 2025). However, it is unclear how saliency signals from different visual feature dimensions (e.g., color, motion, shape) combine to influence attentional priority, as spatial attention may differentially affect interference from task-irrelevant color- and motion-defined distractors (Leonard et al., 2015; Liu & Mance, 2011). To test this, we had participants covertly search an 8-item array for a unique target item in a predefined feature dimension (e.g., color, motion, shape) and report the orientation of a line (horizontal or vertical) overlaid on the target. On most trials, a valid, central cue indicated the relevant hemifield of the search array where the target would appear (top, left, bottom, right; 4 of 8 items; 100% validity). On half of all trials, a singleton distractor in a task-irrelevant feature dimension (e.g., motion target and color distractor) appeared, equally split between appearing within vs outside the cued hemifield. Singleton distractors were operationalized as values with maximum stimulus contrast: exact opposite color or shape along a 360-degree feature space (Li et al., 2020) and perpendicular motion (Chetverikov & Jehee, 2023). Cueing task-relevant locations reduced interference from singleton distractors outside attended regions, however this differed across target- and distractor-defined feature dimensions. Specifically, color was a strongly distracting feature and spatial cues attenuated interference, while motion and shape distractors did not disrupt visual search. These results indicate that top-down spatial attention may lessen interference from distractors to guide visual search, but the effectiveness of spatial attention may differ based on the feature dimensions defining distraction. This motivates future studies on the neural mechanisms mediating computations of attentional

priority within and across feature dimensions, and how these mechanisms sculpt neural representations in feature-selective regions of the cortex.

**Disclosures: S.E. Purnell:** None. **D.D. Thayer:** None. **T.C. Sprague:** None.

**Poster**

**PSTR198: Cognitive and Neural Mechanisms of Attention in Humans**

**Location:** WCC Halls A-C

**Time:** Monday, November 16, 2026, 1:00 PM - 5:00 PM

**Program #/Poster #:** PSTR198.15/II10

**Topic:** I.01. Attention

**Title:** Transcranial random noise stimulation reduces behavioral and electrophysiological attentional bias to negative facial stimuli

**Authors: *R. KANAZAWA**[1], H. AOKI[2], D. SAWAMURA[3], Y. ONO[4];
[1]Meiji Univ. Grad. Sch., Setagaya-ku, Japan; [2]Meiji Univ. Grad. Sch., Kanagawa, Japan;
[3]Hokkaido Univ., Sapporo, Japan; [4]Meiji Univ., Kanagawa, Japan

**Abstract:** Attentional bias refers to preferential attention toward negative emotional stimuli, impairing cognitive control. This study investigated the modulatory effects of high-frequency transcranial random noise stimulation (tRNS) over the left dorsolateral prefrontal cortex on attentional bias. Twenty healthy adults performed an emotional Stroop task using angry, disgusted, and neutral facial expressions during simultaneous EEG recording and tRNS or sham stimulation. Seven participants exhibited attentional bias, defined by prolonged reaction time (RT) to negative versus neutral faces during sham stimulation. In this biased subgroup, baseline accuracy for negative faces did not significantly differ from that for neutral faces during sham stimulation. tRNS ameliorated attentional bias by significantly increasing accuracy for disgusted faces (87.4% to 90.2%, $p = 0.042$), whereas RT and accuracy for angry faces remained unchanged. Event-related potential analyses showed that tRNS reduced the face-related N170 amplitude bias, defined as the difference in N170 amplitude relative to neutral-face condition, for both emotional faces at the left parieto-occipital region (P7). Furthermore, tRNS-induced changes in N170 amplitude bias were positively correlated with changes in RT bias in occipito-central regions (disgusted-face condition: $r = 0.827$ at POz; angry-face condition: $r = 0.860$ at O2 and $r = 0.824$ at Cz) and negatively correlated with those in the right parietal region (disgusted-face condition: $r = -0.782$ at P4). Conversely, in participants who did not exhibit RT delays for negative faces ($n = 13$), tRNS significantly altered the N170 amplitude bias specifically for angry faces at CPz. However, this neural modulation did not translate into behavioral benefits, as no significant tRNS-related changes were observed in RT, accuracy, or the relationship between neural and behavioral changes in this subgroup. These findings suggest that, although tRNS broadly modulates early visual processing, its behavioral benefits are specific to individuals with baseline attentional bias. Opposite correlations between tRNS-induced N170 modulation and RT bias changes across occipito-central and right parietal regions suggest distinct neural mechanisms for the attenuation of emotional interference.

**Disclosures: R. Kanazawa:** None. **H. Aoki:** None. **D. Sawamura:** None. **Y. Ono:** None.

**Poster**

**PSTR198: Cognitive and Neural Mechanisms of Attention in Humans**

**Location:** WCC Halls A-C

**Time:** Monday, November 16, 2026, 1:00 PM - 5:00 PM

**Program #/Poster #:** PSTR198.16/II11

**Topic:** I.01. Attention

**Support:** RRID:SCR_024556

**Title:** Straddling attention between items in short-term and long-term memory

**Authors: *W. NARHI-MARTINEZ**, K. CHIU, A. C. NOBRE;
Dept. of Psychology, Yale Univ., New Haven, CT

**Abstract:** Many contexts in daily life are associated with both working/short-term memory (STM) and long-term memory (LTM) content. We sought to understand how attention operates when directed to content from one versus both of these internal domains. For LTM, participants learned the identities and locations of two objects within various scenes. The next day, the same scenes appeared with two new objects encoded into STM. At the end of the trial, participants made a decision about an item associated with the scene, either in STM or LTM. However, before the response stage, a retrocue could indicate which side the upcoming target had previously been located within the scene, from either STM or LTM. Experiment 1 ($N = 32$) revealed significant performance benefits of attention for both STM and LTM targets. Experiment 2 ($N = 32$) showed that performance for LTM targets was impaired when retrocues prioritized items from both domains compared to when contents from only LTM were prioritized. Neuroimaging results from Experiment 3 ($N = 26$) indicated dorsal frontoparietal regions exhibited significant increases in activation when participants were cued to combined STM and LTM contents, compared to when they were cued to contents purely from STM or LTM. Together, these findings reveal that internal attention can be effectively guided to contextually associated content across domains, but that straddling attention to items across these domains has differential behavioral and neural consequences compared to attending to items from only one domain.

**Disclosures: W. Narhi-Martinez:** None. **K. Chiu:** None. **A.C. Nobre:** None.

**Poster**

**PSTR198: Cognitive and Neural Mechanisms of Attention in Humans**

**Location:** WCC Halls A-C

**Time:** Monday, November 16, 2026, 1:00 PM - 5:00 PM

**Program #/Poster #:** PSTR198.17/II12

**Topic:** I.01. Attention

**Title:** The Fully Engaged Brain: Electrophysiological Correlates of Flow State

**Authors:** E. D'ENTREMONT, D. HENDERSON, A. WALKER, A. KIRWIN, F. SCHAUER, C. NGUYEN, E. MCGOVERN, ***G. SHEN**;
Psychology, Rutgers Univ., Camden, NJ

**Abstract:** Flow state is characterized with high level of control, concentration and rewards, as well as reduced level of self-referential thoughts and worrying. It is usually experienced during creative and automatic tasks, or during engaging daily activities under optimal conditions. The positive effects of flow state on task performances and psychological well-being attracted a vast body of research in recent years, but the neural mechanism is poorly understood. In this EEG study, we simulated real-life-like conditions of flow state using popular video games on tablets. EEG data were recorded while subjects underwent three conditions: Flow State (an engaging video game with self-adjusted difficulty level), Overload (an overly frustrating and difficult game), and Resting State (viewing a silent video of abstract slow-moving stars). One game ("Free Flow") was selected for flow station condition, based on the scores of the Flow State Scale (FSS) questionnaires obtained during the pilot test. The order of conditions was randomized, and each lasted 5 minutes followed by FSS survey. The results showed increased theta-band activity and reduced alpha power in frontal and parietal regions during Flow and Overload conditions, compared to Resting State. In individuals with high FSS scores, Flow State condition induced stronger frontal theta activity than Overload or Resting conditions. The findings provide insights into the electrophysiology of being fully engaged, and highlight the potential application of EEG in studying real-world flow experiences and their implications for learning and well-being.

**Disclosures: E. D'Entremont:** None. **D. Henderson:** None. **A. Walker:** None. **A. Kirwin:** None. **F. Schauer:** None. **C. Nguyen:** None. **E. McGovern:** None. **G. Shen:** None.

**Poster**

**PSTR198: Cognitive and Neural Mechanisms of Attention in Humans**

**Location:** WCC Halls A-C

**Time:** Monday, November 16, 2026, 1:00 PM - 5:00 PM

**Program #/Poster #:** PSTR198.18/II13

**Topic:** I.01. Attention

**Support:** PAPIIT-UNAM #IN221724

**Title:** Cognitive reserve predicts suppression of irrelevant information during working memory performance

**Authors:** ***E. LÓPEZ-GONZÁLEZ**[1], U. CABALLERO SANCHEZ[3], T. V. ROMAN-LOPEZ[4], E. DE HARO HERNÁNDEZ[1], S. HERNÁNDEZ-MÁRQUEZ[5], I. GÓMEZ GONZÁLEZ[6], A. LÁZARO-FIGUEROA[2], S. LUCERO[1], M. ARIAS-GARCÍA[7], I. SANTOYO[1], A. RUIZ-

CONTERARAS[1];
[1]Facultad de Psicología, Univ. Nacional Autonoma de Mexico, Mexico City, Mexico; [2]Facultad de Psicología, Univ. Nacional Autonoma de Mexico, Mexico, City, Mexico; [3]INMEGEN, Mexico City, Mexico; [4]Inst. de Neurobiologia, UNAM, Ciudad de Mexico, Mexico; [5]Facultad de Psicología, Univ. Autonoma de México, Mexico city, Mexico; [6]Facultad de Psicología, Univ. Nacional Autónoma de México, CDMX, Mexico; [7]Facultad de Psicología, UNAM, Mexico City, Mexico

**Abstract:** Cognitive reserve (CR) is a construct that refers to the brain's resilience to age-related changes and neuropathology, shaped by lifelong experiences such as education, occupation, and leisure activities. Two attentional mechanisms are critical for working memory (WM) performance: enhancement of relevant information and suppression of irrelevant information, the later being known to decline in older age; however, our lab has shown that it happens only with low cognitive reserve. It remains unclear whether CR differentially modulates both mechanisms during working memory execution. This study aimed to examine whether CR predicts attentional enhancement and suppression mechanisms, as well as WM efficiency. Forty-two adults (21 women; 20-59 years) completed the CRIq (questionnaire to assess CR, and the MoCA (to evaluate global cognitive functioning). Participants solved the letter-number task designed to dissociate neural responses to relevant and irrelevant stimuli; the task consisted of presenting letters and digits alternatively; participants were asked to respond to one of two categories, answering if the second relevant stimulus was lower or higher than the first relevant stimulus. Event-related potentials were detected offline associated to the execution of the letter-number task. The frontal P2 (enhancement), frontal N2 (suppression), and parietal P3b (working memory updating) components were analyzed as a function of CR group (high vs. low). The high CR group exhibited greater N2 negativity for the first irrelevant stimulus compared to the first relevant stimulus, but this effect was absent in the low CR group. Moreover, CR negatively predicted N2 amplitude, while no group differences were found for P2 or P3b components. These findings showed that CR selectively predicted the suppression mechanism associated with irrelevant information during the performance of WM, without affecting the enhancement mechanism or memory updating. Our results suggest a selective relationship between CR and inhibitory attentional control in adulthood.

**Disclosures: E. López-González:** None. **U. Caballero Sanchez:** None. **T.V. Roman-Lopez:** None. **E. de Haro Hernández:** None. **S. Hernández-Márquez:** None. **I. Gómez González:** None. **A. Lázaro-Figueroa:** None. **S. Lucero:** None. **M. Arias-García:** None. **I. Santoyo:** None. **A. Ruiz-Conteraras:** None.

**Poster**

**PSTR198: Cognitive and Neural Mechanisms of Attention in Humans**

**Location:** WCC Halls A-C

**Time:** Monday, November 16, 2026, 1:00 PM - 5:00 PM

**Program #/Poster #:** PSTR198.19/II14

**Topic:** I.01. Attention

**Support:** NSF Grant SBE-2342847
NIH Grant U01NS13979575
NIH Grant S10OD025025
NIH Grant S10OD030220
NIH Grant S10RR028821
NIH Grant R01DC004290
NIH Grant P50MH132642
NIH Grant RO1 EY017699
NIH Grant R01 MH137624

**Title:** The pulvinar's role in auditory cognition: Speech-in-noise and selective attention effects in human intracranial recordings

**Authors: *J. A. CARUANA**[1], J. I. BERGER[1], A. E. RHONE[1], I. CHOI[2], S. KUMAR[1], B. J. DLOUHY[1], B. MCMURRAY[2], N. HARRISON[1], T. D. GRIFFITHS[3], H. KAWASAKI[1], S. KASTNER[4], M. A. HOWARD, III[1], R. M. CALMUS[1], C. I. PETKOV[1];
[1]Neurosurg., [2]Communication Sci. and Disorders, Univ. of Iowa, Iowa City, IA; [3]Newcastle Univ., Newcastle upon Tyne, United Kingdom; [4]Princeton Neurosci. Inst., Princeton Univ., Princeton, NJ

**Abstract:** The pulvinar is a higher-order thalamic nucleus implicated in visual cognition and brain-wide cortico-thalamic circuit functions. Auditory selective attention engages auditory cortex and subcortical auditory structures, such as the medial geniculate nucleus of the thalamus, but evidence on the role of the pulvinar in auditory cognition is sparse (PMID: 30037997). To test whether the human pulvinar exhibits auditory attention-selective responses, and how these compare to those of auditory cortex, we studied local field potentials (LFPs) and single-unit responses in intracranial recordings from neurosurgical patients during their epilepsy monitoring period. During the recordings, patients performed two auditory tasks: 1) selective attention to auditory spatial location or the voice identity of individuals producing spoken words; and 2) speech-in-noise detection of a spoken word among two different levels of background noise. Recordings were acquired from clinically placed electrode contacts in sites that included auditory cortex (Heschl's gyrus, HG, and Superior Temporal Gyrus, STG) and the pulvinar. Neurophysiological recordings demonstrated significant sound-driven responses in the pulvinar, complementary to those in auditory cortex. In the selective attention task, LFPs in the pulvinar exhibited phase- and time-locked deflections at around 250 ms, particularly when participants were cued to attend to the spatial location of the sounds. In the speech-in-noise task, the high signal-to-noise ratio (SNR) speech stimuli on average elicited larger evoked responses in the pulvinar than those of the low SNR condition, whereas some HG and STG responses to the speech sounds were comparatively less sensitive to SNR. In single-unit recordings from the pulvinar, spiking activity demonstrated consistent responses to the speech sounds embedded in noise. Spectral analyses of pulvinar LFPs showed low-frequency (including theta) modulation during both auditory tasks, as has been reported in the pulvinar during visual cognition (PMID: 30644391). In summary, we report the first in human direct comparisons between neurophysiological signals in the pulvinar and auditory cortex. The results demonstrate robust auditory-driven neurophysiological responses to naturalistic sounds in the human pulvinar at both the population and single-unit levels that vary during speech-in-noise and auditory selective attention. *RC, SK, & CP joint senior authors.

**Disclosures: J.A. Caruana:** None. **J.I. Berger:** None. **A.E. Rhone:** None. **I. Choi:** None. **S. Kumar:** None. **B.J. Dlouhy:** None. **B. McMurray:** None. **N. Harrison:** None. **T.D. Griffiths:** None. **H. Kawasaki:** None. **S. Kastner:** None. **M.A. Howard:** None. **R.M. Calmus:** None. **C.I. Petkov:** None.

**Poster**

**PSTR198: Cognitive and Neural Mechanisms of Attention in Humans**

**Location:** WCC Halls A-C

**Time:** Monday, November 16, 2026, 1:00 PM - 5:00 PM

**Program #/Poster #:** PSTR198.20/II15

**Topic:** I.01. Attention

**Support:** ERC Synergy fund 810580

**Title:** Paying attention under fluctuating multitasking demands: Enhanced P3m but impaired response execution

**Authors: *B. TIAN**[1], J. DAMAS[1], D. WANG[2], D. POEPPEL[3], D. BAVELIER[1];
[1]Univ. of Geneva, Geneva, Switzerland; [2]Beihang Univ., Beijing City, China; [3]Psychology & Neural Sci., New York Univ., New York, NY

**Abstract:** Executing multiple tasks concurrently is typical in many naturalistic settings. Multitasking demands, however, vary over time, such as when one drives while listening to directions. This involves times during which we actually face two different tasks - such as negotiating traffic as we control the car trajectory and also listen to GPS instructions - as well as times during which we carry out only one task - such as when one waits at the red light while still listening to GPS instructions. The focus of the present work is to characterize and better understand our attentional abilities as we fluctuate between these two modes. Thirty-five participants performed an active auditory oddball task while intermittently engaging in a visuomotor pressing task. During pressing, participants controlled the elevation of a visual disk with their right hand while detecting rare auditory targets with a left-hand button press. During inter-trial intervals (ITIs), only the auditory task was carried. Using MEG (306-sensor MEGIN system), we compare dual-task and single-task periods embedded within this same sustained multitasking context.
As expected from load theory (Lavie, 1995, 2004), responses to auditory targets were slower and response-locked ERF smaller during pressing than during ITI, indicating interference from performing concurrent visuomotor demands. Neither the early auditory N1m nor the mismatch negativity (MMN) differed between pressing and ITIs, indicating little selective modulation of early auditory processing as dual-tasking demands varied in this multi-tasking context. Of note, auditory targets elicited a larger P3m during pressing than during the ITI. Source-level analyses localized this enhancement to the posterior cingulate cortex, opposite the RetroSplenial cortex. Rare, unique environmental novel sounds, which were salient but required no response, similarly elicited a larger P3m during pressing in that same area. These latter results indicate that the same auditory detection task results in a larger P3m under dual than single tasking condition, owing in

part to a larger contribution from the Posterior Cingulate/RetroSplenial cortex, one of the major P3m generator.
These findings shed light on the P3 complex, its generators and its relative independence from response-locked mechanisms that more directly mirror behavioral results.

**Disclosures: B. Tian:** None. **J. Damas:** None. **D. Wang:** None. **D. Poeppel:** None. **D. Bavelier:** None.

**Poster**

**PSTR198: Cognitive and Neural Mechanisms of Attention in Humans**

**Location:** WCC Halls A-C

**Time:** Monday, November 16, 2026, 1:00 PM - 5:00 PM

**Program #/Poster #:** PSTR198.21/II16

**Topic:** I.01. Attention

**Support:** NIH Grant P01-AG055365
NIH Grant R01-DC019394
NIH Grant T32-DC000046
Brain and Behavior Institute Seed Grant

**Title:** Concurrent EEG and MEG Shows Differences Between Monolinguals and Bilinguals in Auditory Stream Segregation

**Authors: *C. FISHER**[1], M. A. JOHNS[2], M. A. BELCHER[3], S. ANDERSON[4], N. B. PANDŽA[5], S. E. KUCHINSKY[6], J. Z. SIMON[3];
[1]Univ. of Maryland, Col. Park, Lanham, MD; [2]Inst. for Systems Res., [3]Electrical and Computer Engin., [4]Hearing and Speech Sci., [5]Univ. of Maryland, College Park, MD; [6]Natl. Military Audiol. and Speech Pathology Ctr., Walter Reed Natl. Military Med. Ctr., Bethesda, MD

**Abstract:** Knowing a second language has been associated with better executive control, yet bilinguals show poorer speech-in-noise performance compared to monolinguals. However, language proficiency may bias speech-in-noise performance, often measured by linguistic-based tasks. As a significant portion of the population know more than one language, this presents a need to measure auditory stream segregation, a prerequisite skill for speech-in-noise listening, without inherent language biases. In this study, we utilized concurrent electroencephalography (EEG) and magnetoencephalography (MEG) to compare auditory attentional differences between monolinguals and bilinguals using a tone-based auditory stream segregation task, the stochastic figure-ground (SFG) task, that removes linguistic confounds.18 native English speakers (monolinguals) and 23 non-native English speakers (bilinguals) enrolled in this study. Neural data was recorded using EEG/MEG while participants listened to ~6 second long SFG stimuli under three conditions: target plus distractor (easier), target plus distractor (harder), or distractor only. The distractor background of the SFG stimuli is made up of septotemporal random tones. Targets are made of temporally coherent, inharmonic tones (a “chord”) and varied in difficulty (easier vs. harder) based on the number of temporally coherent tones. To analyze

neural responses, temporal response functions (TRF) were used to characterize responses to each chord index. Generalized additive mixed models (GAMM) were used to quantify temporal dynamics of TRF with statistical analysis.Preliminary results show no behavioral differences in performance among bilinguals and monolinguals on the SFG. However, neural differences emerge for the N100-like response for both target conditions where bilinguals had a larger N100-like response. This difference occurs for earlier chords (~chord index 3-4) for the easier condition and later chords (~chord index 6-7) for the harder condition. This result suggests that knowing a second language may impact neural processes during auditory stream segregation. However, behaviorally, the SFG task may provide a better measure of auditory attention among the broader population.

**Disclosures: C. Fisher:** None. **M.A. Johns:** None. **M.A. Belcher:** None. **S. Anderson:** None. **N.B. Pandža:** None. **S.E. Kuchinsky:** None. **J.Z. Simon:** None.

**Poster**

**PSTR198: Cognitive and Neural Mechanisms of Attention in Humans**

**Location:** WCC Halls A-C

**Time:** Monday, November 16, 2026, 1:00 PM - 5:00 PM

**Program #/Poster #:** PSTR198.22/II17

**Topic:** I.01. Attention

**Support:** P50MH132642
RO1 EY017699
R01MH137624

**Title:** Rhythmic dynamics of overt attention shifts during naturalistic search

**Authors: *A. A. SCHEIBE**[1,2,3], R. BOSHRA[1], Y. WU[1], F. BARTSCH[1], X. LIU[3], P. DE WEERD[2], S. KASTNER[1,3];
[1]Princeton Neurosci. Inst., Princeton, NJ; [2]Cognitive Neurosci., Maastricht Univ., Maastricht, Netherlands; [3]Psychology, Princeton Univ., Princeton, NJ

**Abstract:** Spatial attention has been shown to sample the environment rhythmically, producing periodic fluctuations in perceptual sensitivity. Neurophysiological evidence has linked these fluctuations to theta oscillations in attention networks, with opposing phases favoring either perceptual sampling at the currently attended location or attentional shifts. Evidence for this framework has primarily come from covert attention tasks, in which attention is directed to peripheral stimuli while central fixation is maintained. We hypothesized that similar theta-rhythmic dynamics also constrain the timing of overt attentional shifts, leading to phase-dependent suppression or facilitation of eye movements. If so, saccade timing during free visual exploration should exhibit statistical signatures consistent with theta-rhythmic models. Primates indeed generate ~3-4 saccades per second during free viewing, a rate within the lower theta range. However, the temporal and spectral structure of their timing remains poorly characterized, and the extent to which it reflects intrinsic rhythmic dynamics is still debated. Importantly, much

of this debate relies on oscillatory saccade-generation models that assume biologically implausible constraints, including the absence of a refractory period and questionable stationarity of both modulation frequency and saccade rate. Here, we acquired a large dataset of saccadic sequences during free visual exploration, quantified their temporal and spectral structure, and developed more biologically realistic saccade-generation models for comparison. In total, we analyzed more than 165,000 saccades from 33 participants engaged in complex real-world scene search. Despite substantial variability in visual input, saccade timing exhibited a consistent low-theta rhythm across participants, with elevated spectral power in the 3-5 Hz range. Temporal structure was well captured by models combining oscillatory modulation with modest trial-to-trial variability in frequency and a post-saccadic refractory period. However, under high saccade-rate conditions, reflecting high exploratory drive, oscillatory and purely inhibitory models became largely indistinguishable in their predictions. Together, this study provides a large-scale characterization of saccade timing during natural vision. It also highlights the dependence of conclusions on modeling assumptions and the limits of behavioral analyses alone, motivating future neural investigations into circuit-level mechanisms of saccade rhythmicity.

**Disclosures: A.A. Scheibe:** None. **R. Boshra:** None. **Y. Wu:** None. **F. Bartsch:** None. **X. Liu:** None. **P. De Weerd:** None. **S. Kastner:** None.

**Poster**

**PSTR198: Cognitive and Neural Mechanisms of Attention in Humans**

**Location:** WCC Halls A-C

**Time:** Monday, November 16, 2026, 1:00 PM - 5:00 PM

**Program #/Poster #:** PSTR198.23/II18

**Topic:** I.01. Attention

**Support:** National Institutes of Health
National Institute on Deafness and Other Communication Disorders
Marie-Josée and Henry R. Kravis Foundation

**Title:** Spatial-Spectral Organization and Directed Connectivity of Selective Auditory Attention in the Human Temporal Cortex

**Authors: *Y. MA**[1], G. MISCHLER[2], C. SCHEVON[3], G. M. MCKHANN, II[4], S. BICKEL[5], A. D. MEHTA[6], N. MESGARANI[1];
[2]Electrical Engin., [1]Columbia Univ., New York, NY; [3]Columbia Univ. Irving Med. Ctr., New York, NY; [4]The Mind/Brain Inst., Johns Hopkins Univ., Baltimore, MD; [5]Neurosurg. - Neurol., Feinstein Inst., Manhasset, NY; [6]Neurosurg., Hofstra Northwell Sch. of Med., Manhasset, NY

**Abstract:** Selective auditory attention enables listeners to follow one speaker in noisy, multi-talker environments, yet the spatial and frequency-specific organization of its neural mechanism in the human cortex remains poorly understood. We recorded human intracranial Electroencephalography while subjects listened to single and multi-talker speech, and we quantified attention-related modulation of neural activity across low, mid, and high-frequency

bands in the temporal lobe. We found a robust spatial-frequency gradient: anterior temporal regions showed relatively stronger low-frequency modulation, whereas posterior Superior Temporal Gyrus (STG) exhibited the strongest modulation in the high-frequency range. To characterize the network architecture of these effects, we used frequency-resolved Granger causality, which revealed that attention strengthens high-frequency recurrent loops in posterior auditory cortex while driving low-frequency interactions in the anterior temporal lobe. Together, these results show the spatial-spectral organization of auditory attention to speech, highlighting STG as a central hub that coordinates these distinct channels, and offering a connectivity-based framework for relating frequency-specific modulation to large-scale cortical networks.

**Disclosures: Y. Ma:** None. **G. Mischler:** None. **C. Schevon:** None. **G.M. McKhann:** None. **S. Bickel:** None. **A.D. Mehta:** None. **N. Mesgarani:** None.

**Poster**

**PSTR198: Cognitive and Neural Mechanisms of Attention in Humans**

**Location:** WCC Halls A-C

**Time:** Monday, November 16, 2026, 1:00 PM - 5:00 PM

**Program #/Poster #:** PSTR198.24/II19

**Topic:** I.01. Attention

**Title:** Beyond the P300: Alpha-Band Dynamics Surrounding Successful Target Detection in Naturalistic Visual Search

**Authors: *S. K**;
Humanities and Social sciences, Indian Inst. of Technology, Bombay, Powai, India

**Abstract: Background:** Target detectionduringrapidvisualsearch iscommonly characterizedthroughtarget-evoked neural responses, such as the P300, and short-timescaleneural predictorsofperception.However, less attentionhas been givento how ongoingneural activityvariesacrossextended periodssurroundingsuccessful target detectionduringcontinuousnaturalisticvisualsearch. Usingan open-access EEG dataset, we examinedneural activityimmediatelyprecedingand followingsuccessful target detectionina rapidserialvisualpresentation(RSVP)task.**Methods:** EEG recordingsfrom 10 healthy adults were obtainedfrom the publiclyavailableTHINGS-EEG dataset. Participantsviewedsequences of 20 naturalisticobjectimageswhilemonitoringfor rare appearances of the target character Buzz Lightyearand respondingviakeypress. Images were presented for 100 ms witha 200 ms stimulusonset asynchrony. Sixtarget-containingsequences (“n”)occurred pseudo-randomly withineach session.Analysesfocused on the sequence immediatelypreceding(n−1)and immediatelyfollowing(n+1)eachtarget-containingsequence. EEG data were preprocessed, and epoched. Event-related potentialswere computed to verifytarget detectioneffects. Time-frequencyrepresentationswere estimatedusingMorlet wavelets, and alpha-band (8–13Hz)activitywas compared between n−1 and n+1usingcluster-based permutationtesting.**Results:** Target stimulieliciteda robust parietalP300response relativeto standard stimuli,replicatingcanonicaltarget-detectioneffects.Time-frequencyanalysisrevealed a

significantalpha-band cluster differentiatingn−1 and n+1sequences. Specifically, alpha power was reduced inn−1 relativeto n+1, indicatingsystematicdifferences inneural activitysurroundingsuccessful target detection.**Conclusion:** Successfultarget detectionduringcontinuousnaturalisticvisualsearch was associatedwithdifferences inongoingalpha-band dynamicsextendingbeyond the target event itself.These findingssuggestthat successful detectionsmay occur withindifferent patterns of attentionalengagement and maybe followed by changes inongoingneural processing.Ongoingwork isinvestigatingwhethermultivariatemachine-learningapproaches can reliablydecode pre- and post-detectionactivity,providingfurther evidencefor distinctneural signaturessurroundingsuccessful target detection.

**Disclosures: S. K:** None.

**Poster**

**PSTR199: Human Perception, Imagery, and Imagination I**

**Location:** WCC Halls A-C

**Time:** Monday, November 16, 2026, 1:00 PM - 5:00 PM

**Program #/Poster #:** PSTR199.01/II20

**Topic:** I.02. Perception and Imagery

**Support:** NIH grant R01EY028535
NIH grant R01NS089069
Distinguished Postdoctoral Fellowship (CMU Neuroscience Institute)

**Title:** Contextual role modulates object representational geometry in the human brain

**Authors: *J. DIRANI**[1], S. CHAWLA[2], L. WEHBE[3], B. MAHON[4];
[1]Neurosci. Inst., [2]Dept. of Psychology, [3]Machine Learning Department; Neurosci. Inst., [4]Dept. of Psychology; Neurosci. Inst., Carnegie Mellon Univ., Pittsburgh, PA

**Abstract:** The human brain represents objects in a way that is both invariant across instances and flexible enough to support different contexts and tasks. Yet it remains unknown how object representations are dynamically remapped as the same object shifts across contextual roles. Here we combined fMRI with naturalistic movie viewing to investigate how the same objects are represented when they are passive elements in the scene versus the targets of goal-directed actions. Six healthy human adults underwent fMRI while viewing videos filmed in the first-person perspective where a common set of objects appeared as either passive scene elements or targets of goal-directed actions. Voxel-wise banded ridge encoding models were fit across five feature spaces (passive objects, target objects, action labels, hand synergy weights, motion energy), allowing to test the functional dissociation of object contexts. Representational similarity analysis was then used to compare object representational geometries against four models: visual similarity, semantic similarity, action affordances, and hand posture affordances. When objects were action targets, they engaged a parietal action network centered in the supramarginal and postcentral gyri, while passive objects recruited a distributed occipito-

temporal network involved in visual object recognition (FDR-corrected, $q<.05$). Within the networks most strongly encoding objects in their respective contexts, representational geometry showed a double dissociation: target object representations were organized by action affordance ($p<.001$) and hand posture affordance dimensions ($p<.001$), while passive object representations aligned with semantic dimensions ($p<.01$; all one-sample t-tests, FDR-corrected). In addition, visual representational structure was invariant to context ($p = .613$). Outside those context-specific brain networks, representational content retained context-invariance, indicating that flexibility and invariance operate at different levels of the same representational system. Together, these findings demonstrate neural remapping of object representational geometries in a manner that depends on moment-to-moment changes in the contextual relevance of objects within a naturalistic scene.

**Disclosures: J. Dirani:** None. **S. Chawla:** None. **L. Wehbe:** None. **B. Mahon:** Other; Inventor of US patents US12437878B2 and US12178591B2, and cofounder and Chief Science Officer of MindTrace Technologies Inc which licenses US12437878B2 from Carnegie Mellon University.

**Poster**

**PSTR199: Human Perception, Imagery, and Imagination I**

**Location:** WCC Halls A-C

**Time:** Monday, November 16, 2026, 1:00 PM - 5:00 PM

**Program #/Poster #:** PSTR199.02/II21

**Topic:** I.02. Perception and Imagery

**Support:** Tiny Blue Dot Foundation

**Title:** The hollow mask illusion results from reduced feedforward and feedback inputs to fusiform face areas: a laminar fMRI study

**Authors: *E. ROWE**[1], T. COLGAN[1], J. REEVES[1], R. GLARIN[1], T. SAVA[1], S. SUNDRAM[2], E. CHEN[1], B. NELSON[3], N. TSUCHIYA[2], S. WOOD[4], M. I. GARRIDO[1];
[1]The Univ. of Melbourne, Parkville, Australia; [2]Monash Univ., Clayton, Australia; [3]The Natl. Ctr. of Excellence for Youth Mental Hlth., Orygen, Melbourne, Australia; [4]Swinburne Univ., Hawthorn, Australia

**Abstract:** Visual perception involves the integration of two sources of information: bottom-up incoming sensory information and top-down prior expectations (or past experiences). To probe how these integrate to form our perception of the world, many researchers use visual illusions. One such example is the ‘hollow mask illusion’ in which an observer watches a rotating mask and perceives the concave back of the mask as convex (with the nose ‘popping out’ towards them). Past studies suggest that top-down mechanisms largely contribute to the illusion (that is, the prior expectation that faces should appear convex), while others hint at an interplay between top-down and bottom-up signalling. However, no study has imaged the laminar interactions that occur during this illusion and which would allow empirical testing of these theories. Accordingly, we conducted high resolution fMRI (1 mm isotropic) using 3D echo-planar

imaging on 30 neurotypical individuals at 7T while they completed a rotating hollow-mask task, in a laminar-based study design. We aimed to determine how activity differed (using a 2 x 3 design comparing Mask Reality: front or back of the mask and Layer activation: superficial versus middle versus deep layers) in three face-selective regions of interest that were identified a priori as: the primary visual cortex (V1), the fusiform face area (FFA) and the posterior superior temporal sulcus (pSTS). Importantly, to ensure we were examining the effects of the illusion, we excluded individuals (N = 10) who did not report observing the back of the mask 'popping out' on >50% of trials.
Results (for N = 20) in V1 showed no main effect of Mask Reality but a main effect of Layer for trials where the front of the mask was presented ($F = 10.38$, $p = 0.0008$). This finding was driven by greater activity in the superficial compared to the middle ($t = 2.83$, $pcorr = 0.033$) and deep ($t = 3.73$, $pcorr = 0.0042$) layers. In FFA, we observed a main effect of Mask Reality ($F = 21.72$, $p = 0.0002$), a main effect of Layer ($F = 4.16$, $p = 0.023$) and an interaction ($F = 8.72$, $p = 0.0007$), driven by greater activation overall when individuals viewed the front versus back of the mask. Specifically, during front trials the activation was greatest in the superficial layer compared to the deep ($t = 3.57$, $pcorr = 0.008$) layers and was greater in the middle compared to deep layers ($t = 3.44$, $pcorr = 0.006$). However, there were no significant differences between the layers during back trials. Finally, we observed no significant effects in pSTS. Our findings suggest that in FFA, activation in all layers is reduced during the illusion (i.e., when the back of the mask was perceived as convex) compared to when viewing the front of the mask.

**Disclosures: E. Rowe:** None. **T. Colgan:** None. **J. Reeves:** None. **R. Glarin:** None. **T. Sava:** None. **S. Sundram:** None. **E. Chen:** None. **B. Nelson:** None. **N. Tsuchiya:** None. **S. Wood:** None. **M.I. Garrido:** None.

**Poster**

**PSTR199: Human Perception, Imagery, and Imagination I**

**Location:** WCC Halls A-C

**Time:** Monday, November 16, 2026, 1:00 PM - 5:00 PM

**Program #/Poster #:** PSTR199.03/II22

**Topic:** I.02. Perception and Imagery

**Title:** Electroencephalographic decoding of oscillatory activity during auditory imagery

**Authors: *K. KOJIMA**, R. KATAYAMA, R. ISHIBASHI, A. AOYAMA;
Keio Univ., Fujisawa, Japan

**Abstract:** Auditory imagery, the internal generation and maintenance of sound without external auditory input, is essential for studying internal auditory representations. Although auditory imagery has been suggested to involve distributed networks including both auditory and motor-related regions, the neural representations supporting information transfer during active auditory imagery remain poorly understood. We thus analyzed electroencephalographic (EEG) oscillatory activity during pitch imagery using phase synchronization analysis and evaluated whether these neural dynamics contain information sufficient for pitch discrimination within a decoding

framework.Ten healthy male participants participated in the experiment. Seven pitches from C3 to B3 were randomly presented through speakers for 3 s, followed by a 3-s imagery period in which participants were instructed to actively imagine the previously presented pitch. EEG data were recorded throughout the experiment, and data during the imagery period were analyzed. After preprocessing, phase synchronization in each frequency band was quantified across frontal electrode pairs to evaluate frontal functional connectivity and to extract features for decoding analyses.Overall, phase synchronization increased in both beta (14-30 Hz) and gamma (30-50 Hz) bands during the imagery period. Based on these synchronization patterns, imagined pitch was decoded above chance level, reaching up to 81.3% accuracy with a nonlinear classifier. Pitch-specific analysis revealed differences in classification performance across imagined pitches, with the highest accuracy for C3 (85.0%) and the lowest accuracy for D3 (71.1%).These results demonstrate that frontal phase synchronization carries information related to internally generated pitch representations during auditory imagery. The ability to decode imagined pitch from these synchronization patterns suggests that oscillatory coupling provides a useful neural marker for characterizing auditory imagery dynamics. Together, these results indicate that phase synchronization reflects functionally relevant network organization that encodes information for pitch discrimination during auditory imagery and supports decoding of auditory representations.

**Disclosures: K. Kojima:** None. **R. Katayama:** None. **R. Ishibashi:** None. **A. Aoyama:** None.

**Poster**

**PSTR199: Human Perception, Imagery, and Imagination I**

**Location:** WCC Halls A-C

**Time:** Monday, November 16, 2026, 1:00 PM - 5:00 PM

**Program #/Poster #:** PSTR199.04/II23

**Topic:** I.02. Perception and Imagery

**Title:** Electroencephalographic decoding of scene and object representations during audiovisual imagery

**Authors: *Y. YOSHIMURA**, E. NAKAJIMA, T. GOTO, A. AOYAMA;
Keio Univ., Fujisawa, Japan

**Abstract:** Humans can vividly imagine visual and auditory information from everyday environments. Although recent electroencephalographic (EEG) studies have succeeded in decoding oscillatory representations of these contents during visual and auditory imagery, how category-specific information is represented during audiovisual imagery remains largely unknown. To address this question, we recorded EEG activity while participants imagined audiovisual scenes and objects, and examined decoding of category-specific information across imagery conditions. Participants were presented with stimuli from scene and object categories, each lasting for 10 s in visual-only, auditory-only, or audiovisual conditions. After a 2-s delay, participants imagined the same content in the corresponding modality for 10 s. EEG data recorded during the imagery period were analyzed in the time-frequency domain, and trial-wise spectral features were extracted for early and late imagery stages. Scene and object categories

were then classified separately for visual, auditory, and audiovisual imagery conditions using support vector machine classifiers. Time-frequency analysis revealed a decreasing trend in alpha-band activity across imagery conditions, particularly in the late stage of audiovisual imagery, irrespective of category. For scene classification, no consistent changes in accuracy were observed for audiovisual imagery relative to other imagery conditions across frequency bands or imagery stages. In contrast, for object classification, accuracy was relatively higher during the late stage of audiovisual imagery, particularly when using theta-band features, with higher feature selection rates in the frontal and parietal regions. Since alpha-band activity is generally associated with cortical state changes, the late decreasing trend may reflect task-related neural changes during stable imagery. Moreover, the audiovisual enhancement in accuracy for objects based on theta-band features is considered to involve stronger audiovisual correspondences during imagery-related processing. Considering the feature selection rates, we suggest that category-specific information during audiovisual imagery is differentially represented across brain regions for scene and object categories, with object representations more effectively supported by multisensory mechanisms.

**Disclosures: Y. Yoshimura:** None. **E. Nakajima:** None. **T. Goto:** None. **A. Aoyama:** None.

**Poster**

**PSTR199: Human Perception, Imagery, and Imagination I**

**Location:** WCC Halls A-C

**Time:** Monday, November 16, 2026, 1:00 PM - 5:00 PM

**Program #/Poster #:** PSTR199.05/II24

**Topic:** I.02. Perception and Imagery

**Support:** National Science and Technology Innovation 2030 Major Program (2022ZD0204802)
National Natural Science Foundation of China (T2421004, 32400874)
Beijing Natural Science Foundation (5244044)
Young Scientists Fund of the Humanities and Social Science Foundation of Ministry of Education of China (23YJCZH071)

**Title:** Geometric integration of cortical abstraction and hippocampal specificity supports dynamic prediction

**Authors: *Z. ZHAO**[1,2,3,4], T. HE[5,6,7,8], F. FANG[9,1,2,3,4];
[1]Peking-Tsinghua Ctr. for Life Sciences, Peking Univ., Beijing, China; [2]Sch. of Psychological and Cognitive Sci. and Beijing Key Lab. of Behavior and Mental Health, Peking Univ., Beijing, China; [3]IDG/McGovern Inst. for Brain Research, Peking Univ., Beijing, China; [4]Key Lab. of Machine Perception (Ministry of Education), Peking Univ., Beijing, China; [5]Sch. of Cognitive Sci. and Allied Hlth., Beijing Language and Culture Univ., Beijing, China; [6]Inst. of Life and Hlth. Sciences, Beijing Language and Culture Univ., Beijing, China; [7]Key Lab. of Cognitive Sci. of Language (Ministry of Education), Beijing Language and Culture Univ., Beijing, China; [8]Sch.

of Cognitive Sci. and Allied Health, Beijing Language and Culture Univ., Beijing, China; [9]Peking Univ., Beijing, China

**Abstract:** Prediction is fundamental to adaptive behavior. In dynamic environments, accurate prediction requires the brain to track multiple task-relevant variables over time while balancing flexibility and precision. Flexible prediction depends on abstract representations that generalize across contexts, whereas precise prediction requires context-specific episodic representations. How these complementary representational demands are organized to support dynamic prediction remains unclear. Here, we recorded fMRI signals while participants performed a dynamic visual prediction task. Participants viewed a rotating stimulus that subsequently disappeared. They were instructed to internally extrapolate its ongoing rotation and report its predicted final orientation. Stimulus identity, speed, and direction were independently manipulated. Using an inverted encoding model (IEM), we found that early visual cortex (EVC) reconstructed the predicted orientation trajectory during the blank period in a time-resolved manner, indicating that orientation predictions were actively maintained and updated in the absence of visual input. Representational geometry analyses revealed distinct cortical and hippocampal coding schemes. Across cortex, task variables were represented in anatomically distributed abstract geometries. Specifically, stimulus identity was primarily represented in EVC, direction in sensory-motor regions including EVC and area MT, and speed in a fronto-parietal network including prefrontal cortex (PFC) and intraparietal sulcus (IPS). In contrast, the hippocampus maintained context-specific representations of task variables. Critically, the geometry of these neural representations predicted behavioral precision. Compared with high-error trials, low-error trials showed greater cluster distance for speed representations in sensory-motor regions, together with reduced variance for stimulus-identity representations in the hippocampus and IPS. These findings suggest that precise dynamic prediction depends on both discriminable cortical representations of prediction-relevant abstract variables (e.g., speed), and compact hippocampal representations of the current episodic context. Together, our findings demonstrate that dynamic prediction emerges from the integration of two complementary geometric schemes: cortical abstraction that supports flexible generalization and hippocampal specificity that preserves contextual precision. This cortico-hippocampal geometric organization provides a potential neural mechanism for balancing flexibility and specificity during adaptive behavior.

**Disclosures: Z. Zhao:** None. **T. He:** None. **F. Fang:** None.

**Poster**

**PSTR199: Human Perception, Imagery, and Imagination I**

**Location:** WCC Halls A-C

**Time:** Monday, November 16, 2026, 1:00 PM - 5:00 PM

**Program #/Poster #:** PSTR199.06/II25

**Topic:** I.02. Perception and Imagery

**Support:** The William H. Neukom Institute for Computational Science

**Title:** pRF Amplitude along the Ventral Visual Processing Stream in Autism

**Authors:** ***C. A. LEFERINK**[1], Y. B. CHOI[1], P. A. ANGELI[1], A. D. STEEL[2], C. E. ROBERTSON[1];
[1]Psychological and Brain Sci., Dartmouth Col., Hanover, NH; [2]Univ. of Illinois Urbana-Champaign, Champaign, IL

**Abstract:** Retinotopic activation patterns in visual regions have been shown to differ between autistic and neurotypical individuals (Schwarzkopf et al., 2014), and are thought to contribute to differences in perception and memory characteristic of the condition (Robertson and Baron-Cohen, 2017). This is further supported by recent work showing a role for retinotopy in patterning visual-mnemonic interactions (Steel et al., 2021; Steel*, Silson*, et al., 2024). Specifically, a bivalent retionotopic code consisting of positive and negative amplitude pRFs structures communication between adjacent scene perception and scene memory regions (Steel*, Silson*, et al., 2024). Here, we explored whether there are differences in this novel bivalent code between autistic and neurotypical individuals within the ventral visual stream to the hippocampus using fMRI and voxel-level modeling. In total, 49 adults ($n$ = 24 autism; $n$ = 25 neurotypical; mean age = 27) participated in a fMRI retinotopic mapping task. Probabilistic parcels from Steel et al. (2025) were used to extract responses within PPA and the ventral place-memory area (VPMA) on the ventral surface, while hippocampal voxels were extracted using FreeSurfer's segmentation. Consistent with prior work (Silson et al., 2021), our results show the proportion of retinotopic voxels significantly decreases along the visual hierarchy from PPA to the hippocampus ($p < .001$). The transition from perception to memory is also marked by an increase in negative valence retinotopic voxels: we found a significantly lower proportion of negative retinotopic voxels in visual (PPA) as compared with mnemonic areas (HPC and VPMA), ($p < .001$). An analysis for group differences found no difference between ASC individuals and neurotypical controls in the pattern of retinotopic voxels ($p = .13$) or proportion of negative valence voxels ($p = .89$), and there was no significant interaction between group and ROI ($p = .69$). This suggests that differences in low-level retinotopic organization in autism do not generalize to differences in valence of retinotopic properties along the ventral visual stream to the hippocampus.

**Disclosures: C.A. Leferink:** None. **Y.B. Choi:** None. **P.A. Angeli:** None. **A.D. Steel:** None. **C.E. Robertson:** None.

**Poster**

**PSTR199: Human Perception, Imagery, and Imagination I**

**Location:** WCC Halls A-C

**Time:** Monday, November 16, 2026, 1:00 PM - 5:00 PM

**Program #/Poster #:** PSTR199.07/II26

**Topic:** I.02. Perception and Imagery

**Support:** Office of Naval Research grant N00014-24-1-2325

**Title:** Shared neural representations during cue-guided imagination in the default mode network

**Authors:** ***S. S. PARK**[1,2], X. SHAO[2,4], M. FELEYEH[3], S. SUDHARSAN[3], D. L. SCHACTER[5], C. RANGANATH[1,2];
[1]Dept. of Psychology, [2]Ctr. for Neurosci., [3]Univ. of California, Davis, Davis, CA; [4]Beijing Normal Univ., Beijing, China; [5]Dept. Psychol, Harvard Univ., Cambridge, MA

**Abstract:** We use abstract mental models to understand, remember, and simulate events (Ranganath & Ritchey, in press). Several findings have shown that, when different subjects recall the same event in a film or story, similar activity patterns are evoked in the default mode network (DMN; cf. Chen et al. 2017). Imagination — generating mental imagery guided only by sparse cues, without any visual stimulus — is often thought to be a more idiosyncratic process, and it is not clear whether imagined events would also be associated with shared neural patterns. Given that episodic memory retrieval and episodic simulation share the fundamental process of flexibly recombining memory elements (Schacter and Addis, 2007), we hypothesized that DMN regions would exhibit shared neural representations across individuals during imagination. During fMRI, subjects (n = 29, 16 female) performed an episodic simulation task. On each trial, they viewed cues (4.5s) specifying a person, place, and action (e.g., “teacher, eating a salad, museum”), followed by a silent period when they imagined an event using these elements (15.5s). Data were spatially normalized to a MNI template and single-trial estimates were derived using a least-squares-separate approach. Pattern similarity was computed by calculating the Pearson correlation between each subject's activation pattern and group average from the remaining subjects for every possible trial combination. We performed an inter-subject pattern similarity searchlight analysis to identify brain regions with shared multivariate activation patterns across subjects during 24 silent imagination trials. Statistical significance was assessed via a 10,000-permutation test with FDR correction (q=0.05). Preliminary analyses revealed evidence that inter-subject pattern similarity during imagination of the same event was higher than for imagination of different events within regions of the DMN, particularly the posterior medial cortex. These findings suggest that even without shared perceptual input, cue-guided imagination may drive convergent neural patterns across individuals within the DMN.

**Disclosures: S.S. Park:** None. **X. Shao:** None. **M. Feleyeh:** None. **S. Sudharsan:** None. **D.L. Schacter:** None. **C. Ranganath:** None.

**Poster**

**PSTR199: Human Perception, Imagery, and Imagination I**

**Location:** WCC Halls A-C

**Time:** Monday, November 16, 2026, 1:00 PM - 5:00 PM

**Program #/Poster #:** PSTR199.08/II27

**Topic:** I.02. Perception and Imagery

**Support:** National Research Foundation of Korea (NRF) grant funded by the Korea government (MSIT) (RS-2025-00522357).

**Title:** Decoding melodic contour from human electroencephalography during music listening, imagery, and production

**Authors: *C. YOON**, S.-P. KIM;
Ulsan Natl. Inst. of Sci. and Technol., Ulsan, Korea, Republic of

**Abstract:** Music brain-computer interfaces (BCIs) promise to offer new artistic communication in people with paralysis. While studies have demonstrated the feasibility of decoding specific songs, genres or affective characteristics of music from brain signals, it remains relatively unknown whether it would be possible to decode melodic structures. Especially, decoding of melodic contour, the most basic unit of melodic structure, can provide a general basis for synthesizing melody via BCIs. To explore this possibility, we recorded 31-channel electroencephalography (EEG) from 30 participants while they listened to, mentally imagined, or sang four most primitive melodic contours (Ascending, Descending, Convex and Concave) at four starting pitches (C4, D4, E4 and F4). We found that the temporal pattern of gamma power across diverse brain regions represented the shape of the melodic contour. By examining per-contour grand-average gamma activity traces during music production, we found a sequential note-by-note code: Convex-Concave divergence emerged first near the first note transition, Ascending-Descending divergence emerged at the second note, and the Convex-Concave contrast reversed polarity around the second note transition. The code was concentrated at frontal and parieto-occipital regions. Multiple combinations of EEG frequency bands and electrodes also showed contour-pair differences that were most pronounced for opposite-polarity contour pairs. Informed by these observations, we constructed pooled spatiotemporal templates from polarity-paired EEG differences and projected each trial onto them to obtain features classified by shrinkage linear discriminant analysis with per-subject adaptive band selection. All three tasks yielded significant above-chance four-class decoding (30.5 ± 0.4 % for listening, 30.9 ± 0.6 % for imagery and 39.2 ± 1.6 % for production). Also, decoding of contour could be generalized across different starting pitches for production, while it was less evident for listening and imagery. In addition, we found correlations between imagery and production decoding accuracy across subjects. These findings demonstrated neural representations of melodic contour in EEG spectral patterns, and the plausibility of decoding primitive melodic contour from them. Also, partial representational overlap between imagery and production suggests that an active vocal imagery protocol, silent humming with subtle laryngeal motor engagement, could serve as a promising direction for music BCIs.

**Disclosures: C. Yoon:** None. **S. Kim:** None.

**Poster**

**PSTR199: Human Perception, Imagery, and Imagination I**

**Location:** WCC Halls A-C

**Time:** Monday, November 16, 2026, 1:00 PM - 5:00 PM

**Program #/Poster #:** PSTR199.10/II29

**Topic:** I.02. Perception and Imagery

**Support:** JSPS Kakenhi 23K21851

**Title:** Decision confidence in 3-D structure-from-motion under perceptual uncertainty is reflected in large-scale brain activity

**Authors: *S. IWAKI**[1], A. OTSUKA[2], T. MIMURA[2], H. NISHIMOTO[3], Y. UESUGI[4]; [1]Natl. Inst. of Advanced Industrial Sci. and Technol. (AIST), Tsukuba, Japan; [2]Natl. Inst. of Information and Communications Technol. (NICT),, Suita, Japan; [3]Natl. institute of communications technology, Suita, Japan; [4]Univ. of Tsukba / Natl. Inst. of Advanced Industrial Sci. and Technol., Tsukuba, Japan

**Abstract:** Two-dimensional optical flow in retinal images provides an important cue for perceiving the three-dimensional structure of objects, known as three-dimensional structure-from-motion (3D-SFM). Previous neuroimaging studies using fMRI and MEG have shown that 3D-SFM perception relies on interactions between the dorsal and ventral visual subsystems (Orban 1999, Iwaki 2013). However, how perceptual decision confidence is represented in large-scale brain activity during 3D-SFM under perceptual uncertainty remains unclear. In this study, we investigated how subjective confidence in perceptual decisions during 3D-SFM is reflected in event-related brain activity measured with MEG. Eighteen participants viewed visual stimuli consisting of 1,000 randomly positioned dots with motion coherence ranging from 0 to 100%, which were perceived as a rotating three-dimensional sphere with varying levels of perceptual certainty. During the interstimulus interval, participants reported the tilt angle of the rotation axis and rated their confidence using a scale from 0 to 10. MEG signals were recorded using a 360-channel whole-head system (MEGIN, Helsinki) at a sampling rate of 1 kHz. Source-level brain activity was estimated using a minimum L2-norm inverse solution and summarized across 450 regions of interest (ROIs) defined by the APARC-sub parcellation. Correlation analyses between source activity and subjective decision confidence revealed significant positive associations in the posterior cingulate cortex, lateral occipital cortex, precuneus, and supramarginal gyrus, particularly within the latency range of 700 to 900 ms. These findings suggest that decision confidence during 3D-SFM under perceptual uncertainty is reflected in distributed large-scale brain activity across regions implicated in visuospatial processing and perceptual integration. In particular, medial parietal regions, including the posterior cingulate cortex and precuneus, may contribute to integrating motion and shape information and to stabilizing perceptual judgments. References Orban GA et al, *Neuron* 24: 929-940, 1999. Iwaki S et al., *J. Integr. Neurosci.* 12: 355-367, 2013.

**Disclosures: S. Iwaki:** None. **A. Otsuka:** None. **T. Mimura:** None. **H. Nishimoto:** None. **Y. Uesugi:** None.

**Poster**

**PSTR199: Human Perception, Imagery, and Imagination I**

**Location:** WCC Halls A-C

**Time:** Monday, November 16, 2026, 1:00 PM - 5:00 PM

**Program #/Poster #:** PSTR199.11/II30

**Topic:** I.02. Perception and Imagery

**Title:** Neural representational alignment in developmental prosopagnosia differs from controls beyond visual regions during naturalistic visual processing

**Authors: *A. KIDDER**[1], C. SAVA-SEGAL[2], E. FINN[3], B. DUCHAINE[3], C. I. BAKER[4]; [1]Dartmouth College/NIMH, Hanover, NH; [2]Psychological and Brain Sci., [3]Dartmouth Col., Hanover, NH; [4]Lab. Brain and Cognition, NIH, Bethesda, MD

**Abstract:** Although developmental prosopagnosia (DP) is defined by difficulty recognizing faces, the severity and specificity of this deficit varies widely, with some DPs also reporting atypical perception of other stimuli. The physiological correlates underlying this variability are largely unknown and typically investigated by averaging univariate responses to stimulus categories within visual regions. To address these methodological constraints, we compared whole-brain neural alignment during movie-watching using pairwise inter-subject correlations (ISC). We compared inter- and intra-group neural variability in DPs (N=28) and controls (N=45) using an open fMRI dataset where participants watched Game of Thrones (GoT; Noad et al., 2024). We found that controls were more aligned than DPs in several regions within and outside visual regions, such as right early visual areas and bilateral superior temporal sulcus (STS). DPs had stronger alignment in left early visual areas. When separating participants within each group who were familiar and unfamiliar with GoT, we replicated that familiar controls had greater alignment in right STS compared to familiar DPs (Noad et al., 2024), and showed that unfamiliar DPs had greater alignment in several regions across the cortex. Familiar controls (N=22) had the most whole-brain alignment, followed by unfamiliar controls (N=23), unfamiliar DPs (N=13) and familiar DPs (N=15). To further characterize the relationship between neural variability and face recognition, we used inter-subject representational similarity analysis (IS-RSA). When collapsing across groups, participants who were better at face recognition were more similar in temporal regions, such as the temporal pole. Additionally, regions in the control group that had more neural alignment when face recognition is more similar tend to be less aligned in DPs with similar face recognition. Future analyses will explore how neural alignment changes dynamically during perception, and what visual information is driving those differences. Preliminary results suggest that peak differences between groups were driven by faces conveying social information. Altogether, DPs had greater whole-brain neural variability during visual processing compared to controls, and this effect was primarily driven by DPs familiar with the stimulus.

**Disclosures: A. Kidder:** None. **C. Sava-Segal:** None. **E. Finn:** None. **B. Duchaine:** None. **C.I. Baker:** None.

**Poster**

**PSTR199: Human Perception, Imagery, and Imagination I**

**Location:** WCC Halls A-C

**Time:** Monday, November 16, 2026, 1:00 PM - 5:00 PM

**Program #/Poster #:** PSTR199.12/II31

**Topic:** I.02. Perception and Imagery

**Support:** Florida Department of Health 25A16

**Title:** Fusiform gyrus integrates visual and conceptual object features in young and older adults

**Authors: *C. A. DAVIS**[1], V. SAINTERANT[2], S. D. ALLEN[4], S. CALIRI[1], C. B. MARTIN[3]; [1]Psychology, Florida State Univ., Tallahassee, FL; [2]Psychology, Florida State Univ., Orlando, FL; [3]Dept. of Psychology and Neurosci., Florida State Univ., Tallahassee, FL; [4]Yale Univ., New Haven, CT

**Abstract:** A significant body of research in cognitive neuroscience is aimed at understanding how objects and object concepts are represented in the human brain, with a particular emphasis on structures comprising the ventral visual pathway. Within this context, a central goal is to determine the kinds of features that shape the representational structure of object-evoked responses across regions. Evidence from lesion studies and neuroimaging research, in humans and non-human primates, has revealed clear representational biases related to visual and conceptual object features. Specifically, representational structure in more posterior ventral pathway sites is most strongly influenced by visual similarities, whereas more anterior sites are most strongly influenced by conceptual similarities. Less is known about whether and where visual and conceptual features are integrated. Relevant prior evidence suggests that these fundamentally different kinds of features may be integrated at the level of perirhinal cortex. However, words were used as stimuli in that experiment, which limits the generalizability of claims about cross-modal integration. We addressed this in the current study by using an image-based stimulus set that was carefully crafted to ensure that visual and conceptual features were not confounded across stimuli. Two groups of participants (young adults, older adults) completed an fMRI experiment in which they made trial-wise judgements about the visual or conceptual features of each object image. We used a representational similarity analysis which involved comparisons among neural similarities in object-evoked fMRI responses and behavior-based models that independently captured the visual and conceptual similarities among the stimuli. In both populations, results from an ROI-based approach revealed evidence for task-invariant integrative coding in right fusiform gyrus. The neuroanatomical specificity of this effect was highlighted by converging evidence from searchlight analyses performed in both groups. Combined with our previous research with words as stimuli, this pattern of results suggests that integrative coding of visual and conceptual object features can be seen at multiple sites in the ventral visual pathway; integration plays out in more anterior regions when object concepts are activated by verbal stimuli, and more posterior regions when images are used as stimuli. More generally, these results indicate that integrative coding is not a privileged feature of any one cortical structure. Rather, it is a foundational computation supported by multiple regions in a context-dependent manners.

**Disclosures: C.A. Davis:** None. **V. Sainterant:** None. **S.D. Allen:** None. **C.B. Martin:** None.

**Poster**

**PSTR199: Human Perception, Imagery, and Imagination I**

**Location:** WCC Halls A-C

**Time:** Monday, November 16, 2026, 1:00 PM - 5:00 PM

**Program #/Poster #:** PSTR199.13/II32

**Topic:** I.02. Perception and Imagery

**Title:** Face Blind and Neurotypical Individuals Show Similar Functional Topography During Memory Recall of People and Places

**Authors: *A. HARALANOVA**[1], A. KIDDER[2], C. I. BAKER[1];
[1]Lab. Brain and Cognition, NIH, Bethesda, MD; [2]Dartmouth College/NIMH, Akron, NY

**Abstract:** Developmental prosopagnosia (DP), or face blindness, is a condition characterized by severe impairment in face recognition ability despite typical early visual processing and the absence of any known brain lesions (McConachie, 1976). The underlying causes of atypical face recognition are unclear, though theories include problems with perceptual encoding, memory recall, or connectivity in the temporal lobe. Prior neuroimaging work has primarily focused on perceptual encoding, reporting the presence of the typical face-selective regions in DP participants, but with reduced selectivity. Here, we focused on memory recall for familiar people and places. In neurotypicals (NT), we have previously described alternating regions along the medial parietal cortex (MPC) which preferably responded to self-generated recall of people or places (Silson, Steel, et al. 2019). For this study, we asked both NT (n = 13) and DP (n = 7) participants to recall and visualize personally familiar people and places from memory without any visual input besides written name prompts. The people and places that the participants recalled were selected by the participants prior to the scan. We also functionally localized visually-selective regions, including those responsive to faces, bodies, objects, and scenes. Consistent with prior reports, we could localize the major visually face-selective regions in both NT and DP participants, although the DP participants often showed more activation in frontal cortex. During memory recall, we were also able to find the expected alternating patterns of activation along MPC in most participants, as well as strong activation of anterior scene-selective cortex in ventral temporal regions for recall of places. In addition to preserved functional topography between DPs and NTs, both groups showed similar response magnitude during the recall and localizer tasks in MPC and visual cortex. Future analyses will explore the relationship between univariate activation in visual and recall regions with self-reported vividness of imagery for the selected people and places, and will use multivariate analysis to further elucidate patterns of brain activity that may drive differences in face processing.

**Disclosures: A. Haralanova:** None. **A. Kidder:** None. **C.I. Baker:** None.

**Poster**

**PSTR199: Human Perception, Imagery, and Imagination I**

**Location:** WCC Halls A-C

**Time:** Monday, November 16, 2026, 1:00 PM - 5:00 PM

**Program #/Poster #:** PSTR199.14/JJ1

**Topic:** I.02. Perception and Imagery

**Title:** Framing Moderates Environment-related Distress and Brain Function

**Authors: *J. CHEN**[1], P. KIRK[2], A. HALL[3], S. LOPEZ-GUZMAN[4];
[1]Natl. Inst. Of Mental Hlth., Bethesda, MD; [2]Natl. Inst. of Mental Hlth., Bethesda, MD; [3]Univ. Col. London, London, United Kingdom; [4]Unit on Computat. Decision Neurosci., Natl. Inst. of Mental Hlth. (NIMH), Bethesda, MD

**Abstract:** Negative framing is common in communication and coverage of extreme-weather events but may counterproductively increase distress during information processing. We tested whether negatively framed environmental videos, relative to positively framed videos, increase subjective stress and alter brain responses during naturalistic viewing. In an online sample (N=54), participants viewed positively- and negatively-framed videos about the environment, while providing continuous ratings of distress. We also quantified self-reported environmental attitudes, such as concerns, level of personal responsibility, and belief that one should do more to help. A one-sample t-test on participant-level change in distress before and after the video confirmed greater distress increases for negative compared to positive framing (Δ mean = 33.84, SD = 33.96, t53 = 7.32, p < .001). For each environmental attitude, a linear mixed-effects model predicted mean distress from different framing, attitude, and their interaction. Negative framing increased stress across models (e.g. in concern model: Est. = 25.70, $t_{51}$ = 9.44, p < .001). Moderation analyses showed that climate concern (Est. = 8.48, t51= 3.10, p = .003) and belief that one should do more (Est. = 9.22, t51= 3.43, p = .001) amplified the negative-versus-positive framing effect, with personal responsibility showing a similar trend (Est. = 5.63, t51= 1.96, p = .056). In a separate fMRI sample (N=36), participants viewed the same videos during BOLD acquisition. To isolate a distress-related neural map, we regressed the group-level stress time series against BOLD during the video watching. To account for low-level sensory variation in the naturalistic stimuli, we also included audiovisual feature regressors. Our confirmatory analyses revealed activations in the auditory and visual cortices related to the audiovisual regressors, validating our pipeline. We also found that the sensory area activations differed between positive and negative framing, which suggests contextual modulation during sensory processing. The stress time series covaried with activity in bilateral hippocampus, amygdala, thalamus, and inferior frontal junction. Moreover, our results reveal framing moderates the impact of stress on medial frontal cortex, anterior cingulate and precuneus (which form part of salience and default mode networks). Taken together, our results show that environmental attitudes heighten distress to negative framing. Additionally, fMRI results indicate negative framing shifts how environmental information are processed through sensory, medial temporal, salience and default-mode regions.

**Disclosures: J. Chen:** None. **P. Kirk:** None. **A. Hall:** None. **S. Lopez-Guzman:** None.

**Poster**

**PSTR199: Human Perception, Imagery, and Imagination I**

**Location:** WCC Halls A-C

**Time:** Monday, November 16, 2026, 1:00 PM - 5:00 PM

**Program #/Poster #:** PSTR199.15/JJ2

**Topic:** I.02. Perception and Imagery

**Title:** Questioning brain (re)organization in the motor system: fMRI information connectivity

**Authors: *A. JAIN**[1,2], M. LIN[2,3], A. M. D'MELLO[1,4,5];
[1]Psychiatry, [2]Bioinformatics, [3]Cecil H. and Ida Green Ctr. for Systems Biol., [4]Peter O'Donnell Jr. Brain Inst., UT Southwestern Med. Ctr., Dallas, TX; [5]Psychology, UT Dallas, Dallas, TX

**Abstract:** Decades of neuroimaging research have relied on functional connectivity (FC) to uncover principles of brain organization and test how organization is altered in disease or damage. For instance, in the motor system, FC approaches have revealed a distinct homunculus (aligning with electrophysiological descriptions) with discrete regions for specific effectors (hand, foot, mouth), connections between effectors and premotor/execution areas across cortex and cerebellum, and even novel inter-effector regions. Although FC has been invaluable for characterizing large-scale brain networks, it is fundamentally limited by reliance on correlations between regional time courses, which may not accurately reflect information transfer and can be influenced by noise and other confounding factors. Furthermore, FC-based networks often depend on thresholding procedures that impose arbitrary boundaries on network structure, and FC cannot determine whether correlated regions interact directly or indirectly through intermediary regions. Here we introduce a novel information-theoretic approach, "information connectivity" (IC), which we validate with a focus on the motor system. Through a maximum-likelihood Chow-Liu tree approach that leverages mutual information to estimate the network's joint distribution to second order, we extracted sparse, interpretable graphs of information sharing in the motor system. Using virtual brain simulations, we showed that these graphs (1) capture nonlinearities to supersede correlation assumptions, (2) derive a maximum spanning tree without thresholding, and (3) infer intermediary pathways via a sparse subgraph. We then validated IC in 10 healthy Midnight Scan Club (MSC) participants (~5 hrs rsfMRI, ~1.3 hrs motor task each). IC recapitulated simulated ground truth best among several sparsity-matched FC methods (correlation MST, partial correlation, graphical lasso), and was the only method that recovered strong connections between bilateral effector homologues in 100% of cases. We then asked whether IC provides insights into other fundamental brain properties, like brain re-organization following disuse or injury. In 2 MSC participants who wore a right-arm cast for two weeks (~27-43 hrs each, scanned pre/during/post), FC found that effectors became "functionally disconnected" with large-scale cortical reorganization even on short timescales. However, IC indicated that topology was preserved and information sharing remained stable despite disuse. These findings suggest IC could yield new insights into brain (re)organization and challenge accepted beliefs about reorganization following damage or disuse.

**Disclosures: A. Jain:** None. **M. Lin:** None. **A.M. D'Mello:** None.

**Poster**

**PSTR200: Prefrontal Mechanisms of Executive Function in Humans and Animals**

**Location:** WCC Halls A-C

**Time:** Monday, November 16, 2026, 1:00 PM - 5:00 PM

**Program #/Poster #:** PSTR200.01/JJ3

**Topic:** I.04. Executive Functions

**Support:** Blackrock Neurotech
Hewitt Foundation Gift
CU ASPIRE award
NIH U01NS123127
The T&C Chen BMI Center
Boswell Foundation

**Title:** Neural Dynamics of Interference Control in Human Prefrontal and Parietal Cortex

**Authors: *J. KOWALCZYK**[1], I. ROSENTHAL[2], D. A. BJANES[3,5,4], R. N. TIEN[2], B. LEE[3,6,7], K. PEJSA[3,4], C. LIU[3,6,7,8], R. A. ANDERSEN[3,4], J. A. THOMPSON[2], D. KRAMER[2], L. BASHFORD[1,2];
[1]Newcastle Univ., Newcastle upon Tyne, United Kingdom; [2]Dept. of Neurosurg., Univ. of Colorado Anschutz Med. Campus, Aurora, CO; [3]Biol. and Biol. Engin., [4]T&C Chen Brain-machine Interface Ctr., Caltech, Pasadena, CA; [5]Dept. of Neurosurg., Univ. of Utah, Salt Lake City, UT; [6]Dept. of Neurolog. Surgery, [7]USC Neurorestoration Ctr., Keck Sch. of Med. of USC, Los Angeles, CA; [8]Rancho Los Amigos Natl. Rehabil. Ctr., Downey, CA

**Abstract:** Navigating the environment around us requires the ability to ignore irrelevant information and conduct goal-direct behaviour accordingly. This is underpinned by interference control, a core component of executive function. Here, we investigated the neural dynamics of interference control in two tetraplegic human participants implanted with microelectrode arrays (Blackrock Neurotech). Participants performed two variants of a Stroop color-word task while neural activity was recorded in dorsolateral prefrontal cortex (dlPFC) and supramarginal gyrus (SMG). Participants respond to either the ink color, or the text of the word presented in the stimuli, which can be either congruent (e.g. “RED” written in red ink) or incongruent (e.g. “RED” written in blue ink). In the first task variant, the cue (respond to stimuli text/color of the stimulus) was stable across all trials, whereas in the second, it varied randomly, requiring reactive adaptation. At the single-channel level, neural spiking activity encoded trial condition, varying between text, color, congruent and incongruent conditions. The dominant text-response showed no difference, however, non-dominant color responses differed significantly, both compared against text responses and between congruent and incongruent trials. Population-level activity also distinguished between task conditions, with significant classification accuracy for color responses from the dlPFC and SMG. Notably, latent space trajectories for the dlPFC, but not for the SMG, showed statistically significant divergence between congruent and incongruent conditions. Lastly, we also observed statistically significant encoding of task-switching across single-channel and population level activity in the SMG. The temporal dynamics across the two regions also differed, with dlPFC showing later but more sustained population activity changes, whereas SMG showed an earlier and more transient response. These findings demonstrate circuit-level dynamics underlying response inhibition and interference control in human prefrontal and parietal cortex. We found differential roles of the dlPFC and SMG in the neural dynamics of executive function, with the dlPFC showing later but more sustained activity indicative of top-down control or response inhibition required for correct task performance, and SMG showing more transient and earlier activity, suggesting its role in sensory integration or rule application/task-switching. Future work will examine how closed-loop stimulation could modulate these dynamics and consequently, performance on cognitive tasks.

**Disclosures: J. Kowalczyk:** None. **I. Rosenthal:** None. **D.A. Bjanes:** None. **R.N. Tien:** None. **B. Lee:** None. **K. Pejsa:** None. **C. Liu:** None. **R.A. Andersen:** None. **J.A. Thompson:** None. **D. Kramer:** B. Contracted Research/Research Grant (principal investigator for a drug study, collaborator or consultant and pending and current grants). If you are a PI for a drug study, report that research relationship even if those funds come to an institution.; Blackrock Neurotech. C. Other Research Support (receipt of drugs, supplies, equipment or other in-kind support); Blackrock Neurotech. **L. Bashford:** B. Contracted Research/Research Grant (principal investigator for a drug study, collaborator or consultant and pending and current grants). If you are a PI for a drug study, report that research relationship even if those funds come to an institution.; Blackrock Neurotech. C. Other Research Support (receipt of drugs, supplies, equipment or other in-kind support); Blackrock Neurotech.

**Poster**

**PSTR200: Prefrontal Mechanisms of Executive Function in Humans and Animals**

**Location:** WCC Halls A-C

**Time:** Monday, November 16, 2026, 1:00 PM - 5:00 PM

**Program #/Poster #:** PSTR200.02/JJ4

**Topic:** I.04. Executive Functions

**Support:** Blackrock Neurotech
Hewitt Foundation
CU ASPIRE award
NIH Grant U01NS123127
The T&C Chen BMI Center
Boswell Foundation

**Title:** Uncovering the role of dorsolateral prefrontal cortex (dlPFC) in the updating of working memory with a human brain-computer interface

**Authors: *I. A. ROSENTHAL**[1], R. N. TIEN[3], D. A. BJANES[4,6], J. KOWALCZYK[7], K. NEUMAN[2], J. SMITH[2], P. DAVID GERECHT[2], K. PEJSA[4], B. LEE[8,4], C. LIU[8,4], R. A. ANDERSEN[5], J. A. THOMPSON[9], L. BASHFORD[7,2], D. R. KRAMER[10];
[1]Neurosurg., [2]Univ. of Colorado Anschutz, Aurora, CO; [3]Neurosurg., CU Denver | CU Anschutz, Aurora, CO; [5]BBE, [4]Caltech, Pasadena, CA; [6]Univ. of Utah, Salt Lake City, UT; [7]Newcastle Univ., Newcastle upon Tyne, United Kingdom; [8]USC, Los Angeles, CA; [9]Neurosurg., Univ. of Colorado, AMC, Aurora, CO; [10]Univ. of Colorado Sch. of Med., Aurora, CO

**Abstract:** Task completion requires content revision which relies on working memory, a core component of executive function. Neuroimaging and animal studies have suggested that the dorsolateral prefrontal cortex (dlPFC) enables the updating of working memory. Here, we pair a classic executive function paradigm, the N-Back task, with the high spatiotemporal precision of electrophysiology, to better understand the dynamics of working memory and cognitive load in the human brain. A C5 tetraplegic human participant implanted with 64-channel microelectrode arrays (Blackrock Neurotech) performed two versions of the N-back task (0-back, 1-back) while

neural activity was recorded in dlPFC. Pseudo-random letters (e.g. ‘K’) were displayed sequentially, and the participant was instructed to report either every time a target letter appeared (0-back) or every time the current letter matched the last letter presented (1-back). In the 1-back task, working memory must be updated on every trial to compare a current stimulus with the most recent one, while the 0-back task does not require this updating process. Using linear discriminant analysis, task identity (0-back vs 1-back) was highly decodable at every trial timepoint based on multi-unit firing rate data from dlPFC. Given that the visual stimuli in the two tasks are identical, this indicates that dlPFC encodes the difference in working memory demands between the tasks. It was also possible to decode if a stimulus was a target match 0.25s after stimulus presentation in both the 0-back and 1-back tasks, suggesting that dlPFC represents task requirements as they interface with working memory. In an examination of the latent space of neural activity in dlPFC with PCA, the neural trajectories of the two tasks were similar in the first and second dimensions but highly separable in the third dimension, suggesting that the tasks are encoded similarly to some degree but that the difference in working memory is sufficient to explain a major amount of the variance in firing rates. Individual channel firing rates were also examined though a linear regression tuning analysis. In both tasks, there was an increase in tuned channels relative to baseline firing rates in dlPFC starting 200ms following cue presentation during match trials. During non-match trials in the 1-back task, there was an increase in tuned channels 0.5-1s post-cue onset, indicating a potential encoding of the cue in working memory. In sum, this study contributes to our understanding of dlPFC as a hub for executive function by showing that neural activity encodes working memory demands acutely following stimulus presentation as well as more generally across the duration of a n-back task.

**Disclosures: I.A. Rosenthal:** A. Employment/Salary (full or part-time):; Blackrock Neurotech. C. Other Research Support (receipt of drugs, supplies, equipment or other in-kind support); Blackrock Neurotech. **R.N. Tien:** A. Employment/Salary (full or part-time):; Raynor Cerebellum Project. **D.A. Bjanes:** None. **J. Kowalczyk:** None. **K. Neuman:** None. **J. Smith:** None. **P. David Gerecht:** None. **K. Pejsa:** None. **B. Lee:** None. **C. Liu:** None. **R.A. Andersen:** None. **J.A. Thompson:** None. **L. Bashford:** None. **D.R. Kramer:** C. Other Research Support (receipt of drugs, supplies, equipment or other in-kind support); Blackrock Neurotech, Raynor Cerebellum Project.

**Poster**

**PSTR200: Prefrontal Mechanisms of Executive Function in Humans and Animals**

**Location:** WCC Halls A-C

**Time:** Monday, November 16, 2026, 1:00 PM - 5:00 PM

**Program #/Poster #:** PSTR200.03/JJ5

**Topic:** I.04. Executive Functions

**Support:** McDonnell Center for Systems Neuroscience at Washington University in St. Louis
McDonnell Center for Cellular and Molecular Neurobiology at Washington University in St. Louis

**Title:** Contextual modulation of working and episodic memory in naturalistic experience

**Authors: *H. SONG**[1], J. PARK[2], Q. LU[4], G. VEDOVATI[3], M. D. ROSENBERG[5], Z. M. REAGH[3], S. CHING[3];
[1]Univ. of Texas at Austin, Austin, TX; [2]Washington Univ. in St. Louis, St. Louis, MO, ; [3]Washington Univ. in St. Louis, St. Louis, MO; [4]City Univ. of Hong Kong, Kowloon, Hong Kong; [5]Univ. of Chicago, Chicago, IL

**Abstract:** The prefrontal cortex (PFC) represents contexts using distinct patterns of activity. These context representations are used by the lateral PFC to maintain relevant information in working memory (WM) and by the medial PFC to retrieve context-congruent episodic memories (EM) via interactions with the hippocampus. While work continues to elucidate PFC function and circuitry, the computational mechanisms by which context modulates memory is less understood. To address this, we designed several context modulation models and compared them against naturalistic fMRI data (Song et al., 2025). Recurrent neural networks (RNN) were trained to receive audiovisual inputs from movie scenes at each time step and predict semantics of the next scene, including characters present and time and location. Models were trained on all but one episode of *This Is Us* Season 1 and tested on the held-out episode. Episodes consisted of four interleaved character narratives. The narrative each scene belonged to served as a context signal provided during training. At test, the model inferred context via Bayesian inference. The model in which context modulated WM (i.e., the RNN recurrence) in a low-rank manner (Mastroguiseppe & Ostojic, 2018) achieved the highest representational similarity to cortical activity of fMRI participants who watched the same episode, outperforming RNN variants in which context modulated either inputs or outputs, and a model without low-rank constraints. This suggests that WM may be gated by contexts through low-rank modulation of connectivity in the lateral PFC. Turning to EM, we augmented this WM-modulated RNN with an EM buffer that encodes and retrieves memories via self-attention. In addition to encoding scene contents, the inferred context was encoded into the EM at every time step, and pattern similarity between past and current contexts was computed. This context similarity was multiplied by the self-attention outcome (i.e., content similarity), biasing retrieval of context-congruent memories. Of all EM variants tested, this model exhibited the most human-like memory retrieval. This benefit was most pronounced early in learning and observed only when both WM and EM were modulated. This architecture simulates the mPFC-hippocampus interaction, where the hippocampus encodes both content and context information and the mPFC uses context representations to selectively retrieve congruent memories. Together, our results suggest that context modulates WM by engaging different low-rank connectivity and EM by preferentially retrieving context-congruent memories—shedding light on the functional roles of the lateral and medial PFC, respectively.

**Disclosures: H. Song:** None. **J. Park:** None. **Q. Lu:** None. **G. Vedovati:** None. **M.D. Rosenberg:** None. **Z.M. Reagh:** None. **S. Ching:** None.

**Poster**

**PSTR200: Prefrontal Mechanisms of Executive Function in Humans and Animals**

**Location:** WCC Halls A-C

**Time:** Monday, November 16, 2026, 1:00 PM - 5:00 PM

**Program #/Poster #:** PSTR200.04/JJ6

**Topic:** I.04. Executive Functions

**Support:** NIH Grant R01MH133637

**Title:** Systematic Variation in Representational Geometries Supporting Relational Reasoning Across Lateral Prefrontal Cortex

**Authors: *M. VASHEL**[1], A. CHEN[1,2], S. A. BUNGE[1,3];
[1]Dept. of Psychology, Univ. of California, Berkeley, Berkeley, CA; [2]Interdepartmental Neurosci. Program, Univ. of California, Irvine, Irvine, CA; [3]Helen Wills Neurosci. Inst., Berkeley, CA

**Abstract:** Higher-order reasoning about relationships between relationships has been consistently associated with rostrolateral prefrontal cortex and adjacent regions of lateral prefrontal cortex (LPFC), consistent with influential theories of rostro-caudal organization supporting increasingly abstract cognition. An important open question is how relational and stimulus information are organized across LPFC subregions during reasoning. Characterizing this representational organization may help explain how LPFC supports flexible cognition across diverse task domains. Here, we examined representational geometry and dimensionality across LPFC during relational reasoning using a 2×2×2 fMRI design crossing sensory modality (auditory, visual), stimulus domain ("what", "where"), and relational complexity (1st-order, 2nd-order). Consistent with domain-general accounts of relational reasoning, conjunction analyses revealed robust overlapping activation for 2nd-order relational processing across stimulus conditions within rostrolateral and dorsolateral/multiple-demand prefrontal regions (N = 59). To characterize representational organization within these regions, we conducted representational similarity analysis (RSA) across 11 left LPFC parcels. Regression RSA revealed broad representation of multiple task dimensions across LPFC, including relational complexity, sensory modality, and stimulus domain. However, targeted analyses quantifying representational separation along each task dimension revealed systematic differences in representational geometry across LPFC subregions. Ventrolateral regions exhibited stronger separation by stimulus properties, whereas more rostral regions showed relatively greater separation between 1st- and 2nd-order relations. Effective dimensionality, quantified using participation ratio, increased rostrally along a rostrocaudal gradient and ventrally along a dorsoventral gradient, tracking increases in representational separation across task dimensions. Together, these findings suggest that broad domain-general LPFC recruitment during relational reasoning coexists with distinct patterns of representational organization across LPFC subregions. Rather than reflecting a unitary hierarchy of abstraction, LPFC organization may be better characterized as systematic variation in representational geometry across subregions that differentially emphasize relational and stimulus information.

**Disclosures: M. Vashel:** None. **A. Chen:** None. **S.A. Bunge:** None.

**Poster**

**PSTR200: Prefrontal Mechanisms of Executive Function in Humans and Animals**

**Location:** WCC Halls A-C

**Time:** Monday, November 16, 2026, 1:00 PM - 5:00 PM

**Program #/Poster #:** PSTR200.05/JJ7

**Topic:** I.04. Executive Functions

**Support:** NIH Grant T34GM136467
NSF Grant 2425075
NSF Grant 2322436

**Title:** Manipulating control mode reorganizes delay-period gaze dynamics during the AX-CPT

**Authors: *D. M. DIAZ**[1], V. BHATT[2], J. MARTINEZ[3], G. HERNANDEZ[3], V. ARRIZON[3], I. CRAWFORD[3], C. HALL[3], J. K. JIN[2], K. ROSALES[4], J. REIMER[3];
[1]Departments of Psychology and Computer Sci., [2]Dept. of Computer Sci., [3]Dept. of Psychology, [4]Dept. of Child, Adolescent, and Family Studies, California State University, San Bernardino, San Bernardino, CA

**Abstract:** Proactive cognitive control is associated with sustained dorsolateral prefrontal cortex (DLPFC) activity that maintains task goals before expected demands, yet its moment-to-moment behavioral implementation is less understood. We tested whether manipulating control mode reorganizes delay-period gaze dynamics in 120 undergraduates performing a spatial AX-CPT with eye tracking. Participants completed three conditions: a baseline condition, a proactive-instruction condition that encouraged cue maintenance across the delay, and a reactive no-go condition. We analyzed cue-probe delay gaze using three complementary model-based approaches: time-resolved decoding of cue identity, TCN/GRU trajectory clustering linked to individual differences, and a 6-state Gaussian hidden Markov model (HMM). Across analyses, the control-mode manipulation produced systematic differences in gaze dynamics. Cue identity was decodable from gaze throughout the delay, with proactive control producing higher accuracy and earlier emergence of cue information than baseline or reactive control. The HMM decomposed gaze into latent states related to cue maintenance, anticipatory spatial orienting, saccade/transit, and central/other gaze. Relative to baseline, proactive control shifted state occupancy away from cue maintenance and toward anticipatory orienting, with orienting emerging earlier in the delay. Compared with reactive control, proactive control did not simply increase total orienting; gaze was more selectively directed toward the cue-predicted probe location, indicating greater spatial precision. Clustering further showed that these gaze dynamics were behaviorally meaningful and architecture-general: TCN and GRU models recovered the same cue-congruent orienting structure, and greater cue-fixation with reduced cue-congruent orienting predicted lower working memory capacity, especially under reactive demand. Cross-condition regressions showed that condition-specific gaze deployment predicted baseline proactive behavioral indices beyond trait-like gaze tendencies. Together, these findings show that experimentally induced control modes are reflected in time-resolved latent gaze states. Proactive control did not merely increase maintenance or gaze movement; it reorganized when cue information emerged, which gaze states dominated the delay, and how precisely gaze was directed toward expected task demands.

**Disclosures: D.M. Diaz:** None. **V. Bhatt:** None. **J. Martinez:** None. **G. Hernandez:** None. **V. Arrizon:** None. **I. Crawford:** None. **C. Hall:** None. **J.K. Jin:** None. **K. Rosales:** None. **J. Reimer:** None.

**Poster**

**PSTR200: Prefrontal Mechanisms of Executive Function in Humans and Animals**

**Location:** WCC Halls A-C

**Time:** Monday, November 16, 2026, 1:00 PM - 5:00 PM

**Program #/Poster #:** PSTR200.06/JJ8

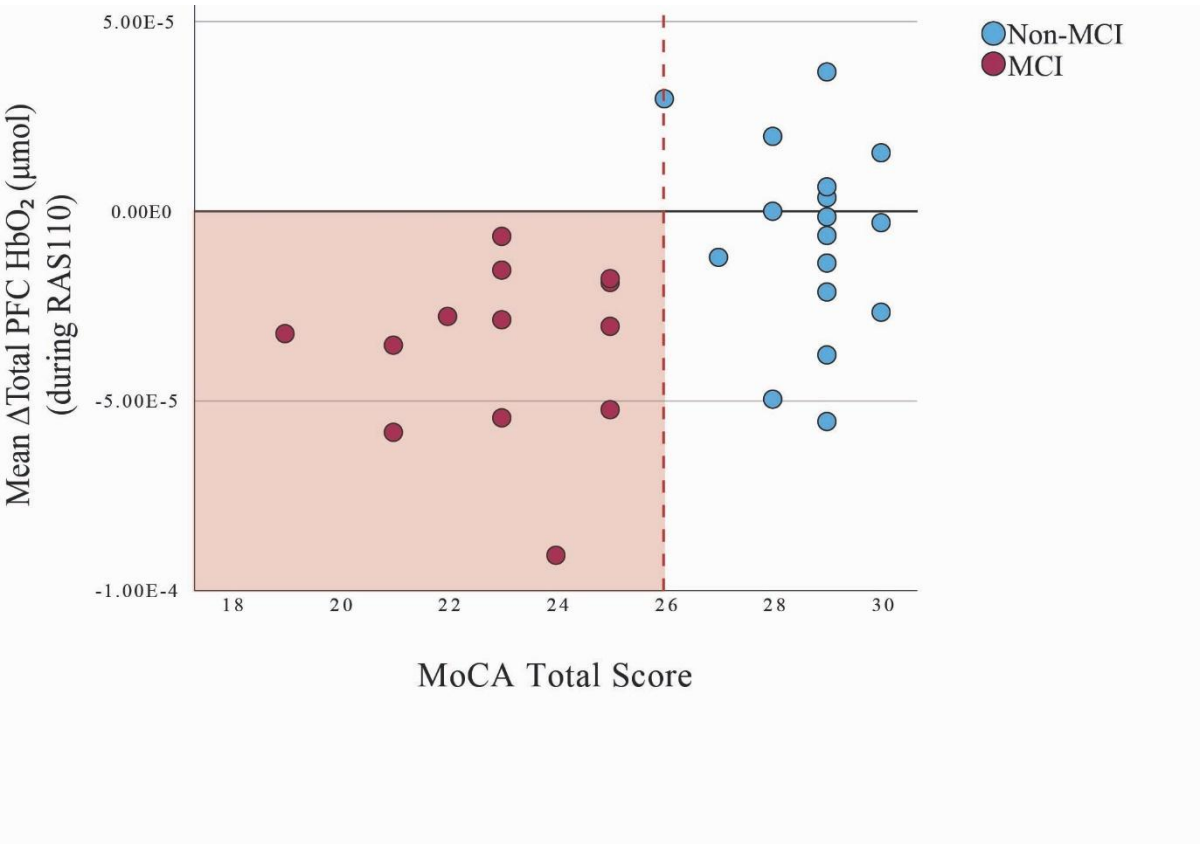
**Topic:** I.04. Executive Functions

**Support:** American Parkinson Disease Association

**Title:** Rhythmic Auditory Stimulation Reduces Prefrontal Cortex Activity during Walking in Cognitively-Impaired People with Parkinson Disease

**Authors: *N. MARRERO**, T. NORDAHL, R. SLOUTSKY, L. AWAD, A. CRONIN-GOLOMB, J. CAVANAUGH, M. A. YUCEL, T. ELLIS, F. PORCIUNCULA;
Boston Univ., Boston, MA

**Abstract:** People with Parkinson disease (PwPD) lose walking automaticity and rely on cognitive resources supported by the prefrontal cortex (PFC). Rhythmic auditory stimulation (RAS) may improve walking automaticity, though its effect may vary with cognitive ability. We hypothesized that PwPD with poorer cognition would have greater reductions in PFC activation during RAS-assisted walking, relative to usual walking, indicating reduced cognitive load. Thirty people with mild-moderate PD participated. Functional near-infrared spectroscopy (NIRx NIRSport2) measured PFC activation during RAS-assisted walking at 100% and 110% of usual cadence (RAS100, RAS110), relative to usual walking. Data were processed in Homer3 with motion correction and drift regression within the general linear model. Changes in oxygenated hemoglobin ($HbO_2$) were averaged across frontal regions to calculate total PFC activation. Global cognition was assessed using the Montreal Cognitive Assessment (MoCA). Spearman correlations assessed the relation between PFC activation and MoCA scores. Participants were dichotomized into mild cognitive impairment (MCI; MoCA <26; n=13) and Non-MCI (MoCA ≥26; n=17) groups. Between-group differences in PFC activation were examined using repeated-measures analysis of covariance, with comfortable walking speed as a covariate. PFC $HbO_2$ in the full sample decreased in both RAS conditions, indicating reduced cognitive load. Lower MoCA scores (poorer cognition) correlated with greater $HbO_2$ decreases during RAS110 ($\rho$=.48, $p$=.007) (Fig. 1). Between-group comparisons revealed that the MCI group, relative to the Non-MCI group, had greater $HbO_2$ reductions during both RAS conditions, with a significant difference during RAS110 ($d$=.92, $p$=.005). Reduced PFC $HbO_2$ during RAS suggested decreased attentional demands, with cognitively-impaired PwPD showing more robust responses, as cognitive limitations may facilitate greater engagement of alternative pathways. RAS shows promise for reducing cognitive load during walking, particularly in cognitively-impaired PwPD.




**Disclosures: N. Marrero:** None. **T. Nordahl:** None. **R. Sloutsky:** None. **L. Awad:** None. **A. Cronin-Golomb:** None. **J. Cavanaugh:** None. **M.A. Yucel:** None. **T. Ellis:** None. **F. Porciuncula:** None.

**Poster**

**PSTR200: Prefrontal Mechanisms of Executive Function in Humans and Animals**

**Location:** WCC Halls A-C

**Time:** Monday, November 16, 2026, 1:00 PM - 5:00 PM

**Program #/Poster #:** PSTR200.07/JJ9

**Topic:** I.04. Executive Functions

**Support:** NIH R01 MH125497
ONR MURI N00014-23-2792

**Title:** Changes in Representational Geometry Explain Improvements in Multi-tasking

**Authors: *A. V. SRINIVASAN**[1], A. KIKUMOTO[2,3], K. SHIBATA[4], D. BADRE[5];
[1]Psychology, Yale Univ., New Haven, CT; [2]Brown Univ., Providence, RI, ; [3]Univ. of Maryland, College Park, MD; [4]Ctr. for Brain Sci., RIKEN, Chikusa-ku, Nagoya-shi, Aichi, Japan; [5]Neurosci. Inst., Carnegie Mellon Univ., Pittsburgh, PA

**Abstract:** Behavioral costs associated with multitasking can be reduced with extended practice. These improvements have been explained by increased separability of the task representations, suggesting that practice reduces interference by minimizing overlap between representations. However, it is unknown how practice transforms the underlying geometry of task representations to do so. To characterize these changes, we had participants (n=24) complete 6 sessions of a PRP paradigm. On each trial, participants saw and made responses to 2 stimuli. Stimuli were colored digits that varied along *color* (Red or Blue, Bold or Faint) and *number* (High or Low, Odd or Even) feature dimensions. The correct responses (Left or Right) were determined by which stimulus features were cued (e.g., a bold, blue "7" is "Bold", "Blue", "High", and "Odd"). In Single Task blocks, participants responded to the same feature in both stimuli, while in Dual Task blocks, they were cued to respond to a different feature for the second stimulus. The set of 16 stimuli spanned the entire stimulus feature space thereby creating feature overlap between tasks and maximizing the potential for overlapping task representations. Participants showed increases in reaction time and error rates for the second stimulus in Dual Task blocks compared to Single Task blocks. Additionally, these costs decreased over sessions, consistent with behavioral improvement reported in the multitasking literature. For the sessions with EEG recordings, we trained and tested a decoder in a time-resolved manner on various task features in the preprocessed EEG data, time-locked to participant responses. We were particularly interested in task representations in the period leading up to the second response. Decoding accuracy for task (High/Low, Odd/Even, Red/Blue, Bold/Faint), response decision (Left/Right), and the unique conjunction of task and decision all showed significantly greater improvement over sessions in Dual-Task trials than in Single-Task trials; however, only improvements in decoding of the task x decision conjunction predicted behavioral improvement in the second response time. Consistent with previous literature on conjunctive representations in action selection, these preliminary results suggest that improvement in multitasking is related to greater access to high-dimensional conjunctive representations of task features.

**Disclosures: A.V. Srinivasan:** None. **K. Shibata:** None. **D. Badre:** None.

**Poster**

**PSTR200: Prefrontal Mechanisms of Executive Function in Humans and Animals**

**Location:** WCC Halls A-C

**Time:** Monday, November 16, 2026, 1:00 PM - 5:00 PM

**Program #/Poster #:** PSTR200.08/JJ10

**Topic:** I.04. Executive Functions

**Support:** NRF Grant RS-2025-00562132
TIPS Program RS-2024-00508829
NST Grant GTL25071-000

**Title:** Real-time modulation of glymphatic-lymphatic transport and cognitive function by taVNS in mice and humans

**Authors: *S. KIM**[1], H. YOON[1], G. CHUNG[2];
[1]Dept. of Physiol., Kyung Hee Univ. Col. of Korean Med., Seoul, Korea, Republic of; [2]Dept. of Physiol., Chungbuk Natl. Univ. Sch. of Med., Cheongju, Korea, Republic of

**Abstract:** Transcutaneous auricular vagus nerve stimulation (taVNS) has recently gained attention as a non-invasive neuromodulatory approach with potential to reorganize brain physiology and enhance cognitive function, yet its mechanistic underpinnings remain incompletely understood. In mice, fluorescent cerebrospinal fluid (CSF) tracers were injected into the cisterna magna and monitored using transcranial macroscopic imaging and deep cervical lymph node (DCLN) imaging to assess glymphatic-lymphatic transport under taVNS. Behavioral outcomes were evaluated with novel object recognition (NOR). In parallel, twenty-three healthy adults were randomized to taVNS or sham stimulation during Stroop task performance. Electroencephalography (EEG) was recorded before, during, and after stimulation to examine oscillatory activity associated with cognitive demand. In vivo imaging revealed that taVNS accelerated CSF tracer redistribution in the middle cerebral artery region and facilitated downstream lymphatic drainage, accompanied by improved NOR discrimination without changes in locomotor activity. In humans, taVNS enhanced Stroop accuracy under incongruent conditions and attenuated the escalation of high beta-band (20-30 Hz) power at frontal sites, particularly Fp1, compared to sham stimulation. Together, these results highlight a mechanistic link between autonomic regulation of brain clearance pathways and modulation of cortical oscillatory dynamics, positioning taVNS as a promising intervention for optimizing cognition.

**Disclosures: S. Kim:** E. Ownership Interest (stock, stock options, royalty, receipt of intellectual property rights/patent holder, excluding diversified mutual funds); Neurogrin Inc. **H. Yoon:** A. Employment/Salary (full or part-time):; Neurogrin Inc. **G. Chung:** E. Ownership Interest (stock, stock options, royalty, receipt of intellectual property rights/patent holder, excluding diversified mutual funds); Neurogrin Inc..

**Poster**

**PSTR200: Prefrontal Mechanisms of Executive Function in Humans and Animals**

**Location:** WCC Halls A-C

**Time:** Monday, November 16, 2026, 1:00 PM - 5:00 PM

**Program #/Poster #:** PSTR200.09/JJ11

**Topic:** I.04. Executive Functions

**Support:** NIH K12GM081266

**Title:** Psilocybin’s effects on cognitive flexibility depend on the underlying circuit dysfunction

**Authors: *C. LIU**[1], E. M. HO[2], A. S. ENOS[2], B. BAUBLYTE[1], I. M. LUNA[3], A. R. KOSCHE[2], V. S. SOHAL[2];
[2]Dept. of Psychiatry, [1]UCSF, San Francisco, CA; [3]Univ. of California, San Francisco, San Francisco, CA

**Abstract:** Psychedelic drugs show immense potential for treating some psychiatric symptoms, but their effects are not always therapeutic. Whether or not treatment is efficacious may depend on the specific neural mechanisms underlying superficially similar behavioral symptoms. By leveraging mouse models and optogenetic manipulations, we can target distinct neural circuits to impair performance in an extradimensional rule shifting task through multiple pathways and compare the effects of systemic psilocybin administration. Building upon prior work in the lab, we induced cognitive inflexibility by targeting 2 distinct neural pathways: 1) stimulation of dopaminergic projections from the ventral tegmental area (VTA) to the medial prefrontal cortex (mPFC) or 2) inhibition of cross-hemispheric mPFC parvalbumin (PV) projections. We found that acute 2 mg/kg psilocybin rescues deficits in mice caused by stimulation of VTA → mPFC TH+ projections. Psilocybin also continued to prevent impairment 24 hours after treatment, suggesting a lasting, protective effect. In contrast, animals with optogenetic inhibition of mPFC cross-hemispheric PV projections continued to perform poorly after acute psilocybin administration. Photometry recordings of a genetically-encoded calcium sensor in L5 mPFC cells that project to the mediodorsal thalamus (MD) reveal abnormally heightened neuronal activity after VTA à mPFC stimulation. Psilocybin treatment attenuated elevated mPFC-MD calcium activity acutely and 24 hours after treatment. Whole-cell electrophysiology recordings performed in corticothalamic (CT) L5 mPFC cells revealed that D2R-dependent afterdepolarization is prevented by psilocybin 24 hours after treatment. Psilocybin also potentiates MD inputs to L5 mPFC CT cells, evidenced by increased amplitude of optogenetically-evoked EPSPs and EPSCs. Altogether, our work suggests that psilocybin induces plasticity in L5 mPFC-MD cells that restore normal activity during aberrant activation of VTA à mPFC inputs, rescuing cognitive flexibility when caused by mesoprefrontal circuit dysfunction.

**Disclosures: C. Liu:** None. **E.M. Ho:** None. **A.S. Enos:** None. **B. Baublyte:** None. **I.M. Luna:** None. **A.R. Kosche:** None. **V.S. Sohal:** None.

**Poster**

**PSTR200: Prefrontal Mechanisms of Executive Function in Humans and Animals**

**Location:** WCC Halls A-C

**Time:** Monday, November 16, 2026, 1:00 PM - 5:00 PM

**Program #/Poster #:** PSTR200.10/JJ12

**Topic:** I.04. Executive Functions

**Support:** NIH R01MH129835
NIH R01NS116594

**Title:** Prefrontal-insular gamma synchrony promotes modality specific cognitive flexibility

**Authors: *L. L. HAGOPIAN**[1], A. J. PHENSY DOS SANTOS[2], V. S. SOHAL[3];
[1]Univ. of California, San Francisco, San Francisco, CA; [2]Psychiatry, Univ. of California, San Francisco, San Mateo, CA; [3]Dept. of Psychiatry, Univ. of California, San Francisco, San Francisco, CA

**Abstract:** The ability to alter decision-making strategies in order to account for changes in the salience of sensory cues which indicate the availability of potential rewards is critical for behavioral adaptation. The medial prefrontal cortex (mPFC) is important for this cognitive function (Miller et al., 2001) and produces gamma synchrony that is necessary for behavioral flexibility in mice (Cho et al., 2015; Cho et al., 2020; Cho et al., 2023). However, it is unclear whether this gamma synchrony is restricted to the mPFC, or whether it might also play a role in communication with other brain structures that is necessary for flexible and adaptive behavior. In particular, the insula is also known to be necessary for many cognitive functions (Gehrlach et al., 2020; Menon et al., 2010; Kayyal et al., 2021) and has bidirectional connectivity with the mPFC (Gehrlach et al., 2020). Here we use optogenetic inhibition of medial insular cortex (mIC)-to-mPFC projecting (mIC-mPFC) cell bodies and axon terminals during a rule shifting task in mice. We find that this projection is necessary for learning rule shifts specifically when the sensory cue which signals the location of a hidden reward shifts from a texture to an odor. We further assayed gamma synchrony between parvalbumin interneurons (PVIs) in the mIC and mPFC during this task using a novel recording technique called transmembrane electrical measurements performed optically (TEMPO) (Marshall et al., 2016; Cho et al., Nat Neurosci, 2020; Phensy et al., Neuron, 2026). We find that mIC-mPFC PVI gamma synchrony increases during shifts to odors, but decreases during shifts to textures. Finally, this gamma synchrony was shown to be necessary for rule shifts to odor cues by comparing the effects of optogenetically stimulating mIC and mPFC PVIs either in or out-of-phase. Overall, the results show that mIC-mPFC communication is necessary for optimal learning of shifts from texture to odor-based rules, and that gamma synchrony is a critical component of this communication.

**Disclosures: L.L. Hagopian:** None. **A.J. Phensy dos Santos:** None. **V.S. Sohal:** None.

**Poster**

**PSTR200: Prefrontal Mechanisms of Executive Function in Humans and Animals**

**Location:** WCC Halls A-C

**Time:** Monday, November 16, 2026, 1:00 PM - 5:00 PM

**Program #/Poster #:** PSTR200.11/JJ13

**Topic:** I.04. Executive Functions

**Support:** Cure Syngap1
NIH Grant R01MH129835
BBRF Young Investigator Grant

**Title:** Prefrontal Long-Range Parvalbumin Circuit Dysfunction Underlies Cognitive Inflexibility in Syngap1 Haploinsufficient Mice

**Authors: *X. ZHU**[1], L. HAGOPIAN[2], V. S. SOHAL[3];
[1]UCSF, San Francisco, CA; [2]Psychiatry, [3]Dept. of Psychiatry, Univ. of California, San Francisco, San Francisco, CA

**Abstract:** *Syngap1* loss-of-function mutations cause intellectual disability, epilepsy, and autism spectrum disorder. Although *Syngap1* haploinsufficient mice exhibit multiple learning abnormalities, mechanisms underlying cognitive inflexibility remain unclear. We recently identified a long-range inhibitory projection from prefrontal callosal parvalbumin interneurons (cPV) that supports extradimensional rule shift learning. Notably, rule shift learning normally strengthens cPV synapses, inhibiting cPV synapses prevents rule shift learning, and 40Hz stimulation cPV synapses can rescue rule shifting deficits. Here, we tested whether this circuit is disrupted in Syngap1+/- mice, contributes to their impaired cognitive flexibility and can be targeted to improve their cognitive flexibility. In a rule shift (RS) task, Syngap1+/- mice showed increases in the trials needed to reach the learning criterion and perseverative errors, indicating cognitive inflexibility. To elucidate circuit mechanisms, we used pathway-specific slice optogenetics and found impaired cPV synaptic plasticity in Syngap1+/- mice after RS learning, including reduced synaptic strength and paired-pulse depression. These changes resembled those produced by optogenetic inhibition of cPV terminals in wild-type mice, suggesting convergence on a cPV circuit deficit. We next applied *in vivo* behavioral optogenetics and found that both bilateral 40Hz in-phase stimulation of cPV somata and 40Hz cPV terminal stimulation restored RS performance in Syngap1+/- mice, indicating that enhancing cPV circuit activity is sufficient to rescue cognitive inflexibility. Together, these findings reveal a cognitive flexibility deficit in Syngap1 haploinsufficient mice, implicate impaired cPV plasticity as an underlying circuit mechanism, and identify cPV synapses as a potential therapeutic target for rescuing cognitive flexibility in neurodevelopmental disorders.

**Disclosures: X. Zhu:** None. **L. Hagopian:** None. **V.S. Sohal:** None.

**Poster**

**PSTR200: Prefrontal Mechanisms of Executive Function in Humans and Animals**

**Location:** WCC Halls A-C

**Time:** Monday, November 16, 2026, 1:00 PM - 5:00 PM

**Program #/Poster #:** PSTR200.12/JJ14

**Topic:** I.04. Executive Functions

**Support:** R01NS116594
R01MH129835

**Title:** Prefrontal astrocytes coordinate interhemispheric parvalbumin interneuron γ-synchrony and plasticity to enable cognitive flexibility

**Authors: *A. J. PHENSY DOS SANTOS**[1], L. SHINDY[2], X. ZHU[5], L. HAGOPIAN[3], R. VIGNESH[6], V. S. SOHAL[4];
[1]Univ. of California, San Francisco, San Mateo, CA; [2]Univ. of California, San Francisco, Duarte, CA; [3]Psychiatry, [4]Dept. of Psychiatry, Univ. of California, San Francisco, San Francisco, CA; [5]Psychiatry and Behavioral Sci., UCSF, San Francisco, CA; [6]Indian Inst. of Sci., Bengaluru.

**Abstract:** Astrocytes are increasingly recognized as active regulators of neuronal signaling, yet how they coordinate neuronal activity during cognitive behavior remains largely unknown. Here, we show that prefrontal astrocytes are recruited during the updating of behavioral strategies and required for gamma (γ)-frequency synchronization of prefrontal parvalbumin interneurons (PVI), learning-induced GABAergic synaptic plasticity, and flexible behavior.
Using bulk calcium photometry during a rule-shift task, we found that prefrontal astrocytes exhibited outcome-related calcium responses that were strongest when mice altered their choice behavior to deviate from an outdated strategy. Intriguingly, this was the same behavioral epoch in which we observed enhanced γ-synchrony between PVI across the left and right prefrontal cortices. To test whether astrocyte activity was required for this behavioral deviation and increase in PVI γ-synchrony, we used astrocyte-targeted hM3Dq DREADDs, which we confirmed suppressed task-evoked astrocytic calcium events following CNO administration. Suppressing astrocyte activity impaired extradimensional rule-shift performance, leading to an increase in perseverative errors and a delay in deviation from the old strategy. This behavioral deficit was also accompanied by a loss of the task-evoked γ-synchrony in prefrontal PVI, suggesting that astrocytes are necessary for coordinating high-frequency inhibitory network dynamics during flexible behavior. Importantly, 40Hz optogenetic entrainment of PVI across the left and right prefrontal cortices rescued the behavioral deficit induced by astrocyte suppression, supporting a mechanism in which astrocyte activity influences cognitive flexibility by modulating PVI γ-synchrony.
Finally, our lab has recently shown that performing an extra-dimensional shift potentiates callosal GABAergic synapses from PVI onto neurons in the contralateral prefrontal cortex which target the mediodorsal thalamus (PFC→MD neurons). Here, using slice electrophysiology following the rule-shift task, we reveal that astrocyte suppression abolishes this learning-induced GABAergic synaptic plasticity from long-range PVI onto contralateral PFC→MD neurons. Together, these findings reveal that prefrontal astrocytes support cognitive flexibility by coordinating both interhemispheric γ-synchrony and GABAergic synaptic plasticity in prefrontal circuits.

**Disclosures: A.J. Phensy dos Santos:** None. **L. Shindy:** None. **X. Zhu:** None. **L. Hagopian:** None. **V.S. Sohal:** None.

**Poster**

**PSTR200: Prefrontal Mechanisms of Executive Function in Humans and Animals**

**Location:** WCC Halls A-C

**Time:** Monday, November 16, 2026, 1:00 PM - 5:00 PM

**Program #/Poster #:** PSTR200.13/JJ15

**Topic:** I.04. Executive Functions

**Support:** NCI CA224672
NCI CA285183
DICR POST-BACC-24-1341392-01-DPBACC

**Title:** The multimodal antidepressant vortioxetine rescues cognitive deficits induced by androgen deprivation therapy but not by prostate cancer

**Authors: *G. TORRES**[1], S. E. BULIN[3], D. ARENAS[4], B. W. LATIMER[2], D. A. MORILAK[3]; [1]Pharmacol., [2]Univ. of Texas Hlth. Sci. Ctr. at San Antonio, San Antonio, TX; [3]Pharmacol., UT Hlth. Sci. Ctr. San Antonio, San Antonio, TX; [4]Univ. of Texas Hlth. San Antonio, San Antonio, TX

**Abstract:** Prostate cancer is the most common type of cancer in American men after basal cell and squamous cell carcinoma, and it's the leading cause of cancer death after lung cancer. Androgen deprivation therapy (ADT) is an effective treatment for prostate cancer and as an adjuvant to treat localized tumors. Unfortunately, more than half of patients treated with ADT experience a decline in cognitive domains, such as cognitive flexibility and memory, mediated by the medial prefrontal cortex (mPFC) and hippocampus, respectively. Vortioxetine (VTX) is a multimodal antidepressant that has been shown to improve cognition independently when compared to other antidepressants. We have previously shown that ADT induces deficits in cognitive flexibility and visuospatial memory in healthy cancer-free rats, and that chronic administration of VTX rescued these deficits. However, the effects of VTX on cognition after ADT in the context of prostate cancer pathophysiology remain unexplored. To address this, adult male Copenhagen rats were ectopically implanted with syngeneic prostate tumors, treated with the GnRH antagonist Degarelix (DGX) for ADT, and administered VTX (40mg/kg/day) via the diet. The novel object location (NOL) test and attentional set-shifting test (AST) were conducted starting 21 days after ADT onset. Results from the hippocampal-mediated NOL indicate that animals with either tumor alone or tumors treated with DGX displayed impaired visuospatial memory ($F(4, 81)=x.xx$; $p <0.01$; n=14-20/grp). When compared to the sham control group, the tumor-DGX group treated with VTX was not significantly different ($p=0.88$), indicating a rescue in hippocampal deficits. Similarly for the mPFC-mediated AST, rats with tumor alone or tumor treated with ADT had significantly impaired cognitive flexibility ($F(4, 81) =x.xx$; $p <0.001$, n=16-21/grp), and these deficits were reversed by VTX only in the tumor-DGX group ($p<0.01$). In conclusion, ADT and prostate tumor presence both independently resulted in impairments to hippocampal and mPFC-dependent cognition. Further, impairment induced by ADT, but not tumor alone, was reversed by chronic administration of VTX. This evidence suggests that ADT and cancer induce similar cognitive deficits but through separate mechanisms. Ongoing experiments focus on evaluating the effects of acute VTX treatment on ADT-induced cognitive deficits, providing us insight into its immediate mechanisms of action, the early pharmacodynamic effects in the mPFC, and its potential suitability as a fast-acting treatment to alleviate cognitive deficits observed in patients with prostate cancer who receive ADT treatment.

**Disclosures: G. Torres:** None. **S.E. Bulin:** None. **D. Arenas:** None. **B.W. Latimer:** None. **D.A. Morilak:** None.

**Poster**

**PSTR200: Prefrontal Mechanisms of Executive Function in Humans and Animals**

**Location:** WCC Halls A-C

**Time:** Monday, November 16, 2026, 1:00 PM - 5:00 PM

**Program #/Poster #:** PSTR200.14/JJ16

**Topic:** I.04. Executive Functions

**Support:** NIH Grant R01 CA285183

**Title:** Cognitive Effects of Ondansetron and Citalopram On Androgen Deprivation Therapy-Induced Deficits in a Rat Model of Prostate Cancer

**Authors: *D. ARENAS**[1], S. E. BULIN[2], D. A. MORILAK[2];
[1]Pharmacol., Univ. of Texas Hlth. San Antonio, San Antonio, TX; [2]Pharmacol., UT Hlth. Sci. Ctr. San Antonio, San Antonio, TX

**Abstract:** Androgen deprivation therapy (ADT) is an effective treatment for prostate cancer, helping increase five-year survival rates to >98%. However, ADT also causes adverse effects, including cognitive deficits mediated in the medial prefrontal cortex (mPFC) and hippocampus, that impact quality of life for patients and increase the risk for age-related cognitive decline. We have shown previously that ADT impairs visuospatial memory and executive function in healthy male Sprague-Dawley rats and male Copenhagen rats implanted with syngeneic prostate tumors. Vortioxetine (VTX), a multimodal antidepressant, reversed these impairments. However, the specific mechanism underlying the beneficial effects of VTX remains unknown. To address this, we are testing drugs that act selectively at two high-affinity targets of VTX: ondansetron (OND), a 5-HT3 receptor antagonist, and citalopram (CIT), an SSRI that blocks SERT. To determine if either or both of these targets are responsible for the beneficial effects of VTX, we will test if cognitive deficits in Copenhagen rats with prostate cancer treated with ADT are reversed by OND or CIT.As VTX was previously administered in the diet, we first confirmed that OND and CIT in the diet would produce clinically relevant blood and brain levels. Rats were fed OND (7.5 mg/kg) or CIT (20/mg/kg) chow for 3 weeks, after which they were sacrificed, and blood and brains collected. Clinically relevant drug levels were observed in blood (OND: 22.97 ng/mL ± 5.95; CIT: 538.67 ng/mL ± 70.27), and brain for CIT (3.19 ng/mL ± 0.439). Brain levels of OND were low but detectable three hours after ingestion (0.0132 ng/mL ± 0.004 SEM), consistent with its rapid metabolism. For behavioral testing, male Copenhagen rats were implanted subcutaneously in the flank with syngeneic prostate tumors derived from Dunning R3327-G rat prostate cancer cells. After 3-4 weeks, tumors were palpable at approx. 1 $cm^3$, at which time tumor- and sham-implanted rats were treated with the GnRH antagonist, degarelix (DGX; 3 mg/kg, s.c.) for ADT or vehicle (5% mannitol). On the same day, rats were started on OND, CIT, or control diet. Behavioral tests were conducted starting 21 days after giving DGX.The Attentional Set-Shifting Test (AST) was used to measure deficits in cognitive flexibility, an index of mPFC function, and the NOL tested visuospatial memory for hippocampal function. Preliminary data in ongoing studies replicate the deficit in set-shifting in rats with tumors ($F_{(1,18)}$=4.031, p=0.059) and tumors + DGX ($F_{(1,19)}$=3.124, p=0.09). While still preliminary, it appears OND may reverse impairments in rats with tumors + DGX, but not with tumor alone, and CIT appears to have no effects.

**Disclosures: D. Arenas:** None. **S.E. Bulin:** None. **D.A. Morilak:** None.

**Poster**

**PSTR200: Prefrontal Mechanisms of Executive Function in Humans and Animals**

**Location:** WCC Halls A-C

**Time:** Monday, November 16, 2026, 1:00 PM - 5:00 PM

**Program #/Poster #:** PSTR200.15/JJ17

**Topic:** I.04. Executive Functions

**Title:** Universal Geometry of Compositional Construction in Prefrontal Cortex

**Authors: *M. MANAKOV**[1], M. PROSKURIN[1], H. WANG[2], E. KULESHOVA[1], A. Y. KARPOVA[3];
[1]Janelia Res. Campus, Ashburn, VA; [2]HHMI Janelia, Janelia, Ningbo, China; [3]HHMI/ Janelia Res. Campus, Ashburn, VA

**Abstract:** Compositional generation underlies the systematic and essentially unlimited construction of complex concepts from simpler parts, as is foundational to intelligent behavior, but its underlying neural mechanisms remain unclear. Here we reveal a neural implementation of hierarchical compositional construction of abstract sequences. We demonstrate that in an open-ended setting with very sparse feedback, rats innately utilize hierarchical composition to construct adaptive action sequences that would have been difficult to discover from scratch. Prefrontal neural population representations of these abstract sequences adhere to a low-dimensional format that encodes the orderly progression of elemental units comprising the sequence while converging to a sequence-general endpoint. Higher-level compositions in the hierarchy are systematically related to their lower-level constituent parts, reusing much of the representation, while providing context separation and satisfying format constraints. These neural representations are geometrically identical across animals, pointing to a convergent solution for how knowledge is hierarchically assembled via a compositional mechanism.

**Disclosures: M. Manakov:** None. **M. Proskurin:** None. **H. Wang:** None. **E. Kuleshova:** None. **A.Y. Karpova:** None.

**Poster**

**PSTR200: Prefrontal Mechanisms of Executive Function in Humans and Animals**

**Location:** WCC Halls A-C

**Time:** Monday, November 16, 2026, 1:00 PM - 5:00 PM

**Program #/Poster #:** PSTR200.16/JJ18

**Topic:** I.04. Executive Functions

**Support:** Medical Research Council Grant
NIH Oxford-Cambridge Scholarship

**Title:** Prefrontal layer 6 Drd1a-Cre+ neurons mediate dopaminergic cortical network activation and facilitate reversal learning in mice

**Authors: *M. ABUELEM**[1,2,3], L. MESSORE[2], Y. CHEN[2], W. SILVER[2], D. A. LEOPOLD[3], T. AKAM[2], E. O. MANN[2], Z. MOLNÁR[2];
[1]Natl. Inst. of Hlth. / Univ. of Oxford, Oxford, United Kingdom; [2]Univ. of Oxford, Oxford, United Kingdom; [3]NIH, Bethesda, MD

**Abstract:** Cortical layer 6 (L6) neurons play an important role in driving cortical arousal via the higher-order corticothalamic system. Many of these L6 neurons are remnants of the transient developmental subplate, which contains some of the earliest generated cortical neurons involved in thalamocortical circuit development and implicated in neurodevelopmental disorders like autism and schizophrenia. In the murine somatosensory cortex, a subpopulation of L6 neurons expressing the dopamine D1 receptor (L6-*Drd1a*) selectively projects to higher-order thalamic nuclei and is highly sensitive to the wake-promoting neuropeptide orexin, playing an important role in gating cortical arousal and anxiety behavior. However, in the prefrontal cortex (PFC), the functional circuitry of L6-*Drd1a* neurons and their role in dopaminergic cortical network activation and reward learning remain poorly understood. Thus, we investigated the effects of chronic genetic 'silencing' of L6-*Drd1a* neurons using a *Snap25* conditional knockout mouse model (*Drd1a-Cre*$^{+/-}$*;Snap25*$^{fl/fl}$*;tdTomato*$^{STOPfl/fl}$), along with the effects of optogenetic stimulation of L6-*Drd1a* neurons, on dopaminergic modulation of PFC network activity in acute slices using high-density multielectrode arrays and whole-cell patch clamp recordings. We then investigated *in vivo* L6-*Drd1a* activity compared to L5-*Rbp4* neurons using freely-moving fiber photometry recordings, along with the effects of bilateral caspase-mediated PFC L6-*Drd1a* neuronal ablation, during operant conditioning and probabilistic reversal learning. We found that dopamine D1 receptor agonist SKF-81297 selectively increased L6-*Drd1a* intrinsic excitability compared to other L6 neurons, which induced regional patterns of PFC network activity that was eliminated upon 'silencing' L6-*Drd1a* neurons. Optogenetic stimulation of L6-*Drd1a* neurons evoked excitatory postsynaptic potentials in nearby L5 pyramidal neurons that also induced PFC network activation. During operant conditioning and probabilistic reversal learning, we found that L6-*Drd1a* neurons responded to reward while L5-*Rbp4* neurons responded to movement initiation. Caspase-mediated PFC L6-*Drd1a* ablation selectively impaired reversal learning compared to initial acquisition by significantly increasing perseveration to previously rewarded stimuli. These findings provide novel insight into the role of PFC L6-*Drd1a* neurons in mediating dopaminergic cortical network activation and facilitating reversal learning in a laminar, cell type-specific manner, with relevant therapeutic implications for learning-related disorders.

**Disclosures: M. Abuelem:** None. **L. Messore:** None. **Y. Chen:** None. **W. Silver:** None. **D.A. Leopold:** None. **T. Akam:** None. **E.O. Mann:** None. **Z. Molnár:** None.

**Poster**

**PSTR200: Prefrontal Mechanisms of Executive Function in Humans and Animals**

**Location:** WCC Halls A-C

**Time:** Monday, November 16, 2026, 1:00 PM - 5:00 PM

**Program #/Poster #:** PSTR200.17/JJ19

**Topic:** I.04. Executive Functions

**Title:** Prefrontal neural dynamics with differential reward structures in goal-directed navigation

**Authors: *Y. LIANG**, W. LI, Y. WANG, X. ZHAO;
Tsinghua Univ., Beijing, China

**Abstract:** To achieve different goals, animals need to flexibly switch behavioral strategies in the same environment. To do so, the brain is required to generate differential dynamics to fit specific behavioral needs. In goal-directed navigation, neurons in the prefrontal cortex have been shown to encode progression to the goal. However, it remains unclear how prefrontal neural representations dynamically reshape following alteration of goal structures. To address this question, we trained mice to collect rewards following two different rules in a linear track in virtual reality (VR) containing several visual patterns presented at random slots trial-by-trial. The reward was associated with a specific visual pattern under the 'pattern rule', whereas fixed at a certain position under the 'position rule'. We find that a subset of mPFC neurons exhibited preparatory activities that encoded progression to potentially rewarded slots under the 'pattern rule'. Such representation pattern became more prominent after mice learned to flexibly shift between the two rules. Together, our findings suggest that the mPFC undergoes experience-dependent reorganization to reflect potential goal structures in an environment, which may support flexible action switching.

**Disclosures: Y. Liang:** None. **W. Li:** None. **Y. Wang:** None. **X. Zhao:** None.

**Poster**

**PSTR200: Prefrontal Mechanisms of Executive Function in Humans and Animals**

**Location:** WCC Halls A-C

**Time:** Monday, November 16, 2026, 1:00 PM - 5:00 PM

**Program #/Poster #:** PSTR200.18/JJ20

**Topic:** I.04. Executive Functions

**Support:** NINDS R01NS120987

**Title:** Dorsoventral gradients in prefrontal ramping activity during interval timing

**Authors: *X. DING**[1], M. A. WEBER[1], A. BOVA[1], S. GUERRERO[2], Y.-C. KIM[1], N. S. NARAYANAN[3];
[1]Univ. of Iowa, Iowa City, IA; [2]Univ. of Iowa, Aurora, IL; [3]Neurol., Univ. of Iowa, Iowa City, IA

**Abstract:** Neurons in the prefrontal cortex (PFC) exhibit highly dynamic activity during cognitive processes, with individual neurons encoding multiple task-related variables. We studied how prefrontal neurons encode a single variable: time. Our previous work has shown that PFC neurons represent temporal information through monotonic changes in firing rate, or ramping, across temporal intervals. However, it remains unclear whether ramping and other temporal signals are homogeneously distributed throughout the PFC. To address this question, we used high-density electrophysiological recordings spanning broad regions of the mouse PFC

during an interval timing task. These recordings allowed us to map neuronal activity to dorsoventral and laminar positions within the PFC. We found that PFC neurons exhibited heterogeneous ramping activity, including increasing, decreasing, and non-ramping patterns. Ramping slope was positively correlated with dorsoventral (DV) position, with neurons located in more dorsal regions exhibiting stronger ramping activity. Furthermore, the association between DV position and ramping slope was more pronounced in superficial than deep cortical layers. Together, these findings highlight the potential contribution of spatial organization to functional dynamics in the PFC during interval timing.

**Disclosures: X. Ding:** None. **M.A. Weber:** None. **A. Bova:** None. **S. Guerrero:** None. **Y. Kim:** None. **N.S. Narayanan:** None.

**Poster**

**PSTR200: Prefrontal Mechanisms of Executive Function in Humans and Animals**

**Location:** WCC Halls A-C

**Time:** Monday, November 16, 2026, 1:00 PM - 5:00 PM

**Program #/Poster #:** PSTR200.19/JJ21

**Topic:** I.04. Executive Functions

**Support:** NIMH R01MH128344
NIMH R01MH110594
NIMH R01MH116937
Conte Center on the Neurocircuitry of OCD MH10643

**Title:** Thalamic Population States Coordinate Long-Range Prefrontal Functional Connectivity

**Authors: *T. TANG**[1], M. YUN[3], S. ANAND[4], G. TAVONI[5,6,7], I. E. MONOSOV[1,2]; [1]Neurosci., [2]Zanvyl Krieger Mind/Brain Inst., Johns Hopkins Univ., Baltimore, MD; [3]Inst. of Med., Univ. of Tsukuba, Tsukuba, Japan; [4]Washington Univ. in St. Louis, St. Louis, MO; [5]Neurosci., [6]Electrical and Systems Engin., [7]Physics, Washington Univ. in St. Louis, Saint Louis, MO

**Abstract:** Human and animal behavior unfolds across short and long timescales. A driver returning from work may react to a changing traffic light while simultaneously being guided by slower internal conditions—such as engagement with external stimuli and responsiveness to them, commonly referred to as arousal. Arousal can shift flexibly, even abruptly, and is thought to rely on widespread, coordinated neural processes. Yet which large-scale spiking regimes instantiate arousal-related internal states, and how they are coordinated across the brain, remain unclear. Functional connectivity (FC) measured by fMRI and local field potentials is known to fluctuate with arousal and reflect multi-region coordination, but how neuron-level FC changes across long-range connections and how such changes are coordinated across brain areas remains unclear. The mediodorsal (MD) thalamus is a compelling candidate for this coordinating role: it projects broadly to prefrontal areas important for regulating internal states, including the anterior cingulate cortex (ACC) and ventral lateral prefrontal cortex (VLPFC). While MD neurons are

sensitive to arousal states, how MD activity regulates prefrontal networks remains unclear. To study the neuronal basis of arousal, we recorded population activity from MD and its downstream prefrontal areas, ACC and VLPFC, and examined FC across them. We found distinct ACC-VLPFC FC patterns across arousal states: neurons fired more synchronously in rest-like states, resulting in increased FC. Surprisingly, neuron-by-neuron FC patterns were uncorrelated across arousal states, suggesting a state-dependent functional structure. Crucially, MD inactivation causally exerted state-dependent remapping in prefrontal FC and unexpectedly produced new functional connections. Post-inactivation networks were similar to each other but different from pre-inactivation states. We next investigated how MD inactivation may cause these changes through detailed analyses of MD neurons and computational modelling. We found that MD neurons shift from uncorrelated firing to synchronized population bursty patterns, producing large-scale, low-dimensional thalamic states during rest-like state. A spiking network further uncovered how thalamic synchrony induces different prefrontal connectivity across states. Modelling shows that a specific thalamocortical projection structure is required to recapitulate our results. *In vivo* retrograde tracing results supported this structure. Overall, our results reveal a thalamus-driven mechanism for coordinating distributed prefrontal networks and structuring the architecture of internal states.

**Disclosures: T. Tang:** None. **M. Yun:** None. **S. Anand:** None. **G. Tavoni:** None. **I.E. Monosov:** None.

**Poster**

**PSTR200: Prefrontal Mechanisms of Executive Function in Humans and Animals**

**Location:** WCC Halls A-C

**Time:** Monday, November 16, 2026, 1:00 PM - 5:00 PM

**Program #/Poster #:** PSTR200.20/JJ22

**Topic:** I.04. Executive Functions

**Title:** Optogenetic Manipulation of Catecholamines in the Prefrontal Cortex Influences Three Choice Serial Reaction Task Performance

**Authors: S. L. BOZARTH**, A. E. O'SHALL, C. J. E. DENNING, E. A. WEST, *M. NIEDRINGHAUS;
Rowan Univ., Stratford, NJ

**Abstract:** The medial prefrontal cortex (mPFC) is a critical brain region that supports executive function. Specifically, norepinephrinergic and dopaminergic inputs to the mPFC contribute to key executive processes, including attention and behavioral inhibition. Disruptions in these inputs, such as those observed in neuropsychiatric, neurodegenerative, and neurodevelopmental disorders, may contribute to executive dysfunction. Previously, we used fiber photometry during a 3-choice serial reaction time task (3-CSRTT) to correlate mPFC catecholamine dynamics with executive function deficits. The 3-CSRTT was selected because it provides a multidimensional assessment of executive function. Trials were self-initiated via a nose poke and began with an 8-s delay, after which one of three target ports was briefly illuminated. Nose pokes into any target

port during the delay immediately terminated the trial and were classified as premature responses. A correct response consisted of a poke into the illuminated port, whereas responses into either non-cued port were classified as incorrect. Failure to respond within 5 s of cue presentation was scored as an omission. Using this task, we previously found that elevated mPFC dopamine (DA) in the delay period was associated with premature responding. Logistic regression analyses further revealed that increased mPFC norepinephrine (NE) early in the delay predicted omissions, whereas coordinated increases in both DA and NE approximately 2s before cue presentation predicted correct responses. Here, to establish a causal relationship between mPFC catecholamine signaling and executive function, we combined optogenetic stimulation with the 3-CSRTT. A cocktail of AAV-FLEX-ChrimsonR and AAV-TH-Cre (4:1) was injected into either the locus coeruleus (LC; primary source of mPFC NE; n = 3) or the ventral tegmental area (VTA; primary source of mPFC DA; n = 3), followed by implantation of an optical ferrule targeting the mPFC. During task performance, optical stimulation (625 nm, 5-8 mW, 20 Hz, 10% duty cycle, 4-s duration) was delivered either during the first half of the delay period (early stimulation), the second half of the delay period (late stimulation), or not delivered (no stimulation). Early NE stimulation increased omission rates, whereas late DA stimulation increased premature responding relative to non-stimulated trials. These findings suggest that dysregulated mPFC NE and DA signaling may contribute to attentional lapses and behavioral disinhibition, respectively.

**Disclosures: S.L. Bozarth:** None. **A.E. O'Shall:** None. **C.J.E. Denning:** None. **E.A. West:** None. **M. Niedringhaus:** None.

**Poster**

**PSTR200: Prefrontal Mechanisms of Executive Function in Humans and Animals**

**Location:** WCC Halls A-C

**Time:** Monday, November 16, 2026, 1:00 PM - 5:00 PM

**Program #/Poster #:** PSTR200.21/JJ23

**Topic:** I.04. Executive Functions

**Support:** U01NS108680

**Title:** Prefrontal cortex modulates motor encoding during natural behavior

**Authors: *X. NIU**[1], M. SLAPIK[2], A. G. MCCONNELL[3], V. DRAGOI[4];
[1]Rice Univ., Houston, TX; [2]McGovern Med. Sch., Houston, TX; [3]Houston Methodist Res. Inst., Houston, TX; [4]Neurobio. and Anat., Methodist/Rice and Weill Cornell Med. Col., Houston, TX, TX

**Abstract:** Prefrontal cortex is thought to bridge sensory processing and motor execution through cognitive control, yet it remains unclear how it directly shapes motor representation during natural behavior. Here we studied freely moving macaques performing a naturalistic foraging task by wirelessly recording neural activity from dorsolateral prefrontal cortex and visual cortex while tracking full-body movements. We found that prefrontal populations encoded ongoing and

upcoming behavioral states, including posture and location, in a way that is modulated by task variables. Reward expectation preferentially enhanced the encoding of future actions, whereas reward outcome strengthened the encoding of past actions. These results indicate that task variables do not simply coexist with motor signals in prefrontal cortex, but dynamically shape motor encoding during natural behavior.

**Disclosures: X. Niu:** None. **M. Slapik:** None. **A.G. McConnell:** None. **V. Dragoi:** None.

**Poster**

**PSTR200: Prefrontal Mechanisms of Executive Function in Humans and Animals**

**Location:** WCC Halls A-C

**Time:** Monday, November 16, 2026, 1:00 PM - 5:00 PM

**Program #/Poster #:** PSTR200.22/JJ24

**Topic:** I.04. Executive Functions

**Support:** NIH Grant R01MH129641

**Title:** Selective $M_4$ Positive Allosteric Modulator VU6008055 Enhances Higher Executive Functions in the Nonhuman Primate: a Multitask Assessment

**Authors: *X. WEN**[1], S. SHEHREEN[2], A. NEUMANN[2], C. LINDSLEY[5], C. K. JONES[3], T. WOMELSDORF[4];
[1]Vanderbilt Brain Inst., Nashville, TN; [2]Vanderbilt Univ., Nashville, TN; [3]Vanderbilt Univ., NASHVILLE, TN; [4]Dept. of Psychology, Vanderbilt Univ., Nashville, TN; [5]Pharmacol., Vanderbilt Univ. Med. Ctr., Nashville, TN

**Abstract:** Muscarinic cholinergic receptors have been implicated to mediate some of the pro-cognitive effects of cholinergic drugs, but the specific contributions of the $M_4$ muscarinic receptor subtype have remained unclear in higher order species. We set out to close this knowledge gap by addressing two key challenges. First, we utilized VU6008055 representing a new generation of highly selective and potent $M_4$ positive allosteric modulators (PAMs) that avoid common cholinergic side effects. Second, we leverage a novel multi-task assessment battery for nonhuman primates (NHPs) that assessed, in the same pharmacological paradigm and with the same subjects, multiple executive functions aimed to match diagnostic human test batteries for schizophrenia.VU6008055 was administered to six healthy, adult rhesus macaque monkeys at three doses plus vehicle with seven determinations over 28 weeks. Following dose administration, subjects performed in ~80 min long experimental sessions of four cognitive tasks out of a set of 7 tasks including: visual search (indexing attention), set shifting (cognitive flexibility), working memory updating, antisaccade (indexing cognitive control), object-sequence learning (indexing visual planning), and hidden Maze-learning (indexing visuospatial skills). Tasks were performed in touchscreen task stations mounted to the home cage of pair-housed NHPs.Dose-specific improvements were observed across subjects for attention, cognitive flexibility, inhibitory control, visuo-spatial skills and visual planning. There were no adverse side effects noted across the dose range tested. Extracting the best- and worst- doses for subjects

relative to vehicle showed a prevalence of best-dose cognitive improvements across domains with only few, non-systematic worst-dose effects. Across tasks, improvements were more prevalent for the more challenging task conditions. These findings provide evidence for the contribution of the $M_4$ muscarinic receptor in mediating major higher-order, domain-general cognitive functions in the NHPs. The wide pro-cognitive effects support the potential development of $M_4$PAMs for the treatment of cognitive symptoms in psychiatric disorders.

**Disclosures: X. Wen:** None. **S. Shehreen:** None. **A. Neumann:** None. **C. Lindsley:** None. **C.K. Jones:** None. **T. Womelsdorf:** None.

**Poster**

**PSTR200: Prefrontal Mechanisms of Executive Function in Humans and Animals**

**Location:** WCC Halls A-C

**Time:** Monday, November 16, 2026, 1:00 PM - 5:00 PM

**Program #/Poster #:** PSTR200.23/KK1

**Topic:** I.04. Executive Functions

**Support:** Army Research Office W911NF2410228
Freedom Together Foundation
The Picower Institute for Learning and Memory
Office of Naval Research MURI N00014-23-1-2768

**Title:** Theta gates and routes information in the frontal cortex

**Authors: *M. B. BROSCHARD**[1], S. L. BRINCAT[2], R. LOONIS[3], E. K. MILLER[4];
[2]Picower Inst., [3]The Picower Inst. for Learning and Memory and Dept. of Brain and Cognitive Sci., [4]The Picower Inst. for Learning and Memory, [1]MIT, Cambridge, MA

**Abstract:** Theta (4-10 Hz) oscillations are well-suited for coordinating neural activity. Many studies have focused on theta's role in long-range coordination across brain regions (e.g., connectivity between the prefrontal cortex and the hippocampus). It remains unclear how theta coordinates neural activity more locally within prefrontal subareas. We examined neural activity in three frontal areas (i.e., dorsolateral prefrontal cortex (dlPFC), ventrolateral prefrontal cortex (vlPFC), and frontal eye fields (FEF)) as non-human primates categorized dot patterns. We found that theta flexibly coordinated spiking activity and higher-frequency oscillations within and between frontal areas. First, theta phase in all areas was coupled to spiking information in the FEF and seemed to gate information that was behaviorally relevant. Second, theta influences were routed in opposite directions depending on feedback. Theta flowed in a posterior direction to the FEF during choices and after correct outcomes. Theta influences reversed directionality and flowed in an anterior direction after incorrect outcomes. Third, theta organized nested cross-frequency, phase-amplitude interactions. Theta was coupled to beta (15-30Hz) oscillations, both within and between areas. Beta, in turn, was coupled to gamma (40-90Hz) oscillations, but mainly locally. Together, our results position theta as a critical mechanism that flexibly and dynamically coordinates neural activity within and across the frontal cortex.

**Disclosures: M.B. Broschard:** None. **S.L. Brincat:** None. **R. Loonis:** None. **E.K. Miller:** None.

**Poster**

**PSTR200: Prefrontal Mechanisms of Executive Function in Humans and Animals**

**Location:** WCC Halls A-C

**Time:** Monday, November 16, 2026, 1:00 PM - 5:00 PM

**Program #/Poster #:** PSTR200.24/KK2

**Topic:** I.04. Executive Functions

**Support:** Army Research Office W911NF241022
Freedom Together Foundation
The Picower Institute for Learning and Memory
Office of Naval Research MURI N00014-23-1-2768
Research Council VR 2022-02328

**Title:** Low-dimensional prefrontal representations of objects during working memory

**Authors: *D. G. SAKELLIADOU**[1], S. L. BRINCAT[1], L. LUNDQVIST[2], E. K. MILLER[1]; [1]The Picower Inst. for Learning and Memory, MIT, Cambridge, MA; [2]Dept. of Clin. Neurosci., Karolinska Institutet, Stockholm, Sweden

**Abstract:** There is an ongoing debate regarding the dimensionality of neural representations. Some accounts emphasize representation within low-dimensional subspaces or manifolds, while others suggest high-dimensional neural codes where neurons respond independently. Here, we investigate the dimensionality of prefrontal cortex (PFC) representations of visual objects held in working memory. We found that object representations are low-dimensional, occupying only 3-6 effective dimensions during both encoding and maintenance in working memory. Control analyses indicate this dimensionality was not limited by the number of objects tested (40) or neurons sampled (~100). We also compared PFC dimensionality to that of a well-established deep neural network model of its inferotemporal (IT) inputs and found an approximately 7-fold dimensionality reduction in PFC. These results suggest object representations are compressed into a low-dimensional manifold in PFC, which might be related to attractor dynamics for working memory, and might facilitate interaction with other variables and cognitive control.

**Disclosures: D.G. Sakelliadou:** None. **S.L. Brincat:** None. **L. Lundqvist:** None. **E.K. Miller:** None.

**Poster**

**PSTR200: Prefrontal Mechanisms of Executive Function in Humans and Animals**

**Location:** WCC Halls A-C

**Time:** Monday, November 16, 2026, 1:00 PM - 5:00 PM

**Program #/Poster #:** PSTR200.26/KK4

**Topic:** I.04. Executive Functions

**Support:** McDonnell Center for Systems Neuroscience

**Title:** Systematic and Dynamic Task coding in Primate Frontal Cortex

**Authors: *J. PARK**[1], H. PARK[2], C. D. HOLMES[4], S. CHING[3], L. H. SNYDER[5]; [1]Washington Univ. in St. Louis, St. Louis, MO; [2]Neurosci., Washington Univ. in St. Louis, SAINT LOUIS, MO; [3]Electrical and Systems Engin., Washington Univ. in St. Louis, Saint Louis, MO; [4]Cognitive Sci., Univ. of California San Diego, SAINT LOUIS, MO; [5]Dept of Neurosci., Washington Univ. Sch. Med., Saint Louis, MO

**Abstract:** Humans and other primates can perform and rapidly switch between many tasks. Prefrontal cortex (PFC) has been implicated in task representation, with baseline firing rates differing across tasks. We used a neural geometry approach to ask whether PFC baseline activity (1) is organized or is idiosyncratic across neuronal populations; (2) encodes a single task-related variable or multiple; and (3) anticipates task performance or follows from it. We trained two rhesus monkeys to perform six cognitive tasks in explicitly cued, 16-trial blocks, and recorded hundreds of neurons per session with a Neuropixels probe in the frontal eye field, dorsolateral PFC, or premotor cortex. Mean firing rates were analyzed during an initial 1-s fixation period before any task-relevant stimulus or planned response, isolating activity that could only reflect task context. In each area, population baseline activity for each task occupied a distinct location in a neural subspace (i.e., "task space") and the upcoming task could be decoded from a single held-out trial, while decoding accuracy was degraded on error trials, linking the population state to behavior. The task space was multidimensional, with each dimension carrying independent information; no single global factor such as reward rate or difficulty could account for the geometry. Remarkably, consistent task geometry was observed across independently sampled neuronal populations, providing evidence of a shared organizing principle rather than an idiosyncratic representation. This shared geometry was strongly conserved within an area but only partly across areas, suggesting each frontal region may configure a distinct preparatory state. Still, such geometry could reflect the task just completed rather than anticipate the one to come. Examining trial-by-trial dynamics revealed that the population state switched abruptly on the very first trial of a new block, before the task had been performed, and persisted when the explicit color cue was removed mid-block, indicating that the population state encodes the upcoming task rather than the color cue or an echo of prior performance. Together, these findings support a model in which frontal cortex holds a rich, structured representation of task context that is partially area-specific, analogous to motor preparatory activity, but for cognitive tasks.

**Disclosures: J. Park:** None. **H. Park:** None. **C.D. Holmes:** None. **S. Ching:** None. **L.H. Snyder:** None.

**Poster**

**PSTR200: Prefrontal Mechanisms of Executive Function in Humans and Animals**

**Location:** WCC Halls A-C

**Time:** Monday, November 16, 2026, 1:00 PM - 5:00 PM

**Program #/Poster #:** PSTR200.27/KK5

**Topic:** I.04. Executive Functions

**Support:** Supported by Howard Hughes Medical Institute

**Title:** Compositional computations in the primate frontal cortex

**Authors: *C. TANG**[1], M. JAZAYERI[2,3];
[1]Brain and Cognitive Sci., MIT, Cambridge, MA; [2]Brain and Cognitive Sci., Massachusetts Inst. of Technol. Dept. of Brain and Cognitive Sci., Cambridge, MA; [3]Howard Hughes Med. Inst., Cambridge, MA

**Abstract:** A hallmark of intelligence is the ability to apply known functions to new variables without additional learning, such as applying translation and rotation to new images. Yet how neural systems perform such compositional computations is not understood. We addressed this by recording neural activity in the frontal cortex of monkeys performing a vector composition task. On each trial, animals combined a start location with a displacement specified by the direction and duration of an optic-flow stimulus. We initially trained animals on a small subset of start-flow combinations. Neural responses for the training set were highly structured, with separable representations of start, flow direction, and flow duration supporting accurate composition. We then confronted animals with novel start-flow combinations. Animals composed new vectors successfully when the neural dynamics preserved this representational structure in new regions of state space, and failed predictably when the structure was distorted.We hypothesized that successful generalization requires compatibility between the format in which task variables are encoded and the operation that reads them out. Modeling identified two general ways this compatibility can fail. First, when the encoding manifold is curved, variables far from the training set accumulate distortion, degrading compatibility with distance. Second, when the encoding format and the readout assume different coordinate systems, composition fails even for well-represented variables; for example, the model fails when the input is Cartesian but the readout is polar. Consistent with the model, distortion in the neural representation grew lawfully with distance from the training set, and behavioral errors increased in parallel, an effect we term the proximity effect. In addition, delay-period activity encoded targets in Cartesian rather than polar coordinates.Behavioral experiments in humans confirmed both principles. Subjects carried a strong Cartesian prior: they generalized when stimulus and operation were both Cartesian and failed when a Cartesian stimulus was paired with a polar operation. Critically, this failure was graded rather than all-or-none. Where the Cartesian cue was locally consistent with the polar operation, subjects adopted the correct polar solution, reverting to the Cartesian default as that consistency fell away, the behavioral signature of the same proximity effect seen in the model and neural data. These findings establish a framework for how the primate brain performs compositional computations and the conditions under which this capacity breaks down.

**Disclosures: C. Tang:** None. **M. Jazayeri:** None.

**Poster**

**PSTR200: Prefrontal Mechanisms of Executive Function in Humans and Animals**

**Location:** WCC Halls A-C

**Time:** Monday, November 16, 2026, 1:00 PM - 5:00 PM

**Program #/Poster #:** PSTR200.28/KK6

**Topic:** I.04. Executive Functions

**Support:** R01 MH121480

**Title:** Effects of mnemonic chunking on neurons and oscillations in primate lateral prefrontal cortex

**Authors: *F.-K. CHIANG**, E. L. RICH;
Ctr. for Neural Sci., New York Univ., New York, NY

**Abstract:** Temporal segmentation and ordering are important for performing sequential behaviors. However, it remains unclear how such ordering is modulated when behaviors are structured into chunks. Here, we investigated how neural ensembles and local-field potentials (LFPs) in primate lateral prefrontal cortex (LPFC) structure information during sequential behaviors organized by chunking strategies. To do this, we trained two monkeys to perform a spatial self-ordered target selection task. Monkeys were trained to saccade to eight identical targets on a screen, one at a time in any order, to collect a one-time reward from each target. This required them to use working memory to update reward-target contingencies and prepare for the next target selection. From target selection patterns, we quantified chunking tendencies and assigned targets to two chunks. Behaviorally, we found that reaction times were longer when transitioning between subgroups than within subgroups, suggesting an abstract chunking boundary can be identified. Error rates were lower within the same chunk compared to those transitioning between chunks, and negatively correlated with chunking tendency, suggesting that stronger chunking improved task performance. The activity of single-neurons and LFPs were recorded from the LPFC, including dorsal principal sulcus and prearcuate gyrus. In total, we had 4132 and 3786 single-units from two monkeys and extracted LFPs of theta (4-8 Hz) and low gamma (35-50 Hz) bands from each channel for further analysis. Using a multivariate regression model we identified neurons selectively encoding either spatial information at the hold target epoch (26.9%) or sequential information at the fixation epoch (26.4%) across target selections. We also found a small subset of sequential-selective neurons encoded the serial position of the chunk boundary. We are quantifying measurements of spike-phase coupling and phase-phase coupling among target-selective and boundary-selective neurons. Our working hypothesis is that boundary-selective neurons may increase spike-phase coupling as the boundary becomes more behaviorally relevant with stronger chunking. Overall, our study aims to examine how mnemonic chunking strategies modulate coupling between neural ensembles and LFPs.

**Disclosures: F. Chiang:** None. **E.L. Rich:** None.

**Poster**

**PSTR201: Hippocampal-Cortical Interactions I**

**Location:** WCC Halls A-C

**Time:** Monday, November 16, 2026, 1:00 PM - 5:00 PM

**Program #/Poster #:** PSTR201.01/KK7

**Topic:** I.08. Learning and Memory

**Title:** Network-Targeted Continuous Theta-burst Stimulation Modulates Resting-State Hippocampal-Cortical Connectivity in Humans

**Authors: *F. BANIASAD**, M. S. HERMILLER;
Psychology, Florida State Univ., Tallahassee, FL

**Abstract:** The hippocampus supports episodic memory through coordinated interactions with distributed cortical regions, forming a hippocampal-cortical network (HCN). Transcranial magnetic stimulation (TMS) provides a noninvasive approach for modulating brain networks, and repetitive TMS has been shown to influence hippocampal-cortical connectivity and memory performance. Theta-burst stimulation (TBS) may be particularly relevant for memory networks because it engages stimulation patterns related to intrinsic theta-nested-gamma frequencies. In this study, we examined whether individualized HCN-targeted continuous TBS (cTBS) can selectively modulate hippocampal connectivity compared with out-of-network stimulation. Twenty participants completed a within-subjects design involving two non-consecutive sessions. Each session included pre-encoding resting-state fMRI, in-scanner encoding, post-encoding resting-state fMRI, out-of-scanner cTBS, post-stimulation resting-state fMRI, and in-scanner cued retrieval. cTBS was delivered either to an individualized HCN-connected left lateral parietal target or to an out-of-network sensory/motor foot (SMF) control site, with stimulation conditions counterbalanced across participants. Analyses focused on post-stimulation resting-state functional connectivity, using hippocampal seed-based and network-level approaches to compare HCN versus SMF targeted stimulation. Preliminary findings suggest that HCN-targeted cTBS selectively enhanced hippocampal network connectivity and produced patterns distinct from out-of-network stimulation. Specifically, HCN-targeted stimulation increased left hippocampal connectivity with the right hippocampus and bilateral parahippocampal cortex. Network-level analyses further showed increased connectivity within the hippocampal-cortical network and across broader networks, including the primary visual network. Together, these findings suggest that theta-burst, network-targeted stimulation of the lateral parietal cortex can selectively modulate hippocampal network connectivity and produce distinct connectivity patterns compared with out-of-network stimulation. These results highlight targeted neuromodulation as a promising approach for influencing memory-related brain networks.

**Disclosures: F. Baniasad:** None. **M.S. Hermiller:** None.

**Poster**

**PSTR201: Hippocampal-Cortical Interactions I**

**Location:** WCC Halls A-C

**Time:** Monday, November 16, 2026, 1:00 PM - 5:00 PM

**Program #/Poster #:** PSTR201.02/KK8

**Topic:** I.08. Learning and Memory

**Support:** NIH R00MH119320

**Title:** Developmental differences in Ventral Hippocampal to Prelimbic Cortex projecting neurons involved in safety learning

**Authors: *V. CASTRO**[1], S. FRANCISCO[2], S. PRABHU[3], H. C. MEYER[2];
[1]Boston Univerity, Boston, MA; [2]Psychological and Brain Sci., [3]Boston Univ., Boston, MA

**Abstract:** Affective regulation is critical for survival as it permits organisms to flexibly respond to emotionally salient stimuli. An example is fear learning, where an organism learns that a stimulus predicts an aversive event. The antithesis is safety learning, where a learned cue predicts the absence of an aversive event. Substantial previous research has highlighted developmental differences in how mice regulate fear. Our lab has shown that neurons projecting from the Ventral Hippocampus (VH) to the Prelimbic Cortex (PL) are critical for inhibiting fear in the presence of a safety cue. This study examined how VH-PL neural ensembles linked to fear or safety differ across development. Male and female mice underwent stereotaxic surgery, where a doxycycline (DOX)-inducible cFos-tTa and cre-dependent TRE-DIO-eYFP virus cocktail was bilaterally infused into the VH and a cre-expressing retrograde-dtomato virus was infused bilaterally into the PL. Following recovery, adolescent (PND 35-36) and adult mice (PND 70-75), underwent discriminative conditioning. Both ages learned to discriminate between a fear tone paired with a shock and an unpaired safety tone across four days. After conditioning, mice are taken off the DOX diet, and 48 hours later undergo a safety memory tagging session, after which the DOX diet is reinstated. 24 hours later mice undergo a second tagging session, where they are presented with a safety, fear, or novel cue. Brains are collected 90 minutes later and subsequently processed for expression of the immediate early gene cFos. During both tagging sessions, mice maintained high freezing for fear cues and lower freezing for safety cues, and intermediate freezing for novel cues, indicating sustained memory of cue valence. Adults have significantly more eYFP+ (safety engram) cells than adolescents, suggesting that adults recruit more VH-PL cells for safety processing. Additionally, adults and adolescents have similar counts of dTomato+ projection cells, indicating similar circuit infrastructure. Lastly, the VH is more responsive (significantly more cFos+ cells) to fear cues than safety or novel cues. Overall, this study informs how fear regulation circuitry develops across adolescence.

**Disclosures: V. Castro:** None. **S. Francisco:** None. **S. Prabhu:** None. **H.C. Meyer:** None.

**Poster**

**PSTR201: Hippocampal-Cortical Interactions I**

**Location:** WCC Halls A-C

**Time:** Monday, November 16, 2026, 1:00 PM - 5:00 PM

**Program #/Poster #:** PSTR201.03/KK9

**Topic:** I.08. Learning and Memory

**Title:** Hippocampus over-represents reward-predicting feature dimensions

**Authors: *W. LI**, Y. LIANG, Y. WANG, X. ZHAO;
Tsinghua Univ., Beijing, China

**Abstract:** Rewards are behaviorally significant and therefore demand special attention from animals. As a result, neurons in multiple brain areas disproportionately encode rewards. In particular, the hippocampus, a brain region essential for spatial navigation, has been shown to over-represent rewards during goal-directed navigation. However, it remains unclear whether the hippocampus preferentially represent rewards and reward-associated cues per se or feature dimensions that indicate reward availability. In another word, if a cue from one sensory modality is associated with reward, are non-rewarded cues from the same modality over-represented? To address this question, we trained mice to perform virtual navigation in the same environment under different rules, in which rewards were associated either with specific visual cues or positions. We find that hippocampal activity carries enhanced visual and spatial information in visually and positionally guided tasks, respectively, even at non-rewarded locations. These findings suggest that the hippocampus over-represents reward-predicting feature dimensions rather than rewards themselves.

**Disclosures: W. Li:** None. **Y. Liang:** None. **Y. Wang:** None. **X. Zhao:** None.

**Poster**

**PSTR201: Hippocampal-Cortical Interactions I**

**Location:** WCC Halls A-C

**Time:** Monday, November 16, 2026, 1:00 PM - 5:00 PM

**Program #/Poster #:** PSTR201.04/KK10

**Topic:** I.08. Learning and Memory

**Title:** Activity-dependent transsynaptic labeling of hippocampal-prefrontal circuitry in rats

**Authors: *J. W. Y. YUEN**[1], D. MATROV[2], H. HUANG[3], D. B. ARNOLD[4], Y. CHUDASAMA[2];
[1]NIMH, [2]Section on Behavioral Neurosci., NIH, Bethesda, MD; [3]NGP, [4]USC, Los Angeles, CA

**Abstract:** The ventral hippocampal CA1 (vCA1) can potentially relay information from the dorsal hippocampal CA3 (dCA3) to the PFC in rats. Whether contextual representations generated in dCA3 influences high-order cognitive processing via vCA1 is unclear. In this study, we first characterized the dCA3-vCA1-PFC circuit with a recently developed anterograde viral tracer called ATLAS (Anterograde Transsynaptic Label based on Antibody-like Sensors). In addition to unidirectionality, ATLAS is capable of monosynaptic delivery of Cre recombinase in an activity-dependent manner. To verify the location of potential relays, we injected Long-Evans rats of both sexes with ATLAS in dCA3 and retrograde Cre-dependent viruses in the dorsal and ventral prefrontal cortex. This revealed abundant labeling of presynaptic neurons projecting from the dCA3 injection site that terminated in the lateral septum (LS) and along the CA1 axis of caudal hippocampus. Importantly, these terminals were in close proximity to the dendrites

labeled by the postsynaptic retrograde tracers, suggestive of synaptic connections. To compare ATLAS with existing AAV1 methods of anterograde tracing, we repeated the experiment with AAV1-Cre injected into dCA3, in a separate group of rats. Results show AAV1-Cre mediated postsynaptic labeling was denser and more dispersed along dorsal to ventral CA1 compared with ATLAS. Finally, to assess compatibility with transgenic models, we injected ATLAS into the dCA3 in ZsGreen-expressing transgenic animals. We found ATLAS delivered Cre recombinase to postsynaptic vCA1 neurons, with no co-labeling of ATLAS and ZsGreen in dCA3 soma. As ATLAS is activity-dependent and labels only excitatory neurons, the present experiments demonstrate that the dCA3 is connected to the PFC via excitatory synapses in the LS and vCA1. Taken together, our findings provide anatomical evidence of relays in the LS and vCA1 linking dCA3 to PFC. Future experiments will aim to manipulate neuronal activity levels within the dCA3-vCA1-PFC circuitry to potentially restore excitation-inhibition (E-I) balance, as E-I imbalance contributes to cognitive deficits characteristic of neuropsychiatric disorders.

**Disclosures: J.W.Y. Yuen:** None. **D. Matrov:** None. **H. Huang:** None. **D.B. Arnold:** None. **Y. Chudasama:** None.

**Poster**

**PSTR201: Hippocampal-Cortical Interactions I**

**Location:** WCC Halls A-C

**Time:** Monday, November 16, 2026, 1:00 PM - 5:00 PM

**Program #/Poster #:** PSTR201.05/KK11

**Topic:** I.08. Learning and Memory

**Title:** Anatomical Dissection of Calbindin- and Calretinin-Defined Circuits in the Nucleus Reuniens of the Thalamus

**Authors: *J. WOODSON**[1], Y. CHUDASAMA[2];
[1]Natl. Inst. of Mental Hlth., Bethesda, MD; [2]Section on Behavioral Neurosci., NIH, Bethesda, MD

**Abstract:** The Nucleus Reuniens (NRe) is the largest of the midline thalamic regions and one of the main sources of thalamic inputs to the hippocampal formation (HPF) and medial prefrontal cortex (mPFC). Dual projecting neurons in the NRe are thought to synchronize mPFC and HPF activity, a circuit essential for cognitive flexibility, contextual encoding, associative learning and spatial navigation. Although midline thalamic regions are difficult to organize molecularly, previous studies have identified distinct distributions of calcium binding proteins, Calbindin (CALB1) and Calretinin (CALB2) within the Re. Interestingly, NRe neurons that project to both mPFC and HPC are lacking in both CALB1 and CALB2 expression, and are instead surrounded by populations of CALB1 and CALB2-positive neurons suggesting a potential modulatory role for these molecularly defined cell populations. To investigate the anatomical contributions of these CALB1 and CALB2 circuits, we used retrograde tracing methods to characterize afferent inputs to CALB1- and CALB2 -expressing neurons withing the NRe. Preliminary findings reveal subtype- and location-specific patterns of connectivity, indicating that molecularly defined NRe

populations receive distinct sources of input. This work provides new insights into the cellular organization of thalamocortical circuits and the mechanisms by which the NRe integrates information to coordinate high order behaviors. Disruption of hippocampal-prefrontal communication is implicated in major depressive and stress -related disorders and understanding how inputs to the NRe shape activity within this circuit may identify novel targets for therapeutic intervention.

**Disclosures: J. Woodson:** None. **Y. Chudasama:** None.

**Poster**

**PSTR201: Hippocampal-Cortical Interactions I**

**Location:** WCC Halls A-C

**Time:** Monday, November 16, 2026, 1:00 PM - 5:00 PM

**Program #/Poster #:** PSTR201.06/KK12

**Topic:** I.08. Learning and Memory

**Support:** Brain Research Foundation BRFSG-2021-11
Norman H. Anderson

**Title:** Lasting influence of experience on prefrontal cortical task representations

**Authors: *S. SHRIDHAR**, H. XU, N. ZHOU, Z. LEVERONI, B. FENG, K. KHANNA, J. Y. YU;
The Univ. of Chicago, Chicago, IL

**Abstract:** Our experiences fundamentally shape our future behavior, yet it remains unclear how prior experience influences the structure of neural representations. The role of experience in shaping neural representations has been highly debated. On one hand, the structure of neural representations for ongoing experience is thought to match the ongoing experience rather than influenced by prior experience. In contrast, pre-existing network configurations are thought to constrain the structure of future neural representations. To reconcile these perspectives and determine the contribution of prior experience in shaping future neural representations, we designed an experiment in which two groups of rats were trained on the same spatial task, but the two groups differed in their prior experience. We analyzed spiking activity from the medial prefrontal cortex during the tasks and tested two specific predictions. If the ongoing experience had a strong influence on the structure of neural task representations, we would predict that both groups express similar task representations despite their distinct prior experience. However, if prior experience constrains future neural representations, we would predict distinct task representations between the groups despite both performing the same task. At both the single-cell and population levels, we observed that the prefrontal task representations for both groups had distinct properties. This was not due to differences in behavior, since both experience groups learned the task at the same rate. Our findings suggest prior experience provides the scaffold for building future neural representations. This supports the idea that the current state of the brain is

a product of changes from an individual's unique experience history that in turn shapes neural representations for new experiences.

**Disclosures: S. Shridhar:** None. **H. Xu:** None. **N. Zhou:** None. **Z. Leveroni:** None. **B. Feng:** None. **K. Khanna:** None. **J.Y. Yu:** None.

**Poster**

**PSTR201: Hippocampal-Cortical Interactions I**

**Location:** WCC Halls A-C

**Time:** Monday, November 16, 2026, 1:00 PM - 5:00 PM

**Program #/Poster #:** PSTR201.07/KK13

**Topic:** I.08. Learning and Memory

**Support:** Start-up and pilot funding HJWRSZTNC
Esther A. & Joseph Klingenstein
Simons Foundation
CureSHANK
Citizens United for Research in Epilepsy
National Institutes of Health (NIH) (NS126725)
Harvard Brain Science Initiative Bipolar Disorder Seed Grant

**Title:** State-Dependent Hippocampal-Retrosplenial Coordination in Health and Alzheimer's Disease

**Authors: *S. ABBASPOOR**[1,3], D. KALLOOR[2,3], K. URIARTE[3], J. S. FARRELL[2,3];
[1]Neurobio., Harvard Med. Sch., Brookline, MA; [2]Harvard Med. Sch., Boston, MA; [3]Neurobio., Boston Children's Hosp., Boston, MA

**Abstract:** The hippocampus and granular retrosplenial cortex (gRSC) form an interconnected spatial-memory network, but how their coordination changes across behavioral and brain states in health and Alzheimer's disease remains unclear. We performed simultaneous high-density recordings from dentate gyrus (DG), CA1, and gRSC in C57BL/6J, 5xFAD+ and age-matched control mice (4-8 months) during spontaneous running on a circular belt and rest. A state-space Bayesian decoder showed accurate ensemble position coding in controls, whereas decoding error was significantly elevated in 5xFAD mice. We defined representational congruence as the absolute difference between positions decoded independently from HPF and gRSC. In controls, congruence during running was high and centered near 0 cm, indicating aligned spatial representations. During rest, congruence decreased significantly, with intermittent periods in which HPF and gRSC represented different, often remote, positions even after controlling for spike counts, suggesting offline representational flexibility. In 5xFAD mice, congruence was reduced during running, although alignment near 0 cm remained significant; during rest, congruence was nearly abolished. We next examined gRSC firing-rate modulation during sharp-wave ripples (SWRs) and dentate spikes (DSs). In controls, gRSC firing increased during SWRs only in putative narrow-spiking inhibitory neurons (nIN), whereas during DSs, gRSC activity

increased across all putative neuronal classes. In 5xFAD mice, SWRs were associated with little to no change in gRSC firing among putative pyramidal neurons (PYR) and wide-spiking interneurons (wIN), along with reduced firing in nIN. During DSs, wIN activity increased, nIN activity decreased, and PYRs remained unchanged. DS rates were significantly elevated in 5xFAD mice, which also showed interictal epileptiform discharges and seizures, indicating hippocampal hyperexcitability. To explain these findings, we estimated short-latency connectivity (<5ms) from parallel spike trains. In 5xFAD mice, Local HPF excitatory and local HPF and gRSC inhibitory connections were largely unchanged, whereas interregional excitatory and inhibitory connection gains significantly changed. Accordingly, HPF firing rates increased, whereas overall firing rates in gRSC significantly decreased. These findings suggest that amyloid pathology induces hippocampal hyperexcitability and altered hippocampal-retrosplenial circuit gain, leading to degraded spatial coding, disrupted congruence, and altered gRSC cell-type recruitment during memory-related hippocampal events.

**Disclosures: S. Abbaspoor:** None. **D. Kalloor:** None. **K. Uriarte:** None. **J.S. Farrell:** None.

**Poster**

**PSTR201: Hippocampal-Cortical Interactions I**

**Location:** WCC Halls A-C

**Time:** Monday, November 16, 2026, 1:00 PM - 5:00 PM

**Program #/Poster #:** PSTR201.08/KK14

**Topic:** I.08. Learning and Memory

**Support:** Medical Research Council scholarship MR/N013867/1 to M.T.
Biological Sciences Research Council Research grant BB/T005475/1 to D.B.
Biological Sciences Research Council Research grant BB/Z51665X/1 to D.B.
Biological Sciences Research Council Research grant BB/Y010345/1 to D.B.
Sir Henry Dale Fellowship from the Wellcome Trust and Royal Society 200501 to A.B.S
Human Frontier in Science Program RGY0076/2018 to A.B.S
Biotechnology and Biological Sciences Research Council grant R004765 to A.B.S
Biotechnology and Biological Sciences Research Council grant BB/W01579X/1 to A.B.S
UKRI Frontier Research grant EP/Y024656/1 to A.B.S

**Title:** Sleep neural oscillations enhance coordinated memory reactivation between cortex and hippocampus

**Authors: *M. TAKIGAWA**[1], D. TONG[2], E. A. B. HORROCKS[2], A. B. SALEEM[2], D. BENDOR[2];
[2]Dept. of Exptl. Psychology, Institue of Behavioural Neurosci., [1]Univ. Col. London, London, United Kingdom

**Abstract:** Memory consolidation during sleep requires that specific experiences are reactivated simultaneously across the hippocampus and cortex during non-rapid eye movement (NREM) sleep. NREM sleep is dominated by three fundamental oscillations — cortical slow oscillations (SO, 0.5-4 Hz), thalamocortical spindles (9-17 Hz), and hippocampal sharp-wave ripples (SWRs, 125-300 Hz) — whose temporal coupling is implicated in consolidation. However, whether these rhythms selectively coordinate which memories reactivate together across regions, or merely reflect a general increase in communication, remains unknown. To address this, we physically segregated competing memory traces in primary visual cortex (V1) by training mice on two visually distinct virtual reality tracks, each restricted to one visual hemifield, rendering track-specific representations hemispherically lateralized. This design created a situation in which a given local cortical oscillation was strongly biased to interact with one memory trace over the other. Using chronically implanted bilateral Neuropixels probes, we recorded large-scale spiking activity from V1 and hippocampal CA1 during NREM sleep following experience. For each SWR, we independently decoded the relative likelihood of tracks being reactivated in hippocampus and V1. This allowed us to quantify coherence of the reactivation content between V1 and hippocampus and examine how cortical and hippocampal oscillatory dynamics modulate this coherence. We found that V1 and hippocampus preferentially reactivated the same memory - with the cortical memory trace before and after a ripple event coherent with which memory hippocampus reactivated. Crucially, this cortico-hippocampal reactivation coherence was highest when three sleep neural oscillations act in concert: 1) high ripple power in the hippocampus, 2) high spindle power localised to the reactivating memory trace in cortex (i.e. dominant hemisphere) and 3) slow oscillation phase:when the dominant hemisphere is in a SO trough phase, while the non-dominant hemisphere is in a SO peak phase.These findings establish that sleep oscillations orchestrate content-specific cortico-hippocampal dialogue, with local cortical dynamics actively shaping which memories are selected for consolidation.

**Disclosures: M. Takigawa:** None. **D. Tong:** None. **E.A.B. Horrocks:** None. **A.B. Saleem:** None. **D. Bendor:** None.

**Poster**

**PSTR201: Hippocampal-Cortical Interactions I**

**Location:** WCC Halls A-C

**Time:** Monday, November 16, 2026, 1:00 PM - 5:00 PM

**Program #/Poster #:** PSTR201.09/KK15

**Topic:** I.08. Learning and Memory

**Title:** Inactivation of hippocampal-frontal circuitry impairs spatial working memory under conditions of increased visual interference in mice

**Authors: *M. HARARI**, H. L. HALLOCK;
Lafayette Col., Easton, PA

**Abstract:** Rodent spatial working memory tasks typically require navigation to physical locations and depend on hippocampal-frontal circuitry. In contrast, human spatial working

memory tasks usually involve remembering locations presented on a computer screen and are thought to rely more heavily on non-hippocampal networks. This distinction raises questions about the translational relevance of traditional rodent spatial memory assays. To address this issue, we used the touchscreen-based Trial-Unique Nonmatching-to-Location (TUNL) task, which models screen-based visuospatial working memory in mice. Unlike maze-based paradigms, TUNL requires animals to remember the locations of stimuli presented on a touchscreen, providing a closer analogue to human computerized cognitive tests. We selectively inhibited hippocampal projections to the frontal cortex using Designer Receptors Exclusively Activated by Designer Drugs (DREADDs) and assessed task performance across conditions that varied spatial separation between stimuli and delay length. We hypothesized that disrupting hippocampal-frontal communication would impair performance if this pathway is required for maintaining visuospatial information in working memory. Inhibition of hippocampal-frontal projections produced a selective deficit in performance when stimuli were positioned close together on the touchscreen, a condition associated with increased spatial interference. This impairment was observed only in female mice. In contrast, increasing delay length had no effect on performance following circuit inhibition, indicating that hippocampal-frontal projections are not required for maintaining visuospatial information across short delays in this task. Instead, these projections appear to contribute specifically when animals must distinguish between highly similar spatial representations. These findings suggest that hippocampal-frontal circuitry plays a more limited role in touchscreen-based spatial working memory than has been inferred from navigation-based tasks. Rather than supporting short-term memory maintenance, this pathway may be engaged primarily under conditions of high spatial interference. Our results support the translational validity of TUNL as a rodent model of screen-based visuospatial working memory and highlight the importance of task design when investigating the neural mechanisms underlying working memory across species.

**Disclosures: M. Harari:** None. **H.L. Hallock:** None.

**Poster**

**PSTR201: Hippocampal-Cortical Interactions I**

**Location:** WCC Halls A-C

**Time:** Monday, November 16, 2026, 1:00 PM - 5:00 PM

**Program #/Poster #:** PSTR201.10/KK16

**Topic:** I.08. Learning and Memory

**Support:** National Science Foundation Graduate Research Fellowship Program
NIH Grant R01-EY035826

**Title:** A semi-chronic non-human primate platform for longitudinal hippocampal-neocortical recording across behavior and states

**Authors: *D. PHAM**, K. WINGEL, J. STEFANOWICZ, E. MIRZAKHALILI, J. A. WOLF, B. L. FOSTER, B. PESARAN;
Neurosurg., Univ. of Pennsylvania, Philadelphia, PA

**Abstract:** Complementary learning system theory suggests that learning relies on two distinct but complementary systems: a fast-learning hippocampal system that rapidly captures transient experiences, and a slow-learning neocortical system that integrates those experiences over time. While this theory is central to systems neuroscience, recent debate questions the rigidity of these distinct learning timescales, suggesting a nuanced interplay between fast and slow dynamics across hippocampus and neocortex. However, investigating these learning dynamics is limited in non-human primates (NHPs), which offer a translational bridge to humans given their highly conserved brain structures. To investigate hippocampal and neocortical learning timescales, we developed a semi-chronic, longitudinal experimental setup to track neural population dynamics spanning hippocampal and neocortical networks across days and states in NHPs. To capture these multi-scale dynamics, we designed a custom microdrive that interfaces with NHP cranial recording chambers. The microdrive is engineered to actuate high-density laminar probes to target deep structures such as the hippocampus, while simultaneously capturing neocortical signals (Diagnostic Biochips Deep Array and Neuropixels probes). This design permits repeated implantation of recording probes in the same animal, critical for examining how learning-related dynamics shift and stabilize across days without probe drift. Using this platform, we sought to study the roles of the hippocampus and cortex during motor sequence learning, given growing interest and debate surrounding their respective contributions. NHPs perform an adapted center-out motor sequence learning task containing both random and fixed target sequences. During task engagement, we recorded hippocampus and neocortical signals, including laminar field potentials and single-unit spiking across multi-day sessions. With these recordings, we captured hippocampal sharp-wave ripples, a key mechanism of memory consolidation, and single-unit spiking during task engagement. Critically, to evaluate the offline processing underlying systems-level consolidation, our setup also incorporates untethered overnight recordings to capture naturalistic sleep using a wireless datalogger (Neuralynx Freelynx) and a customized head chamber. Ultimately, our semi-chronic, longitudinal experimental setup allows us to capture hippocampal and neocortical signals across multi-day sessions and states. This framework is uniquely positioned to elucidate complementary learning dynamics and reveal how these networks coordinate to stabilize memory.

**Disclosures: D. Pham:** None. **K. Wingel:** None. **J. Stefanowicz:** None. **E. Mirzakhalili:** None. **J.A. Wolf:** None. **B.L. Foster:** None. **B. Pesaran:** None.

**Poster**

**PSTR201: Hippocampal-Cortical Interactions I**

**Location:** WCC Halls A-C

**Time:** Monday, November 16, 2026, 1:00 PM - 5:00 PM

**Program #/Poster #:** PSTR201.11/KK17

**Topic:** I.08. Learning and Memory

**Support:** R01NS039456
R01NS102537
Kavli NDI postdoctoral fellowship

**Title:** Congruence between Visual and Path-integration Cues Gates Landmark Control of Directional and Spatial Cells in Retrosplenial Cortex and Postsubiculum

**Authors: *Y.-Q. ZHOU**[1], Y. XIONG[6], Y. SUEOKA[2], N. J. COWAN[3], K. ZHANG[4], J. KNIERIM[5];
[2]Neurosci., [3]Dept. of Mechanical Engin., [4]Dept Biomed Engin., [5]Zanvyl Krieger Mind/Brain Inst., [1]Johns Hopkins Univ., Baltimore, MD; [6]Janelia, Ashburn, VA

**Abstract:** The head direction (HD) network functions as an internal compass that maintains an animal's sense of orientation. Ring attractor models propose that this compass is maintained by recurrent population dynamics, with self-motion signals continuously updating the location of the activity bump to keep the internal HD estimate aligned with the external world. However, path integration can accumulate systematic errors. Even though external landmarks are thought to correct this error, experiments suggest that landmark control may fail when the conflict between external and idiothetic cues becomes too large. How the HD attractor resolves conflict between path-integration error and dynamic landmark input remains poorly understood. It is unknown whether this process is governed solely by the magnitude of the error between internal and external directional estimates, or whether the directional relationship between landmark motion and ongoing self-movement signals also shapes the integration of these competing sources of information. We used simultaneous dual-site Neuropixels recordings from retrosplenial cortex (RSC) and postsubiculum (PoS) in 3 rats navigating a circular track in a virtual reality dome. In each session, visual landmarks were displaced by a series of 10 escalating jumps (15°-87°) in either the same or opposite direction as the animal's movement. We combined RSC and PoS HD and spatially tuned cells into a single Bayesian population decoder per session (16-136 cells, 518 cells in 8 sessions) to track the decoded head direction on a moment-by-moment basis. For each jump, we computed a capture index measuring the change in the decoded HD signal relative to the jump of the landmarks (1 = full following, 0 = no change). When landmark displacement was in the same direction as the rat's movement (i.e., creating an illusion that the rat was transported backwards), capture declined sharply and reached near zero at 40° (mean capture $\leq$ 32° landmark jump: 0.51; mean capture $\geq$ 40° jump: −0.15). In contrast, when landmark motion was in the opposite direction as the rat's movement (i.e., creating an illusion that the rat was transported forward), capture remained strong across all jump magnitudes (mean = 0.42). Capture differed significantly between the two conditions (Wilcoxon rank-sum, $p = 0.0001$; $n = 80$ jumps). These results demonstrate that landmark control of the HD ring attractor is not determined by the magnitude of the visual-self-motion discrepancy alone. Instead, when the direction of the landmark jump was consistent with forward movement of the rat, the degree of landmark control was greater than when the direction of jump was inconsistent with its movement.

**Disclosures: Y. Zhou:** None. **Y. Xiong:** None. **Y. Sueoka:** None. **N.J. Cowan:** None. **K. Zhang:** None. **J. Knierim:** None.

**Poster**

**PSTR201: Hippocampal-Cortical Interactions I**

**Location:** WCC Halls A-C

**Time:** Monday, November 16, 2026, 1:00 PM - 5:00 PM

**Program #/Poster #:** PSTR201.12/KK18

**Topic:** I.08. Learning and Memory

**Support:** JST ERATO (JPMJER1801)
the Institute for AI and Beyond of the University of Tokyo
JSPS KAKENHI (22K21353)
AMED Brain/ MINDS 2.0 (24wm0625207s0101; 24wm0625401h0001; 24wm0625502s0501).
JSPS KAKENHI (25K18705)
Kobayashi foundation

**Title:** Aripiprazole attenuates hippocampal theta oscillations during sleep in mice

**Authors: *K. KAKEHI**[1], H. SUZUKI[1], K. IZUMO[1], Y. IKEGAYA[1,2], N. MATSUMOTO[1,2]; [1]Grad. Sch. of Pharmaceut. Sciences, The Univ. of Tokyo, Tokyo, Japan; [2]The Univ. of Tokyo, Inst. for AI and Beyond, Tokyo, Japan

**Abstract:** Aripiprazole, an atypical antipsychotic, functions as a partial agonist at both dopamine D2 and serotonin 5-HT1A receptors, and it is primarily prescribed for the treatment of schizophrenia and bipolar disorder. While functional dopamine D2 receptors are widely expressed in the hippocampus, the neurophysiological effects of aripiprazole on the hippocampus remain largely unclear. Furthermore, because the prior pharmacological research on aripiprazole has been predominantly limited with disease models, its basic neurophysiological impact on the hippocampus during sleep in healthy mice remains poorly understood. Therefore, we aimed to elucidate the effects of aripiprazole on hippocampal local field potentials (LFPs) during sleep in healthy male mice aged 8 to 10 weeks.After implantation of recording electrodes in the hippocampus and prefrontal cortex, either aripiprazole (10 mg/kg) or control vehicle solution was administered intraperitoneally, and electromyograms (EMGs) and LFPs were recorded for 80 minutes after administration in freely behaving mice. Sleep and awake states were classified based on the amplitude of the EMG signals, and then rapid eye movement (REM) sleep states and NonREM sleep states were defined by the prefrontal LFPs. Following vigilance state scoring, we conducted frequency analysis on the hippocampal LFPs for each state to evaluate the changes in LFP power. Especially, our analysis focused on specific frequency bands associated with hippocampal network activity during sleep: the theta (4-12 Hz), low-gamma (30-50 Hz), and high-gamma (50-80 Hz) bands. Compared with the vehicle-treated group, the aripiprazole-treated mice exhibited a significant increase in both REM and NonREM sleep time. In addition, the aripiprazole-treated group demonstrated significant attenuation in the power of the hippocampal theta band during both REM and NonREM sleep.Our results suggest that neural plasticity and cognitive function are impaired even in healthy mice by aripiprazole-attenuated theta oscillations, as hippocampal theta oscillations are involved in memory processing. Our study presents a novel aspect of the working mechanisms of antipsychotic drugs and serves as basic evidence for managing side effects and considering their impacts on cognitive function in clinical settings.

**Disclosures: K. Kakehi:** None. **H. Suzuki:** None. **K. Izumo:** None. **Y. Ikegaya:** None. **N. Matsumoto:** None.

**Poster**

**PSTR201: Hippocampal-Cortical Interactions I**

**Location:** WCC Halls A-C

**Time:** Monday, November 16, 2026, 1:00 PM - 5:00 PM

**Program #/Poster #:** PSTR201.13/KK19

**Topic:** I.08. Learning and Memory

**Support:** NIH R01 NS121764-03
NIH R01 NS132041-02

**Title:** Spatial representations are preferentially encoded in superficial layers across primary sensory and association cortices

**Authors: *W. NING**[1,2], J. L. SHOBE[2], R. SAXENA[3], B. L. MCNAUGHTON[1,2,4];
[1]Ctr. for the Neurobio. of Learning and Memory, [2]Neurobio. and Behavior, Univ. of California, Irvine, Irvine, CA; [3]Kavli Inst. for Systems Neuroscience, Ctr. for Algorithms in the Cortex, Norwegian Univ. of Sci. and Technol., Trondheim, Norway; [4]Canadian Ctr. for Behavioral Neurosci., Univ. of Lethbridge, Lethbridge, AB, Canada

**Abstract:** The brain creates an internal representation of the world by extracting knowledge about the context (where) and content (what) of experiences. The indexing theory postulates that the hippocampus (HPC) generates unique contextual codes that associatively link to sensory content stored in the neocortex. Recent studies have shown that place cell sequences are also observed across multiple neocortical regions, including retrosplenial cortex, posterior parietal cortex (PPC), primary and secondary motor cortices. However, the relative coding of context versus content information in superficial (L2/3) versus deep (L5/6) cortical layers remains elusive. To investigate this, we developed a treadmill behavioral paradigm for head-fixed mice that integrates virtual reality (VR) environments with discrete tactile cues. On recording day, mice experienced two distinct familiar VR contexts and two novel tactile cues. The novel tactile cues were swapped in position, allowing us to decouple cue activity from location-specific activity in a double dissociation design. Using high-density (512-channel) silicon probes, we recorded neural activity across superficial and deep layers of the primary somatosensory cortex (S1), PPC, and dorsal CA1 of HPC (N=10 mice). As expected, population vector correlation analyses showed that S1 had higher tactile cue discrimination, whereas PPC exhibited greater selectivity for spatial position, similar to HPC. Interestingly, laminar analyses revealed greater global remapping in superficial compared to deep layers in both S1 and PPC, indicating more distinct spatial representations. Cue detection was primarily encoded in PPC superficial layers, whereas S1 deep layers showed a trend toward stronger cue detection. PPC exhibited higher lifetime sparsity and information scores relative to S1. Experience within a session increased lifetime sparsity and information in both cortical regions. These increases occurred across successive VR context and cue swap transitions and were observed in superficial and deep

layers. Together, our data reveal that spatial representations are preferentially encoded in superficial than deep layers in both primary sensory and association cortices, and that experience refines cortical representations across layers.

**Disclosures: W. Ning:** None. **J.L. Shobe:** None. **R. Saxena:** None. **B.L. McNaughton:** None.

**Poster**

**PSTR201: Hippocampal-Cortical Interactions I**

**Location:** WCC Halls A-C

**Time:** Monday, November 16, 2026, 1:00 PM - 5:00 PM

**Program #/Poster #:** PSTR201.14/KK20

**Topic:** I.08. Learning and Memory

**Support:** VA MERIT RR&D, RX002705
NIH R01NS101108

**Title:** Chronic TBI elevates hippocampal interneuron firing and disrupts hippocampal-amygdala coordination during fear extinction

**Authors: *E. R. HALTER**[1], E. MIRZAKHALILI[2], C. D. ADAM[4], J. A. WOLF[3];
[2]Neurosurg., [1]Univ. of Pennsylvania, Philadelphia, PA; [3]Univ. of Pennsylvania, Wayne, PA;
[4]Neurosci., Icahn Sch. of Med. at Mount Sinai, Astoria, NY

**Abstract:** Traumatic Brain Injury (TBI) and Post-Traumatic Stress Disorder (PTSD) frequently co-occur, yet their interaction remains poorly understood. To examine how TBI affects fear memory circuitry, rats underwent lateral fluid percussion injury (FPI) and were tested in contextual fear conditioning (CFC) at acute (2 weeks) and chronic (6 months) timepoints. A subset of chronic animals were implanted with 64-channel electrodes in the hippocampus (HC) and basolateral amygdala (BLA) for electrophysiological recordings in their homecage, and before, during, and after CFC and other behavioral paradigms. All animals showed similar abilities to acquire fear and pattern separate between the shock context and a second context. Injured animals showed less extinction and more freezing compared to shams when placed back into the shock context 24 hours later, indicating insufficient consolidation of extinction memory between the first and second days of the paradigm but was comparable in later sessions. At 6 months post-injury extinction deficits were not present, however significant electrophysiological changes were observed. HC firing rates increased while BLA single-unit activity decreased. HC interneuron firing nearly tripled following injury while pyramidal cell rates were unchanged, indicating interneuron hyperactivity rather than loss. However, cell composition based on waveform and firing-rate classification supported a loss of pyramidal cells without significant interneuron loss in the HC. Oscillatory activity was also disrupted, with persistent reductions in HC theta power and corresponding losses of theta and gamma in the BLA. HC-BLA coherence at theta frequencies was altered, suggesting desynchronization of limbic circuits. Phase-amplitude coupling (PAC) was also reorganized: sham animals showed strengthened coupling between HC theta phase and BLA low gamma post-acquisition, whereas injured animals

exhibited coupling to high gamma that decreased after acquisition. Overall, theta-gamma PAC was decreased in injured animals as previously reported 2 weeks post injury. These data suggest a loss of coordination of neuronal activity and oscillatory interactions within and between HC and BLA, loss of coordination of cell firing and oscillations, and potential pathway reorganization at chronic time points post TBI. These alterations may underlie observed behavioral differences which appear to compensate at chronic time points despite the dysfunction in limbic circuitry. These findings highlight the importance of measuring electrophysiological deficits in addition to behavioral paradigms to understand changes to the brain post TBI.

**Disclosures: E.R. Halter:** None. **E. Mirzakhalili:** None. **C.D. Adam:** None. **J.A. Wolf:** None.

**Poster**

**PSTR201: Hippocampal-Cortical Interactions I**

**Location:** WCC Halls A-C

**Time:** Monday, November 16, 2026, 1:00 PM - 5:00 PM

**Program #/Poster #:** PSTR201.15/KK21

**Topic:** I.08. Learning and Memory

**Support:** NIH grant R01MH129294
NIH grant R01MH130367

**Title:** Supramammillary regulation of hippocampal CA1 cholecystokinin-expressing interneurons and ivy cells

**Authors: *W. GUO**, Y. JIANG, Q. SUN;
Neurosciences, Case Western Reserve Univ., Cleveland, OH

**Abstract:** The hippocampus and its associated neural circuits are critical in memory processes. Dysfunction of these networks contributes to numerous neuropsychiatric disorders. The supramammillary nucleus of the hypothalamus (SuM) sends dense projections to hippocampal subregions. While previous studies primarily focused on SuM projections to the dentate gyrus and CA2, the SuM-CA1 pathway remains poorly understood. Our previous work demonstrated that SuM projections preferentially target the border of stratum radiatum (SR) and stratum lacunosum-moleculare (SLM) layers in CA1, where they innervate vasoactive intestinal peptide-expressing and unknown subclasses of interneurons (INs). In this study, we aim at defining the subclasses of CA1 interneurons targeted by SuM projections and how SuM regulates CA1 IN microcircuits. Given that SuM comprises both glutamatergic and GABAergic neurons, we first used anterograde viral vectors to trace glutamatergic and GABAergic projections from SuM to CA1 in *Vglut2*-Cre and *Vgat*-Cre mice. We detected the dense glutamatergic, but not GABAergic, fibers at the SR/SLM border of CA1, indicating that SuM-CA1 pathway is primarily glutamatergic. As cholecystokinin-expressing (CCK+) INs constitute a major subclass of INs located in SR/SLM, we next asked whether CCK+ INs are targeted by SuM inputs. We identified CCK+ INs by injecting FLP-dependent AAV-mCherry into *Sncg*-FLP mice. We additionally injected AAV-channelrhodopsin2 into the SuM and performed ex vivo whole cell

patch clamp recording in CA1 CCK+ INs. Optogenetic activations of SuM terminals evoked EPSCs in all CCK+ INs at the SR/SLM border (100%), followed by SR (90%) and SO/SP layers (54.5%). Furthermore, optogenetic stimulation elicited action potentials in 46.6% of recorded CCK+ INs in SR/SLM. Strikingly, we found that Ivy INs in CA1 SR, identified by their distinct morphology and unique barrage firing patterns in response to depolarizing current injections, received no excitation but were suppressed by SuM terminal stimulation. The long-latency inhibitory responses (>3 ms) indicate that SuM excitatory inputs suppress Ivy cells through a polysynaptic feedforward inhibitory circuit. Together, this study demonstrates that SuM-CA1 glutamatergic inputs simultaneously activate CA1 CCK+ INs and suppress Ivy INs, highlighting the cell-type-specific tuning of hippocampal CA1 inhibitory networks by SuM.

**Disclosures: W. Guo:** None. **Y. Jiang:** None. **Q. Sun:** None.

**Poster**

**PSTR201: Hippocampal-Cortical Interactions I**

**Location:** WCC Halls A-C

**Time:** Monday, November 16, 2026, 1:00 PM - 5:00 PM

**Program #/Poster #:** PSTR201.16/KK22

**Topic:** I.08. Learning and Memory

**Support:** NS126725
Harvard Brain Science Initiative Bipolar Disorder Seed Grant
Simons Foundation

**Title:** Supramammillary Coordination of Exploration and Hippocampal Spatial Map Formation

**Authors: *D. KALLOOR**, S. ABBASPOOR, J. S. FARRELL;
Harvard Med. Sch., Boston, MA

**Abstract:** Exploration is a fundamental behavioral state in which locomotion, arousal, and spatial cognition must be tightly coordinated to navigate an environment. While hippocampal circuits underlying spatial cognition are well characterized, the upstream signals that link internal state with spatial representations remain poorly understood. One major upstream input that has been understudied compared to its cortical counterparts is the hypothalamic supramammillary nucleus (SuM). Previous work demonstrated that *Tac1-expressing* neurons in the SuM not only control locomotion and promote arousal but also provide a potential speed signal to the hippocampus. Preliminary data show that SuM Tac1 activity predicts hippocampal spatial decoding accuracy even after controlling for locomotor speed, suggesting that this circuit supports the precision of hippocampal spatial maps. Given the known role of SuM in novelty processing, we test the hypothesis that SuM Tac1 neurons coordinate an exploratory brain state with hippocampal spatial map formation. To determine whether SuM Tac1 activity controls exploratory behaviors beyond locomotor speed, we combine cell type specific neural recordings and bidirectional optogenetics with quantitative behavioral decomposition during exploration of novel and familiar environments in freely moving mice. To test whether SuM Tac1 projections

to the dentate gyrus regulate place cell formation and stability, we combine 2-photon calcium imaging of dentate granule cells with optogenetic manipulation of Tac1 axons during exploration of a novel environment. Together, these experiments help define how a hypothalamic circuit links internal behavioral state with hippocampal spatial coding. By identifying an upstream mechanism that coordinates exploration with hippocampal map formation, this work advances our understanding of how brain states shape cognitive processing during behavior. More broadly, defining how the "cognitive hypothalamus" contributes to memory-related hippocampal function may reveal new circuit targets for cognitive impairments associated with neurological and psychiatric disorders.

**Disclosures: D. Kalloor:** None. **S. Abbaspoor:** None. **J.S. Farrell:** None.

**Poster**

**PSTR201: Hippocampal-Cortical Interactions I**

**Location:** WCC Halls A-C

**Time:** Monday, November 16, 2026, 1:00 PM - 5:00 PM

**Program #/Poster #:** PSTR201.17/KK23

**Topic:** I.08. Learning and Memory

**Support:** R21MH134016

**Title:** Median raphe -to- Dorsal Hippocampus Pathway in Flexible Discrimination-Avoidance Learning

**Authors: *W. HUANG**[1], D. V. WANG[2];
[2]Neurobio. and Anat., [1]Drexel Univ. Col. of Med., Philadelphia, PA

**Abstract:** Flexible survival behavior requires animals to integrate sensory cues with contextual information to select appropriate actions under changing conditions. The dorsal hippocampus, particularly dorsal CA1 (dCA1), is thought to support this process by organizing contextual representations and trajectory-related activity, yet the circuit mechanisms that shape these computations behind flexible behaviors remain poorly understood. This work investigates how the median raphe nucleus (MnR), a major subcortical input to the dorsal hippocampus, regulates dCA1 population dynamics during flexible discrimination-avoidance learning. We hypothesize that MnR input enhances the accuracy and stability of hippocampal spatial coding across changing task conditions, thereby facilitating context-dependent avoidance learning. To test this, we developed a novel discrimination-avoidance (D-A) task in mice that dissociates cue, action, and post-action phases, enabling fine-scale analysis of neural activity during learning and decision-making. Using tetrode recordings, pathway-specific manipulations, and population-level analyses, this project will define how dCA1 activity is organized during flexible avoidance behavior and determine how the MnR→dCA1 circuit contributes to contextual discrimination, route-related coding, and adaptive learning. These studies will reveal a circuit-level mechanism by which subcortical input shapes hippocampal dynamics to support cognitive flexibility.

**Disclosures: W. Huang:** None. **D.V. Wang:** None.

**Poster**

**PSTR201: Hippocampal-Cortical Interactions I**

**Location:** WCC Halls A-C

**Time:** Monday, November 16, 2026, 1:00 PM - 5:00 PM

**Program #/Poster #:** PSTR201.18/KK24

**Topic:** I.08. Learning and Memory

**Support:** NSF GRFP
NARSAD Brain & Behavior Research Foundation Young Investigator Award

**Title:** Hormonal Contraceptive Use Modulates Medial Temporal Lobe Activation and Connectivity During Emotional Memory

**Authors: *J. M. SIMONSON**[1], M. CASTRO[3], B. BRANDAO[4], S. L. LEAL[2];
[2]Integrative Biol. & Physiol., [1]UCLA, Los Angeles, CA; [3]Psychological Sci., [4]Rice Univ., Houston, TX

**Abstract:** Despite strong evidence that sex hormones influence cognitive and neurobiological function, the effects of hormonal contraceptives (HC) on memory and medial temporal lobe (MTL) function remain unclear. Using high-resolution fMRI during an emotional mnemonic discrimination task that taxes hippocampal pattern separation, we examined how hormonal status shapes gist (target recognition) and detail (lure discrimination) memory measures, hippocampal and amygdala subregion activation, and hippocampal-amygdala functional connectivity. Young adult (age 18-35) female participants taking hormonal contraceptives (HC) or who were naturally-cycling (NC) were included in the study. Behaviorally, we found that hormonal status differentially impacted gist and detail memory. While there were no differences in target recognition between groups, lure discrimination performance for neutral and negative stimuli varied as a function of hormonal status. When examining activity in the MTL, hippocampal subregion engagement differed by hormonal status and emotional valence. Additionally, functional connectivity analyses revealed valence-dependent group differences in connectivity patterns between the hippocampus and amygdala. Together, these findings demonstrate that endogenous hormones and HC use differentially modulate emotional memory, hippocampal recruitment during emotional pattern separation, and valence-sensitive network dynamics.

**Disclosures: J.M. Simonson:** None. **M. Castro:** None. **B. Brandao:** None. **S.L. Leal:** None.

**Poster**

**PSTR201: Hippocampal-Cortical Interactions I**

**Location:** WCC Halls A-C

**Time:** Monday, November 16, 2026, 1:00 PM - 5:00 PM

**Program #/Poster #:** PSTR201.19/KK25

**Topic:** I.08. Learning and Memory

**Support:** Fulbright-COMEXUS Garcia Robles grant
Diversity Grant of the Psychological Science Research Grant
Rice Social Sciences Research Insitute Seed Grant
James T. Wagoner Foreign Study Scholarship
Building Research on Inequality and Diversity to Grow Equity (BRIDGE) Seed Grant

**Title:** Toward More Inclusive Models of Cognitive Aging: Sociocultural Determinants of Memory and Hippocampal Function

**Authors: *M. MEDINA**[1,2], F. MORALES-CALVA[2], S. L. LEAL[1];
[1]UCLA, Los Angeles, CA; [2]Psychological Sci., Rice Univ., Houston, TX

**Abstract:** Latino older adults are approximately 1.5 times more likely to develop Alzheimer's disease (AD) than non-Latino White adults, yet they remain underrepresented in cognitive aging research. Understanding how sociocultural experiences influence memory and its neural mechanisms is critical for developing equitable approaches to AD detection and prevention. Mnemonic discrimination tasks (MDTs), which assess fine-grained memory processes dependent on hippocampal function, provide a sensitive framework for examining cognitive aging. We developed a culturally inclusive MDT using ratings of emotional arousal, valence, and lure similarity matched across Latinos and non-Latinos. This study investigated whether sociocultural risk factors contribute to differences in memory performance and hippocampal function among cognitively normal Latino and non-Latino adults. Participants completed an emotional, culturally inclusive MDT alongside assessments of social, genetic, and cognitive risk factors for AD. High-resolution functional MRI was used to examine hippocampal subfield activation during memory encoding and retrieval. Memory performance varied according to sociocultural factors, including Latino subgroup, minority status, and region of origin, suggesting that environmental and experiential influences contribute to cognitive outcomes beyond ethnicity alone. Neuroimaging analyses revealed divergent patterns of hippocampal subfield activation across Latino and non-Latino participants that further interacted with emotion and memory processes. These findings demonstrate that sociocultural experiences shape both memory performance and its underlying neural mechanisms in cognitively normal adults. These results highlight the importance of considering cultural context when interpreting cognitive and neuroimaging outcomes and underscore the need for more inclusive models of cognitive aging and AD risk. Such approaches may improve the sensitivity and equity of early detection efforts in historically underrepresented populations

**Disclosures: M. Medina:** None. **F. Morales-Calva:** None. **S.L. Leal:** None.

**Poster**

**PSTR201: Hippocampal-Cortical Interactions I**

**Location:** WCC Halls A-C

**Time:** Monday, November 16, 2026, 1:00 PM - 5:00 PM

**Program #/Poster #:** PSTR201.20/Web Only

**Topic:** I.08. Learning and Memory

**Title:** Is there a relationship between otolith function and hippocampal-dependent memory?

**Authors: *S. SHAHSAVARANI**;
Audiol., San Jose State Univ., San Jose, CA

**Abstract:** The otolith organs within the inner ear have known neural projections to the hippocampus, suggesting a potential functional link between otolith integrity and hippocampal-dependent memory performance. However, this specific relationship remains underexplored. We hypothesized that poorer otolith function, indicated by greater interaural asymmetry, would negatively correlate with hippocampal-dependent memory performance. In a preliminary pilot study, data were collected from 7 participants. Otolith function was assessed using cervical and ocular Vestibular Evoked Myogenic Potentials (cVEMP and oVEMP), which measure the neurophysiological reflex pathways of the saccule and utricle, respectively. The asymmetry ratio (ASR) between the right and left ears was calculated as the primary measure of otolith function, where a higher ASR indicates greater unilateral dysfunction. Hippocampal-dependent memory was evaluated using the Mnemonic Similarity Task (MST), a behavioral assessment designed to test pattern separation (the ability to distinguish between highly similar memories). The Lure Discrimination Index (LDI) derived from the MST was used as the specific measure of hippocampal-dependent memory performance. In addition, we used the Montreal Cognitive Assessment (MoCA) to screen participants and a comprehensive Cognivue battery screening Memory, Executive Function/Attention, Discrimination, Visuospatial skills, Reaction Time, and Processing Speed to evaluate global cognition. Pairwise Spearman's rank correlations ($\rho$) were used to evaluate the relationships between vestibular and cognitive variables. Our primary hypothesis was not supported by this preliminary dataset. MST LDI scores did not show the expected negative correlation with either oVEMP or cVEMP ASR. However, exploratory analysis of broader cognitive measures revealed a strong, statistically significant negative correlation between oVEMP ASR and general cognitive status as measured by the MoCA ($\rho = -0.76$, $p = 0.05$). No other specific Cognivue domains reached statistical significance with VEMP ASRs. While these initial data did not support our primary hypothesis, the findings offer valuable insights. The significant association with MoCA scores suggests that utricular dysfunction may be linked to broader, global cognitive decline rather than isolated memory deficits. Furthermore, this implies that the utricle may play a distinct role in cognition compared with the saccule. Future studies using larger, targeted vestibular cohorts (e.g., Meniere's disease) are necessary to fully assess the specific relationships between otolith organs and cognitive function.

**Disclosures: S. Shahsavarani:** None.

**Poster**

**PSTR201: Hippocampal-Cortical Interactions I**

**Location:** WCC Halls A-C

**Time:** Monday, November 16, 2026, 1:00 PM - 5:00 PM

**Program #/Poster #:** PSTR201.21/KK26

**Topic:** I.08. Learning and Memory

**Support:** NIH Grant R01DC021663
NIH Grant R01DC015426
NIH Grant R01DC018539

**Title:** Respiratory and hippocampal theta rhythm interactions during associative memory mediated by olfactory cortex

**Authors: *A. SHERIFF**[1], G. LANE[1], A. DEDE[1], J. K. HSIEH[2], J. ROSENOW[2], S. SCHUELE[1], C. KARAKAS[3,4], C. OLUIGBO[5], M. Z. KOUBEISSI[3], C. ZELANO[1];
[1]Dept. of Neurol., [2]Dept. of Neurosurg., Northwestern Univ. Feinberg Sch. of Med., Chicago, IL; [3]Dept. of Neurol., George Washington Univ., Washington, DC; [4]Dept. of Neurology, Epilepsy and Clin. Neurophysiol., Children's Natl. Hosp., Washington, DC; [5]Div. of Neurosurg., Children's Natl. Med. Ctr., Washington, DC

**Abstract:** Respiration has been widely shown to couple to brain rhythms in a way that has been theorized to play a role in memory. The olfactory system is implicated here, as respiration is inextricably linked to olfaction; olfactory sensory neurons mechanically sense airflow, and olfactory bulb oscillations track respiratory frequencies in rodents. In rodents and humans, the respiratory rhythm couples to neural oscillations in olfactory cortical areas including piriform cortex and the hippocampus, which is important for memory. Bypassing nasal airflow in rodents and humans disrupts respiratory coupling with downstream brain regions, and nasal breathing in humans was linked to improvements in memory over oral breathing, together suggesting olfactory system activation is necessary for respiratory modulation of brain rhythms in a way that supports memory processing. For high temporal and spatial recordings of local field potentials (LFPs) in human olfactory cortex and hippocampus, these rare recordings will be conducted using intracranial EEG (iEEG) in patients undergoing invasive monitoring for epilepsy. We hypothesize that nasal respiration promotes memory performance by coordinating oscillations between the olfactory system and hippocampus. We predict the magnitude by which neural oscillations in hippocampus and olfactory cortex interact with each other via respiratory coordination will be correlated to memory performance. We have collected preliminary data using an associative memory task with simultaneous recordings of nasal airflow and iEEG, with very promising results. The participant significantly coupled their breathing to images later remembered, but not for images later forgotten ($p<0.05$, Rayleigh's test). In other words, when the participant spontaneously inhaled at image onset, they later remembered that image. Hippocampal theta amplitude was also significantly increased for images later remembered (FDR-corrected $p<0.05$, permutation test against pre-stimulus baseline) and not for images later forgotten. Moreover, theta oscillations were coherent between olfactory (piriform) cortex and hippocampus. Thus, there is a relationship between associative memory performance, breathing, and hippocampal theta oscillations, potentially driven by the olfactory system. We will test this further to see how the olfactory system might be mediating these effects. This work was funded by the NIDCD of the NIH under awards number R01DC015426, R01DC018539, and R01DC021663 to C.Z. The content is solely the responsibility of the authors and does not necessarily represent the official views of the NIH.

**Disclosures: A. Sheriff:** None. **G. Lane:** None. **A. Dede:** None. **J.K. Hsieh:** None. **J. Rosenow:** None. **S. Schuele:** None. **C. Karakas:** None. **C. Oluigbo:** None. **M.Z. Koubeissi:** None. **C. Zelano:** None.

**Poster**

**PSTR201: Hippocampal-Cortical Interactions I**

**Location:** WCC Halls A-C

**Time:** Monday, November 16, 2026, 1:00 PM - 5:00 PM

**Program #/Poster #:** PSTR201.22/KK27

**Topic:** I.08. Learning and Memory

**Support:** R35NS132342

**Title:** Offline generative network reconfiguration guides insight-like accelerated learning by assimilation into schema

**Authors:** B. BHATTARAI, ***G. DRAGOI**;
Yale Univ. Sch. of Med., New Haven, CT

**Abstract:** Complex cross-modal de-novo associative learning generally requires numerous encoding exposures, but acquisition of the underlying mental schema of associative abstract rules enables insight-like accelerated new learning. Reports indicate that post-encoding sleep/rest offline epochs play an active role in insight learning, but the supporting neuronal ensemble mechanisms remained elusive. We developed a complex cross-modal learning task where six cue-place paired-associations (PAs) learned by male rats over weeks created a mental schema that enabled rapid within-day acquisition of 3-6 novel PAs. Simultaneous electrophysiological recording of hippocampus (HPC)-medial prefrontal (mPFC) ensembles across exploration-rest-sleep states indicated that accelerated learning of new PAs combined inferential activation of HPC map-based cue-place abstract associations and offline generative network reconfiguration in coordination with mPFC generalized outcome coding. HPC network reconfiguration during post-encoding sleep/rest predicted insight-like accelerated learning of 3-6 new PAs that consolidated and transferred rapidly via ripple-coordinated cell-assembly co-activation to mPFC. HPC ripple disruption during post-encoding sleep/rest prevented schema-based accelerated learning. Our findings reveal that map-based associative inference via offline predictive HPC-mPFC generative network reconfiguration supports insight-like accelerated learning by assimilation into schema and systems consolidation.

**Disclosures: B. Bhattarai:** None. **G. Dragoi:** None.

**Poster**

**PSTR201: Hippocampal-Cortical Interactions I**

**Location:** WCC Halls A-C

**Time:** Monday, November 16, 2026, 1:00 PM - 5:00 PM

**Program #/Poster #:** PSTR201.23/KK28

**Topic:** I.08. Learning and Memory

**Support:** National Science Foundation Grant 2520821

**Title:** Retinotopic coding in the hippocampus predicts memory-guided eye movements

**Authors: *M. GUMUS**[1], S. E. FAVILA[2], M. ALY[1];
[1]Univ. of California Berkeley, Berkeley, CA; [2]Dept. of Cognitive and Psychological Sci., Brown Univ., Providence, RI

**Abstract:** Memory and perception share a common challenge: selecting relevant features while suppressing competing ones. The hippocampus addresses this challenge by differentiating competing memories. This differentiation predicts both the precision of preparatory spatial representations in early visual cortex (EVC) and the accuracy of memory-guided eye movements. A burgeoning line of work has examined spatially precise retinotopic codes in the hippocampus itself, raising the possibility that anticipatory retinotopic coding in hippocampus may shape memory-guided attention by prioritizing relevant spatial locations and communicating spatial signals with visual cortex. Here, we tested how such hippocampal retinotopic coding may resolve competition during memory-guided attention. We leveraged population receptive field (pRF) modeling to characterize anticipatory retinotopic coding within the hippocampus during a memory-guided visual search task (N=32, fMRI with concurrent eye tracking). Participants learned associations between similar scenes and distinct spatial locations, creating memory competition, and then used these memories to predict upcoming search target locations during a blank inter-trial interval. Using pRFs estimated from independent retinotopic mapping scans, we binned hippocampal voxels by their spatial selectivity relative to target and competitor locations and examined their preparatory responses. Hippocampus showed reliable retinotopic coding, with a mixture of positive and negative pRFs (showing enhancement and suppression when stimuli enter their receptive field, respectively). This spatially precise coding predicted upcoming search behavior. During the preparatory interval, hippocampal voxels with negative pRFs showed relative suppression at the upcoming target location prior to successful searches. These hippocampal signals coupled with EVC through a push-pull dynamic: negative hippocampal pRFs showed anticorrelated activity with spatially matched EVC voxels at the target location prior to successful searches. Conversely, positive hippocampal pRFs were positively correlated with spatially matched EVC voxels at the competitor location prior to interference errors. These findings show that hippocampal contributions to memory-guided attention extend beyond representing the relevant memories: the hippocampus shows retinotopically structured signals that precede upcoming eye movements, revealing a mechanism by which the hippocampus bridges memory and perceptual systems to guide adaptive behavior under competition.

**Disclosures: M. Gumus:** None. **S.E. Favila:** None. **M. Aly:** None.

**Poster**

**PSTR201: Hippocampal-Cortical Interactions I**

**Location:** WCC Halls A-C

**Time:** Monday, November 16, 2026, 1:00 PM - 5:00 PM

**Program #/Poster #:** PSTR201.24/KK29

**Topic:** I.08. Learning and Memory

**Support:** NIH R61 DC021925
NIH R21 MH141420

**Title:** Intracranial EEG correlates of human recollection modulation via hippocampal indirectly targeted stimulation

**Authors: *A. SAN AGUSTIN**, R. B. BAUDO, J. E. KRAGEL, J. L. VOSS;
Univ. of Chicago, Chicago, IL

**Abstract:** Hippocampal Indirectly Targeted Stimulation (HITS) uses transcranial magnetic stimulation (TMS) applied to parietal regions within the hippocampal network to noninvasively modulate hippocampal activity and associated memory functions. Prior work has shown that HITS delivered using a theta-burst stimulation (TBS) pattern enhances recollection and increases hippocampal-network functional MRI activity relative to HITS with a high-frequency (13-20-Hz) stimulation pattern and to sham stimulation. It is hypothesized that TBS more effectively interacts with endogenous theta-band activity in hippocampus than high-frequency stimulation. However, the time-resolved electrophysiological responses that support the effects of HITS remain unknown. Here, we addressed this question by examining the effects of HITS in five patients with refractory epilepsy undergoing intracranial EEG (iEEG) recordings with electrodes implanted in hippocampus. Motivated by prior work demonstrating stronger effects of TBS than 20-Hz stimulation and sham, we tested three stimulation conditions in separate blocks: TBS, 20-Hz stimulation, and sham TBS. Following each stimulation block, patients performed an episodic memory task involving recognition of naturalistic scenes with self-reported recollection and familiarity judgments. Recollection rates varied among the three stimulation conditions (main effect of Condition in a linear mixed-effects model, $p = 0.009$). Recollection occurred the most following TBS (79.5% correct). It was higher than recollection after 20-Hz repetitive stimulation (68%, $q = 0.38$) and significantly higher than after sham TBS (71.3%, FDR-correct test vs. TBS, $q = 0.041$). These findings indicate that a single session of HITS delivered with a TBS pattern is sufficient to increase episodic recollection in epilepsy patients undergoing iEEG monitoring, thereby replicating effects previously noted in healthy individuals. Ongoing analyses of simultaneously acquired iEEG data aim to characterize the neural dynamics by which TBS HITS modulates hippocampal-dependent memory.

**Disclosures: A. San Agustin:** None. **R.B. Baudo:** None. **J.E. Kragel:** None. **J.L. Voss:** None.

**Poster**

**PSTR201: Hippocampal-Cortical Interactions I**

**Location:** WCC Halls A-C

**Time:** Monday, November 16, 2026, 1:00 PM - 5:00 PM

**Program #/Poster #:** PSTR201.25/KK30

**Topic:** I.08. Learning and Memory

**Support:** Spanish Ministerio de Ciencia, Innovación y Universidades Grant
Spanish Ministerio de Ciencia, Innovación y Universidades Grant PID2022 140426NB - I00
HFSP Grant LT0037/2024-L

**Title:** Hippocampal and cortical oscillations support the encoding of event memories during movie watching

**Authors: *M. SILVA**[1], X. WU[3], M. SABIO-ALBERT[4], E. CONDE BLANCO[5], P. ROLDAN RAMOS[6], M. CARRENO[6], L. FUENTEMILLA[7], C. BALDASSANO[8], J. JACOBS[2]; [2]Dept. of Neurol., [1]Univ. of Chicago, Chicago, IL; [3]Ludwig-Maximilians-Universität München, Munich, Germany; [4]Univ. of Barcelona, Barcelona, Spain; [5]5Department of Neurol., [6]Dept. of Neurol., Hosp. Clínic de Barcelona, Barcelona, Spain; [7]CRAI Univ. de Barcelona, Barcelona, Spain; [8]Psychology, Columbia Univ., Pelham, NY

**Abstract:** Ongoing experience depends on the integration of temporally extended information into coherent event representations that can be stored and later retrieved. While oscillatory activity has been implicated in episodic encoding and temporal organization for simple isolated stimuli, the neural dynamics supporting the encoding of continuous naturalistic experience into memorable events remain unclear. Using iEEG recordings, we investigated the oscillatory mechanisms supporting successful episodic memory during the encoding of a 50-min film focusing on hippocampal-cortical power and synchrony dynamics across an unfolding event. We hypothesized that distinct neural mechanisms contribute to memory formation depending on both the timing within an event and the brain region involved. Our results indicate that indeed, successful encoding was associated with distinct, frequency-specific oscillatory signatures across hippocampal, temporal, and frontal regions, as well as differentiated patterns of inter-regional synchrony throughout the event. At the onset, correct encoding required reduced gamma activity in all regions, increased temporal theta and reduced frontal activity in the beta and theta ranges. Additionally, the hippocampus revealed increased beta synchronization with temporal cortex and extended synchronization with the frontal cortex within most frequency bands. Within an event, distinct trajectories of oscillatory activity and hippocampal-cortical synchrony was associated with successful encoding, such as increased temporal gamma activity and hippocampal-temporal synchrony, whereas forgotten events showed stronger increases in theta/beta activity and hippocampal-frontal coordination. Finally, at the end of an event, the hippocampus revealed an increase in theta activity, phase resets and reduced gamma activity supporting memory for the just-concluded event. Temporal cortical activity showed an opposite pattern: gamma power and synchrony with hippocampus was higher, while theta power and synchrony were reduced. In frontal cortex, lower beta power at event boundaries was associated with better memory. Together, these results suggest that episodic memory formation during naturalistic experience depends on a dynamic division of labor across brain regions and frequencies, in which stable oscillatory states support ongoing representation, and transient, boundary-driven reorganization of hippocampal-cortical networks enable the switch between consolidation of past events and encoding of new ones.

**Disclosures: M. Silva:** None. **X. Wu:** None. **M. Sabio-Albert:** None. **E. Conde Blanco:** None. **P. Roldan Ramos:** None. **M. Carreno:** None. **L. Fuentemilla:** None. **C. Baldassano:** None. **J. Jacobs:** None.

**Poster**

**PSTR201: Hippocampal-Cortical Interactions I**

**Location:** WCC Halls A-C

**Time:** Monday, November 16, 2026, 1:00 PM - 5:00 PM

**Program #/Poster #:** PSTR201.26/KK31

**Topic:** I.08. Learning and Memory

**Support:** NIH Grant 5R01MH074692

**Title:** Boundary reactivation during retrieval of event sequences: evidence from hippocampal subfields

**Authors: *V. SCHELKUN**, L. DAVACHI;
Columbia Univ., New York, NY

**Abstract:** Though our experiences unfold continuously, they are remembered as individual episodes. It is well established that ongoing experience is discretized into episodes according to the stability of contextual features present at encoding that is disrupted at event boundaries. Evidence additionally suggests that context encoding is enhanced at event boundaries, and that retrieval of context aids in the retrieval of event details. In this study, we sought to further investigate the mechanism by which context supports episodic memory retrieval. Participants (N=32) encoded sequences of images that were organized into events defined by an associated auditory and motor context while being scanned by high-resolution fMRI. Participants were then tested for item and temporal memory. When prompted to recall the temporal order of items within an event, we find that subregions of the hippocampus that are sensitive to event boundaries reinstate patterns of activity most similar to that of the items' respective event boundary during encoding. The extent of pattern reinstatement differentially supports correct memory decisions across hippocampal subfields. These results suggest a mechanism in which contextual information is reinstated to facilitate the retrieval of memory details independent of contextual cues.

**Disclosures: V. Schelkun:** None. **L. Davachi:** None.

**Poster**

**PSTR202: Hippocampal-Cortical Interactions II**

**Location:** WCC Halls A-C

**Time:** Monday, November 16, 2026, 1:00 PM - 5:00 PM

**Program #/Poster #:** PSTR202.01/KK32

**Topic:** I.08. Learning and Memory

**Support:** The Jane Coffin Childs Fund for Medical Research
NIMH grant F30MH126483
NIH grant T32GM007618
HHMI Investigator Award
Simons Collaboration on the Global Brain grant 521921
UCSF Discovery Fellowship
Phi Beta Kappa Graduate Award

**Title:** Cross-environment generalization of task representations in prefrontal cortex supports accelerated learning

**Authors: *S.-Y. TSENG**[1], J. A. GUIDERA[2], D. GRAMLING[3], P. THOMPSON[4], J. HERNANDEZ[4], A. M. YORITA[4], R.-U. HAQUE[5], L. M. FRANK[6];
[1]Physiol., [2]Med., Univ. of California, San Francisco, San Francisco, CA; [3]Univ. of Tübingen, Tübingen, Germany; [5]Ctr. for Bioengineering, [4]Lawrence Livermore Natl. Lab., Livermore, CA; [6]Departments of Physiol. and Psyciatry, UC San Francisco, San Francisco, CA

**Abstract:** The ability to generalize knowledge across similar circumstances to facilitate learning is a hallmark of intelligent behavior, and the prefrontal cortex has long been implicated in this process. Previous reports demonstrated prefrontal codes that generalize across distinct environments, but it remains unclear which components of task information are abstracted, how this generalized code is structured relative to physical space, and how it is deployed during learning of a new environment. To address this, we trained rats on a series of spatial alternation tasks across distinct mazes with shared geometric structure, while simultaneously recording from the medial prefrontal cortex (mPFC) and hippocampus (HPC). Animals learned more rapidly when encountering familiar tasks in new environments, providing a behavioral signature of task generalization. We decoded a range of task-relevant variables from population activity in both regions, including maze position, path progression, path identity, departure and goal location, actions, and rule-relevant trial history. Comparing representations across mazes revealed critical regional differences: HPC codes remained largely environment-specific, whereas mPFC codes were shared across environments. Importantly, these shared mPFC codes did not reflect a direct mapping of corresponding physical locations between geometrically identical mazes. Instead, they generalized over task features that played equivalent roles in the abstract alternation rule, indicating that mPFC abstracts the computational structure of the task rather than its physical layout. Within individual trials, the generalized mPFC code was dynamically modulated to reflect changing computational demands, taking the form of conjunctions between abstract task states and upcoming actions and thereby expressing policy-like representations. During learning in new mazes, these generalized representations emerged alongside their environment-specific counterparts, indicating rapid deployment of pre-existing task codes to scaffold new learning. Finally, across both new-maze learning and stable performance with environment switching, trial-by-trial decoding accuracy of task variables from both environment-specific and generalized decoders predicted the correctness of the animal's behavioral output with high fidelity, relating faithful expression of task information by the neural population to successful task performance. Together, these findings show that mPFC abstracts shared task features to form schema-like codes supporting efficient generalization to new environments.

**Disclosures: S. Tseng:** None. **J.A. Guidera:** None. **D. Gramling:** None. **P. Thompson:** None. **J. Hernandez:** None. **A.M. Yorita:** None. **R. Haque:** None. **L.M. Frank:** None.

**Poster**

**PSTR202: Hippocampal-Cortical Interactions II**

**Location:** WCC Halls A-C

**Time:** Monday, November 16, 2026, 1:00 PM - 5:00 PM

**Program #/Poster #:** PSTR202.02/KK33

**Topic:** I.08. Learning and Memory

**Support:** Simons Foundation grant 542981
NIA K99AG068425
Howard Hughes Medical Institute

**Title:** Beyond trajectory replay: spatial-temporal sequence learning modulates Sharp Wave Ripples with fragmented spatial content

**Authors: *S. GU**[1], Z. ZHOU[2], C. LIU[4], A. GILLESPIE[5], M. E. COULTER[6], R. NEVERS[7], M. G. MATTAR[3], L. M. FRANK[8];
[1]UC Berkeley/UCSF, San Francisco, CA; [3]Cognitive Sci., [2]New York Univ., New York, NY; [4]Univ. of Chicago, Chicago, IL; [5]Biol. Structure, Univ. of Washington, Seattle, WA; [6]Ctr. for Integrative Neurosci., Univ. of California San Fransisco, San Francisco, CA; [7]Univ. of California, San Francisco, San Francisco, CA; [8]Departments of Physiol. and Psyciatry, UC San Francisco, San Francisco, CA

**Abstract:** Hippocampal sharp wave ripples (SWRs) are thought to support memory consolidation through sequential replay of place cell activity[1-3]. SWRs lacking coherent trajectory-like spatial representations have typically been excluded from analysis (but see [3]). Here we challenge the implicit view that these events serve no clear purpose by demonstrating that such events — which we term fragmented replay — are behaviorally relevant, physiologically distinct, and encode structured spatial information complementary to trajectory replay (continuous replay). Animals were trained on a spatial sequence task[4] while we recorded CA1 place cell ensembles across multiple days. The task features a home arm as a start location for each trial, a central platform as a decision point, and four choice arms, where rewards follow a hidden spatial-temporal structure requiring animals to visit arms in a specific sequential order. SWR-associated neuronal population activity was decoded using a Bayesian approach and classified as continuous or fragmented. The ratio of fragmented to continuous replay time was positively correlated with behavioral performance, suggesting that fragmented replay facilitates sequence learning. Fragmented and continuous replay events encoded distinct spatial content. Continuous replay was dominated by home-arm representations, whereas fragmented replay contained substantially more content from choice arms. In addition, the spatial contents are concentrated near reward locations — arguing against fragmented events being merely degraded trajectory replays. At the single-unit level, fragmented events exhibited higher ripple power and recruited more neurons. A distinct subpopulation of place cells fired preferentially during

fragmented replays, and over the course of a day, fewer neurons remained exclusive to them, suggesting learning-dependent integration into continuous replays. Cell assembly analyses revealed cross-arm co-activation during fragmented events, consistent with binding of distributed spatial elements. On the other hand, continuous replay content of arm choices showed a sequential gradient, with the next arm choice most strongly represented, followed by the next, and so on, consistent with preferential encoding of choices into the future. These findings suggest that SWRs lacking continuous spatial representations participate in learning through reward-anchored spatial consolidation and ensemble-level binding — complementary to trajectory replay. 1. Jadhav, S. P. et al., 2012, Science. 2. Fernández-Ruiz, A. et al., 2019, Science. 3. Liu et al., 2023, Science. 4. Gu et al., bioRxiv, 2026.

**Disclosures: S. Gu:** None. **Z. Zhou:** None. **C. Liu:** None. **A. Gillespie:** None. **M.E. Coulter:** None. **R. Nevers:** None. **M.G. Mattar:** None. **L.M. Frank:** None.

**Poster**

**PSTR202: Hippocampal-Cortical Interactions II**

**Location:** WCC Halls A-C

**Time:** Monday, November 16, 2026, 1:00 PM - 5:00 PM

**Program #/Poster #:** PSTR202.03/KK34

**Topic:** I.08. Learning and Memory

**Support:** NEI Grant 5K99EY036953
Howard Hughes Medical Institute

**Title:** Visual inputs gain-modulate internal path-progress representations in primary visual cortex

**Authors: *K. LEE**[1], P. ADENEKAN[2], F. GAO[3], A. M. YORITA[4], R.-U. HAQUE[5], K. KAY[6], M. SCANZIANI[6], L. M. FRANK[7];
[1]UCSF, San Francisco, CA; [2]Univ. of Rochester, Rochester, NY; [3]Physiol., Univ. of California San Francisco, San Francisco, CA; [4]Lawrence Livermore Natl. Lab., Fremont, CA; [5]Ctr. for Bioengineering, Lawrence Livermore Natl. Lab., Livermore, CA; [6]Univ. of California, San Francisco, San Francisco, CA; [7]Departments of Physiol. and Psyciatry, UC San Francisco, San Francisco, CA

**Abstract:** Taking in and interpreting sensory information is critical for an organism's ability to interact successfully with its environment. Efforts to understand the computations underlying sensory information processing typically begin by identifying the stimulus features that each neuron encodes. But bottom-up feature encoding alone does not explain how sensory signals become meaningful to an animal. To guide behavior, sensory input must be interpreted relative to other "top-down" variables, including the animal's state, goals, and task structure. For example, a visual landmark is useful to a navigating animal not simply because of its visual features, but because it can anchor or update the animal's estimate of its location. Where and how this integration of bottom-up and top-down information occurs remains only partially

understood. Primary visual cortex (V1) is an especially salient place to ask this question. V1 is classically associated with retinotopic maps and low-level visual features, making a sensory-feature account especially compelling. Yet V1 is also influenced by locomotion, head position, spatial position, and other variables. Critically, these influences are usually studied in the presence of visual input and interpreted as top-down gain modulation of visually evoked responses. Here we show that, in a large population of neurons in rat V1, this relationship is inverted. We simultaneously recorded large populations of V1 and CA1 neurons in rats performing a spatial alternation task on a W-track in darkness and in the presence of visual landmarks. In darkness, V1 population activity was organized by directional path progression: neurons tiled matched phases of physically distinct routes that shared turn direction. Visual cues then reshaped this code, making it more place- and route-specific. Quantitatively, visual input modulated the gain of the underlying dark-active path-progress scaffold. V1 neurons encoding path progression were also preferentially coordinated with CA1 ensembles during hippocampal ripples, indicating engagement with a hippocampal-cortical network. Together, these findings indicate that for many V1 neurons, top-down inputs can be primary, and visual input modulates these signals to drive spiking outputs. This combination of internally generated path-progress signals with visual cues could allow sensory input to anchor an internal estimate of task state to specific visual environments during active behavior. More broadly, our results identify a mechanism by which sensory cortex can embed sensory input within an internal coordinate system for behavior.

**Disclosures: K. Lee:** None. **P. Adenekan:** None. **F. Gao:** None. **A.M. Yorita:** None. **R. Haque:** None. **K. Kay:** None. **M. Scanziani:** None. **L.M. Frank:** None.

**Poster**

**PSTR202: Hippocampal-Cortical Interactions II**

**Location:** WCC Halls A-C

**Time:** Monday, November 16, 2026, 1:00 PM - 5:00 PM

**Program #/Poster #:** PSTR202.04/KK35

**Topic:** I.08. Learning and Memory

**Support:** NIH R01MH136875
HHMI

**Title:** Thoughts to actions: behavioral report on self-generated activity in a hippocampal-cortical network

**Authors: *D. SHIN**[1], S. CHIANG[2], E. BROYLES[3], M. E. COULTER[4], K. LEE[5], R. HABIB[2], A. M. YORITA[6], R.-U. HAQUE[7], J. HERNANDEZ[8], L. M. FRANK[9];
[1]Univ. of California San Francisco, San Francisco, CA; [2]Univ. of California San Francisco, SAN FRANCISCO, CA; [3]Ophthalmology, Univ. of Michigan, Ann Arbor, MI; [4]Ctr. for Integrative Neurosci., Univ. of California San Fransisco, San Francisco, CA; [5]Physiol., UCSF, San Francisco, CA; [6]Lawrence Livermore Natl. Lab., Fremont, CA; [7]Ctr. for Bioengineering,

[8]Lawrence Livermore Natl. Lab., Livermore, CA; [9]Departments of Physiol. and Psyciatry, UC San Francisco, San Francisco, CA

**Abstract:** The brain has a remarkable ability to self-generate meaningful distributed activity patterns that are behaviorally accessible to the subject ("thoughts"). We sought neural activity closest to thought, and identified four key features: 1) internal generation: thought can be generated without immediate sensorimotor drive, 2) behavioral accessibility: thoughts can direct actions; 3) conceptual specificity: thoughts can involve knowledge or abstract representations; and 4) distinguishability: thoughts can be distinguished from actual experiences.
To identify such activity, we focused on the hippocampus, a brain area known to be capable of internally generating conceptually specific activity patterns. However, past work has not tested whether such patterns fulfill the four criteria above.
Therefore, we developed a closed-loop content discrimination task where rats' choices depend on access to self-generated representations remote from immediate experience, decoded in real time from hippocampal spikes. Rats first navigated a Y-maze while we chronically recorded spiking activity from several hundreds (~400 to 1200) of hippocampal and medial prefrontal cortical (mPFC) neurons. During the testing phase, rats remained in the maze center. A real-time decoder identified remote representations (RRs) of one of two target locations (~1m from rat). When either target location representation was detected, rats were cued to initiate navigation, but not to which location. Rats were rewarded only if they navigated to the represented location.
We found that all four rats we trained learned the task and generated coherent representations often including the path to the target location. Notably, stronger spatial and path representation predicted correct choices, demonstrating behavioral accessibility and that rats are not simply accessing arbitrary patterns. Interestingly, current source density analysis revealed that remote representations during the task did not typically occur during classical CA3-driven sharp-wave ripple events, but instead began with input from the entorhinal cortex. We also found that a large subset of simultaneously recorded mPFC neurons were activated immediately following the hippocampal target representations. Many mPFC cells showed concordant activity during the hippocampal RRs and during navigation, demonstrating associational specificity. Meanwhile, a subset of mPFC cells were selectively activated during hippocampal RRs but not during actual navigation, a potential mechanism to distinguish thought from experience. These findings identify a specific pattern of hippocampal RRs that could support thoughts.

**Disclosures: D. Shin:** None. **S. Chiang:** None. **E. Broyles:** None. **M.E. Coulter:** None. **K. Lee:** None. **R. Habib:** None. **A.M. Yorita:** None. **R. Haque:** None. **J. Hernandez:** None. **L.M. Frank:** None.

**Poster**

**PSTR202: Hippocampal-Cortical Interactions II**

**Location:** WCC Halls A-C

**Time:** Monday, November 16, 2026, 1:00 PM - 5:00 PM

**Program #/Poster #:** PSTR202.05/KK36

**Topic:** I.08. Learning and Memory

**Support:** NIA P01 AG009973

**Title:** Learning of context-dependent odor-place associations stabilizes rat lateral entorhinal cortex odor code

**Authors: *Y. CHEN**[1], V. ZHU[1], N. MUDRIK[4], A. CHARLES[5], M. GALLAGHER[6], A. BRANCH[2], J. J. KNIERIM[3];
[2]Psychological and Brain Sci., [3]Zanvyl Krieger Mind/Brain Inst., [1]Johns Hopkins Univ., Baltimore, MD; [4]Allen Inst. & Univ. of Washington, Seattle, MD; [5]Johns Hopkins Univ. - Homewood Campus, Lutherville-Timonium, MD; [6]Dept Psych & Brain Sci., Johns Hopkins Univ. Dept. of Psychological and Brain Sci., Baltimore, MD

**Abstract:** The lateral entorhinal cortex (LEC) is a major hippocampal input critical for episodic-like memory (Wilson et al., 2013; Persson et al., 2022). Paradoxically, LEC activity exhibits fast-scale temporal drift, even during sleep (Tsao et al., 2018; Kanter et al., 2025). Reconciling this drift with its role in long-term memory is crucial for a mechanistic understanding of LEC. We investigated how LEC codes, binds, and reorganizes odor content and spatiotemporal context in an odor-place-context associative memory task. Three freely moving Long-Evans rats were trained to associate two odors with left vs. right ports in one context and were then trained in both the learned context and a new context until reaching criterion (80% correct) in both. Neuropixels recordings were obtained on 'day 1' (well-trained in the original box; first exposure to the new box with reversed odor-place associations; n=437 well-isolated units) and 'day N' (after achieving criterion in both contexts; n=241 units). Rats maintained initial odor-place associations and successfully learned the second context with minimal interference. LEC population activity during odor sampling allowed decoding of spatial context (day 1: 96.86% ± 1.03%; day N: 95.92% ± 1.45%; chance = 50%) and elapsed time (day 1: 52.15% ± 9.63%; day N: 42.58% ± 4.02%; adjusted chance = 0%) at both learning stages, but decoding of odor identity was significant only on day N (day 1: 55.49% ± 2.48%; day N: 69.75% ± 2.92%). Autoregressive moving average modeling showed that, even after accounting for temporal drift, single neurons exhibited little to no odor selectivity on day 1 (0%, 0%, and 1.11% significantly odor-tuned, by rat) compared to day N (4.26%, 4.62%, and 5.32%). The findings suggest that LEC maintains a reliable spatiotemporal scaffold of experience but supports a stable, sparse content code only after learning. Theoretical work proposes drift mitigates interference from noise and continual learning (Natrajan & Fitzgerald, 2025). Future work will test whether odor codes are embedded in population drift during early learning and investigate LEC coding principles underlying this learning-driven transition.

**Disclosures: Y. Chen:** None. **V. Zhu:** None. **N. Mudrik:** None. **A. Charles:** None. **M. Gallagher:** None. **A. Branch:** None. **J.J. Knierim:** None.

**Poster**

**PSTR202: Hippocampal-Cortical Interactions II**

**Location:** WCC Halls A-C

**Time:** Monday, November 16, 2026, 1:00 PM - 5:00 PM

**Program #/Poster #:** PSTR202.06/KK37

**Topic:** I.08. Learning and Memory

**Support:** NIH Grant R01 NS102537
NIH Grant R01 MH118926
NIH Grant T32 GM007057
Johns Hopkins Kavli Neuroscience Discovery Institute (NDI) Distinguished Postdoctoral Fellowship (G.S.)
Johns Hopkins Kavli Neuroscience Discovery Institute (NDI) Distinguished Doctoral Fellowship (B.K.)

**Title:** Dynamic coupling between visual landmark processing in area 29e and parahippocampal path integration circuits of the rodent cortex

**Authors: *B. KRISHNAN**[1,2,3], G. SECER[4,1,3], N. J. COWAN[5,4,3], J. J. KNIERIM[1,6,3];
[1]Zanvyl Krieger Mind/Brain Inst., [2]Dept. of Biomed. Engin., [3]Kavli Neurosci. Discovery Inst., [4]Lab. for Computat. Sensing and Robotics, [5]Dept. of Mechanical Engin., [6]Solomon H. Snyder Dept. of Neurosci., Johns Hopkins Univ., Baltimore, MD

**Abstract:** How are internal representations of space anchored to the external world? Parahippocampal circuits maintain an updated estimate of the animal's position by integrating self-motion cues over time, a process termed path integration (PI). Like other inertial navigation systems, PI accrues error that must be corrected by stable sensory landmarks. The neural pathways by which landmark signals anchor internal position estimates remain unknown. Area 29e, a relatively unexplored region putatively homologous to primate prostriata, is well positioned to relay landmark signals: it receives direct geniculate and V1 inputs and projects to the medial entorhinal cortex (MEC) and presubiculum (PR). We performed simultaneous electrophysiological recordings across five parahippocampal regions—area 29e, MEC, PR, parasubiculum, and postrhinal cortex—as rats (n = 5) navigated a virtual-reality apparatus that created conflicts between internal PI computations and external visual landmarks. When these conflicts disrupted landmark anchoring of most spatially tuned cells in other regions, many 29e cells remained tightly anchored to landmarks.

Given this persistent landmark anchoring in 29e, we investigated how landmark-PI conflict altered functional connectivity between 29e and MEC, a region considered central to PI computations. When landmarks were stationary, 29e and MEC LFPs were coherent in the theta and gamma bands. Granger causality analyses revealed frequency-specific information flow: 29e drove MEC in the gamma band, whereas MEC drove 29e in the theta band. When landmarks failed to anchor parahippocampal PI, the 29e→MEC gamma drive decreased, whereas the MEC→29e theta drive increased. The decline in 29e→MEC gamma drive preceded the loss of landmark control. Spike-LFP coupling mirrored these dynamics: 29e spikes were coupled to MEC gamma, whereas MEC spikes were coupled to 29e theta. Moreover, coupling of 29e spikes to MEC gamma declined before landmark control was lost. Within 29e, cells' landmark-anchor scores were positively correlated with their coupling to MEC gamma and negatively correlated with their coupling to MEC theta.

These findings suggest a model in which visual landmark signals in area 29e anchor the parahippocampal PI system to the external world via closed-loop communication with MEC. Specifically, gamma-band 29e→MEC signaling conveys feedforward landmark information, whereas theta-band MEC→29e signaling conveys feedback information about PI-based

estimates of position, consistent with predictive-coding models in which feedforward sensory information and feedback predictions are routed through distinct frequency channels.

**Disclosures: B. Krishnan:** None. **G. Secer:** None. **N.J. Cowan:** None. **J.J. Knierim:** None.

**Poster**

**PSTR202: Hippocampal-Cortical Interactions II**

**Location:** WCC Halls A-C

**Time:** Monday, November 16, 2026, 1:00 PM - 5:00 PM

**Program #/Poster #:** PSTR202.07/KK38

**Topic:** I.08. Learning and Memory

**Support:** NIH Grant R01 NS039456
NIH Grant F31 MH134596
NIH/NINDS Grant T32NS091018

**Title:** Backward shifting dynamics of one-trial place field formation predicted by attentive head scanning in rats

**Authors: *P. OZEL**[1,4], G. RAO[1], V. MULLER[1], V. PULIYADI[2], Y.-Q. ZHOU[1,3], J. J. KNIERIM[1,2,3,4];
[1]Zanvyl Krieger Mind/Brain Inst., [2]Dept. of Psychological & Brain Sci., [3]Kavli Neurosci. Discovery Inst., Johns Hopkins Univ., Baltimore, MD; [4]Solomon H. Snyder Dept. of Neurosci., Johns Hopkins Sch. of Med., Baltimore, MD

**Abstract:** Animals rely on internal cognitive maps to navigate to goal locations. Hippocampal place cells are implicated in this function and overrepresent goals and landmarks (Hollup et al., 2001; Manns & Eichenbaum, 2009; Deshmukh & Knierim, 2013), but it remains unclear how these representations are added to these maps. One candidate mechanism is rapid place field potentiation, where a place field appears or strengthens after a single attended experience. This form of plasticity can be predicted by "head scanning," where animals pause and move their heads laterally to gather information from the environment (Monaco et al., 2014). However, how hippocampal circuit dynamics support this form of representational plasticity and whether these dynamics differ when head scans are coupled with salient reward events remains unknown. Here, we asked how backward shifting dynamics differ across place field potentiation events predicted by reward-evoked versus spontaneous head scans. We recorded CA1 and CA3 neurons with Neuropixels 2.0 probes while rats (n = 8, 3 female, 5 male Long Evans rats) navigated clockwise on a circular track. Rats received 2-3 rewards per lap at pseudorandom locations via medial forebrain bundle stimulation, allowing us to compare spontaneous and reward-evoked head scans. Across 1821 place cells, 291 showed field potentiation, identified using methods from Monaco et al. (2014). Of these potentiation events, 41 were predicted by reward-evoked and 54 by spontaneous head scans. After potentiation, head scan predicted fields shifted their center of mass across subsequent laps. This effect was strongest for reward-evoked head scan predicted fields, which shifted backward with a steeper slope than other potentiation events (Wilcoxon

rank-sum test, Reward-evoked vs spontaneous: -1.49 cm/lap; p = 0.008; Reward-evoked vs non scan: -0.99 cm/lap; p = 0.026). Therefore, salient experience during attentive head scanning may preferentially strengthen inputs that promote backward shifting following potentiation over events predicted by head scanning alone. Enhanced backward shifting of place fields after head scanning at a rewarded location may strengthen predictive coding to that location, after rapidly incorporating events onto the spatial cognitive map.

**Disclosures: P. Ozel:** None. **G. Rao:** None. **V. Muller:** None. **V. Puliyadi:** None. **Y. Zhou:** None. **J.J. Knierim:** None.

**Poster**

**PSTR202: Hippocampal-Cortical Interactions II**

**Location:** WCC Halls A-C

**Time:** Monday, November 16, 2026, 1:00 PM - 5:00 PM

**Program #/Poster #:** PSTR202.08/KK39

**Topic:** I.08. Learning and Memory

**Support:** NIH grants R01 MH079511
NIH grants R01 NS102537
NIH grants R01 MH118926
NIH grants R21 NS095075
NIH grants R01 NS039456
Johns Hopkins Kavli Neuroscience Discovery Institute
Johns Hopkins University Discovery Award

**Title:** Estimating path integration during visual landmark-guided navigation via hippocampal theta frequency

**Authors: *S.-B. PARK**[1], M. S. MADHAV[1,2,3,7], R. P. JAYAKUMAR[1,2,4,5], N. J. COWAN[2,3,4], J. J. KNIERIM[1,3,6];
[1]Zanvyl Krieger Mind/Brain Inst., [2]Lab. for Computat. Sensing and Robotics, [3]Kavli Neurosci. Discovery Inst., [4]Dept. of Mechanical Engin., [5]Psychological and Brain Sci., [6]Solomon H. Snyder Dept. of Neurosci., Johns Hopkins Univ., Baltimore, MD; [7]Sch. of Biomed. Engin., Univ. of British Columbia, Vancouver, BC, Canada

**Abstract:** Path integration, a navigation strategy utilizing idiothetic cues, is crucial to form cognitive maps. Recent virtual reality studies have shown that systematic manipulations of visual landmarks can lead to the recalibration of path-integration gain, the multiplicative factor relating an animal's motion in physical space to the updating of its internal representation of position. However, recalibration was not observable when landmarks were present, as landmarks dominated the hippocampal representation. Here, we reveal that the real-time path-integration gain dynamics can be indirectly estimated through hippocampal theta frequency while landmarks are present. We examined changes in theta frequency in 5 rats during a task where landmark gain (the experimental factor relating an animal's physical locomotion to its updating of position

relative to landmarks) was dynamically ramped, stabilized, and followed by a landmark off event. We hypothesized that landmark gain changes increase the error between the path integration gain and the landmark gain. Once the landmark gain change stops, this error should gradually decrease, as the path integration gain recalibrates to more closely match the landmark gain. Mirroring this predicted error pattern, hippocampal theta frequency exhibited a V-shaped profile, progressively decreasing during the landmark gain change and recovering once the change ceased (slope difference in V-shape = 0.05, p=0.003 compared to shuffled data).
To determine if these changes could be utilized to estimate recalibrated path-integration gain, we investigated the theta frequency change between the landmark-dominated hippocampal gain (the gain represented by hippocampal place cells) just before the landmarks were extinguished and the path integration-driven hippocampal gain immediately after. We found that both (a) the net theta frequency change ($\beta = -0.52$, $p<0.05$, linear-mixed effects model) and (b) the degree to which the theta frequency recovered to its initial baseline value ($\beta = 0.07$, $p<0.05$, linear-mixed effects model) successfully predicted the amount of path-integration gain recalibration. The error between path-integration gain and hippocampal gain could be robustly estimated via theta frequency on a lap-by-lap basis in 24 out of 35 sessions. Using a continuous attractor neural network model, we propose a mechanistic framework for how the magnitude of the error between gains is expressed in the theta frequency. Thus, theta frequency provides a real-time readout of internal gain error signals, offering a novel methodology to estimate hidden cognitive variables through observable physiological oscillations.

**Disclosures: S. Park:** None. **M.S. Madhav:** None. **R.P. Jayakumar:** None. **N.J. Cowan:** None. **J.J. Knierim:** None.

**Poster**

**PSTR202: Hippocampal-Cortical Interactions II**

**Location:** WCC Halls A-C

**Time:** Monday, November 16, 2026, 1:00 PM - 5:00 PM

**Program #/Poster #:** PSTR202.09/KK40

**Topic:** I.08. Learning and Memory

**Support:** AN-AR-Cross Species-00004875-02
SFI-AN-AR-Cross Species-00023278-02

**Title:** Divergent cortical-hippocampal sleep dynamics in adolescent autism-associated rodent models

**Authors: *M. DING**[1], S. P. JADHAV[2];
[1]Dept. of Psychology, [2]Psychology, Brandeis Univ., Waltham, MA

**Abstract:** Sleep disturbances are reported in up to ~80% of children with autism spectrum disorder (ASD), and are often associated with poorer daytime functioning, including social, behavioral, and cognitive difficulties (Oyane and Bjorvatn, 2005; Veatch et al., 2017; Mazurek and Sohl, 2016). Recent human studies suggest that disrupted communication through sleep-

related brain rhythms may contribute to these impairments. In particular, the coordination of cortical slow oscillations (SOs), thalamocortical sleep spindles, and hippocampal sharp-wave ripples (SWRs) is critical for sleep-dependent memory consolidation (Latchoumane et al., 2017). Consistent with altered sleep physiology in ASD, children and adolescents with ASD show reduced spindle density and disrupted SO-spindle coordination, suggesting abnormal thalamocortical sleep dynamics (Mylonas et al., 2022). However, detailed investigation of circuit-level mechanisms remains limited in human studies. To complement human sleep biomarker research, we used recently developed monogenic rodent models associated with autism-related conditions—Fragile X (FX) and Shank3—combined with in vivo electrophysiology.We recorded from hippocampal CA1 and medial prefrontal cortex (mPFC) in adolescent male rats (P45-P60) during sleep. We found that REM sleep episodes were shorter in FX animals, although NREM sleep and other sleep quality metrics were not different. SO density and spindle density were lower in FX animals compared with wild-type (WT) animals, and the consistency of SO-spindle coordination was reduced. Shank3 animals did not exhibit detectable deficits in sleep architecture or oscillatory patterns. In addition, spiking activity in FX animals showed weaker recruitment by local oscillations, including decreased participation during SWRs and cortical spindles. Together, these preliminary results reveal broad alterations of cortical and hippocampal sleep activity in FX animals, whereas Shank3 animals did not show similar changes. These findings suggest that sleep neurophysiology differs across genetic syndromes associated with ASD. Future work will include additional animal lines and deeper analysis of oscillatory signatures and region-specific spiking activity.

**Disclosures: M. Ding:** None. **S.P. Jadhav:** None.

**Poster**

**PSTR202: Hippocampal-Cortical Interactions II**

**Location:** WCC Halls A-C

**Time:** Monday, November 16, 2026, 1:00 PM - 5:00 PM

**Program #/Poster #:** PSTR202.10/KK41

**Topic:** I.08. Learning and Memory

**Support:** NIH Grant R01DC020640

**Title:** A novel open-field foraging task reveals rapid and flexible taste-guided spatial learning in rats

**Authors: *R. G. GABRIEL, III**[1], D. B. KATZ[2], S. P. JADHAV[2];
[1]Neurosci., [2]Psychology, Brandeis Univ., Waltham, MA

**Abstract:** Foraging is an adaptive, goal-directed behavior that maximizes resource intake through spatial memory and sensory evaluation. Efficient foraging requires memory of food locations and assessment of food quality, processes that likely involve cortical taste processing and integration with hippocampal circuits for spatial memory and navigation. Taste-place associations have been demonstrated in the hippocampus, yet existing paradigms often rely on

extensive training or passive tastant delivery, limiting the ability to track rapid, flexible taste-guided decisions during naturalistic navigation. We developed a novel open-field foraging task to measure rapid taste-place learning in freely moving Long Evans rats. Rats shuttle between a central water well and eight peripheral wells assigned to palatable or aversive tastants. Each day includes forced sampling to ensure experience with all tastant-location contingencies, followed by free foraging to test memory-guided choice. Tastant locations are then remapped to assay flexible updating. During water-only training, rats (n=4, male) learned the home-reward shuttle rule over 3 days and increased reward collection from 30 ± 6.6 to 131.5 ± 11.0 rewards/session. Despite equivalent water availability across wells, rats showed idiosyncratic spatial biases. After tastants were introduced, these biases were overridden by palatability. During forced sampling, reward caps promoted relatively balanced tastant sampling, with palatable reward fractions of 58.8 ± 1.6% and 57.9 ± 1.8% across the two taste configurations. During free foraging, rats biased reward collection toward palatable sucrose or NaCl wells, collecting 96.6 ± 1.9% and 94.7 ± 4.2% of peripheral tastant rewards before and after tastant-location remapping. To quantify memory-guided choice, we measured the fraction of the first three free-foraging visits directed toward palatable locations. Rats preferentially visited palatable wells early in free foraging (0.85 ± 0.07, chance = 0.5), indicating memory for recently sampled taste-place associations. After remapping, rats shifted choices toward newly palatable locations within the same session: a sliding three-visit update index, defined as (palatable visits − aversive visits)/3, increased from 0.00 ± 0.04 to 0.41 ± 0.13 late. These findings establish a novel open-field assay for quantifying rapid taste-place associative learning and taste-guided decision making, providing a framework for future circuit-level experiments testing whether gustatory cortical input to entorhinal-hippocampal circuits is required for sensory-spatial learning and adaptive foraging decisions.

**Disclosures: R.G. Gabriel:** None. **D.B. Katz:** None. **S.P. Jadhav:** None.

**Poster**

**PSTR202: Hippocampal-Cortical Interactions II**

**Location:** WCC Halls A-C

**Time:** Monday, November 16, 2026, 1:00 PM - 5:00 PM

**Program #/Poster #:** PSTR202.11/KK42

**Topic:** I.08. Learning and Memory

**Support:** NIH Grant R01MH112661

**Title:** Modeling wake/sleep state-dependence of cortical acetylcholine and reactivation in memory consolidation.

**Authors: *M. SATCHELL**, S. P. JADHAV, P. MILLER;
Brandeis Univ., Waltham, MA

**Abstract:** Acetylcholine (ACh) is a necessary component of memory acquisition, and its reduction in states such as quiet wake and NREM sleep enable hippocampal sharp-wave ripples (SWRs) to drive memory consolidation. However, how the direct influence of ACh on cortical

activity shapes memory consolidation across quiet wake, NREM, and REM sleep remains unknown. Using a biophysical spiking network of 2,000 Hodgkin-Huxley neurons with ACh-dependent dynamics that match experimental observations from our and other labs [1,2], we show that changes in ACh impact the reactivation of cortical assemblies in a manner that is relevant for learning and memory. Applying stimuli with properties based on SWRs from quiet wake and NREM sleep [3], we show that moderate ACh paired with quiet wake-like SWR input is ideal for the initial strengthening of assemblies, while subsequent low ACh periods with NREM-like SWR input enable slower, more extensive assembly growth. Interspersed high ACh states (REM sleep) weaken the cross connections between assemblies to preserve the memory structure of the network, averting catastrophic forgetting. Our work illustrates how each of the major physiological brain states during both wake and sleep following a learning experience contributes to the creation of a functional, pattern-completing memory network.
[1] Shin JD, Satchell M, Miller P, Jadhav SP. “REM sleep prefrontal high-frequency oscillation chains mediate distinct cortical - hippocampal reactivation patterns compared to NREM sleep.” eLife preprint. 2026.
[2] Stiefel KM, Gutkin BS, Sejnowski TJ. “The effects of cholinergic neuromodulation on neuronal phase-response curves of modeled cortical neurons.” J. Comput. Neurosci. 2009.
[3] Tang W, Shin JD, Frank LM, Jadhav SP. “Hippocampal-Prefrontal Reactivation during Learning Is Stronger in Awake Compared with Sleep States.” J. Neurosci. 2017.

**Disclosures: M. Satchell:** None. **S.P. Jadhav:** None. **P. Miller:** None.

**Poster**

**PSTR202: Hippocampal-Cortical Interactions II**

**Location:** WCC Halls A-C

**Time:** Monday, November 16, 2026, 1:00 PM - 5:00 PM

**Program #/Poster #:** PSTR202.12/KK43

**Topic:** I.08. Learning and Memory

**Support:** NIH R01 MH140009-01

**Title:** Hippocampal Cognitive Maps of Social Territories in a Natural Environment

**Authors: *P. PAUDEL**, Z. ZHAO, R. JOE, X. MEI, A. YU, R. NIRAULA, W. ZHENG, E. ZHAO, J. SHEN, R. E. HARVEY, C. C. VOGT, M. SHEEHAN, A. FERNANDEZ-RUIZ, A. OLIVA GONZÁLEZ;
Neurobio. and Behavior, Cornell Univ., Ithaca, NY

**Abstract:** Territoriality is a common social behavioral trait that emerges in large enough environments across many mammals. For instance, for male mice, holding a territory provides access to food, shelter, and mates. Yet, whether and how, the brain represents a territory has remained unknown. Stablishing and keeping track of territories requires an integration of spatial and social information, both aspects encoded in the hippocampus. In this study, we rewilded lab mice (C57/FVB, 9 males and 9 females) in a ~35 x 15 m outdoor enclosure with nine shelters.

We recorded up to ~150 CA1 and CA2 neurons and simultaneously tracked the positions of freely behaving mice across the development of territories. Implanted male mice established and defended territories. We found that the hippocampus generates an integrated socio-spatial cognitive map during territorial behavior. First, place cell's representation of the territories increased in parallel to the establishment of territories. Second, the cognitive map had representations of spatial and social information. Third, spatial information of the place fields located around the territory boundaries was higher compared to other place fields. Importantly, performing a semi-controlled territory-intruder assay, we found that these boundaries were ecologically meaningful, as fights and chasing behavior clustered sharply at territory boundaries. Finally, we found that the structure and location of territories, i.e., whether mice sheltered inside the shelters or out in the paddock, differently modulates spatial information of place cells. Our data show, for the first time, the development of an ecological cognitive map of the environment during territorial behavior.

**Disclosures: P. Paudel:** None. **Z. Zhao:** None. **R. Joe:** None. **X. Mei:** None. **A. Yu:** None. **R. Niraula:** None. **W. Zheng:** None. **E. Zhao:** None. **J. Shen:** None. **R.E. Harvey:** None. **C.C. Vogt:** None. **M. Sheehan:** None. **A. Fernandez-Ruiz:** None. **A. Oliva González:** None.

**Poster**

**PSTR202: Hippocampal-Cortical Interactions II**

**Location:** WCC Halls A-C

**Time:** Monday, November 16, 2026, 1:00 PM - 5:00 PM

**Program #/Poster #:** PSTR202.13/KK44

**Topic:** I.08. Learning and Memory

**Support:** NIH grant R01MH130367
Whitehall Foundation
NIH grant R01MH136355
NIH grant DP2MH136496
Sloan Fellowship
Klingenstein-Simons Fellowship
Pershing Square Foundation's MIND Prize
Klarman Fellowship

**Title:** Rapid formation of hippocampal replay depends on experience-induced plasticity in theta sequences

**Authors: *W. TANG**[1], Y. SAITO[1], X. MEI[1], T. ASABUKI[2,3,4], A. OLIVA[1], A. FERNANDEZ-RUIZ[1];
[1]Neurobio. and Behavior, Cornell Univ., Ithaca, NY; [2]Hierarchical Neural Computation RIKEN ECL Res. Unit, RIKEN Ctr. for Brain Sci., Saitama, Japan; [3]RIKEN Pioneering Res. Inst., Saitama, Japan; [4]Dept. of Life Sci. and Med. Biosci., Waseda Univ., Tokyo, Japan

**Abstract:** During navigation, animals can adapt to novel environments with minimal exploration. The hippocampus is believed to support this rapid learning process by encoding temporal relationships among locations and events, thereby enabling predictions about future experiences. Theta sequences are proposed as a potential mechanism for this process: within each theta cycle, hippocampal place cells fire in a compressed sequence that represents the animal's current and upcoming trajectory. This precise temporal structure is ideally suited to facilitate experience-dependent plasticity and to seed the sequential activity subsequently expressed as offline replay. However, both theta sequences and replay can emerge after limited experience, raising questions regarding how theta sequences can be learned so rapidly in the hippocampal network and how they contribute to replay formation. In this study, we manipulated theta sequences by optogenetically activating local CA1 interneurons in a theta-phase-specific manner in rats. This closed-loop protocol reliably suppressed place-cell firing during the prospective "sweep-ahead" phase of theta oscillations. Conversely, the development and properties of place fields, as well as signatures of behavioral timescale synaptic plasticity (BTSP), remained intact. On a novel linear track, disruption of theta sequences impaired subsequent replay during both awake immobility and sleep. Notably, theta sequences rapidly emerged after optogenetic stimulation was discontinued, and only a limited number of unstimulated trials with intact theta sequences were adequate to support replay formation. To elucidate the mechanisms by which hippocampal sequences develop within this timeframe, we developed a computational model that investigates the interplay between synaptic plasticity rules, including spike-timing-dependent plasticity (STDP) and BTSP, to explain place field development, theta sequences, and replay. Collectively, these findings indicate that intact theta sequences serve as a plasticity-relevant scaffold for the rapid formation of hippocampal replay, a mechanism dissociated from BTSP-dependent place field formation.
*WT and YS have contributed equally to this work.

**Disclosures: W. Tang:** None. **Y. Saito:** None. **X. Mei:** None. **T. Asabuki:** None. **A. Oliva:** None. **A. Fernandez-Ruiz:** None.

**Poster**

**PSTR202: Hippocampal-Cortical Interactions II**

**Location:** WCC Halls A-C

**Time:** Monday, November 16, 2026, 1:00 PM - 5:00 PM

**Program #/Poster #:** PSTR202.14/KK45

**Topic:** I.08. Learning and Memory

**Support:** NIH Grant R01MH136355
NIH Grant DP2MH136496
Sloan Fellowship
Whitehall Research Grant
Klingenstein-Simons Fellowship
Pershing Square Foundation's MIND Prize
Pew Biomedical Scholars Award
NIH Grant R01MH130367

**Title:** Causal dissection of bidirectional hippocampal-cortical interactions supporting replay selection, memory consolidation, and retrieval

**Authors: *X. MEI**, R. E. HARVEY, W. CHEN, Z. ZHAO, E. CARBAJAL LEON, T. NETZER, A. OLIVA, A. FERNANDEZ-RUIZ;
Cornell Univ., Ithaca, NY

**Abstract:** How are memory representations encoded, stored, and selected for context-appropriate retrieval remains largely unknown. Classical models posit that memories are first encoded in the hippocampus (HPC) during experience and later transferred to the neocortex for long-term storage. Initially, some experiences are proposed to be "tagged" or prioritized for consolidation, a process believed to depend on the hippocampus. However, often the relevance of an experience depends on prior knowledge, current goals, or potential future use, which requires abstract knowledge encoded in associative neocortical areas such as the prefrontal cortex (PFC). We simultaneously recorded hundreds of neurons in both the PFC and the HPC of rats during a learning task and sleep. Coupled with an event-specific optogenetic closed-loop manipulation system, we causally identified the time windows in which the PFC is involved in memory "tagging" and in selecting the appropriate memory for replay, consolidation, and retrieval. Rats were trained to perform a spatial learning task on a "cheeseboard" maze. Each day, rats were trained in two sessions on two distinct novel reward configurations in the same maze, followed by post-task sleeps. They were tested next day of the previous configuration. We silenced the PFC during post-task sleep based on the specific phase of the cortical Up-Down cycle, upon detection of hippocampal sharp-wave ripples, or at random times. Theta-dependent PFC silencing during the acquisition session did not affect learning, but the same manipulation applied during the retrieval test severely impaired performance. On the other hand, transient PFC silencing triggered by delta waves or hippocampal sharp-wave ripples (SWRs) significantly impaired goal-directed hippocampal replay and selective memory consolidation. We identified precise temporal windows in which 1) the hippocampus elicits ensemble reactivation in the PFC and 2) the PFC sends a top-down selection signal that bias which memory traces are replayed in the hippocampus based on behavioral demands. In summary, our findings indicate that bidirectional hippocampal-cortical communication is essential for replay, memory consolidation and recall. These results highlight the essential contribution of PFC to hippocampal replay selection and memory consolidation much earlier than assumed by prevailing models.

**Disclosures: X. Mei:** None. **R.E. Harvey:** None. **W. Chen:** None. **Z. Zhao:** None. **E. Carbajal Leon:** None. **T. Netzer:** None. **A. Oliva:** None. **A. Fernandez-Ruiz:** None.

**Poster**

**PSTR202: Hippocampal-Cortical Interactions II**

**Location:** WCC Halls A-C

**Time:** Monday, November 16, 2026, 1:00 PM - 5:00 PM

**Program #/Poster #:** PSTR202.15/KK46

**Topic:** I.08. Learning and Memory

**Support:** NIH grant R01MH130367
Whitehall Foundation
NIH grant R01MH136355
NIH grant DP2MH136496
Sloan Fellowship
Klingenstein-Simons Fellowship
Pershing Square Foundation's MIND Prize
Klarman Fellowship
Eric and Wendy Schmidt AI in Science Postdoctoral Fellowship

**Title:** Dynamic regulation of hippocampal critical regimes during sleep

**Authors: *H. CHANG**[1], W. CHEN[1], L. KARABA[2], X. MEI[1], R. E. HARVEY[3], W. TANG[2], A. FERNANDEZ-RUIZ[2], A. OLIVA[1];
[2]Neurobio. and Behavior, [3]Dept. of Neurobio. and Behavior, [1]Cornell Univ., Ithaca, NY

**Abstract:** Systems operating near the critical point benefit from flexible and efficient computational properties. As a complex biological system, the brain must balance the ability for flexible computations with maintaining network stability. Here, we examined how critical dynamics in the hippocampus are regulated during sleep-dependent memory consolidation. During post-learning NREM sleep, the hippocampal network shifted away from criticality into a more ordered, subcritical regime. This shift was specifically associated with memory replay: distance to criticality increased with replay probability and replay-associated sharp-wave ripples (SWRs) rate, but not with non-replay ripple events. NREM substates with higher rate of replay events also showed reduced branching ratio and lower firing entropy, consistent with a more ordered network state. Using a biophysically inspired network model we predicted that slow integrating inhibitory neurons would restore criticality in the hippocampus. We further found that hippocampal barrage events (BARRs), which recruit a CA2 to CA1 cholecystokinin interneurons (CCK) circuit during sleep, shifted the network back towards criticality. BARRs were associated with reduced distance to criticality, increased branching ratio, and higher entropy. Moreover, optogenetic silencing of CA1 CCK interneurons during BARRs prevented this restoration. Together, our results reveal a circuit mechanism which allows the hippocampus to dynamically balance memory consolidation with homeostatic processes for stable network dynamics.

**Disclosures: H. Chang:** None. **W. Chen:** None. **L. Karaba:** None. **X. Mei:** None. **R.E. Harvey:** None. **W. Tang:** None. **A. Fernandez-Ruiz:** None. **A. Oliva:** None.

**Poster**

**PSTR202: Hippocampal-Cortical Interactions II**

**Location:** WCC Halls A-C

**Time:** Monday, November 16, 2026, 1:00 PM - 5:00 PM

**Program #/Poster #:** PSTR202.16/KK47

**Topic:** I.08. Learning and Memory

**Support:** NIH grant R01MH130367
Whitehall Foundation
NIH grant R01MH136355
NIH grant DP2MH136496
Sloan Fellowship
Klingenstein-Simons Fellowship
Pershing Square Foundation's MIND Prize

**Title:** Transforming value beliefs into flexible foraging in rats

**Authors: *Y. SAITO**[1], H.-Y. LIM[1], K. GUPTA[1], W. ASTORGA-WISTER[1], N. MILLER[1], K. ZHU[1], J. ROMANO[1], A. OLIVA[2], A. FERNANDEZ-RUIZ[1];
[1]Neurobio. and Behavior, Cornell Univ., Ithaca, NY; [2]Neurobio. and Behavior, Cornell Univ., New York, NY

**Abstract:** To forage flexibly in dynamic environments, animals must infer which goal is currently valuable from outcomes and translate this belief into spatial choices. However, it remains unclear how animals use such latent value beliefs to guide navigation rather than relying on fixed place-reward associations. We developed a probabilistic foraging task in a fully automated 2D arena to study how rats update value beliefs and transform them into spatial choices. Rats chose between two goal identities, A and B, associated with different spatial locations. In each task block, one goal was assigned a high reward probability and the other a low reward probability. After rats reached criterion performance, the reward contingencies were reversed, requiring animals to update which goal was currently more valuable based on recent reward outcomes. After multiple reversals, the spatial locations of A and B were changed while preserving their current value relationship. This manipulation allowed us to distinguish a foraging strategy based on goal identity from one based on previously rewarded locations. Rats flexibly adapted their choices after both reward-probability reversals and changes in the spatial locations of A and B, continuing to preferentially choose the currently high-value goal. These results suggest that rats selected goals according to value beliefs. A hierarchical reinforcement learning framework formalized this transformation by updating latent value beliefs from reward history and mapping them onto spatial choices based on the current locations of the goals. We performed large-scale neural ensemble recordings in hippocampal and cortical regions to investigate the neural mechanisms supporting value-guided navigation in this task. Preliminary analyses revealed neural population dynamics at two timescales, with slow across-trial fluctuations associated with evolving value beliefs and faster within-trial dynamics related to individual decisions. Together, these results establish a behavioral, computational, and neural framework for studying how abstract value beliefs are transformed into flexible navigation. The findings provide a basis for identifying neural mechanisms that transform "what is currently valuable" into "where to go."

**Disclosures: Y. Saito:** None. **H. Lim:** None. **K. Gupta:** None. **W. Astorga-Wister:** None. **N. Miller:** None. **K. Zhu:** None. **J. Romano:** None. **A. Oliva:** None. **A. Fernandez-Ruiz:** None.

**Poster**

**PSTR202: Hippocampal-Cortical Interactions II**

**Location:** WCC Halls A-C

**Time:** Monday, November 16, 2026, 1:00 PM - 5:00 PM

**Program #/Poster #:** PSTR202.17/KK48

**Topic:** I.08. Learning and Memory

**Support:** NIH Grant R01MH130367
Whitehall Foundation
NIH Grant R01MH136355
NIH Grant DP2MH136496
Sloan Fellowship
Klingenstein-Simons Fellowship
Pershing Square Foundation's MIND Prize
Klarman Fellowship

**Title:** Naturalistic outdoor foraging enhances mixed selectivity and expands population dimensionality in hippocampal place cells

**Authors: *J. SHEN**, C. LIU, W. TANG, Z. ZHAO, H. CHANG, M. AURELIO, E. CARBAJAL LEON, G. TSIMIS, Z. SUHAIL, A. FERNANDEZ-RUIZ, A. OLIVA; Neurobio. & Behavior, Cornell Univ., Ithaca, NY

**Abstract:** Hippocampal neurons encode position together with movement and other variables. Current theories of hippocampal function range from a primacy of spatial coding to the generation of multimodal representations of behaviorally relevant internal and external variables, supported by mixed selectivity. To test contrasting predictions on hippocampal codes, we compared single cell tuning and population dynamics across laboratory and outdoor natural enclosures. We recorded large CA1 ensembles from freely moving rats during random foraging indoors and outdoors. We employed custom neuro-loggers with inertial measurement unit (IMU) sensors. To extract kinematic and postural variables, and perform automatic behavioral classification, we developed a custom semi-supervised deep learning pipeline that took advantage of fused IMU and video features. Using this approach and generalized linear models (GLMs), we quantified neuronal tuning to position, speed, and head orientation, and summarized each neuron's mixed selectivity score across these factors. CA1 neurons recorded outdoors showed stronger mixed selectivity than those recorded indoors, with a larger contribution from behavior related head orientation variables. This enhanced mixed selectivity contributed to a higher population dimensionality, suggesting an expanded activity manifold rather than simple firing rate rescaling. These results indicate that outdoor exploration enhances existing mixed selectivity in CA1 and expands the dimensionality of its population code. We also found striking differences in outdoor foraging strategies that showed a more efficient energy use and search structure outdoors compared to indoors. Outside navigation bouts, rats exhibited a richer behavioral repertoire outdoors, including behavioral motifs rarely observed indoors. Naturalistic environments may therefore reveal a more distributed hippocampal representation of exploratory state, integrating spatial position with movement, head orientation, and behavioral context.

**Disclosures: J. Shen:** None. **C. Liu:** None. **W. Tang:** None. **Z. Zhao:** None. **H. Chang:** None. **M. Aurelio:** None. **E. Carbajal Leon:** None. **G. Tsimis:** None. **Z. Suhail:** None. **A. Fernandez-Ruiz:** None. **A. Oliva:** None.

**Poster**

**PSTR202: Hippocampal-Cortical Interactions II**

**Location:** WCC Halls A-C

**Time:** Monday, November 16, 2026, 1:00 PM - 5:00 PM

**Program #/Poster #:** PSTR202.18/KK49

**Topic:** I.08. Learning and Memory

**Support:** NIH grant R01MH130367
Whitehall Foundation
NIH grant R01MH136355
NIH grant DP2MH136496
Sloan Fellowship
Klingenstein-Simons Fellowship
Pershing Square Foundation's MIND Prize

**Title:** High-dimensional, multiplexed, hippocampal cognitive maps of natural environments

**Authors: *C. LIU**[1], J. SHEN[1], W. TANG[2], Z. ZHAO[2], H. CHANG[2], M. AURELIO[1], E. CARBAJAL LEON[3], G. TSIMIS[1], Z. SUHAIL[1], A. OLIVA[1], A. FERNANDEZ-RUIZ[2]; [2]Neurobio. and Behavior, [1]Cornell Univ., Ithaca, NY; [3]Neurobio. and Behavior, Cornell Univ., Brooklyn, NY

**Abstract:** Controlled laboratory experiments have been essential for defining core principles of hippocampal function. Yet the brain evolved to support behavior in complex, changing environments, leaving open the question of how these principles operate when animals navigate the real world. To bridge this gap, we recorded hippocampal CA1 activity as rats freely foraged in two large arenas matched in size and task: a controlled indoor enclosure and an outdoor natural field site with rich real-world sensory structure. Neural activity was recorded with silicon probes and custom wireless dataloggers. Despite identical arena size and task demands, hippocampal spatial coding differed markedly across environments. At the single-neuron level, outdoor sessions contained fewer significant place cells. Among neurons that remained spatially selective, place fields per cell were more numerous but smaller, producing a more local and granular spatial representation. This granularity persisted as environment size increased outdoors, contrasting with the field expansion observed when indoor environments are scaled up. At the population level, however, place decoding accuracy remained similar indoors and outdoors, indicating that spatial information was preserved despite changes in single-neuron coding. This dissociation suggests that outdoor hippocampal activity does not simply degrade under naturalistic conditions but instead redistributes information across a higher-dimensional population code. Consistent with this interpretation, we found an approximately two-fold increase in neuronal population dimensionality outdoors. This higher dimensionality could be

explained by an increase in single unit mixed selectivity and a greater diversity in hippocampal assembly patterns outdoors. Behaviorally, rats also showed altered spatial sampling and higher foraging efficiency outdoors, suggesting that increased environmental pressure or sensory richness promoted different motor plans and behavioral strategies. Together, these results show that naturalistic environmental complexity reshapes both behavior and hippocampal coding in ways not accessible in conventional laboratory experiments. In contrast to the low-dimensional, primarily spatial representations commonly reported indoors, natural environments are represented by higher-dimensional, multiplexed hippocampal cognitive maps.

**Disclosures: C. Liu:** None. **J. Shen:** None. **W. Tang:** None. **Z. Zhao:** None. **H. Chang:** None. **M. Aurelio:** None. **E. Carbajal Leon:** None. **G. Tsimis:** None. **Z. Suhail:** None. **A. Oliva:** None. **A. Fernandez-Ruiz:** None.

**Poster**

**PSTR202: Hippocampal-Cortical Interactions II**

**Location:** WCC Halls A-C

**Time:** Monday, November 16, 2026, 1:00 PM - 5:00 PM

**Program #/Poster #:** PSTR202.19/KK50

**Topic:** I.08. Learning and Memory

**Support:** NIH grant R01MH130367
Whitehall Foundation
NIH grant R01MH136355
NIH grant DP2MH136496
Sloan Fellowship
Klingenstein-Simons Fellowship
Pershing Square Foundation's MIND Prize
Cornell Neurotech Mong Fellowship

**Title:** Longitudinal place cell recordings with high-channel count, flexible probes in freely-moving mice

**Authors: *J. PARK**[1], Z. ZHAO[2], L. KARABA[2], Y. SAITO[3], W. TANG[4], S. PEREZ HERNANDEZ[2], A. KWON[2], C. SHON[5], M. AURELIO[2], W. ZHENG[6], A. OLIVA GONZÁLEZ[2], A. FERNANDEZ-RUIZ[2];
[2]Neurobio. and Behavior, [3]Ctr. for Brain Sci., [1]Cornell Univ., Ithaca, NY; [4]Cornell Univ., Ithaca, NY, ; [5]Neurobio. and Behavior, Cornell Univ., NY, NY; [6]Neurobio. and Behavior, Cornell Univ., Ithaca, MA

**Abstract:** Chronic in vivo electrophysiology in freely moving small animals has enabled the study of the neural circuit mechanisms of behavior. Despite its high spatio-temporal resolution and recent advances in high-density silicon probes, stable tracking of the same neurons across long periods of time has remained a challenge. This limitation has prevented the study of the neural mechanisms of learning and memory process that unfold over multiple days or weeks. To

overcome this barrier, we have implemented several technical innovations: 1) high-channel count, ultra-high density, flexible neural probes, 2) miniaturized active electronics, 3) analytical approaches to reliably track the same neurons across months. We integrated this technology into a scalable platform and performed longitudinal, large-scale recordings of the same hippocampal place cells and cortical cell assemblies over months in freely-moving mice. Flexible probes were fabricated ina 5-µm-thick parylene-C thin film and contained pedot:pss coated Pt 64 recording sites per shank with a double-sided architecture. This design resulted in the largest electrode density to date enabling us to record large numbers of neurons across different brain areas, and stably track them over months. We integrated the flexible probes with a 128-channel CMOS-based unit module and implemented a scalable headstage architecture. Multiple modules can be connected in parallel to expand the system to 512 channels. A single 128-channel unit weighs ~0.8 g, and the full 512-channel headstage weighs approximately ~4.4 g, our system supports 512-channel recording through a single USB-C tether, reducing cable torque, tether drag, and head-pulling artifacts.Using this platform, we recorded from large numbers of hippocampal place cell and cortical neurons during mouse navigation to investigate the dynamics of representational drift within and across regions. We compared these dynamics with the structure of cell assemblies and pyramidal-interneuron monosynaptic interactions to elucidate how functional circuit architecture constrain representational dynamics over time. This platform provides a new approach for chronically tracking distributed memory-circuit dynamics across single-neuron, local micro-circuit, and brain-wide network scales during learning.

**Disclosures: J. Park:** None. **Z. Zhao:** None. **L. Karaba:** None. **Y. Saito:** None. **W. Tang:** None. **S. Perez Hernandez:** None. **A. Kwon:** None. **C. Shon:** None. **M. Aurelio:** None. **W. Zheng:** None. **A. Oliva González:** None. **A. Fernandez-Ruiz:** None.

**Poster**

**PSTR202: Hippocampal-Cortical Interactions II**

**Location:** WCC Halls A-C

**Time:** Monday, November 16, 2026, 1:00 PM - 5:00 PM

**Program #/Poster #:** PSTR202.20/KK51

**Topic:** I.08. Learning and Memory

**Support:** NIH grant R01MH130367
Whitehall Foundation
NIH grant R01MH136355
NIH grant DP2MH136496
Sloan Fellowship
Klingenstein-Simons Fellowship
Pershing Square Foundation’s MIND Prize
Mong Fellowship

**Title:** WILDX: A wireless neurologger for Neuropixel recordings and closed-loop optogenetics in behaving mice

**Authors: *Z. ZHAO**[1], J. PARK[2], M. AURELIO[2], A. OLIVA[3], A. FERNANDEZ-RUIZ[2]; [2]Neurobio. and Behavior, [1]Cornell Univ., Ithaca, NY; [3]Neurosci. Dept., New York Univ., New York, NY

**Abstract:** Understanding the neural mechanisms underlying natural behavior requires the ability to record and manipulate brain activity in animals moving freely through rich, unrestrained environments. Extracellular electrophysiology is a powerful approach for studying these mechanisms, but high-channel-count recordings are typically constrained by tethering, whereas wireless systems are often limited by channel count, payload weight, battery life, and lack additionalcapabilities ,such as closed-loop optogenetic manipulations. These limitations restrict the study of naturalistic behaviors such as long-range exploration, social group interactions, and behavior in large-scale environments. We previously developed the Wireless, Interactive, Lightweight Datalogger (WILD), a sub-1.5 g wireless neurologger that combines 64-channel electrophysiological recording, multimodal behavioral sensing, and responsive neural stimulation for real-time monitoring and closed-loop perturbation in freely behaving animals. However, its limited channel count constrained the study of large-scale neural dynamics across distributed brain circuits. To address this challenge, we developed WILDX, a lightweight wireless platform that supports simultaneous recording from two Neuropixels 1.0 or 2.0 probes or 384 channels flexible probe connected to a custom Neuropixels 1.0 NRIC pre-amplifier through either USB streaming or onboard microSD storage. Weighing less than 1.8 g, WILDX also features multimodal sensing and closed-loop optogenetics functionalities enabling recordings and manipualtions of neural activity in freely behaving mice and other small animals. In addition, we implemented a real-time spike-based inference engine for onboard neural decoding and responsive stimulation. We demonstrated how WILDX achieved low-noise in vivo recordings and enabled 768-channel electrophysiological recording in freely moving mice. Together, this platform provides a powerful tool for mechanistic investigation of brain activity during complex, naturalistic behaviors, and will be a valuable resource for the community.

**Disclosures: Z. Zhao:** None. **J. Park:** None. **M. Aurelio:** None. **A. Oliva:** None. **A. Fernandez-Ruiz:** None.

**Poster**

**PSTR202: Hippocampal-Cortical Interactions II**

**Location:** WCC Halls A-C

**Time:** Monday, November 16, 2026, 1:00 PM - 5:00 PM

**Program #/Poster #:** PSTR202.21/KK52

**Topic:** I.08. Learning and Memory

**Support:** NIH grant R01MH130367
NIH grant R01MH136355
NIH grant DP2MH136496
Whitehall Foundation
Sloan Fellowship

Klingenstein-Simons Fellowship
Pershing Square Foundation's MIND Prize

**Title:** Hippocampal-cortical maps across modes of adaptive behavioral control

**Authors: *K. GUPTA**, Y. SAITO, G. LEE, C. CHENG, K. ZHU, W. ASTORGA-WISTER, N. MILLER, A. OLIVA, A. FERNANDEZ-RUIZ;
Dept. of Neurobio. and Behavior, Cornell Univ., Ithaca, NY

**Abstract:** In order to survive in natural environments, animals must exploit learned foraging routes to food sources, while flexibly adapting their strategies upon environmental changes. This adaptive capacity is theorized to depend on cognitive maps: internal representation of spatial, temporal, and abstract relational structures that can be leveraged for guiding behavior. Within the hippocampal-cortical networks, neural representations of these relational variables are often interpreted as the neural substrate for such maps. However, much of the existing literature examines these representations without distinguishing the forms of behavioral control under which such maps are formed and subsequently utilized. Here, we asked how cognitive maps built during habitual navigation in a static environment are modified and repurposed during value-guided patch choice. Rats were trained in a foraging task that dissociated traversal between learned deterministic patches from stay/switch decisions under unpredictable costs into different task phases. We performed large-scale neural ensemble recordings in hippocampal and cortical areas to investigate the underlying neural representations in this task. Behavioral analyses indicated that animals learned stable inter-patch trajectories indicative of procedural behavior and, upon the imposition of variable costs, demonstrated adaptive, value-based decision-making reflecting optimal foraging behavior. Initial neural analyses revealed stability in neural representations across task phases suggesting a shared scaffold of relational structure shared between two modes of behavioral control. Moreover, further analyses demonstrated that such representational stability across tasks phases cannot be explained by a purely spatial code, but instead is tied to the reward configuration. These findings support a model in which hippocampal-cortical maps are not static allocentric descriptions of space, but behaviorally gated representations that integrate task-relevant variables as animals navigate between different modes of behavior control.

**Disclosures: K. Gupta:** None. **Y. Saito:** None. **G. Lee:** None. **C. Cheng:** None. **K. Zhu:** None. **W. Astorga-Wister:** None. **N. Miller:** None. **A. Oliva:** None. **A. Fernandez-Ruiz:** None.

**Poster**

**PSTR202: Hippocampal-Cortical Interactions II**

**Location:** WCC Halls A-C

**Time:** Monday, November 16, 2026, 1:00 PM - 5:00 PM

**Program #/Poster #:** PSTR202.22/KK53

**Topic:** I.08. Learning and Memory

**Support:** Eric and Wendy Schmidt AI in Science Postdoctoral Fellowship
Whitehall Foundation
NIH grant R01MH136355
NIH grant DP2MH136496
Sloan Fellowship
Klingenstein-Simons Fellowship
Pershing Square Foundation's MIND Prize
NIH grant R01MH130367

**Title:** Transient Scale-Free Dynamics in Hippocampus Facilitate Flexible Spatial Learning

**Authors: *W. CHEN**, H. CHANG, L. KARABA, X. MEI, R. E. HARVEY, W. TANG, A. FERNANDEZ-RUIZ, A. OLIVA;
Dept. of Neurobio. and Behavior, Cornell Univ., Ithaca, NY

**Abstract:** Theoretical studies suggest that neural systems operating at criticality exhibit optimal computational properties. However, it remains unclear whether and how self-organized dynamics emerge in the hippocampus and how it relates to distinct cognitive processes. We used temporal renormalization group theory to analyze large-scale electrophysiological recordings from behaving rats and investigated how proximity to criticality in the CA1 region of the hippocampus relates to spatial learning. We found that the hippocampus operated near criticality during the initial stages of a goal-directed, spatial learning task. We built a biophysically inspired CA1 network and ran computational simulations to predict that initializing the network with near-critical dynamics would enable better spatial learning in a complex task. Indeed, in our experimental data we found that the near-critical state displayed higher flexibility of neural representations and correlated with the learning of distinct spatial contexts. Importantly, our experimental data showed that the network's distance to criticality adjusted with cognitive demands and was modulated by both upstream inputs and local circuitry. Together, our results provide a biological substrate for how critical dynamics enable flexible learning in neural networks.

**Disclosures: W. Chen:** None. **H. Chang:** None. **L. Karaba:** None. **X. Mei:** None. **R.E. Harvey:** None. **W. Tang:** None. **A. Fernandez-Ruiz:** None. **A. Oliva:** None.

**Poster**

**PSTR202: Hippocampal-Cortical Interactions II**

**Location:** WCC Halls A-C

**Time:** Monday, November 16, 2026, 1:00 PM - 5:00 PM

**Program #/Poster #:** PSTR202.23/KK54

**Topic:** I.08. Learning and Memory

**Support:** NIH grant R01MH130367
NIH grant DP2MH136496
NIH grant R01MH136355

Whitehall Foundation
Sloan Fellowship
Klingenstein-Simons Fellowship
Pershing Square Foundation's MIND Prize

**Title:** Linking Metabolic State to Hippocampal Sharp-Wave Ripples Through Hypothalamic AgRP Neurons

**Authors: *A. GRUZDEVA**, A. KWON, R. TODOROVA, L. KARABA, N. YAPICI, A. FERNANDEZ-RUIZ, A. OLIVA;
Neurobio. and Behavior, Cornell Univ., Ithaca, NY

**Abstract:** Internal metabolic state shapes behavior, yet how metabolic signals interact with hippocampal network activity associated with memory processing remains poorly understood. Agouti-related peptide (AgRP) neurons in the hypothalamus are key regulators of energy balance, whereas hippocampal sharp-wave ripples (SWRs) and CA2 barrages (BARRs) are network events implicated in memory processing. To determine whether metabolic state influences hippocampal network activity, we compared SWR occurrence in ad libitum-fed and 24-hour-fasted mice. Fasted animals showed reduced SWR rates during sleep and awake immobility, consistent with the possibility that metabolic state influences the occurrence of these coordinated network events. Next, to examine interactions between metabolic signaling and hippocampal network dynamics, we performed simultaneous fiber photometry recordings of AgRP neurons and electrophysiological recordings from hippocampal CA1 and CA2. We found that AgRP neuronal activity was coupled to both SWRs and BARRs across behavioral states. AgRP activity increased around SWR onset and decreased around BARR events in both fed and fasted animals. Because SWRs involve coordinated activation of neuronal ensembles across the hippocampus and distributed brain networks, we hypothesize that AgRP neurons may reflect the metabolic demands associated with these events. To test this, we are currently examining the impact of SWR generation using optogenetics on AgRP photometry signals. Together, these findings suggest that hippocampal sharp-wave ripples are influenced by metabolic state and raise the possibility that metabolic signaling contributes to the regulation of memory-associated network activity.

**Disclosures: A. Gruzdeva:** None. **A. Kwon:** None. **R. Todorova:** None. **L. Karaba:** None. **N. Yapici:** None. **A. Fernandez-Ruiz:** None. **A. Oliva:** None.

**Poster**

**PSTR202: Hippocampal-Cortical Interactions II**

**Location:** WCC Halls A-C

**Time:** Monday, November 16, 2026, 1:00 PM - 5:00 PM

**Program #/Poster #:** PSTR202.24/KK55

**Topic:** I.08. Learning and Memory

**Support:** NIH/NIGMS P30GM149405
NIH S10OD036341

**Title:** Representational transformations from perception to recall in human early visual cortex

**Authors: *F. ZOU**, S. E. FAVILA;
Dept. of Cognitive and Psychological Sci., Brown Univ., Providence, RI

**Abstract:** Recalling an event from the past is thought to rely on reactivation of cortical activity patterns initially evoked during perception. However, accumulating evidence suggests that memory recall involves systematic representational transformations rather than faithful reinstatement of perceptual activity. In particular, recent fMRI studies examining spatial tuning in human visual cortex have documented systematic differences between perception and recall, with the largest effects observed in early visual cortex (EVC). Yet, the mechanisms underlying these representational changes remain unclear. Prior work has focused primarily on simple visual features in highly practiced memories. This leaves open two critical questions: whether these changes generalize to complex natural visual inputs and, more importantly, whether these changes emerge immediately during recall or develop gradually through repeated recall. To test this, we used fMRI to track how neural representations of natural scenes transform from perception to recall across repeated retrieval attempts. During perception, human participants (N = 12) were presented with pairs of natural scene images and arbitrary auditory word cues. During recall, participants heard an auditory word cue and were instructed to recall the associated image. Images were assigned to either a repeated condition (4 recalls) or a control condition (2 recalls). Using representational similarity analysis combined with deep neural network vision models, we found that EVC representations aligned most strongly with early model layers during image perception, consistent with the representation of low-level visual features. Strikingly, recall exhibited the opposite pattern with EVC representations showing greater correspondence to deeper model layers associated with high-level, abstract visual features. In contrast, higher visual cortex (ventral occipitotemporal cortex) exhibited similar representational profiles during perception and recall, showing the strongest correspondence with deeper model layers in both tasks. Moreover, preliminary analyses revealed that representational transformations in EVC were greater in the repeated condition than in the control condition, suggesting that these changes are amplified by repeated recall. Together, these results suggest systematic transformations in EVC representations arise from perception to recall and these transformations continue to evolve with repeated recall.

**Disclosures: F. Zou:** None. **S.E. Favila:** None.

**Poster**

**PSTR202: Hippocampal-Cortical Interactions II**

**Location:** WCC Halls A-C

**Time:** Monday, November 16, 2026, 1:00 PM - 5:00 PM

**Program #/Poster #:** PSTR202.25/KK56

**Topic:** I.08. Learning and Memory

**Support:** NSF National Graduate Research Fellowship
NIH R01 MH129436

**Title:** The emergence of memory systems through meta-learning

**Authors: *Z. ZHOU**[1], A. C. SCHAPIRO[2];
[1]Dept. of Psychology, New York Univ., New York, NY; [2]Psychology, Univ. of Pennsylvania, Philadelphia, PA

**Abstract:** Long-term learning and memory in the primate brain rely on a series of hierarchically organized subsystems extending from early sensory neocortical areas to the hippocampus. The components differ in their representational attributes and plasticity, with evidence for sparser, more decorrelated activity and faster plasticity in regions higher up in the hierarchy. Within the hippocampus, parallel pathways further differ in plasticity, sparsity, and recurrence. How and why did the brain arrive at this organization? We explore the principles that allow such an organization to emerge by simulating a hierarchy of learning subsystems in artificial neural networks (ANNs) using a meta-learning approach. As ANNs optimized weights for a series of tasks, they concurrently meta-learned layer-wise plasticity and sparsity parameters. This approach enhanced the computational efficiency of ANNs, promoting hidden activation sparsity while benefitting task performance. Meta-learning gave rise to a brain-like hierarchical organization, with higher layers displaying faster plasticity and a sparser, more pattern-separated neural code than lower layers. Early layers peaked early in their plasticity and stabilized, whereas higher layers continued to develop and maintained elevated plasticity over time, mirroring empirical developmental trajectories. We explored whether brain-like organization emerges in parallel, in addition to serial, circuits by training two parallel recurrent pathways at the top of a hierarchy, analogous to intra-hippocampal pathways. ANNs with initially identical parallel recurrent pathways trained on dual tasks requiring item-specific encoding and categorization spontaneously differentiated, with one pathway developing higher learning rates, sparser activity, and stronger recurrence than the other. Pathway lesions revealed a double dissociation that generalized to novel categories, with the faster-learning pathway selectively supporting item encoding and the slower-learning pathway supporting categorization. Ablating only the recurrence in the faster-learning pathway impaired item encoding while ablating it in the slower-learning pathway had minimal effect. These emergent properties mirror those observed empirically in the hippocampus. These results suggest that the macroscale organization and development of heterogeneous learning subsystems in the brain may emerge in part from optimizing biological variables that govern plasticity, sparsity, and recurrence.

**Disclosures: Z. Zhou:** None. **A.C. Schapiro:** None.

**Poster**

**PSTR202: Hippocampal-Cortical Interactions II**

**Location:** WCC Halls A-C

**Time:** Monday, November 16, 2026, 1:00 PM - 5:00 PM

**Program #/Poster #:** PSTR202.26/KK57

**Topic:** I.08. Learning and Memory

**Support:** NIH Grant R01 MH126183

**Title:** Developmental changes in the impact of real-world exploration on task-based memory performance

**Authors: *W. YU**, S. L. BENEAR, C. A. HARTLEY;
New York Univ., New York, NY

**Abstract:** Environmental exploration increases over the course of development. While prior research has suggested that environmental enrichment and novelty enhance memory, other work has highlighted the beneficial effects of familiarity and contextual consistency. How these factors jointly impact memory and how these effects change over development remain unclear. Moreover, the majority of existing evidence comes from in-laboratory experiments, leaving it understudied how real-world experiences affect memory in both adults and developing populations. We recruited participants aged 12-25 (N=94) and continuously tracked their real-world GPS locations over 90 days. Twice per week, participants completed a mini Mnemonic Similarity Task (MST) on their phones, during which they were asked to discriminate previously encoded images from perceptually similar lures and new foils. We also recorded participants' geolocations at both memory encoding and retrieval. Results showed that greater real-world exploration positively predicted mood and subjective novelty. Relating real-world exploration and memory performance, we found that encoding and retrieving MST images in consistent geolocations facilitated memory specificity, particularly on days with high exploratory variability, and that this effect emerged over development. Further, we examined the mnemonic errors participants made on the lure images that were similar to the previously viewed items. Consistent with the notion that novelty biases memory systems away from pattern completion, we found that judgments following novel items in the task context, in novel real-world geolocations, and on days of greater subjective novelty were significantly biased towards "new" rather than "old" errors for similar lures; the effect of subjective novelty also trended stronger in older than younger participants. Together, these findings illuminate how laboratory-based characterizations of memory development generalize to ecological settings.

**Disclosures: W. Yu:** None. **S.L. Benear:** None. **C.A. Hartley:** None.

**Poster**

**PSTR203: Grid Cells and Spatially Modulated Cells**

**Location:** WCC Halls A-C

**Time:** Monday, November 16, 2026, 1:00 PM - 5:00 PM

**Program #/Poster #:** PSTR203.01/KK58

**Topic:** I.09. Spatial Navigation

**Support:** Kavli Foundation
Synergy grant from the European Research Council (KILONEURONS, grant 951319)

Centre of Excellence grant from Research Council of Norway (Centre for Algorithms in the Cortex, grant 332640)
National Infrastructure grant from Research Council of Norway (NORBRAIN, grant 295721)

**Title:** Geometry and dynamics of remapping across the spatial navigation system

**Authors: *J. CARPENTER**[1], R. J. GARDNER[1], M. GUARDAMAGNA[1], C. LYKKEN[1], B. DUNN[2], M.-B. MOSER[1], E. I. MOSER[1];
[1]Kavli Inst. for Systems Neurosci., Trondheim, Norway; [2]Dept. of Mathematics, Norwegian Univ. of Sci. and Technol., Trondheim, Norway

**Abstract:** Spatial navigation requires an internal model of space, and the brain holds many such models at once, bringing the appropriate one online as the world changes. These models are the joint code of several functional cell populations across the spatial navigation circuit: head-direction (HD) cells in the pre-subiculum, grid cells in the medial entorhinal cortex (MEC), and the place cells in the hippocampus (HPC). Between environments, each population reorganizes in its own way: place cells remap, HD cells rotate with environmental cues, and grid modules re-anchor independently of one another. However, how these different populations work together to store many maps, and the dynamics governing their retrieval remain unknown. Here, we record simultaneously across the HPC-EC circuit with 3-4 Neuropixels 2.0 probes while rats foraged in five distinct environments with enough cells per region to support population analysis on the millisecond timescale. For each population, we leverage the code's geometry to build decoders that require no real-space coordinates, and these methods recover more distinguishable states (~12 maps) than rate-map methods. With this data, we give the first experimental evidence that the product space of multiple grid modules occupies a high-dimensional, high-capacity toroidal manifold, which we call the "mega-torus." Each position in space is a point on this manifold; each environment is a well-separated, twisted sheet through it. A handful of unlabeled phase samples in time is enough to identify which map is engaged and the animal's position within it. Long predicted as the state space of the grid system's multi-modular code, this manifold is the geometry on which the brain places its spatial memories. Additionally, by tracking fine-timescale dynamics across the product grid manifolds and the state spaces for the other functional populations, we find that recalling a familiar spatial map was not immediate. In fact, for several seconds, both the grid and place populations fire as if still in the wrong map. We observe that head direction stabilizes its mapping to the external environment first, the grid network follows shortly after, and lastly, the hippocampal place code. Together, these results demonstrate the role of the navigation circuit as a memory substrate and define the dynamics by which stored maps are recalled.

**Disclosures: J. Carpenter:** None. **R.J. Gardner:** None. **M. Guardamagna:** None. **C. Lykken:** None. **B. Dunn:** None. **M. Moser:** None. **E.I. Moser:** None.

**Poster**

**PSTR203: Grid Cells and Spatially Modulated Cells**

**Location:** WCC Halls A-C

**Time:** Monday, November 16, 2026, 1:00 PM - 5:00 PM

**Program #/Poster #:** PSTR203.02/KK59

**Topic:** I.09. Spatial Navigation

**Support:** Kavli Foundation
Synergy grant from the European Research Council (KILONEURONS, grant 951319)
Centre of Excellence grant from Research Council of Norway (Centre for Algorithms in the Cortex)
National Infrastructure grant from Research Council of Norway (NORBRAIN, grant 295721)

**Title:** A hot spot of grid cells in the medial entorhinal cortex

**Authors: *M. POFAHL**[1], N. L. DE JONG[2], H. A. OBENHAUS[3], H. ENEQVIST[1], M. P. WITTER[4], W. ZONG[5], M.-B. MOSER[6], E. I. MOSER[6];
[1]Kavli Inst. for Systems Neurosci., Trondheim, Norway; [2]Kavli Inst. for Sys. Neurosci., NTNU, Trondheim, Norway; [3]Moser Group, Kavli Inst. For Systems Neurosci., Trondheim, Norway; [4]Kavli Inst. Systems Neurosci., NTNU Norwegian Univ. of Sci. and Technology, Trondheim, Trondheim, Norway; [5]Kavli institute of systems neuroscience, NTNU, Trondheim, Norway; [6]Kavli Inst. Systems Neurosci, Trondheim, Norway

**Abstract:** The medial entorhinal cortex (MEC) encodes spatial information through a set of canonical cell types, including grid cells, object-vector (OV) cells, head-direction (HD) cells, and boundary-vector (BV) cells. While these functional cell types are co-located within the superficial layers of MEC and the adjacent parasubiculum (PaS), the exact anatomical distribution of these cell types within the MEC remains to be determined. Previous studies showed that grid cells form discrete modules of increasing scale along the dorsal-ventral axis of MEC. Additionally, imaging studies found a non-uniform distribution of grid cells across MEC and suggested a clustering of grid cells towards the dorsomedial MEC, whereas OV, HD, and border cells appeared more uniformly distributed. However, technical limitations have restricted the simultaneous mapping and quantification of these cell types across extended anatomical regions in individual animals. To overcome these limitations, we performed two-photon calcium imaging via miniscopes (MINI2P) and combined multiple field of views (FOVs) obtained in freely moving mice across a 1.3mm wide square prism implant covering MEC and PaS. The imaging area includes the three most dorsal modules with all of module M2 and parts of dorsal M1 and ventral M3. Each grid cell module forms a distinct anatomical cluster (´hot spot´) in the dorsomedial MEC, near the PaS border with an average diameter of 330 um. The estimated fraction of grid cells in the M2 hot spot of layer II is in the order of 30-50%. Combining recordings from multiple depths of layer II we can estimate the absolute number of grid cells for one module in one hemisphere around 500-650. The 300-400 um wide band of grid cell modules is anticorrelated to the anatomical locations of other functional cell. We find more and sharper tuned HD cells in PaS but also find a stable fraction of weakly head direction modulated cells across MEC, often in conjunction with other functional properties. We find OV cells and BV cells in both PaS and lateral MEC. However, BV and OV cells in MEC possess longer animal to border/object vectors than cells in PaS. Further we find a dorsoventral gradient in both cell types with increasing vector lengths towards the ventral part of MEC. Our data allows us to define a general functional map of the superficial layers of MEC and PaS and quantify the total number

of layer II grid cells for one module. Our findings reveal a previously unrecognized tight anatomical clustering of grid cells and suggest a structured spatial relationship between grid and non-grid cells, with implications for the organization and integration of spatial signals within the entorhinal-hippocampal circuit.

**Disclosures: M. Pofahl:** None. **N.L. de Jong:** None. **H.A. Obenhaus:** None. **H. Eneqvist:** None. **M.P. Witter:** None. **W. Zong:** None. **M. Moser:** None. **E.I. Moser:** None.

**Poster**

**PSTR203: Grid Cells and Spatially Modulated Cells**

**Location:** WCC Halls A-C

**Time:** Monday, November 16, 2026, 1:00 PM - 5:00 PM

**Program #/Poster #:** PSTR203.03/KK60

**Topic:** I.09. Spatial Navigation

**Support:** Kavli Foundation
Synergy grant from the European Research Council (KILONEURONS, grant 951319)
Centre of Excellence grant from Research Council of Norway (Centre for Algorithms in the Cortex, grant 332640)
National Infrastructure grant from Research Council of Norway (NORBRAIN, grant 295721)

**Title:** Development of sweeps and toroidal dynamics in the entorhinal cortex

**Authors: *M. GUARDAMAGNA**[1], J. CARPENTER[2], E. HERMANSEN[3], B. DUNN[4], E. I. MOSER[5], M.-B. MOSER[5];
[2]Kavli Inst. for Systems Neurosci., [1]Kavli Inst. for Systems Neurosci., Trondheim, Norway; [3]Dept. of Mathematical Sci., Norwegian Univ. of Sci. and Technol., Oslo, Norway; [4]Dept. of Mathematics, Dept. of Mathematics, Trondheim, Norway; [5]Kavli Inst. Systems Neurosci, Trondheim, Norway

**Abstract:** The medial entorhinal cortex (MEC) is a central hub for the coding of spatial experiences. Grid cells and head direction (HD) cells are essential elements of the navigation system. At the population level, the activity of these cells traverses low-dimensional manifolds, torus and ring manifolds respectively, consistent with the predictions of continuous attractor network theories. We recently showed that these manifolds are already present in rat pups before the onset of spatial navigation, when the eyes and ear canals are still closed (Guardamagna et al., 2026).
While the early emergence of these rigid manifolds is established, it remains unknown whether the fast-timescale dynamics that govern adult spatial coding are present from the beginning or if they mature later. In adult networks, grid cell activity is organized into millisecond-timescale, theta-paced sequences that sweep through the nearby environment in a rigid left-right-alternating pattern, hypothesized to be crucial for memory encoding and retrieval and the sampling of

surrounding space (Vollan et al., 2025). To determine the developmental timeline of these sequential dynamics, we tracked large neural populations and local field potentials (LFP) in the MEC of developing rats from P10 to P21 using chronic Neuropixels 2.0 recordings.
We first established that toroidal manifolds are detectable prior to the presence of consistent theta oscillations (4-12 Hz), confirming that theta is not a prerequisite for toroidal formation. Theta oscillations emerge around P12, coinciding with the appearance of fast-spiking interneurons, and gradually increase in both frequency and power through P21. This maturation of fast-spiking inhibitory dynamics is further reflected in a significant increase in slow gamma (20-45 Hz) burst power at P21, accompanied by a sharp increase in spike-LFP locking to both slow gamma and theta.
Crucially, although regular grid firing is already observable at P19-21, we found that early sequential activity lacks the consistent, left-right alternation characteristic of adult entorhinal sweeps even at P21. We are currently investigating the presence of alternating sequences directly on the toroidal manifold from P10 to P14, independent of physical spatial reference frames. These findings indicate that the ontogeny of entorhinal sweep dynamics is a multi-stage process, gated by precise physiological changes, in which spatial coding emerges well before theta-coordinated alternating sequences. The late emergence of organized sweeps raises critical questions about the specific circuitry required for the emergence of temporal coding in the hippocampal-entorhinal network.

**Disclosures: M. Guardamagna:** None. **J. Carpenter:** None. **E. Hermansen:** None. **B. Dunn:** None. **E.I. Moser:** None. **M. Moser:** None.

**Poster**

**PSTR203: Grid Cells and Spatially Modulated Cells**

**Location:** WCC Halls A-C

**Time:** Monday, November 16, 2026, 1:00 PM - 5:00 PM

**Program #/Poster #:** PSTR203.04/KK61

**Topic:** I.09. Spatial Navigation

**Support:** Kavli Foundation
Centre of Excellence grant from Research Council of Norway (Centre for Algorithms in the Cortex, grant 332640)

**Title:** Spatial representations of curved surfaces: Distances on the grid cell torus approximate local physical distances

**Authors: *V. KARGÅRD OLSEN**[1], A. LAUTRUP[1], M. SCHELLENBERGER[1], B. DUNN[2], M.-B. MOSER[1], E. I. MOSER[1];
[1]Kavli Inst. for Systems Neurosci., Trondheim, Norway; [2]Dept. of Mathematics, Trondheim, Norway

**Abstract:** The hexagonal pattern of grid cells, and their resulting flat toroidal manifold, appears adapted to represent a position on a flat surface. As the real world is not perfectly flat, a natural

question is how grid cells represent position on non-flat surfaces extending into 3D space. Previous studies have recorded grid cells on ramps, walls, and other 3D mazes. These environments are either flat or provide ample realignment cues, leaving open the question of if and how grid cells map curved and continuous spaces.
There are at least two strategies grid cells could use to accommodate curved environments: they could (1) break the environment into several approximately flat patches, each with its own local alignment, or (2) continuously morph the hexagonal pattern, and thus the torus, to accommodate the shape of the surface. Here, we explore these options by recording large numbers of cells in the medial entorhinal cortex using high-density Neuropixels probes, while mice freely explore a flat ramp, a large spherical dome, and a steep cone. We then leverage the toroidal manifold of grid cells to investigate how the toroidal phases changes across the surface. This allows us to quantify toroidal distances between nearby (within one grid spacing) locations, revealing how a grid cell module measures distances in an environment.
In preliminary data, we find that grid cells align to the surface of a ramp, using the same strategy as in flat horizontal environments. On the dome and cone, however, grid cell rate maps and toroidal phases appear morphed. On the dome we see an almost hexagonal pattern, while the pattern is less regular on the cone. We show that this morphing is structured, as we can approximate the physical shape of the environment by embedding the geodesic toroidal distances in 3D space. Next, we investigate the morphing by formulating an objective function that determines how the torus might map arbitrary surfaces: the torus assigns toroidal phases to locations such that physical distances between nearby locations are reproduced by distances on the torus. This is consistent with our recordings, where we find that distances between decoded toroidal phases closely match local physical distances, across all recorded environments. Thus, while grid cell rate maps and toroidal phases sometimes look irregular, they correspond to an optimal way of maintaining local physical distances.
The proposed objective function unifies grid cell responses across different 3D environments, while maintaining the hexagonal pattern in 2D environments. Additionally, it can make predictions in new environments, which we are currently collecting data to test.

**Disclosures: V. Kargård Olsen:** None. **A. Lautrup:** None. **M. Schellenberger:** None. **B. Dunn:** None. **M. Moser:** None. **E.I. Moser:** None.

**Poster**

**PSTR203: Grid Cells and Spatially Modulated Cells**

**Location:** WCC Halls A-C

**Time:** Monday, November 16, 2026, 1:00 PM - 5:00 PM

**Program #/Poster #:** PSTR203.05/KK62

**Topic:** I.09. Spatial Navigation

**Support:** Kavli Foundation
Synergy grant from the European Research Council (KILONEURONS, grant 951319)
Centre of Excellence grant from Research Council of Norway (Centre for Algorithms in the Cortex, grant 332640

National Infrastructure grant from Research Council of Norway (NORBRAIN, grant 295721)

**Title:** Attentional modulation of theta sweeps

**Authors: *M. F. SCHELLENBERGER**, A. Z. VOLLAN, R. SAXENA, R. J. GARDNER, M.-B. MOSER, E. I. MOSER;
Kavli Inst. for Systems Neurosci. and Ctr. for Algorithms in the Cortex, Trondheim, Norway

**Abstract:** Grid cells support navigation by forming an internal map of self-position. By observing the position encoded by populations of grid cells on a theta timescale while rats were foraging in an open field box, Vollan and Gardner et al. (2025) showed that the encoded position does not rigidly adhere to the animal's position but rather rhythmically sweeps ahead of the animal. In each 125 ms theta cycle, these sweeps first represent the animal's position and then move alternatingly towards the front-left or front-right of the animal. Upstream internal direction neurons in the parasubiculum are thought to generate the stereotypic, experience-independent theta sweep pattern. Sweeps could act as an optimized sampling mechanism for the internal map, since left-right alternation provides maximal uniform coverage of upcoming space at the subsecond time scale. However, while uniform sampling is efficient in free exploration, directing theta sweeps towards regions of interest may be more beneficial during more structured tasks with localized cues and rewards. Recently, we found that the rigid left-right alternation pattern of sweeps observed in free exploration is dynamic and adaptable. Sweeps track a piece of bait when rats orient towards it during chasing and they point in the movement direction when rats walk backwards or are transported passively (Vollan et al. 2026). Bait-tracking sweeps can be interpreted as a form of bottom-up spatial attention, whereas sweeps that point in the movement direction can be seen as top-down action planning. To test these possibilities, we have developed a novel paradigm in which rats navigate towards discrete locations, cued by brief auditory and visual stimuli. By combining this new paradigm, as well as chasing and backwards walking, with DREADD-induced unilateral inactivation of the parasubiculum, we are probing whether interfering with sweep directions has consequences for subsequent behavior. Taken together, these experiments will elucidate how sweeps are related to attention and what role they play in supporting navigation.

**Disclosures: M.F. Schellenberger:** None. **A.Z. Vollan:** None. **R. Saxena:** None. **R.J. Gardner:** None. **M. Moser:** None. **E.I. Moser:** None.

**Poster**

**PSTR203: Grid Cells and Spatially Modulated Cells**

**Location:** WCC Halls A-C

**Time:** Monday, November 16, 2026, 1:00 PM - 5:00 PM

**Program #/Poster #:** PSTR203.06/KK63

**Topic:** I.09. Spatial Navigation

**Support:** Kavli Foundation
Synergy grant from the European Research Council (KILONEURONS, grant 951319)
Centre of Excellence grant from Research Council of Norway (Centre for Algorithms in the Cortex, grant 332640)
National Infrastructure grant from Research Council of Norway (NORBRAIN, grant 295721)
EMBO Postdoctoral Fellowship

**Title:** A bihemispheric circuit mechanism underlies left-right alternating grid cell theta sweeps

**Authors: *R. SAXENA**[1], A. Z. VOLLAN[1], M. F. SCHELLENBERGER[1], V. A. NORMAND[2], M.-B. MOSER[2], E. I. MOSER[2];
[1]Ctr. for Algorithms in the Cortex, Kavli Inst. for Systems Neurosci., Trondheim, Norway; [2]Ctr. for Algorithms in the Cortex, Kavli Inst. for Syst. Neurosci., Trondheim, Norway

**Abstract:** Navigation relies on entorhinal-hippocampal network dynamics, such as theta sweeps, in which decoded positions from medial entorhinal cortex (MEC) grid cells alternately extend left and right of the animal's location on successive theta cycles. Theta sweeps are guided and aligned to a left-right alternating internal direction (ID) signal from the upstream parasubiculum (PaS). Theta sweeps may serve as an optimal sampling mechanism enabling rapid map formation; but the circuit mechanisms underlying this alternation remain unknown. Across species (zebrafish and *Drosophila*), movement of directional activity, such as head-direction (HD), is thought to arise from multi-ring shifter networks, in which opposing shifter rings drive HD in opposite directions. We reasoned that a related architecture, combined with a central pattern generator (CPG)-like mechanism, could generate left-right alternating theta sweeps in rats. Specifically, rhythmic switching between two internally coupled shifter rings could alternately bias sweep trajectories towards the left and right.
Using Neuropixels 2.0 recordings from MEC/PaS in rats, we identified novel lateralized internal-direction (L-ID) cells in PaS, which exhibit conjunctive HD and ID tuning and strong hemispheric lateralization. Left-hemisphere L-ID cells preferentially fire during rightward sweeps and display a clockwise shift of ID relative to HD tuning, whereas right-hemisphere L-ID cells show the opposite pattern. Cross-correlogram analyses reveal a cross-hemispheric inhibitory circuit in which L-ID cells recruit contralateral fast-spiking interneurons that suppress the opposing L-ID population ipsilaterally, providing a candidate mechanism for alternation. Consistent with this, unilateral chemogenetic inactivation of CaMKIIα-expressing MEC/PaS neurons biases both ID signals and theta sweeps toward the contralateral side. In addition, L-ID cells form monosynaptic connections with non-lateralized (pure) ID cells in both hemispheres, with tuning offsets centered near ±30 degrees.
Based on these findings, we propose a "copy-and-shift" architecture that combines a shifter network with a CPG-like mechanism. Driven by a common head-direction (HD) input, reciprocally inhibiting bilateral L-ID populations provides phase-shifted drive to pure ID cells, forming a multi-ring shifter network in which cross-hemispheric inhibition generates alternating dynamics that bias successive theta sweeps. This architecture suggests a conserved computational motif across species and brain regions, adapted in rodent parahippocampal circuits to generate left-right alternating theta sweeps.

**Disclosures: R. Saxena:** None. **A.Z. Vollan:** None. **M.F. Schellenberger:** None. **V.A. Normand:** None. **M. Moser:** None. **E.I. Moser:** None.

**Poster**

**PSTR203: Grid Cells and Spatially Modulated Cells**

**Location:** WCC Halls A-C

**Time:** Monday, November 16, 2026, 1:00 PM - 5:00 PM

**Program #/Poster #:** PSTR203.07/KK64

**Topic:** I.09. Spatial Navigation

**Support:** Kavli Foundation
Synergy Grant from the European Research Council (KILONEURONS, grant 951319)
Centre of Excellence grant from the Research Council of Norway (Centre for Algorithms in the Cortex, grant 332640)

**Title:** Organization of grid modules across the dorsal-to-ventral axis of MEC

**Authors: *C. LYKKEN**[1,2], V. A. NORMAND[3], R. GARDNER[4], B. DUNN[5], M.-B. MOSER[6], E. I. MOSER[6];
[1]NTNU, Trondheim, Norway; [2]Kavli Inst. Systems Neurosci, NTNU, Trondheim, Norway; [3]Kavli Inst. for Syst. Neurosci., Trondheim, Norway; [4]Kavli Inst. For Systems Neurosci., Trondheim, ; [5]Dept. of Mathematics, Dept. of Mathematics, Trondheim, Norway; [6]Kavli Inst. Systems Neurosci, Trondheim, Norway

**Abstract:** Grid cells in the medial entorhinal cortex (MEC) are organized into discrete modules that differ in spatial scale and are thought to collectively support a multi-scale representation of space. Along the dorsal-ventral axis of MEC, grid spacing has been shown to vary from ~30-40 cm to several meters. However, most recordings have been limited to dorsal or intermediate MEC, and simultaneous recordings spanning more than 3-4 grid modules remain rare. Thus, it is unclear whether large-scale modules exist in ventral MEC and whether previously reported scale ratios between neighboring modules are preserved across the full range of grid scales. To address this, we used Neuropixels probes to simultaneously record from grid modules spanning the dorsal-ventral axis of MEC across a range of behavioral conditions, including the exploration of large environments (4 ×4 m). Using a latent variable model (LVM) with a toroidal prior enabled the identification of grid modules across an extended range of spatial scales, including modules with periods larger than the width of the recorded environment. Within each animal, we localized the anatomical position of each identified module and estimated the scale ratios between neighboring modules. We identified a larger number of modules than the 3-4 previously identified in the dorsal two-thirds of the MEC, some of which had grid periods of several meters. We are currently mapping the full extent of modules, including the full dorsoventral range of MEC. Together, the results will illustrate how grid modules are organized and coordinated along the entire dorsal-ventral extent of MEC, providing insight into the dynamic range and coding capacity of the grid cell system.

**Disclosures: C. Lykken:** None. **V.A. Normand:** None. **B. Dunn:** None. **M. Moser:** None. **E.I. Moser:** None.

**Poster**

**PSTR203: Grid Cells and Spatially Modulated Cells**

**Location:** WCC Halls A-C

**Time:** Monday, November 16, 2026, 1:00 PM - 5:00 PM

**Program #/Poster #:** PSTR203.08/KK65

**Topic:** I.09. Spatial Navigation

**Title:** What are predictive grid cells for?

**Authors:** A. SINHA[1], O. FASEHUN[2], ***W. REDMAN**[2];
[1]Eon Systems PBC, Katy, TX; [2]Johns Hopkins Univ., Baltimore, MD

**Abstract:** The computational role of grid cells in the hippocampal-entorhinal cortex has been the subject of intensive investigation over the past two decades, with dominant theories attributing them to supporting path integration and serving as a basis for predictive coding. Recent electrophysiological recordings of medial entorhinal cortex (MEC) in rodents have found a subpopulation of neurons that have grid-like tuning, not with respect to where the animal currently is, but where the animal will be (Ouchi & Fujisawa, 2024). These "predictive grid cells", which are distinct from the subpopulation of grid cells, appear consistent with the hypothesis that MEC supports predictive coding. However, a detailed investigation of this has not been performed. To begin to answer the question of what predictive grid cells are for, we first analyze an independent, previously recorded, MEC dataset (Gardner et al., 2022), finding robust evidence of predictive grid coding across rats and grid modules. This suggests that predictive grid cells are a general feature of MEC. We then interrogate the emergent representations of recurrent neural networks (RNNs) trained to path integrate. We find that these RNNs, which have previously been shown to develop units with grid cell-like representations (Banino et al., 2018; Cueva & Wei, 2018; Sorscher et al., 2022), develop units with predictive grid cell-like tuning, even though the RNNs are not explicitly trained with a predictive objective. The predictive grid units that emerge in the RNN models are functionally involved in path integration, as ablating them leads to significantly worse performance, relative to randomly ablating RNN units. In addition, we find that units in the RNN that have representations analogous to band cells in MEC (Krupic et al., 2012) have greater predictive grid tuning than expected by chance. As band units have been shown to play an important role in velocity integration in path integrating RNNs (Chu et al., 2025), we hypothesize that predictive grid cells may be involved in supporting continuous attractor dynamics in MEC, as opposed to only being involved in predictive coding. We find preliminary evidence of this in the MEC neural dataset, where predictive grid cells maintain their average firing rates and firing rate correlation structure even in sleep, demonstrating that their coding may persist across behavioral states.
Banino et al., Nature (2018), Chu et al., NeurIPS (2025), Cueva & Wei, ICLR (2018), Krupic et al., Science (2012), Gardner et al., Nature (2022), Ouchi & Fujisawa, Science (2024), Sorscher et al., Neuron (2022)

**Disclosures: A. Sinha:** None. **O. Fasehun:** None. **W. Redman:** None.

**Poster**

**PSTR203: Grid Cells and Spatially Modulated Cells**

**Location:** WCC Halls A-C

**Time:** Monday, November 16, 2026, 1:00 PM - 5:00 PM

**Program #/Poster #:** PSTR203.09/LL1

**Topic:** I.09. Spatial Navigation

**Title:** Comparison of retrosplenial cortex and hippocampal spatial representations in dynamic environments

**Authors: *X. LIN**[1], A. S. ALEXANDER[2];
[1]Univ. of California, Santa Barbara, Santa Barbara, CA; [2]Psychological and Brain Sci., UC Santa Barbara, Goleta, CA

**Abstract:** Successful navigation requires tracking static and dynamic features of the external world. The retrosplenial cortex (RSC) and hippocampal formation (HPF) are known to encode multiple spatial variables across distinct egocentric and allocentric coordinate systems, yet these data have been typically collected in free foraging conditions that lack the ethological richness of true experience. In order to explore how these areas contribute to spatial cognition under more naturalistic conditions, we performed recordings in the hippocampus, subiculum and RSC while mice either freely foraged or pursued dynamic, moving visual stimuli in the same arena. Because subiculum is a major hippocampal output with direct projections to RSC and is implicated in flexible spatial behavior, we hypothesized that it may represent an intermediate stage between hippocampal map stability and RSC task-dependent reorganization. Specifically, we predicted that hippocampal activity would remain more strongly anchored to allocentric variables, including position, head direction, environmental geometry, and stimulus location, whereas RSC activity would more strongly reflect egocentric variables, including boundary bearing, stimulus bearing, stimulus distance, and relative stimulus motion. We further examined whether subicular activity showed hippocampal-like stability, RSC-like task dependence, or mixed coding across these variables. To test this, we quantified tuning strength, receptive field organization, and spatial stability within each region, with cross-region coordination assessed in simultaneously recorded sessions. These findings provide insight into how interconnected navigation circuits preserve environmental maps while transforming dynamic sensory information into egocentric, action-relevant codes.

**Disclosures: X. Lin:** None. **A.S. Alexander:** None.

**Poster**

**PSTR203: Grid Cells and Spatially Modulated Cells**

**Location:** WCC Halls A-C

**Time:** Monday, November 16, 2026, 1:00 PM - 5:00 PM

**Program #/Poster #:** PSTR203.10/LL2

**Topic:** I.09. Spatial Navigation

**Support:** ZIA NS009415

**Title:** Flexible and stable entorhinal representations jointly support spatial memory

**Authors: *D. YUSUFI**[1], Y. MA[1], G. WANG[1], L. CHEN[1], T. MALONE[1], K. CEKADA[2], K. ZHANG[1], J. KIM[1], F. SHAHID[1], E. BARCELON[1], Y. GU[1];
[1]Natl. Inst. of Neurolog. Disorders and Stroke, Bethesda, MD; [2]Univ. of California, Santa Barbara, Santa Barbara, CA

**Abstract:** Learning a new environment requires neural codes to remain plastic enough to incorporate new information while becoming stable enough to support long-lasting memory. How neural circuits balance these demands of flexibility and stability is unknown. We addressed this question in the medial entorhinal cortex (MEC), a key region for forming cognitive maps that support memory-guided navigation. Using longitudinal two-photon calcium imaging, we tracked thousands of excitatory neurons in head-fixed mice across 15 days as they learned multiple novel virtual reality environments. Novelty produced a transient increase in excitatory activity that decayed with learning. Session-averaged activity revealed an experience- and environment-invariant axis that separated weakly and strongly active cells with distinct properties during learning. Weakly active cells were preferentially recruited by novelty, were less enriched for canonical MEC cell types, such as grid, object-vector, and speed cells, and showed greater spatial tuning plasticity. As a population, weakly active cells preferentially encoded salient environmental features and reorganized flexibly during learning, shifting from landmarks to the reward location, coincident with a simultaneously recorded reward-predictive dopamine ramp. Strongly active cells were less feature-selective but instead maintained stable, information-rich environmental representations. MEC interneuron activity decreased upon novel-environment exposure before increasing with learning, underlying excitatory neuron novelty dynamics. Transient chemogenetic activation of MEC interneurons during novel-environment exposure delayed the excitatory novelty response, impaired the transition of weak-cell representations from landmarks to reward, disrupted stable coding by strongly active cells, and slowed behavioral learning on a similar timescale. Together, these results reveal how MEC reconciles flexibility and stability during spatial learning: distinct excitatory neuron populations arranged along a preconfigured activity axis separately support flexible updating and stable coding, while inhibitory and dopaminergic signals coordinate these codes to enable goal-directed spatial memory.

**Disclosures: D. Yusufi:** None. **Y. Ma:** None. **G. Wang:** None. **L. chen:** None. **T. Malone:** None. **K. Cekada:** None. **K. Zhang:** None. **J. Kim:** None. **F. Shahid:** None. **E. Barcelon:** None. **Y. Gu:** None.

**Poster**

**PSTR203: Grid Cells and Spatially Modulated Cells**

**Location:** WCC Halls A-C

**Time:** Monday, November 16, 2026, 1:00 PM - 5:00 PM

**Program #/Poster #:** PSTR203.11/LL3

**Topic:** I.09. Spatial Navigation

**Support:** NIH 1R01MH126904-01A1
NIH R01MH130452

**Title:** Inter-regional variability and interactions across the navigational circuit in a shifting reward task

**Authors: *S. J. LEVY**, L. M. GIOCOMO;
Neurobio., Stanford Univ., Stanford, CA

**Abstract:** Neural activity in the hippocampus (HPC), medial entorhinal cortex (MEC) and retrosplenial cortex (RSC), among other brain regions, closely tracks an animal's movement through an environment alongside other task and behavioral variables, and 'remaps' to encode changes in the task, the environment or the animal's behavior. These neural representations and the memory-guided navigation behaviors they are linked to depend on interactions across HPC, MEC and RSC, but most prior studies compared activity from brain regions recorded individually in separate groups of animals. In order to track task coding and remapping across brain regions at a fine time-scale, we acutely implanted Neuropixels probes to simultaneously record spiking activity and the local field potential from HPC, MEC and RSC in mice performing a virtual-reality task where the location of a hidden reward shifted frequently. This preparation enables comparisons within each region and across each pair of brain areas for the exact same events. In line with prior studies, we find neurons have region-specific patterns of spatial tuning, multiplexing of other variables (including the animal's speed, proximity to specific environmental cues, and the current location of the hidden reward), and coding stability, resulting in a distinct spatial map associated with each reward location. Mice are able to learn the new reward locations, though typically required several trials to adapt their licking and deceleration to each reward location shift. Similarly, we found that remapping was also delayed following each reward location shift, and in HPC, MEC and RSC proceeded at a different time-course and with a different relationship to the rate of learning each new reward location. In the local field potential, inter-regional coordination between each pair of regions also displayed a unique relationship to reward shifts and behavioral adaptations. These simultaneous, multi-region recordings improve our ability to understand how spatial learning behaviors are supported by cross-region interactions at a fast timescale.

**Disclosures: S.J. Levy:** None. **L.M. Giocomo:** None.

**Poster**

**PSTR203: Grid Cells and Spatially Modulated Cells**

**Location:** WCC Halls A-C

**Time:** Monday, November 16, 2026, 1:00 PM - 5:00 PM

**Program #/Poster #:** PSTR203.12/LL4

**Topic:** I.09. Spatial Navigation

**Support:** NIH R01MH130452
NIH 1R01MH126904-01A1
NIH BRAIN Initiative U19NS118284
NIH Grant P50 DA042012
The Vallee Foundation
The Simons Foundation 542987SPI
NIH F32NS138225
Stanford Jump Start Award

**Title:** Coordination of Task- and Sensory-Driven Remapping Across the Entorhinal-Hippocampal Circuit

**Authors: *F. S. CHO**[1], X. CHENG[1], L. M. GIOCOMO[2];
[1]Stanford Univ., Stanford, CA; [2]Neurobio., Stanford Univ., Chevy Chase, MD

**Abstract:** Flexible navigation requires spatial maps that remain anchored to sensory cues while adapting to learned task demands that make specific locations behaviorally relevant. In MEC, spatial representations reorganize when animals navigate to a remembered, unmarked goal, showing that entorhinal maps reflect task demands as well as physical space. However, it remains unclear whether task- and sensory-driven remapping recruit similar transformations within MEC, and whether learned task demands produce coordinated or region-specific reconfiguration across the entorhinal-hippocampal circuit. To address these questions, we adapted a rat hidden goal-zone task for freely moving mice in a 1 x 1 m open arena (Butler et al., 2019). A brief tone signaled trial onset, after which mice navigated to an unmarked 15 x 15 cm goal zone and remained there for 1 s to trigger reward delivery. The pellet was then dispensed at a variable location, separating memory-guided navigation to the goal from subsequent pellet search and consumption. Across training, mice increased goal-zone success and path efficiency, and after learning one goal zone rapidly adapted to new goal locations. We combined this behavior with chronic Neuropixels recordings targeted to MEC and hippocampus. To isolate task-driven remapping, mice completed paired hidden goal-zone and random-foraging sessions in visually distinct arenas in the same familiar room. Both conditions required search for randomly dispensed pellets, but only the hidden goal-zone task required memory-guided navigation to a learned, unmarked location, enabling comparison of neural activity across overlapping reward-seeking behavior but different learned task demands. In a subset of animals, we compared these task-driven changes with sensory-driven remapping across arenas with different geometries. Preliminary analyses reveal task-dependent changes in spatial firing across MEC grid, nongrid spatial, and border cells, as well as hippocampal place cells, with examples of global and goal-relative rate remapping. Ongoing analyses will test whether task demands and environmental geometry drive distinct forms of remapping across MEC and hippocampus, from changes in single-cell spatial tuning to broader reorganization of population activity. We will also examine the stability of these representations across repeated sessions, their reorganization after changes in goal location, and their expression during offline periods including sleep. Together, this paradigm distinguishes task- and sensory-driven contributions to entorhinal-hippocampal remapping and tests how spatial maps update to support flexible navigation.

**Disclosures: F.S. Cho:** None. **X. Cheng:** None. **L.M. Giocomo:** None.

**Poster**

**PSTR203: Grid Cells and Spatially Modulated Cells**

**Location:** WCC Halls A-C

**Time:** Monday, November 16, 2026, 1:00 PM - 5:00 PM

**Program #/Poster #:** PSTR203.13/LL5

**Topic:** I.09. Spatial Navigation

**Support:** 1R01MH126904-01A1
R01MH130452
U19NS118284
Howard Hughes Medical Institute
5P50DA042012-02

**Title:** Hierarchy-dependent disruption of spatial coding during ketamine-induced dissociation

**Authors: *C. LI**[1], N. PORTER[2], M. NGUYEN[3], Y. WU[4], M. K. LO[3], K. DEISSEROTH[3], L. M. GIOCOMO[2];
[1]Stanford Univ. Neurosci. PhD Program, Palo Alto, CA; [2]Neurobio., [3]Bioengineering, [4]Stanford Univ., Stanford, CA

**Abstract:** Ketamine produces a dissociative state characterized by profound spatial disorientation and cognitive impairment, yet the circuit mechanisms underlying this state remain poorly understood. Prior work has revealed that ketamine-induced dissociation involves a 1-3 Hz oscillation most prominent in the retrosplenial cortex (RSP) (Vesuna et al., 2020) that selectively disrupts recurrent integration in higher-order regions while leaving feed-forward sensory processing relatively intact (Kauvar et al., 2025), producing a hierarchy-dependent collapse of internal spatial representations. To test this, we performed simultaneous Neuropixels recordings from the dorsal lateral geniculate nucleus (dLGN), primary visual cortex (V1), RSP, medial entorhinal cortex (MEC), and CA1 hippocampus (HPC) in head-fixed mice navigating a virtual reality environment during saline, sub-dissociative (10 mg/kg), and dissociative (35 mg/kg) ketamine administration. In N=10 wild-type female mice, population cosine similarity analyses revealed a hierarchy-dependent collapse at the dissociative dose, with primary sensory regions retaining greater representational structure (dLGN: 0.24; V1: 0.29) compared to higher-order integrative regions (RSP: 0.14; MEC: 0.10; HPC: 0.06), arguing against a global network shutdown. Spectral analyses revealed a ~22-fold ketamine-specific increase in RSP delta power, with RSP-referenced spike-phase locking showing hierarchical entrainment strongest in HPC (MVL=0.065) and weakest in dLGN (MVL=0.039). Local phase locking analyses confirmed RSP as the rhythm's pacemaker. Coherence analyses revealed a 4.24x increase in RSP-MEC delta coherence alongside reduction of MEC-HPC 11-15 Hz coherence to 0.26x baseline. To probe molecular mechanisms, we recorded from CaMKIIα::Grin1 and CaMKII α::HCN1 conditional knockout mice. NMDAR (Grin1) knockout reduced RSP delta power by ~73% and HCN1 knockout reduced RSP delta power by ~49%, indicating that both channels may

contribute to generating the dissociative oscillatory state. Together these findings identify a hierarchy-dependent circuit mechanism of ketamine-induced dissociation and elucidate molecular contributions to RSP rhythmogenesis.

**Disclosures: C. Li:** None. **N. Porter:** None. **M. Nguyen:** None. **Y. Wu:** None. **M.K. Lo:** None. **K. Deisseroth:** E. Ownership Interest (stock, stock options, royalty, receipt of intellectual property rights/patent holder, excluding diversified mutual funds); Maplight, Stellaromics. F. Consulting Fees (e.g., advisory boards); Allen Institute, Modulight, RedTree, Maplight, Stellaromics. **L.M. Giocomo:** None.

**Poster**

**PSTR203: Grid Cells and Spatially Modulated Cells**

**Location:** WCC Halls A-C

**Time:** Monday, November 16, 2026, 1:00 PM - 5:00 PM

**Program #/Poster #:** PSTR203.14/LL6

**Topic:** I.09. Spatial Navigation

**Support:** Stanford Interdisciplinary Graduate Fellowship
Stanford Graduate Fellowship in Science & Engineering
HHMI Investigator Program

**Title:** State-dependent grid cell spatial maps

**Authors: *L. MARK**[1], C. ROSE[1,3], D. M. ZOLTOWSKI[2], S. LINDERMAN[2], L. M. GIOCOMO[1,3];
[1]Neurobio., [2]Dept. of Statistics and Wu Tsai Neurosciences Inst., Stanford Univ., Palo Alto, CA; [3]Howard Hughes Med. Inst., Stanford, CA

**Abstract:** The medial entorhinal cortex (MEC) contains an internal map of external space, constructed from the activity of spatial cells encoding for the animal's position, head-direction, and speed. Rather than representing a static spatial map, however, MEC neurons can change the location or firing rate of their spatial fields in a process termed remapping. Remapping can occur in response to external changes in the environment's sensory (color, shape, size) or task features (reward location). Recently, remapping was discovered to occur spontaneously without any changes in the external environment (Low et al. 2021). We hypothesized that spontaneous remapping reflects changes in an animal's latent internal state. We performed in vivo electrophysiology and multi-camera behavioral recordings of mice performing a virtual-reality random foraging task. We found that internal state changes (measured by pupil size and facial motion) predict grid cell remapping in an unchanging sensory environment. Moreover, modeling the moment-to-moment grid cell attractor state demonstrated that spontaneous remapping reflects differences in how strongly landmarks entrain the grid cell attractor state. To determine if state transitions are sufficient to drive spontaneous remapping, we drove state transitions via transcranial optogenetic stimulation of norepinephrine releasing neurons (TH+) in the locus coeruleus (using ChRmine, Chen et al. 2021). These state transitions induced time-locked spatial

coding changes in the MEC: changes in firing rate, spatial field locations, and landmark pinning not visible in control mice. Norepinephrine-driven spatial coding changes were detectable at the population-level, and thus state switches may play a role in driving network-wide spatial map switches. Future work will assess changes in visual neurons' coding fidelity during map switches, and the contribution of MEC subpopulations to state-dependent remapping.

**Disclosures: L. Mark:** None. **C. Rose:** None. **D.M. Zoltowski:** A. Employment/Salary (full or part-time):; Deepmind. **S. Linderman:** None. **L.M. Giocomo:** None.

**Poster**

**PSTR203: Grid Cells and Spatially Modulated Cells**

**Location:** WCC Halls A-C

**Time:** Monday, November 16, 2026, 1:00 PM - 5:00 PM

**Program #/Poster #:** PSTR203.15/LL7

**Topic:** I.09. Spatial Navigation

**Support:** NIH 1R01MH126904-01A1 (LMG)
NIH R01MH130452 (LMG)
BRAIN Initiative U19NS118284 (LMG)
The Vallee Foundation (LMG)
The James S. McDonnell Foundation (LMG)
The Simons Foundation 542987SPI (LMG)
Howard Hughes Medical Institute (LMG)
Wu Tsai Interdisciplinary Postdoctoral Fellowship(Jha, A.)

**Title:** Investigating entorhinal cortex dynamics in a naturalistic cricket-hunting-homing task

**Authors: *K. SHI**[1], A. JHA[2], S. LINDERMAN[2], L. M. GIOCOMO[3];
[2]Dept. of Statistics and Wu Tsai Neurosciences Inst., [3]Neurobio., [1]Stanford Univ., Stanford, CA

**Abstract:** The entorhinal cortex(EC) contains neurons that encode an animal's position, direction, speed, and proximity to boundaries or objects. These neural representations are hypothesized to build an internal cognitive map of the external world, enabling animals to navigate and interact with their environment. However, navigation is not a static behavior; it requires flexibility to adapt to the animal's current goals. To explore how the brain's cognitive map supports flexible behavior in naturalistic settings, we developed a freely moving cricket-hunting-homing task that places mice in an ethologically relevant scenario: actively searching for and pursuing moving prey, and bringing it back to a shelter for safe consumption. Our preliminary results demonstrated that mice exhibit distinct trajectories and kinematic profiles during exploration, hunting, and homing phases.
To analyze the prey-predator interaction as an expression of time-varying goal-directed behavior, we implemented an inverse reinforcement learning framework to unsupervisedly characterize the underlying time-varying goal states of the animals as well as goal-associated reward functions. This approach allows us to capture the internal organization of the animal's actions, including

transitions between exploration, pursuit, and homing. To investigate the EC dynamics across goal states, we chronically implanted Neuropixel 2.0 in the mouse EC while mice performed the cricket-hunting-homing task. Ongoing work will characterize the encoding and decoding of distance and direction related to the cricket, the shelter, and environmental boundaries. Additionally, we will determine whether chemogenetic inactivation of the EC influences animal behavior and/or alters goal representations in other brain regions. All together, this work will provide new insights into classic EC cell types——such as grid cells, head direction cells, speed cells, border cells, and object-related cells—— and reveal how they exhibit behaviorally adaptive coding strategies that support the animal's current goals.

**Disclosures: K. Shi:** None. **A. Jha:** None. **S. Linderman:** None. **L.M. Giocomo:** None.

**Poster**

**PSTR203: Grid Cells and Spatially Modulated Cells**

**Location:** WCC Halls A-C

**Time:** Monday, November 16, 2026, 1:00 PM - 5:00 PM

**Program #/Poster #:** PSTR203.16/LL8

**Topic:** I.09. Spatial Navigation

**Support:** National Institute of Health 1R01MH126904-01A1 (LMG)
National Institutes of Health R01MH130452 (LMG)
BRAIN Initiative U19NS118284 (LMG)
The Vallee Foundation (LMG)
The James S. McDonnell Foundation (LMG)
The Simons Foundation 542987SPI (LMG)
The Howard Hughes Medical Institute (LMG)

**Title:** The role of norepinephrine signaling in the medial entorhinal cortex during navigation

**Authors: *C. ROSE**[1,2], L. MARK[1], L. M. GIOCOMO[1,2];
[1]Stanford Univ. Sch. of Med., Stanford, CA; [2]Howard Hughes Med. Inst., Stanford, CA

**Abstract:** Internal states influence neural activity across the brain, yet how they shape spatial representations in navigation circuits remains poorly understood. The medial entorhinal cortex (MEC) contains neurons that encode position, direction, and speed, collectively supporting a spatial map of the environment. Building on our prior work showing that behavioral state transitions predict spontaneous MEC remapping, we hypothesize that state-linked neuromodulatory signals may help shift the MEC neural state between spatial maps. We focus on norepinephrine (NE), released by the locus coeruleus (LC), as LC-NE signaling plays a key role in arousal, behavioral flexibility, and exploration-exploitation trade-offs through tonic and phasic modes of activity. We previously found that LC-NE activation induces changes in MEC spatial coding. However, direct measurement of endogenous NE activity in MEC in vivo remains technically challenging and poorly characterized. To address this gap, we developed a tapered fiber photometry approach to measure NE signals across the dorsoventral axis of MEC during

navigation. Using genetically encoded fluorescent NE sensors, we record NE dynamics during spontaneous and sensory-evoked state transitions and compare multiple sensors to characterize their kinetics and sensitivity across tonic and phasic LC signaling modes. We also use transcranial optogenetic LC activation to test how tonic and phasic stimulation patterns affect MEC spatial coding. Together, this work establishes a framework for linking norepinephrine signaling to state-dependent changes in MEC spatial representations.

**Disclosures: C. Rose:** None. **L. Mark:** None. **L.M. Giocomo:** None.

**Poster**

**PSTR203: Grid Cells and Spatially Modulated Cells**

**Location:** WCC Halls A-C

**Time:** Monday, November 16, 2026, 1:00 PM - 5:00 PM

**Program #/Poster #:** PSTR203.18/LL10

**Topic:** I.09. Spatial Navigation

**Support:** 1R21MH135232-01

**Title:** Hippocampal Oscillations in Juvenile Rats Are Impacted Differentially by Allocentric and Egocentric Behaviors

**Authors: *E. VINOKUROV**[1], D. GONZALEZ[1], T. C. DUMAS[2];
[2]Psychology, [1]George Mason Univ., Fairfax, VA

**Abstract:** Hippocampus-dependent memory abilities develop relatively late in humans, around two to three years of age, paralleling the delayed emergence of hippocampus-dependent spatial memory in rodents at roughly three postnatal weeks. Previous in vivo investigations of the neurobiology underlying hippocampal maturation in rodents have focused on the first postnatal week while pups are still nesting, utilized linear tracks with no behavioral assessment, or recorded during random foraging. These studies have shown that as juvenile rodents develop, there are substantial changes in the oscillatory network dynamics in the hippocampus, particularly area CA1. Recording of LFPs in this area shows a significant increase in power as the animal matures in a few key oscillatory bands, such as theta and slow gamma. However, there has been limited work connecting any changes in these oscillation bands to distinct cognitive or behavioral states in juvenile rodents during spatial navigation. To address these limitations, we implanted electrodes and recorded LFPs from hippocampal area CA1 in rats just before and just after three weeks of age and examined spontaneous alternation in a Y-maze. In our prior studies, we found no age effect on theta or slow gamma power or event rate in relation to position in the maze or alternation rate. However, phase-amplitude coupling (PAC) between theta and slow gamma, which supports spatial navigation and encoding of spatial context, was not investigated. Currently, investigation of theta/slow gamma PAC during bouts of mobility and immobility revealed no age effects. Given the transient and behavior-dependent nature of these oscillatory events, particularly the theta-modulated emergence of slow gamma rhythms, we are separately examining grooming and rearing behaviors during immobility and inward (toward the

maze center) versus outward movement trajectories during mobility. We will also investigate periods of immobility at the center of the Y-maze. We expect to see age effects on theta/slow gamma PAC during rearing and inward movement trajectories, as well as for immobility epochs at the center of the maze. Our findings will reveal relationships between postnatal changes in theta/slow gamma PAC hippocampal-dependent navigation abilities.

**Disclosures: E. Vinokurov:** None. **D. Gonzalez:** None. **T.C. Dumas:** None.

**Poster**

**PSTR203: Grid Cells and Spatially Modulated Cells**

**Location:** WCC Halls A-C

**Time:** Monday, November 16, 2026, 1:00 PM - 5:00 PM

**Program #/Poster #:** PSTR203.19/LL11

**Topic:** I.09. Spatial Navigation

**Support:** NSF grant 2424326

**Title:** A Medial Septal-Entorhinal Circuit Model of Path Integration

**Authors: *X. SHI**, H. DANNENBERG;
Bioengineering, George Mason Univ., Fairfax, VA

**Abstract:** Grid cells in the medial entorhinal cortex (MEC) support path integration by encoding position from self-motion cues. Existing continuous attractor network (CAN) and oscillatory interference (OI) models can generate grid-cell firing patterns through integrating velocity signals. However, these models often lack biological realism by (i) requiring hand-crafted asymmetric connectivity (CAN) or finely tuned velocity-controlled oscillators (OI), (ii) using head direction as a proxy for movement direction, and (iii) ignoring medial septal inputs despite their importance for grid cell firing. Recent work proposed that velocity integration generates trajectory-coding cell sequences that may give rise to grid-cell firing (R.G. et al., 2025). However, whether this framework can be implemented in a computational simulation with biologically grounded medial septal inputs and MEC connectivity motifs remains unclear. Here, we provide proof of principle using a simplified septo-entorhinal circuit model, in which an innate MEC motif receives theta-rhythmic GABAergic medial septal input that provides a theta-phase code for movement direction. We developed a MATLAB-based MEC ring attractor model with 448 stellate cells and 42 inhibitory interneurons connected through distance-dependent excitation and organized inhibitory feedback. Medial septal GABAergic input rhythmically modulated interneurons at theta frequency. We quantified network dynamics by tracking stellate and interneuron firing rates, activity bump movement, and cell sequence evolution across theta cycles. Our preliminary data show that a 1-D trajectory code can be implemented through cell sequences in this simplified MEC circuit motif. Theta-rhythmic medial septal GABAergic input moved the activity bump across the stellate cell population. Within each theta cycle, bump activity waxed and waned as sequential stellate cell activity unfolded. Partial overlap of active sequences across successive theta cycles suggests continuity of trajectory-related activity over

longer timescales. Together, these results advance our understanding of how medial septal theta input may generate trajectory-coding sequential activity in the MEC, providing a foundation for future integration of cholinergic and theta-frequency speed signals in 2-D trajectory coding.

**Disclosures: X. Shi:** A. Employment/Salary (full or part-time):; George Mason University. **H. Dannenberg:** A. Employment/Salary (full or part-time):; George Mason University.

**Poster**

**PSTR203: Grid Cells and Spatially Modulated Cells**

**Location:** WCC Halls A-C

**Time:** Monday, November 16, 2026, 1:00 PM - 5:00 PM

**Program #/Poster #:** PSTR203.20/LL12

**Topic:** I.09. Spatial Navigation

**Support:** Proyecto de Colaboración Internacional PCI2023-145967-2
NIH R01 NS119503

**Title:** The emergence of spatial fields in mouse CA1 underlies learning of self-motion integration for estimating distance

**Authors:** Z. YE[1], G. CECCHINI[2], J.-B. EPPLER[2], Y. WANG[1], ***A. ROXIN**[3];
[1]Max Planck Florida Inst. for Neurosci., Jupiter, FL; [2]Ctr. de Recerca Matemàtica, Bellaterra, Spain; [3]Ctr. De Recerca Matemàtica, Bellaterra, Spain

**Abstract:** When rodents perform tasks requiring spatial navigation, spatially selective place cells emerge in area CA1 of hippocampus. Similarly, when animals must keep track of a delay, temporally selective cell activity emerges, known as internally generated sequences (IGS). However, the mechanisms by which animals learn to estimate distance travelled from self-motion cues alone remain unknown. Here we analyzed hippocampal Ca2+ imaging data from mice performing a VR task, in which animals estimated distance by integrating self-motion cues in the absence of external landmarks (Heldman et al. (2025)). Mice ran on a treadmill in a virtual environment with minimal visual cues and no intermediate landmarks, requiring them to rely on internally integrated self-motion signals to estimate distance. In each trial, after an initial cue, the mice had to run 180 cm to reach a reward zone where they could collect a water reward. We tracked the behavior and neuronal activity in CA1 as animals learned the task over the course of up to three weeks of training. Unlike in many spatial navigation tasks where place fields emerge immediately, this paradigm allowed us to investigate how spatial representations develop gradually during learning. Over sessions the animals' licking became more tightly focused near the reward zone indicating they had learned its location. We found concomitant changes in the selectivity of neuronal responses. To test whether neuronal activity encoded elapsed time or traveled distance along the virtual track, we trained decoders on Ca2+ imaging data. Specifically, a decoder for the distance traveled by the animal was initially near chance level during the first session, but showed continual improvement over sessions. Interestingly, a decoder for time elapsed from run onset, reflecting the temporal structure of IGS activity, was already above

chance on the first session. Nonetheless, the performance of the temporal decoder did not change significantly over sessions. At the behavioral level, animals also developed increasingly stereotyped running trajectories over learning, linking elapsed time and traveled distance more reliably. This suggests that temporal dynamics in CA1 may provide a substrate which is utilized to learn spatially selective representations during path integration.

**Disclosures: Z. Ye:** None. **G. Cecchini:** None. **J. Eppler:** None. **Y. Wang:** None. **A. Roxin:** None.

**Poster**

**PSTR203: Grid Cells and Spatially Modulated Cells**

**Location:** WCC Halls A-C

**Time:** Monday, November 16, 2026, 1:00 PM - 5:00 PM

**Program #/Poster #:** PSTR203.21/LL13

**Topic:** I.09. Spatial Navigation

**Title:** Task-dependent reorganization of medial entorhinal grid-cell activity during goal-directed route learning

**Authors: *J. TIAN**, C. MIAO;
Peking Univ., Beijing, China

**Abstract:** The entorhinal-hippocampal circuit provides a core substrate for spatial navigation. In the medial entorhinal cortex (MEC), grid cells are classically described as forming stable, periodic maps of two-dimensional space, but accumulating evidence indicates that grid representations can be reshaped by sensory inputs, prior experience, rewards, and behavioral demands. How MEC grid cells reorganize when an animal shifts from unconstrained exploration of a complex environment to goal-directed route navigation remains unclear.We used miniaturized two-photon calcium imaging to record MEC activity in male C57BL/6 mice as they learned to navigate a square maze containing irregular corridors and seven decision points. The maze had a single correct path from a start box to a goal. Each imaging day began with an open-field session to classify spatially-modulated cells. Mice were then tested in two maze paradigms. During a two-day free-exploration stage, the start and goal were blocked, rewards were scattered throughout the maze, and mice explored the entire maze. During the following goal-directed stage, mice entered from the start and received reward only after reaching the goal through the correct path; over training, behavior became progressively restricted to this route.During free exploration, a subset of grid cells retained two-dimensional grid-like activity within the maze, sometimes with altered grid spacing, whereas others lost regular firing patterns. After the task changed to goal-directed navigation, grid-cell activity reorganized rapidly even in the same physical environment. Within one to two days of learning, many grid cells developed multiple reliable firing fields along the correct route that recurred across trials. These fields were better aligned to route position relative to the start along the correct path than to elapsed time or travelled distance, suggesting that grid cells contribute to a task-relevant representation of progress along the learned path. Across approximately one week of training, however, grid-cell

activity became sparser and less stable once animals reached high task proficiency. These results reveal a rapid, behavior-dependent transformation of MEC grid-cell representations from two-dimensional spatial maps to one-dimensional route codes, followed by a late-stage reduction in grid-cell engagement after extensive learning.

**Disclosures: J. Tian:** None. **C. Miao:** None.

**Poster**

**PSTR203: Grid Cells and Spatially Modulated Cells**

**Location:** WCC Halls A-C

**Time:** Monday, November 16, 2026, 1:00 PM - 5:00 PM

**Program #/Poster #:** PSTR203.22/LL14

**Topic:** I.09. Spatial Navigation

**Title:** A Micropeptide CTXND1 rescues hippocampal dysfunction in Alzheimer's disease by modulating calcium homeostasis

**Authors: *Y. LI**, C. MIAO;
Peking Univ., Beijing, China

**Abstract:** The selective vulnerability of hippocampal CA1 pyramidal neurons is a hallmark of Alzheimer’s disease (AD), but the neuron-intrinsic factors linking early pathology to circuit failure remain elusive. Through a spatial transcriptomic screen, we identified *Ctxnd1* (Cortexin-Domain Containing 1) as a highly enriched gene in CA1 pyramidal neurons. Its expression was significantly downregulated in the hippocampus of aged 5xFAD mice and in the CA1 of post-mortem human AD brains. We further showed that *Ctxnd1* encodes a conserved 59-amino-acid micropeptide, CTXND1. Functionally, CTXND1 overexpression in 5xFAD mice improved spatial learning and memory in the Y-maze and Morris water maze, reduced Aβ plaque burden, and enhanced synaptic intensity in the hippocampus. *In vivo* calcium imaging further revealed that CTXND1 overexpression improved spatial coding in CA1 neurons, as reflected by increased spatial information and enhanced discrimination between distinct environments. Mechanistically, CTXND1 localized to the endoplasmic reticulum and interacted with sarco/endoplasmic reticulum calcium ATPase 2 (SERCA2), thereby promoting calcium reuptake into the ER and maintaining intracellular calcium homeostasis. Consistent with this, CTXND1 overexpression shortened the half-decay time of calcium spikes, indicating an attenuation of abnormal calcium dynamics in AD. Together, these findings identify CTXND1 as a CA1-enriched micropeptide that alleviates AD-related behavioral, pathological and neuronal activity deficits, highlighting a therapeutic target focused on bolstering neuronal homeostasis downstream of core pathology.

**Disclosures: Y. Li:** None. **C. Miao:** None.

**Poster**

**PSTR204: Multi-Omics**

**Location:** WCC Halls A-C

**Time:** Monday, November 16, 2026, 1:00 PM - 5:00 PM

**Program #/Poster #:** PSTR204.01/LL15

**Topic:** J.02. Systems Biology and Bioinformatics

**Title:** SCALPEL: Enabling Platform-Independent, Multi-Age Analysis of Whole-Brain Spatial Transcriptomics Datasets

**Authors: *L. CHING**, J. QUON, R. MATHIEU, M. HEWITT, S. C. SEEMAN, A. AYALA, E. GELFAND, B. R. LONG, N. MARTIN, J. NAGRA, P. OLSEN, A. OYAMA, N. VALERA CUEVAS, C. M. PAGAN, S. SUNKIN, J. ARIZA TORRES, K. SMITH, D. MCMILLEN, H. ZENG, J. WATERS, M. KUNST;
Allen Inst., Seattle, WA

**Abstract:** Spatial transcriptomics enables precise mapping of gene expression within tissue architecture, offering unprecedented insights into cellular interactions, tissue heterogeneity, and developmental dynamics. Here we present SCALPEL (Spatial Cell Analysis, Labeling, Processing, and Expression Linking), a standardized, fully reproducible pipeline designed for whole-brain spatial transcriptomics at scale. SCALPEL incorporates advanced 3D segmentation optimized for dense and heterogeneous tissues, refined filtering criteria, and transcriptome-based doublet detection to remove low-quality or artifactual cells. Cell type label transfer from existing taxonomies is performed with robust filtering thresholds. Spatial domain detection captures local transcriptomic organization, and tissue sections are registered to the Developmental Mouse Brain Atlas (DeMBA) for precise anatomical alignment. Genome-wide expression is imputed from single-cell RNA-sequencing data to enrich the dataset.
We apply SCALPEL to 16 whole mouse brain datasets acquired across two imaging platforms, MERSCOPE and Xenium, demonstrating platform-independent processing from raw imaging data to analysis-ready output. Critically, this pipeline enables multi-age analysis spanning postnatal timepoints from P0 to P28, producing a developmental mouse brain atlas that captures transcriptomic and spatial changes across early postnatal development. All code is deployed on Code Ocean, a cloud computing platform that enables reproducible pipeline execution with built-in containerization and pre-configured AWS Batch integration. Output data are stored in a standardized format, enabling straightforward integration and cross-dataset comparison. SCALPEL and the resulting whole-brain developing mouse atlas provide a robust resource for studying the mouse brain across development.

**Disclosures: L. Ching:** None. **J. Quon:** None. **R. Mathieu:** None. **M. Hewitt:** None. **S.C. Seeman:** None. **A. Ayala:** None. **E. Gelfand:** None. **B.R. Long:** None. **N. Martin:** None. **J. Nagra:** None. **P. Olsen:** None. **A. Oyama:** None. **N. Valera Cuevas:** None. **C.M. Pagan:** None. **S. Sunkin:** None. **J. Ariza Torres:** None. **K. Smith:** None. **D. McMillen:** None. **H. Zeng:** None. **J. Waters:** None. **M. Kunst:** None.

**Poster**

**PSTR204: Multi-Omics**

**Location:** WCC Halls A-C

**Time:** Monday, November 16, 2026, 1:00 PM - 5:00 PM

**Program #/Poster #:** PSTR204.02/LL16

**Topic:** J.02. Systems Biology and Bioinformatics

**Title:** A comprehensive single-nucleus transcriptomic atlas of the mouse medial vestibular nucleus

**Authors: *J. JIAN**, Y. XU, L. TU;
Univ. of South Florida, Tampa, FL

**Abstract:** The medial vestibular nucleus (MVe) in the brainstem plays a critical role in processing sensory information about motion, head position and spatial orientation, and yet the cellular composition remains incompletely characterized. To systematically define the cellular landscape, we performed single-nucleus RNA sequencing (snRNA-seq) using mouse MVe tissue and generated a transcriptomic atlas comprising 33,696 nuclei. Unsupervised clustering identified 8 major neuronal and non-neuronal cell populations, including glutamatergic and GABAergic neurons, microglia, astrocytes, oligodendrocyte precursor cells, oligodendrocytes, endothelial cells, and vascular smooth muscle cells. Further analysis resolved multiple transcriptionally distinct neuronal subtypes within each major neurotransmitter class, indicative of substantial molecular heterogeneity in the MVe. Cell-type-specific marker genes were identified in each population, which thus provides a framework for future studies implicating in vestibular circuit organization and function. Together, these findings establish a comprehensive single-nucleus atlas of the mouse MVe and provide a valuable resource for investigating the cellular and molecular basis of vestibular system.

**Disclosures: J. Jian:** None. **Y. Xu:** None. **L. Tu:** None.

**Poster**

**PSTR204: Multi-Omics**

**Location:** WCC Halls A-C

**Time:** Monday, November 16, 2026, 1:00 PM - 5:00 PM

**Program #/Poster #:** PSTR204.03/LL17

**Topic:** J.02. Systems Biology and Bioinformatics

**Support:** Swedish Research Council (Vetenskapsrådet) (2021-03293)
Vetenskapsrådet (2022-04732)
Swedish Brain Foundation (Hjärnfonden) (FO2025-0275)
Åhlén Foundation (Stiftelsen Maja & J.P Åhlén) (253016)
Swedish Parkinson Foundation (Parkinsonfonden) (1636/25)
Magnus Bergvalls Foundation (2025-618)
Swedish Alzheimer's Disease Foundation (Alzheimerfonden) (AF-1031855)

**Title:** Overcoming endogenous autofluorescence in aged fresh-frozen human brain tissue for immunofluorescence-based spatial proteomics

**Authors: *I. SUTEVSKI**;
KTH The Royal Inst. of Technol. - SciLifeLab, Stockholm, Sweden

**Abstract:** Multiplex immunofluorescence enables spatially resolved analysis of complex human brain tissue at cellular to subcellular resolution. These approaches hold great potential for unravelling the complex pathophysiology of neurodegenerative diseases, which span molecular, cellular, and tissue scales and are difficult to capture with bulk methods alone. However, applying these technologies to aged post-mortem fresh-frozen brain sections remains technically challenging. Over the past three years, we have systematically optimised a multiplex immunofluorescence workflow for studying neurodegeneration in aged human fresh-frozen brain tissue, addressing several key technical limitations, with a particular focus on controlling endogenous autofluorescence. A major challenge when applying fluorescent microscopy tools to the aged human brain is strong endogenous autofluorescence, which can interfere with marker detection and downstream image analysis. Chemical quenching approaches are often incompatible with cyclic immunofluorescence workflows, while photobleaching protocols developed for formalin-fixed paraffin-embedded tissue can cause region-specific tissue damage. Therefore, we first established a photobleaching strategy that robustly reduces autofluorescence while preserving tissue integrity and antigen detectability across multiple brain regions. Second, we designed a 28-plex antibody panel to detect major cell types in human brain sections using the PhenoCycler-Fusion platform. Third, we developed an analysis pipeline that integrates protein marker expression, spatial organisation, and cellular morphology, thereby leveraging the multidimensional nature of spatial proteomics datasets. We then applied this optimised workflow to characterise autofluorescence patterns across the caudate-putamen, hippocampus, parietal cortex, and prefrontal cortex. We observed region-specific variation in the size, density, and spatial distribution of autofluorescent particles and found that these particles exhibit distinct associations with specific cell types and tissue compartments. Our work provides an optimised experimental and computational framework for studying neurodegenerative diseases in human post-mortem fresh-frozen brain tissue using spatial proteomics. We are now applying this workflow in several ongoing projects focused on Lewy body diseases, Alzheimer’s disease, and frontotemporal dementia.

**Disclosures: I. Sutevski:** None.

**Poster**

**PSTR204: Multi-Omics**

**Location:** WCC Halls A-C

**Time:** Monday, November 16, 2026, 1:00 PM - 5:00 PM

**Program #/Poster #:** PSTR204.04/LL18

**Topic:** J.02. Systems Biology and Bioinformatics

**Support:** Syracuse University Start-Up Grant

**Title:** Comparative Proteomics Reveals Cell Type-Specific Heterogeneity of Human Neural Cell-Derived Extracellular Vesicles

**Authors: *X. CHEN**[1], C. LO[2], J. ZENG[1];
[2]Biol., [1]Syracuse Univ., Syracuse, NY

**Abstract:** Extracellular vesicles (EVs) are key mediators of intercellular communication and promising platforms for biomarker discovery and drug delivery. However, systematic comparisons of EV proteomes across central nervous system (CNS) cell types under identical conditions remain limited. Such comparisons are critical for defining cell-type-specific EV signatures and establishing reference datasets for disease-related changes. Here, we used tandem mass tag (TMT)-based quantitative proteomics to characterize EVs from three human CNS cell lines: SH-SY5Y neurons (N-EV), astrocytes (AS-EV), and HMC3 microglia (MG-EV). EVs were isolated by differential ultracentrifugation and validated by nanoparticle tracking analysis, electron microscopy, and protein quantification. All EVs showed similar size (80-150 nm), zeta potential (~−30 mV), and protein content per vesicle. However, N-EV exhibited higher particle concentration ($2.57 \times 10^{11}$ vs. $1.31 \times 10^{11}$ vs. $0.75 \times 10^{11}$ particles/mL per $10^7$ cells) and protein yield ($35.3 \pm 8.4$ μg vs. $13.6 \pm 1.0$ μg vs. $11.4 \pm 4.1$ μg per $10^7$ cells) than AS-EV and MG-EV. EV proteins were analyzed by TMT-based quantitative LC-MS/MS proteomics. Differentially expressed proteins were identified using predefined significance thresholds. Principal component analysis showed clear separation by cell type. Comparison with ExoCarta and Vesiclepedia databases confirmed ~88% overlap with known EV proteins, and canonical cell-type markers were enriched in corresponding EVs. Functional enrichment analyses revealed distinct signatures: AS-EV were enriched in cell adhesion and extracellular matrix pathways; N-EV in membrane dynamics and cytoskeletal organization; and MG-EV in chromatin and epigenetic regulation. This study provides a comprehensive reference of CNS cell-derived EV proteomes under physiological conditions, offering a foundation for studying disease-associated EV alterations.

**Disclosures: X. Chen:** None. **C. Lo:** None. **J. Zeng:** None.

**Poster**

**PSTR204: Multi-Omics**

**Location:** WCC Halls A-C

**Time:** Monday, November 16, 2026, 1:00 PM - 5:00 PM

**Program #/Poster #:** PSTR204.05/LL19

**Topic:** J.02. Systems Biology and Bioinformatics

**Title:** Cortical spreading depolarization activates neuronal cell-matrix interaction and cytoskeletal remodeling programs

**Authors:** N. BELDER[1], ***M. CELEBI-CINAR**[2], A. MERSIN[3], M. SAHIN[4], T. DALKARA[5];
[1]Ankara Univ. Biotech. Inst., Ankara, Turkey; [2]Dept. of Mol. Biol. and Genetics, Bilkent Univ., Ankara, Turkey; [3]Dept. of Computer Engineering, Bilkent Univ., Ankara, Turkey; [4]Departments

of Neurosci. and Mol. Biol. and Genet., Bilkent Univ., Ankara, Turkey; [5]Departments of Neurosci. and Mol. Biol. and Genetics, Bilkent Univ., Ankara, Turkey

**Abstract:** Cortical spreading depolarization (CSD) is a propagating wave of neuronal and glial depolarization that underlies migraine aura. While CSD is known to induce neuronal swelling in addition to the profound changes in neuronal excitability and synaptic signaling, the molecular mechanisms underlying the associated structural remodeling remain insufficiently investigated. To characterize neuronal molecular responses to CSD, we secondarily analyzed a previously generated RNA-seq data (Kaya et al., 2025) generated from enriched neuronal populations isolated from mouse brain collected one hour after CSD induction. Differential gene expression analysis identified over 800 genes in neurons that were significantly altered following CSD. KEGG pathway enrichment analysis revealed biologically relevant 17 pathways. Consistent with previously established associations with CSD, pathways related to glutamatergic synaptic transmission, calcium signaling, and long-term potentiation were significantly enriched. In addition, several previously uncharacterized pathways associated with cell adhesion and structural plasticity were found to be enriched, including focal adhesion, extracellular matrix (ECM)-receptor interaction, and integrin-associated signaling pathways (adjusted p-value < 0.05). Regulation of the actin cytoskeleton was also one of the enriched pathways at the significance level of p-value < 0.05, adjusted p-value = 0.10. Furthermore, gene-level analysis revealed alterations in essential transcripts associated with cytoskeletal organization and cell-extracellular matrix communication, including upregulation of collagen family genes, myosin-related genes, and members of the Arp2/3 actin complex that have a vital role in formation of actin cytoskeleton, while other myosin family members were downregulated, suggesting reorganization/restoration of neuron cytoskeleton following CSD. These findings suggest that CSD induces molecular changes in neurons involving structural remodeling/repair and extracellular matrix interactions as well as synaptic overactivation. The convergence of these molecular changes associated with focal adhesion, ECM signaling, integrin-related pathways, and cytoskeletal regulators implies previously underappreciated roles for neuron-matrix communication and cytoskeletal plasticity as a response to CSD induced swelling of neurons including their dendrites and spines.

**Disclosures: N. Belder:** None. **M. Celebi-Cinar:** None. **A. Mersin:** None. **M. Sahin:** None. **T. Dalkara:** None.

**Poster**

**PSTR204: Multi-Omics**

**Location:** WCC Halls A-C

**Time:** Monday, November 16, 2026, 1:00 PM - 5:00 PM

**Program #/Poster #:** PSTR204.06/LL20

**Topic:** J.02. Systems Biology and Bioinformatics

**Support:** NIH Grant R01 DA063090 (B. Herb, C. Colantuoni)
NIH Grant U01 DA053629 (P. Kenny, D. Volsky)

NIH Grant U01 DA056003 (H. Zeng, P. Kenny, D. Volsky)
NIH Grant UM1 DA052244 (O. White)

**Title:** Cell-type specific effects of Opioids in the Nucleus accumbens of macaques, rats, and mice, and their translatability to SUD in humans.

**Authors: *M. A. PROKHORENKO**[1], C. COLANTUONI[1], B. R. HERB[1], L. WILLS[2], S. A. AMENT[3], P. J. KENNY[2];
[1]Inst. for Genome Sci., Univ. of Maryland Baltimore, Baltimore, MD; [2]Neurosci., Icahn Sch. of Med. At Mount Sinai, New York, NY; [3]Dept. of Psychiatry and Inst. for Genome Sci., U Maryland Sch. of Med., Baltimore, MD

**Abstract:** The nucleus accumbens (NAc) mediates rewarding properties of addictive substances and undergoes lasting changes in substance use disorders (SUDs). An ongoing challenge in addiction medicine is to develop new therapies that help decrease cravings and addictive behaviors *that work with an individual's personal addictive experience.* The SCORCH consortium has generated rich multi-omic single-cell data of post-mortem NAc dissections from control and SUD donors from diverse populations and varied history of drug use. However, making sense of this complex and individual impact of opioid use needs to be paired with carefully constructed animal model experiments to get clear molecular effects of opioids on specific cellular populations. The NAc is structured into discrete functional domains with medium spiny neurons (MSNs) projecting topographically to downstream brain regions. However, the molecular diversity, spatial organization, and functional adaptations of MSNs in SUDs remain elusive. To address this, we constructed a comparative multi-omic and spatial atlas of the NAc in humans, macaques, rats, and mice, integrating single-cell multi-omic and spatial transcriptomic data from over one million NAc cells. Our analyses revealed deep evolutionary conservation of many MSN subtypes, as well as human- and primate-specific specializations. Projection mapping revealed previously unrecognized, topographically arranged MSN projections to brain regions regulating reward and aversion. In humans, the dynamics of MSN subtype-specific gene networks reflected complex patterns of polysubstance use that are inherent to SUDs. Comparisons to animal models enabled us to link SUD-associated gene networks to specific substances and stages of addiction. We used Structured Joint Decomposition (SJD) to compute components of variation across samples, cross-species common cell types, and datasets to identify NAc SUD gene patterns shared between species/experimental modalities and unique to each. Additionally, after gene set enrichment analysis of pseudobulked and single-cell differential expression, we analyzed semantic similarity of gene ontologies (GOs), then scored and correlated consensus SUD GOs to SJD patterns. This analysis identified conservation of biological responses to addictive substances that underly SUD in humans, contributing to the translatability of these findings. This work provides a blueprint for identifying key molecular and circuit mechanisms underlying addiction and developing targeted interventions.

**Disclosures: M.A. Prokhorenko:** None. **C. Colantuoni:** None. **B.R. Herb:** None. **L. Wills:** None. **S.A. Ament:** None. **P.J. Kenny:** None.

**Poster**

**PSTR204: Multi-Omics**

**Location:** WCC Halls A-C

**Time:** Monday, November 16, 2026, 1:00 PM - 5:00 PM

**Program #/Poster #:** PSTR204.07/LL21

**Topic:** J.02. Systems Biology and Bioinformatics

**Support:** Robert Campeau Family Foundation/Dr. C.H. Tator Chair in Brain and Spinal Cord Research at UHN

**Title:** Cell-Type-Resolved Ionic Reprogramming After Spinal Cord Injury

**Authors: *Z. H. PATEL**[1,2], A. D. MODI[1,2], K. PATEL[1,2], Y. CHAMPIRI[1,2], J. HONG[1], M. G. FEHLINGS[1,2];
[1]Div. of Exptl. & Translational Neurosci., Krembil Brain Institute, Univ. Hlth. Network, Toronto, ON, Canada; [2]Inst. of Med. Sci., Temerty Fac. of Medicine, Univ. of Toronto, Toronto, ON, Canada

**Abstract:** Spinal cord injury (SCI) triggers ionic dysregulation that contributes to secondary damage, and single-cell transcriptomics has revealed substantial cellular heterogeneity within the injured spinal cord. How distinct cell populations differ in their expression of ion-homeostatic machinery, and how those programs shift across injury phases, has not been systematically characterized. Transcriptomic profiles alone are difficult to interpret functionally, because the contribution of a given channel or transporter depends on biophysical properties, such as single-channel conductance, permeability ratios, and auxiliary-subunit dependencies, which gene counts do not capture. To make expression data more interpretable, we developed a computational framework that combines cell-type-resolved ion channel and transporter expression with curated biophysical parameters to derive a relative ionic-capacity index for each population: a transcript-weighted estimate of potential ionic flux rather than a direct measure of membrane physiology. Applying this framework to a publicly available single-cell SCI dataset across acute, subacute, and chronic post-injury phases, we found that SCI is associated with broad but cell-type-specific remodeling of ion-homeostatic programs rather than uniform changes, spanning both neuronal and glial populations. Surviving neuronal populations, particularly ventral interneurons, showed an early reduction in predicted sodium-conductance capacity, while astrocyte populations showed marked reductions in GABA-transporter capacity, suggesting potential disruption of extracellular GABA handling and tonic inhibitory regulation at tripartite synapses. Oligodendrocyte-lineage populations, particularly progenitors and newly formed oligodendrocytes, showed injury-associated induction of mechanosensitive and volume-regulatory channel transcripts, consistent with a mechanically responsive injury state. These transcriptionally inferred changes generate testable hypotheses — pending electrophysiological or proteomic validation — and suggest that restoring ionic homeostasis after SCI may require targeting specific glial populations and their interactions with neurons.

**Disclosures: Z.H. Patel:** None. **A.D. Modi:** None. **K. Patel:** None. **Y. Champiri:** None. **J. Hong:** None. **M.G. Fehlings:** None.

**Poster**

**PSTR204: Multi-Omics**

**Location:** WCC Halls A-C

**Time:** Monday, November 16, 2026, 1:00 PM - 5:00 PM

**Program #/Poster #:** PSTR204.08/LL22

**Topic:** J.02. Systems Biology and Bioinformatics

**Support:** VHA VISN 1 Career Development Award

**Title:** Defining cell-type-specific mechanisms in the prefrontal cortex for genomic variants associated with PTSD

**Authors: *M. JENSEN**[1,2], N. PANDEY[3], M. GERSTEIN[4], M. GIRGENTI[2,1];
[1]Natl. Ctr. for PTSD, US Dept. of Veterans Affairs, West Haven, CT; [2]Psychiatry, [3]Computat. Biol. and Bioinformatics, [4]Mol. Biophysics and Biochem., Yale Univ., New Haven, CT

**Abstract:** Post-traumatic stress disorder (PTSD) and related stress disorders, such as major depressive disorder (MDD), represent a major public health concern, particularly among veteran populations. PTSD presents clinically with a wide range of symptoms, including intrusive thoughts, hyperarousal, and avoidance, and is often comorbid with other psychiatric disorders. Additionally, dozens of genomic variants have been linked to PTSD susceptibility after trauma exposure. Many of these variants disrupt regulatory elements in non-coding regions of the genome, potentially leading to complex changes in gene regulation across diverse cell types in the brain. However, the specific molecular mechanisms and cell types affected by gene dysregulation remain unclear, especially for individual symptoms of PTSD. Here, we used a deep-learning framework to integrate single-cell RNA-Seq, ATAC-Seq, and spatial transcriptomic data in 229 post-mortem prefrontal cortex samples from individuals with PTSD or MDD and matched controls to determine cell-type-specific gene regulation and prioritize genomic variants within biobank-scale populations of affected individuals. After uniform data processing of RNA and ATAC-Seq data, we identified expression quantitative trait loci (QTLs) and gene regulatory networks (GRNs) for 28 distinct neuronal and non-neuronal cell types in the prefrontal cortex, highlighting dysregulation patterns in known PTSD-associated cell types such as Sst inhibitory neurons. We then re-trained LNCTP, a conditional energy-based deep learning framework for integrating single-cell functional datasets, on PTSD-specific genomic variants, QTL, and GRN datasets. LNCTP produced sets of prioritized variants, genes, and cell types important for predicting PTSD disease state, thus assigning cell types to known and potential new candidate PTSD genes. We finally validated the clinical relevance of prioritized variants and genes using whole-genome sequencing data of >17,500 veterans with PTSD and controls in the US Department of Veterans Affairs' MVP Biobank. In addition to confirming associations between genes and PTSD status in affected individuals, we linked variants and cell types to individual PTSD symptoms by clustering Veterans per validated ICD-10 codes and PCL-C surveys and assessing for enrichment of prioritized variants in each cluster. Thus, we identified cell types and molecular pathways in the prefrontal cortex for top candidate variants associated with PTSD and its clinical sub-features, potentially allowing for personalized diagnosis and development of future therapeutic targets for affected individuals.

**Disclosures: M. Jensen:** None. **N. Pandey:** None. **M. Gerstein:** None. **M. Girgenti:** None.

**Poster**

**PSTR204: Multi-Omics**

**Location:** WCC Halls A-C

**Time:** Monday, November 16, 2026, 1:00 PM - 5:00 PM

**Program #/Poster #:** PSTR204.09/LL23

**Topic:** J.02. Systems Biology and Bioinformatics

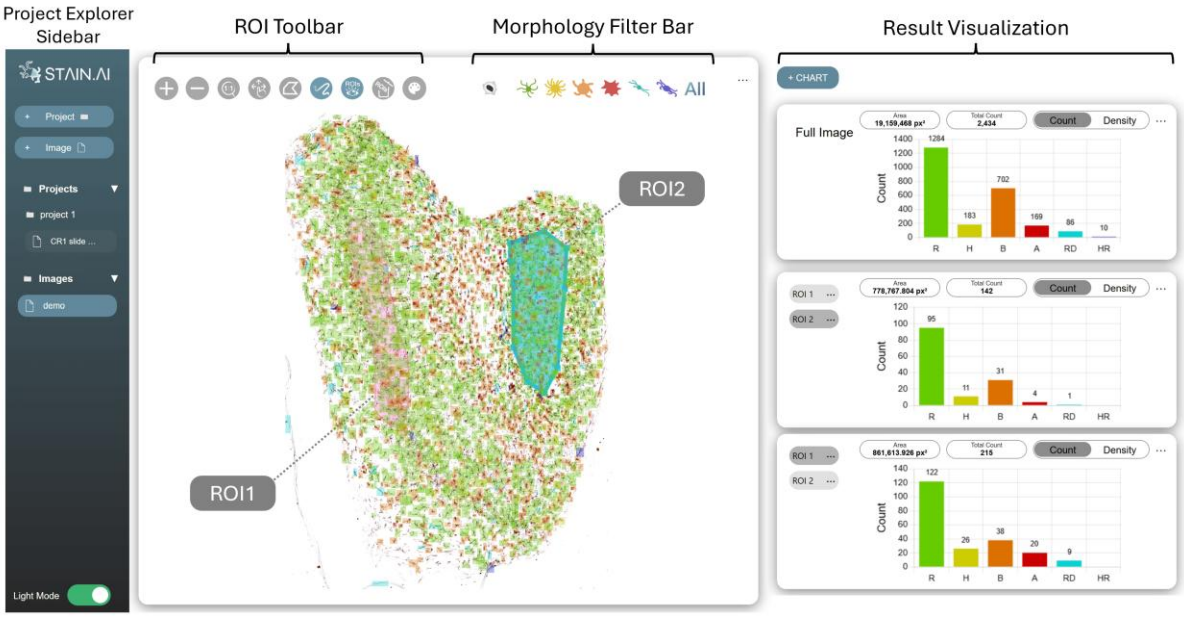
**Support:** NIMHD U54MD007597
NINDS R01NS112294
NINDS R01NS123442
NICHD P50HD105328
NSF grants of HRD 2200489
CNS 2200585

**Title:** StainAI-Web: A Free Online Platform for Automated Whole-Slide Microglial Morphology Mapping for Neuroinflammation Analysis

**Authors: *D.-Y. LIU**[1,2], H.-J. CHUANG[1], C.-H. HSU[1,3], B.-M. CHANG[1], E.-A. ETTE[4], M. SHIH[1,5], Y.-A. LIAO[6,1], P. WANG[1,7], T.-W. TU[1,8];
[1]Mol. Imaging Laboratory, Dept. of Radiology, Howard Univ., Washington, DC; [2]UCSD, La Jolla, CA; [3]Dept. of Computer Sci., Virginia Tech., Alexandria, VA; [4]Neurosci., Boston Univ., Allston, MA; [5]Miin Wu Sch. of Computing, Natl. Cheng Kung Univ., Tainan City, Taiwan; [6]New York Univ., New York, NY; [7]Dept. of Physics, Fu-Jen Catholic Univ., New Taipei City, Taiwan; [8]Dept. of Pediatrics, George Washington Univ., Washington, DC

**Abstract:** Microglial morphology analysis has emerged as a critical approach for investigating neuroinflammatory dynamics across physiological and pathological conditions. The growing availability of high-resolution and whole-slide histological images has increased the demand for robust, scalable frameworks that process large datasets while preserving spatial specificity. Existing approaches are hindered by local computation, slow inference and manual quantification, limiting scalability for whole-slide image analysis. Previously, we introduced StainAI, a multi-stage deep learning system for whole-slide microglial image analysis that classifies individual microglia by morphology. It accurately processed millions of cells across multiple brains and slices, generating morphology-coded color maps that revealed both known and novel neuroinflammatory activation patterns following cardiac arrest. In this study, we advance StainAI-Web as a free, web-based, publicly accessible AI platform for rapid, automated microglial morphology analysis in whole-slide immunohistochemistry (IHC) images. The platform integrates the YOLO model with an overlap-aware, patch-based deep learning strategy for efficient large-scale inference while preserving spatial consistency. Users can upload images or access platform datasets for flexible workflow integration. The platform shifts IHC image analysis from conventional counting to ROI-based quantification, which enables unbiased, systematic comparison of microglial populations across any defined regions. The interactive

web-based interface enables real-time visualization, dynamically updating morphological distributions as regions are selected or modified (Fig. 1). Outputs include microglial morphology maps and structured quantitative charts for downstream statistical analysis. Collectively, these capabilities establish StainAI-Web as a comprehensive resource for whole-slide microglial morphology analysis, facilitating neuroscience research.




**Disclosures: D. Liu:** None. **H. Chuang:** None. **C. Hsu:** None. **B. Chang:** None. **E. Ette:** None. **M. shih:** None. **Y. Liao:** None. **P. Wang:** None. **T. Tu:** None.

**Poster**

**PSTR204: Multi-Omics**

**Location:** WCC Halls A-C

**Time:** Monday, November 16, 2026, 1:00 PM - 5:00 PM

**Program #/Poster #:** PSTR204.10/LL24

**Topic:** J.02. Systems Biology and Bioinformatics

**Support:** National Institute of Mental Health (R01MH129343)
Maryland Stem Cell Research Fund (2026-MSCRFD-6688)
NIMH R37MH080046 to TAB
BBRF Young Investigator Award to STB
2-T32-NS063391-21 award to YG

**Title:** SCIT-seq: A multimodal platform integrating calcium imaging, immunofluorescence, and spatial transcriptomics in human iPSC-derived neurons

**Authors: *Y. GERA**[1], Y. AHMED[2], S. P. ARJONA[3], M. E. CORTES-GUTIERREZ[3], S. T. BARLOW[5], T. A. BLANPIED[6], S. A. AMENT[4];

[1]Univ. of Maryland, Baltimore Inst. of Genomic Sci., Baltimore, MD; [2]Univ. of Maryland, Baltimore, Baltimore, MD; [4]Dept. of Psychiatry and Inst. for Genome Sci., [3]U Maryland Sch. of Med., Baltimore, MD; [5]Sch. of Medicine, Physiol., Univ. of Maryland Baltimore, Baltimore, MD; [6]Dept. of Physiol., Univ. of Maryland Sch. of Med., Baltimore, MD

**Abstract:** Neuropsychiatric and neurodevelopmental disorders are associated with molecular, cellular, and circuit-level abnormalities. However, it remains challenging to directly link these phenotypes within the same cells. New approaches are needed to define how molecular states give rise to functional and structural variation across heterogeneous neuronal populations. To address this challenge, we developed SCIT-seq (Spatial Cellular Imaging and Transcriptomics sequencing), a multimodal platform that integrates live-cell calcium imaging, high-content immunofluorescence, and spatial transcriptomics within the same neural cell culture. SCIT-seq enables direct association of neuronal activity, morphology, protein expression, and transcriptomic state across thousands of individual human induced pluripotent stem cells (hiPSC)-derived neurons in a single experiment, providing a framework for investigating multiscale mechanisms of neuronal development and disease. As an initial application, we established SCIT-seq in NGN2-induced excitatory neurons derived from hiPSCs. Neurons were loaded with a calcium indicator (Rhod-4AM), fixed and stained for dendritic, pre-synaptic, and postsynaptic protein markers, and subjected to spatial transcriptomic profiling (VisiumHD). Protocol development focused on preserving RNA integrity while maintaining compatibility with functional imaging and spatial transcriptomics protocols. Ongoing studies are evaluating computational approaches for cell segmentation, multimodal data integration, and linkage of transcriptomic states with measures of neuronal activity and morphology. Future applications will leverage SCIT-seq to characterize the cellular consequences of neuropsychiatric disease-associated genetic variants, including variants that influence neuronal maturation, connectivity, and network function. More broadly, SCIT-seq provides a scalable platform for multimodal phenotyping of hiPSC-derived neurons and for elucidating relationships between molecular states and emergent cellular phenotypes.

**Disclosures: Y. Gera:** None. **Y. Ahmed:** None. **S.P. Arjona:** None. **M.E. Cortes-Gutierrez:** None. **S.T. Barlow:** None. **T.A. Blanpied:** None. **S.A. Ament:** None.

**Poster**

**PSTR204: Multi-Omics**

**Location:** WCC Halls A-C

**Time:** Monday, November 16, 2026, 1:00 PM - 5:00 PM

**Program #/Poster #:** PSTR204.11/Web Only

**Topic:** J.02. Systems Biology and Bioinformatics

**Title:** Updating the Reference Genome from mRatBN7.2 to GRCr8 Improves Single-Nucleus RNA-Sequencing Sensitivity in the Rat Brain

**Authors: *Z. HASAN**[1], T. BENOUKRAF[2], Q. YUAN[3];
[2]Biomed. Sciences, Fac. of Med., [1]Mem. Univ. of Newfoundland, St. John's, NL, Canada;
[3]Biomed. Sciences, Fac. of Med., Mem. Univ. of Newfoundland, St John's, NL, Canada

**Abstract:** The reference genome assembly determines how sequencing reads are aligned and how gene expression is quantified, making it a fundamental determinant of downstream single-cell and single-nucleus RNA-sequencing analyses. Yet the practical consequences of reference genome updates are rarely systematically evaluated. In 2024 the rat reference advanced from mRatBN7.2 to GRCr8, a more complete, long-read-based assembly with expanded gene annotation. To quantify how this transition affects snRNA-seq inference, we used a previously published snRNA-seq dataset of 36 hippocampal samples from a pretangle tau rat model, spanning six experimental groups and both sexes. We aligned each sample to both the mRatBN7.2 and GRCr8 (Ensembl release 115) references using identical CellRanger parameters, with matched downstream processing in Seurat and Scanpy.
Relative to mRatBN7.2, GRCr8 substantially increased transcriptomic recovery. Reads confidently assigned to the transcriptome increased from 25.9% to 31.5%, exonic mapping increased from 13.1% to 18.4%, and intergenic mapping decreased from 12.8% to 7.9%, indicating reassignment of reads to annotated gene features. These improvements translated into a ~51% increase in detected genes (21,152 vs. 31,943), together with modest increases in recovered nuclei, median genes per nucleus, and median UMI counts, while overall genome mapping remained essentially unchanged. Despite substantial gains in transcript recovery, downstream biological interpretation remained highly consistent. Differential expression analyses showed strong agreement in effect direction and magnitude for shared genes, although GRCr8 identified a somewhat larger set of significant genes, consistent with improved sensitivity.
These results demonstrate that adoption of GRCr8 substantially improves transcript recovery and gene detection in rat snRNA-seq while preserving the principal biological conclusions. We therefore recommend GRCr8 for future rat transcriptomic studies and suggest that previously published mRatBN7.2-based analyses remain broadly robust despite reduced sensitivity. Because these improvements occur at the alignment and annotation stage, similar benefits are likely to extend to scRNA-seq and other rat sequencing workflows.

**Disclosures: Z. Hasan:** None. **T. Benoukraf:** None. **Q. Yuan:** None.

**Poster**

**PSTR204: Multi-Omics**

**Location:** WCC Halls A-C

**Time:** Monday, November 16, 2026, 1:00 PM - 5:00 PM

**Program #/Poster #:** PSTR204.12/LL25

**Topic:** J.02. Systems Biology and Bioinformatics

**Support:** NIH Grant U01 DA051947
NIH Grant R21 DA048554
NIH Grant UM1 DA052244

**Title:** Molecular adaptations of ventral pallidum neurons and glia in the context of heroin abstinence

**Authors: *B. GRISSOM**[1], M. E. CORTES[1], S. MITRA[2], R. R. CAMPBELL[3], M. GREEN[4], D. M. DIETZ[5], M. LOBO[6], S. A. AMENT[7];
[1]Univ. of Maryland Sch. of Med., Baltimore, MD; [2]Biomed. Sci., OSU-CHS, JENKS, OK; [3]Anat. and Neurobio., Univ. of Maryland Sch. of Medicin Program In Neurosci., Baltimore, MD; [4]Univ. of Maryland Sch. of Med. Program In Neurosci., Baltimore, MD; [5]Univ. of Kansas, Lawrence, KS; [6]Anat. and Neurobio., Univ. of Maryland SOM, Baltimore, MD; [7]Dept. of Psychiatry and Inst. for Genome Sci., U Maryland Sch. of Med., Baltimore, MD

**Abstract:** The ventral pallidum (VP) is a critical node of the mesolimbic reward circuit in mammalian brains, yet its cellular diversity and cell type-specific adaptations after exposure to addictive substances are poorly characterized. To address this, we sequenced the nuclear transcriptomes (snRNAseq) of 92,978 cells and chromatin accessibility states (snATAC-seq) of 47,050 cells from the VP of rats in the context of heroin self-administration and forced abstinence. We generated a multimodal atlas for the diversity of neuronal and non-neuronal cells, including 48 transcriptionally distinct neuronal subtypes in the VP and surrounding regions. Cell types were assigned spatial domains within the ventral pallidum by comparing the snRNAseq dataset to a subcellular resolution spatial transcriptomics of mouse VP using CosMx. Vglut1 neurons and Microglia in the VP both showed strong responses to forced abstinence from heroin at a transcriptomic and regulatory level. Responses differed greatly between acute (day 1) and chronic (day 14) phases of forced abstinence for these cell types. Pseudotime analyses using monocle3 revealed the trajectory of shifting cell states across these two time points. Gene regulatory networks reconstructed from the snRNA-seq and snATAC-seq data identified key transcription factors for the mediation of neuroplastic and desensitization responses of neurons and microglia respectively.

**Disclosures: B. Grissom:** None. **M.E. Cortes:** None. **S. Mitra:** None. **R.R. Campbell:** None. **M. Green:** None. **D.M. Dietz:** None. **M. Lobo:** None. **S.A. Ament:** None.

**Poster**

**PSTR204: Multi-Omics**

**Location:** WCC Halls A-C

**Time:** Monday, November 16, 2026, 1:00 PM - 5:00 PM

**Program #/Poster #:** PSTR204.13/LL26

**Topic:** J.02. Systems Biology and Bioinformatics

**Support:** NIH R24MH114788
NIH UM1DA052244
NIH U24MH130968

**Title:** The Neuroscience Multi-Omic Archive (NeMO): A public resource for single cell transcriptomic and epigenomic data from the mammalian brain

**Authors: *J. RECEVEUR**[1], S. A. AMENT[2], R. ADKINS[3], M. G. GIGLIO[4], D. GONZALEZ BRAVO[3], B. HERB[3], T. HODGES[3], O. IFEONU[3], R. LABOULAYE[3], D. LESPERANCE[3], S. NADENDLA[3], D. OLLEY[3], J. ORVIS[3], M. SCHOR[3], R. P. HERTZANO[5], O. WHITE[6], A. MAHURKAR[7];
[1]Inst. for Genome Sciences, Univ. of Maryland Baltimore; Sch. of Med., Baltimore, MD; [2]Dept. of Psychiatry and Inst. for Genome Sci., U Maryland Sch. of Med., Baltimore, MD; [4]Med., [3]Inst. for Genome Sciences, Univ. of Maryland Sch. of Med., Baltimore, MD; [5]Neurotology Br., NIDCD/NIH, Bethesdsa, MD; [6]Inst. for Genome Sciences, Univ. of Maryland Baltimore; Sch. of Med., Baltimore, MD; [7]Univ. of Maryland Sch. of Med., Baltimore, MD

**Abstract:** Scalable technologies to sequence the transcriptomes and epigenomes of single cells are transforming our understanding of cell types and cell states. Large consortia projects and individual research groups are applying these technologies at unprecedented scale in the mammalian brain but there is a critical need for harmonization and tools for interfacing with these data objects. The Neuroscience Multi-Omic Archive (NeMO) serves as the primary sequence data repository for the BRAIN Initiative, SCORCH consortium, and a number of other high-profile efforts exploring the mammalian brain. To date, NeMO hosts over three petabytes of sequencing data from 25 species and 55 different techniques, with over nineteen petabytes of data downloads. Data available at NeMO includes raw data from human and model organisms, as well as summary data processed uniformly through consensus pipelines (for BRAIN Initiative and SCORCH consortia derived data). Archive tools include a searchable web portal allowing cross study and program data searches, API interfaces for large-scale data access, and an interactive analysis platform, NeMO Analytics. NeMO Archive continues to expand with new data and features, and serves as a critical public resource for the neuroscience community.

**Disclosures: J. Receveur:** None. **S.A. Ament:** None. **R. Adkins:** None. **M.G. Giglio:** None. **D. Gonzalez Bravo:** None. **B. Herb:** None. **T. Hodges:** None. **O. Ifeonu:** None. **R. Laboulaye:** None. **D. Lesperance:** None. **S. Nadendla:** None. **D. Olley:** None. **J. Orvis:** None. **M. Schor:** None. **R.P. Hertzano:** None. **O. White:** None. **A. Mahurkar:** None.

**Poster**

**PSTR204: Multi-Omics**

**Location:** WCC Halls A-C

**Time:** Monday, November 16, 2026, 1:00 PM - 5:00 PM

**Program #/Poster #:** PSTR204.14/LL27

**Topic:** J.02. Systems Biology and Bioinformatics

**Support:** NIH 1R25AI175017

**Title:** Peripheral Immune Dysfunction and Microglial Neuroinflammation in HIV-Associated Neurocognitive Disorders

**Authors: *S. MUTUA**[1], J. RECEVEUR[2], B. HERB[2], E. MOCCI[2], S. A. AMENT[3];
[2]Inst. for Genome Sci., [3]Dept. of Psychiatry and Inst. for Genome Sci., [1]Univ. of Maryland Sch. of Med., Baltimore, MD

**Abstract:** Human immunodeficiency virus (HIV) infection remains associated with a high prevalence of neurocognitive impairment even with effective antiretroviral therapy (ART). Approximately one in two people with HIV (PWH) on suppressive ART develop mild to moderate neurocognitive impairments, collectively referred to as HIV-associated neurocognitive disorders (HAND). HAND is thought to be driven in part by persistent neuroinflammation within the central nervous system. HIV enters the brain early in infection through infected T cells, macrophages, and monocytes that traverse the blood-brain barrier and establish long-lived CNS reservoirs. Once in the brain, the infected cells can interact with resident microglia, promoting a sustained inflammatory state that likely contributes to neuronal dysfunction and cognitive decline. However, the mechanisms by which peripheral immune dysfunction in HIV propagates CNS inflammation and cognitive decline remain poorly understood. We hypothesize that peripheral immune dysfunction in HIV is associated with distinct microglial neuroinflammatory gene expression patterns that drive neurocognitive impairment. To test this hypothesis, we leveraged clinical, immunologic, and neurocognitive data from PWH who donated their brains to the National NeuroHIV Tissue Consortium (NNTC), along with transcriptional profiles of microglia in the prefrontal cortex derived from single-nuclei RNA sequencing by the Single-Cell Opioid Responses in the Context of HIV (SCORCH) consortium. We constructed linear regression models to evaluate associations between peripheral HIV markers such as CD4 nadir and microglial neuroinflammatory gene expression profiles, adjusting for age, sex, and ethnicity. We then assessed whether identified expression patterns predicted neurocognitive impairment severity. These analyses may help to explain how systemic immune dysfunction mediates neuroinflammation in HIV, addressing a critical gap in HAND pathophysiology. The microglial pathways identified through this work may represent novel therapeutic targets for neuroprotective interventions that may preserve cognitive health in PWH.

**Disclosures: S. Mutua:** None. **J. Receveur:** None. **B. Herb:** None. **E. Mocci:** None. **S.A. Ament:** None.

**Poster**

**PSTR204: Multi-Omics**

**Location:** WCC Halls A-C

**Time:** Monday, November 16, 2026, 1:00 PM - 5:00 PM

**Program #/Poster #:** PSTR204.15/LL28

**Topic:** J.02. Systems Biology and Bioinformatics

**Support:** JST ERATO grant (Hiroki R. Ueda, no. JPMJER2001),
JST [Moonshot R&D] (Katsuhiko Matsumoto, no. JPMJMS2023)
MEXT Quantum Leap Flagship Program (MEXT QLEAP) (Hiroki R. Ueda, no. JPMXS0120330644)
JSPS KAKENHI grant-in-aid for scientific research (S) (Hiroki R. Ueda, no.

JP18H05270)
JSPS KAKENHI grant-in-aid for scientific research (C) (Katsuhiko Matsumoto, no. 20K06885)
JSPS KAKENHI grant-in-aid for Early-Career Scientists (Shota Y. Yoshida, no. 26K18578)
grant-in-aid from the Human Frontier Science Program (Hiroki R. Ueda)

**Title:** A three-dimensional single-cell-resolution atlas of the adult rat whole brain (CUBIC Rat Brain Atlas)

**Authors: *S. Y. YOSHIDA**[1,3], K. MATSUMOTO[3,4], K. YAMASHITA[5,2], H. R. UEDA[3,4]; [1]Dept. of Pathology, The Univ. of Tokyo, Bunkyo-ku/ Tokyo, Japan; [2]Dept. of Systems Pharmacol., The Univ. of Tokyo, Tokyo, Japan; [3]Dept. of Systems Pharmacol., the Univ. of Tokyo, Tokyo, Japan; [4]Dept. of Systems Biol., Kurume Univ., Kurume, Japan; [5]Osaka Univ., Suita-shi, Osaka, Japan

**Abstract:** The mammalian brain is composed of diverse anatomical regions that support sensory processing, motor control, memory, emotion, arousal, and higher-order cognitive functions. These regions form highly interconnected networks, and brain function emerges from the coordinated activity of distributed cellular populations. Therefore, understanding brain states requires a quantitative framework that can capture both the anatomical organization of the whole brain and the spatial distribution of activated cells at single-cell resolution. Recent advances in tissue clearing, light-sheet microscopy imaging, and computational image analysis have enabled the mouse brain to be visualized in three dimensions at single-cell resolution (Murakami et al., *Nature Neuroscience*, 2018). These approaches are particularly powerful for whole-brain activity mapping using immediate early genes such as c-Fos (Yamashita et al., *Science*, 2025). However, most whole-brain imaging approaches have been developed in mice, and the rat remains less well explored despite its broad use in behavioral neuroscience, pharmacology, physiology, and disease model research. The larger size of the rat brain provides advantages for behavioral and translational studies, but also poses technical challenges for uniform staining, high-resolution whole-brain imaging, large-scale data processing, and automated cell detection. To address this challenge, we constructed the CUBIC Rat Brain Atlas, a whole-brain, single-cell-resolution cellular atlas of the adult rat brain, using tissue clearing, nuclear staining, light-sheet fluorescence microscopy, and computational cell detection. We further applied this rat whole-brain single-cell analysis platform to whole-brain c-Fos immunostaining and explored its application to brain-wide activity mapping. By spatially aligning c-Fos-positive cells with the CUBIC Rat Brain Atlas, this workflow enables region-wise analysis of activity patterns across the entire rat brain at single-cell resolution. This platform provides a scalable anatomical and functional framework for analyzing brain states in rat models of behavior, circadian regulation, pharmacological intervention, and neurological or psychiatric disease.

**Disclosures: S.Y. Yoshida:** A. Employment/Salary (full or part-time):; CUBICStars. Inc. **K. Matsumoto:** A. Employment/Salary (full or part-time):; CUBICStars. Inc. **K. Yamashita:** None. **H.R. Ueda:** A. Employment/Salary (full or part-time):; CUBICStars. Inc.

**Poster**

**PSTR204: Multi-Omics**

**Location:** WCC Halls A-C

**Time:** Monday, November 16, 2026, 1:00 PM - 5:00 PM

**Program #/Poster #:** PSTR204.16/LL29

**Topic:** J.02. Systems Biology and Bioinformatics

**Support:** JST ERATO grant (JPMJER2001),
JST (Moonshot R&D,JPMJMS2023),
MEXT Quantum Leap Flagship Program,JPMXS0120330644
JSPS KAKENHI grant-in-aid for scientific research (S) 20K06885
JSPS KAKENHI grant-in-aid for Early-Career tists (20K16626)
grant-in-aid from the Human Frontier Science Program
the Science and Technology Platform Program for Advanced Biological Medicine

**Title:** Whole-Organ and Whole-Body 3D Imaging and Analysis Using CUBIC Technology

**Authors: *K. MATSUMOTO**[1], S. YOSHIDA[2], H. R. UEDA[3];
[1]Dept. of Systems Pharmacology, the Univ. of Tokyo, Tokyo, Japan; [2]Dept. of Pathology, The Univ. of Tokyo, Bunkyo-ku/ Tokyo, Japan; [3]The Univ. of Tokyo / Kurume Univ., Kurume, Japan

**Abstract:** Tissue clearing-based whole-organ and whole-body imaging has enabled quantitative analysis of cellular organization and inter-organ relationships across many mouse organs, including the central nervous system. In particular, whole-organ cell atlases of various mouse organs provide a framework for assessing the effects of drugs, inflammation, and other perturbations at single-cell resolution beyond the brain (S. Y. Yoshida, *et., al*., Cell, 2026). Focusing on the central nervous system, a circadian neural activity atlas was generated by mapping c-Fos immunostaining across the entire mouse brain(K. Yamashita, *et., al.*, Science, 2026). This atlas revealed that neuronal activity fluctuates over time in many brain regions, suggesting that the timing of administration may be an important factor when evaluating drugs that act on the central nervous system. Based on these atlases, we administered several central nervous system-active compounds, including caffeine, and quantitatively analyzed drug-induced changes in whole-brain c-Fos activity in mice (n = 6). This approach enabled the identification of brain regions whose activity was significantly altered by each compound. Because drugs may also affect organs beyond their known therapeutic targets, systemic side-effect analysis using whole-organ cell atlases of organs such as the kidney, liver, and heart is also important. We will present strategies for evaluating drug effects and potential adverse responses using these whole-organ cell atlases. High-quality three-dimensional imaging requires highly optimized tissue clearing protocols. To construct whole-organ cell atlases across diverse mouse organs, highly cleared samples must be prepared reproducibly, and each organ requires specific technical considerations. Therefore, we will also present detailed protocols and practical tips for preparing high-quality cleared samples suitable for whole-organ and whole-body 3D imaging and quantitative analysis.

**Disclosures: K. Matsumoto:** A. Employment/Salary (full or part-time):; CUBICStars.inc. E. Ownership Interest (stock, stock options, royalty, receipt of intellectual property rights/patent holder, excluding diversified mutual funds); CUBICStars.inc. **S. Yoshida:** None. **H.R. Ueda:** E.

Ownership Interest (stock, stock options, royalty, receipt of intellectual property rights/patent holder, excluding diversified mutual funds); CUBICStars.inc.

**Poster**

**PSTR204: Multi-Omics**

**Location:** WCC Halls A-C

**Time:** Monday, November 16, 2026, 1:00 PM - 5:00 PM

**Program #/Poster #:** PSTR204.17/LL30

**Topic:** J.02. Systems Biology and Bioinformatics

**Title:** Z-HARMony: robust 3D cell segmentation for brain spatial transcriptomic profiling

**Authors:** *L. WU, A. WARDHANI, J. PHAN, A. L. HECK, K. YOUNG, **J. NULL**, J. BEECHEM;
Bruker Spatial Biol., Seattle, WA

**Abstract:** Brain spatial transcriptomic profiling requires accurate assignment of molecular signals to individual cells in densely packed, three-dimensional neural tissue. Because neurons and glia extend across the z-axis, purely 2D analysis can mix signals from vertically adjacent cells and distort cell-level measurements. This problem is especially acute in brain tissue, where close cell packing and fine anatomical organization make precise cell delineation essential for interpreting spatial gene expression. However, existing 3D segmentation methods remain difficult to deploy in routine, high-throughput workflows because sparse axial sampling and optical anisotropy disrupt object continuity, while full 3D inference often requires costly isotropic resampling. To address this challenge, we present Z-HARMony (Z-guided Hybrid Assembly for Robust Mapping in z), a model-agnostic method for 3D cell segmentation in anisotropic, sparse-z imaging datasets. Z-HARMony combines two complementary streams on the same volume: per-Z 2D segmentation to preserve accurate XY boundaries, and a cross-view volumetric prior generated by aggregating predictions from the same 2D model across XY, XZ, and YZ views. Rather than serving as the final output, this prior guides assembly of slice-level masks into z-continuous 3D cell instances. We compute overlap profiles between adjacent slices and prior volumes, build a correlation graph to link coherent objects across planes, and then cluster these links to anchor the stitching of 2D labels along z. Optional nuclear/cytoplasmic cues can be incorporated to further reduce segmentation errors. Tested on brain spatial transcriptomic datasets with large z-steps collected from the CosMx® SMI platform, Z-HARMony improves z-continuity and reduces split and merge errors relative to heuristic stitching and direct cross-view aggregation. Because the volumetric prior can be computed on a down-sampled z-stack while XY segmentation runs at native resolution, the method avoids the high computational cost of isotropic resampling required by many full 3D approaches. Together, these features improve 3D cell delineation in brain sections, enabling more accurate assignment of spatial transcriptomic signals to neurons and glia and supporting more reliable cell-type mapping, laminar and regional analysis, and interpretation of cellular organization in neural tissue.

**Disclosures: L. Wu:** A. Employment/Salary (full or part-time):; Bruker Spatial Biology. E. Ownership Interest (stock, stock options, royalty, receipt of intellectual property rights/patent holder, excluding diversified mutual funds); Bruker Spatial Biology. **A. Wardhani:** A. Employment/Salary (full or part-time):; Bruker Spatial Biology. E. Ownership Interest (stock, stock options, royalty, receipt of intellectual property rights/patent holder, excluding diversified mutual funds); Bruker Spatial Biology. **J. Phan:** A. Employment/Salary (full or part-time):; Bruker Spatial Biology. E. Ownership Interest (stock, stock options, royalty, receipt of intellectual property rights/patent holder, excluding diversified mutual funds); Bruker Spatial Biology. **A.L. Heck:** A. Employment/Salary (full or part-time):; Bruker Spatial Biology. E. Ownership Interest (stock, stock options, royalty, receipt of intellectual property rights/patent holder, excluding diversified mutual funds); Bruker Spatial Biology. **K. Young:** A. Employment/Salary (full or part-time):; Bruker Spatial Biology. E. Ownership Interest (stock, stock options, royalty, receipt of intellectual property rights/patent holder, excluding diversified mutual funds); Bruker Spatial Biology. **J. Null:** A. Employment/Salary (full or part-time):; Bruker Spatial Biology. E. Ownership Interest (stock, stock options, royalty, receipt of intellectual property rights/patent holder, excluding diversified mutual funds); Bruker Spatial Biology. **J. Beechem:** A. Employment/Salary (full or part-time):; Bruker Spatial Biology. E. Ownership Interest (stock, stock options, royalty, receipt of intellectual property rights/patent holder, excluding diversified mutual funds); Bruker Spatial Biology.

**Poster**

**PSTR204: Multi-Omics**

**Location:** WCC Halls A-C

**Time:** Monday, November 16, 2026, 1:00 PM - 5:00 PM

**Program #/Poster #:** PSTR204.18/LL31

**Topic:** J.02. Systems Biology and Bioinformatics

**Support:** NIH RF1MH125933

**Title:** Cell-Type Specificity of Brain Gene-Network Associations Reveals Convergence on Limbic Excitatory Neurons and Oligodendrocyte Precursors

**Authors: *N. SARDARIPOUR**[1], N. HOANG[2], A. GONG[1], A. ZALESKY[3], J. CAPRA[4], M. RUBINOV[1];
[1]Biomed. Engin., [2]Vanderbilt Univ., Nashville, TN; [3]Melbourne Neuropsychiatry Ctr., Melbourne, Australia; [4]UCSF, San Francisco, CA

**Abstract:** Objective: The cell types mediating the relationship between genetically regulated gene expression and large-scale brain network organization remain largely unknown. We identified the cell-type and regional specificity of gene expression by integrating transcriptomic, morphological, and connectomic data at biobank scale. Methods: We developed a non-negative regularized multiview canonical correlation analysis with recursive feature pruning. We applied this framework to identify stable cross-modal associations between genetically regulated gene expression and brain organization in a European-ancestry subset of 39,565 UK Biobank subjects

(mean age 64.4±7.7 years, 52% female). We integrated imputed regional gene expression (Joint-Tissue Imputation/GTEx) with MRI-derived regional morphometry (FreeSurfer, Desikan-Killiany atlas) and diffusion tractography network features (Schaefer 100-parcel/7-network and Melbourne Subcortical atlases). For cell-type specificity, we mapped 132 selected genes against the Whole Human Brain snRNA-seq atlas (~3.37M cells; 31 superclusters, 14 anatomical divisions) using 10,000 stratified permutations against TWAS-retained genes. Results and Conclusions: Multiview analysis revealed significant cross-modal associations (Region-Network: R=0.56, Region-Gene: R=0.15, Network-Gene: R=0.09; p<0.001), with dominant morphometric weights in dorsolateral prefrontal and anterior cingulate cortices and network weights spanning sensory-motor, default mode, attention, and limbic circuits. Cell-type analysis showed the strongest enrichment in committed oligodendrocyte precursors across 11 regions (e.g., cerebellum, p=0.0049; cortex, p=0.0081) and mature oligodendrocytes across 12 regions. The primary excitatory neuronal signal was localized to thalamic excitatory neurons in the amygdaloid complex (p=0.0096), implicating thalamolimbic circuitry in gene-network associations. Upper rhombic lip progenitors, the developmental precursor cells predominantly associated with the cerebellum, were also enriched across multiple regions. Collectively, these network-mediating genes converge primarily on myelination and thalamolimbic excitatory circuits, demonstrating that population-scale connectivity variation is heavily grounded in distributed glial and support cell populations.

**Disclosures: N. Sardaripour:** None. **N. Hoang:** None. **A. Gong:** None. **A. Zalesky:** None. **J. Capra:** None. **M. Rubinov:** None.

**Poster**

**PSTR204: Multi-Omics**

**Location:** WCC Halls A-C

**Time:** Monday, November 16, 2026, 1:00 PM - 5:00 PM

**Program #/Poster #:** PSTR204.19/LL32

**Topic:** J.02. Systems Biology and Bioinformatics

**Title:** High-Plex Spatial Proteomics and AI-Based Image Analysis Reveal Multicellular Architecture of Alzheimer's Disease Human Tissue

**Authors:** *H. LAI[1], A. KARPATI[2], E. LOCHE[2], S. STRUBLE[1], W. HOWAT[2], R. HEIL-CHAPDELAINE[1], N. FERNANDEZ DIAZ GRANADOS[1], **A. BOSE**[1];
[1]Leica Microsystems, Waltham, MA; [2]Abcam Inc., Cambridge, United Kingdom

**Abstract:** Alzheimer's disease (AD) is characterized by complex spatial interactions among neuronal, glial, synaptic, and pathological components that contribute to neurodegeneration and tissue remodeling. Conventional histopathological approaches capture key disease hallmarks but are limited in resolving the high-dimensional spatial organization of multicellular interactions within the brain microenvironment. Spatial multiplex imaging combined with artificial intelligence (AI)-driven computational analysis enables systematic interrogation of tissue architecture underlying AD progression and identify spatial biomarkers associated with disease

pathology. In this study, formalin-fixed paraffin-embedded (FFPE) human AD brain tissue sections from multiple cortical regions, including occipital lobe, frontal lobe, temporal lobe, and postcentral gyrus, were analyzed using the Cell DIVE multiplexed imaging platform by Leica Microsystems. A directly conjugated antibody panel obtained from Abcam was used to profile major AD-associated pathological and cellular classes, including neuronal populations, synaptic integrity, glial populations, and amyloid- and tau-related pathology. Spatial analysis workflows integrating high-dimensional image registration, AI-assisted cell segmentation, and spatial quantification were performed using Aivia image analysis software. AI-based spatial modeling approaches characterized multicellular spatial organization, plaque-associated microenvironments, regional tissue heterogeneity, and cell-cell interaction networks across distinct anatomical brain regions. Spatially resolved computational analyses enabled identification of disease-associated tissue architectures and neuroinflammatory niches within the AD brain microenvironment. This work establishes a scalable framework integrating high-plex spatial proteomics with AI-enabled computational pathology for the investigation of neurodegenerative disease biology and spatial tissue organization in human AD brain tissue. These approaches may support the discovery of spatial biomarkers, disease-associated cellular microenvironments, and molecular interaction networks relevant to AD and related neurodegenerative disorders.

**Disclosures: H. Lai:** A. Employment/Salary (full or part-time):; Leica Microsystems. **A. Karpati:** A. Employment/Salary (full or part-time):; Abcam. **E. Loche:** A. Employment/Salary (full or part-time):; Abcam. **S. Struble:** A. Employment/Salary (full or part-time):; Leica Microsystems. **W. Howat:** A. Employment/Salary (full or part-time):; Abcam. **R. Heil-Chapdelaine:** A. Employment/Salary (full or part-time):; Leica Microsystems. **N. Fernandez Diaz Granados:** A. Employment/Salary (full or part-time):; Leica Microsystems. **A. Bose:** A. Employment/Salary (full or part-time):; Leica Microsystems.

**Poster**

**PSTR204: Multi-Omics**

**Location:** WCC Halls A-C

**Time:** Monday, November 16, 2026, 1:00 PM - 5:00 PM

**Program #/Poster #:** PSTR204.20/LL33

**Topic:** J.02. Systems Biology and Bioinformatics

**Support:** RF1AG059778
R01AG057914
ZEN-21-846037
#5P30AG072931

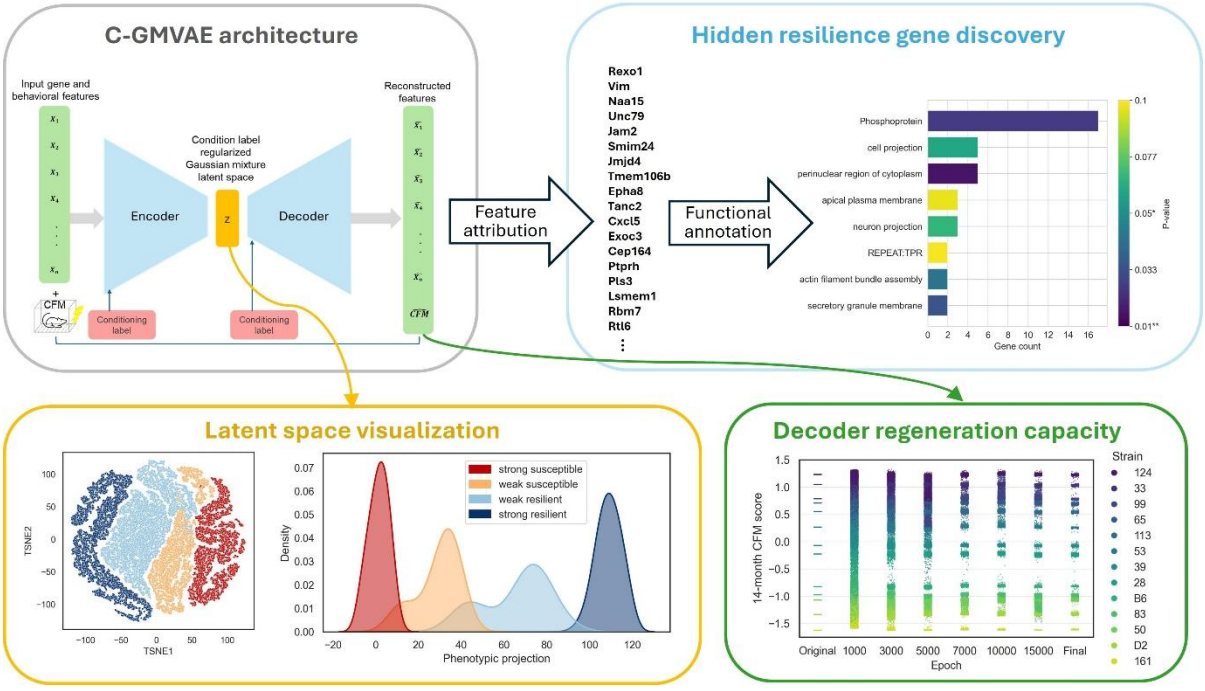
**Title:** Identifying Hidden Factors of Cognitive Resilience in Alzheimer's Disease with a Deep Generative Model

**Authors: *Y. CAO**[1], V. UMASHANKAR[2], R. IRITANI[2], A. DRAELOS[3], C. C. KACZOROWSKI[4];

[1]Univ. of Michigan, Ypsilanti, MI; [3]Biomed. Engin., [2]Univ. of Michigan, Ann Arbor, MI; [4]Neurol., The Univ. of Michigan, Ann Arbor, MI

**Abstract: Identifying Hidden Factors of Cognitive Resilience in Alzheimer's Disease with a DeepGenerative Model**Alzheimer's disease (AD) exhibits heterogeneous cognitive decline despite similar pathology,suggesting that genetic variation influences cognitive resilience. Traditional transcriptomicapproaches often focus on individual genes and may fail to capture coordinated molecularprograms underlying resilience. Discovering hidden and coordinated molecular programsunderlying cognitive resilience may reveal novel therapeutic targets. We developed aConditional-Gaussian Mixture Variational Autoencoder (C-GMVAE), a deep generative modelconsisting of an encoder that learns low-dimensional latent representations and a decoder thatreconstructs transcriptomic profiles. The model was trained using integrated hippocampal andprefrontal cortex snRNA-seq data from the genetically diverse AD-BXD mouse panel. Resiliencelevel, derived from contextual fear memory (CFM), was used as the conditioning label (Figure1). The learned latent space revealed multiple resilience-associated dimensions that were notapparent using conventional dimensionality reduction methods. Several latent variables exhibitedhigh heritability, suggesting that they represent genetically regulated programs. A phenotypicextremal projection dimension was constructed by projecting samples onto an axis betweenresilient and susceptible latent-space states, generating a continuous resilience score. To explorehidden gene signatures associated with AD cognitive resilience that emerge from coordinatedgene activity captured by these resilience-associated latent variables, we applied IntegratedGradients, a feature attribution method, to the model encoder to quantify gene-level contributionsto latent representations. Together, these analyses demonstrate that C-GMVAE can identifyhidden and heritable molecular factors associated with cognitive resilience and prioritizecandidate resilience-associated genes.

Figure 1. C-GMVAE Workflow



**Disclosures: Y. Cao:** None. **V. Umashankar:** None. **R. Iritani:** None. **A. Draelos:** None. **C.C. Kaczorowski:** None.

**Poster**

**PSTR204: Multi-Omics**

**Location:** WCC Halls A-C

**Time:** Monday, November 16, 2026, 1:00 PM - 5:00 PM

**Program #/Poster #:** PSTR204.21/LL34

**Topic:** J.02. Systems Biology and Bioinformatics

**Title:** Multi-Omic Network Effects of 5-Me0-DMT and Non-Hallucinogenic TBG Via Interrogation of Foundational Model Transformer Heads

**Authors: *E. FENTON**;
Univ. of California, Davis, Davis, CA

**Abstract:** Analysis of multimodal snRNAseq data between experimental conditions is challenged by both data quality and analysis method. Foundational models enable utilization of data from millions of cells from the research community, but the underlying biological complexity still hinders detection of the effects of perturbations. Pleiotropic genes and overlapping and interconnected functional networks means that even within single cells, changes in gene expression can be obscured by the involvement of that same gene in unperturbed functions in the same cell. Transformer based models have internal attention matrixes that enable network modeling akin to coexpression matrixes. However, these can conceptually extend the functionality of traditional module based approaches by enabling the detection of arbitrarily complex relationships between genes beyond correlation enabled by backpropagation, and crucially, using multiple parallel attention head to find multiple networks within the same cell thus enabling the ability to focus on different biological networks and allowing a gene to have multiple functions highlighted. Here, we show the ability of attention weights from scGPT to enable differential expression analysis that recapitulates and extends current methods and discovers divergent and convergent modulated pathways 1 hour after administration of a single dose of 5-MeO-DMT or Tabernanthalog in mouse mPFC.

**Disclosures: E. Fenton:** None.

**Poster**

**PSTR204: Multi-Omics**

**Location:** WCC Halls A-C

**Time:** Monday, November 16, 2026, 1:00 PM - 5:00 PM

**Program #/Poster #:** PSTR204.22/LL35

**Topic:** J.02. Systems Biology and Bioinformatics

**Title:** scMOBA: a conversational single-cell multi-omics brain foundation model across species

**Authors: *Z. ZHANG**[1,2], R. WEI[3], J. SUN[4,5], Y. SUN[1,2], Y. SUN[1,6,7];
[1]Ctr. for Excellence in Brain Sci. and Intelligence Technology, Chinese Acad. of Sci., Shanghai, China; [2]Univ. of the Chinese Acad. of Sci., Beijing, China; [3]Peking Univ., Beijing, China; [4]Carnegie Mellon Univ., Pittsburgh, PA; [5]Shanghai Artificial Intelligence Lab., Shanghai, China; [6]State Key Lab. of Genet. Evolution & Animal Models, Shanghai, China; [7]Shanghai Key Lab. of Precision Gene Editing and Clin. Translation, Shanghai, China

**Abstract:** Single-cell and spatial multi-omics atlases are transforming neuroscience, but fragmented modalities, species, ages, and disease states limit integrated interpretation. In this exploratory study, we developed scMOBA, a conversational single-cell multi-omics brain foundation model that links molecular feature profiles to natural-language queries. scMOBA combines a Geneformer-initialized gene encoder, a cross-attention projector, and a modular large language model (LLM) component, and was pretrained with a feature-question-answer framework on approximately 133 million brain profiles from human, macaque, marmoset, and mouse snRNA-seq, snATAC-seq, and spatial transcriptomic datasets spanning development, aging, and disease. Across held-out and external datasets, scMOBA enabled direct zero-shot inference and interpretable embeddings. In unseen human motor cortex snRNA-seq, it predicted major cell classes with >99% accuracy and cell subclasses with 93.1% accuracy, outperforming CellWhisperer and assigning high attention to canonical marker genes. For integration, scMOBA aligned donor, species, RNA/ATAC, and spatial datasets while preserving biological cell identities, outperforming conventional integration methods and other single-cell foundation models. Cross-species analyses generalized to chimpanzee and macaque cell subclasses and identified reptilian ependymoglial astrocyte-like programs and primate-specific L4 glutamatergic neurons. scMOBA embeddings also captured biological dynamics: predicted developmental stages correlated with chronological age (Spearman R=0.98), reconstructed glutamatergic lineage branching, and identified KCNIP4 as a V1-enriched L4 IT marker validated by MERFISH. In aging analyses, a spatial transcriptomic clock trained on mouse MERFISH data generalized across 14 cell types and detected rejuvenation signatures after Yamanaka-factor induction and exercise. Finally, scMOBA predicted Alzheimer's disease status in an independent snRNA-seq cohort with 0.96 accuracy and resolved AD-associated lipid-processing MG4, inflammatory MG8, and reactive GFAP+/NEAT1+/CLU+ astrocyte states, with MG8 attention-gene scores increasing from control to early- and late-stage AD. These results support scMOBA as an extensible and interpretable framework for brain atlas integration and discovery across development, aging, and disease.

**Disclosures: Z. Zhang:** None. **R. Wei:** None. **J. Sun:** None. **Y. Sun:** None. **Y. Sun:** None.

**Poster**

**PSTR204: Multi-Omics**

**Location:** WCC Halls A-C

**Time:** Monday, November 16, 2026, 1:00 PM - 5:00 PM

**Program #/Poster #:** PSTR204.23/LL36

**Topic:** J.02. Systems Biology and Bioinformatics

**Support:** NIH Grant 1R01HG014190
NIH Grant 1RF1MH133703

**Title:** Spatial Transcriptomic Niche Trajectories Reveal Coordinated Gene and Cell-Cell Communication Dynamics Across the Whole Mouse Brain

**Authors: *W. WANG**, S. SHIN, J. CHAVEZ, G.-C. YUAN;
Icahn Sch. of Med. at Mount Sinai, New York, NY

**Abstract:** The mammalian brain is organized by spatially patterned microenvironments in which diverse neuronal and non-neuronal cell types coexist, communicate, and jointly support region-specific function. Recent spatial transcriptomics atlases provide an unprecedented opportunity to study this organization at whole-brain scale, but most analytical methods partition tissue into discrete domains or analyze cell types separately, limiting the ability to model continuous microenvironmental variation. Here, we applied ONTraC, a graph neural network-based niche trajectory framework, to a brain-wide MERFISH spatial transcriptomics dataset to construct a continuous reference map of whole mouse brain microenvironments.

Using niches—spatially localized multicellular units—as the basic analytical unit, ONTraC reconstructed brain-wide and region-specific niche trajectories that captured major anatomical organization while preserving fine-scale intra-regional heterogeneity. We further extended the analysis from structural mapping to dynamic functional interpretation by identifying genes whose expression changes along each niche trajectory. These trajectory-associated genes revealed functionally coherent programs shared across multiple cell types. For example, in the isocortex, Gad2 and Slc6a1, two genes involved in GABA synthesis and transport, showed coordinated negative expression dynamics along the niche trajectory. Notably, GABA-A receptor genes in distinct neuronal populations displayed matched trajectory-dependent patterns: Gabra1 and Gabrg2 in IT CTX glutamatergic neurons followed Slc6a1 dynamics in Pvalb GABAergic neurons, whereas Gabra2 in Pvalb GABAergic neurons and Gabra1, Gabra4, and Gabrb2 in Sst GABAergic neurons followed Gad2 dynamics in Pvalb GABAergic neurons. These findings suggest coordinated pathway-level regulation across cell types within spatially changing cortical microenvironments.

Together, these results suggest that brain spatial organization is not simply a mosaic of discrete regions, but a continuum of multicellular niches coupled to coordinated transcriptional and intercellular communication dynamics. This updated ONTraC analysis demonstrates the value of spatial transcriptomics-based niche trajectory modeling for linking anatomical structure, cell-type-specific gene programs, and multicellular signaling across the whole mouse brain.

**Disclosures: W. Wang:** None. **S. Shin:** None. **J. Chavez:** None. **G. Yuan:** None.

**Poster**

**PSTR204: Multi-Omics**

**Location:** WCC Halls A-C

**Time:** Monday, November 16, 2026, 1:00 PM - 5:00 PM

**Program #/Poster #:** PSTR204.24/LL37

**Topic:** J.02. Systems Biology and Bioinformatics

**Title:** Resolving neuronal diversity and cellular microenvironments from archive to atlas: Segmentation-free, unbiased transcriptome-scale profiling of FFPE mouse cortex at single-cell resolution

**Authors: *C. R. UYTINGCO**[1], A. BARRETT[1], A. SAPRE[2], A. SALVINO[2], G. GALLARETA OLIVARES[2], V. TRAN[2], J. PANGALLO[2], C. XIA[1], J. WILHELMY[1], C. DODATI[1], J. SAKKOS[1], A. SHAHRAVAN[1], D. KOOL[1], W. WANG[1], S. KHARE[1], B. BELL[1], C. CHANG[1], C. ROCO[2], A. ROSENBERG[2], A. FARMER[1];
[1]Takara Bio USA, San Jose, CA; [2]Parse Biosci., Seattle, WA

**Abstract:** Mapping the cellular architecture of the brain at single-cell resolution demands spatial transcriptomic tools that are sensitive, accessible, and compatible with archival tissues. Most platforms require complex segmentation pipelines, proprietary instrumentation, or fresh-frozen samples that limit adoption and obscure the full diversity of cell-type classification. Furthermore, existing FFPE-compatible approaches rely on probe-based profiling methods, fundamentally restricting transcriptome coverage and discovery potential. To address these limitations, we present Trekker™, a next-generation single-cell spatial transcriptomics platform delivering unbiased whole transcriptome spatial resolution with the simplicity of standard single-nucleus RNA sequencing (snRNA-seq), powered by the Parse Biosciences Evercode™ WT FFPE combinatorial barcoding chemistry. Building on a spatial tagging approach pioneered by Russell et al. (2023), Trekker spatially indexes nuclei directly within intact FFPE tissues and supports same-section H&E staining for direct histological correlation. The workflow requires no specialized instrumentation and seamlessly integrates with established snRNA-seq protocols, eliminating the need for cell segmentation, spot deconvolution, spatial binning, and specialized bioinformatics pipelines. Applied to FFPE mouse cortex, Trekker with Evercode WT FFPE generated high-resolution spatial maps of excitatory and inhibitory neurons, astrocytes, oligodendrocytes, microglia, vascular cells, and other rare subtypes. Beyond cell-type mapping, the single-cell spatial resolution enabled characterization of cellular microenvironments, revealing layer-specific associations between neuronal and glial cells reflecting the structural organization of cortical circuitry. Same-section H&E staining further allowed spatially resolved gene expression to be correlated directly with cytoarchitectural landmarks, bridging molecular and histological characterization in a single workflow. Together, Trekker — powered by Evercode WT FFPE — is a uniquely accessible and unbiased spatial transcriptomics platform for mapping the nervous system across archival tissues, atlas construction, and disease characterization, without dedicated hardware, computational expertise, or probe-panel limitations.

**Disclosures: C.R. Uytingco:** A. Employment/Salary (full or part-time):; Takara Bio USA. **A. Barrett:** A. Employment/Salary (full or part-time):; Takara Bio USA. **A. Sapre:** A. Employment/Salary (full or part-time):; Parse Biosciences. **A. Salvino:** A. Employment/Salary (full or part-time):; Parse Biosciences. **G. Gallareta Olivares:** A. Employment/Salary (full or part-time):; Parse Biosciences. **V. Tran:** A. Employment/Salary (full or part-time):; Parse Biosciences. **J. Pangallo:** A. Employment/Salary (full or part-time):; Parse Biosciences. **C. Xia:** A. Employment/Salary (full or part-time):; Takara Bio USA. **J. Wilhelmy:** A.

Employment/Salary (full or part-time):; Takara Bio USA. **C. Dodati:** A. Employment/Salary (full or part-time):; Takara Bio USA. **J. Sakkos:** A. Employment/Salary (full or part-time):; Takara Bio USA. **A. Shahravan:** A. Employment/Salary (full or part-time):; Takara Bio USA. **D. Kool:** A. Employment/Salary (full or part-time):; Takara Bio USA. **W. Wang:** A. Employment/Salary (full or part-time):; Takara Bio USA. **S. Khare:** A. Employment/Salary (full or part-time):; Takara Bio USA. **B. Bell:** A. Employment/Salary (full or part-time):; Takara Bio USA. **C. Chang:** A. Employment/Salary (full or part-time):; Takara Bio USA. **C. Roco:** A. Employment/Salary (full or part-time):; Parse Biosciences. **A. Rosenberg:** A. Employment/Salary (full or part-time):; Parse Biosciences. **A. Farmer:** A. Employment/Salary (full or part-time):; Takara Bio USA.

**Poster**

**PSTR204: Multi-Omics**

**Location:** WCC Halls A-C

**Time:** Monday, November 16, 2026, 1:00 PM - 5:00 PM

**Program #/Poster #:** PSTR204.25/LL38

**Topic:** J.02. Systems Biology and Bioinformatics

**Support:** Cure Alzheimer's Fund
Alzheimer's association fund

**Title:** Operon: Democratizing Multi-Omic Analysis with AI

**Authors: *V. SWARUP**;
Univ. of California, Irvine, Irvine, CA

**Abstract:** Multi-omic technologies such as single-nucleus RNA-seq (snRNA-seq), snATAC-seq, spatial transcriptomics, and proteomics now enable cell-type-resolved interrogation of brain tissue in health and disease. Yet the computational expertise required to analyze these datasets remains a critical bottleneck. Most neuroscience labs lack dedicated bioinformatics support, and trainees face a steep learning curve before they can independently analyze their own data, concentrating analytical power in a few specialized groups and slowing discovery across the field.We developed Operon (swaruplab.bio.uci.edu/operon), an open-source, AI-powered desktop application that pairs an autonomous AI agent for multi-step computational analyses with a visual workspace for navigating files, editing code, and monitoring jobs. Operon offers three modes. Agent runs end-to-end autonomous execution, Plan provides step-by-step review designed for trainee learning and Ask supports literature-grounded Q&A with integrated PubMed search. It ships with over 180 curated protocols spanning snRNA-seq, snATAC-seq, spatial transcriptomics, GWAS fine-mapping, proteomics, and multi-omic integration, encoding best practices for quality control, cell-type annotation, differential expression, and regulatory network inference. Operon connects directly to institutional HPC clusters via SLURM and natively recognizes genomic file formats (FASTQ, BAM, VCF, h5ad).Operon is already in use by researchers at multiple institutions, including UC Irvine, UCLA, Harvard, and the University of Pennsylvania. It enables neuroscientists with no programming experience to run complete

multi-omic workflows using natural language, from raw data to publication-quality visualization, while Plan mode supports trainee learning by surfacing each analytical decision before execution. By lowering technical barriers and embedding reproducible best practices, Operon empowers the next generation of neuroscience genomics researchers across a rapidly expanding data landscape.

**Disclosures: V. Swarup:** None.

**Poster**

**PSTR205: Sensors and Probes**

**Location:** WCC Halls A-C

**Time:** Monday, November 16, 2026, 1:00 PM - 5:00 PM

**Program #/Poster #:** PSTR205.01/LL39

**Topic:** J.01. Molecular, Biochemical, and Genetic Techniques

**Support:** National Natural Science Foundation of China (32525003)
New Cornerstone Investigator Program
National Key R&D Program of China (2021YFF0502904)
NIH BRAIN Initiative (1U01NS120824)

**Title:** A chemigenetic far-red norepinephrine sensor for in vivo multiplex imaging

**Authors: *Y. CUI**[1], Y. ZHENG[1], H. DONG[1], S. XIE[1], L. WANG[1], J. HU[1], T. PATRIARCHI[2], Y. ZHAO[1], J. FENG[1], Y. LI[1];
[1]Peking Univ., Beijing, China; [2]Inst. of Pharmacol. and Toxicology, Univ. of Zurich, Zurich, Switzerland

**Abstract:** Norepinephrine (NE) is a key neuromodulator in the mammalian nervous system and interacts extensively with other neuromodulatory systems. Elucidating these interactions requires simultaneous monitoring of NE and other neurochemicals within the same brain region, creating a need for developing an NE sensor that is spectrally compatible with established green and red sensors. However, conventional far-red fluorescent proteins are often limited by low brightness, restricting their utility for *in vivo* applications, whereas synthetic fluorophores provide substantially brighter far-red fluorescence. Here, we developed a chemigenetic far-red NE sensor by integrating the G protein-coupled receptor activation-based (GRAB) strategy with a circularly permuted HaloTag (cpHaloTag), namely HaloNE1.0. We demonstrate that HaloNE1.0 reliably detects endogenous NE release evoked by optogenetic stimulation and during the tail suspension test. In addition, we used HaloNE1.0 for mesoscopic imaging, achieving large-scale recording with high spatiotemporal resolution. Finally, by combining HaloNE1.0 with other genetically encoded neuromodulator sensors and calcium indicators, we achieved six-channel multiplex recording, enabling simultaneous tracking of coordinated neuromodulatory and neuronal activity dynamics across distinct brain states. Collectively, these results establish HaloNE1.0 as a versatile chemigenetic sensor for far-red NE imaging and provide a powerful platform for multiplexed interrogation of neuromodulatory dynamics and neuronal activities *in vivo*.

**Disclosures: Y. Cui:** None. **Y. Zheng:** None. **H. Dong:** None. **S. Xie:** None. **L. Wang:** None. **J. Hu:** None. **T. Patriarchi:** None. **Y. Zhao:** None. **J. Feng:** None. **Y. Li:** None.

**Poster**

**PSTR205: Sensors and Probes**

**Location:** WCC Halls A-C

**Time:** Monday, November 16, 2026, 1:00 PM - 5:00 PM

**Program #/Poster #:** PSTR205.02/LL40

**Topic:**

**Support:** National Natural Science Foundation of China (32525003)
Beijing Municipal Science & Technology Commission (Z220009)
NIH BRAIN Initiative (1U01NS120824)
New Cornerstone Science Foundation through the New Cornerstone Investigator Program

**Title:** Development of a near-infrared chemigenetic dopamine sensor for multiplex imaging in vivo

**Authors: *E. JI**[1], S. FU[2], Y. ZHENG[2], Y. LI[3];
[1]Sch. of Life Sciences, Peking Univ., Beijing, China; [2]Sch. of Life Sci., [3]Sch. of life sciences, Peking Univ., Beijing, China

**Abstract:** The brain comprises tens of billions of neurons that communicate primarily through neurotransmitters and neuromodulators. Dopamine (DA), one of the most important neuromodulators, plays a pivotal role in learning, reward, motivation, and motor control. Its actions are tightly coordinated with other neurochemicals and involve complex integration of downstream signaling pathways. To systematically decipher these dynamic interactions and functions, there is an urgent need for tools that can monitor multiple neurochemicals simultaneously *in vivo*. To address this challenge, we expanded the spectral range of sensors and developed a near-infrared (NIR) GRAB sensor, $GRAB_{TMP\text{-}DA1.0}$ (TMP-DA1.0 for short). This sensor integrates the G protein-coupled receptor activation-based (GRAB) strategy with a circularly permuted TMP-tag (cpTMP-tag) based chemigenetic approach. Upon labeling with a NIR dye, TMP-DA1.0 exhibits high sensitivity to DA, with emission above 700 nm. Critically, it is spectrally orthogonal to existing green, red, and far-red neurochemical sensors, enabling multiplex imaging and simultaneous real-time monitoring of the dynamics of up to four distinct neurochemicals in freely moving animals. This platform is highly tunable and can be readily extended to create a family of NIR sensors for other neuromodulators, including norepinephrine (NE) and oxytocin (OT). Moreover, these sensors display substantial fluorescence-lifetime changes upon ligand binding, offering strong potential for real-time, quantitative measurement of neuromodulator dynamics independent of intensity-based artifacts.

**Disclosures: E. Ji:** None. **S. Fu:** None. **Y. Zheng:** None. **Y. Li:** None.

**Poster**

**PSTR205: Sensors and Probes**

**Location:** WCC Halls A-C

**Time:** Monday, November 16, 2026, 1:00 PM - 5:00 PM

**Program #/Poster #:** PSTR205.03/LL41

**Topic:**

**Support:** NIH BRAIN Initiative 1U01NS120824
National Key R&D Program of China 2023YFE0207100
National Natural Science Foundation of China (32525003)

**Title:** Improved green and red GRAB sensors for monitoring acetylcholine dynamics in vivo

**Authors: *S. XIE**[1], X. MIAO[4], G. LI[5], Y. ZHENG[1], J. FENG[2], Y. LI[3];
[2]Sch. of Life Sci., [3]Sch. of life sciences, [1]Peking Univ., Beijing, China; [4]Dept. of Anesthesiology, Beijing Chaoyang Hosp., Beijing, China; [5]Peking Univ. Chengdu Acad. for Advanced Interdisciplinary Biotechnologies, Chengdu, China

**Abstract:** The neurotransmitter acetylcholine (ACh) is essential in both the central and peripheral nervous systems. Recent studies highlight the significance of interactions between ACh and various neuromodulators in regulating complex behaviors. The ability to simultaneously image ACh and other neuromodulators can provide valuable information regarding the mechanisms underlying these behaviors. Here we developed and optimized a series of green and red fluorescent G-protein-coupled receptor activation-based ACh ($GRAB_{ACh}$) sensors, featuring improved sensitivity, expanded detection range and diverse spectral profiles for monitoring acetylcholine release. These includes the green variants gACh4h, gACh4m, and gACh4l, and the red-shifted sensors rACh1h, rACh1m, and rACh1l. The high-affinity sensors, gACh4h and rACh1h, reliably detect ACh release in various brain regions, including amygdala, hippocampus, and cortex. Moreover, rACh1h can be co-expressed with green fluorescent sensors to record ACh release together with other neurochemicals in various behavioral contexts using fiber photometry, mesoscopic imaging and two-photon imaging, with high spatiotemporal resolution. In summary, these new green and red fluorescent ACh sensors significantly expand our ability to monitor ACh release with high sensitivity and spatiotemporal resolution. Moreover, their wide detection range and spectral compatibility with other fluorescent sensors provide a powerful set of tools for deciphering the complexity of the cholinergic system.

**Disclosures: S. Xie:** None. **X. Miao:** None. **G. Li:** None. **Y. Zheng:** None. **J. Feng:** None. **Y. Li:** None.

**Poster**

**PSTR205: Sensors and Probes**

**Location:** WCC Halls A-C

**Time:** Monday, November 16, 2026, 1:00 PM - 5:00 PM

**Program #/Poster #:** PSTR205.04/LL42

**Topic:** J.01. Molecular, Biochemical, and Genetic Techniques

**Support:** Beijing Municipal Science & Technology Commission (Z220009)
New Cornerstone Investigator Program
NIH BRAIN Initiative (1U01NS120824)

**Title:** Quantitative acetylcholine detection with a novel chemigenetic lifetime-based sensor

**Authors: *X. JING**[1], Z. WANG[1], H. R. FARRANTS[3], E. R. SCHREITER[3], S. XIE[1], Y. LI[2];
[2]Sch. of life sciences, [1]Peking Univ., Beijing, China; [3]Janelia Res. Campus, HHMI, Ashburn, VA

**Abstract:** Acetylcholine (ACh) is a key neurotransmitter involved in many physiological and pathological processes. To understand the complex functions of acetylcholine in different conditions, it is important to measure acetylcholine levels quantitatively. Based on the GRAB (GPCR Activation Based) strategy, our lab has previously developed a series of green and red fluorescent acetylcholine sensors ($GRAB_{ACh}$ sensors). However, intensity-based fluorescent sensors can pose challenges for quantitative imaging due to intensity-related artifacts. To address this limitation, we developed a new chemigenetic lifetime-based sensor, GRAB-WHalo-ACh-1.0, using circularly permutated WHaloTag (HaloTag with a tryptophan mutation) for quantitative detection of acetylcholine. Fluorescence lifetime is an intrinsic property of fluorophores that is independent of fluorophore concentration and excitation power, enabling robust quantitative imaging with high spatiotemporal resolution. The chemigenetic strategy enables the use of synthetic fluorophores that exhibit superior brightness and red-shifted spectra compared to traditional fluorescent proteins, providing the flexibility for deep-tissue and multiplex imaging. In this study, we demonstrate that GRAB-WHalo-ACh-1.0 is capable of detecting ACh dynamics with high sensitivity and quantifying ACh concentrations across a physiological range in cultured cell lines and cultured primary neurons. Moreover, our *in vivo* data confirm its ability to detect real-time ACh dynamics in behaving mice. Importantly, GRAB-WHalo-ACh-1.0 maintains affinity and dynamic range across different systems, providing a powerful new tool for ACh quantification in the brain.

**Disclosures: X. Jing:** None. **Z. Wang:** None. **H.R. Farrants:** None. **E.R. Schreiter:** None. **S. Xie:** None. **Y. Li:** None.

**Poster**

**PSTR205: Sensors and Probes**

**Location:** WCC Halls A-C

**Time:** Monday, November 16, 2026, 1:00 PM - 5:00 PM

**Program #/Poster #:** PSTR205.05/LL43

**Topic:** J.01. Molecular, Biochemical, and Genetic Techniques

**Support:** NIMH RF1MH130391

**Title:** High-Throughput Engineering of Genetically Encoded μ-Opioid Sensors with Enhanced Sensitivity and Neuronal Expression for Detecting Opioids in vivo

**Authors: *Y. WANG**[1], L. TORP[2], S. WAIT[3], M. LOVELESS[1], A. SUKO[4], J. H. LEE[5], M. R. BRUCHAS[6], M. E. SODEN[7], A. BERNDT[2];
[2]Bioengineering, [3]Mol. Engin., [1]Univ. of Washington, Seattle, WA; [5]Bioengineering, [4]Univ. of Washington, Kirkland, WA; [6]Dept. of Anesthesiol. and Pain Med., [7]Pharmacol., Univ. of Washington, Seattle, WA

**Abstract:** The μ-opioid receptor (MOR) regulates diverse physiological processes including analgesia, reward, stress responses, and affective signaling through endogenous opioid peptides. However, directly monitoring MOR activation in living systems remains challenging. Genetically Encoded Fluorescent Indicators (GEFIs) provide a powerful strategy for real-time visualization of receptor activity, but optimizing sensor performance requires balancing fluorescence dynamic range, ligand sensitivity, and pharmacological properties. Using iterative sensor engineering approaches, we developed successive generations of MOR-based fluorescent sensors with progressively improved performance. Previously developed μMASS1.5 and μMASS1.7 were designed to enhance fluorescence output and exhibited substantially increased dynamic range relative to μMASS1.0. Across multiple opioid ligands, these sensors produced approximately 1.5-3-fold greater maximal fluorescence responses, with μMASS1.7 showing particularly strong signal enhancement toward ligands including met-enkephalin, leu-enkephalin, dynorphin, and fentanyl in mammalian cells. Building upon these advances, we developed μMASS2.0, a next-generation sensor optimized for improved pharmacological performance, with particular emphasis on endogenous ligand sensitivity and receptor response characteristics. Functional characterization revealed refined EC50 profiles across multiple opioid peptides. μMASS2.0 demonstrated improved sensitivity toward met-enkephalin and leu-enkephalin, exhibiting EC50 values of approximately 72 nM and 230 nM, respectively. Robust responses were also maintained toward additional endogenous ligands including β-endorphin and dynorphin, supporting improved pharmacological tuning for endogenous opioid sensing. Together, these studies establish a progressive engineering framework in which distinct μMASS generations independently optimize fluorescence performance and receptor pharmacology. To further accelerate biosensor discovery and optimization, we developed Opto-MASS, a high-throughput screening platform enabling functional evaluation and selection of genetically encoded sensor libraries. By integrating iterative engineering with scalable screening approaches, this platform provides a versatile toolkit for investigating endogenous opioid signaling and advancing next-generation genetically encoded biosensor development in cellular, neuronal, and in vivo systems.

**Disclosures: Y. Wang:** None. **L. Torp:** None. **S. Wait:** None. **M. Loveless:** None. **A. Suko:** None. **J.H. Lee:** None. **M.R. Bruchas:** None. **M.E. Soden:** None. **A. Berndt:** None.

**Poster**

**PSTR205: Sensors and Probes**

**Location:** WCC Halls A-C

**Time:** Monday, November 16, 2026, 1:00 PM - 5:00 PM

**Program #/Poster #:** PSTR205.06/LL44

**Topic:** J.01. Molecular, Biochemical, and Genetic Techniques

**Support:** NIH UM1MH138543

**Title:** Machine Learning-Guided Optimization of Red Fluorescent Protein-Based Genetically Encoded Calcium Indicators for in vivo Imaging

**Authors:** ***S. LI**[1], S. WAIT[2], C. K. KIM[3], H. DANA[4], A. BERNDT[1];
[1]Dept. of Bioengineering, [2]Mol. Engin., Univ. of Washington, Seattle, WA; [3]Princeton Neurosci. Inst., Princeton Univ., Princeton, NJ; [4]Dept. of Neurosciences, Cleveland Clin. Res., Cleveland, OH

**Abstract:** Red fluorescent genetically encoded calcium indicators (GECIs) are important tools for monitoring calcium dynamics in living cells, especially in experiments requiring spectral separation from green reporters or compatibility with blue-light activated opsins. However, most current red GECIs are limited by low baseline fluorescence, slow kinetics, and poor photostability, which reduce their utility in deep brain regions. Additionally, the engineering process remains a time- and resource-intensive challenge due to the vast sequence space of possible protein variants. To address these challenges, we adapted ProteiML (Wait et al. 2024), an ensemble machine learning framework developed in the Berndt Lab, to predict mutation-dependent changes in red GECI performance and prioritize candidate variants for experimental testing. By introducing gain-of-function mutations into jRGECO1a and systematically evaluating in HEK293 cells, iPSC-derived cardiomyocytes, and primary cultured neurons, we identified multiple variants with improved performance. These variants reliably detected single action potentials in neurons and spontaneous calcium transients in cardiomyocytes. Among these, we observed distinct functional improvements: one variant exhibited a 1.75-fold increase in dynamic range while maintaining baseline fluorescence comparable to the parental construct, another showed enhanced calcium sensitivity with an EC50 of 134 nM in purified protein assays, and the third one displayed faster kinetics across multiple experimental contexts. These improvements were further validated by in vivo imaging. Additionally, by transferring ProteiML-predicted mutations to related red GECI scaffolds generally improved indicator kinetics and dynamic range, demonstrating the broader utility of this optimization strategy. Together, our results demonstrate that machine learning-guided protein engineering can accelerate the optimization of red GECIs by efficiently prioritizing functional variants for validation. This approach reduces the experimental burden of navigating large protein sequence spaces and provides a scalable strategy for developing improved fluorescent biosensors for neuroscience, genetics, and bioengineering applications.

**Disclosures: S. Li:** None. **S. Wait:** None. **C.K. Kim:** None. **H. Dana:** None. **A. Berndt:** None.

**Poster**

**PSTR205: Sensors and Probes**

**Location:** WCC Halls A-C

**Time:** Monday, November 16, 2026, 1:00 PM - 5:00 PM

**Program #/Poster #:** PSTR205.07/LL45

**Topic:** J.01. Molecular, Biochemical, and Genetic Techniques

**Support:** 1F31DA064352-01
R01GM139850-01
U01NS128537

**Title:** Engineering genetically encoded fluorescent opioid sensors for characterizing fentanyl and exogenous opioid pharmacology in vivo

**Authors: *L. TORP**[1], Y. WANG[1], H. ZHANG[8], K. S. GIRVEN[2], A. SUKO[3], J. H. LEE[4], M. E. SODEN[5], B. LI[9], M. R. BRUCHAS[6], A. BERNDT[7];
[2]Anesthesiol. and Pain Med., [1]Univ. of Washington, Seattle, WA; [4]Bioengineering, [3]Univ. of Washington, Kirkland, WA; [5]Pharmacol., [6]Dept. of Anesthesiol. and Pain Med., [7]Bioengineering, Univ. of Washington, Seattle, WA; [8]Cold Spring Harbor Lab., Cold Spring Harbor, NY; [9]Westlake Univ., Hangzhou, China

**Abstract:** Opioid-based analgesics are the most widely used treatments for chronic pain. However, opioid use and misuse have resulted in a national overdose crisis fueled by untreated opioid use disorder (OUD). Within the past decade, fentanyl has infiltrated the drug supply, leading to a rise in OUD cases and opioid overdose deaths. Fentanyl is a potent synthetic opioid and, like other exogenous opioids, binds to the μ-opioid receptor (μOR), a G protein-coupled receptor. The μOR is expressed throughout many subcortical brain regions and regulates pain perception, reward, stress, and emotion. However, the pharmacological and spatiotemporal profile of fentanyl distribution in the brain is currently poorly understood. Traditional tools to monitor opioid accumulation in the brain often fall short in terms of sensitivity, specificity, and real-time kinetics. To address this need, the Berndt Lab developed μMASS, a genetically encoded μOR-based sensor that couples real-time opioid detection to an increased fluorescence response. However, μMASS detects both endogenous and exogenous opioids, making it difficult to discern the presence of specific ligands. We hypothesized this was due to μMASS recapitulating the native μOR's promiscuous ligand binding. As a solution, we tested whether structural analysis of μMASS-fentanyl binding may elucidate residues within the binding pocket governing specificity. We generated AlphaFold2 μMASS models and docked fentanyl using AutoDock4, and observed fentanyl did not maintain a critically conserved salt bridge in the opioid binding pocket. Introducing mutations in this region rendered μMASS specific only for fentanyl while greatly reducing affinity for endogenous opioid peptides, and we dubbed this sensor FentSense1.0. This tool detects fentanyl *in vitro* in HEK293 cells and primary cortical neurons with nanomolar affinity. The fluorescence signal is rapid and reverses upon application of μOR antagonist naloxone. To enhance FentSense1.0 signal we introduced μOR receptors from alternative species. This resulted in FentSense1.7, which demonstrated increased dynamic range while maintaining fentanyl specificity. In vivo experiments in the OFC of WT female mice revealed FentSense1.7 displays a dose dependent response to IP fentanyl injections. Additionally, in the CeA of WT male mice, FentSense1.7 rapidly detects IV infused fentanyl, and does not respond to morphine or naloxone infusions. Future in vivo experiments can determine fentanyl pharmokinetics in the brain during various stages of fentanyl use to link real-time pharmacology measurements to behavioral phenotypes in freely behaving animals.

**Disclosures: L. Torp:** None. **Y. Wang:** None. **H. Zhang:** None. **K.S. Girven:** None. **A. Suko:** None. **J.H. Lee:** None. **M.E. Soden:** None. **B. Li:** None. **M.R. Bruchas:** None. **A. Berndt:** None.

**Poster**

**PSTR205: Sensors and Probes**

**Location:** WCC Halls A-C

**Time:** Monday, November 16, 2026, 1:00 PM - 5:00 PM

**Program #/Poster #:** PSTR205.08/LL46

**Topic:** J.01. Molecular, Biochemical, and Genetic Techniques

**Support:** Intramural Research Program of the National Institutes of Health (NIH)

**Title:** Split intein-mediated AAV delivery of an oversized fluorescence lifetime cAMP biosensor for monitoring intracellular signaling in freely behaving mice

**Authors: *J. LEE**[1], H. L. PUHL, III[2], M. H. SHAH[3], A. HOLDER[3], N. SHARMA[3], D. M. LOVINGER[3];
[1]NIAAA, [2]Lab. of Biophotonics and Quantum Biol., [3]NIH, Rockville, MD

**Abstract:** Genetically encoded fluorescent biosensors enable cell-type-specific measurements of intracellular signaling in vivo. While fluorescence intensity-based sensors are widely used in neuroscience, Förster resonance energy transfer (FRET)-based biosensors offer modular architectures and absolute measurement of fluorescence lifetime that are independent of optical systems. However, many FRET biosensors exceed the ~4.7 kb packaging limit of adeno-associated virus (AAV), restricting their in vivo application.To overcome this limitation, we developed a split intein-mediated protein reconstitution strategy for AAV delivery of oversized biosensors. Using an EPAC-based cAMP sensor as a model, we engineered a fluorescence lifetime biosensor (G-Champ) consisting of mNeonGreen and mCherry fluorophores flanking an EPAC1-derived sensing domain. Structural analysis identified a flexible linker region suitable for splitting the biosensor into two fragments, each packaged into a separate AAV vector. Following co-expression, split inteins catalyzed efficient reconstitution of the full-length biosensor. Reconstitution was confirmed by fluorescence imaging and electrophoresis, and sensor functionality was validated in HEK293 cells using pharmacological and receptor-mediated cAMP stimulation.Both biosensor fragments were subsequently delivered to mouse striatum using AAVs. Fluorescence lifetime fiber photometry in freely moving mice revealed robust cAMP increases in D1 receptor-expressing medium spiny neurons (MSNs) following D1 receptor agonist administration and cocaine exposure. Antagonist pretreatment blocked both behavioral and cAMP responses, confirming receptor specificity. During Pavlovian conditioning, cue presentation evoked cAMP elevations in nucleus accumbens D1-MSNs and unexpectedly revealed rapid cAMP transients in dorsolateral striatal D1-MSNs. Long-term recordings in D2-MSNs demonstrated correlations between cAMP levels, locomotor activity, and circadian state over 24-hour periods. The sensor was also compatible with fiber-bundle fluorescence lifetime imaging, enabling single-cell measurements in freely behaving animals.These results establish

split intein-mediated biosensor reconstitution as a general strategy for overcoming AAV packaging constraints and expanding the use of quantitative fluorescence lifetime biosensors for in vivo neuroscience.

**Disclosures: J. Lee:** None. **H.L. Puhl:** None. **M.H. Shah:** None. **A. Holder:** None. **N. Sharma:** None. **D.M. Lovinger:** None.

**Poster**

**PSTR205: Sensors and Probes**

**Location:** WCC Halls A-C

**Time:** Monday, November 16, 2026, 1:00 PM - 5:00 PM

**Program #/Poster #:** PSTR205.09/LL47

**Topic:** J.01. Molecular, Biochemical, and Genetic Techniques

**Title:** Development of an Optical Biosensor for Measuring GPR88 Activation

**Authors: *S. BARANWAL**, E. MATTHIESSEN, P. DONTHAMSETTI;
Pharmacol., Vanderbilt Univ., Nashville, TN

**Abstract:** G protein coupled receptors (GPCRs) represent the largest superfamily of membrane proteins (>800 members) and are targeted by ~35% of clinically approved drugs. Among these receptors, GPR88 has gained considerable attention due to its near exclusive expression in the striatum, a brain structure that plays key roles in diverse central nervous system disorders (addiction, schizophrenia, Parkinson's Disease). Recent pharmacological and genetic studies indicate that GPR88 can regulate striatum-associated behaviors (motor control, reward processing, and learning). However, GPR88 is a member of a subset of GPCRs called orphan receptors, for which no endogenous ligand has been identified. Thus, little is known about the relationship between the activation dynamics of GPR88 and its corresponding role in behavior, limiting our understanding of the biological role and clinical potential of this receptor due to the lack of tools for monitoring its activity in living systems. To address this problem, we are developing a novel optical biosensor to measure changes in GPR88 activation *in vivo*. Prior structural studies indicate that upon activation, GPR88 undergoes a conformational change wherein its transmembrane segments 5 and 6 (TM5 and TM6) move apart, allowing signaling proteins to bind the receptor. Using a structure-guided analysis of GPR88, we replaced the third intracellular loop that connects TM5 and TM6 with the environmentally sensitive fluorophore circularly permutated green fluorescent protein (cpGFP). In proof-of-concept studies, the synthetic positive allosteric modulator 2-PCCA induces a change in the fluorescence of a GPR88-cpGFP prototype, confirming that this biosensor functions as intended. To enhance the dynamic range, we generated variants with randomized linkers flanking the cpGFP insertion site in GPR88 and screened their function using a novel high-throughput plate-reader based assay. Further validation using confocal microscopy indicated that GPR88-cpGFP can detect dynamic changes in GPR88 activity. This screen identified an optimized sensor exhibiting a ~30% decrease in fluorescence following 2-PCCA treatment. These findings establish the first genetically encoded fluorescent biosensor for GPR88 and provide a platform for investigating

GPR88 signaling in live animals. This approach may also facilitate the discovery of novel GPR88 modulators and provide a template for interrogating other elusive orphan receptors in living animals.

**Disclosures: S. Baranwal:** None. **E. Matthiessen:** None. **P. Donthamsetti:** None.

**Poster**

**PSTR205: Sensors and Probes**

**Location:** WCC Halls A-C

**Time:** Monday, November 16, 2026, 1:00 PM - 5:00 PM

**Program #/Poster #:** PSTR205.10/LL48

**Topic:** J.01. Molecular, Biochemical, and Genetic Techniques

**Support:** Brain Canada Platform Support Grant

**Title:** Real-time detection of NMDA receptor co-agonists D-serine and glycine using genetically encoded fluorescent sensors

**Authors: *R. DALANGIN**[1], B. LEONARDON[4], L. FROUX[2], A.-M. LAUZIER[1], R. MORIN-PELCHAT[5], P. LARQUÉ[9], L. PAQUET[6], A. BARBEAU[1], L.-E. LORENZO[3], Y. DE KONINCK[10], M. DROBIZHEV[11], A. G. GODIN[7], T. NEVIAN[4], J.-P. MOTHET[12], M.-E. PAQUET[8];
[1]CERVO Brain Res. Ctr., Quebec, QC, Canada; [2]CERVO Brain Res. Ctr., Québec, QC, Canada; [3]CERVO Brain Res. Ctr., Quebec City, QC, Canada; [4]Univ. of Bern, Bern, ; [6]Fac. of Sci. and Engin., [5]Univ. Laval, Québec, QC, Canada; [7]Univ. Laval, Quebec City, QC, Canada; [8]Dept. of Anesthesiol. and Intensive Care, Univ. Laval, Quebec, QC, Canada; [9]CERVO- Ctr. for Brain Research, Laval Univ., Quebec, QC, ; [10]Univ. Laval / CERVO Brain Res. Ctr., Quebec, QC, Canada; [11]Montana State Univ., Bozeman, MT, ; [12]Neurodiderot, Univ. Paris Cité, Paris, France

**Abstract:** In the nervous system, N-methyl-D-aspartate (NMDA) receptors are widely recognized as the key receptor for synaptic plasticity and require not just depolarization and glutamate for activation but also one of its two co-agonists, D-serine and glycine. Additionally, D-serine has also been historically considered as a key molecule released by astrocytes, while glycine is the main inhibitory neurotransmitter in the spinal cord, brain stem and cerebellum. Accordingly, aberrations in the signalling of these two molecules have been consistently associated with several pathological conditions, including schizophrenia and developmental disorders. However, despite our understanding of their roles in the nervous system, the molecular mechanisms that govern their dynamics remain unclear, thus, limiting our understanding of their roles in both healthy and disease states. To address these gaps in knowledge, tools with the requisite spatiotemporal resolution, such as genetically encoded indicators, are necessary to monitor D-serine and glycine dynamics. To date, the only genetically encoded indicators for D-serine and glycine are FRET-based indicators, called DserFS and GlyFS, respectively, based on bacterial periplasmic binding proteins (PBPs) that were computationally redesigned to bind their targets. PBPs are ideal scaffolds for sensor engineering because they are orthogonal to neurons,

offer large changes in fluorescence in response to ligand binding, and can be targeted to arbitrary cellular compartments. However, these FRET indicators show limited dynamic range relative to single fluorescent protein-based indicators and require exogenous addition of purified protein for imaging, significantly limiting their potential use. Here we present our work on engineering single fluorescent protein-based indicators for D-serine and glycine. Indeed, our results indicate that our sensors are bright, show large fluorescence changes in response to their targets, and have good membrane localization. We anticipate that our new indicators will open new avenues for investigating D-serine and glycine dynamics within the nervous system.

**Disclosures: R. Dalangin:** None. **R. Morin-Pelchat:** None. **L. Paquet:** None. **L. Lorenzo:** None. **Y. De Koninck:** None. **A.G. Godin:** None. **M. Paquet:** None.

**Poster**

**PSTR205: Sensors and Probes**

**Location:** WCC Halls A-C

**Time:** Monday, November 16, 2026, 1:00 PM - 5:00 PM

**Program #/Poster #:** PSTR205.11/LL49

**Topic:** J.01. Molecular, Biochemical, and Genetic Techniques

**Support:** GR059810

**Title:** Engineering protein-based fluorescent sensors for real-time monitoring of both transient and long-form estrogen dynamics in the brain.

**Authors: *A. MOGHADASI**[1], J. H. LEE[2], B. A. BRIONES[1], V. CHAVAN[1], M. TRZECIAK[1], G. D. STUBER[3], A. BERNDT[4];
[1]Univ. of Washington, Seattle, WA; [2]Bioengineering, Univ. of Washington, Kirkland, WA; [3]Pharmacol., [4]Bioengineering, Univ. of Washington, Seattle, WA

**Abstract:** Neurosteroids like estrogens are synthesized locally and can target the brain from peripheral organs, influencing synaptic plasticity, cognitive processes, and behavior. Despite their significance, tissue- and cell-type-specific studies of steroids in vivo remain challenging due to the absence of tools capable of monitoring steroid levels and dynamics with spatio-temporal resolution. Optical tools enable the detailed characterization of steroid signaling in the brain across different physiological and disease-relevant contexts. Here we present eNOVA, a genetically encoded fluorescent sensor for real-time monitoring of estradiol (E2). In vitro characterization of the sensor in HEK cells demonstrated a 180% fluorescence increase in response to E2 stimulation at saturating concentrations, sensitivity extending to picomolar range, and estrogen specificity. We observed similar biophysical properties when the sensor was expressed in primary rat cortical neurons. Furthermore, we performed stereotactic injection of AAV1-DIO vector containing the sensor into the medial preoptic area of the hypothalamus in Cre-ESR1 mice, where we validated the sensor's compatibility for two-photon ex-vivo imaging and in vivo fiber photometry. We also engineered a sensor variant with improved on- and off-kinetics, enabling the detection of transient and rapid estrogen dynamics.The estrous cycle in

mice spans approximately four days, requiring tools capable of long-term and non-continuous monitoring of E2 fluctuations. To address this, we engineered a ratiometric sensor variant by integrating a red fluorescent protein (RFP) to serve as a reference point. This design enables normalization of signal variation from expression variability, photobleaching, or motion artifacts. Characterization of this variant revealed fluorescence resonance energy transfer (FRET) under blue-light excitation, resulting in E2-dependent signals in both fluorophores. In contrast, direct excitation of RFP provides an E2-insensitive signal that serves as a reliable reference for ratiometric measurements. This variant also exhibits FRET-based fluorescence lifetime change upon E2 binding, enabling high-resolution imaging applications.Ultimately, these sensors offer promising potential for visualizing estrogen signaling in the brain. By enabling the real-time monitoring of estrogen with high spatio-temporal resolution, they also provide a powerful platform for exploring broader biological questions, including the regulatory roles of estrogen in maintaining homeostasis, mediating brain-body communication, and influencing disease progression.

**Disclosures: A. Moghadasi:** E. Ownership Interest (stock, stock options, royalty, receipt of intellectual property rights/patent holder, excluding diversified mutual funds); Inventor on a patent for the sensor design. **J.H. Lee:** E. Ownership Interest (stock, stock options, royalty, receipt of intellectual property rights/patent holder, excluding diversified mutual funds); Inventor on a patent for the sensor design. **B.A. Briones:** None. **V. Chavan:** None. **M. Trzeciak:** None. **G.D. Stuber:** E. Ownership Interest (stock, stock options, royalty, receipt of intellectual property rights/patent holder, excluding diversified mutual funds); Inventor on a patent for the sensor design. **A. Berndt:** E. Ownership Interest (stock, stock options, royalty, receipt of intellectual property rights/patent holder, excluding diversified mutual funds); Inventor on a patent for the sensor design.

**Poster**

**PSTR205: Sensors and Probes**

**Location:** WCC Halls A-C

**Time:** Monday, November 16, 2026, 1:00 PM - 5:00 PM

**Program #/Poster #:** PSTR205.12/LL50

**Topic:** J.04. Physiological Methods

**Support:** Brown OVPR
Carney Institute

**Title:** Optimizing CaBLAM, a new bioluminescent $Ca^{2+}$ indicator, to detect depolarization-induced $Ca^{2+}$ signals in living cells

**Authors: *M. CUNNINGHAM**[1,2], G. LAMBERT[3], U. HOCHGESCHWENDER[5], C. I. MOORE[1], N. C. SHANER[4], A. ANDRADE[2], D. LIPSCOMBE[2,1];
[1]Neurosci., [2]Carney Inst. for Brain Sci., Brown Univ., Providence, RI; [3]Neuroscieces, [4]Neurosciences, Univ. of California San Diego, La Jolla, CA; [5]Neurosci., Central Michigan Univ., MT Pleasant, MI

**Abstract:** Calcium is a ubiquitous intracellular messenger often used to monitor cell activity. The source, location, amplitude, and time course of a $Ca^{2+}$ signal contribute to the cellular response. The most widely used $Ca^{2+}$ indicators are genetically encoded and fluorescence-based, but depending on the specific application, photobleaching, autofluorescence, tissue heating, and phototoxicity can complicate their use. Bioluminescent (BL) $Ca^{2+}$ indicators are advantageous for longitudinal imaging in living cells and in vivo as they do not require excitation light for activation. However, until recently, BL $Ca^{2+}$ indicators have had limited use in living cells because of their low $Ca^{2+}$-dependent signals relative to baseline. CaBLAM is a novel genetically encoded BL $Ca^{2+}$ indicator with substantially improved properties capable of detecting $Ca^{2+}$ signals in neurons and *in vivo* comparable to GCaMP6s. Here we use CaBLAM to visualize voltage-dependent $Ca^{2+}$ signals in tsA201 cells expressing the voltage-gated $Ca_V2.2$ and Kir2.1 ion channels. Kir2.1 lowers the resting membrane potential of tsA201 cells, thereby increasing the number of $Ca_V2.2$ channels available for activation. We compare the ability of CaBLAM to GCaMP6 constructs that are targeted to different subcellular regions to detect high K-induced intracellular $Ca^{2+}$ signals. We compare c-CaBLAM (cytoplasmic), p-CaBLAM (palmitoylated, plasma membrane), voltage-gated calcium channel subunit $\beta_3$-CaBLAM (plasma membrane colocalized with $Ca_V2.2$), and $Ca_V2.2$-CaBLAM. All constructs respond reliably to ionomycin application, and both c-CaBLAM and p-CaBLAM detect rapid $Ca^{2+}$ signals in tsA201 cells expressing $Ca_V2.2$ in response to high K. The time course and signal-to-noise ratios of c-CaBLAM and p-CaBLAM were similar to the equivalent GCaMP6 constructs. To optimize CaBLAM to detect $Ca^{2+}$ signals close to the plasma membrane, we are testing versions of CaBLAM and GCaMP6 that target the plasma membrane and have lower $Ca^{2+}$ binding affinities. Our data expand the utility of CaBLAM as a BL Ca2+ indicator and show that it compares favorably to GCaMP6s in living cells.

**Disclosures: M. Cunningham:** None. **G. Lambert:** None. **U. Hochgeschwender:** None. **C.I. Moore:** None. **N.C. Shaner:** None. **A. Andrade:** None. **D. Lipscombe:** None.

**Poster**

**PSTR205: Sensors and Probes**

**Location:** WCC Halls A-C

**Time:** Monday, November 16, 2026, 1:00 PM - 5:00 PM

**Program #/Poster #:** PSTR205.13/LL51

**Topic:** J.04. Physiological Methods

**Support:** NIH Grant R56NS131373

**Title:** Blood-Brain Barrier Permeable Small Molecule Astrocyte Specific Probes for Imaging

**Authors: *S. SINGH**[1], N. GUNAWARDHANA[2], D. CERVASIO[3], O. HAPUTHANTHRIGE DON[1], X. CHEN[4], S.-J. TANG[5], S. T. LAUGHLIN[1];
[1]Chem., Stony Brook Univ., Stony Brook, NY; [2]Chem., Stony Brook Univ., East Setauket, NY; [3]Stony Brook Univ., Stony Brook, NY; [4]Stony Brook Univ. Pain and Analgesia Res. Ctr. (SPARC), Saint James, NY; [5]Anesthesiol., SUNY Stony Brook Univ., Stony Brook, NY

**Abstract:** Astrocytes, closely associated with neuronal cell bodies, axons, blood vessels, and other glial cells, play a vital role in central nervous system development and maintenance. Recent evidence linking astrocyte dysfunction to neurodegenerative diseases underscores the importance of studying these cells and their interactions with neurons and other glial cells. This necessitates the development of cell-specific, non-toxic, and blood-brain barrier (BBB) permeable imaging probes. By leveraging synthetic chemistry, we developed a library of astrocyte specific cationic fluorophores by incorporating methyl pyridinium targeting moiety. This targeting moiety facilitates the delivery of these small molecules through the organic cation transporter into the astrocytes *in vitro* (in primary cells and mouse spinal cord slices) and *in vivo* (in zebrafish). We achieved robust labeling at low concentrations and with short incubation times. We further characterized their BBB permeability and demonstrated their subcellular localization to mitochondria. This new class of small molecules exhibits astrocyte specificity, enhanced photostability and increased brightness across multiple wavelengths, enabling their utility for imaging applications. These advancements can provide new opportunities to study astrocyte function and development in the brain.

**Disclosures: S. Singh:** None. **N. Gunawardhana:** None. **D. Cervasio:** None. **O. Haputhanthrige Don:** None. **X. Chen:** None. **S. Tang:** None. **S.T. Laughlin:** None.

**Poster**

**PSTR205: Sensors and Probes**

**Location:** WCC Halls A-C

**Time:** Monday, November 16, 2026, 1:00 PM - 5:00 PM

**Program #/Poster #:** PSTR205.14/LL52

**Topic:** J.04. Physiological Methods

**Support:** McCamish Parkinson's Disease Innovation Program Blue Sky Seed Grant
Burroughs Wellcome Fund Career Award at the Scientific Interface
David and Lucile Packard Foundation Fellowship
Sloan Foundation Fellowship

**Title:** An optogenetics-compatible red fluorescent calcium indicator with negligible blue light photoactivation

**Authors:** X. ZHANG[1], B. ADDISON[2], E. ULUTAS[6], C. DENG[3], S. DOSHI[4], S. NABHAN[5], A. J. EMANUEL[7], J. E. MARKOWITZ[6], ***D. KOVEAL**[8];
[1]Emory Univ. Sch. of Med. Neurosci. Grad. Program, Atlanta, GA; [2]Georgia Inst. of Technol., Atlanta, GA; [3]Georgia Inst. of Technol., Chicago, IL; [4]Georgia Inst. of Technol., Louisville, KY; [5]Georgia Inst. of Technol., Austin, TX; [6]Biomed. Engin., Georgia Tech. and Emory, Atlanta, GA; [7]Cell Biol., Emory Univ. Sch. of Med., Atlanta, GA; [8]Emory Univ. Sch. of Med., Decatur, GA

**Abstract:** Red genetically encoded calcium indicators (GECIs) are important tools for live cell and in vivo imaging. However, their application in optogenetic experiments has been limited by

their complex photophysics, which can yield blue-light-induced artifacts. These photophysical drawbacks arise from the fluorescent protein used to construct the GECI. To address these limitations, we engineered novel red GECIs based on photostable red FPs, including mScarlet variants. After testing multiple design topologies and screening for calcium responses, we identified a lead variant, named ScaRCaMP-1.0. ScaRCaMP-1.0 exhibits moderate Ca2+ responses (DF/F0 = -13%) relative to other red GECIs, a tradeoff that has enabled remarkable blue light photostability at power densities exceeding 200 mW/mm2. We validated the performance of ScaRCaMP-1.0 in an optogenetic regime in cells, and in vivo in mice via fiber photometry. Finally, guided by structural predictions, we identified a pair of lysine residues on the surface of the fluorescent protein that are important for controlling Ca2+ responses. Mutation of one residue (K132Y) notably increased the response size (DF/F0 = -22%) without compromising blue light photostability. We call the improved variant ScaRCaMP-2.0. Taken together, these results establish ScaRCaMP as an optogenetics-compatible red GECI and demonstrate the potential of mScarlet-based fluorophores as a basis for generating photostable red biosensors.

**Disclosures: X. Zhang:** None. **B. Addison:** None. **E. Ulutas:** None. **C. Deng:** None. **S. Doshi:** None. **S. Nabhan:** None. **A.J. Emanuel:** None. **J.E. Markowitz:** None. **D. Koveal:** None.

**Poster**

**PSTR205: Sensors and Probes**

**Location:** WCC Halls A-C

**Time:** Monday, November 16, 2026, 1:00 PM - 5:00 PM

**Program #/Poster #:** PSTR205.15/LL53

**Topic:** J.01. Molecular, Biochemical, and Genetic Techniques

**Support:** NIH Grant UM1 MH136462

**Title:** Multiplexing novel genetically encoded indicators to simultaneously measure time-resolved absolute norepinephrine and high-fidelity GABAergic transients

**Authors: *Y.-S. WANG**, Y. HUA, A. ANDREONI, L. TIAN;
Max Planck Florida Inst. for Neurosci., Jupiter, FL

**Abstract:** Norepinephrine (NE) and inhibitory neurotransmitters like GABA coordinate complex brain functions, including arousal and sensory processing. Biologically, tonic NE release sets baseline arousal and engages transmodal associative cortical areas, whereas phasic NE bursts bias networks toward lower-level sensory processing. Theoretically, NE is proposed to regulate the exploration-exploitation balance, signaling unexpected uncertainty to act as a network reset during environmental state changes. This noradrenergic activity heavily modulates the thalamocortical pathway, distinctly gating interneuron excitability across different cortical areas. However, determining exactly how phasic NE transients regulate local GABA release relative to different baseline tonic NE levels remains a major technical challenge. To address this, we engineered two novel genetically encoded indicators. First, we developed a red-shifted, time-

resolved NE sensor that utilizes fluorescence lifetime to enable absolute concentration measurement independent of photobleaching or concentration artifacts. Second, we engineered a high-sensitivity GABA indicator exhibiting a markedly superior dynamic range compared to iGABASnFR2. Simultaneous imaging of these multiplexed sensors allows us to capture high-fidelity GABAergic transients alongside precise, absolute NE concentrations. This quantitative approach provides a robust framework to test computational predictions at the microcircuit level, dissecting how tonic and phasic NE signals differentially gate thalamocortical sensory inputs via local inhibitory interneurons. Finally, this will reveal the underlying principles governing how neuromodulators dynamically coregulate brain state and sensory processing.

**Disclosures: Y. Wang:** None. **Y. Hua:** None. **A. Andreoni:** None. **L. Tian:** None.

**Poster**

**PSTR205: Sensors and Probes**

**Location:** WCC Halls A-C

**Time:** Monday, November 16, 2026, 1:00 PM - 5:00 PM

**Program #/Poster #:** PSTR205.16/LL54

**Topic:** J.04. Physiological Methods

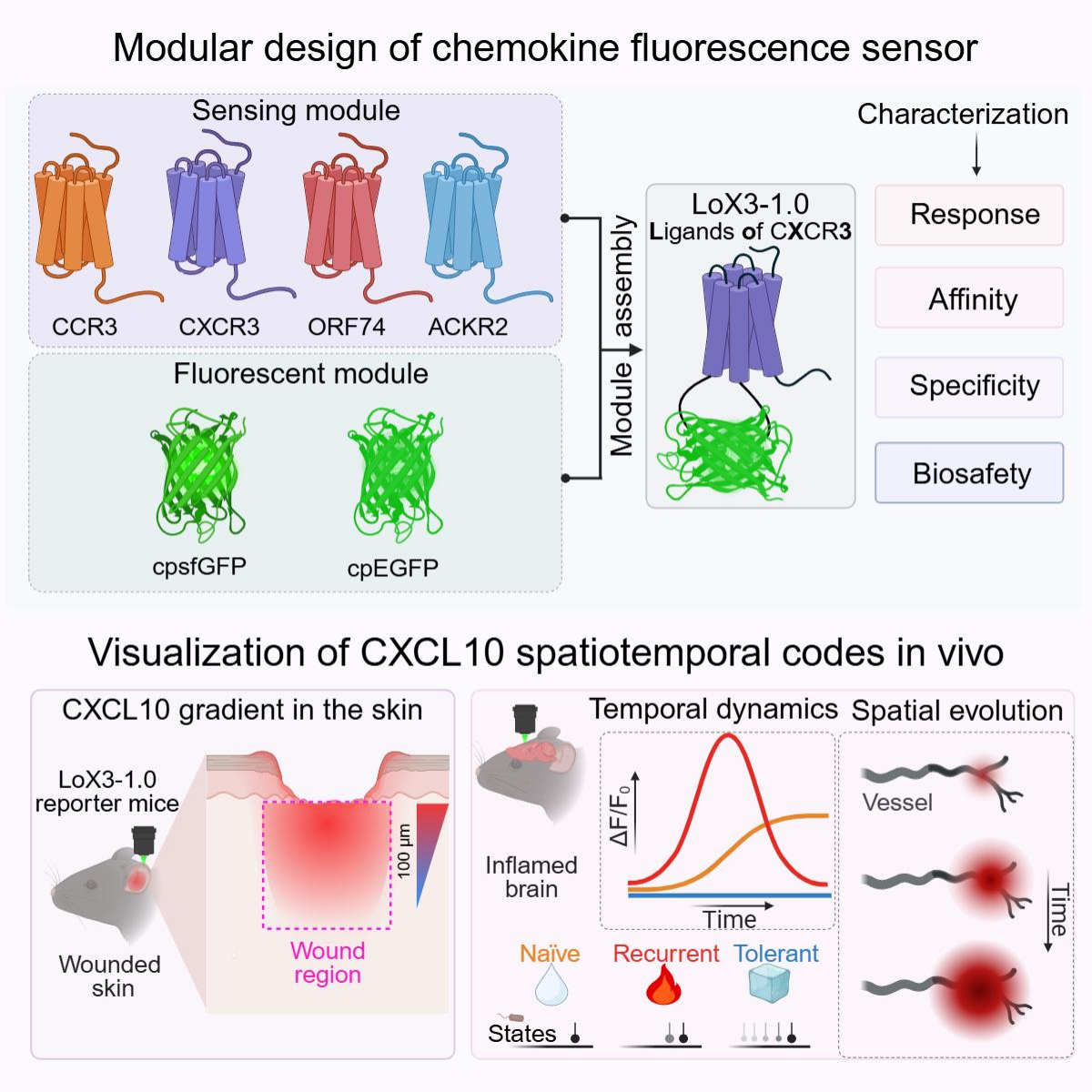
**Support:** STI 2030–Major Project Grant No. 2021ZD0202200 ; Subject 2021ZD0202203
National Natural Science Foundation of China (NSFC) Grant No. 32371150
National Key Research and Development Program of China Grant No. 2024YFA0916800
CAMS Innovation Fund for Medical Sciences (CIFMS) Grant No. 2024-I2M-3-023

**Title:** Spatiotemporal dynamics of CXCL10 encode contextual neuroimmune information revealed by genetically encoded fluorescent sensors

**Authors: *F. XI**, M. JING;
Chinese Inst. for Brain Research, Beijing, Beijing, China

**Abstract:** Chemokines are key extracellular signals that mediate development and inflammatory responses, and also be able to modulate the activity of neurons and glial cells and participate in neuroimmune crosstalk. However, their precise spatiotemporal dynamics and function in living tissues remain largely unexplored. Here we developed LoX3-1.0, a genetically encoded fluorescent sensor for chemokine CXCL10 by inserting a circularly permuted fluorescent protein into the chemokine receptor CXCR3. LoX3-1.0 exhibited robust fluorescence responses ($\Delta F/F_0$ of ~200%), nanomolar affinity, tens-of-milliseconds kinetics, and submicrometer spatial resolution, enabling real-time visualization of endogenous CXCL10 signaling both *in vitro* and *in vivo*. Using LoX3-1.0, we uncovered distinct spatiotemporal patterns of CXCL10 signaling across multiple neuroinflammatory contexts and quantitatively characterized the multidimensional features of CXCL10 that represents environmental information. To further improve sensor performance, we engineered LoX3-2.0 that retained the high affinity to CXCL10

while exhibiting substantially enhanced fluorescence responses ($\Delta F/F_0$ of ~800%). Together, the LoX3 sensors provide a novel and powerful tool to dissect chemokine signaling and their function in living tissues, and reveal context-dependent spatiotemporal organization of CXCL10 dynamics during neuroimmune responses.




**Disclosures: F. Xi:** None. **M. Jing:** None.

**Poster**

**PSTR205: Sensors and Probes**

**Location:** WCC Halls A-C

**Time:** Monday, November 16, 2026, 1:00 PM - 5:00 PM

**Program #/Poster #:** PSTR205.17/LL55

**Topic:** J.04. Physiological Methods

**Support:** Whitehall Foundation
McDonnell Center for Systems Neuroscience
Research Foundation for Opto-Science & Technology

**Title:** Next-Generation Near-Infrared Fluorescent Protein for Non-Invasive Imaging of Genetically Defined Deep-Brain Circuits

**Authors: *M. HALL**[1], M. KURENS[1], D. POLSINELLI[1], G. SUDHAKAR[1], S. FANG[1], H. LEE[1], L. VON ROHR[1], M. INOUE[2];
[2]Radiology, [1]Washington Univ. in St. Louis, St. Louis, MO

**Abstract:** Genetically defined deep-brain populations mediate motivation, adaptive behavior, and disease-related circuit remodeling, yet how these populations reorganize across distributed brain regions remains poorly understood. Progress has been limited by the challenge of repeatedly monitoring deep-brain populations with genetic specificity while preserving intact brain physiology. With current technologies, long-term, non-invasive imaging of genetically defined deep-brain circuits remains a key unmet goal. Non-invasive imaging modalities such as functional MRI provide brain-wide access but lack cellular specificity and have limited temporal resolution, whereas genetically encoded fluorescent reporters provide cell-type specificity but are constrained by tissue scattering and limited optical access to deep structures. Near-infrared (NIR) fluorescent proteins offer improved tissue penetration compared with visible-wavelength reporters, but currently available NIR fluorescent proteins remain limited by insufficient brightness and in vivo sensitivity for deep-brain imaging.

To address this challenge, we developed NIR20e, a next-generation NIR fluorescent protein engineered through genome mining of bacteriophytochrome sequences combined with machine-learning-guided protein design. Biophysical characterization demonstrated substantially improved brightness and photostability relative to the current state-of-the-art NIR fluorescent protein. In mice, we introduced viral NIR20e expression and used a custom wide-field NIR imaging system to demonstrate non-invasive, through-scalp fluorescence detection from deep-brain structures. Compared with GFP, NIR20e enabled robust transcranial visualization of striatal and nucleus accumbens signals through intact scalp and skull. Furthermore, NIR20e expression in midbrain dopaminergic neurons demonstrated transcranial detection of sparse, genetically defined deep-brain populations.

Longitudinal NIR imaging also enabled visualization of neurodegeneration dynamics in a kainic-acid model of hippocampal injury. Repeated transcranial imaging captured progressive neuronal signal loss and delayed bilateral changes consistent with circuit-level reorganization, demonstrating the utility of NIR20e for longitudinal tracking of distributed circuit remodeling within the same animal.

Together, these findings establish NIR20e as a versatile genetically encoded reporter for non-invasive, longitudinal imaging of genetically defined deep-brain circuits and distributed neural populations.

**Disclosures: M. Hall:** None. **M. Kurens:** None. **D. Polsinelli:** None. **G. Sudhakar:** None. **S. Fang:** None. **H. Lee:** None. **L. Von Rohr:** None. **M. Inoue:** None.

**Poster**

**PSTR205: Sensors and Probes**

**Location:** WCC Halls A-C

**Time:** Monday, November 16, 2026, 1:00 PM - 5:00 PM

**Program #/Poster #:** PSTR205.18/LL56

**Topic:** J.04. Physiological Methods

**Support:** NIH Grant 5U19 NS123719
NIH R01 NS129888

**Title:** Engineering Novel Red-Shifted Glutamate Sensors to Record Neural Dynamics

**Authors: *M. MARTIN**[1,3], A. ANDREONI[3], R. D. BLAKELY[2], L. TIAN[3];
[1]Col. of Sci., [2]Col. of Med., Florida Atlantic Univ., Jupiter, FL; [3]Max Planck Florida Inst. for Neurosci., Jupiter, FL

**Abstract:** Glutamate is the primary excitatory neurotransmitter in the brain: fast acting, ubiquitous, and its dynamics are certainly intertwined with other neurochemicals and neuromodulators. Genetically encoded fluorescent sensors (*e.g.* iGluSnFR) have become a widespread analytical tool for the visualization of glutamatergic release that coupled with various detection modalities, from fiber photometry to fast two-photon imaging, has helped reveal new details on this neurotransmitter's role on directing the flow of information through neural networks down to the synaptic level. To expand on this, our group has set out to engineer a suite of red-shifted versions of reporters to enable and expand multiplexed imaging of glutamate in parallel with neuromodulators: our pioneering work in iHaloGluSnFR provided the framework for dual imaging of Glu/$Ca^{2+}$ and Glu/DA with demonstrated applications in 2-photon and fiber photometry. However, the great sensitivity and flexibility of this chemigenetic reporter is undercut by the limitations imposed using a synthetic dye. To overcome this, we aimed at producing the very first fully genetically encoded, positive responding, red-shifted glutamate sensor by engineering an RFP-version of iGluSnFR. Our current prototypes show performance bettering the first generation of GFP-based reporters, and we have several versions with dynamic range, affinity and kinetic performances tuned for multiple purposes. Here, we present the characterization, benchmarking and application of this new generation of sensors for future in vivo application for all optical interrogation of neuronal dynamics of multiple neurochemicals to provide insights into input-output coupling, as well as their interactions.

**Disclosures: M. Martin:** None. **A. Andreoni:** None. **R.D. Blakely:** None. **L. Tian:** None.

**Poster**

**PSTR206: Electrophysiology Techniques II**

**Location:** WCC Halls A-C

**Time:** Monday, November 16, 2026, 1:00 PM - 5:00 PM

**Program #/Poster #:** PSTR206.01/LL57

**Topic:** J.04. Physiological Methods

**Support:** RS-2024-00460266

**Title:** Depth-resolved impedance profiling as a label-free approach to assess maturation-associated tissue organization in human retinal organoids

**Authors: *J. SEO**[1], T. KIM[2], J. BAEK[3], S. PARK[4], S. KIM[5], S. HA[3];
[1]Provalabs. Inc., Seoul, Korea, Republic of; [2]R&D, [3]ProvaLabs, Inc., Seoul, Korea, Republic of; [4]ProvaLabs, Inc., Seongnam-si, Korea, Republic of; [5]Seoul Natl. Univ., Seoul, Korea, Republic of

**Abstract:** Retinal organoids (ROs) have emerged as a powerful in vitro model for retinal neurogenesis and laminated sensory circuit formation. During maturation, ROs generate the major classes of retinal neurons, including photoreceptors, retinal interneurons, and retinal ganglion cells (RGCs). These populations self-organize into a radially stratified architecture extending from the apical (outer) region toward the organoid core. This structural lamination enables synaptic transmission of light-evoked signals to spike-generating RGCs. However, real-time assessment of internal RO architecture is difficult in live samples. Electrophysiological analysis is also challenging because the RGC layer is thin and deep. Since current maturation assays rely largely on destructive methods, label-free, depth-resolved assessment is needed to accurately evaluate internal organization and circuit maturation in situ. To address these challenges, we engineered OrganoInsight, a neural probe-based platform for depth-resolved electrochemical impedance profiling of three-dimensional retinal organoids. The silicon-based neural probe, featuring 16 pairs of microelectrodes (15μm × 10μm) along the needle axis, performs precise, controlled micrometer-scale penetrations from the surface to the organoid core while recording local impedance between adjacent electrode pairs. Impedance spectra from 125 Hz to 10 kHz were acquired to generate radial line scans, which were subsequently normalized to the medium. These scans detected and distinguished medium-to-tissue entry points and depth-dependent changes in normalized magnitude and phase. Intra-organoid profiles were heterogeneous, exhibiting regional plateaus, slope transitions, and frequency-dependent variations reflecting differences in cellular packing, extracellular space, and membrane-rich retinal architecture. Across D60 to D150 ROs, profile morphology and impedance parameters showed stage-dependent trends, indicating maturation-associated remodeling of internal tissue organization. Comparison with immunostained RO sections validated that region-specific impedance signatures reflect variations in cell density and the distribution of canonical retinal markers. Overall, OrganoInsight enables label-free, depth-resolved assessment of RO architecture by linking local impedance signatures to maturation-associated layer-like organization. This approach complements histology and can support RO maturation evaluation, targeting of functionally relevant internal regions, and detection of developmental or drug-induced changes in retinal tissue organization.

**Disclosures: J. Seo:** A. Employment/Salary (full or part-time):; ProvaLabs. **T. Kim:** E. Ownership Interest (stock, stock options, royalty, receipt of intellectual property rights/patent holder, excluding diversified mutual funds); ProvaLabs. **J. Baek:** A. Employment/Salary (full or part-time):; ProvaLabs. **S. Park:** A. Employment/Salary (full or part-time):; ProvaLabs.. **S. Kim:**

None. **S. Ha:** E. Ownership Interest (stock, stock options, royalty, receipt of intellectual property rights/patent holder, excluding diversified mutual funds); ProvaLabs.

**Poster**

**PSTR206: Electrophysiology Techniques II**

**Location:** WCC Halls A-C

**Time:** Monday, November 16, 2026, 1:00 PM - 5:00 PM

**Program #/Poster #:** PSTR206.02/LL58

**Topic:** J.04. Physiological Methods

**Support:** JSPS KAKENHI 23H03023
JSPS KAKENHI 24K20854
JSPS KAKENHI 25H02600
JSPS KAKENHI 25K22825
JSPS KAKENHI 26H02517
AMED 24wm0625401h0001
JST JPMJPR22S8
JST JPMJSP2108
The Asahi Glass Foundation
Secom Science and Technology Foundation

**Title:** Longitudinal high-density CMOS microelectrode array recordings reveal spatial reorganization of spontaneous activity in cultured cortical networks

**Authors: *K. TAKEHANA**[1], H. IKOMA[1], W. KAWAKAMI[1], Y. KAWAHARA[1], D. AKITA[1], H. TAKAHASHI[1,2];
[1]Grad. Sch. of Information Sci. and Technology, Dept. of Mechano-Informatics, [2]Intl. Res. Ctr. for Neurointelligence (WPI-IRCN), The Univ. of Tokyo, Tokyo, Japan

**Abstract:** Spontaneous activity in cultured neuronal networks reflects an evolving balance between stability and reorganization. Longitudinal high-density electrophysiological recordings are therefore essential for capturing how network activity develops, stabilizes, and transitions across time. However, such recordings require both stable culture-recording conditions for prolonged measurements and recording strategies that can follow non-stationary spatial activity patterns. Here, we addressed two challenges in longitudinal high-density CMOS microelectrode array recordings: maintaining a stable culture-recording environment for prolonged measurements and adapting electrode selection to evolving spontaneous activity. Dissociated cortical neurons from embryonic Wistar rats (E18) were cultured on a CMOS-based high-density microelectrode array containing 26,400 electrodes, with 1,024 electrodes routable at a time. We quantified spontaneous activity using firing-rate maps, active-electrode distributions, synchronized network bursts, center-of-activity trajectories, and measures of population-level coordination. Under these recording conditions, we obtained 34 h densely routed recordings from local 529-electrode regions and analyzed the temporal stability of highly active electrode sets. Across nine recordings from eight different cultures, the top-100 active electrode set changed

progressively over time, reaching 47.8% turnover at 34 h (95% CI, 34.4-61.2%), indicating that nearly half of the electrodes most representative of current activity were replaced during the recording period. Consistent with this spatial reorganization, adaptive electrode selection captured more activity than static selection under the same channel budget, exceeding static selection by 17.2 percentage points in oracle-relative attainment at 34 h (paired sign-flip test, $p = 0.004$). Longitudinal recordings also captured the emergence of synchronized network bursts and enabled center-of-activity trajectory analysis of population activity. Together, these findings indicate that cultured cortical networks preserve organized spontaneous activity while reorganizing over time. Longitudinal high-density CMOS microelectrode array recordings provide a framework for characterizing the stability, reorganization, and coordinated dynamics of cultured neuronal networks over extended periods.

**Disclosures: K. Takehana:** None. **H. Ikoma:** None. **W. Kawakami:** None. **Y. Kawahara:** None. **D. Akita:** None. **H. Takahashi:** None.

**Poster**

**PSTR206: Electrophysiology Techniques II**

**Location:** WCC Halls A-C

**Time:** Monday, November 16, 2026, 1:00 PM - 5:00 PM

**Program #/Poster #:** PSTR206.03/LL59

**Topic:** J.04. Physiological Methods

**Title:** A Refined Microelectrode Arrays System for Long-Term Electrophysiological Recordings in Cerebral and Retinal Organoids

**Authors: *G. PORTUGAL**;
Harvard Biosci., Holliston, MA

**Abstract:** Organoids provide three-dimensional (3D) models that mimic features of human physiology, enabling the study of developmental processes, disease mechanisms, and therapeutic interventions. Microelectrode arrays (MEA) allow non-invasive monitoring of the electrical activity of organoids. Nonetheless, conventional (planar) MEA are restricted to surface-level recordings and fail to capture activity within the 3D architecture of organoids. To overcome this problem, we developed a Mesh MEA platform that integrates directly within the organoid structure, preserving cellular organization while enabling stable, long-term recordings of electrical activity.
We investigate the performance of the Mesh MEA for electrophysiological recordings from cerebral organoids (COs) and retinal organoids (ROs). COs and ROs were cultured using dedicated protocols and carefully transferred to the MEA platform (MultiChannel Systems) for electrophysiological recordings.
After 3 weeks, COs displayed higher electrical activity on the Mesh MEA compared to planar MEA and 3D-electrode (spike) MEA. The data suggests that the scaffold Mesh MEA plays a role in preserving the electrophysiology of COs. Moreover, immunofluorescence experiments showed that COs on the Mesh MEA expressed more synapses and a more intact architecture of

neuronal projections compared to planar and 3D-electrode MEAs.
ROs flattened on the surface of planar and 3D-electrode MEA. However, the Mesh MEA preserved multi-structured ROs. Consequently, the amplitude of the local field potential detected was higher in Mesh MEA-cultured ROs, indicating stable, long-term access to inner retinal layers (up to 46 days).
The present work demonstrates that the Mesh MEA is a more refined system for studying COs and ROs.

**Disclosures: G. Portugal:** A. Employment/Salary (full or part-time):; Harvard Bioscience.

**Poster**

**PSTR206: Electrophysiology Techniques II**

**Location:** WCC Halls A-C

**Time:** Monday, November 16, 2026, 1:00 PM - 5:00 PM

**Program #/Poster #:** PSTR206.04/LL60

**Topic:** J.04. Physiological Methods

**Title:** A scalable HD-MEA workflow for multiscale functional phenotying of human midbrain organoids

**Authors: *L. D'IGNAZIO**, F. GALLUZZI, E. GUELLA, P. MANOGARAN;
MaxWell Biosystems, Zurich, Switzerland

**Abstract:** Human 3D midbrain organoids hold promise as physiologically relevant in vitro models to capture selected features of developing human midbrain tissue, including dopaminergic identity, tissue-like organization, and emerging circuit activity. These properties make them well suited to investigate Parkinson's disease (PD)- and synucleinopathy-relevant alterations in neuronal excitability, network synchronization, and axonal output, which may precede overt neurodegeneration. However, resolving these phenotypes in 3D tissues requires non-invasive electrophysiological methods that combine longitudinal access, high spatial sampling, and reproducible acquisition across wells and timepoints to detect low amplitude signals, quantify network bursting, and track axonal propagation at subcellular resolution. Here, in collaboration with STEMCELL Technologies, we used high-density microelectrode arrays (HD-MEAs) to longitudinally profile the functional maturation of commercially available human midbrain organoids. Organoids were plated at 77 days of age onto PEDOT-coated MaxTwo HD-MEA 24-well plates, each containing 26,400 electrodes per well, and spontaneous activity was tracked for approximately one month. Organoids showed progressive strengthening of firing activity, including increased firing rate, spike amplitude, and active area, indicating neuronal maturation and improved tissue-electrode coupling. At the network scale, we tracked the emergence of increasingly organized synchronized bursting, with increased burst cadence and enhanced neuronal recruitment over time. To assess pharmacological responsiveness, organoids were challenged with 4-AP and TTX, which respectively enhanced and suppressed firing activity in a highly reproducible manner. Finally, AxonTracking enabled label-free extraction of soma-to-axon propagation patterns at the organoid-electrode interface, providing a complementary

readout of intra-organoid axonal functionality. Together, these results establish a scalable, non-invasive multiscale electrophysiology workflow for human midbrain organoids that captures spontaneous network maturation, pharmacological modulation of excitability, and axonal propagation phenotypes. By supporting consistent acquisition, processing, and interpretation of functional readouts across wells and timepoints, this approach provides a foundation for Parkinson's disease-relevant phenotyping in 3D human neural models using HD-MEAs.

**Disclosures: L. D'Ignazio:** None. **F. Galluzzi:** None. **E. Guella:** None. **P. Manogaran:** None.

**Poster**

**PSTR206: Electrophysiology Techniques II**

**Location:** WCC Halls A-C

**Time:** Monday, November 16, 2026, 1:00 PM - 5:00 PM

**Program #/Poster #:** PSTR206.06/LL62

**Topic:** J.04. Physiological Methods

**Support:** ALS Scholars in Therapeutics awarded to EVO
SURFiN Fellowship awarded to GVI

**Title:** Chronic High-Density Neural Recordings in an Ovine Model Using Neuropixels-NHP-1.0 45 mm Probes

**Authors: *E. V. OKOROKOVA**[1], G. IZABAL[3], I. MARTINEZ[4], D. E. BROWN, Jr.[5], E. TRAUTMANN[3], A. LESNESKI[3], S. LUCERO[3], D. BRANDMAN[6], S. D. STAVISKY[2]; [2]Neurolog. Surgery, [1]Univ. of California Davis, Davis, CA; [3]Univ. of California, Davis, Davis, CA; [5]Neurolog. Surgery, [4]Univ. of California, Davis, Sacramento, CA; [6]Neurolog. Surgery, UC Davis Hlth., Sacramento, CA

**Abstract:** High-density neural probes, such as Neuropixels, offer transformative potential for neuroscience research and clinical neurotechnology, enabling simultaneous recording from thousands of electrodes across multiple cortical depths with single-neuron resolution. This technology represents the state of the art for animal neuroscience, including in both acute [Trautmann et al. 2025] and chronic recordings in rodents [e.g., Steinmetz et al. 2021; van Beest et al. 2024, Juavinett et al. 2019]. Neuropixels have also been used for brief intraoperative recordings during neurosurgical procedures in humans, including recently with the longer 45 mm variant [Brown et al. 2026]. However, the viability of chronic Neuropixels implantation in large animals and humans, where there is, for example, greater brain motion that may deteriorate the ability to detect single units in the immediate vicinity of the probe, remains unknown. Here we present results from an ongoing preclinical study validating chronic Neuropixels-NHP-1.0 (45 mm, 4,416 electrodes) implantation in awake behaving sheep as a translational model for future semi-chronic human clinical deployment. We developed a complete chronic implant system comprising a modified cannulated FDA-approved surgical bolt mounted through a 5 mm burr hole, a custom-fabricated chronic probe holder and a custom microdrive to deliver the probe to the brain target. Recordings were obtained from two animals 2-3 times per week using a portable

acquisition setup from 1,536 electrodes spanning approximately 15 mm of cortical depth. We performed automated spike sorting and developed semi-automated unit curation techniques. Across two implanted subjects, we demonstrate stable isolation of well-defined single unit and multi-unit activity sustained over multiple weeks post-implantation. To characterize the tissue response to chronic implantation, we conducted histological analysis of post-explant brain tissue, examining markers of neuroinflammation, glial scarring, cell death, and vascular disruption along the probe tract. Collectively, these results establish a robust large animal model for evaluating the chronic performance of high-density probes, with direct translational implications for human applications including intraoperative cortical mapping, epilepsy source localization, and long-term brain computer interface systems.

**Disclosures: E.V. Okorokova:** None. **G. Izabal:** None. **I. Martinez:** None. **D.E. Brown:** None. **E. Trautmann:** None. **A. Lesneski:** None. **S. Lucero:** None. **D. Brandman:** E. Ownership Interest (stock, stock options, royalty, receipt of intellectual property rights/patent holder, excluding diversified mutual funds); University of California. F. Consulting Fees (e.g., advisory boards); Globus Medical Inc. **S.D. Stavisky:** E. Ownership Interest (stock, stock options, royalty, receipt of intellectual property rights/patent holder, excluding diversified mutual funds); Stanford University, University of California. F. Consulting Fees (e.g., advisory boards); Subsense, Neuralink.

**Poster**

**PSTR206: Electrophysiology Techniques II**

**Location:** WCC Halls A-C

**Time:** Monday, November 16, 2026, 1:00 PM - 5:00 PM

**Program #/Poster #:** PSTR206.07/LL63

**Topic:** J.04. Physiological Methods

**Support:** NIH R00EY030528

**Title:** Exploiting the smooth temporal dynamics of action potentials for improved extracellular spike sorting

**Authors: *M. O. JONES**, D. J. HERZFELD;
Dept. of Neurosci., Univ. of Wisconsin-Madison, Madison, WI

**Abstract:** Understanding neural circuit function during behavior requires measurement of single neuron activity. Current methods for spike-sorting are largely empirical, with sophisticated pipelines for single-spike identification and assignment built on signal processing and clustering techniques. Here, we derive a complementary theoretical approach for identification of single-spikes built on the observation that neuron action potentials are determined by relatively fixed biophysical parameters. Thus, the action potential's waveform is consistent and mathematically predictable across spikes from the same neuron. We take advantage of these facts to embed single action potentials in a delay-coordinate space, where each axis represents the signal at successive time delays. In delayed coordinates, action potentials appear smooth, owing to their

continuous nature, while noise and artifacts produce jagged trajectories. For each putative action potential in an extracellular recording, we embed a clip of voltage in delay-coordinate space and quantify smoothness using a scalar waveform curvature (WC) metric. Then, we derive a recording-specific threshold for separation of neuronal from non-neuronal signals by fitting a two-component Gaussian mixture model to the WC distribution and placing the decision boundary at the between-component valley. We quantitatively tested this approach using 16 paired recordings of 16 neurons across 4 public datasets. Our results demonstrate that WC reliably discriminates ground-truth action potentials from unverified events with a mean F1 score of 0.92 ± 0.04 (precision = 0.95, recall = 0.91), indicating high precision and recall. Second, when used as a pre-processing step before conventional spike-sorting on the same datasets, overall F1 scores increased as well. Finally, we applied this approach to extracellular recordings from the cerebellar flocculus of behaving monkeys, ultimately showing substantial improvement in post-processing unit-level quality metrics. Taken together, WC represents an improved metric for neuronal spike identification and, crucially, is agnostic to probe type, brain region, and species. Because WC is based on the intrinsic dynamics of action potentials, rather than their amplitude or shape, it requires no templating, training data, or a priori specification of amplitude thresholds. We propose implementing WC as a pre-processing step prior to clustering in conventional sorters, where lower thresholds for putative spike identification allow for a more complete analysis of neuronal activity in extracellular recordings.

**Disclosures: M.O. Jones:** None. **D.J. Herzfeld:** None.

**Poster**

**PSTR206: Electrophysiology Techniques II**

**Location:** WCC Halls A-C

**Time:** Monday, November 16, 2026, 1:00 PM - 5:00 PM

**Program #/Poster #:** PSTR206.08/LL64

**Topic:** J.04. Physiological Methods

**Support:** R21NS111202
R01EB025819

**Title:** Network connectivity dynamics in human iPSC-derived neurons with Huntington's disease

**Authors: *G. CANNESTRO**[1,2,3], T. SAROVICH[2,3], J. GIORDANO[1,3], J. WEI[1,2,3];
[1]Ctr. for Complex Systems and Brain Sci., [2]Dept. of Biomed. Science, Charles E. Schmidt Col. of Med., Florida Atlantic Univ., Boca Raton, FL; [3]Stiles-Nicholson Brain Inst., Florida Atlantic Univ., Jupiter, FL

**Abstract:** Huntington's disease (HD) is a neurodegenerative disorder characterized by motor, cognitive, and psychiatric symptoms. While multi-electrode array (MEA) recordings have revealed abnormalities in neuronal firing, bursting, and synchrony in HD models, disease-related network alterations are largely unknown. As functional connectivity is fundamental to information processing and circuit function, its disruption may contribute directly to HD

pathophysiology. In this study, we used MEA recordings to characterize alterations in functional network connectivity in human neuronal cultures and determine how these connectivity patterns are remodeled in response to chemical stimulation, providing new insights into circuit-level dysfunction in HD. iPSC-derived forebrain neurons (control and HD) were cultured on 24-well MEA plates, and spontaneous network activity was recorded between DIVs 20 and 40. Immunocytochemical analyses confirmed comparable neuronal composition, enabling direct comparison of network properties. Functional connectivity was assessed using spike time tiling coefficients, with significant electrode pairings used to construct network graphs and calculate clustering coefficients (CCs). Two-way ANOVA revealed a significant effect of time ($F(2,103)=36.14$, $p<0.0001$) and time × disease interaction ($F(2,103)=3.11$, $p=0.0487$), but no main effect of disease state. Post hoc analyses demonstrated a increase in network clustering with maturation, with significantly higher CCs at DIV40 compared to DIV20 (Control: $p<0.0001$; HD: $p=0.0004$) and DIV30 (Control: $p=0.0004$; HD: $p=0.0230$). These findings indicate that network connectivity becomes increasingly organized during neuronal maturation. To assess network responsiveness, DIV40 cells were challenged with picrotoxin (PTX), a GABA receptor antagonist, and connectivity changes were quantified relative to pre-treatment levels. While control networks exhibited an increase in CC following PTX exposure, HD networks showed a significant reduction ($p = 0.0026$ ; fold change: Control, $1.09 \pm 0.03$; HD, $0.91 \pm 0.17$). Furthermore, HD displayed greater variability in their responses, with a coefficient of variation (CV) nearly twofold higher than controls (18.7% vs. 9.5%). These findings indicate that although network emergence was similar in control and HD cultures under basal conditions, HD networks exhibited impaired functional reorganization in response to disinhibition. The reduced recruitment of local network connectivity and increased response heterogeneity suggest deficits in circuit adaptability that may contribute to HD pathophysiology.

**Disclosures: G. Cannestro:** None. **T. Sarovich:** None. **J. Giordano:** None. **J. Wei:** None.

**Poster**

**PSTR206: Electrophysiology Techniques II**

**Location:** WCC Halls A-C

**Time:** Monday, November 16, 2026, 1:00 PM - 5:00 PM

**Program #/Poster #:** PSTR206.09/LL65

**Topic:** J.04. Physiological Methods

**Support:** National Research Foundation of Korea funded by the Ministry of Science and ICT (Project No. 2022M3C1A3091627),
the Ministry of Trade, Industry and Energy (MOTIE) and Korea Institute for Advancement of Technology (KIAT) through the International Cooperative R&D Program (Project No. P0028313)
the Korea Government (MOTIE) (Project No. RS-2025-03612975),
the Institutional Program of the Korea Institute of Science and Technology (KIST) (Project Nos. 26E0172 and 26E0154).

**Title:** Contact-pair screening of intraneural vagus nerve stimulation and recording for glycemic modulation in rats

**Authors:** W. CHOI[1], S. OH[2,3], D.-H. OH[5], H. PARK[2], D. YOON[4], I.-K. JEONG[5,6], ***J. KIM**[7]; [1]Korea Inst. of Sci. and Technol., SEOUL, Korea, Republic of; [2]Korea Inst. of Sci. and Technol., Seoul, Korea, Republic of; [3]Korea Univ., Seoul, Kosovo, Republic of; [4]Korea Univ., Seoul, Korea, Republic of; [5]Kyung Hee Univ. Hosp. at Gangdong, Seoul, Korea, Republic of; [6]Kyung Hee Univ. Sch. of Med., Seoul, Korea, Republic of; [7]KIST (Korea Inst. of Sci. & Technology), Seoul, Korea, Republic of

**Abstract:** Selective bioelectronic control of metabolic function may require access to distinct neural populations within the vagus nerve, but conventional cervical vagus interfaces provide limited spatial access and few opportunities for simultaneous recording. We developed a bidirectional cylindrical intraneural interface for the rat cervical vagus nerve, integrating 16 addressable sites around a within-nerve electrode structure. The device was used to examine whether different bipolar contact pairs could influence glucose responses and whether intraneural recordings could capture neural features associated with glucose and insulin perturbations. After electrochemical characterization and accelerated aging, the interface was implanted in rats fed a normal chow diet or high-fat diet. During intraperitoneal glucose tolerance testing, multiple bipolar contact pairs were screened within each animal under identical stimulation parameters. The contact pair associated with the strongest attenuation of glucose excursion was then used for glucose-only, glucose plus vagus nerve stimulation (VNS), glucose plus insulin, and glucose plus VNS plus insulin sessions. In parallel recording experiments, multichannel vagal activity was aligned to glucose injection and insulin administration. Bipolar contact pairs produced different glycemic responses within the same animal, supporting within-animal contact-pair screening rather than reliance on fixed anatomical alignment. The screening-selected contact pair was associated with attenuated glucose excursion in both diet groups and, when combined with exogenous insulin, showed a greater glucose-lowering trend than either intervention alone in this dataset. VNS was also accompanied by measurable changes in circulating insulin. Intraneural recordings yielded sortable spike activity across multiple channels, and firing-rate features differed between glucose-only and glucose-plus-insulin sessions in a diet- and condition-dependent manner, with clearer divergence around the insulin phase in high-fat-diet rats. These findings support the cylindrical intraneural interface as a proof-of-concept platform for contact-pair-guided vagus neuromodulation and concurrent intraneural recording, providing a basis for future closed-loop studies of vagus-mediated glycemic regulation.

**Disclosures: W. Choi:** None. **S. Oh:** None. **D. Oh:** None. **H. Park:** None. **D. Yoon:** None. **I. Jeong:** None. **J. Kim:** None.

**Poster**

**PSTR206: Electrophysiology Techniques II**

**Location:** WCC Halls A-C

**Time:** Monday, November 16, 2026, 1:00 PM - 5:00 PM

**Program #/Poster #:** PSTR206.10/LL66

**Topic:** J.04. Physiological Methods

**Support:** Horizon 2020 ERC

**Title:** Neuromorphic Communication for Scalable Wireless Transmission of High-Density Neural RecordingsTransmission of Distributed High-Density Neural Recordings

**Authors: *Y.-H. LIU**, J. LIU, Y. HE, P. RUSSO;
Imec, Eindhoven, Netherlands

**Abstract:** Brain-computer interfaces (BCIs) increasingly rely on high-density neural recordings to capture distributed neuronal dynamics at single-unit resolution. However, the wireless transmission of such large-scale data remains a fundamental bottleneck due to stringent power, bandwidth, and thermal constraints in implantable and freely moving systems. Here, we present a neuromorphic compressive telemetry platform that combines event-driven encoding with an ultra-low-power wireless link to enable scalable neural data streaming. The proposed system integrates a neuromorphic compression front-end with a duty-cycling impulse-radio ultra-wideband (IR-UWB) transmitter, achieving a co-design of data reduction, communication protocol, and power efficiency. Neural signals are first encoded using a delta-based, event-driven representation and packetized via an Address-Event-µPacket (AEµP) scheme, which exploits the temporal sparsity of neural activity to minimize data rate and memory access. These events are transmitted using a duty-cycled IR-UWB link with non-coherent DBPSK modulation, enabling high data throughput with relaxed synchronization requirements and efficient multi-node operation. Fabricated in 65 nm CMOS, the system supports 384-channel neural recordings and achieves 11.5× data compression with minimal signal distortion (3.6 µV RMS error, below typical recording noise). The transmitter consumes 1 mW while maintaining a communication range exceeding 6.6 meter and supports multi-access networking via frequency-division multiplexing. The event-driven operation results in low duty cycles (~9%), enabling substantial reductions in energy consumption compared to continuous streaming approaches. We validate the system using in vivo datasets from high-density Neuropixels probes, demonstrating faithful reconstruction of neural spiking activity across channels. By jointly optimizing neural compression, packet-based communication, and wireless transmission, this work provides a scalable pathway toward distributed and multi-node neural recording systems, supporting emerging neuroscience paradigms such as freely moving experiments and networked BCIs

**Disclosures: Y. Liu:** None. **J. Liu:** None. **Y. He:** None. **P. Russo:** None.

**Poster**

**PSTR206: Electrophysiology Techniques II**

**Location:** WCC Halls A-C

**Time:** Monday, November 16, 2026, 1:00 PM - 5:00 PM

**Program #/Poster #:** PSTR206.11/LL67

**Topic:** J.04. Physiological Methods

**Title:** Functional analysis of iPSC-derived three-dimensional neural models on novel microelectrode arrays

**Authors:** B. STREETER[1], D. SULLIVAN[2], ***A. PASSARO**[2], S. A. CHVATAL[2], D. C. MILLARD[2];
[1]Axion Biosystems, Atlanta, GA; [2]Axion BioSystems, Atlanta, GA

**Abstract:** *In vitro* neuronal models are valuable tools for studying function, pathophysiology, and toxicology of the brain. Numerous efforts to refine induced pluripotent stem cell (iPSC) neural differentiation methods have produced 3D models that better represent *in vivo* biology than traditional 2D cultures. These models, referred to as neural organoids or spheroids, better recapitulate the cellular diversity and spatial architecture of in vivo tissue. Therefore, it is necessary to develop methods to accurately measure electrophysiology from these new, advanced 3D models. Here, novel microelectrode array (MEA) methods were used to characterize the electrical activity of 3D neural models. To facilitate recording from smaller (≤500 µm diameter) spheroids, an Ibidi 4 Well Fultrac micro-insert was adhered to a microelectrode array chip, with each microwell positioned over an array of 16 high-density (50 µm spacing) electrodes. Neurospheres formed from 16,000 iCell Glutaneurons, 6,500 Gabaneurons, and 2,500 Astrocytes (25,000 cells total) were seeded into each microwell of the MEA chip, termed SpheroHD MEA, and neurosphere electrophysiology was measured on the Maestro Pro system. From Day 3 to Day 14 on the SpheroHD, neurosphere mean firing rate (MFR, 0.017 Hz to 0.362 Hz) and area under the normalized cross correlation (AUNCC, 0 to 0.016) increased. To measure from larger neural organoids (>1 mm in diameter), we used a flexible MEA with 64 electrodes arranged on cantilevers that bend to conform to the organoid surface. As a proof of concept, a Day 99 midbrain organoid was plated onto this MEA, termed 3DMap™, and recorded on the Maestro Pro for 19 days, during which both MFR (0.0086 to 1.57 Hz) and AUNCC (0 to 0.0397) increased. Further, dosing with potassium channel blocker 4-AP at Day 12 on the 3DMap led to marked increases in these same metrics. Mean firing rate increased from 0.51 Hz to 1.141 Hz, and AUNCC increased from 0.0054 to 0.027. To investigate if other organoid types could be measured on the 3DMapTM, a Day 51 dorsal forebrain organoid was also plated and measured over 15 days. Dorsal forebrain organoid MFR increased from 0.024 Hz at Day 7 to 0.028 HZ at Day 15, and AUNCC increased from 0.00049 to 0.0031. In total, the novel MEAs demonstrated here helped circumvent the challenges associated with measuring electrophysiology from complex, 3D neural cell models without disrupting their cytoarchitecture. Future work will apply these methods to other 3D neural models and will build more comprehensive datasets of these models' electrophysiology.

**Disclosures: B. Streeter:** A. Employment/Salary (full or part-time):; Axion BioSystems. **D. Sullivan:** A. Employment/Salary (full or part-time):; Axion BioSystems. **A. Passaro:** A. Employment/Salary (full or part-time):; Axion BioSystems. **S.A. Chvatal:** A. Employment/Salary (full or part-time):; Axion BioSystems. **D.C. Millard:** A. Employment/Salary (full or part-time):; Axion BioSystems.

**Poster**

**PSTR206: Electrophysiology Techniques II**

**Location:** WCC Halls A-C

**Time:** Monday, November 16, 2026, 1:00 PM - 5:00 PM

**Program #/Poster #:** PSTR206.12/LL68

**Topic:** J.04. Physiological Methods

**Title:** Development of a neural network formation assay for iPSC-derived glutamatergic neurons

**Authors: D. SULLIVAN**[1], B. STREETER[2], P. J. ELLINGSON[1], S. BARNES[1], A. PASSARO[1], *S. A. CHVATAL[1], D. C. MILLARD[2];
[1]Axion BioSystems, Atlanta, GA; [2]Axion Biosystems, Atlanta, GA

**Abstract:** Understanding how neural networks form and communicate is essential for understanding the mechanisms underlying brain development and disease. However, the field lacks standardized approaches to evaluate the functional maturity and connectivity of human iPSC-derived neuronal models. Here, we developed a neural network formation assay using human iPSC-derived neurons cultured on microelectrode arrays (MEAs) to characterize network maturity, synaptic connectivity and excitatory-inhibitory (E:I) balance. Neuronal populations with defined ratios of glutamatergic to GABAergic neurons (100/0, 90/10, 75/25, 50/50, 10/90, and 0/100) were co-cultured with iPSC-derived astrocytes to examine how E:I composition influences *in vitro* network development. Spontaneous activity was monitored for up to 43 days, and cultures were sequentially dosed with a panel of compounds to assess functional synaptic activity. Bicuculline was applied to block GABAergic inhibition, followed by co-application of CNQX and APV to block AMPA and NMDA receptor-mediated glutamatergic transmission, and finally 4-AP to block voltage-gated potassium channels and probe membrane excitability independent of synaptic drive. Two metrics (Network ISI CoV and Synchrony Index) were selected for their stability across the full range of E:I compositions. At baseline, Network ISI CoV increased from 0.98 in 100% GABAergic cultures to 2.31 in 100% glutamatergic cultures, reflecting a shift from tonic firing toward more structured network bursting. Synchrony index showed nearly a 10-fold increase across the same range, consistent with excitatory synaptic drive coordinating population level activity. Bicuculline increased Network ISI CoV that scaled with glutamatergic content, while CNQX/APV subsequently collapsed Network ISI COV and synchrony index towards baseline levels in excitatory-dominant cultures. These results help to establish a defined MEA assay for functional quality assessment of human iPSC-derived neuronal models to indicate whether a culture's network is mature, connected, and excitatory-, inhibitory-, or balanced.

**Disclosures: D. Sullivan:** A. Employment/Salary (full or part-time):; Axion BioSystems. **B. Streeter:** A. Employment/Salary (full or part-time):; Axion BioSystems. **P.J. Ellingson:** A. Employment/Salary (full or part-time):; Axion BioSystems. **S. Barnes:** A. Employment/Salary (full or part-time):; Axion BioSystems. **A. Passaro:** A. Employment/Salary (full or part-time):; Axion BioSystems. **S.A. Chvatal:** A. Employment/Salary (full or part-time):; Axion BioSystems. **D.C. Millard:** A. Employment/Salary (full or part-time):; Axion BioSystems.

**Poster**

**PSTR206: Electrophysiology Techniques II**

**Location:** WCC Halls A-C

**Time:** Monday, November 16, 2026, 1:00 PM - 5:00 PM

**Program #/Poster #:** PSTR206.13/LL69

**Topic:** J.04. Physiological Methods

**Support:** AFOSR FA9550-22-1-0078
AFOSR FA9550-23-1-0701
NIH DP2MH136494

**Title:** The NanoNeedle NET: A 3D Transparent NeuroGrid for Simultaneous Electro-Optical Circuit Mapping Across Cortical Volume

**Authors: *O. KOLHE**[1,2], D. L. GONZALES[1,2], D. AAKER[1,2], K. JAYANT[1,2];
[1]Biomed. Engin., Purdue Univ., West Lafayette, IN; [2]Purdue Inst. for Integrative Neurosci., West Lafayette, IN

**Abstract:** Sensory processing and decision-making arise from neural computations distributed across three-dimensional cortical networks, organized across both cortical layers and the cortical surface, where coordinated activity links local and long-range circuits. Technologies capable of simultaneously resolving neural activity across both depth and spatial extent remain lacking. Here, we introduce NanoNeedle Net, a soft, transparent multimodal neural interface featuring high-density, ultra-high-aspect-ratio electrodes for conformal, minimally invasive volumetric cortical recording. Fabricated using a scalable nanoscale three-dimensional metal-printing process, the NanoNeedles achieve aspect ratios approaching 100:1, submicron-diameter tips, and layer-specific depth targeting. Their mechanical compliance and optical transparency enable truly simultaneous electrophysiology and two-photon calcium imaging, combining millisecond temporal resolution with cellular spatial resolution across cortical volumes. In awake, behaving mice, NanoNeedle Net simultaneously captured single-unit activity, local field potentials (LFP), and calcium dynamics across the somatosensory and motor cortices. In the somatosensory cortex, we resolved spatiotemporal traveling waves and showed how layer-specific spiking and LFP dynamics map onto wave structure to modulate sensory perception. In the motor cortex during locomotion, simultaneous Layer 2/3 and Layer 5 electrophysiological recordings combined with two-photon imaging of the same neuronal population directly linked cellular calcium dynamics to underlying wave patterns and spiking activity across cortical layers. NanoNeedle Net thus establishes a scalable platform for volumetric cortical mapping and for dissecting how three-dimensional neural activity gives rise to perception and behavior.Funding: This material is also based upon work supported by the Air Force Office of Scientific Research under award numbers FA9550-22-1-0078 and FA9550-23-1-0701. Any opinions, findings, conclusions, or recommendations expressed in this material are those of the author(s) and do not necessarily reflect the views of the United States Air Force. This work was also supported by the National Institutes of Health New Innovator Award (DP2MH136494).

**Disclosures: O. Kolhe:** None. **D.L. Gonzales:** None. **D. Aaker:** None. **K. Jayant:** None.

**Poster**

**PSTR206: Electrophysiology Techniques II**

**Location:** WCC Halls A-C

**Time:** Monday, November 16, 2026, 1:00 PM - 5:00 PM

**Program #/Poster #:** PSTR206.14/LL70

**Topic:** J.04. Physiological Methods

**Support:** NIH/NINDS ZIA NS003144

**Title:** Hierarchical activity and coding in local modules of the human temporal lobe

**Authors: *J. I. CHAPETON**[1], K. SWIFT[2], S. K. INATI[3], K. A. ZAGHLOUL[3];
[1]Surgical Neurol. Br., NIH, Natl. Inst. of Neurolog. Disorders & Stroke (NINDS), Bethesda, MD; [2]MIT, Cambridge, MA; [3]NIH, Bethesda, MD

**Abstract:** Networks in the cortex exist are organized at multiple spatial scales. In a previous study we used recordings from micro-electrode arrays (MEAs) implanted in human participants undergoing seizure monitoring to show that at the scale of local circuits, the temporal lobe is organized into functional modules about 1mm in diameter, and these modules shape the underlying patterns of neural activity. In our current work we are testing if this organization is consistent with the idea of hierarchical coding at different spatial scales.Models of modular organization in higher-order cortical regions posit that coding is hierarchical in nature; specific spatio-temporal patterns of neuronal spiking are needed to distinguish two stimuli belonging to the same category, but information at the scale of cortical columns is sufficient for decoding the category of a stimuli. We tested this hypothesis by analyzing MEA recordings from human participants engaging in a visual categorization task where they are asked to categorize images into 4 categories. Importantly, in a subset of blocks they are asked to distinguish between exemplars belonging to the same category, allowing us to test the prediction that the category of an image can be decoded from course-grained activity at the scale of cortical modules, whereas discriminations between exemplars of the same category require detailed knowledge of the activity of neurons within modules.We find that the category of the stimuli can be decoded at a rate significantly higher than chance by using course-grained activity at the scale of cortical columns, decoding is better when course-graining based on module boundaries compared to averaging random groups; individual exemplars from the same category cannot be decoded as well when using module level activity, but can be decoded similar to the categories by using the activity of the individual neurons. Together, these results support the hypothesis of hierarchical coding.

**Disclosures: J.I. Chapeton:** None. **K. Swift:** None. **S.K. Inati:** None. **K.A. Zaghloul:** None.

**Poster**

**PSTR206: Electrophysiology Techniques II**

**Location:** WCC Halls A-C

**Time:** Monday, November 16, 2026, 1:00 PM - 5:00 PM

**Program #/Poster #:** PSTR206.15/LL71

**Topic:** J.04. Physiological Methods

**Title:** Ultra-Flexible Microelectrode Arrays for High-Density Single-Neuron Recording in the Peritumoral Cortex During Awake Craniotomy

**Authors:** ***Y. TIAN**[1], Z. ZHAO[2], Y. ZHANG[1];
[1]Southern Med. Univ., Guangzhou, China; [2]Chinese Acad. of Sci., Shanghai, China

**Abstract:** During awake craniotomy for brain tumor resection, ultra-flexible implantable neural electrode (uFINE) arrays provide a robust platform for high-density single-neuron recordings in the peritumoral cortex. In the present study, dual-shank uFINE arrays were stereotactically implanted into the peritumoral cortex at a depth of 5-6 mm in six patients undergoing resection of various brain tumors, including meningiomas, cavernous hemangiomas, and gliomas. Owing to their exceptional mechanical compliance, the arrays dynamically conformed to intrinsic brain pulsations, thereby substantially attenuating motion artifacts and single-neuron instability typically induced by cardiorespiratory cycles when conventional rigid electrodes are employed. From the acquired signals, 163 high-quality clusters were isolated through automated spike sorting with Kilosort, followed by rigorous manual curation. Throughout the recording sessions, key electrophysiological parameters—including spike amplitude, firing rate, inter-spike interval variability, and signal-to-noise ratio—remained stable. The inverse current source density (iCSD) algorithm was applied to characterize the laminar discharge patterns of peritumoral neurons, revealing laminar-specific differences in neuronal dynamics across distinct tumor types. This minimally invasive approach, characterized by superior biocompatibility and minimal tissue disruption, enables precise real-time investigation of heterogeneous peritumoral neuronal dynamics and facilitates intraoperative functional mapping. Moreover, it provides a valuable framework for elucidating tumor-induced alterations in neural plasticity and excitability, with significant implications for clinical translation and the advancement of next-generation brain-machine interface technologies.

**Disclosures: Y. Tian:** None. **Z. Zhao:** None. **Y. Zhang:** None.

**Poster**

**PSTR206: Electrophysiology Techniques II**

**Location:** WCC Halls A-C

**Time:** Monday, November 16, 2026, 1:00 PM - 5:00 PM

**Program #/Poster #:** PSTR206.16/LL72

**Topic:** J.04. Physiological Methods

**Support:** Technology Platform UZH TPF Fund
SNSF Sinergia Grant 10000131
URPP ITINERARE UZH Fund

**Title:** Cell-type-specific electrophysiology at scale: automated patch-clamp with correlative imaging in heterogeneous neuronal populations

**Authors: *D. COLAMEO**[1], A. GIRARD[2], A. SCHUMACHER[1], G. SCHRATT[3], I. CANALS[2], D. PENTON RIBAS[1];
[1]Electrophysiology Core Facility, Univ. of Zurich, Zurich, Switzerland; [2]Univ. Children's Hosp. Zurich, Zurich, Switzerland; [3]ETH Zurich, Zurich, Switzerland

**Abstract:** Understanding how distinct cell types contribute to neural circuit function requires resolving their electrophysiological properties within heterogeneous populations — a challenge that has remained difficult to address at scale. Whole-cell patch-clamp electrophysiology provides unmatched functional resolution, but existing approaches face a fundamental trade-off: manual recordings offer cell-type specificity but are low-throughput, while high-throughput automated patch-clamp (HT-APC) platforms sacrifice cellular identity for scale. Here, we present a fully integrated pipeline that resolves this trade-off by combining HT-APC with correlative fluorescence imaging. Cells are recorded on a Synchropatch 384 platform and subsequently identified through fluorescent cell-type markers or in situ immunostaining, followed by automated high-content microscopy. An open-source R package with an interactive interface handles data integration, quality control, and cell classification based on electrophysiological and imaging features, including dimensionality reduction approaches that reveal population structure across functional and morphological axes. We validate the pipeline in three biological contexts. First, using engineered mixed populations with known electrophysiological and fluorescent properties, we benchmark classification performance and establish ground-truth sensitivity and specificity. Second, in rat primary cortical cultures containing virally labelled excitatory neurons, inhibitory neurons, and astrocytes, we show that hyperactivity-induced homeostatic plasticity differentially affects the current densities of voltage-gated sodium (Nav) and potassium (Kv) channels in excitatory and inhibitory neurons. Third, longitudinal profiling of human iPSC-derived cortical tri-cultures reveals cell-type-specific trajectories of electrophysiological maturation, uncovering differential development of voltage-gated ion channels in neuronal neurons from Sanfilippo syndrome patient and control lines. Together, these applications demonstrate the ability to disentangle functionally distinct neural subpopulations and track their developmental trajectories — capabilities previously inaccessible at this throughput. This pipeline provides a scalable framework for functional phenotyping in complex neural preparations, with broad applicability to disease modelling and drug discovery in the context of neurological disorders.

**Disclosures: D. Colameo:** None. **A. Girard:** None. **A. Schumacher:** None. **G. Schratt:** None. **I. Canals:** None. **D. Penton Ribas:** None.

**Poster**

**PSTR206: Electrophysiology Techniques II**

**Location:** WCC Halls A-C

**Time:** Monday, November 16, 2026, 1:00 PM - 5:00 PM

**Program #/Poster #:** PSTR206.17/LL73

**Topic:** J.04. Physiological Methods

**Support:** NIMH Grant No. R01MH134828
NIMH Grant No. R01MH110487
NIMH Grant No. R21MH132035

**Title:** Automated high-throughput patch clamp electrophysiology of hiPSC derived neuronal models

**Authors: *G. SHIM**[1], I. OSTLUND[2], F. FARINELLI[2], D. DAS[2], S. SRIPATHY RAO[3], S. MYUNG[1,4], R. E. STRAUB[3], B. J. MAHER[6,5,4];
[1]Lieber Inst. for Brain Develop., Baltimore, MD; [2]Lieber Inst. for Brain Develop., BALTIMORE, MD; [3]Lieber Inst. For Brain Develop., Baltimore, MD; [4]Solomon H. Snyder Dept. of Neurosci., [5]Dept. of Psychiatry and Behavioral Sci., Johns Hopkins Univ. Sch. of Med., Baltimore, MD; [6]Lieber Inst. For Brain Develop. / Johns Hopkins Univ. Sch. of Med., Lutherville Timonium, MD

**Abstract:** The advent of human induced pluripotent stem cells (hiPSCs) and their differentiation into neurons and brain organoids has revolutionized our ability to model brain disorders in a human context. However, current technologies to assay the electrophysiological properties of human neurons in these models remain limited by throughput, as single-cell manual patch clamp is laborious and resource intensive. Here, we provide methods to perform automated high-throughput patch-clamp (APC) on hiPSC-derived neurons. We describe how to dissociate and perform voltage-clamp recordings on human neurons from three well-established protocols - 2D directed differentiation of cortical neurons, NGN2-induced neurons, and 3D cortical organoids - using a commercially available high-throughput APC system. Using this approach, we investigated the biophysical properties of voltage-gated sodium channels (VGSCs) and provide direct comparisons between manual and APC recordings across all three hiPSC-derived model systems. We demonstrate the capability of this automated system for pharmacological analysis of native human VGSC isoforms, which will enable compound screening approaches. Lastly, we provide methods to sort specific cellular populations within these hiPSC models using fluorescence-activated cell sorting (FACS) followed by APC. These methods and results provide a transformative and novel high-throughput technique for quantifying passive and active membrane properties in cell-type specific and/or genetically modified hiPSC-derived neurons.

**Disclosures: G. Shim:** None. **I. Ostlund:** None. **F. Farinelli:** None. **D. Das:** None. **S. Sripathy Rao:** None. **S. Myung:** None. **R.E. Straub:** None. **B.J. Maher:** None.

**Poster**

**PSTR206: Electrophysiology Techniques II**

**Location:** WCC Halls A-C

**Time:** Monday, November 16, 2026, 1:00 PM - 5:00 PM

**Program #/Poster #:** PSTR206.18/LL74

**Topic:** J.04. Physiological Methods

**Title:** Advancing Automated Electrophysiology: Single-Channel Recordings in the Cell-Attached Configuration

**Authors: *P. M. VAELLI**[1], K. R. ROSHOLM[2], M. P. KORSGAARD[3];
[1]Res. and Develop., Sophion Biosci., Bedford, MA; [2]Res. and Develop., [3]Sophion Biosci. A/S, Ballerup, Denmark

**Abstract:** Automated patch clamp (APC) platforms have evolved substantially over the past 25 years and are now widely used to address diverse research questions in ion channel pharmacology and physiology. Nevertheless, applications of APC have largely been confined to whole-cell or perforated patch configurations, limiting their utility for investigating channel gating at the single-channel level. Here, we report the establishment of a single-channel recording assay on the QPatch II APC platform. An updated amplifier in this system, with approximately 10-fold lower noise variance than earlier amplifiers, permitted resolution of current steps down to 2 pA. Using this configuration, single-channel activity of recombinantly expressed large-conductance calcium-activated potassium (BK) channels was recorded in HEK293 cells under cell-attached conditions. Channel openings were detected under basal conditions, and open probability increased following addition of ionomycin to the external solution, consistent with calcium-dependent activation. The BK activator, hydrochlorothiazide (HCTZ) and the inhibitor tetraethylammonium (TEA) were used to characterize the channel pharmacologically. Further investigation of other large conductance channels, such as P2X7, TRPV4, and SWELL-1, highlight the variety of single-channel recordings that can be measured on this platform. These results demonstrate the feasibility of performing single-channel assays in the cell-attached mode on an automated patch clamp system using mammalian cell lines. This advancement broadens the scope of APC technologies to include mechanistic studies of channel gating and pharmacology at the single-channel level.

**Disclosures: P.M. Vaelli:** A. Employment/Salary (full or part-time):; Sophion Bioscience Inc. **K.R. Rosholm:** A. Employment/Salary (full or part-time):; Sophion Bioscience A/S. **M.P. Korsgaard:** A. Employment/Salary (full or part-time):; Sophion Bioscience A/S.

**Poster**

**PSTR206: Electrophysiology Techniques II**

**Location:** WCC Halls A-C

**Time:** Monday, November 16, 2026, 1:00 PM - 5:00 PM

**Program #/Poster #:** PSTR206.19/LL75

**Topic:** J.04. Physiological Methods

**Support:** NIH Grant R01NS126143

**Title:** Latent temporal sequences in human cortex are amplified and reorganized by electrical stimulation

**Authors: *A. DULANEY**[1], S. RAJESH[1], H. MOORE[1], E. ZABEH[3], A. H. FREELIN[4], G. KONOPKA[4], B. C. LEGA[2];

[2]Neurosurg., [1]Univ. of Texas Southwestern Med. Ctr., Dallas, TX; [3]Brain Engin. Res. Ctr., Columbia Univ., NewYork, NY; [4]Neurosci., UCLA, Los Angeles, CA

**Abstract:** Temporal sequences, ordered patterns of multi-neuron firing in which order itself carries information, are central to cortical computation, yet whether they are intrinsic to human cortex and how electrical stimulation reshapes them remain unknown. We recorded single-unit activity with high-density microelectrode arrays from ex vivo human temporal neocortex resected during epilepsy surgery (8 patients, 233 neurons), across pre- and post-stimulation epochs separated by 15 min of focal stimulation (bipolar square pulses, 200 μs per phase, 300 mV). Temporal sequences were detected with SPADE (Spike Pattern Detection and Evaluation), its first application to human cortical tissue, and effective connectivity was inferred with a recurrent spiking neural network model. We identified significant temporal sequences (FDR < 0.05 against firing-rate-preserving surrogates) in naive, unstimulated tissue, present in 5 of 8 patients, establishing them as intrinsic to human cortical circuits. Stimulation increased sequences in all 8 patients (Wilcoxon signed-rank, p=0.0078; pooled fold change 9.3, 95% CI 2.7-31.8), an effect not explained by firing rate, as raising rates 2- to 4-fold under high-potassium perfusion produced no comparable rise in sequences. Stimulation recruited previously quiet neurons (1.45 Hz) into sequences while displacing more active ones (3.07 Hz), with net recruitment positive in all 8 patients (Wilcoxon, p=0.0078); 85% of displaced neurons kept firing, indicating reorganization rather than silencing. Pairs that later formed sequences already showed elevated co-firing before stimulation (Fisher's combined $p=6\times10^{-5}$), indicating that the reorganized sequences drew on latent coordination already present in the network. Most post-stimulation sequences were confined to a single cortical layer (17 of 25 groups; Fisher's exact p=0.003), and excitatory neurons disproportionately initiated them (74% of first-firing neurons vs 59% expected; binomial $p=1.3\times10^{-5}$). A recurrent spiking network model fit to each patient (mean r=0.87) revealed a consistent shift toward excitatory effective connectivity in all 8 patients (Wilcoxon p=0.039), providing a mechanism for this excitatory drive. These results establish temporal sequences as an intrinsic feature of human cortical circuits and show that stimulation reorganizes them by recruiting latent neurons and connections through a shift toward excitatory coordination. By converting pre-existing latent structure into organized temporal activity, electrical stimulation may reshape human cortical network dynamics through a targeted mechanism of circuit reorganization.

**Disclosures: A. Dulaney:** None. **S. Rajesh:** None. **H. Moore:** None. **E. Zabeh:** None. **A.H. Freelin:** None. **G. Konopka:** None. **B.C. Lega:** None.

**Poster**

**PSTR206: Electrophysiology Techniques II**

**Location:** WCC Halls A-C

**Time:** Monday, November 16, 2026, 1:00 PM - 5:00 PM

**Program #/Poster #:** PSTR206.20/LL76

**Topic:** J.04. Physiological Methods

**Title:** High-throughput automated patch-clamp electrophysiology of native lysosomes enables scalable functional characterization of lysosomal ion channels

**Authors:** M. RAPEDIUS[1], N. MURCIANO[1], N. PONATH SADANANDAN[2,3], B. MASSON[4], A. SANTINHO[5], H. GAUTIER[5], A. THIAM[5], A. R. OBERGRUSSBERGER[1], ***E. DRAGICEVIC**[1], M. GEORGE[1], C. GRIMM[2,3,6,7], N. FERTIG[1];
[1]Nanion Technologies GmbH, Munich, Germany; [2]Fac. of Medicine, Ludwig-Maximilians-University, Walther Straub Inst. of Pharmacol. and Toxicology, Munich, Germany; [3]Immunology, Infection and Pandemic Res. IIP, Fraunhofer Inst. for Translational Med. and Pharmacol. ITMP, Munich/Frankfurt, Germany; [4]Oria Biosci., Paris, France; [5]ORIA Biosci., Paris, France; [6]Dept. of Pharmacol., Fac. of Medicine, Univ. of Oxford, Oxford, United Kingdom; [7]Member of the German Ctr. for Lung Res. (DZL), Comprehensive Pneumology Ctr. Munich, Munich, Germany

**Abstract:** Intracellular ion channels in lysosomes and mitochondria regulate cellular homeostasis, signaling, and neurodegenerative pathways, making them attractive therapeutic targets. However, direct electrophysiological characterization in native organelles remains challenging due to the low throughput of manual approaches. To address this limitation, we developed specialized consumables and protocols enabling high-throughput automated patch-clamp (HT-APC) recordings from isolated native lysosomes and mitochondria using the SyncroPatch 384. Lysosomes were obtained either from highly purified microfluidics-based preparations (Lyso-Prep™, ORIA Bioscience) or by modified differential ultracentrifugation. Biochemical analyses confirmed lysosomal purity for both approaches. Automated recordings achieved lysosome capture rates of 88.2 ± 2.7% and giga-seal rates of 79.6 ± 1.6%, corresponding to ~300 patched lysosomes per run. Following predefined quality-control criteria, 45-55% of recordings were accepted for analysis, yielding >100-200 simultaneously recorded lysosomes per experiment and supporting ~1,500-2,000 recordings per day. Both isolation methods yielded comparable electrophysiological and pharmacological results. Using lysosomes expressing TRPML1, TMEM175, or TPC2, we performed pharmacological characterization with established agonists and antagonists. TRPML1 activation by MLSA-1 produced concentration-dependent current increases with EC50 values of 3-6 µM, consistent with manual lysosomal patch clamp. TMEM175 recordings suggested temperature-dependent regulation, whereas pharmacological potency remained unchanged (DCPIB/TUG-891 $EC_{50}$: 8.6 ± 3.8 µM at 21°C, n=50; 8.7 ± 4.4 µM at 35°C, n=38). TPC2 currents displayed expected activation by $PI(3,5)P_2$ and inhibition by ATP, consistent with observations from manual lysosomal patch clamp. The workflow was transferable to isolated mitochondria, demonstrating the applicability of HT-APC to intracellular organelles. Recordings from isolated mitochondria (Mito-Prep™, ORIA Bioscience) overexpressing MCU revealed inward currents that increased in the presence of extracellular $Ca^{2+}$ and were inhibited by 1 µM Ruthenium Red. Population analysis (n=50) demonstrated a significant increase in current amplitude at −150 mV following $Ca^{2+}$ application and reversal by Ruthenium Red. Collectively, these results establish HT-APC on native lysosomes and mitochondria as a robust and scalable platform for organelle-level pharmacology, target validation, and drug discovery.

**Disclosures: M. Rapedius:** A. Employment/Salary (full or part-time):; Nanion Technologies GmbH. **N. Murciano:** A. Employment/Salary (full or part-time):; Nanion Technologies GmbH. **N. Ponath Sadanandan:** None. **B. Masson:** A. Employment/Salary (full or part-time):;

Oria Bioscience. **A. Santinho:** A. Employment/Salary (full or part-time):; ORIA Bioscience. **H. Gautier:** A. Employment/Salary (full or part-time):; ORIA Bioscience. **A. Thiam:** A. Employment/Salary (full or part-time):; ORIA Bioscience. **A.R. Obergrussberger:** A. Employment/Salary (full or part-time):; Nanion Technologies GmbH. **E. Dragicevic:** A. Employment/Salary (full or part-time):; Nanion Technologies GmbH, Oria Bioscience. **M. George:** A. Employment/Salary (full or part-time):; Nanion Technologies GmbH. **C. Grimm:** None. **N. Fertig:** A. Employment/Salary (full or part-time):; Nanion Technologies GmbH.

**Poster**

**PSTR206: Electrophysiology Techniques II**

**Location:** WCC Halls A-C

**Time:** Monday, November 16, 2026, 1:00 PM - 5:00 PM

**Program #/Poster #:** PSTR206.21/LL77

**Topic:** J.04. Physiological Methods

**Support:** NIH Grant R15NS133861

**Title:** Automatic Machine-Controlled AI-Driven Fabrication of Customizable Microwire-based Microelectrode Arrays for Electrophysiological Recordings

**Authors:** K. LAT[1], M. JOVIC[1], J. HARTNER[2], B. O. WATSON[2], ***L. CHEN**[1];
[1]Dept. of Mechanical and Industrial Engin., Univ. of Massachusetts Lowell, Lowell, MA; [2]Dept. of Psychiatry, Univ. of Michigan, Ann Arbor, MI

**Abstract:** Microwire-based microelectrode arrays (MEAs) have long been a powerful tool for electrophysiological recordings due to their low cost, customizability, and superior long-term recording performance. However, compared with alternative neural interfaces such as MEMS-based probes, microwire MEAs are constrained by labor-intensive fabrication processes that rely on manual wire placement and visual alignment. These methods result in low yield and throughput, particularly for complex, large-scale arrays. To address this challenge, we developed a custom machine that automates fabrication of microwire-based MEAs using advanced wire tip preparation, direct-ink-writing (DIW)-based circuit printing, and image recognition and machine-learning control algorithms for assembly alignment. This system enables neuroscience laboratories to fabricate custom microwire MEAs in-house with minimal engineering expertise.Key enabling technologies include: (1) laser-based contactless tip preparation for cellular-scale microwires, including 7 μm carbon fibers and 12 μm tungsten wires, performing simultaneous wire cutoff, conical tip sharpening, and insulation stripping in a single pass; (2) DIW-based circuit creation on both rigid and flexible substrates; and (3) open-source computer-vision and AI-driven motion control for alignment between MEA substrates, printing nozzles, and microwires. The fabrication machine consists of low-cost linear and rotary stages, USB cameras with lighting, and easily replicated 3D-printed fixtures and actuators, enabling low-cost deployment in neuroscience laboratories for in-house custom microwire MEA fabrication. Proof-of-concept MEAs fabricated from carbon fiber (4–9 μm diameter) and metal wire (tungsten and stainless steel, 12–100 μm diameter) on FR4 and Kapton substrates under various configurations

achieved the desired impedance range (20–200 kΩ at 1 kHz) with yields exceeding 90%.Chronic electrophysiological recording results in Nile grass rats demonstrated that fully automated machine-fabricated microwire arrays (8-wire MEAs) provided stable, high-quality neural recordings for over multiple months. Robust multi-unit activity persisted for several weeks post-implantation, while local field potential analysis revealed normal sleep–wake dynamics, including elevated delta power during non-REM sleep and elevated theta power during active states. These findings indicate that machine-fabricated MEAs achieve chronic recording performance comparable to conventionally hand-made arrays.

**Disclosures: K. Lat:** None. **M. Jovic:** None. **J. Hartner:** None. **B.O. Watson:** None. **L. Chen:** None.

**Poster**

**PSTR206: Electrophysiology Techniques II**

**Location:** WCC Halls A-C

**Time:** Monday, November 16, 2026, 1:00 PM - 5:00 PM

**Program #/Poster #:** PSTR206.22/LL78

**Topic:** J.04. Physiological Methods

**Support:** NSF Grant 2347299

**Title:** Title: Piezoelectric Actuator-Based Incremental Insertion Robot for Buckling-Free Membrane Penetration and Deep Implantation of Neural Interfaces

**Authors:** K. LAT[1], X. CHEN[1], J. HARTNER[4], ***B. O. WATSON**[5], N. JAFFERIS[2], L. CHEN[3]; [2]Electrical and Computer Engin., [3]Dept. of Mechanical and Industrial Engin., [1]Univ. of Massachusetts Lowell, Lowell, MA; [4]Univ. of Michigan Molec & Behav Neurosci Inst. (MBNI), Ann Arbor, MI; [5]Univ. of Michigan, Ann Arbor, MI

**Abstract:** Minimally invasive neural interfaces, such as cellular-scale microwires and flexible polymer probes, can improve chronic recording quality by reducing tissue damage and immune response. However, their small size and flexibility also make the implantation process challenging, as the electrodes often buckle when penetrating brain membranes using conventional stereotaxic methods. Previous approaches to prevent buckling via shuttles and backbone supports (permanent or temporary) typically increase insertion damage and/or surgical complexity, while other alternatives rely on bulky insertion systems unsuitable for high-density implants.To address electrode buckling during implantation, we developed a miniaturized piezoelectric inchworm insertion robot that incrementally advances neural electrodes through a cyclic grip-insert-release motion, minimizing unsupported electrode length and increasing buckling resistance. The robot employs three custom piezoelectric unimorph actuators functioning as two alternating grippers and one insertion actuator, enabling automated electrode advancement with high precision in a compact 14 × 5.8 × 3.6 mm, 250 mg package suitable for use within the confined space of rodent neurosurgery. The piezoelectric actuators provide programmable insertion increments as small as 10 µm, up to 80 µm insertion stroke per cycle,

insertion speeds up to 14 mm/s, and gripping/insertion forces approaching 950 mN. The actuator-driven design also enables automated depth control and compatibility with a wide range of neural interfaces, including microwires and multi-shank silicon probes.Benchtop validation studies using a multi-layer dura-pia-brain phantom demonstrated buckling-free insertion of ultra-thin tungsten microwires (12-25 μm diameter) and 15 μm-thick silicon probes through both dura and pia membrane layers. Compared with conventional static insertion approaches, the inchworm mechanism reduced membrane rupture force and dimpling depth while enabling penetration of membrane layers that are typically difficult or impossible for ultra-flexible electrodes to traverse.Results from animal tests showed that the developed inchworm insertion robot could (1) insert 15 μm thick silicon probes into Nile Grass Rats through both the dura and pia mater without buckling, (2) accurately target medial prefrontal cortex (mPFC) and CA1 of the dorsal hippocampus via the robot's precise increment control, and (3) generate high quality PFC and CA1 recordings from the inchworm-implanted probes for multiple weeks with normal local field potential and spiking activity.

**Disclosures: K. Lat:** None. **X. Chen:** None. **J. Hartner:** None. **B.O. Watson:** None. **N. Jafferis:** None. **L. Chen:** None.

**Poster**

**PSTR206: Electrophysiology Techniques II**

**Location:** WCC Halls A-C

**Time:** Monday, November 16, 2026, 1:00 PM - 5:00 PM

**Program #/Poster #:** PSTR206.23/LL79

**Topic:** J.04. Physiological Methods

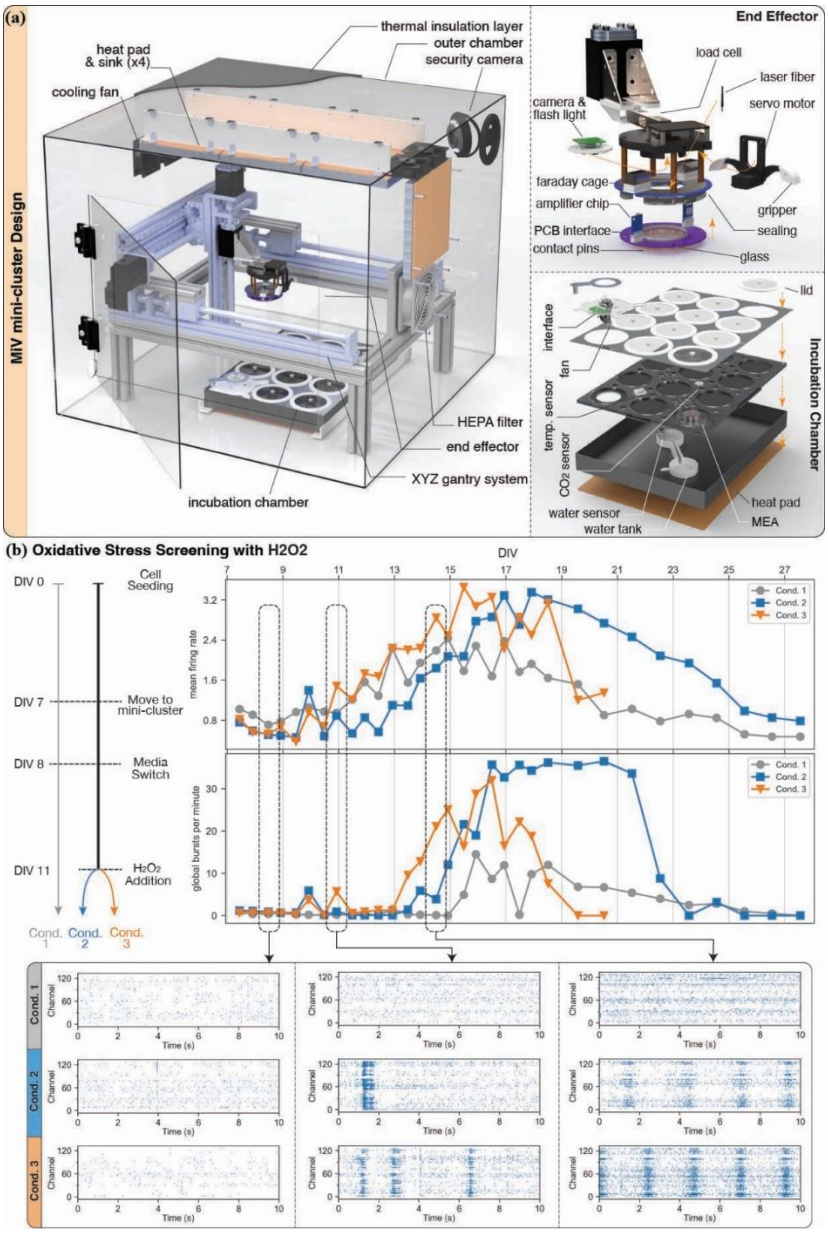
**Support:** NSF Grant 2123781

**Title:** Mind in Vitro Mini-Cluster: An automated electrophysiology platform for high-throughput screening and modulation

**Authors: *H. YUAN**, Z. SONG, M. GAZZOLA;
Univ. of Illinois Urbana-Champaign, Urbana, IL

**Abstract:** In vitro electrophysiology is a reduced yet valuable testbed for studying neural network maturation, perturbation responses, and disease-relevant dynamics. Current microelectrode array (MEA) workflows rely on manual sample handling and force a trade-off between throughput and flexibility. To address this gap, we developed MiV Mini-Cluster, an automated platform combining incubator-like environmental control with robotic access to neuronal cultures. The system integrates a robotic interface for bidirectional communication with neural substrates and a distributed culture-maintenance system around an incubation chamber. For system validation, we quantified culture viability during incubation and spontaneous network activity after robotic access. Environmental control maintained viability comparable to standard incubators, and robotic end-effector access did not perturb spontaneous activity. Cultures could be recorded without waiting for activity to re-equilibrate, as required after conventional manual

transfer. We then used MiV Mini-Cluster for longitudinal oxidative-stress screening in mouse embryonic stem cell-derived motor neuron cultures exposed to 0, 50, or 100 µM hydrogen peroxide (H2O2; n=6 cultures/condition). Cultures were monitored for >16 consecutive days. Higher H2O2 concentration increased network burst rate, demonstrating detection of long-term, concentration-dependent functional changes. Optical stimulation was validated by using the integrated fiber to reliably evoke network bursts in optogenetic motor neuron cultures. These results establish MiV Mini-Cluster as an automated interface for maintaining, accessing, stimulating, and repeatedly recording from in vitro neuronal networks, providing a hardware foundation for autonomous neuroscience workflows.




**Disclosures: H. Yuan:** None. **Z. Song:** None. **M. Gazzola:** None.

**Poster**

**PSTR206: Electrophysiology Techniques II**

**Location:** WCC Halls A-C

**Time:** Monday, November 16, 2026, 1:00 PM - 5:00 PM

**Program #/Poster #:** PSTR206.24/LL80

**Topic:** J.04. Physiological Methods

**Title:** Modulation of Theta-Gamma Phase-Amplitude Coupling Following Hippocampal Transcranial Focused Ultrasound

**Authors: *Y. CHEN**, M. MONTENEGRO, Y.-H. WANG, Z. HUANG, Y. LEI;
Kinesiology and Sport Mgmt., Texas A&M Univ., College Station, TX

**Abstract:** Transcranial focused ultrasound stimulation (tFUS) is an emerging noninvasive neuromodulation technique capable of targeting deep brain structures, such as the hippocampus, with high spatial precision. Cognitive functions mediated by the hippocampus, such as memory consolidation and information routing, depend heavily on the precise cross-frequency synchronization of multi-scale neural oscillations. To capture these dynamics, this study characterized theta-gamma phase-amplitude coupling (PAC)—a mechanism reflecting the integration of widespread, long-range network coordination (theta) with localized cortical computation (gamma). Consequently, PAC serves as a critical electrophysiological marker of hippocampal-cortical communication. However, whether these deep-brain network dynamics can be modulated by tFUS—and subsequently detected using noninvasive scalp EEG—remains poorly understood. To address this, we aimed to validate the utility of scalp EEG in tracking the network-level effects of a hippocampal tFUS protocol. A cohort of healthy adults underwent resting-state EEG recordings before and after stimulation. Ultrasound was delivered through the left temporal acoustic window to target the right hippocampus. Power spectral density (PSD) was analyzed for theta and gamma frequency bands, and theta-gamma PAC was quantified across cortical regions of interest using a modulation index approach. Analyses revealed significant post-stimulation shifts in resting-state oscillatory activity. Specifically, tFUS induced a marked reduction in theta-gamma PAC following stimulation, a decrease that was prominently localized to the temporal, parietal, and central cortical regions. These findings demonstrate that hippocampal tFUS alters large-scale neural dynamics that are directly detectable via scalp EEG. Moreover, characterizing localized alterations in theta-gamma coupling provides a robust, noninvasive readout of deep-brain neuromodulation, highlighting the utility of EEG in mapping the network-level effects of focused ultrasound in humans.

**Disclosures: Y. Chen:** None. **M. Montenegro:** None. **Y. Wang:** None. **Z. Huang:** None. **Y. Lei:** None.

**Poster**

**PSTR206: Electrophysiology Techniques II**

**Location:** WCC Halls A-C

**Time:** Monday, November 16, 2026, 1:00 PM - 5:00 PM

**Program #/Poster #:** PSTR206.25/LL81

**Topic:** J.04. Physiological Methods

**Support:** Beijing Municipal Natural Science Foundation "Qiyan" Program for Undergraduates QY26448
Tsinghua University "Undergraduate Academic Research Promotion Program" Level A
Tsinghua University WeiXian College "Pioneer Program" for Undergraduate Research

**Title:** A light-weight wireless brain-computer interface for multimodal neural recording and real-time state decoding in freely moving mice

**Authors: *W. ZHANG**[1], Y. ZHANG[2];
[2]Life Sci., [1]Tsinghua Univ., Beijing, China

**Abstract:** Electrophysiological monitoring during natural behavior requires lightweight instrumentation that minimizes tethering and head-borne load while preserving signal quality and supporting rapid state analysis. We developed an integrated wireless brain-computer interface for freely moving mice that combines a configurable flexible printed circuit (FPC) cortical electrode, an ADS1299 low-noise front end, an ESP32 microcontroller, Bluetooth Low Energy transmission, triaxial accelerometry, a desktop graphical interface, and lightweight neural-state classifiers. The standard FPC layout targeted visual, somatosensory, and motor cortices, while recording sites could be reconfigured for specific experiments. Custom 316L medical-grade stainless-steel skull screws provided corrosion-resistant, biocompatible contacts, and a 3D-printed headpiece enabled removal and reuse of the PCB after recording. The head-mounted PCB measured 14 × 17 mm, the complete device weighed 1.2 g, and up to eight biopotential channels could be configured for EEG, EMG, or ECG acquisition at 1 kHz. Adult male C57BL/6J mice (n=10) contributed 30 sessions totaling approximately 10 h; sex differences were not assessed. Under matched bench-test conditions, input-referred noise was 0.8 μV RMS versus 8.2 μV RMS for a commercial wired reference system, and BLE packet loss remained below 2% under the tested conditions. The software supported real-time waveform visualization, filtering, spectral analysis, asynchronous storage, and host-side model inference. An offline workflow performed artifact screening, re-referencing, signal-to-noise quantification, band-power analysis, and functional-connectivity analysis. Feasibility was evaluated during social interaction, open-field exploration, steady-state visual evoked potential stimulation, and simultaneous ECG-EEG recording. Lightweight deep learning models for sleep- and seizure-state classification were trained, exported to ONNX, and validated through offline replay; the sleep-stage classifier achieved 92.3% accuracy. These results demonstrate the feasibility of a lightweight, modular platform for wireless multimodal electrophysiology and real-time state analysis in freely behaving mice. By integrating reconfigurable sensing, continuous multimodal monitoring, and real-time brain-state decoding, this platform provides a flexible foundation for investigating diverse neural dynamics and behavior, with potential extension to event-triggered closed-loop neuromodulation.

**Disclosures: W. Zhang:** None. **Y. Zhang:** None.

**Poster**

**PSTR206: Electrophysiology Techniques II**

**Location:** WCC Halls A-C

**Time:** Monday, November 16, 2026, 1:00 PM - 5:00 PM

**Program #/Poster #:** PSTR206.26/LL82

**Topic:** J.04. Physiological Methods

**Support:** JST K Program Grant JPMJKP25Y2

**Title:** Reproducible, lateralized movement-related cortical activity measured non-invasively with a novel magnetic field biased probe (MBP) : a whole-head feasibility study

**Authors: *K. KUWABARA**, M. YANAGIDA, N. MUKAE, O. HIWAKI, K. YOSHIMOTO; Dept. of Neurosurgery, Grad. Sch. of Med. Sciences, Kyushu Univ., Fukuoka, Japan

**Abstract:** Non-invasive readout of cortical activity is central to systems and clinical neuroscience, yet existing modalities trade off temporal and spatial resolution. MBP is a novel magnetic brain-function method applying a weak static bias field, hypothesized to detect neural-current-related signals largely from cortex beneath each coil without inverse-problem reconstruction, in principle distinct from magnetoencephalography (MEG). We asked whether a whole-head MBP system can reproducibly capture lateralized, movement-related cortical responses. Five healthy adults performed metronome-paced index-finger movements (right, left, and bimanual) during whole-head recording with a 159-channel MBP system. Movement onset was detected with an infrared sensor, and trials were block-averaged after standard preprocessing. Responses were examined over regions of interest set a priori near left and right primary motor cortex (M1). We assessed within-subject reproducibility, cross-subject similarity of the contralateral waveform, the timing of the early steepest-rise component via temporal differentiation, and contralateral versus ipsilateral M1 polarity, including bimanual effects. Movement elicited a clear, time-locked response near contralateral M1 in every subject, with high within-subject reproducibility in waveform and topography. Across subjects, the contralateral response showed appreciable similarity, strongest in an early post-movement window (within roughly the first 150 ms), while later activity was more variable. Because raw peak latencies varied, we used temporal differentiation to index the steepest rise; the rate-of-change peaked within an early window common to all subjects, and this early component was consistent across subjects and hands, broadly compatible with early movement-related activity reported with MEG. Responses near M1 showed a roughly symmetric polarity structure: contralateral M1 was predominantly one polarity (a putative primary motor component), whereas ipsilateral M1 tended toward the opposite polarity in many subjects. This ipsilateral activity, and the modulation of lateralization during bimanual movement, varied across subjects and hands and were more variable than the contralateral component, compatible with interhemispheric inhibition. These exploratory results indicate that whole-head MBP can reproducibly capture lateralized, polarity-structured movement-related cortical activity, including a consistent early

component and signs of interhemispheric inhibition. The sample is being expanded, with MRI co-registration planned to confirm M1 and examine the signal mechanism.

**Disclosures: K. Kuwabara:** None. **M. Yanagida:** None. **N. Mukae:** None. **O. Hiwaki:** None. **K. Yoshimoto:** None.

**Poster**

**PSTR206: Electrophysiology Techniques II**

**Location:** WCC Halls A-C

**Time:** Monday, November 16, 2026, 1:00 PM - 5:00 PM

**Program #/Poster #:** PSTR206.27/LL83

**Topic:** J.04. Physiological Methods

**Title:** Assessment of Drug-Induced Calcium Oscillations in hiPSC-Derived Neuron-Astrocyte Cocultures Using FDSS

**Authors: *D. KURGANOVA**[1], B. FRAHER[1], C. TICAS RODAS[1], A. MANTEY[2], L. AGBOR[1], C. KETTULA[1], T. TANAKA[1];
[1]Ricoh Biosci., Baltimore, MD; [2]Ricoh Biosciences, Inc, Baltimore, MD

**Abstract:** Human induced pluripotent stem cell (hiPSC)-derived models provide a physiologically relevant alternative to traditional animal systems for investigating neuronal network function and its pharmacological modulation in vitro. In this study, excitatory neurons and astrocytes generated from hiPSCs were co-cultured in a 96-well format for up to 42 days, during which spontaneous network activity was monitored using fluorescence-based calcium imaging with the Functional Drug Screening System (FDSS). Calcium signals were recorded for 1,000 s at 1 s intervals, and all experimental conditions were evaluated in three independent replicates. FDSS recordings revealed stable, synchronized spontaneous calcium oscillations over time, consistent with the formation of mature and functionally connected neuronal networks. Network activity was quantified using oscillation amplitude and the number of peaks. To evaluate the functional maturation of the neuronal networks, the following panel of pharmacological agents that induce known neuronal responses were applied to the culture at three increasing doses: the neurotransmitters glutamate and GABA, the AMPA/kainate receptor antagonist CNQX, and the ion channel modulators carbamazepine and 4-aminopyridine (4-AP).Vehicle controls (0.1% DMSO or water) produced minimal changes in either oscillation amplitude or peak frequency. GABA completely suppressed spontaneous calcium activity at all tested concentrations. Glutamate produced little effect at 3 μM but abolished network activity at 30 and 300 μM, consistent with network-level excitotoxic suppression. Carbamazepine significantly reduced activity at 30 μM and completely suppressed calcium oscillations at 300 μM.CNQX induced a progressive, concentration-dependent reduction in both oscillatory activity and peak frequency across concentrations ranging from 5 to500 μM. In contrast, 4-aminopyridine increased calcium peak frequency at 1 and10 μM, consistent with enhanced neuronal excitability. These findings demonstrate that hiPSC-derived neuron-astrocyte co-cultures develop robust spontaneous network activity and exhibit reproducible, mechanism-

consistent drug-induced responses that can be quantified using complementary measures of calcium oscillation amplitude and event frequency. This quantitative assay provides a scalable approach for investigating neuronal network physiology, evaluating the effects of pharmacological agents on neural excitability, and characterizing disease-associated functional phenotypes in patient-derived hiPSC models for translational neuroscience and drug discovery.

**Disclosures: D. Kurganova:** None. **B. Fraher:** None. **C. Ticas Rodas:** None. **A. Mantey:** None. **L. Agbor:** None. **C. Kettula:** None. **T. Tanaka:** None.

**Poster**

**PSTR207: Computational Methods for Experimental Neuroscience**

**Location:** WCC Halls A-C

**Time:** Monday, November 16, 2026, 1:00 PM - 5:00 PM

**Program #/Poster #:** PSTR207.01/LL84

**Topic:** J.06. Computation, Modeling, and Simulation

**Title:** Examining the Generalizability of Deep Learning Methods for Perivascular Space Segmentation

**Authors: *S. TANG**[1,2], P. THROPP[3], K. YOUNES[4], D. TOSUN[3];
[1]Univ. of California - Berkeley, Berkeley, CA; [2]Bioengineering, [3]Radiology, Univ. of California San Francisco, San Francisco, CA; [4]Neurol., Stanford Univ., Palo Alto, CA

**Abstract:** Introduction: Perivascular spaces (PVS) are increasingly recognized as biomarkers of neurological disease. Automated segmentation methods circumvent manual labeling, but often struggle on external datasets despite strong internal performance. We evaluated three nnUNet-based methods across multiple datasets, clinical, and acquisition categories to assess generalizability.
Methods: Models included mcPVS-Net (Huang et al., 2024), T1w and T1w+FLAIR nnUNet (Pham et al., 2026) and an in-house nnUNet (Tang et al., 2026). Datasets included 60 3T T1w+FLAIR images from ADNI-3, an Alzheimer's-focused dataset (CU=20, MCI=20, AD=20) and 12 from the publicly available VALDO dataset (3T: n=6, 1.5T: n=6). Performance was assessed using precision, recall, dice (DSC), and count/volume correlations, stratified by brain region, diagnostic, scanner and clinical groups, and via weighted kappa (k) and percent agreement (PA) for the latter.
Results: Summarized in Table 1. On ADNI-3, the in-house model performed best (DSC=0.61), followed by T1w nnUNet (DSC=0.27), mcPVS-Net (DSC=0.24), and T1w+FLAIR nnUNet (DSC=0.21). It also ranked the highest across region, diagnostic, scanner and clinical groups, and had the best agreement with clinical ratings (k=0.9, PA=82%). Count/volume correlations were similar across the top three models ($r \sim 0.73$-$0.83$, $p<0.001$). All models performed better in white matter and in higher-burden images. Performance decreased markedly on VALDO, with the in-house model scoring lowest (3T DSC=0.002, 1.5T DSC=0.001).
Discussion: This study highlights generalizability gaps that persist despite controlling for dataset heterogeneity during model development. Model robustness also varied by categories,

underscoring the need for validation using task-specific metrics. These results suggest caution in deploying PVS models without external validation, especially when the research aim depends on robust performance across specific categories. Further development with large, diverse datasets are likely needed to advance PVS segmentation toward clinical use.

Table 1a. Overall Segmentation Performance

| Dataset | ADNI-3 (n=60) | | | | | VALDO 3T (n=6) | | | VALDO 1.5T (n=6) | | |
|---|---|---|---|---|---|---|---|---|---|---|---|
| Model | Sensitivity | Precision | DSC | Count r | Volume r | Sensitivity | Precision | DSC | Sensitivity | Precision | DSC |
| mcPVS-Net | 0.72±0.21 | 0.15±0.10 | 0.24±0.13 | 0.83* | 0.79* | 0.18±0.06 | 0.47±0.21 | 0.23±0.09 | 0.21±0.14 | 0.02±0.02 | 0.03±0.03 |
| T1w nnU-Net | 0.56±0.23 | 0.20±0.13 | 0.27±0.14 | 0.79* | 0.76* | 0.14±0.08 | 0.34±0.17 | 0.17±0.07 | 0.10±0.07 | 0.01±0.00 | 0.02±0.01 |
| T1w+FLAIR nnU-Net | 0.21±0.20 | 0.31±0.23 | 0.21±0.16 | 0.49* | 0.44* | 0.02±0.01 | 0.30±0.21 | 0.03±0.03 | 0.03±0.02 | 0.02±0.02 | 0.02±0.01 |
| In-house nnU-Net | 0.62±0.20 | 0.66±0.17 | 0.61±0.13 | 0.80* | 0.73* | 0.001±0.002 | 0.350±0.505 | 0.002±0.004 | 0.000±0.001 | 0.006±0.010 | 0.001±0.001 |

** p<0.001. DSC = Dice similarity coefficient; r = Spearman correlation. All scores reported as mean ± SD.*

Table 1b. Categorical Performance (reported as DSC scores) (ADNI-3, n=60)

| Category | Region | | Diagnostic | | | Scanner Type | | | Clinical Rating | | | | Clinical Rating Agreement | |
|---|---|---|---|---|---|---|---|---|---|---|---|---|---|---|
| Model | WM | BG | CU (n=20) | MCI (n=20) | AD (n=20) | GE (n=13) | Philips (n=8) | Siemens (n=39) | Rating 1 (n=6) | Rating 2 (n=5) | Rating 3 (n=11) | Rating 4 (n=38) | Kappa (k) | % Agree (PA) |
| mcPVS-Net[c] | 0.21±0.12 | 0.20±0.15 | 0.23±0.12 | 0.24±0.16 | 0.24±0.10 | 0.23 ± 0.12 | 0.30 ± 0.14 | 0.18 ± 0.10 | 0.23±0.12 | 0.11±0.04 | 0.18±0.10 | 0.29±0.11 | 0.00 | 63% |
| T1w nnU-Net[s,c] | 0.25±0.14 | 0.20±0.17 | 0.25±0.14 | 0.29±0.14 | 0.27±0.12 | 0.27 ± 0.13 | 0.36 ± 0.12 | 0.13 ± 0.07 | 0.27±0.13 | 0.22±0.10 | 0.21±0.12 | 0.32±0.12 | 0.33 | 70% |
| T1w+FLAIR nnU-Net[s,c] | 0.22±0.16 | 0.04±0.10 | 0.23±0.15 | 0.19±0.15 | 0.19±0.17 | 0.24 ± 0.14 | 0.04 ± 0.07 | 0.29 ± 0.14 | 0.24±0.14 | 0.08±0.17 | 0.21±0.12 | 0.22±0.15 | 0.31 | 37% |
| In-house nnU-Net[s] | 0.54±0.19 | 0.34±0.24 | 0.57±0.18 | 0.61±0.08 | 0.60±0.11 | 0.58 ± 0.15 | 0.62 ± 0.06 | 0.64 ± 0.09 | 0.58±0.15 | 0.59±0.12 | 0.60±0.11 | 0.62±0.09 | 0.90 | 82% |

*All DSC reported as mean ± SD. k = weighted Cohen's kappa. Clinical ratings were based on Potter et al. (2015) following STRIVE criteria. Ratings are based on counts of PVS and binned as follows: rating 1=1-10, rating 2=11-20, rating 3=21-40, rating 4=40+. WM = white matter; BG = basal ganglia; CU = cognitively unimpaired; MCI = mild cognitive impairment; AD = Alzheimer's disease. Superscripts on model names indicate significant performance differences between scanner (s) or clinical rating groups (c) (Kruskal-Wallis test, p<0.05).*

**Disclosures: S. Tang:** None. **P. Thropp:** None. **K. Younes:** None. **D. Tosun:** None.

**Poster**

**PSTR207: Computational Methods for Experimental Neuroscience**

**Location:** WCC Halls A-C

**Time:** Monday, November 16, 2026, 1:00 PM - 5:00 PM

**Program #/Poster #:** PSTR207.02/LL85

**Topic:** J.06. Computation, Modeling, and Simulation

**Support:** NIMH L70-MH134315
NIMH T32-MH015144
NIMH K08-DK132493
NY Obesity and Nutrition Research Center Pilot and Feasibility Grant
BBRF-NARSAD Young Investigator Award
Russell Berrie Foundation Frontiers Program in Diabetes Research
NIGMS K99-GM153720

**Title:** A two-timepoint pipeline for sensitive and specific single-cell activity screening

**Authors: *E. J. KYZAR**[1], A. RAMIREZ[1], L. ROGERSON[1], R. SETARA[1], M. EISENGART[1], S. VIRKAR[1], E. RODRIGUEZ[1], L. A. HAMMOND[2], C. D. SALZMAN[1];
[1]Columbia Univ., New York, NY; [2]The Ohio State Univ., Columbus, OH

**Abstract:** Neural activity screening to identify brain areas where neurons are activated in response to specific stimuli or internal states typically rely on immediate early gene (IEG) expression. However, intrinsic variability in IEG expression across subjects and brain areas often necessitates large sample sizes to detect differences in stimulus-evoked activity. Further, IEG expression alone cannot determine whether the same or different neurons are activated in response to two distinct stimuli or states. To overcome these challenges, we developed a brain screening method - two timepoint statistical inference with subtraction (TTP-S) - to identify brain areas on the basis of activity at two timepoints, not one. Our approach involves exposing Trap2:Ai14 mice to two presentations of the stimulus of interest, followed by whole-brain staining for IEGs. We then utilize automated cell-counting methods to detect overlapping cells active at both timepoints, which allows us to compute whether neurons in a particular brain area demonstrate more or less overlap than would be expected by chance. One can also expose mice to distinct opposing stimuli (such as fasting and re-feeding) to explore regions with intermingled, functionally-opposed neural populations. Applying this statistical approach across 500+ brain areas vastly increases the sensitivity and specificity of screens for stimulus-evoked activity across brain areas, thereby reducing required sample sizes. The TTP-S pipeline is designed to be modular, open-source, and to accommodate multiple use cases and imaging/staining methodologies. Coupled with graph theoretical analyses, we use this method to analyze hunger, satiety, GLP1 receptor agonist treatment, alcohol consumption and alcohol withdrawal, identifying known relevant brain areas and implicating other novel areas. In the case of alcohol withdrawal, we show how TTP-S can be combined with individual-level behavioral data to link specific brain areas to alterations in exploration. Taken together, TTP-S offers a new tool to analyze the engagement of regions across nearly the entire brain in response to numerous stimuli and internal states.

**Disclosures: E.J. Kyzar:** None. **A. Ramirez:** None. **L. Rogerson:** None. **R. Setara:** None. **M. Eisengart:** None. **S. Virkar:** None. **E. Rodriguez:** None. **L.A. Hammond:** None. **C.D. Salzman:** None.

**Poster**

**PSTR207: Computational Methods for Experimental Neuroscience**

**Location:** WCC Halls A-C

**Time:** Monday, November 16, 2026, 1:00 PM - 5:00 PM

**Program #/Poster #:** PSTR207.03/LL86

**Topic:** J.06. Computation, Modeling, and Simulation

**Support:** Wellcome Trust (grant no. 226486/Z/22/Z, Principal Investigator F. Pestilli)
NINDS UM1NS132207, BRAIN CONNECTS: Center for Mesoscale Connectomics (Principal Investigator K. Ugurbil)
NINDS U24NS140384, BRAIN CONNECTS: The Axonal Projectome EXchange

(APEX) (Principal Investigator F. Pestilli)
Amazon Web Services Open Data Sponsorship Program

**Title:** Benchmarking generalizability in deep learning-based white matter tract segmentation

**Authors: *J. KWON**, G. AMOROSINO, F. PESTILLI;
Psychology, The Univ. of Texas at Austin, Austin, TX

**Abstract:** White matter tracts form the brain's structural pathways for information transfer, and accurate white matter tract segmentation (WMTS) from diffusion MRI is essential for studying brain connectivity. Since TractSeg, deep learning models have become central to voxel-wise WMTS, yet benchmarks have largely relied on a single manually curated set of 105 Human Connectome Project subjects, leaving generalization across protocols and populations unclear. We built and released through brainlife.io a reproducible 1,455-subject benchmark spanning three public datasets: 1057 HCP young adults, 288 Cam-CAN adults, and 110 PING pediatric/adolescent participants. Using a standardized brainlife.io pipeline, we generated fODF peak maps and 61 tract masks per subject with CSD, tractography, and WMQL segmentation. We trained four WMTS architectures: TractSeg, MedNeXt, SwinUNETR, and MA-SAM adapted from Segment Anything Model. Models were evaluated across 15 training-test combinations spanning three settings: homogeneous within-domain training, with training and testing in the same dataset; heterogeneous within-domain training, with pooled training and separate testing on each dataset; and out-of-domain transfer, with one or two source datasets tested on a held-out target. Performance was quantified by Dice, and predictions were combined using majority voting and STAPLE. Within-domain homogeneous training achieved the highest accuracy on HCP data (Dice = 0.792 ± 0.019), with lower performance on PING (Dice = 0.736 ± 0.025) and Cam-CAN (Dice = 0.674 ± 0.040). CNN-based models performed best within-domain, consistent with the local spatial structure of fODF peak data. Heterogeneous within-domain training did not reliably outperform homogeneous training on each target dataset, showing that adding heterogeneous data does not guarantee better target-dataset performance. Out-of-domain transfer caused substantial degradation, especially across diffusion shell composition and age. The largest failure occurred when adult-trained HCP models were applied to pediatric PING data (Dice = 0.196). Under domain shift, transformer-based models showed smaller relative performance drops than CNN-based models, suggesting greater tolerance to domain shift. On the hardest transfer, HCP to PING, STAPLE improved Dice from 0.18 to 0.30 compared with majority voting (67% improvement, $p < 0.001$). These results show that current WMTS models generalize poorly under realistic scanner and population shifts. This benchmark exposes cross-cohort failure modes and supports ensemble integration as a practical strategy when no single architecture is robust across domains.

**Disclosures: J. Kwon:** None. **G. Amorosino:** None. **F. Pestilli:** None.

**Poster**

**PSTR207: Computational Methods for Experimental Neuroscience**

**Location:** WCC Halls A-C

**Time:** Monday, November 16, 2026, 1:00 PM - 5:00 PM

**Program #/Poster #:** PSTR207.04/LL87

**Topic:** J.06. Computation, Modeling, and Simulation

**Support:** Alzheimer's Association AARF-23-1148428

**Title:** Generative model as a scalable source of training data for animal behaviors

**Authors: *H. Z. OO**, W. GMACH, C. TAO, G.-W. ZHANG;
Neurosci. and Anat., Virginia Commonwealth Univ. Sch. of Med., Richmond, VA

**Abstract:** Video-based approaches have become central to the study of animal behavior, enabling objective, high-throughput quantification of naturalistic actions that are difficult to capture by manual scoring. Recent advances in computational analysis tools, spanning keypoint-based pose estimation and end-to-end video models, have markedly improved our ability to detect and characterize complex behaviors. Progress nonetheless remains constrained by the scarcity of publicly available, richly annotated animal-behavior datasets. This limitation makes it difficult to establish broadly applicable pretrained models, so analysis pipelines are typically trained from scratch within each laboratory, an approach that is costly, labor-intensive, and limits reusability across labs. Because the mouse is the predominant model organism in neuroscience, we focused on building a scalable, richly annotated dataset of mouse social and individual behavior to broaden model generalization across laboratories, animals, and recording conditions. Here we used a generative video synthesis approach to produce realistic behavioral clips. The generated clips span common social and individual behaviors across a range of recording contexts and include diverse mouse coat colors, capturing much of the visual variability encountered in real experiments. Critically, each video is paired with multimodal annotations, including segmentation masks, animal identity, text-prompt descriptions, and keypoints, making the dataset readily adaptable to a wide range of model architecture and downstream tasks. To evaluate its utility, we trained our recently developed TRACE model on the synthetic data and found that it generalized to real, raw mouse behavior recordings with little or no fine-tuning. This indicates that purely synthetic video can train a behavior tracker that transfers to real recordings, reducing the need for per-laboratory training from scratch. Therefore, generative video is a usable, scalable contributor to a community mouse behavior dataset. The dataset and trained model will be released publicly, with the goal of accelerating neuroscience and behavioral research.

**Disclosures: H.Z. Oo:** None. **W. Gmach:** None. **C. Tao:** None. **G. Zhang:** None.

**Poster**

**PSTR207: Computational Methods for Experimental Neuroscience**

**Location:** WCC Halls A-C

**Time:** Monday, November 16, 2026, 1:00 PM - 5:00 PM

**Program #/Poster #:** PSTR207.05/LL88

**Topic:** J.06. Computation, Modeling, and Simulation

**Support:** European Fund for Regional Development
Province of Gelderland

**Title:** An automated home-cage monitoring platform for multimodal welfare and behavior assessment in rats

**Authors:** E. O. YILMAZ[1], J. R. HOMBERG[3], A. SCHMAL[4], V. SEKHAR[5], A. SPINK[5], B. STOELLER[6], ***L. P. J. J. NOLDUS**[2,5];
[1]Dept. of Med. Neurosci., [2]Donders Inst. for Brain, Cognition and Behavior, Radboud Univ., Nijmegen, Netherlands; [3]Med. Neurosci., Radboud Univ. Med. Ctr., Nijmegen, Netherlands; [4]UNO Life Sci. Solutions, Zevenaar, Netherlands; [5]Noldus Information Technol. BV, Wageningen, Netherlands; [6]Brain Builders BV, Bemmel, Netherlands

**Abstract:** Conventional welfare assessment of laboratory rats relies largely on manual checks during daytime. As rats are nocturnal, this may disrupt their sleep-wake cycles. Due to their low temporal resolution these intermittent checks miss transient behavioral or welfare-related signals. In the ELAN (Efficient Lab Animal moNitoring) project, we are developing an automated home-cage monitoring system for scalable, continuous, multimodal welfare and behavior assessment in socially housed rats. Design and monitoring priorities were identified using a questionnaire completed by 41 stakeholders from academia, pharma industry and CROs. Based on the survey outcome, the first prototype was built and evaluated by researchers and animal-care personnel. The validated sensors included thermal imaging for movement and zone occupancy, an inertial measurement unit for cage-level activity and circadian patterns, an ultrasonic microphone for distress calls, and environmental sensors for ammonia, temperature and relative humidity. The ultrasonic vocalization detection algorithm was benchmarked against two hand-annotated recordings containing 460 calls and VocalMat, using time-frequency bounding-box overlap. Survey results prioritized: social housing with 2-4 rats per cage; larger (than standard), enriched, transparent, washable/autoclavable cages; reliable cage-specific water delivery; mounting in an ergonomically designed rack; and compatibility with routine workflows. Monitoring priorities centered on cage- and individual-level activity, animals' health, cage temperature, and food/water levels. The first prototype successfully quantified cage-level movement and zone occupancy using thermal imaging, while IMU signals tracked activity and matched thermal movement events. The USV detector reliably detected cage vocalizations, reaching F1 scores of 0.89 and 0.93. Ammonia, temperature, and humidity sensors can successfully report subtle changes in the cage environment. ELAN is a home-cage monitoring platform that uses multimodal sensor data to track key behavioral and environmental parameters relevant to rat welfare. The system has strong potential to make welfare monitoring more labor- and cost-effective. Addition of cloud-based data storage, visualization and analysis software, and future validation in research and animal facilities will support broader implementation. ELAN provides a user-validated, research-backed and low-cost solution for continuous, non-invasive welfare monitoring in group-housed laboratory rats, with potential to improve data quality, reduce animal disturbance, and increase translational relevance.

**Disclosures: E.O. Yilmaz:** None. **J.R. Homberg:** None. **A. Schmal:** None. **V. Sekhar:** None. **A. Spink:** None. **B. Stoeller:** None. **L.P.J.J. Noldus:** None.

**Poster**

**PSTR207: Computational Methods for Experimental Neuroscience**

**Location:** WCC Halls A-C

**Time:** Monday, November 16, 2026, 1:00 PM - 5:00 PM

**Program #/Poster #:** PSTR207.06/LL89

**Topic:** J.06. Computation, Modeling, and Simulation

**Support:** ARPA-H H37810000728898

**Title:** ECG-Derived Automated Sleep Staging via Deep Learning: An Artifact-Resilient Computational Pipeline for TBI and Neuroimaging Applications

**Authors: *A. POLLATOU**[1], L. MARINELLI[2], J. WERNER, Jr.[1], N. ABAD[2];
[1]Uniformed Services Univ. of the Hlth. Sci., Bethesda, MD; [2]GE, Niskayuna, NY

**Abstract:** Introduction: Characterizing sleep-dependent neural processes, including sleep-driven glymphatic clearance, during neuroimaging is essential for understanding traumatic brain injury (TBI) recovery and brain health. Concurrent EEG is the standard approach but remains prohibitively resource-intensive in MRI, demanding specialized electrode systems, RF shielding, and technical expertise unavailable at most sites. ECG, by contrast, is routinely acquired in MRI protocols and far less burdensome, making it an attractive substrate for automated sleep staging, yet MRI-induced gradient and magnetohydrodynamic artifacts impose signal quality demands that existing preprocessing pipelines cannot reliably meet.Materials and methods: We developed a deep learning pipeline for automated sleep staging from ECG-derived instantaneous heart rate, incorporating novel preprocessing components for robust unattended deployment: automated ECG polarity detection, multi-level epoch and recording-level artifact rejection tailored for MRI-environment signal corruption, and balanced epoch sampling to address class imbalance. A dilated convolutional neural network was trained on N=1,870 (MESA) and N=7,985 (Sleep Heart Health Study) overnight polysomnography recordings, with prospective validation ongoing in N=50 in-house TBI and sleep-deprived participants.Results: Applied to Sleep Heart Health Study (SHHS; N=7,985), the pipeline achieved 87.7% accuracy (kappa=0.668) for 2-class sleep/wake and 82.1% accuracy (kappa=0.683) for 3-class Wake/NREM/REM staging, meeting benchmarks despite training on a single dataset. Balanced epoch sampling was the critical methodological determinant: deep sleep recall collapsed to 0.00 with standard loss weighting versus 0.49 with balanced sampling. Method rankings generalized across independent Multi-Ethnic Study of Atherosclerosis (MESA) and SHHS cohorts, confirming stability.Conclusions: The proposed pipeline demonstrates accurate, generalizable ECG-based sleep staging designed for fully automated deployment without manual quality review. By enabling sleep characterization in populations intolerant of electrode arrays, it opens a practical path for systems-level sleep assessment in TBI and neuroimaging contexts. Prospective validation in TBI and sleep-deprived cohorts will establish clinical utility, with deployment planned across populations with sleep complaints and cognitive impairment in ongoing MRI studies of glymphatic function where EEG-based staging remains clinically and technically infeasible.

**Disclosures: A. Pollatou:** None. **L. Marinelli:** None. **N. Abad:** None.

**Poster**

**PSTR207: Computational Methods for Experimental Neuroscience**

**Location:** WCC Halls A-C

**Time:** Monday, November 16, 2026, 1:00 PM - 5:00 PM

**Program #/Poster #:** PSTR207.07/LL90

**Topic:** J.06. Computation, Modeling, and Simulation

**Support:** Margaret Q. Landenberger Foundation American Heart Association
P50HD105354 (SAIF)

**Title:** Subject-specific Monte Carlo modeling for optical neuromonitoring and neuroimaging in mice

**Authors:** ***J. ZHANG**[1], A. PALMUCCI[2], H. FISHER[2], R. MENEZES FORTI[2], B. R. WHITE[3]; [1]Univ. of Pennsylvania, Philadelphia, PA; [2]Children's Hosp. of Philadelphia, Philadelphia, PA; [3]Pediatrics, Univ. of Pennsylvania, Children's Hosp. of Philadelphia, Philadelphia, PA

**Abstract:** Optical neuromonitoring and functional neuroimaging in mouse models can help develop biomarkers for assessing brain health. Measuring hemodynamics and fluorescence with mesoscopic methods requires correcting for the semi-diffusive photon pathlength. Prior methods assume semi-infinite geometries, but spatial variance in optical properties can have a large effect. We aimed to create subject-specific head models in combination with Monte Carlo simulation. In addition to improving the accuracy of spectroscopy and fluoroscopy, these methods also aim to align optical data with the Allen Mouse Brain Atlas. We modeled two neuromonitoring systems: (1) widefield optical imaging (WOI) using visible light illumination and detection via a camera and (2) a fiber-based diffuse optical spectroscopy (FD-DOS) system. Both modalities are performed through an acrylic cranial window secured to the intact skull with transparent dental cement. FD-DOS uses a fiber-holder mounted to the window, while WOI is performed with the mouse head held below the imaging system. We created a pipeline to generate subject-specific head models derived from CT anatomy (Fig.1). Monte Carlo modeling was performed to calculate voxel-wise sensitivity for each wavelength at each camera pixel (WOI) or source-detector pair (FD-DOS). Preliminary data shows expected photon propagation patterns. As each mouse has the cranial window in a slightly different location, we are able to model how this variance affects the anatomic sensitivity of different measurements. Future work will explore (1) correcting errors from spatial variation in optical properties (e.g., surface vasculature), (2) aligning data with histology and the Allen Common Coordinate Framework, and (3) accurate modelling of fluorescence.

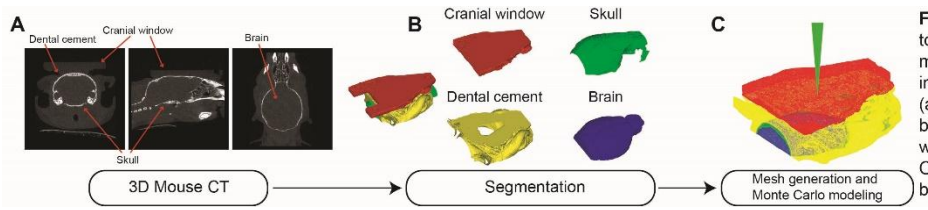



**Figure 1.** We segmented CT scans to generate a realistic mouse head mesh. Segmented volumes included the cranial window (acrylic), dental cement, skull, and brain. Monte Carlo photon transport was then modeled using mmclab. Optical properties were assigned based on previous literature.

**Disclosures: J. Zhang:** None. **A. Palmucci:** None. **H. Fisher:** None. **R. Menezes Forti:** None. **B.R. White:** None.

**Poster**

**PSTR207: Computational Methods for Experimental Neuroscience**

**Location:** WCC Halls A-C

**Time:** Monday, November 16, 2026, 1:00 PM - 5:00 PM

**Program #/Poster #:** PSTR207.08/LL91

**Topic:** J.06. Computation, Modeling, and Simulation

**Title:** Multi-site suprathreshold heat pain calibration algorithm comparison via individualized simulation

**Authors: *A. G. HAGSTRÖM**, E. J. MOANA-FILHO;
Univ. of Minnesota Sch. of Dent., Minneapolis, MN

**Abstract:** Accurate and efficient determination of stimulus intensity evoking suprathreshold pain is needed for many psychophysical protocols. Existing methods are designed to determine the threshold in a single body site. For protocols that include stimulation at two sites within a body region, site-specific pain sensitivity differences and lack of standardized methods pose a challenge for stimulus intensity determination of all testing sites in a body region. To address this, we developed and tested two algorithmic approaches to determine the thermal stimuli required to evoke “moderate pain” (30-69 on a 0-100 visual analogue scale (VAS)) from two sites within a body region using temperatures of 40-49°C. The limit algorithm delivers ascending heat stimuli to each site using adaptive branching logic. The regression algorithm delivers initial heat stimuli at 42 and 47°C to both sites in ascending order, fits a model to each site’s ratings, then tests both sites at three temperatures: the one predicted to evoke a 50 VAS rating at the more sensitive site and two temperatures ±1°C around that prediction. Three regression models were evaluated: linear, quadratic, and power functions. All algorithms are considered successful when each tested site evokes a rating of 30-69 VAS for a tested temperature.To test these algorithms, we developed an open source Python pseudorandom generator with reproducible seeds to generate individualized heat pain ratings from simulated stimuli over the arm (sites: thenar eminence, ventral forearm). Simulated responses are generated by drawing site-specific population-level temperature/rating curves, then adding randomized between- and within-subject variability, derived from 751 research participants. We simulated 100,000 individuals and tested all algorithms to determine their ability to calibrate the heat stimuli evoking “moderate pain” across both testing sites.All three regression algorithms outperformed the limit algorithm. The quadratic regression algorithm achieved the highest calibration success rate (70.3%) with a mean a calibration temperature of 46.2°C ±2.2. The linear regression followed with 67.7% success (mean 46.2°C ±2.1). The power function followed with a success of 63.2% (mean 46.4°C ±2.1) with the limit method least successful at 59.8% success (mean 47.1°C ±2.1).These results suggest quadratic regression-based calibration achieves superior simulated performance compared to its linear and power variants, as well as the limit calibration algorithm, for multi-site

suprathreshold heat pain determination. The next step is to validate these results in a pilot study with actual human participants.

**Disclosures: A.G. Hagström:** None. **E.J. Moana-Filho:** None.

**Poster**

**PSTR207: Computational Methods for Experimental Neuroscience**

**Location:** WCC Halls A-C

**Time:** Monday, November 16, 2026, 1:00 PM - 5:00 PM

**Program #/Poster #:** PSTR207.09/LL92

**Topic:** J.06. Computation, Modeling, and Simulation

**Support:** NIH R61MH135407
NIH R01MH123770
NIH RF1DA056402
NSF CRCNS IIS-2113271
the One Mind Rising Star Award
the Foundation for OCD Research (FFOR)
the Raynor Cerebellum Project (RCP)

**Title:** Cross-Subject Modeling of Widefield Calcium Imaging Enables Zero-Shot Behavior Decoding

**Authors: *M. HOSSEINI**[1], E. ERTURK[2], S. HASHEMI SAFAEI[3], M. M. SHANECHI[4]; [1]Electrical and Computer Engin., USC, Los Angeles, CA, CA; [2]Electrical and Computer Engin., [3]Computer Sci., USC, Los Angeles, CA; [4]Electrical and Computer Engin., Univ. of Southern California, Los Angeles, CA

**Abstract:** Recent large-scale, multi-subject widefield calcium imaging datasets provide unprecedented access to brain-wide cortical dynamics. However, widefield recordings are high-dimensional, exhibit complex spatiotemporal structure, and contain substantial task-irrelevant activity. These challenges have largely restricted modeling efforts to single-session analyses, limiting scalability and generalization across subjects, sessions, and experimental conditions. In particular, zero-shot behavior decoding, in which a model is applied to an unseen subject without retraining, remains a major challenge across neural modalities.
To address this, we introduce WiCAT, a multi-subject modeling framework for widefield calcium imaging that learns subject-invariant, shared brain-wide representations through self-supervised pretraining. WiCAT introduces an atlas-grounded spatiotemporal tokenization scheme without session-specific components, enabling the model to be shared across subjects without subject-specific training or adaptation.
We evaluated WiCAT on multiple large-scale public widefield datasets spanning different subjects, sessions, and behavioral tasks. WiCAT outperforms single-session and multi-session baselines for behavior decoding. In the zero-shot setting, the frozen pretrained representations outperform multi-subject baselines for continuous behavior decoding in held-out subjects.

WiCAT also supports zero-shot reconstruction of activity in left-out brain regions using the rest of the brain as context, showing that it captures transferable spatiotemporal relationships across cortical areas. Taken together, this work establishes a first step toward foundation modeling for widefield neural imaging as larger and more diverse neural datasets become available.

**Disclosures: M. Hosseini:** None. **E. Erturk:** None. **S. Hashemi Safaei:** None. **M.M. Shanechi:** None.

**Poster**

**PSTR207: Computational Methods for Experimental Neuroscience**

**Location:** WCC Halls A-C

**Time:** Monday, November 16, 2026, 1:00 PM - 5:00 PM

**Program #/Poster #:** PSTR207.10/LL93

**Topic:** J.06. Computation, Modeling, and Simulation

**Support:** NIH Grant R01NS123069
1R01AG095248

**Title:** A flexible multi-region depth probe resolves selective CA3→amygdala gamma collapse at seizure onset in mice

**Authors: *B. KHAGHANI**[1], P. OLENIACZ[2], A. LAWYER[1], H. SONTHEIMER[3], X. JIA[1], M. LIU[1];
[1]Virginia Tech., Blacksburg, VA; [2]Univ. of Virgina, Charlottesville, VA, ; [3]Univ. of Virginia, Charlottesville, VA.

**Abstract:** Understanding how seizures reorganize limbic circuit communication requires observing multiple interacting regions simultaneously, yet most in vivo studies sample one or two sites and cannot separate local state changes from network-level shifts in directed information flow. We developed a custom flexible polymer depth-electrode array that records local field potentials simultaneously from cortex, hippocampal CA1, hippocampal CA3, and amygdala in pilocarpine-treated mice across baseline, pre-ictal, and ictal epochs. Brain states were categorically separable: spectral and complexity features distinguished all three epochs with 95.7% accuracy ($\kappa$=0.923, leave-one-mouse-out cross-validation), driven primarily by beta-band dynamics. Against this backdrop, directed connectivity told a more selective story. Gamma-band CA3→amygdala, a constitutive pathway present at baseline and pre-ictally, selectively collapsed at seizure onset, while CA1→cortex gamma persisted across all states. Meanwhile, delta-phase to high-gamma-amplitude coupling rose sharply at onset across every region but showed no directional asymmetry between any inter-regional pair. These findings reveal a dissociation at seizure onset: a specific directed pathway selectively collapses even as cross-frequency coupling becomes globally and symmetrically elevated. Rather than recruiting new hubs, the ictal network simplifies - a distinction visible only with simultaneous multi-region recording enabled by the probe.

**Disclosures: B. Khaghani:** None. **P. Oleniacz:** None. **A. Lawyer:** None. **H. Sontheimer:** None. **X. Jia:** None. **M. Liu:** None.

**Poster**

**PSTR207: Computational Methods for Experimental Neuroscience**

**Location:** WCC Halls A-C

**Time:** Monday, November 16, 2026, 1:00 PM - 5:00 PM

**Program #/Poster #:** PSTR207.11/LL94

**Topic:** J.06. Computation, Modeling, and Simulation

**Support:** NIH 1U24MH130988-01
NIH 1R01MH142410-01
CPRIT RP210045
CPRIT RP170668

**Title:** Digital antibody screening to identify critical targets and epitopes in brain cell clusters

**Authors: *A. SOLANKI**[1], H. ZHANG[2], N. S. MAURYA[1], W. CHEN[1], S. MU[2], Z. WU[2], W. ZHENG[1];
[1]McWilliams Sch. of Biomed. Informatics, UTHealth Houston, Houston, TX; [2]Appel Alzheimer's Dis. Res. Inst., Weill Cornell Med., New York, NY

**Abstract:** Antibodies play an important role in identifying critical targets and epitopes in brain cells. Protein folding AI models such as AlphaFold3 (AF3) allow for quickly screening a diverse set of antibodies against numerous targets to identify binding complexes. On a test set of 3400 antibody-antigen interfaces listed in the Structural Antibody Database, AF3 had 42% recall where predictions with high confidence (calculated using predicted aligned error and interface predicted template modeling score), and the correct epitope were classified as positives. AF3 was observed to prefer X-ray crystallography derived complexes over election microscopy structures. The observations from this structural benchmark were critical for understanding how to screen antibody-antigen complexes with no known structures. Sources such as NeuroMab and CDI Labs freely provide the sequences of numerous antibodies for various target proteins of interest to the neuroscience community: Roughly 2000 and 500 unique antibodies for 400 and 100 different targets respectively. Using AF3, about 300 antibodies were identified as positive binders for these targets in a cross-species prediction assay. Genes such as PVALB, CALB2, MOG, NOVA1, and PPP1R1B reported high KL-divergence scores from gene expression data and had several binding antibodies. For PVALB, molecular dynamics and digital alanine scanning were used to identify residues in the paratope crucial for binding. The binding contributions of these residues were confirmed through alanine mutations in immunohistochemistry assays on mouse brain tissue, validating the digital predictions for these antibodies. These results are necessary for the curation of a free database of antibodies with structural validation. Such a database would be of immense value to neuroscientists for studying the differentiation of brain cell clusters.

**Disclosures: A. Solanki:** A. Employment/Salary (full or part-time):; UTHealth Houston. **H. Zhang:** A. Employment/Salary (full or part-time):; Cornell. **N.S. Maurya:** A. Employment/Salary (full or part-time):; UTHealth Houston. **W. Chen:** A. Employment/Salary (full or part-time):; UTHealth Houston. **S. Mu:** A. Employment/Salary (full or part-time):; Cornell. **Z. Wu:** A. Employment/Salary (full or part-time):; Cornell. **W. Zheng:** A. Employment/Salary (full or part-time):; UTHealth Houston.

**Poster**

**PSTR207: Computational Methods for Experimental Neuroscience**

**Location:** WCC Halls A-C

**Time:** Monday, November 16, 2026, 1:00 PM - 5:00 PM

**Program #/Poster #:** PSTR207.12/LL95

**Topic:** J.06. Computation, Modeling, and Simulation

**Support:** NIH 1U24NS129945-01A1

**Title:** Neuroscience Gateway Enabling Large Scale Modeling, Data Processing and AI/ML Work on Supercomputers

**Authors: *A. MAJUMDAR**[1], S. SIVAGNANAM[2], N. T. CARNEVALE[3];
[1]Univ. of California San Diego, LA JOLLA, CA; [2]San Diego Supercomputer Ctr., UCSD, La Jolla, CA; [3]Neurosci., Yale Univ., New Haven, CT

**Abstract:** The Neuroscience Gateway (NSG) has been in operation for more than 12 years and enables neuroscientists to easily utilize high performance computing (HPC), high throughput computing (HTC) and GPU computing resources for large scale modeling, data processing, and AI/ML work. NSG provides close to 20 neuroscience modeling, data processing and AI/ML tools optimally made available on supercomputer resources. Via NSG's easy to use web-based and programmatic interface neuroscientists can upload input file or data to the NSG, chose the appropriate tool, specify the tool and computing related parameters and submit the computing workload to a supercomputer. Upon completion of the processing, users can download the output results. NSG eliminates administrative and technical barriers to utilize supercomputing resources for modeling, data processing and data analytics work in neuroscience. NSG also provides a software developer platform which neuroscience software developers can use to test, benchmark and scale their software and then release the software on supercomputers where NSG acquires yearly allocation for the neuroscience community. NSG provides a platform for dissemination of neuroscience software. NSG is free and open to any neuroscientist researchers and students. Yearly training and workshops are hosted by the NSG team where NSG users and software developers discuss their research results and software. NSG is utilized by other neuroscience projects, such as the NeuroElectroMagnetic data Archive and tools Resource (NEMAR), Human Neocortical Neurosolver (HNN), the Open Source Brain, as the computational engine for processing of data and simulations. NSG is used in classroom teaching for undergraduate and graduate students. The presentation at SfN will describe the tools that NSG provides, how they are utilized on supercomputers, statistics of NSG's growth, research enabled by NSG and

external projects that are utilizing NSG as the compute engine. NSG has received funding from the National Science Foundation and the National Institutes of Health.

**Disclosures: A. Majumdar:** None. **S. Sivagnanam:** None. **N.T. Carnevale:** None.

**Poster**

**PSTR207: Computational Methods for Experimental Neuroscience**

**Location:** WCC Halls A-C

**Time:** Monday, November 16, 2026, 1:00 PM - 5:00 PM

**Program #/Poster #:** PSTR207.13/LL96

**Topic:** J.06. Computation, Modeling, and Simulation

**Title:** An integrated multimodal virtual surgical planning pipeline for automated eloquent cortex risk assessment and postoperative outcome prediction in refractory epilepsy

**Authors: *T. ZHAO**;
Gnosis Neurodynamics Co. Ltd, Beijing, China

**Abstract:** Epilepsy surgery requires localizing the seizure onset zone (SOZ) while preserving eloquent cortex, yet conventional intracranial EEG (iEEG) biomarker pipelines show low sensitivity and outcome models rarely quantify SOZ-resection geometry. In this retrospective study, we developed a dual-track virtual surgical planning framework combining cortically constrained functional mapping with deep learning on stereo-EEG (SEEG). Functional language and motor territories were localized via resting-functional MRI (fMRI) mapped to T1 cortical vertices to delineate eloquent boundaries. For SOZ localization, a TimeConv-CNN (ResNet18 backbone) was trained on 60-s interictal SEEG segments from the multi-center Omni-iEEG dataset (83 patients, 256 recordings): 1D signals were converted to amplitude spectrograms (10-300 Hz) via short-time Fourier transform (STFT) and classified, with channel-level probabilities aggregated across segments. A patient-level classifier integrated eight SOZ-resection interaction metrics (e.g., Jaccard index, coverage) with clinical variables to predict binary surgical outcomes (favorable [Engel I] vs. unfavorable [Engel II-IV]). Cortically constrained fMRI mapping provided individualized visualization of language and motor boundaries. On a patient-wise independent test cohort (1,791 channels, 27 patients), the model achieved channel-level AUC = 0.791 (sensitivity = 0.51, specificity = 0.84) using only interictal recordings. This outperformed conventional biomarker ensembles (AUC = 0.61) and event-based high-frequency oscillation (HFO) pipelines (channel-level AUC = 0.72), improving sensitivity over ensembles (0.51 vs. 0.40), though absolute sensitivity remains limited. Integrating automated SOZ localization with resection geometry improved patient-level outcome prediction to 68% accuracy, exceeding a clinical baseline (60% accuracy). This framework provides a quantitative foundation for virtual epilepsy surgery planning, offering automated tools to reduce missed epileptogenic tissue while mapping boundaries to assist in eloquent cortex preservation.

**Disclosures: T. Zhao:** None.

**Poster**

**PSTR207: Computational Methods for Experimental Neuroscience**

**Location:** WCC Halls A-C

**Time:** Monday, November 16, 2026, 1:00 PM - 5:00 PM

**Program #/Poster #:** PSTR207.14/MM1

**Topic:** J.06. Computation, Modeling, and Simulation

**Title:** Deep Learning Approach to Video-Based Behavioral Classification with Intracranial Neural Recordings.

**Authors: *C. MACLAREN**[1,3], I. M. BRIGHT[3], O. E. FRUCHET[4], S. N. JACKSON[3], S. K. INATI[2,3], K. A. ZAGHLOUL[3];
[1]Functional Neurosurg. Section, [2]Natl. Inst. of Neurolog. Disorders and Stroke, Bethesda, MD; [4]Neurosurg., [3]NIH, Bethesda, MD

**Abstract:** Intracranial EEG (iEEG) recordings in patients with implanted electrodes who are being monitored for seizures provide an opportunity to examine the neural correlates of cognitive function. These studies and analyses are typically carried out as participants perform specific behavioral tasks. However, patients are monitored for several days, and continuous neural and video recordings are available during their entire monitoring period. Here, we leverage recent advances in deep learning and computer vision to extract and classify human naturalistic behaviors from intracranial seizure monitoring videos and link those behaviors to the recorded neural activity. We used a semi-supervised autoencoder (SS-AE) that can learn the movements of patients from their poses captured on video to create a latent space. By clustering features of this trained latent space, we show that we can successfully group and identify similar natural behaviors. In addition, using this readout of behavioral information, we constructed a classifier to decode behavioral classes from the continuous neural recordings at different spatial scales. Our classifier was able to significantly decode high-level behaviors extracted from our SS-AE in both multi-unit and single-unit spiking activity captured from microelectrode arrays (MEAs) implanted in the anterior temporal lobe in each participant. Together, these results suggest that even at the smallest spatial scale, neural activity from a relatively small region of human cortex is sufficient to represent different high-level natural human behaviors.

**Disclosures: C. MacLaren:** None. **I.M. Bright:** None. **O.E. Fruchet:** None. **S.N. Jackson:** None. **S.K. Inati:** None. **K.A. Zaghloul:** None.

**Poster**

**PSTR207: Computational Methods for Experimental Neuroscience**

**Location:** WCC Halls A-C

**Time:** Monday, November 16, 2026, 1:00 PM - 5:00 PM

**Program #/Poster #:** PSTR207.15/Web Only

**Topic:** J.06. Computation, Modeling, and Simulation

**Support:** NIH U19NS123716-05

**Title:** PhySeqNet: physics-informed deep learning framework for fluorescent spot detection in BARseq spatial transcriptomics

**Authors:** ***N. GOSWAMI**[1], J. HOVER[2], R. GALLUCCIO[3], Y.-C. WU[4], C. ZHAN[3], A. M. ZADOR[5];
[1]Cold Spring Harbor Lab., COLD SPRING HARBOR, NY; [2]MAPseq/BARseq Core Facility, Cold Spring Harbor Lab., Setauket- East Setauket, NY; [3]Cold Spring Harbor Lab., Cold Spring Harbor, NY; [4]Zador, Cold Spring Harbor Lab., Levittown, NY; [5]Zador Lab., Cold Spring Harbor Lab., Cold Spring Harbor, NY

**Abstract:** Spatial transcriptomics methods like BARseq depend on accurate detection of fluorescent foci, yet existing approaches often rely on manually annotated training data or intensity thresholds that miss dim but real signal. Here, we present PhySeqNet, a physics-informed U-Net for fluorescent spot detection trained entirely on semi-synthetic images generated by simulating the optical image-formation process. Simulations were calibrated with channel-specific fluorescent bead measurements and real experimental noise frames. PhySeqNet transfers directly to real BARseq data without fine-tuning, detecting spots based on learned optical characteristics of the imaging system rather than brightness cutoffs. On 10 tiles extracted from full coronal mouse brain BARseq sections, PhySeqNet achieved a mean forward-model normalized cross-correlation of 0.862, significantly outperforming BarDensr (0.780), Piscis (0.754), and classical detectors (0.727-0.754; all $p < 0.001$, paired Wilcoxon, BH-corrected). PhySeqNet recovered approximately 1.55 times more transcripts per cell than BarDensr (median 68 vs. 44 counts) while maintaining comparable genes detected per cell (median 24), with a false-discovery rate of 4.74% compared to 2.51% for BarDensr, estimated via unused codewords. We developed pyBARseq, an open-source Python workflow that integrates PhySeqNet with BARseq registration, basecalling, cell assignment, quality control, and post-processing visualization through a napari plugin. Using scANVI-based label transfer against the Allen Brain Cell Atlas and MERFISH cross-validation, PhySeqNet-based BARseq recovered expected cortical laminar expression and cell-type proportions. Finally, we apply pyBARseq to samples linking in vivo two-photon imaging with post hoc BARseq through vascular-guided registration, providing a route to assign molecular identity to functionally characterized neurons.

**Disclosures: N. Goswami:** None. **J. Hover:** None. **R. Galluccio:** None. **Y. Wu:** None. **C. Zhan:** None. **A.M. Zador:** None.

**Poster**

**PSTR207: Computational Methods for Experimental Neuroscience**

**Location:** WCC Halls A-C

**Time:** Monday, November 16, 2026, 1:00 PM - 5:00 PM

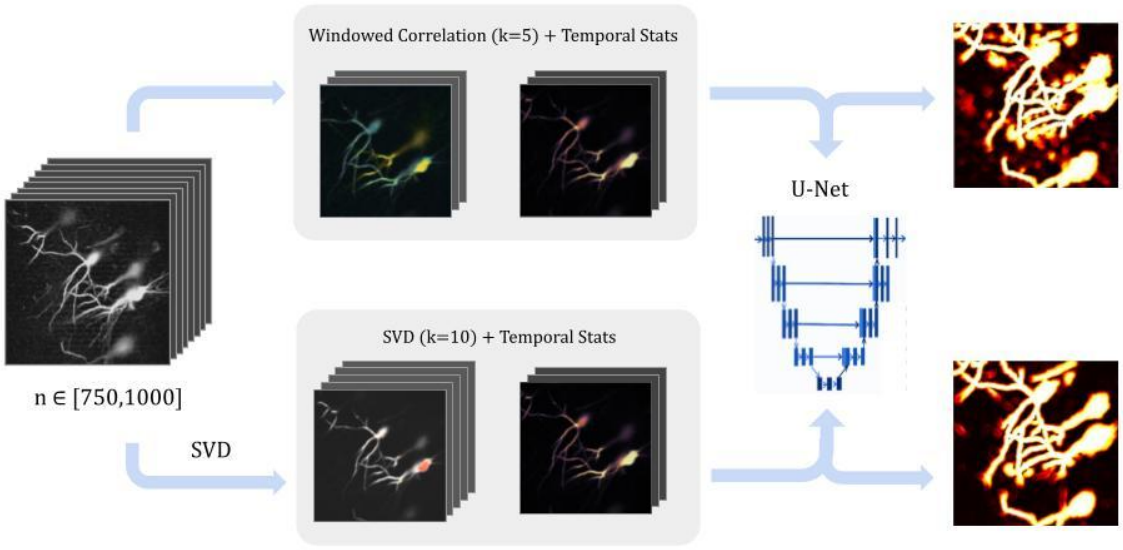
**Program #/Poster #:** PSTR207.16/MM2

**Topic:** J.06. Computation, Modeling, and Simulation

**Title:** Data-driven input representations improve U-Net segmentation of dendritic calcium imaging

**Authors:** ***S. GARCIA**[1], R. A. GONZALES[2,3], K. BINTSI[3], A. SORIANO-VARGAS[2];
[1]Fac. of Computing, Univ. de Ingeniería y Tecnología, Lima, Peru; [2]Fac. of Computing, Univ. of Engin. and Technol. - UTEC, Lima, Peru; [3]Harvard Med. Sch., Boston, MA

**Abstract:** Neurons receive synaptic inputs along thin, branching dendrites, where local calcium transients mark the timing and location of circuit inputs. Two-photon calcium imaging can capture these signals across many dendritic segments, but segmentation is difficult because dendrites are elongated, overlapping, and embedded in correlated neuropil. Standard pipelines assume compact somatic components; dendrites violate that geometry. Constrained nonnegative matrix factorization (CNMF) refinement can miss thin processes or absorb neighboring inactive pixels, a limitation correlation maps cannot fully solve because neuropil can make nearby inactive structures appear correlated. We trained a U-Net to predict binary masks of active dendrites from temporal feature images computed from calcium movies, using the masks to seed active dendritic components and constrain CNMF spatial updates. To identify a compact input prior, we compared different feature sets under identical training conditions on 16 annotated recordings from the Moore et al. 2025 hippocampal dataset (GCaMP6f/7b; C57BL/6J mice, both sexes, 15-25 weeks). Dihedral rotations/reflections and intensity jitter produced 1,200 training and 432 validation patches. Performance was evaluated with Dice and centerline Dice (clDice), capturing pixel overlap and dendritic continuity. Pairing per-pixel temporal statistics with singular value decomposition (SVD) spatial modes yielded higher topological fidelity than the standard windowed correlations (clDice=0.780±0.096 vs. 0.773±0.083, n=6), with comparable pixel-level overlap (Dice=0.648±0.123 vs. 0.665±0.103) and ~1.8× faster feature computation. This trade-off matters for CNMF seeding, where preserving the full trajectory of an active branch is more useful than optimizing exact boundaries. By reducing high-frame-count movies to compact, activity-informative channels, SVD-based inputs provide a practical data-driven prior for active dendrite segmentation and support recovery of subcellular calcium signals across dendritic populations.




**Disclosures: S. Garcia:** None. **R.A. Gonzales:** None. **K. Bintsi:** None. **A. Soriano-Vargas:** None.

**Poster**

**PSTR207: Computational Methods for Experimental Neuroscience**

**Location:** WCC Halls A-C

**Time:** Monday, November 16, 2026, 1:00 PM - 5:00 PM

**Program #/Poster #:** PSTR207.17/MM3

**Topic:** J.06. Computation, Modeling, and Simulation

**Support:** IBACS Summer Fellowship Award

**Title:** A GUI-Based Tool to Improve Interrater Agreement in a Supervised Machine Learning Procedure for Behavioral Classification

**Authors: *E. SHECTER**[1], A. CHRISTENSEN[1], A. SADINSKY[1], G. LAURETANO[1], B. PIERRE PHILIPPE[3], S. KAMMA[1], T. NGUYEN[1], E. J. MARKUS[2];
[2]Psychology, [1]Univ. of Connecticut, Storrs, CT; [3]Univ. of Connecticut - Psychological Sci. & Neurosci. of Hlth. and Behavior, Storrs, CT

**Abstract:** The addition of Machine Learning (ML) based tools in behavioral research has improved the ability to operationalize and classify complex behaviors. Human labeling serves as the scaffolding from which ML builds predictions, making reliable, low-noise labeling critical to the model training process. Traditionally, experimenters ("raters") manually align their labeling decisions until pairwise correlations between them reach at least 0.9; a process requiring

considerable time and effort. Here, we propose a self-paced, GUI-based, independent learning procedure designed to improve inter-rater agreement, used in supplement to DeepLabCut (Mathis et al., 2018) for continuous pose-estimation and behavioral classification. Seven raters, including one designated as “ground-truth”, labeled images extracted from overhead recordings of freely behaving rats. Each rater completed 3 rounds of 400 images (~40 sec of video data), plotting keypoints at 8 unique body parts per image. A GUI-based feedback tool was implemented to compare the decisions made in each round, pairwise against the ground-truth rater's decisions. This tool was designed as an adaptation of a "Hotter/Colder Game" allowing interactive keypoint correction via drag-and-drop, with a heads-up display updating Euclidean pixel error in real time. In between rounds one and two, raters used the interactive tool to adjust each keypoint until achieving < 5px error per keypoint per image. After each implementation of the training tool, raters went on to label a novel set of 400 images from the same recording. Critically, this tool enabled self-paced inter-rater alignment without a human trainer present. Overall error was compared across rounds using a one-way repeated measures ANOVA, which indicated a significant decrease in error across raters following the first round of feedback, with no significant improvement thereafter. To our knowledge, this is the first instructor-less, self-paced method proposed for improving inter-rater agreement, paving the way for efficient, accurate ML-based behavioral classification less prone to noise-induced model deficiency.

**Disclosures: E. Shecter:** None. **A. Christensen:** None. **A. Sadinsky:** None. **G. Lauretano:** None. **B. Pierre Philippe:** None. **S. Kamma:** None. **T. Nguyen:** None. **E.J. Markus:** None.

**Poster**

**PSTR207: Computational Methods for Experimental Neuroscience**

**Location:** WCC Halls A-C

**Time:** Monday, November 16, 2026, 1:00 PM - 5:00 PM

**Program #/Poster #:** PSTR207.18/MM4

**Topic:** J.06. Computation, Modeling, and Simulation

**Title:** In-ear EEG validation using multilayer computational and physical head models

**Authors: *O. N. JAMES**, A. D. NORDIN;
Biomed. Engin., Univ. of Houston, Houston, TX

**Abstract:** In-ear electroencephalography (EEG) is attractive for wearable, ambulatory neural monitoring, but its usefulness for identifying cortical source activity depends on volume-conduction to the ear canal. Prior in-ear EEG forward modeling has mapped source-sensor sensitivity without an independent-solver cross-check or physical ground-truth validation. Our aim was to identify cortical source activity from in-ear EEG using two independent computational forward models: (1) boundary element model (BEM) and (2) finite element model (FEM); and a (3) multilayer physical head model.Our boundary element model (FieldTrip, three-layer Colin27; conductivity: σbrain = σscalp = 0.33 S/m, σskull = 0.0042 S/m) relied on a custom electrode placement montage with external and in-canal ear positions, temporal scalp, and midline channels. Our finite element model (SimNIBS 4.6, CHARM segmentation; ~3×105-

node mesh, five tissues) relied on leadfields computed by reciprocity on a 10-10 electrode placement montage. We tested a single cortical equivalent current dipole in the supplementary motor area (MNI [0, 5, 55] mm) across 10-80 nA·m field strengths and three spatial orientations. Additionally, a brainstem dipole source at matched amplitude served as biological control signal. We compared the predicted source amplitudes against a 2 μV in-ear single-trial noise floor. As a physical validation, we assembled an electrical head phantom device with tissue-equivalent compartments, embedded dipolar sources, and ear-canal contacts.
The computational models showed anatomy- and physics-driven agreement within ~40% among shared channels (Cz, FCz, Fz), within typical inter-method ranges. At 50 nA·m field strength, predicted mean in-ear amplitude was 0.46 μV (peak 3.5 μV at Cz; 5.5 μV FEM peak). The cortical source produced 2.07 times greater in-ear amplitudes compared to the brainstem control signal, confirming the cortical source as a feasible peri-auricular target. Against the 2 μV floor, in-ear signal to noise ratio was 0.23 per single trial, 1.15 at 25 trials, and 2.3 at 100 trials, below detection per trial but recoverable by averaging within realistic protocols.
Two independent computational forward models converged on quantitative in-ear detectability thresholds for a cortical source, establishing cross-validated amplitudes and trial counts. The multilayer physical head phantom device provides physical validation based on computational predictions using experimental ground truth to establish in-ear recording sensitivity and signal recovery.

**Disclosures: O.N. James:** None. **A.D. Nordin:** None.

**Poster**

**PSTR207: Computational Methods for Experimental Neuroscience**

**Location:** WCC Halls A-C

**Time:** Monday, November 16, 2026, 1:00 PM - 5:00 PM

**Program #/Poster #:** PSTR207.19/MM5

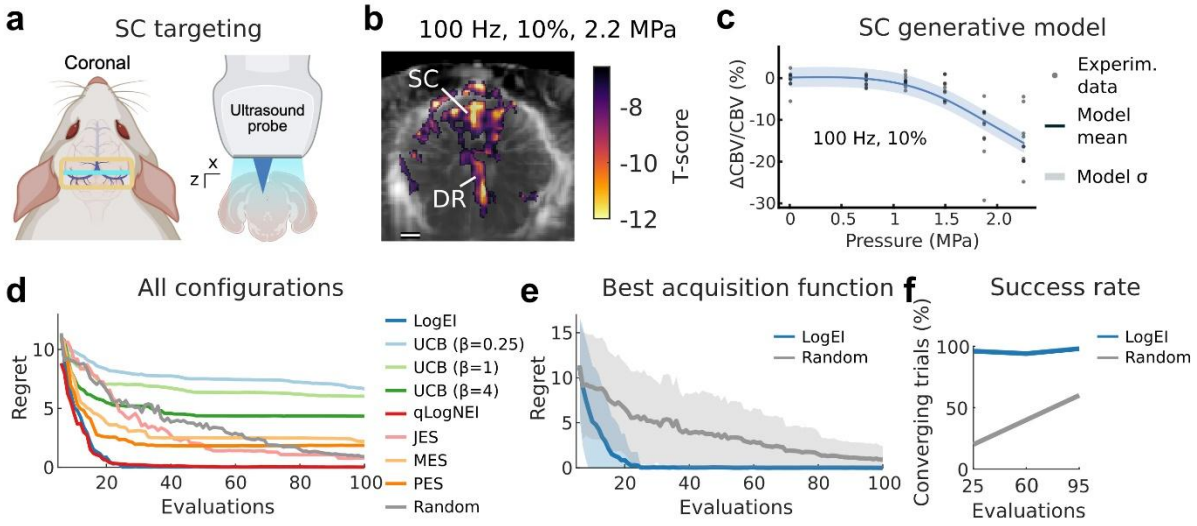
**Topic:** J.06. Computation, Modeling, and Simulation

**Support:** 1R01EB036474 (to TDI)
UCSF RAP Award (to TDI)
John Pritzker Family Fund (to TDI)
Catalyst Award from the UCSF Catalyst Program and UCSF Weill Institute for Neurosciences (to TDI)
National Science Foundation NAIRR Pilot award under grant NAIRR250046 (to TDI)
Brain and Behavior Research Foundation Young Investigator Award (to AB)

**Title:** A Bayesian framework for efficient low-intensity focused ultrasound parameter mapping

**Authors: *A. BOSCUTTI**[1], V. GRASSO[2], T. DI IANNI[3];
[1]Univ. of California, San Francisco, San Francisco, CA; [2]Univ. of California San Francisco, San Francisco, CA; [3]Univ. of California San Francisco, San Francicso, CA

**Abstract:** Low-intensity focused ultrasound (LIFU) is an emerging non-invasive neuromodulation technique whose potential is currently limited by a poorly understood parameter space. Conventional parameter mapping methods rely on grid searches, which are particularly inefficient with large parameter spaces, as in LIFU neuromodulation. Here we developed and validated a Bayesian-optimization (BO) approach for efficient, data-driven mapping of LIFU stimulation parameters. In BO, a Gaussian-process surrogate of the stimulation-response function is iteratively refined, and an acquisition function selects the next parameter set. To validate our method, we built two virtual environments based on real-world LIFU stimulation experiments in rats. The first environment was created from functional ultrasound imaging recordings during LIFU stimulation of the superior colliculus (SC) (*a*-*b*) and had a monotonic landscape with a boundary optimum (*c*). The second environment was based on behavioral readouts recorded during LIFU stimulation of the centromedial thalamus (CMT) and had a non-monotonic landscape with a local optimum. In each configuration, we ran 50 independent BO trials of 100 evaluations under realistic noise levels (1- and 2-fold the estimated experimental noise) and benchmarked the BO against conventional random and grid searches.Comparing eight acquisition functions (*d*), log expected improvement (LogEI) converged most reliably and rapidly (*e*), reaching the optimum in 96% of SC trials within 25 evaluations (*f*) and outperforming the random search ($P < 0.001$). LogEI also outperformed the random search with 2-fold the experimental noise ($P < 0.001$), demonstrating robustness to the variability expected in live experiments. Smaller initialization budgets were most efficient ($P < 0.001$). In the CMT environment, the BO approach outperformed the grid search ($P < 0.001$) and correctly selected the target region. Together, our results support BO as a data-driven and efficient approach for LIFU parameter mapping under realistic experimental conditions.




**Disclosures: A. Boscutti:** None. **V. Grasso:** None. **T. Di Ianni:** None.

**Poster**

**PSTR207: Computational Methods for Experimental Neuroscience**

**Location:** WCC Halls A-C

**Time:** Monday, November 16, 2026, 1:00 PM - 5:00 PM

**Program #/Poster #:** PSTR207.20/MM6

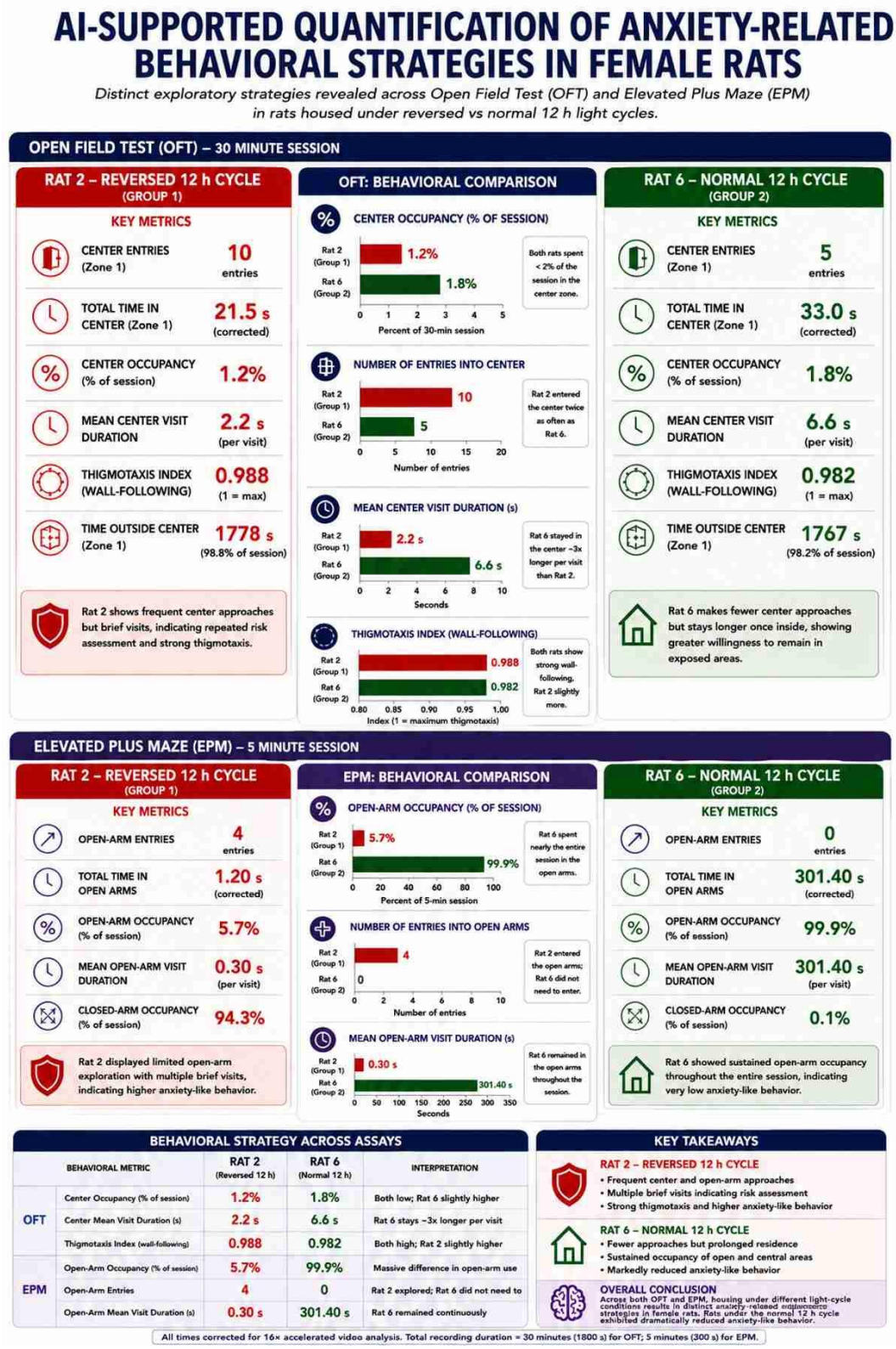
**Topic:** J.06. Computation, Modeling, and Simulation

**Support:** NSF grant 2200489
NSF grant 2200585
NIH grant NINDS R01NS112294
NIH grant R01NS123442
NIMHD U54MD007597
NICHD P50HD105328
CZI NDCF award.

**Title:** AI platform supported quantification of anxiety in female rats

**Authors: *S. ALI**[1], T.-W. TU[2,3], M. SHIH[4];
[1]Howard Univ., Washington, DC; [2]Radiology, Howard Univ., Washington DC, DC; [3]Dept. of Pediatrics, George Washington Univ., Washington DC, DC; [4]Sch. of Computing, Natl. Cheng Kung Univ., Tainin, Taiwan

**Abstract: AI PLATFORM SUPPORTED QUANTIFICATION OF ANXIETY IN FEMALE RATS*AUTHORS:* *S Ali**, M Shih, TW Tu, Department of Radiology, Howard University Washington DC();School of Computing, National Cheng Kung University, Tainan, Taiwan(M Shih)**Disclosures:** S Ali, M Shih, TW Tu: None Behavioral assays remain essential in preclinical research for assessing environmental and experimental effects on animal behavior, yet conventional analyses rely on labor-intensive manual scoring or semi-automatic detector-based apparatus. To address this limitation, we developed an automated video-tracking pipeline based on the YOLO object-detection framework capable of multi-keypoint body segmentation and behavioral quantification.Seven female rats (N = 7; ~1 year old) underwent the Open Field Test (OFT) and Elevated Plus Maze (EPM). Animals were housed under either a reversed 12-hour light cycle (Group 1, n = 3) or standard conditions (Group 2, n = 4). Behavior was recorded using a 4K overhead camera during 30-minute OFT and 5-minute EPM sessions.Representative animals exhibited distinct exploratory patterns during the OFT. Rat 2 (Group 1) entered the center zone 10 times and accumulated 21.5 s of center occupancy (1.2% of the session), whereas Rat 6 (Group 2) entered the center zone five times but accumulated 33.0 s (1.8% of the session), indicating distinct center exploration patterns.EPM analysis revealed marked inter-animal variability, with open-arm occupancy ranging from 0 to 301.4 s. Rats housed under standard conditions exhibited greater mean open-arm occupancy than those maintained under a reversed light cycle (108.2 s vs. 13.7 s), although this difference did not reach statistical significance (Welch's t-test, t = 1.45, df = 3.07, p = 0.241).AI-supported tracking enabled objective quantification of exploratory behavior across OFT and EPM paradigms. Marked inter-animal variability suggests larger cohorts may be required to resolve potential housing-related effects and highlights the utility of YOLO-based tracking for high-throughput analysis of anxiety-related paradigms.




**Disclosures: S. Ali:** None. **T. Tu:** None. **M. shih:** None.

**Poster**

**PSTR207: Computational Methods for Experimental Neuroscience**

**Location:** WCC Halls A-C

**Time:** Monday, November 16, 2026, 1:00 PM - 5:00 PM

**Program #/Poster #:** PSTR207.21/MM7

**Topic:** J.06. Computation, Modeling, and Simulation

**Support:** Pediatric Research Pilot Grant (Marcus Autism Center)
NINDS R01 NS120182
ENPRC P51 OD011132

**Title:** A 3D motion capture and deep learning pipeline for motor abnormality detection in rhesus macaques

**Authors: *N. DESAI**[1], R. RICHARDSON[1], K. LOVE[1], J. RAPER[2];
[1]Emory Univ., Atlanta, GA; [2]Emory Univ., Emory Natl. Primate Res. Ctr., Atlanta, GA

**Abstract:** Precise characterization of motor phenotypes is critical for evaluating neurodevelopmental disorders, but subtle motor impairments induced by early-life viral exposures, including Zika virus (ZIKV), are difficult to detect using standard observational methods. We present an AI-powered pipeline to quantify subtle motor abnormalities in juvenile rhesus macaques (RMs). Utilizing a synchronized 12-camera system and over 30,000 manually annotated frames, we trained a deep learning model to perform robust 3D pose estimation of 17 body landmarks with sub-50mm accuracy. We subsequently deployed this model to infer high-fidelity 3D poses across over 1 million frames of unannotated video (~5h of recording), generating the extensive kinematic time-series data required for behavioral modeling. To bridge the gap between these raw coordinates and biological insight, we apply Keypoint-MoSeq, an unsupervised machine learning framework. Crucially, to adapt this model to the fluid, continuous kinematics of non-human primates, we empirically calibrate the hidden Markov model's state-transition timescale using the autocorrelation of egocentric features. We utilize this calibrated pipeline to decompose high-dimensional tracking data into discrete behavioral 'syllables' that constitute macro behaviors—such as walking, resting, and climbing. We compare syllable usage frequency between ZIKV-infected macaques and age-, sex-, and rearing-matched uninfected controls to identify specific motor patterns that are statistically over- or under-represented. Furthermore, we analyze behavioral transition matrices to determine if ZIKV infection alters the 'grammar' or sequencing of complex motor actions. Specifically, we hypothesize that this unsupervised segmentation will reveal increased motor clumsiness and abnormal kinematic profiles in ZIKV-infected animals, characterized by less stable behavioral transitions and fragmented motor sequences compared to healthy controls. By capturing kinematic and structural differences invisible to the naked eye, this pipeline offers a scalable, objective tool for characterizing motor phenotypes in models of pediatric and neurodegenerative disorders (e.g., Parkinson's disease, HIV infection, early life stress, anesthesia exposure, autism), broadening its impact beyond ZIKV-infected RMs.

**Disclosures: N. Desai:** None. **R. Richardson:** None. **K. Love:** None. **J. Raper:** None.

**Poster**

**PSTR207: Computational Methods for Experimental Neuroscience**

**Location:** WCC Halls A-C

**Time:** Monday, November 16, 2026, 1:00 PM - 5:00 PM

**Program #/Poster #:** PSTR207.22/MM8

**Topic:** J.06. Computation, Modeling, and Simulation

**Support:** Blackrock Neurotech
Wyss Center for Bio and Neuro Engineering
Johns Hopkins University
JHU Applied Physics Laboratory

**Title:** Recent Advances in the ezmsg Ecosystem for Real-Time Neuroscience Applications

**Authors: *G. W. MILSAP**[1], C. BOULAY[2], P. PERANICH[3], K. PILCH[2], K. MCGRAW[2], S. R. NASON-TOMASZEWSKI[3], L. DIAZ[3], H. MARTINEZ[3], M. S. FIFER[3], F. TENORE[3];
[1]Johns Hopkins Univ., Laurel, MD; [2]Blackrock Neurotech, Salt Lake City, UT; [3]Johns Hopkins Univ. Applied Physics Lab., Laurel, MD

**Abstract:** Invasive brain-computer interface (BCI) systems based on electrocorticography (ECoG) and intracortical microelectrode arrays require real-time processing of hundreds to thousands of neural channels sampled at tens of kilohertz while maintaining low-latency operation. Supporting these systems increasingly requires integration of acquisition hardware, signal-processing pipelines, adaptive machine-learning models, visualization tools, simulation environments, and archival data formats within a common software ecosystem.
The ezmsg ecosystem is an open-source (MIT license) collection of Python libraries for constructing modular neural signal-processing applications using a common dataflow programming model. Central to the ecosystem is AxisArray, a coordinate-aware multidimensional array container inspired by xarray's DataArray. AxisArray provides a standardized representation for neural signals and derived features while preserving metadata describing dimensions, coordinates, and sampling relationships. By promoting a common message structure throughout processing pipelines, the ecosystem seeks to reduce fragmentation between acquisition, analysis, visualization, storage, and machine-learning workflows.
More recently, stream-processing components have been implemented independently of the ezmsg runtime through ezmsg-baseproc, which enables processing modules to be developed once and reused in online, offline, simulation, and alternative execution environments. Adaptive modeling capabilities have been introduced through partial_fit-enabled components in ezmsg-learn, supporting continuously updated machine-learning workflows for neural decoding and closed-loop applications. Additional ecosystem packages provide first-class support for Blackrock Neurotech acquisition systems, Lab Streaming Layer (LSL) communication, Neurodata Without Borders (NWB) file generation and logging, event-based processing of sparse or irregularly sampled data streams, real-time system profiling and visualization, and execution across multiple computing nodes.
Although originally motivated by invasive BCI applications, the same abstractions support

noninvasive electrophysiology, multimodal physiology, behavioral sensing, simulation, and closed-loop experimentation. Collectively, these developments extend ezmsg beyond a lightweight messaging framework into a comprehensive ecosystem for prototyping, deploying, sharing, and reproducing real-time neuroscience workflows.

**Disclosures: G.W. Milsap:** None. **C. Boulay:** None. **P. Peranich:** None. **K. Pilch:** None. **K. McGraw:** None. **S.R. Nason-Tomaszewski:** None. **L. Diaz:** None. **H. Martinez:** None. **M.S. Fifer:** None. **F. Tenore:** None.

**Poster**

**PSTR207: Computational Methods for Experimental Neuroscience**

**Location:** WCC Halls A-C

**Time:** Monday, November 16, 2026, 1:00 PM - 5:00 PM

**Program #/Poster #:** PSTR207.23/MM9

**Topic:** J.06. Computation, Modeling, and Simulation

**Support:** University of Minnesota, Interdisciplinary Doctoral Fellowship
University of Minnesota Undergraduate Research Opportunity Funding

**Title:** The Use of Computer Vision to Augment The Assessment of Functional Bilateral Arm Use in Individuals with Chronic Stroke

**Authors: *D. ASANTE**[1], R. L. HAWE[2];
[1]Univ. of Minnesota, Twin Cities, MN; [2]Kinesiology, Univ. of Minnesota, Minneapolis, MN

**Abstract:** The use of both arms in a coordinated way is essential for performing daily functional activities, however, the roles of the arms vary by task. Tasks such as buttoning a shirt require equal contributions from both limbs, while opening a jar of coffee have asymmetric contributions. Stroke results in bilateral arm deficits that are not specifically due to unilateral impairments. However, current clinical assessments focus on unilateral impairments and are mostly subjective. The lack of objective measures limit clinicians' ability to explicitly detect impairments in bilateral tasks as well as track effectiveness of interventions. While computer vision is being increasingly used to quantify movements, functional movements are challenging due to variability in how the tasks can be completed. In this study, we demonstrate the use of computer vision to augment clinical assessments through visualization and quantification of two functional tasks: buttoning a shirt and opening a jar of coffee. We hypothesized that compared to healthy adults, the stroke participant will demonstrate more asymmetrical movements in the buttoning task, however show increased movement of their affected limb in the opening task due to challenges with stabilization. A single camera recorded three healthy older adults and one older adult with stroke while they performed two tasks; buttoning a shirt and opening a jar of coffee. From the videos, individuals' poses were extracted using MediaPipe. For both tasks, participants' poses were visualized using point clouds representing the location of each joint per frame. Poses were quantified using the Minimum Volume Enclosing Ellipse (MVEE) to represent the spatial extent of joint movement. From the MVEE,a laterality index (LI) ranging

from -1 to 1, where zero represents equal bilateral movement, was calculated for each participant's wrists.In the buttoning task, healthy participants had an LI near zero (-0.1 to 0.08), meaning both arms contributed equally, while the stroke participant had a higher LI (0.43), indicating greater asymmetry. In the opening task (asymmetric coordination), the healthy participants had an LI ranging from -0.51 to 0.31, while the stroke participant had a lower LI (-0.05), suggesting impaired ability to differentiate stabilization and manipulation roles.These preliminary results show that our approach was able to detect differences in coordinated arm use between healthy and the stroke participant as well as between tasks, suggesting it could augment clinical assessments of functional bilateral arm use in individuals with stroke.

**Disclosures: D. Asante:** None. **R.L. Hawe:** None.

**Poster**

**PSTR207: Computational Methods for Experimental Neuroscience**

**Location:** WCC Halls A-C

**Time:** Monday, November 16, 2026, 1:00 PM - 5:00 PM

**Program #/Poster #:** PSTR207.24/MM10

**Topic:** J.06. Computation, Modeling, and Simulation

**Support:** TUSEB Grant 39026

**Title:** A bio-inspired catheter system for depth estimation by impedance sensing

**Authors:** A. BOUSTANABADI MARALAN[1], ***E. KÖSE**[1], I. UYANIK[2];
[2]Electrical and Electronics Engin., [1]Hacettepe Univ., Ankara, Turkey

**Abstract:** Minimally invasive neuro-interventional treatments rely on fluoroscopy for catheter navigation, resulting in repeated exposure of neural tissue, patients, and clinicians to ionizing radiation. Inspired by the electrolocation mechanism of weakly electric fish, which sense their surroundings through bioelectric field perturbations, we present a bio-inspired bioelectric sensing system and its experimental validation in 3D-printed neurovascular models. The approach exploits localized bioimpedance variations to estimate vessel geometry and catheter depth without the use of X-ray imaging. To ensure scientific rigor and reproducibility, vascular phantoms incorporating key features such as stenosis, aneurysmal dilations, and bifurcations were designed and fabricated using 3D-printing. Relevant biological variables (e.g., species, sex, age) are not applicable to this study, as the experiments were conducted entirely in-vitro using synthetic models. Custom intravascular catheters with optimized electrode spacing were integrated with a high-gain, low-noise acquisition circuit and advanced through saline-immersed models to replicate conductive biological environments. Results from repeated experimental trials demonstrated that recorded bioimpedance signals showed consistent and repeatable modulation in response to changes in vessel geometry. Specifically, signal amplitude increased in narrowed regions and decreased at aneurysmal and bifurcation sites. Quantitative analysis revealed an inverse relationship between measured voltage and local vessel cross-sectional area, supporting the feasibility of depth and structural estimation based on bioelectric cues. These

results validate the use of bio-inspired electrosensory principles for intravascular sensing in anatomically realistic 3D-printed neurovascular models and establish a foundation for developing radiation-free guidance strategies for future neuro-interventional applications.

**Disclosures: A. Boustanabadi Maralan:** None. **E. Köse:** None. **I. Uyanik:** None.

**Poster**

**PSTR207: Computational Methods for Experimental Neuroscience**

**Location:** WCC Halls A-C

**Time:** Monday, November 16, 2026, 1:00 PM - 5:00 PM

**Program #/Poster #:** PSTR207.25/MM11

**Topic:** J.06. Computation, Modeling, and Simulation

**Title:** Event-related versus block modeling improves detection of single-pulse TMS-evoked fMRI subgenual cingulate response

**Authors: *H. KHALILKHANI**[1,2], D. J. OATHES[3];
[1]Univ. Of Pennsylvania, philadelphia, PA; [2]Perelman Sch. of Med., Univ. Of Pennsylvania, Philadelphia, PA; [3]Perelman Sch. of Med., Univ. of Pennsylvania, Philadelphia, PA

**Abstract:** Concurrent TMS-fMRI measures stimulation-evoked brain responses and is increasingly used to quantify target engagement in therapeutic TMS for depression. The subgenual anterior cingulate cortex (sgACC) is a central target, whose response to prefrontal stimulation may index treatment relevance. Yet, how single-pulse TMS responses should be modeled is underexplored; pulses are typically delivered in interspersed blocks, and treating each pulse as a discrete event versus modeling clusters as sustained blocks may affect sensitivity for capturing circuit engagement evidence such as between cortex and targets like the sgACC. We compared event-related and block first-level designs in 108 single-pulse TMS-fMRI runs from 54 participants, stimulating frontal targets functionally coupled to sgACC. Designs were identical except for the timing model and evaluated averaged over an a priori defined anatomical sgACC region of interest. Both designs revealed a single-pulse-evoked sgACC negative BOLD response (consistent with our prior published work), but event-related modeling was more sensitive, detecting 106 significant ROI voxels (peak $Z=4.36$) versus 7 for block modeling ($Z=3.30$). A threshold-independent per-subject comparison confirmed significantly stronger negative BOLD response under event-related modeling (paired $t=-3.46$, $p<0.001$). A model-free deconvolution, independent of either model, confirmed a negative BOLD response peaking ~8s post-pulse, revealing a rapid per-pulse structure that block modeling captures less effectively. The advantage extended across a whole-brain analysis, indicating an overall sensitivity gain. Stratifying by target valence (positive or negative connectivity), the evoked sgACC negative BOLD response was significant for anticorrelated targets (event-related: $t(53)=-3.65$, $p<0.001$; block: $p=0.004$) but not for positive-correlated targets (both $p>0.1$). Critically, both modeling approaches recovered this same valence pattern, indicating a property of the response rather than a modeling artifact. This localization of negative BOLD primarily to anticorrelated targets contrasts our prior work but may be due to updates in our stimulation parameters, imaging

acquisition or patient cohort. These findings show that event-related modeling more robustly captures single-pulse TMS-evoked sgACC responses, with direct implications for measuring target engagement in neuroscience and therapeutic TMS applications.

**Disclosures: H. khalilkhani:** None. **D.J. Oathes:** None.

**Poster**

**PSTR207: Computational Methods for Experimental Neuroscience**

**Location:** WCC Halls A-C

**Time:** Monday, November 16, 2026, 1:00 PM - 5:00 PM

**Program #/Poster #:** PSTR207.26/MM12

**Topic:** J.06. Computation, Modeling, and Simulation

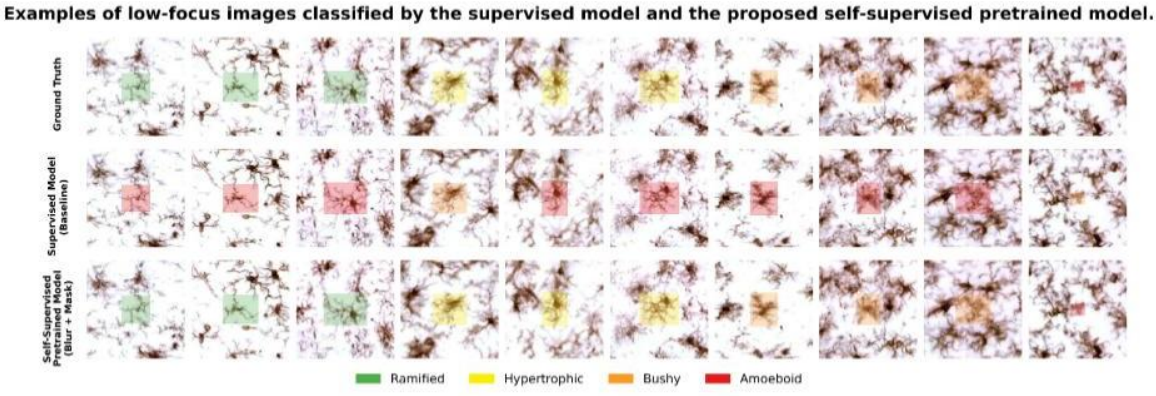
**Support:** NSF grants 2200489 and 2200585
NIH grants NINDS R01NS112294 and R01NS123442
NIMHD U54MD007597
NICHD P50HD105328
CZI NDCF award

**Title:** Self-Supervised Pretraining Improves Microglial Classification in Defocused Immunohistochemistry Images

**Authors: *Y.-A. LIAO**[1,2], M. SHIH[2,3], C.-H. HSU[2], P. WANG[2], T.-W. TU[2,4];
[1]New York Univ., New York, NY; [2]Howard Univ., Washington, DC; [3]Natl. Cheng Kung Univ., Tainan, Taiwan; [4]George Washington Univ., Washington, DC

**Abstract:** Microglial morphology is widely used to quantify neuroinflammation in immunohistochemistry images. Despite advances in deep learning-based automated classification, models remain sensitive to image quality. Defocused regions caused by uneven tissue placement degrade both human annotation reliability and model performance, making large-scale labeling difficult. To investigate whether reconstruction-based self-supervised pretraining can improve robustness to focus degradation, we assessed an approach to reduce reliance on labeled defocused data by training classifiers on high- and mid-focus images and evaluating them on unseen low-focus images. Iba1-stained microglial images (n=1720) from the rat prefrontal cortex were categorized into high- (Brenner's focus measure, FM ≥ 1100), mid- (550 ≤ FM < 1100), and low-focus (FM < 550) groups. A ResNet50 encoder was pretrained using a masked autoencoder-style framework that learns image representations by reconstructing original images from corrupted inputs. To simulate focus degradation typical in microscopy, we compared three corruption strategies: Gaussian blur, random patch masking, or blur plus masking. Following pretraining, the encoder and a linear classification head were fine-tuned to predict four microglial activation states (Ramified, Hypertrophic, Bushy, and Amoeboid) using only high- and mid-focus images. Model performance was evaluated on low-focus images and compared against a supervised baseline without pretraining. The supervised baseline achieved 57% accuracy on low-focus images. Self-supervised pretraining improved performance across all

reconstruction objectives, with blur achieving 62% accuracy, masking 66%, and blur plus masking 74%. Although masking alone produced the highest validation accuracy on high- and mid-focus images (85%), blur plus masking yielded the strongest performance on low-focus images. These findings suggest that incorporating blur-related image corruption during pretraining improves robustness to focus degradation in automated IHC image analysis.




**Disclosures: Y. Liao:** None. **M. shih:** None. **C. Hsu:** None. **P. Wang:** None. **T. Tu:** None.

**Poster**

**PSTR207: Computational Methods for Experimental Neuroscience**

**Location:** WCC Halls A-C

**Time:** Monday, November 16, 2026, 1:00 PM - 5:00 PM

**Program #/Poster #:** PSTR207.27/MM13

**Topic:** J.06. Computation, Modeling, and Simulation

**Support:** NIH R24MH120037
NIH R01NS047293

**Title:** Neuroinformatics infrastructure for human electrophysiology

**Authors: *S. MAKEIG**[1,2], A. DELORME[5], S. SHIRAZI[3], A. MAJUMDAR[4];
[1]Swartz Ctr. for Computat. Neurosci., La Jolla, CA; [2]Inst. for Neural Computation, Univ. of California San Diego, La Jolla, CA; [3]Swartz Ctr. for Computat. Neurosci., Univ. of California San Diego, San Diego, CA; [4]San Diego Supercomputer Ctr., Univ. of California San Diego, LA JOLLA, CA; [5]UCSD Dept. of Neurosciences, La Jolla, CA

**Abstract:** Deep neural network and related methods for modeling complex data radically change the focus of data collection and analysis - from planned hypothesis testing to disjunctive data exploration. Whereas the former requires limited and balanced data collection, the latter can profit from unlimited, highly variegated data sets. Thus, human brain electrophysiology data collected using limited designs can be amassed and mined for more of its latent information

about brain dynamics - if well-labeled then combined into large datasets. We overview a set of interconnected resources to prepare and share data, tools, and compute resources to process human electrophysiology data (EEG, MEG, and iEEG) in new ways: BIDS (Brain Imaging Data Structure) and HED (Hierarchical Event Descriptors) for data annotation, NEMAR (Neuroelectromagnetic data Archive and tools Resource) for data sharing, EEGDASH for data preprocessing and NSG (Neuroscience Gateway) for high-performance computing.

**Disclosures: S. Makeig:** None. **A. Delorme:** None. **S. Shirazi:** None. **A. Majumdar:** None.

**Poster**

**PSTR207: Computational Methods for Experimental Neuroscience**

**Location:** WCC Halls A-C

**Time:** Monday, November 16, 2026, 1:00 PM - 5:00 PM

**Program #/Poster #:** PSTR207.28/MM14

**Topic:** J.06. Computation, Modeling, and Simulation

**Title:** Three-Dimensional Automated Reconstruction of Human Hippocampal Pyramidal Neurons in Ammon's Horn from Serial Whole-Slide Histology

**Authors: *J. CHANG**[1], Y. FARRIS[1], D. W. NAUEN[2];
[1]Johns Hopkins Univ., Baltimore, MD; [2]Div. of Neuropathology, Johns Hopkins Hosp. and Hlth. Syst., Baltimore, MD

**Abstract:** Cellular architecture constrains hippocampal circuit function, but most human histological analyses remain effectively two-dimensional and therefore lose the three-dimensional spatial context of individual neurons. Although volumetric atlases and specialized imaging methods have advanced microscopic human brain mapping, accessible approaches for reconstructing all neuron instances in a volume from serial whole-slide histology remain limited. We developed a computational pipeline to reconstruct pyramidal neuron somata in three dimensions from serial histological sections of human hippocampus. Deidentified tissue from neurologically normal human brain was sectioned into consecutive 5-µm sections, Nissl stained, scanned as high-resolution whole-slide images at 1-µm intervals through the thickness, and registered across adjacent sections. A deep learning segmentation model was trained to identify pyramidal neuron somata in two-dimensional whole-slide image tiles, and segmented somata were linked across adjacent sections using cross-slice spatial correspondences to recover object-level three-dimensional neuron instances. We then quantified soma density, size, shape, orientation, and spatial distribution across hippocampal subregions. The current workflow supports image normalization, registration of serial whole-slide images, tile-level soma segmentation, cross-section instance linking, and export of soma-level morphometric features for downstream analysis. Initial applications demonstrate that this approach preserves local spatial relationships across sections and enables analysis of neuronal morphology and organization in three dimensions. We are applying this workflow to additional hippocampal sections and cases to increase anatomical coverage, evaluate reproducibility, and establish a baseline for future disease comparisons. Because the workflow uses Nissl staining for anatomic delineation, it is compatible

with post-scan immunohistochemistry, allowing immunophenotypic verification of cell identity and future tests of relationships among cellular morphology, protein expression, and hippocampal subregional boundaries. This framework provides a practical strategy for three-dimensional cell-level mapping from human serial histology. Applied to the hippocampus, it can support quantitative studies of cytoarchitectural organization and may help identify structural alterations in disorders such as epilepsy or Alzheimer's disease.

**Disclosures: J. Chang:** None. **Y. Farris:** None. **D.W. Nauen:** None.

**Poster**

**PSTR207: Computational Methods for Experimental Neuroscience**

**Location:** WCC Halls A-C

**Time:** Monday, November 16, 2026, 1:00 PM - 5:00 PM

**Program #/Poster #:** PSTR207.29/MM15

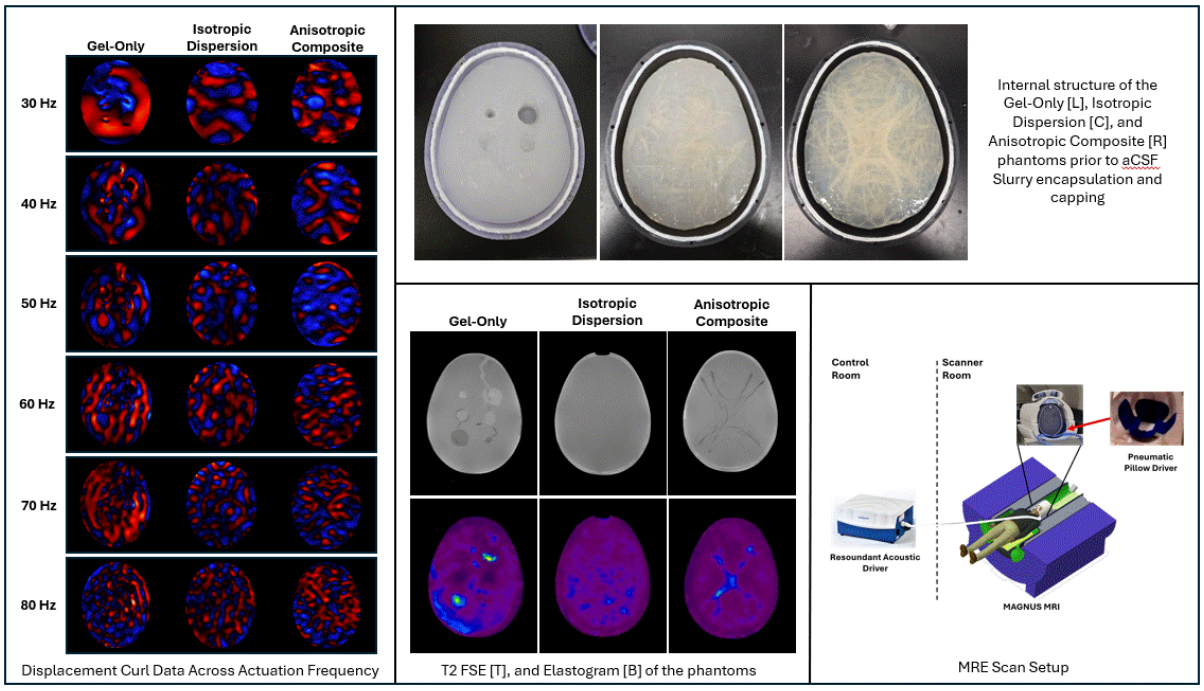
**Topic:** J.06. Computation, Modeling, and Simulation

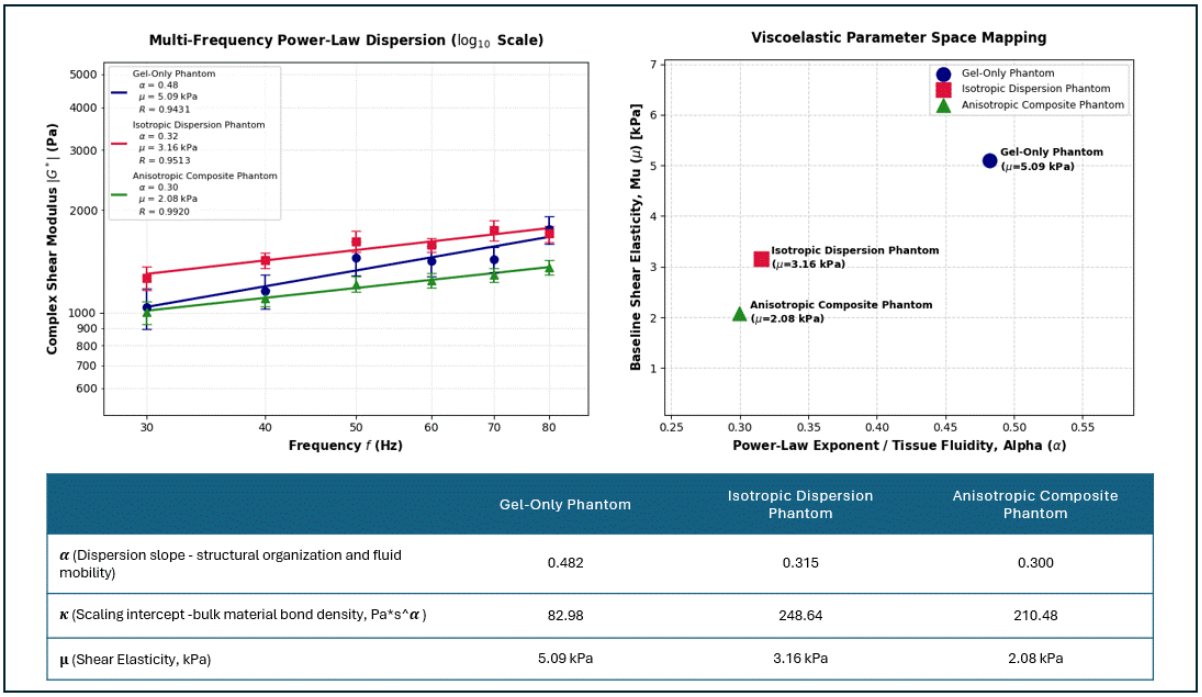
**Support:** HU00012520052

**Title:** Power Law Analysis of Brain Microstructure via Multi-Frequency MRE: Proof of Concept for an Updated Framework Using Phantoms

**Authors: E. R. LONG**, E. CHOW, *T. YUAN, H. MORRIS;
Uniformed Services Univ., Bethesda, MD

**Abstract:** Microstructural geometry and density changes in neural pathology can be characterized via multi-frequency MRE using the power law $G^* = \kappa;(2\pi f)^{\alpha}$. Experimental validation of the structure changes predicted by this model remains open. This work provides evidence for understanding how altered microstructure drives viscoelastic changes, strengthening these metrics as a biomarker for structural remodeling. Three brain-mimicking agar phantoms were scanned at 3T (30-80 Hz): a Gel-Only baseline, an Isotropic Dispersion phantom (random cellulose strips), and an Anisotropic Composite (AC) phantom (aligned nylon bundles). Power-law metrics shifted based on structural layout. The fluid-permissive gel baseline ($\alpha$=0.48, $\mu$=5.09 kPa) shifted when randomly arranged fibrous strands were introduced ($\alpha$=0.32, $\mu$=3.16 kPa) and aligned tracts furthered this shift ($\alpha$=0.30, $\mu$=2.08 kPa), reducing crosslink density as predicted by Sack et. al (2013) and, we hypothesize, restricting fluid mobility. This work provides a direct physical model of a mechanism for the simultaneous drop in $\alpha$ and $\mu$ clinically observed in chronic MS patients. We propose that this dual drop signifies both a reduction in crosslink density and organized structural fluid-pinning. This demonstration strengthens viscoelasticity as a biomarker capable of detecting tissue changes in vivo below imaging resolution and differentiating microscopic tissue degradation from microstructural remodeling (e.g., glial scarring).




| | Gel-Only Phantom | Isotropic Dispersion Phantom | Anisotropic Composite Phantom |
|---|---|---|---|
| $\alpha$ (Dispersion slope - structural organization and fluid mobility) | 0.482 | 0.315 | 0.300 |
| $\kappa$ (Scaling intercept -bulk material bond density, Pa*s^$\alpha$) | 82.98 | 248.64 | 210.48 |
| $\mu$ (Shear Elasticity, kPa) | 5.09 kPa | 3.16 kPa | 2.08 kPa |

**Disclosures: E.R. Long:** None. **E. Chow:** None. **T. Yuan:** None. **H. Morris:** None.

**Poster**

**PSTR208: Computational Modeling of Synaptic Networks**

**Location:** WCC Halls A-C

**Time:** Monday, November 16, 2026, 1:00 PM - 5:00 PM

**Program #/Poster #:** PSTR208.01/MM16

**Topic:** B.07. Network Interactions

**Support:** NSF CRCNS 2508419
NIH MVTP T32

**Title:** Bridging Functional Activity and Synaptic Connectivity through Ensemble Modeling in the Larval Zebrafish Pretectum

**Authors: *S. CHALYSHKAN**[1], T. BISWAS[2], B. JAMES[3], Y. CHEN[4], L. STOCKERT[5], D. FÖRSTER[6], F. KUBO[7], H. BAIER[8], J. E. FITZGERALD[2];
[1]Northwestern Univ., Chicago, IL; [2]Neurobio., Northwestern Univ., Evanston, IL; [3]Neurobio., Northwestern Univ., Chicago, IL; [4]Northwestern Univ., Evanston, IL; [5]Max Planck Inst. for Biol. Intelligence, Martinsried, Germany; [6]Univ. of Cologne, Cologne, Germany; [7]RIKEN Ctr. for Brain Sci., Saitama, Japan; [8]Genes - Circuits - Behavior, Max Planck Inst. of Neurobio., Planegg, Germany

**Abstract:** With the growing use of large-scale activity recordings and advances in anatomical circuit-level reconstructions, researchers can now propose numerous neural network models that tie synaptic connectivity with neuronal activity. However, understanding how well different model classes capture observed neural activity and synaptic connectivity remains a significant challenge in computational neuroscience. Rather than fitting a single model to match observed functional profiles, we examine an ensemble modeling approach that identifies features consistent across all admissible models. We apply this framework to optic flow processing in the larval zebrafish pretectum, taking advantage of a whole-brain connectomics dataset at synaptic resolution alongside recordings of major functional response types. This allows a stringent test of model predictions by comparing inferred structure-function relationships against experimentally measured activity and connectivity. We model the pretectum as a threshold-linear recurrent neural network operating at steady state and use quadratic programming to characterize its solution space. While connectivity predictions remain sensitive to the resolution at which response types are defined and therefore cannot yet be conclusively resolved, robust structure-function relationships emerge at the level of neural activity. Specifically, ensemble modeling predicts neural activity responses to held-out stimulus conditions more accurately than input drives alone. The unresolved structural predictions have motivated parallel efforts to determine whether key functional or structural principles are missing from the model, whether the theoretical assumptions are appropriate, and how theory and experiment can be more effectively aligned. Ongoing work addressing these questions will further test the utility of ensemble modeling as a framework for connectivity prediction.

**Disclosures: S. Chalyshkan:** None. **T. Biswas:** None. **B. James:** None. **Y. Chen:** None. **L. Stockert:** None. **D. Förster:** None. **F. Kubo:** None. **H. Baier:** None. **J.E. Fitzgerald:** None.

**Poster**

**PSTR208: Computational Modeling of Synaptic Networks**

**Location:** WCC Halls A-C

**Time:** Monday, November 16, 2026, 1:00 PM - 5:00 PM

**Program #/Poster #:** PSTR208.02/Web Only

**Topic:** B.07. Network Interactions

**Support:** Sasakawa Scientific Research Grant, The Japan Science Society

**Title:** Biophysical simulation of frequency-dependent cortical circuit responses to repetitive transcranial magnetic stimulation

**Authors: *M. YONEZAWA**[1], T. YAMAZAKI[2];
[1]The Univ. of Electro-Communications, Kashiwa-shi, Japan; [2]The Univ. of Electro-Communications, Tokyo, Japan

**Abstract:** Repetitive transcranial magnetic stimulation (rTMS) is widely used as a non-invasive neuromodulation approach for neurological and psychiatric disorders, but how local cortical circuit activity changes over time under different stimulation frequencies remains incompletely understood. Most modeling studies have focused on single-pulse stimulation or single-neuron responses, leaving circuit-level analyses that integrate morphological detail, synaptic connectivity, and repetitive stimulation limited. Here, we incorporated TMS-induced electric fields into a morphologically detailed local circuit model of mouse primary visual cortex (V1) to examine how rTMS frequency shapes layer- and cell-type-specific activity over time. To reduce the high computational cost of repetitive stimulation in detailed circuit models, we used Neulite, a lightweight biophysical neural circuit simulator. The model included multi-compartment neurons with realistic morphology and synaptic connectivity, and electric fields were computed from the spatial coordinates of each compartment and incorporated into membrane potential calculations as external inputs. We applied repetitive stimulation across multiple frequency conditions and analyzed per-pulse responses, layer-specific firing rates, and changes in activity in excitatory and inhibitory populations. Each pulse evoked a transient increase in firing rate immediately after stimulation, followed by a delayed suppressive response. At higher frequencies (~10 Hz), successive pulses arrived before suppression fully developed, producing repeated overlap of pulse-evoked activation and a net increase in firing rate. At lower frequencies (~1 Hz), delayed suppression developed after each pulse, leading to a net reduction in circuit activity. These frequency-dependent response patterns were particularly pronounced in layer 2/3 (L2/3) pyramidal cells. The observed transient activation followed by delayed suppression is consistent with experimental and multi-scale cortical circuit simulation studies (Romero et al., Nature Communications, 2019; Zhao et al., Brain Stimulation, 2026). Our results suggest that the timing between pulse-evoked activation and delayed suppression may help explain the frequency-dependent effects of rTMS, with low-frequency suppression and high-frequency facilitation. These simulations provide a computational framework for linking rTMS frequency conditions to local cortical circuit dynamics.

**Disclosures: M. Yonezawa:** None. **T. Yamazaki:** None.

**Poster**

**PSTR208: Computational Modeling of Synaptic Networks**

**Location:** WCC Halls A-C

**Time:** Monday, November 16, 2026, 1:00 PM - 5:00 PM

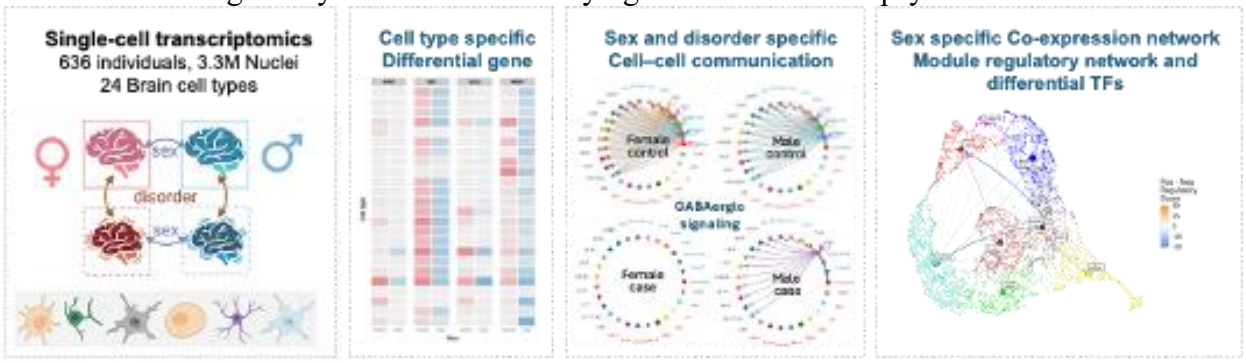
**Program #/Poster #:** PSTR208.03/MM17

**Topic:** B.07. Network Interactions

**Title:** Sex-stratified single-cell transcriptomic analysis reveals molecular and cellular signatures across multiple psychiatric disorders

**Authors: *Y. XIA**;
Yale Univ., New Haven, CT

**Abstract:** Sex differences are pervasive across multiple psychiatric disorders, influencing prevalence, symptomatology, and treatment response. However, the molecular mechanisms underlying these differences remain incompletely understood. Here, we present a comprehensive sex-stratified single-nucleus RNA-seq analysis of 3.3 million nuclei from 636 postmortem brains (PsychENCODE Phase III) spanning schizophrenia, bipolar disorder, autism spectrum disorder, major depressive disorder, post-traumatic stress disorder, and controls. We examined four contrasts: male versus female within cases and controls, and case versus control within males and females. Pseudobulk differential expression was performed using DESeq2, Dreamlet, and glmGamPoi to ensure robustness. Across disorders, we identified numerous sex-specific disease-associated differentially expressed genes (DEGs). Intriguingly, in each disorder, the sex with lower disease prevalence exhibited stronger transcriptional perturbations. These sex-biased DEGs were enriched for synaptic and glutamatergic signaling pathways, particularly within GABAergic and layer 6 excitatory neurons. Moving beyond single-gene analyses, network-level approaches revealed broader mechanistic insights. Key differences emerged in GABAergic signaling networks—including altered NRXN-NLGN interactions—and in gene modules regulated by estrogen-responsive transcription factors such as JUN/FOS. Integration with summary-based Mendelian randomization analyses further linked sex-biased expression to putative causal loci and known drug targets (e.g., *GABRA5*, *SNCA*), revealing sex-specific therapeutic opportunities. Together, these findings highlight the necessity of incorporating sex as a core biological variable and illustrate how integrative, systems-level approaches can illuminate the cellular and regulatory architecture underlying sex differences in psychiatric disorders.




**Disclosures: Y. Xia:** None.

**Poster**

**PSTR208: Computational Modeling of Synaptic Networks**

**Location:** WCC Halls A-C

**Time:** Monday, November 16, 2026, 1:00 PM - 5:00 PM

**Program #/Poster #:** PSTR208.04/MM18

**Topic:** B.07. Network Interactions

**Support:** MUR PRIN 2022 BHISTROT Grant: 2022YZRF4E

**Title:** Computational modeling of biological variability in dendritic spine distribution from high-resolution 3D images of human CA1 pyramidal neurons

**Authors: E. BRUNO**[1,2], I. FERNAUD-ESPINOSA[3], C. MAGLIARO[1,2], R. BENAVIDES-PICCIONE[3,4], J. DEFELIPE[3,4], *M. MIGLIORE[5], N. VANELLO[1,2];
[1]Dept. di Ingegneria dell' Informazione, Univ. of Pisa, Pisa, Italy; [2]Res. Ctr. "E. Piaggio", Univ. of Pisa, Pisa, Italy; [3]Lab. Cajal de Circuitos Corticales, Ctr. de Tecnología Biomédica, Univ. Politécnica de Madrid, Madrid, Spain; [4]Cajal Neurosci. Center, CSIC, Madrid, Spain; [5]Inst. of Biophysics, Natl. Res. Council, Palermo, Italy

**Abstract:** Computational modeling allows us to improve our understanding of neural architecture and to explore pathophysiological hypotheses. One of the most relevant issues currently addressed in this field is the ability of a model to account for the natural variability of neural function, both across different neuron types and within the same neuronal population. This goal is usually pursued by fitting neurophysiological measurements to generic yet adaptive models. Fine anatomical structures, such as spines, can also be segmented from high resolution images; this detailed description can be used to build a model that is replicated along the dendrites or that modulates the neuronal membrane properties. Here we propose a complementary approach, which consists of estimating a full neuron model directly from high-resolution 3D images of real neurons, describing the exact position of spines along the dendrites and estimating their length and size. We tested the approach on human hippocampal tissue from the CA1 region, obtained post-mortem under approved ethical protocols. Pyramidal neurons were intracellularly injected with Lucifer Yellow to label dendritic arbors and spines, and imaged using a Leica TCS 4D confocal microscope (63× glycerol objective, voxel size $0.073\times0.073\times0.28$ μm³). Neuronal structures were reconstructed through SENPAI, a 3D segmentation algorithm leveraging image intensity and Hessian-based second-order derivatives to highlight tubular and protruding structures. A whole pyramidal neuron was fully segmented, preserving fine spine details, and then skeletonized. An SWC file was obtained, containing relevant nodes and corresponding neuronal sections; terminal segments shorter than 5 μm were assigned to spines. A total of 3349 spines were reconstructed. The median spine length was 1.76 μm (median absolute deviation 0.61 μm) and varied along the dendrite, with a minimum in proximal regions (median 1.60 μm) and a maximum at distal regions (approximately 200 μm from the soma, median 1.90 μm). Spine density was very low close to the soma, increased to 0.31 spines/μm within 50 μm, and reached a plateau of 0.47 spines/μm between 100 and 300 μm, decreasing in distal regions (0.25 spines/μm from 350 μm). Although method performances, especially regarding spine density, need further exploration, the spine statistics obtained and their variation along the dendrite are in line with expected values. The proposed approach is therefore

a good candidate for generating computational neuron models that account for the variability of neuronal structure, spine size, and spine distribution, and that can be imported into tools such as NEURON, GENESIS, or NetPyNE.

**Disclosures: E. Bruno:** None. **I. Fernaud-Espinosa:** None. **C. magliaro:** None. **R. Benavides-Piccione:** None. **J. DeFelipe:** None. **M. Migliore:** None. **N. Vanello:** None.

**Poster**

**PSTR208: Computational Modeling of Synaptic Networks**

**Location:** WCC Halls A-C

**Time:** Monday, November 16, 2026, 1:00 PM - 5:00 PM

**Program #/Poster #:** PSTR208.05/MM19

**Topic:** B.07. Network Interactions

**Support:** NIH Grant U24 NS124001-01
NIH Grant R01NS122742

**Title:** Simulations of cortical circuits across the cortical hierarchy

**Authors: *L. GREEN**[1], S. ITO[1], D. HAUFLER[1], C. WANG[1], K. DAIE[2], A. ARKHIPOV[1]; [1]Allen Inst., Seattle, WA; [2]Allen Inst. for Neural Dynamics, Seattle, WA

**Abstract:** The mammalian neocortex is a complex structure with many interacting regions and cell types. Multiple efforts have recently generated large datasets from multiple cortical regions to determine generalizing principles of cortical organization and activity. One such generalizing principle is the concept of a cortical hierarchy - low-dimensional macroscopic gradients of biological properties across cortical areas and a hierarchy of timescales for information processing. Such gradients in properties along a cortical hierarchy may explain how different cortical regions serve different computational roles (i.e. sensory processing versus working memory). We set out to investigate such principles using biologically realistic simulations. Starting from our previously published model of the mouse primary visual cortex (V1) with updated connectivity reflecting recent large-scale connectomics and synaptic physiology datasets, we generate multiple versions of the cortical circuit model with increased connectivity as measured along the cortical hierarchy. We then measure the resulting neural activity in response to a simulated single-cell photostimulation paradigm and thalamocortical inputs. Our findings are as follows: (1) We find that SST cells are most responsive to the stimulation paradigm, due to high excitability of SST cells and relatively weak inhibitory input to SST cells in layer 2/3. (2) Models that are higher along the cortical hierarchy are less responsive to stimulation and receive proportionally more input from SST cells. (3) Time constants in our simulations of isolated cortical areas follow a power law distribution within each region, but decrease along the cortical hierarchy, suggesting that the experimentally observed increase in time constants across the cortical hierarchy is due to long-range connectivity rather than local connectivity. Overall, our results shed light on the mechanisms that determine distinct activity patterns of cortical regions and, thus, likely facilitate their distinct computational roles. Our

findings also link population activity to cell type and circuit properties, generating insight into potential perturbation mechanisms that might be applied to produce desired neural activity.

**Disclosures: L. Green:** None. **S. Ito:** None. **D. Haufler:** None. **C. Wang:** None. **K. Daie:** None. **A. Arkhipov:** None.

**Poster**

**PSTR208: Computational Modeling of Synaptic Networks**

**Location:** WCC Halls A-C

**Time:** Monday, November 16, 2026, 1:00 PM - 5:00 PM

**Program #/Poster #:** PSTR208.06/MM20

**Topic:** J.08. Methods to Modulate Neural Activity

**Support:** R01-MH132592

**Title:** Engineering Programmable Reversible DART Pharmacology

**Authors: *L. LI**[1], B. C. SHIELDS[2], M. R. TADROSS[2,3];
[1]Dept. of Biomed. Engin., [2]Neurosurg., [3]Biomed. Engin., Duke Univ., Durham, NC

**Abstract:** Cell-type-specific neuropharmacology offers a powerful approach to investigate causal links between neural circuits and behavior. It combines the rapid onset of conventional pharmacology with the cellular precision of genetically encoded tools. DART (Drug Acutely Restricted by Tethering) achieves this by expressing HaloTag Protein (HTP) in targeted cell types via a cell-type-specific viral vector, so that only these cells capture and concentrate a drug chemically linked to the HaloTag Ligand (HTL). Notably, the bond between HTL and HTP is covalent, and is therefore ideally suited to rapid-onset, long-lasting perturbations. However, it limits re-dosing flexibility until the protein-ligand complex is endocytosed roughly seven days later.

To enable greater temporal flexibility, we engineered a programmable, reversible HaloTag system that releases ligand with tunable kinetics. Our strategy was to engineer mutations that restore the hydrolytic activity of the dehalogenase upon which HTP was based, and to engineer novel ligands that provide a broad range of chemically programmable release kinetics.

We synthesized HTL variants and used localized surface plasmon resonance (LSPR) to measure rates of ligand capture and release. For our first HTP design, the fastest HTL released the ligand in under one minute, while the slowest released ligand in more than an hour. Thus, we achieved more than sixty fold chemically programmable release kinetics. We next engineered HTP mutants that tuned kinetics globally, slowing or accelerating hydrolysis across all ligands, while retaining a similar fold-change in chemically programmable release. Finally, a live-cell dye-release assay validated these effects in primary neurons. The slow-release ligand dissociated markedly slower than the fast one and the protein variants influenced the kinetics globally, matching the LSPR ranking. Together, these engineered ligand-protein pairs span a broad kinetic spectrum that can be matched to different experimental needs, laying a foundation for reversible, in vivo DART applications.

**Disclosures: L. Li:** None. **B.C. Shields:** None. **M.R. Tadross:** None.

**Poster**

**PSTR208: Computational Modeling of Synaptic Networks**

**Location:** WCC Halls A-C

**Time:** Monday, November 16, 2026, 1:00 PM - 5:00 PM

**Program #/Poster #:** PSTR208.07/MM21

**Topic:** J.08. Methods to Modulate Neural Activity

**Support:** NIH Grant NS110575
NIH Grant DC019916
Novo Nordisk Foundation 0064289
Boston VA Healthcare System BX005959

**Title:** Characterizing Neural Responses to Magnetic Intracochlear Stimulation in a Guinea Pig Model

**Authors: *J.-I. LEE**[1], V. ADENIS[2], S. FRIED[1,3];
[1]Massachusetts Gen. Hosp., Boston, MA; [2]Massachusetts Eye and Ear, Boston, MA; [3]Boston VA Healthcare Syst., Boston, MA

**Abstract:** Cochlear implant (CI) performance remains limited largely by broad current spread during multichannel electrical stimulation, which contributes to spectral blurring and reduces the number of independent spectral channels. This channel interaction limits speech perception in noise and music appreciation. Magnetic stimulation using microcoils may provide an alternative strategy for focal auditory activation by generating localized induced electric fields near target neurons, rather than injecting current directly into the cochlear fluid. Here, we evaluated whether intracochlear magnetic stimulation can evoke spatially restricted and tonotopically appropriate auditory responses in deafened guinea pigs. Acute experiments were performed in anesthetized guinea pigs. A 16-channel recording electrode array was inserted into the inferior colliculus along its tonotopic axis, and placement was confirmed using acoustic pure-tone stimulation. The contralateral cochlea was then acutely deafened by neomycin injection. Magnetic and electrical stimulation were delivered sequentially through arrays inserted into the basal turn of the cochlea via the round window, and spread of excitation profiles were compared at two intracochlear stimulation sites. Intracochlear magnetic stimulation evoked robust multiunit responses in the inferior colliculus. Compared with electrical stimulation, magnetic stimulation produced narrower activation profiles and a clearer shift in the locus of activation when the stimulation site was advanced deeper into the cochlea, consistent with preserved tonotopic organization. These findings suggest that magnetic microcoil stimulation reduces overlap in the neural populations activated by neighboring stimulation sites and may improve channel independence, offering a promising strategy to enhance spatial selectivity and increase the number of independent spectral channels for future CIs.

**Disclosures: J. Lee:** None. **V. Adenis:** None. **S. Fried:** None.

**Poster**

**PSTR208: Computational Modeling of Synaptic Networks**

**Location:** WCC Halls A-C

**Time:** Monday, November 16, 2026, 1:00 PM - 5:00 PM

**Program #/Poster #:** PSTR208.08/MM22

**Topic:** J.08. Methods to Modulate Neural Activity

**Support:** NIH BRAIN Initiative R21EB028055
NIH Grant R44MH131514

**Title:** Low-intensity pulsed ultrasound increases chronic recording yield while reducing microglia activation surrounding the electrode interface

**Authors: *K. A. SNOOK**[1], J. GREASER[2], O. GROVE[2], R. BAGWELL[2], T. THAI[3], V. SINGH[5], A. FORREST[4], Y. SUOFU[3], T. D. KOZAI[3], M. L. MULVIHILL[2];
[1]R&D, [2]Actuated Medical, Inc., Bellefonte, PA; [3]Bioengineering, [4]Univ. of Pittsburgh, Pittsburgh, PA; [5]Bioengineering, Univ. of Pittsburgh, Bioengineering, Pittsburgh, PA

**Abstract:** Neural implants holds great potential as a treatment for various neurological disorders. However, these implants can damage brain tissue during insertion and evoke a foreign body response (FBR). The FBR can damage neurons, and cause glial scarring and neuronal cell loss near electrode sites, which can affect electrode longevity and stability. Efforts to limit insertion damage, such as with flexible implants or incorporating exogenous immunosuppressant chemicals, have some benefit, but more needs done to clear the path for clinical applications. Past work has reported that transcranial focused ultrasound promotes neurotrophic factors in cerebral disease and injury models, and further investigation into these neuroprotective effects was warranted. Current work explores the protective effects of localized low-intensity pulsed ultrasound (LIPUS) to reduce microglia reactivity and preserve electrophysiological quality in rodents following chronic electrode implantation. A reusable head-mounted LIPUS delivery system was developed and tested. Transducers were characterized in water prior to in vivo testing. To record neural activity, NeuroNexus probes were implanted at 45°angle (A4x4-5mm-100-125-703-CM16LP) or vertically (A1x16-5mm-100-703_H16 probes) to record stimulus evoked activity in rats (N=12, Sham=4, Vertical LIPUS=4 Slanted LIPUS=4). Subjects were treated with periodic LIPUS or Sham (Control), daily in Week 1, followed by twice weekly treatments during Weeks 2-6. LIPUS delivered in 3 x 5 min periods with 5 min of quiescence between each period. Stimulation parameters: Burst Duration: 50 ms, Repetition Rate: 2Hz, $I_{ta}$: ~250-300 mW/cm$^2$. Reactivity and neural activity were assayed with two-photon imaging and electrophysiology recordings. Ex vivo and bench tests demonstrated that ultrasound transmitted across the skull without detrimental heating or signal loss. LIPUS-treatment resulted in a lower level of probe coverage around Day 6 and remained consistently lower than Sham (two-sided Šídák's multiple comparisons test, p=0.0187, LIPUS=7; Sham=6. Glial fibrillary acidic protein intensity, whose expression increases in response to neuroinflammation or injury, increased in the Sham compared to LIPUS-treated, 30 µm from the probe. LIPUS treatment significantly decreased average vessel diameter on day 28 (one-sided Tukey’s multiple comparison test,

p=0.02). LIPUS-treated saw an improved signal-to-noise ratio at 28 days, improved single unit detection, reduced capillary diameter, and reduced microglial and astrocytic encapsulation of the probe- all critical factors for improving longer-term neural electrode viability.

**Disclosures: K.A. Snook:** A. Employment/Salary (full or part-time):; Actuated Medical, Inc.. E. Ownership Interest (stock, stock options, royalty, receipt of intellectual property rights/patent holder, excluding diversified mutual funds); Actuated Medical, Inc. **J. Greaser:** A. Employment/Salary (full or part-time):; Actuated Medical, Inc. **O. Grove:** A. Employment/Salary (full or part-time):; Actuated Medical, Inc. **R. Bagwell:** A. Employment/Salary (full or part-time):; Actuated Medical, Inc.. E. Ownership Interest (stock, stock options, royalty, receipt of intellectual property rights/patent holder, excluding diversified mutual funds); Actuated Medical, Inc.. **T. Thai:** None. **V. Singh:** None. **A. Forrest:** None. **Y. Suofu:** None. **T.D. Kozai:** None. **M.L. Mulvihill:** A. Employment/Salary (full or part-time):; Actuated Medical, Inc.. E. Ownership Interest (stock, stock options, royalty, receipt of intellectual property rights/patent holder, excluding diversified mutual funds); Actuated Medical, Inc..

**Poster**

**PSTR208: Computational Modeling of Synaptic Networks**

**Location:** WCC Halls A-C

**Time:** Monday, November 16, 2026, 1:00 PM - 5:00 PM

**Program #/Poster #:** PSTR208.09/MM23

**Topic:** J.08. Methods to Modulate Neural Activity

**Support:** National Research Foundation of Korea(RS-2023-00220237)
the National Research Foundation of Korea(RS-2025-02215354)

**Title:** Implantable microcoil-based magnetic stimulation for neuromodulation in a Parkinson's disease mouse model

**Authors: *S. PARK**[1], S. CHOI[1], S. LEE[1], M. BANG[1], Y. SEO[1], H. YOO[1], T.-I. KAM[2], S. LEE[1];
[1]Korea Advanced Inst. of Sci. and Technology(KAIST), Daejeon, Korea, Republic of; [2]Inst. for Cell Engineering/ Dept. of Neurol., KAIST/Johns Hopkins Univ., ELLICOTT CITY, MD

**Abstract:** Deep brain stimulation (DBS) using electrical currents has been widely used to treat drug-resistant neurodegenerative diseases, including Parkinson's disease. However, conventional elecrical stimulation can suffer from broad current spread and reduced long-term efficacy due to tissue encapsulation around implanted electrodes. Microcooil-based magnetic stimulation has emerged as a promising alternative because it may provide mor localized and durable neuromodulation by inducing electric fields without direct charge injection. Nevertheless, its efficacy has mainly been demonstrated in brain slice experiments and limited cortical-level in vivo studies, and validation in deep brain regions remains necessary.In this study, we investigated the feasibility of implantabe microcoil-based magnetic stimulation targteting the

subthalamic nucleus (STN), a major therapeutic target for Parkinson's disease. Rectangular microcoils were designed based on electric field simulatinos using Ansys Maxwell 3D and fabricated using thin-film micromachining processses. In vivo experiments were performed in a 6-hydroxydopamine-induced Parkinson's disease mouse model, with stimulation applied to the right STN.Microcoil-based magnetic stimulation of the STN reversed the rotation preference from ipsilateral-dominant to contralateral-dominant. In the sham group, ipsilateral and contralateral rotations accounted for 63.8% and 36.2% of total rotaions, respectively. After stimulation, ipsilateral rotations decreased to 32.1% whereas contralateral rotations increased to 67.9%. In addition, c-Fos immunohistochemistry showed an approximately 30% reduction in neural activity within the stimulated STN. These results suggest that microcoil-based magnetic stimulation can modulate disease-related motor behavior and neural activity in deep brain regions in vivo.This study supports the potential of implantable microcoils as a therapeutic neuromodulation platform for Parkinson's disease and other neurodegerative disorders.

**Disclosures: S. Park:** None. **S. Choi:** None. **S. Lee:** None. **M. Bang:** None. **Y. Seo:** None. **H. Yoo:** None. **T. Kam:** None. **S. Lee:** None.

**Poster**

**PSTR208: Computational Modeling of Synaptic Networks**

**Location:** WCC Halls A-C

**Time:** Monday, November 16, 2026, 1:00 PM - 5:00 PM

**Program #/Poster #:** PSTR208.10/MM24

**Topic:** J.08. Methods to Modulate Neural Activity

**Title:** Antidepressant continuation after electroconvulsive therapy and psychiatric readmission in depression: a nationwide Japanese claims database study

**Authors: *T. NISHIKAWA**[1], H. MURAOKA[2], R. SUZUKI[3], M. AKAZAWA[4], K. INADA[2]; [1]Dept. of Psychiatry, Kitasato University, Sch. of Med., Kanagawa sagamihara, Japan; [2]Dept. of Psychiatry, Kitasato University, Sch. of Med., Kanagawa, Japan; [3]Kitasato Univ. Sch. of Med., Sagamihara / Kanagawa, Japan; [4]Dept. of Publ. Hlth. and Epidemiology, Meiji Pharmaceut. Univ., Kiyose / Tokyo, Japan

**Abstract:** Relapse and rehospitalization remain common after electroconvulsive therapy (ECT) for depression, but real-world evidence on post-ECT pharmacotherapy and subsequent outcomes is limited. We examined whether antidepressant prescription patterns at discharge after ECT were associated with psychiatric readmission using a nationwide Japanese health insurance claims database. This retrospective observational study included adults 18 years or older hospitalized with depression, defined by ICD-10 codes F32 or F33, between July 1, 2014 and March 31, 2022 who received ECT during the index hospitalization. Patients were classified by antidepressant prescriptions recorded within 7 days including discharge as no antidepressant, monotherapy, or polypharmacy. The outcome was first psychiatric readmission after discharge, defined by inpatient psychiatric psychotherapy claims and a length of stay of at least 7 days. Associations were assessed using Kaplan-Meier curves, log-rank tests, and Cox models adjusted

for age, sex, lithium, valproate, antipsychotic co-prescription, and antidepressant regimen change. This study was approved by an institutional ethics committee, with informed consent waived for anonymized secondary data.
Among 759 patients, 202 received no antidepressant, 375 received monotherapy, and 182 received polypharmacy. Psychiatric readmission occurred in 196 patients, or 25.8%, during follow-up, including 141 patients, or 18.6%, within 1 year. In the main analysis, readmission risk did not differ significantly by discharge antidepressant pattern, although the no-antidepressant group tended to have higher readmission proportions. In patients receiving antipsychotics, monotherapy was associated with lower readmission risk than no antidepressant, with an adjusted hazard ratio of 0.61 and 95% confidence interval of 0.40-0.92; log-rank P=0.03. A similar association was observed among patients without antidepressant regimen changes within 6 months after discharge, with an adjusted hazard ratio of 0.58 and 95% confidence interval of 0.36-0.94; log-rank P=0.03. In exploratory analyses of monotherapy classes, readmission risk did not differ significantly among selective serotonin reuptake inhibitors, serotonin-norepinephrine reuptake inhibitors, mirtazapine, and tricyclic antidepressants, although serotonin-norepinephrine reuptake inhibitors showed a lower readmission tendency. These findings suggest that continuation antidepressant monotherapy after ECT may be associated with reduced psychiatric readmission in clinically relevant subgroups, while class-specific differences remain uncertain.

**Disclosures: T. Nishikawa:** None. **H. Muraoka:** D. Fees for Non-CME Services Received Directly from Commercial Interest or their Agents (e.g., speakers' bureaus); EA Pharma Co., Ltd., Viatris Pharmaceuticals Japan Inc., Eisai Co., Ltd., MSD K.K., Otsuka Pharmaceutical Co., Ltd., Shionogi & Co., Ltd., Sumitomo Pharma Co., Ltd., Daiichi Sankyo Company, Limited.,. **R. Suzuki:** None. **M. Akazawa:** D. Fees for Non-CME Services Received Directly from Commercial Interest or their Agents (e.g., speakers' bureaus); Astellas Pharma Inc., Janssen Pharmaceutical K.K., Kyowa Kirin Co., Ltd., Mitsubishi Tanabe Pharma Corporation, and MSD. **K. Inada:** D. Fees for Non-CME Services Received Directly from Commercial Interest or their Agents (e.g., speakers' bureaus); EA Pharma Co., Ltd., Viatris Pharmaceuticals Japan Inc., Eisai Co., Ltd., MSD K.K., Otsuka Pharmaceutical Co., Ltd., Ono Pharmaceutical Co., Ltd., Kyowa Kirin Co., Ltd., Kowa Pharmaceutical Co., Ltd.,.

**Poster**

**PSTR208: Computational Modeling of Synaptic Networks**

**Location:** WCC Halls A-C

**Time:** Monday, November 16, 2026, 1:00 PM - 5:00 PM

**Program #/Poster #:** PSTR208.11/MM25

**Topic:** J.08. Methods to Modulate Neural Activity

**Title:** Magnetic Navigation of Janus Particles on the Dura Mater: An In Vivo Proof-of-Concept Study

**Authors: *K. OZMEN**;
Kars Kafkas Univ., Kars, Turkey

**Abstract:** Background-Precise navigation of microscale agents within the CNS could enable targeted therapeutic delivery and minimally invasive interventions. Magnetic actuation provides a wireless and biocompatible approach for controlling microparticles; however, reliable navigation on neural tissue surfaces remains a significant challenge. This study evaluated the feasibility of magnetically controlled Janus microparticles in both biomimetic and in vivo environments.Methos-Janus microparticles with an average diameter of 100 μm were actuated using a custom-built six-coil electromagnetic platform generating a constant magnetic field of 10 mT. The study consisted of both in vitro and in vivo experiments.For in vitro validation, PDMS-based models were fabricated to mimic simplified biological environments. Experiments were performed in an open chamber and a microchannel geometry. Particle displacement, velocity, and trajectory completion were quantified using video-based tracking.For in vivo experiments, cranial window surgery was performed in 18 naive mice. Following exposure of the cranial surface, Janus microparticles were deposited onto the dura mater using a micropipette. Particle motion was controlled by the electromagnetic platform and recorded using a stereomicroscope-based imaging system. Single-particle navigation experiments were analyzed to quantify displacement and velocity on the brain surface under magnetic actuation.Results-Magnetic actuation enabled reproducible navigation of Janus microparticles under both in vitro and in vivo conditions. In PDMS models, 65 of 66 particles successfully completed the intended trajectory, corresponding to a success rate of 98.5%. Particles achieved an average displacement of approximately 770 μm and a mean velocity of 0.78 mm/s.In vivo experiments demonstrated successful magnetic steering of individual microparticles on the dura mater surface. Particles achieved an average displacement of 1119 μm with a mean velocity of 228 μm/s. Real-time imaging confirmed controlled directional movement in response to externally applied magnetic fields without direct mechanical interaction.Conclusions-These findings demonstrate the feasibility of wireless magnetic navigation of 100-μm Janus microparticles on the brain surface using a electromagnetic actuation system. The high trajectory completion rate observed in PDMS models and successful navigation in vivo support the potential of magnetic microrobotic approaches for future CNS-targeted therapeutic delivery and neurosurgical applications. Future studies will focus on closed-loop system and more complex biological models.

**Disclosures: K. Ozmen:** None.

**Poster**

**PSTR208: Computational Modeling of Synaptic Networks**

**Location:** WCC Halls A-C

**Time:** Monday, November 16, 2026, 1:00 PM - 5:00 PM

**Program #/Poster #:** PSTR208.12/MM26

**Topic:** J.08. Methods to Modulate Neural Activity

**Support:** NIGMS R01-GM115384
NINDS R01-NS121776

**Title:** Development of a miniaturized wireless platform for ultrasonic neuromodulation in freely moving rodents

**Authors: *E. HU**[1], Q. ZHANG[2], K. S. GUILLORY[3], T. LEMAIRE[4], S. SHOHAM[1], J. WANG[2];
[2]Anesthesiol., [1]NYU Grossman Sch. of Med., New York, NY; [3]Tech4Health Inst., NYU Langone Hlth., Long Island City, NY; [4]New York Univ., Long Island City, NY

**Abstract:** Transcranial ultrasonic stimulation (TUS) has recently emerged as a landmark technology for noninvasive neuromodulation, owing to its excellent spatial targetability and rapid titratability. Notably, TUS encompasses a broad range of possible stimuli defined by a large set of waveform parameters, and the effects of these parameters on neurophysiology and behavior is an open question. However, one major barrier to conducting TUS experimentation, particularly in freely moving animals, is the need for bulky waveform generation and power amplification setups which hinder subjects' range of motion. Moreover, producing consistent focal pressures across subjects generally requires adjustment of driving voltage and resonant frequency on a per-transducer basis. Finally, existing animal-wearable devices reported in literature do not include mechanisms for high-resolution pulse-shaping, which is known to be vital for preventing auditory confounds during sonication. To address these issues, we hereby present a miniaturized, adult rat-wearable platform for driving sub-MHz ultrasonic transducers. Powered by a single 3.7V lithium-polymer battery, our platform offers high-resolution, real-time wireless programming of drive voltage, fundamental frequency, and timing parameters for pulsed operation. Additionally, the device is capable of time-domain waveform shaping through up-sampled pulse-width modulation using arbitrary duty cycle curves. To maximize accessibility, the device is constructed entirely with low-cost, off-the-shelf electronics. Using a commercially available transducer, we demonstrate that our platform can achieve higher focal pressures than similar competing devices, and provide evidence that it can produce neuromodulatory effects comparable to a traditional wired setup.

**Disclosures: E. Hu:** None. **Q. Zhang:** None. **K.S. Guillory:** None. **T. Lemaire:** None. **S. Shoham:** None. **J. Wang:** None.

**Poster**

**PSTR208: Computational Modeling of Synaptic Networks**

**Location:** WCC Halls A-C

**Time:** Monday, November 16, 2026, 1:00 PM - 5:00 PM

**Program #/Poster #:** PSTR208.13/MM27

**Topic:** J.08. Methods to Modulate Neural Activity

**Support:** NIH (R35GM142490)
NIH (R00NS101065)
JST PRESTO (JPMJPR2386)
RCSA (SA-MBC-2024-080c)
Whitehall Foundation
BrightFocus Foundation (A2021043S)

**Title:** Sleep restores metabolically controlled membrane-potential resilience in sleep-regulating neural circuits

**Authors: *M. TABUCHI**;
Case Western Reserve Univ. Sch. of Med., Cleveland, OH

**Abstract:** Sleep homeostasis implies that wakefulness depletes, and sleep restores, an internal physiological variable, but the biophysical identity of this variable remains unclear. Here we define membrane-potential resilience (MPR) as a history-dependent stability metric that integrates restoring drift, attractor basin size and voltage noise after standardized subthreshold perturbations. In Drosophila sleep-regulating neurons, aging and prolonged wakefulness selectively reduced MPR, whereas conventional excitability measures, including resting membrane potential, input resistance, membrane time constant and firing rate, were insufficient to predict sleep instability. We developed OptoMagForce as a closed-loop MPR clamp to set circuit resilience in vivo. Clamping young circuits to aged MPR induced aging-like sleep fragmentation, whereas restoring aged circuits to youthful MPR rescued delta-like synchrony and consolidated sleep despite persistent age-associated features. Simultaneous DN1p-PI (pars intercerebralis)-R5 recordings further showed matched hysteretic MPR signatures across sleep-circadian pathways. These results identify metabolically controlled membrane-potential resilience as a proximal biophysical substrate of sleep pressure and age-related sleep fragmentation.

**Disclosures: M. Tabuchi:** None.

**Poster**

**PSTR208: Computational Modeling of Synaptic Networks**

**Location:** WCC Halls A-C

**Time:** Monday, November 16, 2026, 1:00 PM - 5:00 PM

**Program #/Poster #:** PSTR208.14/MM28

**Topic:** J.08. Methods to Modulate Neural Activity

**Support:** R01-MH132592
R34-DA059512
ASAP - 020607

**Title:** St3DIO: A Standardized 3D Behavioral Arena for Aiming to Enable Cross Study Pose Estimation and Disease Phenotyping

**Authors: *J. ROACH**[1], S. S.-X. LIM[1], J. WU[2], A. SABATH[1], J. R. RAVENEL[3], A. CHOUDHURY[4], P. NAMBIAR[1], S. SINGH[4], B. C. SHIELDS[5], N. CALAKOS[6], T. W. DUNN[5], M. R. TADROSS[5];
[1]Duke Univ., Durham, NC; [2]Biomed. Engin., Duke Univ., Ann Arbor, MI; [3]Neurobio., Duke Univ., Durham, NC; [4]Duke Univ., Duke University, NC; [5]Biomed. Engin., Duke Univ., Durham, NC; [6]Dept Neurol/Neurobiol, Duke Univ. Med. Ctr., Durham, NC

**Abstract:** Markerless pose estimation has become a cornerstone of modern behavioral neuroscience, yet no consistent standard of comparison exists — preventing direct assay comparison between labs studying the same disease when using pose estimation to its full potential through feature extraction techniques. The core problem is fundamental to using neural networks for pose estimation: networks require fine-tuning on each arena, resulting in subtle tracking differences that compound through feature extraction pipelines and make it nearly impossible to distinguish real biological differences from methodological ones. We built St3DIO (Standardized 3D Integrated Openfield) to solve this at the source. 3D methods offer inherent normalization for camera and arena geometry. Rather than harmonizing data after the fact, St3DIO standardizes the imaging environment itself — delivering consistent optical conditions across laboratories in a portable 30" × 30" enclosed multi-view arena that ships ready to use without on-site assembly. Our patented design captures five synchronized views with a single camera using custom dielectric mirrors optimized for near-infrared illumination. The practical payoff is that pose estimation becomes transferable. A single pre-trained DANNCE model tracked 3D keypoints across all tested St3DIO units without any arena-specific retraining — including two arenas that contributed no frames to training — with errors falling within the range of normal inter-annotator disagreement. The arena's mirror symmetry also enables 8-fold exact data augmentation from a single labeled frame. In an exploratory study using VPS35(D620N) knock-in mice — a progressive Parkinson's disease model that conventional tracking methods have consistently failed to phenotype — standard open-field metrics showed nothing at 13 months. Using our *neuroposelib* analysis library, we identified clear gait abnormalities and an unexpected sex difference in idle posture: female mutants adopted a crouched stance while males sat more upright, a distinction requiring 3D snout elevation data that was invisible to 2D approaches. St3DIO gives behavioral neuroscience a means to increase data transparency and cross-study validity in a field where both the biology and the tools are rapidly evolving.

**Disclosures: J. Roach:** None. **S.S. Lim:** None. **J. Wu:** None. **A. Sabath:** None. **J.R. Ravenel:** None. **A. Choudhury:** None. **P. Nambiar:** None. **S. Singh:** None. **B.C. Shields:** None. **N. Calakos:** None. **T.W. Dunn:** None. **M.R. Tadross:** None.

**Poster**

**PSTR208: Computational Modeling of Synaptic Networks**

**Location:** WCC Halls A-C

**Time:** Monday, November 16, 2026, 1:00 PM - 5:00 PM

**Program #/Poster #:** PSTR208.15/MM29

**Topic:** J.08. Methods to Modulate Neural Activity

**Support:** Duke-Coulter Translational Partnership
NIH Grant R01MH135932

**Title:** Genetically targeted electrophysiology through covalent neuron-electrode coupling

**Authors: *U. GHOSH**[1], L. A. LIGONS[1], I. A. WEAVER[1], B. C. SHIELDS[2], S. YOUSEFZADEH[3], M. R. TADROSS[2];
[2]Biomed. Engin., [3]Psychology and Neurosci., [1]Duke Univ., Durham, NC

**Abstract:** Conventional extracellular electrodes provide millisecond-resolution recordings but have limited sensitivity to small neurons and long-range axons, lack genetic specificity, and often suffer from recording instability. We developed ElectroGLuE (Electropolymer Genetically Linking Neurons to Electrodes), a platform that creates a covalent molecular interface between genetically defined neurons and implanted recording electrodes. ElectroGLuE combines PEDOT-HTL, a conductive electropolymer incorporating HaloTag ligand (HTL), with viral expression of cell-surface HaloTag protein (HTP) in targeted neuronal populations. HTP-expressing neurons covalently bind PEDOT-HTL-coated electrodes. *In vivo* recordings using ElectroGLuE-modified NeuralThread probes in the hippocampus revealed unique high-amplitude waveforms that emerged several weeks after viral delivery, consistent with the expected time course of HTP accumulation at the membrane. These events were approximately an order of magnitude larger and substantially narrower than conventional extracellular spikes, often exceeding 1 mV in amplitude. Their waveform shape, polarity, and time integral were consistent with a capacitive-coupling mechanism, distinguishing them from conventional extracellular field recordings. We next used a cell-type-specific AAV to target HTP expression to midbrain dopamine neurons and implanted probes in the dorsal striatum. ElectroGLuE detected large capacitive-like signals with firing patterns consistent with dopamine neuron activity, demonstrating electrical access to genetically defined long-range axonal processes—a compartment that is typically inaccessible to extracellular recordings. To improve reproducibility and yield, we developed complementary *in vitro* optimization assays. Polymer formulations were assessed using both soluble HTP capture and a cell-based adhesion assay that quantified selective capture of HTP-expressing cells, exclusion of binding-deficient controls, and residual HTP accessibility following adhesion. These assays revealed substantial variability among nominally identical polymer coatings and demonstrated that soluble HTP capture alone does not predict cellular adhesion. Modifications to monomer structure and electropolymerization conditions produced marked improvements in HTP-dependent cell capture and interface formation. Together, these results establish ElectroGLuE as a genetically targeted electrophysiology platform and provide a quantitative framework for engineering reproducible covalent neuron-electrode interfaces.

**Disclosures: U. Ghosh:** None. **L.A. Ligons:** None. **I.A. Weaver:** None. **B.C. Shields:** None. **S. Yousefzadeh:** None. **M.R. Tadross:** None.

**Poster**

**PSTR208: Computational Modeling of Synaptic Networks**

**Location:** WCC Halls A-C

**Time:** Monday, November 16, 2026, 1:00 PM - 5:00 PM

**Program #/Poster #:** PSTR208.16/MM30

**Topic:** J.08. Methods to Modulate Neural Activity

**Support:** This work was supported by the National Research Foundation of Korea(NRF) grant funded by the Korea government(MSIT and MOE) (No. RS-2025-17492968).
This work was supported by the National Research Foundation of Korea(NRF) grant funded by the Korea government(MSIT) (RS-2025-00517742).

**Title:** A Therapeutic and Electrophysiological Monitoring Platform for Nicotine-Induced Substance Use Disorder

**Authors: *S. PAK**, M. CHOO, S.-M. PARK;
IT convergence engineering, POSTECH, Pohang, Korea, Republic of

**Abstract:** Substance Use Disorder (SUD) is currently diagnosed primarily through behavioral observations and self-reported symptoms due to the lack of objective biomarkers. In addition, current treatment strategies largely rely on symptomatic approaches, such as alleviating withdrawal symptoms. However, SUD is not merely a behavioral disorder but a neurophysiological disease characterized by the disruption of the excitation-inhibition (E-I) balance within the brain reward circuitry caused by repeated exposure to addictive substances. Therefore, effective treatment of SUD requires identifying the pathological neural circuit alterations induced by addiction and restoring the impaired reward circuitry to its normal functional state. Herein, we propose a therapeutic strategy based on non-invasive audiovisual gamma oscillation stimulation, which aims to restore the interactions between pyramidal neurons and interneurons, thereby normalize the E-I balance. Furthermore, we present an integrated therapeutic monitoring platform capable of quantitatively evaluating treatment efficacy using electrophysiological biomarkers. Evaluation of the therapeutic effects of audiovisual gamma oscillation stimulation revealed that, unlike the addiction group, both the healthy control group and the gamma-treated group exhibited a state transition characterized by decreased low-frequency delta-band activity and increased high-frequency gamma-band activity in response to drug stimulation. This delta-gamma coupling indicates that the treated group recovered neural response patterns similar to those of healthy controls, suggesting that gamma oscillation stimulation can induce functional restoration of the impaired reward circuitry. Furthermore, recovery assessment in SUD should reflect not only localized changes in specific deep-brain regions but also large-scale functional connectivity and overall network states across the brain. To enable long-term monitoring of these changes, we developed a fully flexible electrode capable of stably recording electrophysiological signals projected to the cerebral cortex that reflect the functional balance of deep brain circuits. Using this electrode, we successfully measured cortical responses and state-transition dynamics induced by nicotine stimulation and demonstrated its ability to effectively distinguish addiction states from recovery states. These findings demonstrate that cortical signals alone can serve as reliable indicators of the functional state of the reward circuitry and the proposed platform enables long-term treatment monitoring and recovery assessment in SUD.

**Disclosures: S. Pak:** None. **M. Choo:** None. **S. Park:** None.

**Poster**

**PSTR208: Computational Modeling of Synaptic Networks**

**Location:** WCC Halls A-C

**Time:** Monday, November 16, 2026, 1:00 PM - 5:00 PM

**Program #/Poster #:** PSTR208.17/MM31

**Topic:** J.08. Methods to Modulate Neural Activity

**Support:** NIH Grant R01-MH132592
NIH Grant RF1-MH117055

**Title:** Cell-Type-Specific Dissociation of Extrapyramidal Side Effects with Haloperidol$^{DART.2}$

**Authors: *J. R. RAVENEL**[1], A. MOGHADAM[2], S. YOUSEFZADEH[3], H. YAN[4], Z. FARAHBAKHSH[6], M. VAN PRAAG[1], V. BRYSON[5], S. S.-X. LIM[4], J. ROACH[4], M. MCDONNELL[7], A. REITZ[7], B. C. SHIELDS[5], M. R. TADROSS[4];
[2]Psychiatry and Behavioral Sci., [3]Psychology and Neurosci., [4]Biomed. Engin., [5]Neurosurg., [1]Duke Univ., Durham, NC; [6]Univ. of North Carolina, Chapel Hill, NC; [7]Fox Chase Therapeut. Discovery Inc., Doylestown, PA

**Abstract:** Antipsychotic drugs that block dopamine D2 receptors (D2Rs) are a frontline treatment for psychosis, but their utility is limited by extrapyramidal side effects (EPS). In rodents, EPS is modeled by bradykinesia and catalepsy, which are canonically attributed to D2R blockade on striatal indirect-pathway spiny projection neurons (iSPNs) and cholinergic interneurons (ChIs), respectively. Cell-type-specific knockout studies attempting to isolate these contributions have been central to the prevailing model that catalepsy is mediated by D2Rs on ChIs, but compensatory mechanisms inherent to constitutive receptor deletion complicate interpretation. Here, we developed haloperidol$^{DART.2}$, a cell-type-specific antipsychotic, and validated its D2R antagonism using TANGO-GPCR reporter assays and slice electrophysiology. Delivering acute D2R blockade to genetically defined populations in the dorsal striatum of mice, we found catalepsy and bradykinesia to be mechanistically dissociable: blockade of iSPNs produced bradykinesia without catalepsy, blockade of thalamostriatal afferents produced catalepsy without bradykinesia, whereas blockade of ChIs or astrocytes produced neither — challenging this longstanding model. To test necessity, we developed and validated sumanirole$^{DART.2}$, a cell-type-specific D2R agonist; delivering it to thalamostriatal afferents prior to systemic haloperidol attenuated catalepsy while sparing bradykinesia, establishing thalamostriatal D2R blockade as both necessary and sufficient for catalepsy. Thus far, we have been unable to identify a cell type in which targeted D2R pharmacology modulates amphetamine-induced prepulse inhibition (PPI) deficits, indicating that antipsychotic-like efficacy is separable from both catalepsy and bradykinesia mechanisms. Finally, to identify a neural signature of catalepsy, we paired local field potential (LFP) recordings with fiber photometry of striatal acetylcholine (gACh4m) or glutamate (iGluSnFr3), comparing systemic haloperidol to thalamostriatal haloperidol$^{DART.2}$. LFP changes tracked behavioral state, from movement to stillness, rather than D2R blockade itself, whereas the neurotransmitter signals revealed a modulation shared by both systemic haloperidol and thalamostriatal haloperidol$^{DART.2}$, representing a candidate circuit signature of catalepsy that we are continuing to define. Together, these results revise the cellular pharmacology of antipsychotic action, demonstrating that

extrapyramidal side effects are not a unitary phenomenon but fractionate into mechanistically independent components defined by the cellular site of D2R blockade.

**Disclosures: J.R. Ravenel:** None. **A. Moghadam:** None. **S. Yousefzadeh:** None. **H. Yan:** None. **Z. Farahbakhsh:** None. **M. van Praag:** None. **V. Bryson:** None. **S.S. Lim:** None. **J. Roach:** None. **M. McDonnell:** None. **A. Reitz:** None. **B.C. Shields:** None. **M.R. Tadross:** None.

**Poster**

**PSTR208: Computational Modeling of Synaptic Networks**

**Location:** WCC Halls A-C

**Time:** Monday, November 16, 2026, 1:00 PM - 5:00 PM

**Program #/Poster #:** PSTR208.18/MM32

**Topic:** J.08. Methods to Modulate Neural Activity

**Support:** NIH NS131069

**Title:** Volumetric Mesoscopic Electrophysiology Reveals Pressure-Dependent Modulation of Visual Cortex by Transcranial Focused Ultrasound in A Nonhuman Primate Model

**Authors: *C.-Y. YEH**[1], K. YU[2,1], H. GAO[1], T. TEICHERT[3], B. HE[1];
[1]Dept. of Biomed. Engin., Carnegie Mellon Univ., Pittsburgh, PA; [2]Dept. of Biomed. Engin., Univ. of Connecticut, West Hartford, CT; [3]Dept. of Psychiatry, Univ. of Pittsburgh, Pittsburgh, PA

**Abstract:** Transcranial focused ultrasound stimulation (tFUS) is a noninvasive neuromodulation technique with high precision and deep brain penetration. Prior work has shown that tFUS can induce regional activity or influence neural activity through cortico-thalamo-cortical interactions in rodent models as assessed by multi-unit activity recordings [1]. It remains unclear how tFUS modulates local field potential (LFP) activity within targeted regions in a large brain. In this study, we investigated tFUS-evoked responses in the primary visual cortex (V1) during resting state in an adult male rhesus macaque using a mesoscopic electrophysiology setup [2], consisting of 992 intracranial electrode contacts across the right hemisphere for LFP recordings. A neuronavigation-guided 128-element ultrasound transducer was used to target V1. Each condition consisted of 320 trials of 300 ms ultrasound stimulation. Trials with excessive artifacts were excluded, and sham stimulation was used to control for auditory and mechanical artifacts. Estimated in situ pressures of 250, 400, and 550 kPa were delivered at a fixed 17% duty cycle and 3 kHz pulse repetition frequency. Time domain analysis identified a 200 ms window immediately following tFUS onset that showed significant differences ($p < 0.01$) between active and sham conditions during 400 kPa tFUS. Within this window, baseline-normalized mean absolute LFP amplitude was significantly modulated in V1, whereas non-targeted regions, including the primary auditory cortex (A1), primary somatosensory cortex (S1), and cerebellum (Cb), showed no significant changes during 400 kPa tFUS. Increasing stimulation pressure reduced the time domain V1 response, with significant reductions observed at 400 and 550 kPa,

as compared to 250 kPa tFUS. In contrast, no significant changes in LFP amplitude were observed in A1, S1, or Cb during V1 sonication with varying pressure levels. Power spectral analysis revealed pressure-dependent changes in V1 across frequency bands, with gamma band power significantly decreased at 400 and 550 kPa. These findings indicate that tFUS can preferentially modulate cortical LFP activity within the sonicated brain region during resting state, and that V1-targeted tFUS produces band-specific, pressure-dependent modulation of neural activity.

**Disclosures: C. Yeh:** None. **K. Yu:** None. **H. Gao:** None. **T. Teichert:** None. **B. He:** None.

**Poster**

**PSTR208: Computational Modeling of Synaptic Networks**

**Location:** WCC Halls A-C

**Time:** Monday, November 16, 2026, 1:00 PM - 5:00 PM

**Program #/Poster #:** PSTR208.19/MM33

**Topic:** J.08. Methods to Modulate Neural Activity

**Support:** EU Grant META-BRAIN 101130650
SNSF Grant 206033
NNSF Grant 52473254

**Title:** A Versatile Magnetoelectric Platform for Targeted Neural Delivery, Regeneration, and Wireless Neuromodulation

**Authors: *E. ZHANG**[1], N. CANCINO FUENTES[2], M. V. SANCHEZ-VIVES[3];
[1]ETH Zurich, Zurich, Switzerland; [2]IDIBAPS, Barcelona, Spain; [3]Systems Neurosci., IDIBAPS (Institut D'Investigacions Biomediques August Pi I Sunyer), Barcelona, Spain

**Abstract:** Achieving precise, minimally invasive control over brain and spinal cord activity requires a stimulation interface that is both spatially targeted and functionally flexible. Here, we present a modular platform based on magnetoelectric nanoparticles (MENPs) that act as deployable nanoscale electrodes. By varying the assembly and delivery of the same MENP material, we demonstrate a multifaceted toolkit for neural intervention across different biological scales. First, we established a macro-scale delivery pipeline using a clinically ready electromagnetic navigation system and dissolvable magnetic capsules, enabling the on-demand, site-specific release of MENPs anywhere within the reachable vasculature. Second, by integrating MENPs into a biohybrid architecture with human-induced pluripotent stem cell-derived neural progenitor cells (NPCbots), we show that these transducers can be localized to spinal cord lesions to drive *in situ* neuronal differentiation and restore motor function. Finally, we demonstrate the capacity for network-scale modulation by utilizing free-floating MENPs to transduce low-intensity static magnetic fields into localized electrical perturbations, reliably and reversibly tuning cortical slow-wave oscillations by compressing Down states. Collectively, these results illustrate the extraordinary flexibility of the MENP platform: by simply altering the delivery vehicle or cellular integration, the same material system can be leveraged to achieve

distinct therapeutic outcomes, from targeted drug delivery and structural regeneration to the wireless tuning of emergent cortical dynamics.

**Disclosures: E. Zhang:** None. **N. Cancino Fuentes:** None. **M.V. Sanchez-Vives:** None.

**Poster**

**PSTR208: Computational Modeling of Synaptic Networks**

**Location:** WCC Halls A-C

**Time:** Monday, November 16, 2026, 1:00 PM - 5:00 PM

**Program #/Poster #:** PSTR208.20/MM34

**Topic:** J.08. Methods to Modulate Neural Activity

**Support:** NIH, NIDA, R01DA052893

**Title:** Electrochemical profiling of dopamine dynamics in chronic pain: mesolimbic circuit modulation via focused ultrasound

**Authors: *L. E. TURNER**, J. VENTON;
Chem., Univ. of Virginia, Charlottesville, VA

**Abstract:** Chronic pain disorders, such as fibromyalgia, represent a major unmet clinical need, as current pharmacological treatments only manage symptoms rather than restoring the underlying neural circuit dysfunction. The pathophysiology of fibromyalgia involves disrupted neurotransmission in mesolimbic pain circuits, particularly pathways with projections to the nucleus accumbens (NAc) and its shell (NAcs), a key region for dopaminergic modulation. Focused ultrasound (FUS) is a non-invasive neuromodulatory technique that employs mechanical energy, in the form of acoustic waves, to target specific brain regions with millimeter resolution. Previous work has shown precise neuromodulatory control of motivation and reward circuits using FUS at the prefrontal cortex to excite and inhibit dopamine release in the NAc core. The ventral tegmental area (VTA) and infralimbic cortex (ILC) represent key afferent inputs to the NAc shell via dopaminergic and glutamatergic projections, respectively, making them distinct circuit targets for FUS-mediated neuromodulation in mesolimbic circuits and chronic pain. However, FUS has not yet been applied to these circuits, leaving the neurochemical effects of acoustic wave stimulation on dopamine dynamics in pain pathways uncharacterized. Using fast-scan cyclic voltammetry (FSCV), changes in dopamine release dynamics can be measured in the NAcs of a reserpine-induced fibromyalgia rat model to establish baseline circuit dysfunction compared to control. FUS is then applied to the VTA and ILC independently to investigate how targeting each node affects NAcs dopamine release and pain sensitivity compared to pharmacological analgesia. Together, this work provides a mechanistic characterization of FUS-mediated neuromodulation within intact mesolimbic pain circuits, supporting its development as a non-addictive therapeutic for chronic pain.

**Disclosures: L.E. Turner:** None. **J. Venton:** None.

**Poster**

**PSTR208: Computational Modeling of Synaptic Networks**

**Location:** WCC Halls A-C

**Time:** Monday, November 16, 2026, 1:00 PM - 5:00 PM

**Program #/Poster #:** PSTR208.21/MM35

**Topic:** J.08. Methods to Modulate Neural Activity

**Support:** NRF Grant RS-2025-00563810
KHIDI Grant HF22C0081

**Title:** Acupuncture inhibits the tolerance of analgesics of morphine

**Authors: *B. LEE**[1], S. CHANG[2], H. JANG[1], N. KIM[1], C. YANG[4], H. KIM[5], S. YOON[3]; [1]Univ. of Daegu Haany, Gyeongsan-si, Korea, Republic of; [3]Dept. of Physiol., [2]Daegu Haany Univ., Gyeongsan-si, Korea, Republic of; [4]Physiol., Daegu Hanny Univ., Gyeongsan-si, Korea, Republic of; [5]Dept of Physiol., Yonsei Univ. Col. of Med., Seoul, Korea, Republic of

**Abstract:** Although opioids have been widely used as potent pain relievers, repeated-use causes side effects such as tolerance and physical dependence. Tolerance results in a decrease in the analgesic effects and an increase in the patient's demand for drugs, therefore finding a way to inhibit the opioid tolerance is an urgent problem and this study examined if opioid tolerance could be attenuated by acupuncture. Male Sprague-Dawley rats were subjected to surgery of chronic catheter implantation into the jugular vein under anesthetization with sodium pentobarbital for the repeated intravenous morphine administration. After recovery, Von Frey test was performed. Stimulation was given at the plantar of the right hind paw and pain perception was recorded 20 min after morphine administration. Following establishment of the baseline for 2 days when the saline was given instead of morphine, morphine hydrochloride was infused intravenously for 14 days. Acupuncture was given bilaterally for 1 min under slight movement restriction, without anesthetization immediately after morphine administration. For the intracerebral injection of naloxone, picrotoxin, and 2-hydroxysaclofen, the guide cannula was implanted into the rostromedial tegmental nucleus (RMTg), and for the injection of SCH23390 and sulpiride, the guide cannula was implanted into the nucleus accumbens (NAc). When repeatedly administered, morphine resulted in the tolerance of analgesic effect at the last half period, however acupuncture at SI5, but not the control acupoint, prevented the development of tolerance. The expressions of c-Fos and tyrosine hydroxylase (TH) and the blood BDNF level showed similar pattern with the behavioral data. When microinjected into the RMTg, naloxone and picrotoxin, but not the 2-hydroxysaclofen, blocked the SI5 acupuncture's effect, and in the NAc injection, sulpiride, but not the SCH23390, blocked SI5. These findings suggest that SI5 acupuncture can be used to prevent the tolerance of opioid analgesic and that this SI5's effect is mediated through the μ-opioid receptor and the $GABA_A$ receptor in the RMTg and through the dopamine D2 receptor in the NAc.

**Disclosures: B. Lee:** None. **S. Chang:** None. **H. Jang:** None. **N. Kim:** None. **C. Yang:** None. **H. Kim:** None. **S. Yoon:** None.

**Poster**

**PSTR208: Computational Modeling of Synaptic Networks**

**Location:** WCC Halls A-C

**Time:** Monday, November 16, 2026, 1:00 PM - 5:00 PM

**Program #/Poster #:** PSTR208.22/MM36

**Topic:** J.08. Methods to Modulate Neural Activity

**Support:** JSPS KAKENHI Grant Number #22H03441
Suzuken Memorial Foundation
SENSHIN Medical Research Foundation
AMED Grant Number #JP21lm0203003
AMED Grant Number #JP22ym0126805
AMED Grant Number #JP26bm1323001

**Title:** Artificially-modified adeno-associated virus vector for the treatment of cerebrovascular diseases

**Authors: *Y. SEHARA**[1], Y. MATSUZAKI[2], A. KONNO[2], R. WATANO[1], T. OHMORI[1]; [1]Div. of Genet. Therapeut., Jichi Med. Univ., Shimotsuke, Japan; [2]Dept. of Neurophysiol. & Neural Repair, Gunma Univ., Maebashi, Japan

**Abstract:** Introduction: Adeno-associated virus (AAV) vectors are widely used for gene transduction. Because AAVs do not proliferate without the existence of adenovirus, non-proliferative tissues are preferable targets for this vector. In the cerebrovascular diseases, vessel wall including smooth muscle cell is one of the therapeutic targets. Generally, AAVs preferably transduce genes into neurons in the central nervous system. In this study, we artificially modified the capsid protein which consists the outer surface of AAVs to change the transduction efficiency to smooth muscle cells. Methods: Shortly, we inserted random seven amino acid sequences into the capsid protein and screened the novel vector using human smooth muscle cells. In detail, we first cloned a reporter and capsid protein-expressing plasmid which contains two main elements flanked by AAV2 inverted terminal repeats (ITRs), including (a) the mCherry cDNA driven by human UBC promoter, and (b) the AAV5 p41 promoter sequence and splicing sequences taken from the AAV2 *rep* gene followed by AAV2 *cap* gene which contains insertion of 21-mer randomized nucleotide sequence in frame after amino acid 587 of VP1. Recombinant AAVs were generated by triple transfection of 293T cells with the above-mentioned plasmid, adenoviral helper plasmid, and assembly-activating protein helper plasmid. Seventy-two hrs after transfection, viral particles were harvested from both the cells and media, and were purified. AAVs were transduced into cultured smooth muscle cells, which were sorted using fluorescence activated cell sorter (FACS). The viral DNA of mCherry-expressing cells was extracted and amplified by PCR using primers interposing randomized nucleotide sequence. The PCR-generated sequence was cloned back into the above-mentioned reporter and capsid protein-expressing plasmid. Using this plasmid, recombinant AAVs were again generated and the screening cycle was performed in the same way as the first round. The nucleotide sequences of *cap* gene in the first and second rounds were identified and the frequency was quantified using the next generation sequencer (NGS). Results: Analysis by the NGS showed that NRPETNP and SHDPSKE identified in the human brain vascular smooth muscle cells were the two of the most

frequent amino acids sequences in frame after amino acid 587 of AAV2 VP1. Conclusions: Using the *in vitro* assay system, we have identified smooth muscle cell-directed variant of AAV2. In the next step, we're going to inject above-mentioned variants of AAVs into nonhuman primates to confirm that the tropism is directed to smooth muscle cells *in vivo*.

**Disclosures: Y. Sehara:** None. **Y. Matsuzaki:** None. **A. Konno:** None. **R. Watano:** None. **T. Ohmori:** None.

**Poster**

**PSTR208: Computational Modeling of Synaptic Networks**

**Location:** WCC Halls A-C

**Time:** Monday, November 16, 2026, 1:00 PM - 5:00 PM

**Program #/Poster #:** PSTR208.23/MM37

**Topic:** J.08. Methods to Modulate Neural Activity

**Support:** NIH grant R01-MH132592

**Title:** Toward Systemic DART: Overcoming Blood-Brain Barrier Constraints for Cell-Type-Specific Pharmacology

**Authors: *S. YOUSEFZADEH**[1], P. JEONG[2], Z. FARAHBAKHSH[1], B. C. SHIELDS[1], J. HONG[2], M. R. TADROSS[1];
[1]Neurosurg., [2]Chem., Duke Univ., Durham, NC

**Abstract:** The DART (Drug Acutely Restricted by Tethering) platform enables cell-type-specific pharmacology in vivo but currently requires intracranial cannulation for ligand delivery, which constrains throughput and limits adoption. To enable systemic DART administration, we engineered ligand variants containing albumin-binding motifs (ABM), reasoning that prolonged plasma residence would increase blood-brain barrier (BBB) penetration. Using Alexa647$^{DART.2}$ as a reporter, we identified ABM-DART candidates that produce substantially greater capture on ventral tegmental area (VTA) dopamine neurons than standard reagents following systemic administration. Anatomical mapping revealed that capture was predominantly localized to the somatodendritic compartment, whereas dopaminergic axons showed little labeling. This pattern mirrors intracerebroventricular delivery, suggesting that systemic ABM-DART enters the brain primarily via the blood-cerebrospinal fluid (CSF) barrier rather than broad capillary penetration. To enhance axonal capture, we developed a complementary strategy to transiently and locally open the BBB, transducing striatal endothelial cells with a Gq-coupled DREADD under an endothelial-specific viral promoter and administering DCZ concurrent with systemic DART delivery. This approach yielded more than tenfold greater striatal DART capture in the DREADD-expressing hemisphere relative to contralateral controls. Ongoing work focuses on refining DREADD signaling parameters and improving ABM-DART potency under BBB-opening conditions. Together, these advances chart a path toward cannula-free, systemically administered DART, broadening the accessibility and applicability of the platform.

**Disclosures: S. Yousefzadeh:** None. **P. Jeong:** None. **Z. Farahbakhsh:** None. **B.C. Shields:** None. **J. Hong:** None. **M.R. Tadross:** None.

**Poster**

**PSTR208: Computational Modeling of Synaptic Networks**

**Location:** WCC Halls A-C

**Time:** Monday, November 16, 2026, 1:00 PM - 5:00 PM

**Program #/Poster #:** PSTR208.24/MM38

**Topic:** J.08. Methods to Modulate Neural Activity

**Support:** Ro1-MH132592

**Title:** Cell-type-specific modulation of voltage-gated sodium channels with DART.2

**Authors: *H. YAN**[1], Y. OH[2], B. C. SHIELDS[1], S. S.-X. LIM[1], P. JEONG[2], J. HONG[2], M. R. TADROSS[1,3,4];
[1]Neurosurg., [2]Chem., [3]Biomed. Engin., [4]Neurobio., Duke university, Durham, NC

**Abstract:** Drug Acutely Restricted by Tethering (DART) is a technology for cell-type-specific pharmacology in which cells are instructed to express the HaloTag Protein (HTP), which captures and locally accumulates a drug linked to the HaloTag Ligand (HTL). Once tethered, these drugs can act on endogenous receptors on the membrane of targeted cells. We recently demonstrated that DART.2 can bidirectionally modulate excitatory and inhibitory synaptic function, and further developed cell-specific opioid-receptor DART.2 reagents capable of manipulating opioid-reward learning. Here we extend this technology to cell-type-specific manipulation of voltage-gated sodium channels, which are responsible for action potential (AP) initiation and propagation in excitable cells. We synthesized a series of candidate DART.2 reagents exploring three recently developed scaffolds that target the sodium channel's voltage-sensing domain, along with various spacers designed to span the distance from the binding pocket to free solution. We then characterized their effects on cultured hippocampal neurons expressing HTP by recording voltage-gated sodium currents in whole-cell voltage clamp and AP firing in whole-cell current clamp. Our results identify JHNaV.2B$^{DART.2}$ as the most potent DART.2 reagent for blocking voltage-gated sodium channels, making it the preferred reagent for applications in which complete neuronal silencing is desired. The variants exhibited a rank-ordered range of antagonistic potency, from strongest to weakest: JHNaV.2B$^{DART.2}$ > JHNaV.2A$^{DART.2}$ > JHNaV.1C$^{DART.2}$ > JHNaV.1B$^{DART.2}$ > JHNaV.1A$^{DART.2}$. The weaker variants provide variable degrees of use-dependent antagonism, which may be useful for suppressing high-frequency burst firing while sparing lower-frequency modes of activity. Together, these reagents provide a unique platform for studying cell-type- and ion-channel-specific contributions to neural circuits, cellular excitability, animal behavior, and neuronal disease.

**Disclosures: H. Yan:** None. **Y. Oh:** None. **B.C. Shields:** None. **S.S. Lim:** None. **P. Jeong:** None. **J. Hong:** None. **M.R. Tadross:** None.

**Poster**

**PSTR208: Computational Modeling of Synaptic Networks**

**Location:** WCC Halls A-C

**Time:** Monday, November 16, 2026, 1:00 PM - 5:00 PM

**Program #/Poster #:** PSTR208.25/MM39

**Topic:** J.08. Methods to Modulate Neural Activity

**Support:** RS-2023-00220237
RS-2025-02215354

**Title:** Distinct Recruitment of Pyramidal and Parvalbumin Neurons by Microcoil-Based Magnetic Stimulation in the Medial Prefrontal Cortex

**Authors: *M. BANG**, J. PARK, J.-T. KWON, S. LEE;
Dept. of Brain and Cognitive Sci., Korea Advanced Inst. of Sci. and Technol., Daejeon, Korea, Republic of

**Abstract:** Microcoil based magnetic stimulation is a promising alternative to conventional electrical stimulation for neural modulation which could induce asymmetric and focal electric fields around the coil, enabling spatially selective neuronal activation without direct metal-to-tissue contact. Previous studies in mouse cortex have demonstrated that microcoil stimulation can evoke both excitatory and inhibitory calcium responses. However, the underlying cellular mechanisms and neuronal populations involved remain incompletely understood. It is unclear whether magnetic stimulation recruits cortical excitatory and inhibitory neurons through mechanisms distinct from conventional electrical stimulation. To address this question, we investigated cell-type-specific responses to magnetic and electrical stimulation in the infralimbic cortex (IL) of the mouse medial prefrontal cortex (mPFC).
Pyramidal neurons were identified using Thy1-GCaMP6f mice, while parvalbumin (PV) interneurons were labeled with Cre-dependent RCaMP expression. Simultaneous calcium imaging was performed during magnetic stimulation and electrical stimulation. This approach enabled direct observation of activity dynamics in excitatory and inhibitory neuronal populations and assessment of both direct and network-mediated responses.
Neuronal responses were quantified by activation probability, activation area, and response latency in each neuron type across different stimulation conditions. Microcoil stimulation elicited robust calcium responses in both pyramidal and PV neurons, indicating recruitment of excitatory and inhibitory components of the local cortical network in IL. Comparison with electrical stimulation revealed distinct response patterns between the two stimulation modalities. Magnetic and electrical stimulation produced different recruitment profiles, and latency distributions in both PV and pyramidal neuron populations. These differences suggest that magnetic stimulation engages cortical circuits through activation patterns that are not fully explained by conventional electrical stimulation. This work could advance the understanding of the circuit mechanisms underlying magnetic neural stimulation by using calcium imaging for dissecting cell-specific network responses.

**Disclosures: M. Bang:** None. **J. Park:** None. **J. Kwon:** None. **S. Lee:** None.

**Poster**

**PSTR208: Computational Modeling of Synaptic Networks**

**Location:** WCC Halls A-C

**Time:** Monday, November 16, 2026, 1:00 PM - 5:00 PM

**Program #/Poster #:** PSTR208.26/MM40

**Topic:** J.08. Methods to Modulate Neural Activity

**Support:** NIH Grant R01-MH132592
NIH Grant DP2-MH1194025
NIH Grant RF1-MH117055

**Title:** Edge-precise tools to dynamically tag and perturb the connectome

**Authors: *B. C. SHIELDS**, H. YAN, J. R. RAVENEL, S. S.-X. LIM, M. R. TADROSS; Duke Univ., Durham, NC

**Abstract:** Understanding how the connectome supports brain dynamics and behavior requires tools that operate at the scale of the synaptic edge - the junction between defined presynaptic and postsynaptic cells. Existing tools remain poorly matched to this scale; they can manipulate one cell type at a time or report apposition between two populations, but cannot make a defined synaptic edge chemically addressable. Previously, our lab developed DART (Drug Acutely Restricted by Tethering), which uses the HaloTag protein (HTP) - HaloTag ligand (HTL) system to deliver dyes or drugs to genetically defined cells. We have now developed EPiC (Edge-Precise Connectomics), a platform for making genetically defined synaptic edges chemically addressable, so they can be labeled, timestamped, and pharmacologically perturbed with our catalog of drug and dye DARTs.

Our central innovation is an engineered protein pair - HSα (Halo-Swap-α) and HSβ (Halo-Swap-β) - where each protein is inactive alone, but upon contact, generates an active HTP. By expressing HSα on the surface of one defined neural population, and HSβ on another, activated HTP becomes localized to the edges where those populations meet. When expressed in cultured neurons or live mice, incubation with a dye-DART produces bright puncta at cell-cell contact sites, with more than 1000-fold brighter dye-DART signal at HSα × HSβ crossings compared with neighboring regions containing HSα or HSβ alone. Moreover, by pulse-labeling pre-existing edges, followed by a chase with a second spectrally distinct dye-DART, we demonstrate that newly formed edges can be detected on the minutes timescale.

Finally, we demonstrate an edge-precise perturbation in a paired-patch electrophysiology experiment. Application of an AMPAR antagonist DART produced robust blockade of HSα→HSβ transmission, when the reconstituted HTP was positioned closer to the postsynaptic face. By contrast, the same antagonist produced no detectable blockade of HSβ→HSα transmission, when HTP was positioned closer to the presynaptic face.

In sum, with EPiC and DART, we can now expand our ability to determine how specific connections in the brain are formed, remodeled, and recruited to support behavior.

**Disclosures: B.C. Shields:** None. **H. Yan:** None. **J.R. Ravenel:** None. **S.S. Lim:** None. **M.R. Tadross:** None.

**Poster**

**PSTR208: Computational Modeling of Synaptic Networks**

**Location:** WCC Halls A-C

**Time:** Monday, November 16, 2026, 1:00 PM - 5:00 PM

**Program #/Poster #:** PSTR208.27/MM41

**Topic:** J.08. Methods to Modulate Neural Activity

**Support:** AFOSR FA95502310461
NSF CSE-2319060

**Title:** Nano-Neuromodulation Enables Amplification of Olfactory Neural and Behavioral Responses

**Authors: A. DEBNATH**[1], V. GARG[2], F. DENG[6], Y. WANG[3], P. GUPTA[7], S. CHAKRABARTY[4], *B. RAMAN[8], S. SINGAMANENI[5];
[1]Washington Univ. in St. Louis, St Louis, MO; [2]Washington Univ., St. Louis, MO; [3]Washington Univ., Saint louis, MO; [4]Washington Univ., Saint Louis, WA; [5]Washington Univ., Saint Louis, MO; [6]Washington Univ. in St Louis, RICHMOND HEIGHTS, MO; [7]Washington Univ. in St. louis, St. Louis, MO; [8]Biomed. Engin., Washington Univ. In St. Louis, Saint Louis, MO

**Abstract:** There is a pressing need for the development of non-genetic techniques that allow reversible control of neural responses. Here, we develop and demonstrate a novel approach based on mesoporous silica-coated polydopamine nanoparticles (mSiO2@PDA NPs) that can function both as nanoheaters, enabling precise focal heating via the photothermal effect, and as nanocarriers, enabling controlled local release of a desired chemical payload to modulate neural activity in a target circuit. We demonstrate this targeted chemo-photothermal neuromodulation approach in the locust (Schistocerca americana).
We delivered mSiO2@PDA NPs onto a specific olfactory neural circuit (antennal lobe or AL; analogous to vertebrate olfactory bulb). Combining odor delivery with optical stimulation of octopamine-loaded mSiO2@PDA NPs enabled tunable gain control of neural signals, amplifying both odor-evoked neural responses and final behavioral outcomes. We show that while odor-evoked responses are altered, the identity of the odor (combination of neurons activated) and the type of behavioral response elicited are preserved. We demonstrate modulation of two types of odor-evoked behavioral responses: an appetitive response (opening maxillary palps near the mouth) and a navigational response (walking). Reversible modulation of both the probability of the behavioral response as well as the intensity of behavioral response (i.e., walking speed) was observed.
Interestingly, even direct chemo-photothermal modulation of mSiO2@PDA NPs without odor delivery elicited neural activity in the targeted antennal lobe circuit. These ‘phantom’ odorants produced behavioral effects similar to those evoked by the natural olfactory stimuli and could be used to evoke both appetitive and walking behavior in locusts. In sum, our results establish

chemo-photothermal neuromodulation as a minimally invasive, non-genetic framework for neural and behavioral control.

**Disclosures: A. Debnath:** None. **V. Garg:** None. **F. Deng:** None. **Y. Wang:** None. **P. Gupta:** None. **S. Chakrabarty:** None. **B. Raman:** None. **S. Singamaneni:** None.

**Poster**

**PSTR208: Computational Modeling of Synaptic Networks**

**Location:** WCC Halls A-C

**Time:** Monday, November 16, 2026, 1:00 PM - 5:00 PM

**Program #/Poster #:** PSTR208.28/Web Only

**Topic:** J.08. Methods to Modulate Neural Activity

**Support:** JP22K01666
JP25K23152

**Title:** Cognitive State Transitions Across Exploratory and Evaluative Task Stages: Evidence from EEG-Derived Indices

**Authors: *M. ISOBE**[1], Y. EDAGAWA[2];
[1]Art and Design, Ritsumeikan Univ., Kyoto, Japan; [2]Grad. Sch. of Technol. Mgmt., Ritsumeikan Univ., Ibaraki, Osaka,, Japan

**Abstract:** Cognitive adaptation requires transitions between exploratory and evaluative stages of processing. Exploratory cognition supports the generation and manipulation of representations, whereas evaluative cognition supports organization, interpretation, and explanation. Although previous studies have identified neural correlates of creative and analytical thinking, less is known about how cognitive states change dynamically during task performance and how such transitions can be characterized through EEG-derived measurements. The present study investigated cognitive state transitions during a model-construction task using electroencephalographic (EEG) measurements. Participants completed a three-stage task consisting of orientation, construction, and explanation. Continuous EEG signals were recorded using a wearable EEG device throughout task performance. To characterize cognitive states, EEG-derived indices were generated primarily from theta (4-8 Hz), alpha (8-13 Hz), and beta (13-30 Hz) frequency-band activity. Relative band contributions were used to derive engagement and load indices. Changes in these indices and their relationships were examined across task stages. Analyses revealed modulation of EEG-derived measures. The engagement-related index increased during construction and decreased during explanation, indicating non-linear and stage-dependent changes in cognitive engagement. Moreover, the relationship between engagement-related and load-related indices changed across stages. During orientation, the two measures showed a positive association. During construction, this association weakened, whereas during explanation the relationship shifted toward an inverse pattern. These findings suggest that cognitive state transitions are characterized not simply by linear increases or decreases in activation, but by dynamic reconfiguration of the relationship between engagement and cognitive

load. The transition from construction to explanation was consistent with a shift from exploratory toward evaluative processing, reflected in changes in the coupling of EEG-derived measures. The observed patterns indicate changes in cognitive organization associated with changing task demands. Taken together, the results suggest that EEG-derived indices may provide a framework for characterizing cognitive state transitions during task performance. This perspective contributes to understanding cognitive flexibility by demonstrating that exploratory and evaluative modes may be distinguished through changes in relationships among cognitive-state indicators rather than activation level alone.

**Disclosures: M. Isobe:** None. **Y. Edagawa:** None.

**Poster**

**PSTR208: Computational Modeling of Synaptic Networks**

**Location:** WCC Halls A-C

**Time:** Monday, November 16, 2026, 1:00 PM - 5:00 PM

**Program #/Poster #:** PSTR208.29/MM42

**Topic:** J.08. Methods to Modulate Neural Activity

**Title:** Radiogenetics: a transformative approach for brain activation.

**Authors: *D. ZANELLA**[1], S. J. MABRY[5], A. M. BUCHANAN[2], C. ROWE[6], C. GONZÁLEZ-ARANCIBIA[1], M. I. HOSSAIN[3], B. D. ROBINSON[3], H. GOFFINETT[3], B. DUYVESTYN[3], S. MENA ORTEGA[8], A. MAROTTA[9], G. GALLI[10], S. A. ANDRABI[3], J. HEINSBROEK[11], P. HASHEMI[12], A. CARTER[7], M. S. BOLDING[4], A. GALLI[13];
[1]Surgery, Univ. of Alabama at Birmingham, Birmingham, AL; [2]Univ. of Alabama at Birmingham, Durham, NC; [4]Radiology, [3]Univ. of Alabama at Birmingham, Birmingham, AL; [5]Psychiatry, Univ. of Pittsburgh, Pittsburgh, PA; [6]Dept. of Surgery, [7]Univ. of Alabama, Birmingham, Birmingham, AL; [8]King's Col., London, United Kingdom; [9]UAB, Milan, Italy; [10]UAB, Brentwood, TN; [11]Neurobio., Univ. of Alabama At Birmingham, Birmingham, AL; [12]Imperial College, London, London, United Kingdom; [13]Surgery, Univ. of Alabama Birmingham, Birmingham, AL

**Abstract:** Current neuromodulation techniques are prized tools in neuroscience research and in clinical settings. However, they present limitations, including requiring permanent implants, being restricted to the region the stimulation apparatus is localized in, and limited regulation of the stimulation intensity. Therefore, developing an approach overcoming these limitations would benefit research and clinical settings alike.
Drosophila shows avoidance of ultraviolet (UV) light mediated by the Transient Receptor Potential Ankyrin type-1 (dTRPA1). dTRPA1 is an evolutionarily conserved detector of reactive oxygen species (ROS) including $H_2O_2$, which are generated by UV irradiation of biological fluids. The dTRPA1 locus has two promoters (A and B) that drive expression of at least five transcripts. The dTRPA1(A)10a and dTRPA1(A)10b isoforms are derived from the A promoter and are highly sensitive to $H_2O_2$ and permeable to calcium and sodium ions.
We hypothesize that the use of a more potent/penetrant ionizing radiation source (X-ray), which

produces ROS, will allow us to use one of these variants (dTRPA1(A)10b) as a flexible tool to establish a novel neuromodulation platform with high penetrance and controlled stimulus intensity (Radiogenetics).
Using X-ray irradiation, we induced neurotransmitters release (i.e. dopamine (DA)) in *ex-vivo* preparations of Drosophila brains, and were able to modify their locomotion. The knockdown of TRPA1 in DA neurons in the fly brains or its pharmacological inhibition impaired the efficacy of X-ray irradiation.
Next, we determined the applicability of the system in a mammalian cell line. Using calcium imaging, we showed that X-ray activate dTRPA1(A)10b, while other splicing variants of dTRPA1 and the murine TRPA1 failed to respond to comparable X-ray stimulations.
Next, we used a lentivirus delivery system to express dTRPA1(A)10b in mouse primary neurons. Upon irradiation, we observed depolarization and firing only in the neurons expressing dTRPA1(A)10b.
Finally, to test Radiogenetics *in vivo*, we injected the lentivirus into the Substantia Nigra (pars compacta) of mice. Using Fast Scan Cyclic Voltammetry, we determined that non-injected mice and control mice (lentivirus carrying mCherry) were insensitive to X-ray irradiation, whereas dTRPA1(A)10b-injected mice released DA in the striatum. Animals treated with the same viral paradigm showed increased grooming when placed in a behavioral arena and irradiated.
X-ray-induced $H_2O_2$ synthesis activated dTRPA1(A)10b both *in vitro*, *ex-vivo* and *in vivo*. This data represents the proof of principle for the use of Radiogenetics as a novel neuromodulation platform.

**Disclosures: D. Zanella:** None. **S.J. Mabry:** None. **A.M. Buchanan:** None. **C. Rowe:** None. **C. González-Arancibia:** None. **M.I. Hossain:** None. **B.D. Robinson:** None. **H. Goffinett:** None. **B. Duyvestyn:** None. **S. Mena ortega:** None. **A. Marotta:** None. **G. Galli:** None. **S.A. Andrabi:** None. **J. Heinsbroek:** None. **P. Hashemi:** None. **A. Carter:** None. **M.S. Bolding:** None. **A. Galli:** None.

**Poster**

**PSTR208: Computational Modeling of Synaptic Networks**

**Location:** WCC Halls A-C

**Time:** Monday, November 16, 2026, 1:00 PM - 5:00 PM

**Program #/Poster #:** PSTR208.30/MM43

**Topic:** J.08. Methods to Modulate Neural Activity

**Support:** NIH R01-MH132592
CBTE Predoctoral Fellowship
AHA Predoctoral Fellowship
NUS Development Grant
NIH RF1-MH117055

**Title:** Subcellular control of dopamine-mediated behavior

**Authors: *S. S.-X. LIM**[1], H. YAN[1], V. G. BRYSON[1], S. YOUSEFZADEH[1], B. C. SHIELDS[1], J. M. ROACH[2], S. SINGH[2], S. C. BURWELL[3], A. CHOUDHURY[2], M. R. TADROSS[1,2,3]; [1]Dept. of Neurosurg., [2]Dept. of Biomed. Engin., [3]Dept. of Neurobio., Duke Univ., Durham, NC

**Abstract:** Neurons are highly polarized cells with distinct anatomical compartments (axon, soma, dendrites). These subcellular compartments are thought to serve distinct functions. However, it remains unknown how the same receptor in different subcellular compartments impacts circuit dynamics and animal behavior. A prototypical example involves the inhibitory neurotransmitter, GABA, whose receptor, the GABAAR, is present throughout all neuronal compartments, each of which receives distinct streams of information and is biophysically positioned for distinct functions. GABAARs on distal dendrites are thought to counterbalance local excitatory inputs, whereas those on the soma are thought to have veto power over action potential output. GABAARs in the axon may further sculpt neural output by decoupling transmitter release from action potential firing, with the potential to individually tune collaterals. Here, we describe the development of somaDART, a new soma-specific variant of DART (Drug Acutely Restricted by Tethering), that makes it possible to deliver pharmaceuticals to genetically specified locales. We demonstrate the utility of this tool across diverse cell types. In particular, by leveraging this approach in dopamine neurons, we identify qualitatively separable behavioral roles for GABAARs in the somatic and distal dendritic compartments.
Finally, we describe extensions of the approach to other subcellular locales, including a method to deliver DART pharmaceuticals to axon projections without diffusion into somatodendritic compartments, enabling axon-specific pharmacology. Altogether, these tools are compatible with use in freely behaving mice, and should provide a modular foundation for subcellular targeting of virtually any drug.

**Disclosures: S.S. Lim:** None. **H. Yan:** None. **V.G. Bryson:** None. **S. Yousefzadeh:** None. **B.C. Shields:** None. **J.M. Roach:** None. **S. Singh:** None. **S.C. Burwell:** None. **A. Choudhury:** None. **M.R. Tadross:** None.